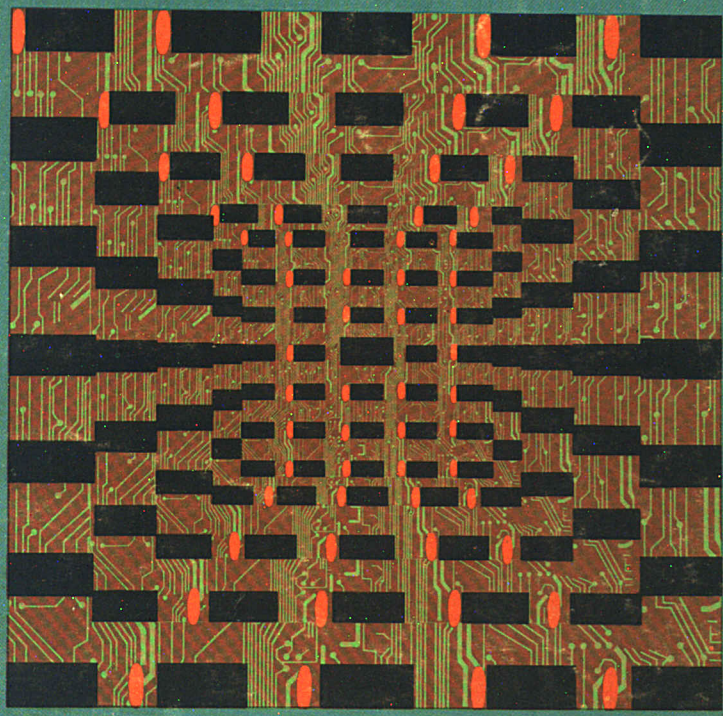
OCTOBER 1974

analytical chemistry



Microprocessors

FACSS—First National Meeting—999A

Thelco Ovens. They stretch your dollars!

How? That's easy. Thelco® Ovens are designed to perform better, look better, last longer. Their trouble-free service and reliability mean less maintenance . . . and your youngest technician may be retired before your Thelco needs replacement. The preference for Thelcos in the scientific community seems to support these facts.

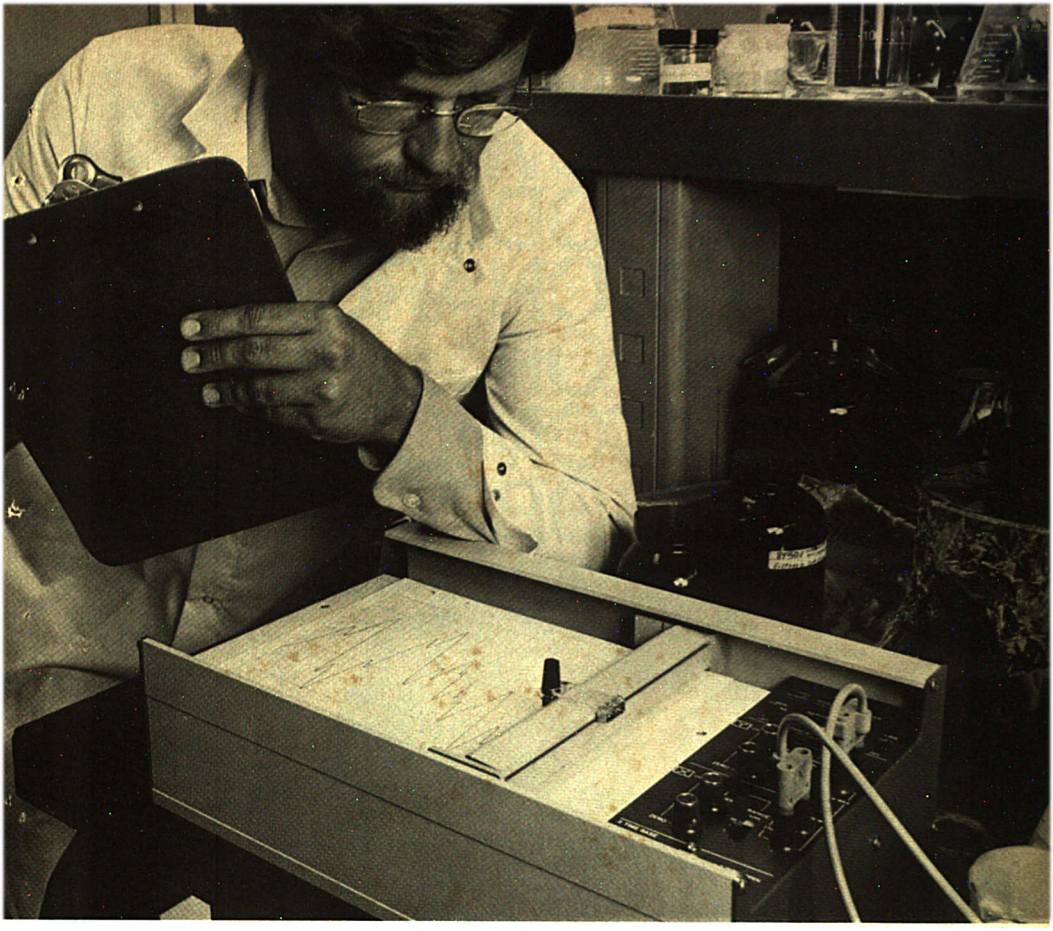
You'll appreciate Thelco's fine styling . . . the all stainless steel interiors . . . the super-safe single-knob dual thermostat . . . the large work chambers with pull-out (but no drop) shelves . . . the smooth working door release. And perhaps most of all you'll like the unequaled temperature uniformity throughout the chamber. It's guaranteed!

Learn more about the Thelco dollar stretchers from your GCA/Precision Scientific Dealer or write us. GCA/Precision Scientific, 3737 W. Cortland St., Chicago, Ill. 60647. Sales offices in Boston, New York, Buffalo, Philadelphia, Charlotte, Atlanta, Cleveland, Chicago, Houston, Los Angeles, San Francisco.

GCA/PRECISION SCIENTIFIC

CIRCLE 89 ON READER SERVICE CARD





HP introduces a new compact 8½ x 11 lab XY recorder.

For labs that really work their recorders, Hewlett-Packard has put together a very appealing group of features in the new Model 7015A.

It starts with the ruggedness and dependability built into every HP recorder. Performance is tight. And this machine is built to keep it that way. Even if the recorder is run off-scale for hours on end, its continuous-duty servo motors will come through without a trace of damage.

The package is small and lightweight. Depending on how you want it, it's economical to equip the recorder with options like internal time base, metric calibration, electric pen lift and carrying case.

For one low price, we've included standard features that help make the 7015A an outstanding value for schools and busy labs. You get three spans from 10mV/in to 1 V/in, front panel vernier and zero controls, electrostatic paper holddown, rear connector and rack mount kit. We supply high quality disposable fiber tipped pens along with a universal holder designed to fit a variety of other brands.

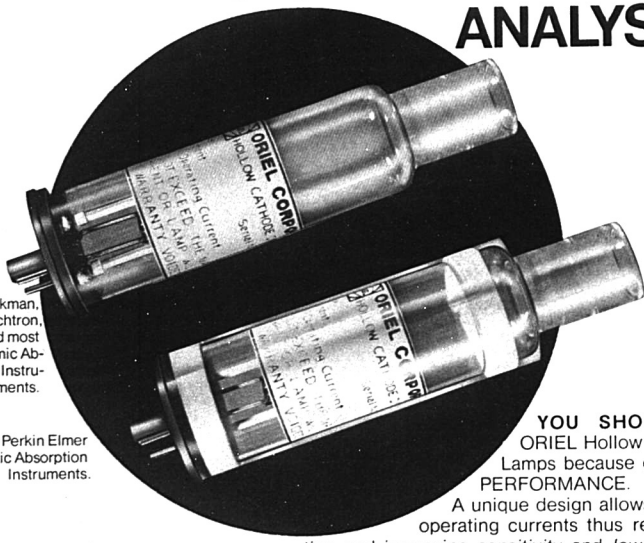
HP's new 8½ x 11 lab XY recorder. At just $945 (domestic USA price only), we built it to be the smartest little investment you ever made. For details, write Hewlett-Packard, 1501 Page Mill Road, Palo Alto, California 94304. 11413

HEWLETT hp PACKARD

CIRCLE 118 ON READER SERVICE CARD

Sales and service from 172 offices in 65 countries.
1501 Page Mill Road, Palo Alto, California 94304

ORIEL HOLLOW CATHODE DISCHARGE LAMPS FOR ATOMIC ABSORPTION ANALYSIS



For Beckman, Varian, Techtron, Jarrell Ash and most other Atomic Absorption Instruments.

For Perkin Elmer Atomic Absorption Instruments.

YOU SHOULD CONSIDER ORIEL Hollow Cathode Discharge Lamps because of their SUPERIOR PERFORMANCE.

A unique design allows high output at low operating currents thus reducing self absorption and improving *sensitivity* and *low-level detectability.*

YOU MIGHT CONSIDER ORIEL Hollow Cathode Discharge Lamps because of their LONG LIFE!
500 hours guaranteed regardless of operating current (under the maximum current of course).

BUT!! YOU MUST CONSIDER ORIEL Hollow Cathode Discharge Lamps because of their EXCELLENT PRICES!!!
Priced from $77.00 these lamps average 20-40% under the competition. WHY PAY MORE?

NOTE: These lamps are made for ORIEL by a leading manufacturer of Hollow Cathode Discharge Lamps.
WRITE TODAY FOR Technical Brochure and Prices!

ORIEL CORPORATION
OF AMERICA
15 MARKET ST. STAMFORD, CONN. 06902
203 357-1600 TWX 710-474-3563

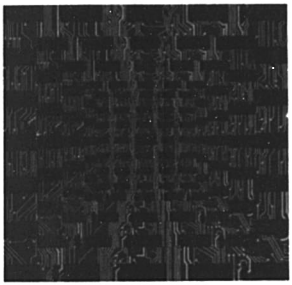
CIRCLE 182 ON READER SERVICE CARD

analytical chemistry

Volume 46, No. 12
October 1974

ANCHAM 46(12) 957A–1084A/1625–1880 (1974)
ISSN 0003-2700

Contents



Our cover design is inspired by the two-part INSTRUMENTATION article on microprocessors which concludes this month with a discussion of the applications of these useful devices to "real world" problems. In Part II the advantages and disadvantages of microcomputers are given, as well as practical suggestions on how to use the simple logical concepts presented in Part I (ANAL. CHEM., September 1974).

The basic microprocessor circuit used in the design was provided by Digital Equipment Corp., Marlborough, Mass.

REPORT

Marvin W. Skougstad of the U.S. Geological Survey describes the many efforts underway to reach national and international agreements on standardization of methods and techniques for evaluating water quality **982 A**

REPORT

R. F. Coleman of London, England, assesses the analytical techniques commonly used to determine inorganic pollutants in food, water, or collected on air filters from the atmosphere **989 A**

INSTRUMENTATION

In Part II of "Microprocessors," Raymond E. Dessy, Jonathan A. Titus, and Peter Janse-Van Vuuren of VPI describe a potential application, spotlight advantages and disadvantages, and summarize instructional possibilities of microcomputers **1055 A**

FACSS

The First National Meeting of the Federation of Analytical Chemistry and Spectroscopy Societies will be held November 18–22, 1974, in Atlantic City, N.J. The technical program, exhibitors, and products are given **999 A**

NEWS AND VIEWS

Sidney Siggia, M. T. Kelley, and Egon Stahl are named winners of 1975 American Chemical Society Awards. Winners of other awards include Jaroslav Sestak, Homer Hagstrum, and Dale Coulson **1031 A**

BOOKS

Books on nonaqueous solvents, vibrational spectroscopy of trapped species, computer-assisted instruction, interpretation of mass spectra, and laboratory administration are reviewed by I. M. Kolthoff, Edward G. Brame, Jr., Harry E. Keller, K. Biemann, and Edward C. Dunlop **1045 A**

EDITORS' COLUMN

A short survey of analytical chemistry in Canada shows that the discipline is "real world" oriented **1053 A**

EDITORIAL

Professor Laitinen discusses some of the problems involved in fundamental research associated with the Nation's energy needs **1625**

Author Index 964 A
Briefs 969 A
Future Articles 1084 A
Call for Papers 1034 A
Meetings 1034 A
Short Courses 1036 A
New Products 1071 A
Chemicals 1078 A
Manufacturers' Literature 1079 A

Articles

Nondestructive Determination of Some Trace Elements in Tantalum by Proton Activation Analysis. *Viliam Krivan, D. L. Swindle, and E. A. Schweikert* **1626**

Multielement Determination in Market-Garden Soils by Instrumental Photon Activation Analysis. *Amares Chattopadhyay and R. E. Jervis* **1630**

Role of Column Parameters and Injection Volume on Detection Limits in Liquid Chromatography. *B. L. Karger, Michel Martin, and Georges Guiochon* **1640**

Disk Conveyor Flame Ionization Detector for Liquid Chromatography. *J. J. Szakasits and R. E. Robinson* **1648**

New Approach to Chromatogram Interpretation by Multiple Detection. *Nedjeljko Ostojic* **1653**

Gas-Complex Chromatography: Substituent and Steric Effects. *R. J. Laub, Vaidhyanathan Ramamurthy, and R. L. Pecsok* **1659**

Polycyclic Aromatic Hydrocarbons in the Environment: Isolation and Characterization by Chromatography, Visible, Ultraviolet, and Mass Spectrometry. *Walter Giger and Max Blumer* **1663**

ห้องสมุด กรมวิทยาศาสตร์
20 ธ.ค. 2517

Contents

Solid Sampling Atomic Absorption Determination of Lead in Rock Samples Using the Iron Screw Rod Technique. *Kuppusami Govindaraju, Guy Mevelle, and Charles Chouard* 1672

Method for the Choice of Optimal Analytical Positions in Spectrophotometric Analysis of Multicomponent Systems. *J. Sustek* 1676

Spectrophotometric Determination of Micro Amounts of Hexathionate in Mixtures with Thiosulfate and Sulfite by Means of Its Sulfitolysis. *Tomozo Koh and Kazuo Taniguchi* 1679

Separation Technique for Mass Spectrometry. Fractionated Evaporation from a Direct Inlet System Which Maintains a Fixed Total Ion Current. *Jochen Franzen, Hendrik Kuper, and Wolfgang Riepe* 1683

Gated Nanosecond Time Resolved Emission Spectroscopy Separation of Mixed Emissions from Carbonyl Compounds. *R. E. Brown, K. D. Legg, M. W. Wolf, L. A. Singer, and J. H. Parks* 1690

Corrected and Automated Spectrophotofluorimeter Employing a Pyroelectric Detector for Correction. *Isaac Landa and J. C. Kremen* 1694

Study of the Precision of an X-Ray Fluorescence Spectrometric Determination. *E. B. Buchanan, Jr., and Foo-Chong Tsai* 1701

Optimization of the Operating Parameters of Chemiluminescent Nitric Oxide Detectors. *D. M. Steffenson and D. H. Stedman* 1704

Analytical Ion Cyclotron Resonance Spectrometry. Sterochemical Effects in Some Cyclic Ketones. *M. M. Bursey, Jar-lin Kao, J. D. Henion, C. E. Parker, and Tai-In S. Huang* 1709

Determination and Comparison of Association Constants for Weak Organic Complexes by Thermodynamic, Resonance, and Optical Methods. *D. E. Martire* 1712

Determination of Rare Earths in Plutonium by X-Ray Emission Analysis. *A. G. Miller* 1720

Simultaneous Determination of Alpha-Emitting Nuclides of Radium through Californium in Soil. *C. W. Sill, K. W. Puphal, and F. D. Hindman* 1725

Radiochemical Separation of Fluorine by Adsorption on Hafnium Dioxide: Application to the Determination of Oxygen by Activation Analysis with Charged Particles. *A. Kohn, J. N. Barrandon, J. L. Debrun, M. Valladon, and B. Vialatte* 1737

Sequential Determination of Radium-226, Radium-228, Actinium-227, and Thorium Isotopes in Environmental and Process Waste Samples. *D. R. Percival and D. B. Martin* 1742

Excited Singlet State Acidity Constants for Hydroxy and Amino Substituted Anthraquinones and Related Compounds: A Comparison of Excited State p*K* Measurement Procedures. *H. H. Richtol and B. R. Fitch* 1749

New Instrumental Approach in Phase-Selective Second Harmonic Alternating Current Polarography. *H. Blutstein, A. M. Bond, and A. Norris* 1754

Voltammetry in Sulfolane: The Electrochemical Behavior of Benzaldehyde and Substituted Benzaldehydes. *N. R. Armstrong, R. K. Quinn, and N. E. Vanderborgh* 1759

Streaming Potentials in Automatic Potentiometric Systems. *Pierre Van den Winkel, John Mertens, and D. L. Massart* 1765

Enzyme Electrode Sensing Oxygen for Uric Acid in Serum and Urine. *M. Nanjo and G. G. Guilbault* 1769

An Automatic Analyzer for the Detection of Dihydroxyphenylalanine Metabolites and Other Reducing Compounds in Urine. *P. W. Banda, A. E. Sherry, and M. S. Blois* 1772

Determination of Uric Acid at the Microgram Level by a Kinetic Procedure Based on a "Pseudo-Induction" Period. *V. V. S. Eswara Dutt and H. A. Mottola* 1777

Identification and Quantitative Measurement of Some *N*-Heterocyclics in Marijuana Smoke Condensates. *M. Zamir-ul Haq, S. J. Rose, L. R. Deiderich, and A. R. Patel* 1781

Simple Digital Method for Resolving Overlapping Electronic Absorption Bands. *B. E. Barker, M. F. Fox, E. Hayon, and E. W. Ross* 1785

© Copyright 1974
by the American Chemical Society

MANUSCRIPT REQUIREMENTS published in December 1973 issue, page 2451, outlines scope and copy requirements to be observed in preparing manuscripts for consideration. Manuscript (4 copies) should be submitted to ANALYTICAL CHEMISTRY, 1155 Sixteenth St., N.W., Washington, D.C. 20036.

The American Chemical Society assumes no responsibility for the statements and opinions advanced by contributors to its publications. Views expressed in the editorials are those of the editors and do not necessarily represent the official position of the American Chemical Society.

1974 Subscription Rates

	1 yr.	2 yr.	3 yr.
Members, domestic and foreign	$ 5.00	$ 9.00	$12.00
Nonmembers, domestic and Canada	7.00	12.00	16.00
Nonmembers, foreign except Canada	15.00	27.50	40.00

Postage: Canada and Pan-American Union, $4.00: foreign, $5.00. Air freight rate available on request. Single copies: current, $2.00 except Annual Reviews, $3.00 each. Rates for back issues and volumes are available from Special Issues Sales Dept., 1155 Sixteenth St., N.W., Washington, D. C. Send all new and renewal subscriptions *with payment* to: Office of the Controller, 1155 Sixteenth Street, N.W., Washington, D. C. 20036. All correspondence and telephone calls regarding changes of address, claims for missing issues, subscription service, the status of records, and accounts should be directed to: Manager, Membership and Subscription Services, American Chemical Society, P.O. Box 3337, Columbus, Ohio 43210. Telephone (614) 421-7230

On changes of address, include both old and new addresses with ZIP code numbers, accompanied by mailing label from a recent issue. Allow four weeks for change to become effective.

Subscriptions should be renewed promptly to avoid a break in your series.

Claims for missing numbers will not be allowed (1) if received more than sixty days from date of issue plus time normally required for postal delivery of journal and claim, (2) if loss was due to failure of notice of change in address to be received before the date specified in (1), or (3) if the reason for the claim is "issue missing from files."

Those interested in joining the American Chemical Society should write to Admissions Department at the Washington Office.

Published monthly with Review issue added in April and a Laboratory Guide in August by the American Chemical Society, from 20th and Northampton Sts., Easton, Pa. 18042; Executive Offices and Editorial Headquarters, 1155 Sixteenth St., N.W., Washington, D. C. 20036; Advertising Office, 142 East Ave., Norwalk, Conn. 06851. ANALYTICAL CHEMISTRY and other ACS periodicals are available on microfilm. For information write to: MICROFILM, Special Issues Sales Dept., American Chemical Society, 1155 Sixteenth St., N.W., Washington, D. C. 20036. Second class postage paid at Washington, D. C. and at additional mailing offices.

Perkin-Elmer's PEP-2 Chromatography Data System now tells you directly if a suspect is drunk.

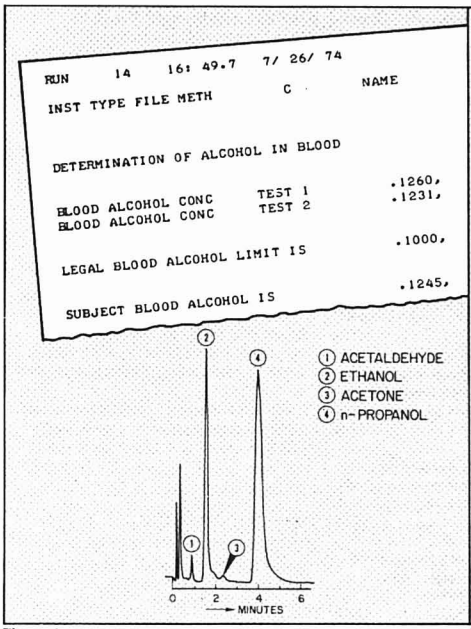


Figure 1

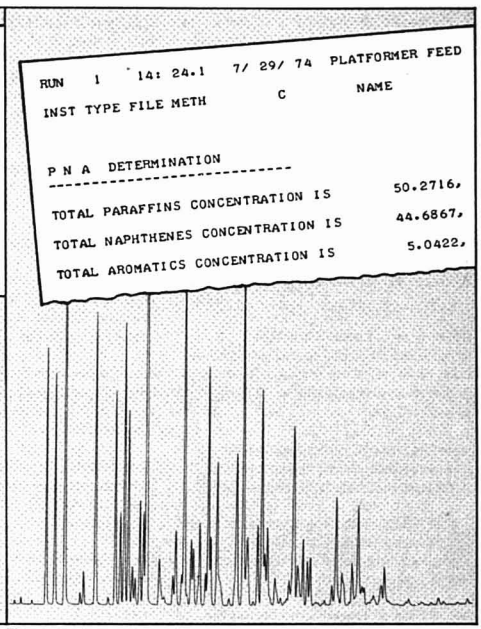


Figure 2

Perkin-Elmer's PEP Chromatography Data System has a well established ability to produce reports where each sample component is listed by name and concentration. Now it can do three more things:

1. It can be used with 16 chromatographs (gas and/or liquid).
2. It can talk over the telephone to other computers.
3. It can be programmed by the operator, though it needn't be.

PEP-2 now sports an interactive programming language (IPL).

Computer people, who can always make the simple sound terrifying, describe IPL as a high-level language employing macro commands. Actually, it's a set of less than a dozen symbols, which a typical noncomputnik can learn in about a day, and which can make PEP manipulate the data in some remarkable ways. For instance:

Before you lock up a drunk, be sure that he is.

When you use an MS-41 Capsule Sampler to inject blood into a GC, you're very likely to get the right answer for alcohol content. The blood stays in the capsule and cannot foul up the injector; there's no possibility of contamination or carryover. Nevertheless, some jurisdictions require that two separate tests be made on drunk driving suspects. The print-out should then display both results, their average, and the legal limit, all in percent concentration. With a little bit of IPL, PEP-2 does it automatically. See Figure 1.

In PNA analysis, all you want is the answer.

A PNA analysis of a feed stock is the measurement of the total concentrations of paraffins, naphthenes, and aromatics. The chromatogram —run in 38 minutes on a Perkin-Elmer Model 3920 Gas Chromatograph equipped with a SCOT column —appears in Figure 2. PEP-2 could easily print out the names and concentrations of all 88 components, if anybody wanted to see them. Instead, IPL is used to make PEP do the sorting and computations and to print out exactly what is wanted —no more and no less.

PEP-2 can talk to the big computer.

There's now a telecommunications link between PEP-2 and most big computers—it's called a dataphone. At last, the user has that rare thing, the best of two worlds. The big computer does what it does best —combines reports, consults histories, changes a process stream, or bills the patient. Meanwhile, the user of the big computer can benefit from the sheer chromatographic power of PEP-2, and need not try to duplicate the five years of very expensive, specialized, and skillful programming that went into it.

For more information write: The Instrument Div., Perkin-Elmer Corp., Main Ave., Norwalk, CT 06856.

PERKIN-ELMER

CIRCLE 193 ON READER SERVICE CARD

Contents

Computerized Pattern Recognition Applications to Chemical Analysis. Development of Interactive Feature Selection Methods for the K-Nearest Neighbor Technique. *M. A. Pichler and S. P. Perone* 1790

Hadamard Transformed Carbon-13 Nuclear Magnetic Resonance Spectra—Pattern Recognition Analysis. *T. R. Brunner, R. C. Williams, C. L. Wilkins, and P. J. McCombie* 1798

Notes

Concise Algorithm for Conversion between Normal and Sequency Ordered Hadamard Matrices. *R. C. Williams, R. M. Swanson, and C. L. Wilkins* 1803

Determination of Sulfur by the Measurement of Molecular Emission in Cool Flames: Conversion of Sample Sulfur to Hydrogen Sulfide. *S. Shiffman and C. W. Frank* 1804

New Discrete Atomization Cell for Atomic Fluorescence Spectrometry. *C. J. Molnar and J. D. Winefordner* 1807

Flame Atomic Fluorescence and Emission Spectrometry with a Microsampling Cup Technique. *J. K. Grime and T. J. Vickers* 1810

Separation of Trace Metal Impurities from Nuclear Grade Uranium by Long-Chain Amine Extraction and Direct Determination by Atomic Absorption Spectrophotometry. *Sergio de Moraes and Alcidio Abrao* 1812

Atomic Absorption Determination of Mercury in Fish Using the Coleman MAS-50 Mercury Analyzer. *Pekka Kivalo, Asko Visapaa, and Runar Backman* 1814

Analytical Applications of the Graphite Braid Nonflame Atomizer. *Akbar Montaser and S R. Crouch* 1817

Detection and Analysis of Protein Functional Group Modification by X-Ray Photoelectron Spectrometry. *M. M. Millard and M. S. Masri* 1820

Determination of Molybdenum in Plutonia Cermets by X-Ray Fluorescence Spectrometry. *H. A. Woltermann and W. W. Strohm* 1822

Quantitative Determination of the Phase I/Phase II Ratio in Sodium Triphosphate by Raman Spectrometry. *Jan Bus* 1824

Spectrochemical Method for Determination of Tellurium in Geological Materials. *Irena Schoenfeld and Armand Berman* 1826

Voltammetry of Bismuth(III) at a Continuously Mercury-Coated Rotating Platinum Disk Electrode. *M. Z. Hassan and Stanley Bruckenstein* 1827

Live Peak Stripping during X-Ray Energy-Dispersive Analysis. *John Parkes, L. J. Rabbitt, and M. J. Hampshire* 1830

Determination of Trace Metals in Aqueous Environments by Anodic Stripping Voltammetry with a Vitreous Carbon Rotating Electrode. *A. H. Miguel and C. M. Jankowski* 1832

Semiquantitative Potentiometric Method for Direct Measurement of Nitrogen Dioxide in Air. *G. G. Barna and R. J. Jasinski* 1834

Electrochemical Technique for the Measurement of Carbon Monoxide. *H. W. Bay, K. F. Blurton, J. M. Sedlak, and A. M. Valentine* 1837

Use of State Variable Active Filters as Differentiators, Rate Meters, and End-Point Locators. *R. H. Callicott and P. W. Carr* 1840

Ion Selective Electrodes Responsive to Anionic Detergents. *Taitiro Fujinaga, Satoshi Okazaki, and Henry Freiser* 1842

Determination of Isocyanates in the Working Atmosphere by Thin-Layer Chromatography. *Jurgen Keller, K. L. Dunlap, and R. L. Sandridge* 1845

Gas Chromatographic Separation of Some Unsaturated Hydrocarbons Using Thallium(I) Tetraphenylborate as Stationary Phase. *G. E. Baiulescu and V. A. Ilie* 1847

Determination of Long Chain Fatty Acids as 2-Naphthacyl Esters by High Pressure Liquid Chromatography and Mass Spectrometry. *M. J. Cooper and M. W. Anders* 1849

Gas Chromatographic Analysis of Ambient Air for Light Hydrocarbons Using a Chemically Bonded Stationary Phase. *H. H. Westberg, R. A. Rasmussen, and M. Holdren* 1852

Synthesis of Reproducible Tin(IV) Based Ion Exchangers: Separation of Lanthanum(III) from Yttrium(III), Europium(III), and Lutetium(III). *Mohsin Qureshi, Rajendra Kumar, and Veena Sharma* 1855

Sampling Errors in the Quantitation of Petroleum in Boston Harbor Water. *S. M. Ahmed, M. D. Beasley, A. C. Efromson, and R. A. Hites* 1858

Triplet State Acidity Constants for Hydroxy and Amino Substituted Anthraquinones and Related Compounds. Comparison of Phosphorescence and Transient Triplet Absorption Measurements. *H. H. Richtol and B. R. Fitch* 1860

Potential Sources of Analytical Error in the Erythrocytic δ-Aminolevulinic Acid Dehydratase Test for Lead Exposure. *T. J. Kneip, Norman Cohen, and Virginia Rulon* 1863

Kinetic Study of the Stabilities of Chloromethyl Methyl Ether and Bis(Chloromethyl)Ether in Humid Air. *J. C. Tou and G. J. Kallos* 1866

Effect of Ethyl Chloroformate on the Dye Combining Capacity of Protein. *Louis Sandler and F. L. Warren* 1870

Evaluation of an Ozone Photometer for Ambient Ozone Measurements. *Leo Zafonte, William Long, and J. N. Pitts, Jr.* 1872

Correspondence

Beryllium Content of NBS Standard Reference Orchard Leaves. *T. M. Florence, Y. J. Farrar, L. S. Dale, and G. E. Batley* 1874

Comments on Ratio Matching. *C. W. Chen* 1876

Aids for Analytical Chemists

Simple Device for Improving the Production of Coiled Glass Capillary Columns. *Eugene Reiner and J. W. Weaver* 1878

Glass-Immobilized 8-Hydroxyquinoline for Separation of Trace Metals from Base Electrolytes Used for Anodic Stripping Analysis. *E. D. Moorhead and P. H. Davis* 1879

Correction. Thermometric Titration Determination of Hydroxide and Alumina in Bayer Process Solutions. *Eric VanDalen and L. G. Ward* 1826

Correction. Correction of Inner Filter Effects in Fluorescence Spectrometry. *V. A. Mode and D. H. Sisson* 1831

Correction. Determination of Fluoride in Coal with the Fluoride Ion-Selective Electrode. *Josephus Thomas, Jr., and H. J. Gluskoter* 1831

plenum
the language of science

Characterization of Solid Surfaces

Edited by **Philip F. Kane**
and **Graydon B. Larrabee**

A brilliant, comprehensive review of surface analysis, this important volume surveys both principles and techniques of surface characterization, describes instrumentation, and suggests the course of future research.
670 pages $32.50

• Critical Stability Constants, Vol. 1
Amino Acids

By **Arthur E. Martell**
and **Robert M. Smith**

An up-to-date compilation of data, this invaluable three-volume treatise provides a thorough guide to metal complex equilibria constants. Dealing with aminocarboxylic acids, the first volume covers values of stability constants and enthalpy and entropy changes for equilibria involving acid-base reactions and the complexation of metal ions with amino acids in aqueous solutions.
469 pages $23.00

The Practice of NMR Spectroscopy
With Spectra–Structure Correlations for Hydrogen-1

By **Nugent F. Chamberlain**

Providing systematic methods and comprehensive data correlations, this important volume offers valuable information on evaluating NMR spectra and measuring spectral parameters to determine molecular structure and to analyze multicomponent systems.
424 pages $29.50

Advances in Experimental Medicine and Biology, Vol. 42

Immobilized Biochemicals and Affinity Chromatography

Edited by **R. Bruce Dunlap**

Offering exciting new techniques for scientists from many disciplines, this invaluable volume examines biochemicals immobilized on a variety of solid supports. This work discusses the potential of this new process in the purification of enzymes and proteins, in the employment of immobilized enzymes as useful catalysts, and in the study of three-dimensional configurations of proteins and enzymes.
377 pages $22.50

Introduction to Bioelectrodes

By **Clifford D. Ferris**

Systematically examining electrodes and electrode systems used in biological, medical, environmental, neurobiological, and physiological research, this introductory volume discusses theoretical aspects of bioelectrodes, their construction, and backup equipment such as amplifier systems.
Approx. 275 pages $19.50

Analytical Calorimetry
Volume 3

Edited by **Roger S. Porter**
and **Julian F. Johnson**

Reporting on original research by leading scientists from industry, government and academia, this timely work deals with such important topics as identification of polymers and inorganic materials by thermal analysis, applications in forensic science, kinetic reaction studies, and quality control applications in industry.
Approx. 800 pages $45.00

• This series is eligible for a SPECIAL CHARTER SUBSCRIBER'S DISCOUNT.
For further information please contact the Publishers.

Visit Booth #E10

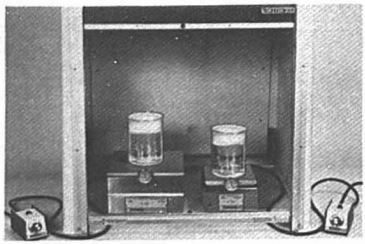
Federation of Analytical Chemistry and Spectroscopy Societies
Atlantic City

PLENUM PUBLISHING CORPORATION, 227 West 17th Street, New York, N.Y. 10011
In United Kingdom: 4a Lower John Street, London W1R 3PD, England

CIRCLE 189 ON READER SERVICE CARD

QUALITY LABORATORY APPARATUS

Remote control



Hot plates

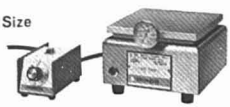
PROVIDE SAFE AND CONVENIENT OPERATION

Types 1900 and 2600 hot plates can now be remotely controlled from outside the fume hood. Controls are removed from corrosive fumes, possible spill damage and flammable vapors assuring safe and trouble-free life. Remote control units can be operated horizontally or mounted vertically on fume hood wall. A 5 ft. control cord and 5 ft. plug-in cord provide sufficient length to operate in most fume hood setups. Optional thermometer available to closely monitor top plate temperature.

Controller reliability allows selection of desired temperature to within ±5°C . . . can easily attain repeatable results up to 900° F. Embedded heating elements provide resistance from fume hood contaminates. Rugged cast iron top plate resists blows, chemical corrosion and thermal shock. For safety and efficiency in your laboratory, select Thermolyne's Remote Control Hot Plates. Available in 120 or 240 Volts 50/60 Hz.

Write for new Laboratory Apparatus Catalog #500.

Type RC1900
6" x 6" Top Plate Size
Price $70.00





Type RC 2600
9" x 9" Top Plate Size
Price $110.00

MEX140 optional dial thermometer Price $20.75

THERMOLYNE
SYBRON CORPORATION
2555 KERPER BOULEVARD, DUBUQUE, IOWA 52001

CIRCLE 223 ON READER SERVICE CARD

Author Index

Abrao, A.	*1812*	Callicott, R. H.	*1840*
Ahmed, S. M.	*1858*	Carr, P. W.	*1840*
Anders, M. W.	*1849*	Chattopadhyay, A.	*1630*
Armstrong, N. R.	*1759*	Chen, C. W.	*1876*
		Chouard, C.	*1672*
Backman, R.	*1814*	Cohen, N.	*1863*
Banda, P. W.	*1772*	Cooper, M. J.	*1849*
Baiulescu, G. E.	*1847*	Crouch, S. R.	*1817*
Barker, B. E.	*1785*		
Barna, G. G.	*1834*	Dale, L. S.	*1874*
Barrandon, J. N.	*1737*	Davis, P. H.	*1837*
Batley, G. E.	*1874*	Debrun, J. L.	*1737*
Bay, H. W.	*1837*	Deiderich, L. R.	*1781*
Beasley, M. D.	*1858*	de Moraes, S.	*1812*
Berman, A.	*1826*	Dunlap, K. L.	*1845*
Blois, M. S.	*1772*		
Blumer, M.	*1663*	Efromson, A. C.	*1858*
Blurton, K. F.	*1837*	Eswara Dutt, V. V. S.	*1777*
Blutstein, H.	*1754*		
Bond, A. M.	*1754*		
Brown, R. E.	*1690*	Farrar, Y. J.	*1874*
Bruckenstein, S.	*1827*	Fitch, B. R.	*1749, 1860*
Brunner, T. R.	*1798*	Florence, T. M.	*1874*
Buchanan, E. B., Jr.	*1701*	Fox, M. F.	*1785*
Bursey, M. M.	*1709*	Frank, C. W.	*1804*
Bus, J.	*1824*	Franzen, J.	*1683*

Continued on p. 967A

Directory of Graduate Research 1973



A valuable guide to graduate schools, research, and personnel in the universities and colleges in the United States and Canada offering an organized curriculum leading to the doctoral degree in chemistry, biochemistry, chemical engineering, and pharmaceutical or medicinal chemistry.

Covers
211 Departments of Chemistry
158 Departments of Biochemistry
104 Departments of Chemical Engineering
32 Departments of Pharmaceutical or Medicinal Chemistry

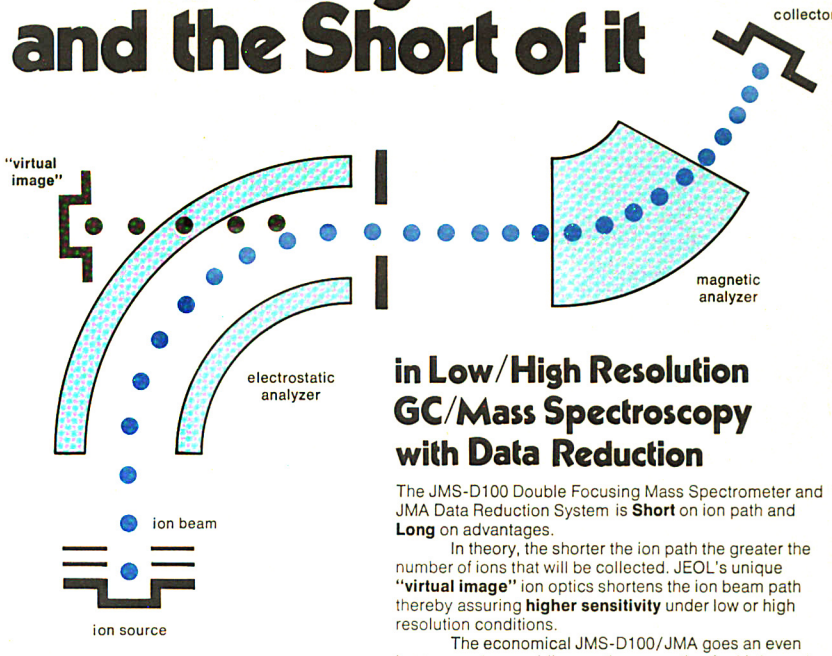
Listings include 8,480 full- and part-time staff members, each with outline of career, teaching and research specialties, and publications for the past two years; interdisciplinary programs and doctoral theses; and statistical data on departments featuring graduate enrollment, number of staff members, number of Ph.D. degrees conferred during the past two years, and number of postdoctoral appointments.

Prepared by the ACS Committee on Professional Training.

Order from:
Special Issues Sales
American Chemical Society
1155 Sixteenth St., N.W.
Washington, D.C. 20036

880 pages including index of names. Paperbound (1974) $20.00 postpaid in U.S., plus 50¢ in Canada and PUAS, 75¢ foreign.

The Long and the Short of it



in Low/High Resolution GC/Mass Spectroscopy with Data Reduction

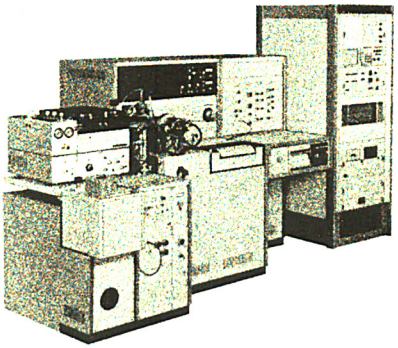
The JMS-D100 Double Focusing Mass Spectrometer and JMA Data Reduction System is **Short** on ion path and **Long** on advantages.

In theory, the shorter the ion path the greater the number of ions that will be collected. JEOL's unique **"virtual image"** ion optics shortens the ion beam path thereby assuring **higher sensitivity** under low or high resolution conditions.

The economical JMS-D100/JMA goes an even longer way by providing routine operation for high resolution on-line **elemental analysis** and conversion to low resolution GC/MS operation is accomplished within minutes. Highest sensitivity GC/MS analysis is assured by the use of a new high efficiency enricher and externally adjustable wide slits. The JMS-D100 is complimented by a complete line of accessories.

The **interactive** JMA Data System, featuring push button operation, provides for low/high resolution on-line analysis. The built-in CRT display and a hardware peak detection system give the operator full control **in "real time"** of data parameter adjustments. Elemental analysis of up to 12 different elements, as well as many other routines, is available.

JEOL also manufactures Mattauch-Herzog instruments for organic and inorganic analysis. For complete details or demonstration contact . . .



JEOL

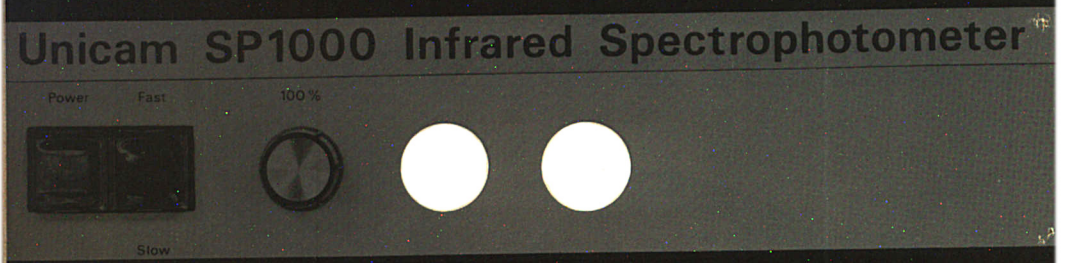
Analytical Instruments, Inc.

235 Birchwood Ave., Cranford, NJ 07016
201—272-8820

INSTRUMENTATION: NMR Spectrometers/Mass Spectrometers/ESR Spectrometers/Laboratory Computers/Scanning Electron Microscopes/Electron Microscopes/X-ray Microprobes/X-ray Diffractometers/Electron Beam Apparatus/Amino Acid Analyzers/Sequence Analyzers.

CIRCLE 139 ON READER SERVICE CARD

Something is missing.



The gain control, for one. You'll never set gain because your sample does. The SP1000 automatically matches gain to sample density.

The slit control is missing, too. A unique high energy detector eliminates the need to open the slit for samples of low transmission.

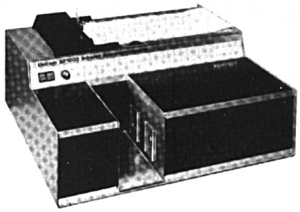
Quick to set up, quick to give results (high resolution scan is only 5 minutes), the SP1000 works well for everyone: student to spectroscopist.

PHILIPS
ELECTRONIC
INSTRUMENTS

A North American Philips Company
750 South Fulton Avenue
Mt. Vernon, NY 10550

Call us today. 914-664-4500.
We'll be glad to arrange for a demonstration.

CIRCLE 191 ON READER SERVICE CARD



What isn't missing is performance.

A solid state detector leads the way.

A solid state pneumatic detector, the IR 50, with unusually high sensitivity and speed of response provides an excellent S/N ratio. This, in turn, permits reduction in monochromator slit width and greatly improved resolution at faster scanning speeds.

Strong price/performance ratio

Resolution	3cm⁻¹ 625 to 2000 cm⁻¹ 6cm⁻¹ 2000 to 4000 cm⁻¹
Wavelength Accuracy & Repeatability	3cm⁻¹ 625 to 2000 cm⁻¹ 9cm⁻¹ 2000 to 4000 cm⁻¹
Accuracy	±1% T
Photometric Repeatability	0.75% T
Dual Scan Speeds	Push Button Selection 2 min or 5⅓ min for full range scanning
Scale Expansion	3X, ordinate
Chart Size	8" x 18.8"

Price, complete: $3950.00

PHILIPS ELECTRONIC INSTRUMENTS

A North American Philips Company
750 South Fulton Avenue
Mt. Vernon, NY 10550

See us at the FACSS Show, Booth numbers 65 and 66.

CIRCLE 192 ON READER SERVICE CARD

Author Index

(Continued)

Freiser, H. *1842*
Fujinaga, T. *1842*

Giger, W. *1663*
Govindaraju, K. *1672*
Grime, J. K. *1810*
Guilbault, G. G. *1769*
Guiochon, G. *1640*

Hampshire, M. J. *1830*
Hassan, M. Z. *1827*
Hayon, E. *1785*
Henion, J. D. *1709*
Hindman, F. D. *1725*
Hites, R. A. *1858*
Holdren, M. *1852*
Huang, T-I. S. *1709*

Ilie, V. A. *1847*

Janinski, R. J. *1832*
Jankowski, C. M. *1834*
Jervis, R. E. *1630*

Kallos, G. J. *1866*
Kao, J-l. *1709*
Karger, B. L. *1640*
Keller, J. *1845*
Kivalo, P. *1814*
Kneip, T. J. *1863*
Koh, T. *1679*
Kohn, A. *1737*
Kremen, J. C. *1694*
Krivan, V. *1626*
Kumar, R. *1855*
Kuper, H. *1683*

Landa, I. *1694*
Laub, R. J. *1659*
Legg, K. D. *1690*
Long, W. *1872*

McCombie, P. J. *1798*
Martin, D. B. *1742*
Martin, M. *1640*
Martire, D. E. *1712*
Masri, M. S. *1820*
Massart, D. L. *1765*
Mertens, J. *1765*
Mevelle, G. *1672*
Miguel, A. H. *1832*
Millard, M. M. *1820*
Miller, A. G. *1720*
Molnar, C. J. *1807*
Montaser, A. *1817*
Moorhead, E. D. *1879*
Mottola, H. A. *1777*

Nanjo, M. *1769*
Norris, A. *1754*

Okazaki, S. *1842*
Ostojic, N. *1653*

Parker, C. E. *1709*
Parkes, J. *1830*
Parks, J. H. *1690*
Patel, A. R. *1781*
Pecsok, R. L. *1659*
Percival, D. R. *1742*
Perone, S. P. *1790*
Pichler, M. A. *1790*
Pitts, J. N., Jr. *1872*
Puphal, K. W. *1725*

Quinn, R. K. *1759*
Qureshi, M. *1855*

Rabbitt, L. J. *1830*
Ramamurthy, V. *1659*
Rasmussen, R. A. *1852*
Reiner, E. *1878*
Richtol, H. H. *1749, 1860*
Riepe, W. *1683*
Robinson, R. E. *1648*
Rose, S. J. *1781*
Ross, E. W. *1785*
Rulon, V. *1863*

Sandler, L. *1870*
Sandridge, R. L. *1845*
Schoenfeld, I. *1826*
Schweikert, E. A. *1626*
Sedlak, J. M. *1837*
Sharma, V. *1855*
Sherry, A. E. *1772*
Shiffman, S. *1804*
Sill, C. W. *1725*
Singer, L. A. *1690*
Stedman, D. H. *1704*
Steffenson, D. M. *1704*
Strohm, W. W. *1822*
Sustek, J. *1676*
Swanson, R. M. *1803*
Swindle, D. L. *1626*
Szakasits, J. J. *1648*

Taniguchi, K. *1679*
Tou, J. C. *1866*
Tsai, F.-C. *1701*

Valentine, A. M. *1837*
Valladon, M. *1737*
Van den Winkel, P. *1765*
Vanderborgh, N. E. *1759*
Vialatte, B. *1737*
Vickers, T. J. *1810*
Visapaa, A. *1814*

Warren, F. L. *1870*
Weaver, J. W. *1878*
Westberg, H. H. *1852*
Wilkins, C. L. *1798, 1803*
Williams, R. C. *1798, 1803*
Winefordner, J. D. *1807*
Wolf, M. W. *1690*
Woltermann, H. W. *1822*

Zafonte, L. *1872*
Zamir-ul Haq, M. *1781*

Now there's a REPIPET® Dispenser and Dilutor for every lab need.

The six REPIPET® Dispensers shown here are but a few of the many models Labindustries can supply you for precise repetitive measurements. Every lab reagent — even corrosives — can be used with REPIPET Dispensers except HF. Choose from 1, 5, 10, 20 and 50 ml sizes, all with 50% lifetime guarantees. Take a moment to circle the reader number for our free new catalog "L/I REPIPETS and Dilutors."

1. Universal REPIPET Dispenser fits any container from ½ ml up to 5 gallons. Simply cut the TEFLON® tubing to fit. 10 ml model $75.



2. NEW Low Silhouette with new 2-opening wide-mouth container. Leave the instrument in place, use the second opening to refill with reagent. This 10 ml unit $66.50 including container.



4. NEW REPIPET Dilutor. This simple, precise and low cost Dilutor now features sturdier construction and low profile container. Many models 1 to 50 ml. 10 ml model with 1 ml aspirator $118.50.





3. NEW REPIPET Jr. Dispenser only $29.50. An unbreakable plastic 0.5% precision dispenser for non-corrosive reagents. We include chemical resistance chart.

5. NEW AUTO-REPIPET Dispenser features air-activated foot-operated pedal — frees both of your hands for other work. The safest way possible to dispense corrosives. Model shown is **$220.**





6. NEW MINI-REPIPET Dispensers. Especially suited for dispensing directly from diagnostic reagent containers ½ ml and larger with 0.1% precision. Avoid the hazards of mouth pipetting! All standard sizes $63.50.

Order from Labindustries or your distributor.

LABINDUSTRIES

1802 Second Street, Berkeley, CA 94710
Phone (415) 843-0220. Cable LABIND, Berkeley

CIRCLE 149 ON READER SERVICE CARD

Briefs

Nondestructive Determination of Some Trace Elements in Tantalum by Proton Activation Analysis

Trace amounts of Ti, Fe, Zr, Nb, Mo, and W are determined simultaneously. Results in the 0.1- to 35-ppm range are given, with an evaluation of the detection limits (0.005 to 0.5 ppm) and the precision of the method (8.5 to 25%).

Viliam Krivan, *Max-Planck-Institut für Metallforschung, Laboratorium für Reinststoffe, D-7070 Schwäbisch Gmünd, West Germany, and* **Dale L. Swindle and Emile A. Schweikert,** *Center for Trace Characterization, Department of Chemistry, Texas A&M University, College Station, Texas 77843*

Anal. Chem., 46, 1626 (1974)

Multielement Determination in Market-Garden Soils by Instrumental Photon Activation Analysis

Thirty elements are determined and the technique, sample preparation, irradiation, activation products, interfering reactions and gamma-rays, and detection limits are described.

Amares Chattopadhyay and R. E. Jervis, *Department of Chemical Engineering and Applied Chemistry, and Institute for Environmental Studies, University of Toronto, Toronto, Ontario, M5S 1A4, Canada*

Anal. Chem., 46, 1630 (1974)

Role of Column Parameters and Injection Volume on Detection Limits in Liquid Chromatography

The general influence of column parameters on solute dilution within a liquid chromatographic system is explored. Optimization for low detection limits is examined. The importance of sample injection volume on detection limits is emphasized.

Barry L. Karger, *Department of Chemistry, Northeastern University, Boston, Mass. 02115, and* **Michel Martin and Georges Guiochon,** *Laboratoire de Chimie Analytique Physique, Ecole Polytechnique, Paris Ve, France*

Anal. Chem., 46, 1640 (1974)

Disk Conveyor Flame Ionization Detector for Liquid Chromatography

A disk-shaped sample conveyor, fabricated of porous alumina, is combined with flame ionization detection to monitor solutes in the column effluent of a liqud chromatographic system.

J. J. Szakasits and R. E. Robinson, *Shell Development Company, MTM Process R&D Laboratory, P.O. Box 100, Deer Park, Texas 77536*

Anal. Chem., 46, 1648 (1974)

New Approach to Chromatogram Interpretation by Multiple Detection

Simultaneous multiple detection is used for interpretation of complex chromatograms without a requirement for high selectivity of the detector system.

Nedjeljko Ostojić, *Institute Rudjer Bošković, Zagreb, Yugoslavia*

Anal. Chem., 46, 1653 (1974)

Gas-Complex Chromatography: Substituent and Steric Effects

Relative formation constants for several aromatic hydrocarbons, amines, and β-ionyl compounds are determined by GLC. Charge-transfer effects are then examined.

R. J. Laub, Vaidhyanathan Ramamurthy, and R. L. Pecsok, *Department of Chemistry, University of Hawaii, Honolulu, Hawaii 96822*

Anal. Chem., 46, 1659 (1974)

Polycyclic Aromatic Hydrocarbons in the Environment: Isolation and Characterization by Chromatography, Visible, Ultraviolet, and Mass Spectrometry

The combination of gel filtration, adsorption chromatography, and charge transfer complexation leads rapidly from crude extracts of environmental samples to polycyclic aromatic ring-type concentrates. Further analysis reveals an unanticipated structural complexity.

Walter Giger and Max Blumer, *Woods Hole Oceanographic Institution, Woods Hole, Mass. 02543* *Anal. Chem., 46, 1663 (1974)*

Solid Sampling Atomic Absorption Determination of Lead in Rock Samples Using the Iron Screw Rod Technique

Trace amounts of lead down to 1 ppm are determined by flame atomic absorption spectrometry without any prior chemical dissolution of silicate rock samples.

Kuppusami Govindaraju, Guy Mevelle, and Charles Chouard, *Centre de Recherches Pétrographiques et Géochimiques (C.N.R.S.), 54500 Vandoeuvre-lès-Nancy, France*

Anal. Chem., 46, 1672 (1974)

Method for the Choice of Optimal Analytical Positions in Spectrophotometric Analysis of Multicomponent Systems

The relative standard deviations of the absorptivities are used as a criterion for the choice of optimal analytical positions. The method is applied to a model system approximated by Lorentzian functions.

J. Šustek, *Research Institute of Agrochemical Technology, 81004 Bratislava-Predmestie, Czechoslovakia*

Anal. Chem., 46, 1676 (1974)

Spectrophotometric Determination of Micro Amounts of Hexathionate in Mixtures with Thiosulfate and Sulfite by Means of Its Sulfitolysis

Hexathionate is stoichiometrically converted to thiosulfate over the pH range 7.5–9.5 when sulfitolyzed for 10 min. The method gives a relative standard deviation of 2.2% for the determination.

Tomozo Koh and Kazuo Taniguchi, *Department of Chemistry, Faculty of Science, Tokai University, Hiratsuka-shi, Kanagawa, Japan*

Anal. Chem., 46, 1679 (1974)

Separation Technique for Mass Spectrometry. Fractionated Evaporation from a Direct Inlet System Which Maintains a Fixed Total Ion Current

Evaporation from a direct inlet system, temperature controlled to maintain a fixed total ion current, is useful for separating mixture components and taking "clean" spectra from less pure substances.

Jochen Franzen, Hendrik Küper, and Wolfgang Riepe, *Institut für Spektrochemie und Angewandte Spektroskopie, Dortmund, Bundesrepublik Deutschland*

Anal. Chem., 46, 1683 (1974)

3M adds another dimension to surface analysis

3M continues to expand the capabilities of the already established ISS technique. As an innovative leader in the field of surface analysis, 3M is constantly seeking new and improved flexibility to meet today's needs.



That's why we've developed an ISS/SIMS combination — to provide a new dimension in sensitivity and analysis. ISS/SIMS is capable of providing Ion Scattering Spectrometry and both positive and negative Secondary Ion Mass Spectrometry to give you three different spectra for a more complete surface analysis.

This new dimension, along with other developments like our new scanning ion beam system module and 8-channel digital multiplexing module, provide great advances in new and updated equipment for surface analysis. And, as always, these advances are modularly designed to adapt to existing ISS equipment.

Analyze ISS/SIMS more closely. For more information, write: Analytical Systems, 3M Company, 3M Center 209-BS, St. Paul, Minnesota 55101; or call 612-733-8193.



3M COMPANY

CIRCLE 156 ON READER SERVICE CARD

Briefs

Gated Nanosecond Time Resolved Emission Spectroscopy Separation of Mixed Emissions from Carbonyl Compounds

A variable nanosecond gated photomultiplier technique capable of separating weak prompt fluorescence from the total radiative emission and identifying E- and P-type delayed fluorescences is described.

Ronald E. Brown, Kenneth D. Legg, Monte W. Wolf, and Lawrence A. Singer, *Department of Chemistry, University of Southern California, Los Angeles, Calif. 90007, and* **Joel H. Parks,** *Departments of Physics and Electrical Engineering, University of Southern California, Los Angeles, Calif. 90007*

Anal. Chem., 46, 1690 (1974)

Corrected and Automated Spectrophotofluorimeter Employing a Pyroelectric Detector for Correction

A state-of-the-art spectrophotofluorimeter is described which provides high sensitivity and resolution, and measures: corrected emission and excitation fluorescence, differential fluorescence, corrected polarization, phosphorescence, absorbance, transmittance, and quantum efficiencies.

Isaac Landa and J. C. Kremen, *American Instrument Company, Division of Travenol Laboratories, 8030 Georgia Ave., Silver Spring, Md. 20902*

Anal. Chem., 46, 1694 (1974)

Study of the Precision of an X-Ray Fluorescence Spectrometric Determination

The precision with which the parameters of voltage drift, goniometer reset, excitation voltage and current reset, the orientation and placement of the specimen in this instrument, as well as the ability to reproduce a specimen are evaluated.

E. B. Buchanan, Jr., and Foo-Chong Tsai, *Department of Chemistry, The University of Iowa, Iowa City, Iowa 52242*

Anal. Chem., 46, 1701 (1974)

Optimization of the Operating Parameters of Chemiluminescent Nitric Oxide Detectors

The relevant optimization parameters are shown to be determined by the kinetic limitations of the $NO + O_3$ reaction, the geometry of photon collection, and the photomultiplier efficiency.

D. M. Steffenson and D. H. Stedman, *Department of Chemistry, University of Michigan, Ann Arbor, Mich. 48104*

Anal. Chem., 46, 1704 (1974)

Analytical Ion Cyclotron Resonance Spectrometry. Stereochemical Effects in Some Cyclic Ketones

Gaseous ionic acetylation of 2-alkylcyclohexanones and α-decalones by $CH_3COCOCH_3^+$ becomes slower as the alkyl group gets larger or the α-decalone more hindered; a factor of 2 in rates for *cis-* and *trans-*α-decalone allows distinguishing between them.

Maurice M. Bursey, Jar-lin Kao, John D. Henion, Carol E. Parker, and Tai-In S. Huang, *Venable and Kenan Chemical Laboratories, The University of North Carolina, Chapel Hill, N.C. 27514*

Anal. Chem., 46, 1709 (1974)

Determination and Comparison of Association Constants for Weak Organic Complexes by Thermodynamic, Resonance, and Optical Methods

Equations are derived, and examples are given, which show that the effects of noncomplexing acceptor–donor interactions and nonideality of the mixed solvent must be considered in analyzing and interpreting measurements.

Daniel E. Martire, *Department of Chemistry, Georgetown University, Washington, D.C. 20007*

Anal. Chem., 46, 1712 (1974)

Determination of Rare Earths in Plutonium by X-Ray Emission Analysis

The relative standard deviation for Sm, Eu, Gd, and Dy at the 1-μg level is measured as 8%, and detection limits are estimated at less than 0.1 μg.

A. G. Miller, *Technical Services Section, Chemical Processing Division, Atlantic Richfield Hanford Company, Richland, Wash. 99352*

Anal. Chem., 46, 1720 (1974)

Simultaneous Determination of Alpha-Emitting Nuclides of Radium through Californium in Soil

A procedure is described for total decomposition of 10 grams of soil and sequential determination of all alpha emitters from radium through californium with yields generally larger than 94%.

Claude W. Sill, Kenneth W. Puphal, and Forest D. Hindman, *Health Services Laboratory, U.S. Atomic Energy Commission, Idaho Falls, Idaho 83401*

Anal. Chem., 46, 1725 (1974)

Radiochemical Separation of Fluorine by Adsorption on Hafnium Dioxide: Application to the Determination of Oxygen by Activation Analysis with Charged Particles

A two-fold study interprets results for the adsorption of F^- from nitric acid solutions, and reports the use of HfO_2 for the determination of oxygen in Ag, Co, and Cu.

A. Kohn, J. N. Barrandon, J. L. Debrun, M. Valladon, and B. Vialatte, *Groupe d'Application Des Reactions Nucleaires a l'Analyse Chimique, Service du Cyclotron, Centre National de la Recherche Scientifique, 45045 Orleans Cedex, France*

Anal. Chem., 46, 1737 (1974)

Sequential Determination of Radium-226, Radium-228, Actinium-227, and Thorium Isotopes in Environmental and Process Waste Samples

The method described permits determinations of the radionuclides with 95% recoveries at 0.1 to 0.001 of Federal concentration guides. Precision, accuracy, and the effects of chemical and radiochemical interferences are discussed.

Donald R. Percival and Don B. Martin, *Health Services Laboratory, U.S. Atomic Energy Commission, Idaho Falls, Idaho 83401*

Anal. Chem., 46, 1742 (1974)

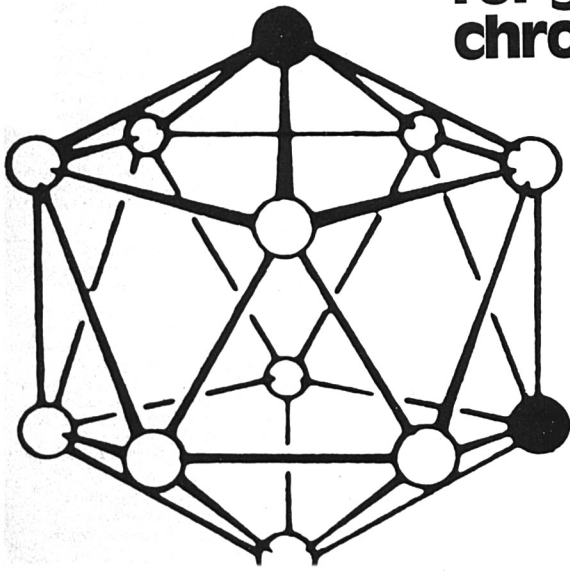
Excited Singlet State Acidity Constants for Hydroxy and Amino Substituted Anthraquinones and Related Compounds: A Comparison of Excited-State pK Measurement Procedures

Excited singlet state acidity constants are determined by 4 different methods. The fluorescence titration method correlates best with fluorescence and absorption energy averaging for pK^* determinations.

H. H. Richtol and B. R. Fitch, *Department of Chemistry, Rensselaer Polytechnic Institute, Troy, N.Y. 12181*

Anal. Chem., 46, 1749 (1974)

DEXSIL®: Superior high temperature phases for gas chromatography



DEXSIL©(s) GC (carborane silicone polymers) are remarkably stable over the temperature range 20° to 500°C. Three different forms of DEXSIL are offered:

DEXSIL 300—(Carborane/Methyl Silicone) highest temperature range...from 50° to 500°C. Non-polar.

DEXSIL 400—(Carborane/Methyl/Phenyl Silicone) temperature range from 20° to 400°C. Slightly polar.

DEXSIL 410—(Carborane/Methyl/2-Cyanoethyl Silicone) temperature range 20° to 400°C. The most polar DEXSIL formulation.

DEXSIL GC has definite advantages at lower temperatures. Lower bleed allows the GC detector to be used at more sensitive settings, thus increasing the range of analysis. Lower bleed also means extended column life. DEXSIL is extremely useful when doing GC mass spectrometry.

Let us send you a detailed report on the properties and uses of DEXSIL polymers, including an annotated listing of reported applications with bibliography.

Analabs, Inc.

A subsidiary of NEN New England Nuclear

80 Republic Drive, North Haven, Connecticut 06473
Telephone: (203) 288-8463 Telex: 96-3518

Canada: NEN Canada Ltd., Dorval, Quebec, H9P-1B3, Tel: (514) 636-4971, Telex: 05-821808
Europe: NEN Chemicals GmbH, D6072 Dreieichenhain, W. Germany, Siemensstrasse 1. Tel: Langen (06103) 85035

DEXSIL is a registered trademark of the Olin Corporation, New Haven, Conn.

CIRCLE 4 ON READER SERVICE CARD

Briefs

New Instrumental Approach in Phase-Selective Second Harmonic Alternating Current Polarography

Electronic multiplication of the ac signal is shown to provide a simple and inexpensive means of obtaining phase-selective second harmonic ac polarograms.

H. Blutstein and A. M. Bond, *Department of Inorganic Chemistry, University of Melbourne, Parkville 3052, Victoria, Australia, and* **A. Norris,** *Clanor Instruments, P.O. Box 75, Balwyn 3103, Victoria, Australia* *Anal. Chem., 46, 1754 (1974)*

Voltammetry in Sulfolane: The Electrochemical Behavior of Benzaldehyde and Substituted Benzaldehydes

The study of the electrochemical reduction of parasubstituted benzaldehydes in sulfolane demonstrates a large solvent effect on these reductions. For example, the rate of the dimerization following reduction of benzaldehyde is lowered to $k_2 = 2.4 \times 10^3$ l./m·sec in sulfolane.

Neal R. Armstrong and Rod K. Quinn, *Sandia Laboratories, Albuquerque, N.M. 87115, and* **N. E. Vanderborgh,** *Department of Chemistry, University of New Mexico, Albuquerque, N.M. 87131* *Anal. Chem., 46, 1759 (1974)*

Streaming Potentials in Automatic Potentiometric Systems

The potential oscillations caused by the proportioning pump in automatic potentiometric systems are found to be due to changes of streaming potentials, set up over the tube connecting the electrode cells.

Pierre Van den Winkel, John Mertens, and Désiré L. Massart, *Farmaceutisch Instituut, Vrije Universiteit Brussel, Paardenstraat 67, B-1640 Sint Genesius Rode, Belgium* *Anal. Chem., 46, 1765 (1974)*

Enzyme Electrode Sensing Oxygen for Uric Acid in Serum and Urine

The plainum electrode with immobilized uricase is used to assay uric acid in serum and urine. The rate of the reaction is measured directly by following the uptake of oxygen during the enzymatic reaction.

M. Nanjo and G. G. Guilbault, *Louisiana State University in New Orleans, Department of Chemistry, New Orleans, La. 70122* *Anal. Chem., 46, 1769 (1974)*

An Automatic Analyzer for the Detection of Dihydroxyphenylalanine Metabolites and Other Reducing Compounds in Urine

An automatic ion-exchange chromatographic system for detecting DOPA metabolites and other reducing compounds in urine, using diphenylpicrylhydrazyl as the colorimetric reagent, is described.

Phillip W. Banda, Arletta E. Sherry, and Marsden S. Blois, *Department of Dermatology, University of California, San Francisco, Calif. 94143* *Anal. Chem., 46, 1772 (1974)*

Determination of Uric Acid at the Microgram Level by a Kinetic Procedure Based on a "Pseudo-Induction" Period

Application of the method to the determination of uric acid in human blood serum and urine is reported.

V. V. S. Eswara Dutt and H. A. Mottola, *Department of Chemistry, Oklahoma State University, Stillwater, Okla. 74074* *Anal. Chem., 46, 1777 (1974)*

Identification and Quantitative Measurement of Some *N*-Heterocyclics in Marijuana Smoke Condensates

Marijuana smoke condensate is shown to contain carbazole, indole, and skatole. The use of internal standards provides accurate quantitative data on these compounds.

M. Zamir-ul Haq, Samie J. Rose, Lisa R. Deiderich, and Appasaheb R. Patel, *Meloy Laboratories, Inc., 6715 Electronic Drive, Springfield, Va. 22151* *Anal.Chem., 46, 1781 (1974)*

Simple Digital Method for Resolving Overlapping Electronic Absorption Bands

A method of resolving electronic absorption bands by simple digital procedures is found to be superior to differential or analog methods and acts as input to minimization methods.

B. E. Barker and M. F. Fox, *City of Leicester Polytechnic, Leicester LE1 9BH, England, and* **E. Hayon and E. W. Ross,** *Pioneering Research Laboratory, U.S. Army Natick Laboratories, Natick, Mass. 01760* *Anal. Chem., 46, 1785 (1974)*

Computerized Pattern Recognition Applications to Chemical Analysis. Development of Interactive Feature Selection Methods for the K-Nearest Neighbor Technique

A systematic operator-interactive computerized approach is developed for feature selection in K-nearest neighbor pattern recognition applications. Applications to binary and multi-category classification problems are described.

M. A. Pichler and S. P. Perone, *Purdue University, Department of Chemistry, Lafayette, Ind. 47907* *Anal. Chem., 46, 1790 (1974)*

Hadamard Transformed Carbon-13 Nuclear Magnetic Resonance Spectra—Pattern Recognition Analysis

The results of pattern recognition studies on Hadamard pre-processed carbon-13 nuclear magnetic resonance data are presented and compared with previously reported preprocessing techniques.

Thomas R. Brunner, Robert C. Williams, Charles L. Wilkins, and Patrick J. McCombie, *Department of Chemistry, University of Nebraska—Lincoln, Lincoln, Neb. 68508* *Anal. Chem., 46, 1798 (1974)*

Notes

Concise Algorithm for Conversion between Normal and Sequency Ordered Hadamard Matrices

An algorithm is derived and a short Fortran program to implement it is developed.

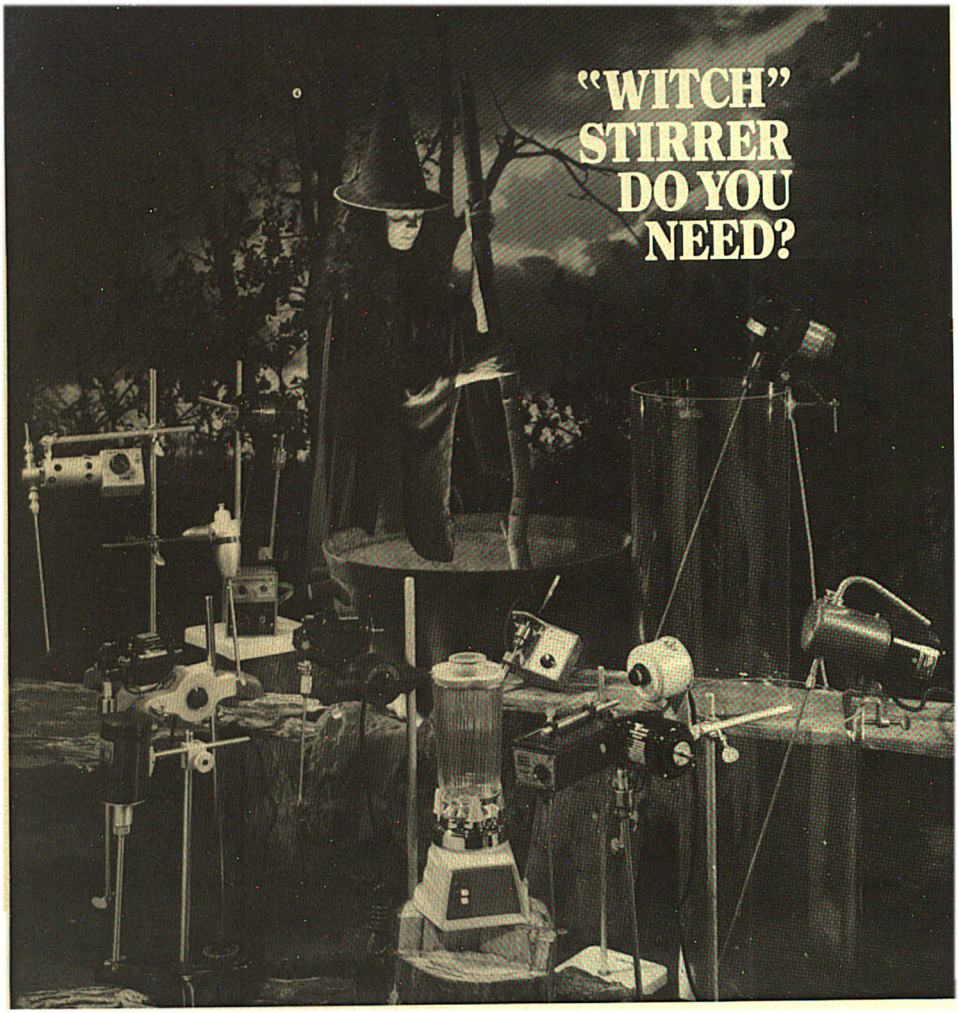
Robert C. Williams, Ray M. Swanson, and Charles L. Wilkins, *Department of Chemistry, University of Nebraska, Lincoln, Neb. 68508* *Anal. Chem., 46, 1803 (1974)*

Determination of Sulfur by the Measurement of Molecular Emission in Cool Flames: Conversion of Sample Sulfur to Hydrogen Sulfide

The intensity of S_2 band emission in cool flames is dependent on the structure of the sulfur-containing molecule as well as the sample matrix. A method for reducing this dependence is described.

S. Shiffman and C. W. Frank, *Department of Chemistry, The University of Iowa, Iowa City, Iowa 52242* *Anal. Chem., 46, 1804 (1974)*

ห้องสมุด กรมวิทยาศาสตร์



We have lab stirrers for every conceivable purpose; in fact, there are over 100 different models to choose from . . . made by such outstanding manufacturers as Brookfield, Corning, Eastern, Eberbach, Heller, Kraft, Lab-Line, "Lightnin", Precision-Scientific, Talboys, Thermolyne and Waring, to name a few.

The stirrers are powered by electricity, air, vacuum or water . . . single speed or variable speed . . . explosion-proof . . . magnetic . . . . with propeller or blades . . . units for blending . . . or for stirring liquids under pressure, in a vacuum, or in a closed or open system. So, "witch" stirrer are you interested in? Please tell us so that we can send literature.

SGA SCIENTIFIC
BLOOMFIELD, N. J. 07003

LABORATORY . . .
♦ APPARATUS
♦ INSTRUMENTS
♦ CHEMICALS
♦ GLASSWARE

Branches: Boston Mass. • New Haven Conn. • Elk Grove Village Ill. • Fullerton Calif. • Philadelphia Penna. • Silver Spring Md. • Syracuse N. Y.

CIRCLE 213 ON READER SERVICE CARD

Briefs

New Discrete Atomization Cell for Atomic Fluorescence Spectrometry

This system allows the use of both pulsed and continuous modes of sampling, which results in improved absolute limits of detection. No deleterious effects to the linear dynamic ranges result.

C. J. Molnar and J. D. Winefordner, *Department of Chemistry, University of Florida, Gainesville, Fla. 32611*
Anal. Chem., 46, 1807 (1974)

Flame Atomic Fluorescence and Emission Spectrometry with a Microsampling Cup Technique

Results are reported for application of a microsampling cup technique in the determination of thallium. The relative standard deviation calculated for ten replicate determinations is 3.4% at the 0.5 μg/ml level.

J. K. Grime and T. J. Vickers, *Department of Chemistry, Florida State University, Tallahassee, Fla. 32306*
Anal. Chem., 46, 1810 (1974)

Separation of Trace Metal Impurities from Nuclear Grade Uranium by Long-Chain Amine Extraction and Direct Determination by Atomic Absorption Spectrophotometry

Solvent extraction separation of trace concentrations of Cd, Ag, Au, Hg, Pb, and Bi in uranium from HCl–KI media is investigated for analytical applications. Direct burning of the organic phase in an AA spectrophotometer provides enhanced absorbance, and precision in the range 2–12%.

Sergio de Moraes and Alcídio Abrão, *Chemical Engineering Department, Instituto de Energia Atômica, Caixa Postal 11.049 e C.E.P. 05.508, São Paulo, Brazil*
Anal. Chem., 46, 1812 (1974)

Atomic Absorption Determination of Mercury in Fish Using the Coleman MAS-50 Mercury Analyzer

The standard deviation of the proposed acid-digestion procedure is ±0.04 ppm Hg at the level of 0.90 ppm Hg. The results agree with those obtained by activation analysis.

Pekka Kivalo, Askó Visapaa, and Runar Backman, *Chemical Laboratory, Technical Research Centre of Finland, 02150 Otaniemi, Finland*
Anal. Chem., 46, 1814 (1974)

Analytical Applications of the Graphite Braid Nonflame Atomizer

Analytical data are presented for 12 elements by atomic absorption spectrometry and for 3 elements by atomic fluorescence spectrometry. Analyses of Cu and Fe in a blood serum matrix are also reported.

Akbar Montaser and S. R. Crouch, *Department of Chemistry, Michigan State University, East Lansing, Mich. 48824*
Anal. Chem., 46, 1817 (1974)

Detection and Analysis of Protein Functional Group Modification by X-Ray Photoelectron Spectrometry

The basis of the method is the introduction of elements with high photoelectric cross-sections or detection sensitivity such as fluorine or mercury into the protein by suitable chemical modification.

Merle M. Millard and Merle Sid Masri, *Western Regional Research Laboratory, Agricultural Research Service, U.S. Department of Agriculture, Berkeley, Calif. 94710*
Anal. Chem., 46, 1820 (1974)

Determination of Molybdenum in Plutonia Cermets by X-Ray Fluorescence Spectrometry

An X-ray fluorescence procedure is developed to determine the weight fraction of molybdenum in $^{238}PuO_2$/molybdenum cermet fuel. This method has a relative standard deviation of approximately 1%.

H. A. Woltermann and W. W. Strohm, *Monsanto Research Corporation, Mound Laboratory, Miamisburg, Ohio 45342*
Anal. Chem., 46, 1822 (1974)

Quantitative Determination of the Phase I/Phase II Ratio in Sodium Triphosphate by Raman Spectrometry

The phase I/phase II ratio in sodium triphosphate correlates (standard deviation 0.02) with the intensity ratio of the Raman lines at 1014 (I) and 945 cm^{-1} (II). $Na_5P_3O_{10}\cdot 6H_2O$ only influences the result at high concentrations.

Jan Bus, *Unilever Research Vlaardingen, Olivier van Noortlaan 120, Vlaardingen, The Netherlands* *Anal. Chem., 46, 1824 (1974)*

Spectrochemical Method for Determination of Tellurium in Geological Materials

This method consists of volatilization of tellurium and dc-arc excitation of the distillate. The precision is about 20%, the accuracy about 10%.

Irena Schoenfeld and Armand Berman, *Soreq Nuclear Research Centre, Yavne, Israel* *Anal. Chem., 46, 1826 (1974)*

Voltammetry of Bismuth(III) at a Continuously Mercury-Coated Rotating Platinum Disk Electrode

Results of cathodic and anodic stripping voltammetry of 2.5×10^{-6}–$5 \times 10^{-9}M$ Bi(III) in 0.1M HNO_3, $HClO_4$, or H_2SO_4 in the presence of 10^{-4}–$10^{-5}M$ Hg_2^{2+} are described.

M. Z. Hassan and Stanley Bruckenstein, *Department of Chemistry, State University of New York at Buffalo, Buffalo, N.Y. 14214* *Anal. Chem., 46, 1827 (1974)*

Live Peak Stripping during X-Ray Energy Dispersive Analysis

Peak stripping during analysis using extremely simple software routines yields excellent peak discrimination for low resolution multi-channel analyzers. Quantitative accuracy is limited by the analyzer, in this case approximately 1%.

John Parkes, L. J. Rabbitt, and M. J. Hampshire, *Electrical Engineering Department, University of Salford, Salford, England* *Anal. Chem., 46, 1830 (1974)*

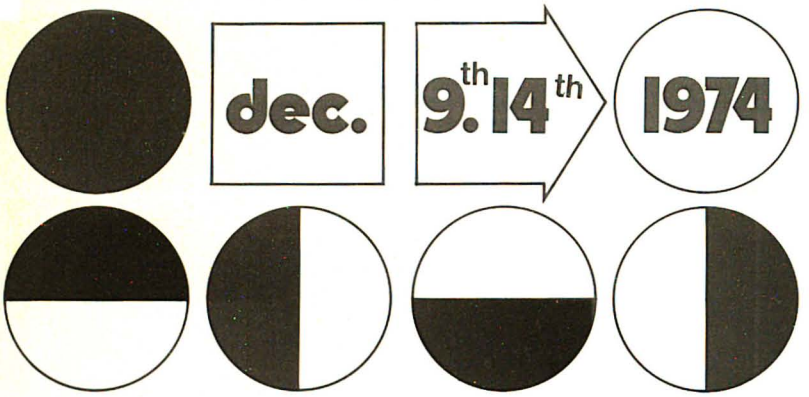
Determination of Trace Metals in Aqueous Environments by Anodic Stripping Voltammetry with a Vitreous Carbon Rotating Electrode

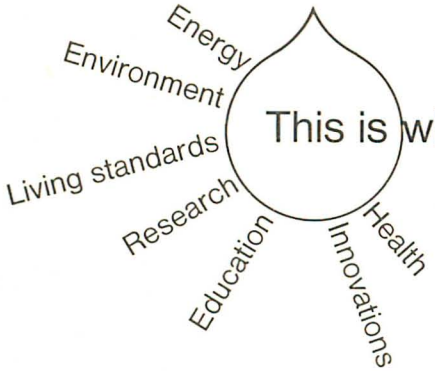
Trace metals are determined at the ppb level by simultaneous deposition of the mercury film and metals for about 5 minutes. Reproducibility is within 2%.

A. H. Miguel and C. M. Jankowski, *Chemistry Department, Northeastern University, Boston, Mass. 02115*
Anal. Chem., 46, 1832 (1974)

salon du laboratoire 1974

Paris, porte de Versailles





This is why Laboratories exist.

The 65th Physics Exhibition is being held along with the Salon du Laboratoire (Laboratory Exhibition); entrance formalities are communal.

The G.A.M.S. (Organisation for the propagation of spectroscopic and physico-chemical methods) will hold its 32nd Congress at the same time and place as the two Exhibitions.

The "Salon du Laboratoire" is organised by the "Association pour le Salon du Laboratoire" 10 avenue Hoche - 75382 PARIS CEDEX 08 - FRANCE - Tel. 622.38.00 ext. 528.

CIRCLE 219 ON READER SERVICE CARD

Briefs

Semiquantitative Potentiometric Method for Direct Measurement of Nitrogen Dioxide in Air

A thermally activated chalcogenide glass is the active element in a potentiometric system for the direct, real-time, semi-quantitative analysis of NO_2 in air.

G. G. Barna and R. J. Jasinski, *Texas Instruments Incorporated, P.O. Box 5936, Dallas, Texas 75222*

Anal. Chem., 46, 1834 (1974)

Electrochemical Technique for the Measurement of Carbon Monoxide

The operating characteristics of an electrochemical sensor for the measurement of carbon monoxide in ambient air are described. A relationship between the signal and the sensor parameters is derived and experimentally verified.

H. W. Bay, K. F. Blurton, J. M. Sedlak, and A. M. Valentine, *Energetics Science, Inc., 85 Executive Boulevard, Elmsford, N.Y. 10523*

Anal. Chem., 46, 1837 (1974)

Use of State Variable Active Filters as Differentiators, Rate Meters, and End-Point Locators

State variable active filters with simultaneous low, band and high pass outputs described and used to obtain the first and second derivatives of titration curves and other time-dependent signals.

Robert H. Callicott and Peter W. Carr, *Department of Chemistry, University of Georgia, Athens, Ga. 30602*

Anal. Chem., 46, 1840 (1974)

Ion Selective Electrodes Responsive to Anionic Detergents

Coated wire electrodes for a number of sulfonate detergents are found to give sensitive and reproducible detergent concentrations in the range 10^{-2}–$10^{-5}M$. The electrodes provide a new and improved approach to critical micelle concentration measurements.

Taitiro Fujinaga, Satoshi Okazaki, and Henry Freiser, *Departments of Chemistry of the Faculty of Science, Kyoto University, Kyoto, Japan, and the University of Arizona, Tucson, Ariz. 85721*

Anal. Chem., 46, 1842 (1974)

Determination of Isocyanates in the Working Atmosphere by Thin-Layer Chromatography

This procedure is based on the determination of the ureas formed from the reaction of the isocyanates with *N*-4-nitrobenzyl-*N*-*n*-propylamine (nitro reagent).

Jürge Keller, *Fabenfabriken Bayer GmbH, OC-Produktion, Organic Analytical Laboratory, 509 Leverkusen-Bayerwerk, West Germany, and* **K. L. Dunlap and R. L. Sandridge,** *Mobay Chemical Company, Division of Baychem Corporation, New Martinsville, W. Va. 26155*

Anal. Chem., 46, 1845 (1974)

Gas Chromatographic Separation of Some Unsaturated Hydrocarbons Using Thallium(I) Tetraphenylborate as Stationary Phase

Useful separations of olefins and aromatic hydrocarbons can be achieved on columns of thallium(I) tetraphenylborate as stationary phase. The strong retention of these compounds should be due to the presence of Tl(I) ions.

George E. Baiulescu, *Department of Analytical Chemistry, University of Bucharest, Romania, and* **Vasile A. Ilie,** *Institute of Chemical Research, Bucharest, Romania*

Anal. Chem., 46, 1847 (1974)

Determination of Long Chain Fatty Acids as 2-Naphthacyl Esters by High Pressure Liquid Chromatography and Mass Spectrometry

The formation of 2-naphthacyl esters of C_{18} and C_{20} polyunsaturated fatty acids is employed for the high pressure liquid chromatographic analysis of these compounds in the nanogram range.

M. J. Cooper and M. W. Anders, *Department of Pharmacology, University of Minnesota, Minneapolis, Minn. 55455*

Anal. Chem., 46, 1849 (1974)

Gas Chromatographic Analysis of Ambient Air for Light Hydrocarbons Using a Chemically Bonded Stationary Phase

A gas chromatographic technique for measuring light hydrocarbons (C_2–C_5) is described. The use of Durapak (*n*-octane/Porasil C) columns provides a simple plus efficient means of monitoring trace quantities of these atmospheric gases.

H. H. Westberg, R. A. Rasmussen, and M. Holdren, *Air Pollution Research, Engineering Research Division, Washington State University, Pullman, Wash. 99163* *Anal. Chem., 46, 1852 (1974)*

Synthesis of Reproducible Tin(IV) Based Ion Exchangers: Separation of Lanthanum(III) from Yttrium(III), Europium(III), and Lutetium(III)

Five reproducible, water insoluble compounds of Sn(IV) are synthesized. The antimonate has highest chemical and thermal stability and the arsenate shows greatest ion-exchange capacity. Stannic selenite columns are used for separation studies.

Mohsin Qureshi, Rajendra Kumar, and Veena Sharma, *Chemical Laboratories, Aligarh Muslim University, Aligarh, U.P., India*

Anal. Chem., 46, 1855 (1974)

Sampling Errors in the Quantitation of Petroleum in Boston Harbor Water

The precision and accuracy of an infrared spectrophotometric method for the quantitation of petroleum in water are evaluated using Boston Inner Harbor as the test case. Sampling errors are large.

S. M. Ahmed, M. D. Beasley, A. C. Efromson, and Ronald A. Hites, *Department of Chemical Engineering, Massachusetts Institute of Technology, Cambridge, Mass. 02139*

Anal. Chem., 46, 1858 (1974)

Triplet State Acidity Constants for Hydroxy and Amino Substituted Anthraquinones and Related Compounds. Comparison of Phosphorescence and Transient Triplet Absorption Measurements

Triplet state acidity constants correlate well for phosphorescence and transient absorbance measurements. Lifetime studies of acidic and basic transients indicate equilibrium has been established.

H. H. Richtol and B. R. Fitch, *Department of Chemistry, Rensselaer Polytechnic Institute, Troy, N.Y. 12181*

Anal. Chem, 46, 1860 (1974)

Potential Sources of Analytical Error in the Erythrocytic δ-Aminolevulinic Acid Dehydratase Test for Lead Exposure

Interferences in the erythrocytic ALA-D analysis are defined. Comparisons between lead concentrations in blood and ALA-D activity can be performed accurately when polystyrene sample containers are employed.

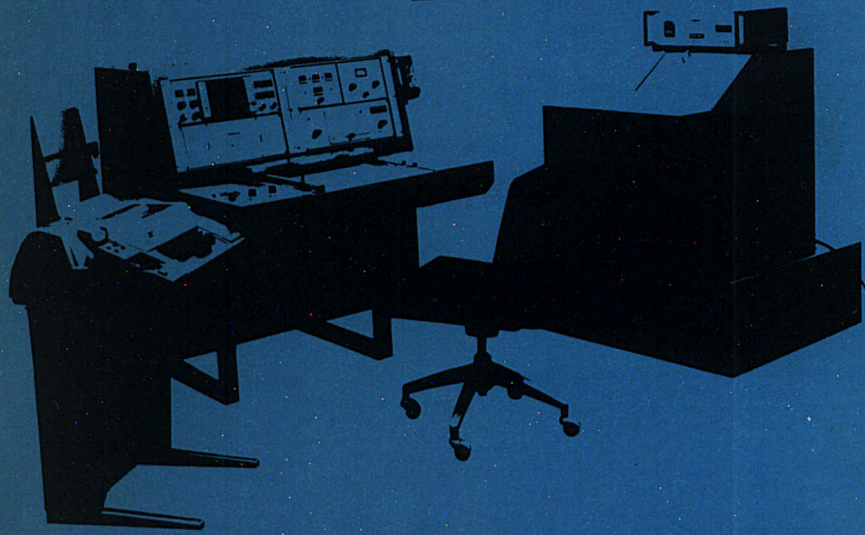
Theo. J. Kneip, Norman Cohen, and Virginia Rulon, *New York University Medical Center, 550 First Avenue, New York, N.Y. 10016*

Anal. Chem., 46, 1863 (1974)

BRUKER

WP 60

The ultimate in low-cost FT NMR Spectroscopy...



- Full multinuclear capability
- Fast, trouble-free changeovers
- 10 mm variable temp for C^{13}
- Superior sensitivity and resolution

See us at the FACSS Show Booth numbers 17 and 18.

PLEASE CONTACT YOUR NEAREST BRUKER REPRESENTATIVE FOR A DEMONSTRATION.

USA

Bruker Scientific Inc.
One Westchester Plaza
Elmsford, N.Y. 10523
Tel. (914) 592-5470
Tlx. 13-1524

Bruker Magnetics Inc.
1 Vine Brook Park
Burlington, Mass. 01803
Tel. (617) 272-9250
Tlx. 94-9493

Bruker Scientific Inc.
1548 Page Mill Road
Palo Alto, Calif. 94305
Tel. (415) 493-3173
Tlx. 34-5533

CANADA

Bruker Spectrospin Ltd.
5200 Dixie Road
Mississauga, Ont. L4W 1E4
Tel. (416) 625-2375
Tlx. 06-961 446

CIRCLE 29 ON READER SERVICE CARD

Briefs

Kinetic Study of the Stabilities of Chloromethyl Methyl Ether and Bis(Chloromethyl) Ether in Humid Air

The rates of hydrolysis of chlormethyl methyl ether and bis-(chloromethyl)ether in the gas phase are found to be proportional to the water concentration and the hydrolysis is highly surface catalyzed.

James C. Tou and George J. Kallos, *Analytical Laboratories, Dow Chemical U.S.A., Midland, Mich. 48640*
Anal. Chem., 46, 1866 (1974)

Effect of Ethyl Chloroformate on the Dye Binding Capacity of Protein

The difference in the amount of dye taken up by fish meal and soya meal before and after treatment with ethyl chloroformate averages to the amount of lysine in the sample.

Louis Sandler, *Fishing Industry Research Institute, University of Cape Town, Rondebosch 7700, Cape, South Africa, and* **F. L. Warren,** *Natural Products Research Laboratory, University of Cape Town, Rondebosch 7700, Cape, South Africa*
Anal. Chem. 46, 1870 (1974)

Evaluation of an Ozone Photometer for Ambient Ozone Measurements

Model 1003A Ozone Photometer is found to be accurate to ±0.02 ppm with a linearity of 1.016 ± 0.017. Airborne operation of this instrument is satisfactory and no interferences are found.

Leo Zafonte, William Long, and James N. Pitts, Jr., *Statewide Air Pollution Research Center, University of California—Riverside, Riverside, Calif. 92502* *Anal. Chem., 46, 1872 (1974)*

Correspondence

Beryllium Content of NBS Standard Reference Orchard Leaves

T. M. Florence, Yvonne J. Farrar, L. S. Dale, and G. E. Batley, *Chemical Technology Division, Australian Atomic Energy Commission Research Establishment, Lucas Heights, New South Wales, Australia* *Anal. Chem., 46, 1874 (1974)*

Comments on Ratio Matching

C. W. Chen, *Mathematics Department, University of Maine at Orono, Orono, Me. 04473* *Anal. Chem., 46, 1876 (1974)*

Aids for Analytical Chemists

Simple Device for Improving the Production of Coiled Glass Capillary Columns

Eugene Reiner and James W. Weaver, *Center for Disease Control, Public Health Service, U.S. Department of Health, Education and Welfare, Atlanta, Ga. 30333*
Anal. Chem., 46, 1878 (1974)

Glass-Immobilized 8-Hydroxyquinoline for Separation of Trace Metals from Base Electrolytes Used for Anodic Stripping Analysis

E. D. Moorhead and P. H. Davis, *Department of Chemical Engineering and Chemistry, University of Kentucky, Lexington, Ky. 40506* *Anal. Chem., 46, 1879 (1974)*

hot tip!

Exclusive PYR-O-SCRIBE—the heated stylus servo and event pen that prevents data loss, needs no ink supply—is just one of your options with Honeywell ElectroniK 195 and 196 Strip Chart Recorders. You can also choose from four models to get precision recording any way you want it—

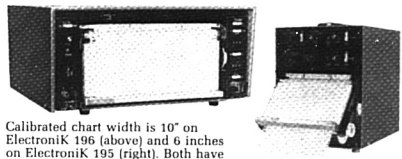
DAZAS (Digitally Adjustable Zero and Span)— Accurate measurements from 1 microvolt to 300 volts.

Selectable Span—1, 5, 10, 50 & 100 mv & volts.

Single Span with interchangeable span cards—0.5 mv to 10 volts.

Single Fixed Volt Span—1 to 10 volts.

For a quick response to your questions, phone any of our 91 offices or Roy Bonsall (215) 643-1300. Honeywell Process Control Division, Fort Washington, PA 19034.



Calibrated chart width is 10" on ElectroniK 196 (above) and 6 inches on ElectroniK 195 (right). Both have tilting chart platen for your convenience in making notations.

Honeywell

CIRCLE 119 ON READER SERVICE CARD

SPECIAL OFFER

pH COMBINATION ELECTRODE

$29.00

BUY NOW & SAVE!

27 1/2%

Use the #9007 for 30 days. If you are not 100% satisfied, send it back with no obligation.

Can be used with most all pH Meters

Note: When ordering specify type of pH Meter or Connector.

Compare Similar Competitive Electrode Prices: $60.00
(Beckman, Corning, & Fischer)



#9007
pH Range 0–14 pH
TEMP RANGE —5°C to 100°C

8 mm DIAMETER
210mm OVERALL LENGTH

■

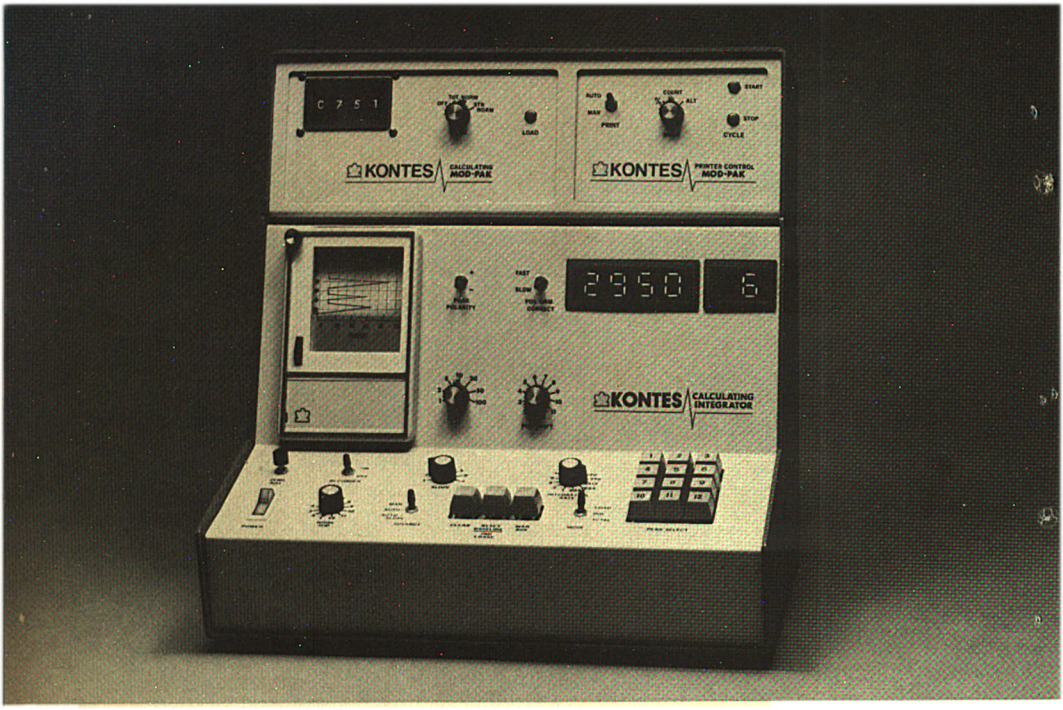
DESIGNED WITH THE USER IN MIND

■

ULTRA FAST RESPONSE & STABILITY

BROADLEY-JAMES Corporation
1714 S. LYON ST. SANTA ANA, CA. 92705 (714) 547-8061
SPECIAL PRICE - LIMITED TIME

CIRCLE 27 ON READER SERVICE CARD



Now for TLC... readin', 'ritin' and 'rithmetic in one package.

This new and unique Kontes Calculating Integrator is the first practical data collection and reduction device designed especially for TLC applications.

Unique solid state circuitry allows selection of any of 12 integration rates to match the rapid run times inherent in TLC scanning. Suitable rates can also be selected for gas or liquid chromatography.

The K-21 Integrator has a built-in strip chart recorder to provide graphic as well as digital pictures of spot readings from any TLC scanner. A memory for storage of data for 12 peaks. And a calculating Mod-Pak module that adds 12 companion memories with thumbwheel entry for dialing-in constants, standards, or variable input for direct calculation of percentage of total unknown, or known.

Our K-21 offers reproducibility and accuracy not previously available for TLC readings. And to maintain this reproducibility, the K-21 includes base line correcting circuitry to overcome the problems of background "noise" and drift.

In its modular form this unique instrument is priced at $2950 for Model K-22, Digital Integrator; and $3750 for Model K-21, Calculating Integrator—as shown. (The Calculating Mod-Pak and Printer Control Mod-Pak can be added to Model K-22 at any time, allowing a modular building approach.)

Whether you want to expand upon the capabilities of our Calculating Integrator or take advantage of separate instrumentation, our line includes a compact Digital Printer, a remarkably efficient Chart Recorder, and a Base Line Corrector that can be used to clean up base line readings on virtually any instrument (all shown below).

For more information on the Integrator or any of our data reduction instruments, contact your Kontes man or write for Bulletin K-21.

KONTES

Vineland, N.J. 08360

CIRCLE 144 ON READER SERVICE CARD

Regional Distributors: **KONTES OF ILLINOIS**, Evanston, Illinois • **KONTES OF CALIFORNIA**, San Leandro, California



RELAX about Federal Regulations- you can comply.

mail coupon for facts.



As you'll see, the Perkin-Elmer Model 55 UV/VIS Spectrophotometer may be precisely what you need to cope with today's stringent regulations. Just mail the coupon and we'll send you 13 good technical reasons why—and one good financial reason. You'll also get a complimentary *Bibliography of Industrial Methods*.

With the Perkin-Elmer 55, you can handle over 95% of the industrial spectrophotometric analyses normally performed. And you can do these with proven accuracy and reliability, getting data that is truly "worry free".

For example, the Model 55 has a higher signal-to-noise ratio than you'll find in any comparably priced instrument. Very important, as you know, when you're working with low concentrations. It allows greater scale expansions, increasing system sensitivity.

Bandpass is a constant 2 nm, eliminating photometric bandpass error in virtually all procedures you run. And photometric error due to stray light is minimal—less than in any other single-monochromator instrument, no matter how much you pay for it. Absorbance to 3A. Drift is less than 0.005A per 8 hours, which means you can relax about the accuracy of your long-term studies.

And finally, you'll appreciate the moderate price. But the best way for you to get the complete story is to mail the coupon. Why not do it now?

PERKIN-ELMER

Coleman Instruments Division
2000 York Road,
Oak Brook, Illinois 60521

Perkin-Elmer is a registered trademark of The Perkin-Elmer Corporation

CIRCLE 38 ON READER SERVICE CARD

COMPLIMENTARY
Bibliography of Industrial Methods

Mail to:
PERKIN-ELMER
2000 York Road
Oak Brook, Illinois 60521

Please send me, without obligation, complete specifications of the Perkin-Elmer Model 55 UV/VIS Spectrophotometer, together with the complimentary *Bibliography of Industrial Methods* I have checked below.

- ○ Agricultural
- ○ Brewing and Liquor
- ○ Metallurgy
- ○ Food and Dairy
- ○ Pharmaceutical

NAME _____ TITLE _____

INSTITUTION _____

ADDRESS _____

CITY _____ STATE _____ ZIP _____

AC-10



Marvin W. Skougstad
U.S. Geological Survey
Denver, Colo. 80225

Water pollution may be considered to be the addition of some substance or material, or the alteration of some physical, chemical, or biological property of water, which either temporarily or permanently renders that water less suitable for a particular use, such as for industrial, domestic, municipal, agricultural, or recreation purposes.

To assess true conditions of water quality, specified chemical, physical, and biological measurements and tests are made on the water body or, commonly, on representative samples of that body of water. It is essential that the best available analytical techniques be used so as to accurately reflect the true condition of the water body. Through continuous monitoring and testing over a period of time, it is possible to determine whether a discharge of wastes has resulted in deterioration of the general condition of the water, or whether appropriate control and management of effluent discharges have resulted in nondeterioration of the water quality.

Moreover, effective cooperation between government regulatory agencies, or between state environmental agencies, and industrial, municipal, agricultural, and other organizations depends on an agreement as to the appropriate analytical method that should be used in order that all parties may have confidence in the results as being a true evaluation of the actual condition of a stream or other body of water. The desirability of such agreements naturally leads to attempts to standardize the analytical methods used. Standardization is obviously desirable on a national basis so that all interested and concerned parties may accept the water-quality data with confidence. It is also desirable internationally, especially when two or more nations share an interest in a single water system or a part of that system.

The need for uniformity in analytical and test methods and for standardization in all aspects of water-quality monitoring has frequently been included within the scope of national standards bodies, such as the American National Standards Institute (ANSI) and the American Society for Testing and Materials (ASTM) in the United States. Technical Committee D-19 of ASTM currently has more than 350 professional people working on the development of standard methods of tests for water-quality data, water characteristics, and water-related materials. The Committee has published more than 135 standard methods and is continually expanding its efforts to meet new needs and conditions.

Organization for Economic Cooperation and Development

Early interests in the development and international standardization of analytical methods for assessing conditions of water quality were evidenced in the late 1950's within the Committee for Applied Research of the Organization for Economic Cooperation and Development (OECD) and the Organization for European Economic Cooperation (OEEC). The first meeting under the sponsorship of this agency was held in 1960 and was titled "The First International Meeting on Scientific Research into Water Pollution." Their initial efforts were directed toward coordinating research on water pollution and "preparing a list of research subjects which could usefully be studied on a cooperative basis." At that time, 22 different laboratories indicated an interest in "methods for the determination of pollution of watercourses and estuaries; standardization of sampling methods and analysis by chemical, biological, or other means."

International Standardization for Water-Quality Evaluation

At the first plenary session of a group of experts to study the methods of determining the "Composition and Condition of the Water of Streams," eight subgroups or working groups were established. Among these was Subgroup No. 8, whose assignment included the preparation of recommendations for the establishment of general sampling criteria and a comparative study of methods of analysis. The subgroup held several meetings, including two general meetings in Paris in December 1962 and in December 1964. The group's activities were terminated in April 1965, and a final report of their activities was prepared in December of that year.

During Subgroup No. 8's tenure, a number of matters were investigated by the participating countries, including dissolved oxygen, biochemical oxygen demand (BOD_5), chemical oxygen demand, chloride, nitrite, nitrate, copper, zinc, residual chlorine, phosphates, and cyanide. Their final report ended with two general conclusions:

"(a) *Sampling.* There is a growing tendency to use sampling systems relying more on statistical principles, either based on a grid of adjacent sections or the speed of the current. More and more automatic sampling and recording stations are being installed for research on major waterways.

(b) *Methods of analysis.* The group compared a large number of tests. Several types of determinations are still under study with a view to improvement or even fundamental modification, but in the great majority of cases the more accepted methods are now practiced. Many laboratories are tending increasingly to exchange the results of the methods in question."

With the report of Subgroup 8, one of the early efforts toward international standardization of water-analysis methods had begun.

Nordic Standards

A few years later, in 1968, the four Scandinavian countries organized among themselves a working group with the aim of developing methods for air and water analysis that would be acceptable to the four countries. The working group consisted initially of experts from leading water-analysis laboratories in Norway, Sweden, Denmark, and Finland. Their activities have been supported by the standards associations in their respective countries. Their early efforts resulted, in October 1970, in the formation of a Nordic Standardization Committee for analytical methods for air and water. Water-analysis methods were given priority, and it was decided to select a limited number of determinations to work on first and to divide the responsibility for developing methods among the four countries. As a result, efforts are being made to agree on methods for determining such quality factors as calcium, chloride, hardness, pH, specific conductance, color, turbidity, ortho- and total-phosphorus, chemical oxygen demand, suspended matter, and a number of others. A given method for a determination is recommended as a Nordic standard only after cooperative testing of the method and after general agreement and acceptance of the method by the four countries.

As with other analytical problems, the water analyst is usually faced with a choice of methods for a particular determination. The Nordic standards generally stress the simpler methods requiring a minimum of instrumentation and expensive equipment. To this end, even atomic absorption spectrophotometric methods are at this time omitted, an omission which may be unfortunate in view of the fact that many toxic metals which occur in water, often at vanishingly small con-



centrations, can conveniently be determined by atomic absorption spectrophotometry. These metals have become increasingly important factors in water-quality characterization; consequently, their determination has also become important and common in many water-analysis laboratories. Because this technique is so useful for the determination of minor constituents, it becomes almost an essential part of the equipment for a laboratory. In light of this, it would seem that atomic absorption spectrophotometric methods might also be specified for the common constituents, too.

The group, however, recognizes the necessity of preparing methods using special equipment and also the urgent need for methods for additional constituents and parameters. Presumably, their work will expand to include these other areas; the start they have made represents an important step in the development of water-analysis methods that can be accepted internationally.

World Health Organization

Other international organizations have, in recent years, given attention to the development and publication of methods for international acceptance. Notable among these is the World Health Organization which has gathered a number of water-analysis methods which are useful in water-quality investigations and in programs of water-pollution assessment. Currently, they are preparing a "Manual on Analysis for Water-Pollution Control," a manual "intended to provide governmental and other agencies, and particularly health administrations, with information and recommendations to assist them in setting up of water-pollution control programmes and the establishment of a unified system for fresh water analysis and recording of results." The manual will include procedures for the determination of a great number of significant water-quality constituents and parameters, including certain radiochemical measurements, and will include a chapter on interlaboratory calibrations.

International Standards Organization

The International Standards Organization (ISO), with headquarters in Geneva, is the international specialized agency for standardization, comprising the national standards bodies of 73 countries. Its work, which covers many fields, is carried out by more than 150 technical committees. The results of ISO technical work are published as International Standards, which represent a global consensus of opinion. ISO initiated activity in the fields of air and water quality in 1971, and the first meeting of two new technical committees (TC 146 and TC 147) organized to deal with these problems was held in Geneva at the end of April 1972.

The establishment of these committees was evidence of the growing worldwide interest and concern for the condition of the human environment and the conviction that something must be done to preserve and improve its quality. About 80 representatives from 19 countries attended this first organizing meeting of the water committee of ISO, which is identified as Technical Committee 147 on Water Quality. Liaison observers from several international organizations attended that first meeting and have continued to offer cooperation in the designation and preparation of urgently needed standards. These include observers from the World Health Organization (WHO), the Food and Agriculture Organization (FAO), the International Union of Pure and Applied Chemistry (IUPAC), and the Economic Commission for Europe (ECE).

The Technical Committee on Water Quality was established by ISO on the premise that major environmental problems are by their very nature international in scope, and that they can, therefore, best be solved at the international level. All national and international regulations relating to water quality should be founded on the same scientific and technological base. By developing the needed, appropriate international standards for pollution assessment, the proper scientific base can be established. Furthermore, it was reasonable that ISO, as the dominant agency for establishing international standards, would be the logical organization to provide the mechanism for preparing and publishing standards that could be accepted worldwide. The American National Standards Institute (ANSI) serves as Secretariat for ISO Technical Committee 147.

The Committee on Water Quality held a second meeting in Washington, D.C., in September 1973, in connection with the Ninth Triennial Meeting of ISO. As a result of these two meetings, the committee has defined the scope of its responsibilities as follows: "Standardization in the field of water quality, including definition of terms, sampling of waters, and the measuring and reporting of water characteristics. Standards of acceptability for water are excluded."

The committee subsequently approved a program of work within the scope established for the committee. The program of work is in two parts, consisting of a preamble and a tabulation of priority work items. The preamble seems worth examining, for it demonstrates the broad categories with which the committee plans to become involved as it pursues its work.

"The program of work of ISO/TC 147 on Water Quality shall include, but shall not necessarily be limited to, the following:

1. Standardization of terminology dealing with all aspects of water-quality characterization, including definition of relevant terms, units of measurement, and reporting results of water analysis.

2. Standardization of general methods for collecting samples of water, sludges, and bottom materials for various purposes, including selection of proper sampling sites, frequency of sampling, appropriate sampling equipment, treatment, preservation, and special handling of samples as may be required, and adequate identification and labeling of samples collected.

3. Standardization of methods for the measurement of water-quality properties and characteristics, including both chemical and physical properties, as well as radiological, microbiological, biological, and biochemical quality factors. Consideration will be given to the analysis and examination of all types of waters, including natural fresh and brackish water, sea water and brines, drinking water, industrial water, municipal and industrial wastewaters, and also sludges and bottom materials.



Table I. Subcommittees of ISO/TC 147 on Water Quality

(1) Terminology
(2) Physical, chemical, biochemical methods
(3) Radiological methods
(4) Microbiological methods
(5) Biological methods
(6) Sampling

4. Standardization of procedures for determining and expressing the comparative precision and accuracy of all test methods proposed as standards."

To accomplish this program of work, the committee established six subcommittees, five of which have been activated and are pursuing their assigned activities. The designated subcommittees are given in Table I. Only Subcommittee 3 on Radiological Methods has not yet been activated. In addition, a Preliminary Study Group was organized to make recommendations concerning committee policies in the matters of precision and accuracy of water-analysis standards. This study group has since become a work group, charged with the responsibility of specifying (1) minimum requirements for determining the precision of a method, (2) minimum requirements for determining the accuracy of a standard method, (3) means of expressing precision and accuracy, and (4) the relationship between significant figures and accuracy.

Subcommittee 1, for which South Africa holds the Secretariat, is preparing a compilation of definitions of terms relating to five categories: (1) types of water, (2) water treatment and storage, (3) water sampling, (4) water analysis, and (5) miscellaneous terms.

Subcommittee 2, for which the United States holds the Secretariat, has addressed itself to the preparation of standard methods in three broad categories: (1) physical properties of water and wastewater, (2) individual inorganic chemical constituents, and (3) individual or groups of organic constituents. Twelve work groups have been established under Subcommittee 2, according to determined priorities of work. These work groups are actively developing methods which can be considered by representatives of the participating member nations for adoption as ISO international standards. The work groups presently working on individual methods include those on nitrogen compounds (United Kingdom), phosphorus compounds (Germany), calcium (Sweden), cadmium (USA), mercury (France), cyanides (Germany), dissolved oxygen (Belgium), biochemical oxygen demand (Belgium), chemical oxygen demand-dichromate (Sweden), total organic carbon (Netherlands), and halogenated hydrocarbons (USA). Other determinations were also assigned high priority, but these twelve were considered urgent and most in need of immediate attention.



Subcommittees 4, 5, and 6, and Work Group A on Precision and Accuracy met in London in March 1974, during which meeting additional work groups under each of these subcommittees were set up to begin preparation of standards. Seven work groups were established under Subcommittee 4 on Microbiological Methods: (1) aerobic mesophilic viable bacteria (France), (2) coliforms, including E. Coli and others (France), (3) pseudomonas including fluorescents and aeruginosa (United Kingdom), (4) fecal streptococci (Netherlands), (5) sulfite-reducing clostridium (Germany), (6) nitrogen-cycle bacteria (Sweden, tentatively), and (7) salmonellae (Hungary).

Subcommittee 5 on Biological Methods now includes three work groups: (1) toxicity-bacteria (Germany), (2) toxicity-daphnia (Hungary), and (3) toxicity-fish (United Kingdom).

Subcommittee 6 on Sampling has divided its activities into three categories and assigned them to work groups as follows: (1) sampling programs (United Kingdom), (2) sampling techniques (USA), and (3) sample handling and preservation (France).

The next meeting of ISO/TC 147 will be in Budapest, Hungary, in the spring of 1975. Presumably, the subcommittees will schedule meetings in the same week as the committee and during the days immediately preceding those on which the full committee will meet. By the time of the planned third meeting of ISO/TC 147, many of the subcommittees and work groups will have significant accomplishments to report, and a number of methods will be ready for consideration and approval as international standards.

Technical Advisory Group

As Secretariat for ISO/TC 147, the American National Standards Institute (ANSI) is responsible to the ISO Council and to the members of the committee, for all the activities of the Technical Committee including its subcommittees and working groups. To assist ANSI in carrying out these responsibilities, a United States Technical Advisory Group (USA-TAG) was organized early in 1972. This TAG provides input to the Secretariat in the matter of proposals for organizing TC 147 and for conducting its work. As Secretariat for TC 147, ANSI acts as an international Secretariat and must not be influenced by national considerations. The Secretariat does rely, however, on counsel and advice from the USA-TAG for guidance in policy matters which are subject to consideration and adoption by all ISO/TC 147 member nations.



The USA-TAG is composed of representatives from organizations and professional societies who have an interest in promoting international standardization in water-quality measurements. Presently active on the USA-TAG are representatives from federal agencies, including the Geological Survey, Environmental Protection Agency, the National Bureau of Standards, Atomic Energy Commission, and the Naval Ship Engineering Center. Several professional societies and organizations are represented, including the American Society of Civil Engineers, American Society of Mechanical Engineers, Manufacturing Chemists Association, Water Pollution Control Federation, American Water Works Association, and the American Society for Testing and Materials. Membership and participation in USA-TAG activities are not restricted but are open to any organization or agency that has an interest in participating in the development of international standards in the area of water-quality assessment. The group ordinarily holds three meetings a year.

The USA-TAG also functions to advise ANSI as Secretariat of TC 147 Subcommittee 2 on Physical, Chemical, and Biochemical Methods, and

serves to establish the United States position relative to technical documents generated by the subcommittees and work groups. These generally consist of Draft Proposals and Draft International Standards.

Liaison

Evidence of the widespread interest in, and the urgent need for, international standards for water analysis is amply demonstrated by the number of international organizations with which ISO/TC 147 has established liaison. Active liaison arrangements have been established with 17 international organizations or agencies, including the World Health Organization, Food and Agriculture Organization of the UN, Economic Commission for Europe, Committee of the European Communities, Inter-Governmental Maritime Consultative Organization, World Meteorological Organization, Council for Mutual Economic Assistance, the International Organization for Hydraulic Research, and the Nordic Standardization Committee for Air and Water. All of these organizations have an interest in standards for water analysis, and active liaison efforts involving at least the exchange of pertinent documents and information have been initiated. In addition, whenever possible, a representative of each of the liaison organizations attends meetings of ISO/TC 147 as observers, and ISO representatives attend meetings of the other agencies in order to maintain an active exchange of information and to keep each other up-to-date on the activities of each relating to water and pollution analysis.

In addition, to facilitate the work of TC 147, liaison has been established and is maintained with nine other ISO and IEC (International Electrotechnical Commission) Technical Committees. These inlcude TC 28 on Petroleum Products, TC 47 on Chemistry, TC 69 on Application of Statistical Methods, TC 113 on Measurement of Liquid Flow in Open Channels, and TC 146 on Air Quality.

The output of ISO and its Technical Committee 147 on Water Quality shows promise of fulfilling an urgent need for international standardization for water pollution assessment.

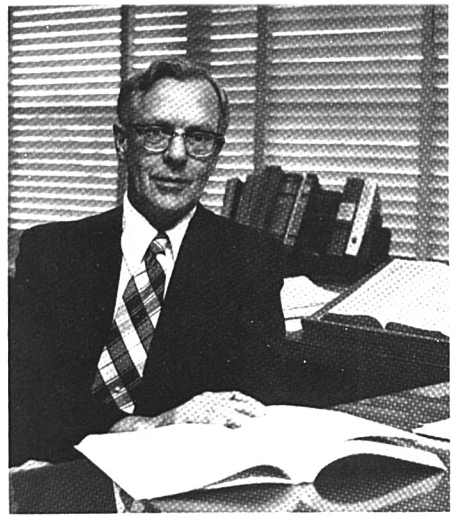
International Association of Hydrologic Sciences

Still another international organization has recently involved itself in matters relating to agreement on uniformity of methods for water analysis. The International Association of Hydrologic Sciences (IAHS) recently organized a subcommittee on water quality. One of this subcommittee's first actions was to recognize the possibility of discrepancies when data from different laboratories are used to evaluate theoretical hydrogeochemical principles. As a part of a program for evaluating the various analytical methods used by leading analytical laboratories around the world, as many as 25 or 30 worldwide laboratories are conducting a round-robin analysis program involving seven natural water samples of widely different types, including both surface and ground waters, and for both common and unusual constituents.

The results of this testing program will be summarized and presented at a Symposium on the Geochemistry of Natural Waters to be held in Burlington, Ont., Canada, in the summer of 1975. Data have already been submitted by participating laboratories for the analysis of three samples, and other samples are being prepared for distribution. Prominent water analysis laboratories in Canada, United Kingdom, Australia, New Zealand, Sweden, Norway, Japan, USA, USSR, and other countries are involved in this round-robin study. This cooperative program should lead to a revelation of interesting facts concerning interlaboratory test data and the reliability of various analytical methods applied to different types of waters.

National and International Standardization

With so many agencies and organizations involved and with so many technical experts participating, both in this country and worldwide, there can be real hope that truly national and international agreement can eventually be reached on standardization of methods and techniques for assessing the real condition of national and international waters. The exchange of technical experience and information that takes place as a consequence of these efforts at standardization serves to assist the member countries in their efforts to deal with water-pollution problems that are common to all.



Marvin W. Skougstad of the Water Resources Division of the U.S. Geological Survey, Denver, Colo., received his BS in chemistry and his PhD in chemistry and metallurgy in 1939 and 1949, respectively, from the University of Wisconsin. He served in chemistry and teaching positions at Washburn Co., Rockford, Ill.; Fairbanks-Morse and Co., Beloit, Wis.; and St. Olaf College, Northfield, Minn., before joining the U.S. Geological Survey in 1958. His research interests are centered on the occurrence and distribution of minor elements in water, development and standardization of methods for water analysis, and methods of determining minor elements in water. He is active in professional societies, including the ACS, SAS, ASTM, and is chairman of Technical Committee 147 on Water of the International Standards Organization.

Reduce cost and increase effectiveness!



Use Engelhard non-wetting platinum alloy 7070

Now you can reduce the cost and increase the effectiveness of the laboratory testing of cements, slags, glasses, bauxites, geological specimens and a variety of other materials with crucibles and other labware made of Engelhard Platinum Alloy No. 7070.

The new alloy is "non-wet" by lithium tetraborate and metaborate fusions used in X-Ray Fluorescent Analysis. This provides longer life for expensive laboratory utensils and more accurate test results. In addition, labware made of this new alloy is ideal for use in the large quantity analyses now possible with the new fused bead production machines.

Crucibles of Engelhard Platinum Alloy 7070 are available in standard laboratory sizes. Specimen holders for casting borax buttons, for X-ray fluorescence and other techniques can be custom made to any specification.

Write or call today for your free catalog of "non-wet" Engelhard Platinum Alloy 7070 dishes and crucibles and hundreds of other platinum implements and equipment.

For further information write or call:
(201) 636-4330 Ext. 232
Ask for John Ven Graitis

ENGELHARD

ENGELHARD INDUSTRIES DIVISION
ENGELHARD MINERALS & CHEMICALS CORPORATION
700 BLAIR ROAD, CARTERET, NEW JERSEY 07008

An Equal Opportunity Employer

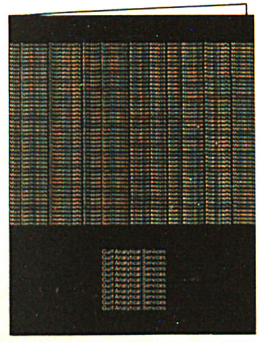
CIRCLE 67 ON READER SERVICE CARD

Atomic Absorption Spectroscopy
Catalyst Testing
Crude Oil Evaluation
Elemental Analysis by Nuclear Techniques
Emission Spectroscopy
Gas Chromatography
Infrared Spectroscopy
Liquid Chromatography
Mass Spectrometry
Organic Elemental Analysis
Radiotracer Services
Unit Operations
Water and Air Quality Studies
X-ray Diffraction and Fluorescence

When you're up against a technique not in your field or an analysis that requires equipment not in your laboratory, think of Gulf Analytical Services.

We can provide you with anything from a one-time evaluation to analytical backup for an entire development program.

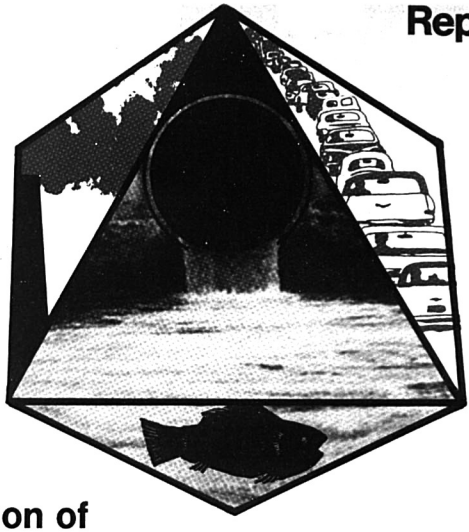
Our laboratory equipment and areas of experience are summarized above. We'll be happy to discuss specific needs and programs with you. Call collect, 412/661-2825. You'll also find more information in our brochure "Gulf Analytical Services". Get a copy from any Gulf Sales Engineer. Or write Gulf Analytical Services, 1161 GBA, Dept.117 P.O. Box 1519, Houston, Texas 77001.



Ask the pro from Gulf.

Gulf Oil Corporation

CIRCLE 86 ON READER SERVICE CARD



Comparison of Analytical Techniques for Inorganic Pollutants

R. F. Coleman
Laboratory of the Government Chemist
London, England

The interest in the concentration of pollutants has never been greater. An increasing number of laboratories are involved in the measurement of a wide range of substances in environmental samples, and much of the current research in analytical chemistry is directed toward improved methods of analysis for this purpose.

The main aim of this paper is to provide some background data which will assist in the selection of the appropriate technique for current and future problems. This is a very wide ranging subject, and I must draw some boundaries, albeit artificial ones, because a pollutant may sometimes be a nutrient, just as to a gardener a weed is merely a plant in the wrong place rather than something inherently undesirable. I shall limit the discussion to inorganic pollutants, but I shall ignore radioactive and also gaseous pollutants such as sulphur dioxide and oxides of nitrogen which require specialised techniques. In effect, this paper will discuss analytical methods which are applied to inorganic pollutants found in food, water, or collected on air filters from the atmosphere. The choice of the appropriate technique depends upon many factors; in addition to the inherent characteristics of that technique, it is very much dependent upon the nature of the requirement for analysis as well as the availability of particular kinds of samples. I propose, therefore, to start off with the kinds of operational requirements which one is likely to meet, follow this by a brief description of sampling techniques and problems which are common to all kinds of analysis, and then discuss the analytical techniques themselves in relation to these requirements and sampling problems.

Operational Requirement

It is of vital importance to try and understand the complete problem. Sometimes analysis is not required at all in the initial stages because the analysis of a few samples may be misleading if the problem has not been properly formulated. All too often, the analysis of samples is requested without any thought being given to the value of the data and the valid conclusions which can be drawn from it.

There are essentially three different kinds of operational requirement in which analysis can play an important part. The first might be the unexpected problem when a known or unknown pollutant is affecting the health of workers or the external population. The analytical chemist is then expected to provide some data rapidly so that necessary appropriate corrective action can be taken. In such circumstances, the appropriate technique should be capable of giving a rapid answer, be comprehensive and wide ranging, and initially, only qualitative or semiquantitative answers may be required. The second typical requirement is to study the effects of a single or, at the most, a few elements or compounds on the environment, for example, lead effluent from an industrial plant or on a larger scale, the lead content of the diet of the whole population. In such cases, one can select a technique which is appropriate for that particular element. If there are a large number of samples, automation may be necessary. Alternatively, several laboratories may collaborate in the study. In this case, it is essential that intercomparison of particular samples is undertaken at the beginning of the survey to ensure compatibility of analytical data. Careful plan-

ning of the sampling programme is also essential. The third requirement involves the analysis of a large number of elements simultaneously. These are often long-term background studies designed to monitor the environment and identify changes which have a health or economic significance. Naturally, multielement techniques are preferred in such surveys, and often some form of automation is necessary to handle the large number of samples generated.

Sampling

Sampling is a difficult and complex problem, and very often insufficient attention is paid to it. The results obtained in many surveys bear little resemblance to the true state of affairs because of changes occurring in the samples, between the source and the laboratory. In some cases, it is possible to avoid sampling altogether by making the measurements in situ. For example, selective ion electrodes may be used for the determination of certain pollutants in flowing streams of liquid. The sampling of water has been reviewed by Spencer and Brewer (*1*), but general solutions to all the problems are not known at the present time. Contamination and loss of trace elements during storage has been responsible for much erroneous data on the concentration of trace elements in the literature. Robertson (*2*) has shown major losses of some elements from unacidified seawater stored in polythene and glass. If it is important to distinguish between ions in true solution and suspended matter, filtration should be carried out as soon as possible. Hamilton and Minski (*3*) showed very significant differences between river waters analysed as sampled and after the addition of acid. The increase in concentration of many elements is attributed to the dissolution of particulate matter. The same authors found that soft water tends to extract more elements from containers than hard water.

Cawse and Pierson (*4*) have described a remote sampling station for airborne dust and rainwater which has been used satisfactorily for several years. Rainwater is collected monthly in a polythene funnel and bottle, while airborne dust is collected by drawing air through a filter paper in a polypropylene duct.

While it is relatively easy to sample in order to measure the concentration of a constituent in a particular foodstuff, sampling of the normal diet of a population is much more difficult. Harries et al. (*5*) have described the organisation of a total diet study which involved local purchase of foodstuffs and cooking in about 20 colleges in different areas of England and Wales in order to give a good geographical coverage of population centres and allow for regional variations in the diet.

Sample Preparation

The sample preparation will naturally depend upon the analytical technique to be used; however, there are some guiding principles which are common. Obviously, care must be taken to avoid contamination of the sample from the laboratory atmosphere, containers, and reagents. Tolg (*6*) reviews procedures involved in sample preparation and also methods of decomposing and dissolving samples for trace analysis. Hamilton et al. (*7*) considers the laboratory environment, sample preparation, and ashing procedures specifically for multielement analysis of biological materials.

Analytical Methods

The analytical techniques which have found the widest application in the study of inorganic pollutants are compared below on the basis of sensitivity, accuracy, precision, multielement capability, and range of application. In addition, where possible, the future trends in each technique will be discussed.

Microscopy. Although neglected by many analytical chemists, optical microscopy is particularly suited to the examination of particulate matter. It is a comprehensive technique capable of detecting as little as 10^{-12} gram quickly and with relatively simple apparatus. In addition, it provides information, not only on the elemental composition, but also the compounds present and in many cases the crystalline form. Identification of particles is greatly assisted by using the classification system of McCrone and Delly (*8*). Each particle is characterised by six parameters, e.g., colour, shape, and birefringence and can be compared with over 1000 substances in "The Particle Atlas." The groups of particles with the same classification can be differentiated on the basis of additional attributes such as density and refractive index and by direct comparison of the unknown with photomicrographs.

The next logical step is to use the scanning electron microscope. It shows the shape and surface of relatively large particles (1–100 μ) better than the polarising microscope because of the superior depth of field, and with magnifications of up to 30,000×, it is suitable for the identification of submicron particles also. A third advantage is the ability to determine the chemical composition of tiny single particles by energy dispersive X-ray analysis. "The Particle Atlas" contains electron micrographs of 100×, 1000×, and 10,000× and the X-ray spectrum of many particles. With transmission electron microscopy diffraction patterns of individual submicron particles may be obtained. With this technique my laboratory identified the presence of traces of talc in maize starch. The latter is used as a lubricant for surgeons' gloves, and talc is forbidden because of the possible deleterious effects of talc inside the body. This is a formidable analytical problem since direct X-ray diffraction on the bulk powder does not reveal talc, and magnesium oxide is also present to improve the free running characteristics of the powder and would greatly exceed the magnesium concentration due to talc. Optical and electron microscopy are particularly suited to troubleshooting and for a preliminary examination of many types of samples.

Atomic Spectroscopy. It is convenient to discuss atomic absorption, atomic fluorescence, and atomic emission together because of their similarities and the complementary nature.

Atomic absorption is particularly suited to the analysis of trace pollutants in studies involving one or a few elements. More than 60 elements can be determined by the technique, and it has become the most widely used technique for such applications. Winefordner et al. (*9*) have written an excellent review of theoretical and experimental aspects of atomic absorption, fluorescence, and emission flame spectroscopy. In addition to comparing the sensitivity of the three techniques, the review discusses the theoretical limitations of different types of excitation and the possible interference effects. Stone and Warren (*10*) review the modern instrumentation available for atomic absorption and give practical advice to assist in the selection of spectrometers from the wide range now available.

Although electrodeless discharge lamps and lasers have been used for atomic absorption, the hollow cathode lamp is still used in the vast majority of applications. The latter are available for over 60 elements and now have a fairly long life and adequate stability. The flame is the most widely accepted method of generating atoms for absorption. A variety of fuels and oxidants have been investigated, but for most purposes, air–acetylene (temperature, 2400°K) and nitrous oxide–acetylene (temperature, 3200°K) are satisfactory. The latter is particularly satisfactory for refractory compounds.

As with any technique, atomic absorption suffers from various types of interference. However, these are not generally serious, and in flames the mechanisms are well understood so that they can be reduced or eliminat-

DON'T TURN THIS PAGE

If Your Problem is Trace Metals

In
air,
water,
food,
soil,
gasoline,
chemicals
or
kids



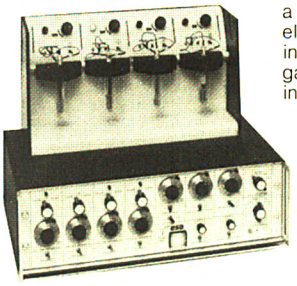
With our Model 3010 Trace Metals Analyzer you can measure trace amounts of lead in macro or micro ($\geq 100\mu l$) samples of blood, ketchup, gasoline, air, water, urine, concentrated acids (and other substances), in 30 to 90 seconds, without sample pretreatment. Throughput is over 200 samples daily, excluding blanks and standards. Direct digital readout is in $\mu g\%$, ppm, ppb, or other specified units. With wet digestion of samples, the Model 3010 can also be used for copper, cadmium, bismuth, thallium, and other heavy metals.

Specify this for fast, routine, repetitive analysis and low cost per sample.

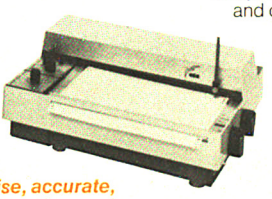


Our Model 2011 Single Cell Analyzer enables you to perform qualitative and quantitative analysis on problem metals in many matrices. The instrument is completely integrated, and, for field use, will operate off a 12v storage battery with an inverter. A typical value for precision (cadmium) is $\pm 6\%$ at the 10 nanogram level. Routine analyses can be performed on samples of 5 to 500 nanograms.

Specify this when your budget and/or the number of daily analyses are limited.



Our Model 2014 is a powerful laboratory tool that can be equipped with extender units to handle up to 12 discrete samples for repetitive analysis of a single or multiple elements. When equipped with peripheral sensors and electronic recorders, this unit can and has been used to measure mercury in the exhaust stack of coal generating stations...lead in air, water, blood, gasoline, food and biologicals...and a wide spectrum of other applications involving the measurement of lead, copper, cadmium, mercury, zinc, antimony, thallium, bismuth, silver, tin, arsenic, indium and other problem elements.



Specify this when you want a precise, accurate, reliable instrument for research or routine analyses.

esa

ENVIRONMENTAL SCIENCES ASSOCIATES, INC.
175 Bedford Street,
Burlington, MA 01803
(617) 272-1200

In Canada: Radionics, Ltd., Montreal, Quebec H4T 1R6; **In Great Britain and Europe:** Joyce-Loebl & Co., Ltd., Gateshead, England; **In Japan and Taiwan:** Nissei Sangyo Co., Ltd., Tokyo; **In Australia:** Tosco PTY, Ltd., Hawthorne; **In New Zealand:** Thomas Hyde, Ltd., Christchurch; **In Central and South America:** Extech International Corporation, Boston, MA.

CIRCLE 70 ON READER SERVICE CARD

ed. Spectral interferences rarely occur in atomic absorption spectroscopy because of the simple absorption spectra and narrow lines emitted by hollow cathode lamps. Variations in the relative proportions of ground state atoms and ionised states can occur if the matrix contains easily ionised elements such as potassium. This is fairly readily avoided by adding a sufficiently large quantity of the element to standards in order to swamp the matrix effect. Chemical interferences owing to compound formation between the element being determined and interfering substances do exist but are often broken down by the use of high-temperatures flames or by adding a releasing agent which preferentially binds the interferent. For example, lanthanum is widely used for this purpose as it will bind a variety of oxy-anions. Physical differences in samples such as viscosity can influence the formation of aerosols and cause errors if the samples and standards are not adequately matched. Samples containing a high salt content can cause scattering of radiation; thus, an absorption effect is detected other than that owing to the element to be measured. Many modern instruments contain a second light source which can eliminate background absorption and substantially increase precision and limits of detection in such samples.

An indication of the sensitivity of current flame atomic absorption procedures is given in Figure 1. Typically, the precision of analysis is 1–3% for concentrations more than 10 times the limit of detection. In principle, the accuracy should be of a similar order because of the limited interference in the technique; however, in practice the sampling and sample preparation procedures often introduce larger errors.

A variety of techniques have been developed to increase the applicability of atomic absorption. For example, the determination of mercury by flame atomic absorption is rather insensitive. However, by reducing mercury to the elementary form, it can be vapourised in a current of air into an absorption tube and then the absorption measured in the cold state. This technique is widely used to determine the mercury level of foods and other biological materials (*11*). The measurement of arsenic can be improved by production of arsine from the solution (*12*), which can then be led directly into the flame and the absorption integrated over time, or by collection in a balloon and subsequently discharged into the flame. Either of these two techniques can determine submicrogram quantities of arsenic. Similarly, the reduction of selenium to hydrogen selenide prior to the introduction into the flame has improved the sensitivity of the technique (*13*). A variety of flameless cells are now commercially available, such as graphite tube furnaces, graphite rod atomizers, and tantalum ribbon atomizers. These devices are electrically heated and produce temperatures up to 3000°K and are suitable for the less volatile refractory elements. The marked improvement in sensitivity of the graphite atomiser methods over flame sources is indicated in Table I. The precision of analysis is much worse than for flame methods, typically 5–25% depending on the type of atomiser and type of sample. The interferences have not been adequately studied, and insufficient information is available on the interaction between solution and gaseous state with carbon. Various physical interferences have been noted in some applications, apparently inhibiting the volatilisation of the sample.

Atomic absorption is widely used within the Laboratory of the Government Chemist for trace analysis of foods, water, and dust samples when the requirement is for one or a few specific elements such as lead, arsenic, cadmium, and mercury. Simultaneous multielement analysis is difficult by atomic absorption, but various

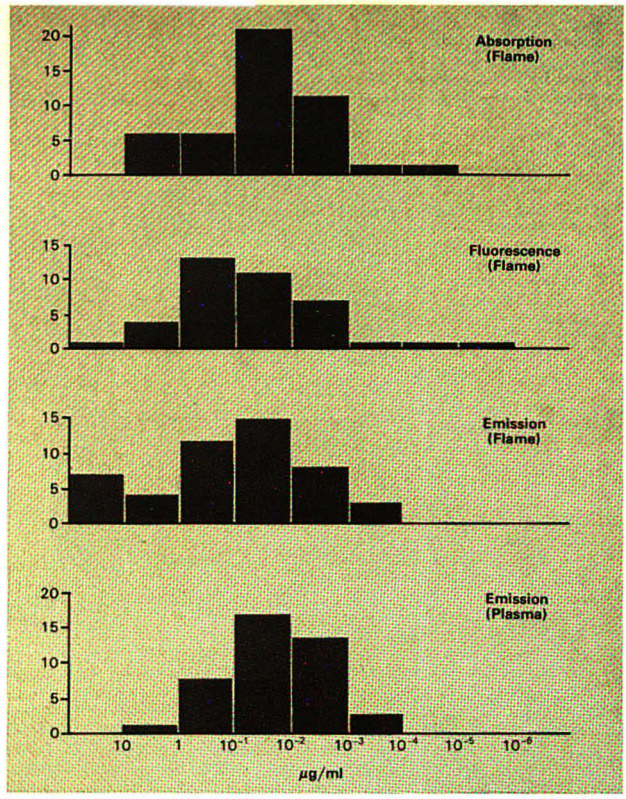


Figure 1. Limits of detection in atomic spectroscopy

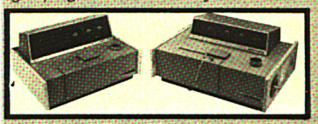
Table I. Comparison of Flame and Graphite Tube Sources

	Detection limits, ng/ml							
	Cd	Co	Cu	Mg	Mn	Ni	Pb	Zn
Flame	2	10	1	0.1	2	2	10	1
Furnace	0.0001	0.004	0.001	0.0001	0.001	0.01	0.006	0.0006

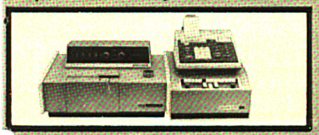
AUTOMATE your spectrophotometry Get 360 results an hour... With the Spectronic® System 400.

Choose the Degree of Automation You Want. The System 400 provides *exactly* the amount of automation you need for your spectrophotometric testing. It can automate clinical testing (end-point or kinetic), drug abuse detection, industrial quality control, water and waste analyses, food sampling, method development, or research studies.

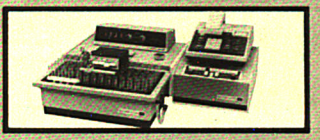
A Quality Spectrophotometer at the Heart of the System. There are two digital spectrophotometers with excellent resolution and stability for the System 400. Choose the Spectronic® 100 for testing in the visible region or the Spectronic® 710 covering the ultraviolet to near IR. Just one of our many sampling options is a micro flow-thru cell compartment that can handle low sample volumes of any chemical reagent, regardless of viscosity.



Automated Data Handling. The Spectronic System 400-2 consists of either spectrophotometer and the DP-110 Data Processor. A unique feature is its ability to print both absorbance *and* concentration for quality control checks. It provides automatic calculations for rate reactions, and samples can be serially identified.



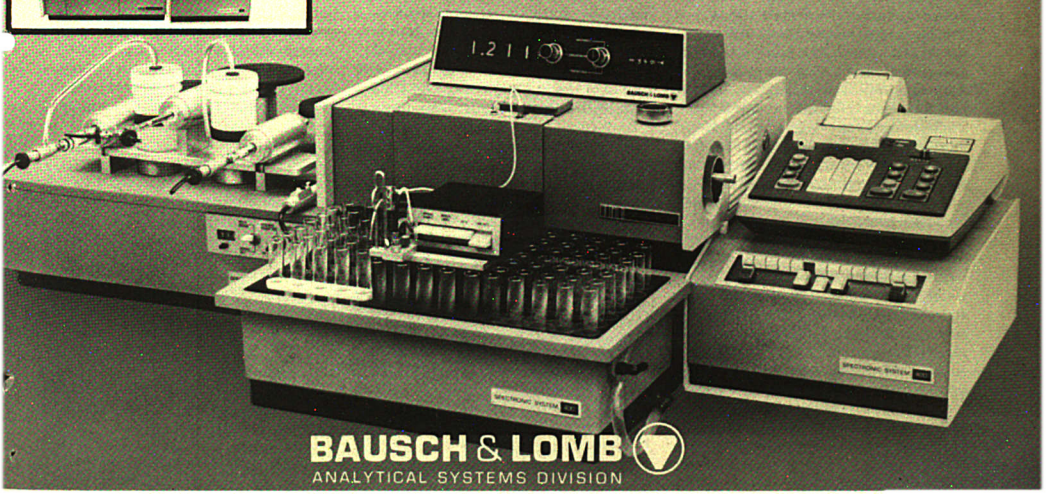
Automatic Sampling. The Spectronic System 400-3 accepts 80 prepared samples in a constant temperature water bath for incubation during color development. Automatic transfer of reaction mixture to the spectrophotometer means *unattended operation.* The operator can work elsewhere while the system produces test results.



Automatic Sample Preparation. Adding the Dilufer/Pipetter gives you the System 400-4, capable of automatically adding a trigger reagent to initiate all chemical reaction. There's no need to use sample cups or waste sample—only the exact amount the test requires is used. An air-jet provides complete mixing of the sample reaction.

If it's time to automate *your* spectrophotometry—no other automatic spectrophotometric system is as flexible or versatile—regardless of price.

we sell more spectrophotometers than any other manufacturer.



BAUSCH & LOMB
ANALYTICAL SYSTEMS DIVISION
ROCHESTER, NEW YORK, U.S.A.

European Headquarters, Bausch & Lomb GmbH, Analytical Systems Division, Munchener Strasse 72, 8043 Unterfoehring, Germany.

CIRCLE 23 ON READER SERVICE CARD

schemes have been reported (*14*) for the rapid sequential analysis of many elements.

Since 1964 when Winefordner and Vickers (*15*) demonstrated analytical applications of atomic fluorescence, many papers relating to this technique have appeared. A review by Browner (*16*) provides a good background description of the technique and allows the reader to make a reasoned choice between this and atomic absorption and flame emission spectrometry. At the present time, there are no commercial instruments available for atomic fluorescent spectrometry which must limit its general availability. It offers considerable improvement in detection capability for many elements, particularly those with principal resonance lines below 320 nm, but the instrumental drawbacks inherent in its nature have delayed its wider acceptance. It is essential to have a high-intensity stable source of the required wavelength. Many workers are now using thermostatic electrodeless discharge lamps, and these seem to offer the best solution at the present time. Atomic fluorescence has the same limited interference problems as absorption; in addition, quenching processes could cause problems. Most of the development work on fluorescence spectrometry uses nonflame cells since this reduces the possibility of quenching and still maintains good atomisation efficiency. Multielement analysis is more readily achieved with atomic fluorescence than absorption, and a spectrometer for the simultaneous determination of up to six elements has been described. As with most multielement techniques, the operating conditions will be a compromise.

Atomic emission has developed significantly in the last decade and is now applied to a large range of elements. The sensitivity, compared with absorption and fluorescence techniques, is indicated in Figure 1. Busch and Morrison (*17*) have reviewed the multielement capability of flame spectroscopy and conclude that emission is the technique most easily adapted for this purpose, although it is not the most sensitive of the three techniques for many elements.

The high-frequency plasma sources for spectroscopy first used by Greenfield et al. (*18*) are now becoming widely accepted, and commercial sources coupled with direct reading spectrometers are available. Scott et al. (*19*) have investigated plasma sources extensively and have developed a compact system ideally suited to practical multielement analysis. A pneumatic nebulizer feeds the aerosol produced from the solution directly into a plasma. The high temperature (7500°K) eliminates most chemical interferences observed with other emission sources; thus, simple standard solutions can be used to calibrate complex mixtures. The stability of the system is good, and precisions of about 1% (relative standard deviation) for sub-ppm solutions have been achieved. The detection limits with a plasma source for most elements are lower than flame atomic absorption or fluorescence. The technique seems well suited to the multielement analysis of biological samples, following removal of organic matter and dissolution of the sample.

Mass Spectrometry. The attraction of mass spectrometry for the analyst is the simplicity of the spectra. In theory, a spectrum of a mixture will contain only discrete lines for each isotopic species present, but in practice, some interference from compounds and hydrocarbons is always present. The spark source is usually used for ionisation for elemental analysis because of the relatively uniform ion formation for all elements. For analysis of environmental samples, it is usually necessary to remove the organic material and mix the residue with graphite in order to prepare conducting electrodes for the spark source. Hamilton et al. (*20*) have studied the procedure extensively for biological materials, and Brown and Vossen (*21*) have applied it to air pollution samples on filters.

Several instruments are available commercially with two-stage magnetic and electrostatic separators and ion detection by photographic plate or electrically by using photomultipliers. The method is most sensitive using photographic plates with exposure times of about 1 hr, and almost all elements can be detected down to ppb levels. Electrical detection is less sensitive but more rapid; in the scanning mode typical sensitivity limits are 0.1 ppm, taking about 10 min for examination of the full mass range, and 0.01 ppm by peak switching to examine specific elements. Direct semiquantitative analysis is possible without standards with an accuracy of about a factor of three. For quantitative analysis it is essential to measure the relative sensitivity of ionisation and detection of each element by using standards prepared in a matrix similar to the sample. In this way, the accuracy can be about ±10–25%—lower for electrical detection and higher for photographic methods.

Although the spark source has been used for many years for elemental analysis, it has serious limitations, and Gray (*22*) has shown that a plasma source has many desirable features for ion formation prior to mass separation. A solution of the sample to be analysed is sprayed directly into a capillary arc plasma, and the gases from the plasma plume directly enter the vacuum system through a small orifice in a thin wall. The ions are focused and directed into a second chamber with a quadrupole filter. The quadrupole mass filter permits only one mass number to pass through it, but by scanning, a complete mass range can be examined and recorded. Currently, the low mass end of the spectrum contains a complex collection of peaks owing to nitrogen, oxygen, and hydrogen compounds, but above mass 55 the background is very small.

Mass spectrometry gives the best coverage of elements at the ppb concentration range (Table II) and is well suited to studies requiring a large number of elements. The careful sample preparation necessary for spark sources limits the rate of analysis, but this may improve with the development of the plasma source.

Isotope dilution procedures are capable of giving some of the most accurate determinations for trace elements. Although not likely to be used on a routine basis for analysis of pollutants, they do offer the possibilities of providing an absolute method suitable

Table II. Typical Detection Limits in Mass Spectrometry (ng/g)[a]

Element	Spark source	Plasma source
Ag	2	2
As	0.6	10
Cd	7	5
Co	0.5	0.2
Cu	2	0.4
K	0.3	0.5
Mg	0.2	0.5
Mn	0.4	0.5
Pb	3	0.2
Zn	2	5

[a] For spark source a 10-g sample was ashed and mixed with carbon to form electrodes; for plasma source residue after ashing was dissolved in 2 ml and sprayed into plasma.

Table III. Comparison of Analytical Methods for Pollutants

Technique	Advantages	Limitations
Microscopy	Excellent for particulate matter Identification of compound and crystalline forms possible Very sensitive Rapid	Not suitable for pollutants in solution Not readily quantified Requires specialised skills and training
Atomic absorption and fluorescence	Applicable to more than 60 elements Simple spectra and instrumentation Sensitive Rapid	Simultaneous multielement analysis difficult
Atomic emission	Multielement analysis feasible Sensitive Rapid Plasma source eliminates most chemical interferences	Flame sources have significant matrix effects
Mass spectrometry	Multielement technique Excellent sensitivity Plasma source promises rapid analysis	Specialised sample preparation techniques for spark source Plasma source still in development phase
Neutron activation analysis	Freedom from contamination Excellent sensitivity for some elements Applicable to wide variety of matrices	Limited availability for routine analysis Total time for multielement analysis may be long
X-ray fluorescence	Direct examination often feasible May be nondestructive Multielement technique Rapid	Limited sensitivity Particle size effects must be carefully controlled
Anodic stripping voltammetry	Simple technique and equipment Excellent sensitivity for some elements	Not suitable for wide range of elements

for the standardisation of secondary techniques. The principle of the method is very simple; the concentration of an element is determined from the change produced in a natural isotopic composition by the addition of a known quantity of the same element, the isotope ratio of which has been artifically altered. A given amount of sample is equilibrated with a known quantity of an isotopically enriched spike; the element is extracted, and its new isotopic ratio measured by mass spectrometry. Since only isotopic ratios are involved, the extraction does not have to be quantitative. Isotope dilution techniques are capable of accuracies of the order of 0.1% for many elements at trace concentrations. The National Bureau of Standards has already used the technique to standardise the determination of calcium in blood and also lead in blood. It is hoped that through certified reference materials and methods such as isotope dilution, it will be possible to obtain compatible data for these elements throughout many laboratories.

X-ray Spectrometry. X-ray fluorescence spectrometry is well suited to the determination of the elemental composition of pollutants because in many cases, limited sample preparation is required, and the technique is nondestructive. All elements of atomic number greater than 11, i.e., sodium, can be analysed. Traditionally, the technique has used wavelength dispersion as a method of separating the X-rays emitted from the sample, but with the recent availability of silicon and germanium X-ray detectors of high resolution, energy dispersive spectroscopy is possible and often simpler. Gilfrich et al. (*23*) have reviewed X-ray spectrometry for particulate air pollution samples and conclude that there are two problems with solid-state detectors which are limiting in that application. First of all, the resolution is not adequate to separate the K-alpha line of one element from the K-beta line of the next lower atomic number in the region of sulphur to nickel; thus, all these elements will require mathematical unfolding to determine X-ray intensities. Also, the solid-state detectors are limited to about 10^4 counts/sec at their best resolution, and long count times would be necessary to get adequate counting statistics for multielement analysis. Because of these limitations, they conclude that large-scale quantitative analysis requires the resolution obtainable from crystal spectrometers, and for routine analysis the only practical approach is the use of multichannel wavelength spectrometers, because of the time required for the wavelength scanning mode.

At our own laboratory we have found X-ray spectrometry very useful for the analysis of food samples; the sample preparation is simple, merely requiring freeze drying followed by grinding at liquid nitrogen temperatures in order to produce a fine powder suitable for presentation to the X-ray beam. It has been particularly useful for light elements, e.g., sulphur and phosphorous, which are difficult to determine by most spectrographic techniques.

The limit of detection for most elements by wavelength dispersive spectroscopy is in the range 0.1–1 μg, with concentration limit depending on the sample size, shape, and physical form. X-ray spectrometry is mainly used for multielement analysis but often does not have adequate sensitivity for all the elements of interest in biological samples.

Neutron Activation Analysis. The radiation of a sample with neutrons transforms some of the atoms of each element present into a radioactive form. These radioactive atoms can be separated and detected more easily than stable atoms. For many years activation analysis was probably the most sensitive analytical technique, but this is no longer the case, and the merits of the technique must be assessed on other properties such as cost, availability, and range of elements analysed. It is not easy to sum up activation analysis because its performance depends upon many different attributes—first of all, the specific nuclear properties of the element concerned, the equipment available for measurement of induced activities, and the nature of the sample itself. One of the prime advantages of activation analysis is its freedom from contamination, provided the sample is not contaminated prior to irradiation; then, one does not have to worry about subsequent contamination from reagents.

After irradiation the measurement

of induced activity may: use direct instrumental methods for discriminating between the radiations emitted from each element present; rely on complete radiochemical separation with simple nonspecific detectors; or use group separations, e.g., Goode et al. (*24*), to reduce the complexity of each sample to more manageable proportions. The improvement in the sensitivity and resolution of germanium detectors over the last five years has encouraged more use of the direct method. However, for biological samples the intense radiation from sodium and chlorine usually makes some preliminary separation essential if a wide range of elements is to be determined.

An example of how the technique can be applied to analysis of pollutants is given by Pierson et al. (*25*) in their work on the composition of rain and dust in the atmosphere. The samples of filter paper or rain were irradiated for 20 sec; then the gamma spectrum of each sample was measured a few minutes after irradiation and at further times over the subsequent 24 hr, with sodium iodide detectors. The spectra were compared with those from standards by the method of linear regression analysis with a computer; about eight elements could be determined in this way. Samples were then irradiated for one week, and gamma spectra obtained over a period of several weeks with germanium detectors, and a further 20 elements determined. This example indicates direct access to a reactor for short and long irradiation; a variety of detection systems and computer data processing are necessary for successful routine multielement analysis by activation techniques. If these requirements cannot be met, then other techniques are likely to offer a better solution to the analytical problem.

Electrochemical Methods. Polarographic methods of analysis have been used for trace analysis of specific trace metals for many years, but the technique has many limitations and has not been so widely used as many spectrographic techniques. However, the related technique of anodic stripping voltammetry has been applied, increasing in recent years to the analysis of water samples and other solutions. The sensitivity of the technique is obtained by initially concentrating the trace elements into a small volume of mercury by electrolysis, at a more negative potential than the reduction potential of the trace element, over a period of 10–60 min. The element is then anodically stripped from the mercury in a few seconds with a linearly varying potential. The current peaks for the metal oxidation of the elements in the mercury are displayed on an X-Y recorder. The technique is particularly useful for elements such as copper, lead, zinc, and cadmium and can be extended to about 12–20 elements, although it is unrealistic to expect more than about six elements to be determined simultaneously in a solution. Multicell units are available commercially and, of the order of 100 samples per day, can be analysed with a precision of 5–10% at the 10–100 nanogram level.

Conclusions

In this review the most practical methods of analysis for pollutants have been discussed. Table III summarizes the advantages and limitations of the various technqiues. There may have been a bias toward multielement techniques, because I believe that most laboratories in the future will need to consider a wider range of elements. A variety of techniques of adequate sensitivity for the trace analysis of bulk samples are available, and it is important to relate the analytical problem to the overall requirement so that a rational and economical choice can be made.

Acknowledgment

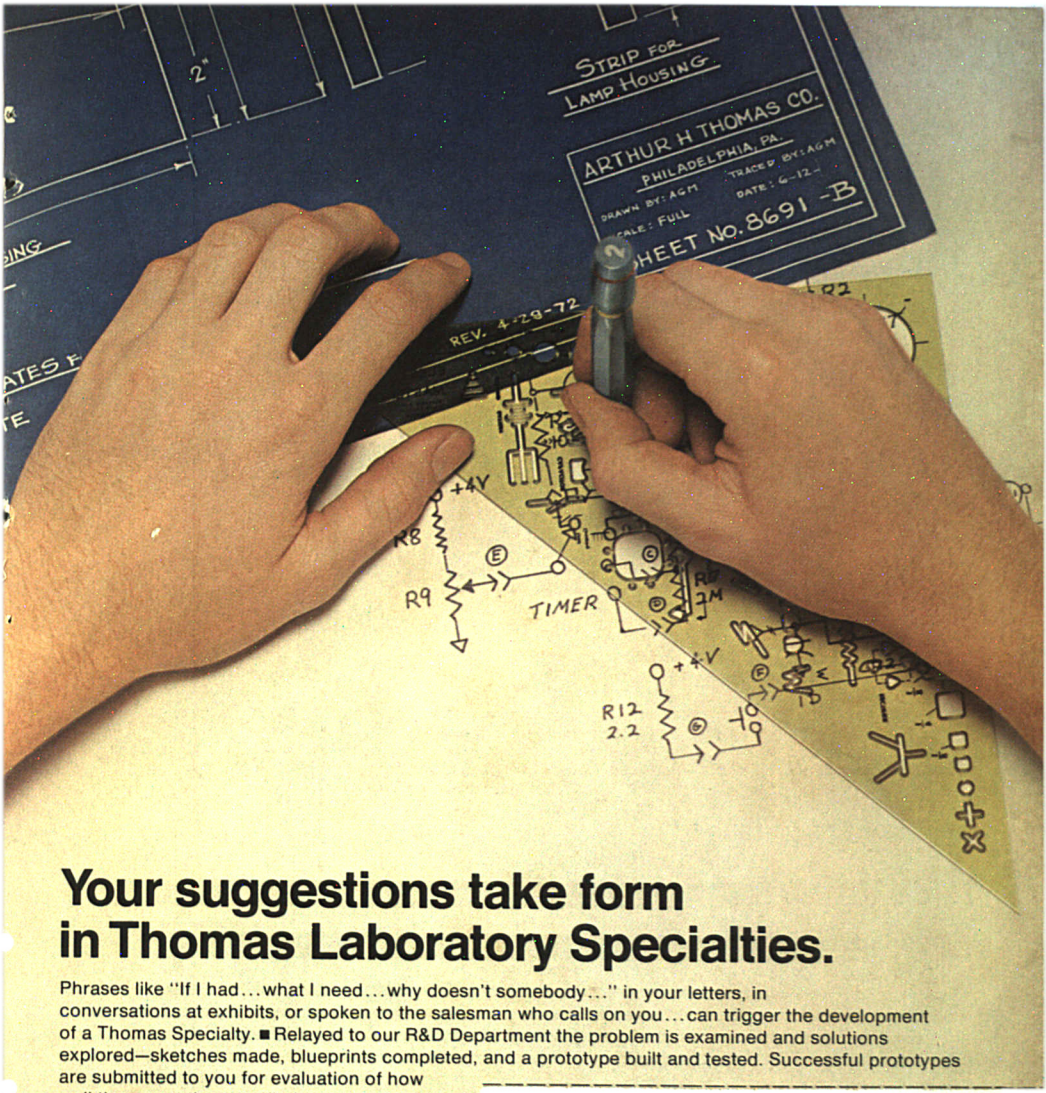
The author acknowledges useful discussions with many members of the staff of the Laboratory of the Government Chemist but particularly R.G. Stone, D.E. Henn, S. Isherwood, and K.L.H. Murray.

References

(1) D.W. Spencer and P.G. Brewer, *CRC, Crit. Rev. Solid State Sci.*, **1**, 401 (1970).
(2) D.E. Robertson, *Anal. Chim. Acta*, **42**, 533 (1968).
(3) E.I. Hamilton and M.J. Minski, *Environ. Lett.*, **3** (1), 53 (1972).
(4) P.A. Cawse and D.H. Pierson, AERE Report R-7134, 1972.
(5) J.M. Harries, C.M. Jones, and J.O'G. Tatton, *J. Sci. Food Agr.*, **20**, 242 (1969).
(6) G. Tolg, *Talanta*, **19**, 1489 (1972).
(7) E.I. Hamilton, M.J. Minski, and J.J. Cleary, *Sci. Total Environ.*, **1**, 1 (1972).
(8) W.C. McCrone and J.G. Delly, "The Particle Atlas," Vols 1–4, 2nd ed., Ann Arbor Sci. Publ., Ann Arbor, Mich., 1973.
(9) J.D. Winefordner, V. Svoboda, and L.J. Cline, *CRC, Crit. Rev. Anal. Chem.*, **1**, 233 (1970).
(10) R.G. Stone and J. Warren, *Lab. Equip. Digest*, 49 (April 1974).
(11) W.R. Hatch and W.L. Ott, *Anal. Chem.*, **40**, 2085 (1968).
(12) E.F. Dalton and A.J. Malanoski, *At. Absorption Newslett.*, **10** (4), 92 (1971).
(13) E.N. Pollock and S.J. West, *ibid.*, **12** (1), 6 (1973).
(14) L.E. Ranweiler and J.L. Moyers, *Environ. Sci. Technol.*, **8**, 153 (1974).
(15) J.D. Winefordner and T.J. Vickers, *Anal. Chem.*, **36**, 161 (1964).
(16) R.F. Browner, *Analyst*, in press (1974).
(17) K.W. Busch and G.H. Morrison, *Anal. Chem.*, **45**, 713 (1973).
(18) S. Greenfield, I.L.W. Jones, and C.T. Berry, *Analyst*, **89**, 713 (1964).
(19) R.H. Scott, V.A. Fassel, R.N. Kniseley, and D.E. Nixon, *Anal. Chem.*, **46**, 75 (1974).
(20) E.I. Hamilton, M.J. Minski, and J.J. Cleary, *Sci. Total Environ.*, **1**, 341 (1972/73).
(21) R. Brown and P.G.T. Vossen, *Anal. Chem.*, **42**, 1820 (1970).
(22) A.L. Gray, *Proc. Soc. Anal. Chem.*, **11**, 182 (1974).
(23) J.V. Gilfrich, P.G. Burkhalter, and L.S. Birks, *Anal. Chem.*, **45**, 2002 (1973).
(24) G.C. Goode, C.W. Baker, and N.M. Brooke, *Analyst*, **94**, 728 (1969).
(25) D.H. Pierson, P.A. Cawse, L. Salmon, and R.S. Cambray, *Nature*, **241**, 252 (1973).



Ronald F. Coleman was appointed head of Research and Special Services at the Laboratory of the Government Chemist in 1973. The laboratory provides analytical service and advice on chemical matters to government departments in the United Kingdom, particularly in the fields of revenue and environmental protection. He obtained a BSc degree from the University of London in 1953 and then spent nearly 20 years at the Atomic Weapons Research Establishment Aldermaston. His research has been mainly connected with nuclear chemistry but he has wandered into many different areas in collaboration with other workers. In the late 1950's, he was studying fast neutron and heavy ion reactions and simultaneously used fast neutrons for activation analysis. In 1963 he started using thermal neutron activation techniques to solve many problems in forensic science, geochemistry, and medicine. He has published about 50 papers in nuclear and analytical chemistry.



Your suggestions take form in Thomas Laboratory Specialties.

Phrases like "If I had...what I need...why doesn't somebody..." in your letters, in conversations at exhibits, or spoken to the salesman who calls on you...can trigger the development of a Thomas Specialty. ■ Relayed to our R&D Department the problem is examined and solutions explored—sketches made, blueprints completed, and a prototype built and tested. Successful prototypes are submitted to you for evaluation of how well they meet the specified requirement. ■ We do independent research, naturally, which also results in other Thomas Specialties. But here also the product is, in effect, suggested by you. It must fill a need that you have. If a product cannot benefit you, it cannot be successful for us. Read about several Thomas Specialties on the next page—and use the detachable postcard to ask for details.



Thomas Laboratory Specialties for the Analytical Chemist.



Thomas-Schöniger Combustion Flasks—simple, quick and inexpensive way to release halogens, sulfur and metals from organic samples. For oxygen combustion of organic samples, replace expensive bombs and trains with Thomas-Schöniger Flasks—original type, or the Ogg or Lisk modifications. Thomas-Ogg Igniter provides remotely triggered infrared ignition with flask inside a safety enclosure. Flasks are available in a variety of sizes. **Circle 125 on Reader Service Card for details.**

Thomas Service Card gone? Use Magazine Service Card or write us direct.

Thomas Printer/Readouts automate data gathering and recording. Obtain analytical data as fast as you can process samples with the Thomas Model 68 Readout. Highly visible illuminated numbers show four-digit reading directly in your reporting units. Get a serial record of readings with the Thomas Model 80 Printer. Features automatic decimal point positioning; uses non-smearing pressure-sensitive tape. **Circle 126 on Reader Service Card for details.**



***Free* Guide to Laboratory Automation.** New Thomas Bulletin points the way to increased lab productivity. Describes modular instrumentation systems to automate sampling, measuring, reading, and reporting. Covers a variety of laboratory procedures including spectrophotometry, titration, pH measurement, and automatic weighing. **Circle 127 on Reader Service Card for details.**



ARTHUR H.
THOMAS
COMPANY
VINE STREET AT THIRD • P.O. BOX 779 • PHILADELPHIA, PA. 19105

First National Meeting

FACSS

Federation of Analytical Chemistry and Spectroscopy Societies

November 18–22, 1974
Chalfonte-Haddon Hall
Atlantic City, N.J.

1st FACSS Meeting Officers

Cochairmen: *George Heinze,* Johnson & Johnson; *James White,* Oak Ridge National Laboratory (Program)

Secretary: *Edward Havlena,* Detroit Edison

Treasurer: *Edward Brame, Jr.,* Du Pont

Arrangements Chairman: *Ivor Simmons,* M & T Chemicals

Publicity Chairman: *Hal Ferrari,* Lederle Laboratories

Budget: *Louis Brancone,* Lederle Laboratories

Employment Chairman: *Leonard Klein,* FMC Corp.

Message Center: *Thomas Kielty,* EXXON Engineering & Research

Registration Chairman: *Richard Knauer,* Armco Steel Co.

Student Awards Chairman: *Anne Donnell*

Technical Films Chairman: *Michael Miller,* NL Industries

Special Events Chairman: *Jerry Lanese,* Stiefel Research Institute

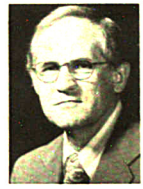
Continuing Education Chairman: *James Lindsay,* U.S. Geological Survey

Exposition Chairman: *George Peterson,* Perkin-Elmer Corp.

Exhibits Manager: *Ed Ruffing,* J & R Assoc.



George Heinze



James White



Edward Brame, Jr.



Ivor Simmons



Hal Ferrari

The first FACSS meeting will be inaugurated with a special session on Monday morning featuring lectures on the analytical problems associated with the energy crisis and analytical concerns in nuclear energy and oil-shale development. The keynote address will be given by C. E. Larson of the U.S. Atomic Energy Commission, Washington, D.C. In all, there will be 33 technical sessions covering a broad range of subject matter from analytical spectroscopy through surface analysis.

The first meeting of FACSS is the culmination of some years of planning and results from the active support and input from representatives of the seven sponsoring organizations: Analytical Chemistry Division, ACS; Society for Applied Spectroscopy; American Microchemical Society; Association of Analytical Chemists, Inc. (Anachems); Eastern Analytical Symposium; Chicago Section, SAS (Mid-America Conference); and the Analytical Instrument Division of the Instrument Society of America.

The technical program includes plenary lectures by J. J. Kirkland, Du Pont; Richard Mack, Kent State University; and award winners: Eugene Sawicki, EPA (Benedetti Pichler); John Mitchell, Jr., Du Pont (Ana-

chem); and H. Kaiser (Hasler). The complete technical program is given on the following pages of the JOURNAL.

In addition to the technical sessions, there are a number of workshops and short courses, including some by ACS that will be given in conjunction with the meeting. See Short Courses, page 1036 A. There will also be a film program, a full complement of social activities, an employment bureau, and an exhibition with over 100 exhibitors. Wednesday afternoon there will be no technical sessions so that all attendees will have a nonconflicting opportunity to visit the exhibits. The exhibitors and their products are listed beginning page 1019 A.

Registration fees are: preregistration, $15; regular registration, $20; one-day registration, $10; student registration, $5; and exhibit only, $1.00.

Preregistrations accompanied by prepayment should be sent to Richard Knauer, Armco Steel Corp., Baltimore, Md. 21203. Hotel registrations should be made directly with Chalfonte-Haddon Hall, North Carolina Ave. and Boardwalk, Atlantic City, N.J. 08404.

Further information on the meeting is available from the publicity chairman, Hal Ferrari, Lederle Laboratories, Pearl River, N.Y. 10965.

Program

Monday Morning, Nov. 18

9:00 Keynote Address: C. E. Larson, USAEC, Washington, D.C.

Special Lectures on Analytical Problems Involved in Obtaining Energy from Nuclear, Coal, and Oil-Shale Sources

Chairman: J. C. White, ORNL

10:20 Analytical Needs Associated with Oil-Shale Development. J. Schmidt-Collerus, Denver Research Institute

11:00 The Analytical Chemist and Nuclear Energy—1974. R. C. Vogel, C. E. Crouthamel, EXXON Nuclear; Carleton Bingham, USAEC

11:40 Energy Crisis. A. L. Jones, Standard Oil Co.

Monday Afternoon

2:00 Plenary Lecture: **Trace Analysis by Modern Liquid Chromatography.** J. J. Kirkland, Du Pont

Liquid Chromatography

Chairman: E. Grushka, SUNY

3:30 Ion Pair Partition Liquid Chromatography. B. L. Karger, Northeastern U

4:15 Adsorption and Partition on Ion-Exchange Resins. R. F. Hirsch, Seton Hall U

5:00 Rapid Liquid Chromatography of Polyamines in Urine, Plasma, and Blood. C. Spitzer, L. R. Snyder, M. Margoshes, H. Adler, Technicon Instruments Corp.

Surface Analysis

Chairman: L. D. Hulett, ORNL

3:30 ESCA Studies of Clean, and Not So Clean, Surfaces. N. E. Erickson, National Bureau of Standards

3:50 Surface Analysis of Metals and Metal–Oxides Using ESCA. N. Winograd, K. S. Kim, Purdue U

4:10 Surface Analytical Techniques—A Comparison. C. A. Evans, Jr., U of Illinois

4:30 High-Energy Ion Backscattering Spectrometry. W. K. Chu, S. S. Lau, J. W. Mayer, M.-A. Nicolet, California Institute of Technology

4:50 Scanning Auger Microanalysis. N. C. MacDonald, Physical Electronics Industries, Inc.

Analytical Applications of Infrared Fourier Transform Spectroscopy

Arranged by Fourier Transform Users' Group

Chairman: R. Jakobson, Battelle Memorial Institute

3:30 Fourier Transform Spectroscopic Analysis of Polymers. J. Koenig, Case Western Reserve U

3:50 Gas Analysis by Infrared Emission Spectroscopy. P. R. Griffiths, Ohio U

4:10 Some Industrial Applications of Infrared Fourier Transform Spectroscopy. R. P. Oertel, Procter & Gamble Co.

4:30 Research and Service Fourier Transform Spectroscopy Usages in an Industrial Analytical Chemistry Department. D. H. Lemmon, Westinghouse R&D Center

4:50 Fourier Transform Spectroscopy in Industry—Taking Full Advantage. J. Lephardt, G. Vilcins, Philip Morris

Analytical Spectroscopy I

Chairman: R. K. Skogerboe, Colorado State U

3:30 Determination of Selenium by Carbon Furnace Flameless Atomization. M. Ihnat, Agriculture Canada, Ottawa

3:50 Determination of As, Se, and Related Elements in Metallurgical Samples by Atomic Absorption. W. B. Barnett, Perkin-Elmer Corp.

4:10 Relative Requirements for Background Correction in Analysis of High Solids Samples by Atomic Absorption. B. R. Culver, Varian Associates; C. J. Rowe, C. R. Parker, Varian Techtron Pty. Ltd., Australia

4:30 Use of a Nitrous Oxide–Acetylene Flame to Minimize Interferences in a Microsampling Cup Atomic Absorption Spectrometer. A. F. Ward, K. M. Aldous, D. G. Mitchell, New York State Dept. of Health

4:50 Sample Preparation of Metal Alloys by Spark Discharge Machining. G. B. Chapman II, W. A. Gordon, NASA

5:10 Emission Spectrometric Arcing Procedure with Minimal Effect of Sample Chemistry. W. A. Gordon, NASA

Tuesday Morning, Nov. 19

9:00 Plenary Lecture: Benedetti Pichler Award Address—American Microchemical Society: **Hazardous Substances in the Environment and Their Analysis.** E. Sawicki, National Environmental Research Center, Research Triangle Park

10:30 Benedetti Pichler Award Symposium: **Application of Heated Vaporization Atomic Absorption to Microanalysis.** W. K. Robbins, EXXON Co.

Liquid Chromatography

10:30 Use of High-Pressure Liquid Chromatography in Pharmacology and Toxicology. P. R. Brown, U of Rhode Island

10:50 Quantitation in Liquid Chromatography. J. N. Little, C. Pidacks, D. W. Skiles, Waters Associates Inc.

11:10 Bonded Phase Packings in Liquid Chromatography. F. Rabel, H. Reeve Angel and Co., Inc.

11:30 Liquid Chromatography (HP)/Infrared Spectroscopy On-the-Fly. K. L. Kizer, Digilab Inc.; L. C. Bonar, Waters Associates

11:50 New Small Particle Reverse Phase Packing—Zorbax—ODS. J. Larmann, D. Baker, R. Williams, Du Pont

12:10 Quantitation in Chromatography: GC Vs. LC. M. T. Jackson, E. Montoya, Spectra-Physics

^{13}C NMR

Chairman: E. D. Becker, NIH

10:30 Survey of ^{13}C NMR: Funda-



Now your rat count won't drown in high water.

Handifluor™ *ScintillAR*® brings you 50 to 100% more counting efficiency at 30 to 50% water content.

You'll like its performance at five per cent water content. At 50% you'll love it. And that includes the tough jobs, like tritium at low concentrations.

A complete cocktail for scintillation counting, *Handifluor ScintillAR* gives you brilliant clear solutions or firm translucent gels on aqueous or non-aqueous samples. Counting efficiency stays high at both low and ambient temperatures.

In case you'd like proof of that efficiency claim, here's how *Handifluor* performed against the two leading competitive cocktails:*

GENERAL AQUEOUS SAMPLES

Ml Aqueous Phase Per 10 ml Base	Approx. Water Percent By Vol.	Absolute Tritium Efficiency (Percent)		
		Handifluor Cocktail Base	Cocktail Base A	Cocktail Base B
None	—	53.7	48.9	50.8
0.5	5	44.5	42.9	44.5
1.0	9	40.5	37.1	39.5
1.5	13	37.5	35.6	36.6
2.5	20	35.0	34.1	32.9
3.5	26	31.0	31.3	32.3
5.0	33	29.8	19.9	28.2
7.5	43	24.1	10.7	22.4
10.0	50	20.7	9.8	19.6

*10 ml of base, tritium equal to 2,000 dpm and aqueous phase giving the indicated percentage of the total cocktail combined and counted by a Packard Model 2425 Tri-Carb® Liquid Scintillation Spectrometer. Instrument efficiency for ^3H by A.E.S. was 97-99%, representing 58-60% absolute tritium efficiency vs. sealed standards. Data represents averages of four successive 10 minute counts. Efficiencies are expressed as percent of the theoretical decompositions per minute actually counted.

After you've read the chart, what more can we say except that it's ready to be delivered to you in Safemor® gallon jugs from your local Mallinckrodt distributor. Catalog No. 4022. If you'd like even more data, ask for our complete comparative data sheet.

Mallinckrodt®

SCIENCE PRODUCTS DIVISION
Saint Louis, Missouri 63147

CIRCLE 158 ON READER SERVICE CARD

Determine additives in polymers

without tedious extractions

A new technique combining GAS CHROMATOGRAPHY and THERMAL ANALYSIS, THERMAL CHROMATOGRAPHY has already found application in the analysis of:

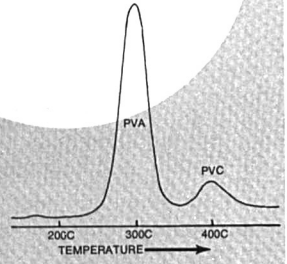
PLASTICIZERS
ANTIOXIDANTS
SLIP AGENTS
UV STABILIZERS
RESIDUAL MONOMERS
RESIDUAL SOLVENTS

in

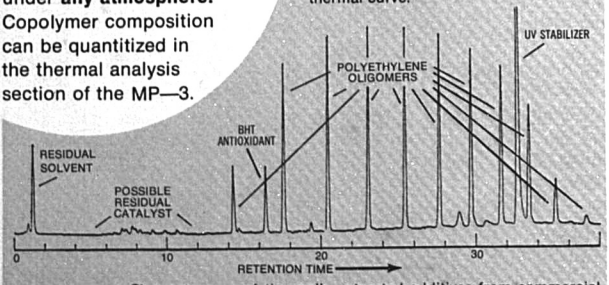
POLYOLEFINS
POLYMETHYL-METHACRYLATES
NYLONS
POLYVINYLCHLORIDE
POLYSTYRENE
OTHER POLYMERS

SEE THE MP - 3 IN ACTION AT FACSS BOOTH H - 14

CHROMALYTICS' MP—3 THERMAL CHROMATOGRAPH provides both qualitative and quantitative results quickly (15-60 min) with high sensitivity (ppm range) and minimum sample preparation. Degradation of polymers can be studied under **any atmosphere.** Copolymer composition can be quantitized in the thermal analysis section of the MP—3.



Thermogram of commercial PVA/PVC copolymer. Amounts of each component can be calculated from areas under the thermal curve.



Chromatogram of thermally extracted additives from commercial polyethylene sample.

CHROMALYTICS CORP.

DIV. OF SPEX INDUSTRIES INC.

ROUTE 82, UNIONVILLE, PA. 19375 • PHONE 215-347-2454

CIRCLE 212 ON READER SERVICE CARD

mentals and Applications to Chemical Problems. G. C. Levy, Florida State U

11:00 Use of Fourier Transform Methods in ^{13}C NMR Studies. E. D. Becker, NIH

11:30 Quantitative Intensity Measurements in ^{13}C NMR. J. N. Schoolery, Varian Associates

12:00 ^{13}C FT–NMR of Micro Samples. K. N. Scott, C. E. Westerman, U of Florida

Surface Analysis

10:30 Problems in Quantitative Ion Probe Microanalysis. K. F. J. Heinrich, National Bureau of Standards

10:50 Catalyst and Corrosion Studies by Photoelectron Spectroscopy. L. D. Hulett, G. A. Nyssen, ORNL

11:10 Auger Electron Spectroscopy of Fracture Surfaces in Irradiated-Type 304 Stainless Steel. R. E. Clausing, E. E. Bloom, ORNL

11:30 Electron Spectroscopy . . . for Surface Analysis. D. M. Hercules, U of Georgia

11:50 Surface Composition Analysis by Ion Scattering Spectroscopy. J. T. McKinney, 3M Co.

General Instrumentation

Chairman: E. C. Dunlop, Du Pont

10:30 Photoacoustic Spectroscopy: A New Analytical Technique. A. Rosencwaig, Bell Laboratories

10:50 Interactive Computer Control as Applied to Clinical Analyzers. W. E. Goldstein, R. W. Rogers, M. A. Genshaw, Ames Co.

11:10 Proton NMR Studies of Butylamine Iodine Systems. M. J. Kogan, Narcotic Addition Control Commission, State of New York, Brooklyn

11:30 Modified Electrode Shape Improves Spectrographic Analysis for Vacuum Cup Method. T. R. Lyon, Allied Chemical Corp.

11:50 Computer-Coupled System for X-ray Fluorescence. J. A. Keenan, Texas Instruments, Inc.

12:10 Off-Line GC Data Reduction with H/P 9830 Programmable Calculator. W. L. Krudop, Shell Development Co.

Tuesday Afternoon

Gas Chromatography

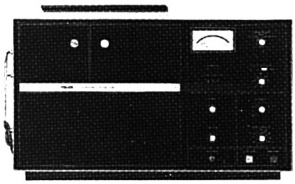
Chairman: S. P. Cram, Varian Aerograph

2:00 Shortening the Bridge over the Technology Gap in Chromatography. L. B. Rogers, U of Georgia

2:30 Physicochemical Significance of Chromatographic Data. E. Grushka, SUNY

Separate fixed gases and hydrocarbons without cryogenic temperature programming

Two columns in series *(one for fixed gases and one for hydrocarbons)*, plus a patented detector work together in the new Model 1200 to save time, money and effort. Just inject the sample and watch the recorder. Signals from both columns are displayed simultaneously. And you don't have to "super cool" the columns like you must in so many conventional instruments. *(You know how expensive coolant gases can be.)*



The price: Just $2300 vs the $5000 price tag you'll find on conventional instruments.

And there's another plus: **You can use liquid samples.**

Want the full story? *Write for a detailed bulletin.*

Fisher Scientific Company

711 Forbes Avenue
Pittsburgh, Pa. 15219

CIRCLE 79 ON READER SERVICE CARD

FREE!

BEL-ART 92 PAGE CATALOG 474



- PLASTIC LAB WARE
- LABORATORY INSTRUMENTS
- PROTECTIVE COATINGS

ALL in our NEW 92-page catalog. THE MOST COMPLETE line of plastic laboratory ware available from one source as well as the complete lines of our subsidiaries, Applied Coatings and TechniLab Instruments. Hundreds of items in various plastics . . . a wide range of scientific instruments . . . plastic coated laboratory ware.

For your copy write Dept. A-10

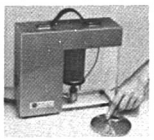
BEL-ART PRODUCTS

Pequannock, N.J.07440 • 201 694-0500

CIRCLE 25 ON READER SERVICE CARD

Bethlehem | the Mercury People

Hg VACUPICK
for picking up Hg droplets



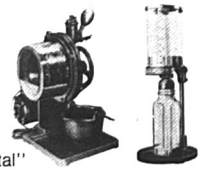
ask for reprint, "How Poisonous Is Mercury"

VACUUM TRIPLE DISTILLED IN PLASTIC DISPENSING-TIP BOTTLES



ask about our Mercury Cleaning Service

OXIFIERS & FILTERS
for cleaning your own Mercury



ask for reprint, "Mercury, The Purest Metal"

BETHLEHEM APPARATUS COMPANY, INC.
Since 1948
Hellertown, Pa. 18055 / (215) 838-7034

CIRCLE 24 ON READER SERVICE CARD

3:00 Applications of Gas Chromatography in Inorganic Analysis. R. E. Sievers, K. J. Eisentraut, Wright-Patterson AFB; W. D. Ross, Monsanto Research Corp.

3:30 Polymer Characterization by Gas Chromatography. M. F. Burke, U of Arizona

4:00 Characterization of Oil Shales by Laser-Induced Pyrolysis. N. E. Vanderborgh, U of New Mexico

4:30 Analytical Characteristics of Plasma Chromatography. R. A. Keller, State College of New York

^{13}C NMR

2:00 Organic Structure Elucidation by ^{13}C NMR. R. J. Highet, NIH

2:40 Use of ^{13}C NMR in Studies of Reaction Kinetics. M. Lana Sheer, R. S. Sudol, Du Pont

3:20 Use of Shift Agents on Large and Small Molecules in ^{13}C NMR. W. M. Ritchey, Case Western Reserve U

4:00 Polymer Microstructure Analysis by ^{13}C FT-NMR. D. W. Ovenall, G. S. Reddy, T.-K. P. Wu, Du Pont

Coblentz Symposium

Chairman: P. R. Griffiths, Ohio U

2:00 Infrared Spectroscopy in the Forensic Laboratory. R. H. Ellis, New York State Police

2:30 Making the Most of the Least in Infrared Spectroscopy. E. C. Sunas, Liggett and Myers, Inc.

3:00 Infrared: A Vital Tool in the Study of Textiles. E. R. McCall, Southern Regional Research Center, New Orleans

3:30 Tracing Source of Oil Slicks by Infrared Spectroscopy. C. W. Brown, U of Rhode Island

4:00 Infrared and Raman Spectroscopy in Surface Chemistry and Catalysis. C. L. Angell, Union Carbide Corp.

4:30 Atmospheric Vinyl Chloride Analysis Using a Miran^{R} Analyzer. R. L. Hudson, Ethyl Corp.

5:00 Low-Temperature Studies of Petroleum Products. P. F. Lynch, S.-Y. Tang, C. W. Brown, U of Rhode Island

General Instrumentation

Chairman: G. Mamantov, U of Tennessee

2:00 Computerized Atomic Absorption Spectrometer for Simultaneous Multielement Analysis. K. M. Aldous, K. W. Jackson, D. G. Mitchell, New York State Department of Health

2:35 An Apparatus to Make Fu-

for

liquid chromatography

reeve angel

reeve angel. in liquid chromatography, **the** source.

Reeve Angel helps people who make or use liquid chromatographs get better results than otherwise possible. We help you to realize optimum performance from your instrument, regardless of make or model.

We engineer reproducible and ready to use columns. And packing media. And virtually everything else you need to operate HPLC instrumentation. (But we don't sell instruments. That helps. We can concentrate on superb media and column performance). Then, we support our products, and the LC discipline in general, with methods, applications, advanced products — all from a staff with scientifically impeccable credentials.

Reeve Angel now has the broadest line of optimized, proven packing media and columns in the industry. Viz:

ADSORBENTS —

Microparticulate silicas (PARTISILS)
Pellicular silicas (PELLOSILS)
Pellicular aluminas (PELLUMINAS)
Pellicular polyamide (PELLIDON)

ION EXCHANGERS —

Pellicular strong anion (AS/AE PELLIONEX SAX)
Pellicular weak anion (AL PELLIONEX WAX)
Pellicular strong cation (PELLIONEX SCX's)
Microparticulate strong anion (PARTISIL SAX)
Microparticulate strong cation (PARTISIL SCX)

BONDED PHASES —

Non-polar microparticulate (PARTISIL ODS)
Non-polar pellicular (CO:PELL ODS)
Polar pellicular (CO:PELL PAC)

With many others on the way. Many others.

And tested HPLC supplies and accessories: injection ports, microsyringes, pressure gauges, low dead volume and standard fittings, septa, frits, etc., etc.

Contact Reeve Angel or the qualified instrument manufacturer handling RA products. (For the name of the manufacturer nearest you, please write or phone.)

A new catalog, applications assistance, literature, prices are all available on request.

Reeve Angel. **The** source for HPLC. Let us help.

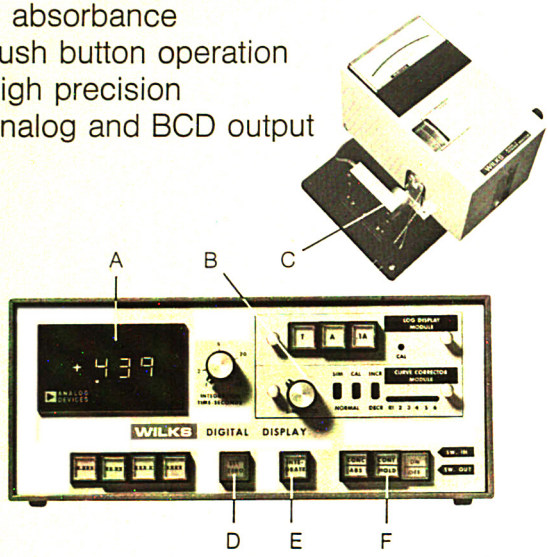
Reeve Angel, 9 Bridewell Place, Clifton, N. J. 07014 ■ Tel. (201) 777-4825 ■ TELEX 133426. Reeve Angel Scientific, Ltd., England; Reeve Angel (France) S.a.r.l., France.

reeve angel

CIRCLE 201 ON READER SERVICE CARD

QUANTITATIVE IR MADE EASY

Direct reading in concentration or absorbance
Push button operation
High precision
Analog and BCD output



A. Display reads linearly in ppm, %, or other concentration units or in absorbance.
B. Curve corrector eliminates errors due to non-linearity in working curves.
C. Flow-through cell for ease of sampling and better reproducibility.
D. Auto zero for push-button setting of zero concentration.
E. Variable-period time integrator for high precision.
F. Continuous/Hold function allows following reading changes or holding average values for improved readability.

The Wilks MIRAN I Digital Display makes semi-automation possible for many quantitative analyses with improved precision. The Digital Display can be used with instruments with an analog output of 10 mv, 100 mv, and 1 volt. The MIRAN I Single Beam Analyzer equipped with a flow-through sample cell and Wilks Scientific New Digital Display can be used for reliable quantitative data.

WILKS SCIENTIFIC CORPORATION
P.O. BOX 449, S. NORWALK, CT. 06856, 203/838-4537

SEE US AT BOOTHS B5-6-7 AT FACSS MEETING
CIRCLE 255 ON READER SERVICE CARD

sion Buttons for X-ray Fluorescence. F. Claisse, University Laval, Quebec

3:10 Impact of Calculator Chips on Design of Analytical Instruments. A. T. Leung, Spectra-Physics, Inc.

3:45 Use of State Variable Active Filters as Differentiators, Rate Meters, and End-Point Locators. R. H. Callicott, P. W. Carr, U of Georgia

4:20 Trace Element Techniques for Energy-Dispersive Fluorescence Analyzers. D. A. Gedcke, L. S. Albrecht, Ortec, Inc.

4:55 Pellet Technique as Aid in Analysis of Uranium and Thorium by XRF. E. C. Snooks, General Atomic Co.

Wednesday Morning, Nov. 20

9:00 Plenary Lecture: Anachem Award Address: **Methods for Determination of Water in Polymers.** J. Mitchell, Jr., Du Pont

Anachem Award Symposium: Recent Advances in Polymer Analysis

Chairman: L. L. Lewis, General Motors Corp.

10:30 Recent Advances in Size Exclusion Chromatography (Gel Permeation Chromatography–GPC) for Polymer Analysis. D. D. Bly, Du Pont

11:05 Polymer Characterization by Thermal Evolution Techniques. J. Chiu, E. F. Palermo, Du Pont

11:40 New Developments in Vibrational Spectroscopy. J. L. Koenig, Case Western Reserve U

12:15 Some Newer Methods for Functional Group Determination on Polymer Systems. S. Siggia, U of Massachusetts

Analysis Instrumentation

Sponsored by Analysis Instrumentation Division of Instrument Society of America

Chairman: J. Williamson, Du Pont

10:30 Infrared Analyzers. W. M. Henebry, Thermal Electron Corp.

11:00 Gas Chromatography. To be announced

11:30 Ultraviolet Analyzers. R. S. Saltzman, Du Pont

12:00 Sampling Systems. W. V. Dailey, Mine Safety Appliances Co.

Analytical Spectroscopy II

Chairman: I. J. Holcomb, Parke, Davis & Co.

10:30 Automatic Background Correction for Trace Analysis in Flame Emission Spectrometry. T. C. Rains, M. S. Epstein, O. Menis, National Bureau of Standards

How to find an ion, measure a "milli-pH" and otherwise simplify life in your lab.

We can help.

With the most complete line of lab liquid analysis meters, electrodes, and recorders available from any single source.

For pH, redox, and specific ions: flouride, nitrate, cyanide. You name it.



Even our least expensive specific ion/pH meter, the 7410, gives you: normal 0-14 pH reading; expanded-scale reading of any two-pH span; a two-decade log scale for monovalent ions; a four-decade log scale for divalent ions; and known-increment and known-decrement scales for simple measurement of ion concentrations.

All told, we have six pH meters for your lab (including one that is a lab unto itself, the 7417 portable).



And our 7421 Digital pH meter, for a good-to-the-last-digit look at a "milli-pH" change.



And all the electrodes and buffer solutions you could ask for. Plus one- and-two-pen recorders, flatbed and low-profile, to serve as willing slaves to the meters. And you.

All ready, right now, to ease your lab life.

Use the reader service card to get the details.

LEEDS & NORTHRUP North Wales, Pa. 19454

To tell you what's happening. To help you control it. Efficiently.

CIRCLE 110 ON READER SERVICE CARD

Replace your obsolete % Transmittance Instrument with a low-cost, direct reading, Linear Absorbance Colorimeter from GLENCO

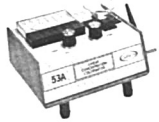
FOR ONLY $275 we offer:

- Direct concentration or absorbance readout
- Narrow Band Pass (7nm)
- 400-1100NM Range
- Broad absorbance range (to over 2 Absorbance Full Scale)
- Fixed Pour-Drain Cell Option

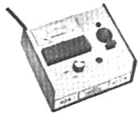
These advanced technology instruments can be used in all methodologies where % T models are being utilized in the visible wavelength range. They are offered in the following models:



MODEL 53A – This model allows the user to read sample directly in units of concentration (0 to 1 units in .02 unit divisions) $275.00



MODEL 53A-FC – Same as 53A but equipped with a pour-drain cell for repetitive readings of samples utilizing the same cell $355.00



MODEL 52A – Same as Model 53A but without concentration pot. Reads sample directly in absorbance units. (0 to 2 O.D. in .05 O.D. Divisions) $275.00

All models are equipped to accept optional adaptors for all standard glass tubes from 10mm to 20mm and for square cuvettes.

For additional information or to discuss application details, write or call

Glenco Scientific, Inc.
2802 White Oak Dr., Houston, Tx.77007
Phone: 713/861-9123
TWX 910-881-6397

GLENCO

CIRCLE 87 ON READER SERVICE CARD

10:50 Recent Developments in Spectral and Chemical Interferences in Flame Spectrometric Methods of Analysis. M. L. Parsons, Arizona State U

11:10 Paper title to be announced. G. Hieftje, Indiana U

11:30 Anion Determination by Inhibition Effects in Emission Flame Spectroscopy. J. R. Sand, C. O. Huber, U of Wisconsin-Milwaukee

11:50 Atomic Absorption Analysis with Graphite Furnace Using Matrix Modification. R. D. Ediger, Perkin-Elmer Corp.

12:10 Matrix Management in Flameless Atomic Absorption (Carbon Rod Atomizer)—Temperature Control and Background Correction. R. L. Stux, C. J. Rowe, Varian Techtron, Australia

12:30 Analyzing High Solids Samples by Atomic Absorption with Carbon Rod Atomizer. R. L. Stux, C. J. Rowe, C. Parker, Varian Techtron, Australia

12:50 Determination of Less Volatile Metals by Atomic Absorption, Using High-Temperature Microsampling Cup Technique. D. G. Mitchell, A. F. Ward, K. M. Aldous, New York State Department of Health

1:10 Image Dissector Echelle Spectrometer—A Rapid Wavelength Access Spectrometer with Single Photon Counting. A. Danielsson, Analytica AB, Sweden

Electroanalytical Chemistry

Chairman: R. A. Osteryoung, Colorado State U

10:30 Bioanalysis with Membrane Electrode Probes. G. A. Rechnitz, State University of New York

11:00 Differential Pulse Polarographic Determination of 1,4-Benzodiazepines in Biological Fluids. M. A. Brooks, J. A. F. de Silva, Hoffmann-La Roche Inc.

11:30 Electroanalytical Chemistry in Ocean Research. D. N. Hume, MIT

12:00 Pulse Stripping Analysis—Theory and Practice. R. A. Osteryoung, Colorado State U

12:30 Cyclic Voltammetry of Adenosine-5′-Monophosphate and Its Iron Complexes in DMF. M. S. Spritzer, Villanova U; P. Kanatharana, Chulalongkorn U, Thailand

Moving Infrared from "Lab" to "Line"

Chairman: P. A. Wilks, Wilks Scientific Corp.

10:30 Role and Responsibilities of Infrared Spectroscopist in Moving Analyses into Plant. D. S. Lavery, Wilks Scientific Corp.

10:50 Sample Handling Problem in Continuous Liquid Analysis. P. A. Wilks, Jr., Wilks Scientific Corp.; A. Bartz, Dow Chemical Co.

11:10 Use of Portable Variable Path Length IR Gas Analyzer During Setting-Up Stage of Gas-Phase Reactor. J. Elliott, EXXON Research & Engineering Co.

11:30 Contaminant Analyzer for Aircraft Oxygen Systems. K. G. Ikels, Brooks Air Force Base

11:50 Continuous Analysis of Viscous Materials. D. G. Burr, General Electric Co.

12:10 Automatic Infrared Analysis. E. G. Brame, Jr., Du Pont

Thursday Morning, Nov. 21

9:00 Plenary Lecture: Hasler Award Address—SAS: **General Problem of Calibration in (Spectro)chemical Analysis.** H. Kaiser, Institute for Spectrochemistry and General Spectroscopy, Germany

Hasler Symposium

Chairman: J. Baldwin, Society for Applied Spectroscopy

10:30 Trace Simultaneous Multielement Analyses by Optical Emission Spectroscopy—Stagnant or Pregnant? (with Apologies to A. Walsh). V. A. Fassel, Iowa State U

11:30 Future of Analytical Spectroscopy. R. K. Skogerboe, P. J. Lamothe, G. Bastiaans, D. L. Dick, Colorado State U

Mass Spectrometry in Industry and Related Topics

Chairman: T. L. Pugh, Du Pont

10:30 Applications of Mass Spectrometry to Problems in Tobacco Industry. N. Einolf, Philip Morris

11:00 Applications of MS in Copying Industry. F. A. Elder, Xerox Corp.

11:30 Application of Mass Spectrometry to Study of Epoxy Resins. M. A. Grayson, R. L. Levy, D. L. Fanter, McDonnell Douglas Corp.

12:00 Mass Spectrometry at Hoffmann-La Roche Inc., Nutley, N.J. F. M. Vane, W. Benz, C. G. Scott, Hoffmann-La Roche Inc.

Enthalpimetric Analysis

Chairman: J. Jordan, Pennsylvania State U

10:30 Progress in Thermometric and Enthalpimetric Analysis. L. S. Bark, U of Salford, England

11:00 Novel Applications for Temperature and Flow Sensitivity of Thermistors in Analysis and Hematology. P. W. Carr, L. D. Bowers, W. D. Bostick, E. B. Smith, U of Georgia

11:30 Titration Calorimetry: Some Recent Advances in Instrumentation and Applications to Biological Systems. R. M. Izatt, L. D. Hansen,

Perkin-Elmer's Model 360 A.A. Spectrophotometer... tomorrow's performance and features at yesterday's prices.

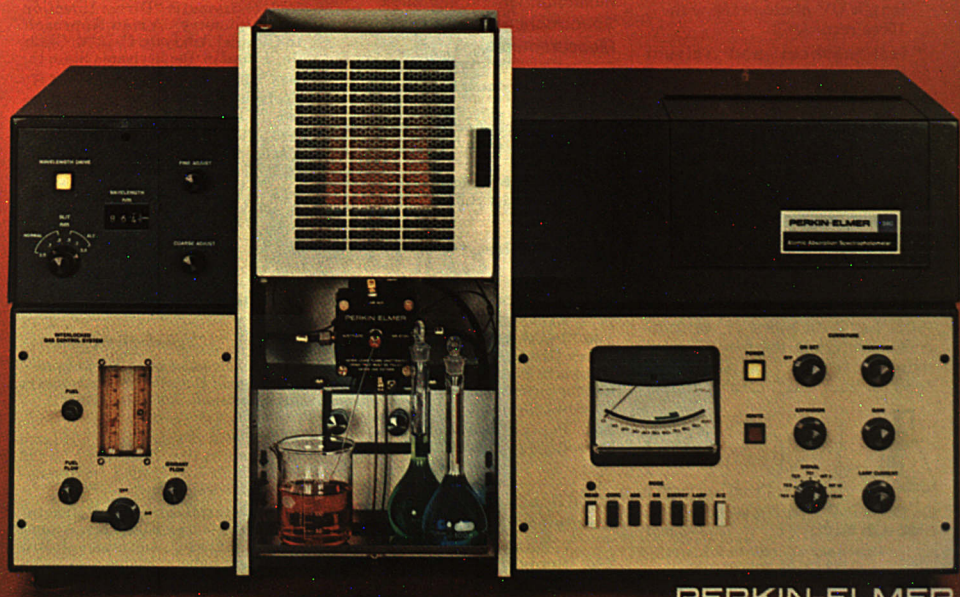
Start with the desirable features in today's A.A. instruments such as double-beam stability, ease of use, and superb performance. Add new features like Automatic Gain Control, double-beam Deuterium Arc Background Correction* with Automatic Intensity Control, and automatic nitrous oxide switching*. Design the optical system to be optimum with flame or flameless sampling just by turning a knob, and let the operator select continuous, integrated, peak area, or peak height readings. A new, high-priced, top-of-the-line instrument?

No, it's the new, low-cost, double-beam A.A. spectrophotometer from Perkin-Elmer—the Model 360.

If you need to determine metallic elements, want the best instrument available, and don't want to spend your yearly budget, the Model 360 is what you're looking for.

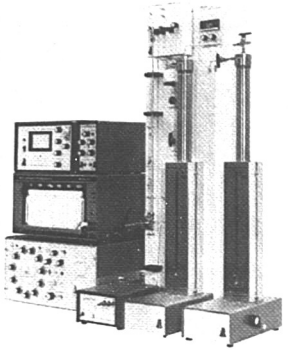
For details, write the Instrument Division, Perkin-Elmer Corporation, Main Avenue, Norwalk, Conn. 06856, or ask your local Perkin-Elmer Sales Engineer to show you the new 10-minute, color/sound movie showing the Model 360 in action. *optional accessory

CIRCLE 195 ON READER SERVICE CARD



PERKIN ELMER

big HPLC prices don't guarantee best performance



An ISCO Model 1440 high performance liquid chromatograph can give you separations and operating convenience identical to other instruments costing twice as much. Ask anyone else to quote on a chromatograph with these ISCO Model 1440 specifications:

- **totally pulseless, noiseless, syringe pump**
- **6 port sample injection valve**
- **high performance multi-wavelength UV photometer with 10cm recorder**
- **fast washout and solvent change.**

These features are all available elsewhere - but only ISCO can provide them for $4795. And for under $9800, ISCO can set you up with a two pump system which produces gradients by multilinear programming, a detector which can monitor two wavelengths at once, a 10'' recorder, a fraction collector, and a digital pressure monitor/controller.

ISCO has built more LC absorbance monitors in the last 12 years than anyone else. Find out why - send for your ISCO catalog today.

ISCO

BOX 5347 LINCOLN, NEBRASKA 68505
PHONE (402) 464-0231 TELEX 48-6453

Please see us at Booth B17, at the FACSS Meeting.

CIRCLE 130 ON READER SERVICE CARD

D. J. Eatough, T. E. Jensen, J. J. Christensen, Brigham Young U

12:00 Enthalpimetry in Biochemistry. J. M. Sturtevant, Yale U

Analytical Spectroscopy III

Chairman: J. D. Winefordner, U of Florida

10:30 Some Considerations on Microwave Electrodeless Discharge. R. Avni, L. P. Hart, J. D. Winefordner, U of Florida

10:50 Constant-Temperature Furnaces with Graphite Crucible Sample Injection. R. Woodriff, Montana State U

11:10 Experimental Verification of Computer Models of Inductively Coupled Plasma Discharge. R. M. Barnes, R. G. Schleicher, U of Massachusetts

11:30 Inductively Coupled Plasma-Optical Emission Spectroscopy—Excitation Temperatures Experience by Analyte Species. D. J. Kalnicky, R. N. Kniseley, V. A. Fassel, Iowa State U

11:50 Inductively Coupled Plasma-Optical Emission Spectroscopy—Application to Determination of Alloying and Impurity Elements in Iron and Steels. R. N. Kniseley, C. C. Butler, V. A. Fassel, Iowa State U

12:10 Inductively Coupled Plasma-Optical Emission Analytical Spectroscopy—A Study of Some Interelement Effects. G. F. Larson, V. A. Fassel, R. H. Scott, R. N. Kniseley, Iowa State U

Multichannel and Multiplex Spectrochemical Methods and Measurements

Chairman: G. Horlick, U of Alberta, Edmonton

10:30 Multichannel Spectrochemical Methods. E. G. Codding, Kent State U

11:30 Transform Multiplex Spectroscopy. T. Hirschfield, Block Engineering, Inc.

Thursday Afternoon

Hasler Symposium

2:00 Physics and Technique of Spark Discharges as Spectrochemical Light Sources. H. Kaiser, Institute for Spectrochemistry and General Spectroscopy, Germany

3:00 Paper title to be announced. V. Mossotti, U of Minnesota

Mass Spectrometry in Industry and Related Topics

2:00 Study of Glass by Mass Spectrometry. V. O. Altemose, S. S. C. Tong, Corning Glass Works

2:35 GC/MS—Computer System Using Time-Sharing Computer Utility. M. A. Grayson, J. M. Putnam, F. J. Yaeger, McDonnell Douglas Corp.

3:10 On-Line Control of High-Resolution Mass Spectrometers. I. Peak Matching. D. W. Bissett, C. Cone, F. C. Maseles, U of Texas

3:30 International Mass Spectral Search System. S. R. Heller, Environmental Protection Agency; R. S. Heller, U of Maryland; H. M. Fales, G. W. A. Milne, NIH; D. C. Maxwell, A. McCormick, Mass Spectrometry Data Centre, UK

3:50 Chemical Ionization Mass Spectrometry—A Powerful Analytical Tool for Problem Solving. A. K. Bhattacharya, Miami U

4:10 Instrumental and Statistical Consideration for Accurate Quantitative Analysis in Gas Chromatograph–Mass Spectrometer Systems. J. N. Gerber, N. D. Young, J. F. Holland, C. C. Sweeley, Michigan State U

Enthalpimetric Analysis

2:00 Investigations of Biochemical and Biological Processes by Batch-Type Microcalorimetry. E. J. Prosen, G. T. Armstrong, R. N. Goldberg, B. R. Staples, National Bureau of Standards

2:35 Application of Stopped-Flow Microcalorimetry to Enzyme Reactions in Biochemistry and Clinical Chemistry. R. L. Berger, NIH

3:10 Enzymatic "Direct Injection Enthalpimetry": A New Approach to Clinical Analysis. C. D. McGlothlin, J. Jordan, Pennsylvania State U

3:45 Thermometric Studies of Hydrolysis of Urea Catalyzed by Urease. N. D. Jespersen, U of Texas

4:20 Biomedical Applications of Enthalpimetric Analysis. H. M. Cullis, American Instrument Co.

4:55 Coagulation Calorimetry. M. A. Marini, Northwestern Medical School

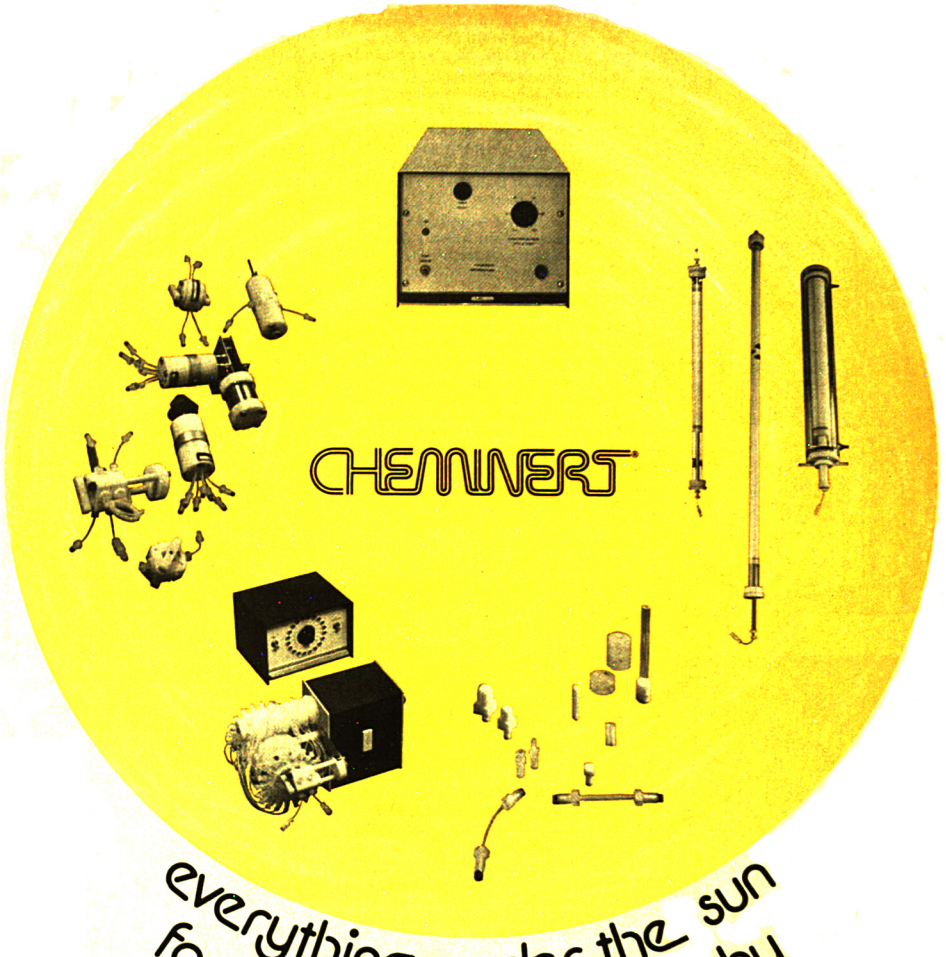
Analytical Spectroscopy IV

Chairman: T. J. Vickers, Florida State U

2:00 Microsampling Technique for Atomic Emission Spectrometry. J. K. Grime, T. J. Vickers, Florida State U

2:20 Critical Evaluation of Flameless Atomization. S. B. Smith, Jr., M. F. Bancroft, J. Y. Hwang, Instrumentation Laboratory Inc.

2:40 Determinations of Refractory Elements by a Flameless Atomizer. J. Y. Hwang, J. J. Sotera, Instrumentation Laboratory Inc.



everything under the sun for liquid chromatography

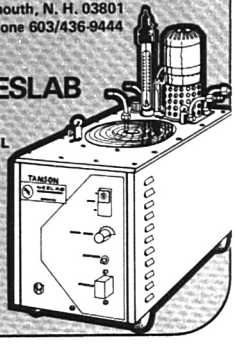
Now you can depend on Laboratory Data Control for *all of your LC component needs*...including Cheminert*. Cheminert*, formerly manufactured and marketed by Chromatronix since 1967, is the chemically-inert connection system proven in laboratories all over the world. Laboratory Data Control is proud to announce the addition of this quality line to its family of products for liquid chromatography.

The Cheminert* System is so outstanding because it is the complete assortment of fittings, connectors, valves, columns, and pumps which may be joined together to form a most versatile and economical LC set-up. Fluid contacts only the tubing itself and the mating part. Absolutely no contamination and virtually no extra-column zone spreading.

Send today for a complete, easy-to-use catalog. Close the loop with Cheminert* pumps, valves, columns, and fittings.

LABORATORY DATA CONTROL
DIVISION OF MILTON ROY COMPANY
P.O. Box 10235, Interstate Industrial Park
Riviera Beach, Florida 33404
Phone: (305) 844-5241 or Telex 513479.

CIRCLE 151 ON READER SERVICE CARD

Constant Temperature Baths / Circulators
12 MODELS
● WINDOWED
● REFRIGERATED
Highest quality at competitive prices.
Contact NESLAB / 871 Islington St.
Portsmouth, N. H. 03801
Telephone 603/436-9444
NESLAB
MODEL TE9

Cooling Breakthrough!
$195.
IMMERSION COOLER

1/6 H.P.
air cooled hermetic compressor
Immersion Head 7/8" x 5" long
Continuous operation
USE WITH ANY BATH TO ACHIEVE BELOW AMBIENT TEMPERATURES
Write us for complete details
UTILE PRODUCTS / DIVISION OF NESLAB
871 Islington Street, Portsmouth, New Hampshire 03801 U.S.A.
Please see us at the FACSS Show
Booths #731 and 733
CIRCLE 170 ON READER SERVICE CARD

3:00 Behavior of Solid Samples in Atomic Absorption Furnaces. D. Bath, R. Woodriff, Montana State U

3:20 Effect of Variations in Heater Tube Carbon on Sensitivity of Certain Elements in Woodriff Furnace. B. Watne, Montana State U

3:40 Some Applications of a Newly Designed DC Argon Plasma to Analysis of Selected Trace Elements. R. J. Karlinski, SMI

4:00 Improved Atomizer for Hydride-Generation Atomic Absorption Selenium Determination. D. D. Siemer, L. Hageman, Montana State U

4:20 Exploding Wires as an Intense Continuum Excitation Source for Atomic Fluorescence. D. W. Brinkman, R. D. Sacks, U of Michigan

4:40 Multielement Analysis by Computer-Controlled, Rapid-Scan Atomic Fluorescence Spectrometry (AFS) Using a Continuum Source. D. J. Johnson, F. W. Plankey, J. D. Winefordner, U of Florida

5:00 Electrical Aspects in C_2H_2–Air Flames. D. J. Johnson, R. Avni, J. D. Winefordner, U of Florida

Multichannel and Multiplex Spectrochemical Methods and Measurements

2:00 Air Pollution Measurements Using Long Path Infrared. B. W. Gay, Jr., EPA, Research Triangle Park

2:50 Application of Vidicon Spectrometer for Molecular and Atomic Spectrometry. H. L. Pardue, Purdue U

3:40 Optical Multichannel Analyzer for Spectrochemical Measurements. D. E. Osten, Princeton Applied Research

4:30 Comparison of Photodiode Array and Fourier Transform Spectrometers for Atomic Spectrochemical Measurements. G. Horlick, U of Alberta, Edmonton

General Organic

Chairman: J. B. Johnson, Union Carbide

2:00 Determination of Dye Carriers in Polyester Fiber and Fabric. E. Hester, E. G. Owens, J. Schulze, M. Tin, CIBA-GEIGY Corp.

2:20 Studies of Interactions of Selected Organic Sorbates at Inorganic Surfaces by GS Chromatography. R. L. Grob, E. J. McGonigle, Villanova U

2:40 Rapid Method for Optimizing TLC Developing Conditions. R. K. Vitek, Camag Inc.

3:00 Analysis of Catecholamines by Resonance Raman Spectrometry. M. S. Rahaman, M. D. Morris, U of Michigan

3:20 Quantitative Determination of Styrene Monomer in Butadiene/Styrene Latexes Using Raman Spectroscopy. P. L. Wancheck, L. E. Wolfram, Standard Oil Co.

3:40 Spectra-Structure Correlations of Alkyl Peroxides. P. A. Budinger, J. R. Mooney, J. G. Grasselli, Standard Oil Co.

4:00 Some Comments on Measurement of Spectral Line Profiles at Wavelengths Below 300 NM. P. N. Keliher, C. C. Wohlers, Villanova U

4:20 Determination of Pentachlorophenol by Ultraviolet Ratio Spectrophotometry. J. E. Fountaine, P. B. Joshipura, P. N. Keliher, Villanova U; J. D. Johnson, Spectrogram Corp.

4:40 Some Applications of Charge-Transfer Complexes (TNF) to Study of Petroleum Arenes. D. M. Jewell, Gulf Research and Development Co.

5:00 Vibrational Spectra and Conformation of Methyl Cyanoacetate. J. E. Katon, D. Sinha, Miami U

Friday Morning, Nov. 22

9:00 Plenary Lecture: **Instrumentation for Environmental Analysis.** R. Mack, Kent State U

Environmental Analysis

Chairman: R. Carrigan, National Accelerator Lab

10:30 Instrumentation for Direct Determination of Phenol, Chromium VI, or APHA Color in Plant Effluent Streams. J. A. Williamson, W. L. Bonam, Du Pont

10:50 Identification of γ-Valerolactone in Waste Water from Oil-Shale In Situ Retort. F. R. McDonald, Bureau of Mines

11:10 Automatic Concentrator/Gas Chromatograph System for Trace Analysis. S. A. Liebman, D. H. Ahlstrom, C. I. Sanders, Armstrong Cork Co.

11:30 Rapid Determination of Lead and Cadmium in Biological Tissues. K. W. Jackson, D. G. Mitchell, New York State Department of Health

11:50 Determination of Selenium in Environmental Samples Using Gas Chromatograph with Microwave Emission Spectrometric Detector. Y. Talmi, ORNL

12:10 FMS Used as Toxic Gas Analyzer. R. E. Gillespie, EOCOM Corp.

12:30 Generation of Aerosol Standards for Evaluation of Filter Media for Air Analysis. J. F. Lech, Varian Associates; R. Woodriff, Montana State U

Analytical Spectroscopy V

Chairman: M. Margoshes, Technicon Instruments Corp.

10:30 Taming of Inductively Cou-

COMPACT, HIGH PRESSURE LIQUID CHROMATOGRAPH

OFFERS MORE FEATURES

Both Constant Flow And Constant Pressure . . .

MICROMERITICS' 7000 Series Liquid Chromatographs operate in either mode by a simple switch selection. This feature, along with others detailed below, lets the chromatographer **completely control the mobile phase.**

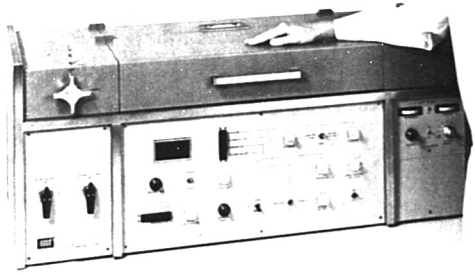
The unique 6000 psi hydraulic pump produces pulseless solvent flow to 10 ml/min **without** pulse dampers, suppressors, or "high frequency noise filters" . . . Any size solvent reservoir may be used . . . Adjustable high and low pressure limits.

Only **one** pump is required for gradient elution . . . Time from 1 to 10,000 minutes . . . Concave, linear or convex curvatures infinitely adjustable from N^5 to N^{-5} . . . Easy reset . . . Start with any initial concentration and finish with any higher concentration . . . Digital display of gradient . . . Simultaneous recorder display of gradient.

Features:

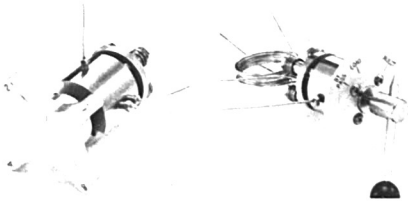
- **Digital Panel Meter monitors pressure, flow rate, oven temperature or percent strong solvent**
- **High Pressure, Septumless Injector Valves . . . Reproducible plug injections . . . Analytical volumes of 1, 2, 4 or 8 microliters . . . Preparative volumes from 15 microliters up**
- **High Pressure, Flow Insensitive, Dual Wavelength UV Detector . . . 0.01 O.D.F.S.**





4000 PSI VALVES FOR INJECTING REPRODUCIBLE VOLUMES

Analytical Injector Valve: One of the most reproducible and accurate ways of injection in high-pressure liquid chromatography. This valve, adjustable to 4000 psi, allows plug injections of 1, 2, 4 or 8 microliter sample volumes by simply turning a handle. The valve has a column bypass position for quick solvent change over. Wetted parts are stainless steel or filled Teflon.®



Preparative Injector Valve: Designed for reproducible sample injection in preparative liquid chromatography. It is essentially identical to the Analytical Injector Valve in construction and specifications. The sample volume, 15 to 1,000 microliters, is determined by loop fitted to the valve. The column bypass position is standard for quick solvent change over.

THESE INSTRUMENTS ON DISPLAY
INTERNATIONAL LC SYMPOSIUM
HOUSTON, TEXAS
4–6 NOVEMBER, 1974
and
FACSS SHOW
ATLANTIC CITY, N. J.
18–21 NOVEMBER 1974

Particle Technology and Liquid Chromatography
micromeritics®
instrument corporation
5680 goshen springs road • norcross, georgia 30071 • U.S.A.
telephone: 404/448-8282 • telex: 70-7450

CIRCLE 163 ON READER SERVICE CARD

Write For Free Booklet "HOW TO GET BETTER TLC RESULTS"



pmd

PROGRAMMED MULTIPLE DEVELOPMENT

. . . is gaining recognition as a new, significant approach to thin layer chromatography.

Among the reasons for this are:

1. At comparable development time, PMD offers greater resolution than conventional TLC with still greater improvement for longer developments.

2. For equal resolution, PMD is faster than conventional TLC.

3. Because PMD developed spots are much narrower, PMD offers sensitivity that is 5 to 10 times greater than conventional TLC for major components, and even more for normally undetectable trace components and longer developments.

The PMD story, complete with photographs and diagrams, is presented in a new booklet entitled "HOW TO GET BETTER TLC RESULTS". The booklet is free upon request.

Also, each month Regis issues "PMD NEWS," a newsletter devoted exclusively to PMD applications and instrumentation.

For a copy of the booklet "HOW TO GET BETTER TLC RESULTS" and/or to receive the free monthly newsletter, "PMD NEWS," write or phone the Regis Professional Service Department.

REGIS CHEMICAL CO.
8210 Austin • Morton Grove, Ill. 60053
Area Code (312) 967-6000

CIRCLE 203 ON READER SERVICE CARD

pled Plasma-Optical Emission Spectroscopy System. S. R. Koirtyohann, W. Freeark, G. Wallace, U of Missouri

10:45 Nonflame, Nondispersive Atomic Fluorescence Spectrometry. B. R. Bartschmid, C. Veillon, U of Houston

11:00 Mechanism of Excitation of Atoms in Electrodeless Discharge Lamps. R. Avni, L. P. Hart, J. D. Winefordner, U of Florida

11:15 Some New Approaches to Atomization for Atomic Spectrometry. T. J. Vickers, W. E. Rippetoe, Florida State U

11:30 Automated Optimization of Pulsed Hollow Cathode Discharge Tubes. E. R. Johnson, T. J. Vickers, Florida State U

11:45 Application of Molecular Emission Cavity Analysis. R. Belcher, S. L. Bogdanski, I. Rix, A. Townshend, U of Birmingham, England

12:00 Exploding-Foil Excitation for Analysis of Trace Metals in Aqueous Media. R. D. Sacks, C. S. Ling, U of Michigan

12:15 Quantitative Energy-Dispersive Analysis Using Scanning Electron Microscope. R. G. Hurley, J. D. Janowski, J. Tabock, Ford Motor Co.

12:30 Applications of Integral and Derivative Thermogravimetry to Analysis of Rubber Formulations. S. J. Swarin, A. M. Wims, General Motors Corp.

General Organic

Chairman: J. G. Grasselli, Standard Oil Co.

10:30 Quantitative Ultrafine Oil Mulling for Infrared Analyses. J. S. Ard, H. Susi, USDA, ARS

10:50 Rapid Determination of Free Amino Groups in Proteins by Absorption Spectroscopy. J. M. Purcell, D. J. Quimby, J. R. Cavanaugh, USDA, ARS

11:10 Spectrofluorometric Determination of Pharmaceuticals Containing Aromatic or Aliphatic Primary Amino Groups as Their Fluorescamine (Fluram®) Derivatives. J. A. F. de Silva, N. Strojny, Hoffmann-La Roche, Inc.

11:30 Applications of Relative Fluorescence Efficiency to Determination of Impurities in Solutions of Complex Fluorescing Molecules. R. B. Blasier, A. Timnick, J. F. Holland, Michigan State U

11:50 Study of Chloranil Charge Transfer Reaction with Amino Acids. K. L. Cheng, U of Missouri

12:10 Fluorometric Determination of Ferricyanide and Thiamine in Water. M. C. Goldberg, J. K. Wilson, U.S. Geological Survey

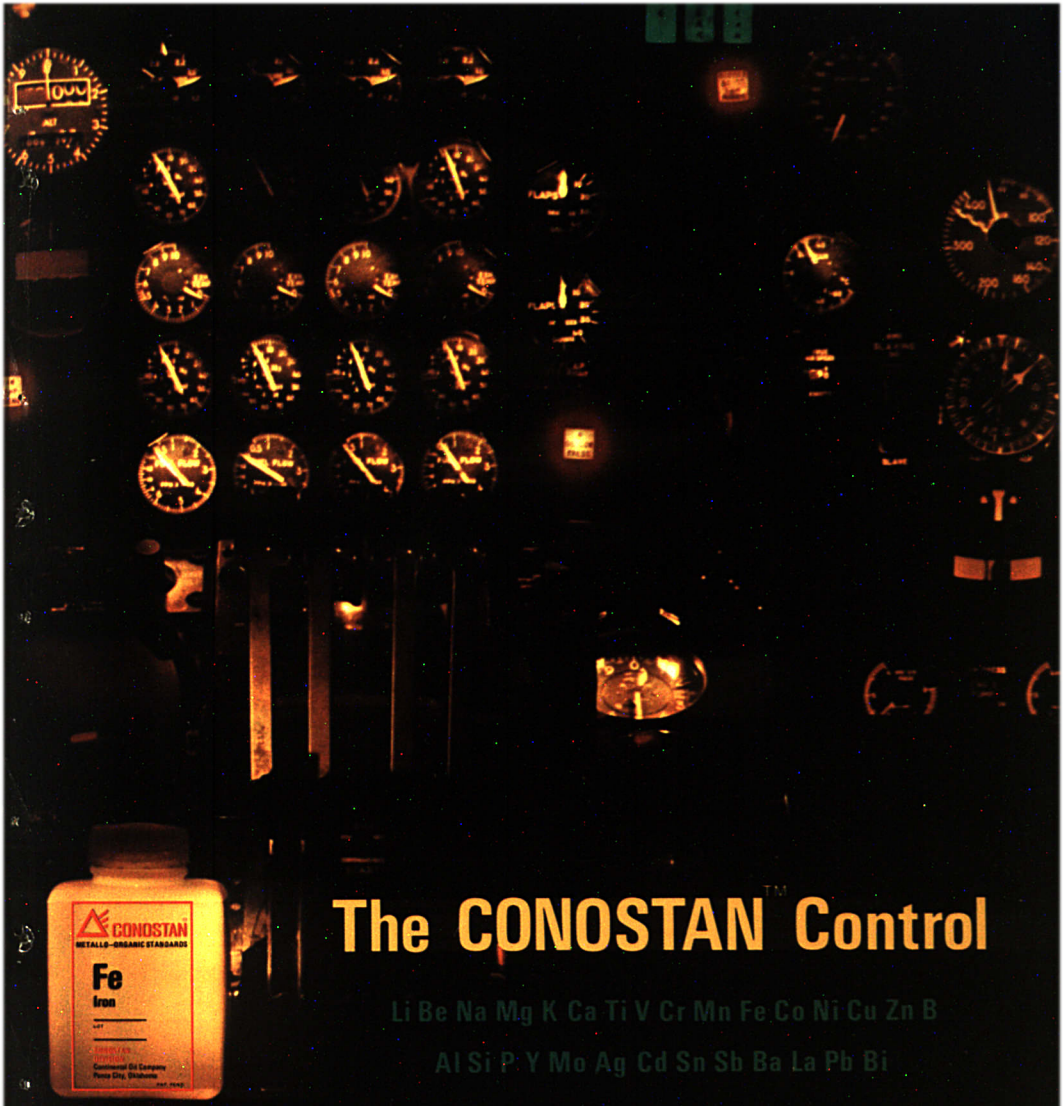
CHOOSE
SAUTER BALANCES

- when you need highest sensitivity, accuracy, reliability . . . from one microgram to one hundred kilograms
- when you want the most rugged and dependable balances
- when you want to select from the widest assortment of models

August Sauter of America, Inc.
80 Fifth Avenue
New York, New York 10011
(212) 685-6659



CIRCLE 2 ON READER SERVICE CARD
CIRCLE 34 ON READER SERVICE CARD →



The CONOSTAN™ Control

Li Be Na Mg K Ca Ti V Cr Mn Fe Co Ni Cu Zn B

Al Si P Y Mo Ag Cd Sn Sb Ba La Pb Bi

The flight control instruments are idle when the engine is in for repair. Today, more than ever, preventive engine maintenance is no luxury. Early detection of potential engine problems saves energy. Oil analysis is a valuable tool in engine maintenance and CONOSTAN standards provide reliability in oil analysis.

Emission spectroscopy or atomic absorption are the flight control instruments in the lab. They work well with CONOSTAN standards. Whatever metals in oil you analyze for, CONOSTAN has reliable standards for you.

If you cannot remember all 29 CONOSTAN standards, ask us for those you want. We have each at 5000 ppm in a light oil for use in atomic absorption or to make your own blends. Also, we have 12 and 20 metal blends in a heavy oil designed for emission spectroscopy.

CONOSTAN

CONOSTAN DIVISION • Continental Oil Company
P.O. Box 1267 • Ponca City, Oklahoma 74601 •
(405) 762-3456



Our Tube-Excited Fluorescence Analyzer combines proven x-ray fluorescence technology with recent advances in computer software, x-ray generation techniques, and high-count-rate amplification. The result is superior performance—analysis of concentrations from ppm to 100%, accuracy of ±1% of the amount present for major elements, and ±0.25% system repeatability.

Fast, easy, and accurate analysis of 82 elements – sodium to uranium

High-level software

TEFA's analytical programs encompass every capability from spectrum smoothing and stripping, to qualitative element identification, to fully-automatic quantitative analysis using matrix corrections.

TEFA is the only computerized x-ray fluorescence analyzer with comprehensive, high-level language. So you can create new programs and modify existing ones as your needs change or new analytical problems arise. And you can do this very conveniently in ORACL—an easy-to-learn language that's as powerful and versatile as modern FORTRAN. Even if ORACL is your first computer language, you can master it in an afternoon.

Flexible excitation

A unique dual-anode x-ray tube and electronically-controlled filter changer solve interference-line problems and let you optimize the analysis for elements of special interest without losing the efficient, broad-spectrum excitation required for determining the sample's overall composition. You can set up any combination of anode and filter at the push of a button.

Fast results

Because our unique x-ray amplifier lets TEFA operate at high count rates without significant resolution loss or peak shift, you can analyze more quickly than ever before with better statistical accuracy. And you can get trace-element data at a respectable rate without the total-sample counting rate getting out of hand.

Is it all for you?

Perhaps this question is best answered by our brochure and technical data bulletin. Get them from your nearby Ortec representative or Ortec Incorporated, 110 Midland Road, Oak Ridge, Tenn. 37830. (615) 482-4411. Ortec Ltd., Dallow Road, Luton, Bedfordshire. 0582 27557. Ortec GmbH, Herkomerplatz 2, 8000 München 86, W. Germany. (089) 98 71 73.

See us at the FACSS Show Booth G13.

ORTEC®

AN EG&G COMPANY

CIRCLE 181 ON READER SERVICE CARD

©ORTEC

5958A

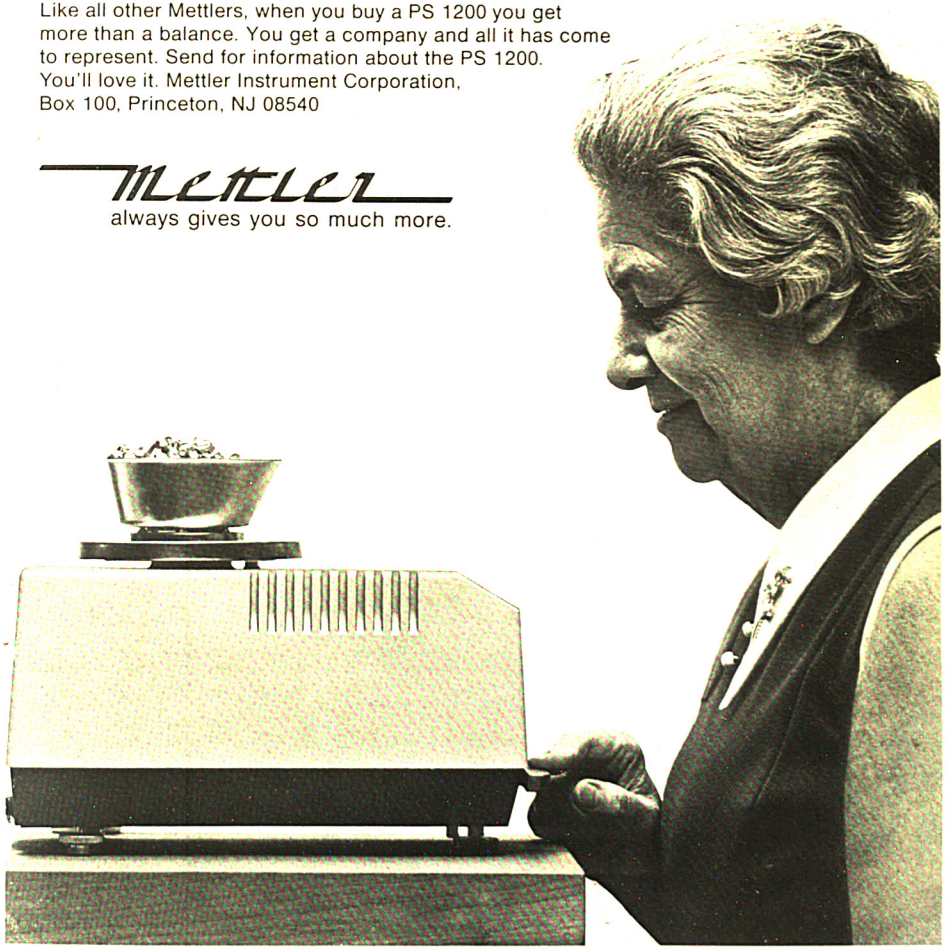
PS, I love you.

Right after we announced the Mettler PS 1200 electronic top-loading balance, orders started pouring in.

Why the instant attachment? Because it's the electronic top loader with just a pan and a result. No knobs. No adjustments. No beam. You simply place your sample on the weighing pan and read the results in less than two seconds. A single control bar performs all operations—on, off, taring. A built-in memory accumulates individual weight values and the total can be read on the digital readout. Additionally, the PS 1200 is equipped with BCD digital outputs—a plus for on-line and on-stream applications. And should an overload occur there is no readout and data transfer is blocked, preventing erroneous inputs. The Mettler PS 1200 has a weighing range of 1200 grams with readability of 0.1 gram.

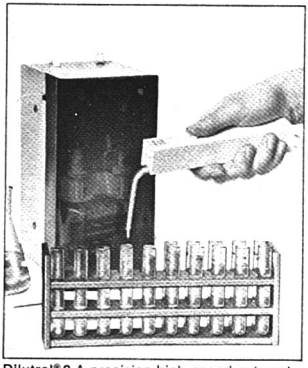
Like all other Mettlers, when you buy a PS 1200 you get more than a balance. You get a company and all it has come to represent. Send for information about the PS 1200. You'll love it. Mettler Instrument Corporation, Box 100, Princeton, NJ 08540

Mettler
always gives you so much more.

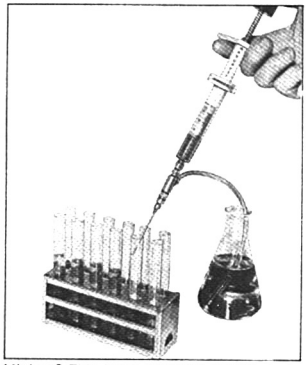


CIRCLE 159 ON READER SERVICE CARD

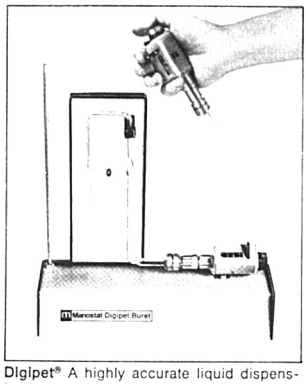
Dispensers?



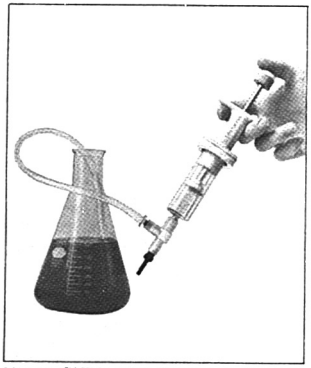
Dilutrol®2 A precision high speed automatic dilutor with volume adjustments from 50 microliter to 30 ml, and ratios up to 3000 to 1. Only Teflon® or glass ever touch sample or diluent for contamination-free operation.



Minipet® This hand operated repetitive pipetting instrument is ideal where multiple preset volumes have to be dispensed. Fully adjustable syringe type dispenser. Also available in low cost all plastic Econopet™ model.



Digipet® A highly accurate liquid dispensing instrument with digital readout. Perform repeated titrations without refilling. Sensitivity of 0.01%. Also available as a mounted Buret, from 0.01 ml capacity.



Manopet™ This large capacity pipetter, adjustable over a range of 1 to 30 ml, is ideal for repetitive pipetting. Especially useful for filling petri dishes and culture tubes. Easy to clean. Chemically resistant.



Varipet® This variable volume transfer pipet is available in 12 models and adjustable over the entire scale of the barrel. Supplied in 0.5, 1, 4, 10 and 30 ml capacities. Ideal for repetitive dispensing.



Accropet® Eliminate the possible dangers of contamination and injury of mouth pipetting. Accropets are available as Ultramicro for pipets up to 0.2 ml and Micro for pipets up to 2 ml. One hand operation.

Manostat!

For complete Dispenser Bulletin. Contact

Manostat Or ask your Dealer

20 North Moore Street, New York, N.Y. 10013, 212-966-1190

CIRCLE 157 ON READER SERVICE CARD

Exhibit

The Exhibition at the 1st FACSS meeting will be located in Chalfonte-Haddon Hall. Exhibit hours are: Nov. 19, 10 a.m. to 7 p.m.; Nov. 20, 10 a.m. to 6 p.m.; Nov. 21, 10 a.m. to 6 p.m. Exhibit only badges are available for $1.00

Academic Press, Inc.
111 Fifth Ave., New York, N.Y. 10003. Books and journals in analytical chemistry and spectroscopy, including Robin, "High Excited States of Polyatomic Molecules," Vol 1; Rao/Ferraro, "Spectroscopy in Inorganic Chemistry," Vol 2; "Methods of Experimental Physics," Vol 3, Williams, Ed., "Molecular Physics," 2nd ed., Pts. A and B; Epstein, "The Variation Method in Quantum Chemistry;" Gawargious, "The Determination of Nitro and Related Functions."

Ace Scientific Supply Co. Inc.
1420 E. Linden Ave., Linden, N.J. 07036. Balances, pH meters, water baths, microscopes, metering pumps for laboratory, pilot plant and production.

Air Products & Chemicals, Inc.
P.O. Box 538, Allentown, Pa. 18105. Specialty gases including calibration standards, zero-grade gases, gas-regulating equipment.

American Elsevier Publishing Co.
52 Vanderbilt Ave., New York, N.Y. 10017. The latest titles from American Elsevier and North Holland Publishing Co. in analytical chemistry and spectroscopy.

American Instrument Co.
8030 Georgia Ave., Silver Spring, Md. 20910. New corrected spectra instrument: produces quanta-corrected or energy-correct excitation and emission spectra without the use of quantum counters; new amine group analyzer, high-speed, high-resolution chromatography system for fluorometric determination of amino acids, peptides, and proteins at picomole level utilizing Fluram.

Anacon, Inc.
30 Main St., Ashland, Mass. 01721. New flame analytical technique: MECA, molecular emission cavity analyzer, for the determination of sulfur, phosphorus compounds, selenium, tellurium, also elements giving oxide and halide emissions. By Arcas, Inc., Div. of Anacon, Inc. New chromatography, COW, chlorinated organics in waste water analyzer, for detection of extremely low levels of organic compounds.

Analabs, Inc. (Sub. New England Nuclear)
575 Albany St., Boston, Mass. 02118. TLC chromatography zonal scraper, TLC thin-layer plates, MLA pipet, Hamilton syringes, Dexsil chromatographic liquid phase, Anasorb-gas chromatographic grade solid adsorbers, Anasil thin-layer absorbents; chromatographic chemicals and equipment for the separation sciences; biochemicals, organic chemicals, pollution standards.

H. Reeve Angel & Co. Inc.
9 Bridewell Place, Clifton, N.J. 07014. Liquid chromatography: broad range of proprietary packings, accessories and supplies for modern HPLC.

Applied Science Laboratories, Inc.
P.O. Box 440, State College, Pa. 16801. Complete line of products for gas, thin-layer, and liquid chromatography plus drug standards, reagents, radiochemicals, clinical standards, high-purity lipids.

Baird-Atomic, Inc.
125 Middlesex Tpke., Bedford, Mass. 01730. Optical emission spectrometers including the Spectromet and Spectrovac; complete line of spectrofluorimeters, including the Fluorimet and Fluorispec.

Beckman Instruments, Inc.
2500 Harbor Blvd., Fullerton, Calif. 92634. Ultraviolet and infrared spectrophotometers, including the ACTA M UV Series, IR Series 4200, Models 24/25 UV/VIS spectrophotometers.

Bel-Art Products
Pequannock, N.J. 07440. Plastic laboratory ware; new developments in instrumentation by TechniLab, a Bel-Art subsidiary.

Bethlehem Apparatus Co., Inc.
Front & Depoe Sts., Hellertown, Pa. 18055. Glass lathes, glass working apparatus, mercury cleaning equipment, mercury vacupick.

Brammer Standard Co.
P.O. Box 339, Aliquippa, Pa. 15001. Analytical standards; spectrographic and chemical standards produced by Brammer Standard and six European sources, including primary standards from the Bureau of Analysed Samples, Ltd; ferrous and nonferrous standards, including alloys of Fe, Ni, Al, Mg, Pb, Sn, Cu, Zn, and Co; ores, slags, ferroalloys, AA standards.

Brinkmann Instruments, Inc.
Cantiague Rd., Westbury, N.Y. 11590. Sartorius balance, Buchi evaporators, Metrohm titrators and pH meters, Brinkmann colorimetric system and TLC apparatus; analytical balances, rotating evaporators, electrochemical apparatus featuring endpoint and printing titrators, curve tracing instrument and probe colorimeter and automated analyzing system; diluters, micropipets, and TLC apparatus.

Bruker Scientific, Inc.
1 Westchester Plaza, Elmsford, N.Y. 10523. WP-60-ft NMR spectrometer.

Buck Scientific, Inc.
11 Ridge Rd., Cos Cob, Conn. 06807. Used scientific instruments; field service for Perkin-Elmer, Hilger Watts, and Barnes Engineering; we buy and sell used instruments; provide service for atomic absorption, infrared, UV–VIS, GC.

Camag Inc.
2855 S. 163rd St., New Berlin, Wis. 53151. Eluchrom for automated elution of TLC samples, in-situ, Vario KS chamber for optimizing TLC developing conditions; new fraction collector that can program typical column chromatographic procedures.

Carle Instruments, Inc.
1141 E. Ash Ave., Fullerton, Calif. 92631. Three models of analytical gas chromatographs (AGC) for high quantitative accuracy with FID and/or TC detectors; low-cost line of Basic gas chromatographs (BGC) for education and industry; micro and mini volume valves for all GC gas sampling and column switching applications; 10-in. recorders for GC.

Chemical Data Systems, Inc.
RD 2, Box 74, Oxford, Pa. 19363. Model 800 reaction systems for rapid determination of kinetic parameters in gas-phase thermal and catalytic pulsed and continuous reactions; Model 1200 elemental analyzer peak identifier for GC effluents; Model 820D controlled atmosphere pyrolysis system, Model 120 pyrolyzer with 1200° option and three-position function selector switch; Model 100 pyroprobe 1000° programmable solids pyrolyzer and Model 210 automatic temperature programmer with cryogenic capability.

Chemtrix Inc.
135 N.W. Adams, Hillsboro, Ore. 97123. pH, oxygen, and conductivity meters; specific ion, pH, and process probes; standard solutions; buffers; colorimeters.

Chromatix, Inc.
1145 Terra Bella Ave., Mt. View, Calif. 94043. New low-priced tunable ultraviolet and visible dye laser; tunable infrared parametric oscillator with 1/1000 cm^{-1} bandwidth; computer-ready, high-resolution, high-flux f/6.8 1-m, coma-corrected spectrometer; new computer-ready 0.4-m additive double spectrometer employing a unique optical geometry which provides unusually high stray light rejection for Raman and fluorescence experiments.

Columbia Scientific Industries Corp.
P.O. Box 6190, Austin, Tex. 78762. High-speed data systems for mass spectrometers; economical digital integrators for gas and liquid chromatography; stone thermal analyzers; portable X-ray analyzers.

Conference Book Service, Inc.
P.O. Box 298, Alexandria, Va. 22314. Cooperative display of new and current professional books and journals.

Coulter Electronics, Inc.
590 W. 20th St., Hialeah, Fla. 33010. Timbrell/Coulter split-image dimension analyzer, Coulter counter Model TA_2 with population accessory, Model MM for direct diametric readout of particle size at selected percentile levels, systems for particle size distribution analysis.

CRC Press, Inc.
18901 Cranwood Pkwy., Cleveland, Ohio 44128. "Atlas of Spectral Data and Physical Constants for Organic Compounds," "Handbook Spectroscopy," "Handbook of Chromatography," *Critical Review Journal*

in Analytical Chemistry, other pertinent titles.

Curtin Matheson Scientific, Inc.
P.O. Box 1546, Houston, Tex. 77001. pH equipment lines of major manufacturers: Coleman, Corning, Orion, Photovolt; glass reference, combination and ion selective electrodes; CMS line of color-coded buffer solutions; complete line of lab equipment; furniture and equipment plus balances and spectrophotometers.

Diano Corp.
2 Lowell Ave., Winchester, Mass. 01890. Latest design in modern miniaturized integrated circuit electronics, control functions from keyboard console.

Digilab, Inc.
237 Putnam Ave., Cambridge, Mass. 02139. Standard line of instrumentation, innovations in the field of Fourier IR spectroscopy.

Digital Equipment Corp.
146 Main St., Maynard, Mass. 01754. Declab 11 computer system for lab instrument automation, Basic Fortran IV, and lab applications-11 software systems, RT-11; AR11 analog, real time interfacing subsystem; included in the AR11 is a 10-bit analog-to-digital converter, two 10-bit digital-to-converters, a programmable clock, scope control, and a 16-channel multiplexer with sample and hold, all on a single printed circuit board.

Dohrmann Div., Envirotech Corp.
1062 Linda Vista Ave., Mountain View, Calif. 94040. Total organic carbon analyzer, trace nitrogen, sulfur, halogen analyzers, high-performance gas chromatographs, specific, quantitative GC detectors, polymer permeation analyzer, sampling accessories, recorder.

Du Pont Co., IPD & Sorvall Div.
1007 Market St., Wilmington, Del. 19898. Electron spectrometer, (ESCA) liquid chromatography systems and packing, new intermediate Model 840 LC, thermal analysis systems, pollution monitoring systems for SO_2 and NO_2.

Elographics, Inc.
1976 Oak Ridge Tpke., Oak Ridge, Tenn. 37830. Model E241 digitizer, a fast and accurate user-oriented digitizing system for data reduction; specific examples will utilize strip charts and point plotter charts and cover the areas of flame photometry, chromatography, polarography.

EM Laboratories
500 Executive Blvd., Elmsford, N.Y. 10523. TLC, HPLC, GC, Ph indicators, reagents, gels.

Encyclopaedia Britannica, Inc.
303 East Ohio St., Chicago, Ill. 60611. New edition of Britannica, the Britannica Junior, other related products.

Environmental Sciences Assoc., Inc.
175 Bedford St., Burlington, Mass. 01803. New instrument for rapid, repetitive analysis of trace metals by anodic stripping voltammetry; system for doing many different analyses with minimum of sample preparation; special system to remove trace metals from reagents down to $5 \times 10^{-10} M$ and lower; standard line of anodic stripping voltammeters.

Extranuclear Laboratories, Inc.
P.O. Box 11512, 250 Alpha Dr., Pittsburgh, Pa. 15238. SpectrEL GC/MS computer system with mass range to 1200 amu, high-resolution quadrupole mass filter, solids probe, and complete computer capabilities; compatible with 16-channel digital mass programmer and multiple ion detection system with one-channel for total ion monitoring.

Farrand Optical Co., Inc.
117 Wall St., Valhalla, N.Y. 10595. Spectrofluorometer with corrected spectra system, VIS–UV chromatogram analyzer, microscope spectrum analyzer, enzyme kinetic system.

Finnigan Corp.
595 North Pastoria Ave., Sunnyvale, Calif. 94086. Model 3100 Series GC/MS with Model 6000 interactive data system; QM 900 X-ray fluorescence analyzer.

Fischer & Porter Co., Lab-Crest Scientific Div.
County Line Rd., Warminster, Pa. 18974. Flow meters, chromatography apparatus, laboratory glassware and glass specialties.

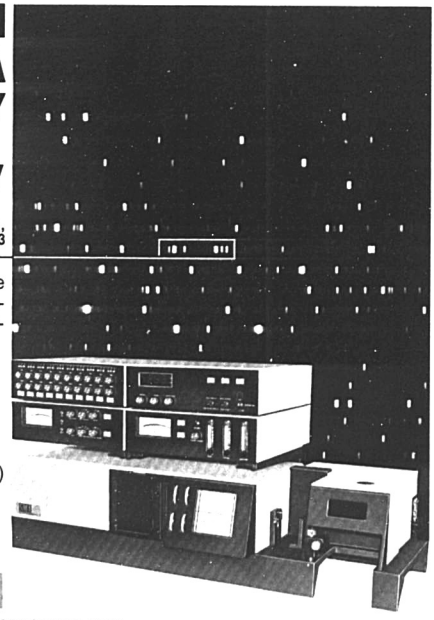
Fisher Scientific Co.
711 Forbes Ave., Pittsburgh, Pa. 15219. Automated chemistry systems with data handling capability; complete line of gas chromatographs, atomic absorption spectrophotometers, pH meters, pH electrodes, ovens, glassware washers, water baths, stirrers, hot plates, pipets and reagent chemicals.

GCA/McPherson Instrument
530 Main St., Acton, Mass. 01720. Com-

SPECTRASPAN PLASMA SPECTROMETRY

proven technology

Wavelengths circled (from left to right) are Fe 2497.82, B 2497.73, W 2497.48, B 2496.78, W 2496.64, Fe 2496.53



SPECTRASPAN's proven high temperature plasma arc and high resolution echelle spectrometer result in sensitive, interference-free elemental analysis. SPECTRASPAN's features:

- Easy to operate
  no explosive gasses, wide dynamic range
- Sensitive, interference-free measurements
  high temperature plasma, high resolution spectrometer
- Analysis of difficult elements (B, P, Al, Si, Ti)
- Economical operation
- Qualitative and quantitative; sequential and multi-channel analysis

SPECTRAMETRICS, INCORPORATED SM
204 ANDOVER ST., ANDOVER, MA 01810

CIRCLE 217 ON READER SERVICE CARD

plete line of spectrophotometers with gel scanning, kinetics, flame photometry, stopped-flow accessories.

GCA/Precision Scientific
3737 W. Cortland, Chicago, Ill. 60647. Constant-temperature circulators, controllers, shaker bath, direct-drive vacuum pump; Freas/Thelco ovens; incubators; water baths; hot plates; Ful-Kontrol heaters; chromatography oven and cabinets; Big Jacks, Swirlite lab supports; PS/Alloy clamps; wet test gas meters; extraction units; automatic Karl Fischer titrator; Vac-Torr pumps.

Gilford Instrument Laboratories Inc.
132 Artino St., Oberlin, Ohio 44074. New Model 250 UV–VIS spectrophotometer and accessories, high-pressure liquid chromatography monitor.

Gilson Medical Electronics, Inc.
P.O. Box 27, Middleton, Wis. 53562. Products which include automatic diluter, dispenser, peristaltic pumps; liquid sample changers to automate your present atomic or molecular absorption spectrophotometers; liquid chromatography UV column monitor, gradient former, fraction collectors.

Glenco Scientific, Inc.
2802 White Oak Dr., Houston, Tex. 77007. High and low-pressure liquid chromatography systems and components, featuring single and dual-channel monitors; columns, pumps, a comprehensive line of valves and fittings including high-pressure and high-temperature sample injection valves; micro and gas tight syringes, reagent dispensers, tissue homogenizers.

Gow-Mac Instrument Co.
100 Kings Row, Madison, N.J. 07940. Liquid and gas chromatographs, gas leak detectors, thermal conductivity detectors, filaments, thermistors.

Hamilton Co.
P.O. Box 17500, Reno, Nev. 89510. Full line of microliter syringes, dispensers, chromatographic accessories, amino acid resins, buffers, calibration standards, valves, needles.

Harrick Scientific Corp.
Croton Dam Rd., Box 867, Ossining, N.Y. 10562. UV–VIS–IR spectrometer attachments and accessories for internal reflection spectroscopy and fluorescence specular reflection and transmission; new beam condensers for microsampling; precision demountable liquid cells; optical windows and precision optical elements; plasma cleaner for ashing ultra clean surfaces; rapid scan spectrometer (1000 spectra/sec) for UV–VIS–NIR; double-beam goniometer spectrometer.

R. J. Harvey Instrument Corp.
123 Patterson St., Hillsdale, N.J. 07642. Infrared accessories; gas chromatography instruments; blood chemistry–hematology instrument; programmed peristaltic reagent dispenser; oxidizer (semi or fully automatic); portable slip-laminate-tensile test device.

Hewlett-Packard, Avondale Div.
Rte. 41, Avondale, Pa. 19311. Gas chromatographs, liquid chromatograph, GC/MS system, integrators, other analytical instruments for research and quality control applications.

Honeywell Inc.
1100 Virginia Dr., Ft. Washington, Pa. 19034. Lab instrumentation for accurate, reliable data recording from chromatographs, spectrometers, other analyzers; models offering flexibility to meet measurement requirements.

Instrumentation Laboratory Inc.
113 Hartwell Ave., Lexington, Mass. 02173. New low-cost 151 and 251 single- and double-beam AA/AE instruments; new 455 flameless sampler.

Interface Technology Corp.
266 Second Ave., Waltham, Mass. 02154. CTi-Cryogenics will operate a Spectrim Cryocooler in a commercial analytical instrument, producing spectra of samples at cryogenic temperatures; Oxford Instruments continuous flow Cryostat.

International Scientific Communications, Inc.
P.O. Box 146, Green Farms, Conn. 06436. Current and past issues of journals and a literature display of laboratory instrumentation and equipment.

ISCO
4700 Superior St., Lincoln, Neb. 68504. Model 1440 high-pressure liquid chromatograph, detectors, fraction collectors, metering and gradient pumps.

Jarrell-Ash Div., Fisher Scientific Co.
590 Lincoln St., Waltham, Mass. 02154.

SPECTRASPAN PLASMA SPECTROMETRY

proven applications

Plasma spectrometry with SPECTRASPAN Systems has proven a simple and routine analytical technique for sensitive analysis in a variety of applications. SPECTRASPAN is in operation in both large and small laboratories world wide performing analytical programs which include:

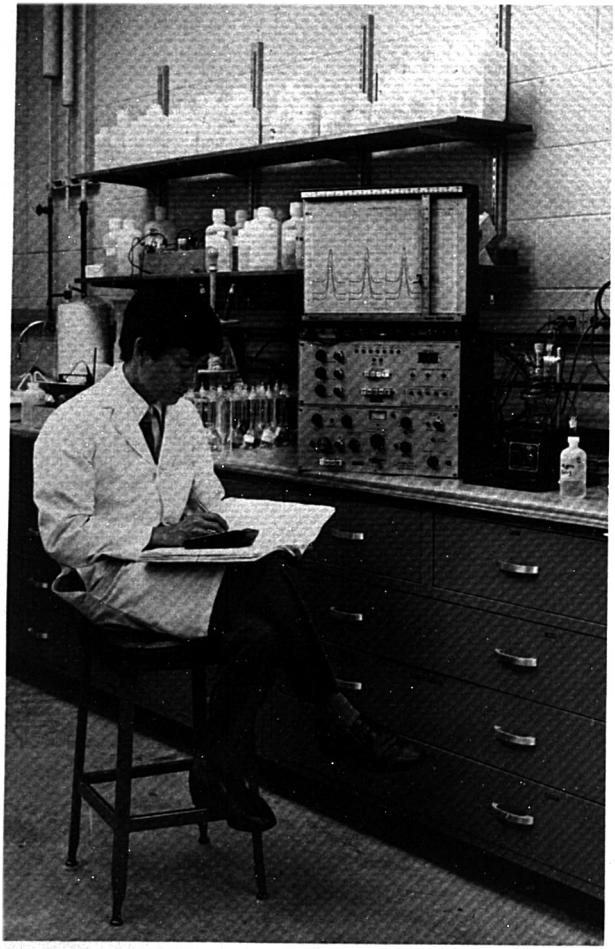
- Water - influent and effluent
- Alloy - including B, P, Si, Al, Ti
- Glass - including Si, B
- Rare Earths, Petroleum Products, Plating Solutions, Precious Metals, Art Objects, Geological Samples



SPECTRAMETRICS, INCORPORATED SMI
204 ANDOVER ST., ANDOVER, MA 01810

CIRCLE 218 ON READER SERVICE CARD

This man is busily doing Pulsed Anodic Stripping Voltammetry



Paper work and telephone calls are just a few of the many interruptions that can steal time from your analytical activities—often time you can't afford to lose. But now you can handle a heavy analytical workload despite these interferences with our **315 Automated Electroanalysis Controller** programming the **174A Polarographic Analyzer** for trace level determinations of metals, anions, organics and pharmaceuticals. The 174A-315 combination:

- **Automatically deaerates the sample**
- **Automatically preconditions the electrodes**
- **Automatically times the deposition for stripping voltammetry experiments**
- **Automatically initiates and terminates the scan**
- **Automatically replicates in triplicate with or without displacement of the recorder Y axis**

So if that telephone rings, if your attention is diverted, if you need more time to reduce data, prep samples, or even have lunch, your analysis will continue without your constant attention.

Before you start losing too much valuable *analysis* time, take some time to investigate the advantages of the 174A-315 combination. Price of the Model 315 is $1,875, the Model 174A is $2,695.

For more information or a demonstration in your lab, write or call Princeton Applied Research Corporation, P. O. Box 2565, Princeton, New Jersey 08540, or telephone (609) 452-2111. In Europe, contact Princeton Applied Research GmbH, D8034 Unterpfaffenhofen, Waldstrasse 2, West Germany.



PRINCETON APPLIED RESEARCH

263

CIRCLE 194 ON READER SERVICE CARD

Don't let someone else's error cost YOU money



You can probably rely on your supplier's inspection and quality control procedures, but how much would just **one** mistake on *their* part cost *you?* Moreover, even the most reliable supplier cannot guarantee that your gas distribution system is fully purged, leak tight and contamination free.

UTI has a way for you to MEASURE composition and total impurities, where it counts . . . and before it hurts. The Q-30C is a mobile, self-contained, automatically operated Precision Mass Spectrometer System uniquely designed for the analysis of electronic specialty gases.

Use it for incoming inspection of silane, arsine, and phosphine. Use it to test the gas as it enters the reactor. Use it to protect yourself.

UTi

UTHE TECHNOLOGY INTERNATIONAL

325 N. Mathilda Ave.
Sunnyvale, CA 94086

Send for the new Q-30C brochure.

CIRCLE 235 ON READER SERVICE CARD

Computer-controlled direct reader, small monochromators, holographic gratings.

JEOL Analytical Instruments Inc.
235 Birchwood Ave., Cranford, N.J. 07016. New low-cost FX-60 FT/NMR system, with light pen control (LPCS) of operating parameters; samples up to 10 mm are standard.

Johns-Manville
Greenwood Plaza, Denver, Colo. 80217. Chromosorb products.

Kevex Corp.
898 Mahler Rd., Burlingame, Calif. 94010. X-ray energy spectrometry systems for rapid, nondestructive multielement analyses; high-intensity X-ray tube excitation subsystem, automatic 16-position sample changer, data processing equipment.

Labconco Corp.
8811 Prospect, Kansas City, Mo. 64132. Freeze dry equipment, fume hoods, glove boxes, carts, lab glassware washer.

Labindustries
1802 Second St., Berkeley, Calif. 94710. Repipet dispensers, repipet diluters, labquake tube shaker, aquametry apparatus water determinations.

Laboratory Data Control
Interstate Industrial Park, Riviera Beach, Fla. 33404. New multiwavelength grating UV detector for HPLC, 5000 psig pulsationless pumping system; complete line of fluorescence, conductivity, refractive index detectors for HPLC; laboratory chart recorders; electrolytic hydrogen generator.

Lear Siegler, Inc./Environmental Technology Div.
1 Inverness Dr., East Englewood, Colo. 80110. SM400 laboratory derivative spectrometer, one of the SM1000 Series ambient air monitors.

Lightner Instrument Co.
431 W. Market St., West Chester, Pa. 19380. Automated thin-layer chromatograph capable of unattended operation of 1–100 samples; standard 5 × 20-cm flexible plastic TLC sheets are used, three modes of detection are available: UV quench, fluorescence, visible absorption.

Linear Instruments Corp.
2930 Grace Lane, Costa Mesa, Calif. 92626. Integrating recorders, X-Y recorders, potentiometric recorders, high-accuracy, reasonably priced recorders.

London Co.
811 Sharon Dr., Cleveland, Ohio 44145. Radiometer pH meters, ion selective electrodes, conductivity meters, potentiometric, photometric titration systems; Heto water baths, shakers, stirrers.

Manostat Corp.
20 N. Moore St., New York, N.Y. 10013. Complete line of peristaltic pumps, multichannel Cassehe pumps, automatic diluters, pipeters, automatic TLC spotters, Labware cleaners.

Mettler Instrument Corp.
Box 100, Princeton, N.J. 08540. Balances, top loading, analytical, electronic; thermal equipment-melting point, differential thermal analyzers; automatic titration equipment; nitrogen analyzer.

Monroe, The Calculator Co.
550 Central Ave., Orange, N.J. 07051. Printing and display programmable calculators.

Neslab Instruments, Inc.
871 Islington St., Portsmouth, N.H. 03801. Temperature-controlled liquid systems

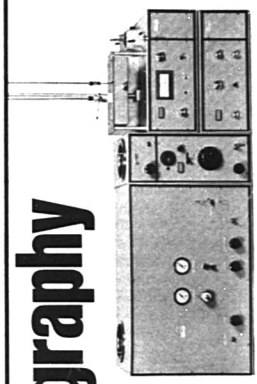
Liquid Chromatography

NEW Universal Modular Liquid Chromatograph

Provides

- Ultra high flow rates for large scale preparative separations
- 2-pump gradient elution operation for wide range of gradient profiles
- 2 or 3 detectors for universality, sensitivity
- Option to split; forming two separate instruments for both analytical and/or preparative applications

All at Surprisingly LOW Cost!

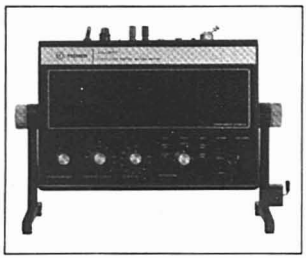


Visit Tracor Exhibit AOAC Booth 38. FACSS B 19, 20.

CIRCLE 227 ON READER SERVICE CARD

Tracor Instruments Tracor, Inc. 6500 Tracor Lane Austin, Texas 78721 Telephone 512/926 2800

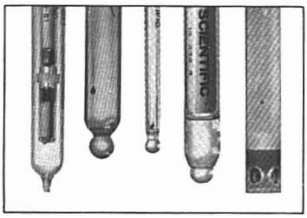
Fisher instruments measure up to your needs ... pH, Surface Tension, Melting Point



Modern, solid-state Accumet® pH Meters

Feature outstanding conveniences: Tilt base for easy viewing. Unique self testing circuit. Easy-to-reach top-mounted terminals. Built-in temperature compensation.

Seven models cover every pH situation. Include: High-accuracy research models with digital readout or expanded-scale analog meter. A unique digital pH meter that reads temperature, too. A low-cost work horse meter for general lab work. For schools and factories, a rugged low-cost model. And, a portable battery-operated model for environmental field work. *For full information on entire Accumet line, circle no. 74 on Reader-Service Card.*



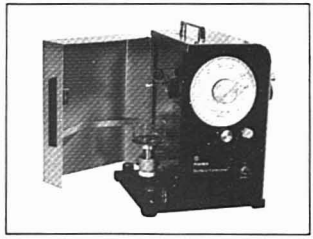
High quality electrodes from our unusually comprehensive line

Glass, reference, combination, micro-combination, metallic. Also: new plastic electrodes as sensitive as glass but a lot more rugged. Ideal for field use. All cover full 0 to 14 pH range and −5° to 110°C temperature range. Can be used with virtually all modern American and European pH meters and potentiometric titrators. *Circle no. 75 for full product bulletin.*



Precisely formulated buffers insure accurate pH

Select convenient ready-made solutions or easy-to-store salts and concentrates. All are certified accurate to ±0.02 pH (at 25°C) . . . carefully standardized on modern instrumentation for highly dependable performance. Packaged for the utmost stability. *Circle no. 76 for product bulletin with complete listing.*

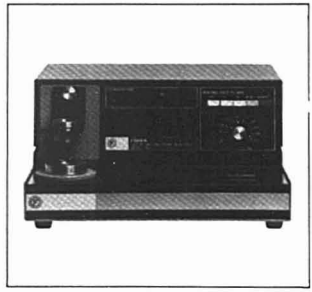


Fisher Tensiometers . . . automated or manual

The Autotensiomat® Tensiometer . . . a fully automatic 2-unit instrument with control-readout and self-contained sample module. For applications that require the highest possible accuracy and reproducibility. Can be connected to a recorder to give you a permanent record of measurements.

The Tensiomat® Tensiometer . . . semi-automatic. A reversible, synchronous motor raises and lowers test ring and sample table.

Model 20 Tensiometer . . . an economical, manually-operated unit for routine measurements. Sensitive enough for research work. *Circle no. 77 for full product bulletin.*



New melting point analyzer with digital readout

Read melting point temperature from ambient to 300°C to the nearest 0.1°C, without guesswork. Simple, accurate determination of melting range, too. Just press HOLD button when melting begins. Record temperature, and release HOLD. Press HOLD again when melting stops. The two readings indicate exact melting range.

Operates by the hot stage melting principle . . . proven to be the simplest, most reliable and accurate method of determining melting points.

Circle no. 78 on Reader-Service Card for product bulletin.

☐ ATLANTA
BOSTON
CHICAGO
CINCINNATI
CLEVELAND
DETROIT
HOUSTON
NEW YORK
ORLANDO
PHILADELPHIA
PITTSBURGH
RALEIGH
RICHMOND
ROCHESTER
SAN FRANCISCO
ST. LOUIS
WASHINGTON
☐ EDMONTON
HALIFAX
MONTREAL
OTTAWA
QUEBEC
TORONTO
VANCOUVER
WINNIPEG

Fisher Scientific Co.

−100°C to +300°C; CryoCool low-temperature coolers, temperature programmers, Utile products; thermostatic baths, circulating baths, coolers.

Nicolet Instrument Corp.
5225 Verona Rd., Madison, Wis. 53711. TT-7 Fourier transform accessory for ^{13}C spectroscopy on T-60A and R-12 spectrometers; NIC-1070 and LAB 80 laboratory data acquisition systems.

Norcon Instruments Inc.
132 Water St., S. Norwalk, Conn. 06854. Model 201 GC Identifier, high-performance package demonstrating on-line, on-the-fly IR identification of GC peaks of samples as small as 1 μg.

Ophthos Instrument Co.
9600 Overlea Dr., Rockville, Md. 20850. Spectroscopic sources, electrodeless lamp system, including microwave generator.

Oriel Corp. of America
15 Market St., Stamford, Conn. 06902. Complete line of hollow cathode lamps for atomic absorption.

Orion Research Inc.
11 Blackstone St., Cambridge, Mass. 02139. Complete line of chemical sensing electrodes, pH electrodes, pH meters, specific ion meters; manuals on analytical procedures and applications.

Ortec Inc.
100 Midland Rd., Oak Ridge, Tenn. 37830. Tube excited fluorescence analyzer (TEFA) with computer option for complete qualitative and quantitative analysis of all elements from Na to U.

Packard Instrument Co., Inc.
2200 Warrenville Rd., Downers Grove, Ill. 60515. Complete line of gas chromatographs and associated equipment.

Perkin-Elmer Corp.
Main Ave., Norwalk, Conn. 06856. Gas chromatography, atomic absorption, UV/fluorescence, microanalytical instruments, infrared spectrometers, microbalances.

Pharmacia Fine Chemicals, Inc.
800 Centennial Ave., Piscataway, N.J. 08854. Sephadex products for gel filtration, ion exchange, affinity chromatography and LH-20 for organic solvents; complete line of liquid chromatography columns, components, valves, gradient mixer, UV, Duo, RI monitors, single- and two-channel recorders; new system for gradient gel electrophoresis, 4-cell gel electrophoresis apparatus, electrophoresis gel destainer, destainer power supply, prepolymerized ready-to-use gradient gels, Pharmacia peristaltic pump P-3.

Philips Electronic Instruments
750 S. Fulton Ave., Mt. Vernon, N.Y. 10550. QXD/QXS quantitative X-ray diffractometry and quantitative X-ray spectroscopy system; Pye Unicam AA, IR, UV spectrophotometers; liquid chromatograph.

Plenum Publishing Corp.
227 West 17th St., New York, N.Y. 10011. Books and journals in the areas of analytical chemistry and spectroscopy; series "Progress in Analytical Chemistry."

Precision Gas Products, Inc.
681 Mill St., Rahway, N.J. 07065. Ultra-high purity carrier and reference gases, highest accuracy liquid-phase and vapor-phase calibration mixtures; custom-engineering gas handling equipment.

Princeton Applied Research Corp.
P.O. Box 2565, Princeton, N.J. 08540. Manual and automatic polarographic analyzers, coulometric analysis equipment, electrochemical equipment, accessories.

Quantachrome Corp.
337 Glen Cove Rd., Greenvale, N.Y. 11548. Instrumentation for research and quality control for physical characterization of powdered materials; Quantasorb, Monosorb, Quantector, null-pycnometer.

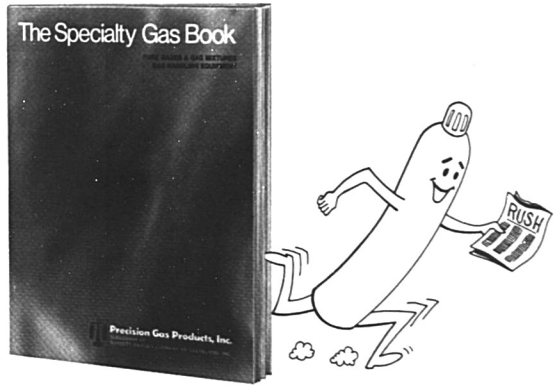
Rigaku/USA
607 N. Ave., Wakefield, Mass. 01880. Fully automatic X-ray spectrometer and portable spectrometer for field use.

Sadtler Research Laboratories, Inc.
3316 Spring Garden St., Philadelphia, Pa. 19104. Standard and commercial collections of reference spectra, including infrared, nuclear magnetic resonance, ultraviolet, Raman, fluorescence, and differential thermal analysis; audiovisual programs on instrumentation analysis and basic chemistry and math; technical books on chemistry and spectroscopy; "Reactiones Organicae"—a documentation of useful organic reactions on slotted punch cards.

Sargent-Welch Scientific Co.
7300 N. Linden Ave., Skokie, Ill. 60076. Recorders, spectrophotometers, pH measuring, recording instruments, vacuum products.

August Sauter of America
80 Fifth Ave., New York, N.Y. 10011. Balances, laboratory research weighing systems, ultrasonic equipment.

What other specialty gas company has grown to meet all your gas needs...



...yet stayed small enough to serve you properly.

Send for our new Specialty Gas Book. This expanded catalog is PRECISION GAS PRODUCT's latest effort to provide from one source a complete answer to your individual specialty gas requirements.

Eighty-four pages from cover to cover. More than 160 gases and purities. An almost infinite number of gas mixtures. An entire section on gases for special applications such as emission control, air pollution, analytical instrumentation and process control, electronic component manufacturing, and gases for producing biological atmospheres and calibrating medical instrumentation. Plus a greatly expanded instrument and gas handling equipment section.

We've been more than a year in the planning of this new specialty gas and equipment catalog and the results are indicative of a continuing desire to improve our services to you.

For your copy of The Specialty Gas Book, use this publication's Reader Service Card, or write:

Precision Gas Products, Inc.
681 MILL STREET, RAHWAY, N.J. 07065

CIRCLE 188 ON READER SERVICE CARD
See us at the FACSS Show Booth D-8

Schoeffel Instrument Corp.
24 Booker St., Westwood, N.J. 07675. Continuously variable wavelength monitor for LC; high-intensity lamp housings; miniature grating, prism monochromators, photodetection equipment.

Scientific Gas Products Inc.
513 Raritan Center, Edison, N.J. 08817. Ultra high-purity gas; gas mixtures; gas-regulating equipment, research-grade gases.

Siemens Corp.
186 Wood Ave. S., Iselin, N.J. 08830. X-ray generator, sequential X-ray spectrometer, electronic panel computer, X-ray diffraction equipment.

Spectrametrics, Inc. (SMI)
204 Andover St., Andover, Mass. 01810. Echelle grating spectrometer, a dc argon plasma, atomic emission system for both qualitative and quantitative analysis; options for single-element or multielement and photographic analysis using a echellogram comparator.

Spectra-Physics, Inc.
1250 W. Middlefield Rd., Mountain View, Calif. 94042. Liquid chromatography systems, components, accessories; digital integrators for laboratory automation of gas, liquid chromatographs.

Spex Industries, Inc.
Box 798, Metuchen, N.J. 08840. MP3 thermal chromatograph, an instrument generating both thermagram and chromatogram for identifying and quantitating ingredients in organic compounds.

Supelco, Inc.
Supelco Park, Bellefonte, Pa. 16823. Column packings for gas chromatography, GC supports, adsorbents, glass, other gas chromatography columns, related accessories for gas, liquid, thin-layer chromatography.

Tekmar Co.
P.O. Box 37202, Cincinnati, Ohio. Homogenizers, analytical mills, recorders, hollow cathode lamps, dispensers.

Arthur H. Thomas Co.
Third and Vine Sts., Philadelphia, Pa. 19105. Stack sampler and glassware, melting-point apparatus with programmer, pollution trace oven, UV–VIS spectrophotometers, electronic balances.

Tracor, Inc.
6500 Tracor Lane, Austin, Tex. 78721. 222/550 gas chromatographs, specific detectors, liquid chromatographs, data handling system.

Tracor Northern
2551 W. Beltline Hwy., Middleton, Wis. 53562. NS-575A signal averager, NS-880 elemental X-ray analyzer, TN-11/1203 computer-controlled signal averager.

Varian Assoc.
611 Hansen Way, Palo Alto, Calif. 94303. New liquid chromatograph with multiwavelength UV detector, gas chromatograph, carbon-13 NMR spectrometer, analytical NMR equipment, atomic absorption spectrophotometer with background corrector, new air microsampler, new mass spectrometer/gas chromatograph with data system, analytical instrument parts and supplies.

VWR Scientific
Box 3200, San Francisco, Calif. 94119. B&L mini-spec 20, B&L spectrophotometers, Bronwill constant-temperature circulators, Bronwill ultrasonic disintegrators.

Waters Associates, Inc.
Maple St., Milford, Mass. 01757. Liquid chromatographs, solvent delivery systems, solvent programmers, LC column packing materials.

Wescan Instruments, Inc.
3018 Scott Blvd., Santa Clara, Calif. 95050. Membrane osmometer, cloud-point apparatus, viscosity timer, conductivity meter, cells.

Wilks Scientific Corp.
P.O. Box 449, S. Norwalk, Conn. 06856. IR accessories including 20, 40-m gas cells, GC–IR attachment; miniature infrared analyzers for laboratory and field analysis of solids, liquids, gases; infrared monitoring systems.

Willey Corp.
720 E. Fee Ave., Melbourne, Fla. 32901. Infrared Fourier transform spectrophotometer.

Wilmad Glass Co., Inc.
Rte. 40 & Oak Rd., Buena, N.J. 08310. Spectroscopic supplies and accessories for NMR, IR, ESR, MS, GC; NMR sample tubes: NMR, IR, general recording charts; deuterated solvents; microliter syringes.

C. N. Wood Mfg. Co.
Newtown Industrial Commons, Newtown, Pa. 18940. Light scattering photometers, differential refractometers, readout equipment.

CSG

CICERO SCIENTIFIC PURE QUARTZ COMBUSTION TUBES



Special annealing process used in making every Cicero combustion tube. Our carbon tubes have heavy-duty built-in jet, give extra hours of lab life. Jetting stems in other tubes allow easier, faster cleaning, reduce capillary opening breakage. All sulfur tube bodies have same dimensions. Unconditionally guaranteed against defects. Instant delivery from stock. Mail coupon or phone collect (616-926-2581) anytime. Ask about our Safety-First Purifying Trains too!

SAVE

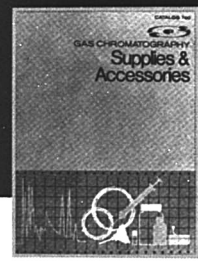
On our bulk-quantity discounts! Mail to: Cicero Scientific Glass, 308 W. Empire, P.O. Box 671, Benton Harbor, Mich. 49022.

Please check for data: ☐ Combustion tubes ☐ Purifying trains ☐ Carbon analyzers ☐ Custom glassware ☐ Please phone.

Name_____
Title_____
Organization/Firm_____
Phone_____
Address_____
City_____
State & zip_____

CIRCLE 40 ON READER SERVICE CARD

Just Released! FOR GAS CHROMATOGRAPHERS



CATALOG 700...

48 PAGES OF CHEMICALS, SUPPLIES AND GADGETS

CRS Catalog 700 lists hundreds of often unique, always useful chemicals, supplies and gadgets of special significance to the gas chromatographer. Everything from **Activated Charcoal** to **Vibrators,** with many exclusive items.

Send for your FREE copy today.

Please send FREE copy of CRS CATALOG 700. AC/10

Name & Title_____
Company/Institution_____
Address_____
City_____ State & Zip_____

Chemical Research Services, Inc.
852 Westgate Drive • Addison, Illinois 60101

CIRCLE 39 ON READER SERVICE CARD

THE GOW–MAC SERIES 550 THERMAL CONDUCTIVITY* GAS CHROMATOGRAPHS OFFER FOUR DETECTOR OPTIONS!



Not only do GOW-MAC's Series 550 offer the following important features for your laboratory,

Sensitive GOW-MAC four filament thermal conductivity detector—the industry standard

Highly reproducible proportional oven temperature controls

Easily accessible detector and column for rapid column change

Rugged compact unit
Maximum economy—basic unit,

But in addition, they offer a choice of four detector systems:

- **Model 69-550** employs a detector specially designed for high resolution, high sensitivity chromatography. It is a low volume, flow through geometry thermal conductivity detector with minimum dead volume. The detector contains four rhenium tungsten (WX) filaments (other filaments available, including nickel, gold-sheathed, etc.)
- **Model 69-560** features a Hex-Nano-Katharometer flow through detector, with four coaxial filaments. Response time is 0.5 seconds. It maintains excellent zero stability over wide flow ranges with negligible noise. Has highest useful signal of any GOW-MAC thermal conductivity cell. Limited to ⅛" columns.
- **Model 69-570** uses a thermal conductivity detector with two 8 K ohm thermistors in a compatible bridge circuit, instead of filaments. This detector is especially suited to low temperature applications and highly oxidizing substances.
- **Model 69-625** incorporates GOW-MAC's exclusive No. 11-625 Gas Density Detector that senses the effect of density variations in the sample gas upon the flow pattern in the cell. The Gas Density Detector permits the chromatography of corrosive substances.

Send for our new technical brochure which will surely convince you that one of these gas chromatographs belongs in your laboratory.

*Strictly speaking, the gas density detector is not a Thermal Conductivity Detector.

See us at the FACSS Show, Booth 338

GOW MAC

GOW-MAC INSTRUMENT CO.
100 Kings Road, Madison, N.J. 07940 Telephone: 201/377-3450 Telex: 136331
Shannon Free Airport, Co. Clare, Ireland Telephone: 61632 Telex: 6254

CIRCLE 88 ON READER SERVICE CARD

CHART PAPER

Finest quality recording charts for use with all spectrometers and other laboratory instruments.

- **NMR CHARTS:** NMR charts are updated to coincide with the newest instrument techniques: Fourier Transformation Hetero-Decoupling, and Time Averaging.
- **IR CHARTS:** Full line of IR charts for most popular instruments.
- **GENERAL RECORDING CHARTS:** We carry a full line of general recording charts for most standard recorders.

• • • •

Wilmad . . . world's largest one-stop source for everything you need for spectroscopic research . . . except the spectrometer. Before ordering chart paper, check our prices and stocks. Like many research organizations . . . *you'll standardize on Wilmad.*

For catalogs and buying data, write today to Wilmad Glass Company, Inc., Route 40 & Oak Road, Buena, N.J. 08310, U.S.A.
Phone: (609) 697-3000
TWX 510-687-8911

WILMAD

Sole distributor of Thompson-Packard products
PIONEERS IN ACCESSORIES AND SUPPLIES FOR SPECTROSCOPY

CIRCLE 254 ON READER SERVICE CARD

SCIENCE MILESTONES - on TAPE from C&EN

☐ **Vitamin B-12—Total Synthesis**
Listen to Dr. R. B. Woodward describe his dramatic work

☐ **Vitamin B-12—Biological Aspects**
International experts discuss biochemistry, biosynthesis, and mechanism of action

—other Science Symposia on Tape also available from ACS—

☐ **The Energy Crisis**
Outlook for oil, gas, coal

☐ **Fuels for the Future—Hydrogen**
Experts discuss solutions to the energy crisis

☐ **Nutrition & Public Policy—Food Quality**
Govt., industry officials spell it out

☐ **Chemical Engineering In Medicine**
—at the frontier of chemical engineering

☐ **Drugs Affecting Learning & Memory**
A hot topic in drug research

☐ **New Solid Waste Disposal Processes**
New processes set to go commercial

☐ **Chemistry of the Moon–I**
Dr. Urey, top experts reveal findings

ABOVE INCLUDE VISUAL MATERIALS

	ACS Members	Non-members
Cassettes only	$14.00	$17.00

10% DISCOUNT if payment accompanies order

Name _____

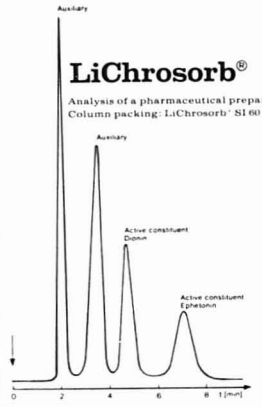
Address _____

_____

Order from:
American Chemical Society
1155 16th Street, N.W.
Washington, D.C. 20036
ATTN: A. Poulos

EM Reagents®

Products for High Performance Liquid Chromatography



LiChrosorb®

LiChrosorb—totally porous HPLC column packings of irregular shape

LiChrosorb SI 60
LiChrosorb SI 100
LiChrosorb Alox T
LiChrosorb SI 60 silanized
mean particle sizes:
5 μm, 10 μm, 30 μm

LiChrospher™

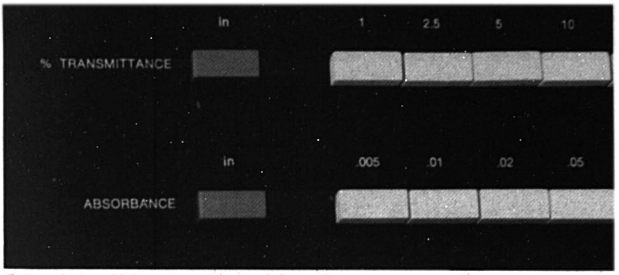
LiChrospher—totally porous HPLC column packings of spherical shape

LiChrospher SI 100
LiChrospher SI 500
LiChrospher SI 1000
mean particle size 10 μm

EM also supplies PERISORB® a porous-layer column packing material for high speed and high resolution LC.

EM Laboratories, Inc.
associate of E. Merck, Darmstadt, Germany
500 Executive Boulevard
Elmsford, New York 10523
Phone 914/592-4660
See us at the FACSS Show, Booth No. F7

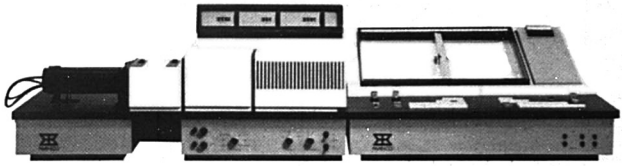
CIRCLE 66 ON READER SERVICE CARD

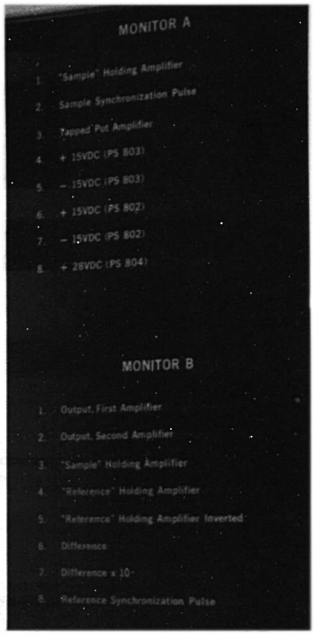


Full scale sensitivity selected by push-button

Take a close look at the DW-2™

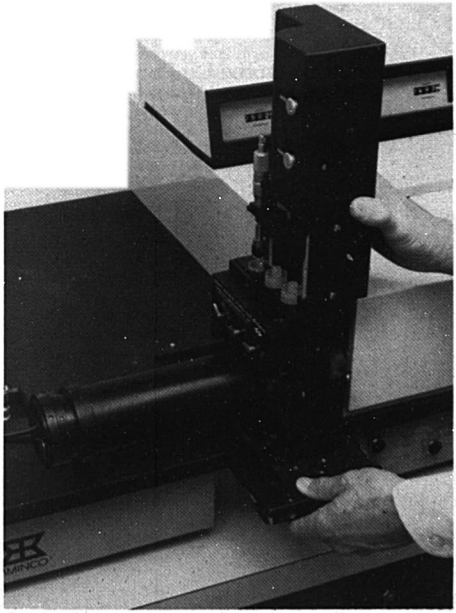
UV-VIS Spectrophotometer





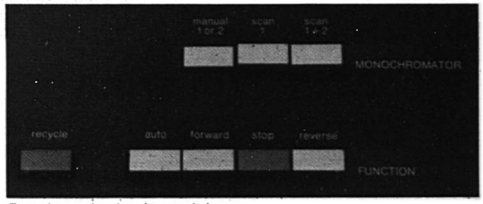


Monitor dials permit easy selection of 16 checkpoints for oscilloscope readout.



Stopped-Flow accessory easily replaces cell compartment. Note open area which allows use of a variety of accessories.

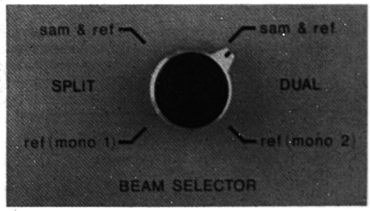
AMINCO®



Function selection by push-button.

For a really close look at Aminco's new DW-2 Bulletin, contact American Instrument Company, Silver Spring, Maryland 20910.

Beam selector permits mode selection at the twist of a dial.



CIRCLE 5 ON READER SERVICE CARD

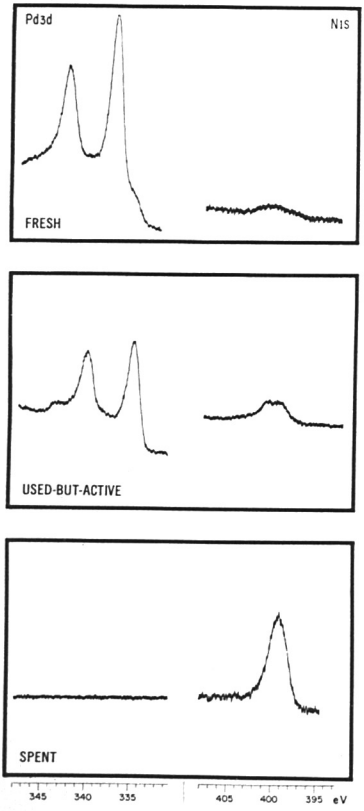
How Du Pont's ESCA solved the case of the poisoned catalyst.

A manufacturer who was using a palladium-on-carbon catalyst in a chemical process to reduce a nitrogen-containing organic compound noted that, after extended use, the catalyst lost its activity.

Using bulk analyses such as x-ray fluorescence, he determined that the total palladium content of the catalyst remained constant after use. He su poison such as sulfur or had no proof.

Surface analysis of Used-but-active, and Sp with a Du Pont 650B Elec produced the following th at left below.

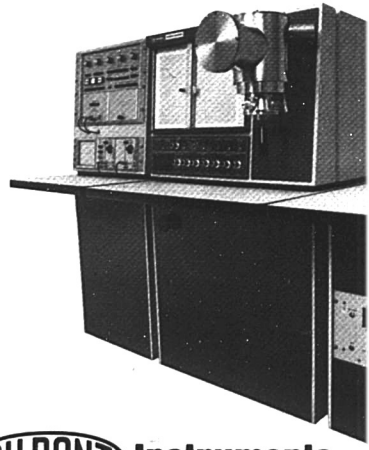
PALLADIUM-ON-CARBON CATALYST



From these data, obtained in le determined that loss of activity w sulfur or halogens. Instead, it was c a nitrogen-containing by-product of coated the surface of the catalyst, l palladium sites.

ESCA—Electron Spectrometry ysis—has proved its unique capacity in the heterogeneous catalyst fiel speed and ease of use of the Du Pon valuable in your field.

For more information on the Du descriptive brochure that takes th ESCA, write Du Pont Instrumen Wilmington, DE 19898.



DU PONT Instruments

REG. U.S. PAT. OFF.

CIRCLE 57 ON READER SERVICE CARD

American Chemical Society 1975 Award Winners

The winners of the 1975 American Chemical Society Awards in Analytical Chemistry, Chemical Instrumentation, and Chromatography were announced at the Fall National Meeting in Atlantic City, N.J. The recipients, their contributions, and brief biographical sketches appear below

Sidney Siggia, professor of analytical chemistry at the University of Massachusetts, Amherst, Mass., has been selected as the 1975 recipient of the ACS Award in Analytical Chemistry, sponsored by Fisher Scientific Co. Dr. Siggia is cited specifically for his "exceptional prominence in fundamental and applied analytical chemical research, in innovative and effective teaching, and in local, national, and international analytical chemical citizenship." His professional career, divided as it is between 23 years in industry and 8 years as an academic scientist, has contributed to his exceptionally broad and perceptive concepts of analytical chemistry and is responsible for his dedication to promoting the interaction between academic and industrial aspects of the science.

Dr. Siggia earned his BS degree from Queens College, New York, in 1942 and his MS and PhD degrees in 1943 and 1944 from the Polytechnic Institute of Brooklyn. He held research and managerial positions at General Aniline and Film Corp. (1944–58) and Olin Corp. (1958–66) research laboratories and joined the University of Massachusetts as a professor in 1966. He is the author of several books, the most recent of which is "Instrumental Methods for Organic Functional Group Analysis," Wiley, 1972.

Dr. Siggia was a pioneer of the functional group approach first by classical methods and latterly through modern instrumental techniques to organic analysis. He has over 50 research publications in this field, many of which have proceeded to adoption as standard methods. Other areas of research interest include reaction rate analysis and chromatographic methods, especially reaction gas chromatography and high-pressure liquid chromatography of molecules of biological significance.



Sidney Siggia



Myron Kelley



Egon Stahl

Active participation in the ACS Analytical Division activities, panels of governmental institutions, service on scientific editorial boards, speaking engagements, and general leadership in the service of the analytical chemistry profession have earned Dr. Siggia international stature. He is much sought after as a speaker and is revered as a teacher.

Recent activities of Dr. Siggia include his participation as opening speaker at the Analytical Division Summer Symposium on "On-Line Process Analytical Chemistry" and as chairman of NSF's Workshop on Shale Oil Analysis, both in June of this year.

Myron T. Kelley, now a consultant to the Analytical Chemistry Division of Oak Ridge National Laboratory and formerly director of this Division for 25 years, has been named winner of the 1975 Award in Chemical Instrumentation sponsored by Sargent-Welch Scientific Co. Under his leadership, the Analytical Chemistry Division at ORNL grew to be one of the largest and most diverse facilities in analytical chemistry in the world. Many highly specialized analytical instruments and techniques that were needed to handle radioactive material were developed during this time. Dr. Kelley's publications cover 13 different areas of specialty. Much of the instrumentation work was used and/or emulated at nuclear installations through the world, and this work also influenced commercial development

of instruments. Specific instruments developed during Dr. Kelley's career include several potentiometric titrators, a fluorophotometer, flame photometers, and especially electroanalytical instrumentation. Developments in electroanalytical instrumentation represented contributions to nearly all the common techniques: polarography, voltammetry, constant-current coulometry, controlled potential coulometry, oscillometry, chronopotentiometry, and stripping techniques. An especially important area in more recent years was the early application of computers to analytical problems.

Dr. Kelley obtained his BS and MS degrees from the University of Nebraska in 1932 and 1933 and earned his PhD at Iowa State College in 1937. After work as an analytical chemist at Monsanto Chemical Co. in St. Louis, he moved to Oak Ridge in the process development section of Clinton Laboratories, later to become the Oak Ridge National Laboratory. In 1948 he was appointed the first director of the Analytical Chemistry Division of ORNL and retained that position until 1972 when he became a senior research advisor.

Dr. Kelley has been active in American Chemical Society affairs, has lectured widely, and participated in the analytical chemistry exhibit in the Geneva Conference on the Peaceful Uses of Atomic Energy (1956).

Currently, Dr. Kelley has been "working" as a consultant to the Software Department of Tennecomp Systems, Inc., with the computer treatment of gamma ray spectra; with Orion, Inc., on the development of computer-based continuous monitoring systems with ion-selective electrodes; and also has been helping the University of Tennessee's Chemistry Department with analytical computerization.

Egon Stahl, professor and director of the Institute of Pharmacognosy and Analytical Chemistry at the University of Saarbrücken, Germany, has been named to receive the 1975 ACS Award in Chromatography, sponsored by Supelco, Inc. Dr. Stahl is cited for his many contributions (including the naming of the techniques) to thin-layer chromatography, gradient thin-layer chromatography, and, more recently, thermofractography. In the latter technique, thermal separation of volatile components is followed by their separation and identification by thin-layer chromatography. He not only developed the necessary equipment to make thin-layer chromatography a universally accepted technique, but also demonstrated a broad range of applications for TLC. As early as 1962, Dr. Stahl and a selected team of authors put together a laboratory handbook which has been translated into Russian and English, "Thin Layer Chromatography, A Laboratory Handbook." His research interests center around micro and ultramicro analysis of natural products, especially medical plants; biochemical procedures in functions in glandular hair of plants; constituents of essential oils; and separation methods, especially chromatography. He is also interested in "chemical races" in medicinal and poisonous plants.

Dr. Stahl earned his MS and PhD degrees at the University of Karlsruhe, Germany, and did postgraduate work at the University of Zurich. He was associated with the Universities of Karlsruhe and Mainz, Germany, until 1958 when he joined the University of Saarbrücken. He is active on the editorial boards of scientific journals, belongs to numerous scientific societies, and has received various medals and prizes from German and Swiss societies. In 1971, he was given an honorary membership in the American Academy of Pharmaceutical Sciences. He is active as an expert for preparing a European Pharmacopoeia and is chairman of the Pharmaceutical-Biological Board of the German Pharmacopoeia Commission. Dr. Stahl is a modern, open-minded European university teacher who gladly fulfills his obligations in teaching.

Awards



Jaroslav Sestak



Homer Hagstrum



Dale Coulson

Jaroslav Sestak, Prague, Czechoslovakia, has been named recipient of the 7th Mettler Award in Thermal Analysis by the North American Thermal Analysis Society. Dr. Sestak was presented the award at the 4th International Conference on Thermal Analysis held in Budapest, July 7–12. He is cited for his outstanding performance in nonisothermal kinetics. After graduation from the University of Chemical Technology at Prague in 1962, Dr. Sestak joined the Institute of Solid-State Physics at the Czechoslovak Academy of Sciences. He received his PhD degree in materials science in 1967, has been a guest scientist at the Swedish Nuclear Center in Studsvik, and is now a principal scientific worker with the Department of Chemistry and Technology of Ferrites at the Institute. He has authored 33 scientific papers, has given lectures, and is an active member in various technical societies. He is also on the editorial board for *Thermochimica Acta.*

This award is sponsored by Mettler Instrument Corp. of Princeton, N.J., and is given each year "in recognition of creative work and distinguished service in the field of kinetic thermal analysis."

Homer D. Hagstrum, head of the Surface Physics Research Dept. at Bell Laboratories, Murray Hill, N.J., will receive the fifth annual Medard W. Welch Award of the American Vacuum Society, on October 10 at the annual symposium of the Society at Anaheim, Calif. Dr. Hagstrum will deliver an address reviewing the development and status of ion-neutralization spectroscopy, a technique which he developed for the examination of solid surfaces. Dr. Hagstrum received his undergraduate and graduate degrees, including the PhD degree in physics, from the University of Minnesota. He has been active in affairs of the American Physical Society and has served on conference committees and editorial boards in the field of surface science.

During his career at Bell which began in 1940, Dr. Hagstrum has

"Two of the best reasons to advertise are...

Chemical & Engineering News and *Analytical Chemistry.*"

"As an advertising executive for 25 years, I urge you to read the new Varian, Camag, Labindustries, and Esterline studies. They substantiate what we've known instinctively for years: advertising is the most efficient way to cover the scientific market when you use the two-magazine combination consisting of *Analytical Chemistry* and *Chemical & Engineering News.*"

Al Emery is president of the Harris D. McKinney advertising agency which specializes in industrial advertising and represents such leading firms as Mettler Instrument Corp., Arthur H. Thomas Co., Honeywell Process Control Division, Sherwin Williams Chemicals, and SunOlin Chemical Co.

Centcom, Ltd., 50 West State St., Westport, CT 06880 • (203) 226-7131
Advertising Management for the American Chemical Society Publications



Al Emery, President
Harris D. McKinney, Inc.

worked on physical research of electron impact on molecules, mass spectroscopy, electron ejection from solids by ions, the development of a spectroscopy of solids and solid surfaces, and surface physics.

Dale M. Coulson, manager of the Analytical, Physical, and Organic Chemistry Group at Stanford Research Institute, has been named winner of the 1974 Harvey W. Wiley Award of the Association of Official Analytical Chemists. The award, $750, will be presented by the AOAC President, F. M. Garfield, at the banquet October 14, during the annual AOAC meeting. Harvey W. Wiley, the "father" of the first Pure Food and Drug Act and Founder of AOAC, is honored by this award given each year for outstanding contributions to analytical methodology in areas of interest to AOAC. Mr. Coulson is recognized for pioneering new analytical methods and designing new analytical equipment. His contributions to pesticide detection by gas chromatography, which resulted in rapid screening methods, is particularly cited by the award selection committee.

PVC Conference

A two-day symposium, scheduled for New York City's Americana Hotel, October 31 and November 1, will deal with problems of concern to those who are processors or converters of polyvinyl chloride. The symposium, which will be educational, will consider current OSHA regulations; methods of detection and monitoring atmospheric concentrations; protective equipment; costs; and regulations and their interpretation.

This symposium is being sponsored by the Palisades Section of the Society of Plastics Engineers, with the cooperation of four divisions of the Society.

Further information is available from the Society at 656 W. Putnam Ave., Greenwich, Conn. 06830. 203-661-4770

ASTM Committee on Lab Apparatus

A new Committee on General Laboratory Apparatus was formed by the American Society of Testing and Materials. The scope of the committee is the preparation of specifications, methods of test, and recommended practices and definitions for general laboratory apparatus. There are ten subcommittees to deal with: glass apparatus, metalware, plasticware, rubber and elastomeric materials, filtration materials, weighing devices, microchemical apparatus, analytical instrumentation, liaison, and executive.

William Gallagher of NBS is chairman of the new committee.

Those interested in the work of this committee should contact Earl R. Sullivan, ASTM, 1916 Race St., Philadelphia, Pa. 19103. 215-569-4200

Editor Moves to University of Florida

Professor H. A. Laitinen, editor of ANALYTICAL CHEMISTRY, has been appointed a Graduate Research Professor at the University of Florida in Gainesville, Fla., beginning October 1, 1974. He will be associated with both the Chemistry Department and the Department of Environmental Engineering Sciences in his new position. Professor Laitinen had been associated with the University of Illinois since 1940.

Call for Papers

Third International Symposium on Liquid Scintillation Counting Bath, Somerset, England. Sept. 15–19, 1975. Sessions on sample preparation, radioimmunoassay, and error. Those wishing to contribute to the scientific sessions or participate in the exhibition, write to M. A. Crook, The Society for Analytical Chemistry, 9–10 Savile Row, London, W1X 1AF, England.

Meetings

- **10th International Symposium on Chromatography.** Sept. 30–Oct. 4. Barcelona, Spain. *Contact: G. Guichon, Ecole Polytechnique, Laboratoire de Chemie Analytique Physique, 17, rue Descartes, Paris (5°), France. Page 811 A, Aug.*
- **21st Canadian Spectroscopy Symposium.** Oct. 7–9. Ottawa, Canada. *Contact: J. L. Dalton, Department of Energy, Mines and Resources, Mines Branch, 555 Booth St., Ottawa, Ont., K1A 0G1, Canada*
- **7th Materials Research Symposium: Accuracy in Trace Analysis (Sampling, Sample Handling, and Analysis).** Oct. 7–11. NBS, Gaithersburg, Md. *Contact: Philip D. LaFleur, B108 Reactor Bldg., National Bureau of Standards, Washington, D.C. 20234. Page 36 A, Jan.*
- **21st National Vacuum Symposium.** Oct. 8–11. Anaheim, Calif. *Contact: L. C. Beavis, Sandia Labs Div. 2413, Albuquerque, N.M. 87115*

News and Views

- **MAC 74, 14th International Exhibition of Equipment for Chemistry, Analysis, and Laboratory Research.** Oct. 8–12, 1974. Milan Fair Ground, Milan, Italy. *Contact: Segreteria Generale via Tiziano, 19, 20145, Milan, Italy*
- **Electrochemical Society.** Oct. 13–17. New York, N.Y. *Contact: The Electrochemical Society, 30 E. 42nd St., New York, N.Y. 10017. 212-867-4430*
- **88th Annual Meeting Association of Official Analytical Chemists.** Oct. 14–17. Marriott Hotel, Twin Bridges, Washington, D.C. *Contact: Luther G. Ensminger, AOAC, Box 540, Benjamin Franklin Station, Washington, D.C. 20044. Page 800 A, Aug.*
- **Pacific Conference on Chemistry and Spectroscopy.** Oct. 16–18. San Francisco, Calif. *Contact: W. J. Eisenlord, 1660 S. Amphlett Blvd., San Mateo, Calif. 94402. 415-929-1100. Page 422 A, Apr.*
- **18th Conference on Analytical Chemistry in Nuclear Technology.** Oct. 22–24. Gatlinburg, Tenn. *Contact: L. J. Brady, ORNL, P.O. Box X, Oak Ridge, Tenn. 37830. Page 884 A, Sept.*
- **NIH Symposium on Recent Developments in Research Methods and Instrumentation.** Oct. 22–24. Bethesda, Md. *Contact: Judith M. Summers, NIH, Bldg. 31, Rm. 1C-02, Bethesda, Md. 20014. 301-496-2315. Page 892 A, Sept.*
- **26th Southeastern Regional ACS Meeting.** Oct. 23–25. Convention Center, Norfolk, Va. *Contact: M. A. Kise, R&D, Virginia Chemicals, Inc., Portsmouth, Va. 27303. 703-484-5000*
- **Instrument Society of America International Conference.** Oct. 28–31. Sheraton Hotel, New York City. *Contact: ISA, 400 Stanwix St., Pittsburgh, Pa. 15222. 412-281-3171*
- **9th International Symposium on Advances in Chromatography.** Nov. 4–7. Sheraton-Lincoln Hotel, Houston, Tex. *Contact: Albert Zlatkis, Chem. Dept., University of Houston, Houston, Tex. 77004. Page 890 A, Sept.*
- **10th Tokyo Conference on Applied Spectroscopy.** Nov. 6–8. Tokyo, Japan. *Contact: The Japan Society for Analytical Chemistry, 1-1-5 Hon-machi, Shibuyaku, Tokyo, Japan 151. Page 326 A, Mar.*

Nalge introduces Dial-a-Solution.

If you have a question about plastic labware call 716-586-8800 and we'll tell you what to use where.

No matter whose labware it is. Ours. Or somebody else's. With the widest line of plastic labware around it stands to reason we know more about plastic.

It may be that you've been holding off on using plastic labware because you didn't know how many different jobs it can do.

But we use ten different resins to make Nalgene® labware with a variety of qualities you need. Transparency. Autoclavability. Accuracy.

We know what each can do and what each can't do. Even if you're using it for a never-before-application.

Our 56-page catalog has a special Nalgene chemical resistance chart covering 192 chemicals from acetaldehyde to zinc stearate. Write for it. Nalgene Labware, Box 365, Rochester, N.Y. 14602. It's a handy reference.

NALGE
SYBRON CORPORATION

CIRCLE 172 ON READER SERVICE CARD



News and Views

■ **10th Midwest Regional ACS Meeting.** Nov. 7–8. University of Iowa, Iowa City, Iowa. *Contact: D. J. Pietrzyk, Chem. Dept., University of Iowa, Iowa City, Iowa 52240. 319-353-4661*

■ **1st Federation of Analytical Chemistry and Spectroscopy Societies (FACSS) Meeting.** Nov. 18–22. Atlantic City, N.J. *Contact: James White, Oak Ridge National Laboratory, P.O. Box X, Oak Ridge, Tenn. 37830. 615-483-8611, ext. 31472. Page 999 A, Oct.*

■ **30th Southwest Regional Meeting.** Dec. 9–11. Astroworld Hotel, Houston, Tex., *Contact: J. M. Fitzgerald, Chem. Dept., University of Houston, Cullen Blvd., Houston, Tex. 77004. 713-749-2639*

The following meetings are scheduled for 1975. Other meetings scheduled for early 1975 are listed in ANALYTICAL CHEMISTRY*'s Sept. issue on page 892 A*

■ **22nd Annual Conference, Western Spectroscopy Assoc.** Jan. 29–31. Asilomar Conference Grounds, Pacific Grove, Calif. *Contact: G. R. Haugen, L-404, University of California, Lawrence Livermore Laboratory, Livermore, Calif. 94550*

■ **Industrial Process Control.** Apr. 23–25. Queen Elizabeth Hotel, Montreal. Theme: "Chemicals Under Control." *Contact: Instrumentation Society of America, Montreal Section, Room 101, 5165 Sherbrooke St. W., Montreal, Que., H4T 1T6, Canada*

Short Courses

ACS Courses. For more information, contact: Department of Educational Activities, American Chemical Society, 1155 16th St., N.W., Washington, D.C. 20036. 202-872-4508

Maintaining and Troubleshooting Chromatographic Systems
St. Louis, Mo. Oct. 11–12. J. Q. Walker, M. T. Jackson, Jr., M. P. T. Bradley. $135; nonmembers, $155

Modern Liquid Chromatography
Washington, D.C. Oct. 12–13. L. R. Snyder, J. J. Kirkland. $140; nonmembers, $160

Chemical Microscopy
Atlantic City, N.J. Nov. 15–17. J. A. Reffner. $135; nonmembers, $155

Gas Chromatography
Atlantic City, N.J. Nov. 16–17. R. A. Keller, M. F. Burke. $125; nonmembers, $145

Solving Problems with Modern Liquid Chromatography
Atlantic City, N.J. Nov. 16–17. J. J. Kirkland, L. R. Snyder. $145; nonmembers, $165

Courses and Workshops at FACSS Meeting
Atlantic City, N.J.
See ACS Courses above

The following workshops require preregistration. Contact: Jim Lindsay, U.S. Geological Survey, 12201 Sunrise Valley Dr., Reston, Va. 22092. 703-860-7543

Atomic Absorption
Nov. 19, all day. T. C. Rains, R. K. Skogerboe. $10

^{13}C NMR Instrumentation
Nov. 19, 6–10 p.m. Ted Becker. $10

Liquid Chromatography
Nov. 21, all day. Hans Veening. $10

SAS Courses following. Contact: W. M. Ritchey, Case Western Reserve University, Cleveland, Ohio 44106

Modern Emission Spectroscopy
Nov. 16–17. Ramon Barnes

Fourier Transform Methods and Applications to Spectroscopy
Nov. 17–18. E. D. Becker

Coblentz following. Contact: J. J. Elliott, Exxon Research & Engineering Co., P.O. Box 121, Linden, N.J. 07036

Introductory Infrared Techniques Clinic
Nov. 20. $35, includes lunch

Liquid Chromatography Seminars
Free seminars will be held in various locations in the U.S. through Oct. and Nov. Covered will be new applications, high-speed, high-resolution GPC and on-stream injection at 6000 psi. *Contact:* Waters Assoc., Maple St., Milford, Mass. 01757. 617-478-2000

Pharmaceutical Analysis Workshops
Chicago, Ill., Oct. 2; Washington, D.C., Oct. 7; Philadelphia, Pa., Oct. 9; Saddle Brook, N.J., Oct. 11. *Contact:* Waters Assoc., Inc., P.O. Box 246, Milford, Mass. 01757. 617-478-2000

Drug Screening
Woodbridge, N.J. Oct. 2–4, Oct. 30–Nov. 2. $295. *Contact:* Center for Professional Advancement, P.O. Box 997, 20 Division St., Somerville, N.J. 08876. 201-722-8111

Recent Advances in Separation Techniques
Edison, N.J. Oct. 7–9. $295. *Contact:* Center for Professional Advancement, P.O. Box 997, 20 Division St., Somerville, N.J. 08876. 201-722-8111

Automatic Control and Applications
North Wales, Pa. Oct. 7–11. $260. *Contact:* D. S. Luppold, Leeds & Northrup, North Wales, Pa. 19454

Applied Polarized Light Microscopy
Chicago, Ill. Oct. 7–11. $325. *Contact:* McCrone Research Institute, 2820 S. Michigan Ave., Chicago, Ill. 60616. 312-842-7105

Photomicrography
Chicago, Ill. Oct. 14–18. $350. *Contact:* McCrone Research Institute, 2820 S. Michigan Ave., Chicago, Ill. 60616. 312-842-7105

Nuclear Magnetic Resonance
Philadelphia, Pa. Oct. 21–25. $275. *Contact:* Sadtler Research Laboratories, 3316 Spring Garden St., Philadelphia, Pa. 19104. 215-382-7800

Techniques of Infrared
Philadelphia, Pa. Oct. 21–25. $275. *Contact:* Sadtler Research Laboratories, 3316 Spring Garden St., Philadelphia, Pa. 19104. 215-382-7800

Identification of Small Particles
Chicago, Ill. Oct. 21–25. $325. *Contact:* McCrone Research Institute, 2820 S. Michigan Ave., Chicago, Ill. 60616. 312-842-7105

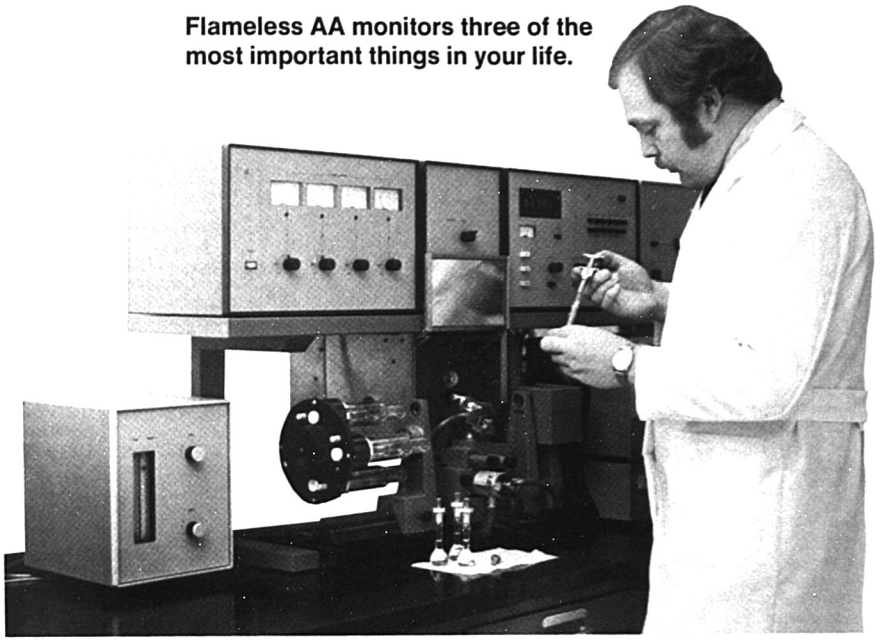
Liquid Analysis Instrumentation, Control, and Applications
North Wales, Pa. Oct. 21–25. $325. *Contact:* D. S. Luppold, Leeds & Northrup Co., North Wales, Pa. 19454

Basic Gas Chromatography
Philadelphia, Pa. Oct. 28–30. $200. *Contact:* Sadtler Research Laboratories, 3316 Spring Garden St., Philadelphia, Pa. 19104

Atomic Absorption
Springfield, N.J. Nov. 6–8, Nov. 13–15. *Contact:* Varian Instruments, #25, Route 22, Springfield, N.J. 07081

Air, Food, Water

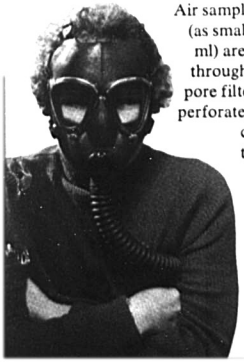
Flameless AA monitors three of the most important things in your life.



This new AA-6CS, *dedicated* to flameless atomic absorption, is *also dedicated* to scientists concerned with traces of toxic metals throughout the environment . . .

. . . in air

Monitoring toxic metals in the atmosphere from industrial plants and engine exhausts is vital to the environmentalist . . . and here's a new, easy, fast method. Air sample volumes (as small as 250 ml) are drawn through a Millipore filter in a perforated carbon cup, which is then placed in the AA-6CS and atomized. Within a minute, you know the concentration of lead, cadmium, or other toxic elements, in parts per billion!





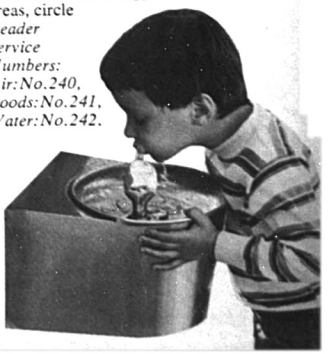
. . . in food

With the AA-6CS, analyzing for lead, cadmium, and other metals in fruits, vegetables and canned baby foods could be no easier! After minimum preparation (simple hydrolysis), sample is atomized and the toxic metal is measured in parts per billion; samples can be injected and analyzed every 90 seconds!

. . . in water

Direct determinations of toxic metals in water and effluents are simply and rapidly carried out on the standard AA-6CS. Little or no sample preparation is needed . . . and the analysis requires only microliter samples. Sensitivity is unmatched! To monitor water pollutants, select the leader in flameless AA . . . the AA-6CS from Varian Techtron!

For AA Methodology books on these areas, circle *Reader Service Numbers: Air: No.240, Foods: No.241, Water: No.242.*



varian

Varian Techtron
Palo Alto, Cal., U.S.A.
Georgetown, Ont., Canada
Zug, Switzerland
Springvale, Vic., Australia

If you use any of these gases



Send for the Specialty Gases and Equipment Catalog from Air Products

Acetylene
Air
Allene
Ammonia
Argon
Arsine

Boron Trichloride
Boron Trifluoride
Bromine Pentafluoride
Bromine Trifluoride
Bromotrifluoroethylene
1,3 Butadiene
Butane
1-Butene
cis-2-Butene
trans-2-Butene
cis- and trans-2-Butene

Carbon Dioxide
Carbon Monoxide
Carbonyl Fluoride
Carbonyl Sulfide
Carrier Gases
Chlorine
Chlorine Trifluoride
Chlorotrifluoroethylene
Cyanogen
Cyclopropane

Deuterium
Dimethylamine
Dimethyl Ether
2,2-Dimethylpropane
Doping Gases

Emission Control Gases
Ethane
Ethyl Acetylene
Ethyl Chloride
Ethyl Fluoride
Ethylene
Ethylene Oxide

Fluorine

Halocarbon—
11, 12, 13, 13B1, 14, 21, 22, 23, 113, 114, 114B2, 115, 116, 142B, 152A, C-318, 1132A
Helium
Hexafluoropropene
Hydrogen
Hydrogen Bromide
Hydrogen Chloride
Hydrogen Fluoride
Hydrogen Sulfide

Iodine Pentafluoride
Isobutane
Isobutylene

Krypton

Methane
Methyl Acetylene
Methyl Bromide
2-Methylbutene-1
2-Methylbutene-2
3-Methylbutene-1
Methyl Chloride
Methyl Fluoride
Methyl Mercaptan
Moisture Mixtures
Monoethylamine
Monomethylamine

Neon
Nickel Carbonyl
Nitric Oxide
Nitrogen
Nitrogen Dioxide
Nitrogen Trifluoride
Nitrogen Trioxide
Nitrosyl Chloride
Nitrous Oxide

Oxygen

Perfluorobutene-2
Perfluoropropane
Phosgene
Phosphine
Phosphorus Pentafluoride
Propane
Propylene

Research Grade Gases

Silane
Silicon Tetrachloride
Silicon Tetrafluoride
Sterilizing Gas Mixtures
Sulfur Dioxide
Sulfur Hexafluoride
Sulfur Tetrafluoride
Sulfuryl Fluoride

Tetrafluorohydrazine
Trifluoromethyliodide
Trimethylamine

Vinyl Bromide
Vinyl Chloride
Vinyl Fluoride
Vinyl Methyl Ether

Xenon

Zero Gases

...Plus customer specified gas mixtures and a complete line of regulators, valves, flowmeters and other accessory equipment.

(Detach and mail this convenient order form today)

Air Products and Chemicals, Inc.
Specialty Gas Department
P.O. Box 538, Allentown, Pennsylvania 18105

Please send the 113-page Specialty Gases and Equipment Catalog listing the industry's leading selection of specialty gases, gas mixtures, and gas handling equipment...available nationally from convenient stock points and 74 district offices.

Name/Title_____

Company_____

Address_____

City/State_____ Zip_____

Air Products and Chemicals INC.

Total Capability and Product Integrity

CIRCLE 6 ON READER SERVICE CARD

News and Views

Gas Chromatography
E. Brunswick, N.J. Nov. 11–13. $295. *Contact:* Center for Professional Advancement, P.O. Box 997, 20 Division St., Somerville, N.J. 08876. 201-722-8111

Industrial Moisture Measurement
S. Plainfield, N.J. Nov. 11–13. $295. *Contact:* Center for Professional Advancement, P.O. Box 997, 20 Division St., Somerville, N.J. 08876. 201-722-8111

Solvent Extraction & Ion Exchange
Edison, N.J. Nov. 11–15. $440. *Contact:* Center for Professional Advancement, P.O. Box 997, 20 Division St., Somerville, N.J. 08876. 201-722-8111

Instrumental Methods for Air and Water Measurements and Monitoring
Gaithersburg, Md. Dec. 14. *Contact:* R. B. Johnson, Materials Bldg. B-348, NBS, Washington, D.C. 20234

For Your Information

Rendering, June 1974, contains an article by Frank Burnham entitled, "Can Yesterday's Labs Do Tomorrow's Job?" The theme of this article is that the analytical and test requirements of the agriculture industry, including rendering, are growing beyond the capabilities of many small, independent labs and also many in-house labs. The cost of the new instrumentation and equipment required and the cost of highly trained personnel are apt to force many small labs out of business. The article cites the types of instruments, costs, etc., involved and suggests trends ahead.

IIT Research Institute has a newly designed facility for safely handling toxic and carcinogenic materials in research studies. The facility, located in Chicago, complies with OSHA and EPA regulations. The latter refer to air and liquid waste leaving the facility. The labs have been designed to serve organizations needing such facilities to work with toxic materials subject to OSHA regulations. Interested persons should contact IIT Research Institute, 10 West 35th St., Chicago, Ill. 60616. 312-225-9630

Du Pont Mass Spectrometers can tell you a lot from little samples.

Discover what makes marine mollusks move.

Using a Du Pont Mass Spectrometer equipped with a Multiple Specific Ion Detection (MSID) accessory, neurobiochemists are discovering what happens in the nerve impulse process by analyzing the ganglia of certain marine mollusks.

The MSID accessory gives Du Pont Mass Spectrometers ultra-high sensitivity and excellent specificity with little or no background noise.

Gas chromatography, for example, showed four different compounds eluted into a single peak. With MSID, however, four peaks are observed—indicating amino acid, alpha methyl amino acid, alpha methyl amine and a primary amine.



Robert Barber, City of Hope Hospital, Duarte, California, photographer

Tell the doctor what an O.D. victim can't.

An unconscious patient can't tell the doctor what's wrong, but a Du Pont Mass Spectrometer often can. Using the Chemical Ionization/Electron Ionization (CI/EI) Source accessory, for example, a hospital is able to analyze the extracted stomach contents of a drug overdose victim.

The CI/EI Source accessory provides additional data for those compounds which do not give molecular ions under EI conditions. Sensitivity is greatly increased by concentrating ionization in a single peak.

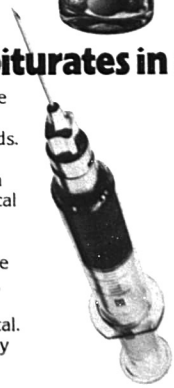
In this case, because CI spectra have few fragment peaks with large spaces between the peaks of interest, it was relatively simple to identify triamterene (M.W. 253), acetylcarbromal (M.W. 278) and benztropine (M.W. 307).



Identify barbiturates in an addict's blood.

Du Pont Mass Spectrometers produce clear, definitive spectra of even small amounts of unknown chemical compounds. Then, using the High Speed Disc Storage Data System accessory, these spectra can be compared with those of known chemical compounds for rapid, positive identification.

In a spectrum of a small blood sample taken from a barbiturate overdose victim, for example, two peaks were quickly identified as pentobarbital and secobarbital. But a third peak did not correspond to any known barbiturate.



The library search accessory identified it, however, as dibutyl phthalate—not a drug, but a plasticizer extracted from a piece of plastic lab apparatus by the solvents used to prepare the sample.

The ion counting interface between the Du Pont Mass Spectrometer and the Data System also gives greater sensitivity for small peaks from low level samples than the analog/digital converters used by most other instruments.

For more information on Du Pont Mass Spectrometers, write Du Pont Instruments, Room 23994, Wilmington, DE 19898.

DU PONT Instruments

REG. U.S. PAT. OFF.

CIRCLE 54 ON READER SERVICE CARD

Why pay £1,000 over the odds for Integrator facilities you may not need...

You won't with Infotronics

Infotronics integrators are built to a modular concept: this means your equipment can be tailored precisely to suit your application–and your budget. You don't pay for facilities you don't need; options can be added when required to existing equipment.

201: SINGLE CHANNEL PROCESSOR — £2250

Infotronic's latest processor incorporates tangential baseline calculations, and response factor entry. Programmable parameter controls optimise the instrument capability for each individual peak without operator intervention. Output is via a desktop calculator provided as standard: internal standard normalisation and multi-programme capability is optional.

204: INTEGRATOR WITH SELECTABLE PARAMETERS — £1895

Push button operation of seventeen parameters, choice of four input sources, and numerous options including tangential baseline calculations for rising and falling baselines and teletype decoder/controller. Price includes desktop calculator.

208: INTEGRATOR WITH PRESET PARAMETERS — £1550

For routine analysis with seven adjustable parameters and the rest preset, and options for tangential baseline calculations and teletype decoder/controller. Price includes desktop calculator.

Infotronics were the first to produce an electronic digital integrator. this long experience ensures reliability; and servicing, already fast because of the modular concept, is guaranteed within 48 hours in the U.K.

Find out more: use this publication's reader reply service, scribble 'Information please' on your letterhead and mail it to our Stockport Office, or better still, phone your nearest office today.



U.K. Infotronics (U.K.) Ltd., 230 Stockport Road, Cheadle Heath, Stockport 061-428 0405 telex 669205
Head Office: Infotronics Ltd., Shannon International Airport, Ireland (061) 61266 telex 6227
Other offices in Switzerland, Australia and U.S.A. Sales and service agents throughout the world.

Techmation is Infotronics in Benelux, France, Germany.

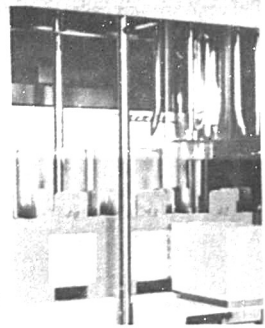
CIRCLE 131 ON READER SERVICE CARD

PRODUCT CAPSULES

Scan this list for products of interest. Then, circle the indicated numbers on the adjacent reply card and selected literature from advertisers in the previous issue will be sent to you.

No.	Product
301	Amplifiers; Power Supplies
302	Balances
303	Baths; Circulators
304	Books
305	Centrifuges
306	Chemicals; Reagents
307	Chromatography, Gas
308	Chromatography, Liquid
309	Chromatography, Thin Layer
310	Computers; Calculators
311	Cryogenic; Refrigeration
312	Elemental Analyzers
313	Filters
314	Furniture
315	Labware, Glass & Plastic
316	Lasers
317	Microscopes
318	Mixers; Stirrers; Blenders; Grinders; Mills
319	Nuclear Instruments
320	Ovens; Furnaces; Heaters
321	Photometers; Colorimeters
322	Polarographic Instruments
323	pH Meters; Ion Meters; Titrators; Electrodes
324	Pipets; Dispensers; Fraction Collectors
325	Recorders; Integrators
326	Pumps; Valves; Fittings
327	Spectrometers, Atomic Absorption
328	Spectrometers, Fluorescence
329	Spectrometers, Infrared
330	Spectrometers, Mass
331	Spectrometers, NMR
332	Spectrometers, UV/VIS
333	Spectrometers, X-Ray
334	Temperature Instruments
335	Thermal Analyzers
336	Vacuum Equipment

Make a manual titrator automatic.



Do it with the new Mettler DV Sample Transport System. It's designed to work with all Mettler titrator modules.

The pneumatically operated system can process 44 samples. Each sample is automatically indexed into position for titration. Once the system is set up, the operator can walk away from the equipment and return later to evaluate the results. In addition, if the equipment is interfaced with a desk-top calculator, all calculations are done automatically.

Mettler

Circle the number for full details.

CIRCLE 166 ON READER SERVICE CARD

FIRST CLASS
Permit No. 25682
Philadelphia, Pa.
19101

BUSINESS REPLY CARD
No postage stamp necessary if mailed in the United States

POSTAGE WILL BE PAID BY

ANALYTICAL CHEMISTRY
P. O. Box 8660
Philadelphia, Pennsylvania 19101

Analytical Chemistry

OCTOBER 1974

Valid through JAN. 31, 1975

NEW PRODUCTS, CHEMICALS, LITERATURE: 401 402 403 404 405 406 407 408 409 410 411 412 413 414 415 416 417 418 419 420 421 422 423 424 425 426 427 428 429 430 431 432 433 434 435 436 437 438 439 440 441 442 443 444 445 446 447 448 449 450 451 452 453 454 455 456 457 458 459 460 461 462 463 464 465 466 467 468 469 470 471 472 473 474 475 476 477 478 479 480 481 482 483 484 485 486 487 488 489 490 491 492 493 494 495 496

ADVERTISED PRODUCTS: 1 2 3 4 5 6 7 8 9 10 11 12 13 14 15 16 17 18 19 20 21 22 23 24 25 26 27 28 29 30 31 32 33 34 35 36 37 38 39 40 41 42 43 44 45 46 47 48 49 50 51 52 53 54 55 56 57 58 59 60 61 62 63 64 65 66 67 68 69 70 71 72 73 74 75 76 77 78 79 80 81 82 83 84 85 86 87 88 89 90 91 92 93 94 95 96 97 98 99 100 101 102 103 104 105 106 107 108 109 110 111 112 113 114 115 116 117 118 119 120 121 122 123 124 125 126 127 128 129 130 131 132 133 134 135 136 137 138 139 140 141 142 143 144 145 146 147 148 149 150 151 152 153 154 155 156 157 158 159 160 161 162 163 164 165 166 167 168 169 170 171 172 173 174 175 176 177 178 179 180 181 182 183 184 185 186 187 188 189 190 191 192 193 194 195 196 197 198 199 200 201 202 203 204 205 206 207 208 209 210 211 212 213 214 215 216 217 218 219 220 221 222 223 224 225 226 227 228 229 230 231 232 233 234 235 236 237 238 239 240 241 242 243 244 245 246 247 248 249 250 251 252 253 254 255 256 257 258 259 260 261 262

PRODUCT CAPSULES: 301 302 303 304 305 306 307 308 309 310 311 312 313 314 315 316 317 318 319 320 321 322 323 324 325 326 327 328 329 330 331 332 333 334 335 336 337 338 339 340

Name_____ Position_____

Company_____

Street_____

City_____ State_____ Zip_____

USE . . .

these postage paid reply cards for free data on all products advertised in this issue.

PRODUCT CAPSULES

Scan this list for products of interest. Then, circle the indicated numbers on the adjacent reply card and selected literature from advertisers in the previous issue will be sent to you.

No.	Product
301	Amplifiers; Power Supplies
302	Balances
303	Baths; Circulators
304	Books
305	Centrifuges
306	Chemicals; Reagents
307	Chromatography, Gas
308	Chromatography, Liquid
309	Chromatography, Thin Layer
310	Computers; Calculators
311	Cryogenic; Refrigeration
312	Elemental Analyzers
313	Filters
314	Furniture
315	Labware, Glass & Plastic
316	Lasers
317	Microscopes
318	Mixers; Stirrers; Blenders; Grinders; Mills
319	Nuclear Instruments
320	Ovens; Furnaces; Heaters
321	Photometers; Colorimeters
322	Polarographic Instruments
323	pH Meters; Ion Meters; Titrators; Electrodes
324	Pipets; Dispensers; Fraction Collectors
325	Recorders; Integrators
326	Pumps; Valves; Fittings
327	Spectrometers, Atomic Absorption
328	Spectrometers, Fluorescence
329	Spectrometers, Infrared
330	Spectrometers, Mass
331	Spectrometers, NMR
332	Spectrometers, UV/VIS
333	Spectrometers, X-Ray
334	Temperature Instruments
335	Thermal Analyzers
336	Vacuum Equipment

Analytical Chemistry **OCTOBER 1974** Valid through JAN. 31, 1975

NEW PRODUCTS, CHEMICALS, LITERATURE: 401 402 403 404 405 406 407 408 409 410 411 412 413 414 415
416 417 418 419 420 421 422 423 424 425 426 427 428 429 430 431 432 433 434 435 436 437 438 439 440 441 442
443 444 445 446 447 448 449 450 451 452 453 454 455 456 457 458 459 460 461 462 463 464 465 466 467 468 469
470 471 472 473 474 475 476 477 478 479 480 481 482 483 484 485 486 487 488 489 490 491 492 493 494 495 496

ADVERTISED PRODUCTS: 1 2 3 4 5 6 7 8 9 10 11 12 13 14 15 16 17 18 19
20 21 22 23 24 25 26 27 28 29 30 31 32 33 34 35 36 37 38 39 40 41 42 43 44 45 46
47 48 49 50 51 52 53 54 55 56 57 58 59 60 61 62 63 64 65 66 67 68 69 70 71 72 73
74 75 76 77 78 79 80 81 82 83 84 85 86 87 88 89 90 91 92 93 94 95 96 97 98 99 100
101 102 103 104 105 106 107 108 109 110 111 112 113 114 115 116 117 118 119 120 121 122 123 124 125 126 127
128 129 130 131 132 133 134 135 136 137 138 139 140 141 142 143 144 145 146 147 148 149 150 151 152 153 154
155 156 157 158 159 160 161 162 163 164 165 166 167 168 169 170 171 172 173 174 175 176 177 178 179 180 181
182 183 184 185 186 187 188 189 190 191 192 193 194 195 196 197 198 199 200 201 202 203 204 205 206 207 208
209 210 211 212 213 214 215 216 217 218 219 220 221 222 223 224 225 226 227 228 229 230 231 232 233 234 235
236 237 238 239 240 241 242 243 244 245 246 247 248 249 250 251 252 253 254 255 256 257 258 259 260 261 262

PRODUCT CAPSULES: 301 302 303 304 305 306 307 308 309 310 311 312 313 314 315 316 317 318 319 320
321 322 323 324 325 326 327 328 329 330 331 332 333 334 335 336 337 338 339 340

Name_____ Position_____

Company_____

Street_____

City_____ State_____ Zip_____

FIRST CLASS
Permit No. 25682
Philadelphia, Pa.
19101

BUSINESS REPLY CARD
No postage stamp necessary if mailed in the United States

POSTAGE WILL BE PAID BY

ANALYTICAL CHEMISTRY
P. O. Box #8660
Philadelphia, Pennsylvania 19101

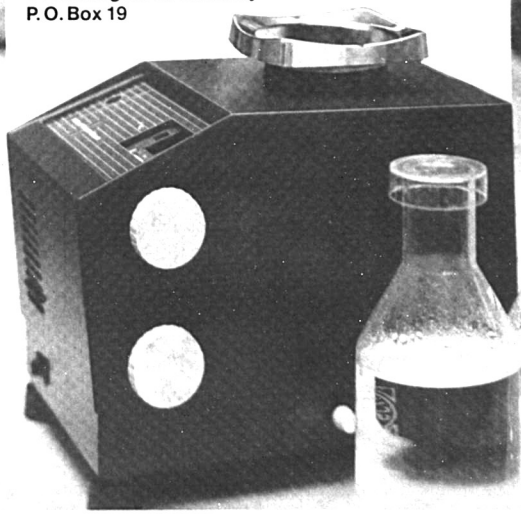
sartorius

Your new helper:
the Sartorius Precision Balance

unpacking - setting up - ready for action

If you're looking for a perfect and reliable helper – why not choose a Sartorius Precision Balance?
It's simplicity itself to handle, extremely versatile, and also saves you time and money.
What's more, it can be fully relied upon to produce accurate results for many years – no matter whether you have to weigh samples of 100 g or 7000 g, either to 0.001 g or 0.1 g precisely.
And it's attractive and well-proportioned. You want it to wear a dress in your favorite color? O.K.!
Ask for an on-the-spot presentation.
Because reliable helpers should always be engaged without hesitation.

Sartorius-Werke GmbH
34 Göttingen/W.-Germany
P.O. Box 19



CIRCLE 215 ON READER SERVICE CARD



GET THE CHEMTECH HABIT

and you won't be able to break it!

and you won't want to either . . . . because CHEMTECH is the lively, stimulating, innovative magazine that you'll read and use and refer to again and again . . .

You'll keep abreast of your own chemical discipline while being informed about others . . .

You'll be exposed to challenging new viewpoints and plain exciting concepts . . .

You'll hear from specialists and learn about their objectives and problems . . .

You'll have months of enjoyable and valuable reading . . .

and all for a very nominal sum.

You can start the rewarding CHEMTECH habit by just checking and returning the order form below. Sign up for three years and you'll save $14.00 and protect yourself against future price raises during the next three years.

Act today!



CHEMTECH
American Chemical Society
1155 16th Street, N.W., Wash., D.C. 20036

	U.S.	Canada, PUAS	Other Nations
* ACS Member, 1 year	☐ $9.00	☐ $13.00	☐ $14.00
Student	☐ $4.50	☐ $8.50	☐ $9.50
Nonmember, 1 year	☐ $18.00	☐ $22.00	☐ $23.00
Nonmember, 3 years	☐ $40.00	☐ $52.00	☐ $55.00

Name _____

Address ☐ Home ☐ Office _____

City _____ State _____ Zip _____

☐ Check enclosed ☐ Bill Company ☐ Bill Me

*ACS member rates are for personal use only.



SARGENT-WELCH INSTRUMENTATION

... when quality really matters

*NEW
XKR RECORDERS

- pH Meters & Electrodes
- Spectrophotometers
- Thermostatic Baths
- POLAROGRAPHS®
- Automatic Titrators
- Oscillometers
- Vacuum Pumps

Sargent-Welch Scientific Company, 7300 No. Linder Avenue, Skokie, Illinois 60076, (312) 677-0600
Anaheim / Birmingham / Chicago / Cincinnati / Cleveland / Dallas / Denver / Detroit / Springfield, N.J. / Toronto / Montreal

For more information about these instruments, circle No. 211 for pH Meters, & Electrodes, No. 212 for Recorders, No. 213 for Spectrophotometers, No. 214 for Thermostatic Baths, No. 215 for POLAROGRAPHS, No. 216 for Automatic Titrators, No. 217 for Oscillometer, No. 218 for Vacuum Pumps.

SPECTROSCOPY IN BIOLOGY AND CHEMISTRY

Neutron, X-Ray, Laser

edited by SOW-HSIN CHEN and SIDNEY YIP

CONTENTS: Introduction to Neutron, X-Ray, and Laser Spectroscopy. Quasielastic Scattering in Neutron and Laser Spectroscopy. Interatomic Forces, Molecular Structure and Molecular Vibrations. X-Ray Crystallography of Biological Molecules. Neutron Diffraction Studies of Hydrogen Bonding in Organic and Biochemical Systems. Comparative X-Ray and Neutron Diffraction from Nerve Myelin Membranes. Neutron Spectroscopy of Chain Polymers: A Critical Review of Polyethylene. Selected Chemical and Biological Applications of Neutron Inelastic Scattering. Neutron Scattering and Optical Studies of Molecular Vibrations. Small Angle Neutron Scattering from Polymers. Tunable Laser Resonance Raman Spectroscopy in Biology. Photon Correlation Spectroscopy in Biology.

1974, 420 pp., $15.00/£7.20

SCIENCE AND TECHNOLOGY OF SURFACE COATING

A NATO Advanced Study Institute on the Science and Technology of Surface Coating held at Imperial College, University of London, in April, 1972

edited by B. N. CHAPMAN and J. C. ANDERSON

As in many other scientific fields of study, there is a good deal of specialization in the techniques of surface coating. So much so, that most workers are familiar with only one or two of the many techniques now available for a very wide range of applications. The aim of this volume is to gather together concisely and under one cover, details of the whole range of surface coating techniques available—some currently in production and others still at the research stage. Although this work is primarily one of a reference nature, it also highlights areas of current research which have only lately appeared in research literature, such as harmonic electric spraying.

1974, 488 pp., $41.50/£14.80

THE DETERMINATION OF NITRO AND RELATED FUNCTIONS

by Y. A. GAWARGIOUS

Number 5 of The Analysis of Organic Materials, An International Series of Monographs

CONTENTS: The Determination of Nitro, Nitroso, and Azo Groups. Recommended Method of Analysis for Nitro, Nitroso, and Azo Groups. Determination of the Azide Group. The Determination of Nitrates and Nitramines. Recommended Methods of Analysis for Nitrate Goups.

1973, 162 pp., $9.75/£3.50

APPLICATIONS OF LIQUID SCINTILLATION COUNTING

by D. L. HORROCKS

CONTENTS: Introduction. Basic Processes. Scintillator Solutions. Liquid Scintillation Counters and Multiplier Phototubes. Particle Counting Techniques. Preparation of Counting Samples. Oxidation Techniques. Counting Vials. Background. Quench Correction Methods. Dual Labeled Counting. Chemiluminescence and Bioluminescence. Radioimmunoassay (RIA). Cerenkov Counting. Pulse Shape Discrimination. Flow Cell Counting. Large Volume Counters. Statistical Considerations.

1974, 364 pp., $29.50/£14.15

COMPUTERS IN CHEMICAL AND BIOCHEMICAL RESEARCH

VOLUME 2

edited by C. E. KLOPFENSTEIN and C. L. WILKINS

CONTENTS: Pattern Recognition in Chemical Research. An On-Line Graphics System as an Instructional Aid in Physical Chemistry. Laboratory Minicomputer Data Systems. Application of Computers in the Clinical Laboratory. Transient Recorders in Automated T-Jump/Stopped-Flow Equipment and Rapid-Scanning Spectrometers. Computers and Automation in Chromatography. Computer Interfacing and Control in Gas Chromatography.

1974, 288 pp., $25.00/£12.50

CHEMICAL ANALYSIS OF ORGANOMETALLIC COMPOUNDS, VOLUME 1

by T. R. COMPTON

Number 4 of The Analysis of Organic Materials, An International Series of Monographs

This book (the first of three volumes) deals with the compounds of lithium, sodium, potassium, copper, silver, gold, beryllium, magnesium, calcium, zinc, cadmium, mercury, boron, gallium and thallium. Each chapter provides a complete review of all aspects of the organo-compounds of the element in question, together with critical comments on the relative importance, merits and demerits of the methods of analysis applicable. Each chapter discusses the determination of the elements and functional groups concerned, and includes sections describing the different techniques—including gas chromatography and spectroscopy—available for the analysis of the different classes of compounds of the elements concerned. Where relevant, sections on topical subjects are included, such as the determination of boron hydrides and organomercury compounds in the environment.

1974, 268 pp., $16.25/£5.80

ACADEMIC PRESS, INC.

A Subsidiary of Harcourt Brace Jovanovich, Publishers
111 FIFTH AVENUE, NEW YORK, N. Y. 10003
24-28 OVAL ROAD, LONDON NW1 7DX

CIRCLE 1 ON READER SERVICE CARD

Plethora of Information on Nonaqueous Chemistry

Physical Chemistry of Organic Solvent Systems. A. K. Covington and T. Dickinson, Eds. x + 823 pages. Plenum Publishing Corp., 227 West 17th St., New York, N.Y. 10011. 1973. $30

Reviewed by I. M. Kolthoff, Department of Chemistry, University of Minnesota, Minneapolis, Minn. 55455

The editors start the preface as follows: "We believe this to be the first monograph devoted to the physicochemical properties of solutions in *organic solvent* systems (italics by me). Although there have been a number of books on the subject . . . ." Advancement of techniques and of the theory of nonaqueous analytical, inorganic, and organic chemistry demands an understanding of and acquaintance with nonaqueous physical chemistry. For this reason, the present monograph, which is primarily concerned with physical chemistry of electrolytic solutions, is of great usefulness to all chemists interested in nonaqueous chemistry.

Each of the seven chapters presents a concise, critical, and clear discussion of the physical chemistry of a particular subject (property) with a generous number of tables giving numerical data, comments on technique, and interpretation of results. At the end of most chapters an appendix tabulates selected numerical data. Both text and appendix contain an abundance of references to the literature. Actually, this book is a collection of a large number of monographs. To impress the reader with the wealth of information to be found, the following breakdown of "contents" is given.

Chapter 1. **Introduction and Solvent Properties** (also includes purification) by A. K. Covington and T. Dickinson, 17 pages; appendix, 4 pages

Chapter 2. **Thermodynamic Measurements.** Part I, Solubility, Calorimetry, Volume Measurements, and Viscosities by C. M. Criss, 104 pages (treatment of experimental data, 12 pages; results, 25 pages; 208 references, 5 pages; appendix, 63 pages). Part 2, Electrochemical Measurements by M. Salomon, 84 pages (52 pages text, 31 pages appendix). Part 3, Precision Cryoscopy by R. Garnsey and J. E. Prue, 31 pages. Part 4, Interpretation of Thermodynamic Data by C. M. Criss and M. Salomon, 65 pages; appendix, 10 pages

Chapter 3. **Acid-base Behaviour** by E. J. King, 57 pages (266 references); appendix, 16 pages

Chapter 4. **Spectroscopic Measurements.** Part 1, Electronic Absorption Spectroscopy by I. R. Lantzke, text, 27 pages. Part 2, Infrared and Raman Spectroscopy by D. E. Irish, 26 pages. Part 3, ESR Spectroscopy by T. E. Gough, 21 pages. Part 4, NMR Spectroscopy by I. R. Lantzke, 38 pages

Chapter 5. **Conductance and Transference Numbers.** Part 1, Conductance by R. Fernandez-Prini, text, 60 pages (247 references); appendix, 27 pages. Part 2, Transference Numbers by M. Spiro, text, 54 pages; appendix, 21 pages. Part 3, Ionic Conductances by M. Spiro, text, 24 pages (181 references); appendix, 11 pages

Chapter 6. **Reaction Kinetics and Mechanism** by D. W. Watts, text, 56 pages (253 references)

Chapter 7. **Electrode Processes.** Part 1, The Electric Double Layer by R. Payne, 12 pages. Part 2, Electrode Reactions by D. R. Brown, 33 pages

Subject Index, 40 pages. Considering the broad scope of this text, this extensive index is particularly welcome.

Depending on his field of specialization, the analytical chemist will find that all chapters contain much of interest. For the electroanalytical chemist, Chapters 5 and 7 are of particular interest, whereas the specialist in acid-base titrations finds much valuable information in King's excellent chapter, "Acid-base Behaviour." Although nothing but deserved praise has been expressed so far, it is customary in a review to mention some shortcomings. In a book of such a broad scope as this, one is likely to find topics which, although they deserve attention, are not mentioned. For example, resolution of acid band base strength, dimsyl solutions in DMSO, and diprotic acids are not discussed in Chapter 3.

The exceptionally low price of this outstanding book is such that workers in the field of nonaqueous chemistry will want to own a copy. This reviewer will keep a copy on his desk for regular consultation.

Nonaqueous Electrolytes Handbook, Vol I. G. J. Janz and R. P. T. Tomkins. xiii + 1108 pages. Academic Press, Inc., 111 Fifth Ave., New York, N.Y. 10003. 1972. $55

Nonaqueous Electrolytes Handbook, Vol II. G. J. Janz and R. P. T. Tomkins. xiii + 933 pages. Academic Press, Inc., 111 Fifth Ave., New York, N.Y. 10003. 1974. $60

Reviewed by I. M. Kolthoff, Department of Chemistry, University of Minnesota, Minneapolis, Minn. 55455

This two-volume handbook, covering more than 2000 pages, is a welcome source of information to all workers in nonaqueous chemistry. Volume I gives numerical data in the following areas: physical properties of solvents, a 17-page nonnumerical section on solvent purification, electrical conductance, diffusion, density, viscosity, transference numbers, and additional references and data sources. It covers the literature to 1972 and includes data for 210 solvents and 650 electrolytes.

Volume II covers the areas: solubilities (including solubility products) of electrolytes, EMF and potentiometric titrations, vapor pressure, cryoscopy,

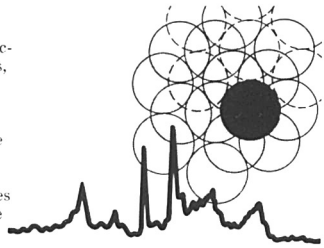
heats of solution, polarography, ligand-exchange rates and electrode reactions, electrical double layer, spectroscopy and structure of electrolytes, organic electrolyte battery systems, and additional references and data sources. This last section not only updates some of the tables in Volume I and presents data with references which had been omitted in Volume I but also contains additional references relative to various sections in Volume II. For the user of the handbook, it would have been preferable to have this appendix available in loose form in two sections, one for Volume I and one for Volume II.

The method of presentation and the symbols used are explained in the preface to each section. Each volume concludes with a compound index, one by solvent and one by solute. "Nonaqueous" refers to organic solvents and their mixtures or mixtures with water; inorganic solvents and fused salts are not considered.

The section on electrical conductance covers 745 pages with six subsections. Some obvious errors in some of the tables may be pointed out, e.g., in the first subsection each table has, among others, one heading, "specific conductance (mho·cm^{-1}) $\times$ 10^8," but in some instances "10^8" has been ignored (e.g., dioxane is listed as 5×10^{-7}, probably instead of 50).

The analytical chemist will find much of interest in these volumes, particularly in the section on EMF data (205 pages) which concludes with three subsections on potentiometric titrations, and in the section on polarography (also 205 pages) which, with "Electrical Double Layer," logically could have followed the EMF section. Since it is impossible to cover potentiometric titrations within a reasonable number of pages, reference is made in a footnote of the preface to W. Huber's book and to the Analytical Reviews in ANALYTICAL CHEMISTRY. This reviewer regrets that no reference is made to the monograph by I. Gyenes which is the most complete to be found in the literature. A more logical and space-saving arrangement of numerical data in the section "Polarography" would have been possible.

These comments do not detract from the great value of having together in the handbook almost complete data of physicochemical properties reported in the widely scattered literature. The editors and the contributors deserve the gratitude of chemists working in the field. The handbook would also be a very helpful source of information for an enterprising scientist who would want to enrich the literature with a set of critically selected data.



Vibrational Spectroscopy of Trapped Species

Edited by
H. E. HALLAM

Survey of Studies from IR to Laser Raman

Vibrational Spectroscopy of Trapped Species. H. E. Hallam, Ed. xii + 430 pages. John Wiley & Sons, Inc., 605 Third Ave., New York, N.Y. 10016. 1973. $29.50

Reviewed by Edward G. Brame, Jr., Elastomer Chemicals Department, E. I. du Pont de Nemours & Co., Wilmington, Del. 19898

According to G. C. Pimentel who wrote the foreword to this book, "the matrix isolation method has now been in active development for almost two decades" but "the method has undoubtedly had its greatest impact in the infrared spectral studies, the subject of this book." The editor writing in the preface states that "this monograph is intended to provide a survey of studies of the vibrational spectra of species trapped in solid matrices." Nine chapters are included in the book. They cover not only the infrared studies that were pioneered by Pimentel and Porter in the early 1950's, but also the more recent developments using laser Raman spectroscopy.

The first chapter in the book covers the background of the method and also a summary description of the other chapters. It was written by the editor. The next chapter, also written by the editor and a colleague at the University College of Swansea, covers the different experimental methods that can be used in performing the infrared or Raman studies at low temperatures. Then, in Chapter 3 the editor describes in a rather extensive way the different infrared studies that have been performed on molecules trapped in low-temperature matrices. Beginning with a description of the matrix effects involved, he goes on to describe the studies performed on diatomic, triatomic, tetra-atomic, and polyatomic molecules. Chapter 4 was written by another colleague at the University College of Swansea, A. J. Barnes, on the theoretical aspects of matrix effects. He describes the various interactive effects which can cause vibrational shifts, for example.

Chapter 5, written by L. Andrews of the University of Virginia, covers the infrared spectra of free radicals and chemical intermediates that can be observed by this method of trapping them in low-temperature matrices. The next chapter, written by A. Snelson of the Illinois Institute of Technology, describes the work that has been done on various halides, oxides, hydroxides, metaborates, nitrates, etc., by infrared following the vaporization of these molecules from being trapped in low-temperature matrices. Chapter 7, written by W. F. Sherman and G. R. Wilkinson of King's College in London, describes the infrared and Raman studies that have been performed on impurities in ionic and covalent crystals. In addition, they make a broad distinction in their discussion between point or atomic defects in a solid which are the defect-distorted vibrations of that solid and polyatomic defects which are the defect-distorted vibrations of the solid, plus those extra effects resulting from their intrinsic vibrational and rotational motion.

Chapter 8, by D. C. McKean of the University of Aberdeen, describes in a rather short account the work that has been done by infrared and Raman on clathrates. The term clathrate is defined as that condition when a small molecular species, the "guest," is enclosed completely within a cage by a crystal lattice of the "host" species. Examples and results are given in the account. Chapter 9 (the last), written by G. A. Ozin of the University of Toronto, covers the use of Raman spectroscopy in matrix isolation. It includes the advantages, the limitations, and the results that can be obtained from the use of this method.

The book gives a good account of the work that has been done in the field of infrared and Raman studies of trapped species. There are few errors. One I noticed is that the sentence on top of page 122 does not follow directly from the end of the sentence at the bottom of page 121. The book can be recommended to anyone interested in the field as well as those involved in cryo studies.

Books

Collection of Articles on CAI for Chemists

Computer-Assisted Instruction in Chemistry, Part A: General Approach. James S. Mattson, Harry B. Mark, Jr., and Hubert C. MacDonald, Jr., Eds. xi + 271 pages. Marcel Dekker, Inc., 270 Madison Ave., New York, N.Y. 10016. 1974. $24.50

Computer-Assisted Instruction in Chemistry, Part B: Applications. James S. Mattson et al., Eds. xv + 258 pages. Marcel Dekker, Inc., 270 Madison Ave., New York, N.Y. 10016. 1974. $26.50

Reviewed by Harry E. Keller, Department of Chemistry, Northeastern University, Boston, Mass. 02115

The area of computer-assisted (or aided or augmented) instruction, CAI, is growing rapidly as the cost of hardware plummets and software sophistication increases. Because of these two factors, educators should familiarize themselves with the use of computers as an adjunct to the instructional process. The two-part volume reviewed here provides a good introduction to the various facets of CAI and could well be used by anyone desiring to know its capabilities and limitations over a broad span of applications in chemistry education.

The chapters are individually authored, primarily by people with experience in CAI. They give many examples from their own experience of how CAI can be used and frequently include sample computer programs. The editors caution the reader that there may be some overlap between chapters, and it is surprising how little overlap actually occurs. There are many separately authored sections, and they are discussed separately here. Both parts of the volume are included in this review, but the reader should recognize that they are available separately.

Part A begins with a very short chapter which serves as an introduction to the volume. Chapter 2 is long and thorough. Replete with examples, it presents many approaches to the use of computers for curriculum enhancement. Costs are analyzed, and a good case is made for teaching students to program in an interactive language.

For those having analog computer systems available, Chapter 3 provides an in-depth discussion of the principles of analog and hybrid computation. Before reading the chapter, one should become familiar with the symbols in the appendix. Also, the author leaves teaching applications, for the most part, to the imagination of the reader.

The fourth chapter is called "Online Classroom Computing," but might have been called "Computation as a Lecture Aid." After a nuts-and-bolts section on how to display computer output in the classroom and the values of such display, a number of computer programs are shown and discussed. The lecture display of printed computer output in an interactive mode can reduce the student-hour load on CAI and, occasionally used, can stimulate increased lecture participation by students. Nevertheless, this reviewer believes that direct student interaction is likely to have a greater positive effect on performance and is to be preferred when possible.

The chapter on information storage and retrieval is well-written and covers the subject from the user point of view. Although such knowledge is useful to chemists, it is unclear how it fits into a book on CAI. The editors state, "As the volume of chemical literature is expanding at an enormous rate, it is important that computerized information storage and retrieval practice . . . be introduced to the students . . . ."

The last chapter in Part A analyzes the cost of a 150-terminal CAI system. The result is about $1.02 per terminal hour for the parameters used.

In summary, the meat of Part A is in Chapters 2–4, and if you have no analog system, you probably will be reading Chapters 2 and 4 for their practical values and the others only for general interest. If you do not have experience in CAI and are contemplating entering the area, you will find the information stimulating and helpful. However, you may find Part B of Volume Four even more so.

Part B is subtitled "Applications." For the individual who has a time-shared computer system available and wants to use it to augment the teaching process, Part B offers practical suggestions and examples based on considerable experience. While each chapter relates examples demonstrated on a specific system, it is clear that the approaches presented are implementable on several systems. Thus, the knowledge gained by reading Part B falls into two areas: types of computer systems available for CAI and examples of uses to which CAI systems can be put.

The first chapter describes the application of APL to analysis of laboratory experiment results. Rapid feedback to the student on the results of an experiment appears to be beneficial, and the computer can do the grading and record-keeping too. The second chapter describes PLATO, a computer-based teaching system. The application is organic chemistry instruction. Ideas on CAI in organic chemistry as well as general lesson-planning strategies for PLATO-like systems are given. The next chapter discusses physical chemistry instruction using FORTRAN. Together, these three chapters constitute Section I of Part B.

Section II includes several uses of the computer to provide an extra dimensionality to teaching. These include repeatable tests, homework preparation and grading, use of prepared programs by students, and organic qualitative analysis simulation. None of these uses of computers is likely to strain or cramp the teaching situation. Ideas from all of the chapters in Section II can be merged and used in a single course. The writing is generally clear in this section, and there are sufficient examples to illustrate the concepts presented.

Overall, this two-part Volume Four of "Computers in Chemical Instrumentation" is well written and informative. Part B appears to contain a greater quantity of useful material. There are many typographical errors, but this reviewer had no difficulty in resolving them. It is good to have a collection of articles on CAI for chemists such as this one available, and it would be even better if it were widely read and the ideas put into practice.

Seventy Percent New or Revised Material

Interpretation of Mass Spectra. Second edition. F. W. McLafferty. xix + 278 pages. W. A. Benjamin, Inc., Reading, Mass. 01867. 1973. Paperbound. $7.50

Reviewed by K. Biemann, Department of Chemistry, Massachusetts Institute of Technology, Cambridge, Mass. 02139

The second edition of McLafferty's introductory text to the interpretation of mass spectra reflects the polishing effect of the use of the first edition in the many short courses the author has conducted during the past few years and for which it was originally written. The publisher's description states that this revised, enlarged, and reset edition consists of 70% of new or substantially revised material. This has been accomplished without changing the general outline, trend, and philosophy. The changes enhance the clarity of the discussion, add some different and better examples, and incorporate findings and developments that have occurred in this fast moving field since the first edition went to press.

The volume was increased from 230 to 278 pages which, when combined with the slightly larger format of the

book, gives a good estimate of the larger content. Fortunately, the author has made a determined effort not to merely add all the new information that has become available, but rather to select those aspects that are most important for the purpose of this book. To a certain extent the choice also reflects his personal interests, such as the theoretical aspects of unimolecular ion decomposition reactions (Chapter 8), which may be of little interest to the majority of the audience to which the book is directed, while relegating important new experimental developments like chemical ionization mass spectrometry to a single paragraph hidden under the heading "Other techniques for molecular weight determination" and given the same attention as the use of the rate of effusion, an obscure special purpose technique.

The most useful parts of this book are the large number of well-chosen examples of spectra that are discussed in detail, as well as the unknowns for which the solutions are discussed in equal detail in Chapter 9. One may at a first glance feel that the examples are too simple, because the vast majority of the compounds are of molecular weight less than 200, and indeed a large fraction are below 100. But one has to keep in mind that this text is directed mainly at those who have little or no prior experience in the interpretation of mass spectra but wish to acquire it through a short course or on their own, in addition to its use in introductory undergraduate or graduate courses. Once someone has gone through all the examples and mastered all the unknowns, he will certainly be in a position to successfully interpret his own mass spectra.

The practitioner will easily notice that all the spectra shown in the book are those of pure compounds carefully recorded and edited and accompanied by tabular relative abundance values down to 0.01%. This is rarely achieved in practice but is necessary if one follows the author's approach of first calculating the elemental composition of the molecule from its isotope peaks. Although the relationship of the abundance of the isotopic species to the number and kind of elements in the molecule is discussed in every textbook, one finds in practice that mass spectra determined under realistic laboratory conditions are generally unsuitable for this purpose.

It is understandable that this approach is used for didactic purposes in this book which addresses itself to classroom situations relatively detached from the chemical inferences of the problem at hand. Thus, while the user will soon find that the assignment of elemental formulas discussed in Chapter 2 is highly unreliable for the direct computation of the number of carbons, nitrogens, and oxygens for a molecule of reasonable complexity, he will realize that the background information that is always available, for example, the origin and the chemical characteristics of the sample, provides other input which narrows down the possible compositions for a particular molecule. The reader will be able to make that transition when he starts to work on experimental mass spectra if he has avoided becoming too dependent on the computation of elemental formulas from isotope peaks.

As in the first edition, a good part of the text is devoted to the fragmentation processes, but these are now greatly expanded and arranged in Chapter 6 according to common compound classes. This chapter, which covers 80 pages, now makes it much easier for the reader to appreciate the structure specificity of mass spectra.

In general, the book is clearly written and relatively free of typographical errors. One may argue with some of the statements like the requirement that the molecular ion must be the ion of highest mass in the spectrum and that it must be an odd-electron ion. First, the isotope peaks are of higher mass, and second, the number of electrons cannot be determined from the mass spectrum of an unknown compound; thus, one cannot use it in the identification of the molecular ion. Most of the typographical errors are recognizable by the reader without confusion and range from the misplacing of arrows or dots indicating electrons to missing atoms like a nitrogen in Equation 6-52. More puzzling may be the statement that toluene-d_1 yields an ion $C_7H_5D_2$ (page 193). The references are a curious mixture of books, chapters, and review articles and references to original papers sometimes in obscure and unaccessible journals. The former may guide the reader who wishes to go beyond what is discussed in the text. The latter appear randomly chosen and often do not refer to the most complete or original publication.

This second edition of the "Interpretation of Mass Spectra" will, like the first, be the textbook of choice for introductory courses or for a reader who wishes to become familiar with the interpretation of mass spectra in the course of his own work. In spite of the large number of books dealing with mass spectrometry, McLafferty's is by far the most useful one for this purpose. The author has clearly summarized the basic principles and illustrated them well with abundant simple examples. In general, he managed not to be sidetracked by the details which would intrigue the advanced worker in this field but only confuse the beginner to which this book is successfully directed. The admirably low price of the book will further aid its use and distribuion.

On the Instruction of Laboratory Managers

Laboratory Organisation and Administration. K. Guy. xi + 527 pages. Crane, Russak & Co., Inc., 52 Vanderbilt Ave., New York, N.Y. 10017. 1973. $22.50

Reviewed by Edward C. Dunlop, Central Research Department, E. I. du Pont de Nemours & Co., Wilmington, Del. 19898

This book deals with the organization and administration of laboratory facilities for instruction of laboratory managers. It is a second edition, and I am unfamiliar with the earlier book. The first three chapters are concerned with equipment and material for the construction of a laboratory building. They represent a fairly good summary, but more up-to-date information can be obtained from equipment suppliers. The description of laboratory services is fairly good, but one noticeable omission is the use of a steam vacuum jet for the laboratory vacuum system. The section on stores items includes a number of unusual things such as shipping instructions, handling of live animals, and postal regulations. However, these would not be pertinent for the United States. A table on available filter papers is a good source of information.

Chapters 4–6 deal with reagents and laboratory maintenance and safety; a number of excellent points are recorded for the teaching of individuals who look forward to having the responsibility of maintaining university science buildings. The reference to perchloric acid does not appear to be sufficient to insure safe use by university students or inexperienced personnel. In general, the chapter on safety is good, and especially the tables on disposal of chemicals represent an important collection.

The section on special needs of a teaching laboratory covers items of personal equipment, some special facilities, and recovery of some expensive items such as silver, platinum, and mercury.

A chapter is devoted to optical projection which is complete but probably more than required for this type of book. It gives a variety of projection techniques, but normal laboratories

It's time someone got specific about LC solvents.

We did.



Up to now, solvents for liquid chromatography really haven't been for liquid chromatography. They were fine solvents, but you paid high prices for unneeded properties.

Now, Mallinckrodt's new *ChromAR*® *Solvents* put an end to this.

ChromAR Solvents are specific for liquid chromatography. The first line of solvents developed, use-tested, controlled and priced particularly for LC.

ChromAR Solvents have: Uniform low UV absorbance. Uniform refractive index. Uniform polarity. Uniform viscosity. And for ready reference, these values are even on our bottle labels. That's how specific we are.

ChromAR Solvents. Specifically for liquid chromatography. Also excellent for column and thin-layer chromatography.

Available at Mallinckrodt distributors nationwide. Call yours to place an order, or write us for technical data.

Mallinckrodt

SCIENCE PRODUCTS DIVISION
Saint Louis, Missouri 63147

CIRCLE 167 ON READER SERVICE CARD

Mallinckrodt, Inc.
Science Products Division
P.O. Box 5439
Saint Louis, Missouri 63147

Send technical data on *ChromAR*® *Solvents*.

Name _____

Title _____

Company _____

Street _____

City _____ State _____ Zip _____

Books

would not have this general requirement. Records, demonstrations, and exhibits are described briefly to show what is required in maintaining a laboratory.

The remainder of the book has to do with the training of technicians, how to keep experimental records, and the use of technical literature. These are brief but present enough on the subject to give the basic material required.

The book will be most valuable for the person who has no experience and finds himself in the position of having to plan for a laboratory building. I was disappointed that the author did not include more information on technical administration and believe the experienced laboratory person will find this book of little use.

New Books

Advances in Nuclear Quadrupole Resonance, Vol 1. J. A. S. Smith, Ed. xv + 434 pages. Sadtler Research Laboratories Inc., Book Division, 3316 Spring Garden St., Philadelphia, Pa. 19104. 1974. $39.50

The first volume of this new review series devoted to all aspects of chemical, physical, and theoretical nuclear quadrupole spectroscopy presents the papers given at the International Symposium on Nuclear Quadrupole Resonance, September 28–29, 1972, Queen Elizabeth College, University of London, England. Major topics covered include halogen resonances, structure and molecular motion, instruments and new techniques, conformational effects, lattice effects, metal resonances, deuteron quadrupole coupling constants, and ^{14}N quadrupole resonance. Attention is paid to the increasing importance of NQR in inorganic chemistry without detracting from the applications in organic and biochemistry.

Quantitative Thin Layer Chromatography. Joseph C. Touchstone, Ed. xiv + 330 pages. John Wiley & Sons, Inc., 605 Third Ave., New York, N.Y. 10016. 1973. $14.95

This multi-authored volume is based on material presented at a symposium on quantitative thin layer chromatography held in Philadelphia in December 1970 and a similar symposium sponsored by the American Oil Chemist's Society in November 1971. To make the book more complete, new authors and subjects were added. The text is reproduced from typed copy.

Systematic Materials Analysis, Vol 1. J. H. Richardson and R. V. Peterson, Eds. xix + 363 pages. Academic Press, Inc., 111 Fifth Ave., New York, N.Y. 10003. 1974. $28

This multivolume work is intended to provide a central source of information on the latest techniques available to materials analysts and to give the reader both theoretical and practical knowledge of a broad range of instrumental methods for a complete analysis. The initial chapter focuses on the selection of analytical methods based on specimen limitations and the information desired. Detailed flow charts list and arrange the entire spectrum of analytical instrumentation to permit the selection of the best method(s). Subsequent chapters focus on specific instruments with emphasis on the practical application of each method, including sample requirements, selectivity, sensitivity, and data output. This first volume covers alpha-particle spectrometry, Auger electron spectrometry, electron diffraction – high energy (HEED) and low energy (LEED), electron microprobe, electron paramagnetic resonance spectrometry, fluorometry, infrared spectrometry, and liquid chromatography.

Batteries, Vol 1: Manganese Dioxide. Karl V. Kordesch, Ed. xi + 566 pages. Marcel Dekker, Inc., 270 Madison Ave., New York, N.Y. 10016. 1974. $47.50

The progress in technology of batteries in the past 10 years has prompted the editor of this series to collect and publish the available information. According to the editor, "This specialized literature is often difficult to obtain, even for technical men. A critical selection is necessary to avoid getting lost in the details." The first volume, "Manganese Dioxide," is dedicated to the most important primary battery system. The text is reproduced from typed copy.

SSIE Research Information Packages

To order the following, write to SSIE, Inc., Room 300, 1730 M St., N.W., Washington, D.C. 20036. (Include code number and title. Add 10¢ postage and handling for orders outside the U.S., Canada, or Mexico.)

FC01S Chemical Information Storage and Retrieval: Chemical compounds classification, chemical structure indexing, computerized chemical information processing systems, chemical data compilation, etc. $35

JK08S Research and Development of Advanced Data Acquisition Systems. $35

KC04S Interface and Technology Studies of Systems for Data Transmission. $35

KC12S Digital Encoding Systems and Digital Computer Simulation for Automatic Pattern Recognition Systems. $35

KC23S Software for Analog-to-Digital or Digital-to-Analog Conversion Studies: AD or DA converter applications. $35

KC37S Interfacing between Computer and Peripheral Equipment. $25

BA13S Bioindicators of Water Quality in Freshwater Lakes and Reservoirs. $35

FA05S Oil Pollution Cleanup: Analysis, separation, and removal of oil from sources such as spills, industrial wastes, etc. $45

FA12S Determination of Organic Substances in Natural Water: Detection and analysis of pesticides, oil, hydrocarbons, etc. $45

FA13S Mercury as a Water Pollutant: Analytical techniques for the detection of Hg levels in fish and water, physiological effects on fish, and potential as a human health hazard. $45

FA14S Lead as a Pollutant: Analysis and removal of lead from air, water, or wastes, plus the sources of the pollutant and related biological studies. $45

FA15S Chemical Oxygen Demand. $35

FA23S Nitrilotriacetic Acid: Analysis, effects, and fate in waters. $35

FA62S Oxides of Nitrogen in Air Pollution: Detection, control, and photochemical reactions involving nitrogen oxides in air pollution. $45

FA65S Sulfur Dioxide in Air: Analysis and removal of sulfur oxides from air by various chemical and physical processes. $45

FL01S Chemiluminescence. $35

FL07S Pulse Radiolysis. $25

FN06S Ion-Exchange Systems: Theory and applications. $45

LA34S Particulate Air Pollutants: Instrumentation and techniques for the detection, sampling, analysis, and control of solid effluents in the atmosphere owing to automobile and power plant emissions, incineration, and various industrial processes (including dust in mine atmospheres). $55

LA35S Atmospheric Sampling and Analytic Devices for Monitoring and Detection of Pollutants. $35

The case for Concentrated Buffers



For your amino acid analysis, have you considered concentrated buffers in the sodium and lithium concentrate forms. There are four good reasons for doing so:

1. They save time, because they're ready for use in minutes. No long hours of preparing and testing a batch.

2. They save money because there is no waste of reagents; no bad buffers; no loss of analysis.

3. They save space, because they take up only 1/5 the space required for diluted buffers.

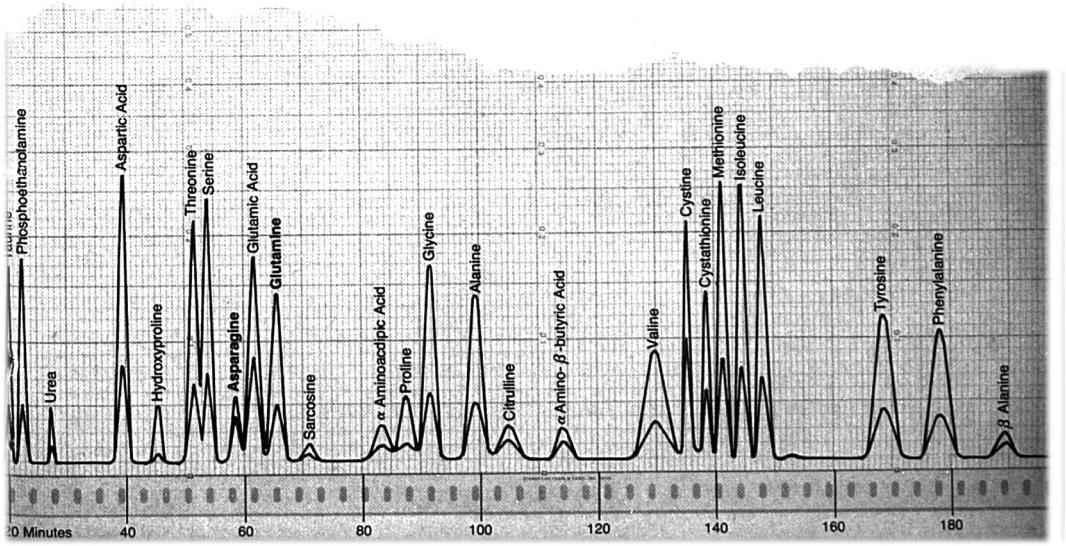
4. They resist mold and contamination in their sealed bottles.

Hamilton concentrated buffers are useful for more than 20 proven chromatographic separations, such as the one below — which was separated with only two buffers in 200 minutes.

We'll be happy to supply our proven methods on request. For more information about Hamilton Concentrated Buffers, write to Hamilton Company, Post Office Box 17500, Reno, Nevada 89510.

HAMILTON

CIRCLE 117 ON READER SERVICE CARD



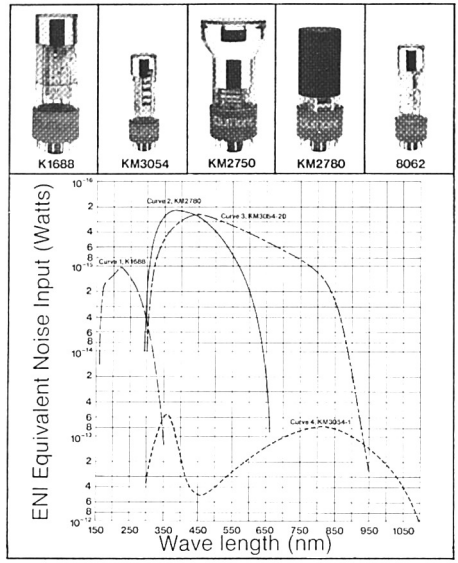
A subsidiary of THOMSON-CSF

How to get low noise at low cost.

We have a whole family of photomultiplier tubes that share one very important family trait; they all provide optimal signal-to-noise ratios and maximum performance-to-dollar ratios at the same time.

One of the better ways to assess PMT performance is its ENI figure* at a specified wave length and an ambient temperature of 25°C, as shown in the graph. For example, our PMT model KM1688 (which is designed to operate in the spectral range from 1600—2600 A°,) is unsurpassed in ENI performance by any comparable PMT, and will meet the most frugal price-to-performance criteria.

The KM1688 is only one example of the kind of performance you can expect from our large family of low noise, low price PMTs. For complete information on any or all of them, contact:



PMT Application Engineering Group, 750 Bloomfield Avenue, Clifton, New Jersey 07015, (201) 773-2000. DuMont

Model	Spectral Range (nm)	Nominal Cathode Diameter	Photo Cathode	* ENI at Peak Sensitivity (watts)	Peak, Cathode Sensitivity (ma/w)	Typical Aged Dark Current at 5×10^5 Gain (amperes)	ENI Factor
K1688	160—260	1¾″	Rb_2Te (S23)	1.05×10^{-15}	18.0	5.5×10^{-10}	Curve 1
KM2780	300—600	1¾″	CsK_2Sb	2.2×10^{-16}	85.0	5.5×10^{-10}	Curve 2
KM2750	300—600	2⅝″	CsK_2Sb	3.1×10^{-16}	85.0	1×10^{-9}	1.4 x Curve 2
KM3054-20	300—900	½″	(S20) $CsNa_2KSb$	2.5×10^{-16}	55.0	3.3×10^{-10}	Curve 3
KM2700	300—900	1¼″	(S20) $CsNa_2KSb$	1×10^{-15}	55.0	5×10^{-9}	4 x Curve 3
KM3054-1	300—1100	½″	(S1) Ag-O-Cs	7.7×10^{-14}	3.0	8.3×10^{-8}	Curve 4
8062	300—1100	1″	(S1) Ag-O-Cs	1.5×10^{-13}	3.0	3.4×10^{-7}	2 x Curve 4

*The ENI or Equivalent Noise Input generally refers to the amount of light in watts necessary to produce a signal-to-noise ratio of unity in the output of the PMT. The ENI can be caculated from:

$$ENI = \frac{\sqrt{2eI_{dk}G\Delta f}}{S}$$

where

Δf = Bandwidth (in this case 1 Hz.)
e = Electronic Charge (1.6×10^{-19} coul.)
I_{dk} = Anode Dark Current at G gain (Amperes)
G = Gain
S = Anode radiant sensitivity (A/w)

CIRCLE 58 ON READER SERVICE CARD

Editors' Column

Analytical Chemistry in Canada

According to information given in the April 1974 issue of *Chemistry in Canada*, analytical chemistry is alive and well in the United States' northern neighbor. Some examples of what is happening around Canada are given below.

The chemistry department at Dalhousie University in Halifax has, since 1971, maintained a Trace Analysis Research Centre (TARC). According to D. E. Ryan, "The basic objectives of the centre are to train specialist analytical chemists and to contribute, through research, to the advancement of analytical chemistry. The long range goal is a centre of research and training excellence in analytical chemistry." Instrumental techniques are stressed with research centered around the creation of new instrumentation, modification of existing instrumentation, and novel applications of existing instrumentation to problems in trace analysis. All 16 alumni (graduate or postdoctoral study) of TARC who have left in the past two years are now working as analytical chemists. In research the group has devised new analytical methods for metals (e.g., Hg), anions (e.g., phosphate), and pesticides (e.g., carbamates) and has developed new instrumentation (e.g., Zeeman-modulated hollow cathode lamp and spectrometer).

At McMaster University in Hamilton, analytical chemistry was given a firm foundation in the mid-1940's and has grown steadily at both the undergraduate and graduate levels. According to A. Corsini, undergraduate "courses are designed to ensure that students in chemistry encounter the fundamentals of analytical chemistry in both theory and practice. As the student gains background knowledge, increasing emphasis is given (via assignments and laboratory projects) to the solution of 'real' problems. Students who complete a four-year chemistry program will have experienced problem-solving techniques" using all important analytical methods. The graduate (MSc and PhD) program attracts students from all over the world. The number of graduate students in analytical chemistry ranges between 10–15 per year. Successful completion of a laboratory course with emphasis on the solution of "real" analytical problems is a requirement for the PhD degree. Areas of research include design, synthesis, and application of selective chelating agents; radiochemistry; trace analysis in ecological and biochemical systems; electroanalytical studies; thermogravimetric studies; determination of polluting trace elements in Great Lake sediments; and the comparison of trace analytical methods for selected elements.

The chemistry department at Queen's University in Kingston also has an active program in analytical chemistry at both the undergraduate and graduate levels. In addition to the usual MSc and PhD programs, a 'nonthesis' analytical MSc program has been set up "in recognition that the analytical specialist must have reasonable familiarity with a wide range of analytical methods if he is to cope with general chemical problems. The aim is not just to consider the analysis of a product by a variety of techniques and say how good or how bad it may be, but be able to look at the whole process, identify the key chemical steps and take positive action to control the product." The program is problem centered and recognizes that analytical problems may be concerned with much more than just elemental composition.

Reports from industry show that research in analytical chemistry is much in vogue. From the Steel Co. of Canada Ltd., Hamilton, we find that "an all-too-common belief that industrial quality control laboratories do nothing but routine mind-numbing analyses" is dispelled. "Rather, because of the economic and other pressures, the need for improvements in analytical procedures is very strong and provides fertile ground for innovative ideas and progress."

A. A. Husovsky

WHEATON
Dry-seal
(U.S. Patent 3,289,879)



THE DESICCATOR THAT SEALS WITHOUT GREASE

Dry-Seal Desiccators seal with a clean, silicone "O" ring – not expensive, messy flange grease ☐ The costs in time, labor, and material of applying and removing grease are eliminated ☐ Lids lift easily without stuck flanges ☐ The lid can be rested on a cabinet top without dust and grit adhering and interfering with the seal as happens with a conventional, greased lid ☐ Since the lid is lifted straight up—not slid sideways, Dry-Seal Desiccators have greater capacity. They can be filled to the underside of the lid ☐ Contours are rounded for greater strength and easy cleaning ☐ Complete with aluminum plate

Dry-Seal Desiccators are available through:

- Ace Scientific Supply Co., Inc.
- Cole-Parmer Instrument Co., Inc.
- Fisher Scientific Company
- Macalaster Bicknell Co.
- Rochester Scientific Co., Inc.
- Sargent-Welch Scientific Co.
- SGA Scientific Inc.
- Arthur H. Thomas Company
- Wards Natural Science Establishment, Inc.

and other leading distributors.

WHEATON SCIENTIFIC
A DIVISION OF WHEATON INDUSTRIES
CIRCLE 253 ON READER SERVICE CARD



Take us to court.

To be admissable evidence in a court of law, the findings of a GC/MS system have to be "right on the button." The mass stability of the CVC 2001 GC/MS gives you results that never miss . . . not even by one amu.

The 2001 is tough. It's designed and quality controlled for heavy continuous usage with little maintenance.

The 2001 is fast. The simultaneous, continuous operation of the oscilloscope, the Total Output Monitor and the analog scan keep the operator fully aware of what's happening to the sample all the time. A lot less time is wasted on re-runs. The active on-line CRT display is also a prime time saver.

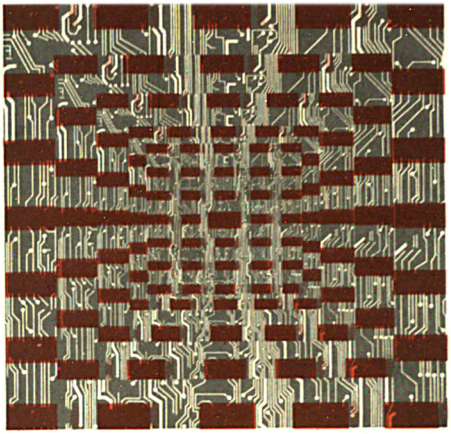
The 2001 is sensitive. It has the largest diameter analyzer of any commercial mass spectrometer for a very high ion transmission. It features a unique patented magnetic electron multiplier. And is the only mass spectrometer that delivers all mass numbers to the output 20,000 per second.

The 2001 is versatile. It offers gas inlets, direct solids inlet probes, and options like Chemical Ionization and Multiple Ion detection. The CVC 2001 will save you time . . . effort . . . mistakes . . . and last but not least—money.

The 2001 is computer compatible. Available with disk storage, CRT display, large compound files, modem for Time-Sharing and computer control of data acquisition.

For complete specifications, contact: CVC Products, Inc., P.O. Box 1886, 1775 Mt. Read Blvd., Rochester, New York 14603 or call (716) 458-2550. CVC Products, Inc., meeting today's needs with worldwide sales and service.

CIRCLE 36 ON READER SERVICE CARD



Microprocessors Part II: Applications

Raymond E. Dessy, Jonathan A. Titus, and Peter Janse-Van Vuuren

Virginia Polytechnic Institute and State University
Blacksburg, Va. 24061

In Part I of this discussion of microprocessors, presented last month (*1*), the rather simple logical concepts of the use of microcomputers in the chemical laboratory were presented. Microprocessors are going to accelerate laboratory automation even more than the introduction of minicomputers did. They are bridging the gap between hardware implementation of control and the use of minicomputers for data acquisition. This month, applications of microprocessors to a "real world" problem are presented. The advantages and disadvantages of such systems are presented, as well as some suggestions on how to get started in the area.

Typical Application

Let us imagine that you want to construct a unit for repetitive analysis of water supplies for trace heavy metal contamination by use of stripping analysis. Hard-wired devices (consisting of logic elements alone) could be built, but most chemists are unfamiliar with their applications. In addition, once built, the units are rather inflexible, and their functions cannot be easily altered. Krause and Ramaley (*2*) have described the background of the method and appropriate circuitry. For the reasons given, the method is not often used. On the other hand, a programmable minicomputer system is a more sophisticated device than is really needed to do the job. A microprocessor is ideally suited to the task.

Since the example was chosen to cover the philosophy of microprocessor usage rather than focus on the method itself, let us first reduce the technique to the barest essentials for those unfamiliar with electrochemistry. An analog voltage signal varying in a complex manner with time is impressed on an electrode, and as the voltage is changed, the corresponding current that flows in the cell is measured.

All we need to add to our basic microcomputer to achieve the intended goal is an analog-to-digital convertor (ADC), a digital-to-analog convertor (DAC), and a clock, as indicated in Figure 1. These elements have been discussed in an earlier article entitled "Computer Interfacing" (*3*).

The analog voltage required is generated first by forming in the A register of the microprocessor its digital equivalent. This is latched out to the DAC by use of the software command OUT1, as described in Part I. (See Figure 1.) Whatever potential is output by the DAC controls a potentiostat made from operational amplifiers. Whatever voltage appears at the DAC output appears at the test electrode. The operational amplifier circuitry is necessary to boost the low current output of the DAC to useful levels. The current passing thru the cell, from test to counter electrode, is amplified to a suitable voltage by another operational amplifier. This voltage is input to an analog-to-digital convertor. The conversion process to digital form is started with the software command OUT6. When the conversion is finished, the ADC signals this fact to the CPU via interrupt request line IR2 by use of the ADC done flag. This is cleared with the corresponding acknowledge signal ACK2. A service routine is entered that acquires the digital equivalent of the current by an INP1 command which activates the gate, transferring the data into the A register. A real-time clock is serviced by IR1 and ACK1 in a manner similar to that of the ADC. It will be used to coordinate the actions of the microcomputer every 0.25 sec in real time.

The actual experiment requires electrolyzing the solution in the cell for a certain TIME at a given POTENTIAL. At the end of the plating time, the computer must generate a voltage ramp to more anodic potentials, upon which is superimposed a square-wave pulse of given AMPLITUDE. Current is sampled at the *bottom* and *top* of each square-wave pulse, and the *difference* measured and recorded [Figure 2 (a)]. If the results of such an experiment were plotted out at the end of a run, they would look like Figure 2 (b). Each peak represents the current necessary to "strip off" a plated metal. The voltage (E) identifies it. The integrated current (i) would give its relative concentration.

The software necessary to perform the operations desired is described in the accompanying flow chart (Figure 3). Five hundred and twelve words of ROM and 250 words of RAM memory would suffice.

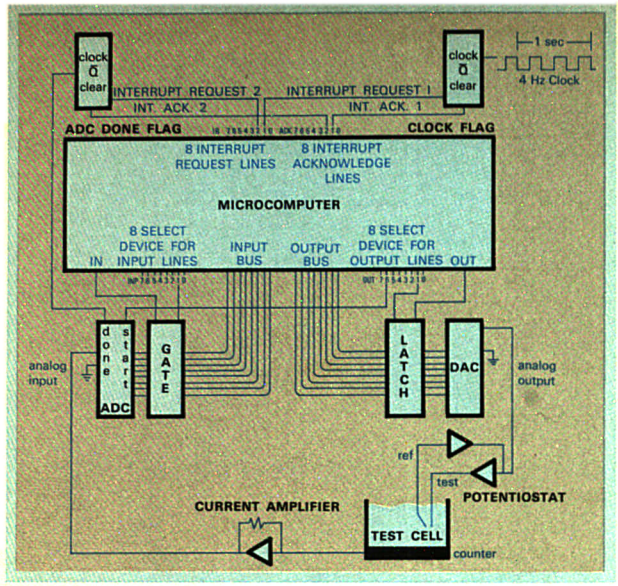


Figure 1. Repetitive stripping analysis unit using a microcomputer

The concept is to have the microcomputer ask for the following parameters, by use of a teletype:

- plating TIME—time plating potential is to be applied to test electrode
- plating POTENTIAL—potential at which solution is to be electrolyzed
- pulse AMPLITUDE—amplitude of pulse to be applied to stripping ramp.

The solution is electrolyzed at the indicated POTENTIAL for the desired TIME, and then a 8-mV/sec ramp to more anodic potentials is applied [Figure 2 (a)]. The scan range is 1.024 V anodic to the plating potential. The linear ramp is modulated by a 1-Hz pulse with the indicated AMPLITUDE.

Plate times of 256 min are accommodated. Stripping time is 2 min. These could be altered by simple changes in the software and the frequency of the clock used. (These parameter limits were chosen for clarity of presentation.)

Implementation of this experiment demonstrates both the computational and control capabilities of microcomputers.

As the plating TIME is typed on a teletype attached to the microcomputer, the data are accepted by the CPU into the A register. The ASCII code transmitted by the teletype is first converted to Binary Coded Decimal (BCD) format as shown. Some microprocessors are designed to handle numbers in BCD format. Others, such as the Intel 8008, require the number to be converted further to a straight binary representation by software (cf ref. *4*). This number is stored in the B register.

No. typed	ASCII codes transmitted		BCD no.	Octal equivalent
23	262	263	23_{10}	27_8

As the plating POTENTIAL and the pulse AMPLITUDE are specified, e.g., 1.20 and 0.10 V, similar conversions are made. However, these numbers will be used in conjunction with a digital-to-analog convertor which has a maximum output of ±2.54 V—the exact output depending on the binary number input to the D/A convertor. It is a common practice in computers to let the most significant bit of a bi-

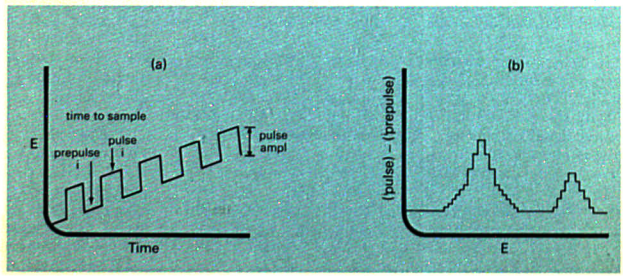
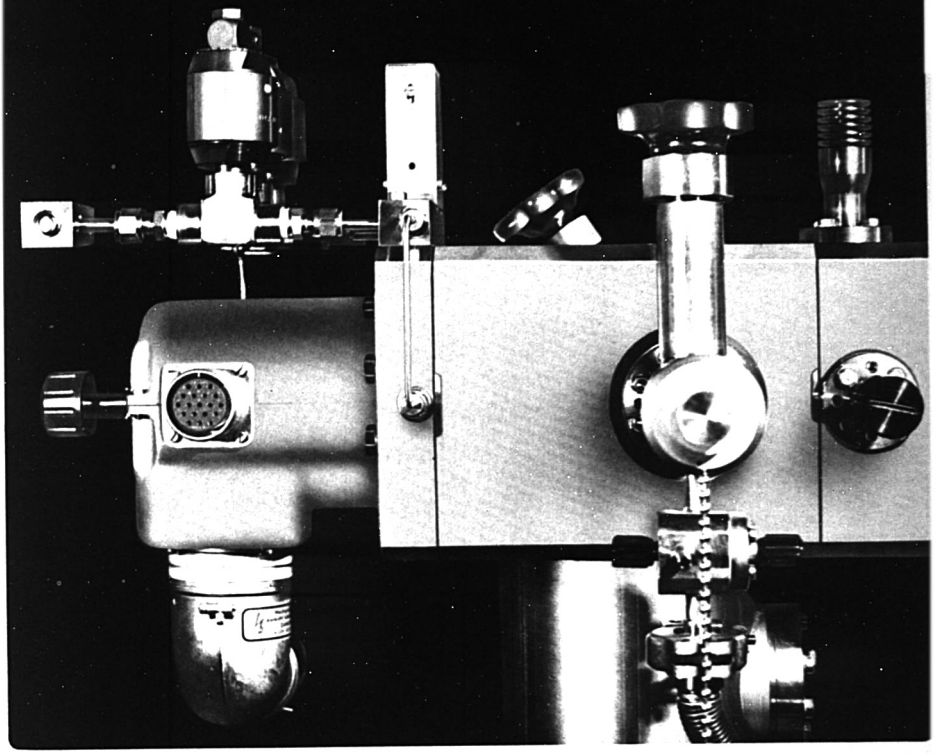


Figure 2. (a) Typical stripping analysis waveform. (b) Typical output current associated with (a)

VARIAN MAT – the leading name in mass spectrometry and MS data systems



Mass Spectrometer MAT 311A
the rugged, routine instrument
for demanding analytical problems

varian

A combined CI/EI source is just one of the many features in this versatile instrument.
Whether your field is environmental research, clinical chemistry, biochemistry, toxicology or forensic science you can routinely perform the most difficult analysis by utilizing:
Low resolution, high resolution, metastable scanning, direct GC coupling, chemical ionization, field desorption, field ionization or automatic data processing.
For more information please write.

VARIAN MAT/U.S. Operations
25 Route 22
Springfield, New Jersey 07081
Telephone 201/467-3660

VARIAN MAT GmbH
28 Bremen 10
P. O. Box 144062
West Germany

052 e 874

CIRCLE 243 ON READER SERVICE CARD

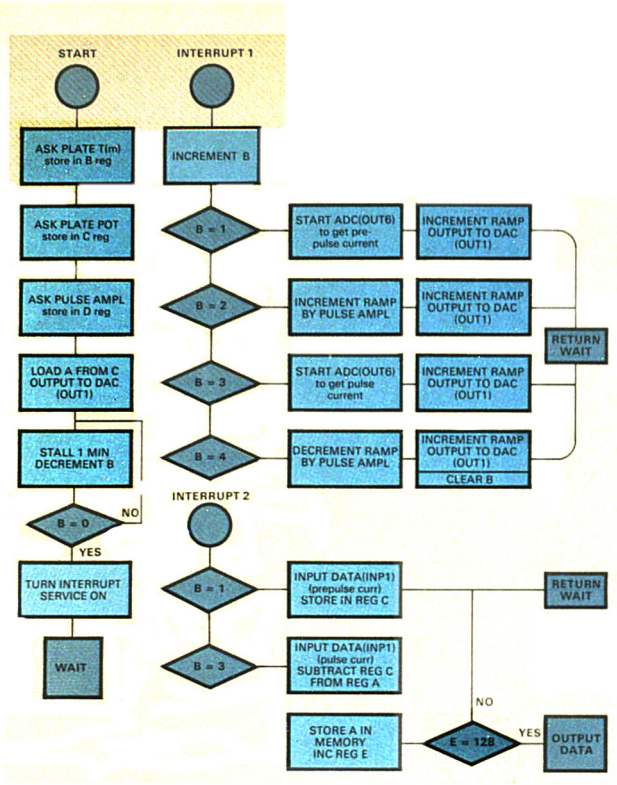


Figure 3. Stripping analysis flow chart

nary number indicate its sign; if it is set to a 1, the number is negative; if it is 0, the number is positive. This means that the following relationship exists between the numbers typed and the numbers to be stored in registers C and D, representing POTENTIAL and AMPLITUDE, respectively.

No. typed	Sign stored temporarily	Octal no. stored temporarily	No. finally stored
+2.54	+	376	177
+1.28	+	200	100
+0.02	+	002	001
0.00	+	000	000
−0.02	−	002	377
−1.28	−	200	300
−2.54	−	376	201

The microprocessor must sense the typed sign, accept the typed number ignoring the decimal point, and convert it to a straight binary representation. If the number is positive, this representation is divided by two since each increment of one in the digital number is equivalent to a 2-mV increase in the analog output of the D/A convertor. Division by two is easily accomplished by rotating the number one place to the right (this is the reason registers are designed to be rotated).

OCTAL 002_8 001_8

—ROTATE ONCE RIGHT→

BINARY $00\ 000\ 010_2$ $00\ 000\ 001_2$

If the number is negative, all of the bits are then complemented (all 1's become 0's; all 0's become 1's), and the result is incremented by one.

OCTAL 200_8 100_8

—— ROTATE ONCE RIGHT ——→

BINARY $10\ 000\ 000_2$ $01\ 000\ 000_2$

COMPLEMENT

277_8

300_8

←—— and ADD 1 ——

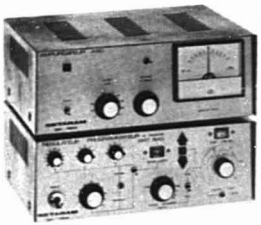
$11\ 000\ 000_2$ $10\ 111\ 111_2$

Try this on another value yourself!



$ 5,100 CIF USA

what less can be said! for a differential thermal analysis system



the D 80 differential thermal analyzer

The D 80 differential thermal analyzer is indispensable to the novice scientist who wishes to familiarize himself with the techniques using this type of equipment.
One practices discussion and interpretation of results.
By reason of its high technical quality, the D 80 differential thermal analyzer is equally able to render numerous services to the DTA specialists, especially in control laboratories.

The total equipment consists of:
- Modular DTA base
- The probe with a set of crucibles
- A furnace
- A quartz analysis chamber
- A program temperature regulator PRT 540 C
- An amplifier A 80
- A recorder with two continuous recording pens.

SETARAM likewise manufactures the G 70 thermoanalyzer. It is designed for the initiation into thermogravimetric techniques and for industrial control laboratories. S 6,026 CIF U.S.A. for the complete system.
(the program unit PRT 540 C and the recorder are identical for the D 80 and the G 70. Thus for a price of S 8,420 CIF U.S.A. the two complete systems can be had utilizing only one program unit and one recorder).

SETARAM
101-103, rue de Séze - 69451 Lyon cedex 3 - France
tél. (78) 24 17 41 - telex 34 924

CIRCLE 211 ON READER SERVICE CARD

With the initial dialog ended, the plate POTENTIAL is loaded from register C into the A register, output to the D/A convertor by use of an OUT1 command, and the electrolysis is started.

But how is time measured? One way is to use the fact that computer operations take known, fixed amounts of time. For example, the following simple program:

Octal command	Mnemonic equivalent	Operation
040	CNTR, INCE	/increment register E
110	JPFZ CNTR	/if E ≠ 0 jump back to CNTR
	(continue)	/if E = 0 perform next instruction instead

involving the incrementing of the E register—001 002 003 . . . . 376 377 000—requires 20 msec in the 8008 CPU. If we did this three times, 1 min in real time would have gone by, AND if we decremented the B register (containing TIME), every time this happens, we could use a similar software routine to determine when to terminate the electrolytic plating! (B would go to zero when the TIME was up.)

At this point, we could turn "on" a clock running at 4 ticks/sec by activating the interrupt service (allowing the CPU to accept interrupts). At each clock tick an interrupt occurs, and the service routine vectored to will perform different functions depending upon which "tick" in each 1-sec cycle is involved. At each clock tick the number output to the D/A convertor would be incremented by 1, increasing the output voltage by 2 mV. In addition, a special function would be performed at each clock tick:

CLOCK TICK	1 + N*4	2 + N*4
SPECIAL FUNCTION IMPLEMENTED	Start ADC to get i before pulse (OUT6 command)	Add pulse AMPLITUDE to number output to D/A conv.
CLOCK TICK	3 + N*4	4 + N*4
SPECIAL FUNCTION IMPLEMENTED	Start ADC to get i during pulse (OUT6 command)	Subtract pulse AMPLITUDE from number output to D/A conv.

The completion of every A/D conversion causes another interrupt of the microprocessor which reads the data in via an INP1 command. In every "4-clock tick cycle," the first value is the prepulse current. This is stored temporarily in C register, which is now free. When the next A/D interrupt occurs, and the data are read into A, representing the pulse current, it is an easy matter to subtract the two:

Octal command	Mnemonic equivalent	Operation
222	SUBC	/subtract C from A

This result is now stored in memory. Space is available for 128 data points, allowing a strip voltage span of 1.024 V. When 128 data points have been taken, the program can "plot" the data out on the teletype, or type the results out and produce a punched tape for later use by using the ASCII format. It could also plot the data out onto a Y/t plotter by using the same D/A convertor used in the voltage sweep. It would be a simple matter to integrate the areas under each peak—simply by adding together data values occurring above a chosen base line. If "voltage windows" were defined in the ROM operating program (e.g., Zn strips from −0.7 to −0.5 V), the program could also locate the maximum in each peak, compare it to the "look-up-table" of known metals, and simply provide a normalized report as in the first two columns:

Metal	Relative concn	Abs concn
Zn	1.00	0.93 E-08
Cu	0.28	0.26 E-08

A calibration run (with known Zn/Cu concentrations) could be run first, letting the microcomputer calculate and remember its own calibration factors, producing the absolute concentrations shown.

Of course, it would also be a simple matter to make a run on supporting electrolyte alone, generating a background file that would be subtracted point by point from the data before it was reported. This would be very difficult to do if a hardware approach had been used.

This system could have been designed to utilize control buttons (read by a SENSE REGISTER) to determine what function (software program) was to be executed. Input-parameters could be entered by a thumb-wheel switch, the BCD data being read into the A register via an input port.

Enter Time	Enter Potential	Enter Amplitude
Start Analysis	Start Calibration	Restart

A simple strip printer could be used for output.

Note that this application utilizes the power of a microcomputer properly. The program is contained in ROM; data entry from the teletype or switches uses RAM as a scratch pad and deposits all necessary operating parameters in the CPU's registers A–E. During stripping almost all of the operations involve these registers, accessing memory mainly for storage of data. The interrupt requirements are not complicated, and the mathematical operations are simple. The data base is small. Table I shows other areas in which microcomputers will find applications. If your area of interest is touched by any of them, the succeeding paragraphs discuss some of the problems in getting started.

Advantages/Disadvantages

Microcomputers should be considered when automation involves primarily control, with minor computation. Memory access in many of these devices is currently relatively slow and awkward. Software floating point packages (to perform four function arithmetic functions with high precision) are available, but they require approximately 1000 words of memory. Hardware math will come (such as the IC's used in calculators), but not for several years. Microprocessors should not be considered *currently* when massive data banks or programs above 3K are needed, because of the cost of the solid-state memories. The system is then approaching available minicomputer prices. Just what are the real advantages of microprocessor systems?

Primarily, the unique advantages in microprocessor systems, in comparison to their currently available competitors, are modularity, programmability, or cost. Most minicomputers, even in their stripped-down forms, are sold as complete systems with operating power and memory often in great excess of what is needed for the proposed task. Microprocessor systems can be purchased with memory increments (ROM or RAM) of 256 words. The interrupt structure can be added and augmented as needed. A control panel is usually not needed. Minicomputers usually are provided with a minimum of 4K of memory, a built-in program interrupt structure, teletype, and operator console. Thus, careful consideration of your actual needs and implementation via microprocessors can lead to considerable cost savings in the initial investment. Hardware implemen-



Altex mix and match LC components

match to make a superb LC system mix perfectly with other components

Chromatographs, UV detectors, columns, valves, fittings, tubing — Altex makes it all. One source for every instrument and accessory you need. Altex components are precisely matched so that you can easily set up the most elaborate or complex LC system. Everything fits. Everything works. And you can mix Altex components into an existing system for added capability since they interface perfectly. Send today for the bulletins you need and your laboratory will be back to doing trouble-free chromatography again!

For free bulletins, circle nos.

8 Chromatographs
9 UV detectors
10 Automatic sample injector
11 High pressure LC accessories
12 Chemical inert fittings, valves and columns

ALTEX **SCIENTIFIC INC.**
1450 Sixth Street
Berkeley, Calif. 94710
(415) 525-5500

Table I. Potential Applications of Microprocessors

Electrochemical experiments
- Pulse polarography
- Stripping analysis
- Programmed triangular voltammetry
- Controlled potential electrolysis

Chromatography
- Liquid chromatography
- Gas chromatography
- Gel permeation chromatography

Optimization
- Mass spectrometers
- Magnetic resonance equipment

Process monitoring
- pH
- Pressure
- Refractive index

Sequencing
- Peptide synthesizers
- GC/LC programmer

Spectroscopy
- Control and data collection in X-ray fluorescence spectroscopy
- Scan control and report generation in densitometers
- Data reduction/correction in absorption/fluorescence spectroscopy

Data handling
- Format changing
  - EBCDIC/ASCII
  - Adapting data tapes to new protocols
- Data compression
  - Peaks to area/position
  - Report changes only
- Data reduction
  - Generate derivative of data
  - Apply calibration factors

Control and data acquisition
- pH-stats
- Automatic titrators
- DTA, TGA
- Autoanalyzers

tation of these needs might be cost-competitive, but any hard-wire implementation requiring 30 IC's or more should be reexamined for potential microprocessor utilization. The reprogrammability of such devices often becomes a deciding factor as future alterations in the system are envisaged.

Who/Where/What?

For those having some capability in-house in software development, hardware design, and troubleshooting (or those willing to develop the necessary skills), the microprocessor opens up the area of instrument development for the analytical chemist in the clinical, quality control, and research laboratories. Most chemists would rightly be hesitant about undertaking the hard-wired development of a wave-form generator suitable for the stripping analysis. But the logical nature of the software used by a microcomputer to accomplish such a task, augmented by the electronic power offered by the microprocessor, without the need to completely understand all of its intimate workings, should liberate the imagination of the analyst. Since the transistor/transistor logic (TTL) levels output by these devices can be current and voltage boosted with new solid-state relays, it is possible to control many items in the laboratory.

In chromatographic experiments, complex sequencing, temperature control, and report generation are obvious applications. Instruments should be capable of calibrating and optimizing themselves to yield the most accurate data and highest S/N ratio. Certainly the lack of imagination in instrument designers is most highly demonstrated in magnetic resonance and mass spectrometric equipment which have $40,000 data processing units attached but which do not automatically optimize themselves. Microcomputers will perform such tasks even in minimum configuration machines.

Correlative process monitoring, in which many transducer types continuously examine a number of system variables and produce a concentrated report, is within the scope of microcomputers. Availability of simple solenoid controlled valves and ion specific electrodes makes construction of closed-loop control devices utilizing microprocessors very simple. pH-stats for biological research controlling deviations in BOTH directions can be built at prices less than current commercial models utilizing hardware alone which control in only one direction. In many of these cases, the system function can be altered on a day-to-day basis by merely plugging in a new ROM program board.

Many of the tensile strength, deformation, and uniformity tests so common to the plastics industry's quality control laboratory will succumb to microprocessors since decentralization will reduce the signal transmission and program development problems associated with the single system. Clinical laboratories will utilize microcomputers in conjunction with autoanalyzers and autotitrators to not only control the data acquisition process but provide data compression before transmission to a central data base. The segregation here will also provide independence in case of system failures elsewhere.

Hospitals in British Columbia are already using them to provide inexpensive, portable data compression units for field monitoring of electrocardiograms. In a similar fashion, remote monitoring devices for effluent control by use of specific ion electrodes can be constructed and connected to a central computer for correlation of data via the telephone lines. A system based on this concept, by use of the respiration rate/cough rate of fish, has been designed at VPI.

Programming

At the present time, programming microcomputers appears to be a formidable problem to the beginner. He is faced simultaneously with the electronic aspect of interfacing AND learning assembly language programming and implementing it. There are cross-assemblers running on commercial time share equipment which can cross-assemble from a sub-set of PL-1 to machine language code that is acceptable to the microprocessor. In many environments such a facility is not easily assessible or cost justifiable if only a few programs are to be developed. Also, despite some vendor's claims, it creates code that uses costly memory inefficiently. On the other hand, production of machine code by an assembler resident in the microcomputer itself is also usually not cost justifiable if the user is involved with only a few microprocessors that are not continuously being altered. These programs are available, but too much ROM and RAM are required for the resident editor/assembler. One avenue that has been successfully employed at a number of installations is to prepare a cross-assembler that will run on available minicomputers. In some cases, these cross-assemblers have been written from scratch; these are available for the PDP-10 and PDP-8. Many laboratories have found it sufficient to take the assembler that is resident in their minicomputer and expunge its permanent symbol table, replacing it with the instruction set for the microprocessor. A few coding tricks and a translation routine to convert from the 12- or 16-bit output of the mini's assembler to the bit format of the microprocessor are all that are needed to generate code rather easily. Documentation and copies of a PDP-8 resident combined editor/assembler called TEACH which will generate code for the Intel 8008 are available from the authors. However, in program development it is also important to have available a set of ROM chip memories containing a basic set of subroutines, callable from the teletype, to aid in program prepara-

We will send you complete information on . . .

Radiometer Quality Electrodes for Chemical Measurements

• pH • glass • combination • reference • metal
• micro • macro • autoclavable
• medical • conductivity
• ion selective



Radiometer produces one of the most extensive lines of electrodes in the industry. Almost 100 different types for analytical, medical and industrial applications are detailed in this new 36 page electrode catalog.

If you use electrodes, you should have this book!

Your free copy is available from . . .

THE LONDON COMPANY
811 Sharon Drive, Cleveland, Ohio 44145
(216) 871-8900

CIRCLE 150 ON READER SERVICE CARD

HELLMA
. . . tomorrow's designs today!



Hellma—the largest assortment of highest precision glass and quartz cells.
Standard · Flow-through · Constant-temperature
Anaerobic · Special Designs
Also available—ULTRAVIOLET LIGHT SOURCES
Deuterium Lamps · Mercury Vapor Lamps
Hollow Cathode Lamps · Power Supplies

HELLMA CELLS, INC.
Write for literature
Box 544
Borough Hall Station
Jamaica, New York 11424
Phone (212) 544-9534

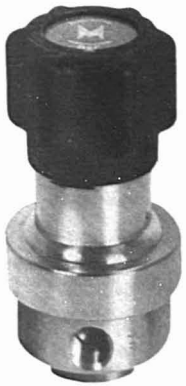
CIRCLE 115 ON READER SERVICE CARD

LOW FLOW INSTRUMENT PRESSURE REGULATORS

IR400 SERIES-20LPM
IR500 SERIES-5LPM

FEATURES:

- Corrosive or non-corrosive high purity service
- 316 stainless steel or brass construction
- Teflon lined 301 stainless steel diaphragm and Kel-F seat
- Max. inlet pressure: 3000 psig
- Adjustable outlet ranges: 0-30, 0-100, 0-300, 0-500 psig



VERIFLO CORPORATION

VERIFLO CORPORATION
INSTRUMENT DIVISION
250 Canal Blvd., Richmond, CA. 94804
(415) 235-9590

CIRCLE 244 ON READER SERVICE CARD



Figure 4. An interface teaching station at VPI&SU

tion and debugging. Some of these are available from vendors, but they vary in quality. A typical set that has been useful at VPI called OPERATE contains:

- paper tape reader routine
- paper tape punch routine
- memory examination/alteration routine
- break point (trap) routine
- single-step (trace) routine

and occupies 768 words of ROM. Documentation and copies are available from the authors.

Software resident in read/write memory can be used to collect data and altered to implement changes in the way data are manipulated or the way data are collected. But the volatility of these programs through operator error or power failure is often a concern, particularly where field work or technicians are involved. Microprocessors have been the focus for the utilization of *r*ead-*o*nly-*m*emories which have their programs "burnt" into them at the factory or in the field by ROM "blasters" which permanently fuse links in the IC device. These are truly nonvolatile memories, but they also cannot be changed. *E*rasable *p*rogrammable *r*ead-*o*nly-*m*emories (EPROMS) are floating gate-MOS circuits which can be biased by avalanche charging near the gate by high currents. Once biased, these devices remain a logic 1 until some conduction pathway is made available to the biasing electrical charge. This requires intensive UV irradiation at the biased junction. EPROMS are provided with quartz lids covering the memory area, and exposure to the UV sources used in TLC will erase their memories in 3–4 min. They may be reprogrammed in the same amount of time with a ROM blaster. Over 200 reprogrammings are possible with current devices. They thus provide FIRMware, less volatile than SOFTware, but more easily changed than HARDware. Vendors will program/reprogram your EPROM's for ~$10 if you provide a paper tape containing the program you want loaded.

Hierarchy

Connecting a microcomputer to a larger minicomputer system (a hierarchical or satellited configuration) is often desired; it might be for the purpose of acquiring a data base from the microcomputer and performing data reduction tasks on it, and then returning the concentrated data to the microprocessor for presentation or action. Alternatively, program preparation in the minicomputer could occur, with subsequent depositing of the program in the microcomputer and initiation of execution. This might be the result of the microprocessor sensing unusual conditions in the experiments it is controlling and requiring an altered operating program to meet these demands. Increasingly, the microprocessor is used to collect and compress a data base from several instruments for passing at a convenient time to the minicomputer at rates of 2–400 words (8 bits) per second. They can be accepted by the minicomputer by a serial interface and, to all intents and purposes, look like a TTY to the minicomputer. The concepts involved are discussed in more detail in the article entitled "Instant Interfacing" (*4*). For higher speeds and more sophisticated interrupt handling, parallel transmission can be used. Details of such a system operating in our VPI laboratories are available.

In the Teaching Lab at Virginia Tech

With their modern architecture, at small cost, microcomputers offer an alluring route to the low-cost introduction of computing philosophy and techniques to undergraduate, graduate, and postgraduate students. This can be accomplished only by a "hands-in" process, in contrast to "hands-on" experience which exposes the student to a teletype and turn-key laboratory data acquisition system. Hands-in experience can only be attained by exposure of the entire I/O bus of the CPU—a process often precluded by cost and extensive use of the computer available in the laboratory.

For $2,000 a complete interface teaching station has been provided, for Virginia Tech students and ACS Short Course participants, centered around microprocessors (Figure 4). The material learned can be extrapolated directly to minicomputers also.

Typically, the student examines the nature and time duration of SELECT DEVICE and IN/OUT pulses and uses them to input and output data. A program in ROM (OPERATE) allows the student to enter small programs into RAM bank and execute them, one step at a time. OPERATE reports the contents of registers A–E at each step.

For example, a typical TTY dialog might be as follows: human response is *underlined;* LF is a line-feed; CR is a carriage return.

TTY dialog	Operation
4100 713 006 LF	Change memory location 4100 to 006
4101 700 014 LF	To load A with 014
4102 000 010 LF	Increment B
4103 777 201 LF	ADD B to A
4104 121 320 CR	Deposit sum in C
4100B CR	Set break point at 4100
4100G CR	Start program at 4100
000 000 000 000 000	All registers (A–E) = 000
S4100	Now do next step
014 000 000 000 000	A = 014
S4102	
014 001 000 000 000	INC B
S4103	
015 001 000 000 000	ADD B to A
S4104	
015 001 015 000 000	And Store in C

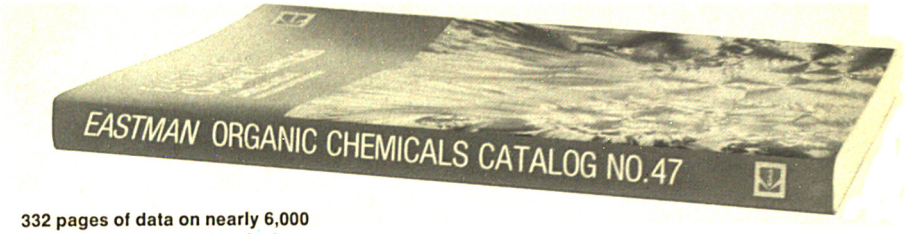
No computer console is involved; therefore, the trauma of operating switches and thinking in binary are not encountered. In addition, the basic program OPERATE is in ROM memory where it cannot be destroyed by the student accidentally.

From this base the student examines sense switch and interrupt operation, printing out data from several sources every 10 sec. In this, as well as all succeeding experiments, the student must generate his own software and hardware.

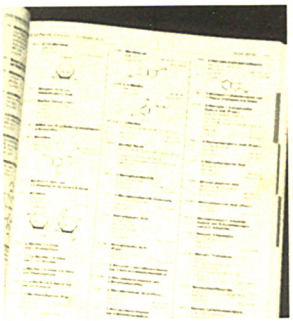
Other typical experiments are:

Eastman Organic Chemicals News

THE NEW *EASTMAN* ORGANIC CHEMICALS CATALOG, NUMBER 47.



332 pages of data on nearly 6,000 EASTMAN Organic Chemicals



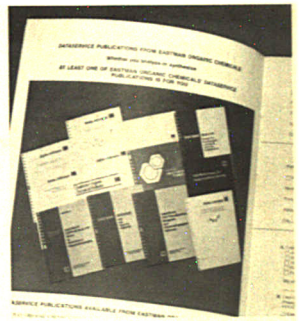
Structural formulas illustrated for more than 1,000 of the chemicals.



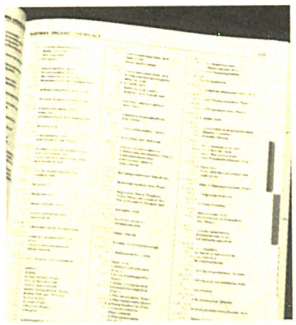
A functional group listing.

Color coding on all pages to help you find what you need fast.

Reader service postcards enabling you to request additional literature, quotes on bulk and custom chemicals, and other information.



Details on the EASTMAN **Dataservice** Publications Program and how you can participate in it.



An empirical formula index.

This new catalog has been sent to everyone on our mailing list. If you don't yet have a copy, we probably don't have your name. To request your own copy, simply return the coupon.

Kodak

10-40

Eastman Kodak Company
Eastman Organic Chemicals
Dept 412L
Rochester, N.Y. 14650



Please send a copy of
EASTMAN Organic Chemicals Catalog No. 47 to:

Name

Affiliation

Address

City State Zip

CIRCLE 65 ON READER SERVICE CARD

Table II. Representative Microprocessor Suppliers

Company	Description
American Microsystems Inc. Santa Clara, Calif.	CK114 microprogrammable serial processor suitable for calculator operations. Seven-chip set. 75 instructions. True microprocessor expected mid-1974
Computer Automation Inc.	16-bit "naked mini" computer built around microprocessor chips is aimed strictly at OEM field. Mounted on single 15 × 17 board, it sells for around $1,000 in lots of 200
Control Logic Inc. Natick, Mass.	Complete microprocessor system available on 3 × 5 pc cards which mount in pre-wired card frame. Built around Intel 8008. Basic 3-card processor set is $335. Basic software available includes loader, ODT, assembler, and editor
Digital Equipment Corp. Maynard, Mass.	Complete microprocessor system on 11 × 8 pc cards which mount in DEC block. Built around Intel 8008. Basic 3-card processor set, plus some memory and interrupt capability, is $745. Cross assembler for PDP-8 family and standard software available
Fairchild Semiconductor Mt. View, Calif.	PPS-25 is a seven-chip parallel BCD set with 93 instructions. True microprocessor anticipated in 1974
General Automation Anaheim, Calif. (Microelectronics Division Rockwell International)	LSI 12/16 series with CPU/memory on 10 × 8 pc board. Software available. $495 in quantities of 1000
General Instrument Co. Hicksville, N.Y.	16-bit parallel processor and control chips available in 1974 as chips or cards
Intel Corp. Santa Clara, Calif.	4-bit (4-chip) parallel processors and 8-bit (1-chip) processors available as chips or systems in a variety of forms. Second generation version of 8008, the 8080, is being shipped. Software available
Motorola Semiconductor Products Phoenix, Ariz.	5-chip 8-bit processor expected 1974
National Semiconductor Corp. Santa Clara, Calif.	4-bit slice (4, 8, 12, or 16 bits) processors on boards or complete systems. IMP-8 card is $800; IMP-16 is $950. Software available
Pro-Log Corp. Monterey, Calif.	4- and 8-bit systems or cards built around Intel microprocessor chips
Rockwell/Microelectronics Anaheim, Calif.	PPS-4 is a 4-bit BCD-oriented system
Teledyne Systems Northridge, Calif.	TDY-52A is an 8-bit microprocessor chip; TDY-52B is a 16-bit version

Other vendors who have microprocessors in development are: RCA, Somerville, N.J.; Signetics Corp., Sunnyvale, Calif.; Western Digital, Newport Beach, Calif., and Raytheon Semiconductor, Mt. View, Calif.

- Digital Control—control 5-V motors (on/off; forward/reverse) for valve control
- Data Acquisition and Display—accepts analog data from GC, converts it to digital data; displays data as it is acquired on CRT; and punches final data file onto paper tape in ASCII format for utilization by a larger computer
- Interrupt Structure—monitor a number of external events (TGA, GPC) at the same time as CPU reports data from a previous run.

At the end of 30 hr of laboratory, the student is aware of the philosophies of interfacing and how he can utilize computers in his laboratory work. Details and courseware materials are available from the authors.

Reading Specifications

Keeping abreast of the microprocessors already available and those that have been announced (but often not even yet designed) is a serious problem. A list of vendors is given in Table II. The bit size (4, 8, 12, 16, etc.) and the number of general-purpose registers should be compared. The word length should easily accommodate your experiment's resolution [8 bits represents 1 part in 256—using two 8-bit words for data storage (double precision) will give a resolution of 1 in 64,000]. The more general-purpose registers there are, the easier programming will be. Current microprocessors can address 16 to 64,000 words of memory, but for most applications, memory limitation is not important, since cost-wise it would be hard to justify such a large microprocessor system in comparison to a minicomputer.

Some microprocessors, particularly the 4-bit versions, are BCD oriented and lend themselves readily to the human entry of data by touch-pads and keyboards. Their instruction set is limited in comparison to 8- and 16-bit machines which are binary.

Some microprocessors have both binary and BCD instructions. A vectored interrupt system is very desirable, since it reduces programming difficulties, but extremely sophisticated designs should be avoided because they lead rapidly to extremely sophisticated software, and another microprocessor might be cheaper in the long run.

Physical configurations are as varied as the internal architecture. Three distinct classes appear to be evident:

- Chips only—the integrated circuit CPU's and control IC's are available for the user to incorporate in his own printed circuit cards. This is definitely only for well-equipped and staffed electronic shops.
- CPU cards—the processor, control circuitry, and some memory are available on a printed circuit card. The user must add device decoding, advanced interrupt service, gates, and latches. A hardware background is essential to use them.
- Systems—the vendor provides a card frame and cards to fit it containing CPU memory in various forms, device decoding, interrupt service, gates, latches, and interfaces for teletypes, other computers (via serial data communication), relays, and A/D and D/A convertors. If you can specify your needs clearly, most chemists will find this route the best.

References

(1) R. E. Dessy, P. J. Van Vuuren, and J. A. Titus, *Anal. Chem.*, **46** (11), 917A (1974).
(2) M. S. Krause and L. Ramaley, *ibid.*, **41** (11), 1365 (1969).
(3) R. E. Dessy and J. A. Titus, *ibid.*, **45** (2), 124A (1973).
(4) R. E. Dessy and J. A. Titus, *ibid.*, **46** (3), 294A (1974).

Enter your personal subscription to the foremost publication in the vital fields of chemical analysis. Treats both theoretical and applied aspects of analysis. Subscription includes "ANNUAL REVIEWS" and "LAB GUIDE" issue. Published monthly.

ANALYTICAL CHEMISTRY

	U.S.	**Canada	**PUAS	**Other Nations
*ACS members	☐ $5.00	☐ $9.00	☐ $9.00	☐ $10.00
Nonmembers	☐ $7.00	☐ $11.00	☐ $19.00	☐ $20.00
Three Year Rates Nonmembers	☐ $16.00	☐ $28.00	☐ $52.00	☐ $55.00

☐ Payment enclosed *(payable to American Chemical Society)* ☐ Bill me ☐ Bill company

Name _____ Position _____

Your Employer _____

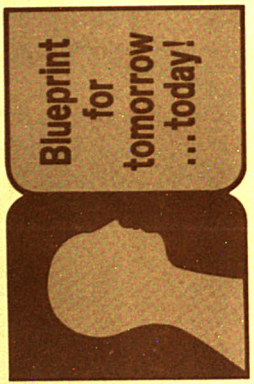
Address ☐ Home
☐ Business _____

City _____ State _____ Zip _____

Employer's Business: ☐ Manufacturing ☐ Government ☐ Academic ☐ Other _____

If Manufacturer, Type of Products Produced _____

*NOTE: Subscriptions at ACS member rates are for personal use only. **Payment must be made in U.S. currency, by international money order, UNESCO coupons, U.S. bank draft, or order through your book dealer.



THE PUBLICATIONS OF THE
AMERICAN CHEMICAL SOCIETY

FIRST CLASS
Permit No. 1411-R
Washington, D.C.

BUSINESS REPLY MAIL
No postage stamp necessary if mailed in the United States

Postage will be paid by

AMERICAN CHEMICAL SOCIETY
1155 Sixteenth Street, N.W.
Washington, D.C. 20036

ATTN: J. MEDINA

analytical chemistry

October 1974, Vol. 46, No. 12

Editor: HERBERT A. LAITINEN

EDITORIAL HEADQUARTERS
1155 Sixteenth St., N.W.
Washington, D.C. 20036
Phone: 202-872-4600 Teletype: 710-8220151

Managing Editor: Virginia E. Stewart

Associate Editor:
Josephine M. Petruzzi

Assistant Editor:
Andrew A. Husovsky

Editorial Assistant: Linda A. Ferragut

GRAPHICS AND PRODUCTION STAFF

Manager: Leroy L. Corcoran

Associate Manager: Charlotte C. Sayre

Art Director: Norman W. Favin

Artist: Linda McKnight

Editorial Assistant: Nancy J. Oddenino

EDITORIAL PROCESSING DEPARTMENT,
EASTON, PA.

Associate Editor: Elizabeth R. Rufe

ADVISORY BOARD: Allen J. Bard, Fred Baumann, David F. Boltz, E. G. Brame, Jr., Warren B. Crummett, M. A. Evenson, Henry M. Fales, A. F. Findeis, Kenneth W. Gardiner, Jack M. Gill, Jeanette G. Grasselli, R. S. Juvet, Jr., Theodore Kuwana, Oscar Menis, Harold F. Walton

INSTRUMENTATION ADVISORY PANEL: Jonathan W. Amy, Stanley R. Crouch, Richard A. Durst, J. J. Kirkland, Ronald H. Laessig, Marvin Margoshes, Harold M. McNair, David Seligson, Howard J. Sloane

Contributing Editor: Claude A. Lucchesi
Department of Chemistry, Northwestern University, Evanston, Ill. 60201

Published by the
AMERICAN CHEMICAL SOCIETY
1155 16th Street, N. W.
Washington, D.C. 20036

Books and Journals Division

John K Crum **Director**

Ruth Reynard **Assistant to the Director**

Charles R. Bertsch **Head, Editorial Processing Department**

D. H. Michael Bowen **Head, Journals Department**

Basil Guiley **Head, Graphics and Production Department**

Seldon W. Terrant **Head, Research and Development Department**

Advertising Management
CENTCOM, LTD.
(for Branch Offices, see page 1083 A)

For submission of manuscripts, see page 960 A

Analytical Chemistry and Energy Related Research

It is heartening to see that analytical sciences are receiving specific recognition as plans go forward to implement research programs related to the nation's energy needs. For example, one of the fifteen areas defined as directly related to chemistry in the supplemental energy program of the National Science Foundation [*C&EN*, May 20, 1974, p 14] is named Chemical Analysis. Several others, such as Instrumentation, Physical and Chemical Separations, and Solid Surfaces have a strong analytical slant, and most of the others will involve analytical research although to a lesser extent. Similarly, the new NSF-RANN program "Environmental Effects of Energy" places a high priority on improving the reliability of analytical measurements.

During the summer and fall of 1974, the Chemical Section of the National Science Foundation is sponsoring a series of workshop conferences (ANAL. CHEM., Sept. 1974, p 881 A) designed to delineate energy-related problem areas to which chemical research could profitably be addressed. An obvious problem here is that, given a sufficiently long time base, practically all fundamental research in chemistry could be envisioned as having at least a tenuous connection with energy programs. But Congress, in funding such research, will surely look for direct and short-range applicability. There is therefore a serious danger that scientists will appear to promise more than they can deliver, and Congress will react in two or three years by deciding that basic research is not worth the cost. It is therefore of utmost importance that any supplemental appropriations for this purpose be channeled to projects showing clear and unmistakable connections to energy-related programs. Analytical research, by its very nature, will have relatively little difficulty in showing such connections. A greater problem appears to be presented by the urgency of timing, to perfect the necessary analytical methodology before a great deal of effort is wasted through the use of inadequate or erroneous measurements.



Nondestructive Determination of Some Trace Elements in Tantalum by Proton Activation Analysis

Viliam Krivan

Max-Planck-Institut für Metallforschung, Laboratorium für Reinststoffe, D-7070 Schwabisch Gmünd, West Germany

Dale L. Swindle and Emile A. Schweikert

Center for Trace Characterization, Department of Chemistry, Texas A&M University, College Station, Texas 77843

Trace concentrations of titanium, iron, zirconium, niobium, molybdenum, and tungsten have been determined nondestructively and simultaneously in high purity tantalum. The determination is based on the analysis of the γ-ray spectra of the radionuclides produced by bombarding thick samples with a 15-MeV proton beam via the following principal reactions: $^{48}Ti(p,n)^{48}V$, $^{56}Fe(p,n)^{56}Co$, $^{90}Zr(p,n)^{90}Nb$, $^{93}Nb(p,n)^{93m}Mo$, and $^{182}W(p,2n)^{181}Re$. The trace elements have been determined at levels comprised between 0.1 to 35 ppm, with a relative precision of 8.5 to 25%. The detection limits for a 5 μA-hr irradiation range from 0.005 ppm for zirconium to 0.5 ppm for tungsten.

The trace characterization of medium and high purity tantalum for metallic impurities is a difficult analytical task. Among the impurities of particular interest in connection with metallurgical and physical studies are titanium, iron, zirconium, niobium, molybdenum, and tungsten. The two most significant trace elements are niobium and tungsten. Niobium, for example, is present at a concentration level of several tens of parts-per-million even in the highest purity tantalum commercially available, prepared by electron beam zone refining. The second main impurity, tungsten, is usually present in the part-per-million range in the same type of material.

Although several sensitive determination methods are available for the elements mentioned, most of them are destructive. Compounding this drawback is the fact that separation procedures applicable in the analysis of tantalum are relatively complicated. Clearly, an instrumental method of analysis would in this case be of significant advantage. Among the instrumental techniques, only emission spectrography (*1–3*) and mass spectrometry (*4*) are applicable, both carrying, however, some inherent limitations (sensitivity and standardization, respectively). Another powerful method, neutron activation analysis, can be used only in connection with radiochemical separations (*5, 6*), mainly because of the high matrix activity induced.

Several studies reported in recent reviews (*7, 8*) and original communications, *e.g.* (*9–12*), have shown the feasibility of highly selective and sensitive determination of medium and high Z elements using charged particle activation analysis. These dealt, however, mostly with destructive or nondestructive single element determinations. In the present study, the application of this technique to the nondestructive multielement analysis in high purity tantalum is presented.

EXPERIMENTAL

Irradiation. Samples and standards were irradiated at the Texas A&M University 88-inch cyclotron. Typical bombarding conditions for thick target yield measurements on Mo, Nb, Zr, W, Ti, and Fe and for standardization purposes were: one-minute irradiations with 15 MeV proton beams of 0.05 to 0.2 μA. Activation curves were established using proton energies up to 30 MeV. High purity tantalum samples for analysis were irradiated in a water-cooled sample holder with beam intensities of 2–4 μA for 1–3 hours. The details of the experimental arrangement have been described previously (*13*).

Samples. Trace characterization was performed on samples of high purity tantalum obtained from Materials Research Corporation, Orangeburg, N.Y. The VP grade tantalum supplied in rod form was cut into sample wafers of approximately 1-mm thickness. A pre-irradiation chemical etch was accomplished with a 3 to 1 mixture of concentrated HNO_3 and HF to remove possible surface contamination.

Counting Equipment. Gamma-ray measurement was performed using an Ortec Ge(Li) γ-ray spectrometer. The detector characteristics included energy resolution of 2.3 keV FWHM for the 1.332 MeV γ-ray of ^{60}Co, photopeak efficiency of 8.0% relative to a 3 × 3 inch NaI(Tl) detector and a peak to Compton ratio of 28:1. The absolute counting efficiency for this detector was determined using calibrated radioisotope sources of ^{57}Co, ^{203}Hg, ^{22}Na, ^{54}Mn, and ^{60}Co supplied by NEN Chemicals. Data were collected on a 4096-channel Canberra multichannel analyzer.

Quantitative Calculations. Quantitation of results was accomplished using thick metal targets of Mo, Nb, Zr, W, Ti, and Fe. These were irradiated and used as reference standards after making the appropriate corrections for both the length of irradiation and the beam intensity.

RESULTS AND DISCUSSION

Trace Element and Matrix Activation by Proton Bombardment. The selection of the type of the bombarding particle and energy is paramount for optimizing the performance of nondestructive multielement charged particle activation analysis. For the trace element–matrix combination considered, proton activation appeared best suited both from the standpoint of sensitivity and selectivity. A bombarding energy of 15 MeV was chosen, based on considerations outlined below.

The trace elements that can be detected in tantalum by

(1) "Methods for Emission Spectrochemical Analysis," Fifth ed., American Society for Testing and Materials, Philadelphia, Pa., 1968, p 580.
(2) L. C. Chandola, V. S. Dixit, and M. D. Sakena, *India, At. Energy Comm., Bhabha At. Res. Cent.*, **BARC-465**, 1970, 5 pp.
(3) N. F. Zakhariya, A. I. Staikov, and I. S. Aubinder, *Spektrosk. At. Mol.*, 88–91 (1969).
(4) K. Sato, N. Yamaguchi, R. Suzuki, and R. Matsumoto, *J. Jap. Inst. Metals*, **34**, 610 (1970).
(5) T. Kawashima, "Proceedings 1965 International Conference: Modern Trends in Activation Analysis," Texas A&M University, College Station, Texas, 1965, p 61.
(6) E. N. Gilbert, V. A. Pronin, and V. G. Torgov, *Radiokhimiya*, **10**, 500 (1968).
(7) E. Ricci, "Charged Particle Activation Analysis," in "Advances in Activation Analysis," Vol. 2, J.M.A. Lenihan, S. J. Thomson, and V. P. Guinn, Ed., Academic Press, New York, N.Y., 1972, p 221.
(8) W. S. Lyon, E. Ricci, and H. H. Ross, *Anal. Chem.* **44**, 438R (1972).
(9) D. L. Swindle and E. A. Schweikert, *Anal. Chem.*, **45**, 2111 (1973).
(10) J. L. Debrun and J. W. Barrandon, *J. Radioanal. Chem.*, **17**, 291 (1973).
(11) D. C. Riddle and E. A. Schweikert, *Anal. Chem.*, **46**, 395 (1974).
(12) B. Parsa and S. S. Markowitz, *Anal. Chem.* **46**, 186 (1974).
(13) H. L. Rock and E. A. Schweikert, *Anal. Chem.*, **41**, 958 (1969)

Table I. Activation Data on the Trace Elements of Interest

Principal reaction	Q-value, MeV	Half-life	Major γ-rays, MeV	Intensity, %	Thick target yield, dps/μA[a]	Experimental threshold energy, MeV
$^{48}Ti(p,n)^{48}V$	−4.8	16.0 d	0.983	100	3.9×10^5	6.5 ± 0.5
			1.312	99		
$^{56}Fe(p,n)^{56}Co$	−5.4	78.5 d	0.847	99	5.1×10^4	8.0 ± 0.5
			1.238	69		
			1.771	15		
			2.598	17		
$^{90}Zr(p,n)^{90}Nb$	−6.9	14.6 h	1.129	89	4.4×10^5	7.5 ± 0.5
			2.319	82		
			0.141	67		
$^{93}Nb(p,n)^{93m}Mo$	−1.2	6.9 h	0.263	53	4.6×10^5	4.0 ± 0.5
			0.685	92		
			1.477	100		
$^{94}Mo(p,n)^{94}Tc$	−5.0	4.8 h	0.702	100	5.4×10^5	8.0 ± 0.5
			0.850	100		
			0.871	100		
$^{95}Mo(p,n)^{95}Tc$	−3.7	4.3 d	0.778	100	2.8×10^5	6.5 ± 0.5
			0.850	97		
			0.812	88		
$^{182}W(p,2n)^{181}Re$	−11.2	19 h	0.366	100	2.2×10^{5b}	11.5 ± 0.5

[a] For 1-minute irradiations of pure metal targets (natural isotopic composition) at the end of irradiation. [b] Assuming $I_\gamma = 100\%$.

Table II. Proton-Induced Reactions on Tantalum

Reaction	Q-value, MeV	Half-life	Major γ-rays, MeV
$^{181}Ta(p,n)^{181}W$	−1.0	121.5 d	0.136
			0.152
$^{181}Ta(p,3n)^{179m,g}W$	−16.7	6 m	0.222
		38 m	0.031
$^{181}Ta(p,4n)^{178}W$	−23.0	21.5 d	no
$^{181}Ta(p,pn)^{180m}Ta$	−7.6	8.1 h	0.093
$^{181}Ta(p,p2n)^{179}Ta$	−14.2	600 d	no
$^{181}Ta(p,p3n)^{178m,g}Ta$	−22.1	9.3 m	0.093
		2.2 h	0.093
$^{181}Ta(p,p4n)^{177}Ta$	−29.0	56.6 h	0.113
$^{181}Ta(p,2p)^{180m}Hf$	−5.9	5.5 h	0.093
$^{181}Ta(p,3p)^{179}Lu$	−13.9	4.6 d	0.217
$^{181}Ta(p,3pn)^{178m,g}Lu$	−20.9	21 m	0.089
		28 m	1.341
$^{181}Ta(p,3p2n)^{177}Lu$	−26.8	161 d	0.115

nondestructive proton activation and pertinent nuclear data (*14–16*) are listed in Table I. Also included are thick target yields for 15-MeV protons. These data indicate the possibility of determining simultaneously the elements listed with a single irradiation. Additional more detailed information was obtained by measuring the activation curves (relative excitation functions) for all of the reactions of interest. The experimental threshold energies observed under used experimental conditions are given in Table I. The activation curves further comfirmed that a proton energy of approximately 15 MeV would be best suited for the combination of trace elements of interest.

In Table II, a listing is given of the proton-induced nuclear reactions on tantalum and their relevant nuclear data. The examination of the Q-values shows that there are only a few reactions energetically possible below ~15 MeV proton energy. For most of them, the γ-ray energies and intensities are low or the half-lives of the product nuclides are long. An important advantageous factor further minimizing the activation of the tantalum matrix is the relatively high Coulomb barrier, which for protons has a value of 15.7 MeV. Experimental evidence confirmed that proton energies ≲15 MeV can indeed be readily used on tantalum.

Nuclear Interferences. At a proton energy of 15 MeV, the following interfering reactions are energetically possible: a) $^{52}Cr(p,\alpha n)^{48}V$ ($Q = -14.2$ MeV), affecting the titanium determination; b) $^{60}Ni(p,\alpha n)^{56}Co$ ($Q = -11.6$ MeV), affecting the determination of iron; c) $^{94}Mo(p,\alpha n)^{90}Nb$ ($Q = -9.0$ MeV), affecting the zirconium determination; d) $^{94}Mo(p,pn)^{93m}Mo$ ($Q = -9.7$ MeV), affecting the niobium determination; e) $^{99}Ru(p,\alpha)^{96g}Tc$ ($Q = +3.1$ MeV), $^{100}Ru(p,\alpha n)^{96g}Tc$, ($Q = -8.4$ MeV), and $^{101}Ru(p,\alpha 2n)^{96g}Tc$, ($Q = -13.4$ MeV), affecting the molybdenum determination; f) $^{184}Os(p,\alpha)^{181}Re$, ($Q = +6.5$ MeV) and $^{186}Os(p,\alpha 2n)^{181}Re$, ($Q = -8.4$ MeV), affecting the determination of tungsten.

These possible interferences were checked experimentally by irradiations of thick targets made from the corresponding elements. In all cases, no measurable interference was observed when the element to be determined and the interfering element were at equal concentrations.

γ-Ray Interferences. Possible interferences due to overlapping γ-rays originating from different nuclides are listed in Table III. This type of interference is most serious in the tungsten determination for which the $^{182}W(p,n)^{182}Re$ reaction combined with measuring the 1.122-MeV and 1.222-MeV γ-rays would be most suitable. Unfortunately, this reaction cannot be used because of a strong interference for both of these lines caused by the presence of ^{182}Ta emitting also γ-rays of exactly the same energies. The formation of ^{182}Ta can only be explained by reaction $^{181}Ta(n,\gamma)^{182}Ta$. The following experimental evidence supports this interpretation: a) this interference occurs only in the presence of a tantalum matrix (Figure 1); b) the γ-ray energies, their intensities and the half-lives indicate the presence of ^{182}Ta; c) the activation curve for the formation of the interfering radionuclide shows that this is not a threshold reaction (Figure 2). The production of ^{182}Ta is not surprising when one considers that by bombardment with protons of medium energy, neutrons can be produced by (p,xn) reactions and that the activation cross

(14) C. M. Lederer, J. M. Hollander, and I. Perlman, "Table of Isotopes," 6th ed., John Wiley & Sons, New York, N.Y., 1967.
(15) K. A. Keller, H. Munzel, and H. Lange, "Q-Values for Nuclear Reactions," Landolt-Bornstein, Neue Serie, Gruppe I, Band 56, Springer, Berlin, 1973.
(16) Ch. Meixner, "Gammaenergien:" Jul-811-RX, Julich, W. Germany, Dec. 1971.

Table III. Gamma-Ray Interferences Encountered in Nondestructive Tantalum Analysis

Principal reaction	$T_{1/2}$	E_γ, MeV	I_γ, %	Interference E_γ, MeV	Interference Nuclide	Interference $T_{1/2}$	Mode of production
$^{182}W(p,n)^{182}Re$	13 h	1.122	strong	1.122	^{182}Ta	115 d	$^{181}Ta(n,\gamma)^{182}Ta$
		1.222	strong	1.222	^{182}Ta		
$^{93}Nb(p,n)^{93m}Mo$	6.9 h	0.264	58	0.265	^{182}Ta	115 d	$^{181}Ta(n,\gamma)^{182}Ta$
$^{56}Fe(p,n)^{56}Co$	77.3 d	0.848	100	0.850	^{96}Tc	4.3 d	$^{96}Mo(p,n)^{96}Tc$
$^{96}Mo(p,n)^{96}Tc$	4.3 d	0.850	100	0.848	^{56}Co	77.3 d	$^{56}Fe(p,n)^{56}Co$
		1.127		1.129	^{90}Nb	14.6 h	$^{90}Zr(p,n)^{90}Nb$
$^{90}Zr(p,n)^{90}Nb$	14.6 h	1.129	97	1.127	^{96}Tc	4.3 d	$^{96}Mo(p,n)^{96}Tc$

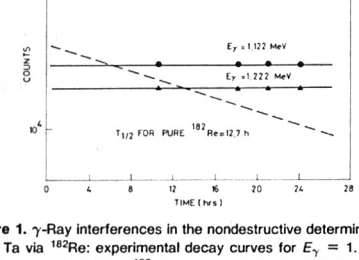


Figure 1. γ-Ray interferences in the nondestructive determination of W in Ta via ^{182}Re: experimental decay curves for E_γ = 1.122 and 1.222 MeV; the decay of ^{182}Re from pure W is given for comparison

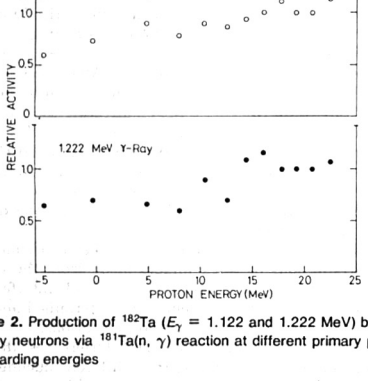


Figure 2. Production of ^{182}Ta (E_γ = 1.122 and 1.222 MeV) by secondary neutrons via ^{181}Ta(n, γ) reaction at different primary proton bombarding energies

section for the reaction $^{181}Ta(n,\gamma)^{182}Ta$ has a relatively high value for neutrons in the MeV range (*17*). A part of the neutrons produced may be thermalized, giving a very high thermal activation cross section for tantalum. These conclusions make it evident that the use of unnecessarily thick samples should be avoided. Consequently the determination of tungsten must in this case be based on the reaction $^{182}W(p,2n)^{181}Re$ and the measurement of a 0.366-MeV γ-ray. Because of the higher threshold energy and the lower thick target yield for 15-MeV protons and also because of high Compton continuum at 0.366 MeV, this determination is less sensitive than that based on the reaction $^{182}W(p,n)^{182}Re$. The ^{181}Re is, however, adequate in the case of a tantalum matrix where the tungsten concentrations are at the ppm level. The detection of ^{181}Re is further aided by the high intensity of its 0.366-MeV γ-ray. It should be emphasized that owing to the complexity of the γ-ray spectra in this energy region, an unequivocal identification of ^{181}Re must be based on both γ-ray and half-life data.

For similar reasons, as discussed above, in the determination of niobium via $^{93}Nb(p,n)^{93m}Mo$, the 0.264-MeV γ-ray cannot be used. In this case, however, there are two other interference-free γ-rays available which, by virtue of their higher energies, have as an added advantage a much lower Compton background.

In the determination of molybdenum, the 0.850-MeV γ-ray of ^{96}Tc can be affected by the presence of the 0.848-MeV γ-ray of ^{56}Co due to iron. These two γ-rays could not be separated by the detector at our disposal. Other interference-free γ-rays of ^{96}Tc were therefore used for the molybdenum assay. Similarly in the case of the determination of iron, specific γ-rays are available, although even the 0.848-MeV γ-ray could be used, provided sufficient waiting time is allowed for ^{96}Tc to decay.

Finally, in the determination of zirconium via the 1.129-MeV γ-ray of ^{90}Nb, a weak interference can occur with the 1.127-MeV γ-ray of ^{96}Tc arising from molybdenum. The error introduced in this case into the zirconium determination is less than 2% when both elements are at the same concentration level. Further, if necessary, the interference-free γ-ray of ^{90}Nb can be used for determining zirconium.

Analysis of Samples. To illustrate the practical usefulness of proton activation, a series of high purity tantalum samples were examined. The nuclides and pertinent γ-ray energies used for the determination of the trace elements sought are indicated in the γ-ray spectrum shown in Figure 3.

The concentrations determined for the six elements of interest are given in Table IV. The results for titanium, iron, molybdenum, and tungsten represent the average of three determinations on replicate samples. Included in these data are the average deviations based on the individual determinations. These results reflect the capabilities of the method on a multielement basis using a single irradiation of 2 to 4 hours and counting periods in excess of 10 hours. The performance of the method in terms of accuracy could not be evaluated because of the lack of tantalum material characterized by another independent method. In this context, the constant concern in this work for assessing possible sources of systematic errors might be emphasized again.

Also listed in Table IV are the estimated limits of detection based on experimental data obtained in a typical tantalum irradiation (2.5-hour bombarding time with a beam intensity of 2 μA followed by a cooling period of 10 to 50 hours). The measured γ-ray peak intensities corresponding to known concentrations were compared with the minimum detectable peaks calculated using the 3σ criterion.

In the case of zirconium and niobium, six additional determinations involving shorter irradiation and counting

(17) M. D. Goldberg, S. M. Mughabghab, S. N. Purohit, B. A. Magurno, and V. M. May, "Neutron Cross Sections," Vol. IIC, BNL 327, 2nd ed., Suppl. 2, Brookhaven National Laboratory, Aug. 1966.

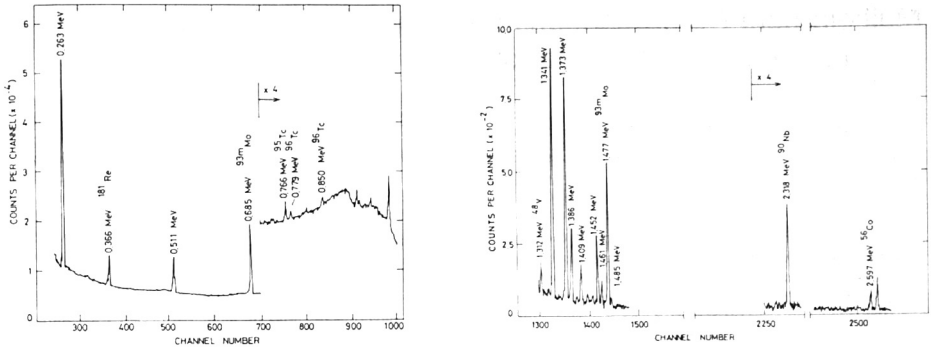


Figure 3. γ-Ray spectrum of a tantalum sample measured under the following conditions: count time of 6 hours, start of count 8 hours after end of bombardment

Table IV. Results of Tantalum Analysis and Experimental Limits of Detection

Impurity element	Concn detd, ppm	Av. dev[a]	Exptl detection limits, ppm
Ti	0.09	±0.02	0.02
Fe	0.77	±0.15	0.10
Zr	0.12	±0.02[b]	0.005
Nb	32.80	±2.80[b]	0.30
Mo	0.67	±0.12	0.20
W	6.60	±1.40	0.50

[a] Based on 3 determinations. [b] Standard deviation calculated from 9 determinations.

Table V. Reproducibility of Niobium and Zirconium Determination in Tantalum (VP Grade)

Detn	Nb content, ppm	Zr content, ppm
1	33.3	0.10
2	35.9	0.10
3	31.0	0.11
4	35.0	0.10
5	37.0	0.12
6	29.7	0.16
7	30.6	0.17
8	37.0	0.12
9	32.4	0.11
Average and σ	32.8 ± 2.8	0.12 ± 0.02

times were carried out to establish the standard deviations. The reproducibility on a total of nine determinations for these two trace elements is illustrated in Table V. The standard deviations were found to be 8.5% for niobium at 30 ppm and 16.6% for zirconium at 0.1 ppm. It should be noted that these repetitive determinations were carried out on nine adjacent samples from the original tantalum rod. Possible inhomogeneities in the trace element distribution would be included in the results obtained and the standard deviations computed.

CONCLUSIONS

Proton activation is well suited for the trace characterization of tantalum. This technique provides a nondestructive assay with high sensitivity and selectivity for most trace elements of major interest. The combination of these important features is particularly attractive when considering currently available methods for the analysis of tantalum.

ACKNOWLEDGMENT

The assistance of the cyclotron operations personnel is gratefully acknowledged.

RECEIVED for review February 5, 1974. Accepted May 1, 1974. This work was supported by the National Science Foundation Grant GP-34877X.

Multielement Determination in Market-Garden Soils by Instrumental Photon Activation Analysis

Amares Chattopadhyay and R. E. Jervis

Department of Chemical Engineering and Applied Chemistry, and Institute for Environmental Studies, University of Toronto, Toronto, Ontario, M5S 1A4, Canada

An instrumental method has been developed for simultaneous photon activation analysis of 30 elements in vegetable crop-growing organic soils using a 45-MeV electron linear accelerator. The method consists of a simultaneous irradiation of a multielement standard and the environmental soil samples at 15, 20, 22, 35, and 44 MeV maximum bremsstrahlung energies for 1 hour to determine concentrations of 27 elements by a high-resolution Ge(Li) detector. Three more elements can be determined by continuing the irradiation for 4 hours at 20 MeV. Guidelines for selecting appropriate activation products and their gamma-rays have been described. The concentrations of several of the elements determined have been independently checked through the use of alternative nuclides and gamma-rays. A comparison of the accuracy of this activation method with other standard analytical techniques, notably atomic absorption spectrophotometry, has been carried out by analyzing a few elements in soils by the latter technique. Agreement among the several analytical methods compared ranged between 2 and 10%. The accuracy of photon activation technique has also been evaluated by analyzing the Standard Reference Materials. The limits of detection for all 30 elements analyzed varied between 10 and 8000 nanograms depending on the nuclide measured.

The determination of trace concentrations of heavy metals in biological and environmental materials has become an important analytical task because of the growing concern about heavy metal contamination of the biosphere as a potential health hazard. Moreover, the toxicity of a particular heavy metal may be increased greatly or decreased by a significant amount of one or more metals present in the sample. Thus multielement determination in a single sample is very valuable for revealing and understanding any such synergistic or antagonistic effects that exist among certain metals at very low concentrations (*1*). Consequently, analytical methods for the simultaneous estimation of a number of trace elements of environmental interest in a single sample are being developed in this and other laboratories. In such analyses, the nondestructive approach has obvious advantages. Recently, instrumental thermal neutron activation analysis (INAA) has been used by Nadkarii and Morrison (*2*) to determine concentrations of up to 36 elements in biological materials. However, not all the elements of environmental interest can be conveniently and sensitively determined by INAA. Photon activation analysis (PAA), the less-studied but developing branch of activation analysis, has an excellent potential for multielement determination on a purely instrumental basis. A few of the significant advantages of PAA of biological materials over its sister technique, NAA, have been summarized by Andersen *et al.* (*3*).

The principles and general features of PAA have been well treated by Engelmann (*4, 5*) and Hoste *et al.* (*6*). As an aid in selecting nuclides on which to base a PAA determination, the gamma-ray energies of nuclides produced by (γ,n) and (γ,p) reactions have been tabulated by Galatanu and Grecescu (*7*). Recently, a number of compilations of photonuclear reactions have been made available. For example, Toms (*8, 9*) compiled photonuclear separation energies, activation products, and their gamma-ray energies in two volumes; Berman (*10*) reported photoneutron cross sections for many nuclides obtained with monoenergetic photons; and Fuller *et al.* (*11*) catalogued photonuclear reaction data. In the past, several authors (*12–17*) have identified a large number of nuclides produced on photon activation and calculated their relative sensitivities. Lutz (*18*) has estimated the specific activities of 60 elements irradiated at 25, 30, and 35 MeV electron energies. Kato (*19–21*) has reported experimental sensitivities for many elements at 30 and 60 MeV bremsstrahlung beams.

Multielement determination in biological materials by instrumental photon activation analysis (IPAA), in particular, has been little studied. Recently, review papers have been presented on photonuclear reaction applications by McNeill (*22*) and on PAA of biological and environmental samples by Hislop (*23*). It is evident from these reviews

(1) J. Parizek, Survey paper, "Nuclear Activation Techniques in the Life Sciences," "Proceedings of an International Atomic Energy Agency Symposium," Bled, Yugoslavia, IAEA, Vienna, 1972, p 177.
(2) R. A. Nadkarni and G. H. Morrison, *Anal. Chem.*, **45**, 1957 (1973).
(3) G. H. Andersen, F. M. Graber, V. P. Guinn, H. R. Lukens, and D. M. Settle, "Nuclear Activation Techniques in the Life Sciences," "Proceedings of an International Atomic Energy Agency Symposium," Amsterdam, IAEA, Vienna, 1967, p 99.
(4) C. Englemann, "Advances in Activation Analysis," Vol. II, J. M. A. Lenihan, S. J. Thomson, and V. P. Guinn, Ed., Academic Press, London, 1972, Chap. I.
(5) C. Englemann, "Photonuclear Reactions and Applications," "Proceedings of an International Conference, Calif.," Vol. II, B. L. Berman, Ed., Lawrence Livermore Laboratory, 1973, p 1137.
(6) J. Hoste, J. Op De Beeck, R. Gijbels, F. Adams, P. Van Den Winkel, and D. De Soete, "Instrumental and Radiochemical Activation Analysis," Chemical Rubber Company Press, Cleveland, Ohio, 1971, p 87.
(7) V. Galatanu and M. Grecescu, *J. Radioanal. Chem.*, **10**, 315 (1972).
(8) M. E. Toms, NRL Report **7554**, Washington, D.C., 1973.
(9) M. E. Toms, NRL Report **7591**, Washington, D.C., 1973.
(10) B. L. Berman, UCRL **74611**, Livermore, Calif., 1973.
(11) E. G. Fuller, H. M. Gerstenberg, H. Vander Molen, and T. C. Dunn, NBS Spec. Publ. **380**, Washington, D.C., 1973.
(12) C. A. Baker, G. J. Hunter, and D. A. Wood, AERE Report **5547**, H. M. Stationary Office, London, 1967.
(13) C. A. Baker and D. A. Wood, AERE Report **5818**, H. M. Stationery Office, London, 1968.
(14) E. A. Schweikert and Ph. Albert, "Radiochemical Methods of Analysis," "Proceedings of an International Atomic Energy Agency Symposium, Salzberg," Vol. I, IAEA, Vienna, 1965, p 323.
(15) T. Oka, T. Kato, K. Nomura, and T. Saito, *Bull. Chem. Soc. Jap.*, **40**, 575 (1967).
(16) T. Kato and Y. Oka, *Talanta*, **19**, 515 (1972).
(17) T. Kato and A. F. Voigt, *J. Radioanal. Chem.*, **4**, 325 (1970).
(18) G. J. Lutz, *Anal. Chem.*, **41**, 424 (1969).
(19) T. Kato, *Res. Rep. Lab. Nucl. Sci., Tohoku Univ.*, **5**, (1), 133 (1972).
(20) T. Kato, *ibid.*, **5** (2), 137 (1972).
(21) T. Kato, "Modern Trends in Activation Analysis," an International Conference, Saclay, France, Paper No. M 65 (1972).
(22) K. G. McNeill, APS Spring Meeting, Washington, D.C., 1973.
(23) J. S. Hislop, "Photonuclear Reactions and Applications," "Proceedings of an International Conference, Calif.," Vol. II, B. L. Berman, Ed., Lawrence Livermore Laboratory, 1973, p 1159.

that with the availability of high-resolution Ge(Li) detectors, the potential for multielement estimation by IPAA is being more widely recognized at present. Air particulates, blood, bone, geological samples, kale, and urine have all been analyzed by this method. On the other hand, little work has been done on soil samples except that reported by the present authors (*24–26*) and by Lutz (27).

Soil can be considered as a sink for metallic contaminants. It can accumulate metals from treated seeds, fertilizers, fungicides, herbicides, insecticides, irrigation waters, and atmospheric fallout, among other sources. These metals, in turn, can be translocated from soil to various parts of edible plants, and may eventually find their way to man. For this reason, the importance of soil analysis to environmental health has recently become more fully recognized. Hence, an IPAA method for estimation of 30 elements using a high-resolution Ge(Li) detector following irradiations of environmental soil samples at different bremsstrahlung energies, has been developed and is reported here. Cultivated soils with high organic matter content, commonly known as "muck" soils, have been collected at the Holland Marsh in Ontario, Canada. Specimens of these soils have been analyzed by the IPAA technique. In this report, emphasis is placed on the nuclear techniques of analysis developed rather than the importance of results obtained to assess the fate of toxic metals in crop-growing areas which will be reported in a separate publication.

EXPERIMENTAL

Samples. Soil samples were collected from the Holland Marsh with the assistance of the Department of Botany, University of Toronto, in June 1970. At each sampling site, two surface scrapings (surface-1 and surface-2) were taken from both sides of a particular plant. Then the whole plant was removed and a soil pit was dug at the site of plant sampling and soils were removed carefully from the surface and depths up to 45 cm at intervals of 7.5 cm. The detailed procedure of soil sampling has been described by Czuba (*28*). About 25 grams of these wet muck soils were air dried at room temperature. Approximately 1 gram of dried soil was packed in a clean polyethylene bag which was then heat sealed. Several such bags were prepared for each soil sample. For IPAA, bags were placed in 5.5-cm long cylindrical polyethylene irradiation capsules fitted with stoppers. The typical sample size was 2 cm long and 1.2 cm in diameter.

Standards. A synthetic soil matrix for use as a support for trace metal standards was prepared by mixing high-purity grade starch powder (46.1%), diammonium hydrogen phosphate (42.8%), silicon dioxide (6.8%), ferric trioxide (2.2%), and calcium oxide (2.1%). To this mixture, microgram quantities of the following elements were added: antimony, arsenic, barium, bismuth, cadmium, calcium, cesium, chlorine, chromium, cobalt, indium, iron, lead, magnesium, manganese, mercury, molybdenum, nickel, scandium, selenium, silver, sodium, strontium, tellurium, thallium, tin, titanium, vanadium, zinc, and zirconium. All the chemical reagents used were "spec-pure" or 99.99% pure. The compounds were mixed homogeneously by rotating in a mixer for 3 days and used as a multielement standard (MES). The homogeneity and accuracy of the MES were later examined by analyzing replicate samples and Standard Reference Materials, and by determining elemental concentrations through alternative techniques. Known quantities of the MES were placed in polyethylene bags and were given the identical shape and volume as the soil samples in the irradiation capsules.

Apparatus. A Vickers 45-MeV electron linear accelerator (Linac) at the University of Toronto was used for IPAA of soils reported here. After considerable improvement during recent years, this Linac is now capable of producing electrons of any energy between 8 and 44 MeV with an energy precision of about ±0.5 MeV, suitable for activation work. The pulse length can be varied from 1.3 nanoseconds to 3.6 microseconds (μsec). A repetition rate of 30 to 480 pulses/sec can be chosen. The maximum power output at a particular electron energy was obtained in this study by using pulses of 2.1 μsec duration at a repetition rate of 240 pulses/sec. The typical average beam currents measured on the tungsten converter by a current monitor were: 25 microampere (μA) at 8 MeV, 35 μA at 10 MeV, 50 μA at 12 MeV, 75 μA at 14 MeV, 80 μA at 15 MeV, 95 μA at 20 MeV, 110 μA at 22 MeV, 125 μA at 25 MeV, 145 μA at 30 MeV, 225 μA at 35 MeV, 190 μA at 40 MeV, and 155 μA at 44 MeV. A peak current of 85 mA was typical. Bremsstrahlung photons for irradiating samples were obtained by converting the electron beam with a 3-mm-thick tungsten plate placed 3 cm away from the face of the beam exit window of the Linac. The size of the electron beam as measured on the converter was 2.3 cm × 1.5 cm. The tungsten converter was water-cooled.

Irradiation. The cylindrical polyethylene irradiation capsules containing sample, MES, a blank polyethylene bag, 2 copper wires (for monitoring photon flux), and a cobalt wire (for measuring thermal neutron flux) were wrapped with a cadmium foil and were put on a rotating sample holder assembly. The design and need for such an assembly have been described elsewhere (*26*). The sample assembly was placed 1 cm away from the rear face of the tungsten converter. Depending on the elements being determined, samples were irradiated at the maximum peak electron energies of 15, 20, 22, 35, and 44 MeV normally for 1 hr in an average flux of 2×10^{13} photons/cm^2 sec. The irradiation energies selected as optimal for determining individual elements are listed in Table II. Both samples and MES were cooled during irradiation by directing a jet of air toward them.

Procedure. The capsules containing sample, MES, and the blank polyethylene bag were removed and opened following irradiation. They were transferred to clean glass counting vials. The sample and MES were given identical geometry without rupturing the polyethylene bag. The copper and cobalt wires were also transferred to counting vials. After a "cooling period" of about 1 hr, the sample and MES were counted under identical geometry conditions using a 60 cm^3 Ge(Li) detector.

Counting Equipment. Gamma-rays were observed with a 60 cm^3 or a 40 cm^3 Ge(Li) detector coupled with a 4096-channel Canberra or Kicksort pulse height analyzer. The full widths at half-maximum of the two detectors were 1.9 KeV and 2.5 KeV at the 1.332 MeV photopeak of ^{60}Co. The peak-to-compton ratios were 30:1 and 18:1, respectively. The efficiencies of the Ge(Li) detectors were measured as 6.7% and 5.8% with respect to a standard NaI(Tl) detector.

METHODOLOGY

The number of events detected in a gamma-ray peak of interest were summed by using the cursor provided in the Canberra PHA. With the Kicksort PHA, a base-line subtraction technique was used. Background counts recorded using the polyethylene bag were subtracted. Decay corrections were made wherever applicable. The concentrations of elements were calculated by the usual relative method by reference to the MES. However, among the large number of well-resolved gamma-rays recorded by a high-resolution Ge(Li) detector in gross gamma-ray spectra of photon-activated soil samples (Figure 1), only a few can be selected for the estimation of the trace concentrations of elements of environmental interest.

At the beginning of this work, a list of prominent gamma-rays emitted by photon-activated products was prepared from the literature (*12, 13, 29*). However, because of lack of reliable data and also to assess problems of mutual interference, some 30 selected elements were irradiated at 8, 10, 12, 14, 15, 20, 22, 25, 30, 35, and 40 MeV maximum electron energies, the bismuth and vanadium were activated at 44 MeV. The gamma-ray spectra of these activated species were recorded as soon as possible by means of a 40 cm^3 Ge(Li) detector. The energy and half-life of each gamma-ray were precisely measured and a nuclide was assigned accordingly to each resolved gamma-ray. This list of

(24) A. Chattopadhyay and R. E. Jervis, *ibid.*, p 1009.
(25) A. Chattopadhyay, L. G. I. Bennett, and R. E. Jervis, *Can. J. Chem. Eng.*, **50**, 189 (1972).
(26) A. Chattopadhyay and R. E. Jervis, *Radiochem. Radioanal. Lett.*, **11**, 331 (1972).
(27) G. J. Lutz, "Nuclear Methods in Environmental Research," "Proceedings of an ANS Topical Meeting," J. R. Vogt, T. F. Parkinson, and R. L. Carter, Ed., University of Missouri, Columbia, 1971, p 144.
(28) M. Czuba, M.Sc. Thesis, Dept. of Botany, Univ. of Toronto, Toronto, Canada, 1972.
(29) C. M. Lederer, J. M. Hollander, and I. Perlman, "Table of Isotopes," 6th ed., J. Wiley and Sons, Inc., N.Y., 1967.

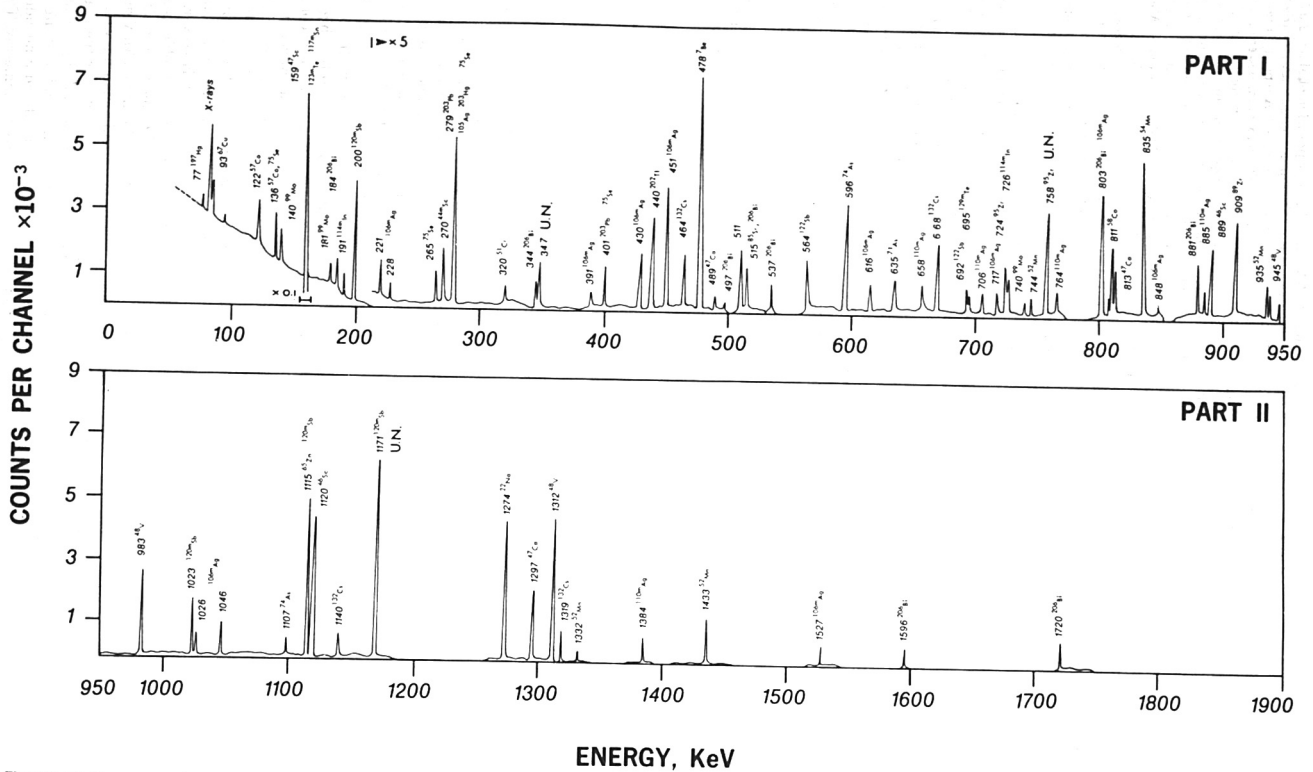


Figure 1. Gamma-ray spectrum recorded with a 60 cm^3 Ge(Li) detector of a "muck" soil sample. E_{rr} = 44 MeV, t_d = 3 w, U.N. = unidentified nuclide

Table I. Interference from Overlapping Gamma-Rays

Element	Data for nuclide analyzed: Target isotope (% abundance)	Activation reaction	Nuclide produced	Half-life of nuclide	Gamma-ray energy in KeV (% intensity)	Interfering nuclides: Gamma-ray energy in KeV (% intensity)	Half-life of nuclide	Method of production	Remarks[a]	Time of analysis[b]
Antimony	^{123}Sb (42.75)	γ,n	^{122}Sb	2.8 d	564.0 (73)	...	...	...	...	R
Arsenic	^{75}As (100)	γ,n	^{74}As	17.9 d	595.8 (61)	592.1 (1.2)	94 d	^{186}Os(γ,n)^{185}Os	A	T
Barium	^{135}Ba (6.59)	γ,γ′	^{135m}Ba	28.7 h	268.1 (16)	592.5 (10)	22 h	^{44}Ca(γ,p)^{43}K	B	
	^{136}Ba (7.81)	γ,n	^{135m}Ba			264.8 (62)	120.4 d	^{76}Se(γ,n)^{75}Se	C	R
Bismuth	^{209}Bi (100)	γ,3n	^{206}Bi	6.24 d	803.1 (99)	270.4 (86)	2.44 d	^{45}Sc(γ,n)^{44m}Sc	D	
					880.8 (73)	804.1 (12.5)	8.4 d	^{107}Ag(γ,n)^{106m}Ag	E	S
Cadmium	^{111}Cd (12.75)	γ,γ′	^{111m}Cd	49 m	246.8 (94)	881.4 (73)	34 d	^{85}Rb(γ,n)^{84}Rb	A	
	^{112}Cd (24.07)	γ,n	^{111m}Cd			248.0 (65)	20 m	^{85}Rb(γ,n)^{84m}Rb	A	P
Calcium	^{44}Ca (2.06)	γ,p	^{43}K	22 h	373.0 (100)	249.7 (3)	56 h	^{79}Br(γ,2n)^{77}Br	A	
Cesium	^{133}Cs (100)	γ,n	^{132}Cs	6.5 d	667.6 (95.6)	374.2 (15)	43 m	^{199}Hg(γ,γ′)^{199m}Hg	B	R
Chlorine	^{35}Cl (75.79)	γ,n	^{34m}Cl	32.4 m	2128.2 (35)	669.6 (9.1)	38 m	^{64}Zn(γ,n)^{63}Zn	B	S
Chromium	^{50}Cr (4.34)	γ,2n	^{48}Cr	23 h	310.2 (100)	...	...	...	...	P
Cobalt	^{59}Co (100)	γ,n	^{58}Co	71.3 d	811.0 (99)	308.4 (15.4)	74.2 d	^{193}Ir(γ,n)^{192}Ir	A	Q
Indium	^{113}In (4.33)	γ,γ′	^{113m}In	100 m	393.1 (64)	808.5 (5.8)	8.4 d	^{107}Ag(γ,n)^{106m}Ag	D	T
Iron	^{54}Fe (5.84)	γ,np	^{52}Mn	5.6 d	1433.2 (100)	397.8 (11)	22 h	^{44}Ca(γ,p)^{43}K	D	P
	^{56}Fe (91.68)	γ,nt	^{52}Mn			1433.5 (100)	3.76 m	^{53}Cr(γ,p)^{52}Mn	B	S
	^{57}Fe (2.17)	γ,p	^{56}Mn	2.58 h	846.8 (99)	847.6 (3.7)	8.4 d	^{107}Ag(γ,n)^{106m}Ag	C	P
Lead	^{204}Pb (1.48)	γ,γ′	^{204m}Pb	67 m	899.1 (100)	898.2 (91.5)	108 d	^{89}Y(γ,n)^{88}Y	A	P
	^{206}Pb (25.1)	γ,2n	^{204m}Pb			...	...	...	...	R
Magnesium	^{25}Mg (10.2)	γ,p	^{24}Na	15 h	1368.5 (100)	...	...	...	...	T
Manganese	^{55}Mn (100)	γ,n	^{54}Mn	303 d	834.8 (100)	...	...	...	...	Q
Mercury	^{198}Hg (10.02)	γ,n	^{197m}Hg	24 h	133.9 (42)	136.0 (60)	120.4 d	^{76}Se(γ,n)^{75}Se	D	Q
Molybdenum	^{100}Mo (9.62)	γ,n	^{99}Mo	67 h	140.5 (92)	...	...	...	...	Q
Nickel	^{58}Ni (67.76)	γ,n	^{57}Ni	36 h	1377.6 (86)	...	...	...	...	P
Scandium	^{45}Sc (100)	γ,n	^{44}Sc	3.92 h	1156.2 (99)	...	...	...	...	P
Selenium	^{82}Se (9.19)	γ,n	^{81m}Se	57 m	103.1 (8)	...	...	...	...	T
Silver	^{107}Ag (51.35)	γ,n	^{106m}Ag	8.4 d	451.1 (28.5)	...	...	...	...	
					717.0 (27)	...	...	...	...	
					1045.6 (29)	1039.5 (100)	1.83 d	^{49}Ti(γ,p)^{48}Sc	B	
Sodium	^{23}Na (100)	γ,n	^{22}Na	2.6 y	1274.4 (100)	...	...	...	...	T
Strontium	^{86}Sr (9.87)	γ,n	^{85m}Sr	70 m	231.7 (86)	228.3 (2.1)	8.4 d	^{107}Ag(γ,n)^{106m}Ag	C	P
Tellurium	^{130}Te (34.49)	γ,n	^{129}Te	69 m	459.2 (7.6)	...	...	...	...	P
Thallium	^{203}Tl (29.50)	γ,n	^{202}Tl	12 d	440.1 (95)	439.1 (100)	13.8 h	^{70}Zn(γ,n)^{69m}Zn	B	T
Tin	^{117}Sn (7.57)	γ,γ′	^{117m}Sn	14 d	158.3 (87)	158.1 (63.6)	43 m	^{199}Hg(γ,γ′)^{199m}Hg	B	T
	^{118}Sn (24.01)	γ,n	^{117m}Sn			158.8 (84)	117 d	^{124}Te(γ,n)^{123m}Te	C	
						160.0 (73)	3.43 d	^{48}Ca(γ,n)β^-^{47}Sc	B	
Titanium	^{49}Ti (5.46)	γ,p	^{48}Sc	1.83 d	1039.5 (100)	...	...	...	...	R
Vanadium	^{50}V (0.25)	γ,2n	^{48}V	16 d	983.3 (100)	983.3 (100)	1.83 d	^{49}Ti(γ,p)^{48}Cs	B	T
	^{51}V (99.75)	γ,3n	^{48}V							
Zinc	^{69}Zn (18.56)	γ,p	^{67}Cu	59 h	184.8 (48)	181.1 (7.6)	67 h	^{100}Mo(γ,n)^{99}Mo	E	Q
						184.0 (21)	6.24 d	^{209}Bi(γ,3n)^{206}Bi	E	
						185.7 (4)	1602 y	^{226}Ra in background	F	
	^{66}Zn (27.81)	γ,n	^{65}Zn	245 d	1115.4 (49)	1115.0 (1.3)	5.7 d	^{121}Sb(γ,n)^{120m}Sb	C	T
Zirconium	^{90}Zr (51.46)	γ,n	^{89}Zr	78.4 h	909.2 (99)	911.2 (100)	67 m	^{204}Pb(γ,γ′)^{204m}Pb	B	R
	^{91}Zr (11.23)	γ,2n	^{89}Zr							

[a] Interfering gamma-rays: A, not observed; B, allowed to decay; C, neglected; D, graphically resolved; E, contribution subtracted; F, background subtracted. [b] Most suitable time of analysis from end of irradiation: P, 2 hours; Q, 12 hours; R, 1 day; S, 3 days; T, 3 weeks or more.

nuclides along with their data was then combined with the other list prepared from the literature to obtain an extensive chart of nuclides produced by photon activation. This chart was kept up to date by consulting recent publications and was used throughout this study for identification of nuclides in activated soils.

Photonuclear Interference: Optimal Selection of Nuclides and Gamma-Rays. In experiments designed to optimize the IPAA determination of selected elements, two types of interfering photonuclear reactions were observed to occur at about the same photon energies. In one type, a gamma-ray which could have been used for determining the exact concentration of a particular element was found to suffer interferences from partial or complete overlap in energy of one or more gamma-rays emitted by other nuclides present in the same matrix. A second type of interference and more serious than the former was due to the competing reactions which could produce the particular nuclide of interest from a number of other elements present in the same sample. If proper precautions were not taken, a third type of interference due to thermal neutron activation could also offer serious problems. These interferences are described below in detail.

Overlapping Gamma-Rays. The choice of a gamma-ray from the nuclide of interest which suffered no interference from other gamma-rays based on the above chart was considered first for measurement. The most abundant gamma-ray of a nuclide was normally selected except when it had interferences from gamma-rays of other nuclides. Gamma-rays falling within ±4 KeV of each other were considered to be mutually interfering under the counting system used in this study. In the case of interferences of all gamma-rays of a nuclide, alternative nuclides produced by photon activation of the same element and that could be used for the determination of that element, were sought. For example, 67-m-nuclide ^{204m}Pb produced by the reactions ^{204}Pb(γ,γ')^{204m}Pb and ^{206}Pb(γ,2n)^{204m}Pb was chosen for interference-free lead analysis by IPAA and the 899.1 KeV (100%) gamma-ray was used. Details of the PAA method for trace lead determination have been reported previously (*26*).

When a number of nuclides were formed from different isotopes of the same element, normally the shorter-lived product was given prior consideration because a superior detection limit could be obtained from it using the standard irradiation period of 1 hr. The abundances of target isotopes, their threshold energies, and cross sections for different photonuclear reactions were also taken into consideration in deciding whether or not to base IPAA determination on particular nuclides. In certain instances, it was possible to select more than one nuclide as well as several gamma-rays satisfying most of the above criteria such as zinc and silver. On the other hand, unavoidable interferences were observed in a few cases. If the interference was due to a short-lived nuclide, it was allowed to decay preferentially to minimize its contribution.

In the opposite situation, *i.e.*, where a longer-lived nuclide interfered, it was produced in a small quantity by limiting the length of irradiation, resolved graphically, or its contribution was calculated and subtracted from the photopeak under consideration. An example of this interference was encountered in the measurement of barium. The observed intensity due to the 268.1-KeV gamma-ray of ^{135m}Ba (28.7 hr) was graphically separated from that due to the 270.4-KeV gamma-ray of ^{44m}Sc (2.44 days) by following their decay curves. On the other hand, the contribution due to the 804.1-KeV gamma-ray of ^{106m}Ag (8.4 days) was calculated and subtracted from the combined photopeak to obtain the bismuth content as measured by the intensity of the 803.1-KeV gamma-ray of ^{206}Bi. The bismuth content was also independently measured by following the 880.8-KeV gamma-ray of the same nuclide.

There are many other examples of interference arising from partial or complete overlap of gamma-rays with nuclides of interest. These are summarized in Table I, along with the nuclides and their gamma-rays which were selected for use in this work.

Competing Photon Induced Reactions. As mentioned above, in some cases competing photonuclear reactions, each producing the particular nuclide of interest, interfered in the selection of a nuclide on which measurements were based. An extensive chart containing the activation reactions of interest and photon induced competing reactions along with their separation energies (E_{sep}) was prepared. A few of these reactions are shown in Table II.

It can be seen from Table II that most of the photon induced interferences were eliminated by choosing an excitation energy below the E_{sep} of interfering reactions. For example, manganese was determined by irradiating soils at 20 MeV which is well above the E_{sep} of 10.2 MeV for the reaction ^{55}Mn(γ,n)^{54}Mn but below the E_{sep} of 20.4 MeV for the competing reaction ^{56}Fe(γ,np)^{54}Mn.

In a few instances, the nuclide with the least interference was selected among several products on the basis of the above criterion. For example, the choice of ^{113m}In was made using this guideline. The reaction ^{115}In(γ,γ')^{115m}In could not be used because of interference from a number of other reactions. The reaction ^{113}In(γ,γ')^{113m}In was also interfered with by the reaction ^{114}Sn(γ,p)^{113m}In (E_{sep}, 8.5 MeV). However, considering the small isotopic abundance of ^{114}Sn (0.75%) and the energy of irradiation used (E_{irr}) of 15 MeV, it was concluded that only a small amount of ^{113m}In could be produced from ^{114}Sn and thus interference from this reaction was neglected.

In a few cases, interfering competing reactions mentioned in the literature were studied in the context of muck soils analyzed. For example, ^{99}Mo–^{99m}Tc used in the determination of molybdenum was also reported to be formed from rhodium and ruthenium isotopes. A search for gamma-rays emitted by alternative products of the latter two elements was made in the gross gamma-ray spectra of muck soils recorded at different time intervals. No such gamma-rays could be identified. It was then concluded that no detectable amount of rhodium and ruthenium was present in muck soils, and thus no interference from these two elements could be observed.

In extreme cases of suspected interference in the photonuclear determination, the elements were measured by other analytical techniques as well. Cadmium in soils was determined by destructive NAA and atomic absorption spectrophotometry as well as by IPAA. The values obtained (Table V) were found to agree well within the experimental errors, *viz.*, about ±10%. Thus, contributions from any interfering reaction producing ^{111m}Cd are thought to be insignificant.

Thermal Neutron-Induced Reactions. The third type of interference, *i.e.*, thermal neutron activation of the soils from stray neutrons produced in the target assembly is also considered in Table II. Thermal neutrons were absorbed by a 0.075-cm-thick cadmium foil in which the sample and MES were wrapped. A cobalt wire was irradiated along with the samples and the neutron-induced ^{60}Co activity recorded with a 7.5-cm × 7.5-cm NaI(Tl) detector was found to be completely negligible. Thus, interferences caused by absorption of thermal neutrons in the soil samples were not considered further.

Positron Annihilation Radiation. A very large number of nuclides with varying half-lives decay by a positron emission. Thus the determination of concentration of any

Table II. Interference from Competing Reactions

Element	Nuclide analyzed: Activation reaction	Nuclide analyzed: E_{sep} (MeV)	Nuclide analyzed: E_{irr} (MeV)	Photon-induced reaction: Activation reaction	Photon-induced reaction: E_{sep} (MeV)	Photon-induced reaction: Remarks[a]	Neutron-induced reaction
Antimony	$^{122}Sb(\gamma,n)^{122}Sb$	9.0	15	$^{123}Te(\gamma,p)^{122}Sb$	8.1	A	$^{121}Sb(n,\gamma)^{122}Sb$
				$^{125}Te(\gamma,t)^{122}Sb$	15.7	B	
				$^{124}Te(\gamma,np)^{122}Sb$	17.5	B	
Arsenic	$^{75}As(\gamma,n)^{74}As$	10.2	20	$^{77}Se(\gamma,t)^{74}As$	18.7	A	...
				$^{76}Se(\gamma,np)^{74}As$	19.8	B	
Barium	$^{135}Ba(\gamma,\gamma')^{135m}Ba$			...		..	$^{134}Ba(n,\gamma)^{135}Ba$
	$^{136}Ba(\gamma,n)^{135m}Ba$	9.1	35				
Bismuth	$^{209}Bi(\gamma,3n)^{206}Bi$	22.5	44	...		..	...
Cadmium	$^{111}Cd(\gamma,\gamma')^{111m}Cd$			$^{115}Sn(\gamma,\alpha)^{111m}Cd$	3.2	A	$^{110}Cd(n,\gamma)^{111m}Cd$
	$^{113}Cd(\gamma,n)^{111m}Cd$	9.4	15	$^{116}Sn(\gamma,n\alpha)^{111m}Cd$	12.8	B	
				$^{113}In(\gamma,np)^{111m}Cd$	15.5	B	
				$^{114}Sn(\gamma,^3He)^{111m}Cd$	16.2	B	
Calcium	$^{44}Ca(\gamma,p)^{43}K$	12.2	20	$^{45}Sc(\gamma,2p)^{43}K$	19.1	B	...
Cesium	$^{133}Cs(\gamma,n)^{132}Cs$	9.0	15	$^{135}Ba(\gamma,t)^{132}Cs$	15.6	B	...
				$^{134}Ba(\gamma,np)^{132}Cs$	17.1	B	
Chlorine	$^{35}Cl(\gamma,n)^{34m}Cl$	12.6	20	$^{39}K(\gamma,n\alpha)^{34m}Cl$	19.8	B	...
Chromium	$^{50}Cr(\gamma,2n)^{48}Cr$	23.3	35	...		..	...
Cobalt	$^{59}Co(\gamma,n)^{58}Co$	10.5	20	$^{60}Ni(\gamma,np)^{58}Co$	20.0	B	...
Indium	$^{113}In(\gamma,\gamma')^{113m}In$		15	$^{114}Sn(\gamma,p)^{113m}In$	8.5	A	$^{112}Sn(n,\gamma)EC^{113m}In$
				$^{115}Sn(\gamma,np)^{113m}In$	16.0	B	
				$^{116}Sn(\gamma,t)^{113m}In$	17.1	B	
Iron	$^{54}Fe(\gamma,np)^{52}Mn$	20.9	35	...		..	...
	$^{56}Fe(\gamma,nt)^{52}Mn$						
	$^{57}Fe(\gamma,p)^{56}Mn$	10.6	20	$^{59}Co(\gamma,^3He)^{56}Mn$	20.3	B	$^{55}Mn(n,\gamma)^{56}Mn$
Lead	$^{204}Pb(\gamma,\gamma')^{204m}Pb$			...		..	...
	$^{206}Pb(\gamma,2n)^{204m}Pb$	14.8	35				
Magnesium	$^{25}Mg(\gamma,p)^{24}Na$	12.1	22	$^{27}Al(\gamma,^3He)^{24}Na$	23.7	B	
Manganese	$^{55}Mn(\gamma,n)^{54}Mn$	10.2	20	$^{56}Fe(\gamma,np)^{54}Mn$	20.4	B	...
Mercury	$^{198}Hg(\gamma,n)^{197m}Hg$	8.3	35	...		..	$^{196}Hg(n,\gamma)^{197m}Hg$
Molybdenum	$^{100}Mo(\gamma,n)^{99}Mo^{99m}Tc$	8.3	35	$^{103}Rh(\gamma,\alpha)^{99m}Tc$	3.1	B	$^{98}Mo(n,\gamma)^{99}Mo$
				$^{100}Ru(\gamma,p)^{99m}Tc$	9.2	B	
				$^{101}Ru(\gamma,np)^{99m}Tc$	16.0	B	
				$^{102}Ru(\gamma,t)^{99m}Tc$	16.7	B	
Nickel	$^{58}Ni(\gamma,n)^{57}Ni$	12.2	35	...		..	...
Scandium	$^{45}Sc(\gamma,n)^{44}Sc$	11.3	20	$^{46}Ti(\gamma,d)^{44}Sc$	19.4	B	...
				$^{46}Ti(\gamma,np)^{44}Sc$	21.7	B	
Selenium	$^{82}Se(\gamma,n)^{81m}Se$	9.3	35	...		..	$^{80}Se(n,\gamma)^{81m}Se$
Silver	$^{107}Ag(\gamma,n)^{106m}Ag$	9.6	20	$^{108}Cd(\gamma,np)^{106m}Ag$	17.7	A	...
Sodium	$^{23}Na(\gamma,n)^{22}Na$	12.4	20	$^{25}Mg(\gamma,t)^{22}Na$	23.0	B	...
Strontium	$^{86}Sr(\gamma,n)^{85m}Sr$	11.5	20	$^{90}Zr(\gamma,n\alpha)^{85m}Sr$	18.2	A	$^{84}Sr(n,\gamma)^{85m}Sr$
Tellurium	$^{130}Te(\gamma,n)^{129}Te$	8.4	20	...		..	$^{128}Te(n,\gamma)^{129}Te$
Thallium	$^{203}Tl(\gamma,n)^{202}Tl$	7.7	15	$^{204}Pb(\gamma,np)^{202}Tl$	14.3	B	...
Tin	$^{117}Sn(\gamma,\gamma')^{117m}Sn$		35	...		..	$^{116}Sn(n,\gamma)^{117m}Sn$
	$^{118}Sn(\gamma,n)^{117m}Sn$	9.3					
Titanium	$^{49}Ti(\gamma,p)^{48}Sc$	11.3	22	$^{50}V(\gamma,2p)^{48}Sc$	19.3	A	...
				$^{51}V(\gamma,^3He)^{48}Sc$	22.6	B	
Vanadium	$^{50}V(\gamma,2n)^{48}V$	20.9	44	$^{50}Cr(\gamma,np)^{48}V$	21.1	C	...
	$^{51}V(\gamma,3m)^{48}V$	31.9					
Zinc	$^{66}Zn(\gamma,n)^{65}Zn$	11.1	35	...		..	$^{64}Zn(n,\gamma)^{65}Zn$
	$^{68}Zn(\gamma,p)^{67}Cu$	10.0	35	...		..	
Zirconium	$^{90}Zr(\gamma,n)^{89}Zr$	12.0	22	$^{94}Mo(\gamma,n\alpha)^{89}Zr$	14.1	B	...
	$^{91}Zr(\gamma,2n)^{89}Zr$	19.2		$^{92}Mo(\gamma,^3He)^{89}Zr$	16.9	B	

[a] Interfering photon-induced reactions: A, negligible contribution; B, not observed; C, observed.

element through the 511-KeV annihilation radiation requires extensive measurements at frequent time intervals and resolution of a very complex decay curve. For this reason, the 511-KeV photopeak was not used in this study. However, in gamma-ray spectra of soils irradiated at 25 to 44 MeV and recorded within an hour from the end of irradiation, the 511 photopeak was so intense that it masked most of the low-energy gamma-rays emitted by many nuclides. On the other hand, high-energy gamma-rays were not interfered with under this condition as was also reported by Aras *et al.* (*30*). However, quite a few gamma-rays could be resolved in a complex gamma-ray spectrum recorded after 2 hr from the end of irradiation at 35 MeV, as reported in our earlier study (*26*). Consequently, it was apparent that most of the 511-KeV radiation was due to the 20-m-^{11}C nuclide produced in the carbon by the reaction $^{12}C(\gamma,n)^{11}C$ (E_{sep}, 18.7 MeV) in the soil matrix itself. The advantage was taken of the relatively high E_{sep} for this reaction in selecting E_{irr} for certain elements to produce short-lived nuclides which emit low-energy gamma-rays during their decay. For example, tellurium was activated at 20 MeV which is well above the E_{sep} of 8.4 MeV for the reaction $^{130}Te(\gamma,n)^{129}Te$, and the 459.2-KeV gamma-ray of 69-m-^{129}Te was assayed without any interference from the ^{11}C positron annihilation radiation. Although the E_{sep} for

(30) N. K. Aras, W. H. Zoller, G. E. Gordon, and G. J. Lutz, *Anal. Chem.*, **45**, 1481 (1973).

Table III. Elemental Concentrations of Soil by Depth (ppm, dry-weight basis)

Element	Soil depth in cm							
	Surface-1	Surface-2	0–7.5	7.5–15.0	15.0–22.5	22.5–30.0	30.0–37.5	37.5–45.0
Antimony	2.11	1.85	1.73	0.66	0.58	0.93	0.75	0.70
Arsenic	1.72	1.61	1.85	0.96	0.78	0.85	0.50	0.42
Barium	285	270	252	293	300	328	295	330
Bismuth	1.52	1.46	1.33	N.D.[a]	~1	N.D.	N.D.	1.21
Cadmium	1.45	1.52	1.71	0.97	0.85	1.15	1.32	0.67
Calcium	20,000	20,000	14,000	11,500	12,300	10,550	11,400	12,200
Cesium	4.82	4.91	2.22	1.95	1.83	2.65	1.78	2.26
Chlorine	72.2	68.5	45.1	32.6	26.0	38.7	11.6	8.42
Chromium	14.3	12.1	18.5	30.2	35.4	45.8	28.6	26.7
Cobalt	8.52	8.65	8.24	7.66	5.48	7.32	4.37	5.28
Indium	2.60	2.12	2.95	1.56	1.12	1.86	0.93	0.56
Iron	28,000	28,350	21,200	18,000	19,750	22,400	24,000	27,750
Lead	32.2	30.0	20.1	18.5	17.8	15.2	12.4	11.6
Magnesium	780	765	640	420	400	525	546	583
Manganese	1,350	1,275	840	625	715	1,120	1,200	1,430
Mercury	1.45	2.50	1.18	1.62	1.80	1.20	1.30	N.D.
Molybdenum	2.12	2.00	1.32	1.05	0.84	1.18	1.25	1.47
Nickel	8.11	7.85	6.21	6.64	5.23	7.55	4.81	3.57
Scandium	3.22	3.41	3.65	3.06	4.31	5.26	5.52	5.88
Selenium	1.10	1.43	1.22	0.81	0.62	1.05	0.91	0.53
Silver	0.92	0.85	0.68	0.52	0.40	N.D.	N.D.	N.D.
Sodium	6,000	5,950	5,000	4,320	4,170	3,860	3,700	3,610
Strontium	80.5	82.8	65.6	52.3	41.4	56.7	75.0	89.3
Tellurium	6.25	6.10	4.33	2.17	~1.2	N.D.	N.D.	N.D.
Thallium	0.22	0.20	0.17	N.D.	N.D.	0.18	N.D.	N.D.
Tin	14.0	13.5	12.2	12.5	10.1	12.3	13.1	14.2
Titanium	101	105	122	145	160	168	173	185
Vanadium	10.5	11.6	15.2	21.4	26.1	30.0	31.4	32.3
Zinc	165	152	148	128	94	65	48	42
Zirconium	200	200	278	323	405	467	500	676

[a] N.D., not detected.

^{11}C for production is 18.7 MeV, it is not expected to interfere seriously at energies only a few MeV above that.

Some of the interferences shown in Tables I and II have been reported and/or discussed by the authors (*24, 26, 31*) as well as in publications of others (*30, 32–42*).

RESULTS AND DISCUSSION

Different types of fertilizer, nutrients, heavy metallic and organic pesticides, fungicides, herbicides, and insecticides were used to varied extends in the Holland Marsh to stimulate plant growth and to combat fungi and weeds. Although this trend of usage of additives has changed in recent years, the present study was undertaken to detect any residues of metallic elements left in the soil from previous agricultural practices. Attempts have been made also to estimate the distribution of elements in soil depth profiles to assess the effects of topical application and cultivating through the years in distributing metals.

Although NAA can be applied for multielement determination, published reports show that it has often been applied to determine single elements (*43*) for various reasons. Recently, however, kay *et al.* (*44*) have reported determination of 23 elements in composite soils by INAA with some preirradiation treatment. In this laboratory, thermal NAA of muck soils for this purpose was very limited because of the large activities of ^{24}Na and ^{56}Mn, and both of these elements are known to be present in soils in large amounts. Consequently, radiochemical separation procedures were developed (*25, 45, 46*) to assist in the determination of certain elements and others were determined nondestructively. Alternatively, in the present work, IPAA has been used to determine the concentrations of 30 elements in soil. Like NAA, IPAA is also not free from interference. However, in most cases interferences observed with IPAA can be elimi-

Table IV. Lead Contents of Surface and Subsurface Soils (ppm, dry-weight basis)

Cultivated soil layers		Virgin soil layers	
Surface-1	7.5–15.0 cm	Surface-1	7.5–15.0 cm
32.1	18.8	35.0	20.2
25.6	12.1	30.6	19.4
27.4	19.3	27.1	18.7
34.6	20.0	21.5	14.3
21.0	8.2	36.2	21.6
34.2	10.4	45.0	23.9

(31) R. E. Jervis, B. Tiefenbach, and A. Chattopadhyay, *Can. J. Chem.*, in press.
(32) Y. Oka, T. Kato, and N. Sato, *Bull. Chem. Soc., Jap.*, **42**, 387 (1969).
(33) H-T. Tsai, T. Kato, and Y. Oka, *ibid.*, **43**, 2582 (1970).
(34) *Ibid.*, p 2823.
(35) R. A. Schmitt, T. A. Linn Jr., and H. Wakita, *Radiochim. Acta*, **13**, 200 (1970).
(36) J. S. Hislop and D. R. Williams, AERE Report **6910**, H. M. Stationery Office, London, 1971.
(37) J. S. Hislop and D. R. Williams, Ref. (*1*), p 51.
(38) J. S. Hislop and D. R. Williams, Ref. (*21*), Paper No. M 67.
(39) T. Kato, I. Morita, and N. Sato, Colloque International du CNRS, Paper No. C30 (1972).
(40) E. Ricci, *ibid.*, Paper No. C 46 (1972).
(41) V. Galatanu, M. Grecescu, and G. Baciu, Ref. (*23*), Vol. II, p 1011.
(42) H. A. Das, G. A. V. Gerritsen, D. Hoede, and J. Zonderhuis, *J. Radioanal. Chem.*, **14**, 415 (1973).
(43) H. J. M. Bowen, Ref. (*1*), p 393.
(44) M. A. Kay, D. M. McKown, D. H. Gray, M. E. Eichor, and J. R. Vogt, *Amer. Lab.*, **5** (7), 39 (1973).
(45) L. C. Bate, "Forensic Activation Analysis, Text of Papers of the 2nd International Conference," Glasgow, U.K., Paper No. 20 (1972).
(46) H. D. Buenafama, Ref. (*39*), Paper No. C 31.

Table V. Concentrations of Elements Determined through Alternative Nuclides of Gamma-Rays

Element	Nuclide	Gamma-ray energy, KeV	Content (ppm, dry-weight basis) Sample No. 1	Sample No. 2	Sample No. 3
Arsenic	^{74}As	595.8	1.72	1.61	1.85
		634.8	1.70	1.64	1.84
Bismuth	^{206}Bi	803.1	1.58	1.49	1.37
		880.8	1.52	1.46	1.33
Iron	^{52}Mn	1433.2	28,000	28,350	21,200
	^{56}Mn	846.8	28,415	28,620	22,000
Silver	^{106m}Ag	451.1	0.92	0.85	0.68
		717.0	0.90	0.88	0.70
		1045.6	0.95	0.89	0.73
Zinc	^{65}Zn	1115.4	170	150	153
	^{67}Cu	184.8	165	152	148

nated instrumentally and by control of bombarding energy as already described in the Methodology Section.

Gamma-Ray Spectrum. A typical gamma-ray spectrum of one of the marsh soil samples irradiated at 44-MeV maximum electron energy for 1 hr and recorded with the 60 cm^3 Ge(Li) detector is shown in Figure 1.

Since many complex photonuclear reactions are observed to occur at about 44 MeV and since many of these reactions can seriously interfere with the determination of a particular element (Table II), therefore, at this energy, only bisuth and vanadium concentrations can be estimated with reasonable accuracy and free of interference. The time of the radiation analysis of a particular nuclide during sample decay is also very important in order to avoid interferences from gamma-rays overlapping in energy. The time of counting of all the nuclides analyzed is shown in Table I.

Half-lives of all nuclides analyzed have been calculated from the gamma-ray spectra recorded at different time intervals and the ones which agreed best to the reported values have been selected. Good counting statistics have been obtained by counting samples for several hours whenever required. It should be pointed out here that there are a few gamma-rays observed in several spectra to which no nuclides can be assigned definitely at this stage.

Elemental Distribution in Soil Depth Profiles. Muck soils were analyzed by using the nuclides and gamma-rays selected as optimal for this purpose and as detailed in Table I. Concentrations of 30 elements at different depths of one muck soil are given in Table III. It can be observed that whereas some elements are concentrated more in surface layers, others are distributed over the entire soil profile. Significance of elemental concentration is better understood by analyzing vegetation species grown on these soils which is beyond the scope of this paper.

Lead, the element of particular interest in several current environmental pollution studies, has been measured in a number of soil samples using IPAA and is shown in Table IV. Nuclear parameters for lead analysis are given in Table I. A radiochemical separation method sensitive to nanogram quantities of lead has been described elsewhere (*26*). The lead content of surface soil scrapings was at least 10 ppm higher than that obtained in subsoils. This is not surprising in view of the fact that the farms are located near two motor expressways. Thus, it is likely that, owing to surface deposition of lead from automobiles, the lead content of surface layers could not be used to understand the distribution of lead in soils. For this reason, we have chosen a surface and a subsurface soil layer at 7.5–15.0 cm depth and have summarized the results in Table IV of lead in 6 cultivated and 6 virgin (uncultivated) soils. Virgin muck soils, in general, contain more lead than the cultivated ones, which may be indicative of uptake of lead by vegetation.

Precision and Accuracy. As stated above, the concentrations of different elements in muck soil were normally measured by using one particular gamma-ray emitted by a characteristic nuclide. The elemental contents shown in Table III were obtained in this manner. However, in certain instances, it was possible to select more than one photonuclear product of the same element such as iron and zinc, and more than one gamma-ray of a particular product such as bismuth and silver for independent assay of soil concentrations. The results of such independent evaluations are shown in Table V. The agreement between different concentration results for the same sample is, in general, quite good, *i.e.*, within ±5% to ±10%. The agreement in iron contents measured through ^{52}Mn and ^{56}Mn indicates that the interfering reaction $^{55}Mn(n,\gamma)^{56}Mn$ could not have contributed an appreciable error in the determination of iron by nondestructive PAA using ^{56}Mn under the experimental conditions already described. Moreover, the agreement in iron concentrations of the same sample measured in two separate irradiations, namely, at 20 and 35 MeV for assaying ^{56}Mn and ^{52}Mn (Table II), respectively, reflects the excellent reproducibility of the method developed in this study.

The muck soils analyzed in this study had 85–90% organic matter content. The complexity of soil organic matter has been described by others (*47–49*). In the preparation of a synthetic soil mixture to be used to support the standard elements for IPAA, no effort was made in this study to simulate the exact soil organic matter, if that were even possible. Instead, a mixture was prepared containing the main constituents of muck soils, namely, carbohydrate, phosphate, calcium, iron, and silicon. Microgram quantities of standard elements were added to it and mixed thoroughly, and used as the MES. To check the accuracy of elemental concentrations determined using this MES in the IPAA, a few elements were also measured by using other standard analytical techniques such as NAA and atomic absorption spectrophotometry. Destructive NAA method for determination of arsenic, cadmium, mercury, and zinc has already been described by the authors (*25*). Atomic absorption measurements were carried out by using a Jarrell-Ash Dial-Atom Mark II spectrophotometer and a standard technique. As can be seen from Table VI, most of the values agreed well within the experimental error of each method, *i.e.*, approximately ±10%, it can be concluded that IPAA is at least as accurate an analytical method as are the other methods listed.

As an additional check on the accuracy of the IPAA tech-

(47) J. L. Mortensen and F. L. Himes, "Chemistry of the Soil," F. E. Bear, Ed., Reinhold Publ. Corp., New York, N.Y., 1964, Chap. 5.
(48) M. M. Kononova, T. Z. Nowakowski, and A. C. D. Newman, "Soil Organic Matter," 2nd ed., Pergamon Press, Oxford, 1966.
(49) T. L. Lyon, H. O. Buckman, and N. C. Brady, "The Nature and Properties of Soils," 5th ed., Macmillan Co., New York, N.Y., 1956, Chap. 6.

Table VI. Intercomparison of Elemental Concentrations by Different Analytical Techniques

Method	Sample No.	Content (ppm, dry-weight basis) As	Cd	Cr	Pb	Hg	Zn
Instrumental PAA	1	1.72	1.45	14.3	32.2	1.45	165
	2	1.61	1.52	12.1	30.0	2.50	152
Destructive PAA	1	...	...	...	31.3	...	...
	2	...	...	...	31.0	...	...
Instrumental NAA	1	...	...	13.5	...	...	170
	2	...	...	12.5	...	...	160
Destructive NAA	1	1.65	1.42	...	...	1.41	161
	2	1.62	1.57	...	...	2.51	150
Atomic absorption[a]	1	...	1.45	...	32.8	...	...
	2	...	1.55	...	31.3	...	...

[a] After chemical separation.

Table VII. Multielement Content of Intercomparison Standards by IPAA[a]

Element	Orchard Leaves This work[b]	Orchard Leaves Cert. values	Coal This work[b]	Coal Infor. value	Fly Ash This work[b]	Fly Ash Infor. value
Sb	3.15 ± 0.26	3.0[c]	3.09 ± 0.26	...	7.14 ± 0.56	...
As	10.2 ± 1.0	11 ± 2[d]	5.75 ± 0.37	5.9 ± 0.4	60.7 ± 2.6	61 ± 3
Ba	51.3 ± 4.5	51[c]	314 ± 20	...	0.261 ± 0.021[c]	...
Bi	...	(0.1)	~1.05	...	~1.08	...
Cd	0.11 ± 0.01	0.11 ± 0.02	0.199 ± 0.02	0.23 ± 0.03	1.52 ± 0.07	1.45 ± 0.06
Ca, %	2.08 ± 0.01	2.09 ± 0.03	...	...	3.92 ± 0.28	...
Cs	...	≤0.06	0.35 ± 0.04	...	0.63 ± 0.06	...
Cl	685 ± 32	(700)	930 ± 48	...	19.6 ± 0.1	...
Cr	2.22 ± 0.20	(2.3)	21.6 ± 2.1	22 ± 2	131 ± 6.1	132 ± 5
Co	...	(0.2)	5.50 ± 0.40	...	35.4 ± 2.8	38
In	...	...	0.23 ± 0.02	...	0.28 ± 0.03	...
Fe	290 ± 12	300 ± 20	0.869 ± 0.041[c]	...	6.08 ± 0.52[c]	...
Pb	44.2 ± 2.1	45 ± 3	32.1 ± 1.8	30 ± 9	70.7 ± 2.6	70 ± 2
Mg, %	0.61 ± 0.01	0.62 ± 0.02	0.160 ± 0.015	...	1.48 ± 0.01	...
Mn	88.2 ± 3.4	91 ± 4	47.1 ± 4.1	47 ± 3	495 ± 25	495 ± 30
Hg	0.14 ± 0.01	0.155 ± 0.015	~0.1	0.11	0.135 ± 0.01	0.15
Mo	2.26 ± 0.21	≤5[c]	0.20 ± 0.02	...	1.52 ± 0.15	...
Ni	1.27 ± 0.08	1.3 ± 0.2	13.5 ± 1.2	15 ± 1	96.8 ± 3.2	98 ± 3
Sc	0.22 ± 0.01	0.205[c]	3.58 ± 0.35	...	20.7 ± 2.1	...
Se	...	0.08 ± 0.01	3.03 ± 0.28	2.8 ± 0.2	9.48 ± 0.8	9.3 ± 1.0
Ag	...	...	1.05 ± 0.1	...	1.32 ± 0.13	...
Na	79.3 ± 5.0	82 ± 6	351 ± 30	...	0.340 ± 0.03[c]	...
Sr	36.2 ± 2.0	(37)	1.33 ± 0.1	...	1373 ± 95	1380
Te	...	...	~1.02	...	2.32 ± 0.20	...
Tl	...	...	0.512 ± 0.06	0.59 ± 0.05	3.64 ± 0.34	4
Sn	...	...	10.2 ± 1.0	...	12.5 ± 1.2	...
Ti	...	...	973 ± 50	...	0.723 ± 0.04	...
V	...	≤0.65[c]	33.9 ± 3.0	35 ± 4	208 ± 12	214 ± 8
Zn	24.2 ± 1.5	25 ± 3	37.5 ± 2.8	37 ± 4	214 ± 16	210 ± 20
Zr	0.21 ± 0.02	...	1.56 ± 0.14	...	301 ± 22	...

[a] Contents expressed in ppm except otherwise mentioned, as-received basis. [b] Average of 3 determinations. [c] Ref. 51. [d] Ref. 52. Contents in %; and values shown in parentheses are noncertified values.

nique reported here, NBS Standard Reference Material 1571 (Orchard Leaves), and the coal and fly ash samples circulated for intercomparison purposes by the U.S. EPA and NBS have been analyzed for several elements. The averages of three such determinations are shown in Table VII along with the supplied probable certified values (*50*). It should be noted that we have measured many elements in all the samples whose concentrations have not yet been supplied.

Errors. There can be a number of potential sources of error in IPAA. The considerable spatial photon flux gradient in the region where samples are irradiated can impart a substantial error. The fluctuations in the integrated photon flux were about ±2.5%, as measured by irradiating known weights of pure copper wires along with samples and MES in the rotating sample assembly described earlier. It was difficult to exactly reproduce all experimental conditions as, for example, the electron beam current showed a variation of ±5 μA between 15 and 22 MeV.

The E_{irr} for any particular analysis was checked regularly before and after the irradiation. Although a precision of ±0.5 MeV of the desired E_{irr} was generally obtained, in a few cases it was about ±1 MeV. The contribution due to interfering competing reactions with E_{sep} within ±1 MeV of E_{irr} of a particular element was found negligible and was considered not to introduce any error in the determination of that element.

If proper precautions are taken, in most cases the total error involved in analysis can be restricted to about ±7–8%

(50) P. D. LaFleur and D. J. von Lehmden, Symposium on Trace Element Analysis of Coal, Fly Ash, Fuel and Gasoline, EPA-NBS, Research Triangle Park, N.C., 1973.
(51) G. H. Morrison and N. M. Potter, *Anal. Chem.*, **44**, 839 (1972).
(52) P. D. LaFleur, National Bureau of Standards, Washington, D.C., private communication, 1973.

and in some instances to ±10% at the most. The agreement between analytical methods (Table VI) is of this magnitude for the elements checked.

Limits of Detection. The limits of detection of all elements analyzed are shown in Table VIII. These limits were calculated on the basis of conditions already described in detail in the Experimental Section. It can be seen in this table that less than or equal to 1000 nanogram quantities of as many as 24 elements can be determined in a single sample by IPAA. By choosing alternative nuclides produced on photon activation of the same element, it has been possible to obtain a superior limit of detection. The best example is the determination of zinc. A 60 times lower detection limit has been achieved by following ^{67}Cu than that by ^{65}Zn for zinc estimation in muck soils. Six more elements have detection limits ranging from 1400 to 8000 nanograms.

The limits of detection of some elements in various materials by IPAA have been reported by many authors (*19, 30, 35, 38*). However, it is difficult to compare them because of different experimental conditions reported, as pointed out by Hislop (*23*). Moreover, these limits of detection are restricted to the particular matrix studied and the concentrations of interfering elements in that matrix.

From the experience of soil analyses by NAA and IPAA in this laboratory, it can be stated that for many trace elements, provided a bremsstrahlung beam of fairly high intensity (*viz.*, 10^{13} to 10^{14}photons/cm^2 sec) is used, the limits of detection of IPAA are in general better that that obtained with INAA. For a few other elements, the sensitivity of both the methods is comparable.

CONCLUSION

Instrumental PAA has been found very useful for the multielement determination in environmental soil samples. It is an invaluable technique for certain elemental analysis because of such factors as the higher specific count rates obtained, minimal interferences from other activity in the matrix, convenient half-life for routine analysis, and lower detection limits. If proper precautions are taken, the accuracy of IPAA is comparable to that of other sensitive methods of analysis. A careful choice of E_{irr} is absolutely essential for IPAA. It is understood that a higher E_{irr} will give a higher yield of the product nuclide; however, it will also enhance interferences from competing reactions and will introduce much error in the measurement. From our experience, we feel that a lower electron energy and a higher beam current are sufficient to estimate a number of elements on a purely instrumental basis with reduced interferences. It should be stressed again that the use of a particular nuclide for elemental determination largely depends on the E_{sep} of the reaction and knowledge of approximate concentrations of interfering elements present in the sample.

Apart from the application of IPAA for determining elemental concentrations in soil samples, we feel that this method has an excellent potential for multielement determination in other matrices of environmental health interest. Consequently, blood, bone, hair, and urine are being analyzed in this laboratory to monitor ingestion, accumulation, and excretion of several toxic metals in the human body.

Table VIII. Detection Limits of Elements Analyzed by IPAA

Nuclide used	Detection limit, ng
^{122}Sb	40
^{74}As	100
^{135m}Ba	300
^{206}Bi	1,000
^{111m}Cd	100
^{42}K	5,000
^{132}Cs	100
^{34m}Cl	100
^{48}Cr	1,000
^{58}Co	3,000
^{113m}In	100
^{52}Mn	2,000
^{56}Mn	1,000
^{204m}Pb	100
^{24}Na	2,000
^{54}Mn	1,400
^{197m}Hg	100
^{99}Mo	100
^{57}Ni	350
^{44}Sc	200
^{81m}Se	200
^{106m}Ag	400
^{22}Na	1,000
^{85m}Sr	10
^{127}Te	1,000
^{201}Tl	150
^{117m}Sn	8,000
^{46}Sc	80
^{48}V	2,500
^{65}Zn	6,000
^{67}Cu	100
^{89}Zr	80

ACKNOWLEDGMENT

We thankfully acknowledge the research group of T. C. Hutchinson, Department of Botany, for assistance in sampling, and J. R. Brown, Environmental Health, School of Hygiene, for continued interest in this project. We also acknowledge the cooperation of the University of Toronto Linear Accelerator Users' Committee and operating staff, and the SLOWPOKE Reactor operating staff for their help in providing irradiation time and assisting in the irradiations.

RECEIVED for review November 26, 1973. Accepted April 30, 1974. This paper was presented at the International Conference on Photonuclear Reactions and Applications, Pacific Grove, Calif., 26–30 March 1973, and a summary is available in the Conference Proceeding, B. L. Berman, Ed., Lawrence Livermore Laboratory, Vol. II, p 1009 (1973). This research was supported in part by an Ontario Ministry of Universities and Colleges grant and by a National Research Council of Canada research operating grant. The award of a University of Toronto Open Graduate Fellowship to one author (A.C.) is gratefully acknowledged.

Role of Column Parameters and Injection Volume on Detection Limits in Liquid Chromatography

Barry L. Karger

Department of Chemistry, Northeastern University, Boston, Mass. 02115

Michel Martin and Georges Guiochon

Laboratoire de Chimie Analytique Physique, Ecole Polytechnique, Paris V^e^, France

This paper examines the role of column parameters and sample size on detection limits in liquid chromatography. A detailed discussion of the meaning of detection limits and its relationship to sensitivity is first presented. Next, the general influence of column parameters on solute dilution within the chromatographic system is explored, assuming a constant sample size sufficiently small that neither retention nor column efficiency is significantly affected. The discussion then focuses on the relationship of these parameters to dilution and resolution. Optimization of detection limits for a given resolution and a constant and small sample size is examined. Next, the influence of sample volume on detection limits is dealt with. It is shown that if a maximum injection volume is defined as contributing a given percentage to the over-all standard deviation of the band eluting from the column, then solute dilution is constant, independent of column parameters. Moreover, 10-fold or greater improvements in detection limits over current typical practice in liquid chromatography are possible without major effects on column performance. This can be achieved in a number of cases through the injection of larger sample volumes. Recognizing the importance of injection volume on detection limits, the last section compares some experimental results on maximum injection volumes in gas and liquid chromatography. These results must be included in a comparison of detection limits for the two methods.

Over the past few years, much effort has been expended to achieve high performance (speed and efficiency) in column liquid chromatography (*1*). While remarkable progress has been made, liquid chromatography is commonly believed to suffer the disadvantage in relation to gas chromatography of poorer sensitivity and detection levels. Workers have at times been limited in their application of the LC method from an inability to detect the components. Further, as pointed out by Scott (*2*), poor detection limits can result in low column peak capacity.

In this paper, we shall examine the optimization of detection limits with respect to the liquid chromatographic system. There are two aspects of this problem, the chromatographic operation and the detector. We shall mainly look into the role of the chromatographic operation on detection limits—in particular, the influence of sample size and column parameters. Obviously, maximization of these factors will be beneficial for the detection of small samples, independent of the dettetector used. We will show that it is sometimes possible to improve detection limits by one or more orders of magnitude over that found for typical chromatographic conditions.

(1) "Modern Practice of Liquid Chromatography," J. J. Kirkland, Ed., Academic Press, New York, N.Y., 1971.
(2) R. P. W. Scott, Jr., *J. Chromatogr. Sci.*, **9**, 449 (1971).

Let us first overview the problem. Chromatography is included in an analysis scheme when it is necessary to separate the components prior to detection. However, a price is paid for this added step—a poorer detection limit—for the components undergo dilution in their transport through the chromatographic column. The best detection level is obtained when no column is used, but, of course, all separation is then lost. Consequently, a compromise must frequently be struck between the desired detection level and the required resolution.

Besides dilution in the column, the amount of injected sample will influence the maximum detectable amount of individual components. We define the injected amount of specific components in terms of weight (grams) and not concentration. The amount of the components injected into the column will then be determined by the volume of injected sample and the concentration of the individual components.

If one has a sample with dilute concentrations of the components of interest and detection is a problem, the first recourse is to concentrate the sample. This is frequently not possible or desirable for the solubility of the components in the solvent may be quite low; preconcentration may be inconvenient or cause losses of material; and/or other components may be concentrated to the point that they will greatly overload the column. (Overloading can be detrimental in that such bands may be greatly broadened and, hence, be overlapped with the components of interest, resulting in a loss in precision, accuracy and detection limits. We assume here that column overloading of the components of interest is not a problem.) Thus, we are often faced with the injection of dilute samples (*i.e.*, trace analysis). We then must turn to the sample volume as a means of improving detection limits. As sample volume is increased, column performance will decrease because the injected volume will cover a more significant fraction of the column (*3-5*). In addition, other species in the mixture may overload the column and interfere with the detection of the compounds of interest. We see again that a compromise must often be made between detection level and resolution. From these arguments, it follows that the better separated the components of interest are from the interfering species, the lower can be the detection limits.

Huber has appreciated the problems of achieving low detection limits in liquid chromatography through the optimization of chromatographic operation (*6, 7*). Additionally, Bakalyar has discussed some aspects of the influence of

(3) E. Glueckauf, *Trans. Faraday Soc.*, **51**, 34 (1955).
(4) P. E. Porter, C. H. Deal, and F. Stross, *J. Amer. Chem. Soc.*, **78**, 2999 (1956).
(5) J. J. van Deemter, F. J. Zuiderweg, and A. Klinkenberg, *Chem. Eng. Sci.*, **5**, 27 (1956).
(6) J. F. K. Huber, J. A. R. J. Hulsman, and C. A. M. Meijers, *J. Chromatogr.*, **62**, 79 (1972).
(7) C. A. M. Meijers, J. A. R. J. Hulsman, and J. F. K. Huber, *Fresenius' Z. Anal. Chem.*, **261**, 347 (1972).

column parameters on sensitivity in modern liquid chromatography (*8*). Previously, Zhukhovitzki (*9*) studied the influence of sample size on minimum detectable concentrations for gas chromatography. It is worth noting that some of t the problems associated with sample size effects are similar to those encountered in preparative scale chromatography. Results from studies on large scale chromatography are thus applicable to the understanding of the role of sample size on detection level. The papers by Sawyer and Purnell (*10, 11*) and Pretorius *et al.* (*12–14*) dealing with preparative scale gas chromatography are particularly useful. Further work on the influence of sample size in preparative scale gas chromatography can be found in work by Verzele (*15*) and Higgins and Smith (*16*). A related problem is the role of injection profile on column performance, as studied by Reilley *et al.* (*17*) and Sternberg (*18*).

SENSITIVITY AND DETECTION LIMITS

There is often a great deal of confusion in the literature on the meaning of sensitivity and detection limits with respect to chromatographic analysis. It is thus important to examine the true meaning of these terms so that our subsequent discussion will be clear.

Consider a gaussian-shaped solute band eluting from a chromatographic column. Detection of this band will depend on our ability to sense the concentration at the peak maximum—C_{max}. This ability will be a function of the sensitivity of the detector for the component and noise level of the base line (*19*). It is not a simple matter to define sensitivity. Since concentration sensitive detectors (*20*) are predominantly used in LC (*e.g.*, UV and RI detectors), we will define the sensitivity S as the millivolt response of the detector to a unit change in solute concentration (in grams/ml). We will assume a linear response of the detector in the range of operation (or else S would not be constant) and an unattenuated signal. This definition represents an empirical response factor and as such is completely arbitrary. The noise level of the base-line G will be defined as the peak-to-peak amplitude of the noise, in millivolts.

The minimum detectable concentration *in the detector* is defined in terms of a multiple of the signal-to-noise ratio. This multiple must be arbitrarily selected, based on the desired precision in either peak height or peak area. [The relative error in peak area is proportional to that in peak height if random noise is the major contributor to imprecision and the band shape is gaussian (*21*).] The larger the multiple, the greater will be the precision of the analysis (*22*). For our purposes, we shall define the minimum detectable concentration as five times the signal to noise ratio. Thus, when

$$C_{max} = 5 \times \frac{G}{S} \tag{1}$$

we have the minimum concentration of the peak maximum eluting from the column for detection. It is clear that one must specify detection limits in relation to either the precision level of the analysis or the multiple of the signal to noise ratio.

The *over-all* detection limit is not the minimum concentration in the detector, but the minimum component amount (in grams) that is injected. Dilution in the column adversely affects the detection level. To take account of this dilution, the relationship between C_{max} and the mass of injected solute m is (*23*)

$$C_{max} = \frac{m(\sqrt{N})}{V_R(\sqrt{2\pi})} \tag{2}$$

where N = number of theoretical plates and V_R = retention volume in ml. [Equation 2 assumes a gaussian profile. Changes from this band shape will alter the factor $\sqrt{2\pi}$; however, gaussian peaks are a good assumption in analytical liquid chromatography (*24*).] Combination of Equations 1 and 2 and substitution of D^*, the detection limit, for m results in

$$D^* = \frac{5(\sqrt{2\pi})V_R G}{(\sqrt{N})S} \tag{3}$$

The detection limit depends not only on the base-line noise level and the sensitivity (detector characteristics), but also on the retention volume and efficiency (column characteristics). It makes no sense to specify detection limits on the basis of Equation 1; we must include consideration of the column characteristics and solute retention. It should also be noted that Equation 3 assumes no problems with band overlap from other components. Band overlap, of course, would lead to worse detection limits than predicted from this equation. Finally, the mass of solute can be expressed as

$$m = C_0 V_0 \tag{4}$$

where C_0 = initial concentration of solute in the sample and V_0 = injected sample volume. Thus, whether a component can be sensed, as predicted by Equation 3, will depend on its initial concentration and the volume of sample injected.

Defining detection limits in terms of the mass of sample rather than concentration eliminates the frequent confusion found in the comparison of gas and liquid chromatographic detection limits *in the detector*. Table I compares detectors on the basis of three different concentration units. In terms of ppm (μgram/gram) average limits are quoted as 10–1 ppm for the refractometer (*2*), 0.1–0.001 ppm for the ultraviolet, depending on the extinction coefficients (*25*), and 1 ppm for the thermal conductivity GC detector (*26*). The ultraviolet detector would then appear to have 1 to 3 orders of magnitude lower limits than the TC detector.

If we convert ppm to gram/ml and assume a roughly 1000-fold greater density for liquids, the average detection limits in Table I become 10^{-5}–10^{-6} gram/ml RI, 10^{-7}–10^{-9} gram/ml UV, and 10^{-9} gram/ml TC detector. The response of the GC detector is now seen to be up to 2 orders of mag-

(8) S. R. Bakalyar, *Int. Lab.*, Jan. 1972, p 36.
(9) V. I. Kalmanovski and A. A. Zhukhovitzki, *J. Chromatogr.*, **18**, 243 (1965).
(10) D. T. Sawyer and J. H. Purnell, *Anal. Chem.*, **36**, (1964).
(11) D. T. Sawyer and G. L. Hargrove, "Progress in Gas Chromatography," J. H. Purnell, Ed., Interscience, New York, N.Y., 1968.
(12) W. J. de Wet and V. Pretorius, *Anal. Chem.*, **32**, 169 (1960).
(13) P. C. Haarhof, P. C. van Berge, and V. Pretorius, *Trans. Faraday Soc.*, **57**, 1838 (1961).
(14) V. Pretorius and K. de Clerk, "Preparative Gas Chromatography," A. Zlatkis and V. Pretorius, Ed., Interscience, New York, N.Y., 1971.
(15) M. Vomaerzele, *J. Chromatogr.*, **15**, 482 (1964).
(16) G. M. C. Higgins and J. F. Smith, "Gas Chromatography, 1964," A. Goldup, Ed., Institute of Petroleum, London, 1965, p 94.
(17) C. N. Reilley, G. P. Hildebrand, and J. W. Ashley, Jr., *Anal. Chem.*, **34**, 1198 (1962).
(18) J. C. Sternberg, "Advances in Chromatography, Vol. 2," J. C. Giddings and R. A. Keller, Ed., Marcel Dekker, New York, N.Y., 1966.
(19) H. W. Johnson, Jr., and F. H. Stross, *Anal. Chem.*, **31**, 1206 (1959).
(20) I. Halasz, *Anal. Chem.*, **36**, 1428 (1964).
(21) H. Barth, E. Dallmeier, G. Courtois, H. E. Keller, and B. L. Karger, *J. Chromatogr.*, **83**, 289 (1973).
(22) M. Goedert and G. Guiochon, *J. Chromatogr. Sci.*, **11**, 326 (1973).
(23) J. H. Purnell, "Gas Chromatography," John Wiley & Sons, New York, N.Y., 1962.
(24) L. R. Snyder, *J. Chromatogr. Sci.*, **10**, 200 (1972).
(25) L. R. Snyder, *J. Chromatogr. Sci.*, **10**, 187 (1972).
(26) T. Johns and J. C. Sternberg, "Instrumentation in Gas Chromatography," J. Krugers, Ed., Centrex Publishing Co., Eindhoven, The Netherlands, 1968.

Table I. Influence of Concentration Units on Detection Limits from the Detectors

Detector	Concentration unit		
	ppm	gram/ml	mole/ml
Ultraviolet (LC)	0.1–0.001	10^{-7}–10^{-9}	10^{-10}–10^{-12}
Refractive index (LC)	10–1	10^{-5}–10^{-6}	10^{-8}–10^{-9}
Thermal conductivity (GC)	1	10^{-9}	10^{-11}

nitude lower than the ultraviolet detector (assuming some UV response by the solute). Presenting the limits in moles/ml again alters the relationships. In general, molecular weights of solutes in LC will be larger than those in GC. For purposes of discussion, assume mol wt = 1000 in LC and 100 in GC for the particular solutes. The limits are altered, as shown in Table I. However, when one elects to report detection limits in terms of the mass of sample (grams) the above problems on unit definitions are not present. (Note again that a true comparison between GC and LC detection limits must include typical column dilutions. We shall point this out in a later section.)

For convenience, we have divided the paper into three sections. First, we examine the influence of column parameters on dilution with a constant sample size (volume and solute concentration). The assumption is made that separation is sufficient such that changes in parameters can be made without regard for changes in resolution and that the sample size is sufficiently small that it does not influence V_R or N. This section will give us an appreciation of the general influence of column parameters on detection limits. In the second section, we examine optimization of detection limits with a constant resolution and a constant sample size. This section will indicate the interrelationship of separation and dilution. The final section will examine the influence of sample size on detection limits. A proper understanding of the role of sample size and column parameters can at times lead to markedly improved detection limits over current practice.

GENERAL DILUTION IN THE COLUMN

In the examination of the role of the chromatographic system on detection limits, we first consider the factors which control solute dilution as a result of solute travel through the column with neglect of changes in resolution. We will assume that the sample size (volume and solute concentration) is maintained constant and small. This situation arises when either the sample is limited or is too complex to be increased in size. From Equations 2 and 4 we may write

$$\frac{C_{max}}{C_0} = \frac{V_0\sqrt{N}}{V_R\sqrt{2\pi}} \qquad (5)$$

The larger the value of C_{max}/C_0, the smaller will be the detection limits (see Equation 3).

It is instructive to estimate dilutions that occur in modern liquid chromatography. Consider first arbitrarily a porous layer bead column of 100 cm and 2-mm i.d. If V_0 = 5 μl, N = 900 plates, and V_R = 20 ml, then C_{max}/C_0, the dilution, will be approximately 1:330. From the quoted detection limits in Table I, this means that the minimum concentration of a 5-μl injected sample must be 3.3×10^{-3} gram/ml or $D^* \approx 16$ μg for the RI detector and $\approx 3.3 \times 10^{-6}$ gram/ml (minimum detector concentration = 10^{-8} gram/ml) or 16 ng for the UV detector. Consider next a porous bead column (particle diameter 10 μm) of 25 cm and 2-mm i.d. With V_0 = 5 μl, V_R = 10 ml, and N = 3600 plates, the dilution is approximately 1:100. Thus, there is a loss of 100-fold or more in detection limits under typical conditions in modern liquid chromatography. We will now examine Equation 5 in depth to search for means of decreasing this dilution effect.

To gain insight into the parameters influencing dilution, we can write the retention volume as

$$V_R = Ft_R = \epsilon_T \pi r^2 NH(1 + k') \qquad (6)$$

where F = volumetric flow rate, t_R = retention time, ϵ_T = total cross-sectional fraction of the mobile phase (inter- and intraparticle), r = inner tube column radius, H = height equivalent to a theoretical plate, and k' = capacity factor. Substitution of Equation 6 into 5 leads to

$$\frac{C_{max}}{C_0} = \frac{V_0}{\sqrt{2\pi}\,\epsilon_T \pi r^2 N^{1/2} H(1 + k')} \qquad (7)$$

This equation in slightly different form has been presented by Huber (7).

By noting that $N = L/H$, it is easy to show from Equation 7 that

$$\frac{C_{max}}{C_0} \sim L^{-1/2} \qquad (8)$$

if V_0, as well as F, are maintained constant for a given solute and column packing. As is well-known, a reduction in column length improves detection limits, if sample size is maintained constant. Relationship 8 also assumes that H is independent of column length which is found to be true if the column packing density does not change with length (26). If change occurs, then one can connect small lengths (*ca.* 25 cm) together with "zero dead volume" connectors. The minimum column length will first depend on the resolution required. Since N decreases with column length, one should use a column just sufficiently long to achieve the desired separation. If resolution is no problem, then the minimum length will be a function of the extra column band broadening effects caused by the injector, detector and associated plumbing (27).

Equation 7 also reveals that if column efficiency is relatively independent of tube radius r, (assuming packing characteristics do not depend on tube radius), then narrower tubes will lead to better detection limits, with constant sample size. It appears that the limiting tube diameter is about 1 mm below which column efficiency is reduced (28). The inverse square dependence makes the column radius a relatively important parameter for detection limits, with V_0 maintained constant and small. (The case of changes in V_0 with radius is discussed later).

Another column parameter that influences dilution is the mobile phase velocity, v. In Equation 5, the retention volume is independent of velocity, but N varies in a complex manner with v in modern liquid chromatography (29). Snyder has proposed the following empirical equation over the range of velocities most often encountered in LC (30):

$$H = Dv^n \qquad (9)$$

where D is a velocity-independent parameter characteristic of a given solute and column, and n ranges from 0.3 (30) to 0.6 (31). This equation is no longer valid when using very

(27) R. E. Majors, *J. Chromatogr. Sci.*, **11**, 88 (1973).
(28) J. J. Kirkland, "Gas Chromatography, 1972," S. G. Perry, Ed., Applied Science Publ., London, 1972.
(29) J. F. K. Huber, *Ber. Bunsenges Phys. Chem.*, **77**, 179 (1973).
(30) L. R. Snyder, "Gas Chromatography, 1970," R. Stock, Ed., The Institute of Petroleum, London, 1971.
(31) R. E. Majors and F. R. MacDonald, *J. Chromatogr.*, **83**, 169 (1973).

low velocities (<0.1 cm/sec) (with ~5-μ particles and very short column lengths). However, for simplicity in examining relationships we shall use Equation 9 with $n = 0.4$. The general conclusions will be valid with Equation 9 as the expression has been shown to be generally a good approximation of the H *vs.* velocity curve over the region of 0.3 to 5 cm/sec (*31–33*).

Substitution of Equation 9 into Equation 5 leads to

$$\frac{C_{max}}{C_0} = \frac{V_0 v^{-0.2}}{(\sqrt{2\pi})\epsilon_T \pi r^2 L^{1/2} D^{1/2}(1 + k')} \qquad (10)$$

Dilution is thus greater, the higher is the mobile phase velocity, although the dependence is not a strong one. It is worth noting that for gas chromatography $C_{max}/C_0 \sim v^{-0.5}$ in the resistance to mass transfer region of the H *vs.* velocity curve; again more dilution at higher velocities. Some workers confuse this point for they reason that since higher velocities result in faster elution times, higher maximum peak heights should be attained. However, it is clear that since column efficiency is generally degraded at higher velocities, dilution must be greater (*i.e.*, the critical retention parameter for dilution is not retention time but retention volume). It is worth noting that these conclusions are valid only for concentration sensitive detectors. For mass flow sensitive detectors—*e.g.*, flame ionization—the peak height increases monotonically with flow rate, so that detection limits are somewhat lower at higher velocities (*34*).

We next turn to the role of particle diameter of the support or adsorbent on dilution as this has been shown to be an important parameter in the performance of liquid chromatographic columns (*e.g., 28, 30, 31, 35*). The constant D in Equation 9 has been empirically shown to be related to particle diameter d_p by

$$D \sim d_p^{\beta} \qquad (11)$$

Experimentally, $\beta \simeq 1.8$ (*31, 36*). Substitution of this relationship into Equation 10 reveals

$$\frac{C_{max}}{C_0} \sim d_p^{-0.9} \qquad (12)$$

or that smaller particles can lead to a sizeable improvement in detection limits. Moreover, since the pressure drop increases with roughly the same power of particle diameter (*31*) (*i.e.*, $d_p^{1.8}$) for constant velocity, we frequently use shorter columns for an even greater gain in detection limits. This point will be brought out more clearly in the next section.

As seen in Equation 10, the capacity factor of the component can also influence dilution. A smaller value of k' always leads to improvement in detection limits when separation is no problem. Frequently, D is found to be independent of k', especially when porous layer bead supports or small particle diameter ($d_p < 10$ μ) adsorbents are employed (*27, 37*). In such cases, mobile phase mixing effects predominate in the band-broadening process. We see that $C_{max}/C_0 \sim (1 + k')^{-1}$ when D is not dependent on k'. When band broadening due to slow diffusion in the stationary liquid or in the stagnant mobile phase within the pores is important, then $D \sim k'/(1 + k')^2$ (*35*) and $C_{max}/C_0 \sim k'^{-1/2}$ again showing improved detection limits at lower k'. Finally, if slow diffusion in the moving mobile phase to the porous matrix is important, then $D \sim k'^2/(1 + k')^2$ (*35*) and $C_{max}/C_0 \sim k'^{-1}$. Thus, we see that in all cases small k' values lead to less dilution. This conclusion is in keeping with our previous discussion that the less chromatographic behavior required to achieve the desired separation, the lower will be the detection limits. Since some retention is necessary for separation, it is clear that optimum k' values will be obtained when dilution and resolution are jointly considered.

Finally, we consider the role of the separation factor α and the required resolution R_s. For two closely spaced peaks of roughly equal area, the standard R_s equation is:

$$R_s = \frac{1}{4}\left(\frac{\alpha - 1}{\alpha}\right)\left(\frac{k'}{1 + k'}\right)(N)^{1/2} \qquad (13)$$

where k' and N refer to the component eluting last. Substitution for N in Equation 7 leads to

$$\frac{C_{max}}{C_0} = \left(\frac{V_0}{4\sqrt{2\pi}}\right)\left(\frac{1}{\epsilon_T \pi r^2}\right)\left(\frac{1}{H}\right)\left(\frac{k'}{[1 + k']^2}\right) \times \left(\frac{1}{R_s}\right)\left(\frac{\alpha - 1}{\alpha}\right) \qquad (14)$$

The first point to notice from Equation 14 is that at constant H and k', dilution is inversely proportional to R_s. This can be seen from Relationship 8 and the fact that $R_s \sim L^{1/2}$. Thus, the more resolution obtained or demanded, the poorer will be the detection limits. Ultimately, the minimum R_s that is satisfactory will depend on the accuracy required for quantitation of the pair of bands. It is thus seen as first pointed out by Zhukhovitzki (*9*) and later by Huber (*6, 7*), that quantitative accuracy and detection limits are inversely related to one another. The more accuracy desired in peak area (or peak height) measurements, the larger R_s that is needed, and the smaller will be C_{max}/C_0.

We further note from Equation 14 that the larger the value of α for a given R_s, H, and k', the greater will be the value of C_{max}/C_0. Changes in α when it is close to unity can have a marked effect on detection limits. For example, if α is increased from 1.01 to 1.05 (*e.g.*, by change of either the stationary or mobile phases), the dilution will be 5-fold less. When we relax the condition that k' remains constant as α changes, the problem of prediction of dilution becomes more complex. Meijers, for example, has found optimum α values—*i.e.*, maxima in curves of C_{max}/C_0 *vs.* α (*38*). Since the relative retention (and its relationship to k') will be specific for a particular solute pair and since control of α may not be possible when dealing with a multicomponent mixture, it does not seem worthwhile in this general discussion to explore this parameter in more detail. In our analyses, we will assume that α has been optimized as much as practically possible.

We see that good column selectivity, short-efficient columns, and narrow tube diameters lead to the best use of the chromatographic system when the injection volume is limited. Of course, the first requirement of chromatography is separation so that it is necessary to examine optimization of detection limits with respect to resolution (at constant V_0). We cover this in the next section.

DILUTION AND SEPARATION

As already noted, the chromatographic column is a dilution device used in the separation of components prior to analysis. The best detection limits are obtained when no column is used, whereas the best separation is achieved when the chromatographic column is employed to a very great extent. Therefore, a compromise must often be struck

(32) J. L. Waters, J. N. Little, and D. F. Horgan, *J. Chromatogr. Sci.*, **7**, 293 (1969).
(33) G. J. Kennedy and J. H. Knox, *J. Chromatogr. Sci.*, **10**, 549 (1972).
(34) G. Guiochon, M. Goedert, and L. Jacobs, "GAS Chromatography, 1970," R. Stock, Ed., Institute of Petroleum, London, 1971.
(35) J. F. K. Huber, *Chimia*, **24**, 24 (1970).
(36) I. Halasz and M. Naefe, *Anal. Chem.*, **44**, 76 (1972).
(37) J. J. Kirkland, *J. Chromatogr. Sci.*, **7**, 361 (1969).
(38) C. A. M. Meijers, Ph.D. Thesis, University of Amsterdam, 1971.

between detection levels and resolution. As in time-resolution optimization (*39*), one can search for maximum resolution for a given detection level or minimum dilution for a given separation. We shall examine the latter case which is perhaps more meaningful in practice.

In order to simplify our discussion, we shall recast Equation 13 as

$$R_s = \frac{1}{4}\left(\frac{\alpha - 1}{\alpha}\right)\left(N_{\text{eff}}\right)^{1/2} \qquad (15)$$

where N_{eff} is the number of effective plates ($= N[k'/(1 + k')]^2$). We see from this expression that we will need a given number of effective plates to make a required separation (R_s) with a constant α value. Substitution of N_{eff} into Equation 5 gives

$$\frac{C_{\max}}{C_0} = \left(\frac{V_0\sqrt{N_{\text{eff}}}}{V_R\sqrt{2\pi}}\right)\left(\frac{1 + k'}{k'}\right) \qquad (16)$$

Substitution of Equation 6 into 16 and noting that $NH = L$, we have

$$\frac{C_{\max}}{C_0} = \frac{V_0\sqrt{N_{\text{eff}}}}{\sqrt{2\pi}\,\epsilon_T\pi r^2 L k'} \qquad (17)$$

Finally, Equation 7 can be modified as:

$$\frac{C_{\max}}{C_0} = \left(\frac{V_0}{\sqrt{2\pi}\,\epsilon_T\pi r^2}\right)\left(\frac{k'}{|1 + k'|^2}\right)\left(\frac{1}{N_{\text{eff}}}\right)^{1/2}\left(\frac{1}{H}\right) \qquad (18)$$

If we assume, as previously, that above 1-mm i.d., the column radius does not affect H, then the same functionality of r to dilution holds as in the previous section. However, most other column parameters affect both $C_{\max}/C_0$ and N_{eff}. Thus, in order to maintain N_{eff} constant, it is necessary to change simultaneously at least two column parameters. This will lead to somewhat different functionalities of the parameters to dilution than found in the previous section.

Let us first consider the simultaneous change in column length and particle diameter, while maintaining mobile phase velocity constant. Equation 17 reveals that

$$\frac{C_{\max}}{C_0} \sim L^{-1} \qquad (19)$$

and Equation 18 with Relationship 11 ($\beta = 1.8$) gives

$$\frac{C_{\max}}{C_0} \sim d_p^{-1.8} \qquad (20)$$

Relationship 19 reveals a stronger dependence of dilution on column length than was previously found when this parameter was varied alone, *cf.* Relationship 8. This arises from the fact that we must maintain N_{eff} constant as column length is reduced. Thus, conversion from a 1-meter column containing a large particle diameter support to a 10-cm column with a very small particle diameter support ($\sim$5 μ) will result in a 10-fold decrease in detection limits, if V_0 is maintained constant and if the sample does not overload the short column. We may also note that the analysis time is much less for the short column.

It is clear then that one should use as short a column as possible with as small a particle diameter as possible for best detection limits (with V_0 constant). As noted by many other authors (*28, 30, 35, 40*), the barrier to improvements will ultimately be the extra column band broadening caused by the injection process and the detector and connector dead volumes.

Comparison of Relationship 20 with Relationship 12 reveals a stronger dependence of dilution on particle diameter when N_{eff} must be maintained constant. The reason for this greater dependence is similar to that discussed above for column length.

A second question is the value of the capacity factor k' that results in minimum dilution for a given N_{eff}. It can be shown from Equation 18 that the maximum value of $C_{\max}/C_0$ occurs at $k' = 1$, if H is independent of k'. This may be compared with $k' = 2$, for time-resolution optimization, with H independent of k' (*41*). On the other hand, when $H \sim k'/(1 + k')^2$ (slow diffusion in the stationary liquid or stagnant mobile phase), then Equation 18 reveals that dilution is independent of k'. This arises from the fact that changes in H with k' are just balanced by changes in a second parameter (*e.g.*, column length) to maintain N_{eff} constant. When $H \sim k'^2/(1 + k')^2$ (slow diffusion in moving mobile phase to the pores), then dilution $\sim k'^{-1}$ or small values lead to improved detection limits.

From this analysis, we reach the conclusion that optimum k' values in consideration of dilution and resolution are smaller than in time-resolution optimization. Whereas a range of $k' = 1.5$–4 is recommended in minimum time analysis, roughly $k' = 0.5$–2 would seem best when detection limits are considered. As previously noted, this discussion neglects changes in α caused by changes in k'. Thus the specific value of k' for minimum dilution may vary somewhat from mixture to mixture; however, the above range should cover most cases.

An important consideration in time-resolution optimization has been inlet column pressure (*30*). Performance has often been thought to be limited by the upper pressure value of the pumping system. However, this parameter may not be a real limitation as quite good performances are possible with low pressures using short columns with small particle diameters (*42*). It is a relatively simple matter to include the role of pressure drop on dilution in a manner previously done on minimum analysis time (*30*). This does not seem a worthwhile effort at this point, and we shall omit this analysis.

INFLUENCE OF SAMPLE VOLUME

Up to this point, we have ignored the role of sample amount on detection limits, assuming constant and small sample sizes. It is clear from Equations 2 and 4 that the sample size plays a central role in the determination of small amounts of material. As noted earlier, we are frequently faced with a limited concentration of the component(s) of interest either from a low solubility in the solvent of the mixture or the complexity of the sample itself. The key factor, then, to enhance the mass of the sample component, m, is the injection volume. We shall now examine this factor and its relationship to dilution in the column.

One of the main considerations for the use of the columns of high performance in liquid chromatography is injection. When the injector is correctly designed and sample delivery is rapid, the injection profile is in the form of a plug with an unretained component covering a volume V_0 (the injected volume) of the column. Plug injection assumes no mixing of the sample with the mobile phase, simply a displacement of mobile phase at the front of the column. Improper injection can lead to mixing between the

(39) G. Guiochon, "Advances in Chromatography, Vol. 8," J. C. Giddings and R. A. Keller, Ed., Marcel Dekker, New York, N.Y., 1969.
(40) J. H. Knox and M. Saleem, *J. Chromatogr. Sci.*, **7**, 614 (1969).
(41) B. L. Karger, "Modern Practice of Liquid Chromatography," J. J. Kirkland, Ed., Interscience, New York, N.Y., 1971.
(42) M. Martin, G. Blu, C. Eon, and G. Guiochon, *Anal Chem.*, in press.

mobile phase and the sample prior to the latter's delivery to the head of the column. An exponential profile (*4, 18*) or other broad-shaped profile will be produced resulting in a significant contribution to band broadening.

Retained components under plug injection clearly displace less mobile phase than unretained species. In most models, it is assumed that the volume at the front of the column covered by a retained solute is $(V_0/1 + k')$, where k' is solute capacity factor for the chromatographic system (*14, 43, 44*). Since the front of the column will be greatly overloaded with this component, as well as all other species in the mixture, it is not good to assume the value of k' found under linear elution conditions. Moreover, less than immediate equilibration will lead to a larger displaced volume than predicted. Since these effects will depend on the particular mixture, method of injection, mobile phase flow rate, etc., we will follow the model used above, while recognizing its limitations. Nevertheless, a clear consequence of the reduced displaced volume for retained components is that greater volumes can be loaded on the column using programming techniques, as k' will be very large at the start of the run. Hence, programming techniques offer a means of lower detection limits (*45, 46*).

As the displaced volume at the head of the column is increased, the effective column length is reduced, resulting in a smaller number of theoretical plates. Following the approach of others (*3, 6, 18, 45*), consider the injection volume V_0 to be proportional to the standard deviation of the injection profile in volume units, $\sigma_{0,v}$, or

$$V_0 = K\sigma_{0,v} \tag{21}$$

K is a parameter characteristic of the method of injection and the conditions upon injection. Clearly, the higher the value of K the better. For a plug injection, $K = 3.5$, while for other injection profiles, K is found to be smaller (*18*). Finally, K is a constant over a sample volume range only if the injection profile does not significantly vary with volume.

If extra column effects beyond injection can be assumed to contribute a negligible amount to band broadening, then the total volume variance as measured on the chromatogram is the sum of the injection and (true) column variances ($\sigma_{c,v}^2$)

$$\sigma_{T,v}^2 = \sigma_{0,v}^2 + \sigma_{c,v}^2 \tag{22}$$

or

$$\sigma_{T,v}^2 = \frac{V_0^2}{K^2} + \sigma_{c,v}^2 \tag{23}$$

Thus, a plot of $\sigma_{T,v}^2$ *vs.* V_0^2 will yield K. This latter parameter is very useful to measure when evaluating an injector design for liquid (or gas) chromatography. The value of K will give some measure of the ability of the injector system to handle large sample volumes, an important characteristic when one wishes to improve detection limits.

We next consider the maximum injection volume that can be delivered to the column, V_0^{max}. This volume can be taken as the amount which degrades the performance of the column by a specified amount; for the moment, let us define V_0^{max} as that point at which $\sigma_{0,v}^2$ is $\theta^2\sigma_{c,v}^2$, where θ is a fraction. Equation 21 then becomes

$$V_0^{max} = K\theta\sigma_{c,v} \tag{24}$$

Substitution of Equation 24 into Equation 5 and noting that $(\sqrt{N}/V_R) = (\sigma_{T,v})^{-1}$, we have

$$\frac{C_{max}}{C_0} = \frac{V_0^{max}}{\sqrt{2\pi}\,\sigma_{T,v}} \tag{25}$$

Now if θ is taken small enough such that $\sigma_{T,v} \simeq \sigma_{c,v}$, we have that

$$\frac{C_{max}}{C_0} \simeq \frac{\theta}{\sqrt{2\pi}} K \tag{26}$$

We see that dilution is constant, independent of column parameters under the above restraints. This is a result of the fact that as a column parameter is varied (*e.g.*, column length, tube radius, etc.), V_0^{max} is appropriately changed.

A careful examination of Equation 26 is required for an understanding of the maximization of detection limits in chromatography. First, if the column is not sample overloaded, the detection limit will depend on the value of θ selected for a given analysis (and injection profile). Following Glueckauf (*3*), some workers have taken $\theta = 0.22$, which represents the point at which the variance due to injection is 5% of the column variance (*11, 23, 43, 46, 47*). Essentially, up to this point V_R and N can be assumed to be independent of sample size, if the mass of other components of the mixture does not affect the chromatographic behavior of the components of interest. (We should note that one could take the condition as $V_0^{max} < 0.7\ \sigma_{c,v}$; however, this is roughly equivalent to a 5% increase in $\sigma_{T,v}^2$, if plug injection is assumed with $K = 3.5$.)

In our previous discussions, we found that dilution was of the order of 1:100 for a small particle diameter, high efficiency column. With $\theta = 0.22$ and $K = 3.5$, we estimate that

$$\frac{C_{max}}{C_0} \sim 0.30$$

or 1:3.3. There is roughly a 30-fold improvement in detection limits if the constraints cited above are valid. From Equation 5, since N and V_R are assumed to be constant with $\theta = 0.22$, it is clear that the enhanced detection limits arise from a larger injection volume—*e.g.*, 150 μl instead of 5 μl.

Kalmanovski and Zhukhovitzki (*9*) and later Huber (*6*) have pointed that $\theta = 0.22$ is often too rigid a criterion upon which to base the maximum injection volume. Depending on the particular mixture, it may be possible to increase θ up to 2–3 times without a precipitous loss in column performance and resolution. Thus, injections of 300 μl or more can often be employed for good detection limits with high performance columns for low retained components (*48*). [We should note that this presupposes that K does not change with sample volume. For high performance, a sample valve is frequently needed for the rapid delivery of the mixture to the column (*49*).] For longer retained components, even higher volumes should be possible. Under proper conditions, $C_{max}/C_0 \simeq 0.65$ or higher (*50*). Thus, the chromatographic column need not be considered as a device producing high dilutions under the proper set of circumstances.

The second factor in Equation 26 is the injector-sample characteristic, K. As we have noted, for an unretained com-

(43) A. Klinkenberg, "Gas Chromatography, 1960," R. P. W. Scott, Ed., Butterworths, Washington, 1961.
(44) L. R. Snyder, *J. Chromatogr. Sci.*, **10**, 187 (1972).
(45) L. W. Hollingshead, H. W. Habgood, and W. E. Harris, *Can. J. Chem.*, **43**, 1560 (1965).
(46) W. E. Harris, *J. Chromatogr. Sci.*, **11**, 184 (1973).
(47) A. B. Littlewood, "Gas Chromatography," Academic Press, New York, N.Y., 1970, p 192.
(48) W. Strubert, *Chromatographia*, **6**, 205 (1973).
(49) L. V. Berry and B. L. Karger, *Anal. Chem.*, **45**, 819A (1973).
(50) V. G. Berezkin and V. S. Tatarinskii, "Gas-Chromatographic Analysis of Trace Impurities," J. E. S. Bradley, Ed., Plenum Publishing Company, New York, N.Y., 1973.

Table II. Influence of Sample Volume on the Volume Variance of the Injected Band in Liquid Chromatography

Component	Velocity, mm/sec	Maximum volume, μl	$K^{(a)}$	$r^{(b)}$
Benzene	1.04	80	2.69	0.97
($k' = 0$)	4.7	100	2.71	0.95
Pyrene	1.00	100	1.86	0.99
($k' = 0.85$)	1.00	190[c]	2.06	0.96

[a] See text for definition of K. [b] r = regression coefficient. [c] Obtained by extension of the 100-μl maximum volume experiments.

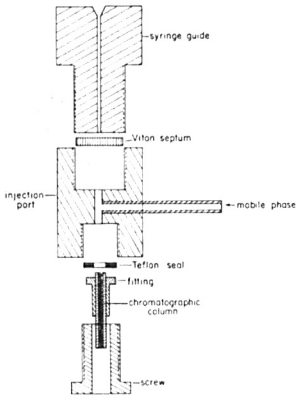


Figure 1. Illustration of the injection design used in this work

ponent with plug injection we expect $K = 3.5$; however, this is an ideal case. For example, calculation from Huber's data (Figure 2 in Ref. 6) reveals a value of 2 for a retained component. From Table II in our results (to be discussed shortly), we find values of 2 and 2.7. This discussion points out that the main approach to improved detection limits is increased sample volumes (assuming that the concentration of the sample cannot be increased). The maximum volume is conditioned by the sample complexity and the performance of the injection system. For mixtures in which the component(s) of interest are well resolved from the other species, we expect that a large volume can be injected. The ability of the injection system to handle these large volumes efficiently becomes the limiting factor. For complex mixtures in which the component(s) of interest are not well resolved from other species, the overloading of the column by the major components may become the limit on sample volume.

Since we are injecting a liquid sample into a liquid mobile phase, no phase changes take place as in gas chromatography. Surprisingly large volumes may be injected in modern liquid chromatography, if the injection system is well designed and if the volume is rapidly delivered to the column. Thus, care needs to be exercised in designing an injection system that can efficiently handle large sample volumes.

INJECTION CHARACTERISTICS

Since the value of K is an important characteristic of the injection system and the solute mixtures, we have examined in a preliminary fashion some typical experimental values one might find in liquid and gas chromatography. The results for LC are shown in Table II and those for GC in Table III.

Table III. Influence of Sample Volume and Injection Mode on the Volume Variance of the Injected Band in Gas Chromatography

Injection mode	Maximum volume, μl	$K_0^{(a)}$	$K_1^{(a)}$	$K_2^{(a)}$	$r^{(b)}$
Gas injection directly in column	500	0.57		0.13	0.86
Liquid injection directly in column	26	0.008	1.85	0.37	0.96
Liquid injection into vaporization tube, $T = 70$ °C	24	0.008	1.95	0.39	0.94
Liquid injection into vaporization tube, $T = 102$ °C	28	0.011	2.75	0.55	0.93

[a] See text for definition of K_0, K_1, K_2. [b] r = regression coefficient.

For on-column injection, the same injector design was used for LC and GC, as shown in Figure 1. In some GC experiments, a vaporization chamber was placed between the injector and the column. This chamber consisted of a stainless steel tube, 10 cm × 1.6-mm i.d., surrounded by a second tube, the temperature of which was controlled by a heating tape wrapped around it. To measure the temperature of the vaporization chamber, a thermocouple was placed between the two tubes.

Both the GC and LC instruments were home-made of standard design. The GC instrument consisted of a column thermostated by an oil bath and a flame ionization detector. The LC apparatus was composed of an Orlita pump, a pressure regulator, the thermostated column and an Uvicord LKB detector with a modified 6-μl cell.

The LC column, 1 meter × 1.6 mm, was filled in the standard manner with neutral N 18 alumina (Woelm), particle diameter = 25–31.5 μ. The GC column, 2 meters × 2.2 mm, contained Spherosil (Rhone-Progil), particle diameter = 80–100 μ, surface area = 77 m^2/gram, impregnated with 10% w/w Carbowax 20 M. The mobile phase for LC was heptane saturated with water, while that for GC was helium.

For samples in LC, we used 10^{-3} v/v benzene ($k' = 0$) in water-saturated heptane and a 2×10^{-5} gram/cm^3 solution of pyrene ($k' = 0.85$), again in water-saturated heptane. For GC, the gaseous sample consisted of 1.3×10^{-4} v/v butane ($k' = 2.2$) in methane, whereas the liquid sample was 10^{-5} v/v benzene ($k' = 13.9$) in pentane ($k' = 3.2$). The column temperature in LC was maintained at 23 °C, while that for GC was 63.4 °C. The mobile phase velocity (outlet) in GC was always 15 cm/sec with an inlet pressure of 5 atm. This was experimentally found to be the optimum velocity (minimum HETP) for the case of butane. The mobile phase velocity of heptane in LC was varied as indicated in Table II.

The procedure followed in the measurement of K values consisted of injecting different volumes of the above solutions and then plotting the resulting total band variance, $\sigma_{T,V}^2$, *vs.* the square of the injection volume, V_0^2. The slope of this plot is the reciprocal value of K^2 (Equation 23). For injection we have used three Hamilton syringes—701N up to 10 μl, 710N up to 100 μl, and 1001 LTN up to 1000 μl. The results in Tables II and III include not only the experimental K values, but also the regression coefficients of the straight lines obtained in the plots. The maximum volumes in these tables should not be confused with V_0^{max} previously discussed with respect to detection limits (Equation 24).

In the tables, the maximum sample volume represents that point beyond which the plot of $\sigma_{T,v}^2$ *vs.* V_0^2 becomes significantly nonlinear.

Turning first to Table II, we see that the K value for benzene, which is unretained, is independent of the mobile phase velocity at these low velocities, and that it is close to the value of 3 predicted for plug injection. The regression coefficients indicate good coherence of the plots to a straight line. The maximum volume of 100 μl was set by the fact that the 1000-μl syringe could not inject very reproducibly at 40 atm (the pressure at v = 4.7 mm/sec). A sample valve would be needed in this case to extend the maximum volume to a higher limit. It may be pointed out that the effects observed are due to the injection band and not to saturation of the column or detector, for a small concentrated sample of the same mass as that in the 100-μl sample revealed no extra band broadening over that of a very dilute sample. Similar checks for the other solutes in Tables II and III revealed that in all cases we are observing injection effects.

The K value for pyrene, a retained component, is lower than that for benzene. The result suggests that equilibration occurs only after full transfer of the sample to the column. With the limited data, it is not possible to further examine the small K value; a more detailed study would be necessary for clarification.

Nevertheless, it is interesting to note that relatively large volumes of sample volume can be injected in LC. Large injection volumes have been successfully employed by Huber (*6, 7*) and Strubert (*48*), among others. As already noted, a sample valve or pressurized syringe injector will rapidly deliver liquid samples to the column. It is expected that these will lead to even larger injection volumes.

Table III presents the results obtained in GC under four sets of conditions: a) on-column injection of a gas; b) on-column injection of a liquid;c) liquid injection into a vaporization tube at 70 °C; and d) liquid injection into a vaporization tube at 102 2 °C. Three different K values are given in this table: i) K_0—from the volume of sample in the syringe, liquid or gas at 1 atm and room temperature; ii) K_1—from the volume of sample corrected to a gas (density correction) at 1 atm and the temperature of the column; iii) K_2—gaseous sample volume at the head of the column (corrected to the inlet pressure and temperature of the column).

Consider first the K_1 values which are comparable to the K values in LC (Table II). The lowest value is obtained for the gaseous sample. This is probably indicative of mixing of the carrier gas with the sample, arising from the relatively slow injection of the large volume from the syringe. In addition, pressure changes might be expected to occur in the syringe as the needle penetrates the septum and at the beginning of the column as the sample is delivered. These pressure effects could cause further mixing of carrier gas with the sample. For liquid injection, the K_1 values approach those obtained in LC. We note that injection on-column is similar to that using a vaporizing chamber at 70 °C; however, as expected, raising the chamber to 102 °C leads to a larger value of K_1. This latter result arises from the fact that a more rapid vaporization of the sample leads to less mixing with the mobile phase prior to the sample's transport to the column.

Conversion to the inlet pressure of the column leads to a compression from 1 atm to 5 atm. From Equation 21 we see that the K values will need to be altered to reflect this compression—*i.e.*, $K_2 = \frac{1}{5}K_1$. At first sight, it might seem that the detection limits are then a function of the definition taken for the injection volume. This is clearly not the case, for the critical sample size is the mass of the solute injected, as this controls the maximum concentration eluting from the column (Equation 2). Of course, dilution will be altered, for C_0 must change with the different definition of V_0 (with maintained constant).

Finally, the K_0 values represent the injection system based on the sample as originally inserted by the syringe. The very low values found for the liquid samples arise from the expansion which must take place as the sample is vaporized. Comparison of Tables II and III either in terms of K_0 and K values or in terms of the maximum injection volume reveals the important point that much larger sample liquid volumes can generally be injected in LC than in GC. In LC, we are injecting a liquid into a liquid mobile phase. As noted, remarkably large sample volumes can be introduced into LC without a precipitous loss in column performance, *e.g.* (*6, 7, 46*).

As we have stated above, the controlling factor on C_{max} is the sample mass, not the volume. Since the maximum mass is fundamentally dependent on the capacity of the column, it would not be correct to say that, for the same detector sensitivity, LC would lead to a lower detection limit than GC. However, since we are often limited in the concentration of the sample in LC, as we have previously discussed, the fact that large volumes can frequently be injected in LC is important as one searches for lower detection levels.

CONCLUSION

In this paper, the role of the chromatographic system on detection limits has been examined. Given a constant sample size, we have seen that the less demands placed on the column, the smaller will be the ensuing chromatographic dilution. The importance of selective separations (*i.e.*, with large α values) is clearly understood on this basis. Moreover, the modern developments of column liquid chromatography with microparticle supports are also seen to lead to improved detection limits. Ultimately, however, the injection volume can be the factor leading to the greatest improvement in detection. It is shown that much larger liquid sample volumes can be injected in liquid chromatography than in gas chromatography. This compensates somewhat for the generally lower detector sensitivities found in LC. For further extensive discussions on trace analysis, references (*50, 51*) should be examined.

RECEIVED for review March 20, 1974. Accepted May 31, 1974. The authors gratefully acknowledge the NIH, for support of this work. During 1972, B. L. Karger was on sabbatical leave at Ecole Polytechnique.

(51) V. Svojanovsky, M. Krejci, K. Tesarite, and J. Janak, *Chromatogr. Rev.*, **8**, 90 (1966).

Disk Conveyor Flame Ionization Detector for Liquid Chromatography

J. J. Szakasits and R. E. Robinson

Shell Development Company, MTM Process R&D Laboratory, P.O. Box 100, Deer Park, Texas 77536

Hydrogen flame ionization, which has gained wide acceptance in gas chromatography for its high sensitivity and linearity, appeared to be a promising detector to adopt for liquid chromatography. However, sample introduction into the detector poses a problem. A number of experimental and commercial systems using chains, etc., of various configurations have been implemented for sample transport with limited success. An alternative concept is to use a highly porous disk-shaped conveyor on which the sample material is firmly held in the pores of the conveyor and carried into the flame of the detector. Spiking and associated problems found with metal sample transports are greatly reduced. The disk conveyor flame ionization detector has a linear response and a minimum detection of ~2 ng/second. The relative standard deviation for ten consecutive injections of a blend containing *n*-eicosane (~0.06 wt %) in benzene was found to be ~1%.

The flame ionization detector (FID) offers high sensitivity, wide linear dynamic-range, quantitative response, and is relatively easily constructed. It has proved useful in gas chromatography and, with the growth of liquid chromatography (LC), various ideas have been implemented by experimenters to adopt the FID to sample LC effluent streams. Sampling a liquid stream creates a problem, since the solvent or mobile phase has to be separated from the solute before detection. This, in turn, places a limitation on the detection of light components in the mobile phase, since the conveyor has to be heated to vaporize the eluent.

Sample transports that have been most successfully implemented are chain (*1–5*), belt (*6*), wire (*7–10*), various forms of disks (*11, 12*) and helix shaped wire (*4*). By and large, with commercially designed detectors, either the total effluent or a portion of it is deposited on a conveyor of some type. The solvent is flash evaporated in a heater leaving the solute on the conveyor. One method of detection involves burning the sample material directly in the flame as the conveyor passes through the detector. An alternative and more involved concept removes the sample material by pyrolysis in a purged enclosure from which the pyrolysis products are swept into a FID. The pyrolyzer design is the more complex of the two but usually gives better broad peak description. Both concepts have been used with varying degrees of success. Nevertheless, the paramount problem of sample diffusion on hot metal conveyors, which manifests itself in the form of signal spikes (spiking), is still present with many of the direct burning and pyrolyzer designs. The noise problem is more evident with all designs when broad peaks are observed, as frequently encountered in gradient elution fractionation (GEF) and gel permeation chromatography (GPC).

A new liquid chromatography detector of the direct burning type has been developed that utilizes a porous disk to transport the sample material into the detector (*13*). For construction of the porous disk, machinable alumina was selected for its excellent resistance to high temperatures and its ability to retain in its pore structure the eluted sample material. Solvent is removed in a heater enclosure from which the vapors are exhausted by a fan. Detection of the sample material takes place in a dual nozzle FID. An oxidizer with two hydrogen nozzles is used to minimize residue build-up in the pores of the conveyor. Background noise caused by impurities in room air currents is eliminated by purging the detector enclosure with nitrogen.

An additional advantage of using porous alumina is that a significant reduction of back-diffusion of the sample occurs. This is evidenced by a stable base line and good signal stability compared to metal conveyors. Furthermore, the conveyor is self-supporting, thereby eliminating the need for pulleys. The sample applicator tip makes contact with the conveyor surface through a liquid interface of the mobile phase, so that wear due to friction is nil. The apparatus is simple and requires little more attention and maintenance than an FID.

EXPERIMENTAL

Apparatus. The vertical disk conveyor flame ionization detector (DC-FID) and electrometer are mounted in a standard 19-inch rack cabinet as depicted in Figure 1. The panel, which contains the pressure regulators, flow controller, etc., is an integral part of the apparatus.

Principal components of the apparatus are the disk conveyor, FID and oxidizer, disk cooler, sample applicator, and the solvent evaporator as shown in Figure 2.

The base plate or the main structural frame of the detector contains the controls for the solvent heater and the exhaust system. Also mounted on the base plate are the detector, conveyor heater, applicator, etc. The base plate is fabricated of structurally sound material (0.5-inch thick aluminum) to maintain good dimensional stability of each major component with respect to the disk conveyor. Close installation of the electrometer and FID is desirable to reduce electrical noise in the connecting line, which has a low signal level.

Disk Conveyor. Solid and perforated metal sample transports were used to fabricate disk conveyors in the early stage of development. Smooth, thin quartz disks roughened by sandblasting and with a narrow band of silica gel or alumina coating were also tried with limited success. A narrow band of sample retaining ring was deposited on the rim of these conveyors to eliminate sample creeping associated with metal or other solid conveyors. Some of the

(1) E. Haahti and T. Nikkari, *Acta Chem. Scand.*, **17**, 2565 (1963).
(2) J. E. Stouffer, T. E. Kersten, and P. M. Krueger, *Biochem. Biophys. Acta*, **93**, 191 (1964).
(3) A. Karmen, *Anal. Chem.*, **38**, 286 (1966).
(4) A. Mrkvicka and S. W. Leslie, "An Evaluation of Detectors for Liquid Chromatography," paper presented at the 17th Pittsburgh Conference on Analytical Chemistry, February 1966.
(5) R. H. Stevens, *J. Gas Chromatogr.*, **6**, 375 (1968).
(6) H. W. Johnson, Jr., E. E. Seibert, and F. H. Stross, *Anal. Chem.*, **40**, 403 (1968).
(7) S. Lieberman, U.S. Patent 3,128,619, April 1964.
(8) A. T. James, J. R. Ravenhill, and R. P. W. Scott, "Gas Chromatography," (Fifth International Symposium) Brighton, England, A. Gouldup, Ed., Institute of Petroleum, London, 1964, p 197.
(9) R. P. W. Scott, British Patent 998,107 (1965); U.S. Patent 3,292,420 (1966).
(10) T. E. Young and R. J. Maggs, *Anal. Chim. Acta*, **38**, 105 (1967).
(11) T. Cotgreave, *Chem. Ind. (London)*, **17**, 689 (1966).
(12) Hanniel Dubsky, Czechoslovakia Patent 5,580 (1970); U.S. Patent 3,744,973 (1973).
(13) J. J. Szakasits, U.S. Patent 3,788,479 (1974).



Figure 1. Vertical disk conveyor flame ionization detector

The simplest and most effective technique was the conditioning of the conveyor *in situ*. A conveyor with stresses or micro-cracks will break in the first few moments in the flame, while a conveyor that has been in service for an hour or longer should not break without external causes. *In-situ* conditioning of a conveyor should not take longer than overnight. A stable base line can be obtained on a 1×10^{-11} A scale of the electrometer.

In routine use, the flame should be left burning and the conveyor rotating continuously overnight to maintain a good base line.

Detector and Oxidizer. The detector and oxidizer design is shown in Figure 4. Detection is accomplished by burning the sample in a hydrogen flame. The edge of the disk on which the sample material has been deposited is enveloped by hydrogen flames produced by dual nozzles impinging on opposite surfaces of the disk edge. Ions formed in the plasma are collected at the nozzles and at the semicircular collector electrode surrounding the edge of the conveyor. The electric field is produced by a 300-volt battery connected in series with the electrometer (Keithley Model 417K). The collector is maintained positive with respect to the two nozzles, which are grounded. The collector consists of semicircular rings (~1.5 cm in diameter and spaced 3 mm apart) positioned ~2 mm ahead of the nozzles. It is mounted on an Amphenol connector that connects through a coaxial line to the battery. In order to minimize thermionic noise, the nozzles and the collector are fabricated of platinum, which has a very low emission ($\sim 10^{-6}$ A cm^2 at 1200 °C). Nozzles have platinum tips of 0.062-inch o.d. and 0.030-inch i.d. The FID nozzles are installed in eccentrically drilled mounts to facilitate positioning with respect to the conveyor. Final positioning of the nozzles with respect to the rim of the conveyor is accom-

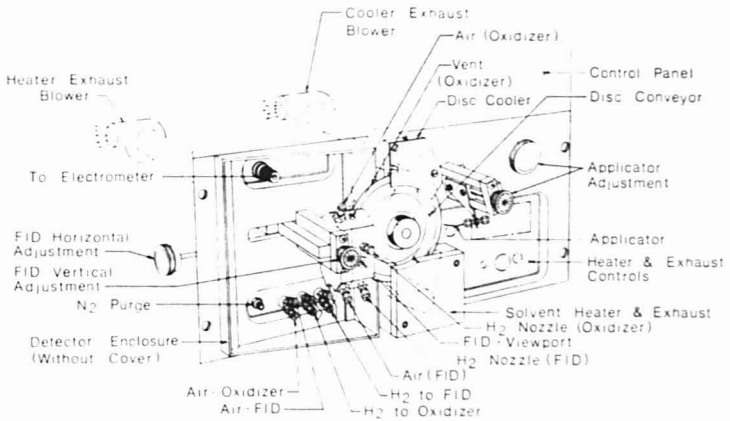


Figure 2. Disk conveyor flame ionization detector. Exploded view of principal components

problems observed with these conveyors were excessive background noise, poor dimensional stability, and flaking of the porous coating.

It became apparent that the sample conveyor should be fabricated from porous, inert, mechanically strong material that had a low expansion coefficient and could withstand thermal shocks. New disks were fabricated from 4.5-inch diameter machinable alumina bar stock on a lathe using a carbide tip tool. The bar stock has an apparent porosity of approximately 40% and is approximately 99% pure alumina (Coors Porcelain Co., Golden, Colo.). The shape and dimensions of the conveyor design is shown in Figure 3.

Before using a new disk, the flat surface (which was clamped to a jig in the final phase of machining) was lightly sanded. After it was washed with acetone and pentane, the disk was dried in a nitrogen-purged oven. Several techniques were tried to pre-condition and test the conveyor prior to installation on the detector. Some were heated in a high temperature furnace (approximately 800 °C) while others were dried in a vacuum oven for 2–3 days. Both procedures produced the same level of background.

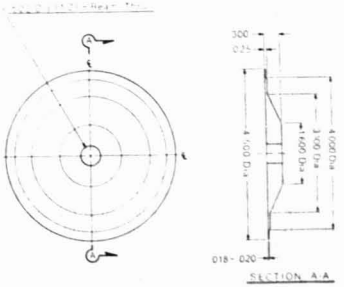


Figure 3. Alumina disk conveyor

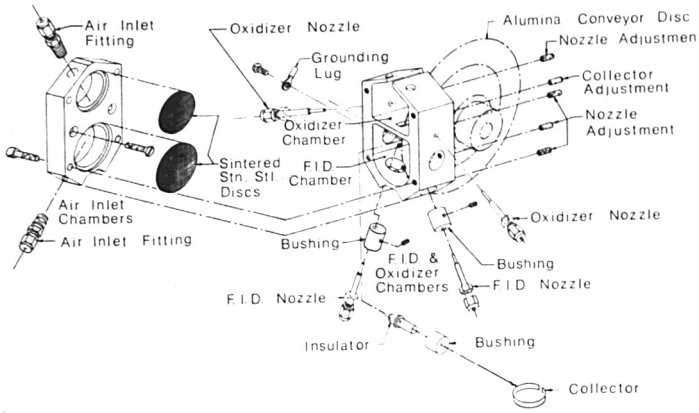


Figure 4. Dual nozzle flame ionization detector and oxidizer combination

plished by horizontal and vertical slides. A port is provided on the side of the FID housing to facilitate the proper positioning of the nozzles and to ignite the hydrogen flames.

The FID housing is machined from aluminum to provide good dimensional stability of nozzles and collector with respect to the conveyor. The oxidizer chamber is an integral part of the FID and is separated from the FID chamber by a baffle, as shown in Figure 4. It is similar in design to the FID cavity, except without an ion collector. Air enters into the FID and oxidizer chambers through sintered stainless steel disks covering small cavities on the side of the housing. A uniform low-velocity air flow is provided through these inlets for combustion and pressurization of the FID cavity to eliminate background noise produced by room air currents; moreover, the detector is installed under nitrogen purged cover, as shown in Figure 1.

Hydrogen and air are fed to the FID and oxidizer through 0.062-inch o.d. by 0.040-inch i.d. Teflon tubing made up with stainless steel Gyrolock fittings. Fixed-ratio splitters are used to divide hydrogen between the front and rear nozzles. Oxidizer hydrogen input is ~75% of the flow rate to the FID.

Solvent Heater. Solvent is vaporized in an aluminum heater block (Figure 2) that surrounds ~20% of the edge of the conveyor. Block temperature is maintaned with a Chromalox 280-watt cartridge heater. This element is positioned in the lower portion of the block close to the solvent vapor exhaust line. A one-inch diameter stainless steel tubing supports the heater block and also serves as the solvent exhaust duct. To prevent solvent vapors from entering the detector enclosure, they are vented via duct and heater blower, as shown in Figure 2. The exhaust duct is cooled with a series of aluminum fins to reduce heat transfer to the main frame of the detector apparatus. The heater block is not insulated. Its cover plate (0.5-inch thick aluminum plate) is easily removable to facilitate disk installation.

Sample Applicator. An ideal applicator uniformly deposits all of the mobile phase on the conveyor without back-diffusion or wetting along the external surface of the applicator tubing. To select a material best suited for sample application, experiments were made with tubing materials readily available. Stainless steel and glass tips showed a higher level of external wetting than Teflon. This behavior causes both sample loss and backmixing. Sample loss occurs when the carrier mobile phase vaporizes and deposits the solvent in the form of rings 3–5 mm above the tip. The extent of this wetting will vary at constant flow rate and is manifested by a slow pulsation along the applicator tube. As a result, a portion or all of the solute deposited by one pulse can be diluted subsequently by a more extensive pulse that dissolves it and carries it down to the applicator tip causing backmixing. This, in turn, places a new sample ring at a higher position. After analysis, a sample ring at "maximum wetting level" is observed on glass and stainless steel applicators.

The extent of solute diffusion is also affected by the conveyor temperature and the viscosity and flow rate of the solvent. Not all these parameters can be readily controlled. The solvent and its flow rate, for example, are fixed for proper operation of the chromatograph. However, applicator material and conveyor temperature are properties of the detector and can be modified to minimize improper applicator performance. In considering other materials for construction of applicators, Teflon was expected to work well. Tips were made by heating and drawing $\frac{1}{16}$-inch o.d. by 0.03-inch i.d. tubing. It was difficult, however, to produce applicators with inside diameters smaller than ~0.015 inch with this technique. Lack of physical strength and excess sample wetting of the conveyor made these applicator tips undesirable and impractical. Teflon-covered syringe needles purchased from Unimetrics have good physical strength, small tip dimensions (about 0.005-inch i.d. and ~0.017-inch o.d. at the tip), and the qualities found with Teflon alone. Excellent solvent deposition and width control can be maintained on the conveyor with these tips. Direct contact of the applicator and disk should be avoided since the applicator tip is covered with Teflon, which is quickly eroded by the alumina disk and can cause plugging. Effluent flow rate should be adjusted to form an ~3–4 mm wide liquid ribbon on the edge of the disk conveyor. Sample flow rates of 200–250 μl/min can be used with a Teflon-coated applicator tip.

Disk Cooler. The disk conveyor as it exits from the oxidizer is at 400–500 °C and must be cooled to near room temperature before the effluent can be applied. An excessively high conveyor temperature will result in partial or complete effluent loss, regardless of its boiling point. In other words, the sample is vaporized along with solvent material. The cooler, shown in Figure 2, is similar in design to the heater. The front half of the cooler is constructed of Plexiglas; the rear, of aluminum for strength. They are supported on insulated one-inch diameter steel tubing that also serves as a duct and connects to an exhaust fan. A large volume of cooling air is drawn over the edge of the disk by this fan. With an exhaust fan rated at ~60 CFM and at ambient temperature, the conveyor can be cooled to a sufficiently low level so that *n*-pentane can be used as solvent. No measurable increase in detector background noise was observed that could be attributed to this cooling system.

DISCUSSION

Initial settings of air and hydrogen flow rates and conveyor speed for optimum response were found by using a rapid spotting technique in which a solution of *n*-eicosane in benzene was spotted onto the rim of the conveyor with a microliter syringe. During these tests, the oxidizer was disconnected. Consequently, any partially combusted sample was allowed to return to the detector, thereby indicating incomplete combustion during the first pass through the

Table I. Optimum Detector Conditions

FID, Hydrogen	~140 ml/min
Air	~1000 ml/min
Oxidizer, Hydrogen	~100 ml/min
Air	~800 ml/min
Nozzle separation	~1 mm for FD ~2 mm for Oxidizer
Nozzle position from edge of conveyor with respect to center line of nozzle tip	Tangent for FID ~3 mm in for Oxidizer
Conveyor speed	10 Inches/min (~0.7 rev/min)
Eluent heater	Varied from room temperature to 200 °C depending on eluent used
Collector polarization	+300 V Nozzles Grounded
Electrometer	Keithley 417K
Detector cover purge	0.5 2 l./min nitrogen

Table II. Detector Repeatability

No. of readings	Response peak area[a]
1	499.92
2	511.58
3	500.02
4	504.35
5	499.03
6	505.34
7	511.95
8	511.10
9	512.70
10	503.90

Average = $\bar{X}$ = 505.89

$$\delta = \pm\sqrt{\frac{\Sigma(X - \bar{X})^2}{n - 1}} = \pm 5.19 \text{ units}$$

$$\delta_{rel} = (\delta / \bar{X})\ 100 = 1.02\%$$

[a] $\bar{X}$ is the arithmetic mean, δ standard deviation, δ_{rel} the relative standard deviation, and n is the number of readings. The peak areas are expressed in arbitrary units. The relative standard deviation at these detector conditions was found to be ~1%.

detector. At the conditions giving maximum response, the effects of nozzle positioning with respect to the conveyor on signal stability were briefly studied. The condition existing at the apex of a sample peak was simulated by percolating a blend of *n*-eicosane in benzene onto the conveyor at a flow rate of ~150 μl/min. Nozzles were positioned at different points on the conveyor for a period of time. The worst condition—*i.e.*, where the most intense noise existed—occurred when the tips of the nozzles were ~3 mm or further inside from the edge of the conveyor. Very little fluctuation in signal level was observed when the nozzles were positioned such that their tips were approximately above or near the edge of the conveyor. In all cases, a uniform flame coverage of the sample rim on the conveyor was observed. No simple explanation of the marked change from a ~3-mm distance to the edge position is apparent at this time.

After establishing the maximum response by spotting and the optimum signal stability by adjusting nozzle positioning, the detector operating parameters were set as summarized in Table I.

For a repeatability check of the detector, a solution of *n*-eicosane (250 ppmw) in benzene was used as a standard blend. To simulate actual LC conditions, benzene (solvent) was percolated onto the disk conveyor through a flow control needle valve fitted in series with a Valco injection valve equipped with a 30-μl sample loop. The sample was picked up with a syringe pump through the 30-μl loop and switched into the line connecting the benzene reservoir with the applicator. Hydrostatic pressure was used to maintain uniform solvent flow, which was set at ~150 μl/min. The solvent heater was set at 100 °C. Ten consecutive injections were made. The resulting peak areas were integrated electronically using a Vidar (Model 240 BR) voltage-to-frequency converter and a Computer Measurements Company (CMC Model 315A) counter. The peak areas obtained for ten consecutive injections of the standard *n*-eicosane/benzene blend are given in Table II.

Precision of the detector was estimated to be ~1%. However, for a detector to give a quantitative response, it must demonstrate accuracy and good linearity. To verify a linear relationship for the DC-FID between response and concentration, a series of blends of known concentrations (weight) of *n*-eicosane in benzene was analyzed. The range of sample concentrations was about the same as expected for practical samples. Five injections were made at each concentration with the 30-μl loop sampling valve. Peak areas were integrated electronically using the voltage-to-frequency converter and CMC counter described earlier. Linearity was checked over four decades, and the slope of the line connecting the data points in the graph was found to be near unity.

The hydrogen FID, similar to other detectors used in chromatography, exhibits differing levels of response for the same weight of various compounds. It will respond to mass flow rate. The peak area is proportional to the total mass of the eluted compound passing through the detector. Response factors have been published by W. A. Dietz (*14*) for a closed FID detector connected to a gas chromatography column. However, when the sample is carried into the hydrogen flame by conveyor, rather than by a gas, the changes in detector and ion-collection geometry can and, in most instances, will be sufficient so that the response factors used with these designs will differ significantly from those reported by Dietz. The compounds of interest are those which cannot generally be vaporized for use with GLC. Detector response relative to *n*-eicosane was briefly studied with a small group of hydrocarbons for the DC-FID.

In addition to the measurement of the relative sensitivities, an attempt was made to investigate the effect of nozzle size (or flame shape) and its positioning with respect to the conveyor and ion collector. Their combined effect on detector response along with the influence of the oxidizer on detector response was also studied. Based on experimental observations, four detector conditions were selected for the measurements. The relative detector responses for a group of compounds under the four differing conditions designated as (A), (B), (C), and (D) are shown in Table III. Condition (A) utilized an FID without the oxidizer and with nozzles of 0.010-inch i.d. Nozzles were positioned so that their tips or ends were near the edge of the conveyor. For (B), conditions were the same as (A) with the exception of nozzle size. A set of larger bore nozzles, 0.030-inch i.d., were substituted for the type used under condition (A) resulting in a more dispersed, broader flame. The results shown under conditions (C) and (D) were obtained with both FID and oxidizer equipped with 0.030-inch i.d. nozzles. Under condition (C), nozzles were positioned so that their tips were ~3 mm inside from the edge and, for (D), the nozzles were above the edge of the conveyor. For all four conditions, (A) through (D), the hydrogen flow rate to the FID was ~140 ml/min.

The response of *n*-alkanes appeared to be the least affected by the choice of nozzle configurations. Responses of aromatic compounds on the other hand were influenced

(14) W. A. Dietz, *J. Gas Chromatogr.*, **5**, 68 (1967).

Table III. Relative Response for Different Detector Conditions

Compound	Relative sensitivities[a] (A)	(B)	(C)	(D)
n-Tetradecane	0.13	0.17	0.12	...
n-Hexadecane	0.72	0.76	0.63	0.83
n-Octadecane	1.00	1.04	0.92	1.09
n-Eicosane	1.00	1.00	1.00	1.00
n-Tetracosane	0.98	0.99	1.06	1.05
n-Tetratriacontane	1.00	0.96	0.89	0.96
Dimethyl naphthalene	0.27	0.27	0.22	0.21
Anthracene	1.31	1.35	1.22	1.38
Phenanthrene	1.13	1.26	1.33	1.32
Pyrene	1.45	1.49	1.33	1.31
Chrysene	1.22	1.14	1.23	1.26
Squalene	1.15	...	1.17	1.18
Ethyl *n*-hexadecyl / Benzene	0.97	0.93	0.97	1.00

[a] (A) FID with 0.010-inch i.d. nozzles, oxidizer disconnected. (B) Same as (A) except with 0.030-inch i.d. nozzles. (C) FID and oxidizer connected, 0.030-inch i.d. nozzles are positioned ~3 mm in from the edge of conveyor. (D) Same as (C) except nozzles are at the edge to the rim of the conveyor.

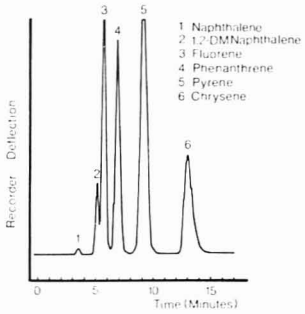


Figure 5. Separation of polynuclear aromatic hydrocarbons by supercritical fluid chromatography

Conditions: 2 m × 2 mm o.d. alumina (120/170 mesh) column; mobile phase, *n*-pentane; column temperature, 211 °C; pressure, 40.9 atm; electrometer, 1.6×10^{-10} AFS

more by changes in nozzle positioning. They were not influenced, however, by the addition of the oxidizer. Thus, the oxidizer, which was installed to maintain conveyor cleanliness, does not appear to affect the detector operation. For certain samples, its need is questionable; however, for samples containing heavy residues (materials which do not produce signal, but nevertheless discolor the conveyor), *e.g.*, pitch, the oxidizer is essential. For routine use, our detector operates with the conditions described under (D). At these conditions various petroleum fractions, *e.g.*, light gas oil (boiling point range ~220–330 °C) and heavy gas oil (boiling point range ~300–440 °C) were successfully analyzed.

A typical chromatogram, as shown in Figure 5, demonstrates the capability of the DC-FID. The chromatogram was obtained with a synthetic blend of aromatic hydrocarbons eluted from a high pressure chromatograph. The total effluent flow rate was 1.78 ml/minute from which about 400 μl/minute (22.5%) was diverted to the disk conveyor through a splitter system. The sample injected was a benzene solution of the aromatic compounds. Small "spikes" on the side of the peaks are attributed to occasional gas bubbles "ejected" at the tip of the applicator. These are thought to be due to periodic flashing of the light carrier solvent (*n*-pentane).

The disk conveyor FID has many similarities in design with the types used in gas chromatography, such as nozzle and electrode arrangements. However, a dramatic deviation is the means of sample introduction into the flame, which necessitates an opening in the side of the detector housing to accommodate the disk. In spite of the added sources of background noise provided by the disk itself and the large opening in the FID housing, the DC-FID is capable of attaining good sensitivity (~3–4 ng/second). Its ability to handle peaks lasting over a long period of time is as good or better than any conveyor FID described in the literature to date.

The DC-FID is a simple device and its operation requires little more technical knowledge and attention than does a typical GLC-FID. The DC-FID described in this paper has been in routine use in our laboratory for close to a year. Except for short periods of time, it has been running continuously and has proved to be a versatile and rugged LC detector.

ACKNOWLEDGMENT

The authors wish to express their indebtedness to R. L. Heller for his assistance in the evaluation of the detector; also to R. E. Wilke for his fine work on the fabrication of the detector.

RECEIVED for review February 4, 1974. Accepted June 3, 1974.

New Approach to Chromatogram Interpretation by Multiple Detection

Nedjeljko Ostojić[1]

Institute Rudjer Bošković, Zagreb, Yugoslavia

The principles of a new method for resolving overlapped peaks in gas and liquid chromatography are given. The method is based on multiple detection but differs from the present use of multiple detection because no highly selective detector system is required. All the necessary information for resolving an overlap involving unknown substances is derived from signal ratios determined continuously as a function of time. Factors influencing accuracy and precision are discussed.

At present, multiple detection in chromatography is used effectively only with detector systems of high selectivity. In the case of an incomplete separation, the proper choice of a detector makes possible the determination of those components for which the sensitivity of that detector is high. The signals of the interfering components are simply neglected. For this, selectivities of a few orders of magnitude are required.

A novel approach, introduced here, utilizes multiple detection in a more complete way. Because of the nature of the operations performed on the signals, this approach can also be considered a contribution to a number of existing mathematical methods for peak overlap deconvolution. These methods range in complexity from simple geometrical operations like the perpendicular drop and shoulder cutting (incorporated in the operation of most commercially available digital integrators), to more sophisticated ones based on curve-fitting the unresolved signals by a variety of analytical or numerical functions as models (*1–10*). All of these methods, however, operate on the signal from only one detector.

The basic element of the new method, named the Signal Ratio Method (SRM), is the characteristic signal ratio. It is defined here as a ratio of the signals of two detectors for a pure substance. All the necessary information for determination of the characteristic signal ratios is contained in the signals from as many different detectors as there are components in the unresolved mixture. Continuous division of these signals yields signal ratios in the form of time dependent functions. The characteristic signal ratios are determined by an analysis of these functions.

[1] Present address, Pollution Control Systems, Division of Geo. A. Hormel & Co., 11501 Yellowbrick Road, Coon Rapids, Minn. 55433.

(1) H. A. Hancock, Jr., L. A. Dahm, and J. F. Muldoon, *J. Chromatogr. Sci.*, **8**, 57 (1970).
(2) H. M. Gladney, B. F. Dowden, and J. D. Swalen, *Anal. Chem.*, **41**, 883 (1969).
(3) A. H. Anderson, T. C. Gibb, and A. B. Littlewood, in "Advances in Chromatography 1970," A. Zlatkis, Ed., Chromatography Symposium, Dept. of Chemistry, University of Houston, Texas, 1970.
(4) D. W. Kirmse and A. W. Westerberg, *Anal. Chem.*, **43**, 1035 (1970).
(5) B. Goldberg, *J. Chromatogr. Sci.*, **9**, 287 (1971).
(6) S. M. Roberts, D. H. Wilkinson, and L. R. Walker, *Anal. Chem.*, **42**, 886 (1970).
(7) S. M. Roberts, *Anal. Chem.*, **44**, 502 (1972).
(8) A. W. Westerberg, *Anal. Chem.*, **41**, 1770 (1969).
(9) Ch. Bosshard, O. Piringer, and T. Gaumann, *Helv. Chim. Acta*, **54**, 1059 (1971).
(10) Y. Mori, *J. Chromatogr.*, **9**, 66 (1972).

The SRM is based on the functional relationship between the characteristic signal ratios and signal ratios of the mixture as experimentally determined quantities, and the signals of the individual components as sought quantities.

The following presentation is an introductory exposition of a new method.

PRINCIPLES OF THE SIGNAL RATIO METHOD

The Signal Ratio Method (SRM) is used to separate the signals of the components of an unresolved mixture. The experimental quantities needed are the characteristic signal ratios of the individual components and the signal ratios of the mixture.

The characteristic signal ratio is here defined as a ratio of the signals of two different detectors for any pure substance. The detectors do not have to be different in the sense that they operate on different principles. The difference may sometimes be achieved by a change in the operating conditions of two identical detectors.

In accordance with the definition, the characteristic signal ratio can be considered a function of the following parameters: physical and chemical properties of the analyzed substance; operating conditions of each detector; and relative amounts/concentrations of the substance fed into each detector.

Whereas all of these parameters influence the numerical value of the characteristic signal ratio, only the first two are of practical importance in the SRM, since only they can influence the selectivity of the detector system. The characteristic signal ratio will be given the following symbol:

$$R_{i,j}^{K} = Y_i^{K}/Y_j^{K} \qquad (1)$$

where R represents signal ratio, Y the signal, while the indices i, j, K indicate detector "i," detector "j," and substance "K," respectively. Here an apology for using superscripts is in place. However, the confusion between powers and superscripts is avoided since no power is used throughout the text.

It should also be noted that, in this text, the word "component" never refers to the solvent. Thus, a binary or two-component mixture is a mixture of two substances, both dissolved in a carrier.

Experimentally, the characteristic signal ratios are determined using a set of simultaneously operated detectors, each of which is receiving a portion of the analyzed substance. For mixtures of known composition, it is possible to determine the characteristic signal ratios using the pure components. If the characteristic signal ratios are determined in this way, not even a partial separation of the components of the mixture is required. In fact, a simple mixture of known composition can be analyzed without any chromatographic columns by feeding the mixture directly into the detectors.

For unknown mixtures, some partial separation must be achieved. Then, the characteristic signal ratios can be determined by analyzing signal ratios of the mixture as func-

tions of time. The steps involved in this procedure are the following: 1) For a total of n detectors used simultaneously in an analysis of an n-component mixture, the signals from $n - 1$ of these detectors are divided with the signal from the nth detector. This division process is carried out throughout the chromatogram and, as a result, $n - 1$ signal ratio curves are obtained as functions of time along with the chromatograms. 2) The signal ratio curves are differentiated. 3) These derivatives are then divided in a way identical to the signal division performed in step 1. 4) The steps involving differentiation and division of the derivatives are repeated in this fashion until sufficient information is furnished for the determination of the unknown characteristic signal ratios. The number of repetitions depends on the number of simultaneously eluting components. 5) Once the characteristic signal ratios are determined, the individual component signals can be obtained by solving a set of linear equations.

For a two-component mixture, only the first step is required; and for a three-component mixture, only the first two steps are required.

The necessary operations are most conveniently carried out on a digitized signal. The basic operation in the SRM, division, is the least suitable operation to be satisfactorily performed by electronic analog computers. Many other necessary operations, such as base-line correction, require or suggest use of a digitized signal.

Theory. A signal ratio of a mixture can be represented as:

$$R_{i,j} = \frac{Y_i^{A} + Y_i^{B} + \ldots + Y_i^{N}}{Y_j^{A} + Y_j^{B} + \ldots + Y_j^{N}} \quad (2)$$

where Y_i^{K} is the signal of the component "K" on the detector "i" measured at any moment in the interval in which the elution of the unresolved mixture takes place. By substituting the characteristic signal ratios, defined by Equation 1, into Equation 2, the expression for the signal ratio of the mixture can be modified into:

$$R_{i,j} = \frac{R_{i,j}^{A}Y_j^{A} + R_{i,j}^{B}Y_j^{B} + \ldots + R_{i,j}^{N}Y_j^{N}}{Y_j^{A} + Y_j^{B} + \ldots + Y_j^{N}} \quad (3)$$

and further into:

$$R_{i,j} = \frac{R_{i,j}^{A} + R_{i,j}^{B}X^{B} + \ldots + R_{i,j}^{N}X^{N}}{1 + X^{B} + \ldots + X^{N}} \quad (4)$$

where

$$X^{K} = Y_j^{K}/Y_j^{A} \quad (5)$$

Expression 4 can be transformed into:

$$X^{B}(R_{i,j}^{B} - R_{i,j}) + X^{C}(R_{i,j}^{C} - R_{i,j}) + \ldots + X^{N}(R_{i,j}^{N} - R_{i,j}) = R_{i,j} - R_{i,j}^{A} \quad (6)$$

Using n detectors for processing a mixture of n components, one can set-up a system of $n - 1$ equations like Equation 6. with $n - 1$ unknowns: $X^{B}, X^{C}, \ldots, X^{N}$:

$$X^{B}(R_{1,n}^{B} - R_{1,n}) + X^{C}(R_{1,n}^{C} - R_{1,n}) + \ldots + X^{N}(R_{1,n}^{N} - R_{1,n}) = R_{1,n} - R_{1,n}^{A}$$

$$X^{B}(R_{2,n}^{B} - R_{2,n}) + X^{C}(R_{2,n}^{C} - R_{2,n}) + \ldots + X^{N}(R_{2,n}^{N} - R_{2,n}) = R_{2,n} - R_{2,n}^{A}$$

$$\vdots$$

$$X^{B}(R_{n-1,n}^{B} - R_{n-1,n}) + X^{C}(R_{n-1,n}^{C} - R_{n-1,n}) + \ldots + X^{N}(R_{n-1,n}^{N} - R_{n-1,n}) = R_{n-1,n} - R_{n-1,n}^{A} \quad (7)$$

Solving for X's, one obtains the signal of component A from:

$$Y_n^{A} = \frac{Y_n}{1 + X^{B} + X^{C} + \ldots + X^{N}} \quad (8)$$

where Y_n is the signal of the mixture from detector "n." Signals of the other components can be found from the definition of the ratio X^{K}, Equation 5.

For a two-peak overlap, the above procedure reduces to solving the following simple equation:

$$Y_1^{A} = Y_1 \frac{R_{2,1} - R_{2,1}^{B}}{R_{2,1}^{A} - R_{2,1}^{B}} \text{ or}$$

$$Y_1^{B} = Y_1 \frac{R_{2,1}^{A} - R_{2,1}}{R_{2,1}^{A} - R_{2,1}^{B}} \quad (9)$$

Signal Y was defined for any particular time in the interval in which the elution of the unresolved mixture takes place. Thus, repeated application of the SRM at successive time points would yield a complete reconstruction of the individual peak shapes. If signal Y was defined as an integral of the signal in the elution interval, which is also possible, the application of the SRM would directly yield the individual peak areas.

Basic Requirements for the Signal Ratio Method. The application of the Signal Ratio Method requires a fulfillment of the following conditions: 1) The number of the detectors is greater than or equal to the number of the unresolved components. 2) All the detectors are used within the range of their linearity. 3) The system of Equations 7 has a nonzero determinant.

The last condition imposes certain restrictions on the values of the characteristic signal ratios. In a system of only two components and two detectors, the two characteristic signal ratios must, of course, differ from each other. When more than two components are present in the mixture, it is not necessary that their characteristic signal ratios be different from each other. For the value of the determinant not to be zero, it is necessary that the following requirements are satisfied: 1) For every detector pair at least one characteristic signal ratio should be different from the others. 2) The number of the corresponding characteristic signal ratios of any two detector pairs, which can be mutually proportional, must be at least one less than the number of the simultaneously eluting components. 3) For every component at least one of the characteristic signal ratios should be different from the others. 4) The following requirement is imposed on the differences between the characteristic signal ratio of one component and the characteristic signal ratios of any other two components on the same detector pair: The ratio of these differences should not be equal for any of the detector pairs. The "forbidden" case is, in other words:

$$\frac{R_{1,n}^{i} - R_{1,n}^{K}}{R_{1,n}^{j} - R_{1,n}^{K}} = \frac{R_{2,n}^{i} - R_{2,n}^{K}}{R_{2,n}^{j} - R_{2,n}^{K}} = \frac{R_{n-1,n}^{i} - R_{n-1,n}^{K}}{R_{n-1,n}^{j} - R_{n-1,n}^{K}} \quad (10)$$

Determination of the Peak Centroids. A chromatographic peak can be thought of as an infinitely thin body of uniform density resting on a time axis. The mass of such a body would be proportional to the peak area. Because of its

uniform density, the center of mass of the body is identical to the centroid of the peak.

In the case of simultaneous multiple detection, a peak has a different amplitude on each chromatogram. However, since the change in amplitude does not affect the peak shape, the peak centroid has a common abscissa on all the chromatograms.

The same holds for a group of overlapped peaks where the abscissa of the centroid of each individual peak does not change because of the change in the peak amplitude. However, the abscissa of the centroid of the group of the overlapped peaks as a whole does depend on the amplitudes of the individual peaks. Therefore, in simultaneous multiple detection, the abscissae of the centroids of a group of overlapped peaks will be different on each chromatogram.

If the whole group of overlapped peaks was thought of as a body of uniform density, the abscissa of the center of mass of this body would be related to the abscissae of the centers of masses of the individual peaks in the following way:

$$C_i \int_{t_1}^{t_2} Y_i \mathrm{d}t = C_i^{\mathrm{A}} \int_{t_1}^{t_2} Y_i^{\mathrm{A}} \mathrm{d}t + C_i^{\mathrm{B}} \int_{t_1}^{t_2} Y_i^{\mathrm{B}} \mathrm{d}t + \ldots + C_i^{\mathrm{N}} \int_{t_1}^{t_2} Y_i^{\mathrm{N}} \qquad (11)$$

Here: C_i = abscissa of the centroid or the "center of mass" of a group of overlapped peaks detected by detector "i," C_i^{X} = abscissa of the centroid or the "center of mass" of peak "X" detected by detector "i," Y_i = observed signal from detector "i" (signal of the mixture), Y_i^{X} = signal of component "X" detected by detector "i," and t_1, t_2 = limits of the interval of elution of the group of overlapped peaks. This equation contains the individual peak areas,

$$\int_{t_1}^{t_2} Y_i^{\mathrm{X}} \mathrm{d}t$$

as known quantities. They must be determined before by SRM or in some other way. The number of the detectors used must equal the number of the components and, consequently, the number of their centroids. For each of the detectors, there is one equation like Equation 11. Abscissae of the centroids of the individual peaks are obtained as a solution of a system of these equations.

DETERMINATION OF CHARACTERISTIC SIGNAL RATIOS

When the constituents of the mixture are known, the characteristic signal ratios can be determined for each of them separately. They could be calculated on the basis of relative molar response data contained in literature, or even calculated for certain detectors from the theoretical expressions for sensitivity. It would only be necessary to experimentally determine the splitting ratio which, once determined, stays the same for all the substances. This way is recommended only for a rough approximation because, as will be shown later, the accuracy of the SRM depends strongly on the accuracy of the characteristic signal ratios.

The determination of the characteristic signal ratios for a mixture of unknown constituents requires their partial separation. It is necessary that there exist zones containing one, two, three, etc. components. A zone corresponding to a group of overlapped peaks contains predominantly one component on its edges. Going towards the middle of the chromatogram, one first encounters a mixture of two components, then three, etc.

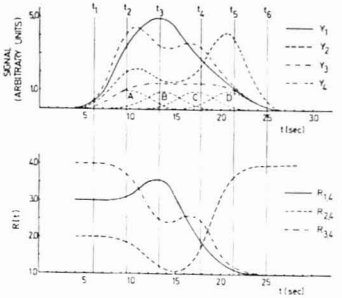


Figure 1. Signals of a four-component mixture from four detectors and the ratios of these signals

The procedure for the determination of the characteristic signal ratios can be best illustrated by an example. Consider a model chromatogram consisting of four overlapping gaussian peaks, shown on the upper part of Figure 1. The standard deviation of each of the four peaks is two seconds. The distance between any two of the neighboring peak maxima is 3.6 seconds or 1.8 units standard deviation. Since there are four simultaneously present components, four detectors are needed for the analysis. The relative amplitudes of the peaks are:

Component	Detector 1	2	3	4
A	3	2	4	1
B	4	1	2	1
C	2	1	3	1
D	1	4	1	1

Since there are four components in the overlap and each of them produces a signal on four detectors, there will be four chromatograms, each containing four overlapped peaks, thus yielding a set of 16 peak amplitudes. Now, if one of the detectors (in our case, detector 4) is chosen to be a reference detector, these sixteen peak amplitudes can be expressed as twelve characteristic signal ratios:

Component	$R_{1,4}^{\mathrm{X}}$	$R_{2,4}^{\mathrm{X}}$	$R_{3,4}^{\mathrm{X}}$
A	3	2	4
B	4	1	2
C	2	1	3
D	1	4	1

where X = A, B, C, or D. From now on these values will be treated as unknowns. They will be determined starting with chromatogram traces Y_1, Y_2, Y_3, and Y_4 from Figure 1 as the only information.

A comment concerning the intervals or zones on the chromatograms, containing only one, two, three, etc. components might be in place. The limits of these intervals are indicated on Figures 1, 3, and 4 as t_1, t_2, t_3, t_4, t_5, and t_6 for the purpose of facilitating the presentation. Although a reference to these limits as to known quantities will be made frequently, they are by no means known at the beginning of an actual analysis. The process of determining these intervals is an integral part of the analysis of the chromatograms, which will be illustrated in the following presentation.

Figure 1 shows time intervals or zones containing an increasing number of components as one approaches the middle of the chromatogram from each side. Further discussion will concentrate on the properties of each of these

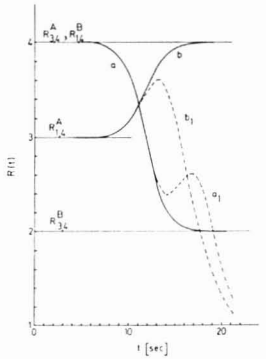


Figure 2. Signal ratio curves for a two-component mixture, (solid lines *a* and *b*) changed by the presence of additional components (broken lines a_1 and b_1)

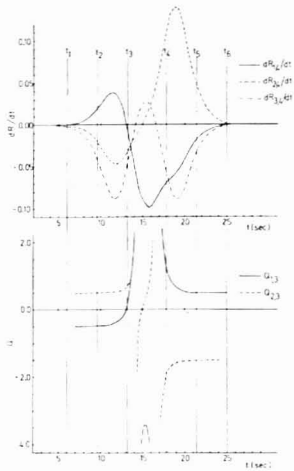


Figure 3. Derivatives of signal ratios and ratios of these derivatives, which are used in analysis of a four-component mixture

zones which make it possible to determine the characteristic signal ratios of all the components. Since each of the four components has one characteristic signal ratio for every detector pair, it will be necessary to determine a total of 12 characteristic signal ratios.

1) The time intervals $t < t_1$ and $t > t_6$ each contain only one component: A and D, respectively. The values of the signal ratios in these intervals should therefore be constant, equal to the characteristic signal ratios of components A and D. The six characteristic signal ratios: $R^{A}_{1,4} = 3$, $R^{A}_{2,4} = 2$, $R^{A}_{3,4} = 4$, $R^{D}_{1,4} = 1$, $R^{D}_{2,4} = 4$, $R^{D}_{3,4} = 1$, can easily be read directly from the constant portions of the corresponding $R(t)$ curves in the considered intervals. The limits of these intervals, t_1 and t_6, are thus chosen as the ends of the constant portions of the $R(t)$ curves.

2) Two components are contained in each of the next coming zones: a mixture of A and B in the interval $t_1 < t < t_2$ and a mixture of C and D in the interval $t_5 < t < t_6$. As the composition of these mixtures changes with time, signal ratios are no longer constant. Going toward the middle of the chromatogram, their values are changing from the constant values of the characteristic signal ratios of components A and D towards the characteristic signal ratios of components B and C. Indeed, if there was a partially resolved mixture of A and B only, the value of $R(t)$ would change from the constant value of R^{A} to the constant value of R^{B} as the composition of the mixture changed from "pure" A to "pure" B. This course of $R(t)$ is shown in Figure 2 for detector pairs 1,4 and 3,4 along with the "real" $R(t)$ curves obtained from our four component chromatograms. In Figure 1, it is easily seen that although the presence of components C and D changes the course of the $R(t)$ curve for a mixture of A and B, there is an initial interval in which the trend of change of $R(t)$ toward R^{B} is unobstructed. Analysis of this trend can yield information leading to the determination of R^{B}'s and R^{C}'s.

This trend is quantitatively characterized by the rate of change of $R(t)$. At a given time t, this rate is a function of the rate of increase of the fraction of component B in the mixture as well as of the difference between R^{A} and R^{B}. This directly follows from the expression for the fraction of the signal of component B in the mixture of A and B (*cf.*, Equation 9):

$$p_i^{B}(t) = \frac{Y_i^{B}(t)}{Y_i(t)} = \frac{R_{j,i}^{A} - R_{j,i}(t)}{R_{j,i}^{A} - R_{j,i}^{B}} \qquad (12)$$

where p_i^{B} represents a fraction of the signal of component B in the signal of the mixture of A and B. From here:

$$R_{j,i}(t) = p_i^{B}(t)(R_{j,i}^{B} - R_{j,i}^{A}) + R_{j,i}^{A}$$

and

$$\frac{dR_{j,i}^{(t)}}{dt} = \frac{dp_i^{B}}{dt}(R_{j,i}^{B} - R_{j,i}^{A}) \qquad (13)$$

On two different detector pairs, both including detector "i," the change of $R(t)$ will occur at a different rate. Since the factor dp_i^{B}/dt in Expression 13 is the same for each detector pair, different rates have their origin in the differences between the characteristic signal ratios. As long as there are only two components in the mixture, the ratio of the derivatives provides a useful relationship involving the unknown characteristic signal ratios. For the detector pairs 1,4 and 3,4 from our example, this relationship is:

$$\frac{dR_{1,4}(t)/dt}{dR_{3,4}(t)/dt} = \frac{R_{1,4}^{B} - R_{1,4}^{A}}{R_{3,4}^{B} - R_{3,4}^{A}} = Q_{1,3}^{AB} \qquad (14)$$

Since the characteristic signal ratios are constants, $Q_{1,3}^{AB}$ is also a constant. It is possible to read this constant directly from the constant portion of the graph of $Q(t)$, Figure 3.

In our case, the three existing detector pairs, 1–4, 2–4, and 3–4 provide two $Q(t)$ curves, each of which contains two such constant portions, one on each side of the chromatogram. This yields four expressions like Equation 14 involving all of the six still unknown characteristic signal ratios. Thus, two additional expressions are needed to bring their total number to six. In the course of an actual analysis, the interval limits t_2 and t_5 are chosen as the ends of the continuous portions of $Q(t)$ curves.

3) Adjacent to the just described zones containing two components, there are two zones containing three components each. On one side of the chromatogram, the three-component mixture involves components A, B, and C, while the mixture on the other side consists of B, C, and D. The analysis of these intervals is based on the approach just used under section 2).

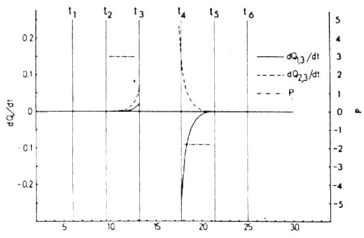


Figure 4. Curves $dQ(t)$ and $P(t)$, which are used in determination of the characteristic signal ratios for a four-component mixture

As long as the mixture contains two components, the function $Q(t)$ has constant values. The presence of a new component causes a deviation from this constant value. If we were dealing with a mixture containing three partially separated components—*e.g.*, A, B, C—the function $Q(t)$ would have constant values in two intervals: Q^{AB} in the interval containing components A and B, and Q^{BC} in the interval containing components B and C. In between, the values of the function would be variable. The rate of change of $Q(t)$ from Q^{AB} to Q^{BC} is a function of the rate of change of the composition and of the difference $Q^{BC} - Q^{AB}$:

$$\frac{dQ(t)}{dt} = f(p^A, p^B, p^C)\ (Q^{BC} - Q^{AB}) \qquad (15)$$

The rate of change of the composition during the detection is equal in all the detectors, and the ratio $(dQ_i(t)/dt)/(dQ_j(t)/dt)$ is a constant since the division eliminates $f(p^A, p^B, p^C)$. This ratio remains constant as long as there are three components in the mixture of changing composition. Each of the two zones we were just analyzing contains three components and, therefore, the function

$$P_{1,2}(t) = \frac{dQ_{1,3}(t)/dt}{dQ_{2,3}(t)/dt} \qquad (16)$$

has constant values in two intervals: $P_{1,2}{}^{ABC}$ in the interval $t_2 < t < t_3$ and $P_{1,2}{}^{BCD}$ in the interval $t_4 < t < t_5$. These intervals correspond to the zones containing components A, B, C and B, C, D, respectively. The constants

$$P_{1,2}{}^{ABC} = \frac{Q_{1,3}{}^{BC} - Q_{1,3}{}^{AB}}{Q_{2,3}{}^{BC} - Q_{2,3}{}^{AB}} \qquad (17)$$

and

$$P_{1,2}{}^{BCD} = \frac{Q_{1,3}{}^{CD} - Q_{1,3}{}^{BC}}{Q_{2,3}{}^{CD} - Q_{2,3}{}^{BC}} \qquad (18)$$

provide the last two expressions necessary for the determination of all the unknown characteristic signal ratios. The numerical values of the constants $P_{1,2}{}^{ABC}$ and $P_{1,2}{}^{BCD}$ can be directly read from the constant portions of the corresponding curves shown in Figure 4. As before, the still unknown "inner" limits of the intervals containing only three components, are determined as the ends of the constant portions of the $P(t)$ curves.

Let's now summarize all the steps performed to arrive at the values of the unknown characteristic signal ratios. First, six out of a total of twelve were read directly from the constant portions of the signal ratio curves. This left six unknown characteristic signal ratios.

The signal ratio curves were then differentiated. Two of the derivatives were divided by the third one to yield $Q(t)$ curves. Constant portions of these curves contained information necessary to formulate a set of four equations involving all of the remaining six unknown characteristic signal ratios. Then, the $Q(t)$ curves were differentiated and one of the derivatives was divided by the other one to arrive at the $P(t)$ curves. This allowed the formulation of two equations involving the six unknown characteristic signal ratios. A total of six equations obtained in this way was sufficient to determine the unknown characteristic signal ratios. In the simple case of an overlap of only two peaks, only two characteristic signal ratios have to be determined. These can be read directly from the constant portions of the signal ratio curve.

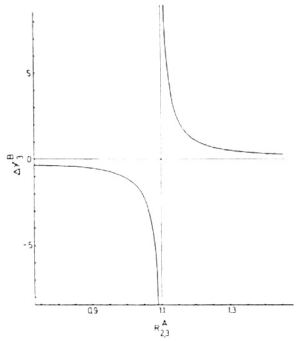


Figure 5. Relative error in the signal of one of the three components of the mixture analyzed by the SRM, as a function of the selectivity of the detector system

For a three-peak overlap, there is a total of six characteristic signal ratios to be determined. Four of these can again be read directly from the constant portions of the signal ratio curves. To arrive at the remaining two, a differentiation of the signal ratio curves followed by a division is necessary.

With four-peak overlaps, the number of the characteristic signal ratios jumps up to twelve and the procedure, as shown in the above example, becomes more complicated.

PRECISION AND ACCURACY

The precision of the Signal Ratio Method is a function of the characteristic signal ratios. It has been pointed out earlier that the array of the characteristic signal ratios used in the SRM must satisfy certain requirements. Arrays which do not meet these requirements cause an infinitely large error when applied in the SRM. The further the configuration of a particular array is from such a "forbidden" configuration, the smaller the error of the SRM.

This is illustrated in Figure 5. for a model mixture composed of equal amounts of three components, where the array of the characteristic signal ratios was arbitrarily chosen to be:

	Detector Pairs	
Component	1,3	2,3
A	1.2	Variable
B	1.9	1.5
C	1.0	1.0

This figure represents the error of determination of the signal of component B, which is caused by a constant error of 0.33% in $R_{2,3}{}^{B}$, as a function of $R_{2,3}{}^{A}$. It is noticed that the error rapidly increases as the configuration approaches the "forbidden" case:

Component	Detector pairs 1,3	2,3
A	1.2	1.1$\dot{1}$
B	1.9	1.5
C	1.0	1.0

in which the ratio of the differences of two characteristic signal ratios (1.2 and 1.9) from the third one (1.0) on one detector pair, is equal to the same ratio on the other detector pair, or:

$$\frac{1.2 - 1.0}{1.9 - 1.0} = \frac{1.1\dot{1} - 1.0}{1.5 - 1.0} = 0.2\dot{2}$$

The precision of the SRM depends on how much the values of an array of the characteristic signal ratios differ from such "forbidden" configurations. This difference could be thought of as selectivity of a group of detectors. However, only in the special case of one detector pair would such a concept of selectivity have a simple mathematical formulation. In that case, the only requirement is that the two characteristic signal ratios be different from each other:

$$s_{2,1}{}^{AB} = \frac{R_{2,1}{}^{A} - R_{2,1}{}^{B}}{R_{2,1}{}^{B}} \qquad (19)$$

Here, $s_{1,2}{}^{AB}$ represents selectivity of detectors 1 and 2 for the substances A and B.

This definition provides for the fact that any amplification of the signal from one of the detectors, which does not increase the signal-to-noise ratio, has no effect on selectivity. Such an amplification would not change the number of significant figures in the signal and, therefore, would not change the number of significant figures in the signal ratio.

It should be said that the procedure used for the determination of the characteristic signal ratios in a mixture of more than two components causes a loss of precision along the way. The procedure involves a repetition of two operations: division followed by differentiation. Relative error in the intermediate results shows the biggest increase in the differentiation step.

The error in differentiation is a function of certain operating parameters such as the frequency of the signal sampling in the process of analog-to-digital conversion. The errors associated with the division of the signals and with the decision-making in resolving a two-peak overlap are dealt with in more detail in Reference (*11*).

Accuracy. Systematic errors in signal ratio determination can be caused by incomplete fulfillment of the two basic requirements of the method: work in the linearity range of the detectors and additivity of the component signals.

As to the first of these two requirements, it should be pointed out that the linear range of the detector system is, at most, as large as the smallest of the linearities of the detectors used. In general, it is even smaller, since only the range of linearity common to all the detectors represents the linearity of the system.

For the majority of gas chromatographic detectors, the additivity of the component signals exists for most practical applications. Some detectors might show deviation for higher concentrations because of an increased probability of mutual interaction of individual particles involved in the detection process. However, deviation from linearity also occurs for the same reason, so that signal additivity problems could be expected near the upper limit of the linearity range where caution is neccessary anyway.

Determination of the characteristic signal ratios in the course of the analysis of an unknown mixture imposes two further requirements, deviation from which would also cause a systematic error of the characteristic signal ratios. The requirements are as follows:

1) In any of the streams going from the splitter to and through the detectors, the deformation of the concentration profile should be the same. Because of processes like lateral diffusion, stream mixing, eddying etc., every moving zone of varying concentration will show certain deformation of its concentration profile. If these processes are not adequately balanced in any two streams, they will lead to an excess deformation in one of the streams as compared to the other. Such a relative deformation would, for instance, manifest itself in a deviation of the $R(t)$ value from a constant for a pure substance.

2) The deformation in transducing a concentration profile into a signal should be equal for all the detectors. This is similar to saying that the dynamic properties of the detectors should be the same. Unsatisfactory fulfillment of this requirement causes similar errors in the determination of the characteristic signal ratios as mentioned under requirement 1. Balancing two detectors with different dynamic properties can be done electronically and pneumatically. It involves introduction of an additional deformation generator, such as a dead volume, into a stream with a relatively less deformed concentration profile. An RC circuit can also be used as a generator of signal deformation.

In addition, the errors inherent in the chromatographic process itself and in the associated signal processing will certainly have their specific effects on the precision and accuracy of this method. Probably the most important of these is the error in base-line determination. Its effect would be the most noticeable in the division of the signals in the zones of a peak distant from the peak maximum.

CONCLUSION

The Signal Ratio Method expands the use of multiple detection in chromatography through a more complete utilization of those detectors whose selectivities are not very high. An analysis of the precision of the SRM applied to a binary mixture shows that an increase in precision, caused by increased selectivity, is significantly smaller for selectivities higher than one (*11*).

To fully utilize the SRM, it will be necessary to pay special attention to the precision in signal processing. This refers to standard operations like base-line correction and peak characterization, as well as to specific requirements of the SRM. The most important among these seems to be the achievement of identical dynamic properties of all the detectors used.

The benefits that the Signal Ratio Method offers to chromatographic data interpretation are multiple:

1) Detection of an overlap when it is not apparent.

2) Resolution of such overlaps using fairly simple algorithms.

3) Characteristic signal ratios determined in the course of an SRM analysis are primarily a function of the physical and chemical properties of the analyzed substances. Thus, they represent a potential aid in identification.

4) While not always necessarily usable as a convenient aid in qualitative analysis, the characteristic signal ratios can provide sufficient characterization of the individual components to facilitate the determination of Kovats' indices on different stationary phases. This valuable tool for identification can thus be obtained in a convenient way which lends itself to automatization (*12*).

5) Because the information contained in signal ratios is

(11) N. Ostojić, work submitted for publication.

(12) N. Ostojić, unpublished work.

complementary to the information contained in the peak shape, a combination of the SRM with the numerical methods utilizing peak models could be expected to widen the range of the applicability of both methods.

6) It is possible for signal processing in the case of a two-peak overlap to be done automatically (*11*). Intervals of the constant signal ratios can be determined by monitoring the slope and the noise level of the signal ratio curve. The values of the characteristic signal ratios can then be obtained by averaging the signal ratio values contained in the appropriate intervals. Once the characteristic signal ratios are determined, the deconvolution of the peak overlap can be easily achieved by means of Equation 9. For more than two components, the process is more involved and less suitable for an automatic execution.

A large number of chromatographic detectors qualify for use in the SRM, provided the differences in their dynamic properties can be satisfactorily balanced. An assembly of dynamically identical detectors offers obvious advantages. Such a system could be created, *e.g.*, from a few photoionization detectors with the source of ionizing radiation separated from the ionization chamber (*13*). The selectivity of this detector system can be achieved by filtration of the ionizing radiation.

ACKNOWLEDGMENT

I wish to thank Zdenko Šternberg of the Institute Rudjer Bošković, Zagreb, Djurdja Deur-Šiftar of the Organsko-Kemijska Industrija, Zagreb, and Juraj Božičević of the Department of Chemical Technology at the University of Zagreb, for their valuable assistance in this work.

RECEIVED for review February 4, 1974. Accepted May 31, 1974.

(13) N. Ostojić and Z. Šternerg, *Chromatographia*, **7**, 3 (1974).

Gas-Complex Chromatography: Substituent and Steric Effects

R. J. Laub, Vaidhyanathan Ramamurthy, and R. L. Pecsok

Department of Chemistry, University of Hawaii, Honolulu, Hawaii 96822

Specific retention volumes (V_g), and relative formation constants (K') are found for aromatic hydrocarbons, amines, and a series of β-ionyl compounds which are twisted diene systems. Di-*n*-butyl tetrachlorophthalate (DBTP) is used as the complexing (electron acceptor) stationary phase. Di-*n*-butyl phthalate (DNBP) and di-isooctyl phthalate (DIOP) were the reference phases. The order of relative formation constants for aromatic hydrocarbons and amines is demonstrated to be as expected. The β-ionyl compounds, however, give anomalous K' values, due to severe out-of-plane deformation effects.

Charge transfer interactions (*1*) have been shown by numerous authors (*2–7*) to enhance GLC separations. However, fundamental solution phenomena may also be investigated with such reagents (*8–20*). Purnell has demonstrated that, in fact, charge transfer phenomena *should* be examined by GLC, rather than UV or NMR spectroscopic techniques (*16*). A measure of the strength of interaction between charge transfer donor and acceptor species is the formation constant, K_f (*1, 21*). For:

$$D + A \rightleftharpoons C$$

$$K_f = \frac{[C]}{[D][A]} \quad (1)$$

where C, A, and D are complex, acceptor, and donor species, respectively. Bracketed terms indicate molar concentrations. Several authors (*8–11*) have shown that K_f may be obtained from GLC data *via* the well-known equation:

$$K_L = K_L^\circ + K_L^\circ K_f[A] \quad (2)$$

where K_L° is the distribution coefficient for a complex-forming solute on an "inert" (noncomplexing) stationary phase, and K_L is for the same solute on the phase which contains a small (0–0.2*M*) concentration of acceptor, [A]. By plotting K_L *vs.* [A], Equation 2 allows calculation of K_f from the slope and intercept of the line. Formation constants for most species investigated thus far are generally small, on the order of 0.1 to 0.5 l./mole. It is therefore essential to chromatograph solutes on several columns of varying acceptor concentration, rather than calculate K_f from a single determination. Formation constants determined from Equation 2 have been measured by the authors to a lower limit of 0.010 l./mole (*22*). This can undoubtedly

(1) R. S. Mulliken and W. B. Person, "Molecular Complexes," Wiley-Interscience, New York, N.Y., 1969.
(2) R. O. C. Norman, *Proc. Chem. Soc., London*, 151 (1958).
(3) S. H. Langer, C. Zahn, and G. Pantazopios, *J. Chromatogr.*, **3**, 154 (1960).
(4) E. Gil-Av, J. Herling, and J. Shabtai, *J. Chromatogr.*, **1**, 508 (1958).
(5) E. Gil-Av and V. Schurig, *Anal. Chem.*, **43**, 2030 (1971).
(6) D. V. Banthorpe, C. Gatford, and B. R. Hollebone, *J. Gas Chromatogr. (J. Chromatogr. Sci.)*, **6**, 61 (1968).
(7) B. H. Gump, *J. Chromatogr. Sci.*, **7**, 755 (1969).
(8) E. Gil-Av and J. Herling, *J. Phys. Chem.*, **66**, 1208 (1962).
(9) M. A. Muhs and F. T. Weiss, *J. Amer. Chem. Soc.*, **84**, 4697 (1962).
(10) N. Kotsev and D. Shopov, *Dokl. Bolg. Akad. Nauk*, **21**, 889 (1968).
(11) H. Schnecko, *Anal. Chem.*, **40**, 1391 (1968).
(12) C. Eon, C. Pommier, and G. Guiochon, *J. Phys. Chem.*, **75**, 2632 (1971).
(13) J. H. Purnell, in "Gas Chromatography—1966," A. B. Littlewood, Ed., Adlard, London, 1966, pp 3–20.
(14) D. F. Codogen and J. H. Purnell, *J. Phys. Chem.*, **73**, 3849 (1969).
(15) D. L. Meen, F. Morris, and J. H. Purnell, *J. Chromatogr. Sci.*, **9**, 291 (1971).
(16) J. H. Purnell and O. P. Srivastava, *Anal. Chem.*, **45**, 1111 (1973).
(17) D. E. Martire and P. Riedl, *J. Phys. Chem.*, **72**, 3478 (1968).
(18) J. P. Sheridan, D. E. Martire, and Y. B. Tewari, *J. Amer. Chem. Soc.*, **94**, 3294 (1972).
(19) J. P. Sheridan, M. A. Capeless, and D. E. Martire, *J. Amer. Chem. Soc.*, **94**, 3298 (1972).
(20) J. P. Sheridan, D. E. Martire, and F. P. Banda, *J. Amer. Chem. Soc.*, **95**, 4788 (1973).
(21) J. Rose, "Molecular Complexes," Pergamon Press, New York, N.Y., 1967.
(22) R. J. Laub and R. L. Pecsok, *Anal. Chem.*, **46**, 1214 (1974).

be improved with the advent of automated and computerized techniques (*23, 24*).

A major disadvantage of this method of K_f determination is that complexing agent solubility is generally low in noncomplexing stationary phases. Only in isolated cases (such as 2,3-dichloro-5,6-dicyanobenzoquinone in di-*n*-butyl phthalate) has this been overcome. It can be argued, however, that for those cases where solubility is not a problem, the *solvated* complexing agent will yield solvent-dependent formation constants. The variation in K_f for different "inert" solvents is not severe, however, especially when contrasted to spectroscopic data (*16*). And, in instances where the solute activity coefficients (or vapor pressures) are known, "relative absolute thermodynamic" formation constants can be calculated. These are said to be solvent-independent (*25*).

An alternative to Equation 2 is the use of pure complexing agent as stationary phase (*3, 17*). Since the concentration of complexor *in itself* is large (3–5*M*), solute–solvent interactions are pronounced. Higher column temperatures can thus be employed. There are several restrictions to this method, however, the most severe being the choice of inert phase. Martire and Riedl (*17*) have shown that the molar volume and London interactions of reference and complexing liquids must be approximately the same. When this is the case, equilibrium formation constants (K_{eq}) can be calculated:

$$K' = \frac{V_g^{A} V_g^{C}}{V_g^{B} V_g^{D}} - 1 \qquad (3)$$

$$K_{eq} = K'/a_A = K'/\gamma_A \bar{A} \qquad (4)$$

where V_g^A and V_g^D are the specific retention volumes for noncomplexing and complexing solutes, respectively, on the reference phase. V_g^B and V_g^C are for the same solutes on the complexing phase. K' is the relative formation constant, and is related to the equilibrium thermodynamic constant, K_{eq}, *via* Equation 4. a_A, γ_A, and $\bar{A}$ represent the activity, activity coefficient, and concentration of pure complexing agent, respectively. γ_A can be estimated by chromatographing several noncomplexing solutes on both complexing and noncomplexing phases (*17*). Thus, K_{eq} can be calculated from data for two columns, and a knowledge of liquid phase molecular weights and densities.

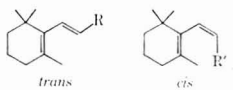
Recently, we reported the determination of vertical ionization potentials (I_v^d) by GLC (*22*). Charge transfer formation constants were determined for several butadienes which have known (photoelectron spectroscopy) I_v^d values. K_f was then plotted against I_v^d to define an empirical curve. Ionization potentials of other butadienes were then found from respective formation constants, and the K_f *vs.* I_v^d plot. Steric hindrance to charge transfer interactions was readily apparent. Substitution of bulky alkyl groups (such as isopropyl) on the end of the butadiene skeleton resulted in an unexpected increase in apparent ionization potentials. The order of increasing hindrance was: methyl < ethyl < propyl < isopropyl. An anomalous compound was 2,4-dimethyl-1,3-pentadiene in which methyl–methyl repulsion causes rotation about the central single bond (*26*). The diene system is then partially deconjugated, causing an increase in I_v^d (from the approximated value of 8.33 eV to the experimental value of 8.83 eV).

To explore possible out-of-plane deformation effects, a series of β-ionyl compounds (*27*) were synthesized for this research. These are diene systems which are highly hindered sterically. Twisting of the conjugated system around the central single bond thus occurs, which can be measured by NMR-spectroscopic decoupling experiments (*28, 29*). Because of the high boiling points (*ca.* 200 °C) of most of these compounds, it was necessary to use a column temperature of 100 °C. Charge transfer interactions become small at elevated temperatures, however, and so the pure complexing agent, di-butyl tetrachlorophthalate (DBTP) was used as the stationary phase. We chose to examine d-*n*-butyl phthalate (DNBP) and di-isooctyl phthalate (DIOP) as reference phases, which do not fulfill the criteria of "suitable" inert solvents, as discussed above, since they do not have the same molar volumes and polarizabilities of DBTP (indicated by very different distribution coefficients of noncomplexing solutes on each of the phases). Therefore, to ensure that charge transfer forces were indeed being examined (as opposed to other solution effects), several well-characterized aromatic hydrocarbons were also run. Relative formation constants were then calculated from Equation 3.

EXPERIMENTAL

Apparatus. A Hewlett-Packard Model 402 dual flame ionization gas chromatograph with a Varian Model A-25 recorder were employed. Two-foot by 2.8-mm i.d. silanized (HMDS) glass U-columns were used.

Reagents. Supelcoport (80/100 mesh) was the solid support. The stationary phases were obtained from Applied Sciences Laboratories, Chemical Research Services, and Supelco. The preparation of *cis*- and *trans*-β-ionyl compounds have previously been described (*27*). Those used in this study are listed below; each was purified by molecular distillation for the NMR experiments.



trans *cis*

R, R' = 1. -CH$_3$
2. -CH$_2$OCCH$_3$
3. -CH(CH$_3$)OCCH$_3$
4. -CO$_2$CH$_3$

Procedure. The GC column temperature was maintained at 100 ± 0.1 °C. Helium at 40 ml/min was the carrier gas. Other experimental details have been described elsewhere (*22, 28, 29*).

RESULTS AND DISCUSSION

Aromatic Hydrocarbons. If Equation 3 is a reflection of charge transfer interactions, then K' values will increase as the ionization potential of donors decreases. To test this, several aromatic hydrocarbons which have previously been characterized (*22*) were used. Specific retention volumes (V_g) and ratios of V_g to V_{g,C_6} (V_g for cyclohexane, the internal standard) on DNBP were extrapolated to 100 °C and are given in Table I. Langer's data at 100 °C (*3*) were used to calculate V_g and $V_g/V_{g,C_6}$ for the same compounds on DBTP. K' values were then calculated from these data, and are also listed in Table I, along with vertical ionization potentials of the aromatic hydrocarbons (*22*).

Several important facts emerge from Table I. The relative formation constants fall in the predicted order: the lower the ionization potential, the larger the charge trans-

(23) M. Goedert and G. Guiochon, *Anal. Chem.*, **42**, 962 (1970).
(24) M. Goedert and G. Guiochon, *Anal. Chem.*, **45**, 1188 (1973).
(25) C. Eon and B. L. Karger, *J. Chromatogr. Sci.*, **10**, 140 (1972).
(26) W. F. Forbes, R. Shilton, and A. Balasubramanian, *J. Org. Chem.*, **29**, 3527 (1964).
(27) V. Ramamurthy, Y. Butt, C. Yang, P. Yang, and R. S. H. Liu, *J. Org. Chem.*, **38**, 1247 (1973).
(28) B. Honig, B. Hudson, S. D. Sykes, and M. Karplus, *Proc. Nat. Acad. Sci. U.S.*, **68**, 1289 (1971).
(29) V. Ramamurthy, T. T. Bopp, and R. S. H. Liu, *Tetrahedron Lett.*, 3915 (1972).

Table I. Ionization Potentials (*22*), Specific Retention Volumes, and Relative Formation Constants for Aromatic Hydrocarbons with DNBP and DBTP at 100°C

Compd	I_v[d], eV	DNBP V_g, ml/g	DNBP $V_g/V_{g,C_6}$	DBTP (7) V_g, ml/g	DBTP (7) $V_g/V_{g,C_6}$	K'
Cyclohexane (reference)	...	30.49	1.000	33.36	1.000	...
Benzene	9.25	63.36	2.078	69.10	2.072	−0.003
Toluene	8.82	131.7	4.320	158.9	4.764	0.013
o-Xylene	8.57	371.8	12.19	451.1	13.52	0.110
m-Xylene	8.57	274.9	9.020	341.8	10.25	0.136
p-Xylene	8.46	263.5	8.641	354.4	10.63	0.230

Table II. Ionization Potentials (*33, 34*) and Relative Formation Constants for Substituted Aromatic Amines

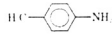
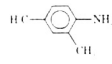
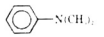
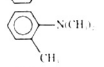
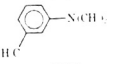
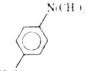
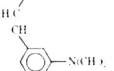
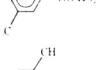
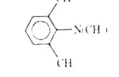
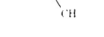
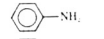
Compd	Stucture	I_v[d], eV	K'_{cis}	K'_{trans}
A. Anilines				
1. Aniline		7.90	33.02	27.18
2. *o*-Toluidine		7.75	35.16	28.93
3. *m*-Toluidine		7.75	37.34	30.73
4. *p*-Toluidine		7.65	40.10	33.00
5. 2,4-Xylidine		...	40.44	33.28
B. *N,N*-Dimethylanilines				
1. *N,N*-Dimethylaniline		...	16.54	13.61
2. *N,N*-Dimethyl-*o*-toluidine		7.37	3.685	3.033
3. *N,N*-Dimethyl-*m*-toluidine		7.35	...	...
4. *N,N*-Dimethyl-*p*-toluidine		7.33	18.86	15.52
5. *N,N*-Dimethyl-3,5-xylidine		7.25	...	...
6. *N,N*-Dimethyl-2,6-xylidine		7.22	2.764	2.275
7. *N,N*-Dimethyl-2,4-xylidine		7.17	3.540	2.913
C. Increased *N*-Substitution				
1. Aniline		7.90	33.02	27.18
2. *N*-Methylaniline		7.60	26.52	21.83
3. *N,N*-Dimethylaniline		...	16.54	13.61

Table III. Approximate Out-of-Plane Deformation Angles and Relative Formation Constants for β-Ionyl Compounds

Compd	Angle, °	Mean, °	K'_{trans}	K'_{cis}
A. *trans*				
R = 1.	26–34	30	1.232	1.283
2.	28–36	32	1.316	1.373
3.	28–36	32	1.247	1.300
4.	26–34	30	1.191	1.242
B. *cis*				
R′ = 1.	30–38	34	1.231	1.284
2.	32–41	37	1.293	1.348
3.	37–50	44	1.267	1.321
4.	33–45	39	1.246	1.299

fer interaction (K'). Langer (*3*), in fact, made use of this phenomenon to separate *m*- and *p*-xylene on di-*n*-propyl tetrachlorophthalate. Compounds with ionization potential greater than 9 eV (illustrated by benzene) give weak charge transfer interactions which are on the order of experimental error. In addition, *o*- and *m*-xylene are not in complete agreement. However, if 0.123 is the correct K' value for both (the mean of the two), the error is only 0.013. Finally, the magnitude of the K' values is probably not of great significance. DNBP has an appreciably different molar volume and likely gives different London interactions than DBTP. Therefore, the relative order and not the magnitude of the K' values is important. These values, which indicate relative charge transfer interactions, increase with decreasing ionization potential, as expected. K' values calculated from Equation 3 thus appear to offer a means of examining charge transfer in other systems.

Substituted Aromatic Amines. To verify that K' is directly related to charge transfer interactions (hence, inversely to I_v^d), we have examined the data of Cooper, Crowne, and Farrell (*30, 31*) who chromatographed several substituted aromatic amines on 2,4,7-trinitrofluorenone (TNF) and silicone oil. We have calculated K' values from their data *via* Equation 3; these are listed in Table II. Since two internal standards (*cis*- and *trans*-decalin) were used, we list both K'_{cis} and K'_{trans} values. Also given in Table II are vertical ionization potentials we have taken from the literature.

K' values for the amines in Table IIA follow the expected trend: lower ionization potentials yield larger relative formation constants. However, the data in Table IIB are erratic. *N,N*-Dimethylaniline (No. 1) and *N,N*-dimethyl-*p*-toluidine (No. 4) fall in the expected order. The former compound has a higher ionization potential and so yields a smaller K' value. However, No. 2, 6, and 7 show no discernible trends, and yield K' values which are appreciably smaller than No. 1 and 4. Substitution in the ortho position is known to cause out-of-plane deformations for *N,N*-dimethylanilines (*32*). Steric hindrance to charge transfer may therefore be responsible for the anomalous behavior of these compounds. Table IIC demonstrates the effect of increasing *N*-substitution at the nitrogen. Apparently, donor–acceptor mutual approachability is hindered by the *N*-methyl group(s). Thus, even though I_v^d decreases, so does K'.

The data in Table II illustrate the very large effects that steric hindrance can cause in charge transfer complexation. When problems of this nature are investigated, therefore, it is crucial to use systems in which steric effects are either negated, or can be determined. For separation purposes, however, these effects can be very advantageous. For example, the relative volatility (α) of *N,N*-dimethyl-2,4-xylidine and *N,N*-dimethyl-2,6-xylidine is 1.13 on silicone oil. However, α = 1.45 on TNF, and the order of elution is reversed.

β-Ionones. The approximate out-of-plane angles for these compounds (which correspond to twisting around the central single bond) are given in Table III. The relative formation constants with *cis*- and *trans*-decalin (K'_{cis} and K'_{trans}) obtained on DBTP (DIOP reference) are also presented.

Angles for the trans compounds are very nearly the same. Hindrance in these systems is due to hydrogen–methyl repulsion in all four cases, and therefore the angles are equal, regardless of R. This is not the case for the cis compounds, however. As the size of R′ increases, the angle becomes larger.

An examination of K' values seems to indicate increased charge transfer for the trans compounds. As the alkyl group changes, the interaction becomes larger in the order: R = 4 < 1 < 3 < 2. Steric effects can be ruled out as the cause, since K' would then be expected to decrease with increasing size of R. However, K' values for the cis compounds increase in approximately the same order as the trans materials. This is not what was expected. As the angle increases, K' values should decrease, when in fact they are erratic. Apparently, charge transfer is not involved (or at least is masked) and other solution effects are responsible for the order in K' values. Work is now in progress on compounds where the out-of-plane deformation angles lie within 0° to about 10–15°, the apparent upper limit of the GLC method.

When out-of-plane twisting or other steric effects are not pronounced, K' values appear to offer a valid measure of charge transfer interactions. Martire and coworkers (*35*) have recently compared K_{eq} values calculated from Equation 4 to K_f values found *via* Equation 2. The agreement was excellent for $\gamma_D = 0.993 \pm 0.002$. Thus, K', K_f, and K_{eq} values found by GLC all offer an internally consistent method of examining charge transfer phenomena. Furthermore, as Purnell has pointed out (*16*), the GLC data certainly appear to be a more valid measure of these interactions than previously-used spectroscopic techniques. It should be noted, however, that much conflicting data have been reported in the literature regarding so-called "charge transfer" interactions. The authors only speculate, therefore, that true charge transfer is operative in the systems reported here, since for example, polarizability and van der Waals interactions may offer an equally plausible explanation for our results. Clearly, much work remains to be done in the elucidation of solution phenomena regarding these effects.

RECEIVED for review April 18, 1974. Accepted June 21, 1974.

(30) A. R. Cooper, C. W. P. Crowne, and P. G. Farrell, *Trans. Faraday Soc.*, **62**, 2725 (1966).
(31) A. R. Cooper, C. W. P. Crowne, and P. G. Farrell, *Trans. Faraday Soc.*, **63**, 447 (1967).
(32) E. G. McRae and L. Goodman, *J. Chem. Phys.*, **29**, 334 (1958).
(33) G. Briegleb and J. Czekalla, *Z. Elektrochem.*, **63**, 6 (1959).
(34) P. G. Farrell and J. Newton, *J. Phys. Chem.*, **69**, 3506 (1965).
(35) H. Liao, D. E. Martire, and J. P. Sheridan, *Anal. Chem.*, **45**, 2087 (1973).

Polycyclic Aromatic Hydrocarbons in the Environment: Isolation and Characterization by Chromatography, Visible, Ultraviolet, and Mass Spectrometry

Walter Giger[1] and Max Blumer[2]

Woods Hole Oceanographic Institution, Woods Hole, Mass. 02543

Polycyclic aromatic hydrocarbons from many sources accumulate in soils, recent and ancient sediments, and in many other environmental samples. They occur at low concentrations and in the presence of other extractable materials. We describe an isolation technique utilizing a sequence of gel filtration, adsorption chromatography, and charge transfer complexation. It leads rapidly to aromatic ring-type concentrates that are sufficiently pure for UV, visible, and mass spectrometry. In combination, these techniques resolve adequately very complex mixtures of aromatic hydrocarbons, for instance from fossil fuels, and provide a detailed insight into the hydrocarbon composition, on a milligram to microgram scale. Analyses of some recent nearshore marine sediments demonstrate an unanticipated complexity of the polycyclic aromatic hydrocarbon fraction. The principal hydrocarbon series extends over a wide molecular weight range; minor series are the naphthenologs and thienologs of the major series. The analytical and biochemical implications are discussed.

Research during the last decade has demonstrated the ubiquity of hydrocarbons in nature. They occur in great structural variety as contributions from many sources, each source differing in the relative proportions of its component hydrocarbons. Their stability spans a wide range, but most hydrocarbons are sufficiently inert to enter into complex pathways of dispersal, involving transport by air, water, particulates, and by the food web.

Much of the research on the origin and fate of hydrocarbons in nature has concentrated on saturated and olefinic hydrocarbons, principally because of the relative ease of analysis by gas chromatography, alone or in conjunction with mass spectrometry. Efforts to study aromatic hydrocarbons in nature are now intensified. The increasing use of fossil fuels and the growing importance of coal and oil shale, whose pyrolysis produces a rich spectrum of aromatic hydrocarbons, pose many environmental and public health questions. However, the formation of aromatic hydrocarbons by geochemical (*1*), industrial, and life processes and their dispersal through the environment are still poorly understood.

In terms of compositional complexity, fossil polycyclic aromatic hydrocarbon (PAH) mixtures range from simple to extremely complex. Thus, nearly pure, crystallized hydrocarbons occur in some mercury ores (*2, 3*), while petroleum is known for the extreme complexity of its homologous and isomeric compounds. The products of incomplete combustion are of intermediate complexity, though the formation temperature and carbon-to-hydrogen ratio of the starting material have a marked influence on the composition of the products.

Environmental samples may contain PAH assemblages from many of these sources. This implies the need for analytical techniques that can resolve adequately the numerous PAH series in fossil fuels. Specific and relatively simple techniques, such as adsorption chromatography with subsequent spectrophotometry or gas chromatography, determine reliably some aromatic hydrocarbons in simple environmental mixtures (*4, 5*). However, no existing method separates and resolves adequately the entire PAH fraction on a milligram to microgram scale and on samples that contain a very large excess of nonhydrocarbons. Even in petroleum analysis, where large samples are available, a complete analytical resolution of the PAH fraction exceeds the capability of any existing combination of analytical techniques. However, adequate characterization is possible, even if it is limited to a description of the molecular weight distribution of the many overlapping homologous series (*6, 7*).

We are involved in a continuing study of the origin and fate of hydrocarbons in nature. This paper reports our methods for the isolation, fractionation, and analysis of PAHs from environmental samples. In addition, we present some analyses of near-shore marine sediments which demonstrate a previously undocumented compositional complexity of the PAH fraction.

EXPERIMENTAL

Sediment Samples. Samples were taken in Buzzards Bay, Mass., with a 1/25 m^2 Van Veen Grab, which was cleaned between uses with water and redistilled methanol, acetone, and pentane. The grab was suspended from polypropylene rope; neither steel cable nor a mechanical winch was used; this prevented sample contamination with lubricants. The sediments were sealed in clean stainless steel containers and frozen until analysis.

Results from two stations in Buzzards Bay are described here, Station A, 1.3 miles from shore at West Falmouth, Mass., in 15 m of water, [location 90 of Blumer and Sass (*8*)], and Station B, 1.8 miles off the entrance to New Bedford Harbor and 0.5 mile from the nearest shore, outside the dredged channel in 7.5 m of water. Both samples were collected in July 1973.

Buzzards Bay is a typical Northeastern U.S. coastal estuary, stretching between the mainland to the northwest and Cape Cod and the Elizabeth Islands to the southeast. Domestic and industrial wastes from the population centers of New Bedford–Fairhaven, Mass., to the north and the commercial and pleasure craft moving through the Cape Cod Canal are the principal sources of pollution. The southern shore of the bay has less or no influx from domestic or industrial wastes, especially along the islands, but it was the site of a 600–700 ton spill of diesel fuel in 1969 (*9*). Except for the polluted areas near New Bedford and the area affected by

[1] On leave from Swiss Federal Institute for Water Resources and Water Pollution Control, CH-8600 Duebendorf.
[2] To whom requests for reprints should be addressed.

(1) M. Blumer, *Pure Appl. Chem.*, **34,** 591 (1973).
(2) T. Geissman, K. Y. Sim, and J. Murdoch, *Experientia*, **23,** 793 (1967).
(3) J. Murdoch and T. A. Geissman, *Amer. Mineral.*, **52,** 611 (1967).
(4) G. Grimmer and H. Hildebrandt, *J. Chromatogr.*, **20,** 89, (1965).
(5) G. Grimmer and H. Boehnke, *Fresenius' Z. Anal. Chem.*, **261,** 310 (1972).
(6) H. J. Coleman, D. E. Hirsch, and J. E. Dooley, *Anal. Chem.*, **41,** 800 (1969).
(7) H. J. Coleman, J. E. Dooley, D. E. Hirsch, and C. J. Thompson, *Anal. Chem.*, **45,** 1724 (1973).
(8) M. Blumer and J. Sass, *Woods Hole Oceanogr. Inst. Tech. Rept.*, 72-19 (1972).
(9) M. Blumer and J. Sass, *Science*, **176,** 1120 (1972).

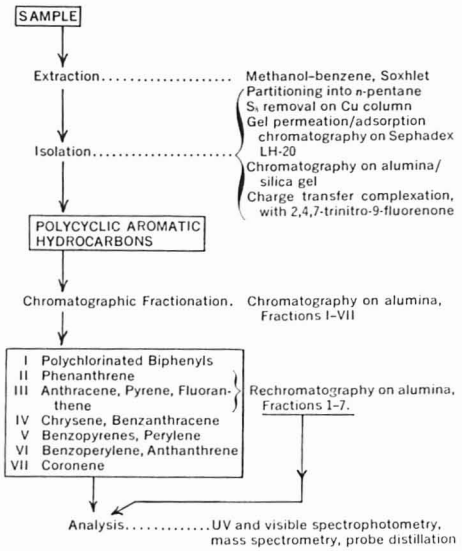


Figure 1. Analysis of polycyclic aromatic hydrocarbons in environmental samples

the 1969 spill, the bay presents a relatively normal bottom ecology (*10*). The biology at Station A was not noticeably affected by the 1969 spill, nor was the fuel oil from that spill detectable by gas chromatography of sediment extracts from that location. The GCs indicate the presence of homologous straight and branched (*e.g.*, pristane) paraffins and of several olefins that exceed all other individual hydrocarbons in concentration. Above C_{15}, odd carbon numbered *n*-alkanes exceed the even homologs.

The chromatograms from both stations have a slowly rising base line, rather than the large unresolved envelope common to the sediments contaminated by the diesel fuel (*8*). While this suggests the absence of major low boiling oil contamination, Station B yielded larger hydrocarbon extracts (84 mg/100 g dry sediment compared to 10 mg/100 g dry sediment at Station A) and a much more complex chromatogram above C_{20}. Neither an odd carbon predominance nor an excess of *n*-alkanes over iso- and cycloalkanes is observed there. This suggests possible hydrocarbon pollution, more likely by lubricants or partly degraded oils, than by a single or recent spill (*11*).

Materials. Analytical grade solvents were used throughout; they were redistilled in an all-glass still. Extraction thimbles, cotton, and anhydrous sodium sulfate ("Baker Analyzed") were extracted with benzene–methanol (1:1) and dried, the latter at 120 °C.

Silica gel (Grade 923, Davison Chemical Company, Baltimore, Md. 22126) and alumina (Catalyst, Al 0102-P, Harshaw Chemical Company, Cleveland, Ohio 44106) were activated for twenty-four hours at 210 °C; subsequently, they were deactivated with various amounts of water to reduce their catalytic activity.

Sephadex LH 20 (Pharmacia Fine Chemicals, Inc., Piscataway, N.J. 08854) was conditioned in benzene–methanol (1:1) and washed with the same solvent, after packing into the column.

PAH references, platinum oxide (K & K Laboratories, Plainview, N.J. 11803) and 2,4,7-trinitro-9-fluorenone (TNF, Eastman Organic Chemicals, Rochester, N.Y. 14650) were used as received, except for phenanthrene, pyrene, fluoranthene, and chrysene, which were purified by column chromatography.

Extraction and Isolation of the PAHs (Figure 1). Wet sediments (100–150 g) were Soxhlet-extracted with methanol (275 ml) for twenty-four hours. Then benzene (75 ml) was added and the extraction was continued (24 hours). The extracted samples were dried to constant weight at room temperature and weighed.

The hydrocarbons were partitioned from the wet benzene–methanol extract into *n*-pentane (125 ml, 3 × 75 ml). After washing with tap water (2 × 250 ml) and drying (anhydrous sodium sulfate), the pentane extracts were concentrated to 1 ml in a rotary evaporator at room temperature. Elemental sulfur was then removed by percolation through a column of copper (*12*), using benzene–pentane (1:1) as eluent. The eluate was evaporated to dryness and subjected to gel permeation chromatography.

Sephadex LH-20 (20 g) in benzene–methanol (1:1) was packed in a column (1.6-cm i.d., 38-cm bed height). Samples were applied in a minimum volume of that solvent, which was also used as eluent at a flow rate of 6 ml/min under slight pressure. The first eluate, 50 ml of colored material, was discarded. The next 50 ml were evaporated to dryness in the rotary evaporator at room temperature. The column was reused after washing with 100 ml of solvent; occasional repacking maintained the flow rate. Reference standards, especially phenanthrene and coronene, were used to establish the cut points and the volume of solvent needed for the regeneration of the column.

The aromatic concentrate from Sephadex in 1 ml of pentane was transferred to a column (1.2-cm i.d., alumina over silica gel, both 4 ml, deactivated with 3% water). The first eluate (20 ml of *n*-pentane) was discarded. The flask which had contained the PAH concentrate from Sephadex was washed with 2 ml of methylene chloride. This, and an additional 13 ml of the same solvent, was added to the alumina-silica gel column, eluting the PAHs.

Trinitrofluorenone (20 mg) was added to the methylene chloride (CH_2Cl_2) eluate. This solution is evaporated to complete dryness in a 100-ml round-bottom flask. The uncomplexed material was removed by washing the walls of the flask with *n*-pentane (5 × 2 ml). These solutions were withdrawn from the flask with a pipet through a cotton pad and discarded. Excess TNF and the complexes were dissolved in methylene chloride and percolated through a silica gel bed (12-ml, 1.2-cm i.d. column, activated, packed in pentane). The PAHs eluted in 75 ml of methylene chloride, which was evaporated to near dryness in a rotary evaporator at room temperature. A small aliquot of the CH_2Cl_2 eluate (1–5%) was transferred with a Hamilton 100-μl syringe to the aluminum pan of a Cahn electrobalance, and weighed after air-drying. The main fraction of PAHs was dried under a stream of nitrogen at room temperature.

Fractionation of the PAH Concentrate and UV Analysis. The PAH fraction in methylene chloride–pentane (0.5 ml, 1:4) was applied to an alumina column (0.6-cm i.d., 5-ml, 1% water). A column load of 200 μg should not be exceeded if optimum resolution is desired. Elution with pentane containing an increasing percentage of methylene chloride (4, 15, 20, 30, 100%, v/v) separated the PAHs into eight ring-type concentrates. Reference standards (12 compounds, 1–3 μg each) have been used to establish the cutpoints (Figure 2).

The resulting fractions were adjusted to 25 ml for the UV measurement (230–450 nm) by partial evaporation or by dilution with the same solvent. Spectra were measured with a Cary Model 14 recording spectrophotometer, using a logarithmic slide wire and 10-cm quartz cells. Absorptivities were measured at those wavelengths (Table I) which are most specific for each hydrocarbon type in the presence of PAHs with comparable chromatographic retention.

Peak absorbances were measured at the wavelengths given in Table I from a base line obtained by straight line interpolation. Specific absorbancies were obtained by spiking sample eluates with known amounts of pure standards; spiking also aided in the qualitative interpretation of the spectra.

The UV spectrum of fraction one was usually poorly defined. The next fractions contained the following major (M) and minor (m) components: Fraction II: phenanthrene (M); Fraction III: pyrene and fluoranthene (M), anthracene (m); Fraction IV: chrysene and benz[*a*]anthracene (M), triphenylene and benzofluorenes were suggested, Fraction V: benzo[*a*]pyrene, benzo[*e*]pyrene and perylene (M), Fraction VI: Benzo[*ghi*]perylene (M), anthanthrene (m), picene and benzo[*k*]fluoranthene were suggested; Fraction VII: coronene (M).

(10) H. Sanders, Woods Hole Oceanographic Institution, personal communication, 1974.
(11) J. W. Farrington and J. G. Quinn, *Estuarine Coastal Mar. Sci.*, **1**, 71 (1973).
(12) M. Blumer, *Anal. Chem.*, **29**, 1039 (1957).

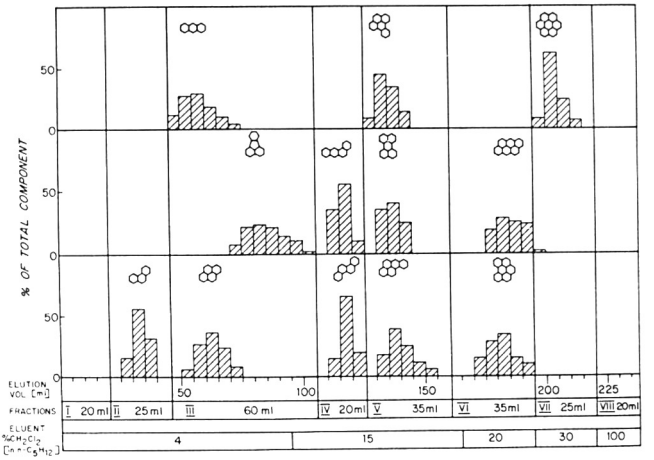


Figure 2. Chromatography of aromatic hydrocarbons on alumina, 1% water; 5 ml in 6-mm i.d. column

Table I. Polycyclic Aromatic Hydrocarbons in Sediments at Stations A and B[a]

Compound	Station A	Station B	Std dev %[b]	Wavelength used, nm
Phenanthrene	33	n.d.[c]	24	293
Anthracene	8	170	37	252
Pyrene	100	960	13	333
Fluoranthene	110	790	14	286
Benz[*a*]anthracene	41	330	27	287
Chrysene	40	240	15	267
Perylene	26	94	14	435
Benzo[*a*]pyrene	75	370	19	383
Benzo[*e*]pyrene	59	310	8	331
Anthanthrene	7	34	34	428
Benzo[*ghi*]perylene	66	280	19	382
Coronene	5	20	34	338
Total, from UV	570	3,600		
Total, actual weight of PAH concentrate	6,700	63,000		
Total actual weight of all fractions in final chromatogram	1,630			

[a] Weight calculated from UV-spectra, μg/kg dry sediment. Calculations based on spectra and molecular weight of unsubstituted hydrocarbons. [b] Three analyses, Station A. [c] Fraction contains much material, but spectra unsuited for quantitative analysis because of excessive peak broadening.

The spectra of fraction VII and more markedly of VIII were poorly defined and may contain contributions from overlapping spectra of unidentified hydrocarbons.

Rechromatography of the Phenanthrene–Pyrene Fraction. The combined phenanthrene–pyrene fractions from several batches of sediment (Station A) were rechromatographed on alumina (with 1% water in 14-mm i.d. column) and eluted consecutively (Fractions 1–8), with 40 ml of pentane, four 25-ml portions of pentane with 2, 2, 3, and 3% CH_2Cl_2, 5 ml of pentane with 3% CH_2Cl_2, followed by 25 ml of pentane with 4% CH_2Cl_2 and, finally, 50 ml of CH_2Cl_2.

The UV spectra indicated no absorbing material in Fraction 1 and weak absorption in Fraction 2; Fractions 3 and 4 contained phenanthrenes, Fraction 5 pyrene and phenanthrene with minor amounts of anthracene and fluoranthene. Fractions 6 and 7 contained pyrenes with increasing amounts of fluoranthenes. The presence of benzofluorenes was suggested in 7 and 8 (weak spectrum).

Hydrogenation. Platinum oxide (1–2 mg) in 100 μl isooctane was reduced to platinum under a hydrogen atmosphere with stirring at room temperature. The sample in isooctane was added and hydrogenated for one hour. Olefins are quantitatively reduced at room temperature; at boiling temperatures, the aromatic rings are partially hydrogenated.

Mass Spectrometry. Spectra were obtained on a CEC 21-104 mass spectrometer (Du Pont Instruments, Monrovia, Calif. 91016), using the low mass heated probe for sample introduction. Samples not exceeding 1 μg total solids in 1–3 μl solvent were injected into a closed-end capillary (15 × 2-mm o.d.; 1-mm i.d.); the solvent was evaporated at room temperature in a stream of notrogen. To minimize premature evaporation during sample introduction, samples were exposed for the shortest possible time to the fore-vacuum in the vacuum lock (30 seconds) and to the high vacuum (40 seconds) before initiating the first scan. The instrument recorded one magnetic scan of 20 seconds duration, every 40 seconds, from 12–350 amu at approximately 500 amu resolution. Radiative heating from the source (200 °C) raised the sample temperature at a rate near 7 °C/minute; after reaching 50 °C, the probe temperature was raised at the same rate by means of the probe heater.

Operating conditions are: 1600-V acceleration voltage, 2720 V on the electron multiplier (17 stages), 35 μA source current at 12 eV ionizing voltage. The detection limit for 4-methyl pyrene at 12 eV is 4×10^{-10} g [(signal + noise)/noise = 2)].

Procedure Blank. A blank of methanol (275 ml) and benzene (75 ml) was refluxed in the Soxhlet apparatus and then carried through the entire procedure, excluding chromatogram B. The fractions from chromatogram A had no measurable UV/Vis absorbance. The fractions were then combined for greater sensitivity in mass spectral analysis, and subjected to probe distilllation. No PAH series was recognizable in the mass spectra.

RESULTS

Isolation Technique. Most environmental samples contain hydrocarbons only as traces and in the presence of many other extractable materials. These hydrocarbons have to be separated and recovered in sufficient purity for subsequent UV and mass spectrometric analysis. The careful application of a single separating technique (*e.g.*, column chromatography) may sometimes yield a sufficiently pure concentrate. However, often mixtures result which resist further resolution by the same method. In general, pu-

Table II. Recovery of Reference Hydrocarbons at Microgram Levels

Compound	Present, μg	Found, μg	Recovery, %
Phenanthrene	3.1	1.2	39
Pyrene	2.4	1.8	75
Perylene	3.0	2.3	77
Benzo[*a*]pyrene	2.6	2.3	88
Benzo[*e*]pyrene	3.2	2.5	78
Coronene	2.4	1.3	54

rity is more rapidly approached through a combination of techniques that respond to different aspects of the physical and chemical properties of the samples.

Our isolation technique utilizes a sequence of gel filtration, adsorption chromatography, and charge-transfer complexation. The resulting analytical scheme (Figure 1), though involving numerous steps, is basically simple and rapid. In all operations, except the final fractionation, only two consecutive fractions are collected. One of these contains the PAH concentrate; the other is rejected.

The initial isolation steps are conventional. Wet sediments are Soxhlet-extracted with methanol, and benzene is added to the refluxing solvent after the initial extraction of the water. This eliminates previous drying of the sample, possible loss of volatile hydrocarbons, and changes the refluxing solvent from methanol to the benzene–methanol azeotrope, which is a good hydrocarbon solvent. From the extract, elemental sulfur, which would chromatograph together with the PAH fraction, is removed by percolation over precipitated copper (*12*).

The subsequent chromatographic separation, on Sephadex LH-20, utilizes the particular properties of that rather polar gel permeation substrate (*13*). True gel permeation chromatography of the nonpolar lipids in the sample is superimposed over the adsorption, and therefore greater retention, of the more polar materials, including the PAH fraction (*14–16*). Most lipids and pigments elute near the column void volume. The greatly retarded PAH fraction elutes later, in order of increasing molecular weight and polarity rather than in the reverse order that would be expected for gel permeation chromatography.

Other authors have used gel permeation substrates to fractionate PAHs, either in an adsorptive separation on Sephadex LH-20 with isopropanol as solvent (*14–16*) or in a gel permeation chromatogram on polystyrene gels in benzene (*6, 7*). However, such a one-step purification is inadequate for complex environmental samples, and the final ring-type separation is more easily and more rapidly accomplished on alumina. Therefore, and because of the high sample capacity of Sephadex LH-20, we apply it in the initial separation of the PAH fraction, at flow rates and with a solvent that favor rapid elution in a single fraction, rather than resolution into ring-type concentrates.

The second chromatography on silica gel–alumina separates the PAH fraction from saturated hydrocarbons and most olefins, which are eluted more rapidly, and from more polar materials, which remain on the column. This separation provides adequate purity of the PAH concentrate for the following TNF-adduction; if the chromatography is omitted, lipids remaining in the PAH fraction solubilize the TNF-adduct or prevent its precipitation entirely. Many soils are rich in long chain methyl ketones (*17, 18*). These follow the PAH fraction through the separation until they are rejected, together with other uncomplexed materials, during the formation of a PAH–trinitrofluorenone charge-transfer complex (*19, 20*).

The TNF-adduct is purified by solvent washing; after dissolution, the adduct is split by percolation over a silica gel column. Column dimensions, elution volumes, and full activity of the silica gel are critical for optimal separation between TNF and especially coronene. Under our experimental conditions, 10 μg coronene is separated from 20 mg TNF with a 97% yield.

The total PAH fraction from the TNF separation is still too complex for UV spectroscopy, but mass spectra recorded during gradual evaporation from a temperature-programmed probe will provide a first indication of sample composition and molecular weight distribution. Much more complete insight into the presence of overlapping homologous series can be obtained after a further chromatographic ring-type separation, by correlation of the UV and mass spectra.

Many published procedures are available for such a final fractionation. We prefer column chromatography on partly deactivated alumina at high adsorbent-to-sample ratio because of the good resolving power (Figure 2), the high flow rate, and the fact that the separation is carried out at room temperature. These features make column chromatography superior to gel permeation and gas chromatography. For safety reasons (dust of PAH loaded silica particles!), we reject thin layer chromatography in spite of its excellent resolution.

Recoveries for six reference PAHs at microgram levels (Table II) and the reproducibility of recoveries from environmental samples (Table I) are adequate for most geochemical and environmental considerations. The quantitative interpretation of the data is limited more by the uncertainties in the evaluation of the UV and mass spectra than by the sample recovery. The low recovery of phenanthrene in the artificial standard may be due to partial volatilization. Actual environmental samples contain lipids in addition to PAH which lower the vapor pressure of the PAH fraction, especially in the early steps of the separation.

Ultraviolet Analysis. Electronic spectra of aromatic hydrocarbons exhibit characteristic absorption bands with considerable fine structure, especially in nonpolar solvents and in the vapor phase (*21*). The spectra are often used for qualitative and quantitative analysis. However, UV analysis, especially of mixtures rich in alkyl derivatives, has severe limitations. Alkylation of the aromatic ring systems leads to bathochromic shifts in the spectra (*22*); the peak displacement increases with the number of substituents. Thus, absorption measurements on mixtures of substituted aromatics with the same basic ring system at a single wavelength assess the contributions from different homologs at different sensitivity levels. An integration of the absorbance over a wider wave length range would provide a more accurate analysis. However, the spectral overlap between various aromatic systems precludes this, except in simple mixtures.

In complex PAH fractions (*e.g.* from fossil fuels), numerous alkyl and cycloalkyl derivatives are present and the spectral overlap is severe; in the resultant spectra, most of the fine structure is lost. The interpretation of such spectra

(13) M. Wilk, J. Rochlitz, anx. Bende, *J. Chromatogr.*, **24**, 414 (1966).
(14) C. A. Streuli, *J. Chromatogr.*, **56**, 219 (1971).
(15) H. J. Kisch and D. Reese, *J. Chromatogr.*, **80**, 266 (1973).
(16) H. H. Oelert, *Fresenius' Z. Anal. Chem.*, **244**, 91 (1969).
(17) M. Streibl and K. Stransky, *Fette, Seifen, Anstrichsm.*, **74**, 566 (1972).
(18) R. I. Morrison and W. Bick, *Chem. Ind. (London)*, 596 (1966).
(19) M. Orchin and E. O. Woolfolk, *J. Amer. Chem. Soc.*, **68**, 1727 (1946).
(20) G. H. Schenk, P. W. Vance, J. Pietrandrea, and C. Mojzis, *Anal. Chem.*, **37**, 372 (1965).
(21) R. A. Friedel and M. Orchin, "Ultraviolet Spectra of Aromatic Compounds," J. Wiley, New York, N.Y. 1951.
(22) E. Clar, "Polycyclic Hydrocarbons," Academic Press, New York, N.Y., 1964.

is difficult. Thus, a crude oil sample, carried through our separating procedure, yielded fractions with smoothed UV spectra that revealed only the presence of the most abundant ring types. This is attributed not to an inadequate separation, but to excessive spectral overlap. Mass spectra confirm both this wide range of alkyl homology and the success of the chromatographic separation.

The quantitative interpretation of the UV spectra requires knowledge of the molecular weights of the PAH. In simple systems, mass spectrometry provides this and, with sufficiently large sample, a direct measurement of the molecular weight or its estimate from the boiling range is possible. In small and complex environmental samples, a reliable determination of the average molecular weight is difficult, even by mass spectrometry, which may not resolve the many overlapping series of homologs into their individual contributions. In particular, the higher ring-number concentrates contain unknown and unidentified PAH components or UV-absorbing non-PAH impurities. Their contribution to the measured absorbance leads to errors that cannot be eliminated by the base-line technique and the incremental addition of standards.

The quantitative UV analysis of PAH in complex environmental samples is limited by the above errors; and the heavy reliance on the UV data in much of the previous work in this area may not be warranted. UV analysis is most reliable where mass spectrometry confirms a simple composition or the predominance of very few components; neither is realized in the samples whose analyses are discussed here.

In our analyses, the summed weights of PAH derived from the UV measurements account for 6–9% of the actual weight of the total PAH fraction or 29% of the weight of the combined fractions of the final PAH chromatogram (at Station A, Table I). The total fraction weight and the weight after the final chromatographic separation step may include non-PAH impurities that have not been rejected by the separating procedure; on the other hand, our UV measurements are based on the absorptivity of the unsubstituted hydrocarbons. Also, the spectra indicate the presence of additional, unidentified aromatics, whose presence is neglected in the sum of weights derived from the UV data. Therefore, the true PAH weight lies between the actual weight of the chromatographic fractions and the weight that has been reconstructed from the individual UV contributions.

In spite of these limitations, omission of the UV measurements from the analytical scheme would severely limit the interpretation of the data. The spectra establish the order of elution, the chromatographic resolution, and the recoveries. They supplement the mass spectral interpretation and often reveal significant trends in analyses of related samples. Thus, the spectrum of the phenanthrenes from Station A exhibits the typical fine structure of that hydrocarbon; however, at Station B, the fine structure is smoothed out and the normally sharp peak at 293 nm is too indistinct to be used for a quantitative measurement of the phenanthrene concentration. This suggests the presence of a wider range of alkylated phenanthrenes at Station B than at Station A. Similarly, at Station B (Table I), the decreasing trend in the concentrations from low to high ring-number aromatics suggests a relatively greater contribution of three- and four-ring aromatics. Not surprisingly, this trend, and that noted above for the alkane distribution, suggests a greater contamination from fossil fuels near New Bedford Harbor.

Mass Spectral Analysis. Mass spectrometry provides much information rapidly, even on small and complex samples, especially in conjunction with ancillary equipment for fractionation during sample introduction—*e.g.*, gas chromatography (GC–MS, mass chromatography) or gradual evaporation from a temperature programmed probe.

In this initial investigation, we preferred not to use GC–MS, since the thermal stability of highly substituted PAH derivatives under GC conditions is poorly known. Pyrolysis of geochemical products occurs often under surprisingly mild thermal conditions (*23, 24*). Programmed temperature probe distillation, though providing a much less efficient separation than GC–MS, fractionates mixtures according to their volatilities, with much shorter and less severe thermal exposure. The separation is performed in the high vacuum of the spectrometer rather than at higher pressure as in GC. Considerable advantage is retained over bulk sample introduction at a fixed inlet temperature; a volatility profile is obtained and good spectra of the more volatile PAH can be measured before the higher boiling non-PAH impurities distill from the probe.

In order to simplify the spectra and their interpretation, we operate consistently at low electron beam energy. At 12 eV, the ionization of impurities and the fragmentation of the alkyl-substituted PAH are minimized. Though this eliminates nearly all except the molecular ions from the spectra, much additional compositional information is deduced from the volatility profiles and from previous sample knowledge, especially from chromatographic behavior and UV spectra.

The mass spectra, even of the chromatographically well separated ring type concentrates, show an abundance of peaks and a wide molecular weight range (Table III). Intense ions at even masses represent principally molecular ions, and weaker peaks at odd masses represent isotope peaks. Nitrogen compounds, which would also give rise to odd mass peaks, are largely removed in the separating procedure, and no major odd-mass series are evident in the spectra.

Most mass spectral peaks contain contributions from overlapping homologous series which represent isomeric hydrocarbons with the same number of aromatic rings (*e.g.*, chrysene, triphenylene, benzanthracene) or aromatic ring structures combined with sulfur containing or naphthene rings ["thienologs" and "naphthenologs" (*7*)]. Neither low voltage mass spectra or UV spectra can resolved this overlap, though the latter permit the identification of the basic isomeric series. An actual measurement of some of the components may be possible by gas chromatography, at least for the lowest boiling members but, at higher molecular weights, the multiple contributions to most masses are unlikely to be resolved by any existing technique.

In probe distillation, the onset of a new homologous series, or of overlapping isomeric series, is often sharp and evident from the sudden appearance of an intense peak at the mass of the unsubstituted parent hydrocarbon of the series (Table IV–V). At the temperature of their first appearance, the contributions from higher homologs are small, but gradually their abundance increases and the maxima of the distribution curves shift toward higher molecular weights. The first members disappear, unless they have been present, initially, in such concentrations that their pump-out is sluggish.

The major hydrocarbon series are readily identified from their mass and UV spectra. They appear chromatographically in the proper elution sequence and, at least the first members of most series, have been identified in environmental samples before. However, a much wider range of alkyl homologs is now described.

(23) M. Blumer and M. Rudrum, *J. Inst. Petrol.*, **56**, 99 (1970).
(24) M. Blumer, *Pure Appl. Chem.*, **34**, 591 (1973).

Table III. Homologous Series of Polycyclic Aromatic Hydrocarbons in Sediments at Station A

Series[a]		Fraction	First mass	Last mass	Tentative identification[b]
−14		2	168	294	Biphenyl, Acenaphthene
		3	182		Tetrahydrophenanthrene, Tetrahydroanthracene
		4	as Fraction 3		
−16		II	180	236	Fluorene, Acenaphthylene, Biphenylene, Benzoindene
		3	as 4		
		4	166	306	As II, also Dinaphthenenaphthalenes (?)
−18		II	178	262	Phenanthrene
		2	weak		
		3	178	290	Phenanthrene
		4	178	276+	Phenanthrene
		5	178	318	Phenanthrene, Anthracene
		6	178	318	Phenanthrene, Anthracene
−20		2	weak		
		3	190	330	Naphthenephenanthrene
		4	190	344	Naphthenephenanthrene
−22		2	weak		
		3	230	328	Dinaphthenephenanthrene
		4	202		Pyrene
		4	230	328	Dinaphthenephenanthrene
		5	202		Pyrene/Fluoranthene
		5	230	328	Dinaphthenephenanthrene
		6	202	342	Pyrene/Fluoranthene
		IV	216	230	Benzofluorene
−24		5	242	284	Trinaphthenephenanthrene
		6	228		Chrysene, Triphenylene, Benzanthracene
		IV	228	312	Chrysene, Triphenylene, Benzanthracene
−16S	or	3	184	338	Dibenzothiophene, Naphthothiophene
−26		3	254		Tetranaphthenephenanthrene
		4	184	338	Dibenzothiophene, Naphthothiophene
		IV	240		Naphthenechrysene
−28		4	280		Pentanaphthenephenanthrene
		IV	252	322	Dinaphthenologs of Tetracyclic Aromatics
		V	252	336	Benzo[*a*]pyrene, Benzo[*e*]pyrene, Perylene, Benzofluoranthene
−30		IV	278	320	Trinaphthenologs of Tetracyclic Aromatics
		VI	278	348	Picene, Dibenzanthracene, Dibenzophenanthrene
−32		VI	276	346	Benzo[*ghi*]perylene, Anthanthrene, Indenopyrene
		VII	276	346	Benzo[*ghi*]perylene, Anthanthrene, Indenopyrene
−34		VII	302	344	Dibenzofluoranthene
		VIII	302	344	Dibenzofluoranthene
−36		VII	300	342	Coronene
−38		VIII	326		Dinaphthenedibenzofluoranthene, Naphthenecoronene

[a] *Z*− number; see text. [b] Listed are identifications which are most consistent with spectra (UV, VIS, MS), chromatographic mobility, and relative volatility. Many series extend beyond the scan limit (350 amu). No last mass is listed if a single peak predominates (as in the first eluates of each major series) or where severe overlap between series occurs.

Table IV. Mass Distribution of the Nominal −12, −26 Series in Fraction 3[a]

	Probe temperature				
amu	<30°	<30°	33°	42°	48°
184	42	71	26	14	
198	42	99	100	35	
212	8	17	26	13	
226	5	8	16	13	
240	1	5	7	11	4
254		5	13	24	37
268		3	5	9	13
282		1	4	5	7
296				4	5
310					4

[a] No strong peaks appear below the first masses of Tables IV–V. Spectra are normalized to the most intense peaks of each series for every probe run. No correction has been applied for sensitivity differences. Relative intensities are comparable within each probe run, but no sample size correction has been applied to different probe runs.

Table V. Mass Distribution of the Nominal −22 Series in Fraction 3

	Probe temperature			
amu	<30°	33°	42°	48°
230	26	50	100	55
244	18	37	67	64
258	13	19	40	64
272	8	18	32	52
286	6	13	22	42
300	3	8	18	27
314		5	10	18
328		5	10	13
342			5	10

Other homologous series appear at lower levels, but well above the chromatographic background; they are offset from the principal series by an even number of mass units. We have arrived at a structural interpretation that considers the chromatographic mobility, the UV and mass spectra, the relative volatility, and the appearance of the initial masses of each series. All of these parameters can be satisfied if the minor series are explained as naphthenologs and thienologs of the basic PAH series, with a preference for cyclo-C_5 over cyclo-C_6 substitution of the aromatic systems. Structures of this type occur abundantly in the higher boiling crude oil distillates (*6, 7*).

CHARACTERIZATION OF FRACTIONS

Station A (Table III). In the discussion of the individual chromatographic fractions the aromatic hydrocarbon series

are classified according to their initial observed masses, the molecular weight range and their hydrogen deficiency or Z number, from $C_nH_{2+Z}S$ (Table III). "Fractions I–VII" refer to the separation of an extract from Station A and "Fractions 1–7" to the rechromatography of the combined phenanthrene–pyrene fractions (II–III) from that chromatogram.

Polychlorobiphenyls are indicated by the mass spectra of Fraction I. There is no strong evidence for PAH series in the mass and UV spectra of this fraction.

The mass spectra of Fraction II are dominated by the −18 series (1st mass 178), extending to 262 atomic mass unit (amu). The same series, predominantly phenanthrene and alkylphenanthrenes according to the UV spectra, extends to 290 amu in Fraction III. That fraction also contains the −22 series (1st mass 202, pyrene/fluoranthene) with homologs to 286 amu.

The numerous other homologous series in Fractions II and III were further resolved by rechromatography into fractions 1–7.

Fraction 1 contains no PAH. Fraction 2 contains a −14 series (observed 1st mass 168 amu, methylbiphenyl/methylacenaphthene). The first member of the series (154 amu), if present, is obscured by the internal standard dimethylnaphthalene. A weak −16 series (1st observed mass 208) may represent the homologs of acenaphthylene/biphenylene (mol wt 152) or fluorene/benzoindene (mol wt 166), or the dinaphthenenaphthalene series.

The spectrum of Fraction 2 is weak and complex, with possiblenvributions from diaromatics and phenanthrene. Correspondingly, a weak −18 series (178, phenanthrene; 192, 206 amu) is observed in the mass spectra. Two additional series (1st masses 204 and 230) are thought to belong to the −20 and −22, rather than to the overlapping −6, −8 and −34, −36 series, because of their chromatographic behavior and the UV spectrum. Corresponding peeeaks reappear at greater intensity in Fraction 3 where we interpret them as begvng to the mono- and dinaphthenephenanthrene series. The same interpretation may apply to the −20 and −22 series in 2. An alternate explanation that they represent polynaphthenediaromatics cannot be rejected without further chromatographic resolution of 2 into fractions with well defined UV spectra.

Ultraviolet and mass spectra of Fraction 3 indicate the predominance of phenanthrene and its homologs. Ultraviolet evidence for anthracenes appears only in Fraction 5. Therefore, the discussion of Fractions 2–4 considers phenanthrene as the typical representative of the tricyclic aromatics and their naphthenologs. Next in abundance, at low probe temperatures, is a −14 series [1st mass 168 (weak), 182], which may represent alkylated biphenyls/acenaphthenes. The intense ion at 182 amu and the predominance within this series of 196 and 210 amu at increasing probe temperatures suggests a contribution from the tetrahydrophenanthrene or tetrahydroanthracene series.

Above 30 °C probe temperature, a −12 or −26 series reaches greater abundance (Table IV). Here, and in the other series discussed, the UV spectra rule out tetracyclic and higher aromatics. The sudden onset of the series at 184 amu and the absence of lower homologs suggest that it represents not alkylnaphthalenes (−12 series) but dibenzo- or naphthothiophenes (1st masses 184, −16S corresponding to −26 series). At low probe temperature, the 198 amu peak is most abundant, and may contain a contribution from dibenzo- or naphthothiopyran (198 mol wt). At higher probe temperature, the series has a bimodal mass distribution, with an intense peak at 254 amu persisting throughout several consecutive spectra. We interpret this as the appearance of a new −26 series. Interestingly, 254 is the molecular weight of the most highly condensed tetranaphthenephenanthrene.

The −20 and −22 series (Table V), already observed in fraction 2, reach greater intensity and cover a wider molecular weight range in 3 (1st masses: −20 series, 190 amu; −22 series, 230 amu). Chromatographic behavior and UV spectra suggest a structural relationship to the phenanthrenes. Highly olefin substituted phenanthrenes, which would fall into these series, are ruled out by negative results of attempted hydrogenations. Similarly, pyrene homologs (−22 series) are unlikely in this fraction; unsubstituted pyrene, which is chromatographically more mobile than the homologs, appears only in Fraction 4. Consistent with the existing data is the assumption of naphthenephenanthrenes (I, −20 series, lowest member: 190 mol wt) and of dinaphthenephenanthrenes (IIa–IIc, −22 series, lowest members 216 and 230 mol wt, depending on degree of condensation and ring size). At higher probe temperature, the −20 series is bimodal with maxima at 204 and 232 amu, corresponding to substitution of phenanthrene by 2 and 4 naphthenic carbon atoms contained in a single C_5 and C_6 ring, or to phenylnaphthalenes.

Fraction 4 still contains predominantly the −18 series. Next in abundance, the −20 series extends from 190 amu beyond the 350 scan limit used in this investigation. In its interpretation, we follow the consideration above without assuming an exact correspondence in the relative concentration of the contributing isomers. Unsubstituted pyrene (202 amu) appears in the mass spectra and its presence is corroborated by the UV spectrum. The unsubstituted PAH are chromatographically more mobile than their homologs and the isomeric methylpyrenes are lacking in this fraction. However, at higher probe temperature homologs of the −22 series appear (1st mass 230 amu, 216 amu missing!). We interpret these peaks again as evidence for the dinaphthenephenanthrene series, discussed in the context of Fraction 3, rather than as a alkylpyrenes. Similarly, the −12 or −26 series, the third in relative abundance, persists in this fraction, but with lesser predominance of the 254-amu peak. Again, these peaks represent benzothiophenes and naphthenephenanthrenes, with a probable shift in the relative contributions of the various isomers.

The −16 series (1st mass 166 amu) observed in Fractions 2 and 3 is now more intense, with a pronounced bimodal distribution (peaks at 180 and 208 amu). At higher probe temperature, the initial members disappear and the series extends beyond 300 amu. The initial mass may represent fluorene, benzoindene, or methylacenaphthylene. The pronounced peaks at 180 and 208 amu may contain a contribution from dinaphthenenaphthalenes.

At lower intensity, the −14 or −28 series is again represented. A bimodal mass distribution is observed at 40° probe temperature; the intense ion at 280 amu may represent the first member of the pentanaphthenephenanthrenes, corresponding to the strong 254 peak in the −26 series of Fraction 3, which was interpreted as tetranaphthenephenanthrene.

In Fraction 5, the phenanthrenes still predominate quantitatively, but unsubstituted pyrene (202 amu) is now abundant. The UV spectra indicate elution in Fraction 5 of anthracene and of fluoranthene, in amounts that are small compared to pyrene. In the mass spectra, most of the features of the previous fractions are retained. Again, methylpyrene is absent but higher homologs of the −22 series, probably dinaphthenephenanthrenes and dinaphtheneanthracenes, are abundant.

In Fraction 6, the −22 (pyrene/fluoranthene) dominates the −18 series (phenanthrene/anthracene).In the course of the chromatogram, the concentration maxima within these

series shift toward higher molecular weights; this reflects the partial separation of the homologs by the column chromatography.

The minor series, except for the naphthenephenanthrenes (−20 series), occur in relatively small amounts. At high probe temperature, the −20 and −22 series again predominate. Within the −24 series, the initial ion (228 amu) is now pronounced, even though this remains the weakest series of this fraction. In view of the low relative concentration and the mixed composition (tetracyclic aromatics, naphthenologs of phenanthrene/anthracene), the absence of a strong indication of tetracyclic aromatics in the UV spectra is not surprising.

In Fraction 7, the pyrene/fluoranthene series predominates again, followed by thephenanthrenes/anthracenes. The same series and general trends as in the previous fractions are observed here.

The discussion now returns to Fraction IV of the main chromatogram. Its spectra are dominated by the intense peak (228 amu) of chrysene/triphenylene/benzanthracene, in agreement with the UV spectra. The parent hydrocarbons of this −24 series predominate to 42 °C probe temperature, with smaller amounts of C_1 to C_5 homologs. At higher temperature, the initial peaks diminish and the series extends to 312 amu.

At lower intensity, the −22 series persists. A strong 216-amu peak in the absence of the lower homologs at 202 amu suggests the start of a new series, presumably benzofluorene (216 mol wt). The −18 series (1st mass 234 amu) and the −26 series (1st mass 240 amu) may represent higher homologs of phenanthrene/anthracene and naphthenologs of chrysene/benzanthracene/triphenylene (lowest member 240 amu).

The appearance of −28 and −30 series in this fraction is of special interest. Elution of picene/dibenzanthracene (−30 series, 1st mass 278 amu) in this fraction is unlikely. Further, the peak at 278 amu in Fraction IV is preceded by the next lower homolog at 264 amu. We suggest that this series represents the trinaphthenologs of chrysene/triphenylene/benzanthracene (lowest member: 264 mol wt).

Correspondingly, the −28 series (1st mass 252 amu) is interpreted as the dinaphthenologs of the same tetracyclic aromatics. A possible contribution of the unsubstituted pentacyclic aromatics, which appear in the next fraction, might be excluded by cautious rechromatography of this fraction.

Fraction V is dominated by the −28 series, appearing above 32 °C probe temperature. The UV spectra confirm the presence of perylene, benzo[*a*]pyrene and benzo[*e*]pyrene. In addition, benzofluoranthenes may be represented in this fraction. The −22, −24, and −26 series (1st masses: 216, 228, and 240) are present, but at lower relative concentrations than in the previous fraction.

Here, and in the succeeding fractions, the minor series occur at considerably lower levels than in II–IV. This and the much wider range of structural possibilities in overlapping homologous series makes interpretation more difficult and speculative.

The principal peaks of Fraction VI belong to the −32 series (1st mass 276 amu, benzo[*ghi*]perylene/anthanthrene/indenopyrene), and at higher probe temperatures to the −30 series (1st mass 278 amu, picene/dibenzoanthracene/dibenzophenanthrene).

The series observed in the previous fraction overlap into Fraction VII. A new −34 series is first observed at 60 °C probe temperature (1st mass, 302 amu, *e.g.*, dibenzofluoranthene) and a −36 series (1st mass 300 amu, coronene) appears at 85 °C. Their homologs extend beyond mass limit of 350 amu used in this work.

Intense spectra of Fraction VIII are obtained only at 120 °C probe temperature. Again, the spectra overlap with those of the previous fraction. The −34 series is particularly strong and an intense first peak of a new −38 series appears (1st mass 326 amu). This may represent the initial member of an unidentified PAH series or, in keeping with the trends observed in previous fractions, a naphthenolog of the most abundant series in this fraction, *e.g.*, a dinaphthenedibenzofluoranthene or a naphthenecoronene.

Comparison of Stations A and B. The quantitative interpretation of the UV spectra (Table I) indicates a greater abundance of PAH in the sediments of Station B, near New Bedford Harbor, and a marked predominance of the lower ring number hydrocarbons.

Similarly, the mass spectra, expecially of Fractions II and III from Station B, indicate a stronger predominance of the more highly substituted 3- and 4-ring aromatics, extending to higher molecular weights than at Station A.

Aside from this and from the much greater predominance of polychlorinated biphenyls at Station B, the differences in the mass spectra are surprisingly subtle, especially in Fractions V–VIII. Even in the lower fractions, the same homologous series occur and correlate in their relative intensities. Thus, in Fractions II–IV from Stations A and B, the representatives of the principal series in the peak clusters at 204–216, 226–238, and 240–252, respectively, present a nearly identical distribution pattern.

CONCLUSIONS

The present paper describes the analysis of very complex PAH mixtures, primarily from soils and sediments. In view of the wide range of lipids, waxes, fatty acids, pigments, etc. occurring in these samples, we expect that the method will be applicable to a wider range of materials, including lipids from plants and animals. The combination of gel permeation and adsorption chromatography with charge-transfer complexation leads rapidly from crude samples to PAH concentrates that are adequately pure for subsequent analysis. The further resolution by moderately efficient chromatography and mass spectral probe distillation and the interpretation of the UV and mass spectra offer a very detailed insight into the hydrocarbon composition of these samples. The method covers compounds from the tricyclic aromatics to coronene. This range is limited by the greater volatility of mono- and diaromatics and the instability of their TNF adducts. An extension of the upper limit for better recovery of coronene and higher ring-number PAH series may be possible through a different choice of operating parameters.

The present method is the first one that resolves adequately any fossil fuel contribution to the PAH fraction in environmental samples. With PAH concentrates in the microgram to milligram range, it yields compositional information comparable to that previously obtained only on crude oil samples in the 1- to 10-kg rannnge (7). Our analytical sensitivity hinges on that of the mass spectrometer; at a nanogram sensitivity, a milligram sample provides a dynamic range of six orders of magnitude. This is adequate to assess the presence of minor series in a mixture that may well contain tens of thousands of different individual compounds.

The analyses of sediment samples from Stations A and B in Buzzards Bay, and a still limited number of similar analyses from other stations, demonstrate an unanticipated complexity of the PAH fraction. The principal series, from which only unsubstituted hydrocarbons and some alkyl derivatives have been known to occur in environmental samples, stretch over a wide molecular weight range. The minor series, previously unknown from recent sediments, cover an

equally wide carbon number range. They are interpreted as the naphthenologs and thienologs of the basic PAH series.

The elucidation of individual structures in such small and complex samples by classical methods is a nearly impossible task. Even for crude oil, where sample size is not limited, few PAH structures have been proved by conventional methods. In spite of this, we believe that our structural assignments and those of Coleman *et al.* (*6, 7*) for crude oil residues, stand on a comparable basis. With their adequately large samples, these authors characterized their fractions further by elemental analysis and NMR spectrometry. This is precluded in our work because of the limited sample size, but we derive additional important information from the chromatographic mobilities, the UV spectra, and the relative sample volatilities.

Especially in the lower molecular weight range, few structural alternatives appear possible. For instance, the strong initial peak of the −20 series at 190 amu in the main phenanthrene fraction is logically attributed to the lowest molecular weight member (I) of the naphthenephenanthrenes. Similarly, the −22 series in the same fraction is suggestive of the isomeric dinaphthenephenanthrenes (IIa–IIc) or, in later chromatogram fractions, of the dinaphtheneanthracene (III) and their alkylhomologs.

All of the compounds encountered in this work occur or must be expected to occur in petroleum. The occurrence of five-ring substituted aromatic systems is geochemically interesting. Fossil aromatic hydrocarbons arise probably from condensation and dehydrogenation reactions during sedimentary diagenesis. The conversion, by cyclization of side chains, to saturated six-membered rings can be expected to be followed rapidly by the thermodynamically favored aromatization. Many five-membered rings, on the other hand, once formed, cannot be aromatized and represent a diagenetic dead end; therefore they accumulate in considerable quantities in crude oil.

The striking complexity of the PAH fraction in these sediments from Buzzards Bay resembles in many respects that of fossil fuels; however, the evidence is still equivocal and a wider range of samples has to be analyzed before we can suggest more definitely the possible sources. Certainly, more than a single source must be considered; polycyclic aromatic hydrocarbons are also formed by incomplete combustion. Other sources may include runoff from land, containing hydrocarbons in solution or on particles, processes of incipient diagenesis in the sediments, and living organisms on the surrounding land or in the water.

The first members of the major hydrocarbon series are more abundant relative to their higher homologs than they appear to be in most crude oils. This may well suggest different sources for the initial and the higher members of the various series. Regardless of the possible contribution of fossil fuels to these sedimentary hydrocarbons, their derivation from the 1969 fuel oil spill at West Falmouth appears unlikely. That particular fuel oil contained a few tricyclic aromatic hydrocarbons (*8*) and could not be the direct source of most of the higher ring-number aromatics and cycloalkyl substituted aromatics at Stations A and B.

To our knowledge, only one reference contains data that can be compared with ours; Tissier and Oudin (*25*) have published a mass spectrum of the heavy aromatic fraction of an "unpolluted mud" in the Seine Bay. Apparently, no extensive chromatography or probe distillation was used and only the principal peaks (178, 202, 228, 252) were assigned to specific compounds. However, the spectrum demonstrates, at what may have been considered background level, the presence of the −18, −20, −22, −24, −26, and −28 series in the 178–300 amu range. This suggests that such a complex PAH composition may not be unique to the sediments of Buzzards Bay.

The complexity of the aromatic fraction in these samples has important implications for the analysis and for the study of the effects of polycyclic aromatic hydrocarbons in nature. A similar PAH complexity must be expected in any sample that may be contaminated with fossil fuels, and possibly in many other instances as well. This paper suggests, and crude oil analyses document, that this implies the presence of tens of thousands of aromatic compounds, mostly of unknown structure, with unknown spectral sensitivities and with unknown biological effects.

At the present time, the complete analytical resolution of such a mixture is not possible; few components, except for the most abundant ones, can be determined with accuracy. The application of simple analytical techniques with low resolving power may provide reproducible but erroneous data, unless preliminary screening by mass spectrometry indicates a very simple sample composition.

Similarly, the prediction, from chemical analyses, of the biological effect of a complex environmental PAH assemblage is tenuous, even if some individual compounds can be determined reliably. Numerous unknown compounds are present, and their biological effect and their influence on the measurements is likely to be unknown. The biological effects of polycyclic aromatic hydrocarbons vary dramatically with minor structural variations (*26*). Therefore, a much more detailed insight into the aliphatic and alicyclic substitution of these aromatic hydrocarbons is required for a quantitative assessment of their biological effects.

Newer analytical techniques, with greater resolving power than those used in the past, call for and make possible a re-evaluation of our knowledge of the geochemistry and of the environmental significance of polycyclic aromatic hydrocarbons. Hopefully, the present method and its combination with other powerful techniques, such as gas chromatography and high resolution mass spectrometry, will point in this direction.

ACKNOWLEDGMENT

We thank J. Sass for the sample collection and initial steps of the sample workup.

RECEIVED for review March 11, 1974. Accepted June 12, 1974. Supported by ONR (NOO 14-66 Contract CO-241) and by the National Science Foundation (Grant GA-35646). W. Giger's efforts at Woods Hole were supported by the Swiss National Research Foundation for the Advancement of Science and the Swiss Department of Commerce (Project COST 64b). Contribution No. 3390 of the Woods Hole Oceanographic Institution.

(25) M. Tissier and J. L. Oudin, Prevention and Containment of Oil Spills, Joint Conference, Proceedings, American Petroleum Institute, Washington, D.C., 205 (1973).

(26) D. Hoffmann, W. E. Bondinell, and E. L. Wynder, *Science*, **183**, 215 (1974).

Solid Sampling Atomic Absorption Determination of Lead in Rock Samples Using the Iron Screw Rod Technique

Kuppusami Govindaraju, Guy Mevelle, and Charles Chouard

Centre de Recherches Pétrographiques et Géochimiques (C.N.R.S.), 54500 Vandoeuvre-lès-Nancy, France

In analytical geochemistry, solid-sampling atomic absorption analysis is very rarely recommended. However, the authors have developed a non-solution flame atomic absorption procedure for the determination of trace levels of lead down to 1 ppm in silicate rock samples. Powdered rock sample is impregnated uniformly on an iron screw rod which is then "burnt" in the air–acetylene flame of an atomic absorption spectrometer. The recorded absorption curve (peak area) is proportional to the lead content of the sample. This solid sampling procedure needs very little sample preparation (no chemical dissolution of samples) and is practically free from matrix effects. The relative standard deviation of the results is about 5% at a level of 70 ppm and about 15% at a level of 10 ppm.

For geochemical prospection of elements of economical interest such as lead, rapid and low cost analytical procedures are necessary. Before the advent of atomic absorption spectrophotometry, the determination of trace amounts of lead (10 to 500 ppm) in silicate rock samples has been mainly by spectrographic and colorimetric methods. Nowadays, atomic absorption procedures are favorably considered for such determinations (*1–8*). In a recent paper, Govett and Whitehead (*5*) have critically studied flame atomic absorption determination of lead for geochemical exploration purposes and have drawn attention to the errors caused by the interfering effects of major elements usually present in geological materials. In order to lower detection limits, Moldan, Rubeska, and Miksovsky (*6*) have used long-path absorption tubes, and Luecke and Emmermann (*7*) the boat technique. Riandey and Pinta (*8*) have used a nonflame atomization procedure and have also studied interelement effects, notably those of Fe and Al.

Whether these analytical procedures are based on flame or nonflame atomization techniques, it is indispensable that the rock sample be first acid-dissolved before its analysis. That such a prior chemical dissolution of samples is not necessary is one of the outstanding features of our proposed solid sampling flame method. This new procedure for lead is based on the iron screw rod technique, previously developed for the rare alkali elements (*9–11*). For the rare alkali elements (Rb, Li, Cs), it is indispensable to mix the rock sample powder with an ionization buffer (NaCl, Na_2CO_3). No such buffer addition is necessary for lead.

Our solid sampling method for lead consists of impregnating uniformly an iron screw rod with rock sample powder, burning the sample-coated rod in the air–acetylene flame of an atomic absorption spectrometer, and recording the absorption curve. The integrated absorption signal is proportional to the lead content of the sample. Despite this simple method of sample preparation, the reproducibility of the results is about 5% at a level of 70 ppm and about 15% at a level of 10 ppm. The accuracy of the results has been verified by the analysis of over twenty geochemical standards. These results show the practical absence of matrix effects. The lower limit of determination is less than 1 ppm.

EXPERIMENTAL

Sample Preparation. Rock samples were ground, if necessary, to reduce them into particle sizes of about 30 to 70 μ. One-gram portions of sample powders were then poured into small polystyrene containers (diameter 20 mm, height 35 mm). Each container was then stoppered with a polyethylene cap provided with it.

Preparation of Rods. Iron screw rods of 3-mm diameter (thread of 0.5 mm), available in lengths of 1 meter, were cut into 8-cm pieces. The ends were ground to obtain even surfaces. The rods were then first cleaned with acetone. After this external decontamination step, the rods were "burnt," one after another, in the air–acetylene flame of the spectrophotometer until the absorption signal for lead returned back to the base-line level. Usually a high intensity absorption peak was observed and the burning time was about 30 sec per rod. This preliminary burning step is necessary to get lead-free iron rods.

Impregnation of Rods. For the impregnation step, the cap of the plastic container was removed and a round hole of 3-mm diameter punched at the central part of the cap with a shoemaker's awl. The container was restoppered. A preweighed (lead-free) iron screw rod was immersed in ethyl alcohol, taken out, and then dipped into the container through the hole in the cap, until the rod touched the bottom. The container was shaken and rotated manually. The rod was pulled out and the same end of the rod reintroduced into the container. These operations of shaking the container and pulling out the rod were repeated three or four times until the rod was uniformly coated with sample powder. The rod was then reweighed in order to calculate the amount of sample fixed in the thread paths of the screw rod. For the same rock sample powder, this amount varied by ±2 mg. Depending on the physical properties (density, particle size) of each sample, the amount deposited on rods varied from 45 to 75 mg.

Equipment. An atomic absorption spectrophotometer, Perkin-Elmer model 303, equipped with a Servogor Recorder (RE 511) operating at 3 cm/min, and a lead hollow cathode lamp were used (wave length, 2833 Å).

Burner Design. In the early stages of our work, we had employed a 5-cm slot burner head (nitrous oxide–acetylene burner head, Perkin-Elmer) with an air–acetylene flame. Later on, we used a round burner head (CRPG) of 6-cm diameter, specially designed for our solid sampling procedure (Figure 1), with a flame aperture in the form of three parallel rows of round holes. The holes were of 1-mm diameter, with 1-mm space between them. The number of holes were 27 for the first and the third rows and 28 for the middle one. The burner head was made of steel (18/10) and a drawing of the burner head can be obtained from the authors. With either burner head, an oxidizing flame was used and was adjusted to give maximum absorption for lead under normal solid sampling working conditions.

(1) F. N. Ward, H. M. Nakagawa, T. F. Harms, and G. H. Vansickle, *U.S. Geol. Surv. Bull.*, **1289**, 45 (1969).
(2) M. Pinta, "Spectrometrie d'Absorption Atomique," Masson and Co, Paris, 1971, Vol. 2, p 332.
(3) H. L. Kahn, F. J. Fernandez, and S. Slavin, *At. Absorption Newslett.*, **11**, 42 (1972).
(4) M. Quintin, B. Hieronymus, A. M. de Kersabiec, A. Martin, and F. Vidot, *III Int. Congr. I.C.S.O.B.A., Nice (France)*, 335 (1973).
(5) G. J. S. Govett and R. E. Whitehead, *J. Geochem. Explor.*, **2**, 121 (1973).
(6) B. Moldan, I. Rubeska, and M. Miksovsky, *Anal. Chim. Acta*, **50**, 342 (1970).
(7) W. Luecke and E. Emmermann, *At. Absorption Newslett.*, **10**, 45 (1971).
(8) C. Riandey and M. Pinta, *Analusis*, **2**, 179 (1973).
(9) K. Govindaraju, G. Mevelle, and C. Chouard, *Chem. Geol.*, **8**, 131 (1971).
(10) K. Govindaraju, G. Mevelle, and C. Chouard, *Bull. Soc. Fr. Ceram.*, **96**, 47 (1972).
(11) K. Govindaraju, R. Hermann, G. Mevelle, and C. Chouard, *At. Absorption Newslett.*, **12**, 73 (1973).



Figure 1. Burner house with rod support assembly (r) and "three rows of holes" burner head (bh). The sample rod (s) is placed just above and within the flame aperture

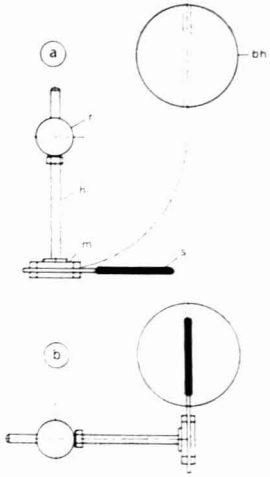


Figure 2. Rod support assembly (r)

a. Position of sample rod (s) before and after analysis. b. Position of sample rod (s) during analysis. bh. "three rows of holes" burner head. r. Rod support assembly. h. Handle. m. Magnetic strip. s. Sample rod

Rod Support Assembly. In order to position the 4-cm sample coated part of a 8-cm rod entirely inside and in parallel to the flame, a rod support assembly (Figure 1) was fixed to the left hand wing nuts of the burner tripod stand. The rod support is pivotable and adjustable, and it permits the placing of rods under practically identical conditions, with the flame aperture oriented either parallel or perpendicular (Figure 2) to the hollow cathode beam. The parallel position is used only for samples containing less than 10 ppm of Pb.

Procedure. The sample rod was first set in its preanalysis position (Figure 2*a*) with the non-impregnated part on the magnetic strip (m). The handle (h) was rotated so as to position the sample-coated part of the rod entirely inside the flame and at about 12 mm above the burner holes (Figure 2*b*). Simultaneously the absorption signal was recorded with the recorder paper running at 3 cm/min. The signal was recorded until it returned to the base line. The time for recording such an absorption curve was about 30 to 100 sec (Figure 3). Initially, with flame on, the recorder was adjusted to give a base line of about 10 divisions on the recorder scale. And then it was adjusted to give a peak height of 70–80 divisions for a natural geochemical standard whose value for Pb was approximately close to the highest concentration expected in the unknown samples.

In the case of the analysis, for instance of 25 samples, the impregnation step was first carried out by preparing 25 sample rods (one rod for each sample) and 5 "standard" rods with one high standard (primary standard). Each rod was weighed before and after the impregnation step. For the analysis of common silicate rock samples, the Diorite DR-N (*12*) with its lead content of 65 ppm was chosen as the primary standard. Beginning with a standard rod, five unknown sample rods were burnt, one after another, and their respective absorption curves recorded. In the same manner, the burning of one standard rod followed by five more sample rods was continued until all the 30 rods were burnt. The absorption curves were then cut from the base line and weighed. Typical recorder tracings of absorption curves are shown in Figure 3.

Because the amount of sample deposited on the rods might differ according to rock sample types, the integrated absorption signal (z) was calculated for a constant sample weight (100 mg). If the weight of the volume of paper under the absorption curve was x mg for y mg of sample on the rod, the z value is 100 x/y. The z values were first calculated for all the unknown samples and the mean z value for the standards. Under normal working conditions, the individual z values for the standards did not differ between themselves by more than 5% of the mean value. If the mean z value for the standard diorite DR-N (Pb, 65 ppm) was 52 mg, 1 mg of z value was equivalent to 1.25 ppm of lead. The z value of each unknown sample was multiplied by 1.25 ppm to determine its lead content.

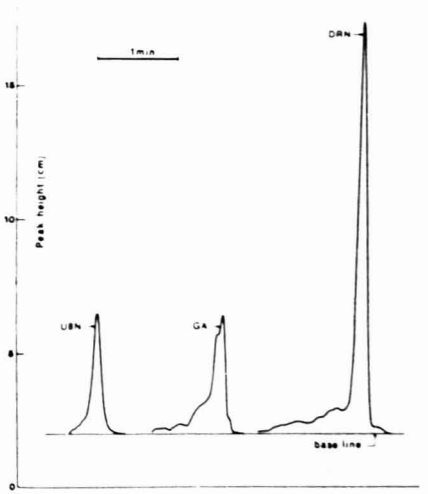


Figure 3. Examples of lead absorption curves for three rock samples: diorite DR-N = 65 ppm; granite GA = 26 ppm; serpentine UB-N = 20 ppm

(12) H. de la Roche and K. Govindaraju, *Bull. Soc. Fr. Ceram.*, **100**, 49 (1973).

Table I. Study of Interelement Effect

Sample mixture[a]	Sample deposited on rod, mg	"Peak volume," mg	z value, mg	Pb, ppm[c]
DR-N + Fe_2O_3	80	40	50.0	30.7
DR-N + Al_2O_3	57	29	50.9	31.3
DR-N + SiO_2	40	22	55.0	33.8
DR-N + MgO	43	24	55.8	34.3
DR-N + $CaCO_3$	58	34	58.6	36.0
DR-N + Na_2CO_3	58	30	51.7	31.8
DR-N + K_2CO_3	60	32	53.3	32.7
DR-N[b]	69	73	105.8	65

[a] Sample mixture containing 300 mg of diorite DR-N (Pb, 65 ppm) and 300 mg of interfering compound. [b] Undiluted diorite DR-N. [c] Pb content calculated with undiluted DR-N as primary standard (Pb, 65 ppm).

RESULTS AND DISCUSSION

In analytical geochemistry, the applications of atomic absorption spectrophotometry are ever-increasing but are strictly limited to acid-dissolved rock sample solutions. Our iron screw rod powder technique is, therefore, a new approach. Some particular problems encountered during the development of this direct method of analyzing rock sample powders are discussed.

Solid Sampling. *Sample Feed.* When sample solutions are fed into flame, a regular sample-feed rate is necessary for recording reproducible absorption signals. In solid sampling analysis, it is difficult to maintain constant feed rates particularly with geological materials which are, in general, of varying physical properties (particle size, density, fluidity). One of the rare procedures proposed for solid sampling analysis is that of Gilbert (*13*) who disperses the powder which is handled like a solution. An eventual routine application of this procedure would require a close control of the uniformity of particle size and also of memory effects between samples.

Instead of trying to maintain a constant sample-feed rate, we introduce, for each sample, a known amount of sample powder impregnated on an iron screw rod and then burn it in the flame to record the total absorption curve. By calculating z values, each absorption signal is related to a constant amount of sample (100 mg).

Burning Conditions. Even with a known amount of sample introduced into the flame, at least two more conditions should be fulfilled for obtaining reproducible results: Maintenance of rod within the flame in a geometrically identical position from sample to sample; and full coverage of the sample-coated part of the rod well within the flame.

The rod support assembly (Figures 1 and 2) permits sample rods to be maintained under practically identical conditions within the flame.

For fully covering the sample-coated part of the rod well within the flame, a new burner head (CRPG, Figure 1) was designed. The cross section of the flame obtained with CRPG burner head is slightly larger than that of the Perkin-Elmer N_2O–C_2H_2 burner head. The time for recording a total absorption curve was less for the CRPG burner head (30 sec) than for the N_2O–C_2H_2 burner head (50 sec). But for all practical purposes, the latter burner could be used.

Peak Area vs. Peak Height. During the development of our solid-sampling procedure for lead, it soon became apparent that the peak area recorded for a given sample represented more truly than the corresponding peak height the concentration of lead in the sample. In fact, for rock samples containing nearly the same amount of lead but of otherwise different chemical composition, the peak areas were nearly equal but the peak heights were much different. It was further observed that, for the same sample, the peak area was directly proportional to the amount of sample fixed on the rods. From these observations, it was decided to calculate the z value for each sample.

Precision of Results. *Reproducibility.* The preceding discussion on solid sampling has been mainly directed toward obtaining reproducible results. In this connection, the particle size of solid samples is also important. A detailed study on particle size effect was carried out on a geochemical standard, granite GH (Pb, 50 ppm), which was available in our laboratory in different particle size ranges. The lead content of the different sieve fractions was determined. Reproducible results in the range of 45 to 55 ppm were obtained for the sieve fractions of less than 100 μ. For particles greater than 100 μ, the results were systematically lower than the recommended value. In addition, it was observed that with coarse particles, the powder did not stick well to the rod and had tendency to fall off on contact with the flame. The peak heights recorded with fine particles (<50 μ) were much steeper than those recorded with coarse particles (>100 μ). The authors recommend the particle size range from 30 to 70 μ. In normal routine work, repeated analyses yield results reproducible to about 5% at a level of 70 ppm and to about 15% at a level of 10 ppm.

Matrix Effect. It has been reported that errors in atomic absorption determination of Pb may occur due to the presence of Fe, Al, Ca, Mg, Na, and K in sample solution with flame (*5*) or nonflame (*8*) methods. In *solution analysis*, it is usual practice to study interelement effects by preparing a set of sample solutions containing both the interfering elements and the element to be determined at different levels of concentration.

In Solid Sampling Analysis, the preparation of powder mixtures containing one or more interfering elements raises several practical difficulties due, in particular, to the differences in physical properties between the added substances and the natural rock sample. For example, the interfering element potassium may be added to the test mixture in the form of K_2CO_3. In the rock sample, K may be present in a particular mineral species (for instance, in potash feldspar). The interfering effect of K, present in the powder mixture as K_2CO_3 may not be the same as that of K in a feldspar-rich silicate rock sample. In addition, it is difficult to prepare homogeneous powder samples, particularly when several interfering elements, at varying levels of concentration, are to be mixed together. In view of these practical difficulties, it was decided to prepare synthetic powder mixtures containing only one interfering element at a time. A set of seven sample mixtures was prepared by mixing one diorite sample (300 mg) with an equal amount of Fe_2O_3, Al_2O_3, SiO_2, MgO, $CaCO_3$, Na_2CO_3, or K_2CO_3. As seen from Table I, the integrated signal measured (z value) for each of the seven test mixtures was approximately half

(13) P. T. Gilbert, *Anal. Chem.*, **34**, 1025 (1962).

Table II. Lead in Geochemical Standards, ppm[a]

Geochemical standards	AA values, this paper	R.V. or P.V.	Published values (*12, 14–19*) SG $\bar{x}$	SG n	FX $\bar{x}$	FX n	CC $\bar{x}$	CC n	CP $\bar{x}$	CP n	SM $\bar{x}$	SM n	AA $\bar{x}$	AA n
C.R.P.G. (*14*)														
Granite GR	36	32	34	12	43									
Granite GA	29	26	24	16	38	2	11	1	30	1				
Granite GH	52	50	42	14	52	2			55	1	58	1		
Basalt BR	6	16	13	10	13	2	8	1	30	1				
Biotite Mica-Fe	12	17	18	8					20	1	10	1		
Phlogopite Mica-Mg	9	...	18	2										
A.N.R.T. (*12*)														
Diorite DR-N	*	65	67	9	47	3			80	1				
Serpentine UB-N	18	20	21	7	28	3			30	1				
Bauxite BX-N	158	...	144	2	186	3	205	1					157	1
Disthène DT-N	34	...	25	4	30	2								
(Granite GS-N)	68													
(Feldspar FK-N)	255													
U.S.G.S. (*16, 17*)														
Granite G-2	32	31.2	29	11	26	4	31	2			30.8	1		
Granodiorite GSP-1	60	51.3	47	11	53	4	63	3			58.7	1	52	1
Andesite AGV-1	40	35.1	32	11	34	4	40	2			36.5	1	40	1
Basalt BCR-1	18	17.6	17	8	13	3	21	2			13.6	1		
Periodotite PCC-1	9	13.3	13	3	7	2	7	1						
Dunite DTS-1	10	14.2	14	3	11	2	12	2						
G.S.J. (*18*)														
Granodiorite JG-1	27	24	25.5	2									23.5	4
Basalt JB-1	8	14	14.5	1									13.5	2
N.I.M. (*19*)														
Lujavrite L	51	45	46	4	44	3			40	1				
Granite G	42	38	30	4	48	3			40	1				
Pyroxenite P	1.5	<10	9	1	6.5	2								
Norite N	1.5	<10			8	2			20	1				
Syenite S	3	13	9	1	4.5	2			10	1				
Dunite D	1.6	<10	9	1	10	2								

[a] R.V. = Recommended value; P.V. = Proposed value. $\bar{x}$ = mean value of n results. Published values taken from Ref. *12, 14–19* and grouped according to the analytical methods employed: SG = spectrography; FX = X-ray fluorescence; CC = Chemical methods; CP = Paper chromatography; SM = Mass spectrometry; AA = Atomic absorption. * Diorite DR-N was used as the primary standard (Pb, 65 ppm) for all the samples except for Bauxite BX-N and Feldspar FK-N. The latter two samples were analyzed with glass standard VS-N (Ref. *15*, Pb, 1100 ppm). Granite GS-N and Feldspar FK-N are new A.N.R.T. standards actually under cooperative study.

that recorded for the diorite sample (Pb, 65 ppm) without dilution, although the recorded peak heights varied greatly between themselves. Apparently, our iron screw rod technique is practically free from matrix effects, provided that z value is calculated for each sample.

Further confirmation on the accuracy of our results for lead comes from the analysis of several geochemical standards. These results are compared with those obtained by different analytical methods (Table II) and also with the recommended or proposed values for these standards.

These reference samples are of widely differing chemical composition and represent a very wide range of silicate rock and mineral samples. In general, our results are in agreement with the values recommended for the geochemical standards of long standing such as those from CRPG (*14*) and USGS (*16*). It is also seen from Table II that agreement between different analytical methods is not always excellent. The problem of valid reference materials for trace elements analysis is not a new one and has been discussed elsewhere (*15*).

To summarize, with an extremely simple method of sample preparation, our solid sampling flame atomic absorption procedure permits the determination of trace amounts of lead down to 1 ppm in rock samples. The method is practically free from matrix effects. The reproducibility of the results is, in general, better than 10%.

RECEIVED for review December 12, 1973. Accepted April 19, 1974.

(14) M. Roubault, H. de la Roche, and K. Govindaraju, *Sci. Terre*, **15**, 351 (1970).
(15) H. de la Roche and K. Govindaraju, *Analusis*, **2**, 59, (1973).
(16) F. J. Flanagan, *Geochim. Cosmochim Acta*, **33**, 81 (1969).
(17) F. J. Flanagan, *Geochim. Cosmochim Acta*, **37**, 1189 (1973).
(18) A. Ando, H. Kurasawa, T. Ohmori, and E. Takeda, *Geochem. J.*, **5**, 151 (1971).
(19) B. G. Russel, R. G. Goudvis, G. Domel, and J. Levis, National Institute for Metallurgy, Johannesburg, Report No. 1351 (1972).

Method for the Choice of Optimal Analytical Positions in Spectrophotometric Analysis of Multicomponent Systems

J. Šustek

Research Institute of Agrochemical Technology, 810 04 Bratislava-Predmestie, Czechoslovakia

The relative standard deviations of the absorptivities are suggested as a criterion for the choice of optimal analytical positions in spectrophotometric analysis of multicomponent mixtures. The method was applied to a 5-component model system simulated by means of a computer. The model spectrum was approximated by the linear combination of ten Lorentzian functions. In the case of overdetermined linear absorption equations, three- to fourfold overdetermination offers satisfactory results. A further increase of the number of analytical positions has no practical significance and in some cases may reduce accuracy and precision of the determination.

If an overdetermined system of linear equations is used in the spectrophotometric analysis of multicomponent mixtures (*1–3*), the problem arises as to what extent the system must be overdetermined in order to obtain sufficiently precise and accurate results.

The influence of the choice of wavelengths on the stability of the system of linear absorption equations was studied by Zscheile *et al.* (*4*), and it has been confirmed that the highest precision for the determination of the component concentrations may be reached by using all available wavelengths. Most of the authors (*5–11*) consider the number of 20–50 analytical positions as sufficient. Drozdov-Tikhomirov (*12*) measured as many as 145 absorbance values on equally spaced wavenumber intervals. With such a procedure, the number of experimental data for processing increases rapidly with increasing number of the analyzed components.

Recently, more and more papers dealing with the choice of the optimal analytical positions have appeared. The authors start from the presumption that for each component, and therefore also for each system, there is a limited optimal number of analytical positions, the increasing of which has no essential influence on the precision of the determination of the component concentrations. Gudym and Vorob'eva (*13*) mention that the increase of the number of analytical positions may lead to a decrease of the analysis precision because errors due to the overlapping of absorption bands are introduced into the system.

The problem is to find the suitable criterion for the choice of the optimal analytical positions. For two-component systems the concentration determination error may be used as a criterion (*5, 14–16*). With a greater number of analytical positions and increasing the number of the components, calculation difficulties appear because the respective functions have to be calculated for all possible combinations. As a simple criterion, the ratios of the absorbances and the absorptivities, respectively, of the components being determined to those of the remaining components were used (*3, 17–19*). Other criteria for the choice of the optimal analytical positions for the determination of multicomponent mixtures are mentioned by Kats in his review (*20*).

In the present paper the procedure for the choice of the optimal analytical positions is described for the case where the system of overdetermined linear equations is solved by the method of least squares. The effectiveness of this procedure was verified with a model system.

THEORY AND CALCULATIONS

Assuming the validity of the Lambert–Beer's law and the additivity of the absorbances of the components, the matrix of the component concentrations in the samples can be calculated from the equation

$$\mathbf{X} = \mathbf{QB} \tag{1}$$

where

$$\mathbf{Q} = (\mathbf{K}^T\mathbf{K})^{-1}\mathbf{K}^T \tag{2}$$

and

$$\mathbf{K} = \mathbf{A}\mathbf{C}^T(\mathbf{C}\mathbf{C}^T)^{-1} \tag{3}$$

It can be seen from Equations 1–3 that the absorptivities matrix **K** has an influence on the results of the determination of the component concentrations in the samples. Moreover, the elements of the main diagonal of the matrix $(\mathbf{K}^T\mathbf{K})^{-1}$ appear in the equation for the calculation of the standard deviation of the particular component concentrations (*3*). To be allowed to eliminate the absorptivities which are subject to measuring errors, it is necessary to know the precision of the calculation of the particular elements of the matrix **K**, characterized by the standard deviations of the absorptivities.

If the number of the analytical positions is greater than the number of components being determined, the system of the linear absorption equations is overdetermined and it is necessary to introduce a further variable, the matrix of the residuals of the mixture absorbances $\mathbf{E}_A$:

$$\mathbf{E}_A = \mathbf{KC} - \mathbf{A} \tag{4}$$

into the relation between absorbance and concentration

(1) A. F. Vasil'ev, *Zavod. Lab.*, **31,** 677 (1965).
(2) Z. Przybylski, *Chem. Anal. (Warsaw)*, **13,** 453 (1968).
(3) J. Šustek, M. Livař, and O. Schiessl, *Chem. Listy*, **66,** 168 (1972).
(4) F. P. Zscheile, H. C. Murray, G. A. Baker, and R. G. Peddicord, *Anal. Chem.*, **34,** 1776 (1962).
(5) J. C. Sternberg, H. S. Stillo, and R. H. Schwendeman, *Anal. Chem.*, **32,** 84 (1960).
(6) I. S. Herschberg and F. L. J. Sixma, *Koninkl. Ned. Akad. Wetenschap. Proc., Ser. B.*, **65,** 244 (1962).
(7) H. Cerfontain, H. G. J. Duin, and L. Vollbracht, *Anal. Chem.*, **35,** 1005 (1963).
(8) I. S. Herschberg, *Fresenius' Z. Anal. Chem.*, **205,** 180 (1964).
(9) J. M. Arends, H. Cerfontain, I. S. Herschberg, A. J. Prinsen, and A. C. M. Wanders, *Anal. Chem.*, **36,** 1802 (1964).
(10) K. Doerffel, P. Kugler, and H. J. Binder, *Z. Chem.*, **6,** 155 (1966).
(11) H. Schmidt, *Erdoel Kohle, Erdgas, Petrochem.*, **19,** 275 (1966).
(12) L. N. Drozdov-Tikhomirov, *Opt. Spektrosk.*, **17,** 683 (1964).
(13) V. K. Gudym and G. A. Vorob'eva, *Zavod. Lab.*, **38,** 778 (1972).
(14) C. E. Berry, *Ann. Math. Stat.*, **16,** 398 (1945).
(15) J. Swietoslawska, *Rocz. Chem.*, **30,** 569 (1956).
(16) A. F. Vasil'ev, *Zavod. Lab.*, **31,** 1331 (1965).
(17) Z. Przybylski, *Chem. Anal. (Warsaw)*, **14,** 1047 (1969).
(18) M. D. Kats and M. Ya. Rozkin, *Zavod. Lab.*, **38,** 688 (1972).
(19) M. D. Kats, *Zh. Prikl. Spektrosk.*, **18,** 508 (1973).
(20) M. D. Kats, *Zavod. Lab.*, **39,** 160 (1973).

(3). The standard deviation of the absorbance at the gth analytical position is then calculated using the equation

$$s_{Ag} = \sqrt{\frac{\sum_{i=1}^{m} e^2_{Agi}}{m - n}} \quad (5)$$

The values $\sum_{i=1}^{m} e^2_{Agi}$ are elements of the main diagonal of the matrix $(\mathbf{E}_A \mathbf{E}_A{}^T)$.

The standard deviation of the absorptivity of the jth component at the gth analytical position is calculated using the equation

$$s_{Kgj} = s_{Ag} \sqrt{h_{jj}} \quad (6)$$

where h_{jj} is the jth element of the main diagonal of the matrix $(\mathbf{C}\,\mathbf{C}^T)^{-1}$.

The values of the standard deviations of the absorptivities are not suitable as a criterion for the choice of the optimal analytical positions. In fact, the same absolute values s_{Kgj} are of different weight for the absorptivities corresponding to the absorption band maxima and for those near the inflection point or in the minima. We used, therefore, the relative standard deviations of the absorptivities

$$r_{Kgj} = \frac{s_{Kgj}}{k_{gj}} \times 100 \quad (7)$$

expressed in per cent, as a criterion for the choice of the optimal analytical positions. The values r_{Kgj} were calculated for each component at all the k analytical positions investigated. The analytical position at which the value r_{Kgj}, calculated for the given component, was the least, was considered as the optimum one for this component.

EXPERIMENTAL

Computer System. All computations concerning the preparation of a model system, the computations of the calibration data and of the concentration of the components in the samples, and the statistic evaluation of the results were carried out on a Gier digital computer (Regnecentralen), equipped with a plotter. The programs were written in ALGOL (version GIER-ALGOL 4).

Model System. The 5-component model system was simulated by means of a computer. The model spectrum, in which two absorption bands, approximated by Lorentzian functions (*21*, *22*), appertain to each component, is shown in Figure 1. The absorptivities of the band maxima a_g and the concentration ranges of the particular components c_{ji} in the calibration mixtures are given in Table I. The concentrations of the components in the calibration mixtures representing the elements of the matrix $\mathbf{C}$ (n = 5, m = 30) were chosen in a way to give the truest possible picture of the technical products composition. The concentration of the components in the model sample were as follows: c_1 = 0.65, c_2 = 0.10, c_3 = 0.05, c_4 = 0.05, and c_5 = 0.15. The computed total absorbances at the analytical positions g = 1–32 (the sum of the absorbances of the components j = 1–5) were assembled into the matrix $\mathbf{A}$ (k = 32, m = 30) and the total absorbances computed for 10 repeat determinations of the model sample were assembled into the matrix $\mathbf{B}$.

The random errors, the values of which were within the interval from 0 to 0.040, were introduced into the matrices $\mathbf{A}$ and $\mathbf{B}$. The distribution of these errors was given by the Gaussian function. The distribution of the errors over the particular analytical positions was carried out by means of a digital computer in a way that their random selection was secured by the program. We considered three variants of the model system: Model System I—without random errors (at the computing only errors due to the rounding off of the absorbances to three decimal places occur, which corresponds to common reading precision); Model System II—random errors at selected analytical positions g = 7, 13, 17, 23, 29 (the maxima of the absorption bands of the particular components); and Model System III—random errors at all analytical positions, g = 1–32.

(21) D. Papoušek and J. Pliva, *Collect. Czech. Chem. Commun.*, **30**, 3007 (1965).
(22) D. Audo, Y. Armand, and P. Arnaud, *J. Mol. Struct.*, **2**, 287 (1968).

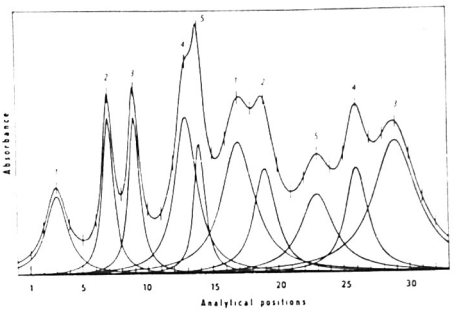


Figure 1. Model spectrum
Numbers at the maxima denote components corresponding to the absorption bands

Table I. Absorptivities and Concentration Range of Component

Component j	Analytical position g	Absorptivity a_g	Concentration range c_{ji}
1	3	0.3	0.6–1.0
	17	0.5	
2	7	0.6	0–0.2
	19	0.4	
3	9	0.6	0–0.1
	29	0.5	
4	13	0.6	0–0.2
	26	0.4	
5	14	0.5	0–0.3
	23	0.3	

Table II. Sequence of Added Analytical Positions

Model system	No. of analytical positions, k	Added analytical positions for the components 1	2	3	4	5		
I	5	17[a]	7[a]	9[a]	13[a]	14[a]		
	10	3[a]	19[a]	29[a]	26[a]	23[a]		
	15	16	6	10	12	22		
	20	4	20	30	25	24		
	25	2	18	28	27	21		
	32	1	5	8	11	15	31	32
II	5	16	19[a]	9[a]	26[a]	14[a]		
	10	18	20	28	12	24		
	15	3[a]	8	30	25	22		
	20	15	6	27	11	21		
	25	2	5	31	10	23[a]		
	32	4	7[a]	32	13[a]	1	17[a]	29[a]
III	5	17[a]	7[a]	9[a]	13[a]	14[a]		
	10	18	19[a]	29[a]	26[a]	23[a]		
	15	16	20	30	12	22		
	20	3[a]	8	28	27	24		
	25	15	6	31	25	21		
	32	4	5	32	11	10	2	1

[a] Analytical positions corresponding to the absorption bands maxima.

RESULTS AND DISCUSSION

For 32 equidistant analytical positions (Figure 1), the values of r_{Kgj} were computed from Equation 7. For each component, the analytical position was chosen to which the lowest value of r_{Kgj} appertained. Analytical positions with higher values of r_{Kgj} were added successively. The sequence of the added analytical positions for Model Systems I–III is given in Table II.

Table III. Relative Accuracy δ_j of Concentrations Means

Model system	No. of analytical positions k	δ_j[%] 1	2	3	4	5
I	5	−0.111	−0.819	−1.460	2.470	−0.903
	10	−0.070	−0.332	−1.614	1.532	−0.432
	15	−0.077	−0.309	−1.380	1.264	−0.197
	20	−0.082	−0.429	−0.738	1.152	−0.051
	25	−0.036	−0.386	−0.702	1.310	−0.099
	32	−0.018	−0.416	−0.490	1.080	−0.039
II	5	−0.106	0.967	−1.614	0.992	−0.655
	10	−0.043	0.480	−1.418	0.574	−0.371
	15	−0.046	0.417	−0.648	0.072	−0.067
	20	−0.020	0.222	−0.398	0.274	−0.043
	25	0.031	0.243	−0.392	1.677	−0.995
	32	0.191	−2.628	4.439	−7.300	0.211
III	5	−0.844	−2.992	4.430	6.725	1.505
	10	−0.622	−1.712	1.660	5.739	0.842
	15	−0.314	−1.338	−1.985	4.831	1.496
	20	−0.070	−2.175	−3.322	3.446	1.355
	25	−0.035	−2.177	−3.777	3.159	1.492
	32	0.013	−2.211	−2.597	3.442	1.377

Table IV. Standard Deviations s_j of Component Concentrations

Model system	No. of analytical positions, k	s_j 1	2	3	4	5
I	5	0.001	0.001	0.001	0.001	0.001
	10	0.000	0.000	0.001	0.001	0.001
	15	0.001	0.000	0.001	0.001	0.000
	20	0.001	0.000	0.000	0.001	0.000
	25	0.000	0.000	0.000	0.001	0.000
	32	0.000	0.000	0.000	0.001	0.000
II	5	0.001	0.001	0.001	0.001	0.001
	10	0.000	0.001	0.001	0.000	0.001
	15	0.000	0.000	0.000	0.000	0.000
	20	0.000	0.000	0.000	0.000	0.000
	25	0.000	0.000	0.000	0.002	0.004
	32	0.004	0.006	0.003	0.008	0.005
III	5	0.013	0.009	0.007	0.010	0.009
	10	0.009	0.007	0.005	0.008	0.009
	15	0.009	0.007	0.004	0.008	0.010
	20	0.012	0.007	0.005	0.007	0.008
	25	0.011	0.007	0.005	0.006	0.008
	32	0.012	0.007	0.004	0.007	0.009

This way we obtained, apart from the absorbances matrix **A** (k = 32), five submatrices $\mathbf{A}_1$–$\mathbf{A}_5$ (k = 5, 10, 15, 20, 25), which were used at the computation of the calibration data. Similarly, the matrix **B** and the submatrices $\mathbf{B}_1$–$\mathbf{B}_5$ were obtained. By multiplying these matrices with the corresponding matrices Q according to Equation 1, the matrix **X** and the submatrices $\mathbf{X}_1$–$\mathbf{X}_5$ were obtained, representing the set of 10 repeat determinations of the component concentrations in the model sample.

The influence of the number of analytical positions on the accuracy of the results was evaluated on the basis of the relative accuracy of the concentration means given by

$$\delta_j = \frac{(c_j - \bar{x}_j)}{c_j} \times 100 \qquad (8)$$

where c_j is the known concentration of the component j in the model sample and $\bar{x}_j$ represents the average of ten determinations of the component j. The values of δ_j, computed for Model Systems I–III, are given in Table III. In Table IV, the standard deviations of the concentrations given by

$$s_j = \sqrt{\frac{\sum_{i=1}^{m} (c_j - x_{ji})^2}{m - 1}} \qquad (9)$$

are presented, by means of which the precision of the determination (m = 10) was evaluated.

No random errors were introduced into the Model System I, and therefore the r_{Kij} values differed from zero only in the case of the lowest k_{ij} values. The other analytical positions were arranged in a sequence of decreasing values of k_{ij}. On the other hand, in the case of Model System III, the random errors were introduced to all analytical positions, their distribution having a statistical character. The values of s_{Aij}, calculated from Equation 5 were very close to each other and the magnitude of the absorptivities at the particular analytical positions had a significant influence on the values of r_{Kij}, which were calculated from Equation 7. As for Model System II, random errors were introduced only into selected analytical positions. Even though these positions appertain to the maxima of the absorption bands of the particular components, the corresponding values of r_{Kij} were of a higher order than in the case of the remaining analytical positions.

From Tables III and IV, it can be seen that, in Model System I, the accuracy and precision of the determination of the component concentrations increases with the increase of the number of analytical positions, which is in accordance with the theory. In Model System III, accuracy and precision are influenced by two factors compensating each other. Apart from the positive influence of the increase of the number of analytical positions, there appears also the negative influence of the random errors which are introduced into the system by successive addition of analytical positions with higher values of r_{Kij}. The increase of accuracy and precision is not so clean-cut as in the case of Model System I. With Model System II, first the positive influence of the increase of the number of analytical positions is predominant and then the negative influence of the random errors. Especially the last adding of analytical positions, which are subject to random errors, significantly decreased accuracy and precision.

From the comparison of the values of δ_j and s_j for Model Systems I–III, it can be seen that a three- to fourfold overdetermination of the system of linear absorption equations offers satisfactory results even in case of overlapping of the

absorption bands. A further increase of the number of analytical positions has no practical significance and, in some cases, it may reduce accuracy and precision of the determination.

NOMENCLATURE

k = number of analytical positions
m = number of mixtures (samples)
n = number of components
$g = 1, 2, \ldots, k$ = sequence of the analytical position
$i = 1, 2, \ldots, m$ = sequence of the mixture (sample)
$j = 1, 2, \ldots, n$ = sequence of the component
$\mathbf{A}$ = absorbances matrix of the calibration mixtures ($k \times m$ matrix)
$\mathbf{B}$ = absorbances matrix of the samples ($k \times m$ matrix)
$\mathbf{C}$ = matrix of the component concentrations in the calibration mixtures ($n \times m$ matrix)
$\mathbf{C}^T$ = transpose of the matrix $\mathbf{C}$ ($m \times n$ matrix)
$\mathbf{E_A}$ = matrix of the residues of the mixture absorbances ($k \times m$ matrix)
$\mathbf{E_A}^T$ = transpose of the matrix $\mathbf{E_A}$ ($m \times k$ matrix)
$\mathbf{K}$ = absorptivities matrix ($k \times n$ matrix)
$\mathbf{K}^T$ = transpose of the matrix $\mathbf{K}$ ($n \times k$ matrix)
$\mathbf{Q}$ = matrix for the calculation of the concentrations ($n \times k$ matrix)
$\mathbf{X}$ = matrix of the component concentrations in the samples ($n \times m$ matrix)
a_{gi} = element of the matrix $\mathbf{A}$ (absorbance of the ith mixture at the gth analytical position)
c_{ji} = element of the matrix $\mathbf{C}$ (concentration of the jth component in the ith mixture)
$e_{\mathrm{A}gi}$ = element of the matrix $\mathbf{E_A}$ (residue of the absorbance of the ith mixture at the gth analytical position)
k_{gj} = element of the matrix $\mathbf{K}$ (absorptivity of the jth component at the gth analytical position)
x_{ji} = element of the matrix $\mathbf{X}$ (concentration of the jth component in the ith sample)
$s_{\mathrm{A}g}$ = standard deviation of the absorbance at the gth analytical position
$s_{\mathrm{K}gj}$ = standard deviation of the absorptivity of the jth component at the gth analytical position
$r_{\mathrm{K}gj}$ = relative standard deviation of the absorptivity of the jth component at the gth analytical position (in per cent)
$\hat{o}_j$ = relative accuracy of the concentration mean (in per cent)
s_j = standard deviation of the concentration

RECEIVED for review October 29, 1973. Accepted April 15, 1974.

Spectrophotometric Determination of Micro Amounts of Hexathionate in Mixtures with Thiosulfate and Sulfite by Means of Its Sulfitolysis

Tomozo Koh and Kazuo Taniguchi

Department of Chemistry, Faculty of Science, Tokai University, Hiratsuka-shi, Kanagawa, Japan

A spectrophotometric method has been developed for the determination of hexathionate in mixtures with thiosulfate and sulfite. The method is based on the formation of thiosulfate equivalent to the hexathionate, and on the spectrophotometric measurement of the excess iodine for reaction with the thiosulfate. The conditions for hexathionate to be stoichiometrically converted to thiosulfate were established by varying the pH, reaction time, and amount of sulfite. A stability of thiosulfate in the presence of sulfite and the effect of pH on masking the excess sulfite with formaldehyde also were examined. The method could be successfully applied to the determination of hexathionate, thiosulfate, and sulfite when mixed in various ratios, and gave a relative standard deviation of 2.2% at the 0.5 μmole level of hexathionate.

It is important and desirable, from a viewpoint of sulfur chemistry, to determine micro amounts of polythionates in mixtures with the other sulfur compounds. For example, when one mole of polythionate (tri-, tetra-, penta-, and hexathionate) reacts with cyanide, sulfite, sulfide, and hydroxide, the mole number of thiosulfate being formed is different in each case. Therefore, the above reactions of polythionate must be studied in detail to determine a specific polythionate in the presence of other polythionates.

With regard to the cyanolysis of polythionates, photometric methods for the determination of trithionate (*1–3*), tetrathionate (*4–7*), pentathionate (*7–8*), and hexathionate (*7, 9*), based on the formation of thiocyanate, have been described. Methods for the determination of polythionates in mixtures with each other (*10*) and total amounts of polythionates in mixtures (*11*) were devised by the authors. They are based, respectively, on the photometric determination of different amounts of thiocyanate formed by the cyanolysis of polythionate in the presence and absence of cupric ions, and on the spectrophotometric measurement of an excess iodine for thiosulfate formed.

Iwasaki and Suzuki have proposed a photometric method (*12*) for the determination of tetrathionate, which is based on the consumption of iodine by thiosulfate formed

(1) P. J. Urban, *Fresenius' Z. Anal. Chem.*, **179**, 422 (1961).
(2) D. P. Kelley, L. A. Chambers, and P. A. Trudinger, *Anal. Chem.*, **41**, 898 (1969).
(3) T. Koh, A. Wagai, and Y. Miura, *Anal. Chim. Acta*, in press.
(4) O. A. Nietzel and M. A. DeSesa, *Anal. Chem.*, **27**, 1839 (1955).
(5) P. J. Urban, *Fresenius' Z. Anal. Chem.*, **180**, 110 (1961).
(6) T. Koh and I. Iwasaki, *Bull. Chem. Soc. Jap.*, **39**, 352 (1966).
(7) T. Koh, N. Saito, and I. Iwasaki, *Anal. Chim. Acta*, **61**, 449 (1972).
(8) T. Koh, *Bull. Chem. Soc. Jap.*, **38**, 1510 (1965).
(9) T. Koh and I. Iwasaki, *Bull. Chem. Soc. Jap.*, **38**, 2135 (1965).
(10) T. Koh and I. Iwasaki, *Bull. Chem. Soc. Jap.*, **39**, 703 (1966).
(11) T. Koh and K. Taniguchi, *Anal. Chem.*, **45**, 2018 (1973).
(12) I. Iwasaki and S. Suzuki, *Bull. Chem. Soc. Jap.*, **39**, 576 (1966).

from tetrathionate by its sulfitolysis, and Blasius and Münch a coulometric method (*13*) for polythionates. However, no consideration has been given to the spectrophotometric determination of hexathionate by means of its sulfitolysis.

In the present study, the following reaction,

$$S_6O_6^{2-} + 3SO_3^{2-} = 3S_2O_3^{2-} + S_3O_6^{2-} \quad (1)$$

was investigated in detail, and the conditions under which hexathionate is stoichiometrically converted to thiosulfate were established. The present method is based on the formation of thiosulfate equivalent to hexathionate, and on the spectrophotometric measurement of an excess iodine for the thiosulfate. A procedure for the analysis of mixtures of hexathionate, thiosulfate, and sulfite also is described.

EXPERIMENTAL

Apparatus. Spectrophotometric measurements were made with a Shimazu Model QV-50 spectrophotometer with 1-mm quartz cells. pH measurements were made with a Hitachi-Horiba Model M-7 pH meter.

Reagents. All other chemicals used, besides hexathionate, were of an analytical grade and were used without further purification.

Hexathionate. Potassium hexathionate was prepared as described by Goehring and Feldmann (*14*). The hexathionate so obtained was recrystallized twice in an acid medium of 2*N* hydrochloric acid, and then dried at room temperature before storage at −10 ± 2 °C. The water content physically adsorbed on the hexathionate was estimated to be 0.29% by the Karl Fischer method. It was confirmed that the hexathionate was pure enough for the present purpose; its purity was estimated by determining the total potassium and sulfur contents (*9*).

StandardHexathionate Solution ($1.0 \times 10^{-3}M$). Dissolve 183.8 mg of potassium hexathionate (water content 0.29%) in redistilled water and dilute to 500 ml. The standard hexathionate solution was stored at 5 ± 2 °C.

Standard Sulfite Solution. Dissolve sodium hydrogen sulfite in freshly boiled and cooled redistilled water, and standardize by iodometry. Prepare working standards by appropriate dilution. Sulfite solution (0.15*M*), which was not standardized and used for the sulfitolysis of hexathionate, proved useful for 2 weeks after its preparation.

Standard Thiosulfate Solution. Dissolve sodium thiosulfate pentahydrate in freshly boiled and cooled redistilled water containing a small amount of sodium carbonate, and standardize by iodometry a week after preparation. Prepare working solutions by suitable dilution. These standards were used to ascertain stoichiometry and completion of the reaction of hexathionate with sulfite. Sodium carbonate was added as a stabilizing agent.

Standard Iodate–Iodide Solution. Add 50.0 ml of $1.0 \times 10^{-2}N$ iodate obtained by diluting 0.1*N* standard iodate to a solution containing 0.2 g of sodium carbonate and 72.2 g of potassium iodide, and dilute to 500 ml to give a $1.0 \times 10^{-3}N$ iodate in 0.87*M* iodide solution.

Iodide Solution (0.87*M*). Dissolve 72.2 g of potassium iodide in a redistilled water containing 0.2 g of sodium carbonate and dilute to 500 ml.

Buffer Solutions. Mix acetic acid (0.1, 0.5, or 1*N*) with sodium acetate (0.1, 0.5, or 1*M*), sodium dihydrogen phosphate (0.2*M*) with sodium hydroxide (0.2*N*), sodium hydrogen carbonate (0.1, 0.3, or 0.5*M*) with sodium carbonate (0.05, 0.3, or 0.5*M*), and sodium monohydrogen phosphate (0.5*M*) with sodium hydroxide (0.5*N*), respectively, in various ratios to obtain buffer solutions of pH as required. The buffer solutions (pH 9.9 and 3.5) used in procedures A and B were prepared by mixing 50 ml of 0.3*M* sodium carbonate with 50 ml of 0.3*M* sodium hydrogen carbonate, and by mixing 80 ml of 0.5*N* acetic acid with 5 ml of 0.5*M* sodium acetate, respectively.

Acetic Acid Solution. Dilute glacial acetic acid as required.

Formaldehyde Solution. Prepare working solutions by suitable dilution of formalin.

Procedures. *Procedure A. Determination of Hexathionate.* Add 2.0 ml of carbonate buffer solution (pH 9.9), 2.0 ml of 0.15*M* sulfite, and then a 10.0-ml of sample solution containing hexathionate to a 25-ml volumetric flask. The pH of the solution is thereby brought to a value of 8.4. Allow the mixture to stand at room temperature for 10 min, to convert hexathionate completely to thiosulfate. Add 2.0 ml of acetate buffer solution (pH 3.5) and 2.0-ml of 0.5*M* formaldehyde to the reaction mixture. In this case, the solution was buffered to pH 5.4. Then, allow it to stand for 5 min to mask the excess sulfite completely. To this mixture, add 2.0 ml of 15*N* acetic acid and 2.4 ml of $1.0 \times 10^{-3}N$ standard iodate in 0.87*M* iodide solution; then fill the flask to the mark with redistilled water. Mix the contents well, and measure the absorbance of the solution of iodine–iodide complex against distilled water at 350 nm within 10 min after the addition of standard iodate-iodide solution.

Procedure B. For Mixtures of Hexathionate, Thiosulfate, and Sulfite. Prepare three reaction mixtures in 25-ml volumetric flasks as follows.

Procedure B-I. For Total Amount of Hexathionate and Thiosulfate in Mixtures. Treat a 10.0-ml aliquot of sample solution containing hexathionate, thiosulfate, and sulfite as in procedure A, in order to convert the hexathionate completely to thiosulfate. Add 2.0 ml of acetate buffer solution (pH 3.5), and 2.0 ml of 0.5M formaldehyde to the reaction mixture; then allow it to stand for 5 min to mask the sulfite completely.

Procedure B-II. For the Amount of Thiosulfate in Mixtures. Add 2.0 ml of carbonate buffer solution (pH 9.9), a 10.0-ml aliquot of the sample solution, 2.0 ml of acetate buffer solution (pH 3.5), and 2.0 ml of 0.5*M* formaldehyde to a 25-ml volumetric flask; then allow the mixture to stand for 5 min.

Procedure B-III. For Total Amount of Thiosulfate and Sulfite in Mixtures. Add 2.0 ml of carbonate buffer solution (pH 9.9), a 10.0-ml aliquot of the sample solution, and 2.0 ml of acetate buffer solution (pH 3.5) to a 25-ml volumetric flask.

Finally, add 2.0 ml of 15*N* acetic acid and 2.4 ml of $1.0 \times 10^{-3}N$ standard iodate in 0.87*M* iodide solution to each mixture; then fill the flasks to the mark with redistilled water. Mix the contents of the flasks well, and measure the absorbance of the solution of iodine-iodide complex against distilled water at 350 nm.

RESULTS AND DISCUSSION

Calibration Graphs. A series of standard solutions of thiosulfate and hexathionate were treated as in procedure A. The resulting graphs are shown in Figure 1. According to Equation 1, when 1 mole of hexathionate undergoes sulfitolysis, 3 moles of thiosulfate are formed. Therefore, if hexathionate is converted to thiosulfate stoichiometrically and completely, the calibration graph of hexathionate should coincide with that of thiosulfate when the molar concentration scale for thiosulfate is drawn to one third of the scale of hexathionate concentration. Figure 1 proves that hexathionate is quantitatively converted to thiosulfate according to Equation 1.

Stability of Thiosulfate in the Presence of Sulfite. A preliminary experiment disclosed that thiosulfate formed by the sulfitolysis of hexathionate was not stable for a long time. Therefore, the stability of thiosulfate in the presence of sulfite was investigated; the thiosulfate solution was allowed to stand for various periods of time at room temperature and various pH levels, and then treated as in procedure A. In all cases the mixture solutions were buffered to pH 4.0–9.1, which is the optimal range for masking the excess sulfite with formaldehyde. The results, Table I, show that the thiosulfate solution was stable for 30 min at pH 6.1, for 45 min at pH 7.5 and 8.4, and for 50 min at pH 9.5, respectively, and thereafter gave progressively higher absorbances. The higher absorbance was thought to be caused by the fact that thiosulfate reacts with sulfite to yield trithionate (*15*) as shown in Equation 2:

$$S_2O_3^{2-} + 4SO_3^{2-} + 6H^+ = 2S_3O_6^{2-} + 3H_2O \quad (2)$$

(13) E. Blasius and J. Munch, *Fresenius' Z. Anal. Chem.*, **261**, 198 (1972).
(14) M. Goehring and U. Feldmann, *Z. Anorg. Chem.*, **257**, 223 (1948).
(15) H. Ishikawa and T. Murooka, *Rikagaku Kenkyushyo Iho*, **6**, 407 (1927).

Table I. Stability of Thiosulfate in the Presence of Sulfite[a]

	Absorbance			
Time, min	pH 6.1 $2.0 \times 10^{-4}M$ $S_2O_3^{2-}$	pH 7.5 $2.0 \times 10^{-4}M$ $S_2O_3^{2-}$	pH 8.4 $2.0 \times 10^{-4}M$ $S_2O_3^{2-}$	pH 9.5 $2.0 \times 10^{-4}M$ $S_2O_3^{2-}$
1[b]	0.203	0.204	0.202	0.203
1	0.205	0.202	0.204	0.205
5	0.203	0.203	0.206	0.204
10	0.206	0.202	0.204	0.206
20	0.207	0.204	0.204	0.204
30	0.207	0.204	0.205	0.207
40	0.211	0.205	0.204	0.205
45	0.216	0.206	0.208	0.206
50	0.220	0.213	0.210	0.208
60	0.230	0.224	0.215	0.210
70	0.236	0.230	0.229	0.228
70[b]	0.202	0.203	0.204	0.205

[a] 2.0 ml of 0.15 M SO_3^{2-} was employed. [b] In the absence of sulfite.

Table II. Rate of Sulfitolysis of Hexathionate at Room Temperature

	Absorbance			
Time, min	pH 6.1 $4.0 \times 10^{-4}M$ $S_2O_3^{2-}$	pH 7.5 $4.0 \times 10^{-4}M$ $S_2O_3^{2-}$	pH 8.4 $4.0 \times 10^{-4}M$ $S_2O_3^{2-}$	pH 9.5 $4.0 \times 10^{-4}M$ $S_2O_3^{2-}$
	0.604[a]	0.605[a]	0.604[a]	0.606[a]
1	0.720	0.628	0.619	0.614
3	0.689	0.616	0.612	0.604
4	0.673	0.611	0.611	0.605
5	0.665	0.610	0.608	0.606
10	0.622	0.605	0.604	0.606
20	0.625	0.603	0.606	0.605
40	0.628	0.606	0.610	0.607
45	0.629	0.608	0.610	0.607
50	0.631	0.608	0.611	0.607
60	0.632	0.612	0.614	0.609
70	0.634	0.621	0.618	0.615
80	0.636	0.623	0.620	0.618
90	0.641	0.638	0.634	0.631

[a] Absorbance for $1.2 \times 10^{-4}M$ thiosulfate.

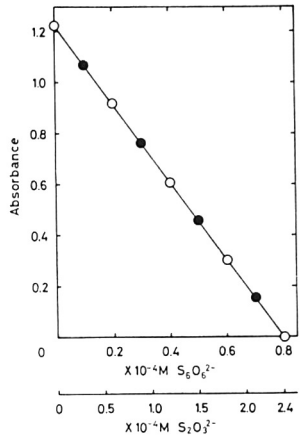


Figure 1. Calibration graphs for thiosulfate and hexathionate
●, $S_2O_3^{2-}$; ○, $S_6O_6^{2-}$

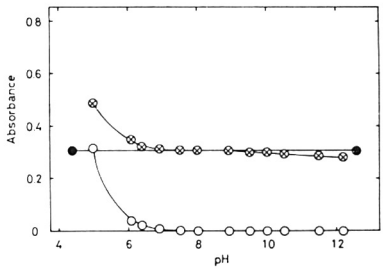


Figure 2. Effect of pH on the sulfitolysis of hexathionate
●, $1.8 \times 10^{-4}M$ $S_2O_3^{2-}$; ⊗, $6.0 \times 10^{-5}M$ $S_6O_6^{2-}$; ○, $8.0 \times 10^{-5}M$ $S_6O_6^{2-}$

However, the thiosulfate in the absence of sulfite did not give any measurable change in absorbance even after a period of 70 min at each pH value.

Rate of Sulfitolysis of Hexathionate. Table II shows that minimal absorbance at pH 6.1 was reached in 10 min, but did not coincide with the expected value. At pH 7.5, 8.4, and 9.5, the absorbance which was in full agreement with the value stoichiometrically sulfitolyzed, was reached in 10 min, in 5 min, and in 3 min, and then remained constant over different intervals of time, respectively. Higher absorbances then ensued because of the reaction of thiosulfate formed with the excess sulfite, deviating from the expected value.

Effect of pH on the Sulfitolysis of Hexathionate. To establish the optimal pH range for the sulfitolysis, hexathionate was allowed to react with sulfite for 10 min at various pH values. Figure 2 shows that hexathionate was stoichiometrically converted to thiosulfate according to Equation 1 over the pH range of 7.5–9.5. A decrease in absorbance at higher pH levels might be attributed to the partial alkaline decomposition of hexathionate (*16*) as shown in Equation 3:

$$2S_6O_6^{2-} + 2SO_3^{2-} + 6OH^- = 7S_2O_3^{2-} + 3H_2O \quad (3)$$

The optimal pH range could be extended to a lower pH value by making sulfitolysis time longer; for example, it was over the pH range of 6.9–9.5 when sulfitoylzed for 20 min. However, sulfitolysis time cannot be made any longer at the lower pH value, because the thiosulfate reacts gradually with the sulfite.

Effect of Amount of Sulfite. In measuring the effect of the amount of sodium hydrogen sulfite on the conversion of hexathionate to thiosulfate, 2.0 ml of 0.01, 0.02, 0.05, 0.1, 0.12, and 0.15M sulfite solution were employed, respectively. In all cases, the solutions were buffered to pH 7.5–9.5, which is the optimal range for the sulfitolysis of hexathionate. As can be seen in Figure 3, the sulfitolysis of hexathionate was incomplete with 2.0 ml of 0.01, 0.02, and 0.05M sulfite, but when 2.0 ml of 0.1, 0.12, and 0.15M were used, the calibration graph of hexathionate was linear and coincided exactly with that of standard thiosulfate when plotted as equivalent concentrations. It was also confirmed that the excess sulfite did not have any effect on the present method because of its being completely masked by formaldehyde as revealed in the next section.

(16) M. Geohring, W. Helbing, and I. Appel, *Z. Anorg. Chem.*, **254**, 185 (1947).

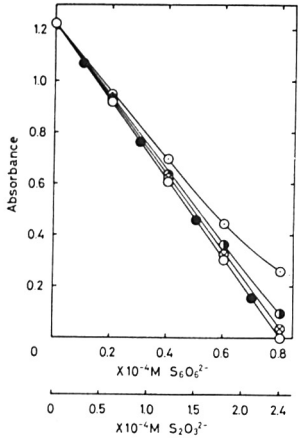


Figure 3. Effect of amount of sulfite on the sulfitolysis of hexathionate

Sulfitolysis time, 10 min; ●, $S_2O_3^{2-}$ with 2.0 ml of 0.15*M* SO_3^{2-}; ⊙, $S_6O_6^{2-}$ with 2.0 ml of 0.01*M* SO_3^{2-}; ◑, $S_6O_6^{2-}$ with 2.0 ml of 0.02*M* SO_3^{2-}; ⊗, $S_6O_6^{2-}$ with 2.0 ml of 0.05*M* SO_3^{2-}; ○, $S_6O_6^{2-}$ with 2.0 ml of 0.1, 0.12, and 0.15*M* SO_3^{2-}

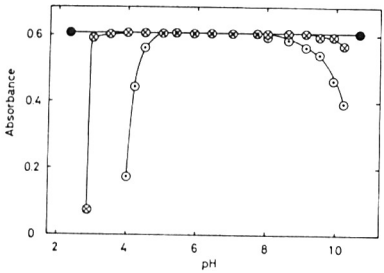


Figure 4. Effect of pH on masking the excess sulfite with formaldehyde

Concentration of thiosulfate was 1.2 × 10^{-4} *M*, and 2.0 ml of 0.50 *M* formaldehyde was employed; ●, no sulfite and formaldehyde were employed; ⊙, sulfite was added as in procedure A (masking time, 1 min); ⊗, sulfite was added as in procedure A (masking time, 5 min)

Masking of Excess Sulfite with Formaldehyde. The sulfite used for the sulfitolysis of hexathionate consumed the iodine completely, as a result of its reaction with the iodine. Therefore, an attempt was made to mask the excess sulfite with formaldehyde (*17*). Figure 4 shows how the sulfite could be msked by varying the pH of the mixture solution. The absorbance was in exact agreement with the theoretical value over the pH range of 5.0–7.7 when the mixture solution was allowed to stand for 1 min, and over the pH range of 4.0–9.1 for 5 min, respectively. The pH of the mixture solution was brought to 5.4 when 2.0 ml of 0.5*M* formaldehyde had been added as in procedure A.

Figure 5 shows how the sulfite could be masked by increasing the amount of formaldehyde added. In ll cases, the

(17) A. Kurtenacker, *Fresenius' Z. Anal. Chem.*, **64**, 56 (1924).

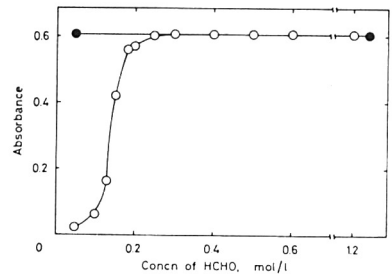


Figure 5. Effect of amount of formaldehyde on masking the excess sulfite

Concentration of thiosulfate was 1.2 × 10^{-4}*M*, and 2.0 ml of formaldehyde solution was employed; ●, no sulfite and formaldehyde were employed; ○, sulfite was added as in procedure A

solutions were buffered to pH 4.0–9.1. It can be concluded from Figure 5 that 2.0 ml of 0.3*M* formaldehyde solution was sufficient for masking the sulfite completely, and that the amount of formaldehyde did not have any effect on this method. Consequently, 2.0 ml of 0.5*M* formaldehyde was used in the present study.

Stability of Iodine–Iodide Complex in the Presence of Sulfite–Formaldehyde Adduct. Iodine–iodide complex is formed in acid medium from an iodate–iodide mixture. The experimental facts showed that 1.0 ml of 15*N* acetic acid was sufficient for the complete liberation of iodine, and that the absorbance remained constant over the volume range of 1.0–3.0 ml. Consequently, 2.0 ml of 15*N* acetic acid was used to make the solution acidic.

The stability of iodine–iodide complex in the presence of sulfite–formaldehyde adduct was examined in an acetic acid medium. According to a previous paper (*11*), the solution of iodine–iodide gave progressively higher absorbances because of the air-oxidation of iodide in acid medium. On the contrary, the solution gave a gradual decrease in absorbance, in the present study, because of the probable reaction of iodine–iodide complex with the adduct formed. However, the solution of iodine–iodide complex was stable enough for a period of 10 min, so all the spectrophotometric measurements were made within at least 10 min after the addition of standard iodate–iodide solution.

Analysis of Mixtures of Hexathionate, Thiosulfate, and Sulfite. The three sulfur compounds in the mixtures give the following equivalents in the three procedures:

$$\text{Procedure B-I} \equiv 3S_6O_6^{2-} + S_2O_3^{2-}$$

$$\text{Procedure B-II} \equiv S_2O_3^{2-}$$

$$\text{Procedure B-III} \equiv S_2O_3^{2-} + 2SO_3^{2-}$$

The absorbance obtained by procedure B-I corresponds to the sum of three times the hexathionate (see Equation 1) and the thiosulfate in mixtures, sulfite being masked by the formaldehyde added for removing the excess sulfite. The absorbance obtained by procedure B-II, where sulfitolysis of hexathionate was not carried out, corresponds to only the amount of thiosulfate. The absorbance obtained by procedure B-III corresponds to the sum of the thiosulfate and twice the sulfite in the mixture solution. Moreover, the calibration graphs for hexathionate, thiosulfate, and sulfite were in full agreement with one another when plotted as equivalent concentrations. Therefore, the following equations can be obtained: $(S_6O_6^{2-}) = (I - II)/3$, $(S_2O_3^{2-}) = II$,

Table III. Analysis of Mixtures of Hexathionate, Thiosulfate, and Sulfite

Taken, μmoles			Found, μmoles		
$S_6O_6^{2-}$	$S_2O_3^{2-}$	SO_3^{2-}	$S_6O_6^{2-}$	$S_2O_3^{2-}$	SO_3^{2-}
0.07	0.30	0.75	0.07	0.31	0.75
0.20	0.50	0.50	0.19	0.51	0.50
0.50	0.40	0.10	0.51	0.39	0.11
0.20	1.00	0.15	0.20	1.01	0.14
0.30	0.50	0.25	0.30	0.52	0.24
0.40	0.50	0.25	0.40	0.52	0.24

and $(SO_3^{2-}) = (III - II)/2$, where I, II, and III indicate the molar concentrations which was determined from the calibration graph for thiosulfate in Figure 1 using the absorbances obtined by procedures B-I, B-II, and B-III, respectively. Table III shows that the above technique can be successfully applied to the determination of hexathionate, thiosulfate, and sulfite mixed in various ratios.

An estimate of the precision was obtained from six results for 10.0 ml of sample solution containing 0.5 μmole of hexathionate, 0.4 μmole of thiosulfate, and 0.1 μmole of sulfite. The method gave a mean value of 0.503 μmole of hexathionate, a standard deviation of 0.011, or a relative standard deviation of 2.2%.

Effect of Diverse Ions. A 10.0-ml aliquot of solution containing various amounts of diverse ion, both in the presence of hexathionate ($4.0 \times 10^{-5} M$) and in its absence, was treated exactly as in procedure A. The results are given in Table IV. Such ions as iron (III), copper(II), and nitrite which oxidize iodide, interfered with the determination of hexathionate, when present in amounts corresponding to that of hexathionate. Sulfide interfered even when present in amount of 0.1 ppm, because it reduces iodine to the iodide. In the case of iron(II), the positive error in absorbance may be due to the oxidation of iodide by the iron(III) ion which was produced by the air-oxidation of iron(II). About 1000 ppm of almost all the other ions listed in Table IV could be tolerated.

Table IV. Effect of Diverse Ions

Ion	Added as	Concn, ppm	Absorbance: Reagent blank	Absorbance: $4.0 \times 10^{-5} M$ $S_6O_6^{2-}$
None		0	1.224	0.613
Na^+	$Na_2SO_4 \cdot 10H_2O$	1000	1.226	0.613
K^+	K_2SO_4	1000	1.224	0.611
NH_4^+	$(NH_4)_2SO_4$	1000	1.224	0.613
Mg^{2+}	$MgSO_4 \cdot 7H_2O$	1000	1.224	0.613
Ca^{2+}	$CaCO_3$	1000	1.244	0.627
Zn^{2+}	$ZnSO_4 \cdot 7H_2O$	1000	1.229	0.620
Cd^{2+}	$Cd(CH_3COO)_2 \cdot 2H_2O$	1000	1.225	0.614
Mn^{2+}	$MnSO_4 \cdot 5H_2O$	1000	1.227	0.614
Al^{3+}	$Al_2(SO_4)_3 \cdot 18H_2O$	500	1.237	0.642
Pb^{2+}	$Pb(CH_3COO)_2 \cdot 3H_2O$	100	1.336	0.830
Fe^{2+}	$Fe(NH_4)_2(SO_4)_2 \cdot 6H_2O$	50	1.654	0.939
Fe^{3+}	$Fe(NH_4)(SO_4)_2 \cdot 12H_2O$	1	1.251	0.642
		10	1.341	0.745
Cu^{2+}	$CuSO_4 \cdot 5H_2O$	10	1.415	0.807
F^-	NaF	1000	1.224	0.611
Cl^-	NaCl	1000	1.227	0.614
Br^-	KBr	1000	1.226	0.613
NO_3^-	KNO_3	1000	1.246	0.650
SO_4^{2-}	Na_2SO_4	1000	1.227	0.613
PO_4^{3-}	$Na_3PO_4 \cdot 12H_2O$	1000	1.225	0.613
$HAsO_4^{2-}$	$Na_2HAsO_4 \cdot 7H_2O$	1000	1.224	0.616
Borate	H_3BO_3	1000	1.225	0.616
Silicate	(as SiO_2)	500	1.230	0.618
NO_2^-	KNO_2	0.1	1.237	0.623
		0.5	1.337	0.712
S^{2-}	$Na_2S \cdot 9H_2O$	0.1	1.192	0.592
		0.5	1.066	0.469

RECEIVED for review March 26, 1974. Accepted June 24, 1974.

Separation Technique for Mass Spectrometry

Fractionated Evaporation from a Direct Inlet System Which Maintains a Fixed Total Ion Current

Jochen Franzen, Hendrik Kuper, and Wolfgang Riepe

Institut fur Spektrochemie und Angewandte Spektroskopie.[1] Dortmund, Bundesrepublik Deutschland

Fractionated evaporation of mixtures from the crucible of a direct inlet system is investigated. The general evaporation behavior of the most frequent types of mixtures is explained theoretically, augmented by results of computer calculations. Crucibles with small apertures show best separation of the different components because the evaporation process is held close to equilibrium. There is no demand for continuously supervising the total ion current since it is maintained constant by an electronic heating control unit. The technique has proved suitable for routinely taking clean spectra from substances contaminated with solvents or by base or intermediary products. In many cases, it can be successfully used also for the easy and rapid separation of mixtures consisting of a few components only. The behavior of the evaporation temperature allows for conclusions about the kind of mixtures.

[1] Supported by the Ministry for Science and Research of Northrhine-Westphalia.

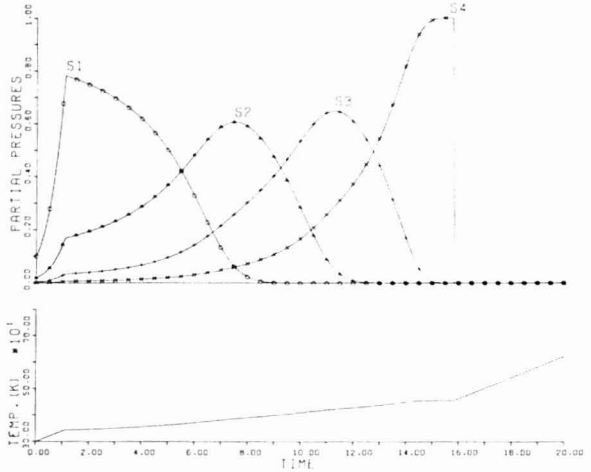


Figure 1. Calculated vapor pressure curves

Four mutually soluble substances, denoted S1 to S4 (only one thermodynamic condensed phase). Amount of substance ratios, 1:1:1:1. Vapor pressure ratios, 125:25:5:1. No adsorbed material

There are several methods which provide a separation of a multicomponent organic substance prior to being evaporated into the ion source (*1–6*). Gas chromatographs are used most extensively and successfully. However, their application is limited to compounds having sufficient volatility. The technique presented here is suitable for the analysis of less volatile substances and is similar to the 'micromolecular distillation' which was introduced at the ASMS meeting in 1970 (*1*).

In a recent paper (*7*), we described an electronic heating control of a direct inlet system attached to a Varian MAT CH7 mass spectrometer. The probe is heated in such a way that the total ion current is held constant at a prechosen value. The system offers different advantages. Once the heating unit is turned on, the complete evaporation of a sample runs automatically without any previous choice of a proper temperature program. No intervention of the operator is required. The peak amplitudes can be fitted optimally to the analog inputs of data acquisition systems or recorders. The constancy of the total ion current prevents the ion source pressure from considerable changes. They would lead to varying space charge conditions which influence the resolving power of the spectrometer and the mass scale. This may cause difficulties when using data acquisition systems, unless the total ion current is continuously supervised.

(1) R. D. Grigsby, R. H. Cole, W. G. Fox, and G. M. Gable, 18th Annual Conf. on Mass Spectrometry and Allied Topics, San Francisco, Calif., 14–19 June 1970; Amer. Soc. for Mass Spectrometry and ASTM Committee E-14, Paper K 8, pp B 273–6, 1970.
(2) R. D. Grigsby, J. S. Bird, and K. E. Bird, 19th Annual Conf. on Mass Spectrometry and Allied Topics, Atlanta, Ga., 2–7 May 1971; Amer. Soc. for Mass Spectrometry and ASTM Committee E-14, Paper H4, pp 110–15, 1971.
(3) R. D. Grigsby, C. O. Hansen, D. G. Mannering, W. G. Fox, and R. H. Cole, *Anal. Chem.*, **43**, 1135–37 (1971).
(4) H. R. Morris and D. H. Williams, *Biochem. J.*, **125**, 189–201 (1971).
(5) Y. Murakami and H. Okamoto, "Transactions of the Tenth National Vacuum Symposium of the American Vacuum Society, 1963," Macmillan, New York, N.Y., 1963, p 93.
(6) W. E. Crosmer, N. C. Thomas, P. H. S. Tsang, and R. J. Duckett, *Rev. Sci. Instrum.*, **44**, 837–43 (1973).
(7) J. Franzen, H. Kuper, and W. Riepe, *J. Mass Spectrom. Ion Phys.*, **10**, 353–57 (1972/1973).

Although originally designed to simplify the heating procedure and to reduce the demand on operator skill, the system was found suitable for fractionated evaporation experiments, a preliminary example of which was presented in the paper cited.

During recent months, we have thoroughly put to test the heating system and the measuring procedure, in daily routine, by taking a large number of clean spectra of substances which were contaminated.

In order to get information about the capabilities and limitations of the technique as a separation method for MS, we have investigated the fractionating process by means of some basic but characteristic examples.

EVAPORATION PROCESS

The theoretical description of the evaporation process of the considered cases of mixtures assumes equilibrium conditions. This can be approximated by fairly small aperture crucibles (Knudsen cells), which show better separation results than open crucibles.

The basic thermodynamic relationships of evaporation equilibria are simple and well-known. A computer program was written which handles a maximum of six substances distributed among up to three condensed phases. An additional adsorption phase is included. The program calculates the partial vapor pressures and the temperature needed to produce a total vapor pressure, which is considered to be constant, as long as the total ion current is held constant. It is assumed that all mixture components have equal evaporation enthalpies. This simplification does not fundamentally influence the behavior of the elimination curves. To closely simulate the experimental conditions, the program limits the heating rate to a maximum temperature gradient. This limitation causes deviations from the constant total vapor pressure if sudden temperature changes are required during the evaporation process.

Figures 1 and 2 show the results of the program for the case of a mixture of substances having complete mutual solubility and thus forming a single condensed phase. The evaporation process of a mixture with four components of equal amounts is illustrated in Figure 1. The partial vapor

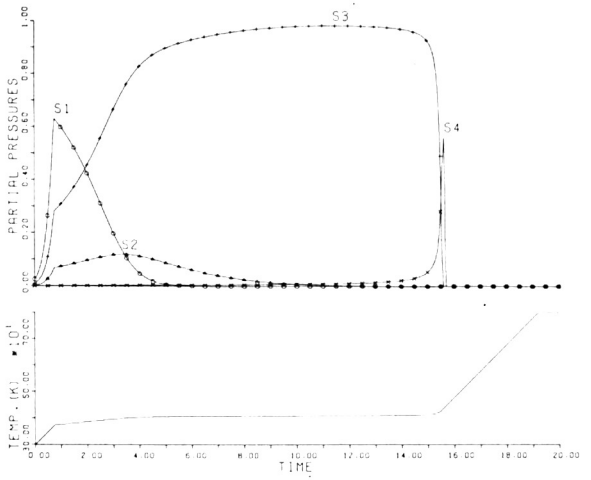


Figure 2. Calculated evaporation process of soluble minor mixture components

One phase. Amount of substance ratios, 10:5:100:2. Vapor pressure ratios, 125:25:5:1. No adsorbed material. The components evaporate in sequence of their vapor pressures

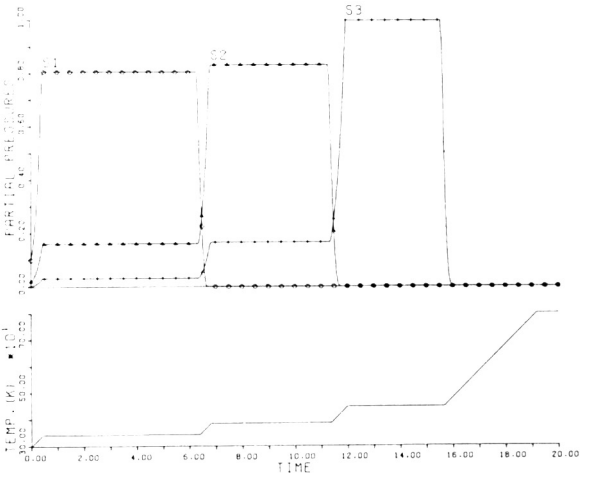


Figure 3. Calculated evaporation process of three substances separated in three distinct thermodynamic condensed phases

Amount of substance ratios, 1:1:1. Vapor pressure ratios, 25:5:1. (Compare with Figure 1)

pressures are geometrically decreasing by a factor of five. After the initial heating-up process, the temperature increases almost linearly with time until it runs into a short plateau when only the last component is evaporating. This "pure state" lasts only a few moments just prior to complete exhaustion. So there may be little time to take a mass spectrum. However, if a substance is contaminated with small amounts of solvents or basic compounds with higher vapor pressures, as is often found in practice, the pure state lasts long enough to take several mass spectra representative of the main component.

From Figure 2 it can be seen that mass spectra may be fatally injured by impurities, although the temperature is nearly constant during a long interval until exhaustion. Contaminants like S2 or S4 remain normally undetected if only a few spectra are taken within an interval between 8.00 and 14.00 time units. In order to recognize the presence of impurities like S4 it is necessary to take spectra until complete exhaustion of the material and look at their deviations near the end of the evaporation.

More favorable for treatment with the technique are mixtures of such components which are not mutually soluble. These components form different separated condensed thermodynamic phases. Partial vapor pressures and temperature remain constant up to the complete exhaustion of one condensed phase. Then, rapidly, a new

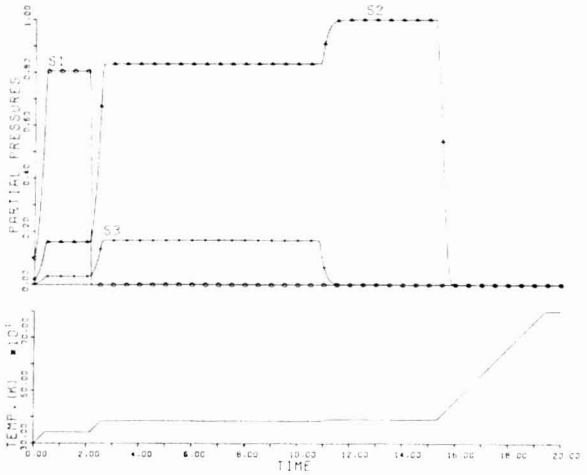


Figure 4. Calculated evaporation process of non-soluble minor mixture components (three phases)

Amount ratios, 10:100:10. Vapor pressure ratios, 25:5:1. Substances with lowest vapor pressure (S3) can exhaust before complete evaporation of the main substance (S2) (Compare with Figure 2)

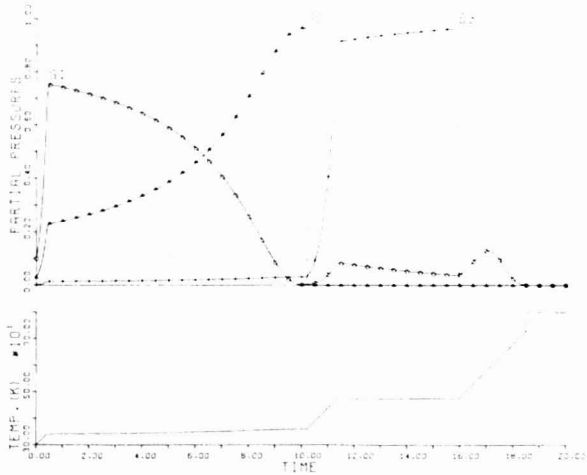


Figure 5. Calculated evaporation process of three substances

The first two (S1 and S2) are mutually soluble and form a common condensed phase, the third (S3) represents a condensed phase of its own. Substance S1 is partially adsorbed (5% of its total amount) at the wall of the crucible and appears preferentially during periods of increasing temperature

equilibrium is established which lasts to the exhaustion of the next phase. As can be seen from Figure 3, the phase evaporating as the last can be measured uninterfered, whereas a separation of spectra taken at earlier periods can be performed easily by subtracting spectra of later periods.

In contrast to the case of complete mutual solubility, small amounts of admixtures of low vapor pressure exhaust before complete evaporation of the main component, so that, in general, uninterfered mass spectra of slightly contaminated substances will be easily obtained (Figure 4).

There is, however, just one case of complete dissolubility which does not allow one to recognize the presence of a mixture. If the ratios of the amounts of substance over their vapor pressures are just constant for all components of the mixture, then the exhaustion takes place at the same moment for all components. No changes in partial

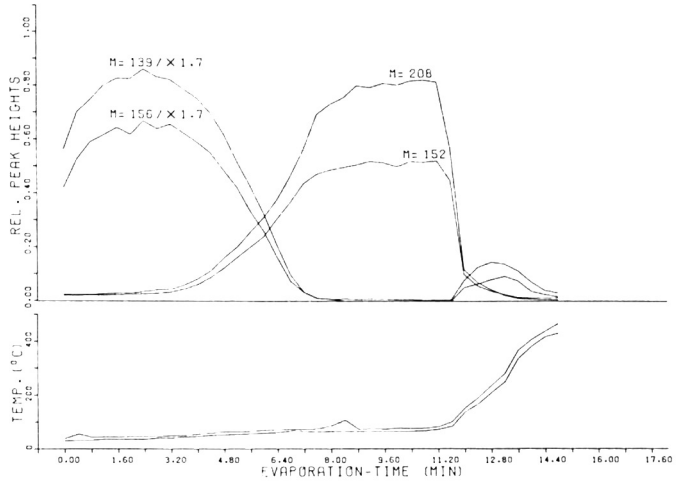


Figure 6. Experimental evaporation curves of chlorobenzoic acid (masses 139 and 156) and anthraquinone (masses 152 and 208)

Open crucible, mixture 1:1. The temperature curves represent minimum and maximum crucible temperatures during the acquisition of one spectrum

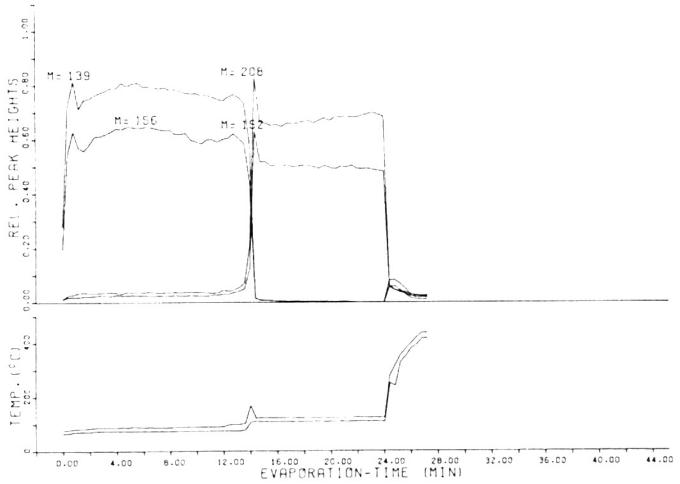


Figure 7. Evaporation curves of a mixture as in Figure 6, but closed crucible

pressures or mass spectra can be observed. This case should be rare, but special care should be taken with substances purified by fractionated evaporation which may produce just such mixtures.

The last computer-calculated example (Figure 5) illustrates the evaporation behavior of a mixture of three components, two of which are mutually soluble and the third forming a separate phase. In addition, the effect of the substance adsorbed by the walls of the crucible or by other surface-active material is seen, forming small vapor pressure bursts during each temperature increase.

In case of partial solubility where, in general, only smaller fractions of a substance are solved within different phases and the larger fraction forms a phase of its own, the evaporation process generally behaves as described above for mutally dissoluble substances.

EXPERIMENTAL

About 5 to 10 μg of material is fed into a Knudsen-cell-like aluminum crucible with a small aperture of only 0.3 mm diameter. The inner surface of the crucible is more than 150 times larger than the cross section of the aperture, so that a state near equilibrium can be expected. The heating unit controls the probe

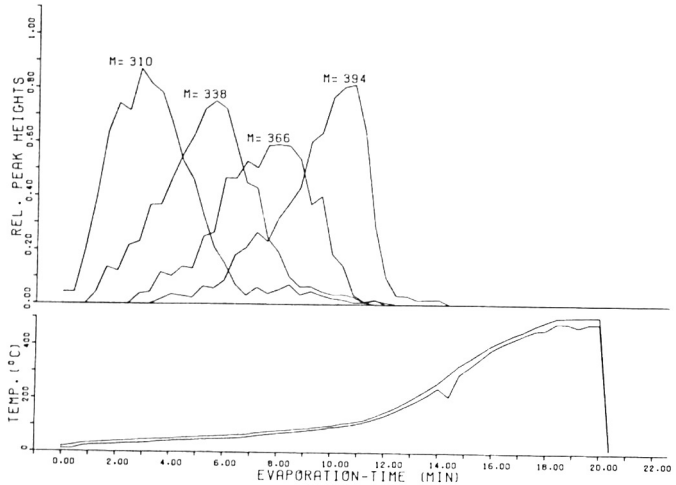


Figure 8. Evaporation process of the four *n*-hydrocarbons C_{22}, C_{24}, C_{26}, and C_{28} Mixture, 1:1:1:1. (Compare with Figure 1)

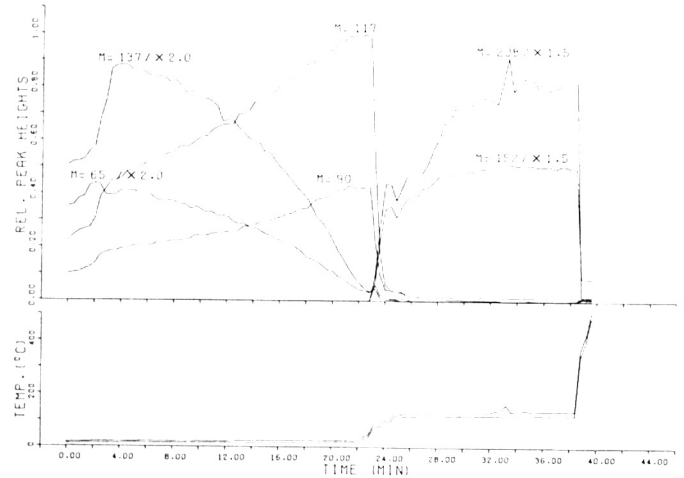


Figure 9. Evaporation process of a mixture of indole (masses 65 and 137), nitrotoluene (masses 90 and 117), and anthraquinone (masses 152 and 208), mixed 1:1:1. (Compare with Figure 5)

temperature to produce a pre-chosen total ion current. (The aluminum crucibles and covers were manufactured by Degen & Co., SA Niederdorf, Switzerland.)

Spectra are taken consecutively, one every 24 seconds by a Varian MAT SpectroSystem 100 data acquisition system from the beginning of the evaporation until complete exhaustion. The acquisition includes the temperature values to add them to mass chromatograms.

RESULTS AND DISCUSSION

It is difficult to estimate whether the technique provides better separation results than other direct probe techniques since no referring experiments were carried out. In order to simulate a technique like that presented in (*1*), the computer program was modified to calculate elimination curves with linearly increasing temperature. These curves as well as those published in (*1*) or (*2*) show comparable resolution, except that the partial pressures may change considerably during evaporation intervals requiring constant temperature to produce a constant total pressure.

First experiments were performed to investigate the difference between "open" crucibles as used normally in mass spectrometry and "closed" crucibles with small apertures. As is evidenced in Figures 6 and 7, closed cru-

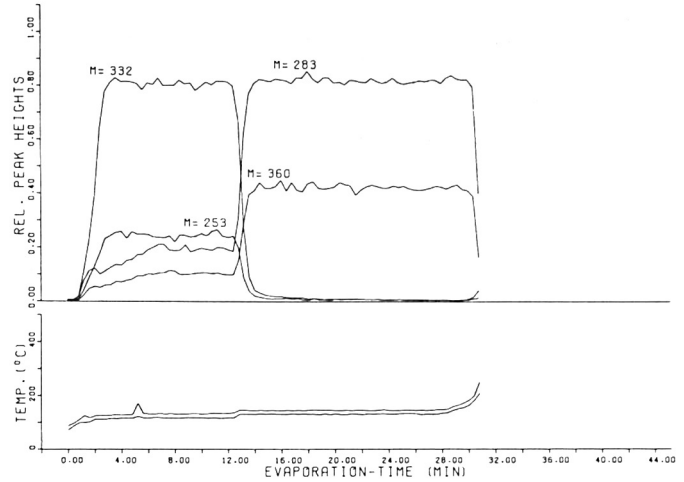


Figure 10. Evaporation process of a synthesis product benzophenoneazene (masses 253 and 332) and tetraphenylethylene (masses 283 and 360)

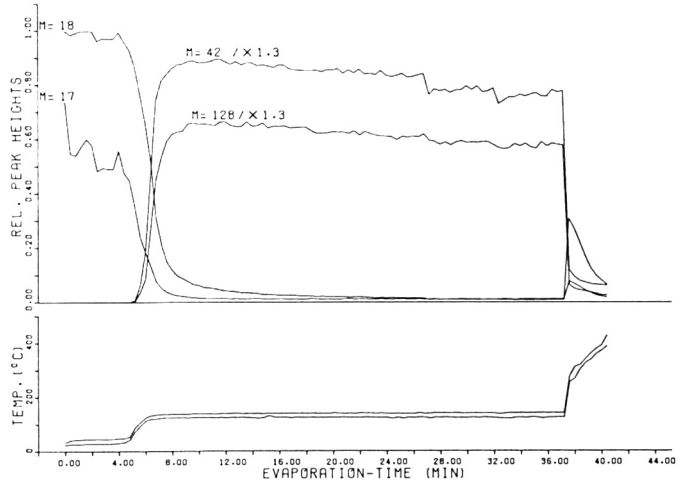


Figure 11. Evaporation process of barbituric acid (masses 42 and 128) with crystal water (masses 17 and 18)

cibles provide better separation results than open ones in case of substances which are not mutually soluble. The elimination and temperature curves of Figure 7 are very similar to those of Figure 3 which are calculated for three substances instead of two. In case of complete mutual solubility, almost no difference in resolution was observed.

Further experimental results obtained with closed crucibles are in good agreement with the theoretical description. For example, Figures 8 and 9 correspond to Figures 1 and 5, respectively. The samples were artificial mixtures. However, mixtures of this kind might exhibit a particularly favorable behavior. Therefore, Figures 10 and 11 were taken as two examples of real mixtures. Benzophenoneazene and tetraphenylethylene were contained at about 50% each in uniformly looking crystals by a laboratory synthesis (by courtesy of H.-P. Ritter, University of Dortmund). The barbituric acid of Figure 11 contained crystal water.

In order to obtain pure component spectra, the behavior of the evaporation temperature is examined. If it remains constant during a time interval preceding immediately the complete exhaustion of the sample, one can expect uninterfered spectra with high probability. The exhaustion is indicated by a vanishing total current causing the temperature to increase rapidly toward a value which is limited to about 500 centigrades to prevent the probe from damage. A computer program module averages successive groups of up to eight spectra and informs about any changes of them.

CONCLUSIONS

The modified direct inlet system has proved useful for the fractionated evaporation of samples not having sufficient volatility to subject them to gas chromatography.

It enables an automatic evaporation procedure without any previous knowledge of the sample behavior. Optimal conditions for data acquisition systems are achieved. Except for some special cases, the technique can be used to check the purity of samples and to obtain uninterfered spectra of contaminated substances. The separation results agree with basic thermodynamic relations and allow for the identification of mixture components by computational methods.

RECEIVED for review September 24, 1973. Accepted April 8, 1974.

Gated Nanosecond Time Resolved Emission Spectroscopy Separation of Mixed Emissions from Carbonyl Compounds

Ronald E. Brown, Kenneth D. Legg, Monte W. Wolf, and Lawrence A. Singer[1]

Department of Chemistry, University of Southern California, Los Angeles, Calif. 90007

Joel H. Parks

Departments of Physics and Electrical Engineering, University of Southern California, Los Angeles, Calif. 90007

A variable nanosecond gated photomultiplier technique capable of separating weak prompt fluorescence from the total emission of carbonyl compounds is described. This technique includes the use of a filtered N_2 laser excitation source and a boxcar integrator for sampling and time-averaging the emission signal. The boxcar enables one to sample segments of the emission as short as 10 nsec at variable time delays. The spectral distributions and quantum yields of prompt fluorescence from benzophenone, 4,4′-dimethoxybenzophenone, acetophenone, and benzil are presented. The utilization of this technique for the identification of E- and P-type delayed fluorescence is demonstrated. A hyposochromic shift in the benzil phosphorescence between 293° and 77° is reported.

The relative disposition (singlet–triplet splitting) and character (n,π^*) of the low-lying excited states in aromatic carbonyls results in a rapid and efficient intersystem crossing from the excited singlet to the triplet state (*1, 2*). As a result, the intensity of the radiative $S_0 \leftarrow S_1$ transition (*i.e.*, prompt fluorescence) often is too weak, relative to phosphorescence, to be detected by conventional spectroscopic techniques. When the fluorescence can be detected, direct measurement of the spectral distribution is prevented because of the overlap of the fluorescence and phosphorescence bands (*3–9*). In addition, because of the relatively small S–T energy splitting, the excited singlet state can be repopulated by thermal reactivation of the triplet (*3, 5–7, 10–12*) as well as by triplet–triplet annihilation (*10, 13–16*). These facile photophysical processes can complicate the quantitative assignment of (i) the $S_0 \leftarrow S_1$ transition energy, (ii) the S–T splitting, (iii) the time dependent singlet and triplet population distributions, and (iv) the effect of concentration, diffusion, and temperature on the triplet deactivation and chemical reactivity. The problems in properly elucidating the emissions from various aromatic carbonyls are exemplified by recent reports of E-type delayed fluorescence (thermal reactivation) from various substituted acetophenones and benzophenones (*3, 5–7, 11, 12*). Consequently, techniques such as time resolved spectroscopy must be used to complement conventional emission spectroscopy in unraveling these competing photophysical processes.

Time resolved spectroscopy refers to techniques capable of providing the time dependence of absorption and emission processes. Some standard techniques are flash photolysis, and flash-fluorimetry and phosphorimetry in which the absorption or emission of electromagnetic radiation is sensed directly and recorded using high speed photographic instrumentation (*e.g.*, streak camera) (*17, 18*) or a photosensor (*e.g.*, photodiode, photomultiplier) coupled to recording instrumentation (*e.g.*, x-y recorder, oscilloscope) (*10*). With the recent advances in ultrashort excitation sources and fast sensing and recording instrumentation, resolution has been extended into the nano- and picosecond time regimes.

[1] Author to whom correspondence should be addressed.

(1) S. K. Lower and M. A. El-Sayed, *Chem. Rev.*, **66**, 199 (1966).
(2) M. A. El-Sayed, *Accounts Chem. Res.*, **1**, 8 (1968).
(3) J. Saltiel, H. C. Curtis, L. Metts, J. M. Miley, J. Winterle, and M. Wrighton, *J. Amer. Chem. Soc.*, **92**, 410 (1970).
(4) S. A. Carlson and D. M. Hercules, *J. Amer. Chem. Soc.*, **93**, 5611 (1971).
(5) P. Jones and A. R. Calloway, *J. Amer. Chem. Soc.*, **92**, 4997 (1970).
(6) P. Jones and A. R. Calloway, *Chem. Phys. Lett.*, **10**, 438 (1971).
(7) N. A. Borisevich and V. V. Gruzinskii, *Proc. Acad. Sci. USSR*, **175**, 587 (1967).
(8) P. M. Rentzepis, *Science*, **169**, 239 (1970).
(9) P. M. Rentzepis and C. J. Mitschele, *Anal. Chem.*, **42** (14), 20A (1970).
(10) C. A. Parker, "Photoluminescence of Solutions," Elsevier, London, 1968.
(11) R. E. Brown, L. A. Singer, and J. H. Parks, *Chem. Phys. Lett.*, **14**, 193 (1972).
(12) M. W. Wolf, R. E. Brown, L. A. Singer, K. D. Legg, and J. H. Parks, Abstracts 167th National Meeting of the American Chemical Society, Los Angeles, Calif., April 1–5, 1974, No. ORGN 76.
(13) H. W. Sidebottom, C. C. Badcock, J. G. Calvert, B. R. Rabe, and E. K. Damon, *J. Amer. Chem. Soc.*, **94**, 13 (1972).
(14) C. C. Badcock, H. W. Sidebottom, J. G. Calvert, B. R. Rabe, and E. K. Damon, *J. Amer. Chem. Soc.*, **94**, 19 (1972).
(15) A. Yekta and N. J. Turro, *Mol. Photochem.*, **3**, 307 (1972).
(16) R. E. Brown, L. A. Singer, and J. H. Parks, *J. Amer. Chem. Soc.*, **94**, 8585 (1972); also see correction, **95**, 3083 (1973).
(17) J. R. Novak and M. W. Windsor, *Science*, **161**, 1342 (1968).
(18) D. J. Bradley, N. H. Hutchinson, H. Koetser, T. Morrow, G. H. C. New, and M. S. Petty, *Proc. Roy. Soc., Ser. A*, **328**, 97 (1972).

Resolution of overlapping absorption or emission spectra of transient species may be accomplished by using onset electronic delays with the sensor or recording instrumentation. This approach permits the monitoring of excited state processes occurring during variable time segments following the initial excitation (*19–27*). We describe our system that couples a high intensity, short duration laser excitation source to a fast, electronically gated photomultiplier detecting system. Further, we present some results on aromatic carbonyls that illustrate the types of photophysical processes that can be investigated by gated time resolved nanosecond spectroscopy.

EXPERIMENTAL

Excitation Source and Optics. A 100-kW nitrogen laser (λ = 3371 Å, pulse duration ~8 nsec, 10 pps) was used as the excitation source. The laser pulse was passed through a Farrand (Foci-flex) monochromator set at 3371 Å, and then through either a Valpey 3371 Å narrow band filter, or a solution filter composed of 15% $KCr(SO_4)_2 \cdot 12H_2O$ in 1*N* H_2SO_4 (*10*) in a 2-cm suprasil cell, as shown in Figure 1. These excitation filters, and the complete isolation of scattered and reflected light, were necessary to prevent nitrogen fluorescence bands (*28*) from entering the sample cell and detector. The emission from the sample at right angles to the excitation beam was passed through a 500-mm Bausch and Lomb "sampling" monochromator onto an RCA 1P21 (S-4 sensitivity) or 1P28 (S-5 sensitivity) photomultiplier tube. If necessary, a 2-cm cell containing 2*M* aqueous KNO_2 (*10*) was placed in front of the monochromator entrance slit to limit the passage of scattered 3371-Å laser radiation.

The transmission characteristics of the chemical filters are fully described elsewhere (*10*). The narrow-band Valpey filter has a center transmission wavelength of 3371 ± 10 Å, a half band width of 50 ± 15 Å, and a minimum transmission of 20%. The Bausch and Lomb 500-mm monochromator has a first-order dispersion of 16 Å/mm, a rated grating efficiency of 65% at 3000 Å, and a first-order range between 2000 and 7000 Å.

Electronics. A Brandenburg Model 472R variable power supply was used as a source of high voltage for the photomultipliers (RCA 1P21 or 1P28). Both of the phototubes have response characteristics of less than 2 nsec. The voltage required for a 10^6 gain is 700 and 750 volts for the 1P21 and 1P28, respectively. Voltage to the phototube was maintained between 700 and 1000 volts depending on the needed sensitivity. The signal from the phototube was fed into a Princeton Applied Research Model 160 Boxcar Integrator ("Boxcar") where it could be stored and averaged, and/or directly displayed on a Hewlett-Packard 183A oscilloscope (250 MHz), with an input termination of 50 ohms.

A common pulse generator was used to trigger the Boxcar and the laser. The applied trigger voltage was maintained above 300 mvolts (not exceeding ±5 volts) and the amplitude-width above 10^{-8} volt-sec to ensure stable triggering. Because of the inherent instrument delay between triggering the PAR 160 Boxcar and the initiation of the time ramp, the trigger signal to the laser was delayed by at least 150 nsec. This delay between triggering and initiation of the time base ramp does not interfere with the recovery of leading edge information.

Signal Processing by the Boxcar Integrator. The Boxcar inputted signal is coupled, amplified, and fed into an FET-gated integrating operational amplifier. The storage characteristics of the amplifier are determined by the time constants which adjust two RC feedback networks. Each time the FET gate opens, the output of the amplifier asymptotically approaches an average level of the input signal. Since the time-averaged value of the noise approaches zero, because of its randomness, the noise associated with the signal is reduced, resulting in an improved signal-to-noise ratio (SNIR).

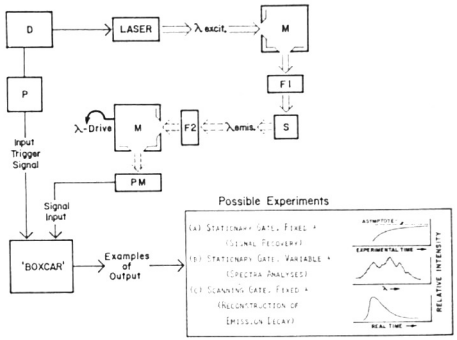


Figure 1. Schematic of experimental arrangement and examples of typical spectroscopic observations

D = electronic delay, F1 = narrow band filter 3371 Å, F2 = cutoff filter 3371 Å, M = monochromator, P = trigger pulse generator, PM = photomultiplier, S = sample

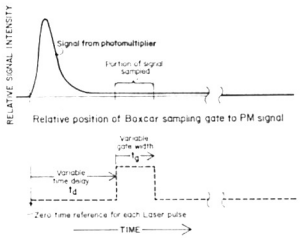


Figure 2. Illustration of variable "Boxcar" sampling gate

$$\text{SNIR} = (2\ \text{TC}_o f)^{1/2} \qquad (1)$$

In Equation 1, TC_o is the observed time constant of the instrument and f is the trigger repetition frequency. TC_o is equal to the effective time constant of the two RC networks divided by the product of the aperture time and the trigger repetition rate. SNIR increases with TC_o, whereas the amplitude of the improved output signal from the Boxcar rises asymptotically, as illustrated in Figure 1(*A*), at a rate inversely proportional to TC_o and directly dependent on f. The time constant also influences the amount of internal noise appearing at the output and affects the duty factor limit. Thus, realistic compromises must be made between signal improvement and experimental time.

The size and position of the aperture can be varied (see Figure 2) so that any time segment of the input signal as small as 10 nsec, and as large as 0.55 sec, can be sampled. During each time base period, the Boxcar averages over the aperture time interval only. For all of the time between aperture pulses, the output of the instrument is expected to "hold" at the level reached during the previous sampling period without leaking. The minimum duty factor (*i.e.*, ratio of aperture time to repetition period) for which the output will change only ±1% with this instrument is 10^{-9}. Thus, unlike conventional photon counting instrumentation which require repetition rates in the kHz regime (*20–25*), it is possible to sample a 10-nsec time width of a signal which recurs only 10/sec with this approach. This retention characteristic of the Boxcar enables one to employ high intensity excitation sources, with low repetition rates, to examine biphotonic processes such as triplet-triplet annihilation. Other aspects of Boxcar performance are discussed in References (*29*) and (*30*).

(19) L. Stryer, *Science*, **162**, 526 (1968).
(20) W. R. Ware, P. Chow, and S. K. Lee, *Chem. Phys. Lett.*, **2**, 356 (1968).
(21) K. Yoshihara, T. Kasuya, A. Inoue, and S. Nagakoa, *Chem. Phys. Lett.*, **9**, 469 (1971).
(22) W. R. Ware, S. K. Lee, G. J. Brant, and P. P. Chow, *J. Chem. Phys.*, **54**, 4729 (1971).
(23) L. Brand and J. R. Gohlke, *J. Biol. Chem.*, **246**, 2317 (1971).
(24) M. De Luca, L. Brand, T. A. Cebula, H. H. Selinger, and A. F. Makula, *J. Biol. Chem.*, **246**, 6702 (1971).
(25) E. Egawa, N. Nakashima, N. Mataga, and C. Yamanaka, *Bull. Chem. Soc., Jap.*, **44**, 3287 (1971).
(26) R. P. Fisher and J. D. Winefordner, *Anal. Chem.*, **44**, 948 (1972).
(27) J. D. Winefordner, *Accounts Chem. Res.*, **2**, 361 (1969).
(28) R. Pease and A. Gaydon, "Identification of Molecular Spectra," J. Wiley and Sons, New York, N.Y., 1963, p 209.
(29) J. O. Weide and M. L. Parsons, *Anal. Chem.*, **45**, 2417 (1973).
(30) R. G. Brewer, *Science*, **178**, 247 (1972).

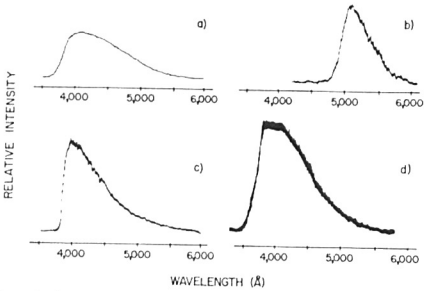


Figure 3. Spectra of ultrafast emissions from benzene solutions, 25 °C, of (a) 0.04*M* benzophenone, (b) 0.05*M* benzil, (c) 0.1*M* 4,4′-dimethoxybenzophenone, and (d) 0.09*M* acetophenone. "Boxcar" sampling gate, t_g = 10 nsec, t_d = 0.0 nsec

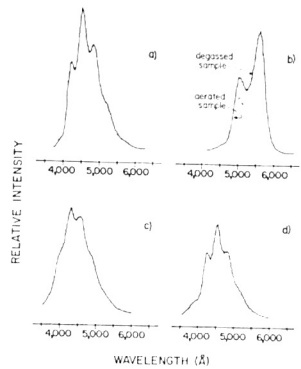


Figure 4. Total emission spectra from (a) 0.05*M* benzophenone, (b) 0.01*M* benzil, (c) 0.01*M* acetophenone, and (d) 0.0001*M* 4,4′-dimethoxybenzophenone, in benzene, 25 °C

Types of Experiments Performed. Two types of experiments are performed with this technique. The emission spectrum in any time segment of a radiative pulse can be determined (a Hewlett-Packard Model 7000A X–Y Recorder was used) by using a stationary sampling gate and a scanning sampling monochromator, see Figure 1(*B*). Second, the decay of an emission at fixed wavelength, but with improved SNIR can be obtained by using a scanning gate, see Figure 1(*C*).

The response characteristics of the monochromator–photomultiplier combination were determined by measuring the output from a Philips Research Laboratory (Netherlands) tungsten filament lamp, and by comparison of the observed quinine sulfate fluorescence spectrum with a reported corrected fluorescence spectrum (*31*). The filament temperature of the tungsten lamp was monitored with a Pyro Optical Pyrometer (Pyrometer Instrument Co.).

Sample Preparation. Benzene was distilled through a 60-cm glass column packed with glass beads and a center cut was taken. Recrystallized and zone-refined benzophenone (Princeton Organic Chemicals) were used with no differences in the emission characteristics from the two samples being noted (*11*). Benzil was recrystallized and 4,4′-dimethoxybenzophenone was recrystallized and vacuum sublimed prior to use. Acetophenone was vacuum distilled and a center cut was taken. Solutions of the above carbonyl compounds in benzene were degassed at 5–10 microns by at least 6 freeze–pump–thaw cycles and sealed in 1-cm² borosilicate glass cuvets.

RESULTS AND DISCUSSION

Separation and Identification of Prompt Fluorescence. It has been reported (*3, 5*) that E-type delayed fluorescence from unsubstituted and substituted benzo- and acetophenones is responsible for the relatively weak emission band on the high energy side of the phosphorescence. Examination of the room and low temperature emissions from benzophenone (*11*), 4,4′-dimethoxybenzophenone (*12*), acetophenone, benzil, and several other carbonyls (*32*) with the gated time resolved system revealed in each case at least two components of emission: (i) an ultrafast emission occurring within the duration of the excitation pulse and (ii) a slower decaying emission (msec at 77 °K and μsec at room temperature). The ultrafast emissions were separated and identified by the following procedures.

A 10-nsec Boxcar gate was used at zero time delay (*i.e.*, superpositioned over the ultrafast pulse). Typical spectra measured from room temperature solutions are shown in Figure 3. A comparison of the spectra in Figures 3 and 4 shows that the ultrafast emissions are quite different from the total emission spectra. The emission spectra in Figure 4 were obtained by use of μsec or wider gates, at zero delay, so as to include the total emission, or by use of an American Instrument Co., Inc. Spectrofluorometer with a 250-W Hg-Xe lamp and 1P21 phototube (excitation at either 3130 or 3660 Å). The total emission spectrum from benzil after aeration (Figure 4b) is identical to the spectrum of the ultrafast emission from benzil. Under aerated conditions, benzil phosphorescence and delayed fluorescence should be totally quenched (*10*). Thus, the ultrafast emissions are identified as prompt fluorescence. By comparing the prompt fluorescence and absorption spectra in the manner suggested by Birks (*33*), the (0–0) transitions of acetophenone, 4,4′-dimethoxybenzophenone, benzophenone, and benzil are estimated to be 2.76, 2.63, 2.63 and 2.12 μM^{-1} in benzene at room temperature.

We observe that the ultrafast emission pulse shapes can be superimposed on the excitation pulse. Therefore, we conclude that the emitting states have lifetimes $<10^{-9}$ sec since longer lifetimes would have led to a distortion of the emission pulse shape relative to the exciting pulse. (*33*). For the case of benzophenone, this observation is consistent with a measured fluorescence lifetime of ~20 psec (*8, 9*). The quantum efficiencies of the prompt fluorescences from these carbonyls are estimated, relative to the phosphorescences, to be between 10^{-3} and 10^{-6} (*11, 32*) by Equation 2.

$$\Phi_f \simeq \left\{\left[\int_0^{t_e} \bar{I}_f dt\right] \Big/ \left[\int_0^{\infty} \bar{I}_p dt\right]\right\} \Phi_p \qquad (2)$$

In Equation 2, t_e is the duration of the excitation pulse, and $\bar{I}_f$ and $\bar{I}_p$ are the emissions integrated with respect to wavelength. Φ_p is the quantum efficiency of phosphorescence determined by comparison with quinine sulfate (*31*). The experimental arrangement shown in Figure 1 was used for determining $\bar{I}_f$ and $\bar{I}_p$ except that the sampling monochromator was bypassed. The *total* emission signal (*i.e.*, total spectral distribution), filtered to eliminate laser radiation, is thus sampled by the photomultiplier. Narrow slits in front of the photomultiplier and a low photomultiplier voltage were used to avoid saturation effects which distort the signal shape. The integrated intensity of the prompt fluorescence $\int \bar{I}_f dt$ is measured using a stationary 10-nsec sampling gate superimposed over the ultrafast emission. $\int \bar{I}_p dt$ is estimated by scanning the 10-nsec gate

(31) C. A. Parker and W. T. Rees, *Analyst (London)*, **85**, 587 (1960).
(32) K. D. Legg, unpublished results, 1974.
(33) J. B. Birks, "Photophysics of Aromatic Molecules," Wiley-Interscience, New York, N.Y., 1970.

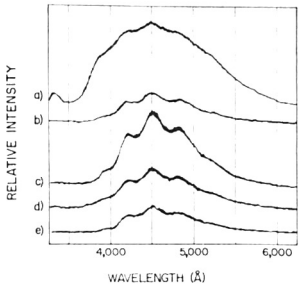


Figure 5. Time resolved emission spectra from 0.05*M* benzophenone, in benzene, 25 °C

t_g = 100 nsec for all. (a) t_d = 0 nsec, (b) t_d = 1 μsec. Relative sensitivity "rs" of the following 2.5, (c) t_d = 1 μsec, (d) t_d = 4.5 μsec, and (e) t_d = 8 μsec

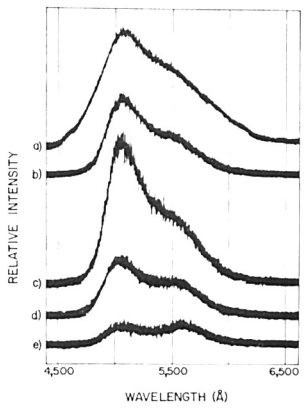


Figure 6. Time resolved emission spectra from 0.30*M* benzil in benzene, 25 °C

t_g = 100 nsec. (a) t_d = 0 nsec, (b) t_d = 200 nsec, rs = 2.0, (c) t_d = 400 nsec, rs = 4.0, and the same for the remaining, (d) t_d = 800 nsec, and (e) t_d = 1.5 μsec

over the remaining portion of the decay curve, under the same Boxcar retention conditions, and integrating the Boxcar output with respect to time. These data, in conjunction with the measured Φ_p, allow calculation of Φ_f.

The limiting resolution of the prompt fluorescence by the above technique can be expressed in terms of the "purity" (F_f) of the ultrafast emission such that

$$F_f = [\Phi_f/\tau_f]/\{[\Phi_f/\tau_f] + [\Phi_p/\tau_p]\} \quad (3)$$

For the case of benzophenone, where $\Phi_f \approx 10^{-5}$, $\tau_f = t_e$, $\Phi_p \approx 10^{-3}$ and $\tau_p \approx 10^{-5}$ sec (*34*), $F_f \approx 0.91$.

Delayed Fluorescence. The high energy emission band observed from these carbonyls consisted of both prompt fluorescence and a slower decaying emission. This evidence was obtained (i) by setting the monochromator on the high energy band and monitoring its decay with a time-scanning Boxcar gate, or (ii) by recording the spectral distribution of the emission with a stationary gate set at various delay times (Figures 5–8). Under conditions of high concentrations and short delay times (after the termination of the prompt fluorescence), the emission decays were non-exponential and the ratio of the "fluorescence" to phosphorescence intensities varied with time. Under conditions of low concentrations and long delay times, the ratio was constant (*i.e.*, the delayed fluorescence decayed with the lifetime of the phosphorescence).

The non-exponential decay and the variation of I_f/I_p is indicative of P-type delayed fluorescence (*16*). The long-lived delayed fluorescence which decays with the lifetime of the phosphorescence, and which is absent at 77 °K, is consistent with E-type delayed fluorescence (*3, 5, 6*).

Low Temperature Phosphorescence. The high energy bands are absent from the low temperature spectra (Figure 9) when the sampling gate is offset from the ultrafast emission pulse (delay times >10 nsec). Under these conditions of temperature (77 °K) and concentration ($\lesssim 10^{-2}$ *M*), delayed fluorescence (E- or P-type) is negligible. Since the prompt fluorescence is excluded by the gate offset, these spectra represent the true phosphorescence spectra from these carbonyl compounds.

Benzil Phosphorescence. Comparison of Figures 4b and 6 reveals a significant hypsochromic shift in the phosphorescence from benzil when the temperature is lowered from 298 to 77 °K. This shift is estimated to be 690 cm^{-1}. A similar shift of 500 cm^{-1} has been observed in the weak

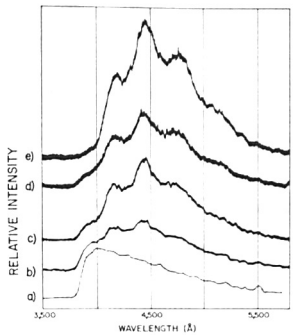


Figure 7. Time resolved emission spectra from 0.1*M* 4,4′-dimethoxybenzophenone in benzene, 25 °C

t_g = 100 nsec. (a) t_d = 0 nsec, (b) t_d = 200 nsec, rs = 5, (c) t_d = 500 nsec, rs = 10, (d) t_d = 1 μsec, rs = 10, and (e) t_d = 5 μsec, rs = 50

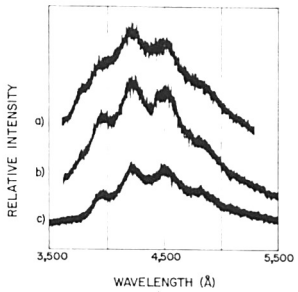


Figure 8. Time resolved emission spectra from 0.01*M* acetophenone in benzene, 25 °C

t_g = 100 nsec. (a) t_d = 0 nsec, (b) t_d = 2 nsec, (c) t_d = 1.6 μsec

(34) L. A. Singer, G. A. Davis, and R. E. Brown, *J. Amer. Chem. Soc.*, **95**, 8638 (1973).

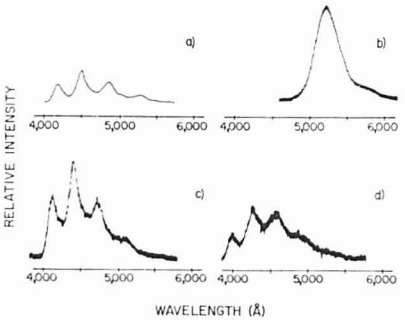


Figure 9. Low temperature, 77 °K, phosphorescence spectra from (a) 0.04*M* benzophenone, (b) 0.001*M* benzil, (c) 0.1*M* 4,4′-dimethoxybenzophenone, and (d) 0.01*M* acetophenone in Mallinckrodt spectrograde methylcyclohexane. $t_d \geq 1$ μsec for all

n,π* absorption band between 201 and 77 °K in EPA (*35*). Similarities in the absorptivities (*36*) and energies of the n,π* transitions of benzil and monocarbonyls such as benzaldehyde and the dissimilarities in the electronic absorption spectra between benzil and α-dicarbonyls which have a *trans*-planar (O=)C—C(=O) orientation in the ground state (*37*, *38*) lead to the conclusion that the molecular orientation in the benzil ground state is skewed. The dihedral angles of the low-lying singlet and triplet states of benzil differ from that of the ground state and are probably *trans*-coplanar based on (i) a comparison of the triplet energies and phosphorescence spectra of benzil and sterically hindered and rigid α-dicarbonyls (*39*), and (ii) the lack of mirror image symmetry between the benzil absorption and fluorescence.

CONCLUSIONS

The technique of gated nanosecond time resolved laser spectroscopy described herein is a valuable tool for the study of emission processes having low quantum efficiencies and/or several competing modes of emission, particularly involving ultrafast emissions. Specifically, with this technique it is possible to (i) separate and time-resolve multi-component radiative processes, (ii) sample and measure weak, low frequency signals, and (iii) improve the signal-to-noise output from a photomultiplier or similar sensing electronics. The limiting time resolution of this instrumentation is 10 nsec. However, by incorporation of faster gated FET signal averagers, and shorter duration excitation sources, the resolution can be extended into the subnanosecond regime.

This technique is invaluable for the investigation of photophysical processes in aromatic carbonyl compounds, since prompt fluorescence, phosphorescence, and E- and P-type delayed fluorescences all occur under certain conditions. This technique may be useful in examining the contribution of triplet → singlet thermal reactivation to photochemical reactivity.

ACKNOWLEDGMENT

We thank Anthony Remeikis for his contributions to the design and assembly of some of the electronic components.

RECEIVED for review January 28, 1974. Accepted June 13, 1974. This work was supported by the U.S. Army Research Office—Durham.

(35) A. Kuboyama, R. Yamazaki, S. Yabe, and Y. Uehara, *Bull. Chem. Soc. Jap.*, **42**, 10 (1969).
(36) H. Suzuki, "Electronic Absorption Spectra and Geometry of Organic Molecules," Academic Press, New York, N.Y., 1967, p 435.
(37) D. J. Morantz and A. J. C. Wright, *J. Chem. Phys.*, **54**, 692 (1971).
(38) D. J. Morantz and A. J. C. Wright, *J. Chem. Phys.*, **53**, 1622 (1970).
(39) T. R. Evans and P. A. Leermakers, *J. Amer. Chem. Soc.*, **89**, 4380 (1967).

Corrected and Automated Spectrophotofluorimeter Employing a Pyroelectric Detector for Correction

Isaac Landa and J. C. Kremen

American Instrument Company, Division of Travenol Laboratories, 8030 Georgia Ave., Silver Spring, Md. 20910

A corrected spectrophotofluorimeter employing a pyroelectric detector for correction is described. The pyro-detector is free from the inherent difficulties associated with quantum counters and thermopiles (stability, purity, drift, fragility, etc.). In this application, it provides reliable and continuous correction of excitation spectra over a wide spectral range. The reliability of correction in the apparatus is further enhanced by the use of a single photomultiplier tube in the system. The capabilities of the instrument are described. These include: Built-in spectrophotometer for direct comparison of absorption and excitation spectra; measurement of differential fluorescence, relative quantum efficiencies, and polarized fluorescence; capability of plotting spectra in energy or quantum units, *vs.* wavelength or wavenumber. Spectra obtained with the instrument are presented to demonstrate its performance in the various modes in which it is operated.

The demand for a spectrophotofluorimeter capable of measuring spectra, independently of instrumental variables, has progressively increased (*1*). The desire for such an instrument is understandable, since it will enable standardization and direct comparison of various spectrophotofluorimetric spectra. The task of developing a fluorimeter

(1) W. H. Melhuish, *J. Res. Nat. Bur. Std., Sect. A*, **76**, 547–60 (1972).

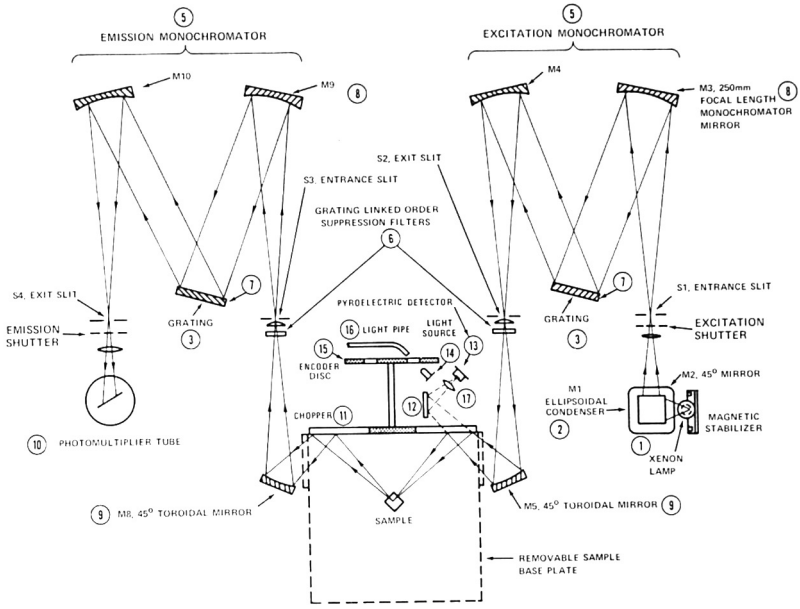


Figure 1. Optical system schematic

is a complicated one due to the large number of instrumental variables involved. The variables that one encounters in fluorimetric studies include variations in source intensity with time and wavelength, spectral dependence of optics with respect to wavelength and state of polarization, sample absorption and scatter, and variation in the sensitivity of detectors.

Various instruments were developed to correct for these variables. In the literature, one finds correction schemes which use electromechanical compensating elements, such as function generators (*2, 3*), while others use computers with programable corrections (*4, 5*). Most of the instruments described were optimized with respect to some given applications. The instrument described in this paper was developed to meet the following goals:

Simplicity and Reliability of Corrections. This goal was achieved by employing a recently developed pyroelectric detector for the excitation correction (*6–9*). Such a detector has distinct advantages over thermopiles and quantum counters; in comparison to a thermopile, the pyroelectric detector has a faster response time, is less sensitive to ambient temperature changes, and has uniform sensitivity over its entire surface (*10*). In comparison to a quantum counter, the pyroelectric detector has a wider wavelength range and is free of the purity and stability problems inherent in quantum counters.

Versatility in Data Presentation. Investigators in different fields have adopted different modes of data presentation. For instance, chemists prefer to see the spectra plotted in units of quanta *vs.* wavenumber, while biologists prefer quanta *vs.* wavelength, and those involved in color studies present their data in watts *vs.* wavelength. To make the instrument versatile, an automatic conversion to the above mentioned units is included and the spectra can be obtained in any of the three formats.

Universality. In attempting to make the instrument useful for the experimentalist, a few important capabilities were included: Measurement of absorbance for direct comparison of excitation and absorbance spectra; integration of corrected emission for measurement of quantum efficiencies; differential fluorescence for automatic subtraction of blank, or scatter peak, and for amplifying small differences in emission between two samples; corrected polarization (depolarizers were included in the optical path to correct for polarization dependence of components); and phosphorescence spectra and lifetimes using a rotating shutter with variable speed.

APPARATUS DESCRIPTION

Optics. Figure 1 shows the optical layout of the system in the corrected excitation mode. The excitation light source is a Hanovia short arc 500-watt xenon lamp that is powered by an IREM power supply, supplying 30 A at 17 V. An ac magnetic stabilizer is mounted perpendicular to the lamp axis to prevent random arc fluctuations. The source also includes an off-axis ellipsoidal condenser system having an energy gathering ability that increases the usable light intensity up to a factor of 10. The light gathered is imaged on fixed bilateral curved slits. The slit width can be adjusted to cover a bandwidth range of 0.1 to 40 nm. The light at the entrance slit is dispersed by a Czerny-Turner monochromator having 250-mm focal length. The gratings used in the monochromators have 600 lines/mm

(2) P. Rosen and G. M. Edelman, *Rev. Sci. Instrum.*, **36,** 809 (1965).
(3) G. R. Haugen and R. J. Marcus, *Appl. Opt.*, **9,** 1049 (1969).
(4) C. F. Grum and D. J. Paine, *Appl. Opt.*, **8,** 1149 (1969).
(5) J. F. Holland, R. E. Teets, and A. Timnick, *Anal. Chem.*, **45,** 145 (1973).
(6) J. Cooper, *J. Sci. Instrum.*, **39,** 467 (1962).
(7) J. Cooper, *Rev. Sci. Instrum.*, **33,** 92 (1962).
(8) R. A. Hanel, *J. Opt. Soc. Amer.*, **51,** 220 (1961).
(9) W. M. Doyle, *Opt. Spectrosc.*, Nov. (1972).
(10) R. G. Johnston and R. P. Madden, *Appl. Opt.*, **4,** 1574 (1965).

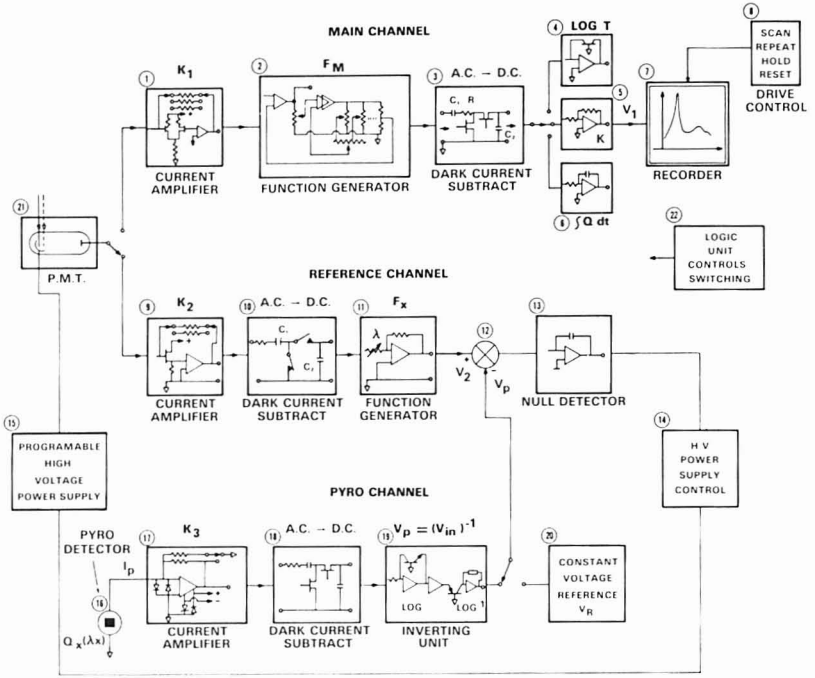


Figure 2. Block diagram of electronics

and are blazed at 300 and 500 nm for excitation and emission, respectively. Higher order suppression filters are linked to the grating drive mechanisms and are automatically inserted during a scan. Toroidal mirrors M5 and M8 focus the excitation monochromator slit in the center of the cell, and the cell on the entrance slit of the emission monochromator. The fluorescence exiting the emission monochromator is imaged on a side-on S20 potted photomultiplier tube. The tube is a Hamamatsu type R446S, specially selected for wide spectral response and high quantum efficiency.

At the sample compartment, the light beam is time shared between the pyroelectric detector 13* and the sample by the use of a rotating chopper mirror 11. The chopper mirror has a dark vane, 3M black coated, which is used to sample the dark current of the photomultiplier tube. The light directed to the pyrodetector channel is reflected from a mirror 12 optically matched to the chopper mirror and is focused by a short focus lens 17 onto the pyroelectric detector. In other ratio configurations, the reference beam is reflected from a white reflector located in front of the pyrodetector and guided through a flexible quartz fiber light pipe 16 to the photomultiplier tube. The flexible pipe is also used to direct the light from a temperature compensated light emitting diode 14 to the photomultiplier tube. The encoding disc 15 is used to time the signal from the constant light source and to generate timing pulses for the logic circuitry.

To use the instrument in the spectrophotometric mode or in the differential fluorescence mode, two mirrors, spectrally matched with the chopper mirror, are mounted behind the chopper (Figure 4, parts D and E). The chopper and the mirrors direct the excitation beam to the sample and blank, and the emission or transmission of the sample and the blank to the photomultiplier tube. To ensure reflectivity match over the spectral range, to within 4%, the chopper mirrors and the two mirrors in the back of the chopper were coated simultaneously. The difference in reflectivity of the mirrors is further compensated by a baseline compensator (function generator).

A few design improvements have been incorporated in the optics. The design of the monochromators follows Fastie (*11, 12*) in that the slit curvatures coincide with the locus of constant wavelength, a necessary condition for improved resolution. Resolution is further improved by a special alignment procedure that uses a target slit to align the mirrors. The positioning of the mirrors was chosen to prevent dispersed light from striking the grating, thus decreasing considerably the stray light found in similar monochromators. To enhance the UV performance, aluminum mirrors were used with a magnesium fluoride coating and UV grade quartz lenses and windows.

Electronics. Figure 2 is block diagram of the electronic circuitry. Light signals are detected and converted into electrical current by the photomultiplier tube and by the pyroelectric detector. The corresponding current signals are processed by the main and reference channels. The electronic sampling of the chopped signals is controlled by an encoder disc mechanically coupled with the mirror chopper. The encoder disc has 40 holes equally distributed

* Numbers without parentheses describe details on the figure under discussion.

(11) W. G. Fastie, *J. Opt. Soc. Amer.*, **42**, 641 (1952).
(12) W. G. Fastie, *J. Opt. Soc. Amer.*, **42**, 647 (1952).

over its periphery. Two holes are plugged and the absence of these holes is monitored by an integrator and serves to synchronize the switching. One revolution of the encoder disc corresponds to two chopping cycles. The rate of chopping is 25 cycles per second. Each hole produces a pulse by opening the light path to a light emitting diode phototransistor combination. The pulses obtained are shaped and referred to a logic circuit that provides output pulses to time the switching in the different modes of operation. The switching circuits serve two main functions: To refer the signal to the appropriate channel and to sample the light and dark current levels. The latter is used to automatically subtact dark currents and drifts.

Main Channel. The emission signal from the photomultiplier tube is referred by the input switch to a low-leakage, low-noise, dual field-effect transistor. The current signal is converted to voltage and amplified to correspond to the desired full scale setting. This signal is directed to a function generator F_M. When used, the function generator multiplies the input signal by the inverse of the spectral response of the emission monochromator and the photomultiplier tube. It also multiplies the input signal by a function of wavelength depending on the units in which the data are to be presented.

The function generator consists of a 10-turn tapped potentiometer with 33 taps. Single turn potentiometers are connecteto the taps and are set to provide the desired functional dependence (*13*). For conversion of units, additional single turn potentiometers (continuous rotation) were included. The tapped and the single turn potentiometers are mechanically coupled to the emission monochromator drive.

The output from the function generator is passed through a dark current subtract circuit 3 which samples the minimum and maximum of the pulsed signal and takes their difference. The dark current circuit performs the following sequence of operations: First, capacitor C1 is charged through a small time constant to SIGNAL + DARK CURRENT; then the dark current is sampled and C2 is charged in proportion to SIGNAL + DARK CURRENT − DARK CURRENT (*i.e.*, proportional to signal only). C2 is large compared to C1 and will reach the final signal value over approximately 25 cycles; C2, therefore, also behaves as a low pass filter with a time constant of 1 sec. The output from the dark subtract circuit is a dc signal that depends only on the intensity of the emitted light. Subsequent processing of this signal depends on the mode of operation. In the absorbance mode, a log module is connected to take the log of the signal; in the quantum efficiency mode, an integrator is introduced to integrate the corrected emission spectra. In all other modes, the signal is amplified. In all modes, the output signal is displayed on an X-Y recorder.

The emission amplifier was designed for wide frequency response. As a result, measurement of phosphorescence decay times as low as 1 msec are possible (see Modes of Operation, paragraph F, Phosphorescence).

Reference Channel. The reference light signal is detected by the photomultiplier tube, amplified 9, and the dark current is automatically subtracted 10. The resulting dc signal is passed through a function generator F_X that is mechanically coupled to the drive mechanism of the excitation monochromator. The function generator controls the gain and converts the signal to the desired units. One can plot the excitation spectra in energy units or in quantum units.

The output voltage from the function generator is compared to a reference voltage. The reference voltage is provided by a fixed voltage source, or by the pyroelectric detector channel V_p. The voltage difference at the output of the summing junction 12 is applied to an integrator, which functions as a null detector. The integrator output controls the gain of the photomultiplier tube to maintain zero voltage at the summing junction.

In analyzing the closed loop response of the system, we found that the open loop gain changes in nearly inverse proportion to the reference signal. A variable time constant was needed to ensure stability of the system over the full dynamic range of the pyrodetector. The variable time constant was obtained by varying the integration rate of the null detector.

Pyroelectric Channel. The pyroelectric detector is basically a dielectric material which shows a strong residual polarization after a polarizing electric field is removed. In this class of materials, the induced polarization depends strongly on temperature, *i.e.*, a change in temperature will cause a change of surface charge. This phenomenon is used to measure light intensity.

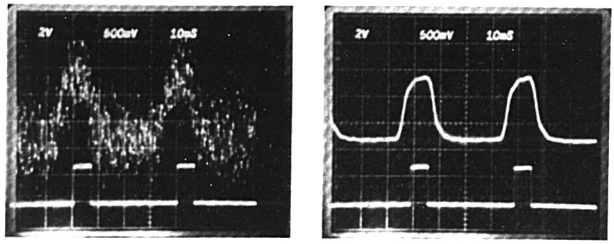
To convert UV-VIS light energy into heat, it is necessary to apply a black coating on the surface of the detector. Therefore, the spectral response of the detector is determined by the black coating. The coating we use is a 3M black velvet. Measurement of total reflectance conducted on this coating (*14*) indicates that the total reflectance varies from 4.9% at 250 nm to 1.9% at 800 nm; thus, the spectral response of the detector is flat to within 3%. The sensitive area is 2 mm in diameter and the responsivity of the detector is 1 μA/watt.

The design of the electronic circuitry for the pyroelectric detector optimizes the signal-to-noise ratio and provides an adequate frequency response for pulse amplification. The frequency response of the detector-amplifier combination depends primarily on the configuration chosen for amplification. Two modes of amplification are possible: voltage and current mode. In the voltage mode, the detector feeds its current into a load resistance and the resulting voltage is then amplified. In this case, the frequency response will be limited by the time constant of the detector capacitance times the load resistance. In the current mode, the detector is feeding the current into a virtual zero resistance (input mode of an operational amplifier); hence, the electric time constant can be assumed zero, and the frequency response will be limited only by the thermal time constant of the coating. To further improve the frequency response, it is necessary to minimize the stray capacitance that exists between leads connecting the components and between the bodies of the components, as well as across the switch structure. Minimization of the stray capacitance was achieved by keeping leads short, by avoiding the location of components in parallel and by grounding switch contacts when not in use. Tests conducted on the pyro input stage showed a rise time of 1–2 msec from 10 to 90% of peak value.

To detect the lowest signal level possible by the detector, it is necessary to keep all noise sources small compared to the NEP of the detector. The noise equivalent power (NEP) is the signal power required to produce a signal-to-noise ratio equal to unity. One has to consider noise sources such as Johnson noise of resistors, the current and voltage noise of operational amplifiers, and noise pick-up from adjacent radiating sources. These noise sources were minimized by proper choice of operational amplifiers and by careful shielding of the input stage. However, in working with the pyroelectric detector we found that the major noise source is due to the piezoelectric properties of the crystal. Mechanical vibrations in the instrument cause the

(13) T. D. S. Hamilton, *J. Sci. Instrum.*, **43**, 49 (1966).

(14) Test Report on 101-C10 Black, 3M Company, Saint Paul, Minn.



– a – – b –

Figure 3. (*a*) Unfiltered pyroelectric detector signal; (*b*) Filtered signal

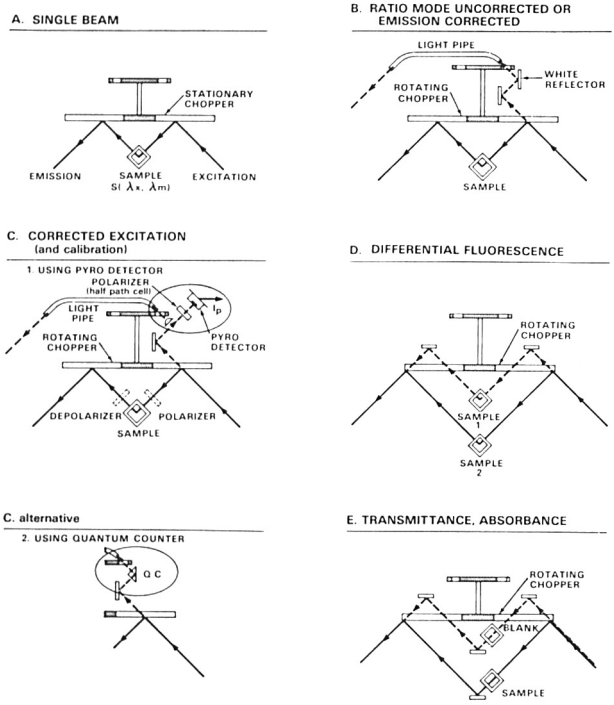


Figure 4. Block diagram of system illustrating modes of operation

output from the detector to be modulated by a resonance frequency typical of the particular structure of the detector. The frequency spectrum of this interference revealed that resonance occurs at about 1 KHz. Therefore, it was possible to remove the interference with a low pass filter. A 6-pole Chebyschev filter with a cutoff frequency of 300 Hz was used for this purpose. Figure 3 shows the signal before and after filtering. The use of 6 poles resulted in a considerable phase shift of the pulsed signal and the timing of the dark current subtract circuitry had to be adjusted accordingly. The dc output from the pyroelectric channel is inverted and summed with the voltage obtained from the photomultiplier tube. This sum is applied to the input of the null detector in the corrected excitation mode.

Modes of Operation. Figure 4 shows the various modes in which the instrument can be operated. In the following, each mode is described separately. The distortion of the displayed spectra due to instrumental variables and the method of correction are given. The equations that follow use the terms defined in Table I and refer to the block diagram shown in Figure 2. It should be noted that the variables used in the equations are only the ones needed to demonstrate the concept used for correction.

A. Single Beam Mode. In this mode, the excitation beam is directed on the sample 100% of the time, providing optimum signal-to-noise ratio for lowest detection limits. Using the notation given in Table I, the following equation can be written to describe the signal output to the recorder,

Table I. Nomenclature

Symbol	Description	Symbol	Description
$E/\Delta\lambda$, $E/\Delta\nu$	Energy emitted per second within a unit wavelength (wavenumber) interval	$S(\lambda_x, \lambda_m)$	Sample response, a function of excitation and emission wavelength
K_1	Gain constants	$T_M(\lambda_m)$	Emission monochromator transfer function
$PM(HV, \lambda)$	PMT gain, a function of high voltage and wavelength	λ_x	Excitation wavelength
$Q/\Delta\lambda$, $Q/\Delta\nu$	Number of photons emitted per second within a unit wavelength (wavenumber) interval	λ_m	Emission wavelength
$Q_x(\lambda_x)$	Number of photons per second exciting the sample		

$$V_1 = K_1 Q_x(\lambda_x) S(\lambda_x, \lambda_m) T_M(\lambda_m) PM(\lambda m, HV) F_M(\lambda_m) \quad (1)$$

F_M, the emission correction function, is set to be inversely proportional to the wavelength response of the emission monochromator times the spectral response of the photomultiplier tube, $F_M \propto [T_M(\lambda_m)\ PM(\lambda_m, HV)]^{-1}$. Inserting the value of F_M into Equation 1 results in

$$V_1 = K Q_x(\lambda_x) S(\lambda_x, \lambda_m) \quad (2)$$

Thus, for fixed high voltage and a given excitation wavelength, the emission scan will depend only on the energy transfer characteristics of the sample resulting in a corrected emission spectra. This mode cannot be used to correct for excitation variation. Consequently, it cannot be used to normalize emission spectra of two different compounds, excited at different wavelengths, for their unequal excitation intensities.

B. Ratio. In practice, one has to deal with intensity fluctuations of the excitation source which causes Q_x to be time dependent. To prevent the distortion in the spectra caused by such fluctuations, the double beam mode is used. In this mode (Figure 4*B*), the excitation beam is divided by a rotating chopper into two beams, a main and reference beam. The main beam excites the sample and the resulting fluorescence is passed through the emission monochromator and detected by the photomultiplier tube. The signal is then processed by the main channel electronics. The reference beam is reflected from a white reflector into the photomultiplier tube and the resulting reference signal is used to control the gain of the photomultiplier tube by varying the high voltage applied to the dynodes. The reference voltage at the summing junction (Figure 2, 12) can be written as,

$$V_2 = K_2 Q_x(\lambda_x) PM(HV) PM(\lambda_x) \quad (3)$$

where it is assumed that $PM(HV, \lambda_x) \propto PM(HV)\ PM(\lambda_x)$. This reference voltage is compared to a fixed voltage V_R, and the difference is used to drive the dynode feedback loop. Thus, in steady state $V_2 - V_R = 0$. As a result the photomultiplier tube high voltage will reach a value such that $P_M(HV) \propto [Q_x(\lambda_x)\ PM(\lambda_x)]^{-1}$. Substitution of the expression of P_M and F_M in Equation 1 results in

$$V_1 = K' S(\lambda_x, \lambda_m)/PM(\lambda_x) \quad (4)$$

It is seen from Equation 4 that ratio operation compensates for the intensity fluctuations of the source. It is also seen that an excitation spectrum will be distorted by the wavelength dependence of the photomultiplier tube. This distortion is eliminated in the corrected ration scheme that employs a pyroelectric detector as the reference element.

C. Corrected Ratio. In this mode (Figure 4*C*), the reference beam is directed to a pyroelectric detector. The detector exhibits nearly constant absorption over the entire wavelength span of the instrument; therefore, the current output will be proportional to the intensity of the excitation source. This output is amplified and inverted (Figure 2) thus, $V_P \propto [Q_x(\lambda_x)]^{-1}$.

A constant light source $Q_R(\lambda_R)$ is directed to the photomultiplier tube and the resulting signal is processed by the reference channel, *i.e.*, $V_2 \propto Q_R\ PM(HV)\ PM(\lambda_R)$. Closed loop action requires V_2 to be equal to V_P; therefore, the photomultiplier tube high voltage reaches a value such that $PM(HV) \propto [Q_R Q_x(\lambda_x)\ PM(\lambda_R)]^{-1}$. Substitution of $P_M(HV)$ and F_M into Equation 1 results in,

$$V_1 = K'' S(\lambda_x, \lambda_m)/Q_R PM(\lambda_R) = KS(\lambda_x, \lambda_m) \quad (5)$$

Note that $Q_R\ PM(\lambda_R)$ is constant at a fixed high voltage and represents the response of the photomultiplier tube to a constant light source with fixed spectral distribution. From Equation 5, it is seen that this mode of operation enables the measurement of corrected excitation. Applying an excitation correction has the same effect as irradiating the sample with an excitation beam that has equal intensity at all wavelengths. Therefore, a direct comparison of the spectra of different chemical species is made possible.

Figure 4*C* also shows the configuration used when correcting the excitation with a quantum counter. This method of correction is the more common approach found in the literature and, therefore, will not be discussed in detail. It was included in our system to provide a direct comparison with previous studies using quantum counters, and also serves as an additional check on the correction.

The corrected ratio mode is also used for calibration. In this mode the two monochromators are scanned with wavelength synchronized. The main beam is reflected off a white refctor (Eastman Kodak White Reflectance Standard) which has a nearly constant reflectance (*15*) for the wavelength range of the instrument. The Emission Correction Function F_M is then adjusted by setting the potentiometers at the corresponding wavelength such that V_1 is maintained constant.

D. Differential Fluorescence. In this mode (Figure 4*D*), the main and reference beams are directed to sample 1 and

(15) F. Grum and G. W. Luckey, *Appl. Opt.*, **7**, 2289 (1968).

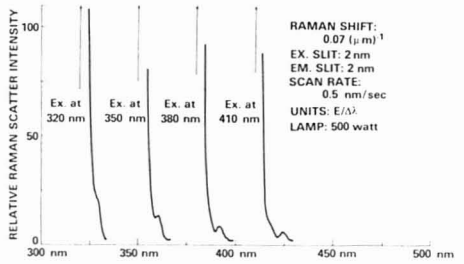


Figure 5. Raman shift of carbon tetrachloride resolved with a continuous xenon source

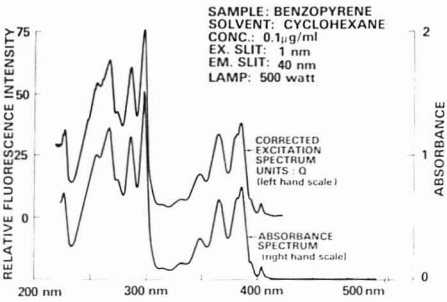


Figure 6. Corrected excitation and absorption spectra of benzopyrene

sample 2, respectively, and the resulting emissions are detected by the photomultiplier tube and processed by the main channel. A double dark subtract circuit is used in this case to obtain the difference between the emissions of the two samples. The differential emission can be corrected by using F_M in the same way as in the single beam mode.

E. Spectrophotometer. Figure 4E shows the configuration used for measuring transmittance and absorbance. In this mode, the reference beam is directed to the blank and the resulting signal is processed by the reference channel. The main beam is passed through the sample and the resulting signal is again processed by the main channel electronics. As shown before, the closed loop action will cause the high voltage of the photomultiplier tube to be inversely proportional to the light intensity of the beam passing through the blank. Hence, the output is proportional to the ratio of the transmittance of sample and blank or to the negative log of this ratio.

F. Phosphorescence. The measurement of phosphorescence is accomplished with the instrument in the Single Beam mode. A special phosphoroscope attachment is inserted at the location of the sample compartment. The phosphoroscope consists of a rotating cylinder (shutter) having two equally spaced ports, driven by a variable speed motor. The test solution in the sample tube is cooled by liquid nitrogen, or other refrigerant, to a temperature of 77 °K. The sample is caused to phosphoresce as the excitation light is admitted to the cell through one port on the rotating shutter. Phosphorescence emission is free to pass through the rotating shutter to the emission monochromator, as the shutter port traverses the optical axis of the emission light. The phosphoroscope attachment enables the measurement of phosphorescence excitation spectra, corrected emission spectra, and decay curves (using an oscilloscope).

G. Corrected Polarization. Figure 4C shows the location of the components used for corrected polarization measurements. These include one polarizer in front of the sample, an additional matched polarizer in front of the pyroelectric detector, and a depolarizer following the sample. These components are required to correct for the difference in efficiency of gratings to vertically and horizontally polarized light. If no correction is applied, these differences in efficiency of the emission monochromator will cause an error in the measurement of polarization ratio. Normally such an error is handled by determining a correction factor at each wavelength and multiplying the measurement by this factor. To avoid measurement of correction factors at several different bandwidths and over a range of wavelengths, a station to mount a quartz achromatic light depolarizer ("scrambler") was included between the sample and the emission monochromator. This is a "pseudo" depolarizer which produces all states of polarization.

Excitation spectra with polarized incident light may be measured by inserting a polarizer in front of the sample. To obtain a corrected spectrum, it is necessary to insert a matched polarizer in front of the pyroelectric detector. The positioning of these polarizers is shown in Figure 4C.

RESULTS

Instrumental Sensitivity. The relative sensitivity of fluorescence instruments is difficult to compare, because of the many variables involved. The variables include: choice of solution, blank purity, slit settings, time constants, etc.

Parker (*16*) suggests a simple test that gives a valuable indication of instrumental performance. Performance in this case refers to a figure of merit proportional to sensitivity combined with resolution. The test is to resolve Raman spectrum of some solutions. According to Parker, "A much more critical test is the resolution of the Raman band of carbon tetrachloride, (frequency shift 0.07 μm^{-1}) from the scattered exciting light. ... Resolution of Raman bands using a continuous source is more difficult and the resolution of the carbon tetrachloride band by this means has not yet been reported." We have applied this critical test to our instrument and the results are shown in Figure 5. As seen, the Raman bands of carbon tetrachloride, using a continuous source, were resolved clearly, with better resolution toward higher wavelength.

To further establish the detection limit of the instrument, the instrument was found capable of measuring 0.5 part in 10^{12} of 9,10-diphenyl anthracene in cyclohexane (at 1:1 signal-to-noise ratio).

Resolution. The wavelength accuracy and resolving power were checked by scanning a mercury pen ray lamp. The scan was done at the lowest scan rate of 0.1 nm/sec, and over a range of 100 nm, expanded to full chart length. The slit was set to 0.1-nm bandwidth. The peaks obtained agree with published data on mercury lines to within 0.2 nm.

Corrected Excitation. The pyroelectric detector corrects the excitation spectra over a bandwidth range of 1 to 40 nm and over a wavelength range of 220 to 800 nm. Figure 6 shows a corrected excitation spectrum of 0.1 μg/ml benzopyrene in cyclohexane. The data are presented in number of quanta emitted per incident quanta *vs.* wavelength. The same solution was used to measure the absorbance spectrum as shown in Figure 6, and the relative peak heights were compared and found to match. Figure 7 shows the

(16) C. A. Parker, "Photoluminescence of Solutions," Elsevier Publishing Co., Amsterdam, 1968, p 406.

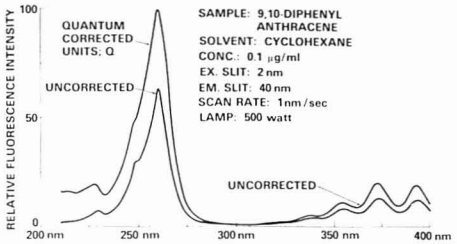


Figure 7. Comparison of corrected and uncorrected excitation spectra

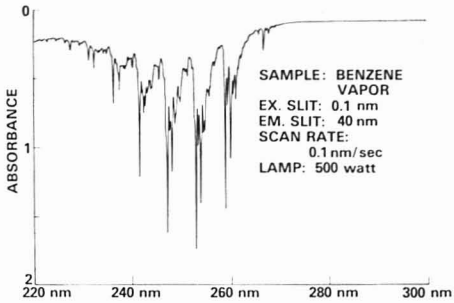


Figure 8. Absorption spectrum of benzene vapor illustrating resolving power

corrected and uncorrected excitation spectra of 9,10-diphenyl anthracene in cyclohexane. The corrected spectrum is presented in number of quanta emitted per incident quanta *vs.* wavelength. The effect of the correction on the relative peak heights is well demonstrated in this figure.

Spectrophotometry. To demonstrate the resolving power of the instrument in the transmittance and absorbance modes, we ran an absorption spectrum of benezene vapor. The results are shown in Figure 8. The high intensity of the xenon lamp enables noise free measurements at densities up to 5 A (absorbance units). This was made possible by providing calibrated absorbance base-line suppression up to 3 A. The use of tandem monochromators ensures sufficiently low stray light levels to make measurements at these high densities possible.

Corrected Emission. The emission was corrected over the range of 275 to 700 nm. A corrected emission spectrum of 0.1 μg/ml of anthracene in cyclohexane is shown in Figure 9. This spectrum is in agreement with the data published by I. B. Berlman (*17*) excluding the peak at 377 nm where the absorption overlaps the emission spectrum. We attribute the difference to the reabsorption of emitted light due to the higher concentration used by Berlman.

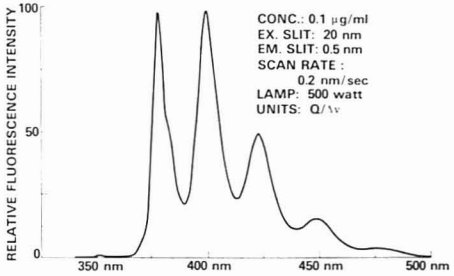


Figure 9. Corrected emission spectra of anthracene in cyclohexane

ACKNOWLEDGMENT

The authors are grateful to W. Donald Finn, president of American Instrument Co. and to C. David Miller, R&D director, for continuous support in the development stages of the project. We are also grateful to F. W. Adler, H. E. Dorman, and M. W. Egerton, Jr., for their valuable contributions to this project.

RECEIVED for review November 27, 1973. Accepted July 16, 1974.

(17) I. B. Berlman, "Handbook of Fluorescence Spectra of Aromatic Molecules," Academic Press, New York, N.Y., 1971.

Study of the Precision of an X-Ray Fluorescence Spectrometric Determination

E. B. Buchanan, Jr., and Foo-Chong Tsai

Department of Chemistry, The University of Iowa, Iowa City, Iowa 52242

Relative standard deviations of the counts accumulated in an X-ray fluorescence spectrometric analysis were evaluated for the several variables affecting analytical precision: instrumental deviation resulting from short-term electronic drift, 0.045%; goniometer reset, 0.030%; excitation voltage–current reset, 0.43%; sample orientation, 0.15%; sample placement, 0.12%; and sample preparation, 0.68%. The total deviation was 0.83%. These values permit the precision of a particular method of X-ray fluorescent analysis to be estimated in advance of other experimentation.

X-Ray fluorescence spectrometry has gained widespread usage in environmental studies of trace metals and as such offers several advantages. It is a relatively fast method of

analyzing the elemental composition of a sample. Spectral line interference is relatively infrequent. Specimens placed in the instrument can be in the form of either solids or liquids. Elaborate sample pretreatment is generally unnecessary, and the specimen is neither consumed nor destroyed during the analysis.

This study was undertaken to determine and evaluate certain sources of error in the X-ray fluorescence analysis. Such an evaluation provides a basis for estimating the types and degree of errors associated with the method.

The key for the successful application of X-ray fluorescence spectrometry to routine analysis as well as to unusual analytical problems lies in the accuracy and precision of the analytical results obtained. The accuracy of the analytical result is the degree of agreement with the "true", accepted, or most reliably-known value. In most cases, standard preparations serve the purpose of providing the most reliably-known values. The precision of the analytical result is the degree of agreement among the replicate determinations made under conditions as nearly identical as possible. The evaluation of the precision of the analytical results will lead us to a more in-depth knowledge of the magnitude and variety of errors affecting an X-ray fluorescent analysis, so that these errors can be revealed and possibly minimized. Furthermore, with the values of these errors known, the precision of a particular method of analysis can often be estimated in advance of the experimentation.

OUTLINE OF THEORY

The precision of an analytical determination is measured as the standard deviations, which are defined as the root mean square of the deviations of a set of measurements from their arithmetic mean. The observed standard deviation calculated from a set of replicate intensity measurements is usually subjected to more than one variable. Therefore, the observed standard deviation is a composite of individual variations and errors. So long as these individual variables are independent, their variances (square of standard deviation) should combine as follows to give the overall observed values.

$$s_{obsd} = (s_1^2 + s_2^2 + s_3^2 + \ldots)^{1/2} \quad (1)$$

This means that the individual variations operate simultaneously to give the total standard deviation. For the method of X-ray fluorescence spectrometry, these variations were considered to originate from sources as follows: X-ray counting errors, instrumental errors due to drifts of current and voltage, operational errors due to the manual reset of the goniometer or placement of the sample in the spectrometer, and technical errors which can result from the inhomogeneity of the sample and the preparation of the sample. Thus,

$$s_{obsd} = (s^2_{\text{X-ray count}} + s^2_{\text{drift}} + s^2_{\text{goniometer reset}} + s^2_{\text{placement}} + s^2_{\text{inhomogeneity}} + s^2_{\text{preparation}})^{1/2} \quad (2)$$

Only s_{obsd} is directly measurable. The proportion of this total that is considered to come from each individual error source must be evaluated by theory or experiment. Theory allows us to evaluate the counting error as $N^{1/2}$, where N is the number of counts accumulated (*1*). The other sources must be evaluated by appropriately designed experiments. This is accomplished by designing the experiment such that all known errors are kept constant except for that variable for which the error is sought.

As the average number of counts may differ in each category for which an error was determined, the percent relative standard deviation, ϵ, where

$$\epsilon = \frac{s}{N} \times 100 \quad (3)$$

was used rather than s to calculate the error.

EXPERIMENTAL

Instrumentation. The instrument was a Philips Universal Vacuum X-Ray Spectrograph equipped with a tungsten-target X-ray tube, LiF(200) crystal monochromator (4 inches × 0.005 inch), collimator, and scintillation counter. The operating conditions were as follows: excitation 50 kV, 45 mA, full-wave; goniometer setting 11.11° 2θ (BaKα); pulse-height selector in integral mode with 5-V base line; and counting time 500 sec.

Specimens. The specimens used in the experiments were chosen to be representative of the samples one would encounter in the analysis of soils or geological materials. The samples were natural sediments. They were ground in an agate mortar to 200 mesh and dried in a muffle furnace at 500 °C for 4 hours. The powdered samples were then packed into a "Somar" aluminum cap (Somar Laboratories, Inc., 54 East 11th Street, New York, N.Y. 10003) and pressed into a pellet at 55,000 lb/in.^{2} pressure.

Evaluation of Errors. Of all the errors listed previously, the counting error is the simplest to evaluate, in that it depends only on the total accumulated counts. The counting error is always present as a variable affecting the overall precision of an X-ray fluorescent analysis. Consequently, it represents the maximum precision attainable in an analysis. The counting error is taken to be equal to the square root of the number of counts obtained. Thus

$$s_{\text{X-ray count}} = N^{1/2} \quad (4)$$

and the percent relative standard deviation is given by

$$\epsilon_{\text{X-ray count}} = \frac{N^{1/2}}{N} \times 100 \quad (5)$$

Incidentally, the particular model of X-ray spectrometer used in these experiments has an internal counter which is not normally read and which has the effect of decreasing the real count N by one order of magnitude to $N' = N/10$. When this internal counter is considered the percent relative standard deviation is given by

$$\epsilon = \frac{(10N')^{1/2}}{10N'} \times 100 \quad (6)$$

Column I of Table I shows a series of successive observations made on the same sample. The average value of the count was observed at 609260. From Equation 6 above, the percent relative standard deviation of the counting error is calculated to be 0.041%.

Error Due to Drift. The ability of the instrument to reproduce X-ray intensity measurements from a given specimen within a period of time may vary. After the spectrometer is allowed to warm up for a period of four hours, instability in the power generator, detector, or other electrical components may cause further drifts. To evaluate the drift error, intensity measurements were obtained for the period of time needed for one normal routine analysis. Successive replicate readings taken within a period of sixty minutes were recorded devoid of any instrument resetting. The individual readings as well as the average and standard deviation are shown as Column I in Table I. Any significant difference between the X-ray counting error and the observed standard deviation may be attributed to some kind of drift within the period of the experiment.

$$\epsilon_{\text{drift}} = (\epsilon^2_{\text{obsd}} - \epsilon^2_{\text{X-ray count}})^{1/2} \quad (7)$$

$$\epsilon_{\text{drift}} = (0.061^2 - 0.041^2)^{1/2}$$

$$\epsilon_{\text{drift}} = 0.045\%$$

Error Due to Goniometer-Reset. There are two important requirements for resetting the goniometer in order that the reset

(1) R. C. Stanley, *Brit. J. Appl. Phys.*, **12**, 503 (1961).

Table I. Series of Measured Accumulated Counts for Evaluation of Six Sources of Error

Readings	I, Drift	II, 2θ Reset	III, Specimen orientation	IV, Specimen placement	V, kV, mA reset	VI, Specimen preparation
1	609332	622239	600706	600399	326215	394361
2	608783	623050	601778	599726	326329	391347
3	609434	622122	600128	598857	327653	390667
4	609722	622007	599220	597804	326179	389519
5	609156	622009	598816	597833	329706	397163
6	609604	622667	600399	597264	329090	393285
7	608788	...	600654	597331	...	...
Av	609260	622349	600243	598459	327529	392724
s	372	422	988	1228	1560	2796
ϵ	0.061%	0.068%	0.16%	0.20%	0.48%	0.71%

error may be minimized. First, it is of marked advantage to have the goniometer setting at the maximum of the intensity peak of an analytical line. At this maximum setting, an error of even 0.01 degree in positioning the adjustment drum corresponds to a change of only about 0.1% in the counting rate (2). It is also of great importance to approach the goniometer setting from the same direction, thus eliminating the backlash in the gears.

A series of six successive readings were taken, with the goniometer reset to the intensity peak maximum each time. These readings are recorded as Column II of Table I. Since no other variables were introduced during these readings, the observed standard deviations calculated from the intensity readings must therefore consist only of errors due to goniometer reset, X-ray counting, and instrumental drift during the time interval of the measurements. Thus

$$\epsilon_{\text{goniometer}} = (\epsilon^2_{\text{obsd}} - \epsilon^2_{\text{counting}} - \epsilon^2_{\text{drift}})^{1/2} \quad (8)$$

$$\epsilon_{\text{goniometer}} = (0.068^2 - 0.041^2 - 0.045^2)^{1/2}$$

$$\epsilon_{\text{goniometer}} = 0.030\%$$

Errors Due to Specimen Inhomogeneity. When the specimen in the form of a pellet possessing inhomogeneous distribution of the analyte or when a pellet with an uneven surface is irradiated, variation of readings will result corresponding to the different orientations of the specimen pellet in the path of the X-ray beam. This variation is not observed when the sample is maintained in precisely the same orientation for all measurements as was done in the preceding experiments. In dealing with a sample where it is necessary to insert and remove it as well as to average over the surface, the single orientation approach used above is impractical. Variation can be kept to a minimum by utilizing the rotating specimen holder. Although the sample was prepared as homogeneously as possible and with as smooth a surface as possible and although the specimen was rotated in the specimen holder, nevertheless the readings shown in Column III of Table I were observed. These readings were taken in such a manner that in addition to the homogeneity error only the drift and counting errors would affect the results. Thus:

$$\epsilon_{\text{inhomogeneity}} = (\epsilon^2_{\text{obsd}} - \epsilon^2_{\text{drift}} - \epsilon^2_{\text{count}})^{1/2} \quad (9)$$

$$\epsilon_{\text{inhomogeneity}} = (0.16^2 - 0.045^2 - 0.041^2)^{1/2}$$

$$\epsilon_{\text{inhomogeneity}} = 0.15\%$$

Specimen Placement Error. It was observed that if the sample were removed from the sample holder and then replaced, an additional error occurred. This was attributed to slight variations in the geometry of the sample holders. The use of the same sample holder throughout the experiment tended to minimize this error. This error is in addition to any error resulting from count, drift, and inhomogeneity. Column IV of Table I lists the results of a set of measurements in which the sample was removed from the instrument and then replaced in the same sample holder.

$$\epsilon_{\text{placement}} = (\epsilon^2_{\text{obsd}} - \epsilon^2_{\text{X-ray count}} - \epsilon^2_{\text{drift}} - \epsilon^2_{\text{inhomogeneity}})^{1/2} \quad (10)$$

$$\epsilon_{\text{placement}} = (0.20^2 - 0.041^2 - 0.045^2 - 0.15^2)^{1/2}$$

$$= 0.12\%$$

The Voltage and Current Reset Error. If the analytical data and the calibration curve are obtained without the necessity of resetting the current or voltage applied to the X-ray tube, then there is no need to consider the reset error involved with these controls. In order to evaluate this reset error, the instrument was turned on, set to the voltage and current values and allowed to warm up for 4 hours, after which time the settings were checked again. The specimen was then inserted and the readings taken. This was done for a period of six consecutive days. The results of the tests are shown in Column V of Table I. All of the previously evaluated errors are present in this experiment. Thus:

$$\epsilon_{\text{reset}} = (\epsilon^2_{\text{obsd}} - \epsilon^2_{\text{count}} - \epsilon^2_{\text{drift}} - \epsilon^2_{\text{goniometer}} - \epsilon^2_{\text{inhomogeneity}} - \epsilon^2_{\text{placement}})^{1/2} \quad (11)$$

$$\epsilon_{\text{reset}} = (0.48^2 - 0.055^2 - 0.045^2 - 0.030^2 - 0.15^2 - 0.12^2)^{1/2}$$

$$\epsilon_{\text{reset}} = 0.43\%$$

Sample Preparation Error. If a sample is assumed to be homogeneous, then the replicate introduction of different specimens in the pellet form prepared from the same sample might cause variations in the X-ray intensity measured. This variation is attributed mainly to the inconsistency in the techniques of sample pretreatment, grinding, pellet pressing, and the differences in the grain size achieved. The intensities of six different pellets prepared from the same sample were observed and recorded in Column VI of Table I.

$$\epsilon_{\text{prep}} = (\epsilon^2_{\text{obsd}} - \epsilon^2_{\text{X-ray count}} - \epsilon^2_{\text{drift}} - \epsilon^2_{\text{placement}} - \epsilon^2_{\text{inhomogeneity}})^{1/2} \quad (12)$$

$$\epsilon_{\text{prep}} = (0.71^2 - 0.050^2 - 0.045^2 - 0.12^2 - 0.15^2)^{1/2}$$

$$\epsilon_{\text{prep}} = 0.68\%$$

(2) H. A. Liebhafsky, H. G. Pfeiffer, E. H. Winslow, and P. D. Zemany, "X-ray Absorption and Emission in Analytical Chemistry," John Wiley & Sons, Inc., New York, N.Y., 1960, p 282.

DISCUSSIONS

The error due to the drift of the X-Ray Spectrometer within a period of one hour was measured to be 0.045%. This value seemed to be in agreement with the value of 0.05% given in the Norelco instrument manual (*3*). For longer preset counting times, although the relative error due to the X-ray counting will decrease, long term instability which usually has several times the magitude of short term instability will start to exert its influence.

The report of the ASTM task group on X-ray Fluorescence Spectroscopy on the first X-ray fluorescence round-robin test (*4*) showed a value of the order of 0.5% for the voltage and current reset error. For each of our measurements, instead of simply lowering the high voltage and tube current and resetting back to the specified values for the measurements, the instrument was turned on, allowed to warm up, set to the specified voltage and current reading, and then turned off after the reading was taken. This was done for six consecutive days. In spite of this, the error of 0.43% thus obtained seemed to be in good agreement with ASTM's value of 0.5%.

The ASTM task group also reported the value for the error of the spectrometer repositioning to be 0.11% (*4*). Our value of 0.030% seemed considerably smaller. The higher ASTM value could be attributed to the differences between the instruments and operators of the ASTM task force.

The errors due to inhomogeneity of the sample, the placement of the sample in the sample holder, and the sample preparation are the most disturbing errors. It appears that pellets prepared from a sample which had been ground to pass a 200-mesh screen and carefully blended still would produce deviations of 0.68%. Still more disturbing was the 0.12% deviation encountered when the same sample was removed and reinserted in the sample holder. Finally, a deviation of 0.15% which resulted from the orientation of the sample in the X-ray beam is extremely difficult to understand; particularly, if the pellet had a smooth face and no measurable difference in thickness from one side to the other.

As expected (*5*), the variations due to sample preparation contribute significantly to the total variation of our method in X-ray fluorescent analysis.

A day-to-day reset of the voltage and current reading contributed to an error of 0.43%. This value seemed to be well within the accepted range, thus allowing the construction of a single calibration curve which would be good for routine determinations on different days.

RECEIVED for review March 14, 1974. Accepted June 26, 1974.

(3) Norelco Electronic Circuit Panel Instruction Manual, p 6, Philips Electronic Industries Corp., 750 South Fulton Ave., Mount Vernon, N.Y. 10550.
(4) ASTM Task Group on X-ray Fluorescence Spectroscopy, *Appl. Spectrosc.*, **13**, 3 (1959).
(5) E. F. Kaelbe, "Handbook of X-rays," McGraw-Hill, New York, N.Y., 1967, Chap. 33, p 4.

Optimization of the Operating Parameters of Chemiluminescent Nitric Oxide Detectors

D. M. Steffenson[1] and D. H. Stedman

Department of Chemistry, University of Michigan, Ann Arbor, Mich. 48104

The parameters that affect the sensitivity of a typical chemiluminescent NO detector have been investigated. Using a 54.8 ppm NO in N_2 calibration gas as the NO source and maintaining a constant flow ratio of cal gas:ozonized oxygen of 2:1 into the reactor, the detector signal was measured as a function of reactor pressure at several different pumping speeds in different reactors. The results are consistent with an analysis of the kinetic limitations on the chemiluminescent intensity, which shows that the Detector Signal = (Reactor Gas Flow/Reactor Pressure) (G) $(1 - \exp(-\tau_{react}/\tau_{NO}))$ where G is the geometry of photon collection of the reactor and $\exp(-\tau_{react}/\tau_{NO})$ is the fraction of NO molecules whose residence lifetime in the reactor (τ_{react}) is short compared to their reactive lifetime with O_3 (τ_{NO}). From this equation, and results using different reactor designs and different photomultipliers, it is shown that the relevant parameters for optimizing the detector are pumping speed, reactor size, O_3 flux, reactor design, and choice of photomultiplier. The choice of these parameters is discussed and they are somewhat different for continuous sampling than for sampling from finite sources.

The use of chemiluminescent nitric oxide detectors has grown rapidly in the past few years, particularly as air pollution monitoring instruments for atmospheric concentrations of NO_x. A recent review of chemiluminescent detectors used in the measurement of air pollutants (*1*) lists nine different manufacturers of commercial NO_x detectors even though the feasibility of such detectors was established by Fontijn *et al.* (*2*) only in 1970, and the prototype for a number of these commercial instruments was developed in 1972 (*3*). Besides their application as monitors for atmospheric NO, these detectors have been used as laboratory analytical instruments for measuring NO as a product or reactant in standard kinetic or photochemical experiments (*4*).

In spite of the growth and rapid development of commercial instruments, there has been little systematic study of the physical and kinetic parameters that determine the optimum sensitivity of the NO detector. The basic design and the components of the detector have been established, but there remains a wide latitude of choice of the operating capabilities of each component. These choices must also be

(1) R. K. Stevens and J. A. Hodgeson, *Anal. Chem.*, **45**, 443A (1973).
(2) A. Fontijn, A. J. Sabadell, and R. J. Ronco, *Anal. Chem.*, **42**, 575 (1970).
(3) D. H. Stedman, E. E. Daby, F. Stuhl, and H. Niki, *J. Air Pollut. Contr. Ass.*, **22**, 260 (1972).
(4) D. H. Stedman and H. Niki, *Environ. Sci. Technol.*, **7**, 735 (1973).

[1] Present address, Department of Chemistry, Albion College, Albion, Mich. 49224.

compatible with the basic kinetic limitations of the chemiluminescent NO–O_3 reaction. Furthermore, operating conditions for use in atmospheric gas monitoring, where the supply of sample is virtually unlimited, are not necessarily ideal for use in the laboratory to detect NO in a limited amount of sample.

In this work we have systematically studied the operating parameters and reactor design that affect the intensity of the chemiluminescence that reaches the photomultiplier tube of the detector. This intensity was found to be a function of pumping speed and the flow parameters of the 54.8 ppm NO calibration gas and ozonized oxygen into the reactor in a way that is quite consistent with the proposed kinetics and mechanism of the reaction. The intensity is also a function of physical parameters, particularly reactor design, that facilitate getting the light to the photocathode of the photomultiplier. Finally, we made a few experiments with a different photomultiplier to demonstrate how important the choice of photomultiplier is to the ultimate sensitivity of the detector.

EXPERIMENTAL

The schematic design of the NO/O_3 chemiluminescent detector used in these experiments is identical to those published earlier (*1*, *3*), and is similar to those of commercial instruments. The photomultiplier used in most of the experiments was an RCA 8852 with an ERMA III response that extended its range to 900 nm. It was Dry Ice-cooled and nitrogen gas from a tank was slowly passed through a small space between the reactor window and the photomultiplier window to prevent frost formation. A Kodak Wratten gelatin filter was used to remove any emission below 600 nm. A few experiments were made using an Amperex 150 CVP photomultipler with an S-1 response, and nitrogen gas vaporized from a Dewar of liquid nitrogen was used for cooling. The power supply for the photomuliplier was a Heath EU-42A variable high voltage power supply with a maximum output of 1500 volts. The photocurrent was measured with a Keithley 414S picoammeter whose output was displayed on a Honeywell 10-mV strip-chart recorder.

A Cenco Hyvac 14 pump was used to maintain the flow of 54.8 ppm NO cal gas and ozonized oxygen through the reactor, and a bellows valve was installed in front of the pump to vary the pumping speed. An ozone killer was placed in front of the bellows valve to protect the pump oil. This was a 20-cm piece of 17-mm o.d. Vycor tubing that had been wound with asbestos tape and several feet of nichrome wire. The wire was connected directly to the 110-volt ac line, and it was turned on simultaneously with the ozonizer. A large piece of copper screen was rolled up and placed in the Vycor tube to provide a hot surface for the ozone destruction.

The flows of the two gases into the reactor were controlled with Teflon needle valves and the flow rates were measured with Gilmont No. 11 or No. 12 flow meters. The flow meters were calibrated with a wet test meter or by displacing water from a volumetric flask.

For these investigations, the instrument was used as an NO detector with a tank of Linde 54.8 ppm NO in N_2 as the NO source for all of the experiments. Oxygen was passed through an ozonizer operated at 9000 volts, through a flow meter, and then into the reactor. The pressure in the reactor was measured with either a mercury or oil manometer using a cathetometer to read the manometer levels to 0.05 mm.

Four different reactors were used in these experiments to test design features that might increase the sensitivity of the detector. The design and dimensions of the two reactors used for most of the experiments are shown in Figure 1. The smallest reactor, referred to hereafter as the "brass reactor", effective volume about 36 cm^3, was designed to facilitate rapid and effective mixing of NO and O_3 with the gases emerging from small jets interspersed with one another and surrounded by a glass cylinder to guide the reactants toward the front window before being pumped down the sides and out the back. The other reactor, referred to hereafter as the "glass reactor", volume about 300 cm^3, was designed to mix the reactant gases as close to the window in front of the photomultiplier tube as possible. The other two reactors were also made of Pyrex glass, and were similar to the glass reactor in Figure 1. One was identical except that the outlet to the pump was two 10-mm tubes exiting at the front of the reactor near the window. The other was larger,

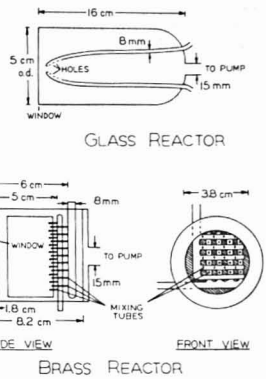


Figure 1. Cross-sectional designs of the two main reactors used in the NO detector

Both the window and the internal glass cylinder of the brass reactor had a diameter of 3.8 cm, which limited the effective reaction volume open to the photomultiplier

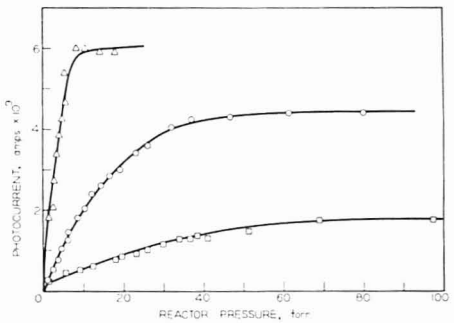


Figure 2. NO detector signal as a function of reactor pressure at three different pumping speeds for the glass reactor

Δ, data at 136 l./min; O, data at 63 l./min; and □, data at 30.5 l./min

about 20 cm long and about 400 cm^3 volume, but the gas inlets had only one hole in the end and they pointed straight forward with a separation approximately four times that of the glass reactor. This reactor provided the poorest mixing of NO and O_3.

With both the glass reactor and the brass reactor, at the highest pumping speed, the maximum photocurrent was obtained with a cal gas:O_3 flow ratio of 2:1 (where O_3 refers to the O_2/O_3 mixture from the ozonizer). This flow ratio was used for all of the experiments. The pumping speed was varied over a range of a factor of ten, so that the total gas flow in the reactor, as measured by the calibrated flowmeters and corrected for the reactor pressure, varied from around 170,000 ml/min to 17,000 ml/min. Thus, the residence time of the gases in the reactor ranged from about 0.11 sec to 1.1 sec for the glass reactor and from about 0.012 sec to 0.12 sec for the brass reactor. In almost all of these experiments, the high voltage power supply for the photomultiplier was set at 1140 volts. A few measurements were made at 1500 volts. Usually the photomultiplier was cooled with Dry Ice, but cooling was not critical since the cooled and uncooled signals were identical and only the dark current was reduced.

RESULTS

The experiments were designed to measure the intensity, I, of the chemiluminescence for the 54.8 ppm NO sample as a function of reactor pressure. This pressure was varied by

Table I. Effect of Reactor Design and Photomultiplier Voltage on the Signal, Dark Current, and Noise of a Chemiluminescent NO Detector

Reactor	1140 volts: Signal, A	1140 volts: Dark current and noise, A	1500 volts: Signal, A	1500 volts: Dark current and noise, A
RCA 8852, ERMA III Response				
1. Brass (36 cm³) (see Fig. 1)	6.0×10^{-9}	$2 \pm \times 10^{-12}$	6.2×10^{-8}	$4 \pm 4 \times 10^{-11}$
2. Glass (300 cm³) (see Fig. 1)	18.0×10^{-9}	n.m.	3.2×10^{-7}	n.m.
3. Glass (300 cm³) (same as 2 with front pumping)	3.2×10^{-9}	n.m.	n.m.	n.m.
4. Glass (400 cm³) (same as 2 with poor gas mixing)	6.5×10^{-9}	$8 \pm 4 \times 10^{-12}$	1.4×10^{-7}	$3 \pm 2 \times 10^{-11}$
5. Glass (300 cm³) (same as 2 with reflective coating)	60.0×10^{-9}	$2 \pm 1 \times 10^{-12}$	n.m.	n.m.
Amperex 150CVP, S-1 Response				
6. Brass (same as above)	70×10^{-9}	$9 \pm 0.4 \times 10^{-11}$ [a]	n.m.	n.m.

[a] The dark current is very dependent on the cooling efficiency and this represents the lowest value found over a four-day period. On other days, it was as much as 20 times higher.

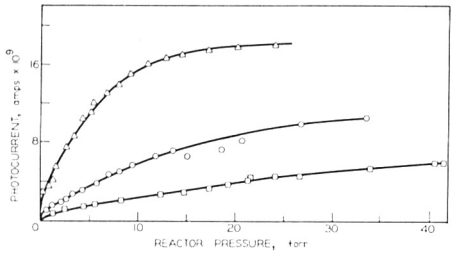


Figure 3. NO detector signal as a function of reactor pressure at three different pumping speeds for the brass reactor

Δ, data at 136 l./min; O, data at 40.5 l./min; and □, data at 16 l./min. The last □ at the 16 l./min pumping speed represents experimental points at 71 and 108 Torr with that ordinate value

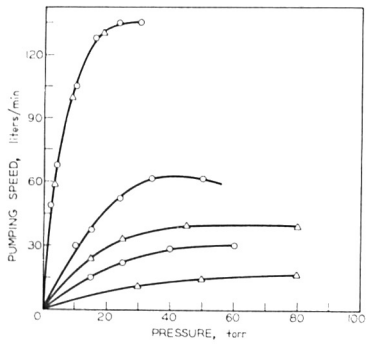


Figure 4. Pumping speed as a function of reactor pressure

These data correspond to the photocurrent *vs.* reactor pressure curves of Figures 2 and 3. O, data collected with the glass reactor; and Δ, data collected with the brass reactor. Pumping speed can be converted to *F/P* in units of $cm^3\ sec^{-1}\ torr^{-1}$ by multiplying the numbers along the ordinate by 7.85

changing the total flow of reactants through the reactor. The results are shown in Figures 2 and 3 for the glass and brass reactors, each at three different pumping speeds. The pumping speeds were determined from the total flow and the pressure in the reactor, and they are plotted in Figure 4 as a function of pressure.

The effect of reactor designs on the sensitivity of the detector is shown in Table I along with data for the dark current and noise of the photomultiplier. Table I also shows the change in signal and dark current achieved by an S-1 response photomultiplier.

DISCUSSION

The main parameters that can affect the signal intensity of the detector can be understood through the kinetics and mechanism of the NO–O_3 reaction, and the relationship of the residence lifetime of the reactants in the reactor to their kinetic lifetime. The mechanism of the reaction between NO and O_3 has been previously established (*5, 6*)

$$NO + O_3 \longrightarrow NO_2^* + O_2 \quad (1)$$

$$NO + O_3 \longrightarrow NO_2 + O_2 \quad (2)$$

$$NO_2^* \longrightarrow NO_2 + h\nu \quad (3)$$

$$NO_2^* + M \longrightarrow NO_2 + M \quad (4)$$

where NO_2^* is an excited electronic state which emits radiation between 600 and 3000 nm with a maximum at 1200 nm. The rate constants for Equations 1 and 2 were measured to be $k_1 = 1.1 \pm 0.6 \times 10^{-15}$ $cm^3\ molecules^{-1}\ sec^{-1}$ and $k_2 = 1.4 \pm 0.6 \times 10^{-14}$ $cm^3\ molecule^{-1}\ sec^{-1}$.

If the only important reactions were 1 and 3, then all of the NO molecules entering the reactor would lead to emitted photons, thus

$$I_{tot} = f_{NO} \quad (5)$$

where I is the intensity of the signal in photons sec^{-1} and f_{NO} is the mass flow of NO into the reactor in molecules sec^{-1}. In fact, the above kinetics impose three constraints on Equation 5. 1) Only a fraction, $k_1/(k_1 + k_2) = 0.073$, of NO + O_3 encounters leads to excited NO_2^*. 2) Quenching of NO_2^* allows only a fraction, $k_3/(k_3 + k_4[M]) = 8.3 \times 10^{-3}$ at 1 Torr (*6*), of the possible photons to be emitted. 3) The rate of reaction of NO + O_3 is relatively slow, which allows a fraction of the entering molecules, $\exp(-\tau_{react}/\tau_{NO})$, to leave the reactor untouched, or allows only a fraction, $(1 - \exp(-\tau_{react}/\tau_{NO}))$, of the entering NO molecules to react inside the reactor. Here τ_{NO}, the reactive lifetime of NO, is the inverse of the pseudo-first-order rate constant for the reaction of NO in the presence of excess O_3,

$$\tau_{NO} = 1/((k_1 + k_2)[O_3]),\ sec \quad (6)$$

(5) M. A. A. Clyne, B. A. Thrush, and R. P. Wayne, *Trans. Faraday Soc.*, **60**, 359 (1964).

(6) P. N. Clough and B. A. Thrush, *Trans. Faraday Soc.*, **63**, 915 (1967).

and τ_{react}, the residence lifetime of the reactants in the reactor, is determined by reactor size and the flow rate in the reactor,

$$\tau_{react} = (A)(d)(P)/F, \text{ sec} \quad (7)$$

where A is the cross sectional area of the reactor in cm^2, d is the reactor length in cm, P is the gas density in the reactor in molecules cm^{-3}, and F is the total flow in molecules sec^{-1}. The above expression for the fraction of unreacted NO molecules derives from the pseudo-first-order kinetics of Equations 1 and 2. The fraction of unreacted NO molecules present at the end of the reactor is

$$\frac{[NO]_{t=\tau_{react}}}{[NO]_{t=0}} = \exp(-\tau_{react}/\tau_{NO}) \quad (8)$$

where $t = \tau_{react}$. Therefore, with the above three constraints on Equation 5, the light emitted from the reaction zone becomes

$$I_{tot} = (f_{NO})\left(\frac{k_1}{(k_1 + k_2)}\right)\left(\frac{k_3}{(k_3 + k_4[M])}\right)\times (1 - \exp(-\tau_{react}/\tau_{NO})) \quad (9)$$

photons per second.

In practice, we cannot collect all of the photons emitted, so the signal from the photmultiplier is not I_{tot}, but has been attenuated by a further factor G which includes the geometry of photon collection and photomultiplier characteristics. Since $k_4[M] \gg k_3$ and [M] is the total gas density in molecules cm^{-3}, Equation 9 can be written

$$\text{Signal} = \left(\frac{f_{NO}}{P}\right)(G)\left(\frac{k_1k_3}{k_1(k_1 + k_2)}\right)\times (1 - \exp(-\tau_{react}/\tau_{NO})) \quad (10)$$

This is the signal measured by the picoammeter and has been plotted as a function of reactor pressure in Figures 2 and 3.

For the moment, assume $\tau_{react} \gg \tau_{NO}$, so that most of the NO molecules react inside the reactor, and we can neglect the exponential portion of Equation 10. In this case, the signal is directly proportional to f_{NO}/P or F_{tot}/P since the NO cal gas flow was a fixed fraction (%) of the total flow. One can enhance the signal by increasing f_{NO}, decreasing P, or increasing f_{NO}/P. For NO detectors with a constant volume vacuum pump, f_{NO} and P are not independent of one another. If one doubles the flow of NO molecules into the reactor, one simultaneously doubles the gas density. One can increase the signal only by increasing f_{NO}/P. Since f_{NO}/P is in units of cm^3 sec^{-1}, it is a measure of pumping speed and it can be increased by increasing the speed of the pump.

Figure 4 shows the different pumping speeds utilized in these experiments. Comparison of these data with the signal intensities in Figures 2 and 3 gives excellent qualitative agreement as predicted by the above analysis. Decreasing pumping speed does decrease the photomultiplier signal.

The fall-off in pumping speed at low pressures, which is matched by an identical fall-off in signal, deserves some comment. The speed pressure curve for the Cenco Hyvac 14 (140 l./min maximum pumping speed) indicates that the pumping speed should be almost constant in this pressure region, and such a fall-off should not occur until 10^{-3} Torr. However, at low pressures, pumping speed is often limited by the resistance of smaller tubing in part of the pumping system (7), and here the tubing from the reactor to the pump, including the ozone-killer section, filled with wire, in front of the pump, causes the early onset of the fall-off in pumping speed at low pressures.

Quantitatively, on the basis of Equation 10, one would expect a plot of signal *vs.* pumping speed to be linear with a zero intercept and a slope that varies with G, the geometry of photon collection for a particular reactor. Such a plot, using the data from Figures 2 and 4 for the glass reactor, was indeed linear with a zero intercept. For the brass reactor, using the data in Figures 3 and 4, only the data for the lowest two pumping speeds falls on a straight line through the origin. As predicted, the slope of this line for the brass reactor was different from that of the glass reactor, but the signal for the highest pumping speed was 2.5 times lower than that predicted by this plot. Clearly, a large fraction of the possible signal had been lost.

To understand the strong attenuation in the signal in the brass reactor at high pumping speeds, we must examine the $(1 - \exp(-\tau_{react}/\tau_{NO}))$ term previously neglected in Equation 10. If the residence lifetime of NO and O_3 in the reactor gets short, compared to the reactive lifetime of NO, as one might find with high pumping speeds in a small reactor, then some fraction of the photons are emitted outside the reactor, and the signal is attenuated by the fact that only a fraction of NO molecules, $(1 - \exp(-\tau_{react}/\tau_{NO}))$ will actually emit light within sight of the photomultiplier. Thus, one cannot increase the sensitivity of an NO detector without limit by just increasing the pumping speed. One must consider the limitations of τ_{react} and τ_{NO} in optimizing the NO detector signal.

From Equation 7, one can see that τ_{react} is inversely proportional to F/P and thus is a constant for a given pumping speed, except at low pressures where it increases as pumping speed falls off. In the experimental section, it was noted that τ_{react} was 0.11 sec for the glass reactor and 0.012 sec for the brass reactor at the highest pumping speeds in the pressure region where F/P is constant.

Equation 6 gives the expression for τ_{NO}, which can be put in a more useful form by expressing $[O_3]$ as

$$[O_3] = (P)(\%\ O_3)fo_2/F \quad (11)$$

where P is the gas density in the reactor in molecules cm^{-3}, % O_3 is the mole fraction of O_3 produced in the oxygen streaming through the ozonizer, and fo_2/F is the fraction of the total flow in the reactor, that is $O_3 + O_2$. Substitution of Equation 11 into Equation 6 gives

$$\tau_{NO} = F/[(k_1 + k_2)(P)(\%\ O_3)(fo_2)] \quad (12)$$

Since $(k_1 + k_2)$ and F/P are constant, the important variable is the product of the oxygen flow in the reactor and the mole fraction of O_3 produced in the oxygen. This, however, is also constant rather than variable.

Using an ozonizer similar to the one we used in our NO detector, Jack Horvath at the Space Physics Research Laboratory at the University of Michigan measured the mole fraction of O_3 in O_2 as a function of fo_2 at several ozonizer voltages. He found that the mole % of O_3 decreased as the flow of oxygen through the ozonizer increased, and the ozonizer produced a constant flux of O_3 (8). At 9000 volts (the operational voltage of our ozonizer), the (% O_3) (fo_2) product was effectively constant at 4.50 ± 0.18 cm^3/min, over an O_2 flow range of 60 to 2160 cm^3/min as measured on the ex-

(7) H. W. Melville and B. G. Gowenlock, "Experimental Methods in Gas Reactions," Macmillan & Co. Ltd., London, 1964, p 41.
(8) J. Horvath, Space Physics Research Lab., University of Michigan, Ann Arbor, Mich., personal communication, 1974.

ternal flow meter. This covers all but the lowest flows of oxygen used in our experiments.

Thus τ_{NO} should be constant for a given pumping speed except at low pressures. For the highest pumping speeds in the pressure region where F/P is constant in either the brass or glass reactor, τ_{NO} is 0.073 sec using the values of (% O_3) (fo_2) from the calibrated ozonizer.

Since both τ_{react} and τ_{NO} are constant when F/P is constant, their ratio is also constant:

$$\tau_{react}/\tau_{NO} = (Ad)(\%\ O_3)(fo_2)P^2/F^2 \qquad (13)$$

The NO detector signal, Equation 10, will be optimized if τ_{react}/τ_{NO} is large so that $\exp(-\tau_{react}/\tau_{NO})$ is negligible. This fraction is negligible in these results except for the brass reactor at the highest pumping speed where the signal is severely attenuated compared to the glass reactor. According to Equations 10 and 13, this signal loss is due to the smaller volume of the brass reactor and the subsequent escape of unreacted NO from the reactor.

The easiest way to keep τ_{react}/τ_{NO} large in an NO detector is to make the reactor volume (Ad) large. This will help compensate for the fact that an increased pumping speed, F/P, which has been shown to directly enhance the signal, can also decrease the signal by lowering this ratio by a factor of $(P/F)^2$. One might further increase this ratio by increasing the efficiency of O_3 production which would increase the % O_3 produced for a given O_2 flow. This would only be important if the detector is operated in a region where Equation 13 is important and the signal thus gained is significant.

At this point, one might be tempted to optimize an NO detector by using a very high speed pump and a large volume reactor, but there is a third important factor, G in Equation 10, that must also be considered. This factor represents the geometry of the photon collection system and the photomultiplier characteristics. These have been studied by varying the reactor design and by changing photomultiplier tubes.

The goal of good reactor design is to mix the entering flows of NO and O_3 very quickly and efficiently and then allow them to react as near the window to the photomultiplier as possible. This is because chemiluminescence is a diffuse source and cannot be focused by lenses or mirrors onto the photocathode. Also, as the reactants flow through the reactor, the intensity of the light reaching the window falls off with the square of the distance. This is the reason one cannot continue to compensate for high pumping speed with large reactors. The ratio of τ_{react}/τ_{NO} may be kept large but some fraction of the reaction occurs far enough from the window to be effectively lost to detection.

The results in Table I with four different reactors support the above analysis. The best reactor was the glass reactor that mixed the reactants well in front of the window and allowed them to flow down the length of the reactor. Pumping them forward and out the side was 5–6 times less effective, and using a larger reactor with less efficient mixing gave only a third of the glass reactor signal. As already indicated, the brass reactor was too small, but its efficient mixing system and forward pumping might work well in a larger reactor. The best improvement in signal was produced by coating the glass reactor with Eastman Kodak reflectance paint which increased the signal by a factor of three.

The choice of photomultiplier tube is very important, but we did not have the resources to undertake any systematic study of this parameter. Ideally, one would like to have a photomultiplier with a spectral response curve that maximally overlaps the chemiluminescence spectrum and one with a low dark current and noise. On the basis of spectral overlap, most photomultipliers fall short of the NO_2* emission which peaks at 1200 nm. The ERMA-III response of the RCA 8852 photomultiplier extends about as far into the infrared as any (900 nm) except the S-1 response of the Amperex 150 CVP, which extends to 1080 nm. This is shown in Table I by an order of magnitude increase in signal using this latter tube with the brass reactor. However, at its best, the S-1 photomultiplier has a dark current 45 times larger than the ERMA-III.

For maximum detector sensitivity for NO samples at ppb concentrations, one must be concerned about the background noise of the photomultiplier, and the important characteristic is the signal/noise ratio of the tube. The noise was such a strong function of cooling efficiency for the S-1 response photomultiplier that its signal/noise ratio varied from 1.7×10^4 to less than 10^3 for the 54.8 ppm NO on N_2 sample. The ERMA-III response photomultiplier has the best signal/noise ratio for this sample for the reflectance painted glass reactor 6×10^4, and it seems to be the better of the two for use in an NO detector. It should be noted in Table I that one can increase the signal by increasing the operating voltage of the photomultiplier, but the noise is increased by the same factor and the signal/noise ratio remains about the same.

CONCLUSIONS

We can now summarize the choice of parameters for the optimization of the signal in an NO detector. They will be somewhat different for a detector designed for continuous sampling of NO where there is an infinite sample of gas available than for a detector designed to measure the NO concentration in a kinetics experiment or in a smog chamber where the amount of sample is finite and one may want to disturb the gases as little as possible.

First, one should maximize the pumping speed within the constraints of being able to supply enough reactants to keep the reactor pressure in the plateau region such as in Figures 2 and 3. For atmospheric sampling, one does not care if the fall-off in pumping efficiency of the system comes at high pressures because one can supply enough sample to keep the pressure above this point. For laboratory sampling, however, one wants to have a high speed pumping system that falls off at a very low pressure so only a minimum of sample is required to keep the reactor pressure in the plateau region.

Second, one should choose a reactor that is large enough to keep the residence lifetime, τ_{react}, large compared to the reactive lifetime, τ_{NO}. There is a compromise between maximizing pumping speed and minimizing τ_{react}/τ_{NO} because the signal intensity decreases by a factor of the inverse of the distance squared of the excited molecules from the photomultiplier, and there may be an upper limit to the usable pumping speed unless one can lower τ_{NO} by increasing the ozone flux into the reactor.

Third, reactor design should provide rapid, efficient mixing as close to the window as possible. Furthermore, the walls of the reactor should be made as reflective as possible by coating with reflectance paint. It is difficult to put a mirror deposit on the inside of the reactor because of the large amount of ozone passing through it.

Finally, choose a photomultiplier with an extended response into the infrared that has a low dark current and low noise. One might be tempted to choose a photomultiplier with a larger diameter photocathode, to collect more light, but the noise increases as the square of the radius and one does not necessarily improve the signal/noise ratio. Ultimately, the quality and characteristics of the photo-

multiplier may be the most important factor in extending the sensitivity of an NO detector to lower NO concentrations.

RECEIVED for review February 19, 1974. Accepted June 17, 1974. The financial support of Grant 802418 from the Environmental Protection Agency is gratefully acknowledged.

Analytical Ion Cyclotron Resonance Spectrometry. Stereochemical Effects in Some Cyclic Ketones

Maurice M. Bursey,[1] Jar-lin Kao, John D. Henion, Carol E. Parker, and Tai-In S. Huang

Venable and Kenan Chemical Laboratories, The University of North Carolina, Chapel Hill, N.C. 27514

The relative rates of acylation by $CH_3COCOCH_3$-$^+$ of 2-alkylcyclohexanones and decalones in the gas phase do not agree with predictions of the three currently used theories. An overriding parameter which correlates well with steric blocking of the carbonyl group exists. Because the α-decalones can be distinguished on this basis, ICR is superior to conventional mass spectrometry, where their differences cannot be predicted on an *a priori* basis.

The potential use of ion cyclotron resonance (ICR) spectrometry for analytical purposes has been explored in several laboratories (*1–3*). One advantage of ICR spectrometry over conventional mass spectrometry lies in its use of ion-molecule reactions (Equation 1) in the gas phase to distin-

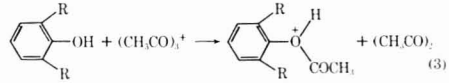
$$A{-}B^{\bullet} + C{-}D \longrightarrow A + B{-}C{-}D^{\bullet} \qquad (1)$$
$$A{-}B^{\bullet} + C{-}D \longrightarrow A + B{-}C^{\bullet} + D$$

guish between compounds whose unimolecular decompositions in a conventional mass spectrometer (Equation 2) are so similar as to preclude easy identification of isomers.

$$A{-}B^{\bullet} \longrightarrow A^{\bullet} + B \qquad (2)$$

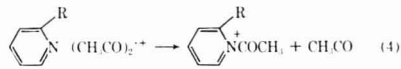
A particularly striking example of the applicability of ICR spectrometry to analysis is the identification of olefinic and cyclic isomers of C_5H_{10}, whose conventional mass spectra are very similar (*2*).

Our own interest in applications of this technique derives from the apparent dependence of some ion-molecule reactions on steric environment. Some ion-molecule reactions, observed in conventional chemical ionization mass spectrometry, lead to ions whose further fragmentation is a strong function of stereochemistry (*4*). We have, on the other hand, been interested in establishing differences between the rates of *formation* of chemically ionized molecules in the ion-molecule reaction. We have shown qualitatively that the acetylation of phenols is a function of the accessibility of the hydroxyl group (Equation 3) (*5*),



(3)

and more recently have found that the acetylation of pyridines is likewise reduced when a 2-alkyl substituent is large (*6*), even when the reaction is somewhat different (Equation 4).



(4)

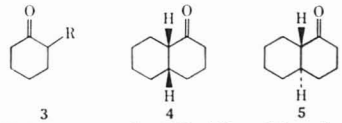
Finally, we have noted that stereochemical differences are observed when the two isomers **1** and **2** are acetylated by the gaseous ion $(CH_3CO)_3^+$, the more hindered **1** reacting more slowly (*7*).



1 **2**

On the other hand, a simple proton transfer from one species to another in the gas phase does not appear, so far at least, to be susceptible to steric effects. The transfer of a proton between alkyl halides does not become appreciably slower when the size of the alkyl group increases (*8*). Perhaps the results should not be compared directly, but a tentative conclusion that might be reached is that groups larger than a proton ought to be transferred in order to detect stereochemical differences. In our studies, we have used either CH_3CO^+ (*3*) or NO_2^+ (*9*).

Transfer of CH_3CO^+ to some 2-alkylcyclohexanones **3** has now been studied. We have also extended our results to the α-decalone isomers **4** and **5.** These last compounds may



3 **4** **5**

a. R = H; b. R = CH_3; c. R = C_2H_5; d. R = n-C_3H_7; e. R = n-C_4H_9

[1] Author to whom correspondence should be addressed.

(1) J. M. S. Henis, *Anal. Chem.*, **41** (10), 22A (1969).
(2) M. L. Gross, P.-H. Lin, and S. J. Franklin, *Anal. Chem.*, **44,** 974 (1972).
(3) M. M. Bursey, T. A. Elwood, M. K. Hoffman, T. A. Lehman, and J. M. Tesarek, *Anal. Chem.*, **42,** 1370 (1970).
(4) T. J. Odiorne, D. J. Harvey, and P. Vouros, *J. Org. Chem.*, **38,** 4275 (1973).
(5) S. A. Benezra and M. M. Bursey, *J. Amer. Chem. Soc.*, **94,** 1024 (1972).
(6) J. D. Henion, M. C. Sammons, C. E. Parker, and M. M. Bursey, *Tetrahedron Lett.*, 4925 (1973).
(7) M. K. Hoffman and M. M. Bursey, *Can. J. Chem.*, **49,** 3395 (1971).
(8) T. Su and M. T. Bowers, *J. Amer. Chem. Soc.*, **95,** 7609 (1973).
(9) M. M. Bursey and W. B. Nixon, *Tetrahedron Lett.*, 4389 (1970).

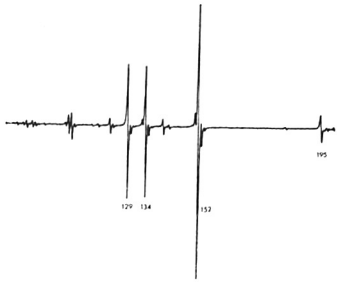


Figure 1. ICR spectrum of 15:1 biacetyl/*trans*-1-decalone; *m/e* 152 = $M^{\cdot+}$ of decalone, *m/e* 195 = $R_2CO(COCH_3)^+$, *m/e* 134 = $[M - C_2H_4]^{\cdot+}$, *m/e* 129 = $(CH_3CO)_3^+$

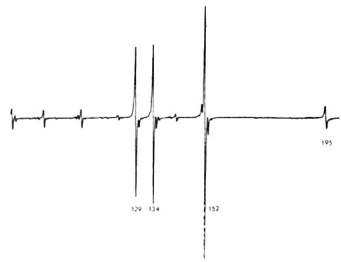


Figure 2. ICR spectrum of 15:1 biacetyl/*cis*-1-decalone. The significant difference between this and Figure 1 is the larger ratio of *m/e* 195 to *m/e* 129 in Figure 1. Quantitative evaluation yields data in the Table.

be likened to a cyclohexanone with a four-carbon alkyl chain which is constrained into a particular position, and therefore form part of the straight-chain series of cyclohexanones explored here. In **4**, the bridgehead hydrogens are cis to each other; in **5** they are trans.

We shall see that the theories of ion-molecule reaction rates do not accommodate our results. The reason presumably is that none of these takes into account parameters such as steric ones which influence reactivity within the collision complex; they are concerned only with the rate of collision of the ion and the molecule. At the moment there are three formulations, which we discuss in historical order.

The first is the theory of Gioumousis and Stevenson (*10*). It takes account only of the attraction between a molecule of electric polarizability α and a singly charged ion. The rate constant is given by Equation 5, where μ is the reduced mass, and the other symbols have their usual significance.

$$k = 2\pi e(\alpha/\mu)^{1/2} \tag{5}$$

The theory of Gioumousis and Stevenson does not take account of the interaction between an ion and a dipole. It would be anticipated that such an interaction would affect the rate; thus Equation 5 really applies only to molecules without a dipole. Moran and Hamill have derived an expression for the rate when the dipole has a fixed orientation induced by the ion (Equation 6) (*11*). In Equation 6,

$$k = (2\pi e/\mu^{1/2})[\alpha^{1/2} + \mu_D(2\pi kT)^{1/2}] \tag{6}$$

μ_D is the dipole moment of the neutral.

However, Equation 6 gives rate constants much larger than found experimentally. This error was interpreted to mean that the dipole is not completely locked by the ion. Su and Bowers have modified the equation to include an adjustable parameter c, which may be altered to give good agreement between experiment and theory (Equation 7) (*12*).

$$k = (2\pi e/\mu^{1/2})[\alpha^{1/2} + c\mu_D(2\pi kT)^{1/2}] \tag{7}$$

This could be interpreted as a measure of the extent to which the ion locks the dipole into a preferred orientation. For a number of well-studied reactions, the value of c is close to 0.15 (*8*, *12*).

(10) G. Gioumousis and D. P. Stevenson, *J. Chem. Phys.*, **29**, 294 (1958).
(11) T. F. Moran and W. Hamill, *J. Chem. Phys.*, **39**, 1413 (1963).
(12) T. Su and M. T. Bowers, *J. Chem. Phys.*, **58**, 3027 (1973).

EXPERIMENTAL

For purposes of comparison with theories, it was necessary to obtain values for α and μ_D for each ketone. The values of α were calculated according to the method of Le Fèvre (*13*) and compared with experimental data where these were available (*14*, *15*). The agreement was within 2%. Likewise, in order to have a uniform set of dipole moments, all these were calculated using an available INDO molecular orbital program (*16*). Again, where experimental data were available (*14*), the agreement was good, within 5%. Data to be quoted in the table in the discussion section are calculated values except that μ_D of cyclohexanone is the experimental value.

The ICR spectra were obtained on a Varian ICR-9 spectrometer using the field modulation mode and a marginal oscillator frequency of 110 KHz. A standard flat cell was used with the following typical cell conditions: trap, 0.30 V; analyzer, split, −0.10 and +0.10 V; source, split, −0.25 and +0.25 V; a typical residence time is 5×10^{-4} sec. The ionizing energy was 15.1 eV. The emission current was operated between 10 and 50 nA. All samples were degassed by several freeze-pump-thaw cycles prior to use and were introduced through separate inlet ports. The pressures were in the range about 2×10^{-6} Torr ketone and 3×10^{-5} Torr biacetyl; they were calibrated with a Datametrics Barocel capacitance manometer. The double resonance and ion ejection experiments were performed as previously described (*17*, *18*).

Representative spectra of mixtures of biacetyl and the decalones are shown in Figures 1 and 2. The ICR spectra of the decalones alone at pressures used in this study are very similar to each other as would be expected from comparison of the conventional mass spectra (*19*), which differ only in the intensity of the peaks of *m/e* 97, 109, and 110.

The 2-alkylcyclohexanones were purchased from Chemical Samples Company and from Pfaltz and Bauer. The *trans*-1-decalone was purchased from the Aldrich Chemical Company and *cis*-1-decalone was prepared according to a reported procedure (*20*).

RESULTS AND DISCUSSION

Because there is concern about the validity of absolute rate constants derived by ICR, we have chosen to publish only the relative rate constants we found and to compare them with the relative rate constants calculated by each of the methods described above. In our hands the rate constant for the well known reaction

(13) R. J. W. Le Fèvre, *Advan. Phys. Org. Chem.*, **3**, 1 (1965).
(14) A. L. McClellan, "Tables of Experimental Dipole Moments," W. H. Freeman and Company, San Francisco, Calif., 1963, p 208.
(15) W. Huckel, *Justus Liebigs Ann. Chem.*, **441**, 1 (1925).
(16) Quantum Chemistry Program Exchange, Bloomington, Ind., Program No. 141.
(17) J. L. Beauchamp, L. R. Anders, and J. D. Baldeschwieler, *J. Amer. Chem. Soc.*, **89**, 4569 (1967).
(18) J. M. S. Henis, *J. Amer. Chem. Soc.*, **90**, 844 (1968).
(19) E. Lund, H. Budzikiewicz, J. M. Wilson, and C. Djerassi, *J. Amer. Chem. Soc.*, **85**, 1528 (1963).
(20) H. E. Zimmerman and A. Mais, *J. Amer. Chem. Soc.*, **81**, 3644 (1959).

$$CH_4 + CH_4^{\cdot+} \longrightarrow CH_5^+ + CH_3\cdot \quad (8)$$

was found to be within 10% of the accepted value, however, and results for several other reactions gave results agreeing with published values within 10% (*21*).

The reaction scheme used is the following. By far the dominant process for acetylation of the ketones under study is Equation 9.

$$CH_3COCOCH_3^{\cdot+} + R_2CO \longrightarrow R_2CO(COCH_3)^+ + CH_3CO\cdot \quad (9)$$

Double resonance experiments show that this is the only significant reaction of $CH_3COCOCH_3^{\cdot+}$ with R_2CO. The self-acetylation of biacetyl (Equation 10) competes favorably with this reaction.

$$CH_3COCOCH_3^{\cdot+} + CH_3COCOCH_3 \longrightarrow (CH_3CO)_3^+ + CH_3CO\cdot \quad (10)$$

Under the conditions employed, this accounts for more than 98% of the reaction of $CH_3COCOCH_3^{\cdot+}$ with $CH_3COCOCH_3$. The collision of $CH_3COCOCH_3^{\cdot+}$ with either R_2CO or $CH_3COCOCH_3$ gives one product in each case, then. At low conversion of the reagent $CH_3COCOCH_3^{\cdot+}$, therefore, the amounts of $R_2CO(COCH_3)^+$ and $(CH_3CO)_3^+$ produced in the instrument are proportional to the rate constants for their formation, provided there is no further decomposition of these products. In fact, no product formed from $R_2CO(COCH_3)^+$ was observed. Therefore all of the rate constants for formation of different $R_2CO(COCH_3)^+$ may be determined, relative to each other, directly from one spectra, after the usual mass corrections (*7*) are made.

There is a minor competing process, Equation 11.

$$(CH_3CO)_3^+ + R_2CO \longrightarrow R_2CO(COCH_3)^+ + (CH_3CO)_2 \quad (11)$$

The inclusion of this pathway in the reaction scheme greatly complicates the kinetic analysis (*22*). However, suitable double resonance and ion ejection experiments indicate, first, that this is a minor process for formation of $R_2CO(COCH_3)^+$ and consumption of $(CH_3CO)_3^+$; and, second, that it contributes nearly the same fraction of the total amount of the $R_2CO(COCH_3)^+$ ion for each ketone when uniform pressures of R_2CO and $CH_3COCOCH_3$ are used for all experiments. Thus, nearly the same small correction term should be applied to the value of the rate constant in each case of R_2CO; and therefore, the ratios of the rate constants for R_2CO compared as a series remain as originally determined. The relative precision of the rate constants (three experiments minimum on different days) ranged between ±1 and ±10%.

Because there is only one channel (*23*) for decomposition of the collision complex, it is pertinent to compare the experimental rate (a rate of product formation) and the calculated rate (a rate of collision of reactants). The experimental and the calculated values of the rate constants are shown in Table I, together with calculated values of α and μ_D as described earlier. See reference (*23*) for examples where the collision complex decomposes through several channels. In such cases the *sum* of the rates of formation is compared with the theoretical value of the rate of collision of reactants.

Table I. Mean Electric Polarizabilities, Dipole Moments, and Calculated and Experimental Relative Rate Constants

Compound	α(Å^3)	μ_D(D)	$k_{(Eq.\ 5)}$[a]	$k_{(Eq.\ 6)}$[a]	$k_{(Eq.\ 7)}$[a]	k_{expt}[a]
3a	10.73	3.98	1.00	1.00	1.00	1.00
3b	12.81	2.91	1.06	0.94	1.01	0.70
3c	14.65	2.89	1.11	0.92	1.03	0.25
3d	16.50	2.87	1.15	0.91	1.04	0.090
3e	18.33	2.86	1.19	0.91	1.06	0.074
4	17.40	2.69	1.17	0.87	1.03	0.031
5	17.55	2.85	1.17	0.90	1.05	0.069

[a] Relative to $k_{3a} = 1.00$.

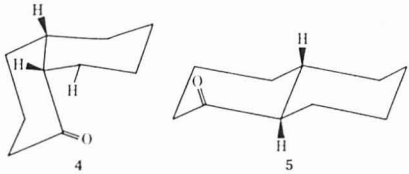
The following conclusions may be drawn about these results. First, none of the models for collision of reactants is capable of explaining the precipitous decline in the rate of the acetylation reaction as one goes from **3a** to **5**. Another factor must be important in these processes, one which, in the case of **4**, must be responsible for a correction factor of thirty in the relative rate. None of the models, it should be noted, assume any interaction in the orbiting complex except (for models) some degree of orientation of the dipole by the charge of the ion. These ions are large and the neutrals are complex, and specific interactions could occur which the simple models cannot predict. Such interactions have not all been present in previously studied ion-molecule reactions.

Double resonance experiments did not uncover any new channels for decomposition of the complex; again the only product observed for the reaction of $CH_3COCOCH_3^{\cdot+}$ and R_2CO was formed according to Equation 9. Therefore a second conclusion can be drawn from the data: for the most part, the decrease in the relative rate constant parallels qualitatively the effect expected for a steric interference by the alkyl group to the approaching $(CH_3CO)_2^{\cdot+}$ ion: the larger the alkyl group adjacent to the carbonyl group, the more it should shield the carbonyl oxygen from attack, and the less likely an orbiting collision is to result in transfer of the CH_3CO^+ group. Thus, the first five compounds react more slowly as the alkyl group becomes longer and longer. This trend is similar to that found experimentally for the reduction of 2-alkylcyclohexanones in isopropranol by $NaBH_4$, in which the relative rates of reduction are: **3a,** 1.00; **3b,** 0.15; **3c,** 0.083; **3e,** 0.065 (*24*). On the other hand, tying back the alkyl group to produce **5** does not produce a significant change from that of **3e** in the rate constant. (We use **5** as a model for a tied-back butyl group because in both **3e** and **5** the 2-butyl group is entirely or predominantly equatorial.) Thus the volume of space available for the approach of the $(CH_3CO)_2^{\cdot+}$ ion is about the same in both cases, but this is not clearly predictable because of opposing trends. On the one hand, one would predict that a freely rotating butyl group would shield the carbonyl more from attack than a group which was tied back. On the other hand, there is only about 2 kcal/mole difference in the free energies of the axial and equatorial forms of 2-butylcyclohexanone; the measured $-\Delta G$ is 1.8 kcal/mole for 2-methylcyclohexanone, and calculations for alkylcyclohexanes show a further change of only 0.3 kcal/mole on going from methyl to *n*-butyl (*25*). The axial alkyl group might permit

(21) D. A. Chatfield, Ph.D. Dissertation, The University of North Carolina at Chapel Hill, Chapel Hill, N.C., 1974.
(22) R. C. Dunbar, D. A. Chatfield, and M. M. Bursey, *Int. J. Mass Spectrom. Ion Phys.*, **13,** 195 (1974).
(23) J. M. S. Henis, M. K. Tripodi, and M. D. Sefcik, *J. Amer. Chem. Soc.*, **96,** 1660 (1974).
(24) D. C. Wigfield and D. J. Phelps, *J. Amer. Chem. Soc.*, **96,** 534 (1974).
(25) E. L. Eliel, N. L. Allinger, S. J. Angyal, and G. A. Morrison, "Conformation Analysis," Wiley-Interscience, New York, N.Y., 1965, pp 44, 114.

more ready attack on the carbonyl in some conformations of the alkyl chain than the equatorial alkyl group, so a significant axial population would tend to increase the overall rate by this mechanism. The degree of correlation with solution chemistry is less than quantitative, in any case, for the *n*-alkylcyclohexanones, though solution chemistry, where it exists, provides a useful qualitative guide to reactivity.

Third, we note a factor of approximately two in the rates of the isomeric decalones **4** and **5**. The trans isomer **5** reacts more rapidly. This is to be expected from examination of the compounds, which exist in the conformations shown below, **4** being able to convert between several stable forms and **5** being constrained to exist in one stable form. In the cis form **4**, the hydrogen at the 8-position



4 5

tends to shield the carbonyl oxygen from attack, as shown, in any stable conformation; thus the rate of this compound should be slower. We again see, therefore, that this sort of ion-molecule reaction parallels effects of stereochemical parameters, and that isomers react at predictably different rates, as we observed once before (*7*). Experiments with non-hindered isomers of the cyclohexanones are under way to confirm the assignment of a steric effect.

These conclusions form the basis of more general remarks. The steric environment of a functional group in a large molecule clearly influences its rate of reaction for a specific ion-molecule process when the reacting species are large enough and competing channels for products do not drain off enough of the collision complex to obscure the reaction of interest. This should be significant for chemical analysis when the mass spectra of isomers are very similar or when the mass spectra differ in ways which cannot be easily predicted.

It now becomes important to study the interactions of more complex acylating reagents to determine if there is a correlation of ionic size with power to discriminate between functional groups of different steric environment. Perhaps more effective gaseous ionic reagents may be found by this route.

It also becomes important to study the effect of ionizing energy on relative rates of reaction of isomeric neutrals. It has been shown that there is a dependence of relative rate constants on ionizing energy (*26*). Optimized conditions should be sought for analysis, perhaps the ideal case where one isomer reacts to produce a detectable amount of product on some set ICR time scale but the other does not.

Studies designed to test these suggestions are in progress.

RECEIVED for review February 19, 1974. Accepted June 12, 1974. This work was supported by the National Institute of General Medical Sciences (GM15994) and the Alfred P. Sloan Foundation. The instrument was purchased through funds from Hercules, Inc., the Shell Companies Foundation, the North Carolina Board of Science and Technology (159), and the National Science Foundation (GU 2059).

(26) M. L. Gross and J. Norbeck, *J. Chem. Phys.*, **54**, 3651 (1971).

Determination and Comparison of Association Constants for Weak Organic Complexes by Thermodynamic, Resonance, and Optical Methods

Daniel E. Martire

Department of Chemistry, Georgetown University, Washington, D.C. 20007

The usual gas–liquid chromatographic (GLC), *i.e.*, thermodynamic, methods of studying "acceptor/donor" systems yield the sum $K_1 + \alpha_1$, where K_1 is the 1:1 AD association constant and α_1 is a measure of the effect of noncomplexing A–D interactions. With weak complexes (small K_1) the latter term may be an important contribution to the sum. α_1 may be interpreted either in terms of the solution nonideality of uncomplexed solute (A or D, as the case may be) or in terms of contact pairing between A and D. The techniques of nuclear magnetic resonance (NMR) spectrometry and ultraviolet/visible (UV/V) spectrophotometry yield K_1 separately. However, with small K_1 values, mixed solvency effects could produce serious error in the NMR and UV/V experiments. Equations are derived and supporting examples are given which illustrate important considerations relative to the analysis, interpretation, and comparison of measurements from GLC, NMR, and UV/V.

This study was prompted by reports (*1*, *2*) that, for a given "acceptor/donor" pair, quite different values for "association constants" are obtained by thermodynamic (gas–liquid chromatography (GLC)) and spectral (nuclear magnetic resonance (NMR) spectrometry and ultraviolet/visible (UV/V) spectrophotometry) means. In one such investigation (*1*), GLC produced seemingly reasonable values for all systems studied, while NMR and UV/V gave much smaller (and sometimes negative) values. In another study (*2*), the GLC results were uniformly larger than the NMR results. The equations derived in the present paper provide a basis for explaining these apparent discrepancies and should serve as a guide to potential pitfalls in determining and comparing "equilibrium constants" from the three methods.

(1) J. H. Purnell and O. P. Srivastava, *Anal. Chem.*, **45**, 1111 (1973).
(2) D. E. Martire, J. P. Sheridan, J. W. King, and S. E. O'Donnell, *J. Amer. Chem. Soc.*, submitted for publication.

We shall consider liquid mixtures containing two neutral organic species, an "acceptor" (A) and a "donor" (D), dissolved in an inert solvent (I), where one of the conditions $C_D \gg C_A$ or $C_A \gg C_D$ obtains and where C_i refers to the concentration of uncomplexed i. As will become evident, the thermodynamic properties of such systems and their spectrometric behavior are governed not only by the extent of complex formation, but also by noncomplexing interactions between A and D.

Complex formation is an association of *definite* stoichiometry between A and D. When we say that a donor and acceptor form a 1:1 complex in an inert solvent, we mean that the number of adjacent DA pairs is in excess of the number to be expected on the basis of random encounters. This complex has a lifetime which is long compared to the duration of a molecular collision. In addition to these longer-lived pairs (which usually require a special mutual orientation of A and D for formation), there also exists a range of loose contacts between A and D, whose lifetimes are of the order of the duration of a molecular collision. (The former are sometimes classified as "chemical" interactions and the latter as "physical" ones.) Orgel and Mulliken (*3*) termed these loose interactions "contact pairs." In their simple model, all AD pairs are arbitrarily divided into two classes, namely, 1:1 complexes and contact pairs, where the former reduces the effective number of free A and free D in solution, while the latter does not. Their model will be applied to the NMR and UV/V procedures for obtaining association constants and will be one of two applied to the GLC approach. It will be shown that, if the number of contact pairs is small compared to the number of complexes, then, under these conditions (*i.e.*, for "strong" complexes), valid equilibrium constants (K) can be obtained directly by any of the three experimental methods. However, with "weak" complexes, the effect of contact pairing must be taken into account, particularly in the GLC experiment.

The concentration of weak complexes in solution cannot be determined from thermodynamic measurements *alone* without the aid of a detailed model. The GLC method provides no exception. In the other model applied to the GLC method, solution theory is used to describe the effect of loose collisions in terms of the solution nonideality of *uncomplexed* solute (D or A, as the case may be). Both models lead to the result that the usual GLC approaches never yield K separately, but always a sum $K + \alpha$, a difference which is unimportant only for strong complexes ($K \gg \alpha$). With the Orgel–Mulliken (*3*) model, α is regarded as a quasi-K for "contact pair formation" (see later), while in the other (and more explicit) model, α is related to combinatorial, energetic, and structural effects in solution. For the spectral methods, it will be shown that the presence of contact pairs affects only the spectroscopic properties of the "complex," and, hence, that K can, in principle at least, be obtained separately. This is in agreement with other workers (*3, 4*). However, wih NMR and UV/V, a potential pitfall in determining K for weak complexes is related to the solution nonideality of D in I (taking $C_D \gg C_A$).

ASSOCIATION CONSTANTS FROM GAS–LIQUID CHROMATOGRAPHY

Let us consider the GLC method utilized by Purnell *et al.* (*1, 5–7*) for obtaining "association constants" of organic complex formation. Let A be the electron acceptor solute, D be the electron donor additive, I be the inert solvennnt, and M be the mixed solvent (D + I) at concentration C_D. The usual condition $C_D \gg C_A$ applies where C_i is the concentration of uncomplexed i. Recently, it was shown (*8*) that the generalized equation relating the apparent partition coefficient of A in M, $(K_R)_M$, to the partition coefficient of uncomplexed A in pure I, $(K_R)_I$, and the 1:1 AD association constant (K_1) is given by

$$(K_R)_M = (K_R)_I \frac{\gamma_I^A v_I}{\gamma_M^A v_M}(1 + K_1\gamma_D C_D) \quad (1)$$

where γ_I^A and γ_M^A are the infinite dilution activity coefficients of uncomplexed A in, respectively, I and M (based on the mole fraction convention that $\gamma_i^A \to 1$ as $x_A \to 1$), γ_D is the activity coefficient of D in M at C_D (based on the convention that $\gamma_D \to 1$ as $C_D \to 0$), and v_I and v_M are the molar volumes of I and M, respectively. Also (*8, 9*),

$$\ln\left(\frac{\gamma_I^A v_I}{\gamma_M^A v_M}\right) = (\chi_I^A - \chi_M^A) + \ln\frac{(\gamma_I^A)^c v_I}{(\gamma_M^A)^c v_M} \quad (2)$$

where χ_i^A is the interaction parameter of uncomplexed A with i (*i.e.*, the sum of the structural and energetic contribution to $\ln \gamma_i^A$ (*9*)), and $\ln (\gamma_i^A)^c$ is the combinatorial or molecular size contribution to $\ln\gamma_i^A$. Previously (*8*), we showed that

$$\ln\frac{(\gamma_I^A)^c v_I}{(\gamma_M^A)^c v_M} = v_A\left(\frac{v_I - v_D}{v_I}\right)C_D \quad (3)$$

Assuming that $v_I \geq v_D$, and letting $\chi_M^A = \chi_D^A\phi_D + \chi_I^A\phi_I - (v_A/v_D)\chi_I^D\phi_D\phi_I$ (*10*), where ϕ_i is the volume fraction of component i in M, one obtains

$$(\chi_I^A - \chi_M^A) = (v_D\chi_I^A - v_D\chi_D^A + v_A\chi_I^D)C_D - (v_A v_D\chi_I^D)C_D^2 \quad (4)$$

where χ_D^A is the interaction parameter of uncomplexed A with D, χ_I^D is the interaction parameter of I with D, and the v's in Equations 3 and 4 represent molar volumes. Thus, Equations 2–4 combined give

$$\ln\left(\frac{\gamma_I^A v_I}{\gamma_M^A v_M}\right) = \left[v_A\left(\frac{v_I - v_D}{v_I}\right) + (v_D\chi_I^A - v_D\chi_D^A + v_A\chi_I^D)\right]C_D + [-v_A v_D\chi_I^D]C_D^2 = \alpha_1 C_D + \alpha_2 C_D^2 \quad (5)$$

where α_1 and α_2, the coefficients of C_D and C_D^2, respectively, are independent of C_D. Note that for the case $v_D \geq v_I$, $\chi_M^A = \chi_D^A\phi_D + \chi_I^A\phi_I - (v_A/v_I)\chi_I^D\phi_D\phi_I$ (*10*), and Equation 5 becomes

$$\ln\left(\frac{\gamma_I^A v_I}{\gamma_M^A v_M}\right) = \left[v_A\left(\frac{v_I - v_D}{v_I}\right) + v_D(\chi_I^A - \chi_D^A + [v_A/v_I]\chi_I^D)\right]C_D + [-(v_A v_D^2/v_I)\chi_I^D]C_D^2 = \alpha_1 C_D + \alpha_2 C_D^2 \quad (5')$$

Assuming that $(\alpha_1 C_D + \alpha_2 C_D^2) \ll 1$, Equations 1 and 5 (or 5′) give

(3) L. E. Orgel and R. S. Mulliken, *J. Amer. Chem. Soc.*, **79**, 4839 (1957).
(4) R. L. Scott, *J. Phys. Chem.*, **75**, 3843 (1971).
(5) J. H. Purnell, "Gas Chromatography," A. B. Littlewood, Ed., Elsevier, Amsterdam, 1966, p 3.
(6) D. F. Cadogan and J. H. Purnell, *J. Chem. Soc. (A)*, 2133 (1968).
(7) D. F. Cadogan and J. H. Purnell, *J. Phys. Chem.*, **73**, 3489 (1969).
(8) H. L. Liao, D. E. Martire, and J. P. Sheridan, *Anal. Chem.*, **45**, 2087 (1973).
(9) D. E. Martire, *Anal. Chem.*, **46**, 626 (1974).
(10) H. Tompa, "Polymer Solutions," Butterworths, London, 1956, p 182, eq 7.22.

$$(K_R)_M = (K_R)_I\Big(1 + \alpha_1 C_D + \left\{\frac{\alpha_1^2}{2} + \alpha_2\right\} C_D^2 + \ldots\Big)(1 + K_1\gamma_D C_D) \quad (6)$$

where γ_D will be taken as the following polynomial in C_D:

$$\gamma_D = 1 + \beta_1 C_D + \beta_2 C_D^2 + \ldots \quad (7)$$

With Equations 6 and 7 and an additional term to allow for the possibility of AD_2 complexes, we have, up through terms in C_D^2,

$$(K_R)_M = (K_R)_I\Big[1 + (K_1 + \alpha_1)C_D + \Big(K_1\{\alpha_1 + \beta_1 + K_2\} + \frac{\alpha_1^2}{2} + \alpha_2\Big)C_D^2\Big] \quad (8)$$

where K_2 is the equilibrium constant for the reaction D + AD $\rightleftarrows$ AD_2 (*5*). It can readily be shown (*2, 5*) that Equation 8 also applies when two isomeric 1:1 complexes, type a and type b, are present. In that event,

$$K_1 = K_{1,a} + K_{1,b} \quad (9)$$

and K_2 would be a more complicated function which need not concern us here.

In the derivation of Equation 8, account was taken of the difference between the partition coefficient of uncomplexed A in M and that in I. This was implemented through an activity coefficient correction (the ratio ${}^{\gamma_I{}^A v_I}/_{\gamma_M{}^A v_M}$ in Equation 1), and led to the α terms in Equation 8. Alternatively, one could account for this difference by utilizing the Orgen–Mulliken model (*3*), which, in effect, would attribute this difference to noncomplexing A–D interactions, or contact pairing, in M. It arbitrarily divides A-type molecules into three classes: (a) unperturbed and uncomplexed A (as in pure I), with its concentration denoted by C_{A^*}, (b) uncomplexed A undergoing loose interactions (contact pairing) with D, and (c) A in complexes with D, the concentration being given by C_{AD}. The concentration of contact pairs ($C_{A\text{-}D}$) is assumed to be proportional (proportionality constant of α_1) to the product $C_A C_D$, where C_i is the concentration of uncomplexed i (*3*). Hence, α_1 may be regarded, roughly, as a quasi-K for short-lived contact pairing. Furthermore, the total concentration of uncomplexed A is the sum $C_{A^*} + C_{A\text{-}D}$, and we have the following equilibrium expressions:

$$A^*(\text{gas}) \overset{(K_R)_I}{\rightleftarrows} A^*(\text{liq}) \quad (10)$$

$$A + D \overset{\alpha_1}{\rightleftarrows} A\text{–}D \quad (11)$$

$$A + D \overset{K_1'}{\rightleftarrows} AD \quad (12)$$

$$AD + D \overset{K_2'}{\rightleftarrows} AD_2 \quad (13)$$

where the prime superscripts denote stoichiometric (concentration units) equilibrium quotients. Correcting the K's for possible nonideality of D in I, and following the derivation set out by Purnell (*5*) for class A(ii) equilibria, with terms higher order than C_D^2 neglected, one obtains from Equations 7 and 10–13:

$$(K_R)_M = (K_R)_I[1 + (K_1 + \alpha_1)C_D + (K_1\{\alpha_1 + \beta_1 + K_2\} + \alpha_1^2)C_D^2] \quad (14)$$

Thus, Equations 8 and 14 are identical in form through first order in C_D and are similar through C_D^2, the only exception being that the sum $(\alpha_1^2/2) + \alpha_2$ in Equation 8 is replaced by α_1^2 in Equation 14. At sufficiently low C_D, $(K_R)_M$ should be a nearly linear function of C_D, enabling one to measure the sum $K_1 + \alpha_1$. Moreover, α_1 may be interpreted either in terms of the nonideal behavior of uncomplexed A in M, or in terms of an "equilibrium quotient" for contact pairing. Note that the former interpretation leads to an explicit relation for α_1 and to the result that α_1 depends not only on A and D, but also on the nature of the "inert" solvent (Equation 5 or 5′).

In Equations 8 or 14, the C_D^2 term can be neglected only at low C_D and/or when the coefficient of the C_D^2 term is sufficiently small. Also, β_1, which is a measure of the nonideal mixing of D and I, can be either negative or positive (see Appendix), whereas K_1, K_2, and α_1 are positive, while α_2 (Equation 8) can be negative or positive ($\chi_I{}^D$ can be negative or positive—see Appendix). Therefore, the C_D^2 term could be positive, negative, or (with fortuitous cancellation) zero. In any event, if a large enough C_D range is studied, the coefficient of the C_D^2 term may be determined empirically from the slope of a plot of $[|(K_R)_M/(K_R)_I| - 1]/C_D$ *vs.* C_D, which also yields $K_1 + \alpha_1$ directly as the intercept.

Thus, in general, GLC studies yield the sum $K_1 + \alpha_1$, and not K_1 separately. With strong complexes ($K_1 \gg \alpha_1$), this need not be worrisome. Similarly, if no long-lived complexes exist ($K_1 = 0$), GLC would yield only the "equilibrium quotient" α_1. With weak complexes (small K_1), however, GLC indiscriminately measures the sum of equilibrium constants for all isomeric long-lived 1:1 AD complexes present (see Equation 9) *plus* short-lived A–D contact interaction pairing. The latter may not be negligible, a situation which can be advantageous or disadvantageous, depending on the molecular information one hopes to infer from the investigation (see Discussion). It should be noted that workers in the field often attempt to account for the α_1 term (or to justify its neglect) by studying an arbitrary noncomplexing (N) solute such as a cycloparaffin or paraffin (*6, 8*). The usual argument that a zero value for α_1 of N implies a zero value for α_1 of A is not justifiable, in general, on theoretical grounds (see Appendix). Under certain circumstances it may be possible to select and study a *proper* nonpolar analog (*11, 12*) of molecule A in order to estimate α_1.

If one neglects the C_D^2 term, Equations 8 (or 14) and 9 give:

$$(K_R)_M = (K_R)_I[1 + (K_{1,a} + K_{1,b} + \alpha_1)C_D] \quad (15)$$

Among the possible combinations that a GLC measurement of "K_1" for a presumed donor/acceptor system might be reflecting are: (i) $K_{1,a} + K_{1,b} + \alpha_1$, (ii) $K_{1,a} + \alpha_1$, (iii) $K_{1,a} + K_{1,b}$, (iv) $K_{1,a}$, or (v) α_1. Spectroscopic and/or dielectric studies can often be used to help distinguish among these various combinations (see later). In addition, the GLC experiment alone might provide circumstantial evidence as to whether one equilibrium constant or the sum of two or more equilibrium constants is being determined. For example, it can be shown (*3*) that with (iii):

$$\Delta H_1 = \frac{K_{1,a}\Delta H_{1,a} + K_{1,b}\Delta H_{1,b}}{K_{1,a} + K_{1,b}} = X_{1,a}\Delta H_{1,a} + X_{1,b}\Delta H_{1,b} \quad (16)$$

where $X_{1,a}$ and $X_{1,b}$ are the fractions of 1:1 complexes which are of type a and type b, respectively, and the ΔH's refer to the enthalpies of complex formation. If the appar-

(11) S. D. Christian, K. O. Yeo, and E. E. Tucker, *J. Phys. Chem.*, **75**, 2413 (1971).

(12) S. D. Christian, R. Frech, and K. O. Yeo, *J. Phys. Chem.*, **77**, 813 (1973).

ent enthalpy of complex formation (ΔH_1) is found to be a function of temperature (*i.e.*, curvature is observed in the ln K_1 *vs.* T^{-1} plot), this would be an indication that K_1 is a sum of two or more terms. This follows from the fact that, while $\Delta H_{1,a}$ and $\Delta H_{1,b}$ should be temperature independent, $X_{1,a}$ and $X_{1,b}$, in general, would not (*3*). The observation that $\Delta H_1 = f(T)$, however, would require good experimental accuracy and a sufficient difference in the values of $\Delta H_{1,a}$ and $\Delta H_{1,b}$. Note also that the preceding argument applies to possibility (ii), *i.e.*, with $\Delta H_1 = (K_{1,a}\Delta H_{1,a} + \alpha_1\Delta H_{\alpha_1})/(K_{1,a} + \alpha_1)$, etc.

Thus far, only the Purnell approach to determining "association constants" by GLC has been discussed; it is the most general (*8*). The method devised by Martire and Riedl (*13*), which is applicable under certain well-defined conditions, employs the following expression for the GLC determination of K_1:

$$\frac{(V_g^\circ)_D^A(V_g^\circ)_I^N}{(V_g^\circ)_I^A(V_g^\circ)_D^N} = \frac{\gamma_I^A\gamma_D^N}{\gamma_D^A\gamma_I^N}(1 + K_1C_D\gamma_D) \quad (17)$$

In the above, D refers to the pure electron donor solvent, I to the pure inert reference solvent (chosen to have approximately the same molar volume, structure, and polarizability as D), V_g° is the specific retention volume, A refers to the electron acceptor solute, and N to an arbitrarily chosen alkane solute, and γ_i^j to the infinite dilution solute (j) activity coefficients (based on the mole fraction convention that $\gamma_i^j \to 1$ as $x_j \to 1$). The other symbols have already been defined. Note that γ_D^A represents the value for *uncomplexed* A in pure D. In the past (*13–15*), it has been argued that the solute activity coefficient ratio on the r.h.s. of Equation 17 should be approximately unity. It is now found that this is not justifiable, in general, on theoretical ground. The value for this ratio turns out to be $1 + \alpha_1C_D + (\alpha_1^2/2)C_D^2$, where α_1 is given by Equation 5 with $v_D \approx v_I$ (see Appendix). Also, γ_D is close to unity (see Appendix). Therefore, with $\gamma_D \approx 1 + \beta_1C_D$, Equation 17 leads to a form similar to Equation 8 and identical to Equation 14 through C_D^2:

$$\frac{(V_g^\circ)_D^A(V_g^\circ)_I^N}{(V_g^\circ)_I^A(V_g^\circ)_D^N} = 1 + (K_1 + \alpha_1)C_D + \left(K_1\beta_1 + \beta_1 + K_2^1 + \frac{\alpha_1^2}{2}\right)C_D^2 \quad (18)$$

The approach based on the above equation has the advantage of requiring only relative retention measurements on two columns, but has the potential disadvantage that the C_D^2 term with pure D may not be negligible (*8*). In any event, with the C_D^2 term assumed negligible, both the less general approach and the Purnell approach give the sum $K_1 + \alpha_1$ as the "apparent association constant."

ASSOCIATION CONSTANTS FROM NUCLEAR MAGNETIC RESONANCEEE AND OPTICAL SPECTROSCOPY

Consider an NMR experiment where the chemical shift of a given proton on the acceptor (A) is observed at various concentrations of the donor (D) in an inert solvent (I), where $C_D \gg C_A$, and C_A is the concentration of *uncomplexed* acceptor. To be completely general, assume that there are four distinct proton frequencies: completely free proton (ν_{A^*}), proton perturbed through collisional contact pairing or loose A–D interaction (ν_{A-D}), proton perturbed by 1:1 complex formation of type a ($\nu_{AD}{}^a$), and proton perturbed by 1:1 complex formation of type b ($\nu_{AD}{}^b$). Because of the assumption of contact pairing, ν_{A-D} should be regarded as an averaged value over all orientations (*3*). Again letting $C_{A-D} = \alpha_1C_AC_D$, one obtains for the time-averaged or observed proton frequency:

$$\nu = \frac{(C_A - \alpha_1C_AC_D)\nu_A{}^* + \alpha_1C_AC_D\nu_{A-D} + C_{AD}{}^a\nu_{AD}{}^a + C_{AD}{}^b\nu_{AD}{}^b}{C_A + C_{AD}{}^a + C_{AD}{}^b} \quad (19)$$

where, as before, $C_A = C_{A^*} + C_{A-D}$.

Rearranging terms, Equation 19 becomes

$$\frac{\Delta}{C_D} = -K_1'\Delta + K_1'\bar{\Delta}_c \quad (20)$$

where

$$K_1' = K_{1,a}' + K_{1,b}' = \frac{C_{AD}{}^a + C_{AD}{}^b}{C_AC_D} \quad (21)$$

$$\Delta = \nu - \nu_A{}^* \quad (22)$$

$$\bar{\Delta}_c = \frac{K_{1,a}'\Delta_{AD}{}^a + K_{1,b}'\Delta_{AD}{}^b + \alpha_1\Delta_{A-D}}{K_{1,a}' + K_{1,b}'} \quad (23)$$

where

$$\left.\begin{aligned}\Delta_{AD}{}^a &= \nu_{AD}{}^a - \nu_A{}^* \\ \Delta_{AD}{}^b &= \nu_{AD}{}^b - \nu_A{}^* \\ \Delta_{A-D} &= \nu_{A-D} - \nu_A{}^*\end{aligned}\right\} \quad (24)$$

To simplify matters, the possibility of termolecular AD_2 complexes has been ignored in the above derivations. For an excellent discussion and treatment of the effect of termolecular complexes the reader is referred elsewhere (*16, 17*). Equation 20 is in the form used by Foster and Fyfe (*18*) for plotting their NMR results. It is equivalent to that suggested by Scatchard (*19*) for treating UV/V data. Deranleau (*16*) demonstrates the clear advantage of this type of plotting equation over the Benesi–Hildebrand or double-reciprocal equation (*20*) and the Scott or half-reciprocal equation (*21*). The latter is given by

$$\frac{C_D}{\Delta} = \frac{1}{K_1'\bar{\Delta}_c} + \frac{C_D}{\bar{\Delta}_c} \quad (25)$$

To convert ths equilibrium quotient K_1' to an equilibrium constant K_1, we assume that A and AD are sufficiently dilute in I, so that $\gamma_{AD}/\gamma_A \to 1$ (based on the convention that $\gamma_i \to 1$ as $C_i \to 0$). Thus, with Equation 7:

$$K_1' = K_1\gamma_D \approx K_1(1 + \beta_1C_D) \quad (26)$$

For analysis of the data from UV/V spectrophotometry, equations of the *same form* as Equations 20 and 25 can be derived (*3*), *i.e.*,

$$\frac{\epsilon_A(\lambda)}{C_D} = -K_1'\epsilon_A(\lambda) + K_1'\epsilon_c(\lambda) \quad (27)$$

(13) D. E. Martire and P. Riedl, *J. Phys. Chem.*, **72**, 3478 (1968).
(14) J. P. Sheridan, D. E. Martire, and Y. B. Tewari, *J. Amer. Chem. Soc.*, **94**, 3294 (1972).
(15) J. P. Sheridan, D. E. Martire, and F. P. Banda, *J. Amer. Chem. Soc.*, **95**, 4788 (1973).
(16) D. A. Deranleau, *J. Amer. Chem. Soc.*, **91**, 4044, 4050 (1969).
(17) B. Dodson, R. Foster, A. A. S. Bright, M. I. Foreman and J. Gorton, *J. Chem Soc. (B)*, 1283 (1971).
(18) R. Foster and C. A. Fyfe, *Trans. Faraday Soc.*, **61**, 1626 (1965).
(19) G. Scatchard, *Ann. N.Y. Acad. Sci.*, **51**, 660 (1949).
(20) H. A. Benesi and J. H. Hildebrand, *J. Amer. Chem. Soc.*, **71**, 2703 (1949).
(21) R. L. Scott, *Recl. Trav. Chim. Pays Bas.*, **75**, 787 (1956).

$$\frac{C_D}{\epsilon_A(\lambda)} = \frac{1}{K_1'\bar{\epsilon}_c(\lambda)} + \frac{C_D}{\bar{\epsilon}_c(\lambda)} \quad (28)$$

where λ is the wavelength of any observed charge-transfer band, $\epsilon_A(\lambda)$ is the apparent molar extinction coefficient of A at λ based on its *total* concentration, and $\bar{\epsilon}_c(\lambda)$ is an effective molar extinction coefficient of the complex given by

$$\bar{\epsilon}_c(\lambda) = \frac{K_{1,a}'\epsilon_{AD}^{a}(\lambda) + K_{1,b}'\epsilon_{AD}^{b}(\lambda) + \alpha_1\epsilon_{A\text{-}D}(\lambda)}{K_{1,a}' + K_{1,b}'} \quad (29)$$

The similarity between the NMR and UV/V equations simplifies the discussion which follows. It should be noted, however, that NMR is a generally more useful tool for complexation studies, since it enables one to investigate complexes stabilized by any combination of electrostatic and charge-transfer forces, whereas the UV/V method obviously requires that there be *some* charge-transfer stabilization.

For the moment, assume that $\gamma_D = 1$ (or $K_1' = K_1$). It is immediately apparent from Equations 20 and 27 that, in principle, it is possible to obtain K_1 *uniquely*, even in the presence of appreciable contact pair interaction. All that is required is that $\bar{\Delta}_c$ [or $\bar{\epsilon}_c(\lambda)$] not be zero. In other words, a change in the chemical shift of A (or the appearance of a charge-transfer band) must occur when D is added. With NMR, *e.g.*, a plot of Δ/C_D *vs.* Δ then gives $-K_1$ directly as the slope. Note that if the Δ term resulted solely from loose A–D interactions ($K_1 = 0$), one would observe a straight line of zero slope and intercept $\alpha_1\Delta_{A\text{-}D}$. The "apparent association constant" ($K_1 + \alpha_1$) obtained through a GLC study on the same system should then be α_1 alone (incidentally, enabling one to estimate $\Delta_{A\text{-}D}$ from the NMR intercept). It also follows that if a nonzero slope is obtained from NMR, and if the NMR result (K_1) and the GLC result ($K_1 + \alpha_1$) are identical (within the combined experimental error), then α_1 is negligibly small. If, in addition, both $\bar{\Delta}_c$ and ΔH_1 of complex formation are temperature independent, then, most likely, only one type of complex (a or b) is present (*3*).

In general, if a nonzero slope ($K_1 \neq 0$) is found in the NMR plot (Equation 20), then comparison with the GLC result allows one to separate the sum $K_1 + \alpha_1$ into its component parts. With $\alpha_1 \neq 0$, the $\bar{\Delta}_c$ term should then be temperature dependent. If, in addition, one observes curvature in the plot of ln K_1 *vs.* T^{-1}, this would indicate that at least two types of complexes are present. Thus, the combination of GLC and NMR (and/or UV/V) measurements over a range of temperatures should aid one in distinguishing among the various possibilities cited in the previous section.

The effect of nonideal behavior of D in M (I + D) on the spectral determination of K_1 merits careful consideration (*22*), especially for weak complexes (small K_1). The NMR and UV/V cases are formally identical; thus, combining Equations 20 and 26, with $\beta_1 C_D \ll 1$, one obtains for NMR

$$\frac{\Delta}{C_D} = -(K_1 - \beta_1)\Delta + K_1\bar{\Delta}_c \quad (30)$$

If K_1 is small and β_1 is positive and small (see Appendix), but greater than K_1, one would obtain an apparently negative "K_1" from a plot of Δ/C_D *vs.* Δ. For example, if the true value of K_1 is 0.10 l. mol^{-1} and $\beta_1 = +0.12$ l. mol^{-1}, one would obtain an apparent "K_1," of -0.02 l. mol^{-1}. Similarly, if β_1 is negative, too high a value of K_1 would be obtained. Note that a β_1 value of 0.12 implies a γ_D of less than 1.05 at $C_D = 0.4$ mol l.$^{-1}$. It would not take very strong I–D interactions to produce this small a β_1 value. The above arguments apply with any of the three plotting procedures mentioned.

DISCUSSION

The results from three recent studies (*1, 2, 23*) will be used to illustrate and support some of the points made in the preceding sections.

Recently completed in this laboratory was a GLC study (10°–40°) of the "association" of various methyl-substituted aromatic "donors" with the "acceptor" CBr_4 (*23*). In this case, the aromatic solutes were the "donors" and CBr_4 was the "acceptor" additive to the inert solvent squalane ($0 \leq C_A < 0.7$ mol l.$^{-1}$). "Association constants" in the range 0.34 to 0.65 l. mol^{-1} and enthalpies in the range 4.5 to 6.6 kJ mol^{-1} were measured. There was no clear trend in the enthalpy values. The plot of $[|(K_R)_M/(K_R)_I| - 1]/C_A$ *vs.* C_A gave a straight line of nearly zero slope for all systems, indicating that the terms in C_A^2 were negligible (see Equation 8). Also, plots of ln "K_1" *vs.* T^{-1} clearly indicated the absence of curvature. These findings were suggestive either of: (a) very weak 1:1 AD complexes of one type, with negligible contact pairing ($\alpha_1 \approx 0$), or, more likely, (b) contact pairing with negligible complex formation ($K_1 \approx 0$). Although paraffin and cycloparaffin solutes gave negligibly small α_1 values, this was discounted as evidence that α_1 was negligibly small for uncomplexed D, as discussed previously.

No discrete charge-transfer (CT) bands were found for mixtures containing CBr_4 and several different aromatics in an inert solvent. Tramer (*24*) observed UV shifts of a CBr_4 absorption edge with the addition of aromatics, an effect which was ascribed to CT transitions, and obtained K_1 values which ranged from 0.01 l. mol^{-1} for benzene/CBr_4 to 0.05 l. mol^{-1} for hexamethyl benzene/CBr_4, certainly indicative of little or no complex formation. We have confirmed the existence of these UV shifts, but were hesitant to attribute them to CT transitions since it appeared that certain artifacts could have caused them (*23*). Moreover, the nuclear quadrupole resonance spectrum of the *p*-xylene/CBr_4 system has been interpreted as being indicative of little, if any, CT interaction in the ground state (*25, 26*). Further, the most current evidence (*27*) indicates that the interaction of CCl_4 with aromatics (systems which *do* yield CT bands) is best described in terms of contact pairing. Hence, it was suspected that our CBr_4/aromatic results from GLC reflected largely, if not totally, loose van der Waals interactions (*i.e.*, "contact pairing" with minimal CT interaction).

To test this suspicion, two additional sets of studies were carried out. Dielectric and refractive index measurements were performed using the procedure described by Guggenheim (*28*) and utilized recently to study tetracyanoethylene/aromatic complexes (*29*). The dipole moments of five aromatics (benzene, toluene, *p*-xylene, mesitylene, and chlorobenzene) in a 0.6 *M* CBr_4 in *n*-decane solution had the same values (within experimental error) as in pure *n*-decane. This was interpreted as indicating that the concentration of complexed species (C_{AD}) in these mixtures was effectively zero, *i.e.*, $K_1 \approx 0$, and corroborated that the

(22) M. W. Hanna and D. G. Rose, *J. Amer. Chem. Soc.*, **94**, 2601 (1972).
(23) G. M. Janini, J. W. King, and D. E. Martire, *J. Amer. Chem. Soc.*, in press.
(24) A. Tramer, *Bull. Acad. Polon. Sci., Ser. Sci. Math. Astron. Phys.*, **13**, 751 (1965).
(25) H. O. Hooper, *J. Chem. Phys.*, **41**, 599 (1964).
(26) D. F. R. Gilson and C. T. O'Konski, *J. Chem. Phys.*, **48**, 2767 (1968).
(27) L. A. Burkhardt, P. R. Hammond, R. H. Knipe, and R. R. Lake, *J. Chem. Soc. (A)*, 3789 (1971).
(28) E. A. Guggenheim, *Trans. Faraday Soc.*, **45**, 714 (1949).
(29) R. K. Chan and S. C. Liao, *Can. J. Chem.*, **48**, 299 (1970).

Table I. Analysis of Spectral (NMR and UV/V) Association Constants (K_1) Listed in Table I of Reference 1[a]

Solvent	Donor solute	Average of observed K_1's	Correction term (β_1)	Corrected K_1 values[b]
DBSUC	Toluene	0.05	−0.07	−0.02
	m-Xylene	0.14	−0.07	0.07
	o-Xylene	0.14	−0.08	0.06
DBAD	Toluene	−0.02	−0.05	−0.07
	m-Xylene	0.09	−0.06	0.03
DBSEB	Toluene	0.02	−0.05	−0.03
	m-Xylene	0.05	−0.04	0.01
	o-Xylene	0.12	−0.05	0.07

[a] Units of l. mol^{-1}. Acceptor, 2,4,7-trinitro-9-fluorenone, 40 °C. [b] Average of this column: $0.01_4 \pm 0.05$.

through Equation 6a (Appendix) using the $(\gamma_D{}^x)^\infty$ data in Table III of Ref. (*1*). With $\chi_I{}^D$ known, β_1 was computed through Equation 8a (Appendix), and the results are given in Table I. The average spectral K_1's corrected for nonideality of D in I through Equation 30 are also listed in Table I. Taking the average value of these corrected K_1's, over all systems, one obtains +0.015 with a standard deviation of ±0.05. For all practical purposes, this suggests true K_1 values of zero (no complexes) for all systems. The implied standard deviation is reasonable, given the observed agreement between the NMR and UV/V results (*1*), and the known difficulty in obtaining reliable data with very small K_1 values (*30*).

It would follow from this reasoning, then, that GLC is yielding α_1 values, which are governed by noncomplexing A–D interactions (or contact pairing) involving charge-transfer and/or electrostatic forces. To examine whether

Table II. Analysis of α_1 Values at 50 °C Listed in Table II of Reference 1[a]

	$v_D\left(\frac{v_I - v_A}{v_I}\right)^b$			$(v_{AX_I}{}^D - v_{AX_A}{}^D + v_{DX_I}{}^A)$			$-v_{AX_A}{}^D + v_{DX_I}{}^A$		
	Solvent			Solvent			Solvent		
Donor solute	DBSUC	DBAD	DBSEB	DBSUC	DBAD	DBSEB	DBSUC	DBAD	DBSEB
Benzene	0.033	0.040	0.050	0.431	0.376	0.259	0.424	0.375	0.271
Toluene	0.039	0.047	0.060	0.482	0.404	0.221	0.472	0.404	0.237
Ethyl benzene	0.045	0.054	0.069	0.399	0.334	0.182	0.381	0.327	0.194
p-Xylene	0.045	0.055	0.069	0.604	0.495	0.312	0.587	0.492	0.330
m-Xylene	0.045	0.054	0.069	0.593	0.507	0.274	0.576	0.503	0.290
o-Xylene	0.044	0.053	0.068	0.627	0.528	0.303	0.611	0.525	0.320

[a] See Equation 31. Acceptor, 2,4,7-trinitro-9-fluorenone. [b] Units of l. mol^{-1}.

GLC experiment is probably giving α_1 values alone. Proton NMR studies were conducted with several aromatic solutes. No significant frequency shifts were observed up to very high CBr_4 concentration. This confirmed that there is no significant withdrawal of electronic charge from the aromatic ring system, *i.e.*, that CT forces play, at best, a minor role in CBr_4/aromatic interactions. Thus, only the GLC experiment provided quantitative information on interactions in CBr_4/aromatic systems. The results were interpreted through the solution model described previously which permitted us to estimate the relative strength of A–D interactions (taken to be electrostatic in nature).

For the second example, consider the GLC, NMR, and UV/V measurements of "K_1" carried out recently by Purnell and Srivastava (*1*). The complexing systems studied by GLC (40°–60°) were methyl-substituted aromatic donor solutes (6 in all) with 2,4,7-trinitro-9-fluorenone (TNF) as the electron acceptor additive in three different "inert" solvents: di-*n*-butyl succinate (DBSUC), di-*n*-butyl adipate (DBAD), and di-*n*-butyl sebacate (DBSEB). With NMR and UV/V, only three aromatics were studied at a single temperature (40°) and the condition $C_D \gg C_A$ applied. Although a few negative "K_1" values were obtained, the NMR and UV/V results agreed moderately well with each other (agreement to within an average of ±0.06 l. mol^{-1}), but they were both much lower than the GLC "K_1" values, which were deemed more acceptable. The authors suggested that the spectroscopic results were unreliable, possibly because the relevant equilibria were wrongly identified, or because the solvents were somehow involved. Based on the derivations and discussion presented thus far, an alternative explanation is offered below.

Listed in Table I is the average value of the spectral K_1's for each of the eight systems studied. With the v_I values from Ref. (*1*) and available v_D data, $\chi_I{}^D$ was calculated

Table III. Least-Squares Results for $\chi_I{}^A$ and $(v_A/v_D)\chi_A{}^D$, and Retrieved α_1 Values[a,b]

Solute	$\Delta\left(-\frac{v_A}{v_D}\chi_A{}^D\right)^c$	α_1 (l. mol^{-1}) DBSUC	DBAD	DBSEB
Benzene	1.485	0.476	0.421	0.292
Toluene	0.996	0.515	0.446	0.292
Ethyl benzene	0.000	0.473	0.395	0.216
p-Xylene	1.312	0.641	0.561	0.378
m-Xylene	1.220	0.627	0.547	0.367
o-Xylene	1.526	0.653	0.574	0.397

[a] See Equation 31. [b] $\chi_I{}^A(\text{DBSUC}) = \chi_I{}^A(\text{DBAD}) + 0.600 \cdot \chi_I{}^A(\text{DBAD}) = \chi_I{}^A(\text{DBSEB}) + 1.383$. [c] $\Delta\left(-\frac{v_A}{v_D}\chi_A{}^D\right) = \left(-\frac{v_A}{v_D}\chi_A{}^D\right)_{\text{Solute}} - \left(-\frac{v_A}{v_D}\chi_A{}^D\right)_{\text{ethylbenzene}}$.

this is a physically realistic proposition, the results in Table II of Ref. (*1*) (called K_C there, but to be referred to as α_1 here) were analyzed using the expression (see Equation 5):

$$\alpha_1 = v_D\left(\frac{v_I - v_A}{v_I}\right) + (v_A\chi_I{}^D - v_A\chi_A{}^D + v_D\chi_I{}^A) \quad (31)$$

With v_A = 0.156 l. mol^{-1} (*31*) and $\chi_I{}^D$ evaluated as described before, the combinatorial and interaction parameter contributions to α_1 at 50 °C were computed through Equation 31, and are listed in Table II, along with the sum $-v_{AX_A}{}^D + v_{DX_I}{}^A$. Note first that the combinatorial contribution by itself cannot account for the observed trends in or magnitude of α_1. The dominant term is clearly $-v_{AX_A}{}^D$

(30) W. P. Person, *J. Amer. Chem. Soc.*, **87**, 167 (1965).
(31) C. Eon and B. L. Karger, *J. Chromatogr. Sci.*, **10**, 140 (1972).

$+ v_D\chi_I^A$: let us focus on it. The systems are too complicated to permit a quantitative prediction of the χ's from solution theory. Furthermore, although there are 18 data points (last three columns in Table II) and nine unknowns (6 χ_A^D's and 3 χ_I^A's), there are only eight independent equations relating these unknowns. Thus, this precludes a least-squares procedure for determining the *absolute* values of χ_A^D and χ_I^A that best fit the experimental results. However, it did prove possible to obtain a least-squares set of relative values, and in the process, to test the validity of Equation 31.

The quantity $-(v_A/v_D)\chi_A^D + \chi_I^A$ was computed from Table II. Since A is fixed, the first term varies with D only and the second with I only. An arbitrary numerical value was assigned to one of the six $-(v_A/v_D)\chi_A^D$ or three χ_I^A terms, and the best-fit values were found for the other eight terms. The results are listed in Table III. The correlation coefficient was computed to be in excess of 0.98. Also, the retrieved α_1 values (last three columns of Table III) agree with the experimental values [Table II of Ref. (*1*)] to within an average of ± 0.014 l. mol^{-1}, which is of the order of experimental error (*8*). Thus, the GLC results of Purnell and Srivastava (*1*) are consistent with the proposed solution model. The indication is that their spectroscopic data are representative of systems with little or no complex formation, while their GLC experiment is yielding solvent dependent α_1 values.

It is difficult to be more specific about these interaction parameters because of the involved nature of the structural contribution (*9*). It is clear, however, that the χ_I^A term (or mixed solvency effect) is responsible for the difference in α_1 values among the three solvents. Furthermore, it would seem that χ_A^D is probably negative, as a consequence of strong A–D interactions (see Appendix).

The last example concerns a recently completed GLC (*14*, *15*) and NMR (*2*) study of the interaction of haloforms with *n* electron donors (di-*n*-octylether (DOE), di-*n*-octylthioether (DOTE), and di-*n*-octylmethylamine (DOMA)). The GLC "association constants" showed no clear trend along the series $CHCl_3$, $CHCl_2Br$, $CHBr_2Cl$, $CHBr_3$. While it had been established that the haloforms undergo complex formation with these donors through hydrogen bonding, the nature of the halogen/*n*-donor interaction was less evident. Existent UV studies of triethylamine with various tetrahalomethanes (*32*) revealed CT bands and a behavior consistent with contact pairing, rather than complex formation. Further, no CT bands were observed with mixtures of CCl_4 or CBr_4 and the ether or thioether. This led us to believe that the halogen/*n*-donor interactions with CHX_3 were noncomplexing, and that GLC was measuring $K_{1,a} + \alpha_1$, where $K_{1,a}$ is the association constant for 1:1 AD hydrogen-bonded complexes and α_1 is a measure of the halogen/*n*-donor contact pairing.

To confirm this supposition, a proton NMR experiment was conducted on the same systems. The NMR K_1 values were all lower than the corresponding values from GLC. Plots of the NMR ln K_1 *vs.* T^{-1} were linear and $\bar{\Delta}_c$ was independent of temperature, for all systems in the range 30 to 60°C. As discussed before, this indicated that NMR was giving the $K_{1,a}$ for 1:1 hydrogen bonding alone, and that the slope of the R ln $K_{1,a}$ *vs.* T^{-1} plot was the ΔH of this complex formation. The constancy of $\bar{\Delta}_c$ with temperature suggested that $\Delta_{A-D} \approx 0$, *i.e.*, when D interacts with A through the halogen atoms, the proton is sufficiently remote as to be virtually unperturbed; hence, $\nu_{A-D} \approx \nu_{A^*}$ (see Equations 20–24). With these $K_{1,a}$ values from NMR, α_1 values for the halogen interaction were then obtained from the GLC composite, $K_{1,a} + \alpha_1$. The plots of ln α_1 *vs.* T^{-1} were linear, and yielded ΔH_{α_1} values. To be brief, whereas the composite GLC values showed no trends and defied interpretation, the separated parameters ($K_{1,a}$ and α_1, $\Delta H_{1,a}$ and ΔH_{α_1}) were of reasonable magnitude, and displayed electronically and sterically plausible trends. The details are discussed in Ref. (*2*).

In the three examples cited above, a case was made that the usual GLC methods measure noncomplexing A–D interactions in addition to any 1:1 AD complexes that may be present. It was also demonstrated how a combination of GLC and UV/V, NMR, and/or dielectric studies can often be used to sort out the various possibilities, and to establish whether a particular interaction is better regarded as a contact pair or as a complex.

APPENDIX

Activity Coefficient of the Additive in the Mixed Solvent. Consider a mixed solvent (M) consisting of an electron donor additive (D) and an inert solvent (I). The mole fraction activity coefficient ($\gamma_i^x \to 1$ as $x_1 \to 1$) of D in M (γ_D^x) is assumed to have the general form (*9*), with $v_I \geq v_D$,

$$\ln \gamma_D^x = \ln \frac{\phi_D}{x_D} + \left(1 - \frac{r_D}{r_I}\right)\phi_I + \chi_I^D \phi_I^2 \quad (1a)$$

where

$$\phi_i = \frac{x_i r_i}{x_I r_I + x_D r_D} \quad (2a)$$

and

$$\chi_I^D = (\chi_I^D)^{en} + (\chi_I^D)^{st} \quad (3a)$$

where x_i, v_i, and ϕ_i are, respectively, the mole fraction, molar volume, and volume fraction of component i, and χ_I^D, the interaction parameter, is a sum of an energetic and a structural term. The energetic term is given by (*9*):

$$(\chi_I^D)^{en} \approx \frac{mr_D}{RT}(\epsilon_{II}^* + \epsilon_{DD}^* - 2\epsilon_{ID}^*) \quad (4a)$$

where m is a positive constant, and ϵ_{II}^*, ϵ_{DD}^*, and ϵ_{ID}^* are the segmental interaction energies for II, DD, and ID interactions, respectively. Thus, $(\chi_I^D)^{en}$ may be negative or positive, depending on whether ϵ_{ID}^* is greater or less than the arithmetic mean $(\epsilon_{II}^* + \epsilon_{DD}^*)/2$. On the other hand, $(\chi_I^D)^{st}$, a more complicated function which need not be discussed here, is always positive (*9*).

Converting γ_D^x to a concentration based activity coefficient γ_D (where $\gamma_D \to 1$ as $C_D \to 0$), one obtains

$$\gamma_D = \gamma_D^x v_D/(\gamma_D^x)^\infty C_D r_I \quad (5a)$$

where $(\gamma_D^x)^\infty$, the infinite dilution mole fraction activity coefficient, is found from Equation 1a to be

$$\ln (\gamma_D^x)^\infty = \ln \frac{r_D}{r_I} + \left(1 - \frac{r_D}{r_I}\right) + \chi_I^D \quad (6a)$$

From Equations 1a, 5a, and 6a:

$$\ln \gamma_D = \phi_D\left(\frac{r_D}{r_I} - 1\right) + \chi_I^D(\phi_I^2 - 1) \quad (7a)$$

When $x_1 \gg x_D$, Equation 7a may be approximated by

$$\ln \gamma_D \approx \left[\frac{r_D}{r_I}(r_D - r_I) - 2\chi_I^D r_D\right] C_D = \beta_1 C_D \quad (8a)$$

Thus, for $\beta_1 C_D \ll 1$, $\gamma_D \approx 1 + \beta_1 C_D$ (see Equation 7). Note that β_1 may be either negative or positive. Since $v_I \geq v_D$, then β_1 will clearly be negative if $(\chi_I^D)^{en}$ is positive, *i.e.*, if $\epsilon_{ID}^* < (\epsilon_{II}^* + \epsilon_{DD}^*)/2$. However, if ID interactions are suffi-

(32) D. P. Stevenson and G. M. Coppinger, *J. Amer. Chem. Soc.*, **84**, 149 (1962).

ciently strong to outweigh the combinatorial and $(\chi_I^D)^{st}$ contributions, then β_1 could be positive. With $v_D \geq v_I$, the term $2\chi_I^D v_D$ in Equation 8 is replaced by $2\chi_I^D(v_D^2/v_I)$ (*10*). However, per the arguments used above, it is clear that β_1 can still be negative or positive, depending on the magnitude and sign of χ_I^D.

In the Martire–Riedl approach (*13*), $v_I \approx v_D$, I and D are structurally similar (hence, $(\chi_I^D)^{st} \approx 0$), and pure donor ($x_D = 1$) is used. Thus, from Equations 3a, 4a, and 7a, one obtains

$$\ln \gamma_D \approx -(\chi_I^D)^{en} \approx -\frac{mv_D}{RT}(\epsilon_{II}^* + \epsilon_{DD}^* - 2\epsilon_{ID}^*) \quad (9a)$$

Since D and I are chosen to have approximately the same molecular polarizability, it is argued (*13*) that $\epsilon_{ID}^* \approx \epsilon_{II}^*$; hence,

$$\ln \gamma_D \approx \frac{mv_D}{RT}(\epsilon_{II}^* - \epsilon_{DD}^*) \approx -(\chi_I^D)^{en} \quad (10a)$$

or

$$\ln \gamma_D \approx \left[\frac{m}{RT}(\epsilon_{II}^* - \epsilon_{DD}^*)v_D^2\right]C_D = \beta_1 C_D \quad (11a)$$

where $v_D C_D = \phi_D = 1$. The r.h.s. of Equation 11a is expected to be quite small and negative, generally leading to values of γ_D slightly less that unity (*14*).

The α_1 Term in Equation 5. According to Equations 5 and 3a:

$$\alpha_1^A = \left[v_A\left(\frac{v_I - v_D}{v_I}\right) + (v_D\chi_I^A - v_D\chi_D^A + v_A\chi_I^D)^{en} + (v_D\chi_I^A - v_D\chi_D^A + v_A\chi_I^D)^{st}\right]$$

where

$$(\chi_i^j)^{en} = \frac{mv_j}{RT}(\epsilon_{ii}^* + \epsilon_{jj}^* - 2\epsilon_{ij}^*) \quad (12a)$$

One can write a similar expression for a nonpolar and noncomplexing solute N:

$$\alpha_1^N = \left[v_N\left(\frac{v_I - v_D}{v_I}\right) + (v_D\chi_I^N - v_D\chi_D^N + v_N\chi_I^D)^{en} + (v_D\chi_I^N - v_D\chi_D^N + v_N\chi_I^D)^{st}\right] \quad (13a)$$

Examining Equations 12a and 13a, and noting the dependence of χ^{st} on solute molecular parameters (*9*), it becomes apparent that $\alpha_1^A \approx \alpha_1^N$ *only if:* (i) N and A are structurally similar, (ii) $v_A \approx v_N$, (iii) $\epsilon_{AA}^* \approx \epsilon_{NN}^*$, and (iv) $(\epsilon_{AD}^* - \epsilon_{AI}^*) \approx (\epsilon_{ND}^* - \epsilon_{NI}^*)$. Hence, any nonpolar analog (NPA) chosen with the expectation of estimating α_1^A in the GLC experiment must satisfy the above four conditions. In the past (*6, 8*), *e.g.,* cyclohexane has been chosen as the NPA of benzene (actually a donor solute, but let us continue to denote it by the symbol A). The observation that $\alpha_1^N \approx 0$ was taken to indicate that $\alpha_1^A \approx 0$. Clearly the weak point in that argument lies in the fact that condition (iv) is probably not satisfied, while the other three conditions are only approximately satisfied, *i.e.,*

$$(\alpha_1^A - \alpha_1^N) \approx v_D\{(\chi_I^A - \chi_D^A)^{en} - (\chi_I^N - \chi_D^N)^{en}\} \approx \frac{2v_D^2 m}{RT}[(\epsilon_{AD}^* - \epsilon_{AI}^*) - (\epsilon_{ND}^* - \epsilon_{NI}^*)] \quad (14a)$$

Thus, even if $\epsilon_{AI}^* \approx \epsilon_{NI}^*$, it is almost certain that $\epsilon_{AD}^* > \epsilon_{ND}^*$. The problem of selecting an appropriate NPA is a difficult, if not an impossible, one. The reader is referred elsewhere (*11, 12*) for discussion of a recently proposed treatment.

With the Martire–Riedl GLC method (*13*) of determining association constants, it was assumed in the past (*13–15*) that the ratio $\gamma_I^A\gamma_D^N/\gamma_D^A\gamma_I^N$ (see Equation 17) was approximately unity. Since D and I are chosen to have approximately the same molar volume and to be similar in structure, the combinatorial and structural contributions to the γ_i^j ratio cancel out, leaving

$$\ln \frac{\gamma_I^A\gamma_D^N}{\gamma_D^A\gamma_I^N} \approx (\chi_I^A - \chi_D^A)^{en} - (\chi_I^N - \chi_D^N)^{en} \quad (15a)$$

Considering the term $(\chi_I^N - \chi_D^N)^{en}$:

$$\ln \frac{\gamma_D^N}{\gamma_I^N} \approx -(\chi_I^N - \chi_D^N)^{en} = \frac{mv_N}{RT}(2\epsilon_{IN}^* - 2\epsilon_{DN}^* + \epsilon_{DD}^* - \epsilon_{II}^*) \quad (16a)$$

Since D and I are chosen to have the same molecular polarizability, then $\epsilon_{DN}^* \approx \epsilon_{IN}^*$ (*13*), and, with Equation 10a:

$$\ln \frac{\gamma_D^N}{\gamma_I^N} \approx \frac{mv_N}{RT}(\epsilon_{DD}^* - \epsilon_{II}^*) \approx \left(\frac{v_N}{v_D}\right)\chi_I^D \quad (17a)$$

Also, with $v_A \approx v_N$, one obtains from Equations 15a–17a:

$$\ln \frac{\gamma_I^A\gamma_D^N}{\gamma_D^A\gamma_I^N} = (\chi_I^A - \chi_D^A + \{v_A/v_D\}\chi_I^D)^{en} \quad (18a)$$

Finally, since $v_D C_D = 1$, we have

$$\ln \frac{\gamma_I^A\gamma_D^N}{\gamma_D^A\gamma_I^N} = [(v_D\chi_I^A - v_D\chi_D^A + v_A\chi_I^D)^{en}]C_D = \alpha_1 C_D \quad (19a)$$

where this α_1 is identical to that in Equation 5 with $v_I \approx v_D$ and $(v_D\chi I^A - v_{DXD}{}^A + v_{AXI}{}^D)^{st} \approx 0$.

Thus, for $\alpha_1 C_D \ll 1$,

$$\frac{\gamma_I^A\gamma_D^N}{\gamma_D^A\gamma_I^N} \approx 1 + \alpha_1 C_D + \frac{\alpha_1^2}{2}C_D^2 \quad (20a)$$

ACKNOWLEDGMENT

Helpful discussions with J. E. Earley (Georgetown University) and C. H. Eon (Ecole Polytechnique, Paris) are gratefully acknowledged. In a conceptually related treatment (in part), Eon (*33*) has also considered the problem of obtaining meaningful association constants from GLC through separation of "chemical" and "physical" effects.

RECEIVED for review December 18, 1973. Accepted May 21, 1974. This research was supported by a grant from the National Science Foundation.

(33) C. Eon, These, Docteur Es-Sciences, L'Universite Paris VI, 1973.

Determination of Rare Earths in Plutonium by X-Ray Emission Analysis

A. G. Miller

Technical Services Section, Chemical Processing Division, Atlantic Richfield Hanford Company, Richland, Wash. 99352

A sensitive and accurate method for measuring trace rare earths in plutonium by X-ray emission analysis has been developed. Plutonium is separated from the rare earths by solvent extraction using tri-isooctylamine. The rare earths are then carrier-precipitated as fluorides and collected on a membrane filter in an "infinitely thin" layer. The rare earths on the filter are counted and ratioed to a terbium internal standard. This work has dealt with samarium, europium, gadolinium, dysprosium, and the elements that produce spectral interferences. However, the method is equally applicable to the other rare earths, assuming spectral interferences are avoided. Detection limits are on the order of 0.1 μg. The relative standard deviation for spike recoveries of the four rare earths at the 1-μg level is 8%.

An important criterion for nuclear reactor fuel materials is the strict control of low levels of neutron-absorbing impurities such as boron, cadmium, and certain rare earths—samarium, europium, gadolinium, and dysprosium. As the Atlantic Richfield Hanford Company (ARHCO) has contracted to supply plutonium for the breeder reactor program, a method for determining low parts-per-million quantities of these rare earths in plutonium was needed. Because of a heavy development and sample load, X-ray emission spectrometry was the choice over emission spectroscopy, which is more commonly used for actinide matrices (*1–7*).

The bulk of X-ray emission work for rare earths (*8–17*) has been at greater than trace levels in samples such as ores and alloys. To be used effectively for trace analysis, three problems must be solved—separation from the plutonium matrix, concentration of the rare earths to produce adequate sensitivity, and elimination of spectral interferences.

Ion exchange, precipitation, and solvent extraction were possible methods of separation. The tendency for dilution of samples in ion exchange procedures, and the difficulty of precipitating trace elements from concentrated plutonium solutions made solvent extraction appear most favorable. Tri-isooctylamine (TiOA) in xylene was used in ARHCO laboratories for plutonium(IV) extraction (*18*). Extraction coefficients for the extraction of plutonium(IV) into 10% tri-*n*-octylamine from nitric ($D = 250$) (*19*) and into 1% tri-*n*-octylamine from hydrochloric (*20*) acids ($D = 50$) indicate the quantitative separation possible with the analogous TiOA system. Trivalent actinides and lanthanides are not appreciably extracted by amines (*19*).

Rare earths in the desired plutonium-free aqueous phase must be collected for X-ray measurement in a way that provides for maximum sensitivity of the elements on the mount. Ideally, this would be a small diameter, "infinitely thin" layer.

The use of ion-exchange membranes as concentration media for X-ray determinations of trace elements was first described in 1955 (*21*), and has recently been used by Walton (*22*) and Eby (*23*) to collect trace rare earths for X-ray emission determination. Rudolph *et al.* (*24*) found greater sensitivities for trace elements by collecting precipitated impurities on filters for X-ray analysis. Luke (*25*) obtained detection limits at nanogram levels for many elements by his "coprex" method (coprecipitation of trace elements for X-ray analysis). Luke used an analogous technique for the indirect determination of fluoride by collecting LaF_3 on a filter membrane for X-ray analysis (*26*). Winters (*18*) prepared X-ray mounts for the determination of lanthanum, cerium, praseodymium, neodymium, and samarium by reversing Luke's fluoride method. The techniques of Luke and Winters have an advantage over ion exchange membranes because element and matrix absorption effects do not occur since an "infinitely thin" layer of precipitate is presented to the incident radiation.

Since the chemical similarity of rare earths makes chemical separation impractical, spectral interferences in the complex L X-ray spectrum of the rare earths are the rule rather than the exception. The lanthanide spectral complexity is evident from Figure 1, which displays relative intensities and wavelengths according to rare earth atomic number. Correction curves (*12, 13, 15, 17, 23, 27, 28*),

(1) T. R. Saranathan and A. P. D'Silva, *India At. Energy Comm., At. Energy Estab. Trombey*, **Rep., AEET-ANAL-23** (1963); *Chem. Abstr.*, **67**, 70302g (1967).
(2) T. R. Saranathan and A. P. D'Silva, *India At. Energy Comm., At. Energy Estab. Trombey*, **Rep., AEET-ANAL-24** (1963); *Chem. Abstr.*, **67**, 87474n (1967).
(3) B. D. Joshi, R. N. Saxena, B. M. Patel, T. R. Bangia, and A. G. Page, *India At. Energy Comm., Bhabha At. Res. Cent., Rep.* **BARC-383** (1968).
(4) R. K. Dhumwad, M. V. Joshi, and A. B. Patwardhi, *Proc. Chem. Symp., 1st, 2*, 298–302 (1969); (Pub. 1970) *Chem. Abstr.*, **74**, 38048n (1971).
(5) B. D. Joshi and B. M. Patel, *Appl. Spectrosc.*, **24**, 573–6 (1970).
(6) A. Butucelea and M. Craiu, *Rev. Roum. Chim.*, **16**, 1287–90 (1971); *Chem. Abstr.*, **75**, 30350a (1972).
(7) R. Ko, *U.S. At. Energy Comm.*, **WHAN-SA-44**; *Chem. Abstr.*, **75**, 71001k (1971).
(8) E. E. Vainshtein and N. V. Turanskaya, *Zhur. Anal. Khim.*, **8**, 346–52 (1953); *Chem. Abstr.*, **48**, 5712e (1954).
(9) T. V. Ternovaya, *Ukr. Khim. Zh.*, **29**, 205–8 (1963); *Chem. Abstr.*, **59**, 3311e (1963).
(10) J. C. Lloyd and J. D. Kuptsis, *Advan. X-Ray Anal.*, **6**, 389–95 (1962).
(11) G. V. Bondarenko and M. A. Blokhin, *Zavodsk. Lab.*, 1337–8 (1964); *Chem. Abstr.*, **62**, 5883e (1965).
(12) A. V. Gordievski and V. N. Kiryushov, *Tr. Mosk, Khim-Teknol. Inst.*, **49**, 167–74 (1965); *Chem. Abstr.*, **65**, 2993g (1966).
(13) B. A. Kushurin, A. V. Gordievski, and V. N. Kiryushov, *Tr. Mosk. Khim-Tekhnol. Inst.*, **43**, 50–4 (1963); *Chem. Abstr.*, **62**, 7097a (1965).
(14) E. A. Hakkila, R. G. Hurley, and G. R. Waterbury, *Appl. Spectrosc.*, **22**, 434–7 (1968).
(15) F. J. Haftka, *Anal. Chem.*, **44**, 1900–02 (1972).
(16) R. R. Freeman, *U.S.***At. Energy Comm., Rep.* **TID-6417** (1960).
(17) H. J. Rose, Jr., and F. Cuttitta, *Appl. Spectrosc.*, **22**, 426–30 (1968).
(18) W. I. Winters, ARHCO, Richland, Wash., unpublished work, 1972.
(19) W. E. Keder, J. C. Sheppard, and A. S. Wilson, *J. Inorg. Nucl. Chem.*, **12**, 327 (1960).
(20) W. E. Keder, *J. Inorg. Nucl. Chem.*, **24**, 561 (1962).
(21) W. T. Grubb and P. D. Zemany, *Nature (London)*, **176**, 221 (1955).
(22) R. D. Walton, *Develop. Appl. Spectrosc.*, **9**, 287–305 (1971).
(23) G. N. Eby, *Anal. Chem.*, **44**, 2137–43 (1972).
(24) J. S. Rudolph, O. H. Kriege, and R. J. Nadalin, *Develop. Appl. Spectrosc.*, **4**,57–64 (1965).
(25) C. L. Luke, *Anal. Chim. Acta*, **41**, 237 (1968).
(26) C. L. Luke, *Anal. Chim. Acta*, **43**, 245 (1968).
(27) A. B. Fuentes and J. B. Polonio, *Junta Energ. Nucl.*, **JEN-214DQ/I-76** (1969); *Chem. Abstr.*, **75**, 29620m (1971).
(28) A. B. Fuentes and J. B. Polonio, *An. Quim.*, **64**, 825–32 (1968); *Chem. Abstr.*, **70**, 83922w (1969).

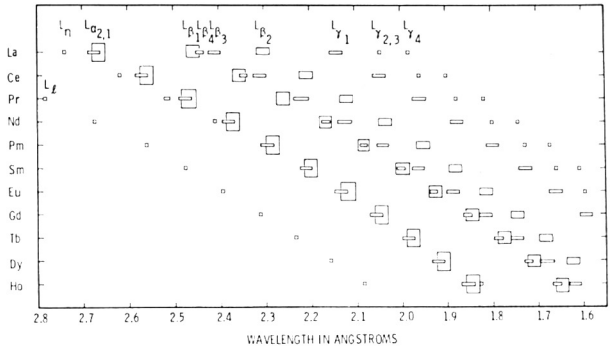


Figure 1. L X-Ray spectra of rare earths
Symbol size is proportional to relative intensity

Table I. Rare Earth Analytical Lines and Backgrounds

Element	Line	2θ	Background 2θ
Sm	$L\alpha_1$	66.22	65.10, 60.22
Eu	$L\alpha_1$	63.56	65.10
Gd	$L\alpha_1$	61.08	60.22
Dy	$2L\alpha_1$	142.90	140.00
Tb	$L\alpha_1$	58.76	
Ce	$L\beta_1$	71.61	74.10
Pr	$L\beta_1$	68.23	74.10
Eu	$2L\beta_1$	145.00	147.00
Gd	$2L\beta_1$	132.98	130.98

Table II. X-Ray Spectrometer Conditions

GE XRD-5	50 KVP, 45 mA
Target	Platinum
Counter tube	$1^2/_3$ atmosphere xenon filled
X-Ray path	Helium
Pulse height selection	
E_L	15% discrimination against La $L\alpha_1$
ΔE	10% discrimination against Fe $K\beta_1$
Soller slit	0.010 inch
Analyzing crystal	LiF 200
Counting time	100 Seconds

among other methods, have been used to surmount difficulties in background determination.

Two major potential sources of rare earths in plutonium are contamination and fission product rare earths. Since plutonium(IV) is easily separated from rare earths during the processing of nuclear fuel elements, fission product rare earths are the less likely.

The method presented here is capable of measuring individual rare earths at the 1-microgram level or less with a precision of better than ±10%.

EXPERIMENTAL

Reagents. One g/l. standard solutions for each rare earth (La–Dy) were prepared from its oxide (99.9% pure or better) obtained from Trona, A. D. McKay, or Spex Industries. The pH 4 acetate buffer is prepared by adding 286 ml of glacial acetic acid to a solution of 125 grams of sodium acetate trihydrate and diluting to 2 liters. The fluoride wash solution is prepared from 4 ml of 15 g/l. NaF, 20 ml of absolute ethanol, and diluted to 100 ml. A solution of 10% TiOA (tri-isooctylamine available from Pfaltz & Bauer, Inc., Flushing, N.Y.) in xylene is equilibrated with an equal volume of 6*N* HCl. Deionized water is used throughout.

Special Equipment. High purity aluminum is used in the sample drawer to eliminate the instrumental background of Cr, Mn, Fe, and Ni, except for about 50 cps (counts per second) due to Fe. Millipore BDWP-2500 0.6-μm filters are used, and mounted by placing between two pieces of ¼-mil Mylar (E. I. du Pont de Nemours), which is then clamped to a Caplug (EP-14, Caplugs Division, Protective Closures, Inc., Buffalo, N.Y.) with a tight fitting curtain rod ring. The Caplugs are cut down to ¼ inch high, with the bottoms punched out.

Calibration. Standard X-ray mounts are prepared by adding the aliquot of standard rare earth and 0.1 ml of 1 g/l. terbium to 5 ml of buffer and 5 ml of ethanol in a 50-ml polyethylene beaker. Dilute to 25 ml, add 1 ml of 15 g/l. NaFl solution, filter, and wrap the filter for X-ray analysis as described in the Procedure.

Procedure. Place 0.1 g of plutonium as dioxide into a glass vial and dissolve in 1–2 ml of 6*N* hydrochloric acid and one drop or less of hydrofluoric acid. The acid will be neutralized, so the quantity used must be minimized. The solution is then transferred to a 20-ml vial containing 0.1 ml of 1 g/l. Tb. Add 8 to 10 ml of 10% TiOA in xylene to the vial and stir vigorously. After the phases separate (centrifuging helps), the organic phase(s) (a middle phase containing the bulk of the plutonium and TiOA may be present) are removed as completely as possible and the extraction is repeated as necessary. After the last extraction, remove the aqueous phase with a 3-ml micropipet and transfer it to a 50-ml beaker; the volume must be estimated to the nearest 0.1 ml. Neutralize the acid (as 6*N* HCl) with 1 ml of 1.5*M* sodium acetate per millimole of acid up to a maximum of 12 millimoles. Neutralize any acid over and above 12 millimoles with sodium hydroxide *before* adding the acetate.

Add 5 ml of ethanol to the solution, dilute to approximately 25 ml and stir. Add 1 ml of 15 g/l. NaF, stir, and let stand a few minutes. Filter, using wash solution to wet filter before filtering and to rinse the beaker and funnel after filtering. Place the filter between two 5- × 5-cm pieces of Mylar lying on a Caplug, and clamp to the Caplug with a curtain rod ring. There should be no exposed radioactivity on the mount. Wrap the mount with at least one additional layer of Mylar, tape it, and label. *Caution:* Americium-trifluoride (AmF_3) and perhaps some residual Pu as plutonium-tetrafluoride (PuF_4) will be present on the filter, so proper care must be taken.

X-Ray Analysis. Count the analytical lines and backgrounds given in Table I under the spectrometer conditions given in Table II. In the event the Nd $L\beta_1$ intensity (65.10° 2θ) equals or exceeds the background at 60.22°, the second-order $L\beta_1$ lines for Eu and Gd are used. The Eu $2L\beta_1$ line is corrected for dysprosium $2L\alpha_2$ and the samarium count is corrected for Ce, Pr, and Nd contributions by the technique described by MacNevin *et al.* (29). One half of the 60.22° count is then used as the samarium background.

Calculations. The ratio, (net rare earth count)/(gross Tb count), varies in a linear way with the quantity of rare earth.

RESULTS AND DISCUSSION

Plutonium Separation. Tri-isooctylamine proved to be an effective extractant for separating Pu(IV) from the rare

(29) W. M. MacNevin and E. A. Hakkila. *Anal. Chem.*, **29**, 1019–22 (1957).

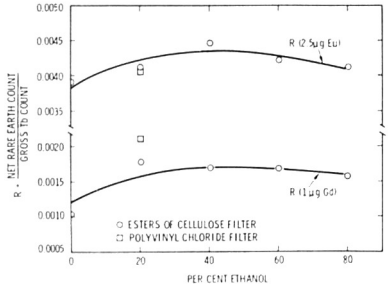


Figure 2. Effects of ethanol on LnF_3 formation

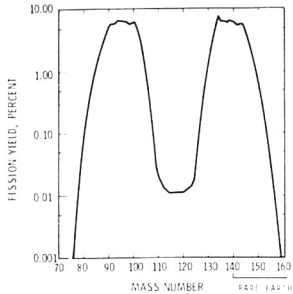


Figure 3. Cumulative yields from ^{235}U thermal fission

Table III. Rare Earth Complexing by Acetate[a]

NaOAC added, mmoles	*M* OAC, final	*M* HOAC, final	mmoles NaOH	Sm cts.	Tb cts.
70	1.31	0.69	0	4,920	8,030
48	0.66	0.69	0	8,460	58,180
36	0.33	0.69	0	14,600	147,230
25	0.03	0.60	0	5,000	4,860
20	0.46	0.12	20	13,980	163,140

[a] Each test contained 24 mmoles HNO_3, 100 μg Tb, 10 μg Sm, and was diluted to 35 ml.

Table IV. Resolution–Intensity Comparisons Using LiF Crystals

Crystal	LiF 200		LiF 220
Order	1	2	1
Deg. 2θ, Dy Lα$_1$	56.59	142.90	84.17
Relative intensity	100%	24.6%	<60%
Separation of FeKα, DyLα$_1$:	0.93°	5.50°	1.55°
Angular dispersion of Fe Kα, Dy Lα$_1$: dθ/dλ	33.2	196.4	55.4
Line widths (full width at half maximum)	0.59°	0.77°	...

earth impurities, leaving the rare earths in a small volume of aqueous phase. Two contacts of about five organic to one aqueous are sufficient to remove essentially all the plutonium.

Concentration of Rare Earths. A method of concentrating and collecting the rare earths in a way analogous to the "coprex" method of Luke (*25*) was developed. Terbium was chosen to function as chemical and spectrometric internal standard, and as a carrier for coprecipitation. In samples, trace Am and unextracted Pu also provide carrier action.

Luke (*26*) precipitated fluoride as LaF_3 in 80% ethanol medium to reduce the solubility. The effect of ethanol was investigated with tests containing 1 μg Gd and 2.5 μg Eu (Figure 2) with the conclusion that 20–60% ethanol is optimum. Since ethanol not only reduces the filtration rate, but also is deleterious to the esters of cellulose filter membrane (0.45-μm pore size) being used, 20% ethanol was chosen for use. Polyvinyl chloride filter membranes (0.6-μm Millipore BDWP-2500 filters) are resistant to ethanol and were subsequently used.

Luke used a pH 4 acetate buffer for precipitating LaF_3. With the concentrations used, rare earth fluorides do not precipitate in greater than 0.1*M* acids. The pH should be maintained above 3 to reduce fluoride attack on the glass frit of the vacuum filter system. At pH levels above 5, hydrolysis of most metals present occurs with a resulting loss in specificity and filterability. Spectral interferences from elements of the first transition series and matrix effects would occur. Sodium acetate (1.5*M*) is used to neutralize the high acid concentrations required for the extraction. An effective buffer system is thus produced.

As noted in the Procedure, the quantity of acid should be minimized to maintain a simpler neutralization step. The presence of molar concentrations of acetate species may result in complexing (and loss) of the rare earths. The results of investigating this effect are found in Table III. No attempt was made to elucidate the complexes formed. Samples with greater than 12 millimoles of acid are partially neutralized with sodium hydroxide (see Procedure).

Spectral Interferences. Rare earths produced by thermal fission of uranium-235 present a difficult analytical situation as, of the spectrum of elements present, the lighter rare earth elements occur near the peak of the fission product production curve, Figure 3. The bulk of the L X-ray spectrum of these high abundance elements extends on the short wavelength side of their analytical lines and among the analytical lines of Sm, Eu, Gd, and Dy (see Figure 1). Better spectral resolution will eliminate many of these interferences and their necessary correction curves, if the attendant intensity loss can be withstood. Plowman (*30*) used the lithium fluoride (LiF) 220 crystal to increase the dispersion. In the absence of such a crystal, the second-order lines of the LiF 200 crystal were investigated as a potential means of avoiding spectral interferences. The gain in angular dispersion was excellent and the sensitivity was adequate (Table IV).

An unexpected spectral interference was found following application of the procedure to plutonium. The plutonium Mα$_1$ X-ray line, at 133.5° 2θ, LiF 200 crystal, significantly overlaps the second-order gadolinium Lβ$_1$. When traces of plutonium are present, pulse height discrimination must be used to eliminate the interference. Energy resolution counter tubes lower than the 1.7 atmosphere xenon counter tubes do not have adequate energy resolution to do this effectively.

Table VA summarizes the relative amounts of fission product rare earths that might be present. An X-ray mount containing the spiked quantities of rare earths listed in Table VB was scanned and its spectrum is displayed in Figure 4. The problem of spectral interference with analytical lines and background measurements is readily apparent. The second-order analytical lines, Eu 2Lβ$_1$, Gd 2Lβ$_1$, and Dy 2Lα$_1$, are used when such a problem occurs. Otherwise, the first-order lines, with the exception of Dy, are used.

(30) C. Plowman, *Analyst (London)*, **96**, (1148), 776–8 (1971).

Table VA. Typical Fission Product Rare Earths (Relative Amounts)

La	47
Ce	90
Pr	43
Nd	156
Pm	1
Sm	30
Eu	2
Gd	1
Tb	0.03
Dy	0.004

Table VB. Synthetic Fission Product Rare Earth Spikes

≥1 μg Sm, Eu, Gd, Dy	Recovered, %	5 μg Sm, Eu, Gd, Dy	Recovered, %
50		50	
100		100	
50		50	
150		150	
0		0	
30	100 ± 1	5	91 ± 8
2	105 ± 11	5	102 ± 4
1	119 ± 13	5	109 ± 2
100		100	
1	75 ± 8	5	104 ± 1

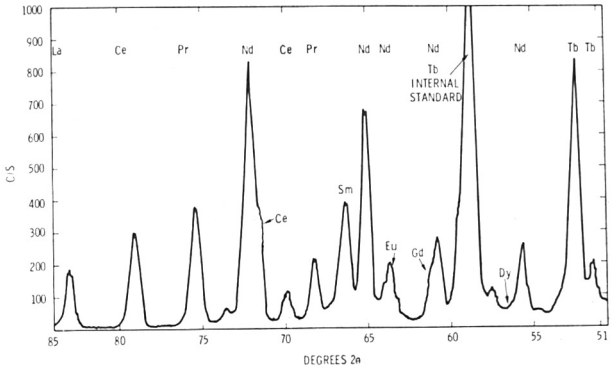


Figure 4. Synthetic sample of fission derived rare earths–Table VB. ≥ 1 μg Sm, Eu, Gd, Dy

The second-order lines of samarium are out of the spectrometer range, so the first-order $L\alpha_1$ line is always used. Cerium, Pr, and Nd interfere somewhat with samarium, and the Dy $L\alpha_2$ line interferes with the Eu $L\beta_1$. Interference correction factors were determined by the technique of MacNevin *et al.* (*29*) and used in these cases.

Analytical Results. Since rare earths derived from fission present the most difficult situation for analysis, synthetic fission product sample mounts were prepared in triplicate to determine recovery of the four elements of interest in such a situation (Table VB). One group of mounts was prepared containing a minimum of 1μg per rare earth (Sm to Dy) and a second group of mounts contained 5 μg per rare earth (Sm to Dy). The spiked quantities and recoveries are tabulated in Table VB. The major source of error is concluded to be incorrect background measurements because of interference by weak X-ray lines *e.g.*, the 1 μg Gd recovery was high due to contributions from Nd $L\gamma_8$ and Sm $L\beta_7$; the 1 μg Dy recovery was low due to a high background measurement caused by the tail from the Sm $L\beta_2$–Nd $L\gamma_1$ peak.

The precision capability of this method was demonstrated by spiking aliquots of solution containing 90 mg of plutonium with trace levels (1, 5, 10, and 20 μg) of the four rare earths of interest. This work was done in triplicate with the results based on standard mounts containing only one of the four rare earths each. The standard deviations for each microgram level for each element were pooled (*31*).

(31) K. A. Brownlee, The Statistical Theory and Methodology in Science and Engineering," John Wiley and Sons, New York, N.Y., 1960, p 231.

Table VI. Precision and Accuracy Data from Spiked Samples

Analytical line measured	Average recovery %	Pooled standard deviation, % 1-μg Level	All-μg levels
Sm $L\alpha_1$	94.9	± 5.7	± 5.0
Eu $L\alpha_1$	95.7	± 8.3	± 6.6
Eu $2L\beta_1$	95.3	± 3.8	± 4.3
Gd $L\alpha_1$	95.4	±10.4	± 7.3
Gd $2L\beta_1$	102.8	±16.0	±10.8
Dy $L\alpha_1$	117.1	±11.1	± 6.8
Dy $2L\alpha_1$	100.7	± 3.6	± 2.9
Sm_1, Eu_1, Gd_1, Dy_2[a]		± 8.6	± 6.6
Sm_1, Eu_2, Gd_1, Dy_2		± 7.5	± 5.9
Sm_1, Eu_2, Gd_2, Dy_2		±10.3	± 7.2

[a] Subscripts indicate diffraction order of X-ray line used.

The results presented in Table VI indicate that slightly better precision is obtainable using first-order lines with the exception of dysprosium. The high recovery of Dy by first-order counting is due to spectral interference by Eu $L\beta_1$. Residual plutonium contributing to the Gd $2L\beta_1$ is the reason for the high recovery and low precision of that measurement. The precision of this method is significantly better than that of Eby (*23*) (10–20%) and less than that of Walton's (*22*) method of standard additions (2.1% at the 10-μg level).

The use of an internal standard in this procedure is very beneficial. When added to the sample solution as the first

Table VII. Analytical Comparisons

	This work		Eby		Walton	
Instrument	G.E. XRD-5		G.E. XRD-6		G.E. XRD-6	
Source	Pt, 50 KV, 45 MA		W, 60 KV, 60 MA		W, 60 KV, 50 MA	
Counter tube	High pressure xenon		Gas flow proportional		Gas flow proportional	
Soller slit	0.010		...		0.020	
Analytical line	Sensitivity cps/μg	D.L., μg	Sensitivity, cps/μg	D.L.,[a] μg	Sensitivity cps/μg[c]	D.L.,[b] μg
La $L\alpha_1$	8	0.1	2.9	0.3		0.2
Ce $L\alpha_1$	8	0.1	3.9	0.3		0.2
Pr $L\alpha_1$	12	0.1	4.7	0.2		0.1
Nd $L\alpha_1$	13	0.09	5.4	0.3		0.3
Sm $L\alpha_1$	16	0.07	7.9	0.2		0.1
Eu $L\alpha_1$	19	0.06	7.5	0.3		0.09
Gd $L\alpha_1$	22	0.09	8.5	0.2		0.1
Tb $L\alpha_1$	25	0.08	10.4	0.2		0.4
Dy $L\alpha_1$	29	0.07	10.4	0.2		0.2
Er $L\alpha_1$	...	...	10.7	0.3	26	0.09
2nd-order						
Eu $L\beta_1$	4.1	0.2				
Gd $L\beta_1$	3.9	0.2				
Dy $L\alpha_1$	7.5	0.1				

[a] Calculated from data presented by Eby. [b] Corrected data–detection limits presented by Walton are in error by a factor of 100 due to calculation error (counting time was included in calculation twice). Calculation: D.L. = 3σ (slope of standard curve as μg/cps)/counting time. [c] Corrected data–standard curve presented by Walton is in error by factor of 10 because of omission of first scalar (obscured on XRD-6).

step, it corrects for chemical yield, mechanical losses, and instrument deviations. Since a ratio of rare earth to terbium standard is taken, the calibration is fixed indefinitely. Recovery of terbium (and hence, all rare earths) through the procedure typically ranges from 60–90%. This loss of rare earths is apparently a combination of loss by extraction and mechanical losses during phase separation and solution transfer.

Sensitivity and detection limits obtained by this method, based on 75% recovery, are satisfactory. They are listed in Table VII along with data from the works of Eby (*23*) and Walton (*22*). Analytical conditions, where different, are also given. Detection limits (D.L.) presented for comparison (including those of Eby), are calculated by: D. L. = 3.3σ (CA/NA), where $\sigma = \sqrt{\text{background}}$, CA = unit of element A, NA = counts of element A, and the confidence interval is 99% (*32*).

CONCLUSIONS

The data presented in Table VII indicate at once that the ion exchange paper disk technique is inferior in sensitivity to the method presented here. Walton and Eby used higher source voltage and currents, and Walton used a coarser collimating slit (increases sensitivity by almost two with an attendant resolution loss). Conversely, the high pressure xenon counter tube has higher efficiency for the heavier rare earths, and the coprex method presents the sample in a geometry free of matrix effects. The tungsten source is optimum for erbium, while the platinum source is optimum for lutetium (less optimum for the lighter elements).

The second-order lines, while substantially less sensitive, offer some advantages over first-order X-ray lines. They are relatively free of spectral interference (and potentially large corrections), which also permits more accurate background measurement. The background is lower and less affected by degraded radiation. The disadvantages are the potential interference of Pu $M\alpha_1$ radiation with the second order Gd $L\beta_1$ and decreased sensitivity.

The use of the carrier, terbium, as an internal standard is a significant improvement to the coprex technique.

(32) R. O. Muller, "Spectrochemical Analysis by X-Ray Fluorescence," Plenum Press, New York, N.Y., 1972.

ACKNOWLEDGMENT

My thanks go to W. I. Winters for making available his prior work on determining rare earths.

RECEIVED for review September 24, 1973. Accepted June 17, 1974. Presented at the 15th Rocky Mountain Spectroscopy Conference, Denver, Colo., August 1973. This work was performed for the U.S. Atomic Energy Commission under Contract AT(45-1)2130.

Simultaneous Determination of Alpha-Emitting Nuclides of Radium through Californium in Soil

Claude W. Sill, Kenneth W. Puphal, and Forest D. Hindman

Health Services Laboratory, U.S. Atomic Energy Commission, Idaho Falls, Idaho 83401

A procedure is described by which virtually all alpha-emitting nuclides can be determined in soil, either singly or in any combination on a single sample. The sample is decomposed completely by a combination of potassium fluoride and pyrosulfate fusions with simultaneous volatilization of hydrogen fluoride and silicon tetrafluoride. The cake is dissolved in dilute hydrochloric acid and all alpha emitters are precipitated with barium sulfate. An option is provided by which uranium can be obtained in a separate fraction to eliminate mutual interference with ^{237}Np. The barium sulfate is dissolved in acidic aluminum nitrate and the elements from thorium through plutonium are extracted into Aliquat-336. Acid-deficient aluminum nitrate is then added to the aqueous phase to reduce the acidity, and americium, curium, and californium are extracted into fresh Aliquat-336. Thorium is removed by scrubbing the first organic extract with 10*M* hydrochloric acid, and protactinium, uranium, neptunium, and plutonium are stripped with a mixture of perchloric and oxalic acids. Americium, curium, and californium are stripped from the second organic extract with 8*M* nitric acid. Each fraction is electrodeposited and analyzed by alpha spectrometry with few interferences. Overall recovery excluding electrodeposition ranges from 88% for protactinium to 99% for plutonium.

The accurate and reliable determination of plutonium in soil is important because of the public attention being focused on current radioactive waste burial practices and the public health impact of any releases of plutonium to the environment. Because of the high sensitivity required, relatively large samples of 10 to 100 grams must be used which introduces problems in obtaining complete sample decomposition. Plutonium oxide becomes extremely refractory and difficult to dissolve when it is heated strongly (*1, 2*) such as occurs during a fire, a reactor incident, or ignition in the laboratory to burn off organic material prior to analysis. Many laboratories analyzing soils for this toxic element ignore these facts and attempt to leach the compound selectively from the insoluble matrix with hydrochloric and/or nitric acids (*3-8*). The results are frequently low and erratic. Occasionally, reproducible results are obtained, but the results can still be shown to be low in many cases by analyzing the insoluble residue remaining after leaching.

Hydrofluoric acid is best known for its ability to dissolve silica but even small quantities exert a marked catalytic effect on the nitric acid dissolution of many refractory oxides including ignited plutonium oxide, due to the high stability of the fluoride complexes. Consequently, use of hydrofluoric acid in leaching procedures generally gives more accurate results. However, erratic results are frequently obtained on larger samples due either to incomplete dissolution of plutonium oxide and/or the siliceous matrix, or to incomplete elimination of fluoride with consequent deleterious effects on the subsequent separations.

The accuracy of any analytical procedure is generally difficult to determine when starting from actual samples whose composition and previous history are unknown rather than from pure solutions using water-soluble tracers. An accurate and reliable analytical procedure should give complete decomposition of the siliceous matrix with complete elimination of insoluble material, but must also guarantee complete conversion of the plutonium to a soluble monomeric ionic form before any chemical separations are attempted. Existing total decomposition procedures employ either sodium carbonate or hydroxide fusions, neither of which can guarantee complete dissolution of refractory components. Subsequent steps generally involve so many precipitations, leachings, repeated ion exchange separations, etc. that the accuracy and reliability of the procedure remains in doubt. Yields are frequently only 50% and sometimes as low as 2% (*8*). While many of these chemical inadequacies can be corrected for by using ^{236}Pu tracer, such technique is of no assistance in correcting for the plutonium remaining undissolved or polymerized because heterogeneous exchange does not occur to any significant extent (*9*). Also, when the time required for complete sample decomposition is prolonged, losses of tracer added in water-soluble form might exceed losses of insoluble sample and high results can be obtained.

The main objective of the present work was to develop an accurate and reliable method for plutonium in soils in which complete dissolution of both the siliceous matrix and the most insoluble forms of plutonium oxide can be guaranteed routinely in a short period of time. It was also desired that the procedure be specifically applicable to the insoluble residues remaining from leaching procedures and to all other analytical fractions, such as ion exchange resins, organic extracts, etc., so that complete material balances on any analytical procedure can be obtained. Analysis of residues is a much more sensitive, direct, and unequivocal way of determining the adequacy of selective leaching than direct comparison of absolute numerical values obtained by different procedures or by different laboratories. Obviously, if complete exchange with the tracer does not occur and plutonium is present in the residue, the quantity found in the acid leach cannot accurately reflect the true concentration in the sample regardless of the precision with which the value can be reproduced. Furthermore, the fact that plutonium can be leached completely from the insoluble matrix is in itself no guarantee that it has been converted to a chemically reactive form.

(1) O. J. Wick, Ed., "Plutonium Handbook," Gordon and Breach, New York, N.Y., 1967.
(2) J. M. Cleveland, *J. Inorg. Nucl. Chem.*, **26,** 1470 (1964).
(3) N. Chu, *Anal. Chem.*, **43,** 449 (1971).
(4) J. H. Harley, *U.S. At. Energy Comm. Doc.*, **HASL 300,** 1972.
(5) G. H. Coleman, "The Radiochemistry of Plutonium," National Academy of Sciences, Nuclear Science Series, **NAS-NS 3058,** 1965.
(6) R. F. Benck, R. J. Smith, J. Bogdan, H. Lada, and H. Mortko, **NDL-SP-7,** U.S. Army Nuclear Defense Laboratory, Edgewood Arsenal, Md., 1964.
(7) M. C. Bortoli, *Anal. Chem.*, **39,** 375 (1967).
(8) Y. Inoue and M. Sakanoue, *J. Radiat. Res.*, **11,** 98 (1970).
(9) C. W. Sill, "Some Problems in Measuring Plutonium in the Environment," presented at "Life Sciences Symposium," Los Alamos Scientific Laboratory, Los Alamos, New Mexico, 1974, *Health Phys.*, in press.

Fusion with anhydrous potassium fluoride in a platinum dish is undoubtedly the simplest, most effective, and reliable method available for the complete dissolution of a wide variety of siliceous materials. The potassium fluoride cake can then be transposed in the same container to a pyrosulfate fusion with rapid and complete volatilization of both hydrogen fluoride and silicon tetrafluoride (*10*). Except for a small quantity of barium sulfate, the pyrosulfate cake will dissolve completely in dilute hydrochloric acid. The resulting pyrosulfate fusion is one of the simplest and most effective methods available for rapid, complete, and dependable dissolution of nonsiliceous materials, particularly high-fired oxides. This fusion has the distinct advantage that the flux can be obtained by simply adding easily purified alkali metal sulfates to sulfuric acid, and the fusion can be carried out in either borosilicate flasks or platinum vessels with very little contamination from either reagents or containers.

There are several other alpha emitters besides plutonium whose identification and determination in the environment is becoming increasingly important, such as the isotopes of uranium, thorium, and the other transuranium elements, particularly ^{241}Am. Because determinations of these other radionuclides have problems almost identical to those encountered with plutonium, it would be particularly helpful and economically desirable to be able to determine most or all of these nuclides simultaneously on a single sample. Consequently, a deliberate effort was made in the present investigation to choose separations that would permit recovery of all alpha emitters from radium through californium. Previous work (*11, 12*) has already demonstrated that virtually all alpha emitters can be carried on barium sulfate with extremely high efficiency from acid solutions containing high concentrations of potassium sulfate. This separation is particularly appropriate for application to the high potassium sulfate solutions resulting from the total sample decomposition employed. In subsequent separations used in the present work, protactinium and neptunium are carried quantitatively in the plutonium fraction. An option is provided by which uranium can be included either in the plutonium fraction or in one by itself. Thorium isotopes and the tervalent actinides are also obtained quantitatively in separate fractions. Because of the high resolution of alpha spectrometers and the large differences in energies of the various nuclides, little mutual interference is encountered because of the presence of several nuclides in the same fraction.

EXPERIMENTAL

Instrumentation. The instrumentation and scintillation technique used for gross alpha counting employing individual die-cut phosphor disks (*13*) has been described previously (*11*). A windowless 2-π proportional flow counter using methane as the counting gas was used in the standardization of the alpha-emitting tracers. Alpha energy spectra were obtained with a 450-mm^2 surface-barrier detector, a charge-sensitive preamplifier, linear amplifier, biased amplifier, pulse stretcher, and either 400-channel or 1024-channel pulse-height analyzers calibrated at 12.5 and 10.0 keV per channel, respectively. The sample holder was machined from aluminum to ensure absolute reproducibility between sample and detector to permit precise quantitative measurements to be obtained from the spectra. The resolution obtained with a ^{210}Po point source electrodeposited on polished platinum was 22 keV full-width-at-half-maximumpeak height (FWHM) at a source-to-detector distance of 1.5 detector diameters. Resolution of acutal samples electrodeposited on stainless steel over a $\frac{3}{4}$-inch diameter is generally about 30 to 40 keV at a distance of $\frac{1}{4}$ inch where the counting efficiency is 28%.

Reagents. *Reprecipitating Solution.* Dissolve 125 grams of anhydrous potassium sulfate in 915 ml of water and 50 ml of concentrated hydrochloric acid with warming to give 1000 ml of solution.

Aliquat-336 (NO_3), 30%. Dissolve 900 ml of Aliquat-336 (Cl) (General Mills, Inc., Kankakee, Ill.) in 2100 ml of xylene in a 5-liter separatory funnel. Shake vigorously for 4 minutes with each of two successive 500-ml portions of 4*M* nitric acid to convert the amine to the nitrate form. Wash the organic solution three successive times with 1 liter of water, again shaking for 4 minutes each time. Draw the organic phase into a suitable bottle for storage.

Aluminum Nitrate, 2.2M. Weigh 825 grams of dry $Al(NO_3)_3 \cdot 9H_2O$ into a 2-liter beaker, add 450 ml of water and warm until the salt dissolves. Add 85 ml of concentrated nitric acid and cool to give 1 liter of solution. Filter the solution through a DM-450 membrane filter (Gelman Instrument Co., Ann Arbor, Mich.) in a filtering chimney to remove insoluble materials, particularly iron. The density of the solution used in the present work was 1.370 grams/ml at 25 °C. If the aluminum nitrate is wet, add enough additional solid to produce this density. The number of grams of additional aluminum nitrate nonahydrate required per liter of solution can be calculated for small differences by multiplying the differences between the measured density and 1.370 by 4400. Do not boil the solution or loss of nitric acid will eventually result in hydrolysis of plutonium and other quadrivalent ions and a decrease in both extraction efficiency and ability to dissolve barium sulfate.

Aluminum Nitrate, 0.75M. Dissolve 280 grams of $Al(NO_3)_3 \cdot 9H_2O$ in 720 ml of water with slight warming as necessary. Add 128 ml of concentrated nitric acid and cool to room temperature to give 1 liter of solution. Filter through a DM-450 membrane filter in a filtering chimney. The density at 25 °C is 1.170 grams/ml. If the density is lower, the number of additional grams of aluminum nitrate nonahydrate to be added per liter of solution is approximately 2700 times the difference in densities.

Aluminum Nitrate, Acid Deficient, 2.5M. Heat 938 grams of solid $Al(NO_3)_3 \cdot 9\ H_2O$ in a graduated 1-liter beaker on an uncovered hot plate until the salt melts and the resultant solution boils. Leaving the beaker uncovered, boil the solution vigorously until the initial volume of 600 ml has been reduced to about 380 ml to volatilize as much nitric acid as possible. Remove the beaker from the hot plate and rinse the walls with several 10-ml portions of water, stirring each into the solution gently to moderate the vigorous evolution of water vapor that occurs. As soon as the vigor of the reaction will permit, add an additional 200 ml of water and boil the solution for a few minutes to redissolve the small quantity of aluminum salts that will have dried on the bottom and sides of the beaker. When the solution is clear, dilute to about 950 ml, cool to room temperature and dilute to 1 liter. Filter the solution through a DM-450 membrane filter. The density of the solution at 25 °C is 1.288 grams/ml and the pH as measured with a glass electrode is 1.6. If the density is lower, weigh a quantity of aluminum nitrate nonahydrate in grams equal to 4300 times the difference in the densities for each liter of solution. Place the salt in a small beaker, evaporate until salts begin to bake out on the bottom, and dissolve in the main solution.

Tracers. Preparation of tracers of elements from thorium through californium of suitable purity for simultaneous use in the present high-sensitivity procedure is described elsewhere (*14*). When prepared as described, all tracers except protactinium can be evaporated directly on stainless steel plates to simplify standardization by eliminating the need for electrodeposition which is time-consuming and less accurate and reliable for quantitative work.

Standardizations. All tracers and counters should be standardized with greater accuracy than is desired in the most accurate work to be accomplished. Otherwise, the uncertainty in the standardization will add substantially to the uncertainty of the determination and will also have to be propagated to each individual analysis.

Standardize the 2-π alpha counter by counting a National Bureau of Standards source containing about 1×10^5 dpm of ^{241}Am electrodeposited on platinum, having a total uncertainty in the certified value of about 1%, for 10 minutes to keep the statistical uncertainty in the counting efficiency less than a few tenths of a percent. The overall accuracy of any subsequent measurement dependent on the 2-π counter will then be limited by the 1% absolute uncertainty of the standard.

Because a point-source standard electrodeposited on platinum cannot be used to calibrate an alpha spectrometer with an external

(10) C. W. Sill, *Anal. Chem.*, **33**, 1684 (1961).
(11) C. W. Sill, *Health Phys.*, **17**, 89 (1969).
(12) C. W. Sill and R. L. Williams, *Anal. Chem.*, **41**, 1624 (1969).
(13) N. A. Hallden and J. H. Harley, *Anal. Chem.*, **32**, 1861 (1960).
(14) C. W. Sill, *Anal. Chem.*, **46**, 1426 (1974).

detector for use with diffuse sources electrodeposited on stainless steel, a secondary standard must be employed. Prepare a source containing about 1×10^5 dpm of ^{241}Am electrodeposited on stainless steel under the exact conditions to be used subsequently for preparation of samples. Standardize the plate by counting in the 2-π counter for 10 minutes. Correct the counting efficiency of the counter for the difference in backscatter between platinum and stainless steel (*15*). Use the diffuse source to calibrate the alpha spectrometer and to recheck the initial calibration of both the spectrometer and the 2-π counter periodically.

For standardization of alpha tracer solutions other than ^{231}Pa, place an appropriate aliquot of the freshly-purified tracer (*14*) on a mirror-finished stainless steel plate using a pipet that has been treated with a silicone water-repellent to eliminate drainage and calibrated "to contain" by blowing residual liquid from the tip. Evaporate the solution carefully to dryness under an infrared lamp, adding 2 or 3 drops of concentrated nitric acid near the end of the evaporation to help in spreading the deposit as uniformly as possible. However, limit the sample to an area not larger than $\frac{3}{4}$ to 1 inch in diameter to minimize the decrease in counting rate that occurs with some 2-π counters when large sources are used. Heat the plate over a blast burner using a strong reducing flame just to the first red glow, and cool immediately by placing the plate on a cold metal surface. Place the cooled plate into the 2-π counter without delay to prevent possible absorption of moisture, and count for sufficient time to give the statistical precision desired. Calculate the total disintegration rate of the tracer solution using the counting efficiency obtained for stainless steel. Also, count the plate in an alpha spectrometer, for approximately the same number of counts, to determine the fraction of the total activity coming from the tracer nuclide of interest, and the fraction coming from other isotopes so that the necessary corrections can be made for the other activities added with the tracer—*e.g.*, the ^{241}Am in the ^{243}Am tracer. Propagate all statistical uncertainties, particularly those from counting the tracer, the standard, and the alpha energy spectrum, to the final tracer solution.

For ^{232}U, ^{236}Pu, and ^{243}Am, which are to be used internally as alpha-emitting isotopic tracers for determining the chemical yield, use 500 μl of a solution containing about 10^3 dpm/ml and a 10^4-minute counting time in the standardization to keep the statistical uncertainty in the quantity of tracer added less than about 0.5% at the 95% confidence level. Prepare working solutions of lower concentrations by exact volumetric or weight dilutions in 10% nitric acid of the standardized stock solutions. The concentration of the working solution is thus known more accurately than if the weaker solution had been standardized directly. Similarly, when restandardization becomes necessary, it will generally be preferable to repurify the stock solution from ingrown daughter activities so that 2-π counting can be used with the solution of high activity than to use alpha spectrometry on the lower concentrations in the presence of daughters.

There are a few cases in which direct evaporation of even specially purified tracers will not permit adequate resolution of the isotopes present. For example, the small quantity of ^{238}Pu generally present in the ^{236}Pu tracer should be determined by alpha spectrometry on an electrodeposited aliquot to determine the correction factor with adequate precision for practical use. Protactinium isotopes are prepared in a strong sodium sulfate–sulfuric acid solution to prevent hydrolysis and must also be electrodeposited to remove the absorbing and corrosive substances. If there is any question as to the energy dependence of the detector, or of the isotopic purity or branching ratios of any of the alpha emitters, the results from direct evaporation should also be verified on electrodeposited sources using the particular alpha-emitter involved.

In the determination of the principal alpha-emitting radionuclides of thorium, protactinium, neptunium, curium, and californium, for which no suitable isotopic, alpha-emitting tracer exists, the activity present on the electrodeposited plate must be determined directly from the known counting efficiency of the spectrometer. Because of the unevenness of electrodeposited sources, this method is less accurate than comparison to an alpha-emitting tracer. The chemical yield must then be determined by a separate measurement of a gamma-emitting tracer, if possible. Except for ^{233}Pa, the tracer can be evaporated directly and its activity compared with that from the electrodeposited sample under identical counting conditions so that the geometry of the irregular source from direct evaporation is not significantly different than that obtained by electrodeposition. The plate must be thoroughly cleaned by boiling for a few minutes in concentrated nitric acid so that the solution will spread uniformly. The volume of tracer used should not be larger than 250 microliters to keep the activity from spreading over an area larger than that obtained from electrodeposition. Best results have been obtained by counting both the sample plate and the tracer standard in a holder over the open top of a 3- by 3-inch thallium-activated sodium iodide well crystal. If the plates are counted in direct contact with a solid crystal, erratic results are obtained, apparently due to differences in thickness of the can and internal reflector.

Electrodeposition is much less accurate or reliable for quantitative standardization of solutions than direct evaporation because of the large and erratic losses that occur. With alpha emitters, the electrolyte and washings must be evaporated and treated to restore the original conditions and the electrodeposition repeated to recover as much as possible of the activity lost initially. If the quantity recovered exceeds a few percent, the recovery process must be repeated until no more activity is recovered. The sum of the activities on all the successive electrodeposited plates invariably agrees within the statistics of counting with that obtained by direct evaporation. The initial plate containing the major portion of the activity is then standardized in the 2-π counter, corrected for loss on electrodeposition to obtain the activity of the solution, or used to standardize the alpha spectrometer. Loss of gamma-emitting tracers on electrodeposition can be determined simply by comparing the activity of the aqueous electrolyte and washings with a standard prepared and counted in a well counter under identical conditions.

Sample Preparation. For soils that are relatively free of roots and other organic debris, dry the soil in an oven for 2 or 3 hours at 120 °C and cool. Grind the sample lightly in a mortar and pestle, using just enough pressure to break up the clods of soil but not enough to grind the small pieces of rock and sand that are inevitably present. Discard all rocks larger than about $\frac{1}{4}$ inch in diameter. If significant quantities of vegetation or root mat are present, heat the sample in a disposable aluminum-foil pan in a muffle furnace at 400 °C for 2 or 3 hours until all organic material is well charred before grinding. Pass the soil through a No. 35 U.S. standard sieve (500-micron opening) to remove the larger remaining rocks. Weigh and record the weight of both fractions to permit evaluation of the bias introduced by screening. Blend the −35 mesh fraction thoroughly by any acceptable method and take an aliquot for analysis. In general, the plutonium present on the surface of the large material removed will be a small and negligible fraction of the total present. However, the larger material can be ground and analyzed if a more accurate estimate of the total quantity of plutonium present is desired.

Procedure. *Sample Decomposition.* Weigh 10.0 grams of the −35 mesh soil into a dry 250-ml semiflat-bottomed platinum dish. Add concentrated nitric acid a few drops at a time at one edge of the powder as fast as frothing and the vigor of the reaction will permit until the entire sample is covered and a free-flowing suspension is obtained. Do not swirl or allow the solution to froth higher than about $\frac{3}{4}$ inch from the top of the dish. Heat the solution gently on a hot plate covered with a clean piece of asbestos cloth until any initial vigorous reaction and/or frothing has subsided. If significant reaction persists, evaporate the solution to dryness. Add enough more concentrated nitric acid to give a thin slurry and ^{236}Pu and/or other tracers as desired. Add 48% hydrofluoric acid carefully a few drops at a time with intermittent heating until the vigorous reaction has subsided. Add an additional 10 ml of hydrofluoric acid and evaporate the solution until all liquid disappears but leave the cake just moist with acid. If allowed to bake, the residue sticks tightly to the bottom of the dish, retarding subsequent dissolution and increasing corrosion of the dish in the presence of phosphates. If the sample is particularly high in iron, rapid and complete dissolution in the subsequent fluoride fusion is facilitated if somewhat more hydrofluoric acid is allowed to remain.

Add 30 grams of anhydrous potassium fluoride to the dish and mix the sample and flux with a stirring rod for a few seconds to give a coarse mixture. Place the platinum dish on a nichrome triangle on a ring stand. Using a Fisher high-temperature blast burner with a 4-cm grid, apply as much heat as possible to the dish until the contents have dissolved completely. About 4 minutes will be required to heat the contents to the fusion temperature of about 900 °C and another 2 minutes to complete the dissolution. As necessary, swirl the melt gently to dissolve the sample present on the sides of the dish. Moderate quantities of organic matter will oxidize smoothly without special attention. Oxidation of larger

(15) J. M. R. Hutchinson, C. R. Naas, D. H. Walker and W. B. Mann, *Int. J. Appl. Radiat. Isotopes*, **19**, 517 (1968).

quantities will be facilitated by addition of 1 gram of solid potassium nitrate although high-iron samples will also then precipitate earlier in the melt. When the sample has dissolved completely, heat the sides of the dish so that any chunks of solidified flux from previous swirling of the dish melt and run down into the bottom of the dish. Cool the dish to room temperature. As the melt begins to solidify, swirl the dish gently to deposit the cake evenly on the bottom and sides up to about ¾ inch from the top to keep the cake uniformly thin to facilitate its transposition and to lessen deformation of the dish.

Add 35 ml of concentrated sulfuric acid, partly around the sides of the dish to transpose the thin layer of potassium fluoride remaining near the top. Place the dish on the covered hot plate and heat gently until the solution begins to froth because of evolution of hydrogen fluoride and silicon tetrafluoride. Set the dish off the hot plate onto a piece of asbestos or other heat-insulatng material until the frothing subsides and more heating is required to restore the reaction. Be prepared to set the dish in a bath of cold water to quench the reaction rapidly to prevent loss of sample if the frothing threatens to go over the top of the dish. Continue heating and cooling the dish alternately as required until the vigorous evolution of gases has subsided. When danger of frothing over is past, heat the dish first on the covered hot plate, then on an uncovered hot plate, until almost all of the potassium fluoride cake has been transposed and most of the water and any excess sulfuric acid has been driven off. Use a 2-inch stainless steel counting disk underneath the platinum dish to protect the dish from direct contact with the iron plate. The solution will become very thick because of precipitation of insoluble metallic sulfates and a thick layer of solid salts will build up on the sides of the dish. When most of the original potassium fluoride cake has dissolved off the bottom and sides, heat the dish over the blast burner until the solid cake on the sides melts and the last few small chunks of fluoride cake dissolve. If the transposition is carried out too rapidly and there are quite large chunks of original potassium fluoride cake still present when the temperature is raised over the blast burner to make the pyrosulfate fusion, hydrofluoric acid will be driven out of the solution faster than the chunks of cake will dissolve and the fluoride remaining will be insufficient to volatilize the last of the silica completely. Consequently, the cake will not transpose completely to give a clear pyrosulfate fusion.

Add 20 grams of anhydrous sodium sulfate, place the dish on the ring stand, and heat with a small flame from the Fisher burner until the thick, almost-solid suspension dissolves to a thin one that is easily boiled. As fast as boiling will permit, increase the temperature until the entire sample has dissolved and a clear pyrosulfate fusion is obtained. Occasionally, if the transposition is taken a little too fast, a slight scum of silica might be present on the surface of the melt but will do no harm. Do not heat the pyrosulfate fusion any hotter or longer than necessary to give a clear melt to minimize dissolution of platinum from the dish. Remove the dish from the flame and swirl the dish gently when the melt starts to solidify so that the cake is deposited in a thin layer around the sides of the dish. Cool the dish and contents to room temperature.

Flex the sides of the dish gently to break the cake loose and empty the contents into an 800-ml beaker. Add 350 ml of water and 25 ml of concentrated hydrochloric acid, rinsing the platinum dish if necessary. Heat the solution as rapidly as possible on an uncovered hot plate with almost continuous stirring to prevent possibly severe bumping and to stir the calcium sulfate into the solution as fast as the cake disintegrates so that the calcium sulfate dissolves as fast as possible. Calcium sulfate becomes distinctly less soluble in dilute acid the longer it is allowed to stand in the crystalline state. If the calcium sulfate dissolves completely, or only a slight turbidity remains, add an additional 50 ml of water, 5 ml of 25% potassium metabisulfite and a couple of 8-mesh silicon carbide boiling chips (not chips made of alumina). Cover the beaker with a watch glass and boil the solution for 15 minutes to hydrolyze condensed phosphates and to ensure complete reduction of plutonium to the quadrivalent state. Proceed with precipitation of barium sulfate as described below.

If the calcium sulfate does not dissolve virtually completely on addition of 25 ml of concentrated hydrochloric acid, and if only the elements from thorium through plutonium are being determined, add as little more acid as possible to a maximum of 50 ml of additional acid until the turbidity decreases to an essentially transparent condition on further boiling for a few minutes. Make up the difference between the additional acid added and 50 ml with water. In the unusual event that the calcium sulfate does not clear up sufficiently with a total of 75 ml of hydrochloric acid, a smaller sample should be used. To avoid having to repeat the sample decomposition, transfer the solution to a 1-liter beaker with 375 ml of water, heat to dissolve the remaining calcium sulfate, adding up to an additional 75 ml of acid and/or water as necessary, and pour into a 1-liter graduated cylinder. Mix and transfer half of the solution back to the 800-ml beaker. Add 35 grams of solid potassium hydrogen sulfate and boil the solution until the solid dissolves before proceeding with the precipitation of barium sulfate.

If the tervalent actinides are to be determined and the calcium sulfate does not dissolve on boiling with the original 25 ml of hydrochloric acid and 350 ml of water, a smaller sample should be used to prevent serious losses on barium sulfate, particularly with curium and californium. Add 500 ml of water and a maximum of 25 ml more of hydrochloric acid only if necessary to dissolve the calcium sulfate. Treat half the solution with 35 grams of extra potassium hydrogen sulfate as described. Use no more hydrochloric acid than is required to dissolve the calcium sulfate, with a maximum of 25-ml total for the tervalent actinides and 75-ml total for the quadrivalent actinides in the volume of about 450 ml.

Barium Sulfate Precipitation. Remove the cover glass momentarily and add 5 ml of a 0.45% solution of barium chloride dihydrate to the boiling solution from a 5-ml Mohr pipet in about 0.5-ml increments every 3 seconds while stirring the solution vigorously and continuously with a stirring rod. Replace the cover glass, heat the solution back to boiling, and boil for 1 minute. Repeat the addition of 5-ml portions of the barium chloride solution followed by a 1-minute boiling period five more times for a total of 30 ml of the barium solution. If determination of curium and californium are of prime importance, increase the number of 5-ml additions of the barium chloride solution by three more to a total of nine. Filter the hot solution through a 47-mm GA-6 membrane filter (0.45-micron pore size, Gelman Instrument Co., Ann Arbor, Mich.) in a filtering chimney. (The Teflon chimney described previously (*12*) is recommended. However, the porous stainless steel support plate recommended should be replaced with a disk machined from a sheet of ⅛-inch coarse porosity polypropylene (Bel-Art Products, Pequannock, N.J.) to eliminate objectionable reactions with acid solutions.) Rinse the beaker and the precipitate with 0.5% sulfuric acid delivered in a forceful jet from a polyethylene squeeze bottle. Do not transfer the boiling chips. Reserve the filtrate for the separate determination of uranium.

Reprecipitation of Barium Sulfate. Place the GA-6 filter containing the barium sulfate into a 250-ml Erlenmeyer flask and add 4 ml of concentrated sulfuric acid, 0.5 gram of anhydrous potassium sulfate, and 3 drops of concentrated nitric acid. Heat the solution gently on a covered hot plate until the sulfuric acid fumes, then more strongly over a blast burner until the barium sulfate has dissolved completely. However, do not permit evaporation of any significant quantity of sulfuric acid or part of the barium sulfate will precipitate in a high-temperature modification that is not readily soluble in the subsequent aluminum nitrate fusion. The particles will become coated with the water-immiscible organic solvent and will transfer to the organic phase giving a pseudo-extraction effect. Add 1 drop of a 1:1 mixture of concentrated nitric and 72% perchloric acids to oxidize the last of the organic matter and the uranium and immediately set the flask off to cool. A yellow color generally forms because of oxidation of the cerium present. The quadrivalent cerium guarantees complete oxidation of the uranium so that it will not carry on barium sulfate but will also oxidize some neptunium and plutonium with the same consequence if not reduced.

Cool the solution to room temperature, add 60 ml of the reprecipitating solution and 1 ml of 25% potassium metabisulfite and set the flask on the hot plate. When the cake has disintegrated, add 1 ml of a filtered 20% solution of ferrous ammonium sulfate in 5% sulfuric acid and boil the solution for 2 minutes to complete reduction of the hexavalent neptunium and/or plutonium that will have been produced in the perchloric acid oxidation. When curium and californium are being determined, add 5 ml of 0.45% barium chloride in increments to increase their recovery. Filter the barium sulfate while still hot on another GA-6 membrane filter and wash with a few milliliters of 0.5% sulfuric acid.

When barium sulfate is to be reprecipitated to retain uranium, add about 100 mg of solid hydrazine sulfate to the hot sulfuric acid solution of the barium sulfate after addition of the 1 drop of nitric–perchloric acids used to oxidize organic material. Heat the sulfuric acid back to near-boiling to destroy the excess hydrazine and cool. Reprecipitate the barium sulfate by adding 60 ml of the reprecipitating solution to which 5 drops of 20% titanium trichloride (Fisher Scientific Co., Fair Lawn, N.J., SO-T-43) has been added imme-

diately before use. Omit addition of both potassium metabisulfite and ferrous ammonium sulfate. Finish as described.

General Dissolution of Barium Sulfate and Extraction. If the tervalent actinides are also to be determined, place the filter containing the barium sulfate in a 150-ml beaker and add 2 ml of a 1:1 mixture of concentrated nitric and 72% perchloric acids immediately after filtration so that the paper and precipitate do not dry. Heat the uncovered beaker gently on a hot plate covered with a piece of asbestos cloth so that spattering does not occur. When strong fumes of perchloric acid are produced, but before the solution begins to dry on the bottom of the beaker, even in local spots, remove the beaker from the hot plate, cool slightly, and add 3 ml of concentrated nitric acid, rinsing the walls. Weigh 50 grams of solid $Al(NO_3)_3{\cdot}9\ H_2O$ into a dry 100-ml beaker and add enough of the salt (about 10 grams) to the beaker containing the sample to give a thick slurry. Swirl the solution vigorously for about 1 minute to grind up the small packed lumps of barium sulfate with the aluminum nitrate crystals. Particularly after having been reprecipitated, barium sulfate tends to pack tightly on centrifuging or filtering with suction. If small lumps of undispersed barium sulfate are allowed to remain, dissolution is markedly retarded, causing an undesirable increase in dissolution time with its increased loss of nitric acid and hydrolysis of quadrivalent elements. An ultrasonic bath is extremely effective in reducing the size of the lumps so that rapid dissolution can be obtained but is generally unnecessary with the grinding technique employed.

Add the remainder of the 50 grams of solid aluminum nitrate nonahydrate. Cover the beaker with a watch glass and heat the solid on the covered hot plate until the salt melts and the solution just begins to boil. Swirl gently to suspend the barium sulfate in the molten flux. Immediately, set the beaker on a clay triangle at the edge of the covered hot plate and maintain the temperature near the boiling point for 5 minutes but allow virtually no movement of the surface of the solution. Otherwise, loss of nitric acid will result in severe hydrolytic precipitation of plutonium. Remove the cover glass and, while swirling the molten salt continuously, add 30 ml of 0.75*M* aluminum nitrate to which 1 ml of 25% sodium nitrite was added immediately before use. Cool the solution to room temperature, pour into a 250-ml separatory funnel and add 50 ml of 30% Aliquat-336 in xylene. Rinse the walls of the beaker with another 20 ml of 0.75*M* aluminum nitrate and cool the rinse thoroughly in a cold water bath. Add 5 ml of 25% sodium nitrite to the cold aluminum nitrate rinse, swirl the beaker gently just once to mix the sodium nitrite without losing any more nitrous acid than necessary, and pour the solution immediately into the separatory funnel. Swirl the separatory funnel just enough to distribute the blue color of the nitrous acid through the aqueous phase and allow to stand for 2 minutes. Shake vigorously for 3 minutes, preferably on a mechanical shaker, but not hard enough to cause formation of stable emulsions. Allow the solution to stand for 10 minutes and draw the aqueous phase into another 250-ml separatory funnel and reserve for determination of the tervalent actinides. Let the solution stand for another 2 minutes and remove the additional aqueous phase that separates because of drainage to obtain maximum elimination of the large quantity of barium and aluminum present.

Scrub the organic phase for 2 minutes with each of three successive 10-ml portions of 8*M* nitric acid to remove the last traces of barium, aluminum, tervalent actinides and lanthanides, particularly cerium. Allow to stand for 2 minutes each time for adequate phase separation. Combine the washes in the same 150-ml beaker in which the fusion was made, without rinsing out the residual aluminum nitrate, and reserve for recovery of the tervalent actinides present. Scrub the organic phase with three successive 50-ml portions of 10*M* hydrochloric acid for about 3 minutes each time to remove thorium. Allow at least 2 or 3 minutes after the phases have separated before drawing off the aqueous phase. Combine the hydrochloric acid washes in another 250-ml separatory funnel and reserve for the determination of thorium isotopes. If more thorium is present than in a normal soil (13 μg/gram), the number of hydrochloric acid scrubs will have to be increased to remove the thorium completely.

Strip the plutonium back into the aqueous phase by shaking the organic layer vigorously for 2 minutes, first with 50 ml of a solution containing 5 ml of 72% perchloric acid and 2 grams of oxalic acid and then with 25 ml of water. Allow the phases to separate for at least 2 minutes each and combine both strips in a 250-ml Erlenmeyer flask. Add 2 ml of a 5% solution of sodium hydrogen sulfate monohydrate in 1-to-1 sulfuric acid and evaporate the solution on a hot plate until most of the perchloric acid has been volatilized. The oxalic acid decarboxylates smoothly without personal attention. Heat the flask over a small flame from the blast burner, keeping the sides hot enough to prevent condensation of the acid, until excess sulfuric acid has been volatilized and a clear, glassy melt is obtained. Remove the flask from the flame before crystallization occurs and cool. Add 1 ml of 0.6*M* sulfuric acid and reevaporate just to fumes on the hot plate. Dissolve the cake and electrodeposit by any acceptable method for analysis by alpha spectrometry. After electrodeposition (*16, 17*), heat the stainless steel plate on an uncovered hot plate for 5 minutes to decrease spontaneous volatility of any ^{210}Po that might be present to prevent subsequent serious contamination of the solid-state detector used in obtaining the alpha spectra (*18*).

Alternate Dissolution and Extraction. If determination of the tervalent actinides is not desired, the above determination of the other elements can be simplified somewhat. Place the filter containing the barium sulfate in a 250-ml Erlenmeyer flask. Add 2 ml of concentrated nitric and 4 ml of 72% perchloric acids and heat the flask on a hot plate until the refluxing perchloric acid reaches the top of the flask. By this time, the paper will have been oxidized and pure barium sulfate will have been dissolved completely. However, barium sulfate precipitated from actual soils does not clear up completely, perhaps because of the presence of other elements, but will dissolve subsequently in the aluminum nitrate. A very fine turbidity visible only by the Tyndall beam of a flashlight might persist, but is apparently silica and does not interfere. Longer boiling with perchloric acid should be avoided because of increased oxidation of both cerium and plutonium in the sample, making complete reduction by sodium nitrite more difficult. If not reduced subsequently, quadrivalent cerium carries through the extraction and causes severe interference in the electrodeposition, and the recovery of plutonium is less complete. When the refluxing perchloric acid reaches the top of the flask, remove the flask from the hot plate for 1 minute and add 50 ml of the acidic 2.2*M* aluminum nitrate solution containing 1 ml of 25% sodium nitrite while swirling the flask continuously. Heat the solution just to the boiling point to redissolve any traces of barium sulfate that might have reprecipitated. Cool the solution to room temperature, pour into a 250-ml separatory funnel, and add 50 ml of 30% Aliquat-336. Rinse the walls of the flask with another 25 ml of the 2.2*M* aluminum nitrate solution, cool thoroughly, and add 5 ml of 25% sodium nitrite to the flask. Transfer the nitrous acid rinse to the separatory funnel and extract, scrub, and strip as described above. Extraction of tervalent actinides is markedly reduced by the larger quantity of perchloric acid present in the alternate method, and the other procedure should be used when their determination is desired.

Determination of Uranium. Cool the filtrate from the original precipitation of plutonium with barium sulfate to room temperature or below and let stand for a few hours, preferably overnight if convenient. Filter the cold solution through a GA-6 membrane filter to remove any alkaline earth sulfates that might have precipitated. Severe loss of uranium will occur if insoluble sulfates are removed after the uranium has been reduced to the quadrivalent state. Add 5 grams of potassium metabisulfite, 1 ml of a 1.25% solution of TeO_2 in 10% HCl, and 2 or 3 silicon carbide boiling chips. Cover the beaker with a watch glass and boil the solution for 5 to 10 minutes to volatilize sulfur dioxide. If particularly large quantities of iron are present, heat the solution just to boiling and remove from the hot plate for 5 minutes to permit more complete reduction of iron before boiling out the excess sulfur dioxide. Tellurium catalyzes the reduction of iron by sulfur dioxide, and the solution will darken and become turbid when most of the iron has been reduced.

When 50 ml or more of hydrochloric acid is used to prevent precipitation of $CaSO_4$, reduction of iron and tellurium are much faster than at the lower acidity, and reduction of tellurium is complete by the time all SO_2 will have been boiled out. Because polonium is not precipitated with SO_2, an additional 0.5 ml of the tellurium solution should be added before addition of $TiCl_3$ to ensure complete carrying of polonium.

When the odor of sulfur dioxide has largely disappeared, add 4 drops of 1% aqueous Safranin-O (National Aniline Division, Allied Chemical and Dye Corp., New York, N.Y., C.I. 841) and 10 drops of 20% titanium trichloride. The bright reddish purple color of the indicator should change to the colorless leuco form, and the tellurium should be reduced to the black elemental form carrying ^{210}Po

(16) K. W. Puphal and D. R. Olsen, *Anal. Chem.*, **44**, 284 (1972).
(17) K. W. Puphal and D. R. Olsen, *Anal. Chem.*, **44**, 1301 (1972).
(18) C. W. Sill and D. G. Olson, *Anal. Chem.*, **42**, 1596 (1970).
(19) R. L. Williams and C. W. Sill, *Anal. Chem.*, **46**, 791 (1974).

quantitatively. Add 15 drops of 3*M* chromous chloride (*19*) from a delivery tube extending under the watch glass to reproduce enough tervalent titanium to serve as a holding reductant for quadrivalent uranium during the subsequent precipitation of barium sulfate from boiling solution in contact with the air.

Boil the solution for 2 or 3 minutes to flocculate the elemental tellurium, cool to about 50 to 70 °C in a cold water bath, and filter through a 47-mm DM-450 membrane filter using an all-glass filtering chimney (Millipore Corp., Bedford, Mass.) rather than the one made of Teflon from which the metallic tellurium is difficult to remove. Rinse the beaker and filtering chimney with a few milliliters of 0.5% sulfuric acid. The filter and tellurium precipitate can be washed with 95% ethanol, dried under a 250-watt infrared heat lamp not closer than 22 inches nor for longer than about 5 min, and alpha counted with a zinc sulfide phosphor (*12*) to determine the ^{210}Po in the solution. However, the results will be somewhat low because of volatilization losses occurring during original sample decomposition.

Scrub the beaker in which the precipitation was made and the filtering chimney with a brush to dislodge small particles of tellurium containing polonium that adhere to the walls if allowed to dry, and rinse with water. Transfer the filtrate from the filtering flask back to the beaker, add 2 more drops of 1% Safranin-O indicator to be sure enough remains undecomposed to indicate complete reduction of uranium. Heat the solution to boiling, precipitate barium sulfate, and finish as described above for plutonium using the alternate procedure employing $HClO_4$ to dissolve the $BaSO_4$.

Determination of Tervalent Actinides. Evaporate the three 10-ml 8*M* nitric acid scrubs of the first Aliquat-336 extract in the 150-ml beaker to about 0.5 ml. Do not permit the solution to evaporate to dryness or the residue will not dissolve completely in subsequent steps. Dissolve the residue in 50 ml of 2.5*M* acid-deficient aluminum nitrate, add 5 ml of 25% sodium nitrite and transfer to the separatory funnel containing the acidic aluminum nitrate solution from the main extraction to neutralize most of the excess acid. Add 50 ml of 30% Aliquat-336 in xylene and shake vigorously for 3 minutes to extract the tervalent actinides. Allow the phases to separate for at least 10 minutes. Reserve the aqueous layer for the determination of ^{226}Ra or discard as desired. Allow 2 more minutes for drainage and remove the small additional aqueous phase that separates. Scrub the organic phase for 2 minutes with each of three successive 15-ml portions of filtered 10.8*M* ammonium nitrate solution to remove the last of the barium and aluminum. Discard the aqueous phases.

Add 30 ml of 8*M* nitric acid to the separatory funnel containing the second organic extract and shake vigorously for 2 minutes to strip the tervalent actinides. Allow the phases to separate for 2 minutes and draw the aqueous layer into a 150-ml beaker. Repeat the strip with 10 ml of 8*M* nitric acid and combine with the first. Discard the organic phase. Add 2 ml of 5% sodium hydrogen sulfate monohydrate in 1-to-1 sulfuric acid, 2 ml of 72% perchloric acid, and 5 ml of concentrated hydrochloric acid to the combined nitric acid strips containing the tervalent actinides and lanthanides. Cover the beaker with a watch glass and evaporate the solution to fumes of sulfuric acid to oxidize ammonium salts and traces of residual organic matter from the extraction. Remove the cover glass and allow the excess sulfuric acid to volatilize. Finally, heat the beaker over a small flame from a blast burner until a pyrosulfate melt is obtained. The melt might not clear completely because of the cerium and lanthanum present but will dissolve subsequently prior to the lanthanide–actinide separation.

With many types of samples such as water, vegetation, etc., the sodium hydrogen sulfate cake can be dissolved in dilute acid and electrodeposited by any appropriate procedure. With soils, the cerium and lanthanum present, about 1 mg in a 10-gram sample (*20*), will be present quantitatively in the tervalent actinide fraction and will interfere seriously with both electrodeposition (*16*) and the resolution of the subsequent alpha spectra. The procedure recommended for the group separation of tervalent actinides from the lanthanides is that of Filer (*21*) which combines extraction chromatography with bis(2-ethylhexyl)phosphoric acid (HDEHP) in the presence of diethylenetriaminepentaacetic acid (DTPA) (*22*) with use of a column of Teflon-6 powder similar to that employed by Moore (*23*). The actinide fraction can then be electrodeposited and analyzed by alpha spectrometry with excellent recovery and resolution. When necessary, Moore's method can also be used to separate ^{242}Cm from ^{252}Cf whose alpha energies are nearly identical and cannot be separated by conventional alpha spectrometry.

Determination of Thorium. Extract the combined hydrochloric acid scrubs of the main Aliquat-336 extract with 10 ml of fresh Aliquat-336 to remove the small quantity of quadrivalent elements that will have been removed from the main extract and discard the organic phase. Add 2 ml of 5% sodium hydrogen sulfate monohydrate in 1-to-1 sulfuric acid, 2 ml of 72% perchloric acid and 2 silicon carbide boiling chips to the aqueous phase in a 250-ml Erlenmeyer flask and evaporate to fumes of perchloric acid. When the solution turns brown, add a few drops of concentrated nitric acid to moderate the oxidation of the waxy flocs of Aliquat-336 remaining from the extraction. Continue heating until all perchloric and sulfuric acids have been removed. Finally, heat the flask over a small flame from a blast burner until a pyrosulfate fusion is obtained. Cool, add 1 ml of 0.6*M* sulfuric acid, and reevaporate just to fumes on the hot plate. Dissolve the cake and electrodeposit thorium by any acceptable procedure. However, a normal soil contains about 130 μg of natural thorium per 10 grams (*20*) which is more than some electrodeposition procedures will handle. An aliquot will give better resolution and higher recovery and is particularly necessary with higher concentrations of thorium, such as in thorium ores.

Determination of Radium-226. Radium-226 can be determined in the aqueous aluminum nitrate phase by the radon emanation technique after removal of the other nuclides.

RESULTS AND DISCUSSION

After all developmental work had been completed, the procedure was rechecked in its final form on actual soils spiked with known quantities of the alpha-emitting nuclides for which the procedure is specifically intended to ensure absence of mass effects due to the long half-lives involved. Each radionuclide was checked individually using approximately 2.5×10^4 cpm per run with a counting time of at least 10 minutes to give a relative standard deviation of 0.2% or less on the major fraction, the standard, and the overall material balance. Every fraction resulting from the procedure was kept separate and analyzed to determine the recovery and distribution of each radionuclide actually obtained under the final recommended conditions. Each fraction was evaporated to a potassium pyrosulfate fusion, the alpha emitter was precipitated on barium sulfate, and the activity was determined by alpha counting under conditions described previously (*12*). Even empty containers were cleaned after each use by pyrosulfate fusion and the contents analyzed. The activity remaining in the empty vessel provides valuable information concerning hydrolysis, sorption effects, etc., and points out sources of contamination of subsequent samples processed in the same glassware. Minor fractions were generally counted for 60 minutes. All fractions were compared *vs.* a standard prepared from another aliquot identical to the one used to spike the soil, and which had been corrected for losses on precipitation by analyzing the filtrate. The zinc sulfide phosphors used for counting the standard and major fraction were selected from a group prescreened for identical counting efficiencies.

The results of the material balance studies are shown in Table I. The numbers not enclosed in parentheses are measured values. The ones enclosed are calculated from the difference between 100% and the sum of the measured values to that point to provide a running description of the course of the analysis. A schematic diagram of the procedure is shown in Figure 1.

Because the final electrodeposition was not properly a part of the present investigation, and many different procedures are available, the material balance study was terminated with the final fraction immediately preceding the electrodeposition step. Losses in the actinide–lanthanide separation are also not included in the data for americium, curium, and californium, but are not more than 1 or 2%

(20) A. P. Vinogradov, *Geochemistry (Engl. Transl.)*, **7**, 641 (1962).
(21) T. D. Filer, *Anal. Chem.*, **46**, 608 (1974).
(22) B. Weaver and F. A. Kappelmann, *J. Inorg. Nucl. Chem.*, **30**, 263 (1968).
(23) F. L. Moore and A. Jurriaanse, *Anal. Chem.*, **39**, 733 (1967).

Table I. Distribution of Activity in Analysis of Ten Grams of Soil

	Radionuclide present, %							
	^{232}Th	^{231}Pa	$^{233}U(IV)$	^{237}Np	^{239}Pu	^{241}Am	^{244}Cm	^{252}Cf
Platinum Dish without Rinsing	0.03	0.02	0.31	0.04	0.09	0.05	0.04	0.05
Main $BaSO_4$ after Reprecipitation	(99.92)	(99.84)	(99.25)	(99.83)	(99.83)	(98.67)	(96.09)	(82.63)
800-ml beaker from main $BaSO_4$ precipitation	0.01	0.03	0.34	0.06	0.01	0.30	0.07	0.19
Second $BaSO_4$ (3 additional portions of $BaCl_2$)	0.01	0.04	0.02	0.01	<0.01	0.52	2.21	8.21
Main filtrate after second $BaSO_4$ precipitation	<0.01	<0.01	<0.01	<0.01	<0.01	0.12	0.96	7.46
Filtrate and wash from repptn of main $BaSO_4$	0.02	0.04	0.06	0.03	0.04	0.34	0.63	1.43
250-ml Erlenmeyer from reprecipitation	0.01	0.03	0.02	0.03	0.03	<0.02	<0.02	0.03
150-ml Beaker from Aluminum Nitrate Fusion	0.01	0.32	<0.01	<0.01	<0.01	0.04	<0.02	0.02
First Aliquat-336 Extract before Scrubbing	(99.78)	(96.00)	(98.51)	(97.12)	(99.53)	(2.72)	(1.19)	(2.70)
First 10-ml 8*M* HNO_3 scrub	0.06	2.43	1.01	0.35	0.01			
Second 10-ml 8*M* HNO_3 scrub	0.07	2.15	1.26	0.40	0.01	2.63*	1.13*	2.62*
Third 10-ml 8*M* HNO_3 scrub	0.06	2.18	1.25	0.37	0.01			
First 50-ml 10*M* HCl scrub after 10-ml ext'n	67.97*							
Second 50-ml 10*M* HCl scrub after 10-ml ext'n	26.20*	0.004	0.02	0.01	0.01	0.09	<0.05	<0.02
Third 50-ml 10*M* HCl scrub after 10-ml ext'n	3.42*							
10-ml extract of combined HCl scrubs	0.79	0.12	0.74	0.41	0.17	(<0.01)	(<0.01)	(<0.01)
First 50-ml $HClO_4$ strip	0.30	(87.29)	(92.35)	(93.59)	(96.72)			
Second 25-ml H_2O strip	0.03	1.12*	1.74*	1.90*	2.50*	<0.02	<0.02	<0.02
Residual organic phase after two strips	<0.01	0.49	0.12	0.06	0.08	<0.02	0.06	0.08
Separatory funnel	<0.01	0.22	0.02	0.03	0.02			
Residual $Al(NO_3)_3$ after First Extraction	(0.13)	(3.52)	(0.74)	(2.71)	(0.30)	(95.91)	(94.90)	(79.91)
Pa-(U)-Np-Pu Fraction from First $HClO_4$ Strip	(0.30)	(87.29)	(92.35)	(93.59)	(96.72)	(<0.02)	(<0.02)	(<0.02)
Main $BaSO_4$ precipitate	(0.30)	86.00*	92.09*	94.00*	95.60*	(<0.02)	(<0.02)	(<0.02)
Filtrate and washes from $BaSO_4$ precipitation		0.06*	0.03*	0.66*	0.04*			
250-ml flask, centrifuge tube, and ethanol transfer liquid from final $BaSO_4$ pptn		0.08*	0.28*	0.06*	0.25*			
Thorium Fraction from Combined HCl Scrubs	(98.47)	(0.004)	(0.02)	(0.01)	(0.01)	(0.09)	(<0.05)	(<0.02)
Main $BaSO_4$ precipitate	(98.05)	(0.004)	(0.02)	(0.01)	(0.01)	(0.09)	(<0.05)	(<0.02)
Filtrate and washes from $BaSO_4$ precipitation	0.07*							
250-ml flask, centrifuge tube, and ethanol transfer liquid from final $BaSO_4$ pptn	0.35*							
Second Aliquat-336 Extract before Scrubbing	(0.13)	(2.49)	(0.74)	(2.51)	(0.30)	(94.43)	(93.76)	(79.41)
Three 15-ml 10.8*M* NH_4NO_3 scrubs combined	0.01	0.04	<0.01	0.17	<0.01	0.82	0.90	1.00
First 30-ml 8*M* HNO_3 strip	<0.01	0.02	<0.01	0.07	<0.01	(92.05)	(91.43)	(77.23)
Second 10-ml 8*M* HNO_3 strip						1.40*	1.43*	1.16*
Residual organic phase after strips	0.12	2.25	0.74	2.27	0.30	0.16	<0.02	0.02
Residual $Al(NO_3)_3$ after Second Extraction	<0.01	1.03	<0.01	0.20	<0.01	1.48	1.14	0.50
Tervalent Actinides from First 30-ml HNO_3 Strip	(<0.01)	(0.20)	(<0.01)	(0.07)	(<0.01)	(92.05)	(91.43)	(77.23)
$Ce(OH)_4$ precipitate	(<0.01)	(0.20)	(<0.01)	(0.07)	(<0.01)	92.14*	90.16*	77.10*
Filtrate from $Ce(OH)_4$ precipitate						0.17*	0.06*	0.17*
Water and ethanol washes of $Ce(OH)_4$						<0.02*	0.04*	0.14*
Centrifuge tube and beaker from $Ce(OH)_4$						0.04*	0.07*	0.12*
Material balance[a]	99.54	98.85	100.05	101.13	99.17	100.30	98.90	100.30
Recovery of each nuclide[b]	98.47	88.41[c]	94.09	95.49	99.22	96.08	93.99[c]	81.01[c]

[a] Sum of all measured fractions. [b] Fractions indicated by asterisks combined as recommended in the general procedure. Indicated recovery and calculated values given in parentheses have been corrected for the difference in material balance from 100%. [c] Recoveries increase to 96.20% and 89.22% for curium and californium, respectively, with three additional portions of barium chloride, and to about 97% for protactinium in the absence of nitrous acid.

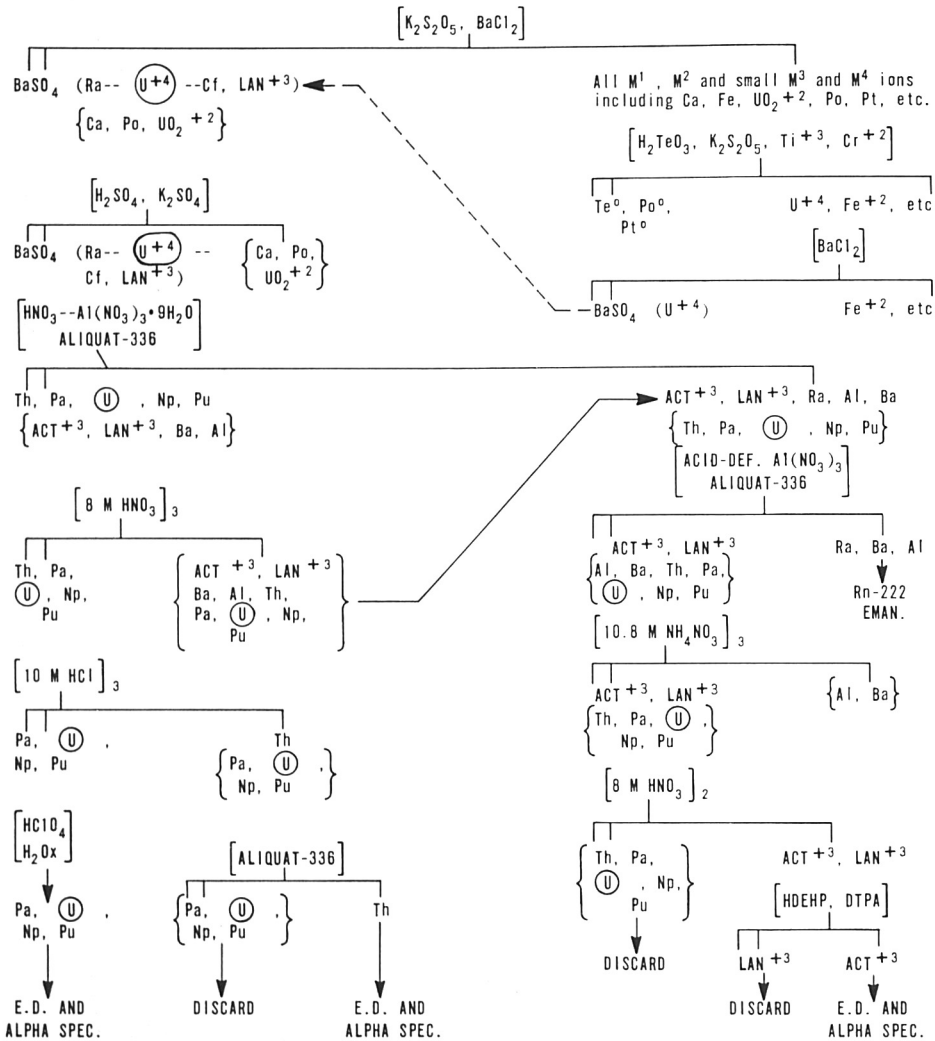


Figure 1. Diagram of procedure. Double vertical lines indicate precipitates or organic extracts; single vertical lines indicate aqueous solutions. Square brackets indicate reagents used; parentheses indicate elements precipitated with barium sulfate; circle around uranium and dotted line indicates option on uranium; and curved brackets indicate small quantities of certain elements that require special attention to eliminate detectable interference

(*21*). Although the final fraction of the three tervalent actinides could have been counted on barium sulfate like the other nuclides, precipitation losses would have been somewhat larger because of the 1 or 2 mg of cerium plus lanthanum present from the soil. Consequently, they were precipitated as hydroxides using the cerium and lanthanum as carriers to show the efficiency and analytical utility of this separation, should the need arise. The salts from the 8*M*

nitric acid strips were dissolved in 8 ml of water, 0.25 ml of 0.25*M* disodium ethylenedinitrilotetraacetic acid and 1 drop of 30% hydrogen peroxide were added, and then 8*M* sodium hydroxide to an excess of 5 ml. After digestion in boiling water for 2 or 3 minutes and cooling, the precipitate was dispersed in an ultrasonic bath and filtered quickly on a 47-mm DM-450 membrane filter to obtain uniform deposition. After washing with water and ethanol, the precipitate was dried and counted.

As shown in Table I, the overall recoveries from 10 grams of soil, excluding the electrodeposition step, range from a remarkable 99.2% for plutonium to the lowest recovery of 88.4% for protactinium. The latter can be increased to 97% by elimination of sodium nitrite as will be discussed below. The principal loss of tervalent actinides occurs in the barium sulfate precipitation, and of protactinium and uranium in the nitric acid scrubs. All the other fractions show remarkably small losses indicating the efficiency and reliability of the individual steps. Radiochemical purity of each of the major fractions can be determined from the quantity of other radionuclides found in each.

Accuracy. To prove the accuracy of the procedure, most of the individual nuclides were determined in samples containing known concentrations of the nuclide. The accuracy of the plutonium determination has been demonstrated previously in connection with the preparation of standard soils (*24*). A standard soil containing 20.2 ± 0.1 dpm/gram of ^{241}Am was prepared similarly and found to contain 20.1 ± 0.4, 20.0 ± 0.4, and 20.0 ± 0.4 dpm/gram on three aliquots. Natural thorium was determined in four standard thorium ores prepared by the New Brunswick Laboratory of the U.S. Atomic Energy Commission having certificate values of 1.01 ± 0.01%, 0.101 ± 0.002%, 0.0102 ± 0.0001%, and 0.0011 ± 0.0001% thorium. The corresponding values obtained were 1.02 ± 0.01%, 0.100 ± 0.001%, 0.0105 ± 0.0002%, and 0.00105 ± 0.00001% thorium, respectively. Statistically identical values for thorium were obtained previously on these same samples by a fluorometric method (*25*).

A standard pitchblende sample containing 0.973 ± 0.004% U_3O_8 was also analyzed. This sample had been analyzed for natural uranium by an accepted volumetric procedure and had also been demonstrated to be in secular equilibrium (*24*). The activities calculated from accepted values for the abundances and half-lives are 6.06 ± 0.04 × 10^3 dpm/gram for the ^{238}U series and 2.83 ± 0.09 × 10^2 dpm/gram for the ^{235}U series. The analytical values obtained were 6.02 ± 0.04 × 10^3 for ^{238}U, 6.02 ± 0.04 × 10^3 for ^{234}U, 6.08 ± 0.04 × 10^3 for ^{230}Th, 2.65 ± 0.11 × 10^2 for ^{235}U, and 2.78 ± 0.03 × 10^2 dpm/gram for ^{231}Pa, all of which are statistically identical to the calculated values at the 95% confidence level.

Sample Decomposition. When potassium fluoride is melted, slow hydrolysis occurs, hydrogen fluoride is volatilized, and the flux becomes progressively more alkaline. When the alkalinity becomes high enough to compete successfully with the soluble fluoride complexes, insoluble hydroxides are precipitated, and the solvent action of the molten flux virtually ceases. The problem becomes worse, the more prolonged the heating and/or the higher the concentration of heavy metals. Although the insoluble hydroxides dissolve in the subsequent pyrosulfate fusion, any siliceous material covered over by the hydroxides and not attacked while the fluoride is still present remains undissolved. Addition of a solid acid such as potassium pyrosulfate is effective in mild cases but the problem is better avoided by keeping the sample from caking so that dissolution is rapid and complete initially. When particularly high concentrations of iron are present, leaving the residue distinctly moist with hydrofluoric acid before addition of potassium fluoride increases the time available for complete decomposition before precipitation begins. However, too much hydrofluoric acid gives potassium hydrogen fluoride which melts at a much lower temperature and causes severe spattering before the final high temperature fusion is reached.

Because the sulfates of most metals other than the alkalis are very insoluble in concentrated sulfuric acid, a very thick immobile mud of insoluble sulfates forms when the fluoride cake is transposed with sulfuric acid and the water removed by evaporation. The mud retains sulfuric acid so tenaciously that it is almost impossible to evaporate to a fusion without severe spattering. High concentrations of iron, aluminum, and calcium are particularly troublesome. However, if a moderate quantity of neutral sodium sulfate is added, the mud suddenly thins to a slurry from which the remaining sulfuric acid can be removed easily and a clear pyrosulfate fusion obtained. Apparently, the excess sulfate ions form anionic sulfato acids with the metals, such as $H[Fe(SO_4)_2]$, which are soluble in concentrated sulfuric acid rather than the neutral salts such as $Fe_2(SO_4)_3$ which are insoluble.

Barium Sulfate Separation. Previous work (*11*, *12*) has shown that small quantities of all ter- and/or quadrivalent ions having ionic radii larger than about 1.0 a.u. can be precipitated quantitatively by barium sulfate. Maximum efficiency of precipitation and minimum interference from other elements are obtained by slow incremental addition of a barium chloride solution not more concentrated than about 0.45% to a boiling solution containing high concentrations of both potassium and sulfate ions. The efficiency decreases with increasing acidity, and nitrates must be absent. Thus, small quantities of lead, bismuth, barium, strontium, lanthanum, cerium, and all elements from radium through californium are precipitated quantitatively, the quantity and efficiency depending on the quantity of barium used. The elements from uranium through americium can be prevented from precipitating by oxidizing them to their highest oxidation states. Strontium, lead, lanthanum, and cerium are almost as efficient as barium in precipitating the other elements. This separation is particularly effective and applicable for the group separation of the large polyvalent ions from all mono-, di-, and the smaller ter- and quadrivalent ions, such as iron, aluminum, titanium, etc.

When present in milligram quantities, those elements precipitated by barium sulfate are their own worst interferences with precipitation of each other, apparently by filling the available lattice positions in a given quantity of barium sulfate. However, the intrinsically serious interferences such as lanthanum, cerium, thorium, etc. produce little loss in the precipitation because the 1 or 2 mg present in 10 grams of soil (*20*) are removed completely in the first couple additions of barium chloride, leaving nothing to interfere with complete precipitation of the actinides sought with the later portions. Calcium is the worst interference to be encountered in soils because of the relatively large quantities present, about 3% for the average (*20*) but considerably higher for individual ones. If allowed to precipitate as calcium sulfate and filtered off, the calcium present in 10 grams of soil will carry virtually all of the large alpha-emitting ions sought. Hydrochloric acid can be added to prevent precipitation of calcium sulfate and keep it from accompanying the barium sulfate, but a significant decrease in efficiency still results, due both to the higher concentration of acid employed and the resulting higher concentra-

(24) C. W. Sill and F. D. Hindman, *Anal. Chem.*, **46**, 113 (1974).
(25) C. W. Sill and C. P. Willis, *Anal. Chem.*, **34**, 954 (1962).

tion of calcium ions in the solution. The loss in efficiency of precipitation is not serious up to about 5% calcium on a 10-gram sample for all elements except the tervalent actinides. As shown in Table I, a progressive decrease in recovery is observed from americium through californium due to the actinide contraction in the size of the ions. The errrors are cumulative, the loss caused by high acidity adding to that caused by calcium ion, etc., with the loss being worse with californium than with curium, etc.

As shown in Figure 1, a small quantity of calcium, polonium, and hexavalent uranium carries in the main barium sulfate precipitation, and must be removed by reprecipitation. Otherwise, the elements carry through the remainder of the procedure, at least in part. Calcium interferes with both the electrodeposition and the resolution of the alpha spectra on the final electrodeposited plate. Polonium does not carry appreciably on barium sulfate in the presence of hydrochloric acid; but the small quantity of ^{210}Po that comes through interferes with the use of ^{243}Am tracer, whose principal alpha energy is different by only about 30 keV. The small quantity of uranium that carries from the hexavalent state interferes with the detection of minimal quantities of ^{237}Np whose alpha energies overlap those of ^{234}U. Enough perchloric acid must be used to oxidize all organic matter from the filter paper or the uranium will remain in the quadrivalent state and will reprecipitate quantitatively with the barium sulfate, defeating the purpose of the reprecipitation as far as uranium is concerned. However, the perchloric acid also oxidizes the cerium present which in turn oxidizes the plutonium present. Because sulfite does not reduce hexavalent plutonium efficiently, ferrous sulfate must be used to avoid serious loss of plutonium during the reprecipitation.

Determination of Uranium. Uranium can be precipitated quantitatively by barium sulfate after reduction to the quadrivalent state, either simultaneously with the other elements from radium through californium or from the filtrate after removal of the other nuclides (*12*). This option is indicated by the dotted line in Figure 1. The uranium will then carry through the remainder of the separations quatitatively. The separate determination is recommended. Quadrivalent uranium is one of the most serious interferences with precipitation of the other alpha emitters on barium sulfate, particularly curium and californium, while hexavalent uranium has an almost negligible effect. The tervalent titanium produced during reduction further adds to the interference. Moderate quantities of uranium also reduce markedly both electrodeposition yield and resolution of the resultant alpha spectrum. Quadrivalent uranium produces much greater interference with both precipitation and electrodeposition of the other alpha emitters than it does with itself. Consequently, it is generally safer to keep the uranium in the oxidized state until after the other elements have been removed and then to recover the uranium from the filtrate by itself. With the normal levels of uranium found in soil, uranium can be determined simultaneously with thorium and plutonium without significant adverse effect on the determination of the latter elements because of their much greater tolerance to interfering elements. However, separate determination of uranium is almost mandatory when the tervalent actinides are being determined to keep losses of these elements from becoming untenably large.

Polonium-210 occurs in normal soils to the extent of about 3 dpm/gram. This radionuclide constitutes a special interference in the isotopic determination of uranium because the energy of its alpha emission is only 20 keV different than that of the ^{232}U tracer used to determine the chemical yield. Although polonium is not precipitated significantly with barium sulfate from hydrochloric acid solution, it is reduced to the elemental state under the strong reducing conditions necessary to reduce uranium to the quadrivalent state and will be filtered off with the barium sulfate. About 1 mg of platinum invariably dissolves from the platinum dish during the initial sample decomposition and will accompany the polonium. Consequently, both platinum and polonium must be removed after reduction of uranium but before precipitation of barium sulfate if ^{232}u is to be used as tracer.

Reduction of uranium to the quadrivalent state in a strongly acid solution containing relatively large quantities of iron is attended by more problems than might be supposed. A Jones reductor is rapid and effective but does not remove polonium quantitatively, causes severe consumption of acid and consequent danger of precipitation of calcium sulfate, and provides great opportunity for contamination from one sample to another unless a new reductor is used each time. Sulfurous acid does not reduce ferric iron completely in strong acid solutions containing chlorides and sulfates, which is a necessary prerequisite to the reduction of uranium. Both titanium trichloride and chromous chloride reduce both iron and uranium quantitatively at room temperature, but the large quantities of either that are required to reduce the iron present in 10 grams of soil introduce other problems. Quadrivalent titanium precipitates as an insoluble potassium sulfatotitanate under the conditions used, and the chromic chloride produced results in an impenetrably dark-colored solution in which the course of the reactions is difficult to follow.

Fortunately, it was discovered that the tellurous acid, which is added to carry the polonium after reduction of both to the elemental state, also catalyzes the reduction of iron by sulfurous acid markedly under the conditions used. A few drops of titanium trichloride then suffices to reduce uranium and the last of the iron, and to precipitate elemental platinum, polonium, and tellurium. A few drops of chromous chloride then restore most of the titanium to the tervalent state to act as a holding reductant for the quadrivalent uranium during the subsequent precipitation of barium sulfate from boiling solution. Without titanium, reduction with chromous chloride again leads to undesirably dark solutions and possible reoxidation of uranium because of rapid oxidation of the excess chromous ion by air, particularly in the boiling solutions required. A low potential indicator, Safranin O, provides positive visual indication that uranium is kept in the quadrivalent state necessary for its quantitative precipitation with barium sulfate.

Extraction. During the early part of this investigation, several unsuccessful attempts were made to extract plutonium and americium simultaneously. At the lower acidity required to extract americium efficiently, plutonium recovery was sometimes as low as 50%. The missing plutonium remained unextracted in the aluminum nitrate solution from which all but about 1% could be recovered by filtration. Increasing the acidity eliminated the loss completely. Obviously, hydrolytic precipitation is indicated. The acidity must be kept relatively high during the first extraction to prevent serious potential losses of plutonium and presumably other quadrivalent elements. Aluminum nitrate solutions and particularly the aluminum nitrate fusion must not be boiled or loss of nitric acid will be significant as evidenced by the effectiveness of boiling in preparing the acid-deficient aluminum nitrate reagent. It should be kept in mind that purification of aluminum nitrate by extraction with Aliquat-336 also removes nitric acid which must be replaced.

When compared with those of Table I, the data of Table II show the pronounced effect of high concentrations of ni-

Table II. Distribution of Neptunium, Plutonium, and Protactinium in the Absence of Nitrous Acid

	Radionuclide present, %		
	^{237}Np	^{239}Pu	^{231}Pa
First Aliquat-336 Extract before Scrubbing	(77.7)	(98.73)	(99.24)
First 10-ml 8*M* HNO_3 scrub	0.27	0.96	0.46
Second 10-ml 8*M* HNO_3 scrub	0.21	0.94	0.26
First 50-ml 10*M* HCl scrub	0.22	0.93	0.10
Second 50-ml 10*M* HCl scrub	0.14	0.39	0.08
First 50-ml $HClO_4$ strip	75.9	94.33	96.63
Second 25-ml H_2O strip	0.92	1.15	1.44
Residual organic phase after two strips	<0.01	0.03	0.27
Residual $Al(NO_3)_3$ after First Extraction	(22.3)	(1.27)	(0.76)
Second Aliquat-336 Extract before Scrubbing	(20.0)	(1.27)	(0.76)
Single 15-ml 8*M* HNO_3 scrub	9.7	0.01	<0.01
Residual organic phase after one strip	10.3	1.26	0.76
Residual $Al(NO_3)_3$ after Second Extraction	2.3	<0.01	<0.01
Recovery of each nuclide	76.8	95.48	98.07

trous acid. Without nitrous acid, the initial extraction of neptunium is about 20% lower. About 10% of the activity not removed in the first extraction is also not removed in the second extraction after adding acid-deficient aluminum nitrate to reduce the acidity. Of particular significance is the fact that about 50% of the neptunium that was extracted at lower acidity is stripped back into 8*M* nitric acid, compared to about 0.3% for the neptunium extracting initially from strong acid solution. Apparently, part of the neptunium is oxidized to the pentavalent state by the high concentration of nitrate ion present. The remaining quadrivalent neptunium is extracted efficiently at high acidity. However, similar to the tervalent actinides, the neptunyl ion does not extract efficiently at high acidity, and much of that extracting at reduced acidity is easily stripped back into 8*M* nitric acid. Nitrous acid, which is one of the few if not the only reducing agent compatible with such high concentrations of nitrate ion, reduces the neptunium back to the quadrivalent state and the extractability increases markedly. The nitrous acid itself is extracted efficiently into Aliquat-336 and provides a holding reductant to prevent loss of neptunium during the subsequent scrubs with nitric acid.

Nitrous acid has little effect on the extraction and scrubbing of thorium and uranium. However, the corresponding small losses of plutonium were almost eliminated, increasing the recovery by about 5.5% for the extraction and three scrubs each with nitric and hydrochloric acids. This effect is probably also due to more complete reduction of plutonium to the more extractable quadrivalent state. Unfortunately, losses of protactinium in both extraction and nitric acid scrubs are increased by about 8.5% by inclusion of nitrous acid for some unknown reason, possibly by formation of a less extractable nitrite complex. However, when protactinium is to be determined alone, the nitrite can be omitted profitably, raising the overall recovery from 88.4% to about 98%, making this procedure one of the better ones available for this very refractory and hydrolytic element.

Because thorium is virtually the only alpha-emitting element that is extractable by Aliquat-336 from a nitrate system and not from chloride, this procedure is virtually specific for thorium nuclides.

Electrodeposition. By far the most serious potential loss of activity occurs during electrodeposition. While pure carrier-free tracers can usually be electrodeposited by any of several methods reliably with good yields, losses increase dramatically in the presence of microgram quantities of other elements (*16, 17*). The losses depend on the radionuclide being deposited, and the kind and quantity of interfering elements present. Electrodeposition of electropositive elements such as the actinides depends on precipitation of hydroxides by hydroxyl ions produced electrolytically at the cathode. Consequently, all metal ions forming insoluble hydroxides might be expected to electrodeposit to some extent, giving degraded spectra and lowered yields if present in appreciable quantities. Particularly, if the extraneous element is allowed to precipitate in the solution during preliminary pH adjustment prior to the beginning of electrodeposition, the radionuclide being determined will be coprecipitated more efficiently than if it were alone and will not be available for electrodeposition on the cathode.

Recent information obtained in this laboratory (*26*) demonstrated that interference from most elements is much greater when methyl red indicator (pH 4.8 to 6.0) is used during the adjustment of pH than when thymol blue (pH 1.2 to 2.8) is used. Apparently, when ter- and particularly quadrivalent ions are present and alkali is added to a pH as high as 6.0, significant precipitation occurs, particularly locally around the drops of alkali, which does not redissolve completely even though the final adjustment is made with dilute acid to the acid side of the indicator range, *e.g.*, pH 4. When thymol blue is used, much less alkali is added, less precipitation occurs, and more acid is present after neutralization to the acid side of the indicator to redissolve any small quantities that might have precipitated. It is strongly recommended that thymol blue be used to a salmon-pink end point (pH 2.0) in place of methyl red recommended in the previous precedure from this laboratory (*17*), and in other procedures employing preliminary neutralization as well.

An interesting discovery is the fact that radium, which does not normally electrodeposit, will do so partially if present in the thorium fraction. For example, if electrodeposition of a thorium fraction containing natural thorium is delayed for several hours after separation to permit ingrowth of ^{224}Ra from the ^{228}Th present, ^{224}Ra will be present on the plate immediately after electrodeposition.

Decontamination of Glassware. During the early stages of application of the present procedure, it became apparent that high and erratic blanks and contamination of low-level samples invariably followed analysis of higher-level samples. This was a particularly frustrating conclusion because all glassware was rinsed routinely with a strong solu-

(26) K. W. Puphal and G. J. McNabb, U.S. Atomic Energy Commission, Idaho Falls, Idaho, personal communication, 1973.

tion of hydrochloric and hydrofluoric acids to avoid this very problem. Consequently, the entire procedure was examined carefully to identify even minute losses of the various radionuclides in the various vessels used and to determine the effectiveness of various methods of decontamination.

By far the most serious source of contamination is the cell, electrode, and "O" ring used in the electrodeposition step. Brief rinsing with a strong solution of hydrochloric acid containing hydrofluoric acid and hydrogen peroxide at room temperature was totally ineffective in producing adequate decontamination. Boiling anode and cell with concentrated nitric acid for 10 to 15 minutes removed virtually all of the activity resulting from analysis of samples containing less than 500 dpm. When larger quantities of activity such as the 2.5×10^4 cpm used in the material balance studies of Table I had been used, a second boiling with clean nitric acid was generally required. However, boiling nitric acid precipitates polonium and other procedures have to be used in its presence. When such high levels of activity have been used, a blank should be run to ensure that decontamination was adequate before the system is permitted to be used in the analysis of subsequent low-level samples. Prudence suggests that a separate system be reserved for low-level samples and good management exercised over the level of samples permitted in the low-level system to minimize the number of blanks and full-length counting times required to determine adequate decontamination.

Other sources of contamination can be identified from the data on empty containers given in Table I. Beakers, flasks, and centrifuge tubes in which barium sulfate has been precipitated must be cleaned by some agent known to dissolve barium sulfate such as boiling perchloric or sulfuric acids or boiling alkaline DTPA. This is a particularly important potential source of contamination, particularly if hot solutions containing freshly-precipitated barium sulfate are allowed to cool without stirring. Some barium sulfate post-precipitates after cooling and adheres to the walls so tenaciously that chemical removal is required. Obviously, the barium sulfate will contain whichever actinide is present, and will not dissolve even in solutions containing hydrofluoric acid. Beakers or flasks in which radionuclides have been evaporated to dryness will invariably contain residual activity which generally requires a pyrosulfate fusion to clean completely and reliably. Separatory funnels can generally be cleaned adequately by rinsing with ethanol and water to remove the organic solvent, and then with hydrochloric–hydrofluoric acids and water to remove traces of hydrolyzed radionuclides. With these precautions, blanks on the total procedure, including reagents and the laboratory environment, are consistently less than 3 counts above the detector background in a 10^3-minute spectrum over the entire energy interval of any given radionuclide.

Alpha Spectrometry. Because of the inability to resolve the energies of ^{240}Pu from those of ^{239}Pu, all references in the present work to the latter are meant to include both isotopes. Differentiation of ^{241}Am from ^{238}Pu, both having energies at about 5.48 MeV, is automatic in the present procedure because the two elements end up in different chemical fractions. With moderate quantities of ^{239}Pu, its spectrum overlaps that of ^{231}Pa, and no resolution is possible. However, because of the small quantity of ^{231}Pa naturally present in soil, the error is never serious at the ^{239}Pu levels at which complete resolution is not obtained. Similarly, the spectra of ^{243}Am and ^{241}Am also overlap at higher levels, particularly if the spectra are slightly degraded due to the presence of absorbing materials. If the two peaks are integrated to the low point in the crotch between them, the results are generally low. Americium-243 has two minor branches at higher energies than the major one which makes resolution even more difficult. Because the problem occurs only when tracer and nuclide being determined are both present in relatively large quantities, sufficient activity will always be present to permit counting at a lower geometry to restore adequate resolution.

Previous recommendations (*18*) should be strictly observed to prevent serious contamination of the solid-state detector by recoiling nuclei, particularly when high levels of activity or large numbers of samples containing ^{228}Th, ^{232}U, or ^{236}Pu are involved. Heating stainless steel plates for 5 minutes on an uncovered high-temperature hot plate is virtually mandatory to fix polonium to prevent spontaneous volatilization and contamination of the detector (*18*). In some cases, particularly with the americium fraction, some improvement in resolution can be obtained by heating the plates over a blast burner momentarily to dull redness and cooling quickly. However, caution should be observed if lead might be present. Lead electrodeposits as metal relatively more rapidly than the more electropositive elements which plate out as hydroxides. Upon ignition, the lead is completely volatilized carrying much of the other deposited nuclides along.

Calculations. When alpha-emitting tracers can be used in the yield determination of the other isotopes being determined, calculation of the results and propagation of the uncertainties is very simple and rapid. Let X, Y, and Z be the total counts obtained in the energy intervals for the ^{239}Pu to ^{236}Pu recovered by the dpm/gram of ^{236}Pu tracer the procedure, and the ^{236}Pu obtained in the standardization for the same quantity of tracer, respectively. Let t_z and E_z be the counting time and efficiency for Z; B_x, B_y, and B_z the corresponding background counts or other corrections in the same counting times; and g the weight of sample taken. The activity of ^{239}Pu in the sample in dpm/gram is found by multiplying the ratio of net counts of ^{239}Pu to ^{236}Pu recovered by the dpm/gram of ^{236}Pu tracer added, or $(X - B_x)/(Y - B_y) \times (Z - B_z)/t_z E_z g$. It should be noted specifically that neither counting time, counting efficiency, nor chemical yield of the sample measurements affects the accuracy of the determination except as they affect the total number of counts obtained. The accuracy of the determination is dependent almost solely on the accuracy with which the tracer is standardized, provided that complete exchange is obtained.

If it is arranged that errors in t_z, E_z, and g do not contribute significantly, the absolute uncertainty in the ^{239}Pu activity in dpm/gram is:

$$[^{239}\text{Pu, dpm/g}] \times \left[\left(\frac{S_x}{(X - B_x)}\right)^2 + \left(\frac{S_y}{(Y - B_y)}\right)^2 + \left(\frac{S_z}{(Z - B_z)}\right)^2\right]^{1/2}$$

where S_x, etc., indicates the standard deviation or uncertainty in the net value of X and will generally be equal to $(X + B_x)^{1/2}$ for equal counting times of sample and background. The equation shows that the total number of counts of ^{236}Pu obtained either in the yield determination on each sample or in the standardization of the tracer affects the uncertainty of each analysis in exactly the same way as does the total number of counts of ^{239}Pu obtained. If the quantity of ^{236}Pu and/or the counting time used in the standardization is sufficiently large, the error function simplifies to the first two terms under the square root sign in the equation. If the quantity of ^{236}Pu tracer used in the sample is sufficiently high, the total uncertainty in the de-

termination will be determined entirely by the uncertainty in the ^{239}Pu count as it should be. Otherwise, the final result must reflect the additional uncertainties contributed by the other variables.

When the quantity of ^{236}Pu used is too small, the uncertainty in the yield determination becomes much greater than the uncertainty in the total count of the ^{239}Pu from the sample. Clearly, the tracer should be standardized more accurately than any subsequent work to be done, and the quantity of tracer used should be at least equal to the total quantity of radionuclide being determined to balance the contribution of each to the total uncertainty.

Most other isotopic tracers are not as ideal and unequivocal in their use in the determination of chemical yields as ^{236}Pu. Americium-243 currently contains about 2.6% ^{241}Am which restricts the permissible quantity to about 3 dpm per sample if maximum sensitivity is to be obtained. Furthermore, ^{243}Am is not a particularly uncommon nuclide and occurs with ^{241}Am in many types of samples, particularly from chemical processing plants. In contrast, ^{232}U is available that is virtually free of ^{233}U and other isotopes and is an excellent tracer for the naturally occurring isotopes of uranium. However, it occurs in products from the thorium breeder in activities equal to or larger than the ^{233}U being traced and must also be determined. Excellent gamma-emitting tracers are available for isotopes of thorium, protactinium, and neptunium, but the yield determination must be made separately from the analysis itself.

Information on leachability of ignited plutonium with and without hydrofluoric acid, sample inhomogeneity due to the particle problem, and a comparison of ^{236}Pu and ^{242}Pu tracers are presented elsewhere (*9*).

ACKNOWLEDGMENT

The authors gratefully acknowledge the assistance and many useful suggestions contributed by their associates, with special thanks to T. D. Filer and G. J. McNabb for electrodeposition of many samples and to J. S. Morton and D. G. Olson for the equipment and many alpha spectra without which this work would not have succeeded.

RECEIVED for review January 14, 1974. Accepted June 6, 1974.

Radiochemical Separation of Fluorine by Adsorption on Hafnium Dioxide: Application to the Determination of Oxygen by Activation Analysis with Charged Particles

A. Kohn, J. N. Barrandon, J. L. Debrun, M. Valladon, and B. Vialatte

Groupe d'Application Des Reactions Nucleaires a l'Analyse Chimique, Service du Cyclotron, Centre National de la Recherche Scientifique, 45045 Orleans Cedex, France

Low concentrations of oxygen in metals and semiconductors are best determined by activation analysis with charged particles. The main problem, in most cases, is to perform a good radiochemical separation of ^{18}F, produced by nuclear reaction on oxygen. Adsorption of fluorine on hafnium dioxide, from nitric acid solutions, is studied here in detail as a possible method to perform this radiochemical separation. Applications in the case of the determination of oxygen in copper, cobalt, and silver are presented.

Because of surface effects (*1, 2*), oxygen is best determined at the part per million level, and below, by activation analysis with charged particles. The particle of choice is generally ^{3}He, and, in most cases, the problem is to develop a suitable radiochemical separation for the ^{18}F produced by nuclear reactions on ^{16}O. In the past, fluorine has often been radiochemically separated by steam distillation of H_2SiF_6, by solvent extraction, by adsorption on metallic oxides, and by numerous other methods (*3–8*).

In our laboratory, we have always been interested in simple, fast, and reliable radiochemical separations for ^{18}F. In view of the good results that we obtained (*9*) with Al_2O_3 in the case of an iron matrix, we decided to study HfO_2, a compound that seemed to be particularly interesting because of the high affinity of hafnium for F^-, and because it is rather insensitive to most chemicals.

This study is two-fold: in the first part, we present our results for the adsorption of F^- from nitric acid solutions, and our interpretation of these results. In the second part, we report the use of HfO_2 for the determination of oxygen in some metals of interest to us—namely, Ag, Co, and Cu.

Only a nitric acid medium has been investigated, since all these metals are readily dissolved in nitric acid.

EXPERIMENTAL

Commercial hafnium dioxide was sieved, and we retained the fraction between 0.2 and 0.5 mm in diameter. All experimental results were obtained by making use of radiotracers prepared in the reactors, the cyclotrons, or the linear accelerator at Saclay.

The experimental curves were obtained by shaking the different solutions in polyethylene vials, in the presence of 1 gram of HfO_2. The fixation of the elements on HfO_2 columns was studied under the same conditions as those described by Girardi (*10*).

(1) J. N. Barrandon, Lino Quaglia, J. L. Debrun, Marc Cuypers, and Guy Robaye, *J. Radioanal. Chem.*, **4**, 115–126 (1970).
(2) J. N. Barrandon, J. L. Debrun, Marc Cuypers, Lino Quaglia, and Guy Robaye, *C.R. Acad. Sci.*, **267**, 1306–1308 (1968).
(3) J. N. Barrandon, J. L. Debrun, and Philippe Albert, Euratom Report, **EUR 3896**, (Proceedings of the 2nd Conference on Practical Aspects of Activation Analysis with Charged Particles, Liège, Belgium, Sept. 21–22, 1967.
(4) Jacques Giroux, Lycen Report No. 6930.
(5) C. K. Kim, *Radioanal. Lett.*, **2**(2), 53 (1969).
(6) Liliane Faure-Mazagol, Thesis, June 1971, University of Lyon, France (Lycen Report No. 7136).
(7) John Robson, *Aust. At. Energy Comm. Rep.*, **AAEC/TM 435** (1968).
(8) P. E. Wilkniss, K. J. Skinner, and C. M. Check, *Radiochim. Acta*, 101–276 (1968).
(9) Gilbert Blondiaux, and Bernard Vialatte, *Radiochem. Radioanal. Lett.*, **8**(4), 251 (1971).
(10) Franco Girardi, R. Pietra, and E. Sabbioni, *J. Radioanal. Chem.*, **5**, 141 (1970).

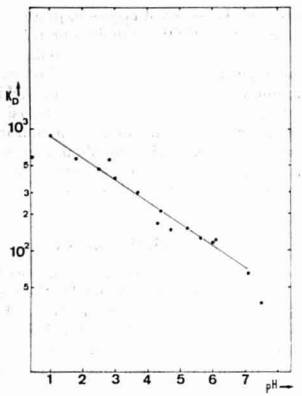


Figure 1. Partition coefficient of F^- between HfO_2 and the liquid phase, for $7 > pH > 1$

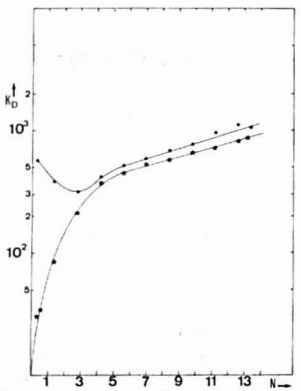


Figure 2. Partition coefficient of F^- between HfO_2 and the liquid phase, for $1 < N_{HNO_3} < 13$

Upper curve: no Al^{3+} in solution. Lower curve: presence of Al^{3+}

RESULTS

Characteristics of HfO_2 for the Fixation of F^-. *Variation of the Partition Coefficient with the pH.* The partition coefficient of fluoride ion between the liquid phase and the hafnium dioxide phase can be defined as $K_d = A_s/A_l$, where A_s is the radioactivity of ^{18}F for 1 gram of HfO_2. A_l is the radioactivity of ^{18}F in one gram of liquid. In this experiment, 10 μg of inactive fluoride ion were added to the carrier-free ^{18}F.

Figure 1 shows the variation of K_d (logarithmic scale) with the pH (linear scale). As can be seen, in the interval pH 7 to pH ~1, this variation is linear, and the slope of the straight line is equal to −0.2. The lower the pH, the better F^- is adsorbed. When $pH < 1$, K_d decreases, then increases again, as shown in Figure 2 (upper curve). It seems that this curve represents the sum of different phenomena. The same variation is observed when ZrO_2 is used in place of HfO_2 (Figure 3).

If Al^{3+} is added to the solution, we see (Figure 2, lower curve) that F^- is adsorbed on HfO_2, but much less at low HNO_3 concentrations, and there is no minimum in the curve.

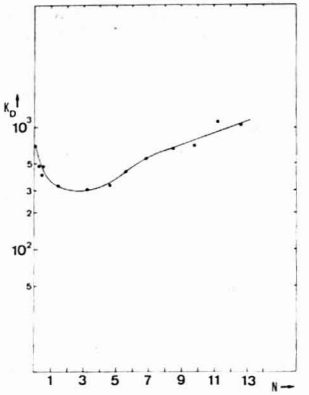


Figure 3. Partition coefficient of F^- between ZrO_2, and the liquid phase, for $1 < N_{HNO_3} < 13$

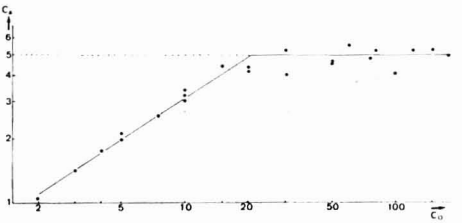


Figure 4. Capacity of HfO_2 for F^-

C_0 is the number of milligrams of F^- at $t = 0$. C_A is the number of milligrams of F^- adsorbed per gram of HfO_2

Table I. Capacity of HfO_2 for F^- for Different Particle Sizes

Diameter ϕ, mm	Amount of F at t_0, mg	Amount of F adsorbed, mg, (1 g HfO_2)
0.5	30	6.6
	75	5.3
$0.05 < \phi \leq 0.1$	30	5.7
	75	7.0
$0.1 < \phi \leq 0.2$	30	5.0
	75	5.2
$0.2 < \phi \leq 0.5$	30	4.0–5.3
	75	4.75

Capacity of HfO_2 for F^-. This parameter was determined in 7*N* nitric acid only. As shown in Figure 4, the capacity of HfO_2 for F^- is roughly equal to 5 mg/g. From the results in Table I, we can deduce that this capacity is apparently independent of the granulometry. It should be noted that there is some loss of fluorine during the experiment because of the continuous shaking of strong acid-solutions, in spite of the fact that we used closed polyethylene vials. A standard solution was then shaken in the same manner to avoid any errors resulting from this loss.

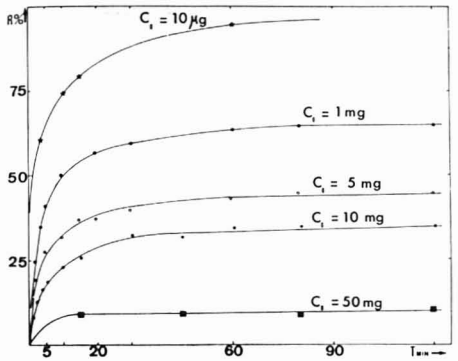


Figure 5. Yield of adsorption of F^- *vs.* the time of shaking, for different values of C_0, for 1 gram of HfO_2

V_A, V_B, V_C, are the speeds of reactions at $t = 0$

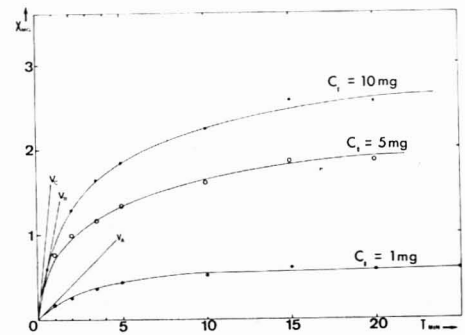


Figure 6. Total amount of fluorine adsorbed on HfO_2 *vs.* the time of shaking, for different values of C_0, for 1 gram of HfO_2

Table II. Value of the Order of Reaction α for the Adsorption of F^- on HfO_2, for Different Initial Concentrations and Different Amounts of F^- Adsorbed

	α		
x mg	a_0 = 1 mg, a_0' = 5 mg	a_0 = 1 mg, a_0' = 10 mg	a_0 = 5 mg, a_0' = 10 mg
0.0	1.00	0.98	0.93
0.1	1.01	1.03	1.00
0.2	1.16	1.07	1.01
0.3	1.18	1.07	
0.4	1.37	0.93	
0.5		1.20	
0.75			1.00
1.0			1.09
1.5			1.34

Kinetics of the Fixation of F^-. The curves in Figure 5 give the percentage of F^- adsorbed as a function of time, for different initial concentrations. Figure 6 shows the quantity of F^- adsorbed per gram of HfO_2 for different initial concentrations. These values and the speeds of reaction are enough to calculate the order of the reaction:

$$n\mathrm{F}^- + m \text{ oxide} \longrightarrow \text{products of reaction}$$

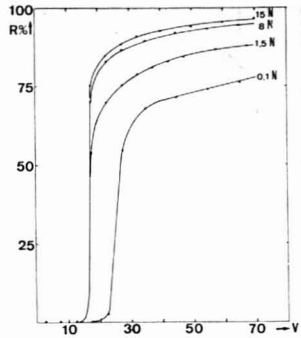


Figure 7. Yield of elution of F^- after adsorption from a 7*N* HNO_3 solution *vs.* the volume of NaOH, for different NaOH concentrations

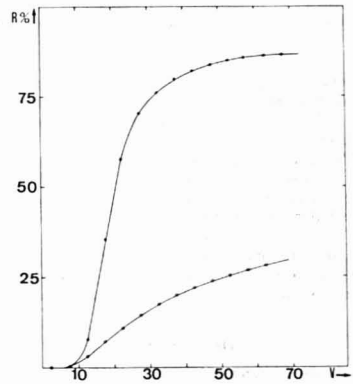


Figure 8. Yield of elution of F^- after adsorption from a 7*N* HNO_3 solution *vs.* the volume of $Al(NO_3)_3$ solution

Upper curve: 1*M* $Al(NO_3)_3$, pure water. Lower curve: 1*M* $Al(NO_3)_3$, 7*N* HNO_3

The speed of reaction is $V = k\ (\mathrm{F}^-)^\alpha\ (\text{oxide})^\beta$

$$V = k(a_0 - x)^\alpha \left(b_0 - \frac{m}{n}x\right)^\beta$$

$$V' = k(a_0' - x)^\alpha \left(b_0 - \frac{m}{n}x\right)^\beta$$

for two different initial concentrations a_0 and a_0' and at $t = 0$

$$\alpha = \frac{\mathrm{Log}\left(\frac{V}{V'}\right)}{\mathrm{Log}\left(\frac{a_0}{a_0'}\right)}$$

Table II gives the values of α at $t = 0$ and as a function of x, the quantity of fluorine adsorbed on HfO_2 (mg of fluorine/g of HfO_2). α is found equal to 1, at least during reaction times of less than 15 minutes.

Elution of F^-. Figure 7 shows the elution of F^- by NaOH solutions of different concentrations, for 10 μg of F^- adsorbed from 7*N* nitric acid and washed with 10 cm^3 of water. More than 95% of the F^- is eluted by concentrated solutions of NaOH.

In Figure 8, we see the elution of F^- by 1*M* aluminum ni-

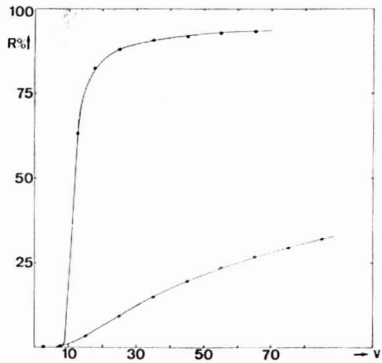


Figure 9. Yield of elution of F^- after adsorption from a 0.28*N* HNO_3 solution *vs.* the volume of $Al(NO_3)_3$ solution

Upper curve: 1*M* $Al(NO_3)_3$, pure water. Lower curve: 0.1*M* $Al(NO_3)_3$, pure water

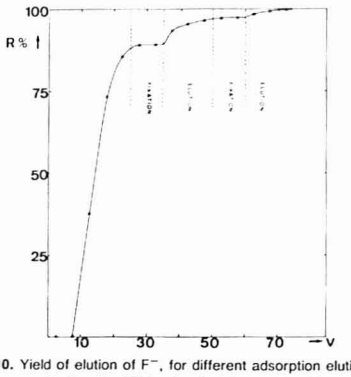


Figure 10. Yield of elution of F^-, for different adsorption elution cycles. In one cycle, inactive F^- is adsorbed from a 0.28*N* HNO_3 solution and eluted with 1*M* $Al(NO_3)_3$ (pure water)

trate solutions after adsorption from a 7*N* nitric acid solution: for the lower curve, the aluminum nitrate was dissolved in 7*N* nitric acid; and for the upper curve, it was dissolved in pure water.

In 7*N* nitric acid, the equilibrium is not reached after 100 ml, and at this moment only 30% of the F^- is eluted. When eluting with aluminum nitrate dissolved in water, the situation is similar, but about 85% of the F^- is eluted.

If F^- is adsorbed from dilute nitric acid solutions (*e.g.*, 0.28*N*), the elution is faster, and 90% of the F^- is eluted, as shown in Figure 9. Complete elution of F^- can be achieved by successive adsorptions and elutions, as shown in Figure 10.

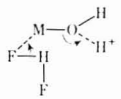
DISCUSSION

The curves in Figures 1 and 2 can be explained as follows: in weak acid medium (pH > 1), an ion-exchange mechanism takes place (*11*):

$$(F^-)\ \text{solution} + (OH^-)\ \text{oxide} \longrightarrow (F^-)\ \text{oxide} + (OH^-)\ \text{solution}$$

$$K_{eq} = \frac{(F^-)\ \text{oxide} \times (OH^-)\ \text{solution}}{(F^-)\ \text{solution} \times (OH^-)\ \text{oxide}}$$

and since $K_d = [(F^-)\ \text{oxide}]/[(F^-)\ \text{solution}]$, $\log K_d$ is proportional to the pH (Figure 2). When Al^{3+} is present, F^- is probably complexed as $(AlF)^{2+}$; this ion is not exchanged with OH^-, and there is no adsorption. In $0.1 < N_{HNO_3} < 3$, F^- is less adsorbed, probably because of the complexation with H^+ ions, more and more numerous in the solution. Above $N_{HNO_3} = 3$, a new mechanism of absorption takes place. We have studied the adsorption of fluoride ion on several oxides in 7*N* nitric acid (*12*) and shown that K_d decreases with the equilibrium constant of the complexes of fluorine with the corresponding metals. For instance, K_d (ZrO_2), K_d (HfO_2) > K_d (Nb_2O_5) > K_d (Al_2O_3) > K_d (SnO_2) > K_d (Sb_2O_5). A first-order mechanism, involving both the concentration of H^+ in the solution and the nature of the metal, should then be considered. It could be a simple nucleophilic substitution:



This explains the fact that in batch experiments, the results are the same with aluminum in solution or not, F^- being more complexed by Hf than by Al. In column experiments, the equilibrium is constantly displaced by formation of the Al complex, and F^- is slowly eluted. In basic medium, OH^- replaces F^-, which is then quickly eluted. It is to be noted that, after reaction on the surface, the penetration of F^- into the grains of HfO_2 is fast; indeed, as shown in Table I, it is apparently independent of the granulometry.

Application to the Determination of Oxygen in Ag, Co, and Cu. ^3He and ^4He are the particles of choice for the determination of oxygen, because they produce a very convenient radioisotope: ^{18}F.

Nuclear reactions also occur on the matrix itself, and if *Z* is the atomic number of the matrix element, radioisotopes of the elements *Z*, *Z* + 1, and *Z* + 2 (and sometimes *Z* − 1) are usually also produced. It is then necessary to perform a radiochemical separation of ^{18}F, to detect its radioactivity. We have shown that complete retention of ^{18}F on HfO_2 can be achieved but a systematic study of the retention of the other elements was also necessary. In Figure 11 we present the experimental results that we obtained for the adsorption from 7*N* nitric acid solution. With the help of this Table, we can tell from which type of matrix ^{18}F can possibly be cleanly separated, or not. For example, a good separation after irradiation of V or Cr (direct production of radioactive Mn) or irradiation of Fe (production of radioactive Mn with secondary neutrons) is not feasible by simple adsorption on HfO_2. On the contrary, such a separation is possible when the matrix is Ag, Co, Cu, or Ni.

After irradiation and etching, the samples were dissolved in concentrated nitric acid and in the presence of carriers of the different radioisotopes obtained. The solutions were brought to a volume of 20 cubic centimeters by addition of water and were divided into two equal parts. On the first part, we performed the solvent extraction of F^- as described in reference (*6*). The second part was passed through a column of HfO_2 as described in reference (*10*); this column was first washed with concentrated nitric acid. 100% of the ^{18}F is retained on the column which is then

(11) C. B. Amphlett, "Inorganic Ion Exchangers," Elsevier, Amsterdam, 1964, p 88.
(12) Bernard Vialatte, Ph.D. Thesis, University of Orsay, France, 1972.

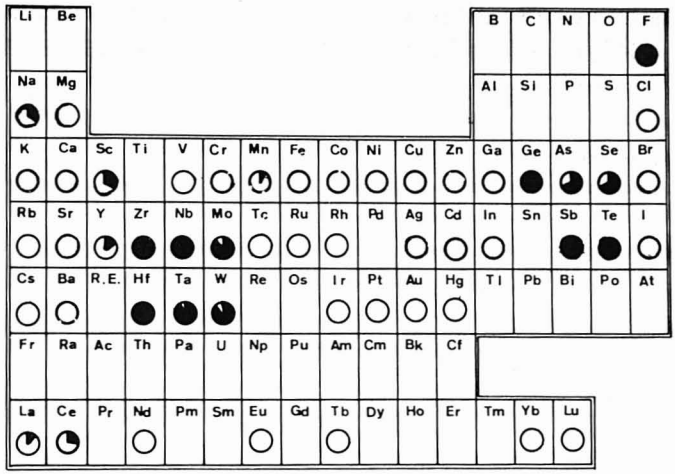


Figure 11. Adsorption on HfO_2 from 7*N* HNO_3

% of element adsorbed is proportional to the dark surface (*10*)

washed with ~40 cubic centimeters of concentrated nitric acid and in the presence of carriers of the radioisotopes produced on the matrix.

In Table III, we give our experimental results for the determination of oxygen in Ag, Co, and Cu; it can be seen that the two methods are in good agreement.

CONCLUSIONS

We have shown that a fast, simple, and reliable method, adsorption of F^- on HfO_2, can be used to determine oxygen in several matrixes. We feel that this method can be more easily automated than the solvent extraction method, and that it is then to be preferred when either of these two methods can be used.

This study is not complete, and we are currently developing it in two different directions: Use of other media (HCl, H_2SO_4), etc.; and elution of F^- after adsorption.

It is highly probable that excellent radiochemical separations of ^{18}F from many matrices will be achieved by fixation of F^- followed by elution with Al^{3+}. Indeed, few elements are adsorbed on HfO_2, and F^- should be eluted alone with an Al^{3+} solution. The problem here will be to be sure of the reproducibility, and of the value of the yield for the recovery of ^{18}F.

Table III. Determination of Oxygen in Ag, Co, and Cu[a]—Results in parts per million, weight

	Ag		Co		Cu	
Sample No.	Extraction	HfO	Extraction	HfO_2	Extraction	HfO_2
1	401	390	0.22	0.17	3.31	3.27
2	128	120	38.2	40.3	3.57	3.12
3	36.3	35.6	722	708	1.14	1.27
4			74.1	72.1	2.2	1.8
5					1.64	1.63

[a] Samples of different origin for the same metal.

RECEIVED for review January 11, 1974. Accepted April 15, 1974.

Sequential Determination of Radium-226, Radium-228, Actinium-227, and Thorium Isotopes in Environmental and Process Waste Samples

Donald R. Percival and Don B. Martin

Health Services Laboratory, U.S. Atomic Energy Commission, Idaho Falls, Idaho 83401

A procedure is described for the sequential determination of ^{226}Ra, ^{228}Ra, ^{227}Ac, thorium isotopes, and, in some cases, ^{231}Pa in environmental and process waste samples at 0.1 to 0.001 of the concentration guides specified by Federal regulations. The radionuclides are separated from gross sample constituents by coprecipitation with lead sulfate. Radium is separated on a small quantity of barium sulfate precipitated from a diethylenetriaminepentaacetate solution of the lead sulfate. Actinium-227 and thorium are then separated sequentially from the barium sulfate supernate by extraction into bis(2-ethylhexyl)phosphoric acid. Any one or more of the radionuclides may be excluded from the analysis by omitting certain independent steps. Over-all recoveries are 99% for radium and 95% for actinium and thorium. Accuracy, precision, and the effects of chemical and radiochemical interferences are discussed.

The radionuclides ^{226}Ra, ^{228}Ra, ^{227}Ac, and ^{230}Th, which concentrate in uranium mill wastes, are subject to stringent control by Federal regulations (*1*) and are included in the "Very Highly Hazardous Group" defined by Morgan *et al.* (*2*). Sensitive and specific radiochemical procedures are required for the detection of the specified nuclides at levels of a few disintegrations per minute in samples of minimum size and with relatively short counting times. The present procedure permits determination of up to eight different radionuclides on a single sample, including ^{231}Pa under certain conditions, and is designed to be applicable to the high concentrations of sulfates generally encountered in process wastes from uranium mills and potassium fluoride and pyrosulfate fusions commonly used to ensure complete sample decomposition (*3*).

Many methods for separating radium with the insoluble sulfates of barium or lead have been reported. Actinium can also be carried efficiently on lead sulfate (*4, 5*). Sill and Willis (*6, 7*) showed lead sulfate to be an efficient carrier for most cations with a charge greater than two and an ionic radius larger than about 1.0 a.u. The present procedure is based in part on a ^{226}Ra method developed previously in this Laboratory (*8*) involving an initial separation of radium with lead sulfate. Work reported previously for barium sulfate (*6, 7, 9–13*) was used to help define the conditions necessary for simultaneously separating actinium and thorium with radium using lead sulfate.

Previous work (*8*) showed that radium could be separated on a small quantity of barium sulfate precipitated by lowering the pH of an ethylenediaminetetraaceticacid or diethylenetriaminepentaacetic acid (DTPA) solution of the lead sulfate carrier. Weaver and Kapplemann (*14*) reported the preferential extraction of lanthanides over trivalent "actinides" (actinium was not included) into bis(2-ethylhexyl)phosphoric acid (HDEHP) from aqueous solutions containing lactic acid and DTPA. The homologous relationship between actinium and lanthanum suggested that actinium might be extracted into HDEHP directly from the barium sulfate supernate following the radium separation of the present procedure. Sato (*15*) showed that thorium was extracted into HDEHP from 10*M* nitric acid. In the present work, the addition of nitric acid and aluminum nitrate to the aqueous phase following the actinium separation makes it possible to recover the thorium in a single extraction with HDEHP.

The procedure provides a sequential separation scheme for radium, actinium, and thorium which is applicable to several important types of samples. The initial separation on lead sulfate discriminates against most of the elements likely to be encountered as gross constituents in environmental and process waste samples. These include the alkali metals and most of the elements in Groups IB through VIIB and Group VIII. The light rare earths and actinides which do carry on lead sulfate are discussed in the sections on chemical and radiochemical interferences. Further discrimination against certain elements is achieved with the HDEHP extractions.

EXPERIMENTAL

Apparatus. Radium-226 was determined by a direct de-emanation method using radon bubblers similar to those described by Rushing *et al.* (*16*) and radon scintillation cells described by Lucas (*17*). The cells are available commercially (Johnston Laboratories, Inc., Cockeysville, Md.).

Counting Techniques. All gross alpha counting was performed using a scintillation technique (*18*) and instruments described elsewhere (*13*). Scintillations from the Lucas cells were detected and recorded by established methods (*16, 17, 19*). Actinium-228, the beta-emitting daughter of ^{228}Ra, was counted on filtered cerium oxalate precipitates using a Beckman Widebeta II counter (Beckman Instruments, Inc., Fullerton, Calif.). Aqueous and organic solutions in polystyrene or glass bottles were gross gamma

(1) "Code of Federal Regulations," Title 10, Part 20, as revised January 1, 1968.
(2) K. Z. Morgan, W. S. Snyder, and M. R. Ford, *Health Phys.*, **10**, 151 (1964).
(3) C. W. Sill, *Anal. Chem.*, **33**, 1684 (1961).
(4) C. K. McLane and S. Peterson in "The Transuranium Elements," G. T. Seaborg, J. J. Katz, and W. M. Manning, Ed., Div. IV, Vol. XIV-B, Part II, McGraw-Hill, New York, N.Y., 1949, p 1371.
(5) N. E. Rogers and R. M. Watrous, *Anal. Chem.*, **27**, 2009 (1955).
(6) C. W. Sill and C. P. Willis, *U.S. At. Energy Comm. Rep.*, **IDO 12034** (1963).
(7) C. W. Sill and C. P. Willis, *Anal. Chem.*, **36**, 622 (1964).
(8) E. R. Ebersole, A. R. Harbertson, J. K. Flygare, Jr., and C. W. Sill, *U.S. At. Energy Comm. Rep.*, **IDO 12023** (1959, revised 1960).
(9) C. W. Sill and C. P. Willis, *Anal. Chem.*, **38**, 97 (1966).
(10) C. W. Sill, *Anal. Chem.*, **38**, 802 (1966).
(11) C. W. Sill, *Anal. Chem.*, **38**, 1458 (1966).
(12) C. W. Sill and R. L. Williams, *Anal. Chem.*, **41**, 1624 (1969).
(13) C. W. Sill, *Health Phys.*, **17**, 89 (1969).
(14) B. Weaver and F. A. Kapplemann, *J. Inorg. Nucl. Chem.*, **30**, 263 (1968).
(15) T. Sato, *J. Inorg. Nucl. Chem.*, **29**, 555 (1967).
(16) D. R. Rushing, W. J. Garcia, and D. A. Clark in "Radiological Health and Safety in Mining and Milling of Nuclear Materials," Vol. 2, *Int. At. Energy Agency Rep.*, **STI/PUB/78**, Vienna, 1964, p 187.
(17) H. F. Lucas, *Rev. Sci. Instrum.*, **28**, 680 (1957).
(18) N. A. Hallden and J. H. Harley, *Anal. Chem.*, **32**, 1861 (1960).
(19) R. L. Blanchard, *U.S. Pub. Health Serv.* **999-RH-9**, 1964.

counted in a 3-in. thallium-activated sodium iodide well crystal. Mounted alpha sources containing a gamma-emitting tracer were placed in a positioning holder at the top of the well crystal for gross gamma counting.

Reagents. *Bis(2-ethylhexyl)phosphoric Acid, 5 and 15%.* Wash 1 liter of 15% bis(2-ethylhexyl)phosphoric acid (V-C Chemical Co., Richmond, Va.) in *n*-heptane twice for 1 min with 200-ml portions of a 1 to 1 mixture of 2*M* diammonium citrate and concentrated ammonium hydroxide and twice with 200-ml portions of 4*M* nitric acid. Release the pressure which builds up with the first alkaline and first acid washes. Dilute 300 ml of the 15% reagent to 900 ml with *n*-heptane and wash twice with 4*M* HNO_3.

Aluminum Nitrate, 2M. Dissolve 750 g of $Al(NO_3)_3{\cdot}9H_2O$ in 450 ml of water plus 50 ml of concentrated nitric acid with heating. Filter the solution through double glass-fiber filters with suction and dilute to 1 liter. If thorium is to be electrodeposited, the traces of iron present in the aluminum nitrate must be removed. Extract the solution for 1 min with 100 ml of 15% HDEHP. Discard the organic and repeat the extraction with another 100 ml of HDEHP. Wash the aqueous phase twice with 100-ml portions of chloroform and once with 100 ml of *n*-heptane. Several hours are necessary for complete separation of the *n*-heptane phase.

Sodium Diethylenetriaminepentaacetate, 0.17M. Dissolve 67 g of diethylenetriaminepentaacetic acid (CHEL DTPA, Geigy Industrial Chemicals, Ardsley, N.Y.) and 32 g of sodium hydroxide pellets in 400 ml of water. Filter through double glass-fiber filters with suction and dilute to 1 liter with water. Adjust the pH to 10 with sodium hydroxide or perchloric acid. Store the solution in a polyethylene bottle.

Actinium Wash Solution. Dissolve 100 g of monochloroacetic acid, 10 g of DTPA, and 33 g of sodium hydroxide in water and dilute to 1 liter. Adjust the pH of the solution to 3 by adding sodium hydroxide pellets.

Cerium Carrier, 5 mg per ml. The cerium carrier is purified from ^{232}Th and its daughters by a procedure similar to one described elsewhere (*20*). Add solid divalent silver oxide (Handy and Harman Company, Bridgeport, Conn.) to 100 ml of 8*M* nitric acid until the solution remains black. Equilibrate 50 ml of this solution for 1 min with 50 ml of 15% HDEHP in a 125-ml separatory funnel and discard the aqueous layer. Dissolve 3.9 g of cerium nitrate hexahydrate, $Ce(NO_3)_3{\cdot}6H_2O$, in 50 ml of 8*M* nitric acid and add divalent silver oxide until the solution remains black. Immediately extract the cerium with the preequilibrated 15% HDEHP for 1 min. Discard the lower aqueous phase, add the remaining 50 ml of 8*M* nitric acid–divalent silver oxide preparation, and mix the phases for 1 min. Discard the aqueous layer and wash the organic phase for 30 sec with 50 ml of 8*M* nitric acid.

Strip the cerium from the organic phase for 1 minute each with two 10-ml portions of 4*M* nitric acid containing 1 ml of 30% hydrogen peroxide. Collect the aqueous layers in a clean separatory funnel, add 20 ml of *n*-heptane to the combined strip solutions, and mix the phases for 1 min. Drain the aqueous phase into a 100-ml beaker. Boil the solution for 5 min and dilute to 250 ml with 0.2*M* nitric acid. Recovery of cerium is about 99%.

Sulfuric–Hydrochloric Acid Solution. Add 100 ml of concentrated sulfuric acid and 40 ml of concentrated hydrochloric acid to 1 liter of water.

Lead Sulfate Wash Solution. Dissolve 25 g of anhydrous potassium sulfate in 1 liter of 1% sulfuric acid.

Tracer Studies. All developmental work was performed using radioactive tracers. The following gamma-emitting nuclides were used to facilitate the large number of experiments required. Thorium-234 was isolated carrier free by applying the present procedure to the wet-ashed eluate from a cation-exchange separation (*21*). The final oxalic acid solution containing the tracer was washed once each with 10 ml of chloroform and *n*-heptane, wet-ashed with perchloric acid, and diluted with 4*M* nitric acid. Actinium-228 was obtained by applying the present procedure to commercially available ^{228}Ra (Nuclear-Chicago, Des Plaines, Ill.), which had been separated and stored on barium sulfate. Americium-241 (New England Nuclear Corp., Boston, Mass.) and ^{239}Np prepared from ^{243}Am (*10*) were used as gamma tracers. Protactinium-233 was obtained as needed from a stock of its ^{237}Np parent (*11*).

The remaining tracers used were essentially pure alpha-emitters. Polonium-210, ^{233}U, and ^{239}Pu were studied only as radiochemical interferences and were determined only in final radium, actinium, and thorium fractions by gross alpha counting. Radium-226, determined both by a direct de-emanation technique and by gross alpha counting, was used to study radium.

Sample Preparation. The use of approximately 10^4 gamma counts per minute of ^{234}Th tracer is recommended to determine the thorium yield. However, uranium ores, mill tailings, and mill effluents sometimes contain enough ^{234}Th to cause a significant positive error in the yield determination. Such samples should be checked for ^{234}Th prior to analysis by gross gamma counting and by gamma spectrometry if necessary.

Ores, Mill Tailings, and Soils. Add 1 ml of ^{234}Th tracer and 2 ml of concentrated nitric acid to a 0.5-g sample in a 75-ml platinum dish and heat to near dryness. Continue the decomposition as described (*3*) beginning with the addition of hydrofluoric acid. Use 4 ml of concentrated sulfuric acid for transposition of the potassium fluoride fusion cake, and when the "cake has been completely disintegrated and the frothing has subsided," add 2 g of anhydrous sodium sulfate. Complete the decomposition as described (*3*).

Remove the pyrosulfate fusion cake (*3*) by flexing the sides of the platinum dish and tapping the bottom on a flat surface. Dissolve the cake in 60 ml of sulfuric–hydrochloric acid solution and 1 ml of 30% hydrogen peroxide in a 250-ml beaker. Boil the solution and continue as described below under "Separations on Lead Sulfate." For 1-g samples, use the same quantities of nitric and hydrofluoric acids but double the quantities of all other reagents including the sulfuric–hydrochloric acid solution.

For increased sensitivity in the determination of natural levels of activity in soils, a 5-g sample can be decomposed by a modification (*22*) to the procedure described above. Treat 5 g of soil with 10 ml of concentrated nitric acid and 10 ml of 48% hydrofluoric acid in a 250-ml platinum dish. Moisten the residue with 2 ml of 4*M* nitric acid, add 30 g of anhydrous potassium fluoride, mix the residue with the potassium fluoride, and fuse the sample. Transpose the potassium fluoride fusion cake with 35 ml of concentrated sulfuric acid and add 20 g of anhydrous sodium sulfate for the pyrosulfate fusion. Dissolve the pyrosulfate fusion cake in 500 ml of water, 30 ml of concentrated sulfuric acid, and 10 ml each of concentrated hydrochloric acid and 30% hydrogen peroxide in a covered 1-liter beaker containing two boiling chips. Heat the sample to boiling and continue as described below under "Separations on Lead Sulfate."

Air Dusts. Decompose polystyrene and cellulose filters as described (*23*) but substitute 1 ml of ^{234}Th tracer for the "lead–bismuth carrier," add 2 g of anhydrous sodium sulfate, and not less than 5 ml of concentrated sulfuric acid. Complete the decomposition of both types of filters by evaporating the solution until about 4 ml of sulfuric acid remains. Add 4.5 g of potassium sulfate and fuse the sample over a blast burner. Any turbidity is probably due to siliceous material and may be ignored at this point. Allow the flask to cool, add a boiling chip, and dissolve the pyrosulfate fusion cake in 60 ml of sulfuric–hydrochloric acid solution with heating. Boil the solution for 1 or 2 minutes and then cool. If decomposition of siliceous material is not desired, filter the solution, transfer the filtrate to a 250-ml beaker, add a boiling chip and 1 ml of 30% hydrogen peroxide, and heat the sample to boiling. Continue as described below under "Separations on Lead Sulfate."

When siliceous material is to be included in the analysis, dissolve the fusion cake as described above and transfer the solution and insoluble material to a 100-ml Lusteroid centrifuge tube with enough lead sulfate wash solution to make the total volume 60 to 70 ml. Centrifuge, decant the supernate into a 250-ml beaker, add a boiling chip and 1 ml of 30% hydrogen peroxide, and save the solution for later use. Transfer the insoluble material from the Lusteroid tube to a 75-ml platinum dish with five 1-ml portions of 48% hydrofluoric acid and evaporate the sample to dryness. Add 3 g of anhydrous potassium fluoride and continue as described above for 0.5-g samples of ores, mill tailings, and soils. Place the pyrosulfate fusion cake in the 250-ml beaker containing the original supernate. Add 60 ml of the sulfuric–hydrochloric acid solution, 1 ml of 30% hydrogen peroxide, heat the sample to boiling, and continue as described below under "Separations on Lead Sulfate."

With glass fiber filters, carry out the initial decomposition with hydrofluoric acid (*23*). Moisten the residue with up to 30 drops of concentrated nitric acid and heat just to dryness. Starting with the potassium fluoride fusion, complete the decomposition as described above for 0.5-g samples of ores, mill tailings, and soils.

(20) *U.K. At. Energy Auth. Rep., PG Rep.*, **685 (W),** Lancashire, England, 1965.

(21) C. W. Sill, *Anal. Chem.*, **36,** 675 (1964).

(22) C. W. Sill, K. W. Puphal, and F. D. Hindman, *Anal. Chem.*, **46,** 1725 (1974).

(23) C. W. Sill and C. P. Willis, *Anal. Chem.*, **37,** 1661 (1965).

Water and Mill Effluents. Acidify water and mill effluent samples in their original containers with 2 ml of concentrated hydrochloric acid for each 100 ml of sample. Mix thoroughly and allow the sample to stand overnight to recover readily acid-soluble forms of radium, actinium, and thorium which might have been adsorbed on the walls of the container or on sediments in the sample.

Place 510 ml of the acidified sample in a 1-liter beaker. Add two boiling chips, 1 ml of ^{234}Th tracer, 30 ml of concentrated sulfuric acid, and 40 g of anhydrous potassium sulfate. Cover the beaker with a watch glass, heat the sample to boiling, and continue as described under "Separations on Lead Sulfate." For other samples in the range of 1 to 0.1 liter, scale the quantities of sulfuric acid and potassium sulfate up or down proportionately.

Separations on Lead Sulfate. The boiling solutions obtained from each type of sample described above provide a common starting point for the separation of radium, actinium, and thorium on lead sulfate. Carry out the separation by adding 5 ml of 3.2% lead nitrate solution over a 20 sec (±5 sec) interval while stirring or swirling the boiling solution continuously. Boil the sample for 1 to 2 min and add a second 5-ml portion of lead nitrate solution in the same manner. Cover the beaker with a watch glass and boil the sample for 10 min with occasional swirling of the smaller samples. Cool the samples to at least room temperature in a bath of cold running water.

With ores, mill tailings, air dusts, and soils up to 1 g, transfer the contents of the beaker, except the boiling chip, to a centrifuge tube with lead sulfate wash solution and centrifuge at 2000 rpm for 5 min with this and all subsequent centrifugations. Continue as described in the last paragraph of this section.

With waters, mill effluents, and 5-g soils, filter the entire sample excluding the boiling chips through a 5.5-cm Whatman-40 paper using suction. Use lead sulfate wash solution to transfer the precipitate to the filter. Fold the filter and place it in a 125-ml Erlenmeyer flask. Wet-ash the filter with 5 ml of concentrated nitric acid and 2 ml of 72% perchloric acid. Add 4.5 g of anhydrous potassium sulfate, 2 g of anhydrous sodium sulfate, 4 ml of concentrated sulfuric acid, and fuse the sample over a high temperature blast burner. Any turbidity is probably due to siliceous material and may be ignored at this point. The best place to interrupt the procedure when the remaining steps cannot be completed on the same day is after the pyrosulfate fusion.

Add a boiling chip, 60 ml of sulfuric–hydrochloric acid solution, 1 ml of 30% hydrogen peroxide, and dissolve the fusion cake with heating. Boil the solution vigorously for 10 min with occasional swirling. Cool in a cold water bath for 10 min, transfer the contents of the flask, except the boiling chip, to a centrifuge tube, and centrifuge.

After centrifugation, decant and discard the supernate. Wash the precipitate with 25 ml of the lead sulfate wash solution, centrifuge, and discard the supernate. The lead sulfate contains radium, actinium, and thorium which are subsequently separated from lead and from one another.

Sequential Separations. Dissolve the lead sulfate in 15 ml of 0.17*M* DTPA with stirring and heating. Centrifuge the solution if silica or other insoluble material is present. If only thorium is to be determined, transfer the solution to a 125-ml separatory funnel with a Teflon stopcock, dilute to 50 ml with water, and continue as described below under "Thorium." Otherwise, transfer the solution to a 40-ml conical centrifuge tube containing 2 ml of 0.45% barium chloride dihydrate solution. Add 25 ml of concentrated nitric acid to the insoluble material centrifuged from the DTPA solution, and reserve for the thorium determination. If the ^{227}Ac separation is to be omitted, use only 20 ml of nitric acid.

Radium. Add 1 ml of 20% sodium sulfate solution to the 40-ml centrifuge tube and dilute with water to 28 ml. While swirling the solution, add 2 ml of 6*M* acetic acid. Heat the sample in a bath of boiling water for 5 min with occasional swirling during the digestion. Cool the sample for 5 min in a cold water bath. While swirling the sample continuously, add 4 drops of 0.45% barium chloride dihydrate solution with 5-sec intervals between drops. Cool for another 10 min and then centrifuge. If ^{227}Ac is to be determined, decant the supernate into a 100-ml beaker; if not, decant the supernate directly into a 125-ml separatory funnel with a Teflon stopcock, and reserve for the thorium determination.

Dissolve the barium sulfate in the 40-ml centrifuge tube in 7.5 ml of 0.17*M* DTPA with heat and stirring. Add 1 ml of 20% sodium sulfate and dilute with water to 19 ml. Reprecipitate the barium sulfate by adding 1 ml of 6*M* acetic acid and record the time of the reprecipitation. Beginning with the 5-min digestion, treat the sample exactly as it was treated with the initial barium sulfate precipitation and combine the second supernate with the first.

If ^{227}Ac is to be determined, filter the combined barium sulfate supernates through a 1-in. vinyl Metricel filter (DM-450, 0.45 μ, Gelman Instrument Co., Ann Arbor, Mich.) with suction. Transfer the filtrate to a 125-ml separatory funnel, add 7 ml of 2*M* monochloroacetic acid, and reserve for the ^{227}Ac determination. The total volume at this point should not exceed about 65 ml including any water used in the transfers and filtration. The reprecipitated barium sulfate contains all radium isotopes.

Radium-228. Add about 1 ml of water to the 40-ml centrifuge tube containing the barium sulfate and allow at least 20 hr for ingrowth of 6.13-hr ^{228}Ac. After the ingrowth period, dissolve the barium sulfate in 15 ml of 0.17*M* DTPA. Add 1 ml of 20% sodium sulfate, dilute to 28 ml with water, and reprecipitate the barium sulfate with 2 ml of 6*M* acetic acid. Record the time of this reprecipitation. Digest, cool, and scavenge with 4 drops of 0.45% barium chloride dihydrate solution as described above. Centrifuge the sample and decant the supernate into a 40-ml conical centrifuge tube, using up to 3 ml of rinse water to complete the transfer. Save the reprecipitated barium sulfate for the ^{226}Ra determination.

Add 2 ml of 0.45% barium chloride dihydrate solution to the centrifuge tube containing the supernate, swirl the tube vigorously, and digest the sample in a bath of boiling water for 5 min. Swirl the tube a few times during digestion. Cool the sample in a cold water bath for 5 min, centrifuge, and decant the supernate into a 125-ml separatory funnel containing 5 ml of 2*M* monochloroacetic acid, again using up to 3 ml of water to complete the transfer. Discard the barium sulfate scavenge.

Wash some 15% HDEHP for 1 min with an equal-volume portion of water and then with a one-half-volume portion of the actinium wash solution. Add 10 ml of the washed extractant to the 125-ml separatory funnel, mix the phases vigorously for 2 min, and discard the aqueous phase. Wash the organic phase for 1 min each with two 10-ml portions of the actinium wash solution and discard the aqueous phases.

Strip the actinium from the organic phase with two 10-ml portions of 1*M* nitric acid using mixing times of 1 min. Collect the strip solutions in a 40-ml centrifuge tube. Add 6 ml of saturated sodium acetate solution and 5 ml of 0.2*M* diammonium oxalate to the centrifuge tube and swirl. Heat the sample for 5 min in a bath of boiling water, add 1 ml of cerium carrier, and continue heating with occasional swirling for another 5 min.

Cool the sample in a bath of cold water for 10 min. Suspend the cerium oxalate precipitate in the solution and pour the contents of the tube into a filtering chimney assembly (*12*) containing a 47-mm DM-450 filter. Use a little 0.02*M* diammonium oxalate to complete the transfer. Apply gentle suction until the liquid has been drawn through the filter. Wash the precipitate by interrupting the suction, adding about 10 ml of 0.02*M* diammonium oxalate to the chimney, and reapplying suction. Repeat the wash with about 20 ml of ethanol and remove the filter while it is still wet. Place the filter in an appropriate holder such as an aluminum disk with a lipped-retainer ring and dry under a heat lamp at a distance of about 10 in. Count the sample in a low-background beta counter and calculate the ^{228}Ra activity.

Radium-226. Radium-226 in the reprecipitated barium sulfate can be determined by gross alpha counting or by an emanation method. The gross counting method is generally adequate for screening purposes.

Gross Counting. Dissolve the barium sulfate in 7.5 ml of 0.17*M* DTPA, filter the solution through a 1-in. DM-450 filter with suction using enough water to bring the total volume to about 20 ml, and collect the filtrate in a 40-ml conical centrifuge tube. Add 1 ml of 20% sodium sulfate and 1 ml of 6*M* acetic acid. Digest, cool, and scavenge with 4 drops of 0.45% barium chloride dihydrate solution as described above. Centrifuge and discard the supernate. Add 2 ml of 0.5% sulfuric acid and disperse the precipitate with a stirring rod. Add about 20 ml of 95% ethanol, mix, filter, and dry the precipitate (*12*). Mount and count the barium sulfate (*13*). Differential decay analysis (*24–26*) or an alpha spectrum of the barium sulfate precipitate is often adequate to determine the isotopic radium composition.

Emanation Method. Dissolve the barium sulfate in 7.5 ml of 0.17*M* DTPA as described above. Transfer the solution to a radon bubbler and proceed using an established method (*16*).

(24) J. Sedlet in "Treatise on Analytical Chemistry," I. M. Kolthoff and P. J. Elving, Ed., Part II, Vol. 4, Interscience, New York, N.Y., 1966, p 309.
(25) H. W. Kirby, *Anal. Chem.*, **26**, 1063 (1954).
(26) J. R. Rosholt, Jr., and J. R. Dooley, Jr., *Anal. Chem.*, **32**, 1093 (1960).

Actinium-227. Beginning with the HDEHP extraction, follow the directions given above for ^{228}Ac in the determination of ^{228}Ra with the following exceptions. Transfer the aqueous phase after the extraction to a 125-ml separatory funnel and reserve for the thorium determination. Precede the two 10-ml washes of the organic phase with a 5-ml wash and add the 5-ml wash to the thorium fraction. Record the time of the first 1*M* nitric acid strip. Place the filter on a 2-in. nylon disk and dry under a heat lamp. Mount the filter for alpha counting (*13*).

A precipitate prior to the addition of cerium carrier indicates the presence of the light rare earths; 0.5 mg of lanthanum or cerium show a very distinct turbidity. If more than a slight turbidity appeared, weigh the filter before it is mounted for counting and compare the weight with that of the blank. Assume that the additional mass is due to cerium indigenous to the sample and correct the counting efficiency for increased self-absorption. Fourteen days after completion of the first strip, the total alpha disintegration rate of the sample will be equal to the disintegration rate of ^{227}Ac. If desired, the build-up of alpha activity may be followed and checked against the theoretical factors in Table XIV of reference (*27*).

Thorium. Centrifuge the tube containing the insoluble material which remained after dissolution of the lead sulfate in DTPA and decant the nitric acid wash into the separatory funnel containing the thorium fraction. If no insoluble material was present, add 20 ml of concentrated nitric acid, or 25 ml if ^{227}Ac was separated, directly to the separatory funnel. Add 10 ml of 2*M* aluminum nitrate and 1 ml of 30% hydrogen peroxide, and shake the funnel vigorously. Loosen the stopper and allow the sample to stand for 10 min.

Wash some 5% HDEHP for 1 min with a one-half-volume portion of 4*M* nitric acid. Add 10 ml of the washed extractant to the separatory funnel and contact the phases vigorously on a mechanical shaker for 15 min. Allow 5 min for phase separation and discard the aqueous phase. Add 10 ml of 4*M* nitric acid and 10 drops of 30% hydrogen peroxide to the separatory funnel, mix the phases for 1 min, and discard the aqueous phase. Repeat the wash with another 10 ml of 4*M* nitric acid but omit the hydrogen peroxide.

Rinse both the inside and outside of the separatory funnel stem with a stream of water from a squeeze bottle. Add 10 ml of toluene and 6 ml of 0.4*M* oxalic acid to the separatory funnel and mix the phases vigorously for 2 min. Allow 5 min for separation of the phases and look for a fine white precipitate. If a precipitate is observed, refer to the section below on "Special Problems from Thorium-232"; if not, transfer the aqueous phase to a cell for electrodeposition of thorium or to a 40-ml centrifuge tube for carrying and counting of thorium on barium sulfate. Repeat the strip with 8 ml of 0.4*M* oxalic acid and combine the second aqueous phase with the first. Discard the organic and treat the combined oxalic acid strip solutions as described below.

Electrodeposition of Thorium. Add 3 drops (*ca.* 0.15 ml) of 1*M* ammonium DTPA and 2 ml of saturated ammonium chloride to the combined oxalic acid strip solutions in the electrodeposition cell. Beginning with the pH adjustment, complete the electrodeposition as described by Puphal and Olsen (*28, 29*). Before alpha-counting the sample, obtain a gamma count and determine the thorium yield.

Carrying and Counting Thorium on Barium Sulfate. Heat the 40-ml centrifuge tube containing the combined oxalic acid strip solutions for 5 min in a bath of boiling water. Add 2 ml of 0.45% barium chloride dihydrate solution and 10 ml of 10% potassium sulfate–20% sulfuric acid with swirling. Continue heating for no less than 15 min with occasional swirling. Cool the sample in a cold water bath for 5 min, scavenge with 4 drops of 0.45% barium chloride dihydrate solution, and cool for another 10 min. Centrifuge and discard the supernate. Wash the precipitate with 10 ml of 0.5% sulfuric acid, centrifuge, and discard the wash supernate. Filter the barium sulfate and mount it for gross alpha counting (*12*). Before alpha-counting the sample, gamma-count it and determine the thorium yield.

Special Problems from Thorium-232. The appearance of a fine white precipitate during the stripping of thorium indicates that the sample contained at least 1.5 mg of ^{232}Th. In such cases, the subsequent electrodeposition or carrying of thorium by barium sulfate will be seriously incomplete. When milligram quantities of thorium are observed, two courses of action may be taken. The first is to reduce the sample size by a factor of at least 20. Alternatively, complete the two oxalic acid strips and then wash the organic phase for 1 min with two 10-ml portions of 9*M* sulfuric acid. Combine the washes with the oxalic acid strips and check the thorium yield by gamma counting. If the yield is satisfactory, add 2 ml of 72% perchloric acid and evaporate the solution until about 5 ml of sulfuric acid remain. Cool and dilute to 25 ml with 0.5% sulfuric acid. Rerun an aliquot of the solution if not more than 0.1 mg of ^{232}Th is present for electrodeposition or 0.2 mg for carrying on barium sulfate.

RESULTS AND DISCUSSION

Distribution Studies. Distributions of the three elements being determined were studied using ^{226}Ra, ^{228}Ac, and ^{234}Th tracers. Material balances of 100 ± 2% accounted for all the tracer added in each study. A schematic diagram of the procedure is shown in Figure 1, and the values in Table I are representative of the approximate distributions to be expected for radium, actinium, and thorium. The variations of the distributions, in most cases, result in an increase or decrease of about 2% in the final recovery of actinium or thorium and about 1% in that of radium.

Radiochemical Interferences. The major radiochemical interferences likely to be encountered in the sample types for which the procedure is intended are members of the three naturally occurring decay series. The procedure was designed with this in mind and special emphasis was placed on separation of the elements being determined from one another. Plutonium-239, ^{239}Np, and ^{241}Am were included to show the limitations of the procedure if applied to samples containing high activities of transuranium elements. The decontamination factors summarized in Table II were obtained on both 500-ml water samples and 0.5-g samples of dunite. Only one value is shown because, in every case, the results were approximately the same for both liquid and solid samples. Decontamination factors for the ^{228}Ac fraction from which ^{228}Ra is determined are greater than those shown for ^{227}Ac. The factors given in the column for radium apply only when radium is gross counted on barium sulfate since an emanation method would provide theoretically infinite decontamination factors. The results shown are the minimum values to be expected when the procedure is applied exactly as described.

Of the elements studied, protactinium, neptunium, and plutonium are potentially serious interferences in the final thorium fraction. Decontamination factors of only 1.3 to 1.1 actually correspond to recoveries of about 70 to 90% for these three elements. In fact, with certain types of samples discussed below, the recovery of protactinium is equal to that of thorium. However, the three elements will not be mistaken for thorium if alpha spectrometry is employed.

Chemical Interferences. The most serious effect of chemical interferences is associated with the recovery of thorium on lead sulfate. In the case of liquid samples, any complexing agent which is effective for lead, radium, actinium, or thorium will interfere with the quantitative recovery of the element(s). However, the low pH and high sulfate concentration employed with the lead sulfate precipitation eliminate the successful competition of most complexing agents for all four elements. One exception is the chloride anion which effectively complexes lead, but the recovery of carrier-free ^{234}Th on 200 mg of lead is unaffected by chloride concentrations as high as 0.6*M*.

Since ^{232}Th was known to be its own worst interference (*7*), it was studied both separately and in combination with other potential interferences. Various quantities of ^{232}Th were carried through the procedure described for 0.5-g solid samples beginning with the pyrosulfate fusion. Losses of thorium in the lead sulfate supernate and lead sulfate

(27) H. W. Kirby in "Analytical Chemistry," H. A. Elion and D. C. Stewart, Ed., Progress in Nuclear Energy Series IX, Vol. 8, Part 1, Pergamon Press, Oxford, 1967, p 89.
(28) K. W. Puphal and D. R. Olsen, *Anal. Chem.*, **44**, 284 (1972).
(29) K. W. Puphal and D. R. Olsen, *Anal. Chem.*, **44**, 1301 (1972).

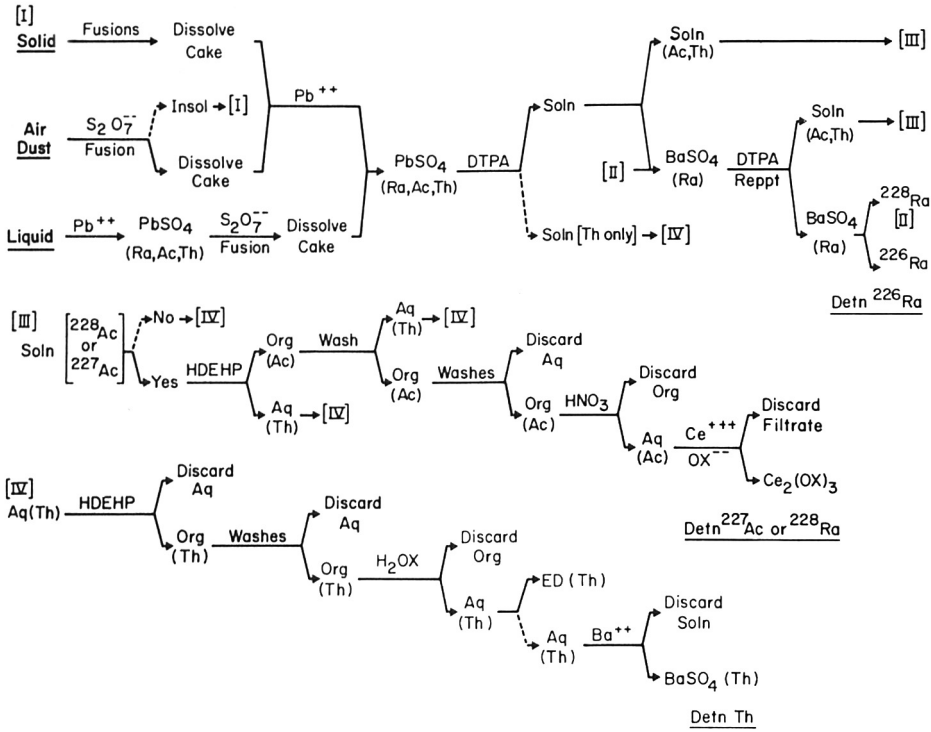


Figure 1. Diagram of radium, actinium, and thorium procedure. Dashed lines indicate options. See text for ^{226}Ra and ^{228}Ra options

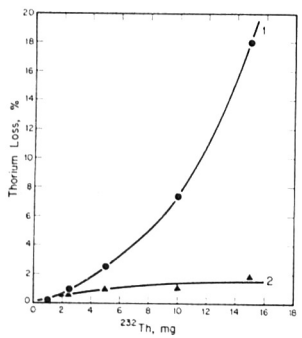


Figure 2. Loss of thorium *vs.* milligrams of ^{232}Th present

(1) Loss in lead sulfate supernate. (2) Loss in wash of lead sulfate

wash are shown in Figure 2. The loss in each fraction is less than 1% up to 2.5 mg of ^{232}Th, a quantity approximately 12 times that which can be carried on 5 mg of barium as the sulfate and 25 times that which can be electrodeposited. Losses of thorium with 500-ml water samples are not as severe as those shown in Figure 2, up to 10 mg of thorium being recovered to the extent of 98 to 99%. Beyond 10 mg, the losses increase rapidly. Additional losses of thorium through the remainder of the procedure are similar to those shown in Table I up to and including the HDEHP extraction. Radium and actinium recoveries on the lead sulfate will be complete, provided that no more than 2.5 mg of thorium is present.

The effects of various elements on the recovery of ^{226}Ra, carrier-free ^{234}Th, and 1 mg of ^{232}Th with lead sulfate are summarized in Table III. Recovery of actinium was as good or better than that of carrier-free ^{234}Th. Losses in the lead sulfate wash solutions were generally less than those shown for the lead sulfate supernates. The studies were carried out as described above for various quantities of thorium. At the levels shown, none of the elements studied interfered seriously with the recovery of radium or thorium. However, some of the elements which precipitate as sulfates or are carried by lead sulfate constitute potential interferences in subsequent steps of the procedure.

Cerium and lanthanum are carried by lead sulfate or, when present above a few milligrams, precipitate as potassium sulfato salts. Both elements accompany ^{227}Ac, precipitate as oxalates, and decrease the alpha counting efficiency for ^{227}Ac and its daughters. Similarly, about 5 mg of an original 100 mg of calcium carries through into the final ^{227}Ac fraction and causes a decrease in counting efficiency.

Strontium and barium indigenous to the sample will be present in the final radium fraction. Therefore, the counting efficiency must be corrected when using gross alpha

Table I. Approximate Distributions of Radium, Actinium, and Thorium in Recommended Procedure for All Sample Types

Fraction	Element present, % Ra	Ac	Th
First $PbSO_4$ supernate	0.6	0.2	0.6
Second $PbSO_4$ supernate[a]	<0.1	<0.1	<0.1
$PbSO_4$ wash	<0.1	<0.1	<0.1
Reprecipitated $BaSO_4$[b]	99 ± 1	1.0	
Combined $BaSO_4$ supernates[c]	0.3		
Aqueous after Ac extraction		0.6	
Combined washes of Ac extract		0.4	0.1
Ac organic after strips		0.5	0.7
$Ce_2(C_2O_4)_3$ supernates and wash		0.3	
$Ce_2(C_2O_4)_3$ precipitate[d]		97 ± 2	
Aqueous after Th extraction			0.4
Combined washes of Th extract			0.2
Th organic after strips			0.2
Separatory funnel and stopper			0.8
$BaSO_4$ supernates and wash			0.9
$BaSO_4$ precipitate			96 ± 2
Aqueous after Th electrodeposition			1.0
Electrodeposition plate			96 ± 2

[a] Corresponds to the only $PbSO_4$ supernate with solid samples except soils. [b] Decrease to 98% when gross counting Ra fraction on $BaSO_4$. The Ac is reduced from 1 to about 0.005% by a second reprecipitation and filtration. [c] Removed by filtration prior to ^{227}Ac extraction. [d] Decrease to 95% for the determination of ^{227}Ac when sample decomposition requires a pyrosulfate fusion in platinum. Decrease to 94% for ^{228}Ac in the determination of ^{228}Ra due to additional losses in $BaSO_4$ reprecipitation and scavenge.

Table II. Radiochemical Decontamination Factors

Tracer	Final fraction Radium	Actinium-227	Thorium
^{226}Ra		1×10^5	$>1 \times 10^5$
^{228}Ac	2×10^4		4×10^4
^{234}Th	1×10^5	1×10^5	
^{210}Po	$>1 \times 10^4$	$>1 \times 10^4$	$>1 \times 10^5$
^{233}Pa	4×10^4	8×10^4	1.1
^{232}U	$>1 \times 10^4$	$>8 \times 10^4$	$>4 \times 10^4$
^{239}Np	1×10^5	1×10^5	1.3
^{239}Pu	$>1 \times 10^5$	$>1 \times 10^5$	1.2
^{241}Am	$>1 \times 10^5$	55	1×10^6

Table III. Effect of Various Elements on the Recovery of Radium and Thorium with Lead Sulfate

Element	Quantity, mg	Losses in lead sulfate supernate, %[a] ^{226}Ra	^{232}Th	1-mg ^{232}Th
Al	100	0.08	0.2	0.1
Ba	10		0.3	0.1
Bi	10		0.01	0.08
	100	0.1	0.01	0.01
Ca	100	0.1	0.2	0.2
Ce	1		0.1	0.5
	25		0.09	0.2
Fe	250	0.07	0.1	0.03
La	0.1		0.01	0.1
	1	0.08	0.05	0.3
	5		0.6	0.8
	10	0.2	0.5	0.6
Mn	100	0.1	0.09	0.09
Nb	100	0.04	0.1	0.02
P	100	0.06	0.2	0.2
Sc	10	0.2	0.01	0.1
Sr	50	0.1	0.05	0.05
Ta	10	0.4	0.1	0.2
Ti	100	0.08	0.1	0.07
Y	100	0.09	0.1	0.1
Zr	50	0.1	0.3	0.3
Th	1	0.1	...	...

[a] Error associated with each result *ca.* 0.03.

counting to determine radium in samples containing significant quantities of these elements—*i.e.*, soils which contain about 0.6 mg of barium and 0.4 mg of strontium per gram of sample (*30*).

If present in the sample at levels equal to or greater than those shown in Table III, some of the niobium, tantalum, scandium, and zirconium accompany the lead sulfate and precipitate in the alkaline DTPA solution. Losses of radium, actinium, and thorium result, the worst case being tantalum whose precipitate will contain about 5% of each of the three elements. Thorium will be recovered when the precipitate is washed with the concentrated nitric acid used in the thorium extraction. However, scandium and zirconium will follow thorium through the remainder of the procedure and might interfere with its electrodeposition or carrying on barium sulfate.

Except for oxygen, sodium, magnesium, silicon, and potassium, all of the more abundant and some of the less abundant elements present in soils (*30*) were studied. High concentrations of sodium and potassium are an integral part of the procedure and silicon from silica and silicates in solid samples is eliminated during transposition of the potassium fluoride fusion cake. Those elements including magnesium which did not interfere under the conditions used by Sill and Willis (*6*) were not reexamined since the present procedure is less sensitive to even the most serious interferences reported for both barium and lead sulfates.

The quantities of each element studied correspond to about two to several thousand times the concentrations likely to be encountered in an average soil. The results for individual elements cannot be directly related to what might be expected from a combination of elements, particularly in ores and mill tailings where composition and concentrations vary widely from those of an average soil. However, the present procedure has been applied without difficulty to 5-g samples of several different soils, up to 1 g of pitchblende and uraninite ores, sand and slime tailings, and many other unclassified tailings from uranium milling operations.

Accuracy and Precision. Accuracy and precision were studied by analyzing samples of a pitchblende ore in which both natural uranium chains were thought to be present in secular equilibrium. Volumetric uranium analyses of the ore gave a U_3O_8 content of 0.973% (*23*) which is equivalent to 6059 dpm of ^{238}U per gram of ore. Replicate analyses for ^{210}Pb and ^{210}Po (*23*) gave results of 5963 ± 25 and 6000 ± 180 dpm/g, respectively. The agreement among the ^{238}U, ^{210}Pb, and ^{210}Po results obtained from three different independent analytical methods indicated that members of the ^{238}U series were at or very near secular equilibrium. Assuming equilibrium in the ^{235}U series, the activity of each chain member was calculated to be 283 dpm/g.

Since proof of secular equilibrium in the two uranium chains would constitute proof of the accuracy of the analytical methods used, various quantities of the ore were analyzed in duplicate for ^{226}Ra, ^{227}Ac, ^{227}Th, ^{230}Th, and ^{231}Pa. The results are summarized in Table IV, and an alpha spectrum of the electrodeposited thorium fraction is shown

(30) V. P. Vinogradov, "The Geochemistry of Rare and Dispersed Chemical Elements in Soils," 2nd ed., Engl. trans., Consultants Bureau Inc., New York, Chapman and Hall Ltd., London, 1959.

Table IV. Results of Pitchblende Analyses

Sample, g	dpm/g				
	^{230}Th	^{226}Ra	^{231}Pa	^{227}Ac	^{227}Th
0.10	6184 ± 95	6088 ± 78	283 ± 11	298 ± 11	279 ± 13
0.10	6044 ± 93	6190 ± 29	297 ± 11	271 ± 11	282 ± 11
0.25	6178 ± 77	6046 ± 20	294 ± 10	274 ± 7	290 ± 9
0.25	6142 ± 76	6046 ± 21	298 ± 10	272 ± 7	296 ± 9
0.50	6224 ± 70	6122 ± 14	270 ± 8	278 ± 5	291 ± 8
0.50	6120 ± 69	6072 ± 12	277 ± 8	277 ± 5	285 ± 8
1.00	6255 ± 61	5994 ± 11	266 ± 6	277 ± 3	284 ± 6
1.00	6224 ± 61	6038 ± 10	276 ± 7	273 ± 3	285 ± 6
$m \pm s$	6174 ± 71	6075 ± 60	283 ± 12	278 ± 9	287 ± 5
$\pm s_m$	± 25	± 21	± 4	± 3	± 2
$(m \pm s_m)$/ calculated[a]	1.019 ± 0.004	1.003 ± 0.003	1.000 ± 0.014	0.982 ± 0.011	1.014 ± 0.007

[a] Calculated dpm/g = 6059 for the ^{238}U series and 283 for the ^{235}U series.

Table V. Results of Process Waste Analyses, Concentration,[a] μCi/ml × 10^7

^{230}Th	^{227}Th	^{229}Th	^{227}Th	^{231}Pa	^{227}Ac	^{228}Ra	^{226}Ra
1260	0.98	0.48	5.45	1.73	5.62	0.44	2.78
1190	1.02	0.46	5.36	4.08	5.84	0.44	2.66
1200	0.82	0.43	4.98	11.08	5.97	0.44	2.61
1130	0.93	0.63	5.08	13.14	6.26	0.46	2.86
1200	1.03	0.52	4.85	9.55	6.08	0.45	2.71
1196 ± 46	0.96 ± 0.09	0.50 ± 0.08	5.14 ± 0.25	...	5.95 ± 0.24	0.45 ± 0.01	2.72 ± 0.10

[a] Values at the bottom of each column are $m \pm s$.

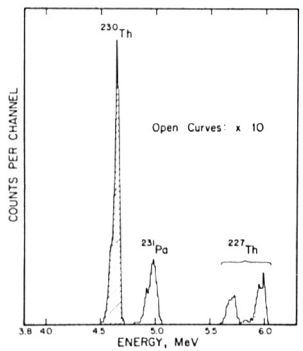


Figure 3. Alpha spectrum of the electrodeposited thorium fraction from a pitchblende ore

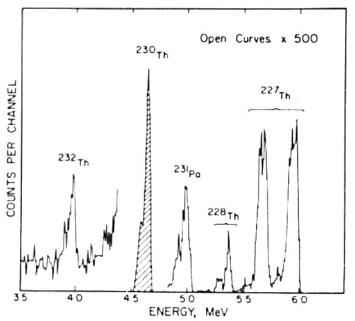


Figure 4. Alpha spectrum of the electrodeposited thorium fraction from a uranium mill effluent

in Figure 3. The mean thorium recovery for the eight samples shown in Table IV was 95.8 ± 1.8% with a range of 94 to 99%. The ^{231}Pa recoveries were assumed to be equal to the corresponding thorium recoveries, and the results were included to demonstrate the reliability of the procedure for the determination of protactinium in solid and air dust samples from which silica has been removed by a potassium fluoride fusion and transposition to a pyrosulfate fusion. Assumed recoveries of 99 ± 1% and 95 ± 2% were used in calculating the results for ^{226}Ra and ^{227}Ac, respectively.

The experimental means (m) and standard deviations of individuals about the mean (s) and of the mean itself (s_m) are shown at the bottom of each column in Table IV. In terms of relative uncertainties of individual results about the mean, the precision for ^{230}Th and ^{226}Ra was 1%, while it was 2 to 3% for ^{231}Pa, ^{227}Ac, and ^{227}Th. The larger uncertainties were due in part to the much lower activities and, therefore, poorer counting statistics for the ^{235}U chain members. The ratios of the means from this series of analyses to the dpm/g values calculated from the volumetric uranium results are sufficiently close to unity to further strengthen the assumption of secular equilibrium for the ^{238}U and ^{235}U chains present in this ore sample. Of equal importance, the ratios indicate that the procedure can provide results which are accurate to within 1 to 2% when a sample is analyzed in replicate. An analysis of variance on the four duplicate results for each radionuclide showed

that their means were equal except for ^{231}Pa where the F ratio was barely significant.

Additional data were obtained on precision by applying the procedure to 500-ml samples of a uranium mill process waste known to contain about 3 mg of cerium and four times the 100-μg limit for the electrodeposition of ^{232}Th. This sample was chosen to represent one of the worst cases for the determination of thorium. The results of the five replicate analyses are summarized in Table V, and an alpha spectrum of the thorium fraction is shown in Figure 4. Alpha spectra were obtained under the conditions described by Sill and Olson (*31*) to minimize recoil atom contamination of the solid state detector. The counting efficiency for the ^{227}Ac fractions was reduced to correct for the additional precipitate formed from cerium present in the sample. Thorium recoveries were determined with ^{234}Th tracer and ranged from only 8 to 25% because of large losses in the electrodeposition.

In spite of the large thorium losses, the relative deviation of an individual result from the mean was only 4% for ^{230}Th, but 9, 16, and 5% for ^{232}Th, ^{228}Th, and ^{227}Th, respectively. A major factor in the variance of the ^{232}Th results was the large correction applied for the contribution of degraded ^{230}Th alpha particles in the ^{232}Th energy region. The relative uncertainties of just the numbers of counts were approximately 8 to 12% and 2 to 4% in the ^{228}Th and ^{227}Th energy regions, respectively. The wide variance of the results for ^{231}Pa was due to its large and erratic losses on silica from the process waste sample and also in the electrodeposition. In such cases, thorium recoveries are not reliable estimates of ^{231}Pa recoveries, and the results were included in Table V merely to emphasize this point. The relative deviations of individual results about the means for ^{227}Ac, ^{228}Ra, and ^{226}Ra were 2 to 4%, about the same as the precision for ^{227}Ac and ^{226}Ra in the series of pitchblende ore analyses.

Sensitivity. The following detection limits for 500-ml liquid and 100-m^3 air samples were calculated for paired observations (*32*) and are merely intended to illustrate the sensitivities of the procedure under the conditions specified.

The blank activity for the determination of ^{226}Ra by either gross-alpha counting or the emanation method is about 25 cph, which results in detection limits for gross counting and emanation counting, respectively, of 1×10^{-9} and 3×10^{-10} μCi/ml for liquid samples and 4.5×10^{-15} and 1.4×10^{-15} μCi/ml for air samples. The ^{228}Ra blank of about 195 counts per 50 minutes is equivalent to a detection limit of 2.5×10^{-9} μCi/ml for a liquid sample and 1.2×10^{-14} μCi/ml for an air sample. However, decay of the 6.13-hour ^{228}Ac used for the indirect determination of ^{228}Ra results in a practical detection limit 1.5 to 2 times these values. The blank for ^{227}Ac is about 7 cph, and the detection limit is 6×10^{-10} μCi/ml for liquid and 3×10^{-15} μCi/ml for air samples. Gross alpha blanks of thorium fractions are roughly 25 cph making the detection limit 9×10^{-10} μCi/ml and 5×10^{-15} μCi/ml for liquid and air samples, respectively. The detection limits for individual thorium isotopes determined by alpha spectrometry may be higher or lower than for gross counting depending on the presence or absence of interferences from higher energy alpha emitters. The detection limits given above represent 1×10^{-4} to 3×10^{-4} of RCG for 500-ml liquid samples and 5×10^{-2} to 7×10^{-4} of RCG for 100-m^3 air samples.

RECEIVED for review December 3, 1973. Accepted June 13, 1974.

(31) C. W. Sill and D. G. Olson, *Anal. Chem.*, **42**, 1596 (1970).

(32) L. A. Currie, *Anal. Chem.*, **40**, 586 (1968).

Excited Singlet State Acidity Constants for Hydroxy and Amino Substituted Anthraquinones and Related Compounds: A Comparison of Excited-State p*K* Measurement Procedures

H. H. Richtol and B. R. Fitch

Department of Chemistry, Rensselaer Polytechnic Institute, Troy, N.Y. 12181

Excited singlet state acidity constants of hydroxy and amino derivatives of anthraquinones, fluorenes, fluorenones, and a xanthone were investigated in 33% dioxane–water. The excited singlet state acidity constants were determined by four methods. Three of these are based on the experimental determination of the energy differences between the excited state acidic and basic forms measured by absorption, fluorescence, and by an average of absorption and fluorescence energies. The fourth method involved the measurement of fluorescence intensity as a function of solution acidity. Experimental values showed increases in acidity of from 5 to 16 orders of magnitude over the ground state. Values obtained from fluorescence titration of both conjugate acid and base forms and from the averaging of fluorescence and absorption data give the best internal agreement.

Initial observation of "abnormal" fluorescence due to protolytic dissociation was reported by Weber (*1*). The effect was interpreted by Förster (*2*) who first demonstrated the occurrence of excited state dissociation with solutions of hydroxy- and amino-pyrene sulfonates.

Weller (*3*) outlined a method whereby the value of pK^* can be estimated from absorption and fluorescence spectra, if equilibrium is established in the excited state. He was able to calculate the value of pK^* provided the value of the ground state pK was known independently.

Bartok, Lucchesi, and Snider (*4*) measured the effects of

(1) K. Weber, *Z. Phys. Chem.* (*Leipzig*), **B15**, 18 (1931).
(2) Th. Forster, *Z. Elektrochem.*, **54**, 42 (1950).
(3) A. Weller, *Z. Elektrochem.*, **56**, 662 (1952).
(4) W. Bartok, P. J. Lucchesi, and N. S. Snider, *J. Amer. Chem. Soc.*, **84**, 1842 (1962).

electronic dissociation of para-substituted phenols, estimating the values of pK^* from spectroscopic data. They found that apart from large increases in acidity as a result of excitation, the dissociation constants of the excited phenols could not be correlated.

Haylock, Mason, and Smith (*5*), carried out a critical examination of the methods employed for determining the prototropic equilibria of electronically excited molecules. Mason *et al.* (*6*) state that the theoretical values of the acid dissociation constant of an excited-state equilibrium calculated from absorption and emission data may differ one from the other by as much as six pK_a units, and both may diverge substantially from the value obtained experimentally from the variation of the fluorescence spectrum with the acidity function of the medium.

Wehry and Rogers (*7*) measured protolytic dissociation of phenol and numerous monosubstituted phenols in the lowest triplet and first excited singlet states by means of fluorescence, phosphorescence, and ultraviolet absorption spectra. It was shown that excited state acidities can be correlated well with ground state substituent constants. Schulman and Fernando (*8, 9*) have measured the excited state pK's of halogenated 8-quinolinols by the fluorimetric titration method. Using the Hammett acidity scale they were able to determine pK^* values as low as minus eleven. Goldman and Wehry (*10*), having disputed the excited state equilibrium hypothesis, studied the fluorescence of 8-quinolinol in several media and concluded that the quenching of 8-quinolinol fluorescence is due to hydrogen bonding by hydrolytic solvents. However, Schulman (*11*) defended the excited state prototropic equilibrium hypothesis stating that while hydrogen bonding is probably of considerable importance in determining the quantum yields of the various species derived from 8-quinolinol in different solvents, the fluorescence phenomena observed in solutions of differing acidities and basicities are due primarily to prototropic equilibria in the lowest excited singlet states of the various prototropic species derived from 8-quinolinol.

Rosenberg and Brinn (*12*) have determined singlet excited state dissociation rate constants for naphthols and rationalized the results on the basis of a change in charge-transfer character.

Recently, Lasser and Feitelson (*13*) have shown that fluorescence of either the acidic or the basic form of a molecule alone does not necessarily yield a pK value of the excited state.

One of the main problems encountered in obtaining acidity constants in the excited singlet state is the method employed in their calculation and the assumptions made in each of these methods. This paper is concerned with the study of excited state acidity constants in the singlet state of certain anthraquinones, fluorenes, fluorenones, and hydroxyxanthone. Each of the acidity constants is measured by several methods, and a comparison is made of the results obtained by each method.

EXPERIMENTAL

Chemicals. Matheson Coleman and Bell spectrograde dioxane was used without further purification. 1-Hydroxyxanthraquinone, 1-aminoanthraquinone, 2-aminoanthraquinone, 1-hydroxyfluorene, 2-hydroxyfluorene, 9-hydroxyfluorene, 2-aminofluorene, 4-hydroxy-9-fluorenone, 1-amino-9-fluorenone were all available commercially from either Aldrich Chemical Company, Chemical Procurement Laboratory, or James Hinton Associates. All were recrystallized three times from ethanol.

1-Hydroxyxanthone and 2-hydroxyxanthraquinone (*14*) were synthesized in this laboratory and recrystallized three times from ethanol.

Buffer solutions of 33% dioxane-water in the pH range 1–14 were prepared by using appropriate mixtures of the following in deionized water solutions: HCl, HOAc, NaOAc, KH_2PO_4, NaOH, H_3BO_3. Each buffer was brought up to constant ionic strength by adding an appropriate amount of KCl. For very weak bases, Hammett indicators were used in H_2SO_4–H_2O mixtures. The pH of the solutions were measured on an Orion Model 801 digital pH meter using glass and calomel electrodes. Calibration was made with Harleco standard buffer solutions.

Absorption measurements were made on a Beckman DK2-A recording spectrophotometer or a Beckman DU spectrophotometer. Fluorescence measurements were obtained on an instrument constructed in this laboratory (*15*), with quinine sulfate in 0.1*N* sulfuric acid used as a standard for relative intensities.

RESULTS

Ground State Acidity Constants. For the measurement in this work of acidity constants in the ground state, a technique introduced by von Halban (*16*) and later simplified by Robinson and Biggs (*17*) was used. Further work by Robinson and Kiang (*18*) and by Biggs (*19*) helped to simplify procedures.

By use of the following equation:

$$K = \gamma_H m_H \frac{\alpha}{1-\alpha} \gamma_A$$

K, the dissociation constant can be obtained, where m_H is the hydrogen ion molality and γ_H, γ_A are the activity coefficients of the hydrogen ion and the respective anions, that of the uncharged molecule being almost unity at the concentrations used. α is the fraction of anion present at the particular pH. As calculated from the data of Robinson and Biggs (*17*), the pH is equal to $-\log \gamma_H m_H$. From the extended Debye–Hückel (*20*) equation, the value of γ_A can be estimated. Therefore, from changes in the absorption spectra at varying pH, the dissociation constant can be calculated. The majority of the compounds studied showed distinct changes in the spectra of the protonated and anion forms of the acids, with clear isosbestic points. The results are tabulated in Table I and compared to literature values which were obtained in different solvent systems.

pK Values of the Excited Singlet State. The dissociation constants of organic acids and bases in the first excited singlet state often differ from the corresponding ground electronic state value by several orders of magnitude because of the redistribution of electronic charge density on excitation (*26*). Various methods are available for the evaluation of these excited state acidity constants and the

(5) J. C. Haylock, S. F. Mason, and B. E. Smith, *J. Chem. Soc.*, 4897 (1963).
(6) S. F. Mason, J. Philip, and B. E. Smith, *J. Chem. Soc.*, 3051 (1968).
(7) E. L. Wehry and L. B. Rogers, *J. Amer. Chem. Soc.*, **87**, 4235 (1965).
(8) S. G. Schulman and Q. Fernando, *J. Phys. Chem.*, **71**, 2668 (1967).
(9) S. G. Schulman and Q. Fernando, *Tetrahedron*, **24**, 1777 (1968).
(10) M. Goldman and E. L. Wehry, *Anal. Chem.*, **42**, 1178 (1970).
(11) S. G. Schulman, *Anal. Chem.*, **43**, 285 (1971).
(12) J. L. Rosenberg and I. Brinn, *J. Phys. Chem.*, **76**, 3558 (1972).
(13) N. Lasser and J. Feitelson, *J. Phys. Chem.*, **77**, 1011 (1973).
(14) A. G. Perkins and T. W. Whattam, *J. Chem. Soc.*, **121**, 289 (1921).
(15) H. H. Richtol and F. H. Klappmeier, *J. Chem. Phys.*, **44**, 1519 (1966).
(16) H. V. Halban and T. Ebert, *Z. Phys. Chem.*, **112**, 359 (1924).
(17) R. A. Robinson and A. I. Biggs, *Trans. Faraday Soc.*, **51**, 901 (1955).
(18) R. A. Robinson and K. Kiang, *Trans. Faraday Soc.*, **51**, 1398 (1955).
(19) A. I. Biggs, *Trans. Faraday Soc.*, **52**, 35 (1956).
(20) E. A. Guggenheim and T. D. Schindler, *J. Phys. Chem.*, **38**, 533 (1934).
(21) H. Treadwell and G. Schwarzenbach, *Helv. Chim. Acta.*, **11**, 386 (1928).
(22) E. Gerasimenko, S. S. Tkachenko and Y. B. Shteinberg, *Reakts Sposbnost Org. Soedin*, **6**, 1065 (1969).
(23) P. H. Grantham, E. K. Weisberger and J. H. Weisberger, *J. Org. Chem.*, **26**, 1008 (1961).
(24) V. P. Kreiter, W. A. Bonner, and R. H. Eastman, *J. Amer. Chem. Soc.*, **76**, 5770 (1954).
(25) L. Sillen, "Stability Constants of Metal-Ion Compounds," 2nd ed., The Chemical Society, London, 1964, p 676.
(26) A. Weller, "Progress in Reaction Kinetics," Vol. 1, G. Porter, Ed., Pergamon, Oxford, 1961, p 189.

Table I. Ground State pK Values

	This Work	Reported (Ref.)		
1-Hydroxyanthraquinone	9.3	8.8	(96% EtOH)	(*21*)
2-Hydroxyanthraquinone	7.1	5.7	(96% EtOH)	(*21*)
1-Aminoanthraquinone	0.52	0.57	(H_2SO_4)	(*22*)
2-Aminoanthraquinone	0.76			
1-Hydroxyfluorene	9.3	11.4	(70% EtOH)	(*23*)
2-Hydroxyfluorene	9.1	11.6	(70% EtOH)	(*23*)
		9.5	(H_2O)	(*24*)
9-Hydroxyfluorene	14.6			
2-Aminofluorene	4.3	4.4	(70% EtOH)	(*23*)
4-Hydroxy-9-fluorenone	8.4			
1-Amino-9-fluorenone	−0.3	−0.3	(70% EtOH) (H_2SO_4)	(*23*)
1-Hydroxyxanthone		10.7	(*25*)	

the ground state pK values. For 1-hydroxyfluorene, 2-hydroxyfluorene, and 9-hydroxyfluorene, the absorption maximum of the acidic form was obtained directly from the absorption spectra. However, the long wavelength absorption band of the basic form was determined more exactly from excitation spectra as it appeared either as a broad band or as the shoulder of a more major peak. Results for all compounds are summarized in Table II where pK is the dissociation constant for the ground state species, pK_s* is the dissociation constant for the species in the lowest excited singlet state, ν_a is the wavenumber of the long wavelength absorption maximum of the acid form, and ν_b is the wavenumber of the long wavelength absorption maximum of the basic form.

From Fluorescence Spectra. If the analogous assumption is made with respect to fluorescence spectra that was made for absorption spectra—*i.e.*, that the maximum of the fluorescence bands of the acid and base occur an equal amount above the O–O transition—then similar computations can be performed using fluorescence data. This method was also attempted and the results are tabulated in Table III. It should be noted that excited singlet state acidity constants could be calculated, using this method, only for those compounds which gave fluorescence of both the acid and its conjugate base.

Table II. Excited Singlet State Acidity Constants Determined from Absorption Spectra in 33% Dioxane–Water Solutions[a]

Compound	pK	ν_a(cm^{-1}) × 10^{-4}	ν_b(cm^{-1}) × 10^{-4}	ΔpK	pK_s*
1-Hydroxyanthraquinone	9.3	2.49	2.04	9.5	−0.2
2-Hydroxyanthraquinone	7.1	2.67	2.12	11.5	−4.4
1-Aminoanthraquinone	0.52	3.02	2.08	19.7	−19.2
2-Aminoanthraquinone	0.76	3.07	2.23	17.6	−16.8
1-Hydroxyfluorene	9.3	3.40	3.19	4.4	4.9
2-Hydroxyfluorene	9.1	3.20	2.94	5.0	4.1
9-Hydroxyfluorene	14.6	3.68	3.17	10.7	3.9
2-Aminofluorene	4.3	3.33	3.13	4.2	0.1
4-Hydroxy-9-fluorenone	8.4	2.34	1.99	7.4	1.0
1-Amino-9-fluorenone	−0.3	3.04	2.31	15.3	−15.6
1-Hydroxyxanthone	10.7	2.27	2.03	5.0	5.7

[a] Precision for all values is ±2%.

Table III. Excited Singlet State Acidity Constants Determined from Fluorescence Spectra in 33% Dioxane–Water Solution[a]

Compound	pK	ν_a(cm^{-1}) × 10^{-4}	ν_b(cm^{-1}) × 10^{-4}	ΔpK	pK_s*
1-Hydroxyfluorene	9.3	2.99	2.44	11.5	−2.2
2-Hydroxyfluorene	9.1	2.97	2.43	11.3	−2.2
9-Hydroxyfluorene	14.6	3.10	2.44	13.8	0.8
2-Aminofluorene	4.3	2.94	2.70	5.0	−0.7

[a] Precision for the above values is ±2%.

values obtained by these methods can also often differ markedly.

From Absorption Spectra. The Förster cycle (*2*) is applicable only to the O–O transition of either absorption or emission spectra. Unfortunately, the position of the O–O band is generally difficult to evaluate in solution. If the assumption is made that the maximum of the absorption bands of the acid and base occur equal amounts above the O–O transition, then absorption spectra alone can be used in a Förster cycle to determine the energy differences between the ground and the excited states and hence to calculate the first excited singlet state pK*. The equation used is

$$\mathrm{p}K - \mathrm{p}K^* = \frac{\Delta E - \Delta E'}{2.303RT}.$$

where ΔE and $\Delta E'$ are the absorption energies of the acid and anion, respectively.

For most of the compounds under investigation, data could be taken directly from the spectra used to determine

From the Average of Absorption and Fluorescence. Bartok, Lucchesi and Snider (*4*) sought a more accurate indication of the O–O transition. They felt this could be achieved by taking an average of the energy values obtained in both absorption and fluorescence. However, this method too has the limitation that it can be applied only to those compounds which fluoresce in both acidic and basic forms. Table IV presents the results for those compounds whose excited singlet state acidity constants were measured by this method. In the table, pK is the dissociation constant for the ground state species; $(\nu_{ab} + \nu_{fl})/2$ is the average value of the wavenumbers of the long wavelength of absorption and the short wavelength of fluorescence for the acidic form; $(\nu_{ab}' + \nu_{fl}')/2$ is the average value of the wavenumbers of the long wavelength of absorption and the

Table IV. Excited Singlet State Acidity Constants Determined from an Average of Absorption and Fluorescence Spectra in 33% Dioxane–Water Solutions[a]

Compound	pK	$\frac{\nu_{ab} + \nu_{f1}}{2}$	$\frac{\nu_{ab}' + \nu_{f1}'}{2}$	ΔpK	pK$_a$*
1-Hydroxyfluorene	9.3	3.20×10^4	2.82×10^4	8.0	1.3
2-Hydroxyfluorene	9.1	3.09×10^4	2.69×10^4	8.4	0.7
9-Hydroxyfluorene	14.6	3.39×10^4	2.81×10^4	12.2	2.4
2-Aminofluorene	4.3	3.14×10^4	2.92×10^4	4.6	−0.3

[a] Precision for all values is ±2%.

Table V. Excited Singlet State Acidity Constants Determined by "Fluorescence Titration"[a]

Compound	pK	pK$_a$*	λ_{max} nm (acid)	λ_{max} nm (base)
1-Hydroxyanthraquinone	9.3	1.2	450	
2-Hydroxyanthraquinone	7.1	−3.5	470	
1-Hydroxyfluorene	9.3	1.4	335	410
2-Hydroxyfluorene	9.1	0.8	337	411
9-Hydroxyfluorene	14.6	2.8	323	410
2-Aminofluorene	4.3	0.4	340	370
4-Hydroxy-9-fluorenone	8.4	1.8	493	
1-Hydroxyxanthone	10.7	5.8	484	

[a] Precision for all values is ±2%.

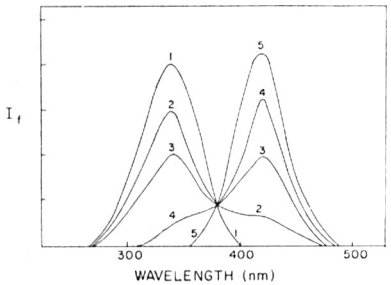


Figure 1. Fluorescence spectral curves of 1-hydroxyfluorene with varying pH in buffered dioxane–water solutions

(1) pH 0.57; (2) pH 1.21; (3) pH 1.56; (4) pH 2.49; (5) pH 3.63

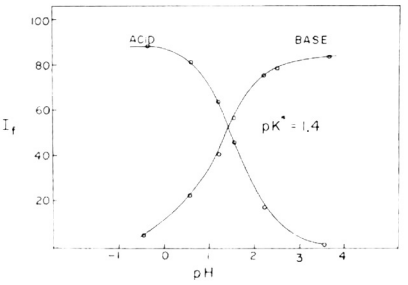


Figure 2. Plot of fluorescence intensity of 1-hydroxyfluorene with varying pH in buffered dioxane–water solutions

short wavelength of fluorescence for the basic form. pK$_a$* is the acidity constant of the excited singlet state.

Fluorescence Intensity as a Function of Acidity. The fourth and final method used for the determination of excited state acidity constants involves a "fluorescence titration" (*8*). If one or both members of a conjugate acid–base pair is fluorescent, the variation in fluorescence intensity of either species can be determined as a function of pH or of the Hammett acidity function, H_0. The necessary condition here is that equilibrium be established within the lifetime of the first excited state which is apparently the case with many compounds having both members of the conjugate acid–base pair fluoresce (*13*). If this condition is met, a plot of the fluorescence intensity *vs.* the solution acidity will give a sigmoid curve whose point of inflection is the same for the acidic and basic form of the molecule (*13*) and is a measure of the dissociation constant in the excited state. The curves are determined for all compounds except 1-aminoanthraquinone, 2-aminoanthraquinone, and 1-amino-9-fluorenone which appear to have excited state activity constants so low they could not be determined by such a method.

Four of the compounds measured fluoresced in both the acidic and basic forms. These were 1-hydroxyfluorene, 2-hydroxyfluorene, 9-hydroxyfluorene, and 2-aminofluorene. Their acidity constants in the first excited singlet state could therefore be determined as a result of the fluorescence intensity in both forms. This was done and the results gave the same inflection point for each form titrated. Figure 1 shows the fluorescence spectral curves for 1-hydroxyfluorene with varying pH. Figure 2 shows the fluorescence titration curves for this compound. The recorded data are presented in Table V along with the λ of maximum intensity of the acid and (or) basic fluorescence. The data presented are the average of at least five runs. The exciting wavelength for all compounds was at a point approximately halfway between the ground state absorption of the conjugate pairs. In those cases where an isosbestic point appeared in the ground state absorption spectra *vs.* pH, the excitation was at the isosbestic point.

DISCUSSION

The ground state pK's in this work were all obtained experimentally in 33% dioxane–water buffered solutions. The 33% dioxane–water buffered solutions were chosen because of the high solubility of all compounds in dioxane and the low solubility of the compounds in pure water. Agreement with literature values was in general quite good. Any ob-

Table VI. Summary of Excited Singlet State Acidity Constants

Compound	pK	pK*(Abs)	pK*(Fluor)	pK*Avg/O–O	pK* (Titration)
1-Hydroxyanthraquinone	9.3	−0.2			1.2
2-Hydroxyanthraquinone	7.1	−4.4			−3.5
1-Aminoanthraquinone	0.52	−19.2			
2-Aminoanthraquinone	0.76	−16.8			
1-Hydroxyfluorene	9.3	4.9	−2.2	1.3	1.4
2-Hydroxyfluorene	9.1	4.1	−2.2	0.7	0.8
9-Hydroxyfluorene	14.6	3.9	0.8	2.4	2.8
2-Aminofluorene	4.3	0.1	−0.7	−0.3	0.4
4-Hydroxy-9-fluorenone	8.4	1.0			1.8
1-Amino-9-fluorenone	−0.3	−15.6			
1-Hydroxyxanthone	10.7	5.7			5.8

served discrepancies in Table I can probably be attributed to differences in the solvent system. For simplicity, all the data are summarized in Table VI and, as evidenced by results presented in this Table, the acidity constant in the first excited singlet state may vary over several orders of magnitude depending upon the method employed in its measurement and, subsequently, the assumptions which must be made for the particular determination.

By assuming that the absorption bands of the acid and base occur an equal amount above the O–O level, the Förster (2) cycle being *a priori* applicable only to the O–O vibrational bands of either absorption or emission spectra, absorption spectra alone can be used to calculate the excited singlet state acidity constant. It must also be assumed, as it must in any application of the Förster cycle, that ΔS, the entropy change, is the same in both the ground and the excited state. This seems to be a rather reasonable assumption. It seems probable (27) that the most important contribution to such a difference would come from differences in solvation.

If one uses absorption spectra alone for calculation of excited singlet state acidity constants, however, the method is valid only if the vibrational spacings of the excited states of the conjugate pair (*i.e.*, the acid form and its corresponding basic form) are alike and if the energy distribution between vibrational subbands is alike. Although no proof for the validity of these assumptions exists, they appear quite reasonable, particularly in rigid aromatic systems chosen for this work where the vibrational structure involves mostly ring deformations and in comparison of absorption bands of similar electronic origin.

Schulman *et al.* (28) state that pK* values, estimated from absorption data alone, are generally somewhat crude, and usually do not account for differences in vibrational structure in ground and excited states of acid and conjugate base or solvent relaxation in the electronically excited state, and may be several log units in error. This is also the case for the compounds studied in this paper. However, as found in this work in the case of 1-aminoanthraquinone, 2-aminoanthraquinone, and 1-amino-9-fluorenone (*cf.* Table VI), compounds which have excited singlet state acidity constants which are too low to be evaluated by fluorescence titration or which do not fluoresce at all, absorption measurement calculations may be the only method available. The pK* values obtained for these three compounds were, respectively, −19.2, −16.8, and −15.6 corresponding to a ΔpK of between 16 and 20 pK units. These values are quite large compared to the ΔpK of between 5 and 10 found for most compounds. However, Jaffe (29) found a ΔpK value of 21.8 for certain bands in azobenzene. Obviously, one of the major troubles encountered in this method is the apparent inability to be certain that corresponding (30) absorption bands are the ones being used in calculations. Care should be exercised in dealing with amino comhounds, since they frequently do not correspond to simple protonation (31).

Absorption measurements alone (32) cannot take into account the difference in destabilization energy of the excited states of the two species due to solvent effects. Therefore $\Delta\nu$ can be measured accurately neither from the absorption nor, for the same reasons, from only fluorescence spectra; only the average of these energies provides a "best value" of the energy gap between the ground and the excited singlet state. This is the method first used by Bartok and Lucchesi (4) in their investigation of substituted phenols. It is also this method which provided the best correlated results with those obtained from fluorescence intensity measurements *vs.* pH in this work (Table VI). Nevertheless, if no other method is available, measurements of the excited singlet state acidity as evaluated from absorption spectra must serve as a crude approximation. Values presented in Table VI do indicate that for certain compounds measured (4-hydroxy-9-fluorenone, 1-hydroxyxanthone), correlation with other methods was reasonable although these may be simply coincidental.

Before discussing the final method of obtaining excited singlet state acidity constants, it is worth noting that while the precision of measurements (2% internal deviation) is quite good, there are still other sources of error. Quite often an error arises in the determination of λ_{max} of absorption. Although wavelength settings are reproducible to within 0.05 nm in the ultraviolet and to within 0.5 nm in the near infrared, an error of 1 nm at 250 nm will produce a difference of 0.35 pK unit. Even at 350 nm, this same error translates into 0.20 pK unit.

For several of the compounds which fluoresce, plots of fluorescence intensity *vs.* pH can be made. The ability to apply these plots to pK* determinations depends on whether or not equilibrium has been established in the excited state. This condition can be guaranteed only for molecules whose acidic and basic forms fluoresce (13). As determined by Weller (33), the back reaction is diffusion controlled in the excited singlet state. Since the natural lifetime of the excited singlet is typically 10^{-8} second, the establishment of equilibrium is dependent solely upon the protonation or deprotonation of the particular molecules involved. Thus, if equilibrium is established within the lifetime of the excited singlet state, a set of fluorescence titration curves such as those shown in Figure 2 can result. Equal inflection points for the 2 curves is the best measure

(27) H. H. Jaffe, H. L. Jones, and M. Isaks, *J. Amer. Chem. Soc.*, **86**, 2934 (1964).
(28) S. G. Schulman, L. B. Sanders, and J. D. Winefordner, *Photochem. Photobiol.*, **13**, 381 (1971).
(29) H. H. Jaffe, D. L. Beveridge, and L. Jones, *J. Amer. Chem. Soc.*, **86**, 2932 (1964).
(30) H. H. Jaffe and H. Lloyd Jones, *J. Org. Chem.*, **30**, 964 (1964).
(31) S. G. Schulman and P. Liedke, *Z. Phys. Chem. (Leipzig)*, **84**, 317 (1973).
(32) E. Lippert, W. Luden, and F. Moll, *Spectrochim Acta*, **15**, 858 (1959).
(33) A. Weller, *Discuss. Faraday Soc.*, **27**, 28 (1959).

of pK^*. As pointed out recently by Lasser and Feitelson (*13*), a single fluorescence titration curve is insufficient for accurate pK^* determinations. This can be the case even if quite a sharp titration curve is obtained for a single fluorescent form. Dual fluorescence titration curves could be obtained from four compounds (*cf.* Table VI) and these probably represent the most accurate pK^* values, since equilibrium in the excited state is assured.

An advantage of the titration method over spectroscopy methods is that none of the previously mentioned assumptions—*i.e.*, that the entropy change is the same in both the ground and excited singlet states or that one is observing O–O transitions—plays any role in this method of determining the excited singlet state acidity constant. However, if only one form is fluorescent, the inflection point in the titration curve may be in error (*13*). Others (*34–36*) have used and compared various methods of calculating excited singlet state acidity constants, all offering different and theoretical reasons for the discrepancies observed. Some variances in the works are as high as 10 pK units. It is apparent that although each method has its limitations and assumptions, the spectroscopic values which internally correlate the best to fluorescence titrations of both acid and basic forms are obtained by averaging absorption and fluorescence measurements (Table VI). However, both these methods require the conjugate acid and basic forms to fluoresce, thereby limiting its general applicability. It is probably best to apply four methods when measuring pK^* values for any molecule, and then examine the data for internal consistency as was done here with the data in Table VI.

RECEIVED for review January 23, 1974. Accepted May 3, 1974.

(34) E. L. Wehry and L. B. Rogers, *Spectrochim Acta*, **21**, 1976 (1965).
(35) E. Vander Donckt, "Progress in Reaction Kinetics," Vol. 5, G. Porter, Ed., Pergamon, Oxford, 1970, p 277.
(36) R. O. C. Norman and P. D. Ralph, *J. Chem. Soc.*, 2221 (1961).

New Instrumental Approach in Phase-Selective Second Harmonic Alternating Current Polarography

H. Blutstein and A. M. Bond

Department of Inorganic Chemistry, University of Melbourne, Parkville 3052, Victoria, Australia

A. Norris

Clanor Instruments, P.O. Box 75, Balwyn 3103, Victoria, Australia

The development of a simple and inexpensive ($10–$20) approach to obtaining the second harmonic response is described using electronic multiplication of the ac reference signal to the phase-selective detector. The principle can be understood by consideration of trigonometric identities of the type

$$\sin^2 \omega t = \tfrac{1}{2}(1 - \cos 2\omega t)$$

The performance of the circuitry is assessed on a commercially available instrument and the theoretical response obtained in both aqueous and nonaqueous solvents. Phase-selective detection is employed and the use of this readout form in analytical work is discussed.

The use of second harmonic alternating current polarography has had limited popularity as an electroanalytical tool (*1–10*). Its major use has been in kinetic studies (*1–3, 11–23*), in which the parameters (rate constant and transfer coefficient) of the electron-transfer step can often be obtained more conveniently than by faradaic impedance measurements.

The relative neglect of second harmonic ac polarography as an analytical technique cannot be justified by limitations arising from its theoretical basis; in fact, the converse is true. Contributions of double layer charging current in second (even) harmonic ac polarography approach the ideal situation of being negligible (*2*) and therefore, in principle, the technique would show a marked advantage over the fundamental mode. In fundamental harmonic ac polarography, the alternating current contains a substantial nonfaradaic component (double layer charging current) and, in view of this, measurements must in general be restricted to the low frequency range or else phase-selective detection used, where the in-phase component contains negligible charging current under ideal conditions. The quadrature component of the fundamental harmonic alternating current contains large charging current contributions. With

(1) D. E. Smith in "Electroanalytical Chemistry," A. J. Bard Ed., Vol. 1, M. Dekker, Inc., New York, N.Y., 1966, Chapter 1.
(2) B. Breyer and H. H. Bauer "Alternating Current Polarography and Tensammetry," Interscience, New York, N.Y., 1963.
(3) D. E. Smith, *C. R. C. Crit. Rev. Anal. Chem.*, **2**, 247 (1971).
(4) H. H. Bauer, *J. Electroanal. Chem.*, **1**, 256 (1960).
(5) D. E. Smith and W. H. Reinmuth, *Anal. Chem.*, **33**, 482 (1961).
(6) R. Neeb, *Fresenius' Z. Anal. Chem.*, **188**, 401 (1962).
(7) J. Dèvay, T. Garai, L. Mészáros, and E. Punger, *Hungr. Sci. Instrum.*, No. 12 (1968).
(8) J. Dèvay, T. Garai, L. Mészáros, and B. Palágyi-Fényes, *Hungr. Sci. Instrum.*, No. 15 (1968).
(9) J. Dèvay, T. Garai, L. Mészáros, and B. Palágyi-Fényes, *Magy. Kem. Foly.*, **75**, 460 (1969).
(10) A. L. Woodson and D. E. Smith, *Anal. Chem.*, **42**, 242 (1970).
(11) J. van Cakenberge, *Bull. Soc. Chim. Belges.*, **60**, 3 (1951).
(12) H. H. Bauer and P. J. Elving, *Anal. Chem.*, **30**, 341 (1958).
(13) H. H. Bauer, *Aust. J. Chem.*, **17**, 591 (1964).
(14) H. H. Bauer *Aust. J. Chem.*, **17**, 715 (1964).
(15) H. H. Bauer and D. C. S. Foo, *Aust. J. Chem.*, **19**, 1103 (1966).
(16) T. G. McCord and D. E. Smith, *Anal. Chem.*, **40**, 289 (1968).
(17) T. G. McCord and D. E. Smith, *Anal. Chem.*, **40**, 1967 (1968).
(18) J. E. B. Randles and D. R. Whitehouse, *Trans. Faraday Soc.*, **4**, 1376 (1968).
(19) T. G. McCord and D. E. Smith, *Anal. Chem.*, **41**, 131 (1969).
(20) T. G. McCord and D. E. Smith, *Anal. Chem.*, **41**, 1423 (1969).
(21) T. G. McCord and D. E. Smith, *Anal. Chem.*, **42**, 2 (1970).
(22) T. G. McCord and D. E. Smith, *Anal. Chem.*, **42** 126 (1970).
(23) T. G. McCord and D. E. Smith, *J. Electroanal. Chem.*, **26**, 61 (1970).

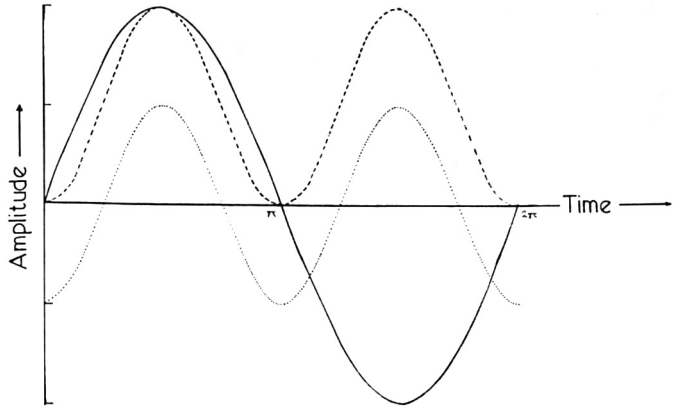


Figure 1. Operation of the multiplier circuitry in terms of trigonometric functions

(———) $\sin \omega t$; (– – –) $\sin^2 \omega t$; (. . .) $-\frac{1}{2} \cos 2\omega t$

the second harmonic, no restrictions are placed, in theory, on the frequency range or use of quadrature or for that matter any other phase components. The magnitude of the second harmonic current is, of course, small. However, with the advent of solid state electronics and associated circuitry, this does not constitute the problem that may have been present at the time the technique was first developed.

One reason for the preference of other analytical polarographic techniques over second harmonic ac polarography has undoubtedly been that little high quality inexpensive instrumentation is available commercially. Furthermore, with the instruments available (*24, 25*) or with a modified instrument using a commercially available lock-in amplifier (*26–28*), little practical advantage or use has appeared in the open literature. Indeed, one of the advantages proclaimed has been the improved resolution which recently has been critically queried by one of us (*29*). Thus, a complete analytical evaluation of the technique and a comparison with existing electroanalytical methods are required. However, this topic will constitute a later communication and the present work deals with the development of an inexpensive method of extending the capabilities of ac polarographs to give a second harmonic readout, and, at the same time, give all the options already available for the fundamental mode.

EXPERIMENTAL

Reagents. All chemicals used were reagent grade purity. Solutions were deoxygenated with argon. Cadmium(II) solutions were prepared from cadmium carbonate in 1*M* hydrochloric acid, which served as the supporting electrolyte. The $Fe(C_2O_4)_3^{3-}$ anion was prepared from the sodium salt with 1.3*M* potassium oxalate and 0.2*M* oxalic acid as supporting electrolyte. Nonaqueous work was undertaken in acetone using bis(π-cyclopentadienyl)*N,N*-dibutyldithiocarbamatovanadium(IV) tetraphenylborate as a model system. Tetraethylammonium perchlorate, 0.1*M*, was used as the supporting electrolyte. Other details are as reported elsewhere (*30*). All solutions were thermostated at 25.0 ± 0.1 °C.

Instrumental. The detailed circuitry for second harmonic work is described separately, immediately below. The circuitry was inserted into a PAR Electrochemistry System, Model 170 (Princeton Applied Research Corporation, Princeton, N.J.).

In aqueous media, the reference electrode was Aq/AgCl (5*M* NaCl). In acetone, a Ag/AgCl (0.1*M* LiCl; acetone) was used. The third electrode was either tungsten or platinum in both solvent systems.

DISCUSSION

New Approach to Obtaining the Second Harmonic Response. The main approach used for obtaining the second harmonic response utilizes a series of tuned amplifiers to give the harmonic of interest (*1, 5, 6, 14, 31, 32*). To obtain phase-selective detection, additional circuitry to generate a second harmonic reference signal is introduced (*1, 31, 32*).

In an early paper, Smith commented (*31*) on the possible use of electronic multiplication of the ac signal as a useful extension of instrumentation in ac polarographic methodology. To date, this has yet to be employed.

The use of multiplication of the sine wave reference signal can readily be seen from the well-known trigonometric equations

$$\sin^2 \omega t = \tfrac{1}{2}(1 - \cos 2\omega t) \quad (1)$$

$$\cos^2 \omega t = \tfrac{1}{2}(1 + \cos 2\omega t) \quad (2)$$

$$\sin \omega t \cdot \cos \omega t = \tfrac{1}{2} \sin 2\omega t \quad (3)$$

Thus, arithmetical squaring of the sine wave reference should lead to the possibility of direct measurement of the second harmonic content, after compensation for the offset introduced in the squaring process. Suitable high-quality inexpensive multipliers are now available commercially, and this approach is now amenable to simple experimentation, at a cost of well below $10. The simplicity of the circuitry involved, coupled with the low cost, makes this approach most attractive.

The theory behind the frequency doubler is readily seen in Figure 1. Figure 2 shows a detailed circuit diagram. By

(24) J. Dévay, T. Garai, B. Juhász, L. Mészáros, and E. Pungor, *Hungr. Sci. Instrum.*, No. 13 (1968).
(25) Amel Milano, Short Form. Catelog (1969–1970).
(26) H. H. Bauer and D. Britz, *Chem. Instrum.*, **2**, 361 (1970).
(27) J. B. Flato, *Anal. Chem.*, **44**(11), 75A (1972).
(28) J. B. Flato, Princeton Applied Research Corporation, Princeton, N.J., private communication, 1972.
(29) A. M. Bond, *J. Electroanal. Chem.*, **36**, 235 (1972).
(30) A. M. Bond, A. T. Casey, and J. R. Thackeray, *Inorg. Chem.*, **12**, 887 (1973).
(31) D. E. Smith, *Anal. Chem.*, **35**, 1811 (1963).
(32) D. E. Glover and D. E. Smith, *Anal. Chem.*, **43**, 775 (1971).

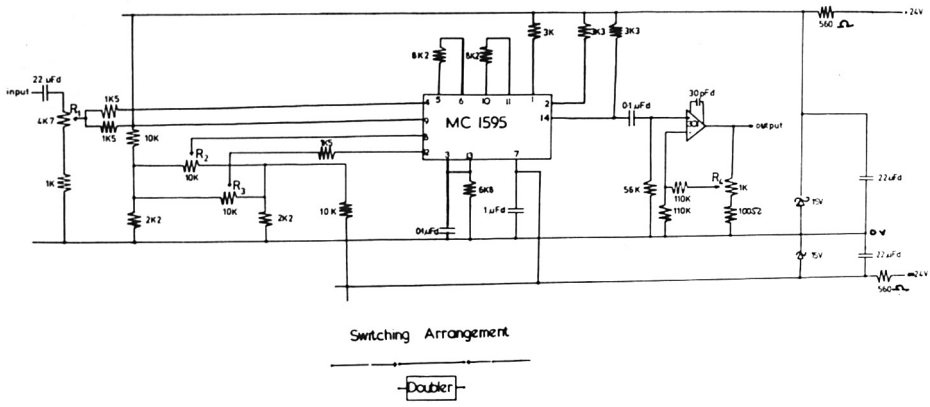


Figure 2. Frequency doubler circuit including offset control and gain adjustment

MC 1595 is a four-quadrant multiplier, Motorola Semiconductor Products Inc., Phoenix, Ariz. Printed circuit board available from authors on request

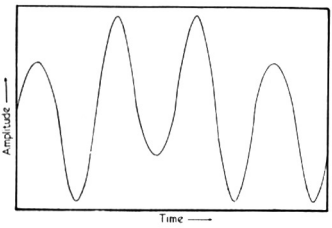


Figure 3. Schematic representation of output signal prior to gain adjustment and trimming

filtering the dc component, *i.e.* ½, out of the $\sin^2 \omega t$ signal, the $-\frac{1}{2} \cos 2\omega t$ signal is obtained. The frequency doubler yields a reference $2\omega t$ signal having a waveform which is correctly related to the input ωt signal as required by Equation 1 and illustrated in Figure 1. The resulting signal contains less than 1% distortion without filtering. This method eliminates the necessity for adjustments required when using tuned amplifiers, and problems associated with oscillator drift, etc. Therefore the frequency doubler can be inserted into any ac polarograph without significantly altering its performance characteristics.

In this work, the second harmonic circuitry was installed into a PAR Electrochemistry System Model 170. The output of the phase shift circuit of the reference oscillator into the mixer or phase-sensitive detector was broken and the circuit inserted. A press button switch was used to provide a choice between either the fundamental harmonic utilizing the existing circuitry or incorporating the second harmonic modification as shown in Figure 2.

To obtain usable output accuracy, several adjustments must be made in the external multiplier circuit. These are also shown in Figure 2.

In setting up the circuit, R_1 is set for less than 5 volts peak-to-peak (1 volt was used in this work) to conform to the manufacturers input specifications. R_4 is adjusted to give the same output amplitude as the input amplitude. Variable resistors R_2 and R_3 are used for offset adjustments by using them to null the outputs to zero volt and trimming the circuit to give an undistorted reference signal (Figure 3). When long leads are used on the input, oscillations may occur and a parasitic suppression network is included by inserting resistors in series with the multiplier at pins 4, 8, 9, and 12.

Verification of Instrumental Approach. The use of a frequency doubler, as outlined in the preceding section, has been investigated to ensure it is a legitimate means of obtaining conditions under which the second harmonic ac polarographic response can be obtained.

The simplest situation for comparison with theory is that in which diffusion of the electroactive species to the electrode is the rate-determining step. Three examples are used in this work:

(i) The reduction of Cd(II) in 1*M* HCl

$$\mathrm{Cd(II)} + 2e \rightleftharpoons \mathrm{Cd(amalgam)} \qquad (4)$$

which strictly speaking is a quasi-reversible process in the ac sense (*31*) but it is adequate for our purposes.

(ii) The reduction of ferric ion in potassium oxalate–oxalic acid supporting electrolytes has been reported to exhibit reversible ac polarographic behavior (*5*).

$$\mathrm{Fe(C_2O_4)_3^{3-}} + e \rightleftharpoons \mathrm{Fe(C_2O_4)_3^{4-}} \qquad (5)$$

(iii) Using acetone as the solvent, the one-electron reduction of bis(π-cyclopentadienyl)vanadium(IV)*N*,*N*-dibutyldithiocarbamate tetraphenylborate in 0.1*M* tetraethyl ammonium perchlorate, has been reported to be totally reversible in the fundamental harmonic experiment (*30*).

$$[\mathrm{cp_2V^{IV}(dbdtc)}]^{+} + e \rightleftharpoons \mathrm{cp_2V^{III}(dbdtc)} \qquad (6)$$

This provides an example in a nonaqueous solvent.

For a reversible reaction

$$\mathrm{O} + ne \rightleftharpoons \mathrm{R}$$

in which both species are soluble, the equation for the second harmonic alternating current ($I(2\omega t)$) has been derived by considering a sinusoidal alternating potential being superimposed on a constant dc ramp potential. Thus,

$$E = E_{dc} - \Delta E \sin \omega t$$

The equation, derived by Tachi and Senda (*33*) can be conveniently written as (*1*, *5*)

(33) I. Tachi and M. Senda, *Bull. Chem. Soc. Jap.*, **28**, 632 (1955).

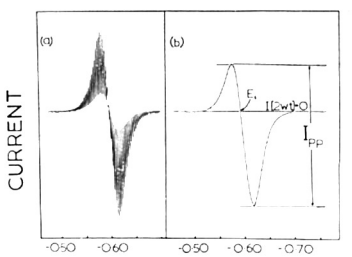


Figure 4. Second harmonic ac polarograms. [Cd(II)] = 1.00 × $10^{-4}M$ in 1M HCl. ΔE = 10 mV, p-p. ω = 400 Hz

(*a*) Natural drop time; (*b*) current sampled

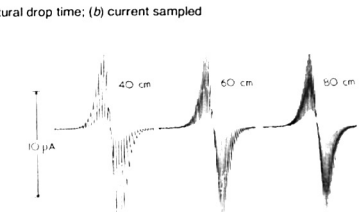


Figure 5. Dependence of the second harmonic ac response for the process Cd(II) + 2e ⇌ Cd(amalgam) on mercury column height when natural drop time is used

[Cd] = 1.00 × $10^{-3}M$. ΔE = 10 mV, p-p. ω = 400 Hz

trode geometry and growth (in the case of a DME) have been ignored. The restriction that $\Delta E \leq 8/n$ mV (*1*) needs also to be noted.

Figure 4 shows second harmonic polarograms obtained by the instrumental modification developed in this work, at both natural drop time and current sampling at the end of the drop. Labeled on this diagram are the variables of interest in this work. The inflection or crossover potential (E_i), [corresponding to the second harmonic minimum potential referred to in nonphase sensitive work (*10*)] is defined as the potential at zero second harmonic current in the phase-selective readout form. The use of the peak-to-peak current (I_{pp}) provides a simple way to test the various aspects of Equation 7. This parameter should be directly proportional to $\omega^{1/2}$, ΔE^2, depolarizer concentration, electrode area and phase angle. The predicted dependence on ΔE (1 to 10 mV, p-p), frequency (10 to 1100 Hz), concentration (10^{-2} to $10^{-6}M$) and phase-angle was obtained.

Dependence of I_{pp} on Area of DME. The magnitude of I_{pp} is directly proportional to the electrode area according to Equation 7 and, therefore, independent of mercury column height (*34*). Figure 5, however, shows that I_{pp} for cadmium varies with the mercury column height. This apparent divergence from theory is accounted for by recalling that Equation 7 is an approximate expression based on a planar-diffusion model which ignored the reality of spherical diffusion to the DME. The spherical-diffusion factor is drop time dependent, resulting in a noticeable height dependence in metal ion–metal amalgam systems (*16, 35*).

For a reversible system in which both species are soluble in solution, the drop curvature is not significant and the electron transfer step can be adequately described by Equation 7. This experiment was repeated for the ferric oxalate system in which both reduced and oxidized species are soluble in the bulk solution. In this case I_{pp} did not vary significantly with mercury column height.

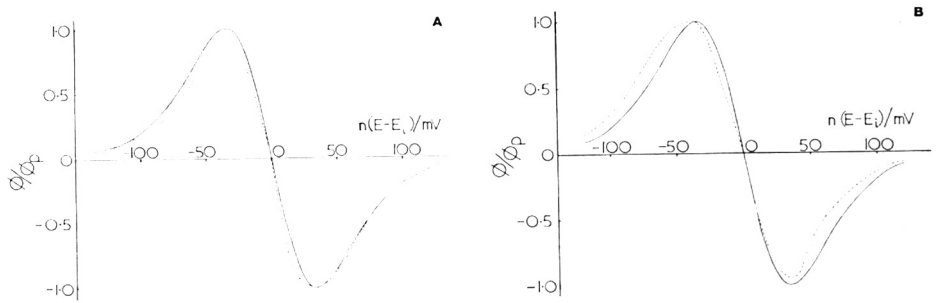


Figure 6. Comparison of theoretical (———) (Ref. *36*) and experimental (– – –) second harmonic ac polarograms

The electrode processes considered are: (*A*) Cd(II) + 2e ⇌ Cd(amalgam), ΔE = 10 mV, p-p. ω = 400 Hz. Concentration = 1.00 × $10^{-4}M$. (*B*) $[cp_2V(IV)dbdtc]^+ + e \rightleftharpoons cp_2V(III)dbdtc(acetone)$. ΔE = 10 mV, p-p. ω = 625 Hz. Concentration = 0.971 × $10^{-3}M$

$$I(2\omega t) = \frac{\sqrt{2}\, n^3F^3AC_0^*(\omega D_0)^{1/2}\Delta E^2 \sinh(j/2)}{16R^2T^2 \cosh^3(j/2)} \times \sin\left(2\omega t - \frac{\pi}{4}\right) \quad (7)$$

where A = electrode surface area, C_o^* = initial concentration of oxidized species, ω = applied frequency, ΔE = sinusoidal amplitude, D_o = diffusion coefficient of oxidized species, E_{dc} = applied dc ramp potential, $E_{1/2}^r$ = reversible half-wave potential, and j = (nF/RT)($E_{dc} - E_{1/2}^r$), and all other terms have their usual meaning. Equation 7 is based on the planar-diffusion mass-transfer model in which electrode geometry and growth (in the case of a DME) have been ignored. The restriction that $\Delta E \leq 8/n$ mV (*1*) needs also to be noted.

Wave Shape. The second harmonic ac wave shape (*36*) obtained for the vanadium complex shows excellent agreement with theory (Figure 6*B*). However, the cadmium system shows divergence (Figure 6*A*) also because of mass-transfer asymmetry (*35*).

Dependence of E_i on Various Parameters. Tables I and II show some relevant data concerning measurement of

(34) L. Meites, "Polarographic Techniques," 2nd ed., Interscience Publishers, New York, N.Y., 1965.
(35) T. G. McCord, E. R. Brown, and D. E. Smith, *Anal. Chem.*, **38**, 1615 (1966).
(36) A. M. Bond, *J. Electroanal. Chem.*, **35**, 343 (1972).

Table I. Variation of E_i and Peak-to-Peak Separation with Frequency for $1.00 \times 10^{-4}M$ Cadmium(II) in $1M$ HCl

Frequency, Hz	E_i, volt	Peak-to-peak separation, mV
10	0.590	37
20	0.593	34
40	0.593	32
60	0.591	34
80	0.591	38
100	0.593	36
150	0.591	33
200	0.592	32
250	0.590	33
300	0.592	38
350	0.591	33
400	0.592	33
450	0.591	37
500	0.591	38
600	0.590	36
700	0.593	37
800	0.591	35
900	0.591	34
1000	0.590	35
Av value:	0.591 ± 0.001 volt	35 ± 2 mV

Table II. Variation of E_i and Peak-to-Peak Separation with Amplitude for $1.00 \times 10^{-4}M$ Cadmium(II) in $1M$ HCl

Amplitude, mV, p-p	E_i, volt	Peak-to-peak separation, mV
	At ω = 100 Hz	
10	0.592	33
5	0.593	35
1	0.591	35
	At ω = 400 Hz	
10	0.593	35
5	0.591	35
1	0.591	36
	At ω = 900 Hz	
10	0.590	34
5	0.591	33
1	0.592	36
Av value:	0.591 ± 0.001 volt	35 ± 2 mV

E_i for the cadmium(II) electrode process. As can be seen, this value is independent of ΔE and frequency within the limit of experimental error. Furthermore, the dc $E_{1/2}$-value, the fundamental harmonic E_p-value, and E_i were all in excellent agreement as required by theory. The separation of peak to peak potentials is also in excellent agreement with theory (*1*) (68.4/*n* mV).

Analytical Applications. The use of phase-selective detection to reduce the charging current component of the alternating current, is not as important in the second harmonic mode because the charging current is negligible under ideal operating conditions (2). The main advantage of phase-selective second harmonic ac polarography relative to the "normal" form results from the shape of the current–voltage curve.

Phase-selective second harmonic ac polarography, in contrast to the nonphase-sensitive readout, gives a waveshape resembling the second derivative of the dc polarographic wave (*36*). This waveshape provides a more accurate and convenient means of preparing an analytical calibration curve by plotting the second harmonic peak-to-peak current against concentration, rather than measuring the height of one of the two peaks obtained from the nonphase-sensitive readout. For some systems with nonphase-sensitive readout, the peaks do not always give a linear response (*10*). The prediction by Woodson and Smith (*10*) that phase-sensitive readout might pose advantages, as far as obtaining a linear concentration response, has been confirmed by this work. In general, the nature of the second harmonic readout allows substantial improvement in precision because of the decrease in uncertainty in measuring the faradaic current. The magnitude of the alternating current is taken from a peak-to-peak measurement rather than from reference to the base line or zero value, as is the case in dc, fundamental harmonic, and nonphase-selective second harmonic ac polarograms. Reference to a base line necessarily introduces uncertainty into the measurement, which is eliminated in the technique under discussion, and even drifting base lines can be tolerated when a peak-to-peak measurement is undertaken. Peak-to-peak currents, in this work, could be measured with a reproducibility of ±1% without difficulty. Unlike peak height, no value judgment of this parameter is required, and a high precision as well as reproducibility is possible.

In other respects, both total and phase-selective second harmonic techniques are almost equivalent for reversible electrode processes in analytical work. A detailed study, optimizing all the parameters, and a complete analytical evaluation of second harmonic methods is currently in progress.

RECEIVED for review August 27, 1973. Accepted May 6, 1974. The authors acknowledge the financial support of the Australian Research Grant Committee in undertaking this work. One of us (H.B.) also received assistance in the form of a Commonwealth Post-Graduate Award.

Voltammetry in Sulfolane: The Electrochemical Behavior of Benzaldehyde and Substituted Benzaldehydes

Neal R. Armstrong and Rod K. Quinn

Sandia Laboratories, Albuquerque, N.M. 87115

N. E. Vanderborgh

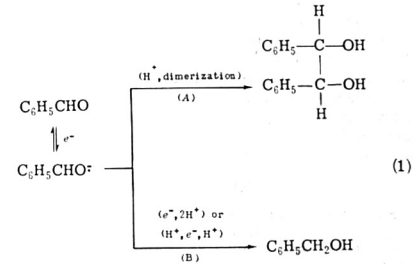
Department of Chemistry, University of New Mexico, Albuquerque, N.M. 87131

The electrochemical reduction of a series of para-substituted benzaldehydes in the aprotic solvent sulfolane has been explored by linear sweep and cyclic voltammetry. A single one-electron process is seen for the carbonyl reduction. The potential for the benzaldehyde reduction is shifted cathodically from previously reported potentials in other solvents and the chemical reaction following reduction is slow enough so that the reoxidation of the benzaldehyde intermediate is detectable at a sweep rate of 83.3 mV/sec. Benzaldehydes with an inductive substituent show an enhanced stability of the reduction intermediate. Rate coefficients for the disappearance of the intermediate are presented (*e.g.*, k_2 for the dimerization following reduction of benzaldehyde $= 2.4 \times 10^3$ l./m·sec). The contribution of the dielectric constant, and low Bronsted acidity of sulfolane to this reduction behavior is discussed.

Several recent studies have described electrochemistry in the aprotic solvent sulfolane, tetrahydrothiophene-1,1-dioxide. The reduction of several metals (*1–4*), and the reduction of oxygen (*5*) have been explored. These papers demonstrate the excellent solvent properties of sulfolane (*3, 5, 6*). The dielectric constant (43.3) (*7*) and wide electrolysis window (≥3.0 volts) (*1*) make this solvent unique for electrochemical investigations.

No previous work has been reported to utilize these solvent properties for an investigation involving a more complicated reduction pathway than those mentioned above. Other dipolar, aprotic solvents such as acetonitrile, dimethyl sulfoxide, and dimethyl formamide have been used with some success to explore reaction pathways which include protonation steps and short-lived intermediates—*i.e.*, free radicals, and radical anions (*8–12*). Electrochemistry in sulfolane should be rewarding in elucidating these pathways.

The electrochemistry of the carbonyl group has been studied extensively in aqueous media (*8–10, 13–19*). Equation 1 shows a summary of the proposed pathways for reduction under several conditions of acidity (*19*). Of particular interest here is the high pH pathway (A); the one-electron transfer to form the anion radical, in the case of benzaldehyde, $C_6H_5CHO^{\cdot-}$, which then undergoes protonation followed by dimerization.



(1)

Large cathodic potential shifts have been observed in the half-wave or formal potentials with increasing pH and with decreasing aqueous mole fraction (*8–10, 13–15*). This behavior is commensurate with a reduction mechanism initiated by a polarization of the functional group immediately prior to electron transfer and followed by protonation immediately after electron transfer, as assumed by Elving and Leone (*17*) (phenyl ketone reductions) and Rudd and Conway (*16*) (acetophenone reduction).

Using a ring-disk electrode in a 0.1*M* NaOH, 40% ethanol water basic media, Nekrasov and coworkers (*8–10*), have shown a single, one-electron process at $E_{1/2} = -1.5$ V *vs.* SCE for the reduction of benzaldehyde. This is a potential shift of some −0.7 V from the potential observed in 1*M* H_2SO_4. The reoxidation of the reduction intermediate could be simultaneously detected at the ring electrode, but the oxidation current was only a small fraction of the reduction current indicating a rapid following chemical reaction. This reduction intermediate was not detected in more acidic media. Stable electrolysis intermediates have also been observed by ESR spectroscopy in dimethyl formamide solutions and acetonitrile solutions (*20, 21*).

There are indications that the dimerization following reaction is a heterogeneous, surface-dependent process.

(1) J. F. Coetzee, J. M. Simon, and R. J. Bertozzi, *Anal. Chem.*, **41,** 767 (1969).
(2) J. F. Coetzee and J. M. Simon, *Anal. Chem.*, **44,** 1129 (1972).
(3) J. B. Headridge, D. Pletcher, and M. Callingham, *J. Chem. Soc.*, **1967,** 684.
(4) J. Desbarres, P. Pichet, and R. L. Benoit, *Electrochim. Acta*, **13,** 1899 (1968).
(5) C. Louis and R. L. Benoit, *Electrochim. Acta*, **18,** 7 (1973).
(6) E. M. Arnett and C. F. Douty, *J. Amer. Chem. Soc.*, **86,** 409 (1964).
(7) R. Fernandez-Prini and J. E. Prue, *Trans. Faraday Soc.*, **62,** 1257 (1966).
(8) L. W. Nekrasov and A. D. Korsun, *Elektrokhimiya*, **4,** 539, 996 (1968).
(9) A. D. Korsun and L. H. Nekrasov, *Elektrokhimiya*, **5,** 212 (1969).
(10) L. H. Nekrasov, D. H. Soshchin, and V. H. Gramenitskaya, *Elektrokhimiya*, **6,** 15 (1970).
(11) V. J. Puglisi and A. J. Bard, *J. Electrochem. Soc.*, **119,** 829 (1972).
(12) A. J. Bard, *Pure Appl. Chem.*, **25,** 379 (1971).
(13) P. H. Given, *J. Chem. Soc.*, **1958,** 2074.
(14) P. H. Given and M. E. Peover, *J. Chem. Soc.*, **1960,** 385.
(15) S. Wawzonek and A. Gunderson, *J. Electrochem. Soc.*, **107,** 537 (1960).
(16) E. J. Rudd and B. E. Conway, *Trans. Faraday Soc.*, **1971,** 440.
(17) P. J. Elving and J. T. Leone, *J. Amer. Chem. Soc.*, **80,** 1021 (1958).
(18) P. Zuman *et al.*, *Collect. Czech. Chem. Commun.*, **33,** 2548, 3090, 3205, 3213 (1968); and "Topics in Organic Polarography," P. Zuman, Ed., Plenum Press, New York, N.Y., 1970, pp 37–48, 49–56, 57–65, 66–79.
(19) B. Kastening and L. Hollack, *J. Electroanal. Chem.*, **27,** 355 (1970).
(20) P. H. Rieger and G. K. Fraenkel, *J. Chem. Phys.*, **37,** 2811 (1962).
(21) H. Steinberger and G. K. Fraenkel, *J. Chem. Phys.*, **40,** 723 (1964).

Table I. Purification Methods

Compound	Origin[a]	Purification method[b]
Tetrabutylammonium perchlorate (TBAP)	(E)	(1)
Benzaldehyde (C_6H_5CHO)	(E)	(2)
p-Nitrobenzaldehyde (PNB)	(A)	(1)
p-Cyanobenzaldehyde (PCNB)	(K)	(1)
p-Chlorobenzaldehyde (PCB)	(A)	(1)
p-Bromobenzaldehyde (PBB)	(A)	(1)
p-Phenylbenzaldehyde (PC_6H_5B)	(K)	(1)
1,2-Diphenyl-1,2-ethanediol	(K)	(1)

[a] E = Eastman White Label, Eastman Kodak Co.; K = K and K Laboratories Inc.; A = Aldrich Chemical Co. [b] (1) = recrystallization from ethanol and vacuum dried at 60 °C. (2) = distilled at reduced pressure from molecular sieves.

Udupa *et al.* (*22*), have shown the products of the aqueous benzaldehyde reduction to be dependent on the current density. At high current densities, high surface coverage, the pinacol predominates, while at low current density, low surface coverage, the alcohol is preferentially formed. Stereochemical analysis of the pinacol of this reduction also indicates a surface dependent formation (*23*).

We report here, the systematic study of the electrochemistry of a series of para-substituted benzaldehydes in sulfolane to demonstrate its novelty as an electrochemical solvent and its effect on these carbonyl reductions.

EXPERIMENTAL

Solvent Purification. Several techniques have been reported for purification of sulfolane (*1, 3, 4*). The solvent used in this study was prepared using a purification scheme which was suited to our electrochemical studies. Purity levels compare favorably to those previously reported (*1, 3*).

Sulfolane, Eastman Chemicals, was heated to approximately 100 °C and maintained at this temperature as it was eluted through a 125 × 4-cm diameter column of separate beds of activated alumina (8–14 mesh), followed by molecular (Linde 4A) sieves. A continuous stream of high purity argon was passed through the heated eluant. The eluant, approximately 3 liters in volume, was subsequently distilled from molecular sieves, using a Norelco stainless-steel, spinning-band still at 80 °C and 10^{-4} atm; the 80% center-cut was retained. This fraction was again distilled under identical conditions; volumes of this distillate were received directly into specially equipped electrochemical cells which served as the final receptacles in the purification scheme (details are given under the equipment section). The purified solvent had a maximum conductivity of 1×10^{-8} ohm^{-1} cm^{-1} and a water content of $<1 \times 10^{-3}M$ (Karl Fischer detection limits). Gas chromatography showed no detectable impurities greater than 0.01% of the solvent peak. The cathodic discharge of the solvent/supporting electrolyte occurred at −2.8 volts and anodic discharge at +0.975 volt *vs.* the Ag/$AgClO_4$ reference couple (see below). Residual currents were less than 0.5 μA through the full potential scan (scan rate = 1 volt/minute) at a stationary platinum disk (0.1064 cm^2). No faradaic components were noted in the residual scan.

The final purification step involved transferring 10 to 15 ml of solvent to the cells into which the supporting electrolyte tetrabutylammonium perchlorate (TBAP) had been previously weighed. Following filling, the cells were reweighed and solute concentrations reported in molal units. All solutions were 0.1 molal in supporting electrolyte. Several cells were prepared at once, filled with argon, and refrigerated until use. All solutions were deaerated with purified argon for 45 minutes prior to a measurement.

Table I shows the origin and method of purification of each of the solutes and the supporting electrolyte. All purified chemicals were kept at 0 °C, in the dark, under an argon atmosphere prior to use.

A three-electrode potentiostat based on the design of Jones *et al.* (*24*), was used for all electrochemical studies. The electrode used was a Teflon shrouded platinum disk (*25*), (area = 0.1064 cm^2, as measured by traveling microscope) coupled directly to a Motomatic E550/E500 rotator-controller. Contact was made to the electrode by means of a spring-pressure carbon brush. The resistance between the electrode and the potentiostat was less than 5 ohms.

Potentials were monitored with a Hewlett-Packard 3439/3443A digital voltmeter, with internal standard. This voltmeter was frequently checked with a Leeds and Northrup potentiometer.

The electrode was cleaned in nitric acid, rinsed in ethanol, polished with Linde Molecular abrasive, and rinsed with ethanol and dried. Following each potential scan, the electrode was stepped to 0.0 volts *vs.* the AgRE (defined below) for 45 seconds. This pretreatment was necessary to ensure reproducible current–voltage behavior. A slightly undersized Teflon male joint was used as a bearing for the rotating disk studies. An argon overpressure was continually maintained throughout the experiments.

The reference electrode (AgRE) was similar to one described previously for use in sulfolane (*1*). A silver plate (0.5 cm × 0.15 cm × 5 cm) was submerged in approximately 2 ml of a 0.1*m* $AgClO_4$/sulfolane solution in a 10-mm (inside diameter) tube terminated by a fine glass frit. This tube was inserted into a solution of 0.1*M* TBAP/sulfolane contained in a 12-mm (inside diameter) tube which tapers down to a 4-mm diameter fine glass frit. The outer tube was ring-sealed to a 14/20 ⅋ ground glass joint and fitted into one of the side joints of the cell. No leakage of Ag^+ ion was detected in the bulk solution. Faradaic currents resulting from the reducton of Ag^+ ion ($E_{1/2}$ = −0.19 V *vs.* AgRE) (*2*) were not observed under our experimental conditions. The distance between the reference electrode outer frit and the working electrode was reproducibly minimized (Figure 1).

The electrochemical cell (Figure 1) was designed to serve as a distillation receptacle as well as a location for electrochemical studies. A small volume is necessary to minimize the required amount of purified solvent. Entrance ports were provided for solute addition, reference, working and auxilliary electrodes, and admission of argon for deaeration and as a protective blanket during the run. This is similar to the technique described by Bard (*12*). The cell was constructed from a three-necked distillation flask, 25 ml in volume (19/20 ⅋ center joint, 14/20 ⅋ side arms). Three additional 7/15 ⅋ female joints were placed symmetrically around the upper center joint to serve as addition and exit ports for argon and to accommodate the auxilliary electrode. The cell was jacketed to maintain a temperature of 50.0 ± 0.1 °C throughout these investigations. Solute was added by a volume addition technique (*26*). A solution of the compound in sulfolane (prepared by weight) was dispensed with a Manostat Digipet sealed into a ground glass joint.

In the cyclic voltammetric experiments, the switching potential was always made at least 300 mV past the cathodic peak potential. Anodic currents for the reoxidation process were measured from the base line created between the switching potential and the onset of the oxidation process.

Apparatus for the controlled potential electrolysis was similar to those described previously (*15, 23*). A platinum gauze cylinder (2 cm high × 3-cm diameter) served as the cathode; a large platinum foil (1 cm × 8 cm) served as the auxilliary electrode. The auxiliary and cathode compartments were separated by a medium porosity frit (4-cm diameter). The reference electrode, a large silver plate, was immersed in a compartment filled with 0.1 molal TBAP in sulfolane, and separated from the cathode compartment by a fine porosity frit. This reference electrode poised approximately 600 millivolts positive of the AgRE, with negligible drift within the time frame of the electrolysis.

Benzaldehyde solutions (0.040 molal, 10-ml volume) were prepared and subjected to controlled potential electrolysis at potentials 300 mV past the reduction peak potential for times up to 350 minutes. The solution was stirred during electrolysis; and was deaerated with a purified argon stream. The concentration of benzaldehyde remaining was periodically checked by cyclic voltammetry at the stationary platinum disk, also mounted in the cathode compartment. Potential scans were made from cathodic to

(22) H. V. K. Udupa, G. S. Subramanian, K. S. Udupa, and K. Hortarajan, *Electrochim. Acta*, **9**, 313 (1964).
(23) V. J. Puglisi, G. L. Clapper, and D. H. Evans, *Anal. Chem.*, **41**, 279 (1969).
(24) H. C. Jones, W. L. Belew, R. W. Stelzner, T. R. Mueller, and D. J. Fischer, *Anal. Chem.*, **41**, 772 (1969).
(25) R. H. Adams, in "Electrochemistry at Solid Electrodes," Marcel Dekker, Inc., New York, N.Y., 1971, pp 267–300.
(26) N. E. Vanderborgh, N. R. Armstrong, and W. D. Spall, *J. Phys. Chem.*, **74**, 1739 (1970).

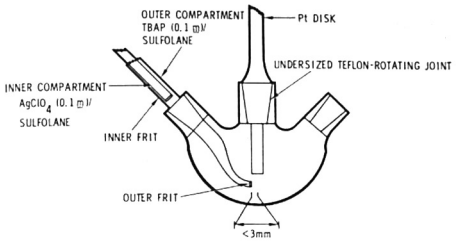


Figure 1. Cross-sectional view of electrochemical cell with working and reference electrodes in position; temperature jacket and auxiliary ports not shown

anodic potential limits to observe the presence of any electroactive species produced during the electrolysis.

Aliquots from the final electrolysis solution were subjected to separation and analysis by a Finnegan 1015D gas-chromatograph/mass spectrometer. Samples of 1.0 μl volume were injected onto an OV-1 column, temperature programmed from 100 to 250 °C at 10 °C per minute, with a helium carrier gas flow of 30 cm^3 per minute. Mass spectra were recorded of each eluted component of the electrolysis solution.

RESULTS AND DISCUSSION

Representative stationary electrode cyclic voltammograms for benzaldehydes are shown in Figure 2. The reduction process showed a single, diffusion-controlled faradaic component. (A small current, a few percent of the reduction wave, occurred at the foot of the current/potential curve.) Similar results were found for each of the substituted aldehydes. Diffusion control for these faradaic processes was ascertained by the linear dependence of peak current

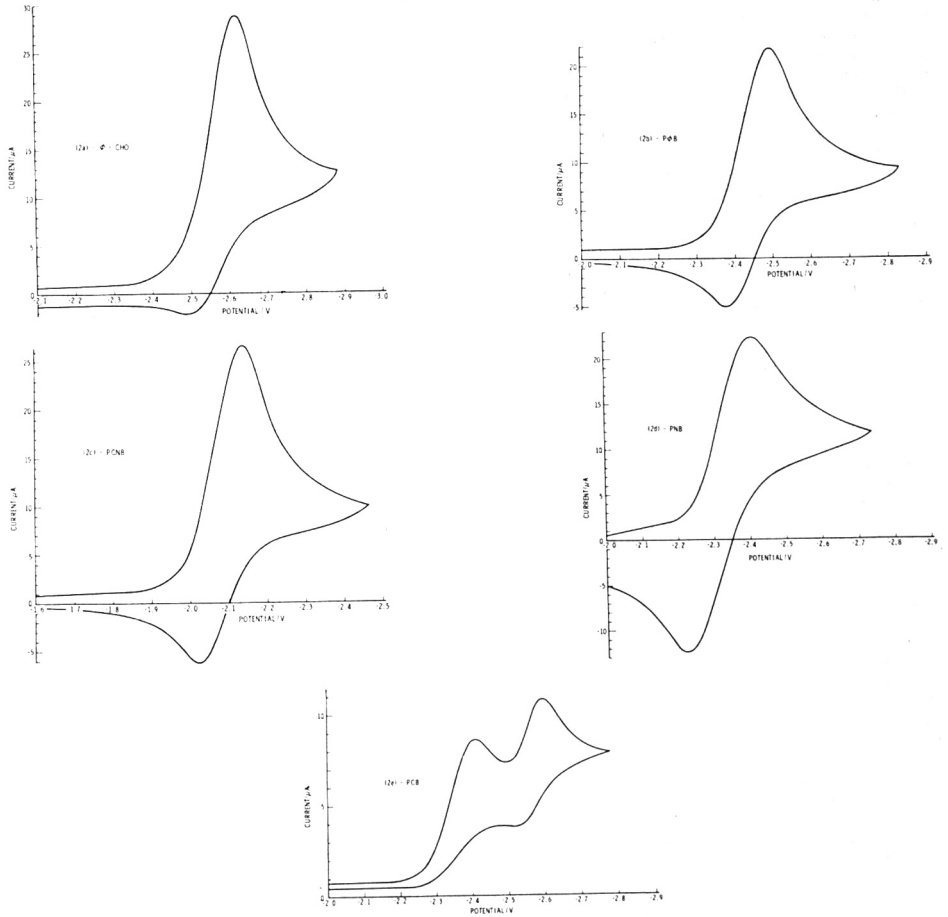


Figure 2. Representative cyclic voltammograms of benzaldehyde reductions at 50.0 °C. Potentials *vs.* AgRE

(*a*) Benzaldehyde, 2.10 m*m*, 167 mV/sec; (*b*) *p*-Phenylbenzaldehyde, 2.16 m*m*, 83.3 mV/sec; (*c*) *p*-Cyanobenzaldehyde, 2.64 m*m*, 83.3 mV/sec; (*d*) *p*-Nitrobenzaldehyde, 2.48 m*m*, 83.3 mV/sec; (*e*) *p*-Chlorobenzaldehyde, 1.19 m*m*, 16.7 mV/sec

Table II. Peak and Half-Wave Potentials and Wave Analysis of the Benzaldehyde Reductions. Shift in Half-Wave Potentials with Hammett Acidity (σ_p) and Inductive (σ_I) Parameters

Compound	$E_{p,c}$[a]	$E_{1/2}$[a,b]	log (i/i_{l-i})[b]	σ_p	σ_I	$\Delta E_{1/2}$[c]
Benzaldehyde (C_6H_5CHO)	$-2.581\,v$	$-2.557\,v$	68.0	0	0	0
p-Phenylbenzaldehyde (PC_6H_5B)	$-2.453\,v$	$-2.439\,v$	66.9	+0.01	+0.10	$0.118\,v$
p-Cyanobenzaldehyde (PCNB)	$-2.065\,v$	$-2.036\,v$	69.2	+0.67	+0.58	$0.521\,v$
p-Nitrobenzaldehyde (PNB)	$-2.114\,v$	$-2.091\,v$	67.6	+0.78	+0.63	$0.466\,v$
p-Chlorobenzaldehyde (PCB)	$-2.396\,v$	$-2.357\,v$	80.8	+0.24	+0.47	$0.200\,v$
p-Bromobenzaldehyde (PBB)	$-2.327\,v$	$-2.312\,v$	98.5	+0.27	+0.45	$0.245\,v$

[a] Volts *vs.* AgRE corrected to zero concentration effect; v = 16.7 mV/sec. [b] Taken while electrode rotated at 600 rpm; v = 16.7 mV/sec. [c] $\Delta E_{1/2} = [E_{1/2(R\text{-}C_6H_4CHO)} - E_{1/2(C_6H_4CHO)}]$.

with concentration and with square root of the scan rate, $(V/sec)^{1/2}$. Pertinent data for these reductions are shown in Table II.

The peak potentials show a slight shift with increasing concentration. For the purposes of comparison, data in this table list those potentials found by the extrapolation of the $E_{p,c}$ *vs.* concentration to zero concentration. These corrections correspond to a 1–15 mV anodic potential shift from the values found at 1m*m*.

More complicated voltammograms result with three of the investigated compounds: *p*-nitro-, *p*-chloro-, and *p*-bromobenzaldehyde. In the first instance, the nitro substituent underwent one-electron reduction prior to the carbonyl reduction. Both of the halo substituents showed an additional current wave past the carbonyl reduction potential, $E_{p,c} = -2.595$ V for PCB (Figure 2*e*) and -2.585 V for PBB. These processes may be due to adsorption (*27*) but more likely represent the reduction cleavage of the halo substituent (*28*). Wave analysis of these halo benzaldehydes showed a larger deviation from Nernstian behavior than found for compounds which did not show this effect (see Table II), probably because of the distortion produced by the second faradaic process.

The *n*-value for these reduction processes in sulfolane was determined by comparison to the reduction of ferrocene obtained under similar conditions. Ferrocene is believed to yield a reversible, one-electron oxidation (*2*); this was confirmed experimentally. Linear sweep voltammograms obtained using a sweep rate of 0.017 volt/sec at the platinum disk, rotated at 600 rpm showed reversible behavior: $E_{1/2} = -0.286$ V *vs.* AgRE and log $(i/i_l - i) = 64$ mV/decade. The diffusion coefficient was estimated to be $D_{RDE} = 1.03 \pm 0.11 \times 10^{-6}$ cm^2/sec from the Levich equation (C_0^b, the bulk concentration of ferrocene, = 0.74 and 1.50m*m*). A similar determination was made using the Stokes–Einstein relationship. Assuming the density for ferrocene to be 1.51 g/cm^3 (*29*), one can estimate a radius (assuming a spherical molecule) of 0.365 nm and, finally, a diffusion coefficient, D_{calcd} equal to 1.06×10^{-6} cm^2/sec. This agreement may be fortuitous since ferrocene is hardly spherical and has a formula weight only slightly larger than that of the solvent. However, the agreement does give some confidence in D_{RDE} as a reliable number.

Using literature values of the densities, spherical radii of 0.300 and 0.342 nm for benzaldehyde and *p*-nitrobenzaldehyde, respectively, were determined. Limiting currents at the rotating platinum disk (at 600 rpm) were compared with those data obtained for ferrocene yielding *n*-values of 0.94 for benzaldehyde and 1.06 for *p*-nitrobenzaldehyde.

Current–potential curves for *p*-phenyl- and *p*-cyanobenzaldehydes indicated similar results; the initial faradaic process is a one-electron step.

The corrected half-wave potentials were correlated with both the Hammett (σ_p) function and the Taft (σ_I) function (*30*). Figures 3*a* and 3*b* show these correlations between σ and $\Delta E_{1/2}[E_{1/2(R\text{-}C_6H_5CHO)} - E_{1/2(C_6H_5CHO)}]$. Of special interest are the trends between the inductive parameter, σ_I and the $\Delta E_{1/2}$ of these compounds with extended conjugation. The decrease in the energy required for the reduction with increasing inductive substituent parallels the facilitated polarization of the carbonyl group by those substituents (*16, 17*). Least squares slopes of Figures 3*a* and 3*b*, 0.589 and 0.782 volt, respectively, indicate a high sensitivity of the reduction process to substituent. This behavior also parallels the enhanced stability of the reduction intermediates discussed later.

The gas chromatographic/mass spectrometric analysis of the controlled potential electrolysis solutions indicates the product of the following chemical reaction of the benzaldehyde reduction to be the pinacol (1,2-diphenyl-1,2-ethanediol). Its identity was determined by a comparison of retention times and mass spectra of the suspected component of the electrolysis solutions and pure pinacol. The above method of separation and product identification requires solution concentrations only up to an order of magnitude greater than normal cyclic voltammetric conditions. These conditions provide microgram per microliter concentrations of product for analysis which is sufficient for GC/MS analysis. Previous identifications have relied on large solution concentrations, large current densities, etc. (*15, 22, 23*). Identification of the product of a massive electrolysis does not unambiguously prove the pathway of the electrode reaction occurring at millimolal concentrations of electroactive species. This low concentration analysis provides a more reliable identification of the product of the electrode reaction.

EC mechanisms have been considered by several authors; the linear sweep or cyclic voltammetric treatments of a dimerization reaction following charge transfer are of specific interest here (*31–36*). Olmstead *et al.* (*31*), have described a method using the ratio of peak currents determined by cyclic voltammetry, $(i_{p,a}/i_{p,c})$, to find values of the dimerization rate coefficient, k_2. Furthermore, Evans (*32*) has described a simulation method which generates

(27) R. H. Wopschall and I. Shain, *Anal. Chem.*, **39**, 1515 (1969); *ibid.*, 1535 (1969).
(28) I. M. Kolthoff and J. J. Lingane, "Polargraphy," Vol. II, 2nd ed., Interscience, New York, N.Y., 1952, p 681.
(29) J. D. Dunitz, L. E. Orgel, and A. Rich, *Acta Crystallogr.*, **9**, 373 (1956).
(30) J. March, "Advanced Organic Chemistry: Reactivity, Mechanisms and Structure," McGraw-Hill Series in Advanced Chemistry, McGraw-Hill Book Co., New York, N.Y., 1968, pp 231–45.
(31) M. L. Olmstead, R. G. Hamilton, and R. S. Nicholson, *Anal. Chem.*, **41**, 260 (1969).
(32) D. Evans, *J. Phys. Chem.*, **76**, 1160 (1972).
(33) L. Nadjo and J. M. Saveant, *J. Electroanal. Chem.*, **33**, 419 (1971).
(34) J. M. Saveant and E. Vianello, *Electrochim. Acta*, **12**, 1545 (1971).
(35) E. P. Andrieux, L. Nadjo, and J. M. Saveant, *J. Electroanal. Chem.*, **27**, 147 (1970).
(36) C. P. Andrieux, L. Nadjo, and J. M. Saveant, *J. Electroanal. Chem.*, **42**, 223 (1973).

values of $(E_{p,c} - E^{0'})$ (the difference between the peak potential and formal potential) as a function of the logarithm of the sweep rate to fit experimentally determined values. Evan's method allows determination of dimerization rates from reactions with quasi-reversible charge transfer rates whereas the cyclic voltammetric method of Olmstead *et al.* (*31*), assumes a reversible charge transfer. The resulting values of k_2 found by each method are listed in Table III. The simulation method requires a previous knowledge of the charge transfer rate. Estimates of the rate were made by the cyclic voltammetric peak potential separation method of Nicholson (*37*), under conditions where the effect of the following chemical step is minimized (highest sweep rates, lowest reactant concentrations). The charge transfer rate found ($k_s = 2 \times 10^{-3}$ cm/sec) seems quite low for these reactions but provides reasonable agreement in k_2 with the values determined by the peak current ratio method. Despite the minimal distance between the working and reference electrodes, uncompensated resistance effects can be a problem at the higher sweep rates and reactant concentrations. This was evidenced by a decrease in fit of the $(E_p - E^{0'})$ *vs.* sweep rate data at these extremes. Therefore, the values of k_2 determined are from the lowest reactant concentrations (1–2 mmolal).

The values of k_2 reported show an overall decreased rate of the following chemical reaction in sulfolane compared to values reported in aqueous and aqueous/alcohol media (*33*). An increase in the inductive character of the parasubstituent causes apparent stabilization of the intermediate. This supports the studies of Nekrasov and coworkers (*8–10*) and Rieger *et al.* (*20*) who showed aromatic character was necessary to stabilize the reduction intermediate so that it had a long enough lifetime to make observation possible. This reduction of the rate of the following chemical reaction is in marked contrast to studies in other solvents (*8–10, 33*), especially since the lifetime of the benzaldehyde is increased to such an extent as to be observable by cyclic voltammetry at relatively low sweep rates.

The second *p*-nitrobenzaldehyde reduction step shows a following reaction that is almost chemically reversible. This confirms the findings of Kargin *et al.*, (*38*) who found the *p*-nitrobenzaldehyde reduction consisted of two successive one-electron reduction steps, both chemically reversible. Interestingly, the nitro group substituent effect (σ_I, σ_P) on the second half-wave potential of *p*-nitrobenzaldehyde is still quite marked (Figure 3), even though the molecule has undergone the prior one-electron reduction.

The data presented here support a one-electron reduction of the benzaldehydes followed by dimerization to the pinacol (Pathway A, Equation 1). A decided solvent effect is evidenced in several parameters. The reduction potential is sufficiently shifted cathodically from previous reported reduction potentials to preclude the observation of subsequent faradaic processes at still more cathodic potentials.

Coetzee estimates the potential of the AgRE (in sulfolane) to be 0.70 volt *vs.* the SCE (*1*). Using this value, it is possible to compare these results with previous studies. The corrected $E_{1/2}$ for the benzaldehyde reduction, −1.857 V, represents a 0.3-V cathodic difference compared to the reduction potential reported in a 0.1*M* NaOH, 40% ethanol medium (*10*). A similar difference is seen between the benzaldehyde peak potentials obtained by linear sweep voltammetry in buffered ethanol medium by Nadjo and Saveant (*33, 39*) and our own data in sulfolane. In addition to differences in liquid junction potentials, a lower Bronsted acidity (*40*) of sulfolane necessitating higher energies for the reduction process would contribute to this increase in reduction potential. Addition of small amounts of water (acidic relative to sulfolane) showed an anodic shift in peak potential, approximately 15 mV/decade for a concentration change of H_2O between 1–5 mm. Addition of stronger acids, benzoic acid and phenol, distorted the current–volt-

Table III. Determination of the Rate Coefficient of the Following Chemical Reaction, k_2. Sweep Rate, Peak Current Function, Peak Current Ratio, and Homogeneous Rate Coefficient k_2 for Benzaldehydes and Substituted Benzaldehydes[a]

Sweep rate, V/sec	$i_{p,c}/v^{1/2} \cdot C_b$ (μA·sec$^{1/2}$/V$^{1/2}$ mm)	$i_{p,a}/i_{p,c}$
Benzaldehyde (C_6H_5CHO) (C = 1.50 mm)		
0.0167	39.3	...
0.0333	37.4	...
0.0833	36.5	0.19
0.1667	35.4	0.21

k_2(A) = 2.4 × 10^3 l./m·sec (Average from 1.50–3.09 mm); k_2(B) = 2.0 × 10^3 l./m·sec

***p*-Phenylbenzaldehyde (PC_6H_5B) (C = 1.15 mm)**		
0.0167	30.9	0.51
0.0333	29.9	0.49
0.0833	28.9	0.50
0.1667	34.0	0.56
(C = 2.16 mm)		
0.0167	34.8	0.37
0.0333	33.3	0.38
0.0833	32.8	0.44
0.1667	31.6	0.53

k_2(A) = 2.0 × 10^3 l./m·sec (Average from 1.15–3.86 mm); k_2(B) = 9.0 × 10^2 l./m·sec

***p*-Cyanobenzaldehyde (PCNB) (C = 1.42 mm)**		
0.0167	31.4	0.49
0.0333	31.9	0.44
0.0833	32.9	0.49
0.1667	34.8	0.49
(C = 4.66 mm)		
0.0167	29.3	...
0.0333	30.1	0.37
0.0833	29.9	0.38
0.1667	29.5	0.45

k_2(A) = 1.0 × 10^2 l./m·sec (Average from 3.71–4.66 mm); k_2(B) = 1.5 × 10^2 l./m·sec

***p*-Nitrobenzaldehyde (C = 1.34 mm)**		
0.0167	28.6	0.95
0.0333	26.4	0.94
0.0833	24.0	0.99
0.1667	25.4	0.89
(C = 3.48 mm)		
0.0167	30.5	0.91
0.0333	28.7	0.91
0.0833	25.9	0.91
0.1667	24.9	0.82

k_2(A) = 3.0 l./m·sec (Average from 1.34–4.35 mm); k_2(B) not determined.

[a] k_2, the calculated, second-order rate coefficient for the disappearance of intermediate, *i.e.*, $d[R^-]/dt = -k_2[R^-]^2$ (*31*). (A) Determined by ratio of peak currents method (*31*). (B) Determined by fitting of experimental $(E_{p,c} - E^{0'})$ *vs.* log a, $a = nFv/RT$. v = scan rate, volts/sec (*32*).

(37) R. S. Nicholson, *Anal. Chem.*, **37**, 135 (1965).
(38) V. Kargin, V. Kondrania, and H. Semakhima, *Tsvet. Akad. Nauk. Ser. Khim.* **2**, 278 (1970).
(39) F. Ammar, L. Nadjo, and J. M. Saveant, *J. Electranal. Chem.*, **47**, 146 (1973).
(40) R. L. Benoit and P. Pichet, *J. Electroanal. Chem.*, **43**, 59 (1973).

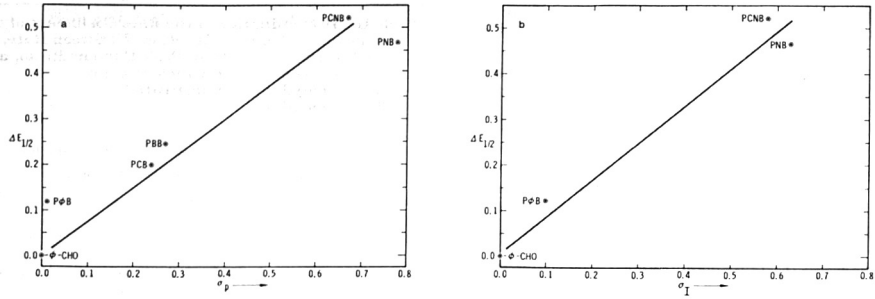


Figure 3. Linear free energy plots of benzaldehyde reductions $\Delta E_{1/2} = [E_{1/2(R\text{-}C_6H_5CHO)} - E_{1/2(C_6H_5CHO)}]$ (*a*) $\Delta E_{1/2}$ *vs.* Hammett acidity σ_p of each para substituent (*29*); Least squares slope = 0.589 volt. (*b*) $\Delta E_{1/2}$ *vs.* Taft σ_I inductive parameter of each para substituent (*29*). Least squares slope = 0.782 volt

age curves for the reduction process. This probably arises from simultaneous hydrogen discharge in these more acidic solutions.

Protonation of the reduction intermediate is intimately involved with the reduction process in all media studied thus far. It is generally agreed that the formation of a pinacol type dimer must be preceded by either a protonation of the one-electron intermediate, followed by dimerization, or dimerization of this intermediate to form the pinacolium dianion and then protonation (*13–19, 22, 23, 33, 39*). One must question the origin of the protons necessary in these steps. In sulfolane, one source is residual water in the solvent. Detection limits of Karl Fischer titrimetry are of the same order of magnitude as the concentrations of electroactive species. There is no reason to assume water concentrations appreciably lower. Although sulfolane itself is considered an extremely weak acid ($pK_a > 31$), the intermediates mentioned may show basicity sufficient for proton abstraction from the solvent. In keeping with their observed lifetimes, the substituted benzaldehydes rank in decreasing basic character with increasing inductive character of the substituent.

Assuming a protonation step, the medium should lose acidity during electrolysis. A test of the base concentration of an electrolyzed solution was performed by fivefold dilution with water and subsequent titration with 0.01*N* HCl. Basic species liberated in the protonation steps (such as the solvent lyate ion) should be convertible to titratable OH^-. In a typical experiment, 5.89×10^{-5} mole of pinacol was formed and 9.29×10^{-5} mole of OH^- subsequently titrated. The average ratio, moles OH^-/moles pinacol = 1.60, deviates negatively from the expected ratio of 2.0. This deviation can represent experimental losses of the basic species or a competitive reaction not requiring protonation. These experiments tend to prove the formation of the pinacol in the dry solvent leaving the solvent deficient in acidity. However, the chemical identity of the protonating agent remains speculative without further experimentation. The observed decrease in the rate of the following chemical reactions can also contribute to the cathodic shift in reduction potential of benzaldehyde between aqueous solvents and sulfolane. As demonstrated previously, an order of magnitude lowering of the rate coefficient can result in a 20- to 30-millivolt cathodic shift in the reduction peak potential (*28, 29*).

Lawrence and Parsons have recently developed a model of the mercury/sulfolane interface (*41*) which may have some applicability to this study. At largely negative potentials, strong adsorption of the hydrocarbon side of the solvent occurs, resulting in an estimated mean dielectric constant of 7 for the inner Helmholtz plane. One would expect inhibition of the approach and polarization of the carbonyl group into such a low dielectric constant and a repulsion of the one-electron intermediate. The exact extent of this effect toward lowering the charge transfer rate and cathodically shifting the reduction potential remains unclear.

The solvent sulfolane can therefore affect both the prereduction state of the benzaldehyde and the state of the reduction intermediate. The benzaldehyde molecule has been assumed protonated prior to reduction in aqueous media (*8–19*), the unprotonated species in sulfolane should be harder to reduce. The solvent also enhances the lifetime of the intermediate via the low hydrogen activity, the low viscosity, which tends to lower collision frequencies for any following chemical reaction, and the reasonably high dielectric constant which would tend to stabilize an anion radical. This enhanced lifetime manifests itself also as a further cathodic increase in the reduction potential.

The further exploration of these reductions in sulfolane is in progress. Use of convective-transport techniques and *in situ* spectroelectrochemical studies appears extremely promising.

ACKNOWLEDGMENT

We are grateful for the assistance of F. J. Conrad with the gas chromatography/mass spectrometry experiments.

RECEIVED for review January 30, 1974. Accepted May 31, 1974. This work was supported by the U.S. Atomic Energy Commission. One of us (NRA) gratefully acknowledges the Associated Western Universities for financial support through an AWU/AEC Graduate Fellowship.

(41) J. Lawrence and R. Parsons, *Trans. Faraday Soc.*, **64** 751 (1968).

Streaming Potentials in Automatic Potentiometric Systems

Pierre Van den Winkel, John Mertens, and Désiré L. Massart

Farmaceutisch Instituut, Vrije Universiteit Brussel, Paardenstraat 67, B-1640 Sint Genesius Rode, Belgium

Several authors have reported oscillations of potential caused by the peristaltic pump in automated potentiometric systems, which were ascribed to differing causes. This article shows that the disturbances are due to streaming potential oscillations. Both, the base-line shift, which is another consequence of the streaming potential, and the oscillations are shown to obey the Helmholtz–Smoluchowski equations. The order of magnitude of both phenomena corresponds with theoretical expectations. Procedures for the experimental elimination or reduction of the oscillations are discussed.

The steadily growing number of commercially available ion selective electrodes has also stimulated research on the automation of measurements with these electrodes and, in particular, the use of autoanalyzer systems (*1–5*).

Potential oscillations caused by the proportioning pump have been observed in all cases. They seem to occur as well for glass electrodes (*3*), as for solid state electrodes (CN^-, Ref. *1*; and F^-, this article and Ref. *5*), for liquid membrane electrodes of the ion exchange type (*2*) or the neutral sequestering type (*4*). They have been variously ascribed to liquid junction potential changes at the reference electrode (*1*) or to static electricity effects (*2*).

Mertens *et al.* (*3, 4*) proposed that these oscillations could be due to changes in streaming potentials. To obtain experimental evidence for this hypothesis, a systematic investigation of the parameters having an influence on the magnitude of the oscillations was carried out, using a system for the automatic analysis of F^-. The results are reported here.

EXPERIMENTAL

The automatic systems used in this study are based on the flow scheme given in Figure 1. Analytical applications of this system were presented at a IUPAC symposium (*6*) and will be published elsewhere. This experimental set-up was adapted to the present investigation where it was, of course, necessary to use varying flow rates, varying electrolyte concentrations, and to work with or without a debubbling system.

Apparatus. Discrete samples are picked up by means of a Technicon sampler II and fed into the manifold by proportioning pumps of different construction such as Technicon pump I, Carlo Erba 1512/20 and Gilson Minipuls. The larger part of the experiments were done with the Minipuls pump which combines the advantages of continuously adjustable flow rate with relative small pressure pulses. When continuous sample pick up was required, the sampler was omitted. In the manifold, the samples of known F^- concentrations were mixed with different electrolyte concentrations. Various flow rates were achieved by adjusting the rotation speed of the pump or by changing the diameter of the pumping tubes. The indicator (Orion F^- 94-09-A and 94-09-00) and reference electrodes (SCE Radiometer K401; solid state Cl^- electrode Beckman 39604; Ag/AgCl internal reference electrode Beckman 39278 and single and double junction Orion reference electrode 90-00-01 and 90-02-01) were mounted in separate home made Perspex cells provided with metallic nipples and connected by plastic tubes of varying length and diameter. A detailed description of the indicator flow through cell is given elsewhere (*6*). An Orion 801 or 601 digital mV meter ($Z_{in} \approx 10^{14}\Omega$) was used. The base-line potential (*i.e.*, the potential recorded at flow rate 0), the base-line shift (*i.e.*, the potential shift observed when the flow rate changes from zero to a predetermined value) and the base-line oscillations (*i.e.*, the periodic potential variations observed at flow rates $\neq 0$) were recorded with a Kipp and Zonen double pen recorder. The correct amplitude response of this recorder was verified under appropriate conditions of sensivity range and paper speed by means of a dual trace oscilloscope PM 3210 (Philips).

Conductivity measurements were carried out in an EA 645 titration cell coupled to an E 365 conductoscope (Metrohm).

RESULTS AND DISCUSSION

Nature of Base-Line Shift and Oscillations. When a liquid is forced through a narrow capillary by a pressure gradient, a potential difference E_S is set up between the ends of the capillary. This potential is called the streaming potential. E_S is given by the Helmholtz-Smoluchowski equation:

$$E_S = \frac{D\zeta}{4\pi\eta} \cdot \frac{\Delta p}{\lambda} \tag{1}$$

where D = dielectric constant (dimensionless), ζ = electrokinetic potential (volt), η = viscosity (poise), Δp = pressure gradient (dyne cm^{-2}), and λ = conductivity ($ohm^{-1}\,cm^{-1}$).

If one assumes that a Poiseuille velocity profile is obtained in the liquid, *i.e.*, when the flow is laminar

$$\Delta p = \frac{8d\eta l}{\pi r^4} \tag{2}$$

where d = flow rate (ml/sec), l = length of the capillary, in this case the length of the tube connecting the electrodes (cm), and r = radius of the capillary (cm). Substitution of Equation 2 in 1 yields:

$$E_S = 2\frac{dD\zeta l}{\pi^2 r^4 \lambda} \tag{3}$$

In the cgs electrostatic system the result must be divided by 9.10^{11} to obtain E_S in volts.

If periodic oscillations in the flow rates occur, these must lead to oscillations ΔE_S in the streaming potentials. Indeed the establishment of the streaming potential must be considered as immediate since it is characterized by a time constant τ

$$\tau = \frac{D}{9.10^{11} 4\pi\lambda} \tag{4}$$

It is probable that these phenomena also occur in continuous automatic systems where the liquid is pressed through a tube connecting the reference electrode to the indicator electrode. As a consequence, one must expect that a streaming potential is set up over the connecting tube which will be added algebraically to the potential

(1) B. Fleet and H. von Storp, *Anal. Chem.*, **43**, 1575 (1971).
(2) J. Ružička and J. C. Tjell, *Anal. Chim. Acta*, **47**, 475 (1969).
(3) P. Van den Winkel, J. Mertens, G. De Baenst, and D. L. Massart, *Anal. Lett.*, **5**, 567 (1972).
(4) J. Mertens, P. Van den Winkel, and D. L. Massart, *Anal. Lett.*, **6**, 81 (1973).
(5) R. T. Oliver, G. F. Lenz, and W. P. Frederick, "Advances in Automated Analysis," Vol. II, Technicon International Congress, 1969, p 309.
(6) International IUPAC Symposium on Ion Selective Electrodes, Cardiff, Wales, April 1973, *J. Pharm. Belg.*, in press.

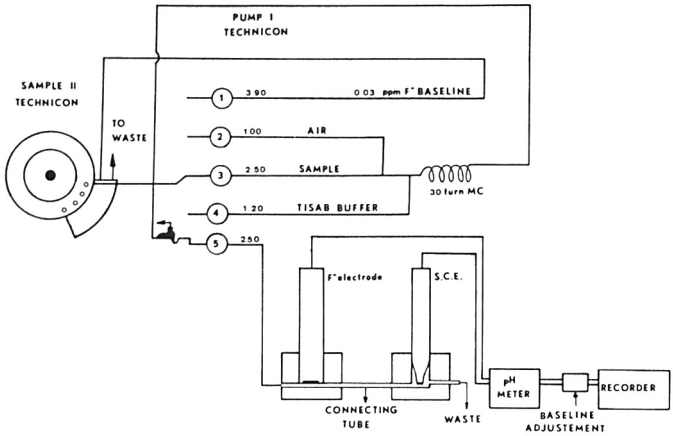


Figure 1. Flow scheme of the automatic system

measured by the electrodes. In the literature (*7-9*), one finds a few references to experimental difficulties encountered or expected in potentiometric measurements in flow systems.

If d represents the average flow rate and since normally all the other parameters entering in Equation 3 remain constant during a run of the automatic system, this will show a dependence of the base line on this parameter. Actually, it is known that flow rates slowly change because of fatigue effects of the pumping tubes so that a drift of the base line will be obtained. Another consequence is that base-line oscillations caused by the pump and corresponding to flow rate oscillations may be expected.

Figure 2 shows the effects which are observed. In going from a static measurement (flow rate = 0) to dynamic measurements, the base line is shifted and the oscillations develop. The frequency of the oscillations of potential is equal to the frequency with which a bar or roller of the propulsing peristaltic pump passes over the pumping tube, *i.e.*, the number of pressure or flow rate pulses. When the rotation speed of the pump is altered, one observes a proportional change in the frequency of the oscillations of potential.

This amply proves the point, which was also taken for granted in earlier articles (*1-4*), that the oscillations of potential are associated directly with the movement of the pump.

In the system studied here, the oscillations are not due to liquid junction potentials. This was proved by carrying out the measurements with several different reference electrodes, some with and some without a liquid junction (see Experimental). No differences were observed.

Instead of measuring the oscillations of potential over the electrodes, one can also measure the streaming potential and the oscillations between the metallic inlet nipple of the reference cell and the outlet nipple of the indicator cell. In this way, one measures the potential over the plastic connecting tube between both flowthrough-cells without any possible interference due to one of the electrodes.

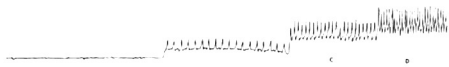


Figure 2. Base-line shift and oscillations. Flow rate in ml/min: *A*, 0; *B*, 0.44; *C*, 0.81; *D*, 1.44

Simultaneous potential measurements over the electrodes and over the ends of the connecting tube, show that the oscillations have the same frequency and the same magnitude (within a few percent) in both kinds of measurements. This is an unequivocal proof that the oscillations of potential are indeed due to streaming potentials. Since the measurement is carried out without intervention of the electrodes, the same phenomenon must occur in all automatic systems.

In the case of liquid ion exchange electrodes, it cannot be excluded that pressure effects on the membrane or streaming potentials across the membrane itself, may also contribute to the oscillations. This was proposed by Fleet and Rechnitz (*10*) in the case of the Ca^{2+} membrane electrode. Moreover they reported that operating at very high flow rates even causes an erratic response of the sensor, probably due to distorsion of the membrane resulting in a change of membrane solution geometry. In other systems, liquid junctions may also play a role. Nevertheless, it is the authors' opinion that in most systems, streaming potentials must be responsible for the larger part of the observed oscillations.

If this is true, both the base-line shift E_S and the magnitude of the base line oscillations ΔE_S must obey Equation 3. Figures 3 and 4 represent $E_S = f(l)$ and $\Delta E_S = f(l)$ when all the other parameters appearing in Equation 3 are constant. As shown, a linear relationship is obtained as expected from Equation 3. The same holds for $E = f(d)$ (Figure 5) and $\Delta E_S = f(d)$ (Figure 6). The relationships $E = f(\lambda)$ and $\Delta E_S = f(\lambda)$ (Figures 7 and 8) are linear in the conductivity range from 10 to 2500 μSiemens corresponding to 5.10^{-4} to $10^{-1}M$ NaCl.

At very low conductivity, however, both the base-line shift and the oscillations are smaller than expected. This is due to the fact that the Helmholtz-Smoluchowski equation takes into account only the volume conduction.

(7) R. A. Gortner, "Outlines of Biochemistry," 3rd ed., Wiley, New York, N.Y., 1949.
(8) W. N. Greer, Leeds and Northrup Co. Tech. Publ. **EN 96(1)**, Philadelphia, Pa., 1962.
(9) G. A. Rechnitz and G. C. Kuchler, *Anal. Chem.*, **39**, 1682 (1967).
(10) B. Fleet and G. Rechnitz, *Anal. Chem.*, **42**, 690 (1970).

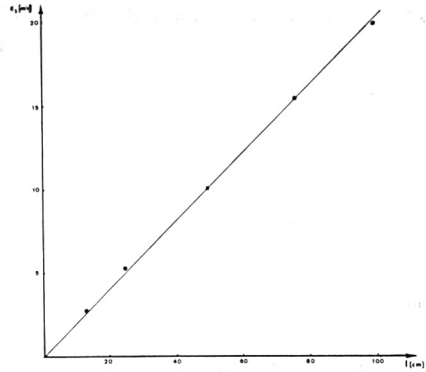


Figure 3. Base-line shift E_S as function of the length l of the connection tube

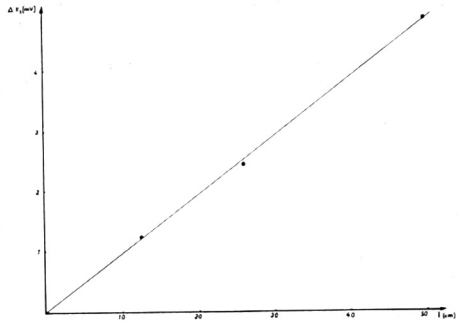


Figure 4. Base-line oscillation ΔE_S as function of the length l of the connection tube

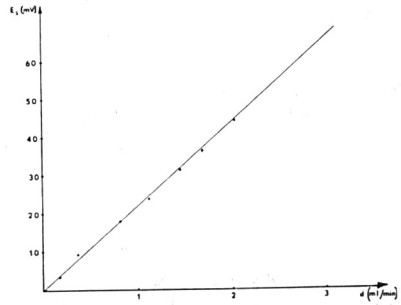


Figure 5. Base-line shift E_S as function of the flow rate d

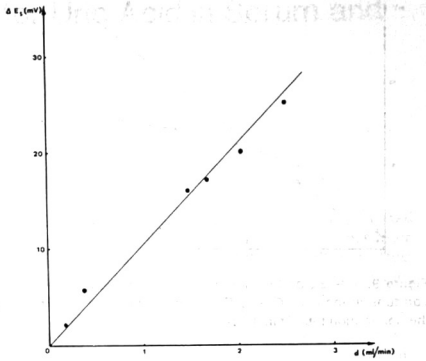


Figure 6. Base-line oscillation ΔE_S as function of the flow rate d

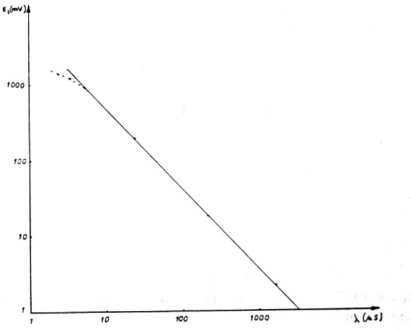


Figure 7. Base-line shift E_S as function of the conductivity λ (in micro-Siemens)

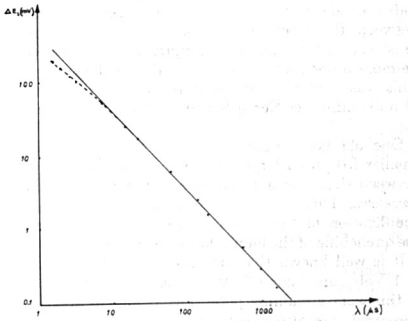


Figure 8. Base-line oscillations ΔE_S as function of the conductivity λ (in micro-Siemens)

At low electrolyte concentrations, an important part of the conduction occurs along the surface of the capillary, so that Equation 1 must become

$$E_S = \frac{D\zeta}{4\pi\eta} \frac{\Delta p}{(1 + 2\lambda_S/r\lambda)} \quad (5)$$

where λ_S represents the surface conduction. As a consequence, the conductivity becomes larger than calculated with Equation 3 and E_S is smaller than expected. It can be concluded that our observations of E_S and ΔE_S as functions of λ are in agreement with the theory.

The base-line shift, E_S, is a function of $(1/r^4)$ as expected from Equation 3 (see Figure 9). However, $\Delta E_S = f(1/r^4)$ is a convex function. It was thought that this could be due

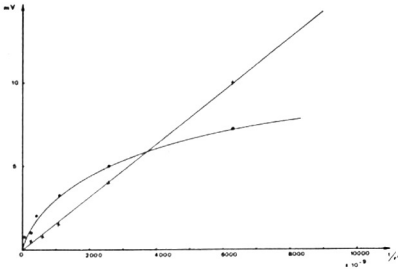


Figure 9. $x = E_S$ as function of $1/r^4$ (r = radius of the connection tube in inches). O = ΔE_S as function of $1/r^4$ (r = radius of the connection tube in inches)

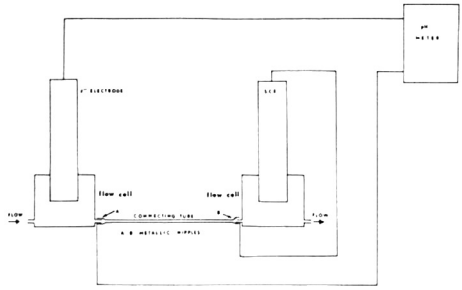


Figure 11. Electronic pulse-suppressing set-up

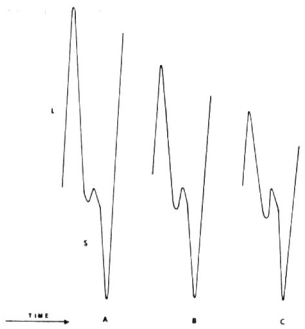


Figure 10. Pulse shape as function of the inner diameter of the connection tube (in inches) *A*, 0.02; *B*, 0.04; C, 0.056

to differences in quenching of the pulses when the liquid stream passes from the narrow bore outlet nipple of the indicator electrode flow cell to the larger connecting tube between the electrode compartments. This larger tube must act as a partial pulse suppressor and the effect must be more pronounced when the radius of the tube is larger. This was verified experimentally by recording the pulses at maximum recorder speed to obtain a more detailed picture.

One observes (Figure 10) that the pulse consists of a smaller (*S*) and a larger (*L*) component and that the ratio between these becomes smaller as the radius of the tubes increases. This is probably to be interpreted as a partial equalization of the flow by local turbulence resulting in the quenching of the larger flow rate pulses.

It is well known that streaming potentials of the order of 1 Volt can occur (7). With the automatic system used in this work streaming potentials as high as 1350 mV were measured (see also Figure 7) for the following conditions: $5.10^{-5}M$ NaCl, $\lambda = 3.10^6$ ohm^{-1} cm^{-1} (*i.e.*, 2.5 μSiemens/cm) at 20 °C l = 12 cm, r = 0.017 cm, d = 0.011 ml/sec. Taking a value of ζ = 0.1 volt (ζ usually has a value between 0.05 and 0.2 V) and D = 80, and calculating E_S with Equation 3, one obtains 1.2 volt. Thus the order of magnitude of the potentials found corresponds with the theoretically expected value. The values of ΔE_S can be even larger because with certain pumps the flow rate varies during a pulse from 0 (or even slightly negative values) to about twice the mean flow rate.

Practical Elimination of Base-Line Oscillations. It is clear that oscillations of 1 volt or even of a few millivolts are very detrimental to the quality of the analyses carried out with automatic systems. They must therefore be suppressed in one way or another. There are several possibilities:

One can vary the parameters in Equation 3, *i.e.* on d, r, l, or λ. The most practical solution is to add a large quantity of electrolyte, so that a larger value of λ is obtained. This is often also required for other reasons. For example: in the automatic analysis of F^-, TISAB buffer (which is $1M$ in NaCl) must be added. However, the addition of large quantities of salt cannot always be tolerated, *e.g.*, in automatic analysis of serum or when low-selectivity electrodes such as the nitrate electrode are used.

One can also vary the magnitude of the flow rate pulses. Peristaltic pumps always give rise to such pulses so that a careful choice of pump will only reduce the effect but will not eliminate it. At the same flow rate, the pulses caused by two Peripumps are inversely proportional to the number of bars passing per unit time. This means that the pump with the larger number of bars and the higher rotation speed will be the most adequate. Furthermore, a pulse suppressor mounted immediately before or after the indicator electrode cell or the pumping of air slugs into the tube connecting the pump to the indicator cell and debubbling just before the latter, reduces ΔE_S by a factor of 100.

Finally a partial suppression of the oscillations can be achieved by transferring the voltage built up between the metallic nipples (see Figure 11) to the reference electrode terminal lead in an appropriate way. Although a complete suppression of the pulse could be expected, reductions of ΔE_S by a factor of only 50 was obtained. This is probably due to a phase shift. Further pulse reduction may be obtained by earthing both nipples or by using a grounded metallic connection between indicator and reference cells.

ACKNOWLEDGMENT

The authors thank W. Rigolle, F. Van de Kerkhove, and A. Rutgers for advice in the interpretation of the results and N. Harford for advice in the redaction of the article.

Received for review September 11, 1973. Accepted February 21, 1974. The authors are grateful to the Fonds voor Geneeskundig Wetenschappelijk Onderzoek for financial assistance.

Enzyme Electrode Sensing Oxygen for Uric Acid in Serum and Urine

M. Nanjo and G. G. Guilbault

Louisiana State University in New Orleans, Department of Chemistry, New Orleans, La. 70122

A direct reaction-rate method is proposed for the sensitive determination of uric acid, based on the uricase (Urate Oxidase, EC 1.7.3.3) catalyzed oxidation of uric acid:

$$\text{Uric acid} + O_2 \xrightarrow{\text{uricase}} \text{allantoin} + CO_2 + H_2O_2 \quad (1)$$

Using a platinum electrode which is covered with an immobilized uricase as a thin reaction layer, the disappearance of dissolved oxygen during the enzymatic degradation of uric acid is directly measured at −0.60 V *vs.* SCE. The initial rate of disappearance of dissolved oxygen is proportional to the uric acid present. By this method, the assay of uric acid in human serum and urine can be performed selectively and rapidly.

The assay of uric acid for the diagnosis and the treatment of hematologic disorders has been well recognized (*1, 2*) and the desire for simplicity, precision, and good selectivity has brought about the development of several methods and modifications (*3–5*).

Those methods fall into two categories: one is based on the non-specific reduction of phosphotungstate by uric acid in an alkaline solution (phosphotungstic acid reagent is reduced also by ferrous salts, glutathion, phenols, ascorbic acid, glucose, tyrosine, tryptophan, cystine, and cysteine) and the second is based on the specific enzymatic oxidation by uricase. In the latter method, that of Praetorius and Poulsen (*6, 7*) and its modifications (*1, 2, 8*), the decrease in the absorbance of uric acid is measured at 293 nm. In this method, prior deproteinization of the blood sample is necessary.

Recently, kinetic methods based on fluorometric (*9*) and photometric (*10*) techniques have been described. Electrochemical methods based on the oxidation of uric acid have been described by Feldman (*11*) and Adams (*12*). Also, Bell and Ray (*13*) reported the rate of oxygen consumption was proportional to uric acid concentration in the bulk solution by means of a glucose analyzer.

This paper describes an enzyme electrode for uric acid based on the direct amperometric measurement of the decrease in dissolved oxygen level by the uricase-catalyzed oxidation of uric acid. The method uses a simple platinum electrode without a membrane and, hence, is different from the previously quoted enzyme electrode for glucose which used an oxygen membrane electrode of the Clark type coated with a layer of physically bound glucose oxidase (*14*). When this electrode is placed into a biological fluid, blood or urine, the uric acid diffuses into the layer of chemically bound uricase where it is oxidized at the expense of dissolved oxygen around the platinum electrode. Thus, the electrode has a high selectivity for uric acid, and no pretreatment of the sample, such as deproteinization is necessary. The method is rapid, reliable, simple, and economical enough to be used in a physician's office or clinical laboratory.

EXPERIMENTAL

Reagents and Solutions. *Uric Acid.* A stock 88 mg % solution was prepared by dissolving uric acid (2,6,8-trioxypurine, monosodium salt, Sigma Chemical Co., St. Louis, Mo.) in 0.04% lithium carbonate solution.

Uricase. Uricase was immobilized according to a modification of the method reported by Brown (*15*) as follows: Uricase (Sigma Chemical Co., Type IV, 2.5 units/mg, from *Candida utilis*) 10 mg, also uricase (Sigma Chemical Co., Type V, 25 units/g, from *hog liver*) 200 mg, and plasma albumin (Sigma Chemical Co., from *Bovine serum*) 200 mg were dissolved into 5 ml of $(NH_4)_2SO_4$ and $Ba_2B_4O_7{\cdot}10\ H_2O$, 0.1*M* solution (pH 9.4). Then five drops of glutaraldehyde (Sigma Chemical Co, 50%) was added into the mixture and stirred. The solution was frozen by Dry Ice–acetone coolant. The frozen mixture was warmed slowly in a refrigerator for a day. The sponge-like copolymer was washed with the buffer and stored in a refrigerator until use.

Buffers. Borate buffer, 0.1*M*, pH 9.2, with ammonium sulfate was prepared by dissolving $Na_2B_4O_7{\cdot}10\ H_2O$ (Mallinckrodt) and $(NH_4)_2SO_4$ (Mallinckrodt) in distilled water.

Glycine buffer, 0.1*M* and 0.3*M* were made from glycine powder (Sigma Chemical Co.) and adjusted pH with NaOH solution.

Uricase Electrode. Platinum disk electrode (Beckman Model 39273) was used as the solid base electrode. The procedure for the preparation of the enzyme electrode is simply as follows: The immobilized uricase was mounted on the surface of the platinum electrode and secured with nylon cloth (Pharmacia Fine Chemicals, Inc., Piscataway, N.J., Nylon Screen No. 0670) and "O" rings; then the electrode was stored in the borate buffer solution with ammonium sulfate 0.1*M*, pH 9.2, at room temperature. Borate–ammonium sulfate buffer has been reported to enhance the activity of uricase by Arima and Nose (*16*).

The electrode response time was proportional to the amount of uricase on the electrode surface; less uricase immobilized gave a faster response time.

Apparatus and Procedures. A Heath Polarograph System (Model EUA-19-2) was used. The uricase enzyme electrode procedure consisted of placing the electrode with a calomel electrode into a stirring buffer solution at −0.6 V *vs.* SCE.

When the current is at a constant level, the sample solutions are pipetted into the buffer solution and the initial rate of change in dissolved oxygen limiting current is recorded with a Heath Recorder Model EU-205-11.

In the assay of serum, 5.0 ml of 0.3*M* glycine buffer (pH 9.2) is

(1) C. A. Dubbs, F. W. Davis, and W. S. Adams, *J. Biol. Chem.*, **218**, 497 (1956).
(2) L. Liddle, J. F. Seegmiller, and L. Laster, *J. Lab. Clin. Med.*, **54**, 903 (1959).
(3) S. Natelson, *Stand. Methods Clin. Chem.*, **1**, 123 (1953).
(4) W. R. Coraway, *Stand. Methods Clin. Chem.*, **4**, 239 (1963).
(5) D. R. Donald, *Stand. Methods Clin. Chem.*, **6**, 1 (1970).
(6) E. Praetorius, *Scan. J. Clin. Invest.*, **1**, 222 (1949).
(7) E. Praetorius and S. H. Poulsen, *Scan. J. Clin. Lab. Invest.*, **7**, 201 (1955).
(8) Sigma Technical Bulletin, 680; Sigma Chemical Co., St. Louis, Mo.
(9) G. G. Guilbault and P. Hodapp, *Anal. Lett.*, **1**, 789 (1968).
(10) Sigma Chemical Company, St. Louis Mo., Enzymatic Assay Procedure for Uricase U-8500.
(11) F. J. Feldman, Electrochemical Approach to Clinical Instrumentation, paper presented at 166th American Chemical Society Meeting, Los Angeles, Calif., August 27–31, 1973.
(12) G. Park, R. N. Adams, and W. R. White, *Anal. Lett.*, **5**, 887 (1972).
(13) R. Bell and R. Ray, *Clin. Chem.*, **17**, 644 (1971).
(14) S. J. Updike and G. P. Hicks, *Nature (London)*, **214**, 986 (1971).
(15) G. Brown, C. T. Thomas, G. Gellfe, D. Domurado, A. M. Berjonneau, and C. Guillon, *Biotech. Bioeng.*, **105**, 359 (1973).
(16) K. Arima and K. Nose, *Biochim. Biophys. Acta*, **151**, 54 (1968).

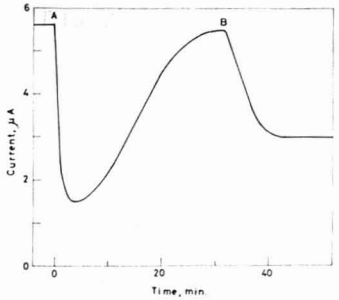


Figure 1. Changes in the dissolved oxygen current during enzymatic reactions

T = 30 °C, borate buffer 0.1*M*, pH 9.4, E = −0.6 V *vs.* SCE. *A*, 22 mg of uricase (Type V) added to 1.0 ml of 8.8 mg % uric acid solution. *B*, Uric acid (1.0 ml, 8.8 mg %) added to the above solution

used and 0.5 ml of serum is added to the buffer solution. In the case of urine, 0.5 ml of urine is added to 10.0 ml of the buffer solution.

These procedures are conducted at 30 °C. The effect of temperature has been reported to be very important for uricase function and the activation energy for the enzymatic reaction was calculated to be 12.4 Kcal/M (*17*) indicating the temperature control was very critical for rate method. After each measurement, the electrode was rinsed with buffer solution and dipped into the buffer solution for 1 or 2 minutes to recover the dissolved oxygen concentration around the enzyme and to eliminate the remaining reaction products. The oxygen content in the buffer solution was constant in this experiment and the starting oxygen contents in sample solution did not affect the rate because of the small amount of samples (less than $\frac{1}{10}$ of buffer solution).

RESULTS AND DISCUSSION

Electrode Response. Uric acid oxidation by dissolved oxygen in the presence of uricase is well known (Equation 1). A fluorometric assay for uric acid based on the Schöenneman reaction has been applied to the system in which hydrogen peroxide is generated (*9*). But, in this study, the amperometric determination of liberated hydrogen peroxide at +0.6 V *vs.* SCE failed; although in the case of a glucose oxidase electrode, hydrogen peroxide was detected by the same procedure (*18*).

The reasons that direct measurement of hydrogen peroxide cannot be used to monitor uric acid are: 1) uric acid itself is also electroactive, and gives a limiting current at the same potential where hydrogen peroxide is oxidized and the i–E curves of uric acid and hydrogen peroxide behave similarly with changes in pH. Hence, the complete separation of the currents is impossible with either a platinum or a gold electrode. 2) The reaction products of Equation 1 are reported as a stoichiometric complex of allantoin and hydrogen peroxide in phosphate or Tris buffer in the pH range between 7.0 and 9.0 as follows (*17*):

$$\text{Uric acid} + O_2 + 3H_2O \xrightarrow{\text{uricase}} \text{allantoin} \cdot H_2O_2 + HCO_3^- \quad (2)$$

Although in borate buffer, urate has been reported to be oxidized to give hydrogen peroxide, we could not detect any peroxide electroanalytically.

Attempts to measure the rate of disappearance of dissolved oxygen according to the Equations 1 or 2 at a negative potential, −0.6 *vs.* SCE, where dissolved oxygen is reduced stepwise to water, yielded a limiting current proportional to the dissolved oxygen concentration.

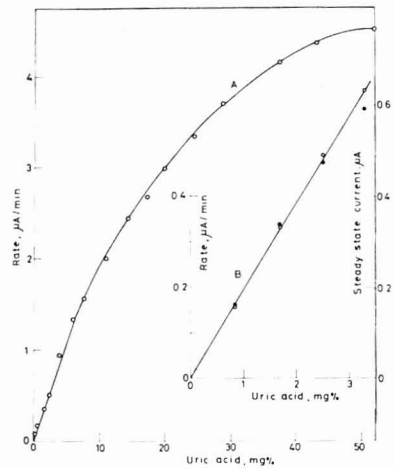


Figure 2. Calibration curves for uric acid

T = 30 °C, 0.1*M* glycine buffer, pH 9.2, E = −0.6 V *vs.* SCE. *A*, Curve for urine assay. *B*, Curve for serum assay. O, Rate method; ●, Steady state method

At the same potential for dissolved oxygen, hydrogen peroxide also gives a cathodic current; however, no hydrogen peroxide formation was detected. In Figure 1, the changes of the current at −0.6 V *vs.* SCE are shown using a platinum electrode. When uricase solution was introduced into a uric solution (A), the current due to the dissolved oxygen was observed to decrease very rapidly. After the uric acid was completely oxidized, the current showed a recovery of the dissolved oxygen level due to adsorption of more oxygen from the air. This phenomena was also observed when uric acid was added to uricase solution (B).

Such a dissolved oxygen consumption during an enzymatic reaction was found not only for uricase, but also in the case of alcohol oxidase (from *Basidiomycete* and *Kloeckera*), glucose oxidase (EC 1.1.3.4, from *Aspergillus niger*), and L-amino acid oxidase (EC 1.4.3.2, from *Bothrops atrox venom*).

Hence, either alcohols, amino acids, or glucose could be measured by the same technique. This will be the subject of a future paper.

In the bulk reaction, the initial rate of disappearance of dissolved oxygen currents and the total current change were proportional to uric acid concentration. Using the enzyme electrode, steady state currents are obtained at the plateau because of an equilibrium between the dissolved oxygen consumption by enzymatic reaction and the supply of oxygen from the bulk solution to the enzyme layer on the surface of the electrode. Instead of the kinetic method, the steady state current method can also be used. A longer time is required (2–3 min.) to obtain a steady state than the time required for the initial slope (1 min).

A linear relationship is obtained up to 8 mg % of uric acid concentration (Figure 2); then a plateau is observed as predicted by the Michaelis-Menten equation. The per cent deviation from linearity at 10 and 15 mg % of uric acid are 10 and 25%, respectively.

(17) H. R. Mahler, G. Hübscher, and H. M. Baum, *J. Biol. Chem.*, **216**, 625 (1955).
(18) G. G. Guilbault and G. J. Lubrano, *Anal. Chim. Acta*, **64**, 439 (1973).

Table I. Initial Rates in Various Buffer Solutions[a]

Medium	Rate, μA/min	Dissolved oxygen current, μA
Glycine 0.1*M*	0.27	2.5
Tris 0.1*M*	0.24	2.1
Borate 0.1*M* + $(NH_4)_2SO_4$ 0.1*M*	0.22	1.9
Britton–Robinson buffer 0.1*M*	0.26	2.3
Borate 0.1*M*	0.25	2.2
0.25*M* Glycine	0.23	2.1
0.50*M* Glycine	0.21	1.4
1.00*M* Glycine	0.15	0.6

[a] E = −0.6 V *vs.* SCE, T = 30 °C, pH = 9.2.

Effect of pH. The effect of pH on the electrode response was studied from pH 7.5 to 11 for 8.0 mg % of uric acid solution. The optimal pH is approximately 9.3, and the electrode response using immobilized enzyme was not observed to be as sensitive to pH change as the soluble uricase reaction.

This optimal pH is in agreement with the reported value for the soluble enzyme: pH 9.0 (*17, 19*) and pH 9.2 (*16*).

The type of buffer solution also had an effect on the initial rate of dissolved oxygen consumption. The effect on the rate was directly proportional to the change of oxygen concentration in the electrolyte solution and indirectly to change of uricase enzyme activity.

Table I shows the initial rates in various buffer solutions at the same pH. As can be seen from the table, the higher oxygen current gives the faster initial rate.

Ammonium sulfate concentration also had an effect on the initial rate in the same pH borate buffer, the rate decreasing with increasing concentration. This means that a low ionic medium is more favorable for measurements with the enzyme electrode.

Effect of Other Compounds Present in Serum and Urine. The various inhibitors of uricase have been investigated in the bulk solution (*16, 17, 19, 20*). In this electrode process, the initial rate and steady state current were affected by two different mechanisms. One is direct inhibition of the enzyme by inhibitors such as heavy metal ions and thiol compounds. The second is interference by oxidizable compounds such as ascorbic acid or cysteine which consume dissolved oxygen.

In this study, the interference of ascorbic acid, cysteine, cystine, methionine, tyrosine, and albumin were examined. Interference was found with ascorbic acid and cysteine, which consume dissolved oxygen very fast in alkaline solution as shown in Figure 3. Other compounds have no effect on the initial rate within the range of concentrations found in blood and urine.

Although the effect of ascorbic acid and cysteine are serious for the assay of uric acid, fortunately, the concentration of these two compounds in human fluid is very low, and they are oxidized before the measurement of uric acid. Hence, there is no effect by these compounds in human fluid on the initial rate when the sample solution was measured by the enzyme electrode.

Therefore, the number of interferences in this initial rate method is considerably less than those in the classical nonenzymatic methods. Furthermore, there is no necessity for dialysis or deproteinization which cause the loss of uric acid as is necessary in spectrophotometric methods and no necessity of the other enzyme, such as peroxidase, as required in fluorometric methods.

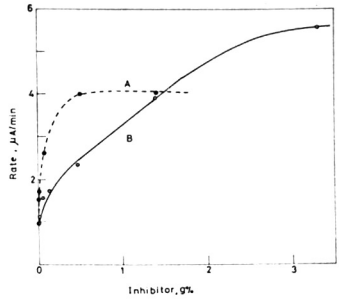


Figure 3. Effect of cysteine and ascorbic acid on the uricase electrode response

T = 30 °C, 0.1*M* glycine buffer, pH 9.2. E = −0.6 V *vs.* SCE. *A*, Ascorbic acid. *B*, Cysteine hydrochloric acid salt

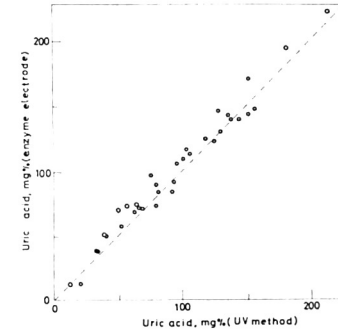


Figure 4. Assay of uric acid in urine

T = 30 °C, 0.1*M* glycine buffer, pH 9.2, E = −0.6 V *vs.* SCE. UV = Spectrophotometric method (decrease of urate at 293 nm). Enzyme electrode: Uric acid electrode (rate method)

Effect of the Applied Potential. In this study, the potential was kept constant at −0.60 V *vs.* SCE. However, the reduction of the dissolved oxygen begins at almost 0 V *vs.* SCE and gives a limiting current between −0.2 and −0.7 V *vs.* SCE on the platinum electrode. This means that any drift in the applied potential between −0.2 and −0.7 V *vs* SCE does not give any significant errors in the initial rate method and it is possible to choose the best proper potential to eliminate other electroactive substances in human fluids.

Assay of Uric Acid in Urine and Serum. The concentration of uric acid in human urine and serum is 2–8 mg % in normal serum and 250–750 mg/day in normal urine (*8*). As can be seen from the calibration curve, the enzyme electrode has enough sensitivity for serum in which the concentration of uric acid is less than one tenth of uric acid in urine.

The results of analysis are shown in Figures 4 and 5, respectively. The regression equations by the method of least squares are as follows for serum (Figure 4) and urine (Figure 5) in mg % (Y means uric acid concentration measured by enzyme electrode and X means that of the spectrophotometric method.

(19) H. M. Baum, G. Hübscher, and H. R. Mahler, *Biochim. Biophys. Acta*, **22**, 514 (1956).
(20) H. R. Mahler, H. M. Baum, and G. Hübscher, *Nature (London)*, **124**, 705 (1956).

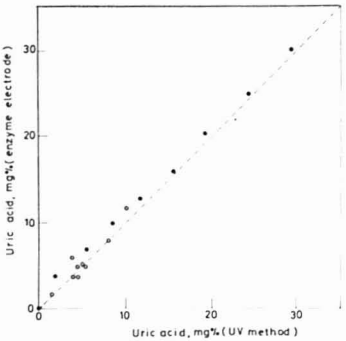


Figure 5. Assay of uric acid in serum

T = 30 °C, 0.3M glycine buffer, pH 9.2, E = −0.60 V *vs.* SCE. ○, Actual serum. ●, Control serum, added uric acid

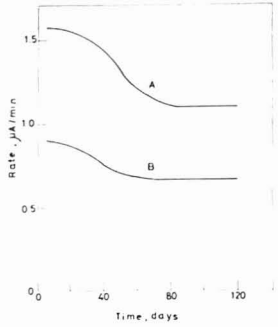


Figure 6. Long-term stability of uric acid electrode using the rate method

T = 30 °C, 0.1M glycine buffer, pH 9.2, E = −0.6 V *vs.* SCE. *A*, 8.0 mg % of uric acid measured. *B*, 4.2 mg % of uric acid measured

$$Y = 0.96X + 0.83 \text{ (serum)}$$

$$Y = 0.97X + 6.5 \text{ (urine)}$$

respectively. The calculated correlation coefficients were 1.02 and 1.00 for serum and urine.

As can be seen from these results, the enzyme electrode gave good agreement with values obtained by the spectrophotometric method (*5*), in which uricase was used and deproteinization is required.

The reproducibility was determined using the same samples, and was found to be (153 ± 7) mg % (4% of relative standard deviation) in the case of urine, and (9.6 ± 0.9) mg % (~9%) in the case of serum.

Long-Term Stability of the Electrode. Soluble enzyme can be used for the enzyme electrode (*21*) but it loses activity very fast. After 4 days, all activity is lost at room temperature. In this study, the long-term stability was examined by testing the response of the electrode to 8.0 mg % and 4.2 mg % uric acid in buffer solution several times a week for several months (Figure 6).

When the electrodes are not used, they were stored in borate buffer, with ammonium sulfate, 0.1M solution (pH 9.2) at room temperature (*ca.* 25 °C).

As can be seen in Figure 6, even after 100 days, the apparent decrease of the response is only about 29% lower at 8.0 mg % of uric acid and about 26% lower at 4.2 mg % uric acid indicating the electrode is still useful for assays.

(21) L. C. Clark, Jr., *Biotech. Bioeng. Symp.*, **3**, 377 (1972).

ACKNOWLEDGMENT

The authors thank S. S. Kuan for his assistance in this project.

RECEIVED for review February 14, 1974. Accepted June 10, 1974. The financial assistance of the National Science Foundation, NSF Grant No. GP-31518, is gratefully acknowledged.

An Automatic Analyzer for the Detection of Dihydroxyphenylalanine Metabolites and Other Reducing Componds in Urine

Phillip W. Banda, Arletta E. Sherry, and Marsden S. Blois

Department of Dermatology, University of California, San Francisco, Calif. 94143

A new cation-exchange chromatographic system has been developed for detecting DOPA metabolites and other reducing compounds in urine. The system is similar in design to an amino acid analyzer, but uses diphenylpicrylhydrazyl as the colorimetric reagent, and has its own unique set of operating parameters. The system was developed to detect catecholic and indolic metabolites in the urine of patients with malignant melanoma. The chromatograms of normal urines show only a few major peaks, while the chromatograms of urines from patients with disseminated disease show a larger number of major peaks which are not observed in normals. The identity of these peaks remains to be determined.

We wish to describe the operation of an automatic ion-exchange chromatographic system that detects and measures a broad range of reducing compounds in urine. The system has a general design similar to an amino acid analyzer, but uses the stable free radical 2,2-diphenyl-1-

picrylhydrazyl (DPPH) as the colorimetric reagent. The system was constructed to identify dihydroxyphenylalanine (DOPA) metabolites in the urine of patients with malignant melanoma, but we believe that it has applications in other clinical and research areas as well.

A number of automated liquid column analytical systems are currently available for detecting various classes of physiologic compounds. The systems range from the amino acid analyzer, where ninhydrin is the class reagent for primary amines, to the high pressure UV analyzers, where detection is based on the absorption of the individual compounds (*1*). More recently, automated column systems have been developed using either inherent or reagent-enhanced fluorescence (*2, 3*) as a class-detecting system for various indoles. A more elaborate system for the simultaneous detection in urine of both amino acids and polypeptides, using the multiple reagents of the Lowry method as the peptide class indicator, has appeared (*4*). Each of these systems has its own applications and advantages, but none of the present automatic systems was particularly suited for our purposes.

We are interested in detecting urinary melanogens, a group of hydroxy- and/or methoxy-substituted indoles and phenols that are associated with the metabolism of melanin pigment, and that are excreted in elevated amounts in the urine of patients with malignant melanoma (*5, 6*). Detection problems arise because the compounds considered as melanogens fall into a broad range of chemical classes: the phenolic and indolic acids, aromatic amino acids, and the catecholamines (*7–10*). Such a range of metabolites is difficult to detect adequately by any single chromatographic monitoring procedure. While ninhydrin will react with DOPA and other amine-containing melanogens, it fails to detect the aromatic acids, such as homovanillic acid (HVA) and the hydroxyindole acids. It is possible, of course, to detect DOPA and related metabolites by their UV absorption, as in the UV analyzer (*11*). The disadvantage of UV absorption is that a large number of metabolites other than catechols and indoles are also detected. The elution of these other metabolites, principally nucleic acid base derivatives and related compounds, makes the UV chromatograms complex and the runs many hours long, with the peaks of interest often comprising only a small portion of the chromatogram. In addition, the molar absorptivity of bases and their analogs is approximately an order of magnitude greater than that of the catechols ($\sim 10^4$ *vs.* 10^3), whereas the DPPH reaction is inherently more sensitive to DOPA than to any base analog (*12*).

Fluorescence is a very sensitive means of detection and, while useful for certain indole metabolites, it is not a property native to all the melanogens, nor is there a single fluorescent reagent that will tag all the compounds of interest. The recent introduction of fluorescamine (*13*)increases the sensitivity of amine detection, but does not broaden the class of compounds identifiable. A new column detection method based on the reduction of cerium(IV) to fluorescent cerium(III) is valuable for organic acids, but requires greater that day-long elution times (*14*). Current procedures for the fluorescent detection of DOPA metabolites extracted from urine (*15*) depend on a partial oxidation of these compounds to an indole derivative, a process not readily adaptable to automatic analysis.

DPPH is a stable free radical that has long been known in the chemical literature. In solutions of organic solvents, DPPH exhibits a deeply violet color with a broad absorbance maximum centered near 520 nm. Upon reaction with suitable electron donors, DPPH solutions lose color stoichiometrically with the number of electrons taken up. We have previously reported that DPPH reacts with a broad range of reducing compounds of biological origin, particularly antioxidants, the catechol acids, and catecholamines; that DPPH is useful as an indicator of elevated levels of melanogens in the urine of melanoma patients; and that DPPH can be used to assay for DOPA in urine fractions isolated from ion-exchange resins (*12, 16, 17*). We, therefore, proceeded to construct an automatic ion-exchange column system, using DPPH as the colorimetric reagent, in order to have an analytical system particularly suited for identifying individual melanogens in urine. The present communication describes the DPPH analytical system in detail.

EXPERIMENTAL

Design of the System. The buffer and reagent flow pattern of the DPPH system is similar to that of an amino acid analyzer, with buffer and reagent reservoirs, pumps, a column, mixing tee, reaction bath, and flow cell detector. The system is unique in the buffer sequence used, the reagent and its concentration, the temperature of the reaction bath, and the class of compounds identifiable. The system was constructed from parts and spare equipment, and is not a commercial instrument.

Detection System. The detection system was built around a B & L Spectronic 20 colorimeter (No. 33-29-40), by adapting a flow cell (6.6-mm pathlength, 0.12-ml volume) to the sample chamber. The colorimeter wavelength was set at 525 nm, and the microammeter was replaced by a resistor across the input terminals of a chart recorder. The recorder attenuation was set at 5 mV, and the chart speed at 15 cm/hr.

Temperature. The resin columns were jacketed and maintained at 51 °C. A separately heated reaction bath, containing approximately 100 feet of $\frac{1}{16}$-inch o.d. heavy wall Teflon tubing, was maintained at 62 °C.

Reagent and Solvent. DPPH (Eastman) is 94% pure and is used without further processing at a concentration of 100 mg/liter in methyl cellosolve. The reagent-solvent mixture is pumped at 75 ml/hr. Purportedly high purity methyl cellosolve from many suppliers turned out to be inadequate for use with DPPH, which decolorized upon dissolving. Methyl cellosolve of purity adequate for stable reagent solutions may be obtained by distilling practical grade solvent.

Buffers. The four sodium citrate buffers used as eluants are, together with their running times: (1) 0.20*N* pH 2.50, 15 minutes; (2) 0.20*N* pH 3.25, 30 minutes; (3) 0.20*N* pH 4.30, 60 minutes; and (4) 0.35*N* pH 5.25, 110 minutes. The buffer flow rate is 75 ml/hr. BRIJ-35, 30% solution, is added to all buffers at 2 ml/liter.

Resins. We have used the following cation exchange resins in our system: Aminex MS-B, Q-15S, and A-6 (Bio-Rad), and H-70 (Hamilton). Each has particular advantages, but the A-6 resin provides the best resolution of the reference compounds with the four-

(1) W. W. Pitt, Jr., C. D. Scott, and G. Jones, Jr., *Clin. Chem.*, **18**, 767 (1972).
(2) D. D. Chilcote, Clin, Chem., **18**, 1376 (1972).
(3) H. H. Brown, M. C. Rhindress, and R. E. Griswold, *Clin. Chem.*, **17**, 92 (1971).
(4) J. A. Klosse, D. Y. Huistra, P. K. De Bree, S. K. Wadman, and J. F. G. Vliegenthart, *Clin. Chim. Acta*, **42**, 409 (1972).
(5) J. Duchon and B. Matous, "Pigment Cell," Vol. 1, Karger, Basel, 1973, p 317.
(6) H. Hinterberger, A. Freeman, and R. J. Bartholomew, *Clin. Chim. Acta*, **39**, 395 (1972).
(7) M. L. Voorhess, *Cancer*, **26**, 146 (1970).
(8) J. J. Vallon, A. Badinand, and C. Bichon, *Clin. Chim. Acta*, **36**, 397 (1972).
(9) J. Duchon and Z. Pechan, *Ann. N.Y. Acad. Sci.*, **100**, Pt. 2, 1048 (1963).
(10) J. Duchon and B. Matous, *Clin. Chim. Acta*, **16**, 397 (1967).
(11) J. E. Mrochek, S. R. Dinsmore, and D. W. Ohrt, *Clin. Chem.*, **19**, 927 (1973).
(12) P. W. Banda, A. E. Sherry, and M. S. Blois, *Anal. Lett.*, **7**, 41 (1974).
(13) S. Udenfriend, S. Stein, P. Bohlen, W. Dairman, W. Leimgruber, and M. Weigele, *Science*, **178**, 871 (1972).
(14) S. Katz, W. W. Pitt, Jr., and G. Jones, Jr., *Clin. Chem.*, **19**, 817 (1973).
(15) H. Weil-Malherbe, *Methods Biochem. Anal.*, **16**, 293 (1968).
(16) M. S. Blois, *Nature (London)*, **181**, 1199 (1958).
(17) L. Taskovich, P. W. Banda, and M. S. Blois, "Pigment Cell," Vol. 1, Karger, Basel, 1973, p 323.

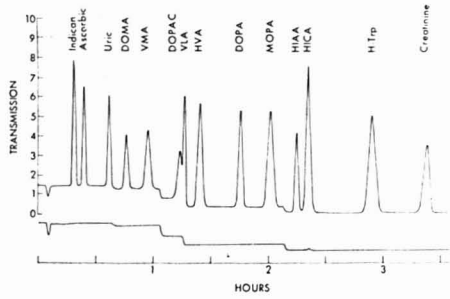


Figure 1. Chromatogram of the reference compounds, with a base line run below

The chromatographic profile represents peaks of transmittance, with the 0–10 scale corresponding to 5–65% *T*

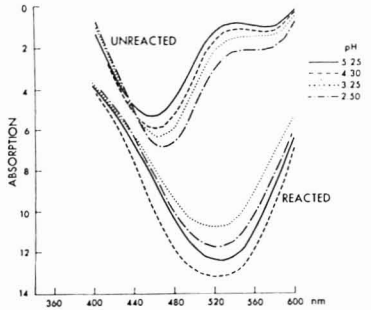


Figure 2. Absorbance spectra of the 1:1 DPPH–solvent:buffer mixture at the pH of the four eluting buffers

Upper family: unreacted spectra. Lower family: reacted spectra. The two families of curves are vertically displaced for the sake of display

Table I. Reference Compounds for the DPPH-Analyzer

Compound		Concn, mg/l.
Indican (3-indoxylsulfate)		40
Ascorbic acid		30
Uric acid		20
3,4-Dihydroxymandelic acid	DOMA	6
3-Methoxy-4-hydroxymandelic acid (vanilmandelic acid)	VMA	80
3,4-Dihydroxyphenylacetic acid	DOPAC	10
3-Methoxy-4-hydroxyphenyllactic acid (vanillactic acid)	VLA	40
3-Methoxy-4-hydroxyphenylacetic acid (homovanillic acid)	HVA	60
3,4-Dihydroxyphenylalanine	DOPA	6
3-Methoxy-4-hydroxyphenylalanine	MOPA	60
5-Hydroxyindole-3-acetic acid	HIAA	30
5-Hydroxyindole-2-carboxylic acid	HICA	40
5-Hydroxytryptophan	H-Trp	40
Creatinine		1600

buffer elution program, and we are currently using A-6 in a 0.9 × 50-cm column.

Reference Compounds and Urine Samples. Solutions of reference compounds are mixed in a liter volumetric flask using buffer 1, with the following exceptions. Uric acid is first dissolved in dilute base (0.1*N* NaOH, 5–10 ml), then transferred to the flask half-filled with buffer 1. 5-Hydroxyindole-3-acetic acid (HIAA) is separately dissolved in absolute ethanol (5–10 ml), then transferred. The other reference compounds are subsequently added. The mixture is divided into aliquots and frozen before use, to conform to our handling of urine samples. A list of the reference compounds and their concentrations is given Table I.

Twenty-four-hour urines were collected in glass containers, refrigerated without added preservatives. Aliquots are acidified to pH 2.50, and routinely frozen at −45 °C for storage before use. An aliquot of thawed urine, 5–10 ml, is passed through a 0.22-micron filter, taken to dryness (60 °C bath and aspirator vacuum), redissolved in 2 ml of buffer 1, and then centrifuged. One ml of solution is applied to the column via a sample loop injection valve.

RESULTS

Reference Compounds. Designing a sequence of eluting buffers for the DPPH system depends on the choice of the reference compounds. Our selection of a reference set is based on the compounds we wished to identify, namely DOPA metabolites, and on the DPPH reactive constituents commonly found in urine, the physiologic fluid of primary interest to us. The reference compounds we have chosen are listed in Table I, and Figure 1 shows their chromatogram, with a base line run underneath. The chromatogram shows peaks of transmittance, since DPPH loses its absorbance upon reaction. It is interesting to note that each 3,4-dihydroxy aromatic elutes before its corresponding 3-methoxy analog.

Certain other physiologic compounds that are DPPH reactive are omitted from the reference set to simplify the chromatogram, and since some are incompletely resolved by the buffer program. These include 3-methoxy-4-hydroxyphenylglycol (MOPEG),3-methoxy-4-hydroxyphenylethanol (MOPET), cysteine, 2,5-dihydroxybenzoic acid (gentisic acid), 2,5-dihydroxyphenylacetic (homogenistic acid), 3,4-dihydroxyphenylserine, and 3,4-dihydroxycinnamic acid.

Recovery. When a reference solution is dried and re-dissolved similar to a urine sample, the recovery of all compounds is quantitative except for ascorbic acid, which shows a subsequent 40% loss in chromatographic peak area. The recovery of DPPH-reacting compounds from urine, after concentration in pH 2.50 buffer, is greater than 90% except for uric acid, less than 50% of which is recovered. Although uric acid can be recovered when in low concentration, as in the reference solution, the uric acid level in urine is too high and the buffer too acidic to permit complete recovery.

Base-Line Shifts. Base-line shifts are observed as the pH of the eluting buffer changes, since the DPPH reaction is pH dependent, and since the DPPH stock solution is not buffered. The shifts in base line are evident in the standard chromatogram of Figure 1, and the accompanying base-line run shows the position and extent of the shifts. We attribute the higher base line at lower pH to a partial decolorization of DPPH by the acidic buffers, thus raising the base line above the level found for a more neutral buffer. Recall that the chromatograms show transmittance, not absorbance.

The small peak at approximately 142 minutes in the base line is of unknown origin and identity. The peak appears in all runs, and may represent some contamination of the buffers and/or columns. The peak is not enhanced by the addition to ammonia to the buffers, in accord with our previous observation that ammonia is DPPH negative (*12*).

DPPH Spectra. The observed base-line shifts might also be attributable to a shift in the DPPH absorbance spectrum as the eluting pH changes. To explore this possibility, we recorded the DPPH spectrum at the pH of the

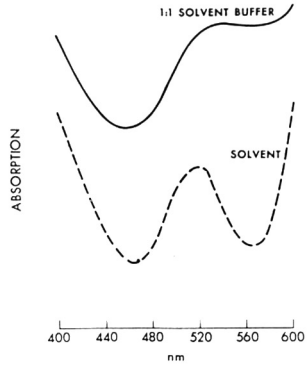


Figure 3. A comparison of the DPPH spectrum in solvent *vs.* solvent: buffer

Below: DPPH in methyl cellosolve. Above: DPPH in 1:1 methyl cellosolve: 0.35*N* citrate, pH 5.25, with the two curves vertically displaced for the sake of display

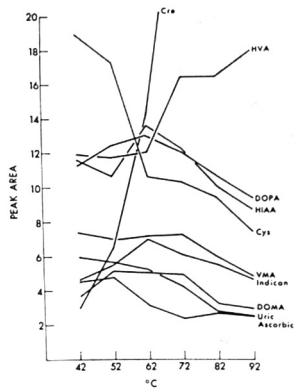


Figure 4. Changes in chromatographic peak areas of the reference compounds as the temperature of the reaction bath increases. Area units are arbitrary

four eluting buffers, both before and after reaction, as shown in Figure 2, where data are plotted as absorbance instead of transmittance spectra. The particular compounds eluted and reacted are ascorbic acid, DOPAC, DOPA, and HIAA at pH 2.50, 3.25, 4.30, and 5.25, respectively.

No significant spectrum shifting is observed as the buffer pH changes, either in the reacted or unreacted families of spectra. The results shown in Figure 2 thus support the view that the base-line shifts in the chromatograms arise from a loss of DPPH due to the acidity of the early buffers. As the pH of the eluting buffer increases, the loss of DPPH decreases. This is evident in the unreacted family of spectra, where the relative absorbance increases (with transmittance thus decreasing) as the pH rises from 2.50 to 5.25.

Figure 2 is also a display of the loss of absorbance that accompanies DPPH reduction. The unreacted family of spectra show that DPPH has a shoulder-type peak in the 1:1 solvent:buffer mixture used in our system with a maximum close to 525 nm, as opposed to the distinct absorbance peak at 520 nm observed in organic solvents. Figure 3 compares the DPPH absorbance spectra in the two media. Despite the absence of a distinct absorbance peak in the solvent:buffer mixture, the reacted family of spectra show a pronounced drop in absorbance at the same wavelength (525 nm). It is this loss of absorbance as DPPH is reduced that accounts for the chromatographic (transmittance) peaks.

Molar Response *vs.* Reaction Temperature. Figure 4 shows the peak areas, in arbitrary units, of the reference compounds chromatographed at a series of reaction bath temperatures increasing in ten degree intervals from 42 to 92 °C. The response for each compound is unique in its temperature dependence and is not constant as the temperature increases. The reference compounds may be categorized as generally decreasing in response as the temperature rises (ascorbic acid, uric acid, VMA, cysteine), as showing a maximum response at an intermediate temperature (indican, DOMA, DOPA, HIAA), or as increasing in response with rising temperature (HVA, creatinine). There is thus no single reaction bath temperature that is optimum for detecting all the reference compounds. A reaction bath temperature of 62 °C has been adopted for all analytical runs as a workable compromise for the range of compounds in which we are interested. Three of the reference compounds (indican, DOPA, HIAA) have a maximum response at this temperature, while the responses of DOMA and VMA are close to their maximal levels, although there is some loss in sensitivity for ascorbic, uric, HVA, and cysteine.

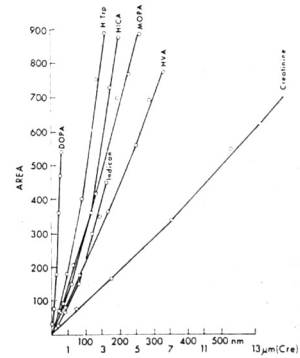


Figure 5. Response curves of the reference compounds

The lower scale in Figure 5 denotes the creatinine concentration

Linearity and Sensitivity. Figures 5 and 6 show the peak areas of a reference solution chromatographed at a series of dilutions. This set of response curves shows that the DPPH reaction is not entirely linear for any of the reference compounds, as measured on our detecting system.

The primary determinant of sensitivity is the molar reaction ratio of a compound with DPPH—*i.e.*, the number of nanomoles of reactant that are required to reduce a given number of nanomoles of DPPH. The reaction ratios are unique for each compound, and are generally different from 1:1 (*12*). The molar reaction ratios are derived from the slopes of the response curves: the steeper the slope, the higher the reaction ratio and the greater the DPPH sensitivity for that particular compound. As previously reported, DOPA has the steepest response slope of all the

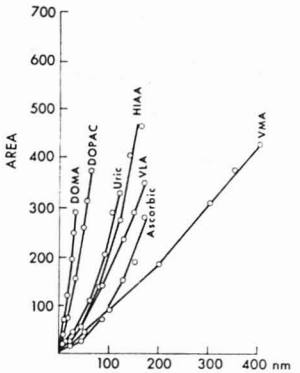


Figure 6. Response curves of the reference compounds

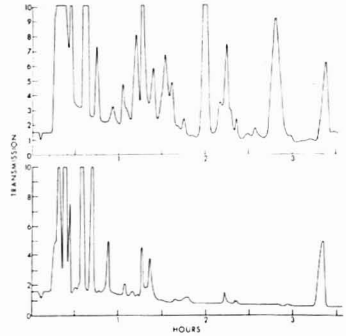


Figure 7. Chromatograms comparing normal (below) and disseminated melanoma urine (above), 5 ml each

reactants tested, and the DPPH system is thus most sensitive in detecting DOPA, while creatinine is the least sensitive reactant.

In addition to the reaction ratios, the operating conditions of the analyzer are important in determining sensitivity. Under the present operating conditions of DPPH concentration, flow rate, cell dimensions, and recorder attenuation, the system has a stable, noise-free base line, and a full scale 0–10 chart deflection corresponding to 5–65% T. A peak as small as 0.2% T in height is readily observable, and in the case of DOPA corresponds to 1 nm. This amount would be increasingly larger for the other reference compounds, in the order of their decreasing slopes of response.

Reactivity of DPPH. The identity of all the physiologic compounds which react with DPPH is only partially known. Although previous reports have identified a large number of organic compounds that react with DPPH (*cf.* *12*), the extent of its reactivity among physiologic compounds is only beginning to emerge. The list of DPPH-positive compounds has continued to grow, but the unknown peaks appearing in the chromatograms of disseminated melanoma urines (see Figure 7) show that more reactants remain to be identified.

It is difficult to neatly characterize the range of reactivity that DPPH possesses toward physiologic compounds. DPPH is a mild oxidizing agent, and all reactants must have the proper oxidation potential to reduce DPPH to the hydrazine form. The requirement of a proper oxidation potential is very simple in principle, but it does not limit DPPH reactivity to any one chemical or structural class of compounds, nor does it provide any facile way to recognize potential reactants, as can be done for ninhydrin (primary amines) or for UV absorption (ring compounds). The list of known DPPH reactants thus appears to represent many different chemical and physiological categories. This may turn out to be one of the principal advantages of DPPH.

Our original interest in DPPH arose because of its reaction with DOPA metabolites and, in particular, because of its high molar reaction ratio with DOPA. The 3,4-dihydroxy and 3-methoxy-4-hydroxy aromatic metabolites are the one structural class of reacting compounds that render DPPH useful from our point of view. DPPH reacts with every such compound tested, regardless of whether the side chain is acidic, amino acidic, basic, or neutral. Although DPPH cannot be considered specific for this class of compounds, it nonetheless provides a simple colorimetric means of detecting and measuring all such metabolites.

A number of reports on DPPH reaction mechanisms with organic compounds in pure solvents have appeared. A four-electron, ring-splitting mechanism has been proposed for the DPPH reaction with catechol (*18*), and it is likely that similar mechanisms are functioning in the reaction of DPPH with DOPA metabolites in an organic solvent–aqueous buffer environment. A mechanism for indole reactions with DPPH has not been explicitly proposed, but may be similar to the mechanism operating during a Fremy's salt oxidation (*19*). Reaction mechanisms with mercaptans have long been known (*20*). However, mechanisms for other DPPH reactants, such as creatinine, remain to be explored.

Clinical Correlations. The most interesting observation that can be derived at this early stage from the urine chromatograms is the striking difference between normal urines and disseminated melanoma cases. Figure 7 compares typical chromatograms from these two categories. While there are similarities between the two during the early stages of the run, and with both showing a final major peak which may correspond to creatinine, the 1½- to 3-hour section of the run shows significant differences. The molecular weights of the compounds appearing in the chromatograms are all less than 1000 daltons, since the chromatographic patterns remain unchanged after ultrafiltration (Millipore PSAC) of the samples. The identification of peaks presents a major and continuing task, and correlations between chromatographic patterns and various stages of melanoma are being developed.

DISCUSSION

The automatic DPPH analytical system described represents the outcome of a program to develop improved procedures for identifying melanogens in the urine of patients seen at the Melanoma Clinic of the University of California, San Francisco. Initially, this work involved the use of DPPH as a colorimetric reagent for assays manually performed on urine samples for the presence of melanogens. Although elevated levels of total melanogens occur in dissemination and can be measured in this way, the usefulness of the manual test is limited due to the reaction of DPPH with other urinary constituents, such as uric acid and creatinine. However, no other single reagent matched DPPH

(18) G. H. Schenk and D. J. Brown, *Talanta*, **14**, 257 (1967).
(19) W. A. Remers, in "Chemistry of Heterocyclic Compounds. Indoles, Pt. 1," W. J. Houlihan, Ed., Wiley-Interscience, New York, N.Y., 1972, p 159.
(20) K. E. Russell, *J. Phys. Chem.*, **58**, 437 (1954).

in its ease of use and sensitivity for DOPA metabolites and, in this respect, DPPH was too valuable to be discarded for alternate methods of detection. The primary motive in developing chromatographic procedures for analyzing urine was to exploit the desirable reactive properties of DPPH for DOPA metabolites by an ion-exchange separation of reactants.

We suggest that the DPPH analytical system will be valuable in other areas of clinical and basic research because of its applicability to detecting a diverse set of important metabolites. The compounds shown in Figure 1 are all well-known, but it is not possible with conventional analytical techniques to identify and measure them together during the course of a single chromatographic run, only a few hours in length. The ability of DPPH to detect a few common physiologic compounds, such as uric acid and creatinine, is particularly useful since their peaks may serve as position markers and as indicators of physiologic function. The DPPH system also appears to provide a much more simple and direct means of detecting ascorbic acid than the titrimetric procedures typically employed (*21*), although the evaporation of urine will have to be avoided in this case. Our experience with the DPPH analytical system opens a new category of detection for ion-exchange chromatography, and brings to the field of melanogen analysis the reliability and precision that has long characterized amino acid analysis.

RECEIVED for review February 25, 1974. Accepted June 21, 1974. This investigation was supported by Public Health Service Research Grant No. CA-12043 from the National Cancer Institute, and by research grant DRG-1168 from the Damon Runyon Memorial Fund for Cancer Research.

(21) L. Pauling, A. B. Robinson, S. S. Oxley, M. Bergeson, A. Harris, P. Gary, J. Blethen, and I. T. Keaveny, in "Orthomolecular Psychiatry," D. Hawkins and L. Pauling, Ed., Freeman, San Francisco, Calif., 1972. p 32.

Determination of Uric Acid at the Microgram Level by a Kinetic Procedure Based on a "Pseudo-Induction" Period

V. V. S. Eswara Dutt and H. A. Mottola

Department of Chemistry, Oklahoma State University, Stillwater, Okla. 74074

The pronounced accelerating effect exerted by oxalic acid on the oxidation of tris(1,10-phenanthroline)iron(II), ferroin, by chromium(VI) is preceded by a "pseudo-induction period" in the presence of low concentrations of uric acid. Kinetic studies show that the oxidation of uric acid is effected by the active oxidant ferriin (the oxidized form of ferroin), produced by the oxidation of ferroin by chromium(VI) in the presence of oxalic acid as promoter. The length of the "pseudo-induction period" is proportional to the uric acid concentration and allows the quantitative determination of 0.85–5.95 μg/ml of this species in aqueous solutions. The application of this method to the determination of uric acid in human blood serum and urine is also reported.

Some reactions used in kinetic methods are characterized by the presence of induction periods (*1*). Generally the length of the induction period is proportional to the reactant's concentration and this allows the development of determination procedures. Most of the analytical methods based on this effect are catalytic in nature and grouped under the classification of "Landolt reactions" (*2*).

In a recently reported reaction rate method for oxalic acid in biological fluids, the accelerating effect of oxalic acid on the oxidation of tris(1,10-phenanthroline)iron(II), ferroin, by chromium(VI) was observed to be preceded by an "induction period" in the presence of low concentrations of uric acid (*3*) Development of a method for the determination of uric acid based on this effect and its application to human blood serum and urine are reported here.

Induction periods are observed in many precipitation reactions; in autocatalytic reactions, such as when time is needed for the accumulation of the desired form of catalyst; and in free radical reactions. Generally in these cases, the reaction occurs in two or more stages (the first one being the slowest) or a given chemical species totally or partially inhibits the reaction. The procedure for uric acid described in this paper results from the concerted action of two independent chemical reactions occurring at drastically different rates. One of these reactions regenerates *instantaneously* the monitored species in the other reaction and this mimics an induction period. As such, and for the lack of a better denomination, we have termed the effect a "pseudo-induction period."

EXPERIMENTAL

Apparatus. The equipment and technique employed to obtain absorbance *vs.* time plots have been described previously (*3*). Determinations were performed in 1-cm glass cells, the reaction being initiated by injection of the chromium(VI) solution. Mixing was accomplished by using the cell holder and air-driven stirrer also described previously (*4*). Temperature control was maintained at 25.0 ± 0.2 °C with a Lauda/Brinkmann Model K-2/R circulator and the use of a thermostatable cell adapter (Cary Instruments).

Reagents and Solutions. All the reagents used were prepared from analytical grade chemicals. The water used was purified by distilling demineralized water in a borosilicate still equipped with a quartz-covered immersion heater. Potassium dichromate: $1.67 \times 10^{-3}M$. Ferroin: $1.60 \times 10^{-3}M$. Sulfuric acid: $5M$. Oxalic acid: $1.0 \times 10^{-4}M$ (freshly prepared from $0.10M$ stock solution). Uric acid:

(1) K. B. Yatsimiriskii, "Kinetic Methods of Analysis," Pergamon Press, Oxford, 1966, pp 16, 50, and 51.
(2) G. Svehla, *Analyst, (London)*, **94**, 513 (1969).
(3) V. V. S. Eswara Dutt and H. A. Mottola, *Biochem. Med.*, **9**, 148 (1974).
(4) H. Hall, B. E. Simpson, and H. A. Mottola, *Anal. Biochem.*, **45**, 453 (1972).

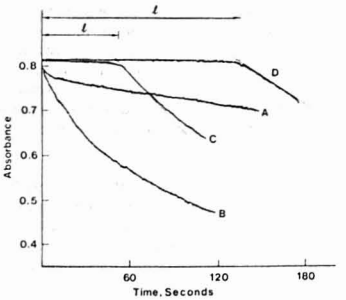


Figure 1. Variation of absorbance with time in the oxidation of ferroin by chromium(VI) in the presence of uric acid

Chromium(VI): 8.33 × $10^{-5}M$, ferroin: 7.40 × $10^{-5}M$, sulfuric acid: 0.25M, oxalic acid: 3.33 × $10^{-5}M$. *A*. No uric acid, no oxalic acid. *B*, No uric acid. *C*, 1.0 × $10^{-5}M$ uric acid. *D*, 3.0 × $10^{-5}M$ uric acid. *I*, Length of induction period

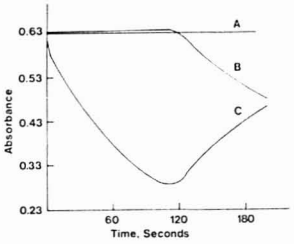


Figure 2. Reaction rate profiles for the oxidation of uric acid

Chromium(VI): 8.33 × $10^{-5}M$, ferroin: 5.65 × $10^{-5}M$, sulfuric acid: 0.25M, oxalic acid: 3.33 × $10^{-5}M$, uric acid: 3.33 × $10^{-5}M$. *A*. Monitored at 285 nm (no ferroin present). *B*. Monitored at 510 nm. *C*. Monitored at 285 nm.

1.0 × $10^{-4}M$ (freshly prepared from 0.010M stock solution). The stock standard solution is prepared by dissolving the uric acid in water in the presence of an equivalent amount of lithium carbonate.

Procedure. Samples of uric acid solution ranging from 0.15 to 1.05 ml in volume were introduced into an absorption cell containing a mixture of 0.15 ml of sulfuric acid, 0.15 ml of ferroin, and 1 ml of oxalic acid. Water was added to bring the total volume to 2.85 ml; 0.15 ml of potassium dichromate solution was injected into the reaction mixture, and the absorbance *vs.* time was recorded at a wavelength of 510 nm until a perceptible change in absorbance was visualized. The length of the "induction period" (Figure 1) was evaluated by extrapolation of the two segments of the reaction curve and measuring the distance from the point of intersection to the origin. The concentration of the uric acid was calculated by reference to a working curve.

RESULTS AND DISCUSSION

Several chemical species promote the oxidation of ferroin (*5*). Oxalic acid is one of these, and was chosen as a component of the indicator reaction for the determination of uric acid since it shows, comparatively, marked accelerating effect, and it does not absorb at the wavelength used to follow the main reaction. The indicator reaction employed then can be represented as follows:

$$\text{Cr(VI)} + \text{ferroin} \xrightarrow{(\text{HCOO})_2} \text{Cr(III)} + \text{ferriin} \quad (1)$$

in which, ferriin = iron(III) complex with 1,10-phenanthroline.

When uric acid is also present in the above system, the accelerating effect of oxalic acid is temporarily masked, the length of the "induction period" being dependent on the concentration of uric acid.

In an attempt to understand the observed "induction period," the chemical reactivity of uric acid toward chromium(VI) was examined. No measurable reaction between Cr(VI) and uric acid took place in sulfuric acid of concentration less than 1.0M. At acidities greater than 1.0M, some oxidation of uric acid occurred, but no detailed studies were made as this does not fall in the region of analytical interest. However, in the presence of oxalic acid, chromium(VI) oxidized uric acid in sulfuric acid at low concentrations, the rate being directly proportional to the concentration of oxalic acid. In fact, at an overall concentration of nearly 1.0 × $10^{-2}M$ oxalic acid, 10–100 mg of uric acid could be determined by measuring the intial rate of the reaction. But when the concentration of oxalic acid was decreased by three orders of magnitude (to 3.33 × $10^{-5}M$), which is that employed in the recommended procedure, no oxidation of uric acid was detected. Thus, uric acid is not oxidized to a measurable extent when only sulfuric acid and oxalic acid are present at the low concentrations described in the procedure. Further, no spectral evidence in the UV-VIS region was obtained for the formation of an intermediate complex of uric acid with oxalic acid or chromium(VI), or with both. These facts indicate that the role of uric acid in the reaction is associated with that of ferroin. When the reaction mixture containing chromium(VI), oxalic acid, sulfuric acid, and uric acid was monitored at 285 nm (λmax for uric acid) against a ferroin blank, rapid decrease in absorbance was noticed initially for a short time, after which it began to increase sharply. This is illustrated in Figure 2. The increase in absorbance was due to the oxidation of ferroin to ferriin, occurring after all the uric acid had been oxidized. Because ferriin has a larger absorbance than ferroin at 285 nm, and the reaction is being monitored against a ferroin blank, the decrease of ferroin concentration in the sample compartment appears as an apparent increase of actual absorbance. The same reaction mixture, when monitored at 510 nm, exhibits an "induction period" followed by the accelerated rate, (Figure 2, curve *B*). It is to be noted that the length of the "induction period" almost exactly equals the time interval during which the absorbance of uric acid decreases.

In light of the above experimental findings, one would presume that uric acid oxidation precedes the oxidation of ferroin. However, this leaves an intriguing question on what chemical species is responsible for the oxidation of uric acid, because it was previously proved that, at the concentrations employed here, chromium(VI) cannot oxidize uric acid even in the presence of oxalic acid. The only other species in the reaction system that has oxidizing capabilities is ferriin, the oxidized form of ferroin, which is generated by Reaction 1. To test this possibility, ferriin (pale blue in color) was prepared by oxidation of ferroin with an equivalent amount of cerium(IV) sulfate [care was taken to ensure no excess of cerium(IV) left] and made to react with uric acid. There was an almost instantaneous formation of ferroin; the reaction is so fast that its kinetic characteristics could not be recorded. Since oxidation of uric acid in acidic medium yields urea and alloxan, we have:

$$\text{uric acid} + \text{ferriin} \longrightarrow \text{urea} + \text{alloxan} + \text{ferroin} \quad (2)$$

By summing up these facts, the sequence of reactions oc-

(5) V. V. S. Eswara Dutt and H. A. Mottola, *Anal. Chem.*, **46**, 1090 (1974).

curring in the analytical procedure could be easily understood. The oxidation of uric acid takes place through the active oxidant ferriin, which is produced from the oxidation of ferroin by chromium(VI) in the presence of oxalic acid as promoter. Reaction 2 regenerates ferroin which subsequently reenters Reaction 1 to produce ferriin again. This cycle is repeated until all uric acid in the reaction is oxidized, after which the accelerated rate of ferroin oxidation appears because the ferriin formed remains as such in the system. Because Reaction 2 is extremely fast, virtually no decrease of ferroin concentration could be perceived, and this appeared as an "induction period" in the reaction rate curves. The length of "induction period" corresponds to the time needed for complete oxidation of uric acid.

Strictly speaking, this time lag does not fit in the chemical definition of "induction period" and, hence, it is termed as "pseudo-induction period." This is because, in the commonly encountered chemical reactions exhibiting an induction period, the reaction is quiescent in the early stages, and rendered fast later. From a different perspective, the reaction is the oxidation of uric acid by chromium(VI), involving two accelerators, oxalic acid and ferroin, operating in succession. To the best of the authors' knowledge, this phenomenon is unique; no reaction rate procedure in analytical chemistry based exactly on a similar principle could be found in the literature. The enzyme-coupled fluorimetric assay for uric acid reported by Bloch and Lata (*6*) has some resemblance to the method reported here, being based on the inhibitory effect of uric acid on the oxidation of scopoletin with hydrogen peroxide and horseradish peroxidase. The "induction period" in this case is due to delay in the oxidation of scopoletin.

Reaction Parameters. The optimum concentrations of chromium(VI) ($8.33 \times 10^{-5}M$), sulfuric acid ($0.25M$), and ferroin ($7.40 \times 10^{-5}M$) for the determination of uric acid were essentially the same as those employed in the determination of oxalic acid (*3*). Systematic variation of oxalic acid concentration has indicated that the determinability of uric acid is inversely proportional to the concentration of oxalic acid. For a fixed concentration of uric acid, as the oxalic acid concentration was gradually decreased, the length of the "pseudo-induction period" progressively increased. This is interpreted in terms of the smaller concentration of ferriin generated with decreasing concentration of the promoter, which evidently increased the time for complete oxidation of uric acid. At oxalic acid concentrations lower than $1.67 \times 10^{-5}M$, the length of the "pseudo-induction period" could not be precisely evaluated. This is because the completion of the induction period and appearance of the accelerated rate did not appear abruptly, but gradually. At oxalic acid concentrations between $1.67 \times 10^{-5}M$ and $3.33 \times 10^{-5}M$, uric acid can be determined with good sensitivity, producing well developed reaction curves with sharp breaks. The reaction between ferriin and uric acid, from an analytical viewpoint, is so fast that temperature effects above 20 °C should introduce no variation in the results. The effect of temperature on the oxidation of ferroin by chromium(VI) in the presence of oxalic acid has been reported earlier (*5*) and indicates that slight changes of temperature should not introduce error.

Careful scrutiny of Figure 1 reveals that, although the same concentration of oxalic acid was used in all runs, the slopes of the accelerated rate curves decrease as the concentration of uric acid is increased. This decrease is caused by gradual depletion of oxalic acid in the reaction system. This is due mainly to its complexation with chromium(III) (produced during the reaction) and partly to decarboxylation (*5*). Evidently, the active concentration of oxalic acid participating will become smaller with progressive increase of uric acid concentration, and the length of the "pseudo-induction period" consequently increases. This is why the plot of uric acid *vs.* length of "pseudo-induction period" is not linear (Figure 3, curve *A*). A plot of square root of the "pseudo-induction period" *vs.* uric acid concentration yields a straight line (Figure 3, curve *B*) with a positive intercept on the ordinate, and this could equally well be used for the determination of uric acid. Because of very good reproducibility of the "pseudo-induction period," either of the two plots could be used as a working curve and the results were independent of the choice. For biological fluids, however, as explained later, the square-root form of the plot is to be preferred, in order to apply the standard addition procedure. Oxalic acid concentrations above $3.33 \times 10^{-5}M$ can be used with some sacrifice in the limit of detection. Using the standard addition procedure, in biological samples, variations in the total oxalate concentration are taken care of.

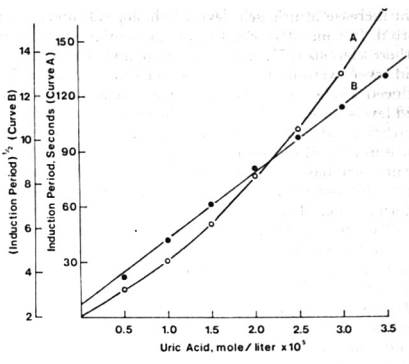


Figure 3. Working curves for the determination of uric acid

The standard deviation for 7 replicate determinations of 2.50 μg of uric acid/ml was 0.02 with an average of 2.54

The possibility of uric acid determination by direct use of ferriin was considered of secondary importance in consideration of the unfavorable characteristics of ferriin as an analytical reagent (*7*).

Determination of Uric Acid in Biological Fluids. Clinical studies have shown that extreme abnormalities of uric acid levels in blood serum and urine are symptoms of several diseases. Elevated uric acid levels have been observed in cases of excessive cell breakdown and catabolism of nucleic acids. Thus in the acute stages of infectious diseases such as pneumonia (*8*), fatal poisoning with chloroform or methanol (*9,10*), extensive exposure to X-rays (*11*), toxemia of pregnancy (*12*), multiple myeloma (*13*), polycythemia vera (*14*), leukemia (*15*), and gout (*16*), signifi-

(6) P. L. Bloch and G. F. Lata, *Anal. Biochem.*, **38**, 1 (1970).
(7) A. A. Schilt, "Analytical Applications of 1,10-Phenanthroline and Related Compounds," Pergamon Press, Oxford, 1969, p 168.
(8) C. W. Wells, *Arch. Internal Med.*, **26**, 443 (1920).
(9) I. M. Rabinowitz, *Arch. Internal Med.*, **29**, 831 (1922); *J. Biol. Chem.* **83**, 333 (1929).
(10) H. J. Stander, *Bull. Johns Hopkins Hosp.*, **35**, 46 (1924).
(11) M. S. Fine and A. F. Chase, *J. Pharmacol. Exp. Ther.*, **6**, 219 (1914–15); *J. Biol. Chem.*, **21**, 371 (1915).
(12) J. F. Cadden and H. J. Stander, *Amer. J. Obstet. Gynecol.*, **37**, 37 (1939).
(13) A. Stewart and F. P. Weber, *Quart. J. Med.*, **7**, 211 (1939).
(14) R. Issacs, *Arch. Internal Med.*, **31**, 289 (1923).
(15) O. Folin and W. Denis, *Arch. Internal Med.*, **16**, 33 (1915).
(16) J. E. Seegmiller, L. Laster, R. R. Howell, *New Engl. Med.*, **268**, 712 (1963).

cant increase of uric acid levels in biological fluids was reported. In congestive heart failure, essential hypertension, artherosclerosis (*17*), and severe uremia (*18*), elevated uric acid levels were noticed in excess of those attributable to reduced kidney function. In contrast, reduced blood uric acid levels were found in acute yellow liver atrophy (*9*), polyarthritis (*19*), and acromegaly (*20*). In view of this importance in clinical diagnosis, the analysis of biological fluids for uric acid has been attempted and described below. Martinek (*21*) reviewed the various methods available for the determination of uric acid in biological fluids and recommended the alkaline phosphotungstate and uricase methods for the routine clinical laboratory work. The recent procedures reported include the automated method using the coupled ferricyanide redox reaction by Klien and Lucas (*22*), fluorescence assay with enzyme coupled approach by Bloch and Lata (*6*), the manual and automated photometric determinations as copper(I)–neocuproine complex with and without enzyme uricase (*23–25*) and the electrochemical methods of Park *et al.* (*26*) and Troy and Purdy (*27*).

Procedure for Human Urine. An aliquot of well-mixed 24-hour urine specimen was diluted with 19 volumes of water. If the urine sample was cloudy, it was warmed at 50–60 °C for 10 minutes (to dissolve any precipitated urate) and dilution was made while the liquid was still warm. A portion (5.0 ml) of the diluted urine sample was transferred into a 20-ml test tube containing 2.50 ml of 10%(w/v) sodium carbonate solution and the mixture allowed to stand for about 10 minutes. The solution was then neutralized with 0.50 ml of sulfuric acid reagent and diluted to 10.0 ml with water after the generated carbon dioxide had been expelled from the system in an ultrasonic cleaner. A sample (0.50 ml) was subjected to determination as described above. The amount of uric acid was evaluated either by interpolation in the working curve or by a standard addition technique. The value so obtained was multiplied by a factor of 80 × volume of urine collected in 24 hours.

Procedure for Human Blood Serum. A serum specimen (2.0 ml) free from hemolytic products was mixed with 4.0 ml of water and 4.0 ml of 10% (w/v) trichloroacetic acid, and the mixture shaken well and set aside for three minutes. The precipitated protein material was removed by centrifugation at 1500 rpm and a 5-ml portion of the supernatant liquid was treated with 3.0 ml of 10% sodium carbonate and allowed to stand for 10 minutes. A 0.25-ml portion of sulfuric acid reagent was then added and the carbon dioxide formed was expelled by immersion of the container in an ultrasonic cleaner. The solution was diluted to 10.0 ml and a 0.50-ml portion was analyzed as described above. The amount of uric acid obtained from the calibration curve was multiplied by 2000 to arrive at the amount of uric acid present in 100 ml of serum.

Because the matrix effects in biological samples are better compensated in the standard-addition technique, this approach is recommended for the determination of uric acid in human urine and blood serum. Since the standard-addition technique is valid only with linear calibration graphs, the plots of square root of "pseudo-induction period" *vs.* uric acid concentration were used for the determination. Further, it should be mentioned that because the working curve obtained using pure uric acid standards has a positive intercept on the ordinate, this value should be subtracted in the standard plots.

Deproteinization of serum samples was carried out using trichloroacetic acid. The conventionally used tungstic acid reagent could not be employed because it interfered in the subsequent determination by forming an insoluble ion-association complex with ferroin. Since urine is usually free from proteins, the analysis could be directly performed after appropriate dilution of the sample.

According to Caraway (*28*), the interference due to ascorbic acid and other labile reducing compounds present in the samples can be eliminated by treatment with sodium carbonate and incubation for ten minutes. In basic media, these compounds are believed to undergo air oxidation, leaving uric acid unaffected. This treatment step was necessary in our method also. We observed that incubation times of 10 to 60 minutes all gave the same values of uric acid, confirming the stability of uric acid in basic media. Larger concentrations of sodium carbonate were employed in serum samples than in urine, to compensate for the high

Table I. Effect of Some Foreign Species[a]

Foreign species	Maximum level tested without observing interference (in μg)
Urea	1000
Creatine	1000
Creatinine	500
Glucose	500
Glycine	300
Tyrosine	500
Tryptophan[b]	90
Glutathione[b]	20
Cystine	100
Ascorbic acid[b]	4
Caffeine	1000
Theophylline-7-acetic acid[c]	1000
7,7PR-(1,4-piperazinodimethyl)-ditheophylline[c]	1000
7-(Morpholinomethyl)theophylline[c]	1000
EDTA	1000
Salicylate	200
Acetate	500
Phosphate	500
Chloride	500
Fluoride	500
Nitrate	500
Formic, tartaric, lactic, adipic, malic, maleic, malonic, fumaric, succinic, and glycolic acids	100
Citric acid[c]	25
Calcium	200
Magnesium	200
Copper(II)	250
Nickel(II)	150
Cadmium	500
Cobalt(II)	200
Mercury(II)	200
Iron(III)	150
Zinc[d]	150
Lead(II)	20

[a] Determination according to procedure in text and in the presence of 2.5 μg uric acid. [b] Interferes at levels higher than indicated by reacting with chromium(VI). [c] Higher levels shorten the induction period. [d] Forms a precipitate with chromium(VI) at higher levels. [e] Analogs of uric acid.

(17) A. M. Fishberg, *Arch. Internal Med.*, **34**, 503 (1924).
(18) W. P. Holbrook and H. D. Haskins, *J. Lab. Clin. Med.*, **12**, 11 (1926).
(19) K. Brohner-Mortensen, *Acta Med. Scand.*, **96**, 438 (1938).
(20) G. Schmidt, *Z. Gesamte Exp. Med.*, **94**, 76 (1934).
(21) R. G. Martinek, *J. Amer. Med. Technol.*, **32**, 233 (1970).
(22) B. Klien and L. B. Lucas, *Clin. Chem.*, **19**, 67 (1973).
(23) D. L. Bittner, S. G. Hall, and M. L. McCleary, *Amer. J. Clin. Pathol.*, **40**, 423 (1963).
(24) H. B. Lofland and L. Crouse, Paper presented at the Technicon Symposium "Automation in Analytical Chemistry," New York, N.Y., Sept. 8, 1965.
(25) S. Morgenstern, V. F. Richard, J. H. Kaufman, and B. Klien, *Clin. Chem.*, **12**, 748 (1966).
(26) G. Park, R. N. Adams, and W. R. White, *Anal. Lett.*, **5**, 887 (1972).
(27) R. J. Troy and W. C. Purdy, *Clin. Chim. Acta*, **27**, 401 (1970).
(28) W. T. Caraway, *Clin. Chem.*, **15**, 720 (1969).

acidity contributed by trichloroacetic acid. Because the determination involves the use of an acidic medium, the reaction mixture was neutralized after incubation and the recommended acidity maintained using sulfuric acid. During the neutralization process, carbon dioxide is liberated; its expulsion from the reaction mixture was essential because bubbles in the cuvet partially blocked the optical path and caused absorbance fluctuations. This difficulty was completely eliminated by keeping the reaction mixture in an ultrasonic cleaner for a few seconds. The modified phosphotungstic acid procedure of Caraway recommended in "Standard Methods of Clinical Chemistry" (29) was used as a reference method for comparison. The average uric acid concentration of six replicas of a pooled human serum sample analyzed by the reference method was 4.80 mg/100 ml, with a standard deviation of ±0.15. Analysis by the present method gave the average value of 5.00 mg/100 ml with a standard deviation of ±0.20. The mean value of uric acid excreted, obtained by the analysis of six replicas of a urine specimen, was 0.73 g/24 hr with a standard deviation of ±0.01 for the reference method and 0.75 g/24 hr with a standard deviation of ±0.01 for the present method. Evaluation of uric acid content in serum and urine by interpolation in the working curve instead of by the standard-addition technique gave substantially lower values in the reference method as well as in the present method. The average values found in this case for serum and urine were 3.90 mg/100 ml (reference method), 4.05 mg/100 ml (method reported here); and 0.59 g/24 hr (reference method), 0.60 g/24 hr (method reported here), respectively, with approximately the same standard deviations as given above. This fact suggests the presence of some interfering substances which inhibit the reaction of uric acid in both serum and urine. In any event, the results obtained with the reference and present methods are in good agreement.

Interferences. The effects of foreign species which are often present in some biological fluids were tested by the analytical method and the results are summarized in Table I.

(29) W. T. Caraway, Uric Acid, in "Standard Methods of Clinical Chemistry," Vol. 4, Academic Press, New York, N.Y., 1963, pp 239–47.

Comparison with Other Methods. The method reported in this paper for the determination of uric acid is equal in simplicity and reproducibility to the alkaline phosphotungstic acid procedure, but lower amounts of uric acid can be determined. A period of 20–30 minutes is necessary for the final color development in the phosphotungstic acid method, whereas only 1–5 minutes reaction monitoring is sufficient in the method reported here. The enzyme-coupled fluorimetric method for the determination of uric acid in picomole quantities reported by Bloch and Lata (6) seems to offer the lowest limit of detection of all those so far reported in the literature. However, the two main disadvantages associated with this method are that elaborate cleaning of the cuvets between assays has to be done by rinsing with water, soaking in 30% hydrogen peroxide for five minutes, and then sequential rinsing in boiling distilled water, acetone at room temperature, and boiling hexane and pentane at room temperature to eliminate the interference of accumulated products; and that horseradish peroxidase substrates, which are found in some biological samples, interfere with the assay. The coulometric determination of uric acid described by Troy and Purdy (27) involves titration with electrogenerated iodine of the total reducing substances before and after treatment of the sample with urate oxidase. The electrochemical procedure of Park *et al.* (26) for the determination of serum uric acid requires no sample manipulation and uses no reagents. The technique is based on oxidation of uric acid at a carbon paste electrode using a digital potentiostat. These authors state, however, that extensive studies would be necessary to establish all potential interferences with the method. Thus, the reaction rate method reported in this paper offers speed, simplicity, selectivity, and adaptability to automation.

RECEIVED for review April 15, 1974. Accepted June 7, 1974. Paper presented at 25th Pittsburgh Conference, Cleveland, Ohio, March 6, 1974. This work was supported by the National Science Foundation (Grant GP-3882X).

Identification and Quantitative Measurement of Some *N*-Heterocyclics in Marijuana Smoke Condensates

M. Zamir-ul Haq, Samie J. Rose, Lisa R. Deiderich, and Appasaheb R. Patel

Meloy Laboratories, Inc., 6715 Electronic Drive, Springfield, Va. 22151

Carbazole, indole, and skatole have been identified and quantitatively determined in marijuana smoke condensates using gas chromatography, mass, and liquid scintillation spectrometry. Methods for the synthesis of carbazole-*5,6,7,8,12,13,*-^{14}C and skatole-*3a,4,5,6,7,7a*-^{14}C are described. These and indole-*2*-^{14}C served as internal recovery standards. The procedure involves partitioning of the condensate and the respective internal standard between hexane and methanol–water (4:1). The ratio of methanol–water is changed from 4:1 to 1:2 and the resulting solution is shaken with hexane. The hexane extract is first washed with 2*N* acetic acid and then with water, dried (Na_2SO_4) and chromatographed on a Florisil column. The concentrate of the appropriate fractions is analyzed for carbazole, indole, and skatole. The average amount of carbazole, indole, and skatole per gram of fresh dry condensate is, respectively, 89 ± 3, 826 ± 4, and 597 ± 7 μg. Effect of aging of the condensate on these components is discussed.

In recent years a great deal of work has been done (*1–12*) on *Cannabis sativa* L. (marijuana) constituents. Although the nationwide consumption of marijuana cigarettes has increased greatly, relatively little attention has been focused (*13–16*) on its smoke constituents. The present study was initiated in view of reported (*17*) tumor-accelerating characteristics of some *N*-alkylated carbazoles and indoles. In this paper, we report the detection and quantitative determination of carbazole, indole, and skatole from marijuana smoke condensates (MSC) using primarily gas chromatography, mass, and liquid scintillation spectrometry.

EXPERIMENTAL

Apparatus. An automatic machine was used for cigarette making. Smoking was carried out on an automatic Process and Instrument, Inc., smoking machine. A Beckman GC-65 gas chromatograph equipped with a flame ionization detector was used for the detection and quantitation of *N*-heterocyclics. A Beckman GC-72-5 with a thermal conductivity detector was used to determine water content of MSC. Conclusive identification of carbazole, indole, and skatole was done on an LKB-9000 gas chromatograph–mass spectrometer. Counting of the radioactive materials was conducted on a Beckman LS-255 liquid scintillation spectrometer. Concentration of solvents was done under reduced pressure below 40 °C. Standard variation and standard error were computed on an Olivetti Programma 101.

Reagents. Analytical reagent grade (Fisher Scientific) organic solvents were used. Carbazole, cyclohexanone, skatole, and propionaldehyde were purchased from Eastman Kodak Co. Indole, phenylhydrazine, and Florisil (60–100 mesh) were bought from Fisher Scientific and 5% palladium on carbon was bought from Matheson, Coleman, and Bell. Column packings, namely 20% Apiezon L on Chromosorb W, 20% SE-30 on Gas Chrom P, 5% OV-225 on Gas Chrom P, 3% OV-17 on Gas Chrom Q, and 3% Silar 5CP on Gas Chrom Q (80–100 mesh) were purchased from Applied Science Laboratories, while Porapak P was available from Waters Associates. Liquifluor was available from New England Nuclear.

Radioisotopically Labeled Compounds. Phenylhydrazine hydrochloride (uniformly labeled-^{14}C) and indole-2-^{14}C (pure on a gas chromatogram) were available from International Chemical and Nuclear Corporation. Carbazole-^{14}C and skatole-^{14}C were synthesized by us.

Synthesis of Carbazole-*5,6,7,8,12,13*-^{14}C. Phenylhydrazine hydrochloride [(ring uniformly labeled-^{14}C; 1.3 mg; specific activity 5.48 mCi/mM)] was dissolved in ethyl alcohol (97%; 1 ml). Cyclohexanone (20 μl) was added to this solution with stirring and the mixture was refluxed for 2 hours. The residue, after the removal of the solvent, was dissolved in mesitylene (1 ml) and palladium on carbon (5%; 3 mg) was added. The suspension was refluxed for 2 hours. The mixture was filtered and the filter paper was washed with *n*-hexane. The filtrate and washings were combined and concentrated. The residue was purified on a Florisil column yielding pure carbazole-^{14}C (0.8 mg; 52% yield; specific activity 5.2 mCi/mM); the purity was determined by gas chromatography.

Synthesis of Skatole-*3a,4,5,6,7,7a*-^{14}C. Phenylhydrazine hydrochloride [(ring uniformly labeled-^{14}C; 2 mg; specific activity 5.48 mCi/mM)] was dissolved in absolute ethanol (1 ml) and after the addition of propionaldehyde (3 μl), the mixture was refluxed for 2 hours. The flask was occasionally shaken to affect dissolution of the solid that deposits on its walls. The solvent was evaporated and the residue was purified on a Florisil column giving 0.79 mg (44% yield) of skatole-^{14}C (sp. activity 5.1 mCi/mM); the purity of this material was confirmed by gas chromatography.

Marijuana Cigarette Making, Smoking, and Condensate Preparation. Marijuana cigarettes of standard specifications (*i.e.*, 85 mm length) were made in our own research facilities. The cigarettes after conditioning at 24° and 60% relative humidity for 48 hours were smoked using the standard conditions of one 35-ml puff of two-second duration per min. The smoke condensate was collected in 4 three-liter jars connected in series and the traps were kept at −78°. The first two traps were partially filled with Pyrex beads and the last two with Teflon filament. The condensate was removed from the traps using distilled acetone. The suspension was concentrated yielding a condensate with less than 5% water content. The wet condensate was mixed with a weighed amount of acetone and the water content of the mixture was determined by gas chromatographic procedures essentially similar to those published by Schultz and Spears (*18*).

Two types of MSC were used—*i.e.*, fresh samples within a month of the condensate production and a composite of all samples collected every 8 weeks over a period of 2 years.

Identification of Carbazole, Indole, and Skatole in Marijuana Smoke Condensate. MSC (2.5 grams; dry) was dissolved in *n*-hexane (70 ml) and methanol–water (4:1; 70 ml). The two layers were shaken and separated. The *n*-hexane layer was extracted three times with 70 ml of methanol–water (4:1). Water (392 ml) was added to the latter bringing the ratio of methanol–water to 1:2. The resulting solution was extracted with *n*-hexane (300 ml ×5). The combined hexane extracts were concentrated *in vacuo* to 200 ml, washed with 2*N* acetic acid (200 ml ×2) and then with water (100 ml ×2). The hexane solution was dried (Na_2SO_4), filtered, and concentrated yielding a residue (0.3 gram). A concentrated solution of the latter in *n*-hexane was chromatographed on a Florisil column (2 × 25 cm; 53 grams). The column was eluted with *n*-hexane (200 ml), benzene–*n*-hexane (1:4; 200 ml), and finally with benzene–hexane (2:3; 300 ml), the volume of each fraction being 20 ml. Gas chromatography indicated that fractions 4–8 (with benzene–hexane, 2:3) contained indole and skatole, whereas fractions 6–10 predominantly showed the presence of carbazole. These fractions were injected in a gas chromatograph–mass spectrometer. Mass spectra of the respective peaks were identical with those of the reference compounds.

Gas Chromatography. Detection of carbazole, indole, and skatole was carried out by gas chromatography with a variety of column packing (see Apparatus). However, all the quantitative work was done on a glass column (6 ft × 2 mm) packed with 3% Silar 5 CP on Gas Chrom Q. For the determination of carbazole, the following conditions were used: column temperature, 220°, detector 300°; injector, 250°; flow rate (helium), 20 ml/min.; sample size, 2 μl; isothermal temperature. Determination of indole and skatole was carried out at the column temperature of 160°; the rest of the conditions were the same as those used for carbazole.

Quantitative Measurement of Carbazole in MSC. The MSC (usually 2–3 grams) and a solution of carbazole-*5,6,7,8,12,13*-^{14}C (100 μl, 20,000 CPM) in *n*-hexane were extracted with methanol–water (4:1) 70 ml 4 times. The rest of the procedure was essentially the same as that described above for the identification of this heterocyclic. Fractions 6–10 (benzene–hexane, 2:3; 20 ml each) from the Florisil column in general showed the radioactivity; these were combined, concentrated, and the volume was made up to 1 ml. The actual amount of carbazole in this solution was determined by gas chromatography using a concentration–peak height calibration curve prepared by the use of authentic carbazole. On an average, the recovery of carbazole-^{14}C was 70% and was obtained by counting 100 μl of the 1-ml solution in 10 ml of liquid scintillation fluid. The handling losses were computed from the loss of the counts in radioactivity.

Quantitative Measurement of Indole in MSC. The amount of indole was determined in the same way as that of carbazole except that indole-2-^{14}C (100 μl; 200,000 CPM) was used as the internal standard. On an average, fractions 4–8 from the Florisil column

(1) L. Grlic, *Eur. J. Toxicol.*, **4**, 43 (1971).
(2) L. Strömberg, *J. Chromatogr.*, **68**, 248 (1972).
(3) R. A. De Zeeuw, Th. M. Malingré, and F. W. H. M. Merkus, *J. Pharm. Pharmacol.*, **24**, 1 (1972).
(4) T. B. Vree, D. D. Breimer, C. A. M. Van Ginneken, J. M. Van Rossum, R. A. De Zeeuw, and A. H Witte, *Clin. Chim. Acta*, **34**, 365 (1971).
(5) K. H. Davis, Jr., N. H. Martin, C. G. Pitt, J. W. Wildes, and M. E. Wall, *Lloydia*, **33**, 453 (1970).
(6) T. B. Vree, *J. Chromatogr.*, **79**, 81 (1973).
(7) R. A. De Zeeuw, *Experientia*, **29**, 260 (1973).
(8) R. A. De Zeeuw, J. Wijsbeek, and Th. M. Malingré, *J. Pharm. Pharmacol.*, **25**, 21 (1973).
(9) A. B. Segelman, *J. Chromatogr.*, **82**, 151 (1973).
(10) C. A. L. Bercht, R. J. J. Ch. Lousberg, F. J. E. M. Küppers, C. A. Salemink, T. B. Vree, and J. M. Van Rossum, *J. Chromatogr.*, **81**, 163 (1973).
(11) C. E. Turner and K. W. Hadley, *J. Pharm. Sci.*, **62**, 1083 (1973).
(12) Y. Gaoni and R. Mechoulam, *J. Amer. Chem. Soc.*, **93**, 217 (1971).
(13) K. O'Brien Fehr and H. Kalant, *Can. J. Physiol. Pharmacol.*, **50**, 761 (1972).
(14) F. Fish and W. D. C. Wilson, *Forensic Sci. Soc. J.*, **9**, 37 (1969).
(15) T. C. Adams, Jr., and A. L. Jones, *J. Agr. Food Chem.*, **21**, 1129 (1973).
(16) A. F. Fentiman, Jr., R. L. Foltz, and G. W. Kinzer, *Anal. Chem.*, **45**, 580 (1973).
(17) D. Hoffmann and E. L. Wynder, *J. Nat. Cancer Inst.*, **48**, 1855 (1972).
(18) F. J. Schultz and A. W. Spears, *Tobacco Sci.*, **10**, 75 (1966).

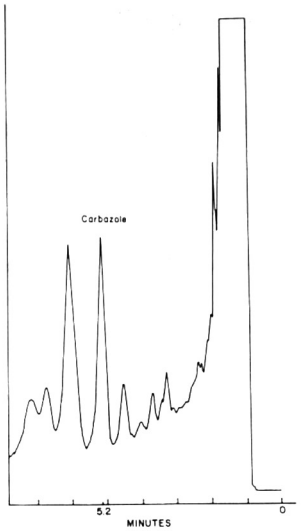


Figure 1. Gas chromatogram of carbazole fraction from MSC

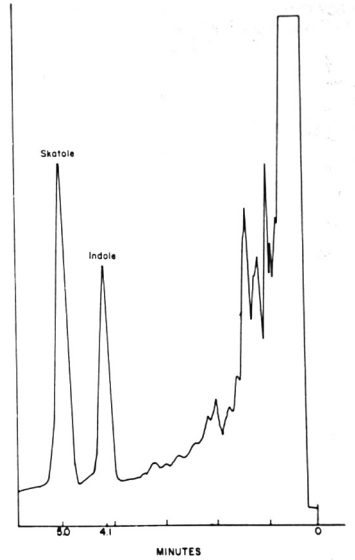


Figure 2. Gas chromatogram of indole–skatole fraction of MSC

were radioactive and were subjected to quantitative determination. The percentage recovery of indole was 30.

Quantitative Measurement of Skatole. The amount of skatole was determined using skatole-*3a,4,5,6,7,7a*-^{14}C as the internal standard (100 μl; 50,000 CPM). The rest of the procedure was the same as that for indole. The recovery of skatole was 40%.

RESULTS AND DISCUSSION

Thirty thousand marijuana cigarettes were smoked in one smoking run in connection with another study. The average yield was 17 mg/cigarette. The dry condensate, after partitioning between two pairs of solvents (see Experimental for details) and column chromatography yielded fractions enriched in carbazole, indole, and skatole. Gas chromatographic analysis on a variety of column packings showed the presence of these heterocyclics in the respective fractions. Preliminary identification was made by comparing the retention time of the peak of interest with that of its authentic counterpart. The retention time of carbazole at 220° (column, 3% Silar 5 CP) was 5.2 min. The retention times of indole and skatole at 160° were, respectively, 4.1 and 5.0 min (see also Figures 1 and 2). The identity of these compounds in MSC was conclusively established by a comparison of the mass spectra of the peaks of authentic reference compounds with those of their respective counterparts in marijuana smoke extracts (Figures 3–5). For this purpose, a gas chromatograph–mass spectrometer was used. One single experiment is sufficient to carry out qualitative determination of carbazole, indole, and skatole in MSC.

For the quantitative analysis, however, separate experiments were done using individual internal standards. This was because of the fact that operational losses of carbazole, indole, and skatole were quite different from each other and thus none of the internal standards could be used for the quantitation of the other component.

In MSC, carbazole was quantitatively determined using carbazole-*5,6,7,8,12,13*-^{14}C as internal standard (see Experimental for details). The use of carbazole-*13*-^{14}C for the quantitation of carbazole in tobacco smoke condensate was

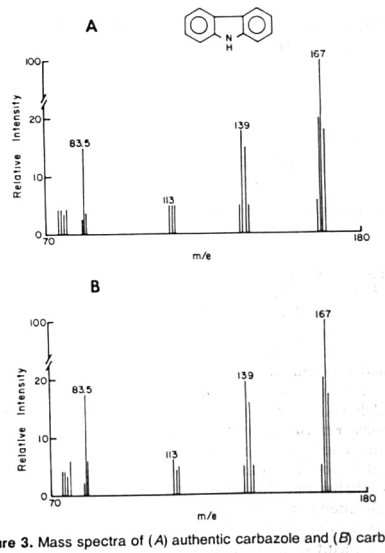


Figure 3. Mass spectra of (*A*) authentic carbazole and (*B*) carbazole from MSC

first reported by Hoffmann and coworkers (*19*). We modified both their method of synthesis and quantitative measurement of this compound.

(19) D. Hoffmann, G. Rathkamp, and H. Woziwodzki, *Beitr. Tabakforsch.*, **4**, 253 (1968).

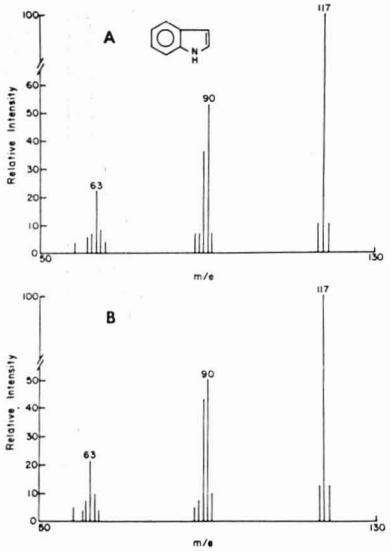


Figure 4. Mass spectra of (*A*) authentic indole and (*B*) indole from MSC

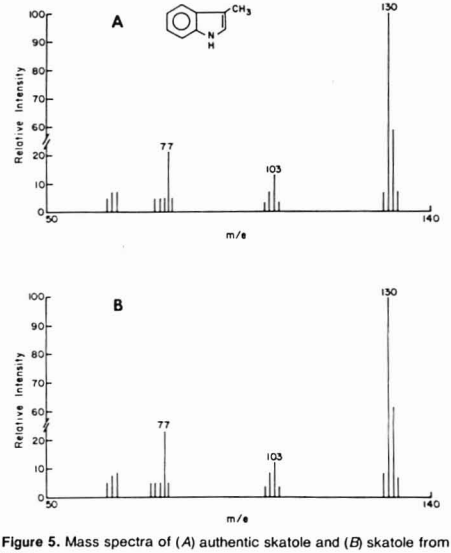


Figure 5. Mass spectra of (*A*) authentic skatole and (*B*) skatole from MSC

Table I. Quantitative Data on Carbazole, Indole, and Skatole of Fresh MSC

Compound	1	2	3	Mean	Std dev	Std error of the mean	Coeff of variation
Carbazole[a]	86	92	89	89	3	2	3.4
Indole[a]	823	826	830	826	4	2	0.4
Skatole[a]	591	604	596	597	7	4	1.1

[a] μg/gram of dry condensate.

Table II. Quantitative Data on Carbazole, Indole, and Skatole of Composite MSC

Compound	1	2	3	Mean	Std dev	Std error of the mean	Coeff of variation
Carbazole[a]	64	65	57	62	4	3	7.0
Indole[a]	737	746	730	738	8	5	1.1
Skatole[a]	797	780	791	789	9	5	1.1

[a] μg/gram of dry condensate.

In a separate experiment, indole was quantitatively measured employing indole-2-^{14}C which is commercially available. The method of Hoffmann *et al.* (*20*) for tobacco smoke condensate was modified for this study of MSC.

The synthesis of skatole-*3a,4,5,6,7,7a*-^{14}C was accomplished by refluxing a solution of phenylhydrazine hydrochloride (ring uniformly labeled-^{14}C) in ethanol with propionaldehyde. Several preliminary experiments were done to optimize reaction conditions. It was necessary to modify the procedure for the synthesis of unlabeled skatole reported in the literature (*21*). Using the pure radioisotopically labeled skatole and following the same procedure as that for indole, we were able to measure quantitatively the amount of skatole in MSC.

As a result of three quantitative analyses (see Table I), the value of carbazole, indole, and skatole in the fresh marijuana smoke condensate was, respectively, 89 ± 3, 826 ± 4, and 597 ± 7 μg per gram of dry condensate. Experimental variations for the determination of carbazole, indole, and skatole were ±3.4, ±0.4, and ±1.1%, respectively.

Another aspect of this investigation was to study the effect of aging of MSC on the levels of these heterocyclics. Quantitative results (Table II) were, therefore, obtained on a composite sample of MSC (collected every 8 weeks over a period of 2 years). As can be seen, levels of carbazole and indole decreased whereas levels of skatole increased on standing.

In this investigation, we have demonstrated that the use of indole as an internal standard for the determination of skatole is not valid. This is primarily because of the higher chemical instability of indole than that of skatole (*20*). Thus, higher operational losses are observed for indole compared to skatole. In any quantitative determination, therefore, the use of internal standard for the quantitation of another structurally related component may be undertaken with caution. Ideally, individual standards should be used as has been done by us.

In summary, we have identified carbazole, indole, and skatole in MSC; quantitatively measured the levels of these compounds in MSC; and synthesized radioisotopically labeled carbazole and skatole. Our method of synthesis for skatole is ideally suited for microgram quantities.

ACKNOWLEDGMENT

The authors thank Richard L. Hawks, National Institute of Mental Health, National Institutes of Health, Bethesda, Md., for carrying out gas chromatographic–mass spectral determinations.

(20) D. Hoffmann and J. Rubin, *Beitr. Tabakforsch.*, **3**, 409 (1966).
(21) L. Marion and C. W. Oldfield, *Can. J. Res., Sect. B*, **25**, 1 (1947).

RECEIVED for review April 15, 1974. Accepted June 17, 1974. This paper was presented at the 9th Middle Atlantic Regional Meeting of the American Chemical Society held in Wilkes-Barre, Pa., April 23–26, 1974 (Abstracts 22). The work was conducted under Public Health Service Contract No. NIH 69-2084.

Simple Digital Method for Resolving Overlapping Electronic Absorption Bands

B. E. Barker and M. F. Fox[1]

City of Leicester Polytechnic, Leicester LE1 9BH, England

E. Hayon and E. W. Ross

Pioneering Research Laboratory, U.S. Army Natick Laboratories, Natick, Mass. 01760

A new method of resolving overlapping electronic absorption bands is described. The method operates through linearizing Gaussian band shapes through derivation of d log $\phi/d\nu$, where ϕ is the absorption band profile absorbance at wavelength ν. The simple, digital, method provides information of individual component peak positions, band heights (intensities), and widths. The limits of applicability for the method are given and extensions to include a visual display presentation are described. Results obtained using the method described are more consistent and accurate than results obtained using an analog curve resolver.

We are concerned with the problem of estimating the position, height, and width of absorption bands in experimentally obtained electronic absorption spectra. Various mathematical methods have been proposed for estimating peak parameters, but each method has its own advantages and disadvantages and no single procedure seems wholly adequate.

The two main types of methods are those which differentiate the spectra and those which rely on a least squares fitting procedure. The former methods include those described by Butler and Hopkins(*1, 2*) and by Morrey (*3*), while the latter methods are exemplified in the work of Tunnicliff and Wadsworth (*4*), Savitsky and Golay (*5*), and Schwartz (*6*). In these papers, the peak forms are usually assumed to be Gaussian, Lorentzian, or Student-T type envelopes. Siano and Metzler (*7*) have proposed a least-squares method based on a log-normal distribution.

The differentiation method is convenient but encounters difficulty if the order of differentiation is high, generally of second or fourth order, and if the spectrum includes noise. The least squares method is capable of great precision but usually depends upon initial estimates of the number of peaks and their parameters. A du Pont Curve Resolver is often necessary for preliminary analysis to obtain the initial peak parameters.

All the methods described require large digital computers for their application and, in most cases, the programs are written for equally-spaced data.

[1] Author to whom correspondence should be addressed.

(1) W. L. Butler and D. W. Hopkins, *Photochem. Photobiol.*, **12**, 439 (1970).
(2) W. L. Butler and D. W. Hopkins, *Photochem. Photobiol.*, **12**, 451 (1970).
(3) J. R. Morrey, *Anal. Chem.*, **40**, 905 (1968).
(4) D. D. Tunnicliff and P. A. Wadsworth, *Anal. Chem.*, **40**, 1826 (1968).
(5) A. Savitsky and M. J. E. Golay, *Anal. Chem.*, **36**, 1627 (1964).
(6) L. M. Schwarz, *Anal. Chem.*, **43**, 1336 (1971).
(7) D. B. Siano and D. E. Metzler, *J. Chem. Phys.*, **51**, 1856 (1969).

THE METHOD

A spectral-resolution method is described that has the following properties: it assumes that the absorption peaks are Gaussian shaped as a function of wavenumber, ν; it uses data taken at equal intervals in wavelengths, λ; it permits filtering of the data to reduce noise without significant distortion; it provides reliable estimates of the peak positions, heights, and widths together with a criterion of accuracy; and it is not excessively long or complicated and is thus suitable for small computers, such as a Honeywell DDP 516 (8K core). It is assumed that the wavelength is perfectly known and the signal/noise ratio in absorbance is at least 200.

The method uses both least-squares fitting procedures and differentiation, and is probably closest in outlook to that of Tunnicliff and Wadsworth (*4*). The fundamental concept arises from the following considerations:

Suppose that the wavelength spectrum, $\phi(\nu)$, consists of a lone Gaussian peak centered at $\nu = A$, with height ϵ and width w, related to the standard deviation S by

$$w = 2S(2 \ln 2)^{1/2} \tag{1}$$

Then,

$$\phi(\nu) = \epsilon e^{-1/2\left(\frac{\nu - A}{s}\right)^2} \tag{2}$$

and the quantity $\psi(\nu)$, defined by;

$$\psi(\nu) = d(-\ln \phi)/d\nu \tag{3}$$

satisfies

$$\psi(\nu) = (\nu - A)/S^2 \tag{4}$$

Hence, in a region where the wavenumber spectrum consists of a single Gaussian peak, the quantity $\psi(\nu)$ is linear in ν with Slope $= S^{-2} > 0$ and $\psi(0) = A$. When more than one peak is present in a spectrum, this will be true only in the regions where one peak dominates all of the other peaks.

Conceptually, the method proceeds as follows. The spectral data are submitted to the transformation Equation 3, the transformed data are plotted, and straight portions with positive slopes are sought. Each of these straight portions denotes a region where one peak dominates all the other peaks. Assuming that one such region can be found, the values of S and A are estimated from the plot and ϵ is estimated by using Equation 2,

$$\epsilon = \phi(\nu)e^{+\frac{1}{2}\left(\frac{\nu - A}{S}\right)^2} \tag{5}$$

With the parameters for that peak available, it is now possible to subtract it from the overall absorption envelope and then repeat the process for the next peak. In this way, the peaks are subtracted sequentially until they are all removed.

This procedure is quite straightforward to carry out when the data consist of spectral ordinates at equal increments in wavenumber ν. Normally one is concerned with the case where the spectral ordinates are available in equal increments of wavelength λ and, therefore, unequal increments in ν. The main problems in practical implementation are then: (i) to design a numerical differentiation procedure for Equation 3 that does not distort the peak shapes too much, and is also not excessively affected by the noise in the spectrum, and (ii) to develop a procedure for estimating A and S from the plot $\psi(\nu)$. Sometimes this can be done by simple graphical means, but it is desirable also to have an analytical method.

In treating problem (i) above, we shall adopt the criterion that our numerical process should be such as to minimize the distortion in a lone Gaussian peak. Naturally, this means that the regions where more than one peak contributes to the spectrum will be slightly distorted. This is not too serious a problem, however, because one can calculate peak parameters only from regions where one peak dominates.

If we define

$$\chi(\lambda) = \phi(\nu) \tag{6}$$

and use the relations

$$\lambda = \nu^{-1},\ d\lambda/d\nu = -\nu^{-2} = -\lambda^2 \tag{7}$$

we obtain,

$$\psi(\nu) = \lambda^2 d(\ln \chi)/d\lambda \tag{8}$$

$$= d(\lambda^2 \ln \chi)/d\lambda - 2\lambda \ln \chi \tag{9}$$

If t is the constant wavelength increment between readings, we shall use the numerical differentiation formula,

$$d(\lambda^2 \ln \chi)/d\lambda = 1/(2t)\{(\lambda + t)^2 \ln \chi(\lambda + t) - (\lambda - t)^2 \ln \chi(\lambda - t)\}. \tag{10}$$

This formula is usually only an approximation, but, when applied to a lone Gaussian peak, it is exact because it is known to be exact for second degree polynomials, and $\lambda^2 \ln \chi$ is a second degree polynomial in λ,

$$\lambda^2 \ln \chi = \lambda^2 \ln \epsilon - {}^1/_2\left(\frac{1 - A\lambda}{S}\right)^2 \tag{11}$$

Hence, we evaluate $\psi(\nu)$ by means of

$$\psi(\nu) = (2t)^{-1}\{\eta(\lambda + t) - \eta(\lambda - t)\} - 2\lambda^{-1}\eta(\lambda) \tag{12}$$

$$\eta = \lambda^2 \ln \chi = \lambda^2 \ln \phi \tag{13}$$

and this formula is exact in regions where a single Gaussian peak dominates the spectrum.

To reduce the effect of noise on the differentiated spectrum, a three-point linear digital filter of the form,

$$\zeta(\nu) = \left(\frac{1 - \gamma}{2}\right)\{\eta(\lambda + t) + \eta(\lambda - t)\} + \gamma\eta(\lambda) \tag{14}$$

$$\psi(\nu) = 1/2t\{\zeta(\lambda + t) - \zeta(\lambda - t)\} - 2\lambda^{-1}\eta(\lambda) \tag{15}$$

is used in place of Equation 12 if desired. γ is a constant which determines the filter properties; for $\gamma = 1$, Equation 15 reduces to Equation 12, and corresponds to no filtering at all. The best choice for noise suppression is $\gamma = {}^1/_5$. Appendix I shows that the result of applying the filter to a lone Gaussian peak is Equation 4, *i.e.*, the filter causes zero distortion of a lone Gaussian peak for any choice of γ.

Problem (ii) above is treated by a least-squares fitting procedure with orthogonal polynomials at equal intervals, see, *e.g.*, Kendall and Stewart (*8*). For this purpose, the wavelengths at which the equally spaced measurements are taken are indexed as:

$$\lambda_j = \lambda_R + jt \qquad j = 0, 1, 2, \ldots \tag{16}$$

where λ_R is the initial wavelength. Then,

$$\nu_j = (\lambda_R + jt)^{-1} \tag{17}$$

and ν_j is not at equal increments. If j_0 be any one of the j-values, we set:

$$\lambda_0 = \lambda_R + j_0 t \tag{18}$$

and obtain:

$$\nu_j = \{\lambda_0 + (j - j_0)t\}^{-1} \tag{19}$$

If $(j - j_0)t \ll \lambda_0$, we have approximately,

$$\nu_j = \lambda_0^{-1} - (j - j_0)t\lambda_0^{-2} \tag{20}$$

or

$$\nu_j = \nu_0 + (j - j_0)\delta_0 \tag{21}$$

where

$$\nu_0 = \lambda_0^{-1}, \text{ and } \delta_0 = -t\lambda_0^{-2} \tag{22}$$

From Equation 21, it can be seen that ν_j is spaced approximately equally for points near j_0, the spacing being δ_0. This will be sufficiently accurate in most cases, provided that $|j - j_0|$ is not too large. As j_0 changes, then both ν_0 and δ_0 change.

The slope and intercept (ν) of the transformed spectrum, $\psi(\nu)$, is estimated by fitting a second degree polynomial to each successive set of five ψ-ordinates, centered at j_0. The method of least-squares (*8*) is applied to the data from the points with indices $j_0 - 2, j_0 - 1, j_0, j_0 + 1, j_0 + 2$, *i.e.*, abscissas $\nu_0 - 2\delta_0, \nu_0 - \delta_0, \nu_0, \nu_0 + \delta_0, \nu_0 + 2\delta_0$. For that j_0, estimates are obtained of the intercept, slope, curvature, and residual squared error. Estimated values of A and S are obtained from the slope and intercept, and ϵ is estimated from Equation 5 by averaging over the five data points. The process is repeated at each j_0 for which sufficient data are available. If this least-squares procedure is used, it may be unnecessary to initially filter the data, using Equation 14, since least-squares is itself a smoothing process. The filter is useful mostly when graphical methods are employed to estimate A and ν.

If ψ_j is assumed to have the behavior:

$$\psi_j = C_0 + C_1(\nu_j - \nu_0) + {}^1/_2 C_2(\nu_j - \nu_0)^2 \tag{23}$$

near ν_0, then we obtain estimates of the C's from

$$C_2 = -2T_2/(7\delta_0^2) \tag{24}$$

$$C_1 = T_1/(10\delta_0) \tag{25}$$

and

$$C_0 = (T_0/5) + (2T_2/7) \tag{26}$$

where,

$$T_0 = \psi_{j_0-2} + \psi_{j_0-1} + \psi_{j_0} + \psi_{j_0+1} + \psi_{j_0+2} \tag{27}$$

$$T_1 = -2\psi_{j_0-2} - \psi_{j_0-1} + \psi_{j_0+1} + 2\psi_{j_0+2} \tag{28}$$

(8) M. G. Kendall and A. Stuart, "The Advanced Theory of Statistics," Vol. 2, Hafner, New York, N.Y., 1961, Chapter 28.

$$T_2 = -\psi_{j_0-2} + {}^1/_2\psi_{j_0-1} + \psi_{j_0} + {}^1/_2\psi_{j_0+1} - \psi_{j_0+2} \quad (29)$$

The sum of squared errors is:

$$E^2 = \sum_{m=-2}^{2}[\psi(\nu_0 + m\delta_0)]^2 - (T_0^2/5) - (T_1^2/10) - (2T_2^2/7) \quad (30)$$

The estimated peak parameters are:

$$S = C_1^{-1/2} = (10\delta_0/T_1)^{1/2} \quad (31)$$

$$A = \nu_0 - (C_0/C_1) \quad (32)$$

and the curvature of the plot is C_2. In general the curvature, e, will be negligible when

$$e = \frac{{}^1/_2|C_2|(2\delta_0)^2}{E} = \frac{2|C_2|\delta_0^2}{E} = \frac{4|T_2|}{7E} \ll 1$$

The presence of a portion of a single Gaussian peak is marked by nearly constant values of A, ϵ, and S over several adjacent values of j_0 and also by low values of e at the same points.

In general, it would be advantageous to remove the higher, wider peaks first. However, these peaks will have low values of ψ, and thus appear suppressed when compared with values of ψ from smaller, narrower peaks. The method will do badly if there is no region in which one peak dominates all of the others. Most methods experience difficulty for the case where no one peak dominates among others in a region. Thus, in differential methods, an illusion of a third peak arises when two peaks are resolved under certain conditions of relative height, width, and peak separation.

It is essential that any new proposed deconvolution methods be tested extensively such that the limits for accurate resolution of two overlapping absorption bands are delineated. All problems of band resolution reduce to the two band problem, and we thus frame the problem in general terms as that of resolving bands A and B, with positions ν_A and ν_B, intensities ϵ_A and ϵ_B and widths at half-height of w_A and w_B. The peak separation, $\nu_A - \nu_B$, is defined as Δ. Resolution of peaks A and B will be determined (in a general sense) by their relative size and the magnitude of Δ. Reduction of the six independent variables proceeds through expressing heights and widths as ratios, thus ϵ_A/ϵ_B and w_A/w_B. If ν_B, and ϵ_B and w_B are fixed and only ν_A, ϵ_A, and w_A varied, then the peak separation/band width properties are determined by the parameter w_A/Δ.

The criterion chosen for accurate resolution was that ν_A and ν_B must be at, or within, 1% of Δ from their actual positions. When the peak parameters are such that this condition is obeyed, the resolution is considered successful. In Figure 1, the limits of conditions for the successful resolution are plotted as a function of w_A/w_B *vs.* w_A/Δ for given ϵ_A/ϵ_B ratios.

The cusp behavior in the region of $w_A/w_B = 1.7$, $w_A/\Delta = 0.6$ for $\epsilon_A/\epsilon_B = 1.0$, occurs when the two peaks overlap such that one peak does not dominate the other completely. When one peak is much larger than the second, and Δ is relatively small, ψ for the first peak provides a background upon which the contribution from ψ for the second may be recognized. The other extreme, *i.e.*, at large Δ, shows ψ's from each peak separately and clearly. The cusp condition arises where the "tail" of the first, larger, peak interferes only partially with the second peak.

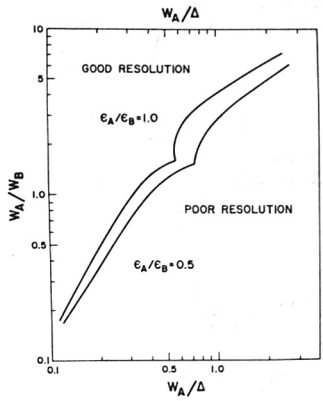


Figure 1. Presentation of the limits of resolution by this method plotted on a logarithmic scale as a function of w_A/w_B *vs.* w_A/Δ for various ϵ_A/ϵ_B ratios

In the region of good resolution, the method successfully resolves two bands to give both values of ν_{max} accurate to less than 1% of Δ. In the region of poor resolution, the method gives progressively more inaccurate values for the band maxima as w_A/Δ increases

APPLICATIONS OF THE COMPUTER PROGRAM

The program of the method described above presents the original absorption profile when called as the appropriate data set number from a backing disc store. The data may be filtered if required, preferably for a graphical analysis only. The program then transforms the data using Equations 14 and 15 and carries out the least mean squares fitting at each j_0.

Output may take two forms. The first form is a table of λ, ν, ϕ, ψ, A, ϵ, S, and e in which peaks are recognized by constant values of A, E, and S and low values of e.

The second form of output gives the original absorption profile, ϕ, and ψ, the first derivative of log ϕ, on a graph plotter from which linear portions of ψ may be recognized. Feedback of the limits of the linear portions of ψ into the program will remove the associated peaks. In practice, several attempts are required to optimize peak removal and plotting each set of graphs requires considerable time.

The alternative version of the graphical output presents the graphs in sequence on a Tektronix 4002A Visual Display Unit, with a joystick control. In this mode, several attempts may be made to remove peaks within a short time and only the optimum peak removal (identification) plotted to give a hard copy.

As an example, the absorption spectrum of iodide dissolved in a range of solvents in the far-ultraviolet region shows a series of overlapping bands (*9*). The example given in Figure 2, is that of tetra-*n*-butyl ammonium iodide in triethyl phosphate at 253 K (*10*). The original spectrum is displayed in Figure 2*A* as ϕ, with normalization 2×10^2. Figure 2*B* shows d log A/dν plotted *vs.* ν, *i.e.*, ψ, with an initial linear region encompassed by the crosswire marks. It is advantageous to look at the linear portion selected, and Figure 2*C* shows the section of ψ which was chosen expanded to full scale. Further selections of ψ may be attempted

(9) M. F. Fox and E. Hayon, *Chem. Phys. Lett.*, **14**, 442 (1972).
(10) M. F. Fox and E. Hayon, to be published.

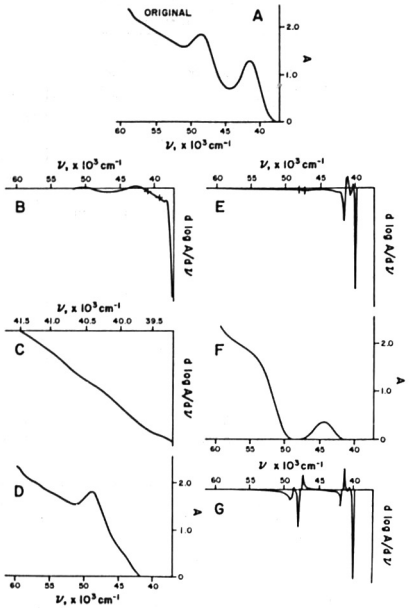


Figure 2. Visual data display for 5 × 10^{-3} tetra-*n*-butylammonium iodide in triethyl phosphate at 253 K

(*A*) Experimentally obtained absorption spectra, ϕ. (*B*) d log *A*/dν of (*A*) plotted *vs.* ν, (ψ), showing crosswires controlled by joystick. (*C*) Expansion of ψ between the crosswires of (*B*) above showing region of interest for peak removal. (*D*) ϕ, *i.e.*, (*A*) with the first peak removed. This spectrum is then made an original data, as ϕ'. (*E*) d log *A*/dν, (ψ) of (*D*) showing linear region denoted by crosswires. (*F*) (*A*) with second peak removed. The remaining data are then treated as an original data set, ϕ''. (*G*) d log *A*/dν for (*F*) giving the band parameter of the small band at approx. 44,000 cm^{-1}

until a decision to remove the band associated with that linear portion is made. The spectrum ϕ, after optimal removal of the first band, Figure 2*D*, contains, among others, a hitherto unsuspected low intensity band. The initial spectrum, ϕ, and the residual spectrum after the first band has been removed, ϕ', may then be plotted to give a hard copy.

The residual spectrum ϕ', is then reprocessed to give ψ' wherein a further linear portion, delineated by the crosswire marks, is noted as in Figure 2*E*. Optional removal of the second large band gives the second residual spectrum, ϕ'' in Figure 2*F* showing the previously described small band in isolation. The parameters of the small band in the region of 44,000 cm^{-1} may be obtained by further processing of ϕ'' to obtain ψ'', Figure 2*F*. Attempts to remove further bands are not successful because the individual components are too overlapped for accurate deconvolution, the "poor resolution" condition of Figure 1 applying. Further band resolution can only be achieved using an analog curve resolver on a subjective basis, using as few bands as is consistent with an acceptable solution.

Comparison with other methods shows the method described here to give more consistent results for a set of spectra recorded over a range of temperature than obtained using the analog curve resolver approach. The advantages of the digital method being that one peak, and thus a small part of an overall absorption profile, is dealt with at each treatment and the parameters are obtained from a least mean squares approach.

Such considerations are the more advantageous when it is realized that a spectral width of 25,000 cm^{-1} is presented on the ten-inch scale of the analog resolver.

On the other hand, the method is not as effective as the iterative least mean squares method of fitting a series of Gaussian (normal) or log-normal curves to an absorption profile. The advantages of the iterative method lie with the absence of differential operators and the small but very effective adjustments which are made to obtain an accurate solution.

A program listing, with worked examples, is available upon request from the authors.

APPENDIX I: DERIVATION OF THE FILTER EQUATIONS

In this Appendix, we shall show that the filter defined by Equations 14 and 15 leads to Formula 4 when applied to a lone Gaussian peak.

For such a peak, Equations 11 and 13 imply

$$\eta_\lambda = \eta(\lambda) = \lambda^2 \ln \epsilon - {}^1/_2\left(\frac{1 - A\lambda}{S}\right)^2 \quad \text{(I.1)}$$

We assume that the filter has the three-point, linear, digital form

$$\zeta_\lambda = \gamma_{-1}\eta_{\lambda-1} + \gamma\eta_\lambda + \gamma_1\eta_{\lambda+1} \quad \text{(I.2)}$$

where

$$\left.\begin{aligned}\zeta_{\lambda+m} &\equiv \zeta(\lambda + ml)\\ \eta_{\lambda+m} &\equiv \eta(\lambda + ml)\end{aligned}\right\} \quad m = \ldots -2, -1, 0, 1, 2, \ldots \quad \text{(I.3)}$$

and γ_{-1}, γ, γ_1 are constants to be specified later. If we substitute the form of η_λ, Equation I.1, into I.2, use I.3 and collect terms, we obtain after some algebra

$$\zeta_\lambda = (\lambda^2\sigma + 2\theta_0\lambda l + \sigma_0 l^2)\ln\epsilon - \frac{1}{2S^2}[\sigma(1 - A\lambda)^2 - 2Al\theta_0(1 - A\lambda) + A^2l^2j_0] \quad \text{(I.4)}$$

where

$$\sigma \equiv \gamma_1 + \gamma + \gamma_{-1}$$
$$\sigma_0 \equiv \gamma_1 + \gamma_{-1}$$
$$\theta_0 \equiv \gamma_1 - \gamma_{-1}$$

Using Equation I.4, we obtain after some more algebra

$$\frac{1}{2l}[\zeta_{\lambda+1} - \zeta_{\lambda-1}] = 2(\lambda\sigma + \theta_0 l)\ln\epsilon - \frac{A}{S^2}[-\sigma + A(\lambda\sigma + \theta_0 l)] \quad \text{(I.5)}$$

Equations 2, 6, and 7 lead to

$$\ln\chi(\lambda) = \ln\chi_\lambda = \ln\epsilon - \frac{1}{2}\left(\frac{\lambda^{-1} - A}{S}\right)^2$$

or

$$2(\lambda\sigma + \theta_0)\ln\chi_\lambda = 2(\lambda\sigma + \theta_0 l)\ln\epsilon - \frac{(\lambda\sigma + \theta_0 l)}{S^2}(\lambda^{-2} - 2A\lambda^{-1} + A^2) \quad \text{(I.6)}$$

Subtracting Equation I.6 from I.5 and simplifying the result, we find

$$Q_\lambda \equiv \frac{1}{2l}[\zeta_{\lambda+1} - \zeta_{\lambda-1}] - 2(\lambda\sigma + \theta_0 l)\ln \chi_\lambda = \frac{1}{S^2}[\sigma(\lambda^{-1} - A) + \theta_0 l\lambda^{-1}(\lambda^{-1} - 2A)] \quad (I.7)$$

We have not yet chosen the filter constants γ_{-1}, γ, and γ_1. We now choose them so that the final form of the filter, given by Q_λ, leads to Equation 4. Equation I.7 tells us that we can do that only by choosing

$$\theta_0 = 0 \quad \text{and} \quad \sigma = 1$$

or

$$\gamma_1 = \gamma_{-1} = (1 - \gamma)/2 \quad (I.8)$$

With this choice we obtain

$$Q_\lambda \equiv \frac{1}{2l}[\zeta_{\lambda+1} - \zeta_{\lambda-1}] - 2\lambda^{-1}\eta_\lambda = \frac{\lambda^{-1} - A}{S^2}$$

or from Equations 7 and 13

$$Q_\lambda \equiv \frac{1}{2l}[\zeta_{\lambda+1} - \zeta_{\lambda-1}] - 2\lambda^{-1}\eta_\lambda = \frac{\nu - A}{S^2} \quad (I.9)$$

Also, combining Equations I.8 and I.2, we find that

$$\zeta_\lambda \equiv \zeta(\lambda) = \left(\frac{1 - \gamma}{2}\right)[\eta(\lambda - l) + \eta(\lambda + l)] + \gamma\eta(\lambda) \quad (I.10)$$

Equation I.10 is the same as Equation 14.

We see from Equations I.9 and I.2 that the quantity

$$Q_\lambda \equiv \frac{1}{2l}[\zeta(\lambda + l) - \zeta(\lambda - l)] - 2\lambda^{-1}\eta(\lambda) \quad (I.11)$$

where $\zeta(\lambda + l)$ and $\zeta(\lambda - l)$ are defined by Equation I.10, gives the number $(\nu - A)/S^2$ when applied to a lone Gaussian peak with parameters A and S. This means that we may interpret Q_λ as the filtered version of $\psi(\nu)$; that is, we may take Q_λ to be the definition of $\psi(\nu)$ when the data are subjected to a three-point, linear digital filter of the form of Equation I.10. This leads to Equation 15.

Notice that the filter gives the correct values for $\psi(\nu)$, namely $(\nu - A)/S^2$, regardless of the choice of the constant γ. The value of γ determines the properties of the filter. If $\gamma = 1$, we obtain

$$\zeta(\lambda) = \eta(\lambda)$$

$$\psi(\nu) = \frac{1}{2\Delta}\{\eta(\lambda + l) - \eta(\lambda - l)\} - 2\lambda^{-1}\eta(\lambda)$$

For this choice of γ, the filter gives the same result, Equation 12, that is obtained when there is no filter. If the noise is low-level, uncorrelated, and Gaussian, and if the peak is sufficiently wide compared to the spacing, it can be shown that $\gamma \approx \frac{1}{5}$ gives the least variance in the filter output. However, filtering can cause originally uncorrelated noise to become correlated and can also cause loss of resolution, so it may be preferable to use a γ-value nearer to unity.

The filter (I.10) can be repeated N times according to the formula

$$\zeta^{(n)}(\lambda) = \frac{1 - \gamma}{2}[\zeta^{(n-1)}(\lambda - l) + \zeta^{(n-1)}(\lambda + l)] + \gamma\zeta^{(n-1)}(\lambda) \quad \text{for } n = 1, 2, \ldots N \quad (I.12)$$

$$\zeta^{(0)}(\lambda) = \eta(\lambda) \quad (I.13)$$

If $\zeta(N)(\lambda)$ is substituted into

$$\psi(\nu) = Q_\lambda = \frac{1}{2l}[\zeta^{(N)}(\lambda + l) - \zeta^{(N)}(\lambda - l)] - 2\lambda^{-1}\eta(\lambda) \quad (I.14)$$

the result is again $(\nu - A)/S^2$ for a lone Gaussian peak. That is, filtering N times according to Equations I.12 and I.13, then substituting the final results, $\zeta(N)(\lambda)$, into Equation I.14 causes no distortion of a pure Gaussian peak. Filtering several times can reduce the noise into a lower level than filtering only once. However, it is risky to filter too many times because of resolution loss.

RECEIVED for review September 24, 1973. Accepted May 28, 1974. One of us (MFF) wishes to thank the National Research Council for a NAS/NRC Senior Visiting Research Associateship at U.S. Army Natick Laboratories.

Computerized Pattern Recognition Applications to Chemical Analysis

Development of Interactive Feature Selection Methods for the K-Nearest Neighbor Technique

M. A. Pichler and S. P. Perone

Purdue University, Department of Chemistry, Lafayette, Ind. 47907

A systematic approach has been developed for feature selection in the application of the K-nearest neighbor (KNN) computerized pattern recognition method. The approach utilizes an operator-interactive computer system. A large number of potentially useful features for classification of patterns can be screened for the most relevant members by a combination of recommended procedures. These include: one-dimensional KNN classification of all patterns using each feature individually; inspection of histogram displays of classification records for each feature; and establishment of consensus classifications from combined one-dimensional results. A computerized trial-and-error procedure can then be implemented to find the best combination of a minimum number of features for accurate classification using the multidimensional KNN method. This overall procedure has been applied here to binary and multicategory pattern recognition problems. The results show that the dimensionality of KNN analyses can be reduced drastically with no loss in classification accuracy, and perhaps with improved accuracy, while at the same time allowing more effective use of available computer time.

Computerized pattern recognition methods have been explored by workers in various areas, including speech analysis (*1–3*), alphanumeric character identification (*4–6*), and image processing (*7*). A recent review (*8*) also shows that these methods have been applied to problems in chemical analysis. Moreover, Isenhour and Jurs (*8*) and Kowalski and Bender (*9, 10*) have introduced the fundamental concepts of pattern recognition on a broad scope and illustrated the potential for interpretation of complex chemical data sets. Previous work in this laboratory has been concerned with pattern recognition applications to the interpretation of electroanalytical data (*11, 12*). In this previous work, learning machine (*13–15*) methods were applied and an interactive laboratory computer system was utilized.

One objective of the work reported here was to explore the applicability of the K-nearest neighbor (KNN) pattern recognition method (*16–18*) to interpretation of overlapped electroanalytical waveforms and compare with results obtained previously with the learning machine method (*12*). Because the conventional application of the KNN method (*16*) does not provide criteria for discriminating between relevant and irrelevant pattern features, it was also our objective to develop a systematic approach for selection of the pattern features most relevant for classification purposes. To accomplish this latter objective, we relied heavily on interactive procedures allowable by the laboratory computer system employed.

BACKGROUND

Learning Machines. Mathematical pattern recognition concepts are geometrical in nature; *i.e.*, d features of a given pattern constitute coordinates of a single point in d-space, and points representing patterns of the same *class* are assumed to occupy the same region in feature space. The object of pattern classification is to find boundaries which discriminate between the different spacial regions. The learning machine (LM) method involves an error-correction procedure to obtain *pattern classifiers*. The mathematical foundation for this approach has been presented elsewhere (*13, 14, 19–22*), and the specific considerations for the work done previously in this laboratory have been described (*11, 12, 15*).

The learning machine method is most easily implemented with binary problems—*i.e.*, where discrimination between two classes is required. Also, the method has been applied primarily to systems where a *linear* discriminant function is utilized and does not work well for patterns which are not dichotomized by a linear classifier—*i.e.*, patterns not linearly separable.

K-Nearest Neighbor Method. The K-nearest neighbor (KNN) classification rule is considered here as an alternative classification procedure which does not suffer from the same limitations as the learning machine approach. Moreover, a firm statistical foundation exists for the KNN method (*16–18*) and it has been suggested as a standard classification procedure (*17*). The KNN classification rule

(1) K. N. Stevens, *J. Acoust. Soc. Amer.* **32,** 47 (1960).
(2) P. Denes and M. V. Mathews, *J. Acoust. Soc. Amer.*, **32,** 1450 (1960).
(3) S. R. Petrick, *New Sci.*, **10,** 370 (1961).
(4) O. G. Selfridge and U. Neisser, in "Computers and Thought," E. A. Feigenbaum and J. Feldman, Ed., McGraw-Hill, New York, N.Y., 1963, p 237.
(5) L. Uhr and C. Vossler, *ibid.*, p 251.
(6) R. G. Casey and G. Nagy, *Sci. Amer.*, **224,** 56 (1971).
(7) G. Nagy, *Proc. IEEE*, **56,** 836 (1968).
(8) T. L. Isenhour and P. C. Jurs, *Anal. Chem.*, **43** (10), 20A (1971).
(9) B. R. Kowalski and C. F. Bender, *J. Amer. Chem. Soc.*, **94,** 5632 (1972).
(10) B. R. Kowalski and C. F. Bender, *J. Amer. Chem. Soc.*, **95,** 686 (1973).
(11) L. B. Sybrandt and S. P. Perone, *Anal. Chem.*, **43,** 382 (1971).
(12) L. B. Sybrandt and S. P. Perone, *Anal. Chem.*, **44,** 2331 (1972).
(13) N. J. Nilsson, "Learning Machines," McGraw-Hill Book Co., New York, N.Y., 1965.
(14) K. S. Fu, "Sequential Methods in Pattern Recognition and Machine Learning," Academic Press, New York, N.Y., 1968.
(15) P. C. Jurs, B. R. Kowalski, T. L. Isenhour, and C. N. Reilley, *Anal. Chem.*, **41,** 690 (1969).
(16) B. R. Kowalski and C. F. Bender, *Anal. Chem.*, **44,** 1405 (1972).
(17) T. M. Cover, *IEEE Trans. Info. Theory*, **IT-14,** 50 (1968).
(18) D. W. Peterson, *ibid.*, **IT-16,** 26 (1970).
(19) "Computer and Information Sciences-II," J. T. Tou, Ed., Academic Press, New York, N.Y., 1967.
(20) J. R. Slagle, "Artificial Intelligence: The Heuristic Programming Approach," McGraw-Hill, New York, N.Y., 1971.
(21) J. M. Mandel and K. S. Fu, Ed., "Adaptive, Learning, and Pattern Recognition Systems," Academic Press, New York, N.Y., 1970.
(22) H. C. Andrews, "Introduction to Mathematical Techniques in Pattern Recognition," Wiley-Interscience, New York N.Y., 1972.

simply states that an unknown pattern is classified according to a majority vote of its K-nearest neighbors in d-dimensional feature space. Computationally, the Euclidian distances between the single d-dimensional point representing the pattern in question and all other pattern points in d-space must be calculated to find the K nearest neighbors. The KNN method can be applied to nonlinear classification problems—*i.e.*, linear separability of classes is not required. Moreover, it is inherently applicable to multiclass categorization. (A recent article by Kowalski and Bender (*16*) considers the factors involved in selecting K, the convergence properties, and the statistical basis for risk estimates with the KNN method.)

The primary disadvantage of the KNN method is that it is very expensive computationally because of the large numbers of d-dimensional distance calculations. For example, the distance, in d-space, between two points i and j is:

$$D_{ij} = \left[\sum_{k=1}^{d} (x_{ik} - x_{jk})^2 \right]^{1/2} \quad (1)$$

Also, one pass through all known patterns is necessary to classify each unknown pattern. This should be contrasted to the LM procedure where, once the weight vector of the linear discriminant function is found by the error-correction procedure, the classification of an unknown pattern requires only a simple series of computations which could be done on a desk calculator.

Another limitation of the KNN method is that it provides no convenient way, except trial-and-error, for eliminating irrelevant or less useful features, and subsequently lowering the dimensionality of the problem. (However, we describe below a new systematic procedure for feature elimination using this method.) The LM approach does allow feature elimination in a systematic and effective manner (*12, 15, 23*).

Classification of Doublet/Singlet Electrochemical Waveforms. In our previous work, pattern recognition was applied to the identification of doublet and singlet peaks in electroanalytical data. Because only peak overlap cases so severe as to preclude the use of conventional identification methods (such as 1st- and 2nd-derivative analysis) were considered, this was a very demanding problem. The approach taken involved the arbitrary selection of a total of 135 features of a voltammetric peak. The LM program was trained to properly categorize various doublet and singlet patterns, each described by these 135 features. Training was designed so that ineffective features could be eliminated. Thus, a total of only about 22 features was required to classify each peak as doublet or singlet. The trained classifier could successfully categorize previously unseen patterns with about 90% accuracy.

The previous work dealt with electroanalytical data generated from theoretical expressions for stationary electrode polarography (SEP) (*24*), and sets were restricted to reversible electrode processes only. Concentration ratios were allowed to vary randomly between a range of about 40:1 and 1:40. Severe peak overlap was allowed where peak separations were in the range of 4- to 16-mV; and the number of electrons in the redox process could vary from 0.92 to 3.08.

FEATURE SELECTION WITH THE KNN METHOD

Learning machine techniques for pattern recognition allow the systematic elimination of features which are less useful (or counter-productive) in solving the particular pattern recognition problem (*12*). Thus, the dimensionality of the problem can be minimized and the most relevant features can be identified. This provides a useful procedure by which the experimental correlations with desired information can be discovered empirically.

Unfortunately, the K-nearest neighbor (KNN) pattern recognition procedure (*16*) does not generate criteria by which less useful features can be identified and systematically eliminated. Thus, reduction of the dimensionality of the problem must be accomplished by some other mathematical means (*25*). However, these approaches are severely limited to a variety of special cases where the user has a great deal of insight into the nature of the patterns and features being studied. Thus, the most effective approach currently appears to be trial-and-error (*16*), where the burden is on the scientist to select features at the outset which are relevant.

Because the KNN method is particularly useful for multicategory classifications and nonlinearly-separable patterns (*16–18, 26, 27*), we consider it essential to utilize this approach in much of the work currently under way in our laboratory. Because we are also concerned with finding the most relevant experimental correlations, it is necessary to identify the most effective features in the pattern recognition procedure. Thus, we have developed an interactive trial-and-error method for feature selection with the KNN technique.

Approach. The feature selection approach is described as follows: (a) Q features are defined for the set of patterns to be classified, with no limitations imposed on the total number, Q, or on the relevancy of each feature; (b) all patterns in the training set are classified on a *one-dimensional* KNN basis, conducting Q classification procedures—*i.e.*, using only one feature at a time; (c) the M features providing the most accurate categorization on a one-dimensional basis are selected for further *multidimensional* classification studies; (d) a series of KNN classification procedures are conducted using Z features for each, where all possible combinations of Z of the M best features are used (for $Z \leq M$); (e) the combination of Z features which provides the greatest accuracy is selected for subsequent categorization applications.

Development of the procedure outlined above showed that the operator must exercise some judgment in determining the magnitudes of M and Z. For example, if M were selected as 10, and Z were selected as 6, the number of possible feature combinations would be over 200, where the number of combinations = $M!/[Z!\ (M - Z)!]$. Clearly, if one started out with 50 or 60 possible features, a reduction to the 10 best features has diminished the magnitude of a trial-and-error procedure for finding the best combinations. However, as shown above, the KNN classification program would need to be executed over 200 times for the entire training set to find the best 6 of 10 features; and a single KNN analysis is very consuming of computer time. Furthermore, how is one to know if Z shouldn't be taken as 7, or 5, or 9? Investigation of all these possibilities would be prohibitively time consuming. Thus, the operator must be arbitrary and selective. However, it is possible to provide the operator with additional information to guide his decisions. For example, the operator can display histograms of the classification records (see Figures 1–5) for the best features from the one-dimensional KNN analyses. From observation of these histograms, it may be possible to reduce

(23) P. C. Jurs, *Anal. Chem.*, **42**, 1633 (1970).
(24) R. S. Nicholson and I. Shain, *Anal. Chem.*, **36**, 706 (1964).
(25) H. C. Andrews, Ref. 22, Chap. 2.
(26) B. R. Kowalski, T. F. Schatzki, and F. H. Stross, *Anal. Chem.*, **44**, 2176 (1972).
(27) T. M. Cover and P. E. Hart, *IEEE Trans. Info. Theory*, **IT-13**, 21 (1967).

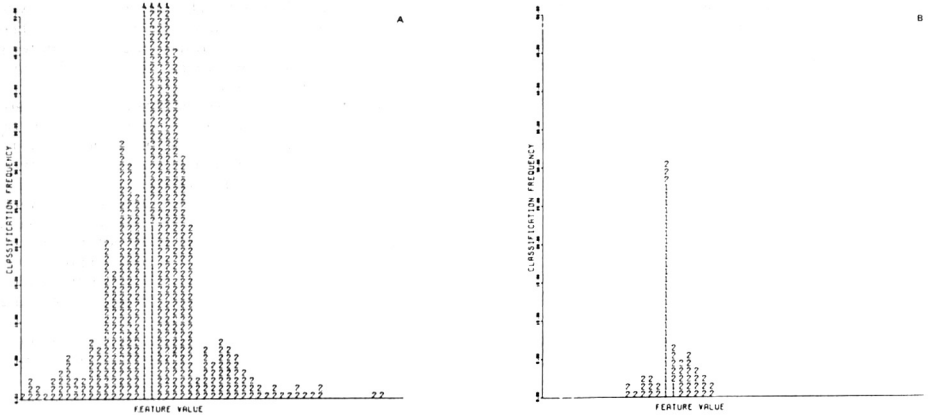


Figure 1. Training set classification histogram for feature No. 2. KNN analysis of SEP data. Good feature. "1" = known singlet class; "2" = known doublet class

(A) Normal scale on frequency axis. (B) Fequency axis scaled by 1/10

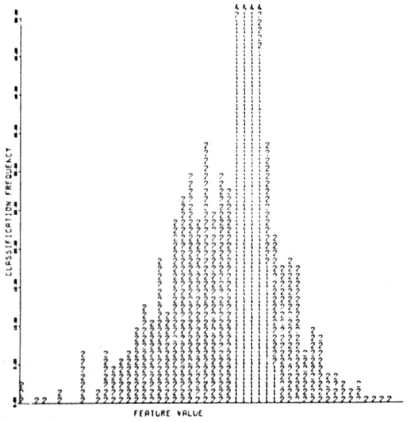


Figure 2. Training set classification histogram for feature No. 28. KNN analysis of SEP data. Less useful feature. "1" = known singlet class; "2" = known doublet class

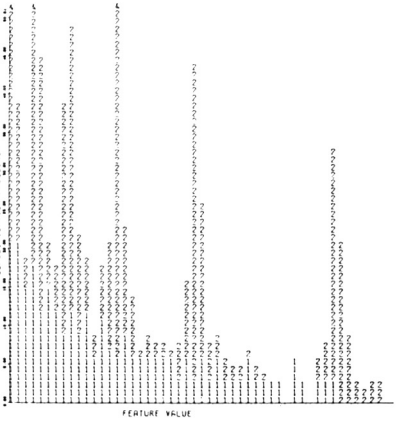


Figure 3. Training set classification histogram of feature No. 121. KNN analysis of SEP data. Poor feature. "1" = known singlet class; "2" = known doublet class

further the number of features considered by selecting only those with obviously better geometrical characteristics (largest separations of classes).

Other interactive possibilities exist. For example, the operator may choose to compare the KNN classification results for Z of the best features, letting Z vary from M to 1, without looking for the best combination of Z features. On the other hand, the operator may choose to select M and Z as low as possible, such that the number of possible combinations is small enough to make exploration computationally feasible. The operator could decide on expanding M and Z if acceptable accuracies are not obtained with the lower dimensions.

Finally, another alternative is simply to compute the *consensus* categorization decisions of the M best features from their individual one-dimensional KNN analyses. This is simple computationally and may provide acceptable accuracy. Furthermore, features may be eliminated on the basis of disagreement with consensus classifications (which would provide a convenient elimination criterion, based on compatibility of features, not obtained easily in any other way).

Advantages. The advantages of the operator-interactive KNN approach described above can be summarized here. First of all, it is possible to start with a large number of features, without regard to whether or not they are the most relevant. Thus, it allows the investigation of problems where little advance knowledge of the nature of correlations between features and classifications can be anticipated, and these can be found empirically. A second advan-

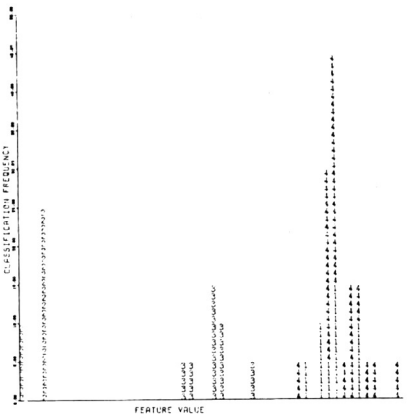


Figure 4. Training set classification histogram of feature No. 3. KNN analysis of archaeological data. Good feature for classification of class 2 and class 3 patterns. Frequency axis scaled by ×5. Numbers plotted refer to known categories

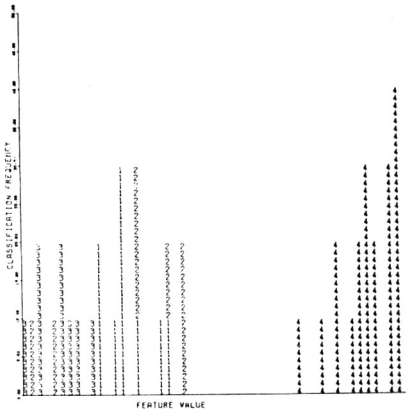


Figure 5. Training set classification histogram of feature No. 1 for KNN analysis of archaeological data. Poor feature. Frequency axis scale by ×10. Numbers plotted refer to known categories

tage is that the approach does allow reduction of the dimensionality of the KNN problem, and this is preferred for higher classification reliability with a limited number of patterns in the training set. A third advantage is that the resultant trial-and-error procedure is based on an operator-interactive system which allows the most effective use of computational time. Finally, the computational approach is orders of magnitude simpler than the standard KNN approach. That is, the one-dimensional analysis requires no auto-scaling (*9*) of features, and classification can be based on a simple ranking procedure, whereas the usual KNN classification program requires Z-dimensional geometrical distance calculations.

RESULTS AND DISCUSSION

In the work described here, the KNN method has been applied to the problem of classifying doublet/singlet patterns from the same stationary electrode polarography (SEP) data base as used in our previous LM work (*12*). This was done for two purposes. One was to compare results for the two pattern recognition techniques for the same data base; of particular interest were the questions of what dimensionality would be required to allow accurate classification and whether the KNN method would be subject to the same limitations on range of pattern characteristics which could be allowed. The other objective was to explore and develop the interactive feature elimination procedure described above. For this purpose, it was particularly useful to work with the large theoretical SEP data base, the composition of which could be varied conveniently in a known fashion.

It was also desirable to apply the feature elimination technique to KNN analysis of a real data base of considerably different nature to help establish the generality of the procedure. For this purpose, B. R. Kowalski of the University of Washington has generously provided us with the data base utilized in a KNN pattern recognition study conducted previously for identification of archaeological artifacts (*26*). The data base includes 74 patterns, with 4 categories, and 10 features defined by Kowalski *et al.* (*26*).

The computer system used for this work was a Hewlett-Packard 2116B with 16K words of core memory, high-speed paper tape input/output, a 7-track incremental magnetic tape unit, a 2.2 million-word moving-head disk, high-speed printer, and interfaced storage oscilloscope. The scope, combined with a teletype and auxilliary keyboard, allowed operator-interactive operations. In addition, the system is provided with a high-speed digital data acquisition and laboratory control panel which allows on-line instrumental measurements. Programming was carried out with disk-based FORTRAN IV, modified for display-oriented operator interaction and on-line data acquisition.

KNN Classification of Doublet/Singlet SEP Data. The SEP data set consisted of features extracted from severely overlapped doublet and singlet SEP curves. These theoretical curves were generated as described by Sybrandt and Perone (*12*). Peak ratios varied randomly from 20:1 to 1:20; peak separations varied randomly between 8 and 12 mV; and electron-transfer values (n) varied randomly between 1.0 and 3.0. Data could be generated such that no prediction set patterns were identical to any training set patterns (*12*). There were a total of 836 training set patterns (303 singlets and 533 doublets) and 900 prediction set patterns (300 singlets and 600 doublets); from each pattern could be extracted 121 features. (The nature of all features is listed elsewhere (*12, 28*). Only 121 of the original 135 defined by Sybrandt (*28*) were used because of disk formatting requirements.)

The first step involved a KNN analysis of the SEP data, using only the minimum 22 features which Sybrandt found necessary for good prediction results (92.5% correct, 2.8% undecided (*12*)). KNN analysis using these 22 features gave 89.2% correct prediction for $K = 1$. Thus, the results were essentially identical for the two approaches. However, it was likely that, due to the inherent differences in the 2 decision algorithms, the features important for LM classification might not be important for KNN analysis. Thus, to achieve good prediction results with KNN, some method of feature selection was necessary.

Feature Selection. Two approaches to feature selection were investigated here. One was to visually observe classification histograms for each feature over all patterns. This allows a visual comparison of the degree of class separation

(28) L. B. Sybrandt, Ph.D. Thesis, Purdue University, Lafayette, Ind., 1972.

Table I. One-Dimensional KNN Classification Results for $K = 1$ (Unautoscaled SEP Data). Percent Correct Prediction

Feature No.	Total accuracy, %	% 2-comp	% 1-comp
2	92.6	95.2	87.3
4	92.9	94.5	89.7
6	89.8	91.7	86.0
8[a]	87.3	90.2	81.7
9[b]	67.3	71.8	58.3
21[a]	88.7	89.5	87.0
26[a]	89.8	94.2	81.0
27[b]	62.9	70.3	48.0
28	85.6	88.3	79.0
63	76.8	81.0	68.3
64[a]	90.1	95.2	80.0
65[a]	76.2	83.7	61.3

[a] This feature was among the final 22 Sybrandt (*12*) found necessary for LM prediction. [b] This feature was selected, from the histogram plot, as a less useful feature.

Table II. Nature of Twelve Most Useful Features of SEP Patterns

Feature No.	Definition[a]
2	E function at 70% i_p
4	E function at 75% i_p
6	E function at 80% i_p
8	E function at 85% i_p
9	Δi at $\Delta E_{ip} = 8$ mV
21	$(E_{3/4} - E_p)/(E_{1/4} - E_p)$
26	i'_{p1}/i'_{p2}
27	$(E_{i'p1} - E_p)/(E_{i'p2} - E_p)$
28	$E(i'_{p1p2} = 0) - E_p$
63	i''_{p1}/i''_{p2}
64	i''_{p1}/i''_{p3}
65	i''_{p3}/i''_{p2}

[a] See Ref. *12* for complete definition of all terms. E function = $(E_2 - E_1)(E_p - E_1)/((E_2 - E_p) - (E_p - E_1))^2$. i' = 1st-derivative peak current. i'' = 2nd-derivative peak current.

provided by each feature, and the better ones could be selected. The other approach involved conducting one-dimensional KNN anlyses for each feature over all patterns. As described above, the most accurate features on a one-dimensional basis could be combined subsequently for a multidimensional KNN classification procedure.

Since some of the original 121 features not found necessary or important in LM prediction might be useful for KNN analysis, one-dimensional classification histograms of all 121 features were obtained for both training and prediction sets. Of the 121 features examined, 10 were selected as being potentially very good features, and 2 others as useful but less important features. Figures 1 to 3 show examples of the three types of histograms observed.

The classification results for one-dimensional KNN anlaysis were obtained also for all 121 features individually. Patterns were not autoscaled (*9*) (since features were used individually on a one-dimensional basis, there was no need to autoscale in order to give all features the same range of magnitude.) For this work a new KNN program was written which, since classification was based on the use of one feature at a time, used a simple ranking procedure rather than time-consuming, multidimensional distance calculations. As a result, time required for classification was decreased by more than an order of magnitude. The following results were obtained (for $K = 1$): 1) Of the 10 features selected as very good on the basis of their histograms, 3 gave overall prediction results better than 90%, 5 gave 85% or better, and 2 gave 75% correct classification (see Table I). 2) Of the 2 other features deemed less useful from their histograms, one gave 67% correct classification, and the other, 63% (see Table I). 3) The remaining 109 features all individually gave prediction results less than 60%. (In most cases, classification accuracy was between 52 and 55%.)

It should be noted that of those 12 features giving the best individual classification results, only 5 had been retained in the final 22 features found important in the LM work done by Sybrandt (*12*). Of the 7 features not retained by Sybrandt but selected as important from their histograms, 2 gave prediction results of better than 90% and 2 gave better than 85% correct classification. (The natures of the 12 features identified in these studies are summarized in Table II.) A correlation matrix for these features is shown in Table III.

Optimum Feature Combinations. The next step taken in this work, to improve prediction results for the SEP data, was to select some of the better features and to determine the prediction results using patterns composed of various combinations of these features. In general, the M best

Table III. Correlation Matrix of SEP Training Set Patterns for 12 Most Useful Features

Feature No.	2	4	6	8	9	21	26	27	28	63	64	65
2	1.00											
4	.99	1.00										
6	.97	.99	1.00									
8	.92	.96	.99	1.00								
9	−.38	−.40	−.42	−.44	1.00							
21	.18	.17	.14	.12	−.08	1.00						
26	−.77	−.73	−.67	−.59	.10	.29	1.00					
27	.75	.78	.80	.79	−.27	.12	−.47	1.00				
28	−.38	−.41	−.43	−.46	.70	−.14	.05	−.26	1.00			
63	−.13	−.14	−.15	−.16	.18	.77	.50	−.06	.02	1.00		
64	−.68	−.63	−.56	−.47	.08	.20	.96	−.31	.04	.47	1.00	
65	.67	.61	.52	.41	.08	.36	−.63	.32	−.03	.30	.67	1.00

Table IV. Z-Dimensional KNN Classification Results (Autoscaled SEP Data) $K = 1$. Percent Correct Prediction

Features[a]	% 1-comp	% 2-comp	Total accuracy, %
2, 4, 6	98.3	98.2	98.2
2, 4, 8	98.3	98.5	98.4
2, 4, 26	99.7	98.7	99.0
2, 4, 28	97.0	98.7	98.1
2, 6, 8	97.7	98.2	98.0
2, 6, 26	99.7	98.5	98.9
2, 6, 28	97.7	98.5	98.2
2, 8, 26	100.0	98.5	99.0
2, 8, 28	99.7	98.7	99.0
2, 26, 28	100.0	98.9	99.2
4, 6, 8	95.0	98.5	97.3
4, 6, 26	98.0	98.5	98.3
4, 6, 28	98.0	98.3	98.2
4, 8, 26	99.7	98.3	98.8
4, 8, 28	99.7	98.5	98.9
4, 26, 28	100.0	98.9	99.2
6, 8, 26	98.3	98.8	98.3
6, 8, 28	99.7	97.8	98.4
6, 26, 28	100.0	98.7	99.1
8, 26, 28	99.3	98.2	98.6

[a] See Table II.

Table V. KNN Classification Results Autoscaled SEP Data for $Z = 6, 8, 12$. Percent Correct Prediction

Features used[a]	% 1-comp	% 2-comp	Total accuracy
2, 4, 6, 8, 26, 28	100.0	99.2	99.4
2, 4, 6, 8, 21, 26, 28, 64	100.0	99.3	99.6
2, 4, 6, 8, 9, 21, 26, 27, 28, 63, 64, 65	100.0	97.2	98.1

[a] See Table II.

features could be chosen on the basis of their one-dimensional prediction results. However, in selecting features, it may be desirable to chose, from among several which give about the same one-dimensional classification accuracy, those which should provide the best multidimensional results. Such decisions can be made more easily by examination of the histograms of the features. In any event, from the M selected features, KNN analysis is then conducted using all possible combinations of Z of these. It is desirable to have Z as small as possible to reduce the dimensionality of the analysis and, hence, to reduce the computation time required. It is desirable to choose M as small as possible to reduce the number of possible combinations of features.

In our work with the SEP data, 6 features were selected from the 12 listed in Table I ($M = 6$). Three-dimensional KNN analysis was done on the autoscaled patterns using all possible combinations of 3 of these 6 features ($Z = 3$). Results (see Table IV) were significantly better than the one-dimensional results of Table I and the LM work done by Sybrandt. Because overall classification accuracy was very high and very nearly the same in all cases, no sound conclusions could be drawn with regard to classification performance as a function of the degree of correlation between features. Because the purpose of the work here was not to maximize the accuracy but to demonstrate the feature selection technique, exhaustive exploration of feature combinations was not conducted, (*e.g.*, for $Z = 4, 5$, etc.). But classification data are shown for the case where Z and $M = 6, 8$, and 12 (Table V).

Table VI. Comparison of KNN ($K = 1$) and LM Classification Results for Patterns Exceeding Training Set Limits

	% Correct	
Peak height	LM[a]	KNN[b]
a) Ratios	(22 features)	($K = 1$)
20–25:1	92.8	100.0
25–30:1	89.6	99.5
30–35:1	88.5	97.0
35–40:1	81.6	90.5
b) Peak Separation		
4–6 mV	86.9	95.5
6–8 mV	90.9	98.0
12–14 mV	89.0	98.0
14–16 mV	86.2	100.0
c) n-value: Two components		
0.98–1.00	90.5	93.0
0.92–0.98	99.5	98.0
3.00–3.08	2.5	94.0
d) n-value: One component		
0.98–1.00	9.1	100.0
0.92–0.98	57.9	100.0
3.00–3.08	98.5	100.0

[a] See Ref. *12*; note that % undecided is not included here. This would lower overall LM accuracy a few percent in each case. [b] 6 Features used, No. 2, 4, 6, 8, 26, 28.

Classification Results for Patterns Exceeding Training Set Limits. The preceding discussion illustrates the effectiveness of the feature selection procedure. Also, the results show that the KNN method provides more accurate classification results with lower dimensionality required than for the LM approach (*12*). This is probably due to the ability of the KNN method to handle nonlinearly-separable patterns. With these encouraging results, we explored next the problem of classifying doublet/singlet patterns which fell outside the ranges of characteristics of those included in the training set. A comparison with the results of similar studies by Sybrandt and Perone (*12*) was made. The results are summarized in Table VI, where the superiority of the KNN method appears obvious. It should be emphasized that exactly the same data base was used here as for the previous studies (*12*).

Consensus Vote Technique. An alternate technique to conventional KNN analyses is to take the consensus vote of the class types assigned when the M best features are used individually on a 1-dimensional basis. The consensus vote of various combinations of these features may also be taken. The advantages offered are: 1) Since patterns are used on a 1-dimensional basis, autoscaling is unnecessary. 2) Features are allowed to work independently of the others in assigning class types to prediction set patterns. 3) Since computation time is greatly reduced in comparison with conventional Z-dimensional KNN analysis, many different combinations of features may be tried in a much shorter time. One major drawback to the technique derives from the fact that all features have equal votes in deciding

Table VII. Classification Results for SEP Data Using Consensus Vote Method (K = 1). Percent Correct Classification

Features	% 1-comp	% 2-comp	Total %
2, 4, 6	95.3	94.7	94.9
2, 4, 8	93.0	95.5	94.7
2, 4, 26	94.7	96.2	95.7
2, 4, 28	94.0	96.3	95.6
2, 6, 8	94.7	92.8	93.4
2, 6, 26	93.7	96.8	95.8
2, 6, 28	93.7	96.2	95.3
2, 8, 26	92.7	97.5	95.9
2, 8, 28	92.7	97.0	95.6
2, 26, 28	91.7	99.0	96.6
4, 6, 8	95.7	92.0	93.2
4, 6, 26	95.0	96.0	95.7
4, 6, 28	93.7	94.8	94.4
4, 8, 26	93.0	97.2	95.8
4, 8, 28	91.7	96.2	94.7
4, 26, 28	91.0	99.2	96.4
6, 8, 26	93.0	94.2	93.8
6, 8, 28	93.0	93.7	93.4
6, 26, 28	90.3	98.0	95.4
8, 26, 28	90.3	98.2	95.6

Table VIII. Classification Results for SEP Data Using Consensus Vote Method (K = 1). Percent Correct Classification for 10 Best Combinations

Features	% 1-comp	% 2-comp	Total %
2, 4, 21, 26, 64	97.0	99.0	98.3
2, 4, 26, 28, 64	97.0	99.0	98.3
2, 6, 21, 26, 64	97.7	99.0	98.6
2, 21, 26, 28, 64	96.0	99.3	98.2
4, 6, 21, 26, 64	97.7	98.8	98.4
4, 6, 26, 28, 64	96.7	99.2	98.3
4, 8, 21, 26, 28	97.3	98.7	98.2
4, 8, 21, 26, 64	98.0	98.8	98.6
4, 8, 26, 28, 64	96.3	99.2	98.2
4, 21, 26, 28, 64	97.0	99.2	98.4

the class types to be assigned to prediction patterns. Correct feature selection becomes much more important. For example, prediction results would be much poorer for the consensus vote technique than for the conventional KNN analysis, if 3 features were used, 2 of which classify only one class-type correctly and one of which classifies all classes equally well.

Initial results for the SEP data using the consensus vote technique are very good (Table VII). It should be noted that the results are slightly poorer than those obtained using the conventional Z-dimensional KNN analysis (Table IV.). However, it should be pointed out that it is much less demanding of computer time to impose trial-and-error methods to find the best Z of M features. Thus, Table VIII was included to show results of one such study. Note that the results were again much better than the LM results obtained previously (*12*) and were not significantly different than those obtained using conventional KNN analysis (Table IV).

Feature Selection Applied to KNN Analysis of Archaeological Data. Results lending support to the feature selection method were obtained with the archaeological data donated by B. R. Kowalski. The data set was derived from measurements taken on archaeological (obsidian) artifacts (*26*). There were 45 training set patterns (9 class-1, 7 class-2, 8 class-3, and 21 class-4 patterns) and 30 prediction set patterns (5 class-1, 5 class-2, 20 class-3). Patterns consisted of 10 features each. A correlation matrix for these features is included in Table IX.

From examination of the histogram plots and the one-dimensional KNN classification results (Figures 4 and 5 and Table X), 6 of the original 10 features were selected (M = 6). Patterns were autoscaled and KNN analysis was carried out using all possible combinations of three of the six features (Z = 3). The results in Table XI show that 5 different combinations each yield 96.7% correct classification, the same results as when all 10 of the original features were used (*26*). In other words, a reduction in dimensionality did *not* degrade classification results. In fact, two different combinations each yielded 100% correct classification; also, a separate study using combinations of 2 of the original 10 features gave 100% correct prediction for 2 different combinations of features (see below). Moreover, the computational requirements are considerably diminished, and the reliability of the classification results are improved with the lowered dimensionality.

All 10 of the features had histograms which showed direct correlations with the one-dimensional KNN results in Table X. As can be seen from the table, no single feature gave good results for all 3 classes in the prediction set pat-

Table IX. Correlation Matrix of Archaeological Training Set Patterns

Feature No.	1	2	3	4	5	6	7	8	9	10
1	1.00									
2	.71	1.00								
3	.96	.70	1.00							
4	.86	.33	.77	1.00						
5	−.88	−.76	−.87	−.61	1.00					
6	.92	.49	.87	.90	−.81	1.00				
7	−.78	−.49	−.81	−.62	.89	−.80	1.00			
8	.52	.36	.51	.39	−.44	.39	−.30	1.00		
9	−.45	−.46	−.48	−.26	.47	−.46	.32	.25	1.00	
10	.83	.31	.75	.87	−.71	.94	−.68	.33	.45	1.00

Table X. One-Dimensional Prediction Results for $K = 1$ (Unautoscaled Archaeological Data). Percent Correct Classification

Feature[a]	Total %	% Class 1	% Class 2	% Class 3
1	70.0	60.0	20.0	85.0
2	73.3	0.0	40.0	100.0
3	83.3	0.0	100.0	100.0
4	76.7	0.0	60.0	100.0
5	66.7	80.0	0.0	80.0
6	43.3	40.0	0.0	55.0
7	36.7	20.0	20.0	45.0
8	43.3	40.0	100.0	30.0
9	16.7	20.0	0.0	20.0
10	60.0	80.0	100.0	45.0

[a] For definition of features see Ref. 26.

Table XI. KNN Classification Results for Combinations of Features (Archaeological Data; Patterns Autoscaled; $K = 1$), Percent Correct

Features[a]	% Class-1	% Class-2	% Class-3	Total %
1, 2, 3	60.0	100.0	100.0	93.3
1, 2, 5	60.0	40.0	100.0	83.3
1, 2, 8	60.0	40.0	100.0	83.3
1, 2, 10	60.0	80.0	100.0	90.0
1, 3, 5	100.0	100.0	100.0	100.0
1, 3, 8	80.0	100.0	100.0	96.7
1, 3, 10	100.0	100.0	100.0	100.0
1, 5, 8	60.0	40.0	100.0	83.3
1, 5, 10	60.0	100.0	100.0	93.3
1, 8, 10	60.0	100.0	100.0	93.3
2, 3, 5	60.0	100.0	100.0	93.3
2, 3, 8	40.0	100.0	100.0	90.0
2, 3, 10	60.0	100.0	100.0	93.3
2, 5, 8	60.0	40.0	100.0	83.3
2, 5, 10	60.0	80.0	100.0	90.0
2, 8, 10	60.0	80.0	100.0	90.0
3, 5, 8	80.0	100.0	100.0	96.7
3, 5, 10	80.0	100.0	100.0	96.7
3, 8, 10	80.0	100.0	100.0	96.7
5, 8, 10	80.0	100.0	100.0	96.7

[a] For definition of features see Ref. 26.

terns. Instead, some features classified members of class 2 with a great deal of accuracy, but failed to classify other patterns correctly. Other features gave good results for class 3, but not class 1 or 2, etc. Examination of the histograms of training set patterns showed, in every case, some region where one class was clustered which could be directly correlated to the classification accuracy for *that* class using *that* feature in a one-dimensional KNN analysis. Classification results for the other overlapped classes could not be correlated directly with the histograms. The poor prediction results obtained with features No. 6, 7, and 9 was evident from the severe class overlap shown by the histogram plots.

Straightforward interpretation of histograms of the archaeological data was not always possible. That is, since the training patterns were comprised of 4 different class-types, the degree of overlap between classes made the histograms much more difficult to interpret (see Figure 5). On the other hand, inspection of histograms for several features might indicate which features should provide good two-dimensional classification accuracy. For example, close examination of the histograms for features 3 and 1 (see Figures 4 and 5) indicate that the 2 features used in combination might give excellent classification. Feature 3 separates class 2 from class 3, and both from classes 1 and 4. Feature 1 would serve to separate class 4 from all others. A 2-dimensional plot of features 3 and 1 for the training set according to class-type indicates the class separation achieved (see Figure 6), and 00% correct classification of the prediction set is obtained. It should be noted, however, that the two-dimensional plots of training set features can be misleading. For example, two-dimensional plots using features 1 and 2 (see Figure 7) and features 3 and 10 (see Figure 8) both show degrees of class separation similar to that for features 3 and 1 (Figure 6). Classification results for the prediction set using these features, however, were 83.3 and 100.0% correct, respectively. Thus, although one- or two-dimensional plots of training set features may indicate very good inter-class separation, classification results may be less than anticipated if the prediction set has a different distribution than that of the training set. The converse may also be true.

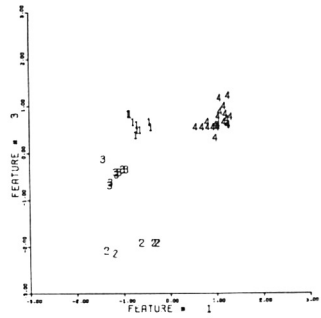


Figure 6. Two-dimensional plot of archaeological training set features No. 3 and No. 1. 100% correct classification of prediction set was achieved using these 2 features. Numbers plotted refer to known categories

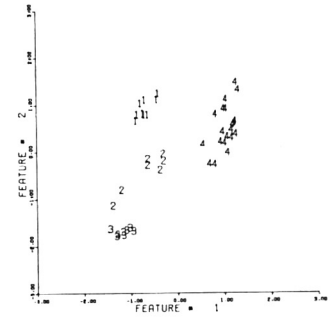


Figure 7. Two-dimensional plot of archaeological training set features No. 1 and No. 2. 83.3% correct classification of prediction set was achieved using these 2 features. Numbers plotted refer to known categories

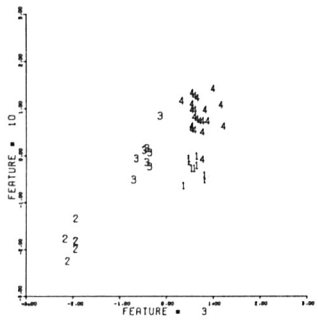


Figure 8. Two-dimensional plot of archaeological training set features No. 3 and No. 10. 100% correct classification of prediction set was achieved using these 2 features. Numbers plotted refer to known categories

Results of the consensus vote method obtained with the archaeological data were less than satisfactory. Much of the problem is that no one feature is able to classify all classes with a relatively high accuracy. Thus, the patterns classed incorrectly with one feature serve to completely cancel the vote of another feature which classifies them correctly. It may be possible to circumvent this difficulty by using one feature to classify members of one class and another to classify patterns of other classes.

CONCLUSIONS

One obvious limitation of the procedure described here is the implicit assumption that one-dimensional classification performance is a valid criterion for feature selection. It does appear intuitively correct to assume that the combined use of *good* "one-dimensional" features in a multidimensional classification procedure would yield high accuracy. However, this does not preclude the possibility that selected combinations of *poor* "one-dimensional" features might provide accurate multidimensional classifications. In fact, this was illustrated here for the archaeological data set.

One interesting possibility arising from the work reported here is a more confident identification of experimental measurements related to desired information. When these features can be reduced reliably to two or three dimensions, the possibility of direct graphical displays and visual classifications of experimental data becomes feasible.

The results of studies with the consensus vote technique indicate that it is useful for binary classification, although not readily applicable to multiclass problems. However, because of the computational simplicity allowed, it should prove useful for appropriate problems.

Both the results with SEP data and with the archaeological data support the use of the methods proposed here for feature selection. It has been shown possible to identify useful features by looking at histograms of training set patterns and/or by comparing tabulated one-dimensional KNN results. Moreover, the methods described here provide an alternative to transform methods for dimensionality reduction as described elsewhere (*29*). Most importantly, the work reported here illustrates the usefulness of operator-interactive computer methods for optimizing pattern recognition procedures using the KNN technique.

ACKNOWLEDGMENT

The authors express their appreciation to B. R. Kowalski, for donating the archaeological data set used in this work, and to F. G. Pater, Jr., who was largely responsible for development of the computer systems used here. The helpful suggestions of S. N. Deming are also gratefully acknowledged.

RECEIVED for review March 4, 1974. Accepted July 1, 1974. This work supported in part by the National Science Foundation under NSF Grant GP-21111, and by the Office of Naval Research under Contract Number N00014-67-A-0026-0021.

(29) B. R. Kowalski and C. F. Bender, *Anal. Chem.*, **45**, 2234 (1973).

Hadamard Transformed Carbon-13 Nuclear Magnetic Resonance Spectra—Pattern Recognition Analysis

Thomas R. Brunner, Robert C. Williams, Charles L, Wilkins,[1] and Patrick J. McCombie

Department of Chemistry, University of Nebraska—Lincoln, Lincoln, Neb. 68508

Carbon-13 nuclear magnetic resonance spectra represented either in binary coded (presence or absence of peaks) or relative intensity form have been subjected to Hadamard Transform processing. Results of linear discriminant function analysis of both Hadamard sequency ordered carbon-13 spectra and Hadamard energy spectra are described. These results are compared to those obtained in a previous study in which Hadamard preprocessing was not used. It is shown that learning machine analysis of the Hadamard domain data is, in general, less efficacious.

Recently, we reported (*1*) the first application of the heuristic pattern recognition method called the "learning machine" (*2*) approach to the analysis of experimental proton noise-decoupled ^{13}C high resolution nuclear magnetic resonance spectra. We found that the general applicability of

[1] Author to whom requests for reprints should be sent.

(1) C. L. Wilkins, R. C. Williams, T. R. Brunner, and P. J. McCombie, *J. Amer. Chem. Soc.*, **96**, 4182 (1974).
(2) N. J. Nilsson, "Learning Machines," McGraw-Hill, New York, N.Y., 1965.

pattern recognition analysis suggested by earlier workers (*3–5*) was further verified for carbon NMR analysis. In particular, we showed that for simple structural analysis questions, the application of this method to ^{13}C spectra was comparable in efficacy to mass spectral and infrared data interpreted in the same way.

Prompted by the observation (*6*) that ^{13}C chemical shifts are enormously sensitive to structural changes, we have begun research directed toward the development of rapid computer-assisted means of interpreting such data. The widespread availability of computer controlled NMR spectrometers for the routine determination of natural abundance ^{13}C NMR spectra makes it highly desirable that such interpretation methods be developed.

In this paper, we report the very first application of Hadamard Transform preprocessing to NMR spectral analysis and compare the results to those obtained in the previous study of linear discriminant analysis of ^{13}C NMR spectra *via* the learning machine method (*1*).

EXPERIMENTAL

Data Base. A recently-published collection of ^{13}C NMR spectra, containing a total of 500 spectra measured on two different instruments and in eight different spectral solvents (*7*) provided the original data. Chemical shifts were referenced to tetramethylsilane and covered a range of about 200 ppm. Eighty of the spectra were obtained in the continuous wave mode and the remainder in the Fourier transform mode. All were proton noise-decoupled. Intensities were digitized manually and added to the original structure-coded, peak frequency list contained in Johnson and Jankowski's collection(*7*).

Computation Method. Binary pattern classification using an error correction feedback method (*5*) and a combination of preprocessing methods was employed to analyze the coded spectral data. Programs were written in FORTRAN IV using algorithms described elsewhere (*1, 8*) or below, and all computations carried out using an IBM 360/65 computer.

Data Representation. The ^{13}C NMR spectra were represented as points in pattern space and hyperplanes (linear discriminant functions) which separated them into binary subsets were found. Typical sets separated by such decision surfaces were the spectra of organic acids and those of all other compounds in the set, or spectra of alcohols and those of the remaining compounds. Categorization was carried out in the general way described previously (*1*) using data in 257 or 130 dimensional hyperspace where the 256 or 129 spectral information elements (*vide infra*) have been augmented by one for computational purposes (*9*). Each spectrum used in the present study was divided in 200 one-ppm resolution elements and, within each interval, the intensities of all peaks appearing were summed. The largest peak appearing in each spectrum was assigned the intensity value 100 and the remaining peaks were assigned intensities relative to that and coded in 1% intervals. Further, each spectrum was then normalized so that the *total* of all peak intensities was 100. Peaks appearing above tetramethylsilane or below 200 ppm were arbitrarily assigned to the nearest interval (*i.e.*, the first or the last resolution element). For peak-no peak ("binary") coding, an integer equal to the number of peaks appearing in each of the respective intervals was used, instead of intensities. These data, subsequently referred to as the *normalized absolute intensity* (NAI) and the *peak-no peak* (PNP) data, were then subjected to Hadamard Transform preprocessing as described below to yield data sets containing either 256 elements per spectrum (Hadamard sequency ordered) or 129 elements per spectrum (Hadamard sequency energy spectra). Error correction feedback training was then applied to the augmented data using 400 transformed spectra in each case for the training set and the remaining 100 spectra for an "unknown" test set.

FEATURE ELIMINATION

Two, admittedly arbitrary, procedures were used to reduce the dimensionality of the problem. For Hadamard sequency (HS) spectra, the effect of using only the positive (HSP) or negative (HSN) data values, followed by further feature elimination based on results obtained from different weight vector initializations was explored. Thus, final weight vectors produced by the ECF analysis resulting from either a +1 or a −1 initialization were compared and those features whose weights changed sign were discarded. This process was repeated iteratively until no further elimination occurred. For the Hadamard sequency energy spectra, only the weight initialization-based feature elimination technique was used. As expected, in most cases reduction of the number of features used improved the predictive ability of the resulting discriminant functions (*10*).

THE HADAMARD TRANSFORM

A generalized approach to fast transform spectral analysis, which included the Hadamard transform as a special case, was developed by Andrews and Caspari in 1970 (*11*). These workers carefully drew the analogies between Fourier transform methods and various others. Subsequently, others published similar analyses (*12*). Kowalski and Bender introduced the use of the Hadamard Transform preprocessing method as a means of improving interpretation of mass spectral data by pattern recognition analysis (*13*). They found a definite improvement in the ability of classifiers to predict carbon number for the data set examined when the data were represented in the Hadamard domain, rather than in the original mass domain. These results encouraged us to carry out the study reported here, transforming chemical shift (frequency) domain ^{13}C NMR to the Hadamard domain for subsequent learning machine analysis. Briefly, a normal Hadamard matrix may be generated recursively by the following algorithm

$$[H(n+1)] = \begin{bmatrix} H(n) & H(n) \\ H(n) & -H(n) \end{bmatrix} \quad (1)$$

$$[H(0)] = [1] \quad (2)$$

where n is an integer power of 2. Since this is simply a Kronecker multiplication, we will call this the Kronecker normal form. (Although Hadamard matrices other than Kronecker and sequency ordered exist, these are the only types with which we are concerned in the present work.) If a waveform is sampled at n discrete equal intervals, the resultant measurement vector, $\mathbf{X}_n$, can be transformed to the Hadamard domain

$$\mathbf{Y} = [H(n)]\mathbf{X}_n \quad (3)$$

an appropriate scaling factor ($1/2^n$) may be included, but is more conveniently included if the inverse transform is used to recover the original waveform. This procedure

$$\mathbf{X} = \frac{1}{2^n}[H(n)]Y \quad (4)$$

avoids round-off or truncation errors, which prevent recov-

(3) P. C. Jurs, B. R. Kowalski, and T. L. Isenhour, *Anal. Chem.*, **41**, 21 (1969).
(4) B. R. Kowalski and C. F. Bender, *J. Amer. Chem. Soc.*, **94**, 5632 (1972).
(5) T. L. Isenhour and P. C. Jurs, *Anal. Chem.*, **43** (10), 20A (1971).
(6) H. J. Reich, M. Jautelat, M. T. Messe, F. J. Weigert, and J. D. Roberts, *J. Amer. Chem. Soc.*, **91**, 7445 (1969).
(7) L. F. Johnson and W. C. Jankowski, "Carbon-13 NMR Spectra," John Wiley and Sons, New York, N.Y., 1972. The computer-readable spectral data were used with permission of the authors and publisher.
(8) R. C. Williams, R. M. Swanson, and C. L. Wilkins, *Anal. Chem.*, **46**, 1803 (1974).
(9) L. E. Wangen, N. M. Frew, and T. L. Isenhour, *Anal. Chem.*, **43**, 845 (1971).
(10) D. N. Anderson and T. L. Isenhour, *Pattern Recog.*, **5**, 2334 (1973).
(11) H. C. Andrews and K. L. Caspari, *IEEE Trans. Comput.*, **19**, 16 (1970).
(12) N. Ahmed, K. R. Rao, and A. L. Abdussattar, *IEEE Trans. Audio Electroacoustics*, **19**, 225 (1971).
(13) B. R. Kowalski and C. F. Bender, *Anal. Chem.*, **45**, 2234 (1973).

ery of the original data if the scaling is carried out when applying Equation 3, rather than when Equation 4 is used, as indicated. If a straightforward matrix multiplication is to be used only a *rearranged form* of the Hadamard matrix generated *via* Equation 1 can result in a *sequency ordered* (by increasing number of zero crossings) (*13*) Hadamard domain data representation. In this case, the transforming matrix is rearranged to sequency order. This may be stored in memory and multiplied by measurement vectors to form the desired data representation. In the present case, 200 spectral resolution elements were augmented by 56 zero valued elements in the frequency domain to yield data vectors of 256 (2^8) elements. Clearly, storage of a 256 × 256 matrix would require excessive computer memory, particularly since minicomputer data processing is planned.

An alternate approach is to compute the sequency ordered matrix an element at a time, as required, using the relations,

$$H(k,j) = \prod_{r=0}^{n-1} (-1)^{(k_{n-r} + k_{n-r-1})j_r} \quad (5)$$

where

$$j = \sum_{r=0}^{n-1} j_r 2^r \quad (6)$$

and

$$k = \sum_{r=0}^{n-1} k_r 2^r.$$

i.e., j_r and k_r are the binary digits of j and k (*14, 15*). Unfortunately, this method requires $\simeq (2^n)^2$ operations whereas a fast Hadamard Transform (FHT), utilizing matrix factorization would use about $2^n \log 2^n$ operations, which is far more efficient.

A method yielding equivalent results is to rearrange the data vector either before or after transformation with a Kronecker normal Hadamard matrix *via* a Fast Hadamard Transform (FHT) algorithm (*16*) adopted from the well-known Cooley–Tukey (*17*) algorithm used for Fast Fourier Transforms (FFT). This technique was chosen because parallel studies of FFT pre-processing were under way and a closely comparable algorithm was desired. If this method is used, it is possible to generate the required transform without storing the matrix elements. Caution must be used in the rearrangement step employed with the FHT since, contrary to Dromey's claim (*16*), the published procedure does not yield a sequency ordered spectrum. To circumvent this, we have developed an appropriate re-ordering algorithm (*8*) which permits either pre- or post-transform reordering of the data vector so that sequency ordered Hadamard domain representations can be obtained from the Kronecker normal form. That procedure was used to transform the two 500 spectra data sets used in the present study.

HADAMARD SEQUENCY ENERGY SPECTRA

As Kowalski and Bender (*13*) note, the Hadamard Sequency Energy Spectrum (HSES) can be generated from the Hadamard sequency spectrum by a simple procedure. The elements of the HSES are defined as

$$P(0) = [Y(\text{cal}, 0)]^2 \quad (7)$$

$$P(i) = [Y(\text{sal}, i)]^2 + [Y(\text{cal}, i)]^2 \quad (8)$$

where

$$0 < i < 2^n/2 \quad (9)$$

and

$$P(2^n/2) = [Y(\text{sal}, 2^n/2]^2 \quad (10)$$

It is therefore clear that the even elements (cal) and the odd elements (sal) bear an obvious analogy to the cos and sin terms of the more familiar Fourier analysis. The second and third elements of the Hadamard sequency spectrum are Y(sal,1) and Y(cal,1). Application of Equations 7–10 yields HSES with $2^n/2 + 1$ elements.

RESULTS AND DISCUSSION

One of the conclusions of our initial study of ^{13}C NMR data pre-processing was that there is no obviously superior pre-processing technique (*1*). In fact, those results suggest that different methods may be optimal, depending on the structrual questions asked. Thus, it was of interest to examine the Hadamard domain representation to determine whether this kind of pre-processing might offer advantages in some, or all, cases. Since the Hadamard transform results in a spreading or "mixing" of the information throughout the data vector (similar to the Fourier frequency to time domain conversion), we reasoned that it might allow significant feature elimination without severe degradation of predictive ability. The success of Kowalski and Bender (*13*) in this regard encouraged us, even though they used a different pattern recognition approach. Accordingly, we explored a number of structural questions using both Hadamard sequency spectra and Hadamard sequency energy spectra as training and test sets *via* a linear learning machine analysis (*2*). The results are summarized in Tables I and II.

Hadamard Sequency (HS) Spectra Results. Two modes of feature elimination were examined for each of the data sets (PNP or NAI). In the first method, the appropriate HS spectra were simply analyzed as described above, discarding features as indicated by the weight intialization elimination procedure. The second technique was to first eliminate all components of the HS spectra which had negative intensities. Subsequently, further feature elimination on these truncated data sets (HSP) was carried out using the first method. For selected examples, a *third* method (elimination of all positive intensity peaks) was also examined. These results which are not included in the Tables did not differ substantially from these obtained for method 2 (HSP). For nearly all the functional group questions, irrespective of which data set was used, the first method (weight initialization elimination) yielded significantly fewer features for the final weight vectors. Predictive abilities of the vectors obtained for both elimination schemes were comparable. Only for phenyl and alcohol did the HSP method give better results.

Clearly, the first feature elimination technique is superior for these data. It should be noted that, in many of the cases, feature elimination resulted in a *degradation of predictive ability* of the classifiers and (often) an increase in the number of feedbacks required for training.

Turning attention to which of the initial data sets was more useful, we observe that PNP data when converted to HS generally result in fewer features and equal or better predictive ability than NAI data treated in the same way. Thus, it appears that if Hadamard domain data are to be used with a linear learning machine analysis of the kind described here, FHT of PNP data represents the best initial

(14) W. K. Pratt, J. Kane, and H. C. Andrews, *Proc. IEEE*, **57**, 58 (1969).
(15) C. H. Chen, "Statistical Pattern Recognition," Hayden Book Co., Rochelle Park, N.J., 1973, pp 44–45.
(16) R. G. Dromey, *Decuscope*, **12** (3), 5 (1973); Digital Equipment Corp., Maynard, Mass.
(17) J. W. Cooley and J. W. Tukey, *Math. Comput.*, **19**, 297 (1965).

Table I. Error Correction Feedback Training for Functional Group Identification from Hadamard Domain ^{13}C NMR Peak-No Peak (PNP) Spectra

Functional group[a]	Pre-processing method	Initial results[b,c] Number of feedbacks +/-	Initial results[b,c] % Correct unknown set +/-	After iterative feature elimination[d] Features retained	After iterative feature elimination[d] Number of feedbacks +/-	After iterative feature elimination[d] % Correct unknown set +/-
Aldehyde and ketone	HS[e]	92/30	100/100	39	110/23	98/99
	HSP[f]	72/34	98/97	78	27/30	98/99
Aliphatic alcohol	HS	941/338	78/91	92	679/598	81/80
	HSP	406/386	90/92	119	276/285	88/84
Carbonyl (any C=O)	HS	536/393	78/76	90	576/442	76/74
	HSP	562/472	70/75	97	450/328	79/79
Carboxylic acid	HS	138/112	92/97	60	375/185	91/90
	HSP	166/130	92/95	97	104/124	91/92
Alkyl bromide	HS	163/194	93/95	50	273/121	96/97
	HSP	169/160	96/95	89	100/168	95/93
Alkyl chloride	HS	106/101	98/98	52	156/78	100/99
	HSP	141/122	96/100	106	79/109	98/98
Phenyl	HS	868/817	70/71	106	1297/871	66/68
	HSP	478/394	77/78	114	409/318	76/72

[a] Total set of spectra is 500 (see experimental); number of spectra containing each of these functional groups are 29, 78, 167, 31, 18, 14, and 130, respectively. [b] Using 400 spectra in the training set; the remaining spectra comprise the unknown set. [c] + designates results from a weight vector initialized to all ones; − designates results from a weight vector initialized to all minus ones. [d] After successively eliminating features whose final weight vectors have different algebraic signs for +/− initialization. [e] Hadamard sequency ordered spectrum; 256 features initially. [f] Hadamard sequency ordered spectrum, positive values only; negative values set to zero; 256 total features; number of nonzero features varies.

Table II. Error Correction Feedback Training for Functional Group Identification from Hadamard Domain ^{13}C NMR Normalized Intensity (NAI) Spectra[a]

Functional group	Pre-processing method	Initial results Number of feedbacks +/-	Initial results % Correct unknown set +/-	After iterative feature elimination Features retained	After iterative feature elimination Number of feedbacks +/-	After iterative feature elimination % Correct unknown set +/-
Aldehyde and ketone	HS	288/151	88/92	63	260/143	94/92
	HSP	164/106	96/93	108	104/92	96/93
Aliphatic alcohol	HS	1829/...[b]	76/69	...	...	...
	HSP	697/796	90/92	138	537/669	92/90
Carbonyl (any C=O)	HS	2079/...[b]	72/58	...	...	...
	HSP	2023/1933	61/68	159	1732/1653	58/61
Carboxylic acid	HS	319/196	94/95	69	325/130	90/91
	HSP	272/203	88/89	107	137/191	90/91
Alkyl bromide	HS	439/205	91/97	66	405/228	96/95
	HSP	206/280	96/95	121	126/212	97/99
Alkyl chloride	HS	220/130	95/100	64	.../...[b]	98/91
	HSP	213/140	97/100	100	82/109	98/99
Phenyl	HS	977/...[b]	74/77	...	...	...
	HSP	386/305	77/83	104	286/229	85/82

[a] See Table I for an explanation of the notation. [b] Perfect performance in the training set did not occur within 3000 feedbacks, or nonconvergence detected; feature elimination was not attempted if the initial set did not converge.

choice for development of new discriminant functions. This buttresses the intuitive suggestion that chemical shift information is, by far, of dominant importance for answering questions of the kind posed here.

Hadamard Sequency Energy Spectra (HSES) Results. When either the NAI and PNP data sets were converted to Hadamard Sequency Energy Spectra and then used to develop linear discriminant functions for the structural questions, the results [in contrast to the previous mass spectral analysis (*13*)] were uniformly unsatisfactory. Complete training was achieved in only two of the fourteen cases and, in those, over 1000 error correction feedbacks were required. Thus, feature elimination using the positive and negative initialization procedure was usually not possible. Even in the two cases (carboxylic acid and alkyl chloride NAI data) where feature elimination was possible, relatively few (24 of 129 and 68 of 129) features were eliminated. Predictive ability of the incompletely trained weight vectors developed for HSES data was either comparable to or, in most cases, significantly worse than those obtained

Table III. Comparison of Binary (PNP) Coded ^{13}C NMR Data Pre-processing Methods for Functional Group Identification

	No pre-processing			Hadamard Sequency Spectral Pre-processing		
Functional group	Average number of feedbacks[a]	Features retained	Av. % Correct, unknown set[a]	Average number of feedbacks[a]	Features retained	Av. % Correct, unknown set[a]
Aldehyde and ketone	21	17	100	67	39	99
Aliphatic alcohol	383	100	90	639	92	81
Carbonyl (any C=O)	236	81	81	509	90	75
Carboxylic acid	...[b]	88	95	280	60	91
Alkyl bromide	...[b]	96	93	197	50	97
Alkyl chloride	...[b]	92	95	117	52	100
Phenyl	443	86	78	1084	106	67

[a] Average of final results using both +1 and −1 initial weighting vectors. [b] Perfect performance in the training set did not occur within 3000 feedbacks, or non-convergence detected.

otherwise. To summarize, the HSES pre-processing mode has little to commend it for ^{13}C NMR data analysis of the kind described here.

Comparison of Hadamard Domain with Frequency Domain Results. Since one of the principal objectives of the research described in this paper is to assess the relative value of Hadamard pre-processing in learning machine analysis of ^{13}C NMR spectra, a comparison of the current results with previous ones is important. Table III contains some of the data appropriate for that comparison. The PNP data which give the most consistently good results throughout the study, show that, for the categorizations attempted, Hadamard sequency spectra are clearly inferior for identification of all but alkyl bromides and chlorides. For the functional groups other than these, HS pre-processing significantly *increases the number of feedbacks required* for training and *decreases the predictive ability* of the classifiers thus developed. The number of features retained either increase or remain about the same for the non-halide functional groups. In contrast, the number of feedbacks required and features retained *decrease* for the alkyl halide questions and the predictive ability increases. It seems clear, that for these structural questions and the present data set, there are cases where Hadamard domain representation can improve the separability of categories. In the majority of cases we examined, however, Hadamard pre-processing did not improve the results, but degraded them.

CONCLUSION

A number of conclusions emerge from this research. First, Hadamard pre-processing when applied to ^{13}C NMR data prior to linear learning machine analysis is of limited utility. For specific questions, it does offer marked improvements. Thus, any general on-line pattern recognition analysis system for ^{13}C NMR data should include this mode of pre-processing as one of the options available to the experimenter. It is equally clear that separability of low information density data such as ^{13}C frequency domain NMR spectra is not generally enhanced by conversion to the Hadamard domain. Further studies of analysis of time domain (free induction decay) ^{13}C NMR data are under way to test the possibility of utilizing spectral data represented in that way to directly deduce structural information.

RECEIVED for review April 29, 1974. Accepted July 8, 1974. Support of this work under Grant GP-41515X from the National Science Foundation is gratefully acknowledged.

Concise Algorithm for Conversion between Normal and Sequency Ordered Hadamard Matrices

Robert C. Williams, Ray M. Swanson, and Charles L. Wilkins[1]

Department of Chemistry, University of Nebraska, Lincoln, Neb. 68508

With increasing frequency, chemists are using pattern recognition as an aid to spectral interpretation (*1–16*). Various techniques of pre-processing spectral data are also of interest, since they often simplify computations and enhance the results (*13–16*). Paramount among these are the Hadamard and Fourier transform approaches, because existing instrumental techniques automatically generate data in the appropriate pre-processed form. The Hadamard transform is less well known than its Fourier analog, but the advantages have been discussed in several recent theoretical papers (*17–21*), and have been experimentally verified for infrared, ultraviolet, and atomic fluorescence spectrometry (*20–22*). Hadamard pre-processing has also been reported to improve the prediction of carbon number in pattern recognition studies of mass spectral data (*13*).

As part of our investigation of pattern recognition analysis of ^{13}C NMR spectra (*1, 2*), we decided to explore the feasibility of Hadamard pre-processing. Experimentally, most Hadamard spectrometers use a cyclic Hadamard matrix. Mathematical calculations are usually performed by permuting the original data, applying a fast Hadamard transform (FHT) algorithm, then re-permuting the computed result. These permutations are necessary because the FHT generates a transform of an alternate Hadamard matrix, rather than that resulting from the cyclic Hadamard matrix; the matrices are equivalent, but the transformation from one to the other is non-trivial (*17*).

For pattern recognition studies, it is most convenient to use yet another equivalent form of the Hadamard matrix, which generates a *sequency-ordered* transform. The appropriate Hadamard matrix is, in this case, a rearranged Kronecker normal form, with the rows re-ordered by increasing *level crossings* or changes of sign.

i.e., Kronecker Normal Hadamard Matrix

$$[H(3)] = \begin{bmatrix} 1 & 1 & 1 & 1 & 1 & 1 & 1 & 1 \\ 1 & -1 & 1 & -1 & 1 & -1 & 1 & -1 \\ 1 & 1 & -1 & -1 & 1 & 1 & -1 & -1 \\ 1 & -1 & -1 & 1 & 1 & -1 & -1 & 1 \\ 1 & 1 & 1 & 1 & -1 & -1 & -1 & -1 \\ 1 & -1 & 1 & -1 & -1 & 1 & -1 & 1 \\ 1 & 1 & -1 & -1 & -1 & -1 & 1 & 1 \\ 1 & -1 & -1 & 1 & -1 & 1 & 1 & -1 \end{bmatrix} \quad (1)$$

Sequency-Order Hadamard Matrix

$$[H(3)] = \begin{bmatrix} 1 & 1 & 1 & 1 & 1 & 1 & 1 & 1 \\ 1 & 1 & 1 & 1 & -1 & -1 & -1 & -1 \\ 1 & 1 & -1 & -1 & -1 & -1 & 1 & 1 \\ 1 & 1 & -1 & -1 & 1 & 1 & -1 & -1 \\ 1 & -1 & -1 & 1 & 1 & -1 & -1 & 1 \\ 1 & -1 & -1 & 1 & -1 & 1 & 1 & -1 \\ 1 & -1 & 1 & -1 & -1 & 1 & -1 & 1 \\ 1 & -1 & 1 & -1 & 1 & -1 & 1 & -1 \end{bmatrix} \quad (2)$$

The results are then similar to the Fourier transform analog, where the transform converts time domain data into a frequency ordered sequence. Algorithms exist for generating the complete sequency ordered Hadamard matrix (*23*), but are prohibitively slow for large matrices. Algorithms which generate sequency ordered transforms also exist (*24–26*); however, our search of the chemical literature failed to yield a permutation algorithm similar to the cyclic case, which would allow us to convert between Kronecker normal and sequency ordered Hadamard matrices. [The

[1] Author to whom requests for reprints should be sent.

(1) T. R. Brunner, R. C. Williams, C. L. Wilkins, and P. J. McCombie, *Anal. Chem.*, **46**, 1798 (1974).
(2) C. L. Wilkins, R. C. Williams, T. R. Brunner, and P. J. McCombie, *J. Amer. Chem. Soc.*, **96**, 4182 (1974).
(3) P. C. Jurs, B. R. Kowalski, and T. L. Isenhour, *Anal. Chem.*, **41**, 21 (1969).
(4) B. R. Kowalski and C. F. Bender, *J. Amer. Chem. Soc.*, **94**, 5632 (1972).
(5) B. R. Kowalski and C. F. Bender, *J. Amer. Chem. Soc.*, **96**, 916 (1974).
(6) T. L. Isenhour and P. C. Jurs, *Anal. Chem.*, **43**, (10), 20A (1971).
(7) L. B. Sybrandt and S. P. Perone, *Anal. Chem.*, **44**, 2331 (1972).
(8) J. B. Justice, Jr., D. N. Anderson, T. L. Isenhour, and J. C. Marshall, *Anal. Chem.*, **44**, 2087 (1972).
(9) P. C. Jurs, *Anal. Chem.*, **43**, 22 (1971).
(10) B. R. Kowalski, P. C. Jurs, T. L. Isenhour, and C. N. Reilley, *Anal. Chem.*, **41**, 1949 (1969).
(11) B. R. Kowalski, P. C. Jurs, T. L. Isenhour, and C. N. Reilley, *Anal. Chem.*, **41**, 1945 (1969).
(12) R. W. Liddell III and P. C. Jurs, *Appl. Spectrosc.*, **27**, 371 (1973).
(13) B. R. Kowalski and C. F. Bender, *Anal. Chem.*, **45**, 2234 (1973).
(14) L. E. Wangen, N. M. Frew, T. L. Isenhour, and P. C. Jurs, *Appl. Spectrosc.*, **25**, 203 (1971).
(15) P. C. Jurs, *Anal. Chem.*, **43**, 1812 (1971).
(16) J. B. Justice and T. L. Isenhour, *Anal. Chem.*, **46**, 223 (1974).
(17) E. D. Nelson and M. L. Fredman, *J. Opt. Soc. Amer.*, **60**, 1664 (1970).
(18) N. J. A. Sloane, T. Fine, P. G. Phillips, and M. Harwit, *Appl. Opt.*, **8**, 2103 (1969).
(19) C. J. Eckhart and M. L. Gross, *Int. J. Mass Spectrom. Ion Phys.*, **5**, 223 (1970).
(20) J. A. Decker, Jr., *Appl. Opt.*, **10**, 510 (1971).
(21) J. A. Decker, Jr., *Anal. Chem.*, **44**, (2), 127A (1972).
(22) F. W. Plankey and J. D. Winefordner, Pittsburgh Conference on Analytical Chemistry and Applied Spectroscopy, Cleveland, Ohio, March 1974, paper No. 200.
(23) C. H. Chen, "Statistical Pattern Recognition," Hayden Book Co., Rochelle Park, N.J., 1973, pp 44–50.
(24) H. C. Andrews and K. L. Caspari, *IEEE Trans. Computers*, **19**, 16 (1970).
(25) J. W. Manz, *IEEE Trans. Audio Electroacoustics*, **2D**, 204 (1972).
(26) W. K. Pratt, J. Kane, and H. C. Andrews, *Proc. IEEE*, **57**, 58 (1969).

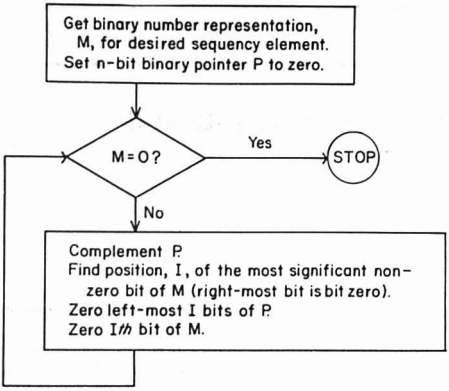


Figure 1. Flow chart for Kronecker normal to sequency-ordered Hadamard permutation algorithm

FHT we used was based on a fast Fourier transform algorithm (27), and generated results in the Kronecker form.] We have therefore derived such an algorithm, and developed a short (25 statement) Fortran program to implement it.

The algorithm consists of a series of bit complements and zeroings, and can be applied to the data vector either before or after application of the Kronecker normal Hadamard transform. It is designed for use with matrices of order $N = 2^n$, whose indices range from zero to 2^n-1, where n is a positive integer. A flow chart for the algorithm is given in Figure 1, but the algorithm is best illustrated by an example. Consider the Hadamard matrix of order 256 (n = 8) whose indices run from 0 to 255. Suppose that we are seeking the sequency order of the data element whose Kronecker normal position is 106; the following procedure allows us to find it. The binary representation (M) of 106_{10} is 01 101 010, and pointer P is set to 00 000 000, then complemented to 11 111 111. The most significant bit of M is the sixth (numbering the right-most bit as *zero*); after zeroing the left-hand six bits, P is 00 000 011, while the remainder in M after zeroing bit six is 00 101 010. Repeating the process for bits 5, 3, and 1 of M yields, P = 00 000 100, 00 011 011, and finally 01 100 100, or decimal 100. Thus, the 106th row of the Kronecker Normal Hadamard matrix contains 100 level crossings; moreover, the 106 element of the data vector produced by the FHT corresponds to a frequency component of 100.

Thus, the algorithm can be used to reorder the Kronecker normal output of the FHT to yield the sequency ordered results. Conversely, if the reverse permutation is applied to the *original* data vector, then the results of the FHT will already be sequency ordered. In this case, the 100th data element would have to be stored in place of the 106th, and the other 255 permutations would also have to be performed. It should be noted that, unlike the Fourier transform analog, it is not possible to reorder in place, as has been erroneously claimed in the literature (27). The permutations involved are not interchanges; the 100th data element corresponds to sequency 59, not sequency 106. In practice, only the even numbered elements need be calculated, since the (I + 1)th odd element is always the N-bit complement of the Ith even element; *e.g.* element 107 corresponds to sequency 155, which is the 8-bit complement (equivalent to Mod 255) of sequency 100.

RECEIVED for review April 29, 1974. Accepted July 8, 1974. Support of this work under Grant GP-41515X from the National Science Foundation is gratefully acknowledged.

(27) R. G. Dromey, "Decuscope," **12** (3), 5 (1973); Digital Equipment Corporation, Maynard, Mass.

Determination of Sulfur by the Measurement of Molecular Emission in Cool Flames: Conversion of Sample Sulfur to Hydrogen Sulfide

S. Shiffman and C. W. Frank

Department of Chemistry, The University of Iowa, Iowa City, Iowa 52242

The fact that the atomic resonance lines of sulfur occur in the vacuum ultraviolet region of the spectrum severely limits the usefulness of atomic absorption spectrometric techniques for the determination of this element. Because of this, a number of researchers have investigated the analytical use of the band emission of sulfur-containing species for sulfur. In particular, the band systems of the diatomic sulfur molecule, S_2, and the CS molecule show the greatest potential for analytical use. Under conditions of low temperature (less than 1000 °C), low oxygen concentration, and in the presence of a low energy species (carrier gas, fuel, or a chilled surface), the predominant band system observed is that of S_2. The CS band system is observed in hotter flames.

The reported analytical use of S_2 band emission has been reviewed by Gilbert (*1*) and Veillon and Park (*2*). A number of difficulties have been noted in these studies. Most of these difficulties are the direct result of the low temperature necessary for the formation of the chemiluminescent S_2 species.

1) Each sulfur-containing compound has a different emissivity. Because of the low temperature of the analytically useful flames, there is a limited amount of energy available for the dissociation of the sulfur in the sample

(1) P. T. Gilbert, in "Analytical Flame Spectroscopy," R. Mavrodineanu, Ed., Springer Verlag, New York, 1970, Chapter 5, pp 181–377.
(2) C. Veillon and J. Y. Park, *Anal. Chim. Acta*, **60**, 293 (1972).

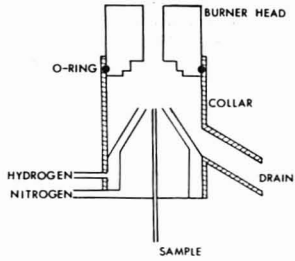


Figure 1. Burner used for N_2/H_2 diffusion flame

molecule. The emissivity is therefore very dependent on the strength with which the sulfur is bound in the molecule. Dagnall *et al.* (*3*) reported the following order of emissive response for sulfur compounds in a sheathed nitrogen-hydrogen diffusion flame:

Sulfide > Sulfite > Thiosulfate ≫ Ammonium Sulfate ≃ Sulfuric Acid ≫ Alkalai-Metal Sulfates

2) There is little S_2 emission from compounds containing carbon–sulfur double bonds or mercaptan groups. Syty and Dean (*4*), studying a shielded air–acetylene flame, reported that in the low temperature flame there apparently is not sufficient energy to break the carbon–sulfur double bond, C=S, or to dissociate the mercaptan group, –C–S–H.

3) In most systems, there is a dependence of the measured intensity of S_2 emission on the square of the sulfur concentration.

4) The presence of an alcohol (or organics) in the sample solvent results in the quenching of the S_2 emission. This quenching is almost total at an alcohol concentration of three per cent in water. In addition, the background emission increases when an alcoholic solvent is used.

5) The evaporation of the solvent and the vaporization of the sample are very inefficient processes under low temperature conditions.

6) Both spectral and chemical interferences are encountered or would be anticipated when metals are present in the sample.

7) The emissive intensity of many compounds is dependent on the hydrogen ion concentration of the sample solution (*3*).

There are two basic methods for overcoming these difficulties. The first is to separate the sulfur-containing species from the matrix and from each other prior to flame photometric determination, as in gas chromatographic measurements using emission as the detection system. This method requires that standards of all of the sulfur-containing species be available so that calibration curves can be prepared. The second method is to convert all of the sulfur in the sample to a single intermediate and to remove this intermediate from the interfering matrix. This is the method that is the subject of this investigation.

The intermediate used in this study is hydrogen sulfide. Hydrogen sulfide has the following properties which cause it to be of interest:

1) It has a high S_2 emissivity.

2) It is a gas at room temperature and is therefore easily removed from the matrix. It also requires no energy for solvent evaporation or sample vaporization.

(3) R. M. Dagnall, K. C. Thompson, and T. S. West, *Analyst, (London)*, **92**, 506 (1967).
(4) A. Syty and J. A. Dean, *Appl. Opt.*, **7**, 1331 (1968).

Table I. Important Properties of the Decomposition Products

$MgBr_2$	Melting point 700 °C
$MgCl_2$	Melting point 708 °C
MgI_2	Decomposes at temperatures over 700 °C
Mg_3N_2	Decomposes at 800 °C
MgO	Melting point 2800 °C
MgS	Decomposes at temperatures over 2000 °C
MgH_2	Decomposes violently in water Decomposes at 280 °C in vacuum
$MgCO_3$	Decomposes at 350 °C
CO_2	Boiling point −78.5 °C

3) There is a linear relationship between S_2 emissive intensity and H_2S flow rate over the range of interest (H_2S flow rate, 0–50 ml/min).

4) The intensity of emission is independent of flame height in the range of interest (flame height between 1.5 and 6.5 cm).

The method chosen for generation of hydrogen sulfide from organic sulfur-containing compounds is that of Terent'ev *et al.* (*5*) involving thermal decomposition of the sample in the presence of magnesium to form magnesium sulfide. Upon acidification, the magnesium sulfide liberates hydrogen sulfide which is then passed through the flame. The reaction is as follows:

Sample (containing C, H, N, O, S, X) + Mg→Products, where X may be Cl, Br, or I

The products of the general reaction are listed in Table I along with their significant properties. If the total sample size does not exceed twenty milligrams, the decomposition can generally be carried out in a sealed glass tube at 600 °C without magnesium hydride forming in sufficient quantity to present difficulty.

The acidification is carried out by the addition of hydrochloric acid.

EXPERIMENTAL

Apparatus. The burner used for the nitrogen–hydrogen diffusion flame, shown in Figure 1, is constructed from a Jarrell-Ash Hetco emission burner to which is attached the collar from the JACO tri-flame burner head. Into this collar is fitted a cylindrical burner head machined from stainless steel.

The sampling apparatus, shown in Figure 2, consists of a device in which the acidification is carried out and a pair of five-liter reservoirs for collection of the evolved gases. Initially, reservoir L is filled with mineral oil which is displaced into reservoir M.

The instrument used for measuring the S_2 emission is a Jarrell-Ash one-half meter monochromator with a reciprocal linear dispersion of 16 Å/mm. The emission was monitored at the 384-nm band head with an effective band width of approximately 3 Å. The high voltage to the 1P28 photomultiplier was supplied by a Super Stable High Voltage Power Supply (Atomic Instrument Co.) and the resultant current measured with a Keithley Model 610 CR electrometer. The signal was recorded with a Sargent SRG recorder equipped with a Disc integrator.

Procedure. The sample, containing approximately three milligrams of sulfur, is placed in a six-inch length of 8-mm o.d. Pyrex tubing which has been sealed at one end. It is then covered with 100 mesh magnesium powder to within one inch of the end of the tube. If, as mentioned previously, the sample size can be kept below twenty milligrams, the tube is then sealed and the sample heated at 600 °C for one hour. If a larger size sample must be used, the tube is left open at one end. The decomposition is then carried out by first preheating the magnesium powder above the sample to 600 °C with a small tube furnace. Subsequently, the sample is

(5) A. P. Terent'ev *et al., Izv. Vyssh. Ucheb. Zaved., Khim. Khim Tekhnol.*, **2**, 54 (1959).

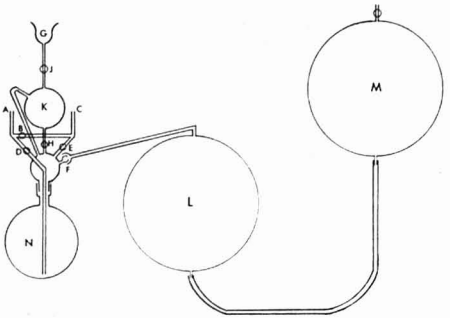


Figure 2. Sampling apparatus for the discontinuous method

(A) Inlet for carrier gas, (B) Stopcock for carrier gas bypass, (C) Outlet to burner, (D) Stopcock to purge sampling cell, (E) Stopcock to outlet and burner, (F) Ball and socket connection to gas reservoir, (G) Funnel for acid addition, (H) Stopcock for acidification of sample (Teflon), (J) Stopcock for filling acid reservoir, (K) Acid reservoir, (L) Gas reservoir, (M) Displacement reservoir, (N) 250-ml round-bottom flask for sample

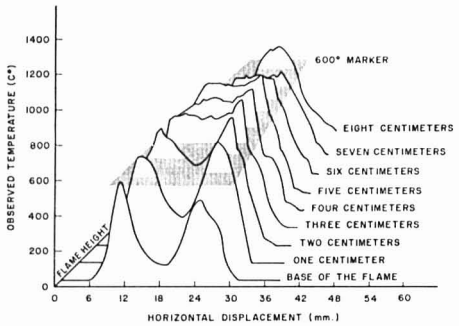


Figure 3. Three-dimensional temperature profile of N_2/ H_2 diffusion flame

slowly vaporized by raising the tube fully into the furnace until the sample completely decomposes.

Once the decomposition is complete, the sample tube is wrapped in a piece of filter paper and crushed and the entire reaction mass is transferred to the 250 ml round bottom flask. The sample is then acidified by the gradual addition of fifty milliliters of concentrated hydrochloric acid. After the evolution of gas has ceased, nitrogen is bubbled through the solution for several seconds to release any trapped hydrogen sulfide. The trapped gases are then allowed to pass through the burner and the resultant emission is monitored at 384 nm. The area under the recorded peak is then integrated to yield the relative amount of sulfur in the sample.

RESULTS

The Diffusion Flame. The three-dimensional temperature profile of the nitrogen–hydrogen diffusion flame is presented in Figure 3. The X axis plots the relative horizontal position in the flame. The Y axis plots the temperature as measured with a chromel-alumel thermocouple. The Z axis locates the height in the flame at which the series of measurements were performed. This profile shows that there is a cool inner core at low flame heights which becomes less significant at greater flame heights as oxygen diffuses into the flame. It can also be seen that the maximum temperature in the flame is in the vicinity of 850 °C, far lower than the temperatures in the commonly used analytical flames.

Table II. Relative Emissivities by Direct Solution Nebulization[a]

Compound	Emissivity
Carbon disulfide	2.4
2-Mercapto ethanol	1.2
Thioacetamide	0.72
Thiourea	0.36
Thiosemicarbazide	0.36
Dimethyl sulfoxide	0.13

[a] Relative emission (measured at 384 nm) per milligram sulfur.

Table III. Analyses of Sulfur-Containing Compounds by the Discontinuous Pretreatment Method

Model compound	Sample size, mg	No. of samples	Relative emissivity
Elemental sulfur	2.4–4.3	4	0.76
Thiourea	10.3–13.8	3	1.00
L-Cystine	11.2–19.7	4	0.93
Thioacetamide	8.5–13.0	6	0.98
Potassium Dithiooxalate	19.1	1	0.75
Thiosemicarbazide	8.0–13.0	5	*a*

[a] Open tube decomposition, run under different experimental conditions.

Direct Solution Sampling. Table II lists the measured emissivities for a number of compounds sampled by direct solution nebulization into the nitrogen–hydrogen diffusion flame. The samples were in aqueous solution at sulfur concentrations of approximately one part per thousand. The range in emissivities, varying by approximately a factor of twenty, is typical for organic compounds sampled by this method.

Magnesium Sulfide Method. Table III lists the results for a series of analyses performed using the pretreatment described previously. Sampling times were between twenty and thirty minutes (excluding the decomposition procedures). Mean deviation of replicate samples were in the range of ±10%. The solubility properties of some of these compounds prevent direct comparison by solution nebulization. The variation of approximately 25% over the range of compounds studied is, however, quite reasonable in light of the results for thioacetamide and thiourea obtained by direct nebulization. These compounds give emissivities differing by a factor of two by direct solution sampling while the results using the magnesium sulfide pretreatment are virtually identical.

CONCLUSIONS

The Diffusion Flame. The nitrogen–hydrogen diffusion flame is a very sensitive device for exciting S_2 emission from organic sulfur-containing compounds. In order to be used as a practical analytical tool, however, a pretreatment step must be employed in conjunction with flame photometric measurements.

The Magnesium Sulfide Method. The conversion of the sulfur in a sample to hydrogen sulfide *via* thermal decomposition in the presence of magnesium, with subsequent acidification, is effective in reducing the dependence of the emissivity on the structure of the sample compound. It also is effective in removing the sulfur from a potentially interfering matrix. It has the additional advantage of using

samples in the solid state, making it useful for samples whose physical properties preclude the use of solution techniques. Considerable handling of the sample is required however, and this is a decided disadvantage. In addition, both the precision and accuracy of the technique are subject to improvement by modification of the experimental procedure and sophistication of the sampling apparatus.

RECEIVED for review February 11, 1974. Accepted June 3, 1974.

New Discrete Atomization Cell for Atomic Fluorescence Spectrometry

C. J. Molnar[1] and J. D. Winefordner[2]

Department of Chemistry, University of Florida, Gainesville, Fla. 32611

Resistively-heated non-flame cells have been operated in either a continuous mode of sampling or a repetitive mode of sampling. However, most atomization systems cannot be operated in both modes without major alterations. Non-flame cells have been extensively reviewed by Winefordner (*1*), Kirkbright (*2*), and Winefordner and Vickers (*3, 4*). Woodriff and coworkers (*5–7*) have used their non-flame (cell) tube furnace in both the continuous mode with a pneumatic nebulizer and in the discrete mode by disconnecting the nebulizer and placing microliter samples in the furnace with a syringe or solids in a suitable holder in the furnace.

Each mode of operation has certain strengths and weaknesses. For instance, sampling in the continuous mode gives the analyst a steady-state signal with the advantage that long integration times may be employed to reduce the system noise. The pulsed (discrete) mode with its concomitant transient signal requires short time constants, but often such a system results in an increase in the observed atomic concentration of analyte and consequently in a decrease of absolute limits of detection. L'vov (*8*) has reviewed the advantages of each form of sampling.

The previously described vitreous-carbon non-flame tube in which the continuous mode of sampling was utilized has been slightly altered to allow the use of pulsed sampling with the consequent improvement in absolute limits of detection; also no deleterious effects to the linear dynamic ranges have resulted. Additional features of the new system are: the vitreous carbon tube's lifetime is increased markedly; operator error due to sample placement is eliminated; and conversion to the continuous mode by altering only the means of sample injection (about 10 sec) is simple to achieve.

[1] Present address, E. I. DuPont de Nemours & Co., Inc., Wilmington, Del. 19898.
[2] Author to whom reprint requests should be sent.

(1) J. D. Winefordner, in "Atomic Absorption Spectroscopy," Plenary Lectures presented at International Atomic Absorption Spectroscopy Conference, Sheffield, 1964, R. M. Dagnall and G. F. Kirkbright, Ed., Butterworth, London, 1970, p 37.
(2) G. F. Kirkbright, *Analyst (London)*, **96**, 604 (1971).
(3) J. D. Winefordner and T. J. Vickers, *Anal. Chem.*, **44**, 150R (1972).
(4) J. D. Winefordner and T. J. Vickers, *Anal. Chem.*, **46**, in press.
(5) R. Woodriff and R. W. Stone, *Appl. Spectrosc.*, **22**, 408 (1968).
(6) R. Woodriff and R. W. Stone, *Appl. Opt.*, **7**, 1337 (1968).
(7) R. Woodriff and G. W. Ramelov, *Spectrochim. Acta*, **23B**, 665 (1968).
(8) B. V. L'vov, *Pure Appl. Chem.*, **23**, 11 (1970).

EXPERIMENTAL

Nebulizer-Atomizer. The resistively-heated vitreous-carbon tube atomization device is identical to the system previously described (*9*) with two minor modifications; the nebulizer was altered to reduce dead volume in the sample transport needle without affecting the critical nebulization cone, angle, diameter, or sample transport needle dimensions, and the sample is forced into the nebulizer which is operated continuously at 60-lb pressure of Ar from a 0.5-ml syringe (Model 1000, Hamilton Co., Reno, Nev.) contained in a repeating dispenser (Model PB-600, Hamilton Co.).

Atomic Fluorescence Spectrometric System. The optics and electronic measurement systems are identical to the system described previously (*9*).

Single element electrodeless discharge lamps (EDLs) were used in all cases as the sources. All EDLs were prepared from the respective reagent-grade iodide form of the element except for Cd and Zn which were prepared from the pure elements.

The EDLs were operated under thermostated mode conditions as previously described (*10, 11*). The operating conditions (microwave power and temperature) for the EDLs are given in Table I.

Stock solutions were prepared with analytical grade reagents at concentrations of 1000 μg/ml. Serial dilutions were then performed with deionized water.

Procedure. The various gases (nebulization Ar, desolvation CH_4, and the Ar–H_2 diffusion flame sheath) were flowing continuously. The temperatures of the vitreous-carbon tube and desolvation chambers were independently adjusted by varying their respective currents (*9*). The desolvation chamber was adjusted so that the exiting gases attained a temperature of 250 °C. The temperatures of the vitreous carbon tube for each element are listed in Table I. The variation of temperature at the hottest point in the vitreous carbon tube with current is given in Figure 1. The temperatures at analytically-useful heights above the carbon tube with an Ar sheath *and* with an Ar–H_2 diffusion flame sheath are also shown in Figure 1. All temperature measurements were performed with 0.010-in. diameter W-26% Re–W thermocouples (Omega Engineering, Inc., Stamford, Conn.) and a digital multimeter (Model 414, Dynasciences) to monitor the electrical potential differences.

RESULTS AND DISCUSSION

Detection Limits. The limit of detection (LOD) for the present studies was defined as that concentration (in μg/ml or amount (in ng) of analyte resulting in a signal-to-noise (rms) ratio of 3. The concentrational detection limits as well as experimental conditions for Ag, Bi, Cd, Co, Mg, Pb, Sb, Sn, Te, Tl, and Zn are given in Table I. A comparison of limits of detection obtained in atomic fluorescence spec-

(9) C. J. Molnar and J. D. Winefordner, *Anal. Chem.*, submitted.
(10) R. F. Browner, B. M. Patel, T. J. Glenn, M. E. Rietta, and J. D. Winefordner, *Spectrosc. Lett.*, **5**, 311 (1972).
(11) B. M. Patel, R. F. Browner, and J. D. Winefordner, *Anal. Chem.*, **44**, 2272 (1972).

Table I. Experimental Conditions and Analytical Results for Measurement of Several Elements by Means of the Pulsed-Sample Introduction Tube Furnace Atomic Fluorescence Spectrometric System

		EDL conditions		Tube furnace conditions					Results		
Element	Wavelength, nm	Temperature, °C[a]	Power, W[b]	Temperature, °C[c]	Ar flow rate, nebulizer, (L./min)	Ar flow rate, external, L./min[d]	H_2 flow rate, external, L./min[d]	CH_4 flow rate, internal, L./min[e]	LOD[f]	RSD[g]	V, μl[h]
Ag	328.1	540	50	1580	0.66	5.3	0.0	0.014	$4. \times 10^{-4}$	0.028	10
Te	213.9	440	30	1550	0.66	5.3	2.2	0.014	$3. \times 10^{-3}$	0.036	10
Sn	303.4	285	90	1720	0.66	5.3	2.2	0.014	$2. \times 10^{-2}$	0.021	10
Tl	377.6	385	50	1540	0.66	5.3	2.2	0.014	$2. \times 10^{-3}$	0.031	10
Bi	307.7	510	50	1540	0.66	5.3	2.2	0.014	$6. \times 10^{-4}$	0.036	10
Pb	283.3	430	40	1580	0.66	5.3	2.2	0.014	$5. \times 10^{-3}$	0.033	10
Co	240.7	200	100	1860	0.66	5.3	0.0	0.014	$3. \times 10^{-3}$	0.031	10
Sb	231.1	125	100	1650	0.66	5.3	2.2	0.014	$1. \times 10^{-2}$	0.035	10
Cd	228.8	360	70	1540	0.66	5.3	2.2	0.014	$4. \times 10^{-5}$	0.022	10
Zn	213.8	480	30	1540	0.66	5.3	2.2	0.014	$2. \times 10^{-4}$	0.026	10
Mg	285.2	410	100	1940	0.66	5.3	2.2	0.014	$5. \times 10^{-2}$	0.036	10

[a] Temperature of air flowing by EDL. [b] Microwave power applied to EDL using thermostated "A" antenna. [c] Temperature of graphite tube furnace walls. [d] Flow rate of Ar and/or H_2 around tube furnace exit. [e] Flow rate of CH_4 through tube furnace. [f] LOD = limit of detection, in μg/ml (see text for definition). [g] RSD = relative standard deviation (taken at a concentration of about 100 × LOD). [h] V, μl = volume size of discrete sample.

Table II. Comparison of Flame and Non-Flame Atomization Atomic Absorption and Fluorescence Limits of

		Tube non-flame cell, this study						
		Continuous LOD		Pulsed LOD		Atomic fluorescence flame LOD		
Element	Wavelength, nm	Concn, μg/ml	Absd, ng	Concn, μg/ml	Abs, ng	Concn, μg/ml	Absd, ng	Ref.
Ag	328.1	$2. \times 10^{-4}$	$2. \times 10^{-2}$	$4. \times 10^{-4}$	$4. \times 10^{-2}$	$1. \times 10^{-4}$	$5. \times 10^{-1}$	(12)
Te	213.9	$2. \times 10^{-3}$	$1. \times 10^{-1}$	$3. \times 10^{-3}$	$3. \times 10^{-2}$	$6. \times 10^{-3}$	$3. \times 10^{1}$	(13)
Tl	377.6	$6. \times 10^{-3}$	$7. \times 10^{-1}$	$2. \times 10^{-3}$	$2. \times 10^{-2}$	$8. \times 10^{-3}$	$4. \times 10^{1}$	(12)
Bi	307.7	$2. \times 10^{-3}$	$2. \times 10^{-1}$	$6. \times 10^{-4}$	$6. \times 10^{-3}$	$5. \times 10^{-3}$	$2. \times 10^{1}$	(13)
Pb	283.3	$1. \times 10^{-2}$	$1. \times 10^{0}$	$5. \times 10^{-3}$	$5. \times 10^{-2}$	$1. \times 10^{-2}$	$5. \times 10^{1}$	(15)
Sn	303.4	$1. \times 10^{-2}$	$1. \times 10^{0}$	$1. \times 10^{-2}$	$1. \times 10^{-1}$	$1. \times 10^{-1}$	$5. \times 10^{2}$	(14)
Sb	231.1	...	...	$1. \times 10^{-2}$	$1. \times 10^{-1}$	$5. \times 10^{-2}$	$2. \times 10^{2}$	(17)
Mg	285.2	...	...	$5. \times 10^{-2}$	$5. \times 10^{-1}$	$1. \times 10^{-4}$	$7. \times 10^{-1}$	(19)
Cd	228.8	...	...	$4. \times 10^{-5}$	$4. \times 10^{-4}$	$1. \times 10^{-6}$	$5. \times 10^{-3}$	(12)
Zn	213.8	...	...	$2. \times 10^{-4}$	$2. \times 10^{-3}$	$4. \times 10^{-5}$	$2. \times 10^{-1}$	(16)
Co	240.7	...	...	$3. \times 10^{-3}$	$3. \times 10^{-2}$	$5. \times 10^{-3}$	$2. \times 10^{1}$	(18)

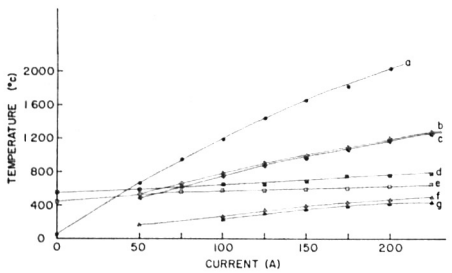


Figure 1. Temperatures of non-flame cell at various points

(*a*) Temperature in center of carbon tube; (*b*) Temperature at grazing incidence to carbon tube, with Ar sheath; (*c*) Temperature at grazing incidence to carbon tube with Ar–H_2 diffusion flame; (*d*) Temperature at 1 cm above carbon tube with Ar–H_2 diffusion flame; (*e*) Temperature at 2 cm above carbon tube with Ar–H_2 diffusion flame; (*f*) Temperature at 1 cm above carbon tube with Ar sheath; and (*g*) Temperature at 2 cm above carbon tube with Ar sheath

trometry with a continuous introduction non-flame cell, with a graphite filament non-flame cell, with a flame cell, and with the present pulsed continuous gas flow non-flame cell are given in Table II (*11–27*). The concentrational LODs obtained with the present pulsed system are similar to those obtained with other non-flame and flame atomizers in atomic fluorescence spectrometry. The absolute

(12) K. H. Zacha, M. P. Bratzel, J. M. Mansfield, and J. D. Winefordner, *Anal. Chem.*, **40,** 1733 (1968).
(13) A. Hell and S. Ricchio, Paper 23 given at the Pittsburgh Conference on Analytical Chemistry and Applied Spectroscopy, Cleveland, Ohio, 1970.
(14) R. F. Browner, R. M. Dagnall, and T. S. West, *Anal. Chim. Acta*, **46,** 207 (1969).
(15) R. F. Browner, R. M. Dagnall, and T. S. West, *Anal. Chim. Acta*, **50,** 375 (1970).
(16) M. P. Bratzel and J. D. Winefordner, *Anal. Lett.*, **1,** 43 (1967).
(17) R. M. Dagnall, K. C. Thompson, and T. S. West, *Talanta*, **14,** 1151 (1967).
(18) B. Fleet, K. V. Liberty, and T. S. West, *Anal. Chim. Acta*, **45,** 205 (1969).
(19) P. L. Larkins, *Spectrochim. Acta*, **26B,** 477 (1971).
(20) M. D. Amos, P. A. Bennett, K. G. Brodie, P. W. Y. Lung, and J. P. Matousek, *Anal. Chem.*, **43,** 211 (1971).
(21) B. M. Patel, R. D. Reeves, R. F. Browner, C. J. Molnar, and J. D. Winefordner, *Appl. Spectrosc.*, **27,** 171 (1973).
(22) R. G. Anderson, I. S. Maines, and T. S. West, *Anal. Chim. Acta*, **51,** 355 (1970).
(23) D. Alger, R. G. Anderson, I. S. Maines, and T. S. West, *Anal. Chim. Acta*, **57,** 271 (1971).
(24) H. Massman, *Spectrochim. Acta*, **23B,** 215 (1968).
(25) Perkin Elmer Literature on AA403, Perkin Elmer Corp., Norwalk, Conn.
(26) P. W. J. M. Bowmans and F. J. De Boer, *Spectrochim. Acta*, **27B,** 391 (1972).
(27) V. A. Fassel, Electrical "Flame" Spectroscopy Plenary Lectures, XVI Colloquium Spectroscopicum Internationale, Heidelberg, 1971, p 61.

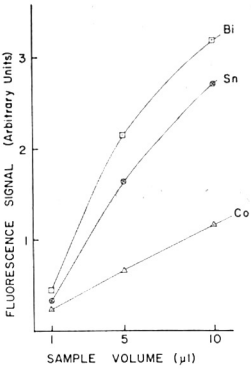


Figure 2. Fluorescence signal *vs.* sample size for Bi, Sn, and Co

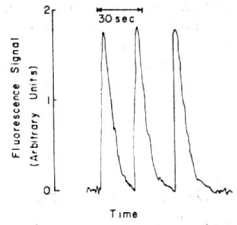


Figure 3. Fluorescence signal *vs.* time for 10 μg/ml Sn at 303.4 nm

μl, while the efficiency drops off slightly with the 10-μl sample size.

Lifetime of Carbon Tube Furnace. Because water aids in the decomposition of hot vitreous carbon, the vitreous-carbon tubes have a greatly extended lifetime in the pulsed mode over the continuous mode of sampling. This is due not only to the fact that smaller values of sample, and

Detection and Plasma Torch Limits of Detection

Atomic fluorescence filament non-flame cell LOD			Atomic absorption flame LOD			Atomic absorption tube non-flame cell LOD			Atomic emission plasma torch LOD		
Concn, μg/ml	Absd, ng	Ref.	Concn, μg/ml	Absd, ng	Ref.	Concn, μg/ml	Absd, ng	Ref.	Concn, μg/ml	Absd, ng	Ref.
$8. \times 10^{-4}$	$4. \times 10^{-4}$	(21)	$2. \times 10^{-3}$	$2. \times 10^{-1}$	(25)	$2. \times 10^{-6}$	$2. \times 10^{-4}$	(25)	$2. \times 10^{-2}$	$1. \times 10^{1}$	(27)
...	...	...	...	...	...	...	...	...	$2. \times 10^{-1}$	$1. \times 10^{2}$	(27)
$4. \times 10^{-2}$	$2. \times 10^{-2}$	(21)	$1. \times 10^{-4}$	$1. \times 10^{-2}$	(25)	$1. \times 10^{-4}$	$1. \times 10^{-2}$	(25)	$2. \times 10^{-1}$	$1. \times 10^{2}$	(27)
$1. \times 10^{-2}$	$1. \times 10^{-2}$	(22)	$1. \times 10^{-4}$	$1. \times 10^{-2}$	(25)	$1. \times 10^{-4}$	$1. \times 10^{-2}$	(25)	$5. \times 10^{-2}$	$3. \times 10^{1}$	(27)
$1. \times 10^{-2}$	$2. \times 10^{-2}$	(20)	$6. \times 10^{-5}$	$6. \times 10^{-3}$	(25)	$6. \times 10^{-5}$	$6. \times 10^{-3}$	(25)	$2. \times 10^{-2}$	$2. \times 10^{-1}$	(26)
$2. \times 10^{-1}$	$1. \times 10^{-1}$	(21)	$1. \times 10^{-2}$	$1. \times 10^{0}$	(25)	...	...	...	$3. \times 10^{-2}$	$3. \times 10^{0}$	(26)
$7. \times 10^{-1}$	$2. \times 10^{-1}$	(24)	$2. \times 10^{-4}$	$2. \times 10^{-2}$	(25)	$2. \times 10^{-4}$	$2. \times 10^{-2}$	(25)	$2. \times 10^{-1}$	$1. \times 10^{2}$	(27)
$1. \times 10^{-3}$	$1. \times 10^{-3}$	(22)	...	...	...	...	...	...	$2. \times 10^{-4}$	$2. \times 10^{-2}$	(26)
$3. \times 10^{-5}$	$3. \times 10^{-5}$	(20)	$1. \times 10^{-6}$	$1. \times 10^{-4}$	(25)	$1. \times 10^{-6}$	$1. \times 10^{-4}$	(25)	$3. \times 10^{-3}$	$3. \times 10^{-1}$	(26)
$2. \times 10^{-5}$	$2. \times 10^{-5}$	(22)	$6. \times 10^{-7}$	$6. \times 10^{-5}$	(25)	$6. \times 10^{-7}$	$6. \times 10^{-5}$	(25)	$9. \times 10^{-3}$	$9. \times 10^{0}$	(27)
$2. \times 10^{-2}$	$2. \times 10^{-2}$	(23)	$4. \times 10^{-5}$	$4. \times 10^{-3}$	(25)	$4. \times 10^{-5}$	$4. \times 10^{-3}$	(25)	$3. \times 10^{-3}$	$2. \times 10^{0}$	(27)

LODs are generally better than or equivalent to (within a factor of 3) those obtained by other non-flame and flame atomizers in atomic fluorescence spectrometry. The concentrational and absolute values obtained by the present pulsed atomizer are also comparable to or better than the best values obtained by flame and non-flame atomic absorption and flame emission spectrometry.

Precision. The relative standard deviation (RSD) for the eleven elements measured by atomic fluorescence spectrometry using pulsed mode atomization for concentrations at approximately 100 × LOD are listed in Table I. For the eleven elements determined, the precision was found to be between 0.021 and 0.036 with an average value of about 0.030. These values are slightly better than those found for the continuous mode (*9*) and for the flame as well as most other non-flame atomizers in atomic fluorescence spectrometry.

Linear Dynamic Range. The linear dynamic ranges (LDR) for three elements (Sn, Bi, Co) were examined. Both Co and Bi had the same large LDRs as in the continuous mode (2000 and 10,000, respectively) after accounting for differences in source intensity. The LDR for Co was even greater—*i.e.*, 3×10^4.

Size of Sample. The increase of fluorescence signal was not linear with increasing sample sizes of 1, 5, and 10 μl for the three elements shown in Figure 2. The figure indicates that the best atomization efficiency is obtained for 1 and 5 hence water, are needed for an analysis, but also because methane is continuously passed through the carbon tube replenishing the decomposed vitreous carbon with pyrolytic carbon. The carbon tube was further replenished by passing a mixture of Ar and CH_4 at flow rates of 0.66 l./min and 0.090 l./min, respectively, while the carbon tube was operated at a temperature of 1900 °C. Using this form of replenishment, only one vitreous carbon tube was used for this entire study. Veillon (*28*) has also used this method of extending tube life in his non-flame cell work.

Form of Signal. A plot of fluorescence signal *vs.* time is given in Figure 3. The temporal characteristics of the signal follow the expected profile expected of an exponential dilution (*29*) of a sample from a chamber—*i.e.*, in our case, the sample can be assumed to completely enter the nebulization chamber before any sample vapor exits to the vitreous-carbon tube and to become diluted by the carrier gas. Although our nebulization chamber is by no means an ideal exponential dilution flask, it is evident that the sample peaks approximately follow the expected exponential dilution behavior. Therefore, one would expect a larger peak signal if the volume of the nebulization chamber were decreased. By reducing the volume of the chamber by about

(28) C. Veillon, University of Houston, Houston, Texas, unpublished data, 1974.
(29) H. P. Williams and J. D. Winefordner, *J. Gas Chromatog.*, **4**, 271 (1966).

20-fold, the detection limits given for the elements in Table I decreased by about 20-fold. Of course, if the nebulization chamber were reduced too greatly, then desolvation would be incomplete resulting in poorer rather than better detection limits. Further studies involving chamber size as well as studies involving emission of atomic species from the hot gases above the vitreous-carbon tube are being carried out.

RECEIVED for review March 11, 1974. Accepted June 3, 1974. This work was supported by AF-AFOSR-74-2574.

Flame Atomic Fluorescence and Emission Spectrometry with a Microsampling Cup Technique

J. K. Grime and T. J. Vickers

Department of Chemistry, Florida State University, Tallahassee, Fla. 32306

For many applications, and especially with biological materials, trace element determinations must be carried out with limited amounts of sample material. Recognition of this need has led to extensive development of microsampling techniques for atomic absorption spectrophotometry. Furnace, rod, strip, and several other types of electrothermal atomization devices have received considerable attention (*1, 2*) and, for several of these devices, very high absolute sensitivities have been demonstrated for a range of elements. There are, however, disadvantages to the nonflame atomization devices: The initial equipment cost is in most cases large; and rapid conversion between nonflame and flame atomization is not possible because the nonflame atomization device must be critically aligned for optimum performance. This is a severe handicap since, when adequate amounts of sample are available, flame atomizers are usable for a larger number of elements, are often more convenient, and provide better precision than the nonflame atomizers.

Probably the best method so far reported for microsample analysis with a flame atomizer is that of Delves (*3*). In this technique, solution residues are vaporized from nickel crucibles into an absorption tube placed in a long path flame. This method appears to have achieved wide acceptance for the determination of lead in blood (*4*), and preliminary results have been reported (*5–8*) for its application to other elements: Ag, As, Bi, Cd, Hg, Se, Te, Tl, Zn. To achieve adequate sensitivity and precision with the Delves cup technique, great care must be exercised in obtaining correct alignment of the cup with respect to the absorption tube (*9, 10*). Because of the consequent long setup time, frequent conversion between normal spraying and Delves cup sample introduction is discouraged.

Sychra *et al.* (*11*) have recently described the use of two atomization techniques, a sampling cup and a hot wire loop atomizer in conjunction with atomic fluorescence spectroscopy. This apparatus has been used to determine cadmium and zinc in serum with good sensitivity, precision, and reproducibility.

The geometry of atomic fluorescence and emission flame spectrometry systems is such that the use of a flame atomizer with a configuration similar to the sampling cup, but without an absorption tube, can be considered. Accordingly, cup alignment becomes less critical and the ready interchange between the microsampling and spraying modes is facilitated. In this report, we describe the results of an evaluation of such a system for the determination of thallium, using a relatively inexpensive adaptation of the Delves technique. With the Delves cup atomic absorption technique, the detection limit for thallium was reported by Kerber and Fernandez (*5*) to be 1 ng, and Shkolnik and Bevill (*12*) reported sensitivities of 0.6 ng and 0.7 ng for thallium in urine and plasma, respectively. Thallium in microsamples has also been determined by atomic absorption spectrophotometry with a carbon rod atomizer (*13*) and with the tantalum sampling boat technique (*5*). With conventional sprayed samples, the detection limit for thallium by atomic fluorescence has been reported by Zacha *et al.* (*14*) to be 0.008 μg/ml.

EXPERIMENTAL

Apparatus. Instrument specifications and operating parameters are listed in Table I. For atomic fluorescence measurements, the source was placed at approximately 90° to the flame–monochromator axis. No lenses or mirrors were employed to focus the radiation, but the source was placed as close as possible to the flame (approximately 7 cm) and the flame was placed as close as possible to the entrance slit of the monochromator (approximately 6 cm).

The sampling cup was identical to that employed in the Delves technique. The cup holder was fabricated locally from 0.25-mm thick nickel sheet. A 6-mm wide band of the nickel sheet was formed into a loop with a double thickness handle approximately 20 mm long. The handle was firmly attached to a 6-mm diameter nickel rod, which was in turn mounted on a rotatable post, as shown in Figure 1. The height of the cup with respect to the monochromator was readily varied by moving the rod holder on the mounting post. The post could be rotated through 90° between fixed stops to provide movement of the cup in the horizontal plane and reproducible placement of the cup in the flame. A brief study indicated that best results were obtained by placing the cup just lower than the bottom of the entrance slit of the monochromator and approximately 5 mm above the burner top.

Optimum operating conditions for the Tl electrodeless discharge lamp were briefly investigated. The lamp was operated in a cylin-

(1) J. D. Winefordner and T. J. Vickers, *Anal. Chem.*, **42**, 206R (1970).
(2) J. D. Winefordner and T. J. Vickers, *Anal. Chem.*, **44**, 150R (1972).
(3) H. T. Delves, *Analyst (London)*, **95**, 431 (1970).
(4) J. M. Hicks, A. N. Gutierrez, and B. E. Worthy, *Clin. Chem.*, **19**, 322 (1973).
(5) J. D. Kerber and F. J. Fernandez, *At. Absorption Newslett.*, **10**, 78 (1971).
(6) M. M. Joselow and J. D. Bogden, *At. Absorption Newslett.*, **11**, 127 (1972).
(7) D. Clark, R. M. Dagnall, and T. S. West, *Anal. Chim. Acta*, **58**, 339 (1972).
(8) R. D. Ediger and R. L. Coleman, *At. Absorption Newslett.*, **12**, 3 (1973).
(9) F. J. Fernandez, *At. Absorption Newslett.*, **12**, 70 (1973).
(10) E. D. Olsen and P. I. Jatlow, *Clin. Chem.*, **18**, 1312 (1972).
(11) V. Sychra and D. Kolihova, *Int. Congr. At. Absorption, At. Fluorescence Spectrom. Pap., 3rd, 1971*, Vol. 1, Wiley, New York, N.Y., 1973, p 265.
(12) G. Shkolnik and R. F. Bevill, *At. Absorption Newslett.*, **12**, 112 (1973).
(13) N. P. Kubasik and M. T. Volosin, *Clin. Chem.*, **19**, 954 (1973).
(14) K. E. Zacha, M. P. Bratzel, J. M. Mansfield, and J. D. Winefordner, *Anal. Chem.*, **40**, 1733 (1968).

Table I. Instrument Specifications and Operating Parameters

Monochromator	Heath/McPherson EU-700 with 1.8-mm slit width, set for 377.6 nm.
Photomultiplier	RCA 1P28 with Heath/McPherson power supply and dc amplifier.
Electrodeless discharge lamp	Tl lamp (Opthos Instruments) operated in cylindrical cavity with heater as described by Ball (*15*). Scintillonics HV15A microwave generator. Lamp operated at 60 watts indicated power with cavity at 410 °K.
Burner	Alkemade type burner (*16*) with circular array of 0.8-mm diameter holes. Array consists of a central hole and 6, 12, 18, 24, 30, 36, 42, 48, 54, 60, and 66 holes on concentric circles of respective diameters of 3.2, 6.4, 9.6, 12.8, 16.0, 19.2, 22.4, 25.6, 28.8, 32.0, and 35.2 mm. The 5 outermost circles of holes are used for the N_2 sheath gas. Flame conditions for microsamples: Air—14.5 l./min, H_2—4.7 l./min, N_2—8.7 l./min. Flame conditions for sprayed samples: Air—11.0 l./min, H_2—3.7 l./min, N_2—6.2 l./min.
Sampling cup	Perkin-Elmer 303-0813.

drical cavity with provision for convective heating as described by Ball (*15*). Figure 2 shows the effect on the fluorescence intensity at 377.6 nm of heating the cavity. It would appear that the chief advantage of heating for the thallium lamp is that peak output can be obtained at a much lower power setting. Our findings seem in general agreement with those of Browner and Winefordner (*17*). The gas flow rates were optimized with respect to peak shape. It was observed that flow rates less than those listed in Table I produced "tailing" of the peaks.

Reagents. A stock solution of approximately 1000 μg/ml Tl was prepared by dissolving the appropriate weight of Tl_2SO_4 in distilled water. Lower concentration standards were prepared by successive dilutions.

Procedure. A cup is placed in the holder and heated in the flame to remove impurities. After cooling, a 10-μl sample is added with a 50-μl glass syringe with Chaney adapter. The holder is rotated to position the cup over the hot plate (at 140 °C), and the cup is heated for 90 sec. The cup is then rotated into the flame, and the atomic fluorescence peak recorded. After removal from the flame, the cup is allowed to cool for at least 60 sec prior to addition of the next sample.

RESULTS AND DISCUSSION

Analytical Curves. In Figure 3, results obtained with the microsampling atomic fluorescence technique are compared with those for normal sprayed samples. Both analytical curves are substantially linear at low concentration. The flattening of the microsampling curve at high concentration is expected for atomic fluorescence measurements. Note that the sensitivity of the microsampling method is approximately 15 times that of the normal sprayed sample method. At concentrations at which the fluorescence curve is nonlinear, the Tl in 10-μl samples is readily determined by thermal emission. Curve *C* in Figure 3 is the analytical curve for emission.

Figure 4 illustrates the appearance of the Tl fluorescence peaks at various concentrations. Tl is clearly detectable at the 0.05 μg/ml level with a 10-μl sample (0.5 ng Tl). At this

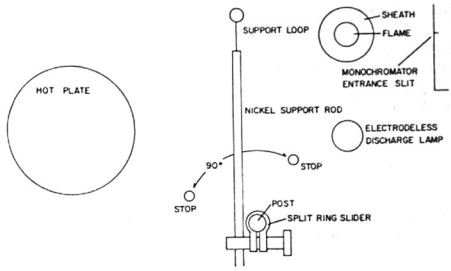


Figure 1. Top view showing arrangement of components for microsampling

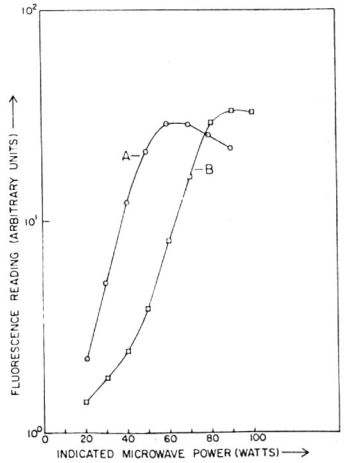


Figure 2. Plots of fluorescence intensity at 377.6 nm for 10 μg/ml Tl as a function of indicated microwave power for the cavity heated to 410 °K (*A*) and the cavity with no auxiliary heating (*B*)

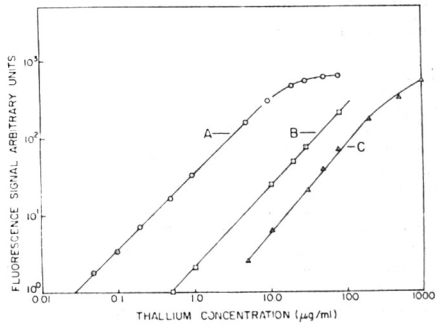


Figure 3. Analytical curves obtained for thallium

A, Atomic fluorescence with the microsampling technique (10-μl sample). *B*, Atomic fluorescence with sprayed samples. *C*, Atomic emission with the microsampling technique (10-μl sample)

(15) J. J. Ball, *Rev. Sci. Instrum.*, **44**, 1141 (1973).
(16) P. J. Slevin, V. I. Muscat, and T. J. Vickers, *Appl. Spectrosc.*, **26**, 296 (1972).
(17) R. F. Browner and J. D. Winefordner, *Spectrochim. Acta, Part B*, **28**, 263 (1973).

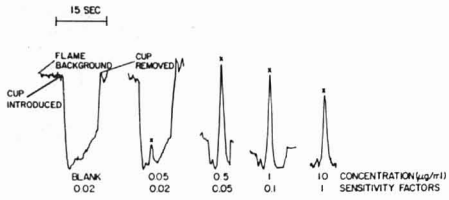


Figure 4. Recorder tracings for blank and fluorescence peaks for various Tl concentrations

X marks the Tl measurement peak. The sensitivity factor is the factor by which the intensity value should be multiplied to place it on the same relative intensity scale as the peak for the most concentrated Tl solution

level, the change in the background signal resulting from introduction of the cup, its heating, and removal is clearly evident. The increase in background signal during cup heating (shown in the blank trace) is due at least in part to incandescent emission from the cup.

Precision. Table II lists the within-run precision of the method expressed as the relative standard deviation at three concentration levels. Standard deviations were computed from 10 determinations at each concentration. The relative standard deviation is approximately that expected due to uncertainty in the micropipetting, and it is clear that adequate reproducibility in cup placement is readily achieved. No sensitivity variations were noted with cup aging, and no deterioration of the cup was apparent even after several hundred determinations. With the burner employed in the present study, the cup is completely immersed in what appears to be a largely homogeneous thermal and chemical environment and, at least in part, this seems to be the origin of the improvement in precision and cup life compared to previously reported atomic absorption studies with slot burners.

Table II. Relative Standard Deviation for Ten Determinations

Tl concn, μg/ml	Rel std dev, %
10.0	2.3
1.00	3.4
0.50	3.4

CONCLUSIONS

The results obtained demonstrate that thallium can be determined by a microsampling cup flame atomic fluorescence technique with a sensitivity at least as good as that achieved with the Delves cup procedure. The precision obtained is somewhat better than that normally obtained with the Delves procedure. With the addition of the flame emission technique, the procedure described can be used to determine Tl to concentrations at least as high as 1000 μg/ml. Cup alignment for the fluorescence procedure is readily and rapidly obtained, and the microsampling device does not interfere with use of the burner in the normal sprayed-sample mode.

RECEIVED for review March 22, 1974. Accepted June 12, 1974. Work supported in part by funds from PHS Grant R01-GM15996.

Separation of Trace Metal Impurities from Nuclear Grade Uranium by Long-Chain Amine Extraction and Direct Determination by Atomic Absorption Spectrophotometry

Sergio de Moraes and Alcidio Abrão

Chemical Engineering Department, Instituto de Energia Atômica, Caixa Postal 11.049 e C.E.P. 05.508, São Paulo, Brazil

The purification and conversion of uranium concentrates to nuclear grade products require the identification and determination of a series of trace metal impurities, some of which have deleteriously high thermal neutron capture cross-sections. The majority of the published literature in this area has approached the problem by an initial separation of the matrix uranium using, for instance, solvent extraction, and determining the trace impurities in the raffinate. Any procedure that could primarily separate the impurities by solvent extraction, or otherwise, from the major constituent, uranium, would be advantageous and attractive. This paper deals with such an approach for the separation, concentration, and determination of microgram quantities of a series of metals present as impurities in high grade uranium.

Long-chain amines have been utilized extensively as extracting agents for various elements, including uranium. The literature on the subject is extensive (*1–9*). Such procedures have also been investigated in this laboratory for isolating trace metal concentrations from hydrochloric acid media (*10*). Of pertinent interest is the use of tri-*n*-octyl

(1) F. L. Moore, Rept. NAS-NS-3101 (1960).
(2) M. Y. Mirza, M. Ejaz, A. R. Sarni, S. Ullah, M. Raschid, and G. Samdani, *Anal. Chim. Acta*, **37,** 402 (1967).
(3) A. D. Nelson, J. L. Fasching, and R. L. MacDonald, *J. Inorg. Nucl. Chem.*, **27,** 439 (1965).
(4) W. J. Maeck, G. L. Booman, M. C. Elliott, and J. E. Rein, *Anal. Chem.*, **30,** 1902 (1958).
(5) W. J. Maeck, G. L. Booman, M. C. Elliott, and J. E. Rein, *Anal. Chem.*, **32,** 605 (1960).
(6) W. J. Maeck, G. L. Booman, M. E. Kussy and J. E. Rein, *Anal. Chem.*, **33,** 1775 (1961).
(7) F. L. Moore, Rept. ORNL-1314 (1952).
(8) F. L. Moore, *Anal. Chem.*, **29,** 1660 (1957).
(9) W. D. Arnold and D. J. Crouse, Rept. ORNL-3030 (1961).
(10) A. Abrão, Ph.D. Thesis, Instituto de Quimica, Universidade de São Paulo, Brazil, 1971.

amine (TOA), diluted with an inert solvent as extracting agent. The extractive separation of cadmium, silver, gold, mercury, lead, and bismuth from aqueous hydrochloric acid solutions of uranyl chloride by use of TOA in benzene was studied. It was demonstrated that, while Au was quantitatively extracted, Cd, Hg, Pb, and Bi were only partially extracted and Ag not at all. Addition of small quantities of potassium iodide to the aqueous acid phase overcame this difficulty and permitted high and reproducible extraction by the amine.

Atomic absorption spectrophotometry indeed appears to be the method of choice for the determination of a variety of trace elements in terms of sensitivity and convenience. In this study, the impurity elements, after extraction from uranium chloride solutions, were determined by atomic absorption by directly burning the organic phase in the spectrophotometer.

EXPERIMENTAL

Apparatus. Absorption measurements were made on a Jarrell-Ash series 82-500 atomic/flame emission spectrophotometer, equipped with a 0.5-meter Ebert-type monochromator. The resolution of the instrument is 0.2 Å in the first order. The spectrophotometer has a HETCO total consumption burner and a multipass optical system to give five passes through the flame. The height of the HETCO burner was adjusted for each element to achieve optimum readings. The following spectral lines were used: (nm) Cd, 228.8; Ag, 328.1; Au, 242.8; Hg, 253.7; Pb, 283.3; and Bi, 306.8. The light source was preheated at least 15 minutes before use. Acetylene–air and hydrogen–air flames were tested. The compressed air was dried through a column of silica gel and finally filtered to remove solid particles and oil mist. Optimum fuel pressures were adjusted for maximum element sensitivities.

Reagents. All chemicals were reagent grade (E. Merck; B&A; Carlo Erba, São Paulo, Brazil) or of the highest purity available. Deionized water was used for the preparation of all aqueous solutions. Tri-*n*-octyl amine (Koch & Light, England) was utilized without any further treatment. It was diluted with benzene to provide a 5% (v/v) working solution. These were used immediately after preparation to avoid possible aging effects.

Procedure. Ammonium diuranate (ADU) was dissolved in hydrochloric acid and adjusted to 0.4*M* in free HCl in the final dilution. Solutions that contained potassium iodide were similarly adjusted to a final 0.4*M* HCl–0.01*M* KI. Fifty-ml aliquots of uranyl chloride solutions (U 300 g/l.), to which were added microgram quantities of Cd, Ag, Au, Hg, Pb, and Bi individually or in mixtures, were extracted thrice with 3-ml portions of TOA–benzene. The organic phase was similarly washed three times with 3-ml lots of 0.4*M* HCl or 0.4*M* HCl–0.01*M* KI, respectively, in the two series of experiments. The final organic phase was filtered and made up to 10.0 ml with benzene.

The TOA–benzene phase was burned directly in the atomic absorption spectrophotometer to determine the concentration of extracted trace elements. Hydrogen–air flame was preferentially used in view of increased sensitivity. A set of standard calibration curves were also run by the same procedure, however omitting the matrix uranium in the aqueous phase. Similarly a blank experiment was performed utilizing a previously purified uranium in which the trace metal impurities were separated by TOA–benzene extraction.

RESULTS AND DISCUSSION

Amine Extraction from HCl Medium. The extraction of metals from hydrochloric acid medium with an organic phase consisting of tri-*n*-octyl amine diluted with benzene, or other diluents, depends mainly on the capacity of the metals to form anionic chloride complexes, and is considerable in the case of several metals, including Cd, Ag, Au, Hg, Pb, Bi, Pd, Cu, Zn, Sn, and U. In such systems, the influence of HCl concentration is of paramount importance on the distribution coefficients of the various metal ions. Mirza *et al.* (*2*), have studied the behavior of several metals toward extraction with tri-*n*-octyl amine diluted with methyl isobutyl ketone from hydrochloric acid solutions. Abrão (*10*) has investigated the use of tri-*n*-octyl amine for the separation of uranium from 24 metals in HCl and UO_2Cl_2–HCl media.

An attempt was made to adapt such solvent extraction procedures for the separation, concentration, and determination of Cd, Ag, Au, Hg, Pb, and Bi from high grade uranium. Whereas the amine extraction of the pure metal ions proceeds quantitatively in HCl solutions (*2, 3, 10*), the presence of relatively large concentrations of uranium in the aqueous media seriously inhibited their extraction. In these experiments, the hydrochloric acid concentration was adjusted to a nominal 0.4*M* (free acidity) to retard appreciable coextraction of uranium. The trace metal concentrations were in the range up to: Cd, 0.67; Ag, 1.64; Au, 1.31; Hg, 191; Pb, 66; and Bi, 134 μg per gram of uranium. These experiments showed that while Au was extracted into TOA–benzene quantitatively, Cd (28%), Hg (72%), Pb (4%), and Bi (4%) were not efficiently extracted and Ag was not at all extracted from the acid–uranyl chloride solution.

Amine Extraction from HCl–KI Medium. The unsatisfactory extractions of the trace metals mentioned above were considerably improved by the addition of iodide ion (as KI) to the uranyl chloride–hydrochloric acid aqueous media. Although the potentiality of solvent extraction of anionic metal iodide complexes by long-chain amines and quaternary ammonium salts was foreseen (*11*), published literature in this area is limited (*12, 13*). In a variation of this approach, Abrão (*10*) demonstrated that the extraction of pure Pb and radiotracer Pb (^{212}Pb in thorium) in TOA–benzene was improved quantitatively by the addition of small quantities of KI to the hydrochloric acid solution. Similarly, while the extraction of Ag diminishes from 97% in 0.08*M* HCl to 3% in 8.3*M* HCl, addition of KI to the acid solution brought about quantitative extractions in TOA–benzene.

Based on these observations, the solvent extraction of Cd, Ag, Au, Hg, Pb, and Bi and separation from uranium was studied. The aqueous phase containing uranium was adjusted to a final 0.4*M* HCl–0.01*M* KI. The trace element concentrations were identical to those mentioned previously. The relative extraction of the metals into TOA–benzene were: Cd, 92%; Ag, 62%; Au, 100%; Hg, 84%; Pb, 21%; and Bi, 88%. While no change in the extractability of Au was expected, considerable improvements in the extraction of Cd, Ag, Hg, and Bi into TOA–benzene were obtained.

Atomic Absorption Determination of Trace Elements. A significant observation in this study is the enhanced absorbance produced by burning the organic phase (TOA–benzene) directly in the atomic absorption spectrophotometer. Then, for the pure elements, the absorbance values were increased by a factor, 1.5 (Cd), 2.0 (Ag), 1.7 (Au), 1.4 (Hg), 1.6 (Pb), and 2.1 (Bi) compared to those obtainable by burning similar concentration of the aqueous acid phase. Additionally, the absorbance of the pure elements extracted into TOA–benzene from 0.4*M* HCl and 0.4*M* HCl–0.01*M* KI, respectively, was identical and reproducible. Calibration curves obtained (absorbance *vs.* concentration, μg element per ml organic phase) for Cd (0.1–1.5), Ag (0.1–1.5), Au (0.2–4.0), Hg (10–200), Pb (10–100), and Bi (10–150) were linear in the entire range. Besides enhancement of absorbance, the possibility of avoiding stripping the organic phase for the extracted elements was another convenient advantage.

(11) A. A. Prokoshev, L. K. Chuchalin, B. Z. Iofa and Yu. A. Zolotov, *J. Anal. Chem. USSR., Eng. Transl.*, **27**, 1230 (1972).
(12) M. L. Good, S. C. Srivastava and F. F. Holland, Jr., *Anal. Chim. Acta*, **31**, 534 (1964).
(13) D. G. Tuck and E. J. Woodhouse, *J. Chem. Soc., Suppl.*, 6017 (1964).

It must be mentioned that the relative extractions of the various metals into TOA–benzene from acid solutions containing uranium, presented above, were computed on the basis of their absorbance with reference to the pure metals similarly extracted from acid media. It is believed that the matrix effect of small concentration of uranium coextracted with the trace elements into TOA–benzene is primarily the reason for an apparent lower than 100% recovery of Cd, Ag, Hg, Pb, and Bi. Repeated extraction from the aqueous raffinate did not improve the "computed" recovery values. To the extent that the calibration for the elements separated from uranium by TOA–benzene extraction and determined by atomic absorption were reproducibly linear in the entire concentration range, the analytical application of the method is evident.

CONCLUSION

The combination of the solvent extraction and atomic absorption determination of a series of trace elements has proved to be a unique approach to the analysis of nuclear grade uranium (ADU and UO_3). While several pure elements are well extracted by long-chain amines from hydrochloric acid solution, the presence of appreciable concentration of uranium and chloride ions constitute serious interference, lowering the activity of the metal chloro complexes. Such an interference is so marked for silver, for example, that TOA–benzene does not extract the element from UO_2Cl_2–HCl medium.

Addition of a small concentration of KI surmounted the difficulty and provided practical and reproducible extraction of the various elements in the presence of uranium. The exact mechanism of the extraction in the presence of iodide ions is not well understood. The possibility exists for the formation of stronger iodide or ever mixed iodo-chloro complexes of the metal ions. It is also pertinent to indicate that even precipitates like the chlorides and iodides of Hg, Tl, Ag, Bi, and Pb are dissolved and extracted by TOA–benzene from hydrochloric acid solution (*10*). Iron and cobalt were not extracted by TOA–benzene; copper was extracted, but it could be stripped quantitatively from the organic phase by washing with HCl-KI solution.

Concentrations of uranium in the aqueous phase have approached up to 300 grams per liter. However, no difficulty in phase separation with TOA–benzene was experienced. Accommodating such high concentration of the matrix uranium necessarily provides for increased analytical sensitivity for the trace elements. The enhanced absorbance obtainable in direct burning of the organic phase is an added advantage of procedure.

The technique outlined in this paper is routinely used for the analysis of Cd, Ag, Au, Hg, Pb, and Bi in uranium. Calibration curves obtained with the uranium matrix have realized relative standard deviations of approximately 2, 4, 6, 2, 12, and 3%, respectively, for these elements in the trace concentration of interest. An extension of this work is in progress for the determination of trace metals in nuclear grade thorium (*14*).

RECEIVED for review October 11, 1973. Accepted April 22, 1974.

(14) A. Abrão and S. de Moraes, Instituto de Energia Atômica, São Paulo, Brazil, unpublished work, 1972.

Atomic Absorption Determination of Mercury in Fish Using the Coleman MAS-50 Mercury Analyzer

Pekka Kivalo, Asko Visapää, and Runar Bäckman

Chemical Laboratory, Technical Research Centre of Finland, 02150 Otaniemi, Finland

In this Research Centre, a large number of mercury determinations of fish samples have been performed by means of neutron activation analysis in conjunction with studies concerned with environmental protection. In 1971, the Coleman Division of the Perkin-Elmer Co. introduced a mercury analyzer, called MAS-50 (*1*), which is based upon cold vapor atomic absorption (*2*) and upon the procedure developed by Hatch and Ott (*3*). In view of the time-consuming and costly nature of activation analysis in mercury determinations, it was decided in this laboratory to investigate the suitability of the MAS-50 analyzer for mercury determinations in fish.

The literature concerning nonflame methods, up to and partially including 1970, has been reviewed by Manning (*4*). Since 1971, a few references to the MAS-50 analyzer have been made in the literature (*5–7*).

(1) Coleman Instruments, Maywood, Ill., Coleman Mercury Analyzer MAS-50, Operating Directions 50-900 (1971).
(2) R. G. Smith, "Methods of Analysis for Mercury and Its Compounds: A Review," in "Environmental Mercury Contamination," R. Hartung and B. D. Dinman, Ann Arbor Science Publishers Inc., Ann Arbor, Mich., 1972.
(3) W. R. Hatch and W. L. Ott, *Anal. Chem.*, **40**, 2085 (1968).
(4) D. C. Manning, *At. Absorption Newslett.*, **9**, 97 (1970).

EXPERIMENTAL

Instrumentation. In this instrument, mercury vapor is constantly circulated by a pump within a closed loop that comprises an external BOD (biological oxygen demand) bottle connected by silicone rubber tubes to a glass absorption cell with plastic windows. The mercury vapor in the cell absorbs the 253.7-nm radiation of a mercury lamp at one end of the cell, and a photoelectric cell with a narrow band-pass filter is placed at the other end. The diminution in intensity is measured. The instrument is equipped with an electronic memory circuit which stops the absorbance reading at the maximum.

In preliminary studies, the original plastic end windows of the absorption cell developed cracks, and rapidly became opaque by reason of the UV radiation of the lamp and the ozone produced by the UV radiation. The original windows were replaced by windows made of quartz.

When the instrument was operated with the memory circuit shut off, it was noted that when a sample containing elemental mercury was being aerated, the maximum absorbance was attained

(5) J. D. Suggs, D. H. Petersen, and J. B. Middlebrook, *Water Pollut. Contr. Res. Ser.* **1690HTD 03/72,** Environmental Protection Agency, Washington, D.C., 1972.
(6) J. E. Longbottom and R. C. Dressman, *Chromatogr. Newslett.*, **2**, 17 (1973).
(7) S. H. Omang and P. E. Paus, *Anal. Chim. Acta*, **56**, 393 (1971).

within 5 to 6 seconds [and not after one minute, as stated in the instrument manual (*1*)]. Subsequently, the reading was found to decrease slowly (Figure 1). Other researchers (*8*) have found a similar phenomenon, which they believe originates in oxidation of the mercury vapor, or adsorption on the walls of the air circulation loop.

With the aim of discovering the reason for the gradual disappearance of mercury from the gas phase, the following experiments were made, all of them with a concentration corresponding to a scale reading of 1 μg Hg:

1) Before aeration, a piece of cardboard was placed between the lamp and the absorption cell, to cut off the radiation. Aeration was begun and, in successive experiments, the cardboard was removed after predetermined times, with the memory circuit on. The readings obtained, as a function of time, were almost the same as those when the radiation was entering the cell continuously with the memory circuit off (Figure 1). Consequently, the diminution in the reading does not result from oxidation of the mercury vapor by the UV radiation or ozone.

2) Since the mercury vapor is not oxidized, its disappearance cannot be caused by absorption into the solution in the BOD bottle. This was confirmed by blowing mercury vapor into an empty and dry BOD bottle as the sample. A similar diminution occurred in the reading after an initial rapid rise, both with the radiation entering the cell, and with the radiation blocked off for given lengths of time, as indicated in 1).

3) When glass wool, with a surface area of about 4000 cm^2—*viz.*, a tenfold increase in the adsorbing surface—was placed in the air circulation loop, no change was observed in the speed of decrease in the reading. When thin silicone rubber slices, about 4000 cm^2 in area, were placed in the air circulation loop, the speed of decrease in the reading became slightly faster. Consequently, the diminution in the reading was not attributable to adsorption of the mercury vapor on the glass surfaces of the air circulation loop. Apparently, the mercury vapor is slightly removed with silicone rubber.

4) When the silicone rubber tubes outside the instrument case were replaced by Teflon tubing, definite retardation in the diminution of the reading was observed (Figure 1). This indicated the escape of part of the mercury vapor through the walls of the silicone rubber tubing. To confirm this, equal amounts of mercury were placed in pieces of tubing, 3 cm in length; made from silicone rubber and Teflon. These pieces were closed by tightly fitting glass rods. Each piece of tubing, containing mercury, was placed in a separate BOD bottle, and the bottles were closed; after these had stood 10 minutes, determinations were made in the usual way, by starting aeration. The results indicated that the amount of mercury vapor diffused through the wall of the silicone rubber tubing was about ten times that diffused through the Teflon tubing wall, although the tube wall thicknesses were 2.2 mm for silicone rubber, and 0.4 mm for Teflon. Thus, a part of the loss of mercury on prolonged aeration arises from diffusion through the walls of the connection tubes.

In the pump, mercury vapor comes into contact with surfaces of nylon, rubber, and hard rubber. Hard rubber, in particular, may induce absorption of mercury vapor as a result of its sulfur content.

A suitable rotameter must be employed for periodic checks of the air flow. Permanent connection of a rotameter in the air circulation loop is unnecessary, as calibration is performed before each series of determinations. Furthermore, permanent connection of a rotameter could lead to more rapid disappearance of the mercury vapor.

However, it must be borne in mind that, despite the causes mentioned for the disappearance of mercury vapor from the gas phase in prolonged aeration, the determination itself is not affected, provided that the tubing material does not allow mercury vapor to escape too rapidly. All the effects (absorption, adsorption, and diffusion) are eliminated in the calibration procedure, and by use of the memory circuit.

Precision and Accuracy of the Instrument. The reproducibility and accuracy of the instrument were checked by means of three concentrations (0.50, 1.00, and 1.50 ppm) of mercury as mercuric chloride, without acid digestion, that is, starting with the addition of permanganate, followed by hydroxylamine hydrochloride, and continuing with reduction by stannous chloride and aeration. Table I presents the results of six parallel determinations for each concentration. It is observable that the degree of accuracy is good at all three concentrations. The values of the relative standard deviation vary between 1 and 3.

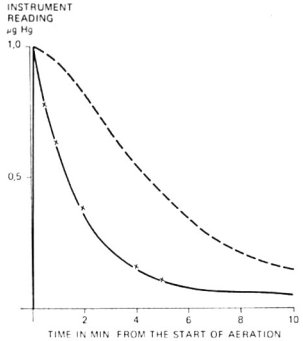


Figure 1. Decrease in the reading as a function of time on aeration of a reduced $HgCl_2$-solution with the memory circuit off

(——) Readings obtained with the original silicone rubber tubing. (– – –) Readings obtained with Teflon tubing replacing the silicone rubber tubing outside the instrument case. (X) Readings obtained after blocking the radiation for 0.5, 1, 2, 4, and 5 minutes

Table I. Parallel Determinations of the Mercury Content of Mercuric Chloride Solutions of Known Concentration without Acid Digestion

Hg added, ppm	0.50	1.00	1.50
Hg found, ppm	0.51	0.97	1.52
	0.52	1.02	1.50
	0.48	0.99	1.49
	0.50	1.00	1.52
	0.49	1.02	1.50
	0.49	0.98	1.49
Mean value	0.50	1.00	1.50
Variance	0.00022	0.00043	0.00019
Std deviation	0.015	0.021	0.014
Rel std dev, %	2.95	2.07	0.91

Acid Digestion Procedure. For investigation of the acid digestion procedure for fish samples, given in the Applications Data Sheet (*9*), several determinations were made with known amounts of mercuric chloride. The precision and accuracy were satisfactory. However, when determinations were made with fish samples of which the mercury concentrations had been determined by neutron activation analysis (*10*), the precision was satisfactory in parallel determinations, although the results obtained were only about 30 to 70% of those with activation analysis. Consequently, it was obvious that the acid digestion procedure was unsatisfactory with respect to organomercuric compounds. In biological samples, mercury is often very strongly bound to the organic material. No complete knowledge is possessed of the exact nature of the bonding (*11*). For biological material, one of the major problems is the separation of mercury from the large mass of organic matter with which it is associated (*2*). Sample digestion constitutes a critical step in quantitative determination of the total mercury. During digestion, errors can arise as a result of the incomplete extraction of mercury, the nonquantitative conversion of organomercury into mercury(II) ions, or the loss of mercury vapor (*12*).

Trials were made with a number of different acid digestion procedures (different acids, mixtures, temperatures, and reaction

(8) J. F. Uthe, F. A. J. Armstrong, and M. P. Stainton, *J. Fish. Res. Bd. Can.*, **27**, 805 (1970).

(9) Perkin-Elmer Co., Coleman Instruments Division, Maywood, Ill., Applications Data Sheet MAS-50-6 (1971).

(10) E. Hasanen, *Suom. Kemistilehti*, **43B**, 251 (1970).

(11) I. M. Kolthoff and P. J. Elving, "Treatise on Analytical Chemistry," Part II, Vol. 3, Interscience Publishers, New York, N.Y., 1961, p 253.

(12) I. K. Iskandar, J. K. Syers, L. W. Jacobs, D. R. Keaney, and J. T. Gilmore, *Analyst (London)*, **97**, 388 (1972).

Table II. Results in ppm, Obtained for Organomercuric Compounds by the Method Proposed with and without Acid Digestion[a]

Compound	Without acid digestion	With acid digestion
Methylmercuric chloride	0.10	1.01
Phenylmercuric acetate	0.10	1.02
Phenylmercuric hydroxide	0.05	0.98

[a] In all cases, the known concentration equals 1 ppm Hg.

Table III. Parallel Determinations of the Mercury Content of Mercuric Chloride Solutions of Known Concentration with Acid Digestion

Hg added, ppm	0.50	1.00	1.50
Hg found, ppm	0.48	0.97	0.48
	0.48	0.94	1.55
	0.50	1.00	1.53
	0.52	0.98	1.50
	0.47	1.04	1.46
	0.49	0.95	1.45
Mean value	0.49	0.98	1.50
Variance	0.00320	0.0013	0.0016
Std dev	0.018	0.036	0.039
Rel std dev, %	3.65	3.71	2.63

times) (*8, 9, 13–16*); that finally adopted, a modification of the procedure published by Häsänen (*10*), was as follows:

About 1 gram of homogenized fish tissue is placed carefully in a 50-ml round-bottom flask, provided with a ground glass joint. The exact weight of the sample (±0.01 gram) is determined by weighing the flask before and after addition of the sample. The sample is transferred to the bottom of the flask; 2 ml of fuming nitric acid is added slowly, followed by 1 ml of sulfuric acid (d = 1.84). The flask is immediately connected to an Allihn reflux condenser, 30 cm in length, which has at its upper end a 15-cm long capillary (0.5–1 mm inner diameter) connected by a ground glass joint to the condenser. The function of the capillary is to prevent mercury and acid losses, and diminish bumping. The sample must always be completely covered by the acid mixture. The mixture is boiled gently for 30 minutes; the clear brown solution is then transferred quantitatively to a BOD bottle, into which the condenser is rinsed with one 10-ml portion, and the flask with two 5-ml portions of distilled water. The volume of the solution in the BOD bottle is adjusted with distilled water to 100 ml. Potassium permanganate crystals are added to the bottle with swirling, until a pink color persists. The determination is then continued according to the Applications Data Sheet instructions (*9*).

One determination takes about 40 minutes.

No frothing occurs in the aeration step after this digestion procedure.

Recovery with Organomercuric Compounds. For investigation of whether organically-bound mercury reacts completely in the acid digestion procedure proposed, methylmercuric chloride, phenylmercuric acetate, and phenylmercuric hydroxide were used as model substances for organomercuric compounds. The acid digestion procedure gave complete recovery (Table II). Without acid digestion (beginning with permanganate oxidation), the recovery was not more than 5 to 10%. For methylmercuric chloride, 1 hour of acid digestion time was required for complete recovery whereas a boiling time of 30 minutes was adequate for phenylmercuric acetate and phenylmercuric hydroxide.

(13) S. H. Omang, *Anal. Chim. Acta*, **63**, 247 (1973).
(14) R. J. Evans and J. D. Bails, *Environ. Sci. Technol.*, **6**, 901 (1972).
(15) W. L. Hoover, J. R. Melton, and P. A. Howard, *J. Ass. Offic. Anal. Chem.*, **54**, 860 (1971).
(16) V. A. Thorpe, *J. Ass. Offic. Anal. Chem.*, **54**, 206 (1971).

Table IV. Six Parallel Determinations of the Mercury Content of One Pike Sample[a]

Detn No.	Hg, ppm
1	0.86
2	0.88
3	0.89
4	0.92
5	0.94
6	0.84
Mean value	0.89
Variance	0.0014
Std dev	0.037
Rel std dev, %	4.18

[a] Result obtained by activation analysis: 0.90 ppm.

Table V. Mercury Concentrations in ppm of Different Fish Samples, Obtained with MAS-50 Analyzer, Applying the Procedure Proposed and Neutron Activation Analysis (10)

Type of fish	MAS-50	Activation analysis
Whitefish	0.17	0.17
Roach	0.25	0.26
Roach	0.26	0.28
Perch	0.33	0.32
Perch	0.34	0.32
Perch	0.40	0.44
Bream	0.46	0.50
Perch	0.46	0.42
Walleye	0.48	0.50
Pike	0.49	0.52
Pike	0.57	0.53
Bream	0.58	0.61
Pike	0.58	0.54
Pike	0.61	0.62
Pike	0.62	0.62
Pike	0.86	0.90
Pike	0.88	0.90
Pike	0.92	0.90

RESULTS AND DISCUSSION

The precision and accuracy of the method proposed (acid digestion, treatment with permanganate and hydroxylamine hydrochloride, reduction, and the determination proper) were ascertained by six parallel determinations with known amounts of mercuric chloride. The results obtained are listed in Table III, and indicate that, at levels of 0.50 and 1.00 ppm Hg, the relative standard deviation is 3.7, and that the precision is satisfactory at all three concentrations used. At a level of 1.50 ppm (seldom encountered in fish samples), the relative standard deviation is 2.6. Consequently, the acid digestion induces a slight increase in the spread of the results (see Table I), but does not affect the accuracy.

The mercury content of one pike sample was determined six times to check the reproducibility and accuracy in determination of the mercury in fish (Table IV). Activation analysis showed that the mercury concentration in this pike sample was 0.90 ppm. It is discernible from this Table, that the mean value obtained was 0.89 ppm Hg: the relative standard deviation was 4.2; this can be considered satisfactory in analysis of this type.

The accuracy of the method proposed was further checked by determination of the mercury content of several fish samples (pike, bream, perch, roach, whitefish, and walleye), both by the method proposed, and by neutron activation analysis (*10*). The activation analyses were con-

ducted in the Reactor Laboratory of this Research Centre. Table V presents typical results. The value of correlation coefficient r was 0.992, and its statistical significance t = 30.96; this indicates that the correlation is significant at the 99% probability level (*17*).

When mercury determinations are being made, the utmost care must be exercised throughout, to ensure that contamination is prevented. Precise analysis is dependent upon avoiding contamination of glassware, reagents, and standards. A reagent blank should be run to confirm the purity of the reagents. When analytically pure reagents are utilized, a typical value found for the reagent blank is 0.01 μg Hg.

(17) K. Doerffel, "Beurteilung von Analysenverfahren und -Ergebnissen," Springer-Verlag, Berlin, 1962.

RECEIVED for review January 21, 1974. Accepted May 7, 1974.

Analytical Applications of the Graphite Braid Nonflame Atomizer

Akbar Montaser[1] and S. R. Crouch[2]

Department of Chemistry, Michigan State University, East Lansing, Mich. 48824

In a previous report (*1*), the graphite braid atomizer (GBA) was introduced as a new filament-type nonflame atomizer for atomic absorption (AA) and atomic fluorescence (AF) spectrometry. The GBA has the advantages of a medium power required to reach high temperatures, a furnace-type environment during the various heating steps, and a low cost (<1 cent for a 30-mm long, 1.5–2 mm diameter braid). The GBA also requires very low sample volumes (1–10 μl), which is highly desirable for trace metal analysis of biological fluids. Since the GBA is a filament-type atomizer, it can be used as an atomic vapor cell for both AA and AF measurements. In the earlier report (*1*), AF data were presented for Cd and Zn, and AA data were reported for Cu and Pb.

Because of its potential advantages over other nonflame atomizers (*2*), a more extensive investigation of the analytical capabilities of the GBA was undertaken and is described in this paper. Detection limits are presented for 12 elements by AA spectrometry and for 3 elements by AF spectrometry. In addition, a brief matrix effect study is reported along with results of the direct analyses of Cu and Fe in a serum matrix. These latter results illustrate the potential applicability of the GBA for the analysis of complex biological samples with no sample preparation steps other than a simple dilution.

EXPERIMENTAL

Instrumentation. The graphite braid atomizer, 30 mm in length and 1.5–2 mm in diameter, was mounted below the optical path of an AA/AF spectrometer by an arrangement similar to that described previously (*3*). The GBA was positioned over an adjustable inert gas sheath which transports the atomic vapor plume to the optical axis, minimizes oxide formation, and reduces quenching of the fluorescence radiation in AF. The gas sheath design consisted of a square piece of 2- × 2-in. stainless steel with separate inner and outer clusters of holes. The inner cluster consisted of a square matrix containing five parallel rows of holes. The holes had a diameter of 0.018 in. and were 0.032 in. apart. The outer cluster consisted of three square matrices of holes. The holes in this group had a diameter of 0.032 in. and were 0.048 in. apart. Argon was used for both inner and outer sheaths. Table I shows the experimental components of the AA/AF spectrometer.

Hollow cathode lamps operated in a dc mode were utilized as AA excitation sources, while computer-controlled pulsed hollow cathode lamps (*5*), with a duty cycle of 1/16, were employed as AF sources. Unless otherwise stated, the radiation from the source was focused at about 1–2 mm above the GBA. Computer integration of the transient absorption or fluorescence signals was used in all cases. The photometric signal was integrated for the duration of the atomization step. Background correction, conversion of transmittance to absorbance, and statistical calculations were performed by the computer, and all results were printed out on a teletype. Electrical heating of the GBA was also performed by a computer-controlled feedback system (*6*). All results were obtained using either a 2- or 3-stage power program (*6*), rather than current-programmed heating. The former has been shown to improve the GBA lifetime and its temperature reproducibility (*6*).

Reagents. Stock solutions were prepared from pure metals dissolved in a minimum amount of HCl or HNO_3. Aqueous standards were prepared with distilled water which had been purified by an "Ultrapure Water System" (Osmonics, Inc., Hopkins, Minn.). For the serum analyses, a serum matrix (Lot No. CALC 102 A-2, Dade Div., American Hospital Supply Corp., Miami, Fla.) was used after tenfold dilution.

Sampling and Procedure. Except for optimization studies, samples were dispensed onto the GBA manually with a 5-μl syringe (Unimetrics Universal Corp., Anaheim, Calif.). For optimization studies, a pneumatically operated automatic sampler (*7*) was employed. For detection limit and matrix effect studies, 2 μl samples were dispensed to the GBA and the integrated AA or AF results obtained. For the serum analyses by AA, 1-μl samples were employed. The rest of the experimental conditions employed in the AF and AA analyses are summarized in Tables II and III, respectively. Measurements of the atomizer temperature were made with an optical pyrometer and had an uncertainty of approximately ±50 °C.

RESULTS AND DISCUSSION

Analytical Curves and Detection Limits. Analytical data were obtained for 13 elements in aqueous solutions. Except for an optimization of the atomization temperature, no other parameters in the system were rigorously optimized in obtaining these data. Analyses of Hg, Cd, and Zn

[1] Present address, Ames Laboratory–USAEC and Department of Chemistry, Iowa State University, Ames, Iowa 50010.

[2] Author to whom reprint rquests should be addressed.

(1) Akbar Montaser, S. R. Goode, and S. R. Crouch, *Anal. Chem.*, **46**, 599 (1974).
(2) G. F. Kirkbright, *Analyst (London)*, **96**, 609 (1971).
(3) S. R. Goode, Akbar Montaser, and S. R. Crouch, *Appl. Spectrosc.*, **27**, 355 (1973).
(4) E. Cordos and H. V. Malmstadt, *Anal. Chem.*, **44**, 2407 (1972).
(5) E. F. Palermo, Akbar Montaser, and S. R. Crouch, *Anal. Chem.*, in press.
(6) Akbar Montaser and S. R. Crouch, *Anal. Chem.*, in press.
(7) Akbar Montaser, Ph.D. Thesis, Michigan State University, East Lansing, Mich., 1974.

Table I. Experimental System for AA and AF Measurements with the GBA

Component	Description and type	Supplier
Radiation sources	Hollow cathode discharge lamps	Fisher Scientific, Pittsburgh, Pa.
	Metal vapor discharge lamps	George W. Gates & Co., Inc., Franklin Square, N.Y.
Source power supplies	DC hollow cathode supply Model EU-703-70	GCA/McPherson, Acton, Mass.
	Pulsed hollow cathode supply, modified EU-703-70 [see reference (4)]	
Monochromator	Model EU-700, 350 mm focal length, f/6.8 aperature, 20 Å/mm reciprocal linear dispersion	GCA/McPherson, Acton, Mass.
Nonflame atomizer	Graphite braid	Union Carbide, Parma, Ohio
Photomultiplier tubes	1P28A	RCA, Electronic Components, Harrison, N.J.
	R166 solar blind	Hamamatsu Corp., Lake Success, N.Y.
Photomultiplier power supply	Model EU-701-30	GCA/McPherson, Acton, Mass.
Current-to-voltage converter	Model 427 current amplifier	Keithley Instruments, Cleveland, Ohio
Minicomputer	PDP Lab 8/e	Digital Equipment Corp. Maynard, Mass.
Optical Pyrometer	Catalog No. 8622-c	Leeds and Northrup Co., Philadelphia, Pa.

Table II. Experimental Parameters Used for AF Measurements[a]

Elements	Radiation source current, mA[b]	Source on Time, msec	Drying power, W[c,d]	Atomization power, W[c]	Atomization temp., °C	Atomization time, sec	Analysis wavelength, nm
Cd	200	2	6	130	1650	1	228.8
Zn	426	4	10	130	1650	1.3	213.86
Hg	400	4	2	130	1650	1.3	253.65

[a] The following parameters were the same for all elements: sheath gas flow rate = 2 l/min; monochromator spectral bandpass = 4 nm; photomultiplier supply voltage = 800 V. [b] Radiation sources were pulsed hollow cathode lamps. [c] Power programmed heating. [d] Drying time = 11 sec.

Table III. Experimental Parameters Selected for AA Measurements[a]

Element	Drying power, W[b]	Drying time, sec	Atomization power, W[b]	Atomization temp., °C	Atomization time, sec	Monochromator spectral bandpass, nm	Analysis wavelength, nm
Tl	10	11	130	1650	1	0.8	276.79
Au	6	21	250	2250	1.6	0.4	242.8
Mn	6	21	250	2250	1.6	0.1	279.48
Fe	6	21	250	2250	2	0.4	248.33
Ni	6	21	250	2250	1.6	0.4	232.0
Ag	6	11	152	1737	1.6	0.4	328.06
Zn	15	11	130	1650	1.6	0.4	213.8
Cd	6	16	130	1650	1.6	0.4	228.8
Co	6	21	250	2250	1.6	0.4	240.73
Mg	6	11	350	2500	0.5	0.4	285.21
Pt	7	11	350	2500	3	0.06	265.95
Sn	3	11	250	2250	1.6	0.4	224.61

[a] The following parameters were the same for all elements: DC hollow cathodes were used as radiation sources; sheath gas flow rate = 2 l/min; PMT supply voltage = 800 V; atomizer cooling period = 10 sec. [b] Power programmed heating.

Table IV. GBA Atomic Fluorescence Detection Limits[a]

Element	Radiation source[b]	Detection limit, μg/ml	Reference
Cd	PHCL	0.002	This work
Zn	PHCL	0.2	This work
Hg	PHCL	0.01	This work
Pb	PHCL	0.005	(5)
Cd	MVL	0.005	(1)
Zn	MVL	0.005	(1)

[a] Signal-to-noise ratio = 2. [b] PHCL = pulsed hollow cathode lamp; MVL = metal vapor discharge lamp.

Table V. GBA Atomic Absorption Detection Limits[a]

Elements	Detection limit, μg/ml[b]
Cd	0.0005
Zn	0.0005
Tl	0.04
Pb	0.01
Cu	0.01
Mn	0.006
Mg	0.002
Sn	0.1
Au	0.02
Ag	0.007
Fe	0.004
Ni	0.02
Co	0.004
Pt	0.9

[a] Signal-to-noise ratio = 2. [b] All detection limits except for Pb and Cu were obtained in this work. The Pb and Cu detection limits were reported in reference (1).

were performed by atomic fluorescence. Table IV summarizes the detection limits (signal-to-noise ratio = 2) obtained for these elements along with those reported previously (1, 5). The high detection limit for Zn with a pulsed hollow cathode lamp is due to the lack of primary source intensity, since a metal vapor discharge lamp gave a significantly lower limit of detection. All of the analytical curves showed good linearity over 1.5–3 orders of magnitude in concentration.

Atomic absorption data were obtained for Cd, Zn, Tl, Mn, Mg, Sn, Au, Ag, Fe, Ni, Co, and Pt using dc hollow cathode lamps as the radiation sources. The detection limits of these elements as well as detection limits for Cu and Pb (1) are summarized in Table V. Analytical curves were obtained for all the above elements except Tl and Pt, and all working curves exhibited good linearity over 1.5–3 orders of magnitude.

The relative standard deviation of measurements both in AA and AF was usually between 4–7% at concentrations one order of magnitude greater than the detection limits. Since the above data were obtained without a rigorous optimization of instrumental parameters, it can be expected that detection limits and the linear dynamic range can probably be improved substantially if the system is fully optimized (3).

Matrix Effect Studies with the GBA. One of the major advantages of the GBA over the other filament-type atomizers is that when the sample is placed on the atomizer, it soaks down between the graphite fibers. Heating the fibers produces a furnace-type environment with a high surface area. Since the sample is trapped by the fibers, the diffusion rate of atomized particles should be influenced, and this should decrease the amount of interference. Because of the high temperature and the furnace-like environment of the GBA, most matrix effect interferences should not occur on the atomizer, but should occur in the cold environment above the filament atomizer.

A brief study was carried out to test for matrix interferences on the atomic absorption of Fe, Ni, Mn, and Cd and on the atomic fluorescence of Cd. The concentration of each analyte element was 200 ppb. Each analyte element was tested for interferences from the following species present in 10-fold excess: $AlCl_3$, $CoCl_2$, $Co(NO_3)_2$, $Cu(NO_3)_2$, $FeCl_3$, $MgCl_2$, $MnCl_2$, $NiCl_2$, $Pb(NO_3)_2$, $Zn(NO_3)_2$, HCl, and HNO_3. A significant depression (10%) of the Fe AA signal was found for cobalt salts, while minor depressions (<5%) of the Ni AA signal were found for Al, Cu, Fe, Mg, and Mn salts. No other significant interferences were noted at these levels. An extensive investigation of the severity and mechanisms of matrix interferences with the GBA is presently being carried out in these laboratories.

Table VI. Experimental Parameters for Analysis of Iron and Copper in Serum with the GBA

Element	Drying temp., °C	Drying time, sec	Ashing temp., °C	Ashing time, sec	Atomization temp., °C	Atomization time, sec	Cooling period, sec
Fe	100	15	600	30	2250	3.0	25
Cu	100	10	500	25	1900	2.5	25

Table VII. Experimental Results for Analysis of Iron and Copper in Serum with the GBA

Element	Supplier values, μg/100 ml	GBA results, μg/100 ml
Fe	204	207 ± 15.6
Cu	220	221 ± 19.8

Application of the GBA to a Real Chemical System. Analyses of Cu and Fe in a serum sample were conducted by AA. The serum sample contained 220 and 204 μg/100 ml copper and iron, respectively, as reported by the supplier. These concentrations, however, are above the linear region of the copper and iron calibration curves. Several methods can be employed to obtain analytical curves that are linear to higher concentrations. These methods include dilution of the sample with either deionized water or an organic solvent; use of a smaller sample volume; increasing the vertical distance between the GBA and the light beam from the hollow cathode lamp; and use of a less sensitive spectral line. Each method exhibits certain limitations. Dilution is time-consuming and use of sample volumes smaller than about 0.2 μl increases the relative error of dispensation and sample deposition, and the danger of non-representative sampling. Increasing the distance between the GBA and the light beam to about 10 mm is satisfactory for simple matrices, but there is the possibility of enhancing chemical interferences with the complex serum matrix.

The technique actually chosen was a combination of the above methods. In both cases, a sample volume of 1 μl was

used, and the vertical distance between the GBA and the light beam was increased to 5 mm. The serum sample was also diluted 10-fold with deionized water. Although the 372-nm iron line has a sensitivity about one-fifth that of the 248.3-nm line, the use of this line was discarded because of continuum emission interference from the GBA.

Using the power technique for heating the GBA and the above conditions, analytical curves were linear to about 3 μg/ml for aqueous standards of copper and iron. The concentrations of copper and iron were then obtained from the standard addition analytical curves under the conditions shown in Table VI. In both cases, the absence of non-specific absorption was substantiated by monitoring nearby non-resonance lines as well as by use of a deuterium continuum source at the analysis wavelengths. The analytical results are summarized in Table VII and again indicate the capability of GBA to handle complex samples.

RECEIVED for review March 22, 1974. Accepted June 24, 1974.

Detection and Analysis of Protein Functional Group Modification by X-Ray Photoelectron Spectrometry

Merle M. Millard and Merle Sid Masri

Western Regional Research Laboratory, Agricultural Research Service, U.S. Department of Agriculture, Berkeley, Calif. 94710

The elemental composition of solids can be determined from X-ray photoelectron spectroscopy (XPS) data (*1–4*). The elemental photoejected core electron line intensity can be related quantitatively to elemental composition by constructing calibration curves for a given instrument and excitation source. The calibration curve is a relationship between the percent elemental composition of known standards and the measured elemental line intensity. The factors affecting the line intensity corrections are discussed by Siegbahn *et al.* (*1*). Using calibration curves and core electron line intensities, Siegbahn was able to determine the elemental composition of organic compounds containing carbon, chlorine, sulfur, and nitrogen such as chlorosulfonates and amino acids, generally within ±5% accuracy (*1*). The copper and zinc content in brass samples was determined to within ±5%.

Klein and Kramer (*2*) determined the nitrogen and sulfur content of grain protein in barley, wheat, oats, and kidney beans from the nitrogen and sulfur core electron line intensities. Instrument elemental sensitivity factors for nitrogen and sulfur line intensities were determined by mixing known amounts of sodium chloride with cystine and measuring the sodium, nitrogen, and sulfur core electron line intensities for these known samples. The agreement between chemical analysis and XPS was quite satisfactory.

Swartz and Hercules (*3*) have employed this core electron line intensity calibration method to analyze mixtures of MoO_2 and MoO_3. A relative standard deviation of 2% was reported in their paper. The sensitivity of detection of different elements by XPS varies considerably. The most important factor determining elemental line intensity is the atomic cross-section for photoelectric absorption of incident photons. The sensitivity for elemental core electron detection is usually determined for a given type of instrument by an empirical calibration procedure. Wagner (*5*) published a table of elemental core electron sensitivities obtained by examining the spectra of a variety of sodium- and fluorine-containing compounds. Sensitivities as estimated by line height and area were determined. The elemental core electron sensitivity varies by a factor less than a thousand for the elements studied. This relative sensitivity of detection can be quite important in terms of analysis time and accuracy when the element to be estimated is present in low concentration. Another problem, especially when long run times are necessary, is the possibility of radiation damage to the sample (*6, 7*). Short sample run times are particularly desirable from this standpoint.

Although the analytical potential of XPS is well documented and current instrumentation is capable of improved accuracy, very little work has been reported in the field of protein chemistry. Siegbahn *et al.* (*1*) determined the elemental composition of insulin to within 5 to 10%. Several binding energy studies of metallo proteins have been reported (*8–10*).

In this note, we report the analysis of modified proteins by XPS. This technique is most accurate when the specific reagent for chemical modification contains elements of high detection sensitivity such as fluorine and mercury. When specific reagents for protein modification are used, it is possible to estimate the functional group content of the protein. Although XPS analyzes only the surface of solids, we believe that this surface analysis is representative of the bulk sample in this case.

EXPERIMENTAL

Core binding energies were determined using a standard Du Pont 650 electron spectrometer with a magnesium anode. The X-ray source was operated at standard voltage and current. Samples were run as ground powder pressed into pellets ¼-inch in diameter. Approximately the entire surface of the pellet was exposed to

(1) K. Siegbahn, C. Nordling, A. Fahlman, R. Nordberg, K. Hamrin, J. Hedman, G. Johnson, T. Bergmark, S.-E. Karlson, I. Lindgren, and B. Lindberg, "ESCA, Atomic, Molecular, and Solid State Structure Studied by Means of Electron Spectroscopy," Almqvist and Wiksells AB, Stockholm, 1967.
(2) M. P. Klein and L. N. Kramer, "Improving Plant Protein Nucl. Tech. Proc. Symposium," *Lawrence Berkeley Lab. Tech. Rep.*, 243–52, (1970); *Chem. Abstr.*, **75**, 105912a (1971).
(3) W. E. Swartz and S. M. Hercules, *Anal. Chem.*, **43**, 1774–9 (1971).
(4) G. O. Kohler, M. M. Millard, S. C. Witt, and H. G. Walker Jr., Abstracts of the 58th annual meeting of the American Association of Cereal Chemists, St. Louis, Mo., November 4, 1973, No. 81, Published in *Cereal Sci. Today*, **18**, 293 (1973).
(5) C. D. Wagner, *Anal. Chem.*, **44**, 1050–53, (1972).
(6) T. A. Carlson, K. L. Cheng, and J. C. Carver, *Inorg. Chem.*, **12**, 1702–4, 1973.
(7) J. A. Ibers, J. P. Collman, C. P. Brock, G. Dolcetti, P. H. Farnham, J. E. Lester, and C. A. Reed, *Inorg. Chem.*, **12**, 1304–13 (1973).
(8) L. N. Kramer, Ph.D. Thesis, University of California, Berkeley, Calif., 1971.
(9) D. Leibfritz, *Angew. Chem., Int. Ed. Engl.*, **11**, 232 (1972).
(10) U. Wesser, G. Jung, M. Ohnad, W. Bohenkamp, and W. Bremeser, *Biochim. Biophys. Acta*, **295**, 77–86 (1973).

Table I. Elemental Core Electron Line Intensity Data for Mercuripapain

	Hg 4f7/2 line intensity	Corrected intensity[a]	Nitrogen 1S line intensity	Corrected intensity[a]	Sulfur 2P line intensity	Corrected intensity[a]
Mercuripapain	384	100	12,420	29,600	576	1,250
Number of scans	400		100		400	
	N/Hg		S/Hg		N/S	
	Calcd[b]	XPS	Calcd	XPS	Calcd	XPS
Atom ratio	302	296	14	12.5	21.7	23.7

[a] Observed intensity divided by Wagner's sensitivity factors (5). [b] Based on the amino acid content established by the structure determined by X-ray diffraction (11).

Table II. Line Intensity Data for Determination of Mercury $4f_{7/2}$ Line Height Sensitivity Factor

Compound	Sulfur line intensity	Corrected intensity[a]	Mercury line intensity	Mercury line height sensitivity factor
HgS	4130	8970	34,490	3.85
	Chlorine line intensity	Corrected intensity[a]		
$HgCl_2$	9240	16800	32,350	3.85

[a] Observed intensity divided by Wagner's (5) sensitivity factor. Wagner's sensitivity scale is normalized to the fluorine 1S line.

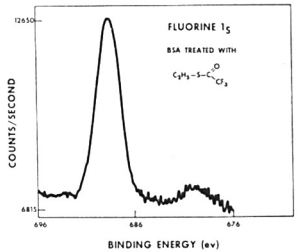


Figure 1. The fluorine 1S line from trifluoroacetylated bovine serum albumin

Table III. Nitrogen and Fluorine Core Electron Line Intensity and Wet Chemical Analysis Data for *N*-Trifluoroacetylated Bovine Serum Albumin

Sample	NIS counts/sec	Corrected intensity[a]	FIS counts/sec	N/F atom ratio	N/F atom ratio, wet chemical analysis
M-196					
Run 1	15,800 ± 100	37,600	9,700 ± 200	3.88	4.45
Run 2	20,800 ± 100	49,600	10,700 ± 100	4.63	
M-197					
Run 1	12,900 ± 100	30,700	6,450 ± 100	4.75	
Run 2	16,700 ± 100	39,750	8,350 ± 100	4.76	5.02

[a] Observed intensity divided by Wagner's sensitivity factor (5).

radiation. A routine scan rate of one electron volt per centimeter was used. The recorder sensitivity was selected so that the amplitude of the peak was almost full scale. The nitrogen 1S and fluorine 1S binding energies were determined by a single scan over the binding energy region. An 18-electron volt scan width was used. The number of scans used to obtain the core electron binding energies for mercuripapain are given in Table I for each element. A box car smooth plot was used for these data.

Line intensities were determined by manually estimating a base line and measuring the peak height at half-width. The nitrogen and fluorine 1S line widths were 2.0 ± 0.1 eV. Atom ratios were determined by dividing the line intensity by sensitivity factors taken from Wagner's data (5). The mercury $4f_{7/2}$ line height sensitivity factor was determined from the data in Table II. Bovine serum albumin (BSA) was supplied by Sigma Chemical Company, St. Louis, Mo. Mercuripapain was supplied by Worthington Inc., Freehold, N.J., BSA was *N*-trifluoroacetylated using ethyl thioltrifluoroacetate according to Goldberger (12). The ethyl thioltrifluoroacetate reagent was prepared according to Hauptschein *et al.* (13).

(11) J. Drenth, J. N. Jansonius, R. Koekoek, A. M. Swen, and B. G. Wolthers, *Nature (London)*, **218**, 929 (1968).
(12) R. F. Goldberger, in "Methods in Enzymology" Vol. 11, C. H. W. Hirs, Ed., 1967, p 317.
(13) M. Hauptschein, C. S. Stokes, and E. A. Nodiff, *J. Amer. Chem. Soc.*, **74**, 4005 (1952).

RESULTS AND DISCUSSION

As an example of the introduction of fluorine into a protein to label and detect a functional group, we *N*-trifluoroacetylated the ϵ-amino group of lysine in bovine serum albumin (BSA). The nitrogen 1S and fluorine 1S core binding energy lines were determined using a single scan over the appropriate electron energy region. The fluorine 1S core electron line obtained on a typical sample of *N*-trifluoroacetylated BSA is shown in Figure 1. The fluorine 1S line is 5800 counts above background and is more than adequate for an accurate line intensity measurement. The *N*-trifluoroacetylated BSA samples were also analyzed for fluorine and nitrogen by wet chemical analysis. The nitrogen to fluorine atom ratio calculated from XPS line intensity data and the nitrogen to fluorine atom ratio obtained from wet chemical analysis are shown in Table III. The average values of the elemental ratios as determined by XPS data and wet chemical analysis agree within 5%. The precision of the atom ratios determined from XPS data for sample M197 was excellent and much poorer for sample M-196. We believe that the agreement among the results for M-197 is more typical of the precision to be expected from XPS

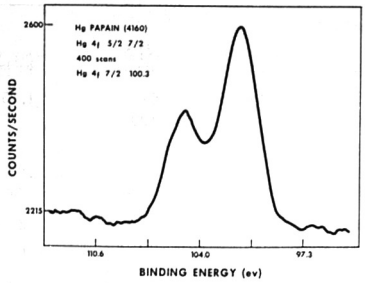


Figure 2. The mercury $4f_{5/2,7/2}$ line from mercuripapain

data. The instrument time required for a single scan is less than five minutes for each element per sample. It should be possible to detect and analyze the fluorine content in modified proteins at considerably lower fluorine levels by multiple scanning.

During the course of studies on the binding of mercury to proteins, we found that mercury has a relatively high sensitivity factor. We determine the peak height sensitivity factor to be 3.85 from electron line intensity measurements on HgS and $HgCl_2$ and the sensitivity determined by Wagner for sulfur and chlorine (*5*). The data necessary for determination of the mercury $4f_{7/2}$ line height sensitivity factor are presented in Table II.

As an example of the detection of mercury in proteins, we present the line intensity data obtained for mercuripapain in Table I. Mercuripapain contains one atom of mercury in approximately 42,000 molecular weight. The mercury $4f_{7/2}$ line is intense enough to allow fairly accurate detection and estimation (Figure 2). The mercury content of mercuripapain is 0.5%.

In cases where mercury reagents react specifically with the sulfhydryl group, the sulfhydryl group content of the protein can be estimated from mercury binding-energy measurements.

RECEIVED for review April 11, 1974. Accepted June 24, 1974. Reference to a company or product name does not imply approval or recommendation of the product by the U.S. Department of Agriculture to the exclusion of others that may be suitable.

Determination of Molybdenum in Plutonia Cermets by X-Ray Fluorescence Spectrometry

H. A. Woltermann and W. W. Strohm

Monsanto Research Corporation, Mound Laboratory, Miamisburg, Ohio 45342

Pressed disks of molybdenum-coated PuO_2 are fabricated at Mound Laboratory for use as heat sources in the Viking and Pioneer space missions (*1*). The molybdenum matrix is intended to contain the highly radioactive PuO_2 in the event of reentry during an abortive space mission.

PuO_2 shards in the size range from 105 to 250 μm are coated with molybdenum metal by reduction of $MoCl_5$ vapors. These coated shards are then pressed into a disk under high temperature and pressure. The resultant disk is in turn coated by $MoCl_5$ reduction.

To obtain the proper containment of plutonium and yet allow the power density needed for the heat source, it is necessary to control the amount of molybdenum coating to 16–19 wt % of the coated shard. Consequently a rapid, reliable molybdenum determination is needed, both prior to pressing the disk, and after the product is finished. Because of the high radioactivity of plutonium-238, this determination must be performed in an alpha box.

An EDTA titration of molybdenum had been employed for this purpose (*2*). However, several serious drawbacks were associated with this method. Lengthy fuming steps with HCl were required to remove the HNO_3 used in dissolving the molybdenum metal. These HCl fumes attacked the stainless steel alpha box, resulting in extremely poor working conditions. Largely because of these conditions, periodic biases were obtained on batches of fuel.

EXPERIMENTAL

X-Ray fluorescence spectrometry affords a reliable, specific method of analysis. In initial attempts using molybdenum-coated ThO_2 as a stand-in for PuO_2, the shards were ground into a fine powder and mounted directly in the X-ray beam of a Siemans X-ray Fluorescence Spectrometer (Siemans America, Inc., 186 Wood Ave. South, Iseline, N.J.). The ratio of Mo Kα to Th Lβ_1 counts was highly dependent on the degree of grinding, and reliable data could not be obtained. This particle size effect could be removed by dissolving the molybdenum metal and counting the resulting molybdenum solution. However, with plutonium samples, containment of the radioactive solution for counting on the nonradioactive spectrometer would be difficult.

A method employing small disks of filter paper as the supporting matrix was then used (*3*). A 1-g sample of the fuel is weighed into a 25-ml volumetric flask. The molybdenum is readily dissolved by addition of 5 ml of 3*N* HCl, then 2.5 ml of concentrated HNO_3. The solution is warmed to dispel excess nitrogen oxides, and diluted to volume with H_2O. After the insoluble PuO_2 settles, a 2-ml aliquot of the molybdenum solution is pipetted into a plastic vial and mixed with a 0.5-ml aliquot of the internal standard niobium solution. Twenty microliters of this solution is then pipetted onto a filter disk (Whatman No. 40 filter paper) of ½-in. diam, which is attached by double-sided tape to a polystyrene sheet of 0.125-mm thickness. After the disks are dried (approximately 1 hr at room temperature), they are pulled from the alpha box into small plastic bags, which are then thermally sealed. The exterior surfaces of the bags are monitored to ensure the absence of alpha activity. The filter disks are counted at 20.25° (Mo Kα), 20.90° (background), and 21.32° (Nb Kα) for 2 min using the LiF crystal on the Siemans X-ray Spectrometer. Calculation of a molybde-

(1) R. R. Jaeger and S. J. Cohen, "Proceedings of the Third International Conference on Chemical Vapor Deposition," F. A. Glaski, Ed., American Nuclear Society, Hinsdale, Del., 1972, pp 500–512.
(2) E. Lasner and R. Scharf, *Fresenius' Z. Anal. Chem.*, **167**, 114 (1959).
(3) J. M. McCall, D. E. Leyden, and C. W. Blount, *Anal. Chem.*, **43**, 1324 (1971).

Table I. Molybdenum Samples

Sample	Percentage of molybdenum	
	Trial 1	Trial 2
231-232	16.00	15.99
237-238	18.94	18.76
233-234-236	20.09	20.16
236-239	19.62	18.77
118B	18.92	19.12
120T	16.44	16.64
223-224	20.34	20.24
244LA1	17.62	17.29
239-240-244	21.78	21.89
238LA3	15.55	15.59
240LA4	17.61	17.99
E. NUNN	15.56	15.77
247LA1	16.61	16.22
248LA3	20.09	19.95
247-248-SA1	18.26	18.27

Standard deviation (4) = $\sqrt{(\Sigma(\text{difference between duplicates})^2)/2n}$ where n = number of sets of duplicates. Relative standard deviation (rsd) = (standard deviation × 100)/mean value. rsd = 1.24%.

Table II. Molybdenum Standards

Standard no.	Amount of molybdenum, Grams		Bias, %[a]
	Theor	Found	
1	0.1146	0.1146	0.00
2	0.1146	0.1165	+1.66
3	0.1146	0.1126	−1.75
4	0.1146	0.1150	+0.35
5	0.1146	0.1149	+0.26
6	0.1146	0.1152	+0.52
7	0.1146	0.1158	+1.05
8	0.1162	0.1155	−0.60
9	0.1988	0.1983	−0.25
10	0.2195	0.2220	+1.14
11	0.2195	0.2195	0.00
12	0.2195	0.2195	0.00
13	0.2195	0.2187	−0.36
14	0.2195	0.2190	−0.23

Standard deviation = $\sqrt{(\Sigma(\bar{X} - Xi)^2/(n-1)}$, where $\bar{X}$ = mean, Xi = individual determinations, n = number of determinations. Relative standard deviation (rsd) = (standard deviation × 100)/mean. rsd on 0.1146-g standard = 1.06%. rsd on 0.2195-g standard = 0.60%.

[a] Av Bias = +0.13%.

num-to-niobium ratio corrected for background (Mo − background/Nb − background), and interpolation of a standard curve, yield the weight of molybdenum present in the sample. Two standard molybdenum samples are run with each series of samples to ensure the reliability of the method.

RESULTS

Table I lists the results of a series of determinations on actual production samples. The relative standard deviations between duplicates is 1.2%, compared to 1.9% typically attained by the EDTA method. Table II shows the results of a series of standards, prepared from 99.99% molybdenum wire and run with these samples. Typical counts accumulated for a 17% molybdenum sample are: Mo Kα = 260,000; background = 110,000; Nb Kα = 220,000. A root mean square propagation of errors due to counting statistics yields a 0.7% relative standard deviation. The counting statistics appear to be the major uncertainty in determination of the molybdenum-to-niobium ratio.

To ensure that molybdenum had been quantitatively dissolved from the fuel, the residue from several molybdenum-coated ThO_2 samples, used as a substitute for the highly radioactive plutonium cermet, was submitted for both emission spectroscopy and atomic absorption spectrophotometry. Less than 0.01% molybdenum was found in the residue. To ensure that small amounts of plutonium would not interfere with X-ray fluorescence determination, 0.02 g of plutonium was dissolved with 0.20 g of molybdenum. Ninety-nine percent of the theoretical molybdenum value was obtained, indicating no serious plutonium interference at this level.

An energy dispersive X-ray system (Kevex Corporation, 898 Mohler Road, Burlingame, Calif.) using a Si(Li) detector and an ^{241}Am exciter source of 10 mCi in an annular ring configuration was evaluated for this measurement. The use of the energy dispersive system offers the advantages that the entire X-ray spectrum, in the desired energy range, is obtained with a single measurement; and that the data can be conveniently reduced by a minicomputer. Data gathered on standard molybdenum samples yielded a precision similar to that from the Siemans unit. However, the actual samples were contaminated with plutonium-238 which has an alpha half-life of 87.78 ± 0.02 years (5). Since the sample is viewed directly by the Si(Li) detector, characteristic uranium X-rays, which follow the alpha decay of plutonium-238, obscured the Mo Kα and the Nb Kα X-ray peaks. Both an exciter source with an intensity a few orders of magnitude greater than the 10 mCi of the ^{241}Am source, and a subsequent mechanical reduction of total radiation (both characteristic X-rays and plutonium caused radiation), are required for these measurements on radioactive samples. Such energy dispersive systems using X-ray tubes are now commercially available (*e.g.*, from Kevex Corp.).

The determination of molybdenum by X-ray fluorescence spectrometry using the Siemans spectrometer and filter disk slides has proved to be a more rapid, specific, and reliable method than the EDTA titration method. This X-ray method has permitted the analysis of radioactive materials on a nonradioactive spectrometer without degenerating the alpha boxes. The method is now used routinely for determination of molybdenum in cermet fuel.

ACKNOWLEDGMENT

The authors thank G. E. Hapner for his work in preparing and counting the slides used in this work, and R. R. Eckstein for his help in the operation of the X-ray equipment.

RECEIVED for review March 1, 1974. Accepted June 19, 1974. Mound Laboratory is operated for the U.S. Atomic Energy Commission by Monsanto Research Corporation under Contract No. AT-33-1-GEN-53.

(4) W. J. Youden, "Statistical Methods for Chemists," John Wiley and Sons, New York, N.Y., 1961, p 16.

(5) K. C. Jordan, "Half-life of Plutonium-238," presented at the Second International Conference of Calorimetry and Thermodynamics, Orono, Me., July 12–14, 1971. [*Phys. Abstr.*, **74**, 63772 (1971)].

Quantitative Determination of the Phase I/Phase II Ratio in Sodium Triphosphate by Raman Spectrometry

Jan Bus

Unilever Research Vlaardingen, Olivier van Noortlaan 120, Vlaardingen, The Netherlands

Sodium triphosphate (STP) is used as a builder in washing powders and it is to be expected that this situation will not change until an acceptable substitute has been developed.

An important step in the production of washing powders is the spray-drying of the slurry which contains all the ingredients. The properties of this slurry depend largely on the ratio of phase I and phase II, the two crystal modifications, in which STP can occur. This is explained in the following way:

Phase I is stable at temperatures >410 °C (*1*) and metastable at room temperature, while phase II is stable at room temperature. This difference in stability is the cause of the much higher hydration rate (to $Na_5P_3O_{10}$·6 H_2O) of phase I than that of phase II.

STP·6H_2O dissolves slowly and the rate of formation from STP determines certain important slurry properties (*e.g.*, viscosity).

Hence, the phase I/phase II ratio is an important parameter for the factory or the pilot plant.

Three different methods exist for the determination of phase I and phase II concentrations in STP samples.

1) The temperature rise test (*2, 3*), in which the temperature increase of a well defined mixture of STP and glycerol is measured after the addition of a known amount of water. It is assumed that in this medium only STP-I reacts with water which causes the temperature rise. The method is easily performed but not very accurate, possibly because this assumption is incorrect.

2) The infrared spectrometric method described by Corbridge and Lowe (*4*) by which the phase I content is determined from the difference in absorbance at 707 and 797 cm^{-1}. As hexahydrate also absorbs at 707 cm^{-1}, the method can only be used for samples containing no hexahydrate which, however, is never the case in commercial samples. A second drawback is the possibility of phase transitions during the pressing of the potassium bromide disks.

3) X-Ray diffraction methods which utilize the intensities of the characteristic diffraction lines of the various components in the mixture. Mabis and Quimby (*5*) were the first to describe an application for STP mixtures, but modified procedures are used as well (*6*). The X-ray method gives serious problems for samples containing STP·6H_2O, due to the usually severe preferred orientation of the hexahydrate crystallites (*6*).

In this paper, the results of an investigation of Raman spectrometry (*7, 8*) as a method for the quantitative analysis of STP samples are presented.

EXPERIMENTAL

Materials. The three STP samples were prepared as described by Troost (*1*) and the remaining materials purchased from Merck, Darmstadt (Na_3PO_4·12H_2O and $Na_4P_2O_7$·10H_2O) and from Riedel-de Haën AG, Seelze-Hannover ($Na_4P_2O_7$). Na_3PO_4 was prepared by dehydration of Na_3PO_4·12H_2O at 100 °C in vacuo.

The weighed components were gently mixed in an agate mortar. Thorough mixing, if necessary, must be carried out in a closed ball mill. Grinding in an open mortar lowers the phase I/phase II ratio.

Apparatus and Procedure. The spectra were measured on a Cary 82 Laser Raman Spectrometer of the Chemical Technology Department of the University of Technology, Eindhoven. The 514.5-nm argon ion line of a Spectra Physics Model 165 laser was used. The small positive lens which normally focuses the laser beam at the sample had to be removed to obtain a larger spot on the sample surface. The *focused* beam may accidentally hit a relatively large crystal of only one of the components which would lead to erroneous results. Most of the measurements were repeated after rotating the sample about 90° along an axis perpendicular to the sample surface.

The standard Raman sample holder for solids was dipped into the phosphate powder until the conical opening was completely filled, and pressed against a piece of glass in order to obtain a flat surface. Only a few milligrams of the sample are needed.

The sample preparation time is less than one minute. If the sample is homogenized in a ball mill for one minute, the total time for sample manipulation becomes about three minutes. The measurement of the spectrum took about 15–20 min in our experiments but this might be different for other types of Raman spectrometers.

RESULTS AND DISCUSSION

Raman Spectra of the Phosphates. Raman spectra were measured of $Na_5P_3O_{10}$-I, $Na_5P_3O_{10}$-II, $Na_5P_3O_{10}$·6H_2O, $Na_4P_2O_7$, $Na_4P_2O_7$·10H_2O, Na_3PO_4, and Na_3PO_4·12H_2O.

Inspection of the STP spectra reveals that the best region for a quantitative determination of the phase I/phase II ratio is that between 900 and 1040 cm^{-1}. Figure 1 shows these spectra of the three individual STPs and an approximate 1:1:1 mixture. Anhydrous Na_3PO_4 shows two bands at 1018 and 936 cm^{-1} (intensity ratio 14:100) and Na_3PO_4·12H_2O gives bands at 1034, 1009, 971, and 943 cm^{-1} (intensity ratios 24:25:55 . 5:100). In the commercial STP samples, no sodium orthophosphate bands could be detected. The situation is quite different for sodium pyrophosphate. In the spectrum of the dehydrated sample, a very sharp band is present at 1032 cm^{-1} (halfwidth 7 cm^{-1}) and the hydrated sample gives a broader band at 1026 cm^{-1} (halfwidth 15 cm^{-1}). One or both of these bands are present in spectra of many samples with variable, but relatively small intensities. See the band at about 1030 cm^{-1} in the two (bottom) spectra of Figure 1 which probably corresponds to a decomposition product of STP. If there is no difference, or only a small difference in intensity per standard quantity for both types of sodium pyrophosphate, then this band can be used for measuring the amount of pyrophosphate in STP mixtures. This was not investigated in the present experiments.

STP-I, which is probably not completely free of its hexahydrate, has a very strong peak at 1014 cm^{-1} which is well separated from the Raman lines of STP-II and STP·6H_2O (Figure 1). The sample of STP-II might also contain a small amount of hexahydrate; both have a 992 cm^{-1} band

(1) S. Troost, Thesis Groningen, **1969**, 14.
(2) J. D. McGilvery, *Amer. Soc. Test. Mater. Bull.*, **191**, 45 (1953).
(3) J. Seiffarth and D. Zobel, *Chem. Technol.*, **20**, 490 (1968).
(4) D. E. C. Corbridge and E. J. Lowe, *Anal. Chem.*, **27**, 1383 (1955).
(5) A. J. Mabis and O. T. Quimby, *Anal. Chem.*, **25**, 1814 (1953).
(6) A. A. W. A. van Eulem, this laboratory, private communication 1973.
(7) P. J. Hendra and C. J. Vear, *Analyst (London)*, **95**, 321 (1970).
(8) H. A. Szymanśky, Ed., "Raman Spectroscopy," Plenum Press, New York, N.Y., 1967.

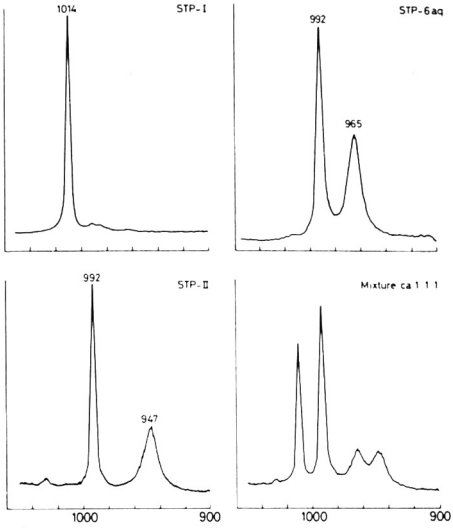


Figure 1. Raman spectra of three STPs and a 1:1:1 mixture of them in the 900–1050 cm^{-1} range

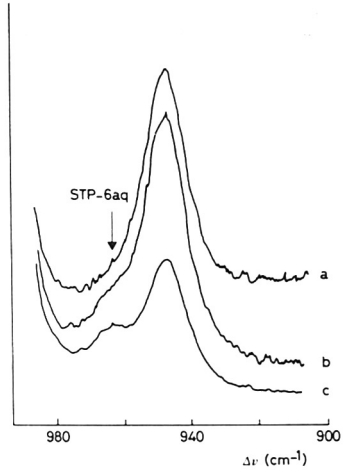


Figure 2. Raman spectra of three STPs with various relative amounts of STP-II and STP·6H_2O; *a* and *b*: ~75% STP-II, *c*: ~40% STP-II

and the broad 965 cm^{-1} band of STP·6H_2O might be hidden in the high-frequency side of the 947 cm^{-1} band of STP-II.

The Phase I/Phase II Ratio of STP. If the mixtures contain only STP-I and STP-II, the ratio between the two can be calculated directly from the ratio of the peak heights or areas by means of a calibration line. Due to the presence of small amounts of STP·6H_2O in many samples (Figure 2; shoulder at ~965 cm^{-1}), it is necessary to use peak heights for the calculation.

From the spectrum of the pure sample, it can easily be concluded that the 965 cm^{-1} peak of STP·6H_2O contributes less than 5% of its maximum height to the signal at 947 cm^{-1}. Moreover, in all industrial samples, the hexahydrate content is much smaller than the phase II content. The 965/947 cm^{-1} peak intensity ratio is approximately the same as the STP-6aq/STP-II ratio (Figure 1, mixture spectrum). The error in the 947 cm^{-1} peak height will be smaller than 2% if this ratio is smaller than 0.40. In a first approximation, the contribution of the hexahydrate signal to the 947 cm^{-1} peak height can be neglected.

Tangential base lines are drawn from about 920 cm^{-1} to about 975 cm^{-1} and from about 975 cm^{-1} to about 1045 cm^{-1}. In the exceptional cases where the minimum between the pyrophosphate peak and the phase-I peak is lower than this line, the tangent is drawn along this minimum; hence from about 975 cm^{-1} to about 1024 cm^{-1}. Now the peak heights (I) are measured. For ease of calculation, the difference in peak height per unit weight for the 1014 cm^{-1} peak (STP-I) and the 947 cm^{-1} peak (STP-II) is corrected fffor with the constant factor 0.326. If $A = 0.326\ I_{1014}$ and $B = I_{945}$, then $100\ A/(A + B)$ is the percentage of STP-I of the total amount of dehydrated STP. The results are given in Table I. A time interval of about one month lies between the measurements shown above and below the dotted line. The deviations from the mean value of duplicate measurements are less than 2% in nearly all cases which makes this method very attractive. The standard deviation is 2.3%.

Table I. Measured Heights for the Raman Lines at 1014 cm^{-1} ($\times 0.326$) (A) and at 945 cm^{-1} (B) for Various Known STP Mixtures. The Fourth Column Shows the Calculated Phase-I Percentages and the Last One, the Differences with the Known Values

STP-I, wt %	A	B	$\frac{100A}{(A+B)}$	Δ
5.2	0.69	10.73	6.0	+0.8
	0.69	9.65	6.7	+1.5
13.9	1.86	10.50	15.0	+1.1
	1.53	10.56	12.7	−1.2
25.0	3.46	10.64	24.5	−0.5
	2.99	10.46	22.2	−2.8
50.3	7.04	7.49	48.5	−1.5
	7.56	6.78	52.7	+2.4
65.9	7.26	3.85	65.3	−0.6
	5.93	3.08	65.9	0
	6.90	2.78	71.3	+5.3
79.7	7.42	1.88	79.8	+0.1
	7.19	2.00	78.2	−1.5
5.2	0.63	9.30	6.3	+1.1
	0.59	9.30	6.0	+0.8
25.0	2.74	10.02	21.5	−3.5
50.3	6.37	5.40	54.1	+4.1
	6.32	5.78	52.2	+1.9

To check the importance of the hexahydrate content, a mixture of 39.8 mg STP-I, 40.5 mg STP-II, and 39.8 mg STP·6H_2O was measured. Using the procedure as outlined above, an experimental phase-I percentage of 50.6 was found. Calculation from the weighed amounts gives 49.6% (again of the total dehydrated STP), which justifies the use of the method described.

CONCLUSION

The Raman spectrometry method for a quantitative determination of the percentage STP-phase I with respect to the total amount of dehydrated STP is very promising. The presence of STP·6H_2O does not influence the result, if its quantity is less than 40% of the phase-II amount. This is always the case in STP made for detergents manufacturing.

Curve resolution of partially overlapping peaks at 947 cm^{-1} and 965 cm^{-1} may make it possible to quantify also the small amounts of STP·6H_2O.

ACKNOWLEDGMENT

I wish to thank E. Strijks of the Chemical Technology Department of the University of Technology, Eindhoven, for measuring the Raman spectra, A. A. W. A. van Eulem and N. J. Pritchard for supplying the phosphate samples, and Th. J. Liefkens for his skillful assistance.

RECEIVED for review March 11, 1974. Accepted April 29, 1974.

CORRECTION

Thermometric Titration Determination of Hydroxide and Alumina in Bayer Process Solutions

This paper by Eric VanDalen and L. G. Ward [*Anal. Chem.*, **45**, 2248 (1973)] contains two errors in the concentrations of the sodium aluminate solutions described on page 2249. In the Reagents section, the 10th word in the 13th line should read 4*N* and not 2*N*. In the caption for Figure 1, the 2nd line of the paragraph, "Titration Conditions," the 9th word should read 12 g/l., and not 24 g/l.

Spectrochemical Method for Determination of Tellurium in Geological Materials

Irena Schoenfeld and Armand Berman

Soreq Nuclear Research Centre, Yavne, Israel

Tellurium is known as an element with a very low Clarke value, *i.e.*, a low mean concentration in the Earth's crust. It is commonly associated with other elements of the sulfur group, but it occurs at lower concentrations. Several values for Se and Te content in geological materials are given in Ref. (*1*). The determination of tellurium at such low concentrations is difficult and involves indirect procedures consisting of the formation of colored complexes of tellurium, their extraction and photometric (*2–4*) or catalytic (*5*) determination. For small amounts of tellurium, these methods require preliminary tedious chemical separation and are subject to the interference of many elements.

The purpose of the present work was to develop a spectrochemical method for the determination of tellurium in geological samples. The two standards, Sulphide-Ore 1 (McGill University, Canada) and Basalt BCR-1 (U.S. Geological Survey, Washington) were chosen as experimental materials, although tellurium had not been previously reported in analytical data for these ores (*6–8*). The presence of sulfur in Sulphide-Ore 1 and selenium in BCR-1 (*9*), however, indicated that tellurium may have been present, but remained undetected because of its low concentration and the insensitivity of the analytical methods hitherto used. Therefore, preliminary separation of tellurium by distillation in air was undertaken. Volatilization is an attractive method because it offers enrichment of trace elements without the use of additional reagents. At a temperature of about 900 °C, the vapor pressure of tellurium oxide is high enough to allow its collection at atmospheric pressure.

(1) "Lösler-Lange Geochemische Tabellen," VEB Deutscher Verlag fur Grundstoffindustrie, Leipzig, 1965, p 190.
(2) C. O. Ingamells and E. B. Sandell, *Microchem. J.*, **3**, 3 (1959).
(3) J. Jankovsky and O. Ksir, *Talanta*, **5**, 238 (1960).
(4) K. L. Cheng, *Talanta*, **8**, 301 (1961).
(5) A. E. Hubert, *U.S. Geol. Surv. Prof. Pap.*, **750-B**, 188 (1971).
(6) G. R. Weber, *Geochim. Cosmochim. Acta*, **29**, 229 (1965).
(7) F. J. Flanagan, *Geochim. Cosmochim. Acta*, **31**, 289 (1967).
(8) N. M. Sine, W. O. Taylor, G. R. Weber, and C. L. Lewis, *Geochim. Cosmochim. Acta*, **33**, 121 (1939).
(9) A. O. Brunfeld and E. Steinnes, *Geochim. Cosmochim. Acta*, **31**, 283 (1967).

EXPERIMENTAL

The analytical procedure consists of the separation and subsequent spectral determination of tellurium.

Separation of Tellurium. The separation of Te is based on distillation, using the apparatus shown in Figure 1. The inner walls of the quartz condenser are first lined with graphite by pouring a suspension of 2 parts (by weight) Aquadag (Aqua Deflocculated Acheson Graphite, Acheson Colloids Corp., Port Huron, Mich.) in 3 parts water into the quartz tube, closed at one end. After 1 minute, the tube is emptied and dried slowly by means of a stream of hot air, in order to obtain a thin uniform layer of graphite. It was experimentally established that a thickness of 0.2–0.3 mg/cm^2 graphite is the most suitable. The tube is then tightly closed with a pure graphite electrode and baked in a high temperature furnace (Type K25A) at 450 °C for 4 hours. The weighed sample (1–10 grams) is placed in a quartz vessel, which is then sealed to the condenser. The entire device is heated at 900 °C in an electric furnace. After 12 hours, the heating is interrupted, the quartz condenser is cut from the volatilization vessel, and the graphite is removed quantitatively from the condenser walls with a special quartz spatula. The graphite is weighed, ground in an agate mortar, and packed into the same electrode that served previously as a stopper. This electrode is then excited in a dc arc.

Spectral Determination of Tellurium. The sample and synthetic standards are excited under conditions given in Table I. The standards are prepared by mixing pure graphite (Specpure Johnson Mathey) with adequate amounts of oxides of Te, Se, Cd, Zn, Hg, In, Ga, Sn, Sb, Bi, Ag, and Tl—*i.e.*, all the volatile elements that can be present in sulfide and quartz sulfide ores.

Photometric measurements were made with a non-recording Jarrell-Ash microphotometer. The photographic emulsion, Ilford Q-2, sensitive to short-wave radiation was applied in order to make use of the most sensitive lines, Te I 2385 Å and Te I 2142 Å. The intensities ratio of these two lines is given in Ref. (*10*) as 1 and in Ref. (*11*) as 1.27; under our conditions the mean ratio, experimentally established, is 1.46. The shorter wavelength line is probably attenuated by the blaze angle of our spectrograph (~3000 Å); however, it has the advantage of being interference-free compared with the Te I 2385.76 Å line, which can be subject to Cr I 2385.74 Å interference. The use of both lines permits more controlled results.

(10) G. H. Harrison, "Massachusetts Institute of Technology Wavelength Tables," Wiley, New York, N.Y., 1939.
(11) W. F. Meggers, C. H. Corliss, and B. F. Scribner, "Tables of Spectral-Line Intensities," Nat. Bur. Stand. Monograph 32, Pt. 1, U.S. Govt. Printing Office, Washington, D.C.

Table I. Spectrographic and Photographic Data

Spectrograph	Jarrell-Ash Grating Spectrograph, Ebert Mounting, 3.4-m focal distance, grating 15,000 grooves/inch, first order
Slit width	40 μm
Mode of illumination	The image of the source on the collimator mirror
Source	Jarrell-Ash modified Standard Varisource, DC-arc, 10 A
Analytical lines	Te I 2385.76 Å, Te I 2142.75 Å
Electrodes	UCP graphite: upper, negative, 4.5-mm diameter with pointed end; lower, positive, 6-mm diameter, Type 1990.
Analytical gap	3 mm
Exposure time	45 sec
Photographic emulsion	Ilford Q-2
Photographic processing	3 min at 20 °C in D-19 Developer, 5 min in Kodak Acid Fixer (Jarrell-Ash Photoprocessor)

Other tellurium lines proposed for analytical purposes (*12*) were found to be too weak for our working conditions.

The separation of tellurium from the bulk of the sample permits the use of one set of standards for various specimens.

RESULTS AND DISCUSSION

The analytical curve is a plot of the log of the ratio of the intensity of the Te line to that of the background *vs.* the log of the tellurium concentration in the synthetic standards. A straight line relation was obtained. The amount of tellurium in the sample was read from the curve and the corresponding concentration calculated using the concentration factor. Since the limit of detection is 10 ppm, a considerable concentration factor is needed for samples with tellurium content at the ppb level.

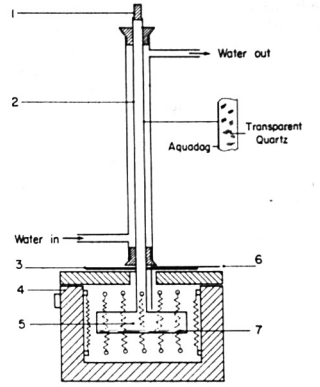


Figure 1. Apparatus for volatilization and collection of Te

(1) graphite electrode, (2) transparent quartz condenser, (3) isolating asbestos plate, (4) electric oven, (5) transparent quartz container, (6) chrome-alumel thermocouple, (7) sample

The results obtained for Sulphide-Ore 1 and Basalt BCR-1 are 0.70 ppm and 0.05 ppm, respectively. The mean standard deviation is about 20%. Since values for the tellurium content in these standards had not yet been published, the samples were submitted for activation analysis and the values 0.730 ± 0.021 and 0.054 ± 0.002 ppm obtained, respectively, confirmed the accuracy of our method (*13*).

In the spectra of the distillates, other volatile elements such as As, Sn, In, Ag, and Zn were also detected.

RECEIVED for review January 21, 1974. Accepted May 10, 1974.

(12) J. W. Mellichamp and G. C. Vezzoli, *Appl. Spectrosc.*, **26**, 106 (1972).

(13) N. Lavi, *Anal. Chim. Acta*, in press.

Voltammetry of Bismuth(III) at a Continuously Mercury-Coated Rotating Platinum Disk Electrode

M. Z. Hassan and Stanley Bruckenstein

Department of Chemistry, State University of New York at Buffalo, Buffalo, N.Y. 14214

In this note, we describe the results of initial voltammetric and anodic stripping voltammetric studies performed with a rotated continuously mercury-coated platinum disk electrode. In these investigations, 2.5×10^{-6}–$5 \times 10^{-9} M$ Bi(III) solutions were studied in acid media containing (10–100)-fold excess of Hg_2^{2+}. In an earlier publication, Mal'kov, Fedoseeva, and Stromberg (*1*) reported the determination of nanogram amounts of Sb and Bi by "amalgam polarography with accumulation" on a mercury graphite electrode. Bi and Sb were concentrated by solvent extraction prior to using anodic stripping voltammetry (ASV).

(1) E. M. Mal'kov, A. G. Fedoseeva, and A. G. Strombe, *Zh. Anal. Khim.*, **25**, 1748 (1970); Eng. transl.: *J. Anal. Chem. (USSR)*, **25**, 1499 (1970).

Florence (*2*) found electrodes formed by *in situ* deposition of Hg on a polished glassy carbon substrate to be very sensitive ($\sim 10^{-10} M$) for the determination of Pb in the presence or absence of Cu and Cd.

More recently, Johnson and Allen (*3*) illustrated the use of stripping voltammetry with collection (SVWC) at a rotating glassy carbon disk and platinum ring electrode for determining $10^{-10} M$ Ag^+ in $0.1 M$ H_2SO_4. These authors have reviewed the stripping voltammetry technique at a single electrode and pointed out some of the advantages of SVWC over conventional single electrode ASV.

(2) T. M. Florence, *J. Electroanal. Chem.*, **27**, 273 (1970).
(3) D. C. Johnson and R. E. Allen, *Talanta*, **20**, 305 (1973).

In anodic striping voltammetry, the use of a plain solid electrode fabricated from Pt or Au has a rather limited applicability for the trace determination of metals, especially in a multicomponent system. The limited applicability is due partially to low hydrogen overvoltage and primarily because of frequent irreproducibility of results and intermetallic compound formation (*4, 5*). Also, the problem of selectively leaching one component of a multicomponent deposit many atom layers thick is formidable (*6*).

A continuously mercury-coated rotating platinum disk electrode (CMCRPDE) can serve as an indicator electrode having properties and reproducibility very similar to a hanging mercury drop (HMD) electrode. A CMCRPDE does not suffer from the main disadvantage of a HMD electrode—*i.e.*, the loss of deposited metal by diffusion into the drop.

It is recognized that, for the maximum sensitivity and selectivity of ASV analyses, the ratio of the area of the indicator electrode to the mercury volume should be as large as possible (*7*). In the case of rotating platinum disk electrode (RPDE) coated with mercury during deposition of the metal ion(s) of interest, the electrode area is quite large compared to a HMD. The thickness (volume of mercury film) can be reproducibly controlled at the optimum value by varying Hg_2^{2+} concentration in the supporting electrolyte, or by controlling the rotation speed of RPDE, or by changing the time of mercury deposition. Polishing the disk of a previously Hg-coated RPDE quickly regenerates the original electrode surface, which removes the necessity of creating complicated and lengthy electrochemical pretreatments.

It has been stated that the reproducibility of ASV depends markedly on the convection pattern around the indicator electrode during the concentration step (*7*). The RPDE reproducibly controls convective-diffusion during electrodeposition. The use of high rotation speeds in the case of a RPDE decreases the diffusion layer thickness and accelerates the mass transfer process in a predictable way, and shortens the deposition time even for very dilute solutions (10^{-8}–$10^{-10}M$) (*3*).

Intermetallic compound formation among Pt, Hg, and/or any deposited metals, considerably complicates the interpretation of ASV data obtained with a CMCRPDE. The complex nature of such results can outweigh some of the advantages of CMCRPDE. As was shown earlier (*8*), Hg–Pt interactions are one of the problems in using mercury-coated platinum electrodes.

EXPERIMENTAL

Electrodes. Experiments reported in this note were performed with platinum disk electrodes of areas 0.5–0.9 cm^2.

Rotators. Low (42–1872 rpm) as well as high (400–10,000 rpm) speed rotators were used as described in reference (*9*).

Reagents. HNO_3, $Hg_2(NO_3)_2$, $Hg(NO_3)_2$, and $Bi(NO_3)_3$ were purified, prepared, and analyzed according to the methods described in reference (*10*).

Equipment. Electrolytic cell, instrument, and automatic linear voltage ramp were the same as those described elsewhere (*11–13*).

Supporting Electrolytes. The supporting electrolytes used were 0.1*M* HNO_3, 0.1*M* $HClO_4$, or 0.2*M* H_2SO_4. They were deoxygenated with purified and H_2O-saturated N_2 as described elsewhere (*13*).

Procedure. *CMCRPDE Formation and Bi Preconcentration.* A freshly pretreated RPDE was prepared in the deoxygenated supporting electrolyte by electrochemical oxidation and reduction as described elsewhere (*13*). Hg_2^{2+} solution was then added to the supporting electrolyte in (10–100)-fold excess over the metal ion to be analyzed, Bi(III). Hg was coated on RPDE either by holding E_D at 0.0 V for five minutes at 400 rpm, or by very slowly (5–10 mV/sec) scanning the RPDE between +0.55 V *vs.* SCE and the hydrogen evolution potential. E_D was then set between −0.5 and 0.0 V, the electrode rotation was stopped, and Bi(III) solution was added to the solution in the cell. Next, both Hg and Bi were plated simultaneously for the desired time on the CMCRPDE. Finally, conventional ASV data were obtained by sweeping the potential anodically at a selected scan rate (50–100 mV/sec) while rotating the electrode at 400 rpm.

Bi(III) Cathodic Voltammogram in Excess Hg(I). Cathodic voltammograms of Bi(III) in the presence of (10–100)-fold excess of Hg_2^{2+} were obtained by compensating for the Hg_2^{2+} reduction current. An anodic current equal in magnitude to the Hg_2^{2+} reduction current at 0.0 V *vs.* SCE was injected into the summing point of the current follower of the conventional 3-electrode polarograph to accomplish this.

The CMCRPDE was scanned slowly between 0.4 V and hydrogen evolution potential. Under these conditions a well-developed current–potential, *i–E*, curve could be obtained for the reduction of Bi(III) to Bi(0) on a MCRPDE. The noise level of CMCRPDE was much less than that found for the previously reported continuously mercury-coated rotated Pt wire electrode (CMCRPWE) (*10*). However, the hydrogen overpotential on a CMCRPDE was ~0.3–0.4 V less than that on a CMCRPWE. As was shown in reference (*8*), low current density in the case of a CMCRPDE is not the only cause of low hydrogen overpotential. Furthermore, studies with disk electrodes of different areas indicated that our low hydrogen overpotential was independent of Pt disk area.

As stated above, the stripping of deposited Bi was performed at 400 rpm. However, the electrolysis step for Bi was performed at higher rpm's (2500–4900 rpm) in low concentrations of Bi(III) solutions. The completion of oxidation of deposited Bi was confirmed by performing a second subsequent scan between the same voltage limits at 0 rpm.

If Bi was deposited in the absence of Hg_2^{2+} using the above procedure the reproducibility and sensitivity of the ASV analysis of the *i–E* curve were lost.

RESULTS AND DISCUSSION

Cathodic Wave for Bi(III) → Bi(0). The cathodic voltammogram of Bi(III) in 0.1*M* HNO_3, H_2SO_4, and $HClO_4$ containing 0.5–2.5 × $10^{-5}M$ Hg_2^{2+} are quite similar for $C_{Bi}^{b} > 5 \times 10^{-7}M$. $E_{1/2}$ is −0.04 V *vs.* SCE and is well-separated from that of Hg_2^{2+}. A typical *i–E* curve actually obtained for 2.5 μM Bi(III) in 0.1 *M* HNO_3 is shown in Figure 1. The large Hg_2^{2+} reduction current of 65 μA at 0.2 V was electronically compensated for as described above. As is seen in Figure 1, the Bi(III) wave is well-formed, and the limiting current region is flat over a 0.5-V range.

The limiting current for the Bi(III) wave was proportional to the bulk concentration of Bi(III) and the square root of the electrode rotation speed. Both of these plots passed through the origin. Thus, according to the Levich equation, the cathodic limiting current for Bi(III) is convective-diffusion controlled. The slope of i (at −0.25 V) *vs.* $\omega^{1/2}$ plot gives a value of 5.3 × 10^{-6} cm^2/sec for the diffusion coefficient, $D_{Bi(III)}$, using the Newman version of the Levich

(4) S. H. Cadle, Ph.D. Thesis, State University of New York at Buffalo, 1972.
(5) V. Vicenti, Ph.D. Thesis, State University of New York at Buffalo, 1973.
(6) G. W. Tindall and S. Bruckenstein, *J. Electroanal. Chem.*, **22**, 367 (1969).
(7) E. Barondrecht, in "Electroanalytical Chemistry," Vol. 2, A. J. Bard, Ed., Marcel Dekker, New York, N.Y., 1967, p 53.
(8) M. Z. Hassan, D. F. Untereker, and Stanley Bruckenstein, *J. Electroanal. Chem.*, **42**, 161–81 (1973).
(9) D. C. Johnson, Ph.D. Thesis, University of Minnesota, Minneapolis, Minn., 1967.
(10) F. L. Marsh, Ph.D. Thesis, University of Minnesota, Minneapolis, Minn., 1965.
(11) D. F. Untereker, Ph.D. Thesis, State University of New York at Buffalo, 1973.
(12) D. C. Johnson, *Talanta*, **16**, 1481 (1969).
(13) M. Z. Hassan, Ph.D. Thesis, University of Minnesota, Minneapolis, Minn., 1973.

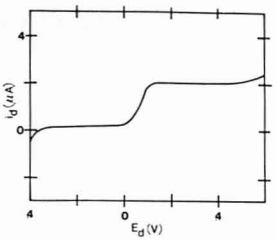


Figure 1. Cathodic *i–E* curve for Bi(III)

CMCRPDE area = 0.62 cm^2; ω = 600 rpm; scan rate = 100 mV sec^{-1}; 2.5 × 10^{-6}*M* Bi(III) in 0.1*M* HNO_3 + 2.5 × 10^{-4}*M* Hg_2^{2+}

equation (*14*), in excellent agreement with the literature (*15*). As expected, if the Hg-current was not compensated, the separate Bi wave could not be obtained.

Anodic Stripping Curve for Bi(0) → Bi(III). At concentrations $C_{Bi(III)}{}^b < 5 \times 10^{-7}M$, it was not feasible to obtain a distinguishable wave for Bi in the cathodic *i–E* curve. For the identification and determination of Bi(III), $10^{-7} < C_{Bi(III)}{}^b < 5 \times 10^{-9}M$, it was necessary to cathodically deposit (and concentrate) it on the CMCRPDE for the requisite time, and obtain, by linear scan voltammetry, the anodic stripping peak (Figure 2). The bismuth deposition (preconcentration) potential used was cathodic to −0.1 V *vs.* SCE. The deposition time depended on ω and $C_{Bi(III)}{}^b$. For example, times of 15–75 seconds for the $10^{-7}M$ studies, and times of 30–45 minutes for 10^{-9}–$10^{-10}M$ studies were used at 600 rpm.

Simultaneous deposition of impurities in the supporting electrolytes cause problems at low Bi(III) concentration. The impurity problem was treated in this study by obtaining a blank ASV curve in the supporting electrolyte (acid + Hg_2^{2+}) before the addition of Bi(III). All data reported below were corrected for this blank which was equivalent to $C_{Bi(III)} \approx 10^{-8}M$.

The primary source of impurities was the acid used to prepare the supporting electrolyte. The Hg_2^{2+} solution used was prepared from chemically purified (wet method) Hg and freshly distilled HNO_3. Furthermore, the mercury concentration in the supporting electrolyte was so low (10^{-5}–$10^{-4}M$) compared to that of the acid (0.1*M*) that impurity contribution from mercury would be electrochemically negligible.

The peak current, i_p, obtained at ~0.05 V during the anodic scan is caused by the oxidation of Bi(0) at CMCRPDE and it was linearly proportional to: (a) the preconcentration time, t_p, (b) the bulk Bi(III) concentration, and (c) $\omega^{1/2}$. Typical peak current data are summarized in Figure 3, in which i_p *vs.* $C_{Bi(III)}{}^b$ and t_p are plotted.

In Figure 2, if the scan was reversed at 0.4 V for ω = 0 rpm, the second and successive scans did not show any appreciable peak for Bi oxidation around 0.05 V, verifying that complete removal of Bi from the Hg-film had occurred. The charge under the peak is 17 μC and that calculated by $i_d \times t_p$ is 18 μC.

(14) J. Newman, *J. Phys. Chem.*, **70**, 1327 (1966).
(15) S. H. Cadle and Stanley Bruckenstein, *Anal. Chem.*, **44**, 993 (1972).

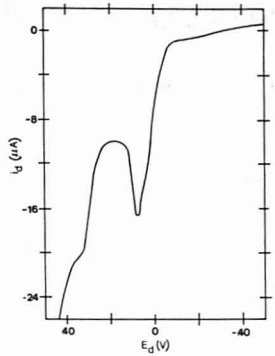


Figure 2. Anodic stripping voltammogram of Bi

Plating time 75 sec in 2.5 × 10^{-7}*M* Bi(III) at −0.5 V. Other conditions same as in Figure 1

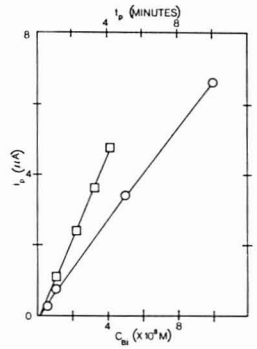


Figure 3. Dependence of Bi anodic peak current on plating time (C_{Bi} = $10^{-8}M$) (upper ordinate) and concentration (lower ordinate) (t_p = 10 min)

ω = 400 rpm. Other conditions same as in Figure 1. O, concentration; □, time

CONCLUSIONS

It is possible to obtain a satisfactory *i–E* curve of 2.5 μ*M* Bi(III) in the presence of a 100-fold molar excess of Hg_2^{2+} by compensation of the Hg_2^{2+} reduction and expanding the current scale. Our anodic stripping voltammetry of Bi(III) at a CMCRPDE is limited by the presence of supporting electrolyte impurities (~$10^{-8}M$).

RECEIVED for review March 11, 1974. Accepted June 24, 1974. M.Z.H. received a Summer Fellowship from Gould, Inc. This work was also supported by the Air Force Office of Scientific Research by AFOSR Grant No. 70-1832 and Grant No. 74-2572.

Live Peak-Stripping during X-Ray Energy-Dispersive Analysis

John Parkes, L. J. Rabbitt, and M. J. Hampshire

Electrical Engineering Department, Univeristy of Salford, Salford M5 4WT, England

There has been considerable growth in the use of Si(Li) detectors connected to on-line computers to provide very rapid X-ray energy-dispersive analysis. Such a system analyzes all channels simultaneously and consequently is very much faster than wavelength-dispersive spectrometers, which usually handle not more than two channels at any one time. However, the resolution of the Si(Li) system is rarely less than 150 eV; this is considerably worse than that of crystal spectrometers, which may typically have a resolution less than 50 eV. Consequently, with the Si(Li) system, it is often the case that peaks from two or more elements are unresolved. Therefore, the capability to strip away peaks is preferable for qualitative analysis, and is essential for quantitative analysis. Often peak stripping is done by fitting a Gaussian distribution, but the peaks are very rarely Gaussian and, when they are not, this procedure produces two unwanted "satellite" peaks. Even more complicated mathematical functions can be used, but if the peak to be stripped is unresolved, it becomes very difficult to match the function to the peak before subtraction. The system described in this note is quick, effective, and does not suffer from any of the above difficulties.

Live Peak-Subtraction System. The analyzer consists of a Kevex 150 eV Si(Li) detector coupled to a Nova 1220 computer, the system being fabricated by A.E.P. (Link Systems). There are two 1000-channel memories, A and B; A is used to store the live spectrum; B is a stored reference memory which can be displayed as a set of dots superimposed on the live memory, which is displayed as a line spectrum. A spectrum can be stored in the reference memory B by any of three ways: transposing the spectrum from memory A after analysis, reading in a spectrum stored on paper tape, or reading in a spectrum from disk or magnetic tape.

To the basic software supplied by the manufacturer, which operates in less than 2K of computer store, the authors have added three functions. The first is a subtraction routine which takes the reference memory B from the live memory A and places the difference in the live memory. This is done by tapping a control button while live analysis is occurring. The second function is the converse, which adds memory B to memory A, and places the sum in the live memory. This ensures that no data are ever lost, since every subtraction can be cancelled by an addition if required. The third function is division of the reference memory by two at each touch of a control button. This enables any reference spectrum to be scaled down to a suitable size prior to subtraction; the good statistics associated with the large count are retained in the scaled-down standard.

During live analysis of the unknown, the standard is subtracted and the live count becomes negative if the standard has a sufficiently high count. The computer used has a 16-bit word, one word being used for each display count. A count of minus x in a particular channel is therefore displayed as a count of $2^{16} - x$, a vertical line of almost the display capability, $2^{16} - 1$. As the analysis is continued, the counts in the channels increase until 2^{16} is reached, when the large vertical line in that particular channel vanishes, indicating that the channel now contains positive counts. The object is to stop the analysis at the time when the state of the background counts shows that an accurate subtraction has been achieved. If the counts increase beyond the required level, the subtraction is repeated, and the counts again accumulate to give a "positive" spectrum. The operation can be repeated several times to provide the remaining peak with the required statistical accuracy. The number of subtractions is recorded on a teletype and, since the addition facility is available, no information has been lost.

Practical Example. To demonstrate the capabilities of this peak-stripping routine, an example is given of a difficult peak-stripping problem, namely K and Sn. The K spectrum has a $K\alpha_{1,2}$ line at 3.31 KeV and a $K\beta_{1,2}$ line at 3.59 KeV, while Sn has several L lines, the main two being $L\alpha_{1,2}$ at 3.44 KeV and $L\beta_{1,3}$ at 3.70 KeV. Both separate spectra, obtained from standards, are displayed in Figure 1, where it is evident that the $K\beta$ peak of the potassium falls between the two strong L lines of the tin.

Figure 2 shows the spectrum of a mixture of approximately equal mass concentrations of KCl and $SnCl_2$ (line spectrum), and also the spectrum of a pure Sn standard (dot spectrum). After multiple subtractions of the Sn standard during live analysis, the count was stopped at the appropriate time, revealing the stripped potassium $K\alpha$ and $K\beta$ peaks, shown as line spectrum in Figure 3. To demonstrate the effectiveness of the technique, a potassium standard spectrum has been scaled down to match the stripped peaks, and is displayed as the dot spectrum. The fit is not perfect, but is nevertheless very good.

DISCUSSION

It is clear from this example that peak stripping in this way greatly enhances the effective resolution of the system, and it is important to emphasize that very little operator skill is required. To achieve accurate results, it is necessary for the energy of a peak not to drift relative to the standard; a relative drift of one channel will produce a significant error in the resulting integral of the stripped peak. The system described here does drift at about 10 KeV up to 40 eV over several days. However, this does not present a problem, providing there is no significant drift during analysis. Two ways are available to compensate for the drift: first, software has been written which enables the memory B reference spectrum to be shifted one channel at a time in either direction: second, the preamplifier gain can be set using a standard target to give the current energy just prior to performing accurate analysis.

It is important to note that the software required to perform the extra functions of addition, subtraction, division, and spectrum shifting only occupies approximately 100 computer memory locations.

The manufacturer's software deals with the problem of background, and this is achieved by the operator setting up a "window" to define the peak. An integral is then evaluated of the area under the peak above a straight line joining the two extremities of the window.

There is, however, one further problem to be solved before accurate *ZAF* (atomic number–absorption–fluorescence) corrections can be used for all elements. With a 150-eV detector, the $K\alpha$ and $K\beta$ peaks are fully resolved with negligible overlap for elements with atomic number

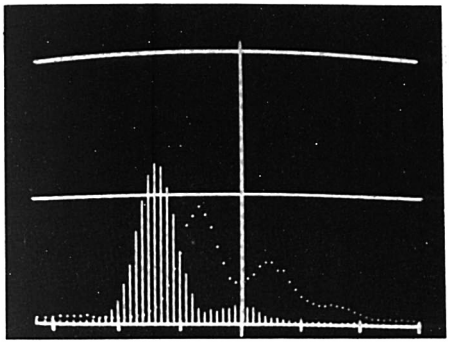


Figure 1. Spectra of the potassium (lines) and tin (dots). Full-scale count $2^{15} - 1$, channel width 20 eV, center line on 3.60 KeV

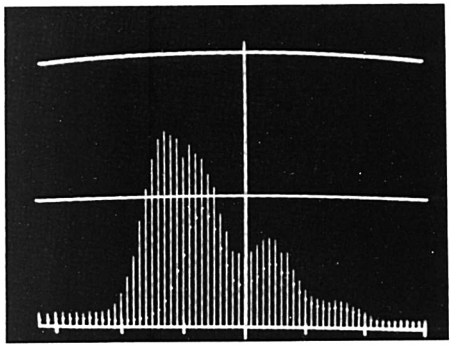


Figure 2. Combined spectrum of potassium and tin chlorides, with the tin spectrum as dots. Scales as for Figure 1

higher than 21. Similarly for Lα and Lβ lines, full resolution is achieved for atomic numbers above 56. For atomic numbers of 14 and below, the Kα/Kβ pairs are less than 90 eV apart, and consequently very little error will be involved in treating this doublet simply as a single K line. Between atomic numbers 14 and 21, the Kα and Kβ peaks may be absorbed by different amounts by other elements in the sample, and treating these as a single peak could give small errors. In the case where an absorption edge falls between the Kα and Kβ lines, a significant error will result. Such a situation occurs in the analysis of potassium with silver or cadmium present, since both these elements have an L_{III} absorption edge falling between the potassium Kα and Kβ peaks.

For the L lines, the problem is more complex because the different peaks arise from ionization of different shells, and the jump ratio and fluorescent yield will be different for each peak. This means that the Lα and Lβ peaks will be affected by flourescence and absorption to a different degree than are K lines.

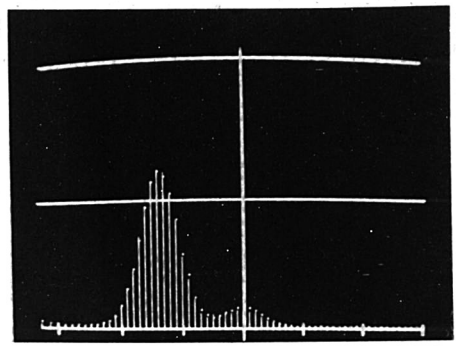


Figure 3. The stripped potassium peak is shown as lines with a scaled-down peak from a potassium standard (dots) for comparison. Scales as for Figure 1

It is obvious that for full and accurate *ZAF* analysis, some way will have to be found to extract an integral of the α peak from the α/β doublet.

RECEIVED for review February 11, 1974. Accepted June 17, 1974.

CORRECTION

Correction of Inner Filter Effects in Fluorescence Spectrometry

In the paper by V. Alan Mode and D. H. Sisson, *Anal. Chem.*, **46**, 200 (1974), Equation 6 (p 201) should read

$$F(V) = \frac{1}{2\pi}\int_0^V \left[\arctan\left(\frac{BC}{BP}\right) + \arctan\left(\frac{AB}{BP}\right)\right] dv \quad (6)$$

and Equation 7 (p 202) should read

$$f(l) = \frac{1}{\pi}\left[\arctan\left(\frac{1}{l}\right) - \frac{l}{2}\ln(l^2 + 1) + l\ln(l)\right] \quad (7)$$

With these corrections, the rest of the text is correct.

CORRECTION

Determination of Fluoride in Coal with the Fluoride Ion-Selective Electrode

In the paper by Josephus Thomas, Jr., and Harold J. Gluskoter [*Anal. Chem.*, **46**, 1321 (1974)], the National Bureau of Standards sample which is designated in Table I and in the text on page 1322 as NBS 1631 should be changed to read NBS 1632.

Determination of Trace Metals in Aqueous Environments by Anodic Stripping Voltammetry with a Vitreous Carbon Rotating Electrode

A. H. Miguel[1] and C. M. Jankowski

Chemistry Department, Northeastern University, Boston, Mass. 02115

Effective performance in the monitoring and control of trace metal pollutants requires the existence of reliable and reproducible methods of analysis at the parts-per-billion level and below.

At present, atomic absorption and fluorescence spectrometry, neutron activation analysis, electroanalytical methods of analysis, and others appear to offer the best promise for the determination of trace metals in natural and waste waters. The applicability of these techniques has been described by Mancy (*1*) and they have been used with varying degrees of convenience, success, and cost.

Among the electroanalytical techniques, differential pulse anodic stripping (DPAS) (*2*) and anodic stripping voltammetry (ASV) with thin film or solid electrodes appear to be most suitable. The advantages over other techniques are that relatively fewer errors are introduced through contamination from glassware and chemical reagents. Of the two techniques ASV requires less expensive and simpler instrumentation and both permit determination of trace metals at the sub-part-per-billion level without preconcentration which, at times, can also be a source of error.

This paper describes the determination of copper and lead in aqueous solution by the simultaneous deposition of Hg and the trace metals of interest directly onto a vitreous carbon rotating electrode. Using this modified version of the Hg film method, we were able to speed up the analytical procedure appreciably and improve the reproducibility to approximately 2%. The method of simultaneous plating was first reported by Florence (*3*) using a glassy carbon electrode. The calculated relative standard deviation for several separate runs on aliquots of the same sample was ±2%, which is about the same precision obtained by Florence.

The useful concentration range for the metals studied is from about 10^{-6} to 10^{-9} *M*.

EXPERIMENTAL

Reagents. All chemicals were reagent grade, with no further purification attempted. Solutions were prepared with water purified by passage through a mixed bed cation–anion exchange resin, then distilled once. High purity nitrogen gas was used for deaeration of the samples.

A mercuric nitrate solution was prepared by dissolving triply distilled mercury in reagent grade nitric acid and diluting to give a $1 \times 10^{-2}M$ solution. Standard solutions of copper and lead were prepared by dissolving high purity metals in reagent grade nitric acid. Excess acid from both solutions was eliminated by evaporation. These solutions were used as standards for known increment measurements and were transferred with disposable micropipets (Micropet).

Apparatus. All measurements were done using the Beckman Electroscan Model 30P Electroanalytical System in the potentiostat mode of operation.

Cell and Electrodes. The cell (Figure 1) used in this study was made from quartz tubing 50 mm in diameter by 50 mm long. By using the quartz cell, absorption of trace metals on the cell walls, usually found with glass and polyethylene containers (*4, 5*) was minimized.

A silver/silver chloride reference electrode was prepared as described by Matson (*4*). The working electrode was a Beckman Rotating Electrode with a vitreous carbon electrode tip (Catalog No. 39084). The counter electrode was made from 0.3-mm high purity platinum wire. Both the reference and the counter electrodes were contained in 3-mm diameter open quartz tubing directly in the solution. These electrodes, together with a 1.5-mm diameter Teflon bubbling tube were held in a machined Teflon head, as shown in Figure 1. This arrangement facilitates the ease of transfer between samples, and maintains a stable configuration of the electrodes and the bubbling tube. In a separate study, we found it to be of paramount importance that the position of the bubbling tube be left unchanged; otherwise irreproducible peak currents are obtained.

Procedures. *Pretreatment of the Working Electrode.* The vitreous carbon rotating electrode (working electrode) surface was cleaned before each set of analyses. This was done simply by polishing the electrode with a fine textured cloth, followed by wiping with wet tissue paper, then giving a final polish with dry tissue paper. These cleaning operations were done while the electrode was rotated.

Sample solutions were deaerated by bubbling nitrogen gas for about 10 minutes. Prior to entering the cell, the nitrogen is saturated, at room temperature, with sample solution or supporting electrolyte contained in a gas saturator to prevent evaporation of the sample in the ASV cell.

A sample of dionized water made 0.5*M* in NaCl (sea water ~0.54*M* NaCl) was selected as a test solution. A 30-ml aliquot of this solution was placed in the quartz cell, followed by the addition of 200 μl of $1 \times 10^{-2}M$ $Hg(NO_3)_2$, making the final concentration of Hg $6.6 \times 10^{-5}M$.

The machined Teflon head containing the reference and counter electrodes and the Teflon bubbling tube was then lowered into the cell. Nitrogen gas was bubbled through the solution for about 10 minutes, at a rate of 70 ml/min. The pre-cleaned working electrode was then inserted into the cell and rotated at the desired speed.

The electrodeposition potential (E_d) was set at −1.0 volt for copper, lead, and cadmium and the simultaneous electrodeposition of the mercury film and trace metals was carried out for exactly 5 minutes. At the end of the electrodeposition period, both the rotating working electrode and the nitrogen bubbling were turned off. A rest period of 5 seconds was allowed before stripping (re-oxidation) of the trace metals from the Hg film was conducted.

Stripping was accomplished by scanning the potential from −1.0 to −0.1 volt. Continuous tracing of stripping potentials and stripping currents were monitored. Potential scanning rates as fast as 100 mV/sec were possible using the Beckman instrument without pen response becoming a problem. Care should be taken not to scan the potential beyond −0.1 volt, as the Hg film starts to strip off.

[1] Present address, School of Chemical Sciences, Department of Chemistry, University of Illinois, Urbana, Ill. To whom correspondence should be addressed.

(1) K. H. Mancy in "Analytical Chemistry: Key to Progress on National Problems," NBS Special Publication 351. W. W. Meinke and J. K. Taylor, Ed., 1972, pp 343–53.
(2) Application Note AN-107 Princeton Applied Research, Princeton, N. J. 08540.
(3) T. M. Florence, *J. Electronanal. Chem.*, **27**, 273 (1970).
(4) W. R. Matson, Ph.D. Thesis, Massachusetts Institute of Technology, Cambridge, Mass., 1968.
(5) D. E. Robertson, *Anal. Chim. Acta*, **42**, 533 (1968).

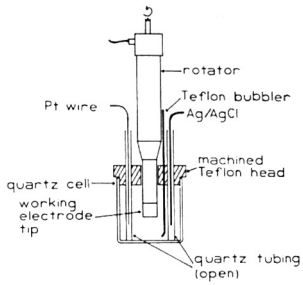


Figure 1. The ASV cell consisting of the rotating electrode, the counter and the reference electrodes, and the bubbling tube

Standard addition aliquots were added via a 1.5-mm diameter hole bored through the machined Teflon head.

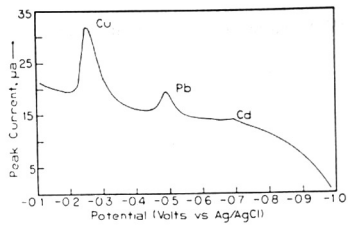


Figure 2. Anodic stripping voltammogram of deionized water 0.5*M* in NaCl

Conditions: 5-min deposition at −1.0 volt, 30 rps, 7.5 ppb Cu^{2+}, 2.6 ppb Pb^{2+}, $6.6 \times 10^{-5}M$ Hg^{2+}, 100 mV/sec, pH 4.1, 26 °C

Table I. Variation of Peak Current with Scan Number for Copper[a]

Scan No.[b]	i_p, μA	$-E_p$, volts
1	2.95	0.264
2	3.11	0.260
3	2.95	0.260
4	2.95	0.260
5	2.95	0.255
Av	$2.98_2 \pm 0.072$	

[a] 0.5*M* NaCl, 100 mV/sec, 30 rps, 100-sec deposition time at −1.0 volt, $6.6 \times 10^{-5}M$ Hg^{2+}, 7.5 ppb Cu^{2+}, pH 4.1, 26 °C. [b] Successive deposition and scans on the same test solution.

Table II. Variation of Peak Current with Scan Number for Lead[a]

Scan No.[b]	i_p, μA	$-E_p$, volts
1	0.98	0.505
2	0.98	0.500
3	0.98	0.495
4	0.98	0.490
5	0.97	0.485
Av	$0.97_8 \pm 0.0045$	

[a] 0.5*M* NaCl, 100 mV/sec, 30 rps, 100-sec deposition time at −1.0 volt, $6.6 \times 10^{-5}M$ Hg^{2+}, 2.6 ppb Pb^{2+}, 26 °C. [b] Successive deposition and scans on the same test solution.

Table III. Variation of Peak Current with Rotational Speed[a]

Rotational speed, rev sec^{-1} [b]	i_p, μA	
	Cu^{2+}	Pb^{2+}
5	2.36	0.91
10	3.52	1.38
20	5.32	2.07
30	7.48	2.66
40	10.1	3.15
50	11.8	3.56

[a] 0.5*M* NaCl, 100 mV/sec, 5-min deposition time at −1.0 volt, $6.6 \times 10^{-5}M$ Hg^{2+}, 2.6 ppb Pb^{2+}, 7.5 ppb Cu^{2+}, pH 4.1, 26 °C. [b] Measurement made on the first scan.

A typical anodic stripping voltammogram is depicted in Figure 2.

To establish the peak current amplitude for the trace metals by standard addition, an aliquot of the trace metal of interest is added to the sample solution contained in the ASV cell and the experimental procedure is repeated. Usually between 3 and 4 consecutive additions of each trace metal was found to be sufficient to define a peak current calibration curve. Peak current measurements from the base-line offset were measured for each standard addition of the trace metal. The *x* intercept obtained by extrapolation of the straight line defines the original concentration of the metal of interest in solution.

RESULTS AND DISCUSSION

The concentration of copper and lead in the test solution was found to be 7.5 and 2.6 ppb, respectively. Values obtained for cadmium were less than 0.1 ppb. The experimental conditions are discribed in the legend of Figure 2.

Reproducibility of peak current for Cu^{2+} and Pb^{2+} are shown in Tables I and II. Conditions are defined in the legends. Relative standard deviation for peak currents were ±2.40% for copper and ±0.46% for lead. This compares favorably with the ±4.98% obtained by Florence (*3*) for a solution containing 41 ppb Pb^{2+} ($2 \times 10^{-7}M$). We attribute this enhancement to the more reproducible mass transfer conditions inherent of rotating electrodes and also to the minimization of wall effects by the elimination of glass from the system. Standard deviation for concentration between several runs on separate aliquots of the same sample was found to be ±2%.

Slight reduction in the value of the peak potentials with scan number was noted; however, reasons for this are not known. A similar observation was made by Florence (*3*). Presumably this is an electrode aging phenomenon. An interesting observation is that our results differ from those of Florence (*3*) in that his results showed a marked increase in the peak current value between the first and second scans. Deviations in our results appear to be random for all scans.

The influence of rotational speed of the rotating electrode is illustrated in Table III for the peak current of copper and lead. High rotational rates give higher peak currents but the relationship is not linear. Also, at high rotational rates, the electrode response deteriorates. Optimum rates were around 30 revolutions per second (rps).

Table IV. Variation of Peak Current with Scan Rate[a]

Scan rate, mV/sec[b]	i_p, μA Cu^{2+}	Pb^{2+}
10	0.98	0.39
20	2.03	0.61
50	5.22	1.58
100	10.0	2.74

[a] 0.5*M* NaCl, 30 rps, 5-min deposition time at −1.0 volt, 6.6 × 10^{-5}*M* Hg^{2+}, 2.6 ppb Pb^{2+}, 7.5 ppb Cu^{2+}, 26 °C. [b] Measurements made on the first scan.

Table V. Variation of Peak Current with Deposition Time[a]

Deposition time, sec[b]	i_p, μA Cu^{2+}	Pb^{2+}
100	2.98	0.98
200	6.02	1.87
300	9.00	2.81

[a] 0.5*M* NaCl, 30 rms, 6.6 × 10^{-5}*M* Hg^{2+}, 2.6 ppb Pb^{2+}, 7.5 ppb Cu^{2+}, deposition at −1.0 volt, pH 4.1, 26 °C. [b] Measurements made on the first scan.

Table IV shows the variation of peak current with scan rate for copper and lead. Peak current amplitudes increased linearly with scan rate as would be expected with this film electrodes (*6*).

We found that high potential scanning rates gave results of the same reproducibility as the low rates. For rapidity of the analyses, fast rates are to be preferred.

Variations of peak current with deposition time are illustrated in Table V. Peak currents were extremely linear with deposition time. For the part-per-billion range, deposition times of approximately 5 minutes were suitable.

CONCLUSION

The method described is simple and very fast for the determination of trace metals at the part-per-billion level and below.

ACKNOWLEDGMENT

The authors express sincere appreciation to D. H. Howling of New College, for his constructive criticism and to E. N. Pollock, L. P. Zopatti, and J. C. Cornwell of Ledgemont Laboratory for furnishing the quartz cells and the high purity reagents used in this study.

RECEIVED for review January 16, 1974. Accepted June 27, 1974. This work was partially supported by the National Science Foundation under Grant No. G.I.–31605.

(6) E. Barendrecht, in "Electroanalytical Chemistry, Vol. 2," A. J. Bard, Ed., Marcel Dekker, New York, N.Y., 1967, p 69.

Semiquantitative Potentiometric Method for Direct Measurement of Nitrogen Dioxide in Air

G. G. Barna and R. J. Jasinski

Texas Instruments Incorporated, P.O. Box 5936, Dallas, Texas 75222

The potentiometric measurement of electroactive gases, in contrast with amperometric measurements such as using a Field Lab O_2 Analyzer (Beckman Instruments, Part No. 100800), a Faristor NO_2 Sensor (Environmetrics, Marina del Rey, Calif.), or the method of Bay *et al.* (*1*), has the inherent advantage of simplicity and low cost, in that the only components required are the electrochemical transducer for the particular species, a reference electrode, and a high impedance voltmeter. There exist, however, only a very limited number of cases where such measurements are performed, and except for O_2 (*2*), those involve the indirect measurement of the aqueous reaction product of the particular gas, via an ion-selective electrode. The determination of SO_2 using an SO_2 electrode (Model 95064, Orion Research Inc., Cambridge, Mass.) or the method of Young *et al.* (*3*), NH_3 with an NH_3 electrode (Model 95-10, Orion), and NO and NO_2 (*4*) has been achieved by these means.

All these techniques involve a preconcentration step to achieve the necessary sensitivity, obtained by purging the air sample through a scrubbing solution; consequently, they do not yield real-time analyses. They are also, in the case of the pH measuring devices, amenable to interference by a range of pH altering gases.

This paper describes the direct potentiometric measurement of NO_2 in air by means of a properly activated Fe–chalcogenide glass electrode. This system avoids the complication of a preconcentration step while still maintaining high sensitivity; achieves selectivity directly via the nature of the chemical interaction between the gas and the sensor material; while it maintains the advantage of simplicity in measurement.

EXPERIMENTAL

The active element of the electrochemical NO_2 sensor is a nonoxide chalcogenide glass with the approximate composition of $Se_{60}Ge_{28}Sb_{12}$ doped with 1.7–2% Fe^0 (the subscripts refer to the mole percentages of the elements). This material is prepared by the direct fusion of the elements, as described in a previous publication (*5*), and will subsequently be designated as "Fe 1173."

The electrode was constructed by attaching a glass disk (7 mm in diameter and 1 mm thick) cut from the melt to a brass screw fitted inside a cylindrical rod of paper-based phenolic resin (A-1 Plastic Supply, Dallas, Texas). This material was chosen for its compatability with the necessary high-temperature air-oxidation

(1) H. W. Bay, K. F. Blurton, H. C. Lieb, and H. G. Oswin, *Amer. Lab.*, No. 7, p 57 (1972).
(2) P. B. Hanh, M. A. Wechter, D. C. Johnson, and A. F. Voigt, *Anal. Chem.*, **45**, 1016 (1973).
(3) M. Young, J. N. Driscoll, and K. Mahoney, *Anal. Chem.*, **45**, 2283 (1973).
(4) B. M. Kneebone and M. Freiser, *Anal. Chem.*, **45**, 449 (1973).
(5) R. Jasinski and I. Trachtenberg, *J. Electrochem. Soc.*, **120**, 1169 (1973).

Table I. Sensor Potentials *vs.* Gas Composition

Gas	Potential shift (*vs.* N_2), mV
Air	+4
NO_2 (350 ppm in N_2)	+324
NO (100 ppm in N_2)	+3
CO (1% in N_2)	+6
SO_2 (100%)	+7
CH_4 (1% in N_2)	+3

activation required by the sensing material (see below) and with the electrolytes. Other details related to the construction of the electrode have been described before (*5*).

The necessary and sufficient procedure required for making the Fe 1173 material reproducibly active toward NO_2, has been established to be a 3 min/300 °C air oxidation of the electrode material. Although various slices of the non-activated material have shown a limited degree of activity towards NO_2, these responses of the non-activated sensors were not reproducible either in rate or in magnitude.

The necessary liquid–solid interface was obtained via the cell configuration, hereafter to be designated as "inverted," shown in Figure 1. The rationale behind this construction will be discussed below. A wick was taped along the body of the electrode such that it was in close contact with the sensing surface of the electrode, which protrudes above the surface of the electrolyte. In this way, the sensing element was directly exposed to the gas being monitored. The electrolyte brought to the exposed surface by the capillary action of the wick, completed the solution circuit between the sensing and reference electrodes. A Beckman Perma-Probe electrode was used as a reference. A piece of ¼-mil perforated Teflon membrane was placed between the gas stream and the sensor, at approximately 3 mm above the surface of the sensor, to retard the evaporation of the electrolyte while allowing the gas an access to the sensor.

The electrolyte, unless otherwise mentioned, was a 0.1*M* solution of $(NH_4)_2HPO_4$ at its natural pH of 8. Identical sensor responses were obtained with 0.1*M* solutions of KNO_3, CsCl, $NaClO_4$, $NaNO_3$, KCl, and NH_4Cl, in the pH range of 3.7 to 8.0. The calibrating gases were pre-analyzed mixtures of NO_2 in air, purchsed from Matheson Company. The flowrate of the gas stream was generally held at 120 cm^3/min; however, a twofold increase in this rate made no appreciable difference. No attempt was made at controlling the relative humidity in the sensing cavity. However, no differences were observed when the fluid electrolyte was substituted by the gelled electrolyte, which necessarily provided a lower partial pressure of water around the sensor.

The response of the system was monitored by measuring the open-circuit voltage between the sensor and reference electrodes by means of a Keithley 610B Electrometer the output of which was fed into a Hewlett-Packard 4340A digital voltmeter, and simultaneously into a TI Servo/Riter II strip-chart recorder.

RESULTS AND DISCUSSION

The chalcogenide glass described in the experimental section has been shown (*5*) to form the basis of an electrode sensitive to ferric ions. With the proper pretreatment, this material also gave a positive potential shift when equilibrated with NO_2 in the presence of air and was insensitive to NO, SO_2, CO, and CH_4. The results of these selectivity experiments are shown in Table I, where potentials (*vs.* Ag/Ag_2SO_4) are listed for a properly activated Fe 1173 electrode exposed to a series of gases. The electrolyte was 7*N* H_2SO_4; however, similar results were obtained with other electrolytes.

Persuant to exploiting this selective activity of the Fe 1173 material to NO_2, a gas cell, similar in design to commercial O_2 cells, was constructed. This configuration, however, was unsatisfactory for the potentiometric measurement of NO_2, because of the unacceptably slow response and purge rates of the device. The remainder of this paper will be devoted to a description of a viable structure and the resulting measurements.

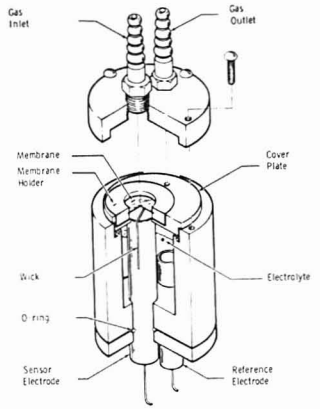


Figure 1. A prototype gas sensor system in the "inverted" configuration

There are two reasons for the poor (equilibrium potential not reached in 30 minutes) response characteristics of the system assembled with a relatively large volume of electrolyte between the gas-permeable membrane and the sensing electrode. First, unlike O_2, NO_2 reacts with aqueous electrolytes as shown in the following equation

$$2\,NO_2 + H_2O \rightleftharpoons HNO_2 + HNO_3$$

Since the potential determining process is some interaction of the NO_2, not NO_2^- or NO_3^-, with the electrode material (*6*), it can be seen that this solution chemistry of NO_2 serves only as an interference in as far as it necessitates the establishment of a gas electrolyte equilibrium prior to the measured equilibrium between the NO_2 and the sensor electrode. Second, in contrast to a commercial amperometric NO_2 sensor, in which NO_2 is reduced electrochemically, the potentiometric measurement allows for no process, other than diffusion, for the elimination of NO_2 from the electrolyte. To overcome these drawbacks, the inverted configuration was developed.

The principle behind this inverted configuration is as follows. In the potentiometric mode of operation, the measured variable is the open-circuit voltage between the sensor and reference electrodes. This voltage is determined by the potentials of the two electrodes. However, the potential is an intensive property of an electrode—*i.e.*, it does not depend on the size of the electrode or, what is more to the point, on the size of the electrode–electrolyte interface. This is in direct contrast to the amperometric mode of operation, where the measured variable is a current. This is an extensive property and is thus directly proportional, at a given gas concentration, to the size of the electrode–electrolyte interface. Thus, while the kinetics of the response, as limited by the solution chemistry of NO_2, are anticipated to improve if the volume of electrolyte between the gas and the sensor is reduced, thermodynamics indicates that such a reduction would have no bearing on the magnitude of the response.

This is demonstrated in an experiment where the gas cell was assembled in a non-inverted configuration: with a 45-mil spacer between the gas permeable membrane and the

(6) R. Jasinski, G. Barna, and I. Trachtenberg, *J. Electrochem. Soc.*, in press.

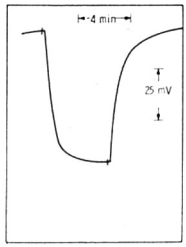


Figure 2. Characteristic response curve

sensor and with only as much electrolyte in this interface as was conducted there by the capillary action of a wick. Compared in Table II are the rates of response of these two systems to a mixture of 290 ppm NO_2 in air. These data clearly illustrate the advantage of minimizing the volume of electrolyte.

Through a minor alteration of the cell configuration, the entire cell was inverted, and the wick thus became the sole conduit for the electrolyte to reach the exposed surface of the sensor electrode. This configuration, however, suffered the problem common to all such gas sensing electrochemical cells—*i.e.*, the drying of the electrolyte in contact with the gas stream. This problem was essentially eliminated by the placement of a piece of perforated ¼-mil Teflon membrane between the gas and the electrode. This membrane prevents the crystallization of the electrolyte on the exposed surface of the electrode, and has been capable of maintaining a "clean" electrode surface during weeks of intermittent operation, while still allowing an equilibrium to be established between the sample and the gas cavity.

It is worth noting that while a membrane has been employed in the final prototype of this cell, the inverted configuration eliminates the inherent need for the use of a membrane with nonporous electrochemical cells. Generally, such a membrane serves as the gas permeable boundary enclosing a limited volume of electrolyte between itself and the electrode surface. By necessity, this membrane can only be a negative contribution to the overall response time of the sensor system. Whatever the couple at the electrode, the rate and amount of response will be a function of the permeability of the gas through the membrane. The response can vary from zero, in the case where the membrane is impermeable to the gas, to a value that is essentially determined by the electrode reaction—*i.e.*, where the membrane is so permeable that permeability ceases to be the limiting factor. With the membrane not essential for the short term operation of the system, studies could be carried out for the permeability of a given membrane for a specific gas, the electrochemical measurement of a gas for which a permeable membrane can not be found, and fundamental gas–electrode interactions, by being able to separate the gas–membrane and the gas–electrode effects.

Having developed a gas cell in which the necessarily adverse effect of the volume of electrolyte has been minimized, it was possible to study the sensor response after various types of chemical pretreatment—*i.e.*, activation. The necessity for the high-temperature air-oxidative activation of the electrode material, as described in the Experimental section, is shown by the data in Table III. Summarized there is the nature of the response for the gas cell assembled under conditions that were identical in every respect other than the treatment of the electrode.

Thus, the activated electrode yields a much quicker and larger response to NO_2 than one that has not been so treated. In line with previously described activation treatments (*5*) for Fe^{3+} sensing, various modes of chemical oxidation were evaluated. A sequential treatment of a freshly etched electrode with H_2O_2, Fe^{3+} and NO_2 did give a response to NO_2. However, both the amount (potential shift for a fixed NO_2 concentration) and the rate of response were very poor; typically, a 150 ppm mixture of NO_2 in air gave an increase in potential of 5 mV in a period of 8 minutes. None of the other combinations of this activation sequence, such as an H_2O_2 plus NO_2 or an Fe^{3+} plus NO_2 treatment, improved the previous results.

The nature of the response to varying NO_2 concentrations obtained from the described prototype of a properly activated NO_2 sensor is summarized in the following Tables and Figures. A typical tracing of the potential *vs.* time, for the system in the inverted configuration, is shown in Figure 2. After a steady state potential had been obtained for air going through the system, a 23-ppm NO_2 mixture was introduced. The vertical bars in Figure 2 represent the

Table II. Response of the Cell as a Function of the Volume of Electrolyte between the Electrode and the Membrane

	Rate of change	
Sequence	45-Mil spacer	Wick
Response (NO_2 On)	+10 mV/3 min	+127 mV/3 min
Purge (NO_2 Off, Air On)	−7 mV/3 min	−70 mV/3 min

Table III. Response of the Sensor to NO_2 in Air

	Result	
Sequence	Nonactivated electrode	Air-oxidized electrode
Air	Steady potential	Steady potential
290 ppm NO_2/Air	3-min delay +58 mV/3 min	30-sec delay +115 mV/3 min

Table IV. Calibration Data for the NO_2 Sensor (Potentials Relative to Air)

Day	1.2 ppm, mV	25 ppm, mV	392 ppm, mV
	Electrode 46-9		
1	6, 10	118, 138	197, 212
2	20	90, 106	200
3	9	91	157, 186
6	17, 20	100, 101	213, 220
7	11, 11	94, 103	205, 210
8	8, 8	79, 80	202, 205
9	14, 14	109, 110	196, 208
10	13, 13	86, 96	210, 222
13	16, 20	106	217, 221
14	14, 14	104, 107	207, 209
15	20, 23	97, 99	205, 207
16	12, 13	95, 97	218, 225
Average	14	100	199
Std dev	4.3	13.0	13.7
	Electrode 46-A		
Day			
1	17, 19	103, 105	178, 183
2	25, 26	124, 127	213, 207
Average	21.7	114.7	193.9
Std dev	4.0	14.8	15.7

times when the NO_2 was turned On and Off. When the NO_2 mixture was turned On, there was an initial 10-second delay, partially due to the time it takes for the gas to travel through the approximately 6 feet of tubing associated with the gas delivery system. Including these initial periods of delay, 90% of the final response to the NO_2 mixture, as well as to the subsequent air purging, was obtained in 1.5 and 2 minutes, respectively.

The magnitudes of the response of two separate sensors to NO_2 in air mixtures in the range of 1.2 to 392 ppm, are demonstrated in Table IV. The numbers represent the differences in potential between air and the specified mixture. While the data with electrode 46-9 were obtained with a fluid electrolyte [0.1*M* $(NH_4)_2HPO_4$], the electrolyte in the cell containing sensor 46-A was immobilized by gelling the above mentioned solution with 0.5 Agar/100 cm^3 electrolyte.

The magnitudes of the response are essentially the same for the two sensors. In the case of the system employing the gelled electrolyte, the advantage of portability has been gained since the possibility of flooding the sensing surface, due to any movement of the cell during the course of the measurement, has been eliminated.

The averages and standard deviations from Table IV are plotted in Figure 3. The curves exhibit slopes of 70 mV/decade. Precedents do exist (*2, 5*) for such a "super-Nernstian" response of an electrochemical process not involving a classical type of redox reaction. Considering the standard deviations, this system, in its current state of development, yields a semiquantitative means for the direct, real-time analysis of NO_2.

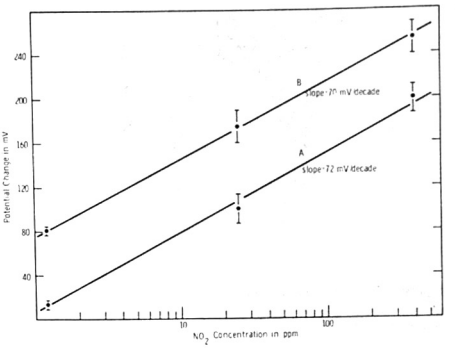


Figure 3. Calibration curves obtained with: (A) electrode No. 46-9 and (B) electrode No. 46-A, curve displaced by +60 mV

RECEIVED for review January 21, 1974. Accepted May 3, 1974.

Electrochemical Technique for the Measurement of Carbon Monoxide

H. W. Bay, K. F. Blurton, J. M. Sedlak, and A. M. Valentine

Energetics Science, Inc., 85 Executive Boulevard, Elmsford, N.Y. 10523

Recently a portable instrument for the measurement of carbon monoxide was described (*1, 2*) and independently evaluated (*3, 4*). Its operating principle is based on electrochemical oxidation of carbon monoxide at a Teflon-bonded diffusion electrode (*5*). This paper reports a theoretical analysis of the mass transfer and electrochemical processes occurring in this electrochemical sensor and describes the experimental data justifying these equations.

EXPERIMENTAL

The sensor consisted of a three-electrode electrochemical cell containing 3.4*M* H_2SO_4 solution (Figure 1). Each of these electrodes (sensing, counter, and reference) were Teflon-bonded diffusion electrodes (*6*) which were catalyzed with Pt. The sensing electrode (anode) was maintained at the potential of 1.2 V (*vs.* SHE) by a conventional potentiostat. This potential was selected to maximize the electrode sensitivity toward CO (*7*) and to minimize the current due to O_2 reduction and water oxidation.

Analyzed mixtures of CO in air in the range 21–385 ppm CO were obtained from Matheson Gas Products Co. The mixtures were certified to ±2% of the stated concentration.

During sensor operation, a CO/air mixture was passed at a constant flow rate over the back (gas side) of the sensing electrode. The current generated due to the electrochemical oxidation of CO was determined by measuring the potential drop across a standard resistor. The values of the current were reproducible to ±1%. All measurements were made in triplicate at a temperature of 22 ± 1 °C.

THEORETICAL ANALYSIS OF SENSOR RESPONSE

A schematic of the sensing electrode face plate is shown in Figure 2. The air stream enters the sensor through ACBD and exits through A′B′C′D′. The sides and top of the sensor element (ACA′C′, BDB′D′, and CDC′D′) are impervious to mass flow. AA′BB′ is the back side of the diffusion electrode through which CO molecules must pass to reach the electrocatalytic surface—*i.e.*, the gas migrates to the catalytic sites in a direction perpendicular to convective flow through the sensor.

The reaction at the sensing anode is

$$CO + H_2O \longrightarrow CO_2 + 2H^+ + 2e \qquad (1)$$

(1) H. W. Bay, K. F. Blurton, H. C. Lieb and H. G. Oswin, *Amer. Lab.*, 4(7), 57 (1972).
(2) K. F. Blurton and H. W. Bay, *Amer. Lab.*, in press.
(3) N. Yamate and H. Inoue, *J. Environ. Contr. (Japan)*, **9**, No. 3 (1973).
(4) C. F/ Smith and G. C. Ortman, Paper presented to 20th Meeting of Instrument Society of America, May 1974.
(5) H. G. Oswin and K. F. Blurton, U.S. Patent **3,776,832** (1973).
(6) J. P. Hoare, "Electrochemistry of Oxygen," Interscience, New York, N.Y., 1968.
(7) K. F. Blurton and J. M. Sedlak, *J. Electrochem. Soc.*, in press.

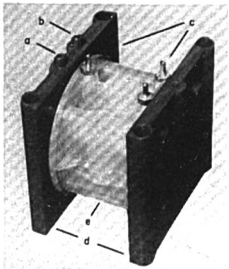


Figure 1. Photograph of assembled sensor
(a) Gas inlet, (b) gas outlet, (c) electrode connections, (d) face plates, (e) housing containing electrolyte

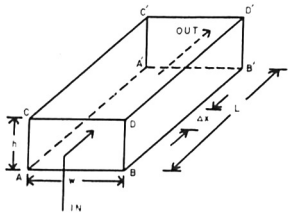


Figure 2. Schematic of gas pathway in sensor

The overall mass transfer–electrochemical reaction process in the sensor is given by

$$\frac{\partial n}{\partial t} = -\nu\frac{\partial n}{\partial x} - k\int\frac{\partial n}{\partial t}\mathrm{d}t \qquad (2)$$

The first term on the right hand side of Equation 2 accounts for convective transport of CO in the x direction and the second term refers to unsteady-state mass transfer of CO through the porous electrode and subsequent electrochemical oxidation. Diffusional transport in the x direction is assumed to be negligible since $D\partial^2 n/\partial x^2 \ll \nu\partial n/\partial x$, and n is taken as independent of h (h is small, *ca.* 0.15 cm).

Equation 2 was solved using techniques appropriate to partial integrodifferential equations (*8*). With the substitution $\nu = G/wh$ and the boundary conditions: $n = 0$, $t = 0$, for all x; $n = n_0$, $t = \infty$, $x = 0$,

$$n = n_0(1 - \exp\{-\lambda t\})\exp(\{\lambda - k\}whx/G) \qquad (3)$$

The change in CO concentration, Δn, in the air stream on passing through the sensor is

$$\Delta n = n(x = L, t) - n(x = 0, t) \qquad (4)$$

If it is assumed that all CO molecules migrating through the back side of the porous electrode undergo electrochemical oxidation (justified below), Faraday's law applies and,

$$i = -z\frac{FG}{V}\Delta n = 2\frac{Fn_0G}{V}[1 - \exp\{-\lambda t\}][1 - \exp(\{\lambda - k\}whL/G)] \qquad (5)$$

As can be seen from Figure 3, when CO is introduced into the sensor the current increases until a steady state

(8) C. R. Wylie, "Advanced Engineering Mathematics," McGraw-Hill, New York, N.Y., 1960.

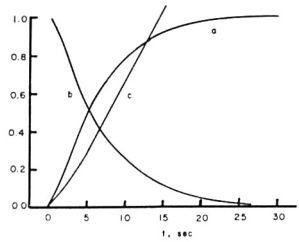


Figure 3. Sensor response characteristics
(a) i/i_{lim} *vs.* t (sec) for signal rise; (b) i/i_{lim} *vs.* t (sec) for signal decay; (c) $-\log(1 - i/i_{lim})$ *vs.* t (sec) for signal rise. Note: All curves are on same ordinate scale

value, $i_{\lim}$ is attained at large values of λt. This is the value measured by the CO instrument (*1, 2*) and it is related to the CO concentration by

$$i_{1\lim} = 2\frac{Fn_0G}{V}\left[1 - \exp\left\{(\lambda - k)\frac{whL}{G}\right\}\right] \qquad (6)$$

Equation 6 shows the parameters which determine the design of a practical electrochemical sensor.

The dependence of k and λ on flowrate could not be predicted but an *a priori* resolution of k into two contributions was possible. The overall process in the sensor involves, first, the transport of CO through the hydrodynamic boundary layer at the gas/solid interface and, second, a series of diffusion, adsorption, and oxidation steps within the electrode system. The first step is dependent on gas flow rate whereas the latter steps are not. On this basis, k is separated into flow-dependent (k_G) and flow-independent (k_∞) portions,

$$1/k = 1/k_G + 1/k_\infty \qquad (7)$$

where the relationship between k_G and G is $k_G = aG^n$.

RESULTS AND DISCUSSION

Electrode Stability. The Pt electrodes underwent a three-week aging period during which the signal decayed to approximately 80% of its original signal. Therefore, these results were obtained after potentiostating the electrode 1.2 V (*vs.* SHE) for 30 days. This decrease in CO signal was attributed to the slow formation of oxide on the catalytic surface (*7*).

Response/Time Curve. Figure 3 (curve *a*) shows a response/time curve for 48 ppm CO using a flow rate of 700 cm^3/min. As predicted by Equation 6, the sensor signal increases with time to a steady-state value at large values of λt.

Figure 3 (curve *b*) shows the current decay with time after CO flow through the sensor had ceased. The rapid return of the current to zero supports the assumption used in the derivation of Equation 5 that all the CO migrating through the porous electrode is electro-oxidized.

Figure 3 (curve *c*) shows the data of curve *a* replotted in the form $-\log(1 - i/i_{\lim})$ *vs.* t. The slope of this plot equals λ. The values calculated from these data were 0.18 ± 0.02 sec^{-1} for $300 < G < 1500$ cm^3/min. Similar semilogarithmic plots were obtained with the current decay results and they gave $\lambda = 0.16 \pm 0.02$ sec^{-1} in the same flow-rate range. Thus, the time constants for rise and decay of sensor signal are essentially equal and are independent of flow rate.

Signal/CO Concentration Relationship. Equation 5 predicts that the steady-state current varies linearly in CO

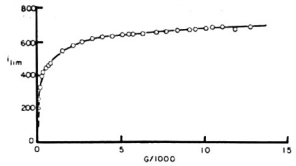


Figure 4. i_{lim} (μA) *vs.* G (cm^3/min ÷ 1000) for n_0 = 48 ppm CO (i_∞ = 700 ± 5 μA)

concentration. Linearity of sensor response has been observed repeatedly by us (*1, 2*) and by independent investigations (*3, 4*). Again, in this work, signal linearity was found. The important implication of this finding is that instruments using this sensor require only a "one point" calibration procedure.

Sensor Response as a Function of Gas Flow Rate. Equation 6 predicts that $i \rightarrow 0$ as $G \rightarrow 0$, and at high flow rates, i_{lim} approaches a maximum current (i_∞) given by

$$i_\infty = 2\frac{Fn_0whL}{\bar{V}}(k_\infty - \lambda_\infty) \qquad (8)$$

Figure 4 shows the steady-state oxidation current for 48 ppm CO as function of flow rate. From these results, i_∞ = 700 ± 5 μA and k_∞ = 6.12 ± 0.05 sec^{-1}.

Also from the results in Figure 4, the overall "constant" k (Equation 6) and k_G (Equation 7) were calculated as a function of flow rate. The plot of log k_G *vs.* log G in (Figure 5) had two linear branches which intersect at G = 1150 cm^3/min. From the slopes of the two segments, α = 0.48 for $G < 1150$ and α = 0.81 for $G < 1150$. The change in α indicates the transition from laminar to turbulent flow in the gas space of the sensor (*9–11*). The transition is not readily apparent in Figure 4 since at G = 1150 the larger portion of the resistance to the overall process is accounted for by the flow-independent term ($1/k_\infty$).

The relative magnitudes of k_G and k_∞ are also shown in Figure 5. Thus, at 50 cm^3/min, 500 cm^3/min, and 5000 cm^3/min, the mass transfer contribution to the overall resistance of the process is 56%, 32%, and 9%, respectively—*i.e.*, the process is controlled by the rate of the electrochemical reaction at the higher flow rates.

(9) F. Kreith, "Principles of Heat Transfer," International Textbook Company, Scranton, Pa., 1961
(10) W. M. Kays, *Trans. ASME*, **72**, 1067 (1950).
(11) D. J. Pickett, *Electrochim. Acta*, **18**, 835 (1973).

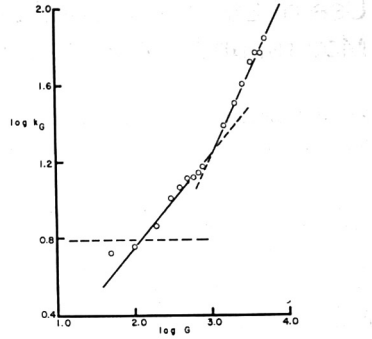


Figure 5. log k_G (sec^{-1}) *vs.* log G (cm^3/min) for n_0 = 48 ppm CO. Note: horizontal – – – represents k_∞

These results demonstrate that the experimentally observed behavior of the electrochemical sensor is in agreement with theoretical predictions. The rapid signal response and decay times, and the large signal per ppm of CO demonstrates that ambient CO concentrations can be measured with this technique.

NOMENCLATURE

a = empirical constant
D = CO diffusion coefficient, cm^2/sec
G = volumetric gas flow rate, cm^3/sec
h = height of gas pathway, cm
i = oxidation current, μA
i_{lim} = steady state oxidation current, μA
k = overall rate constant for transfer of CO to the catalytic surface and the electrochemical reaction, sec^{-1}
k_G = gas flow rate-dependent portion of k, sec^{-1}
k_∞ = gas flow rate-independent portion of k, sec^{-1}
L = total length of gas pathway in sensor, cm
n = concentration of CO in air at any time and position in sensor, ppm
n_0 = concentration of CO in air entering sensor, ppm
t = time, sec
$\bar{V}$ = molar volume of ideal gas
w = width of gas pathway, cm
x = length coordinate of gas pathway in sensor, cm
α = empirical constant
λ = time constant arising from solution of continuity equation, sec^{-1}
v = linear velocity of gas stream through sensor, cm/sec
∞ = subscript for "infinite gas flow-rate conditions"

RECEIVED for review March 4, 1974. Accepted June 24, 1974.

Use of State Variable Active Filters as Differentiators, Rate Meters, and End-Point Locators

Robert H. Callicott and Peter W. Carr[1]

Department of Chemistry, University of Georgia, Athens, Ga. 30602

The ability to precisely measure the various time derivatives of a signal is of considerable importance in several areas of chemical analysis. Many kinetic methods of analysis use the first time derivative of a signal as a direct measure of sample concentration (*1*). Automatic titrators frequently use either the point of maximum slope or the inflection point in the titration curve to locate an end point (*2*).

Although very simple operational amplifier circuits may be used to differentiate a time-dependent signal, such circuits are generally not very useful (*3*) because they tend to selectively amplify the high frequency noise components present in any real signal. To obtain a clean derivative, it is generally essential to limit the circuit's bandwidth as well as its high frequency gain (*4*).

Malmstadt and Crouch have described a very useful multiple operational amplifier differentiator which has several unique features (*5*). Their device constitutes a high-pass single-pole state variable filter (*6*) and is described by the transfer function, $T(s)$, given below:

$$T(s) = \frac{e_0(s)}{e_{in}(s)} = \frac{H_0 s}{s + \omega_0} \qquad (1)$$

where H_0 represents the circuit gain, ω_0 the cut-off frequency, and s is the Laplace transform variable. A high-pass filter (or transfer function) is invariably one in which the highest degree of s in the numerator of the function is equal to the highest degree of s in the denominator. The Laplace transform variable does not appear in the numerator of a low-pass transfer function. The physical result of this is that a high-pass filter has a finite output for high frequency (ac) signals, but a lowpass filter has zero output in the limit of very high frequency. In the limit of long times ($s \ll \omega_0$), the transfer function becomes identical with the differentiation operator—*i.e.*, multiplication by s. The principal advantage of the state variable design is that both H_0 and ω_0 may be tuned independently over very wide ranges.

During the past several years, a variety of "universal" active filters have become available. Since these devices are quite small, have low power requirements, and most importantly are two-pole filters in which high, band and low-pass outputs are simultaneously available, we have investigated their use in several common analytical operations. Inspection of the band-pass and high-pass transfer functions (Equations 2 and 3, respectively) indicates that, at appropriately long time, both the first and second time derivatives may be obtained.

$$T_{BP}(s) = \frac{A_{BP}(\omega_0/Q)s}{s^2 + (\omega_0/Q)s + \omega_0^2} \qquad (2)$$

$$T_{HP}(s) = \frac{A_{HP}s^2}{s^2 + (\omega_0/Q)s + \omega_0^2} \qquad (3)$$

Q in the above equations is the damping ratio: at $Q = 1/\sqrt{2}$, the filter will be critically damped regardless of ω_0. The low frequency behavior of Equation 2—*i.e.*, $s \ll \omega_0$—is identical to the differentiator of Malmstadt and Crouch. Since the denominator is quadratic in s, the filter offers better high frequency noise rejection, at a given ω_0, than the corresponding single-pole device but with the same rise time.

EXPERIMENTAL

A Burr-Brown UAF-11 filter was used throughout this study. A partial schematic diagram is given in Figure 1. All components not housed inside the epoxy encapsulated filter are denoted by an asterisk. Power supply and offset trim connections are not indicated but the procedure advised by the manufacture was followed. Preliminary results were obtained with a ±15-volt power supply; however, better noise characteristics were obtained when power was obtained from a set of four 9-volt transistor batteries. The cut-off frequency, ω_0, was tuned by adjustment of both R_1 and R_2. For the circuit given in Figure 1, it is easily shown that with $R_1 = R_2$ and $C_1 = C_2$ the cut-off frequency is:

$$\omega_0 = 1/R_{eq}C_1 \qquad (4)$$

where

$$R_{eq} = \frac{10^{10}}{R_1} + 2{\cdot}10^5 \qquad (5)$$

With the components used in this study, the time for 99% response could be varied from approximately 3 to 50 seconds by changing R_1 and R_2. Although very low ω_0 values may be obtained by decreasing R_1 below 500 Ω or by increasing the 100 KΩ resistors in the "T" networks at the input of OA2 and 3, we found that this leads to unstable operation and considerable difficulty in adjusting the offset trim. Acceptable results were obtained by adding the 0.5-μF non-polarized capacitors shown in Figure 1. A final practical consideration is that the "Q adjust" resistor which may be placed between point A and common (see Figure 1) was deleted since Q may be adjusted to a critically damped value by means of R_g. It should be noted that critical damping was independent of ω_0—*i.e.*, of variation in R_1 and R_2—provided that care is taken to keep R_1 equal to R_2.

A signal generator (Wavetek, Model 112) was used to test and perform preliminary adjustments of the filter. All signals were recorded on a Hewlett-Packard X-Y recorder (Model 7001-A) in the Y-T mode. The thermometric titrations were carried out with equipment described previously (*7*). Constant rate potentiometric titrations were carried out in a thermostated (25 °C) 100-ml cell with a Radiometer (ABU-11) 2.5-ml buret. A fast response micro combination electrode (Beckman 39505-3C) was used to measure the pH. An electrometer amplifier (Analog Devices Model 523) in a voltage follower configuration was used to monitor the output of the glass electrode.

[1] To whom all correspondence should be addressed.

(1) H. V. Malmstadt, C. J. Delaney, and E. A. Cordos, *Crit. Rev. Anal. Chem.*, **2**, 559 (1972).
(2) J. P. Phillips, "Automatic Titrators," Academic Press, New York, N.Y., 1959, pp 37–40.
(3) H. V. Malmstadt, C. G. Enke, and E. C. Toren, Jr., "Electronics for Scientists," W. A. Benjamin, New York, N.Y., 1963, pp 358–9.
(4) Philbrick Application Manual for Computing Amplifiers, Philbrick Researchers, Inc., Dedham, Mass., 1966.
(5) H. V. Malmstadt and S. R. Crouch, *J. Chem. Educ.*, **43**, 340 (1966).
(6) J. G. Graene, G. E. Tobey, and L. P. Huelsman, "Operational Amplifiers, Design and Applications," McGraw-Hill, New York, N.Y., 1971, p 303.
(7) E. B. Smith, C. S. Barnes, and P. W. Carr, *Anal. Chem.*, **44**, 1663 (1972).

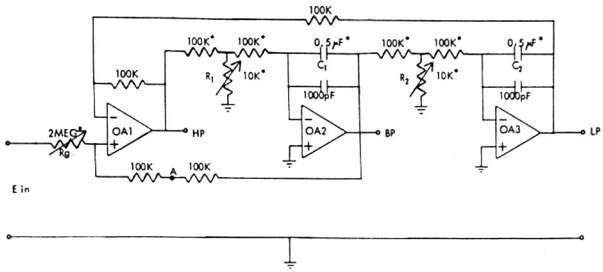


Figure 1. Schematic diagram of active filter

All components shown with an asterisk are external to the monolithic filter. Power supply and offset trims are not shown

Table I. Effect of Cut-Off Frequency on Filter Output

ω_0[a]	Low pass[b] e_0 (V)	Band pass[c] e_{ω_0} (V/sec)	High pass[d] $e_{\omega_0^2}$ (V/sec²)
0.291	3.70	0.0704	0.0437
0.567	3.80	0.0697	0.0523
0.741	3.82	0.0696	0.0547
1.07	3.80	0.0696	0.0577
1.38	3.80	0.0676	0.0515
1.67	3.80	0.0701	0.0498
Average	3.79	0.0695	0.0515
Rel std dev	1.1%	1.4%	8.9%

[a] Cut-off frequency of the filter calculated from Equation 4. [b] Input signal is a 9.1 volt, 0.018-Hz sinusoid. Output is the amplitude of the filtered sine-wave. [c] Input signal is a 0.015-Hz triangle wave. Output is the amplitude of the resultant square wave. [d] Input signal is a 0.019-Hz sinusoid. Output is the amplitude of the resultant sine wave.

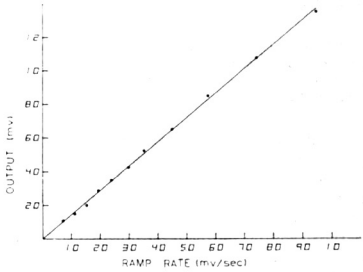


Figure 2. Band-pass output as a function of the input rate

Input is a triangle wave of known rate of charge. Output is the steady-state response; ω_0 = 0.2 Hz

All titrations reported here are 290 μmoles of perchloric acid (Baker Analyzed) with 1*M* sodium hydroxide (Fisher). A 30-ml volume was used in the thermometric titrations and 50-ml volume was used in the potentiometric titrations. The titrant was added at a rate of 9.1 μmoles/sec in all cases.

RESULTS AND DISCUSSION

The transfer function of each output was tested to determine that the device was operating properly. Although this could be easily assessed by varying the frequency of the input function, the filter and its limitations are more effectively checked by varying ω_0. The results of such tests are shown in Table I. The low-pass output was tested by measuring the steady-state response to a 9.1-volt, 0.018-Hz sine wave. As expected (see Table I), the response is independent of the cut-off frequency of the filter. The low-pass and high-pass gains are related to the band-pass gain by the following relationship:

$$A_{LP} = A_{HP} = \frac{A_{BP}}{Q} \quad (6)$$

The relationships in Equation 6 were verified by inputing a sine wave and measuring each of the available outputs.

The low frequency ($s \ll \omega_0$) limits of Equations 2 and 3 are:

$$T_{BP}(s) = \frac{A_{BP}S}{Q\omega_0} \quad (7)$$

and

$$T_{HP}(s) = \frac{A_{HP}S^2}{\omega_0^2} \quad (8)$$

The steady-state band pass and high-pass response to a low frequency triangle and sinusoidal wave are given in Table I. In each case, the expected dependence upon ω_0, see Equations 7 and 8, was obtained. The theoretical relationship between the high-pass and band-pass gains was also verified. Equations 7 and 8 indicate that the steady-state band-pass and high-pass responses correspond to the first and second derivatives of the input signal, respectively. Since the data in Table I indicate that the active filter used does in fact follow Equations 7 and 8, its ability to accurately differentiate a signal was tested.

In kinetic analysis and particularly enzymatic assays, one generally strives to obtain pseudo-zero order kinetics—*i.e.*, a linear signal–time curve. Such assays were simulated by inputing a series of triangle waves of various amplitudes and frequencies so that the rate of change of the input signal was scanned from 1 mV/sec to 500 mV/sec. For the data of Figure 2, the band-pass output was employed with ω_0 = 0.2 Hz. A 99% steady-state response was obtained within 25 seconds (=5/ω_0) and was a linear function of the rate of change of the input signal. Since noise is most apparent at low input rates, only the data from 1 to 10 mV/sec are shown in Figure 2. The mean residual from a least squares line for the points shown is only 2.1%. Data corresponding to input rates between 36 and 500 mV/sec obtained with ω_0 set at 0.7 Hz had an average residual from the least squares line of 0.9%. The band-pass output is therefore precisely tracking the rate of change of the input signal.

The active filter is not the principal noise source at high input rates. A series of experiments with the input shorted indicates that over a range of ω_0 from 0.2 to 1.7 Hz the

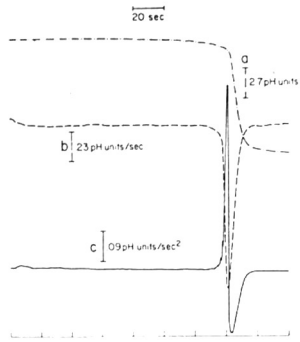


Figure 3. First and second derivative of potentiometric acid–base titration

Sample is 920 μmoles of perchloric acid in 50 ml of distilled water; rate of titrant addition is 9.1 μmole/sec. Curve *a*, low-pass output; curve *b*, band-pass or first-derivative output; curve *c*, high-pass or second-derivative output. Cut-off frequency is 0.39 Hz

magnitude of the rms noise is essentially independent of the cut-off frequency and has an average value of about 0.1 mV; this corresponds to an input standard deviation of ±70 μV/sec at ω_0 = 0.2 Hz. The frequency domain of the noise shifts to lower frequency as ω_0 is decreased.

Since the magnitude of the noise inherent in the amplifier is essentially independent of ω_0, the optimum results with a noisy input signal will be obtained with ω_0 set to as low a value possible commensurate with the desired 99% response time (= $5/\omega_0$). This is a result of two factors. First, the effective gain of the band-pass filter increases as ω_0 is decreased (see Equation 7). Second, noise in the input signal will be filtered more effectively, the smaller is ω_0.

The second derivative or high-pass output was not studied in detail because the quantitative measurement of the second derivative is seldom of interest. However, the end point of an automatic potentiometric titration is frequently located by determining the inflection point in a titration curve. The original along with the first and second derivatives of a constant rate acid–base titration are shown in Figure 3. These curves were obtained from three individual titrations. The inflection point is quite evident and the second derivative curve has the expected shape (*8*). The second derivative curve is not significantly noiser than the

(8) L. Meites and H. C. Thomas, "Advanced Analytical Chemistry," McGraw-Hill, New York, N.Y., 1958, p 45.

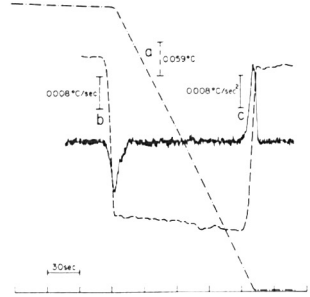


Figure 4. First and second derivatives of a thermometric acid–base titration

All conditions identical to Figure 3 except sample volume is 30 ml. Curve *a*, original unfiltered titration curve; curve *b*, first derivative; curve *c*, second derivative. Cut-off frequency is 0.74 Hz

first derivative curve, and we estimate that the inflection point can be located within ±0.005 pH/sec². Care must be exercised in using the active filter in very rapid titrations since some phase lag does occur. Thus, the titrant delivery system should be calibrated by titrating a standard with the same setting of ω_0 as that used for the unknown. The effect of a decrease in response time is to elongate the titration curve and shift the end point to longer time. A very rapid rise time does not distort the shape of the titration curve but does permit more noise to pass through the filter. We did not encounter any serious difficulty in adjusting ω_0 for the titration curve. One pretitration generally suffices to obtain an appropriate setting of ω_0.

Various derivative thermometric titrations are shown in Figure 4. Since we wanted to compare analyses via two methods on essentially identical samples, the total temperature change in the thermometric titrations were extremely large (~0.5 °C). Much lower concentrations could be determined with the apparatus used in this work. The first derivative titration has the expected step functional form. The shape of the second derivative curve is in qualitative agreement with the first derivative. The width of the second derivative spikes which indicate the start and end of the titration is fixed by ω_0 since no initial or end-point curvature is present in the original titration curve.

RECEIVED for review March 4, 1974. Accepted May 3, 1974. This work was supported in part by a grant (GM 17913) from the National Institutes of Health and one of us (R.H.C.) was supported by a fellowship from the Graduate School of University of Georgia.

Ion Selective Electrodes Responsive to Anionic Detergents

Taitiro Fujinaga, Satoshi Okazaki, and Henry Freiser

Departments of Chemistry of the Faculty of Science, Kyoto University, Kyoto, Japan, and the University of Arizona, Tucson, Ariz. 85721

One of the major problems in attacking environmental pollution is the absence of adequately sensitive, reliable, specific, and convenient analytical methodology. In particular, determination of trace level organic contaminants in water such as that of the detergents is rather difficult because of the absence of functional groups of highly distinctive characteristics. Two of the authors have devoted special attention to contamination due to such surface active

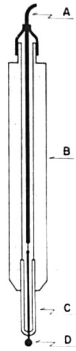


Figure 1. Configuration of electrode

A: Coaxial cable; B: Teflon body; C: Glass tube; D: Pt tip

agents (*1*), now one of the most urgent problems in environmental pollution. It has been recently demonstrated that the ion selective electrode approach can be applied to the determination of organic as well as inorganic ions (*2*). The possibility of extending this to the problem of detergent analysis is most attractive. The recently developed coated-wire ion selective electrode provides an inexpensive and convenient way to do this (*3, 4*).

EXPERIMENTAL

Reagents. Sodium alkyl benzene sulfonates were synthesized by conventional methods and recrystallized three times from benzene. Sodium alkyl sulfonates were also synthesized and recrystallized from ethanol. All other chemicals used were of reagent grade quality.

The ion association complexes were prepared by the following procedures. A 50% (v/v) solution of methyltricaprylammonium chloride (Aliquat 336S) in decanol was shaken with 0.1*M* aqueous solution of the sodium salt of the detergent anion to synthesize the quaternary ammonium salt, and the emulsion, if present, was centrifuged for 3 minutes at 6000 rpm. These procedures were repeated at least 6 times or until chloride ion was no longer detected (as silver chloride) in the aqueous phase. The electrode coating mixture was prepared by making a 3:1 mixture of 10% polyvinyl chloride dissolved in cyclohexanone and decanol solution of the complex.

Apparatus. The electrode assembly, shown in Figure 1, was similar to that described earlier (*3, 4*). The tip of a fine platinum wire (0.7 mm in diameter) was fused to make a ball of *ca.* 1.5 mm in diameter. The exposed part of the platinum wire was dipped several times in the electrode coating mixture.

The electrode was initially conditioned by soaking it for 30 minutes in a $10^{-4}M$ standard solution of the anion to be measured and stored in air at room temperature when not in use. It was reconditioned by soaking in the standard solution for 5 minutes immediately before use.

Surface tension measurements of detergent solutions were carried out with a Du Nouy tensiometer.

RESULTS AND DISCUSSION

The response time of the electrode varied with the concentration, but the equilibrium steady potential was usually achieved within 2–3 minutes and was reproducible to ±0.1 mV.

Figure 2 shows the potential response curve to the concentration of *p*-toluene sulfonate anions. A linear response

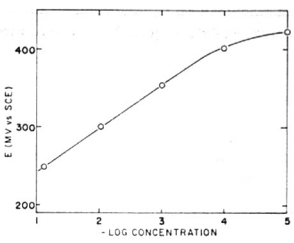


Figure 2. Potential response curve of *p*-toluene sulfonate ion electrode

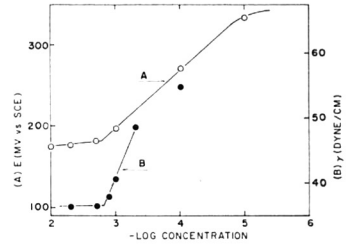


Figure 3. Potential response curve (A) and surface tension–concentration plot (B) of lauryl benzene sulfonate ion electrode

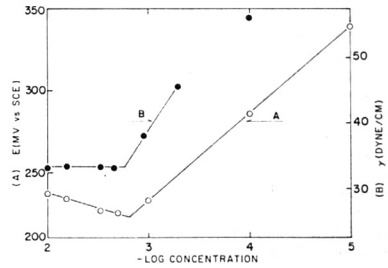


Figure 4. Potential response curve of isolauryl benzene sulfonate ion electrode

was obtained to the logarithmic variation of concentration with the slope of 57 mV/log *a* from $10^{-1}M$ to $2.5 \times 10^{-4}M$, although the electrode can be used down to $10^{-5}M$ after calibration.

With laurylbenzene sulfonate (LBS), the potential response curve to the concentration of LBS is steeper than that expected from the Nernst equation in the concentration range between $1 \times 10^{-3}M$ and $2 \times 10^{-5}M$, and when the concentration of LBS is greater than $1 \times 10^{-3}M$, there is a sharp break in the potential response curve (see curve A in Figure 3).

Because we suspected that the discontinuity and the potential response curve for LBS represented a change of the solution rather than a failure in the electrode, we postulated that the break in the curve arose when the LBS began

(1) T. Fujinaga and S. Okazaki, *Jap. Anal.*, **14,** 832 (1965).
(2) C. J. Coetzee and H. Freiser, *Anal. Chem.*, **41,** 1128 (1969).
(3) R. W. Cattrall and H. Freiser, *Anal. Chem.*, **43,** 1905 (1971).
(4) J. T. Davies and E. K. Rideal, "Interfacial Phenomena," Academic Press, New York, N.Y., 1961.

Table I. Behavior of Detergent-Responsive Electrodes

Electrode	Slope, mV	Concn range of linear response, *M*	Usable concn range, *M*	CMC: Electrode, $\times 10^{-3}M$	CMC: Surface tension, $10^{-3}M$
p-$CH_3C_6H_4SO_3^-$	57	10^{-1}–$10^{-3.6}$	10^{-1}–10^{-5}	...	...
i-$C_{12}H_{25}C_6H_4SO_3^-$	55	10^{-3}–10^{-5}	10^{-3}–$10^{-5.5}$	1.6	1.7
n-$C_{12}H_{25}C_6H_4SO_3^-$	75	10^{-3}–$10^{-4.7}$	10^{-3}–$10^{-5.5}$	1.6	1.5
n-$C_8H_{17}SO_4^-$	55	10^{-1}–$10^{-3.6}$	10^{-1}–10^{-5}	...	...
n-$C_{12}H_{25}SO_4^-$	89	10^{-2}–$10^{-3.7}$	10^{-2}–10^{-5}	12	10

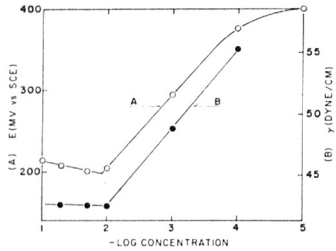


Figure 5. Potential response curve of lauryl sulfate ion electrode

Table II. Selectivity Ratios for Interfering Anions with LBS Responsive Electrode

Interfering anion	K_i
Chloride	0.012
Sulfate	0.006
Nitrate	0.93
Perchlorate	0.81
Acetate	0.59
Lauryl sulfate	1.36
Lauryl sulfonate	0.81
p-Toluene sulfonate	0.75

to associate in micellar aggregates. Solutions or surfactants will form such polymeric aggregates at fairly well defined concentrations, known as the critical micelle concentration (CMC). One of the critical ways of observing CMC is to measure the surface tension of a series of solutions of different concentrations (*4*). A sharp break in the surface tension concentration curve is observed at CMC. It will be noted from comparison of curves A and B in Figures 3, 4, and 5, that the surface tension and electrode response curve breaks coincide, thereby demonstrating the validity of the use of electrode measurements for the determination of CMC (Table I).

The ion selective electrode method is not only more rapid and convenient than the conventional surface tension approach, but it can be also argued that the potential reading of the electrode in solutions having concentrations higher than CMC still reliably measure monomer concentrations. Thus, the use of the anion detergent responsive electrode provides a new and useful tool for studies of behavior of these interesting colloids. The LBS electrode, not surprisingly, is not very selective with respect to other anionic detergents of similar molecular weight. The interferences of this electrode were studied in the previously described (*5*) manner with results as shown in Table II. It is interesting to note that the more commonly encountered inorganic ions of chloride and sulfate are relatively noninterfering. The selectivity ratios for lauryl sulfate and lauryl sulfonate are reasonably close to unity, which suggests that even though LBS could not be determined in a mixture of the three detergents, that the electrode could be used to give a good approximation of the total concentration of the three together.

ACKNOWLEDGMENT

The authors are grateful to the Japanese Society for the Promotion of Science both for sponsoring a visit of one of them (H.F.) to Kyoto University during which time this work was initiated, as well as for the continuing support of this research.

RECEIVED for review April 15, 197. Accepted June 27, 1974.

(5) H. James, G. Carmack, and H. Freiser, *Anal. Chem.*, **44**, 856 (1972).

Determination of Isocyanates in the Working Atmosphere by Thin-Layer Chromatography

Jürgen Keller

Farbenfabriken Bayer GmbH, OC-Produktion, Organic Analytical Laboratory, 509 Leverkusen-Bayerwerk, West Germany

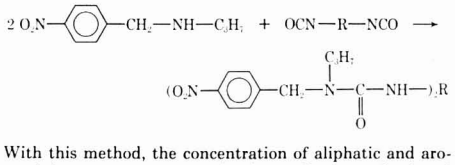
K. L. Dunlap[1] and R. L. Sandridge

Mobay Chemical Company, Division of Baychem Corporation, New Martinsville, W. Va. 26155

With the large usage of isocyanate resins in spraying and foaming applications, and the growing concern over the exposure of workers to isocyanate vapors, there exists the need for a way of determining the isocyanate content of industrial working atmospheres. This includes not only free isocyanate monomers but also isocyanate resin aerosols with free isocyanate groups which may be present in spraying applications. Of the methods currently available, none can be used to estimate both the isocyanate monomer and resin in the working atmosphere.

The colorimetric method described by Ehrlicher and Pilz (*1, 2*) and Marcali (*3*) is widely used to determine toluene diisocyanate (TDI) in the atmosphere. However, this method is applicable only to aromatic isocyanates and is subject to interferences by aromatic amines. Some difficulties have been encountered in applying this method to the determination of 4,4′-diphenylmethane diisocyanate (MDI) in air. The method of von Eicken (*4*) which was later modified by Pilz and Johann (*5*) can be used to determine hexamethylene diisocyanate (HDI) in air. Several laboratories have reported difficulty with this spectrophotometric method due to high blanks and lack of reproducibility. Heuser *et al.* (*6*) have reported a thin-layer chromatographic method for the determination of free HDI monomer in polyurethanes which is based on the reaction of the isocyanate with *N*-methyl-*N*-(4-aminobenzyl)amine.

In this paper, a thin-layer chromatographic method is presented for the analysis of isocyanates in the working atmosphere. The procedure is based on the determination of the ureas formed from the reaction of the isocyanates with *N*-4-nitrobenzyl-*N*-*n*-propylamine (nitro reagent).



With this method, the concentration of aliphatic and aromatic isocyanate monomers in air may be determined, and the concentration of isocyanate resins in the working atmosphere may be estimated.

EXPERIMENTAL

Synthesis of Nitro Reagent. Dissolve 250 g of 4-nitrobenzyl chloride in 1.2 liters of benzene. Bring the solution to boiling under reflux conditions, and add 180 g *n*-propylamine dropwise over a 30-minute period. Reflux for 5 hours. Concentrate the reaction mixture by stripping off the solvent in a rotary evaporator at 50 °C. Dissolve the residue in 400 ml of water, and slowly add 150 ml of a 45% NaOH solution. Add 500 ml of benzene, and stir the mixture for about 5 minutes. Remove the benzene layer, treat with approximately 5 g of charcoal, and filter. Strip off the solvent and excess *n*-propylamine in a rotary evaporator. Dissolve the product in about 250 ml of acetone, and add 170 g of concentrated HCl. Evaporate the mixture to dryness at 50 °C in a rotary evaporator. Purify the HCl salt of the nitro reagent by washing the salt with a 1:1 mixture of acetone:benzene followed by suction filtration. Repeat this purification step several times. Dry the salt in a vacuum oven at 50 °C. *Yield:* 60 to 95%, depending on the quality of 4-nitrobenzyl chloride; *e.g.* 90 to 95% with 99% 4-nitrobenzyl chloride.

Reagents. *Nitro Reagent Solution.* For stability reasons, the nitro reagent is stored as its hydrochloride (mol wt 230.7). Dissolve about 120 mg of nitro reagent hydrochloride in about 25 ml of distilled water; add 13 ml of 1*N* NaOH, whereby the free amine precipitates. Extract the free nitro reagent with 50 ml of benzene (Toluene may also be used as a solvent for the nitro reagent solution.). Dry the benzene layer with Na_2SO_4, and dilute the resulting solution to 250 ml to prepare the $2 \times 10^{-3}M$ solution. Dilute this solution tenfold to obtain the $2 \times 10^{-4}M$ solution which is used as the absorber solution. Store the nitro reagent solution in the dark and do not use the solutions after more than five days storage.

Benzene. Reagent grade has been passed through a column of alumina to ensure that no trace contaminant will interfere with the analysis.

Titanous Chloride Solution. This solution consists of pyridine: 20% $TiCl_3$ solution:glacial acetic acid, 40:40:20 by volume. To prevent the oxidation of the titanous chloride, this solution should be deaerated and stored under nitrogen.

Apparatus. A TELEMATIC portable air sampler, Type C115, (Bendix, Environmental Science Division) or its equivalent is used in conjuction with midget gas impingers containing the nitroreagent absorber solution to collect the air sample. TLC plates used in the analysis are CHROMAR 7GF plates from Mallickrodt Chemical Works or silica gel plates (layer thickness 0.25 mm) from E. Merck, Darmstadt, West Germany.

Procedure. *Air Sampling.* The required volume of air is drawn through two midget gas impingers at the rate of 1–2 liters per minute (Two impingers connected in series should be used unless it has been established that the collection efficiency of the first impinger is such that the isocyanates of interest are quantitatively absorbed in the first impinger.). The impingers are connected in series, and each contains 10 ml of $2 \times 10^{-4}M$ nitro reagent solution. After the air sample is taken, the two solutions are combined and carefully evaporated to 1 ml. This is most easily accomplished by evaporating to dryness in a vacuum oven set at 35 °C, and dissolving the residue in 1 ml of benzene. This solution is then submitted for TLC analysis.

TLC Analysis of the Ureas of Isocyanates. Ten-microliter aliquots of the solutions to be analyzed are spotted with 10-μl disposable pipets on a thin-layer plate. In addition, ten-microliter aliquots of standard solutions which are to be compared with the samples are spotted on the plate. Before the plate is developed, it is treated with HCl vapors for 3 minutes by placing the plate in a developing chamber with a small container of concentrated hydrochloric acid. By impregnation with HCl, the amines (including the excess nitro reagent) will be eluted by the initial development while the ureas remain at the starting point. The plate is first developed using a mobile phase of methanol:water, 10:90 by volume.

[1] Author to whom all correspondence should be directed.

(1) H. Ehrlicher and W. Pilz, *Arbeitsschutz*, **1956**, 276 (Part I).
(2) H. Ehrlicher and W. Pilz, *Arbeitsschutz*, **1957**, 7 (Part II).
(3) Kalman Marcali, *Anal. Chem.*, **29**, 552 (1957).
(4) Sigrid von Eicken, *Mikrochim. Acta*, **1958**, 731.
(5) W. Pilz and Ilse Johann, *Mikrochim. Acta*, **1970**, 351.
(6) E. Heuser, W. Reusche, K. Wrabetz, and R. Fauss, *Z. Anal. Chem.*, **257**, 119 (1971).

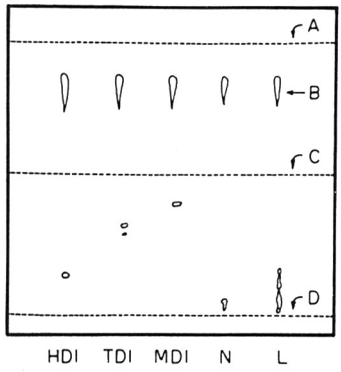


Figure 1. Scheme of chromatogram

HDI = 1,6-hexamethylene diisocyanate; TDI = 2,4- and 2,6-toluene diisocyanate; MDI = 4,4′-diphenylmethane diisocyanate; N = DESMODUR N, Mobay Chemical Company; L = DESMODUR L, Mobay Chemical Company. A = Front for first development; B = Excess nitro reagent; C = Front for second development; D = Start

The length of development is approximately 18 cm, which will require about 1.25 hours.

After the initial development, the TLC plate is dried for exactly 10 minutes in an oven set at 100 °C. The conditions of this drying step should be followed closely since deviations from these conditions will result in changes of the R_f values for the ureas. The plate is developed a second time using a mobile phase of ethyl acetate: acetone:hexane, 10:10:30 by volume to elute the ureas. After the second development, the plate is dried and sprayed with the titanous chloride solution to reduce the nitro groups to amino groups. The plate is dried and treated wtih HCl vapors. The amine hydrochlorides on the plate are then diazotized with nitrous fumes by placing the plate in a developing chamber with a container of $NaNO_2$. Several drops of HCl are added to the container, and the plate is removed from the chamber after a period of 2 minutes. A stream of air is passed over the plate for 2 minutes to remove any residual nitrous fumes, and then the plate is visualized by spraying it with a 0.5% aqueous *N*-1-naphthylethylenediamine solution. By comparing the spots of the sample solutions with those of the standards, the concentration of isocyanate in the solution can be determined. This may then be related to the concentration of isocyanate in air by the volume of air sampled.

Preparation of Standard Solutions. Standard solutions are prepared as needed by adding a weighed amount of the isocyanate of interest to the nitro reagent solution. These standard solutions should be stored in the dark and should not be used if they are more than 5 days old. Normally, the $2 \times 10^{-3}M$ nitro reagent solution is used to make a stock solution which is then diluted to obtain standard solutions in the concentration range of interest. For example, stock solutions for diisocyanates such as TDI, MDI, or HDI would be prepared by weighing out 10 mg of the diisocyanate to the nearest 0.1 mg and diluting to 100 ml with the $2 \times 10^{-3}M$ nitro reagent solution. The stock solution would then be diluted to give standards in the concentration range of interest.

Table I. Concentration Limits for Several Isocyanates[a]

Isocyanate	Lower limit, mg/m³	Upper limit, mg/m³
HDI	0.08	33
TDI	0.08	34
MDI	0.08	50
DESMODUR N	0.40	15
DESMODUR L	0.50	5

[a] Concentration levels are based on a 10-liter air sample and 20 ml of $2 \times 10^{-4}M$ absorbing solution.

RESULTS AND DISCUSSION

This method can be applied to both aliphatic and aromatic isocyanates whether they are in the form of vapors or resin aerosols in the working atmosphere. The method offers both a qualitative identification of isocyanates by R_f values and quantitative determination of the amount of these isocyanates. The scheme of a developed thin-layer chromatogram is given in Figure 1. Upper and lower concentration levels which may be determined by the method are given in Table I for several of the more common isocyanates. These levels are based on taking a 10-liter air sample and using 20 ml of the $2 \times 10^{-4}M$ nitro reagent absorbing solution. The lower limit may be decreased by taking a larger air sample, and the upper limit may be increased by increasing the amount of nitro reagent or by decreasing the volume of the air sample.

For quantitative determinations of the isocyanates, a visual comparison of the sample and standards may be used; however, the use of the scanning densitometer or other scanner designed for the evaluation of TLC plates would eliminate any analyst bias in the interpretation of the results and improve the precision of the method. With the use of a scanner, an absolute calibration or a calibration based on an internal standard could be used, thus avoiding the necessity of preparing standard solutions for comparison every five days.

An important concern in the analysis of isocyanates is the likelihood of undesirable reactions of the collected isocyanate. This possibility is eliminated by the method since the isocyanate is reacted with the nitro reagent to form a stable derivative. The only limitation of the method is that it cannot be applied to atmospheres which decompose the reagent by oxidation or reduction.

In conclusion, this paper presents a highly sensitive TLC method to determine isocyanate levels in the working atmosphere for most types of isocyanates of current industrial interest.

RECEIVED for review March 14, 1974. Accepted June 7, 1974.

Gas Chromatographic Separation of Some Unsaturated Hydrocarbons Using Thallium(I) Tetraphenylborate as Stationary Phase

George E. Baiulescu

Department of Analytical Chemistry, University of Bucharest, Romania

Vasile A. Ilie

Institute of Chemical Research, Bucharest, Romania

Several stationary phases are available for the gas chromatographic separation of olefins, particularly those of the terpene series (*1, 2*); but the best and most commonly used, silver nitrate in diethylene glycol or ethylene glycol (*3, 4*) has considerable drawbacks. Silver ion is rapidly reduced above 65 °C to the detriment of column performance; even at 40 °C, an operating life of only a few days is often obtained, and the column behavior is irreproducible.

At 25 °C, the column is stable for long periods and gives reproducible separation (*3, 4*) but the resulting long retention times for terpenes and other high boiling olefins are inconvenient; attempts to improve the situation by reducing the proportion of silver nitrate in the stationary phase give columns with low capacity that are unsuitable for preparative-scale operation.

Several attempts were made to separate some unsaturated hydrocarbons on lithium caproate (*5*) as well as on transition-metal complexes (*6*). The capacity of Tl(I) in thallium nitrate to interact selectively as the silver ion in silver nitrate with unsaturated hydrocarbons is reported in (*7, 8*).

The present paper studies the behavior as stationary phases of the thallium tetraphenylborate compared with that of sodium in the separation of a series of olefins and aromatic hydrocarbons.

The use of sodium, potassium, rubidium, cesium, and thallium tetraphenylborates as stationary phases in gas chromatography was previously mentioned (*9*).

EXPERIMENTAL

The preparation of thallium(I) tetraphenylborate was made by precipitation from a concentrated solution of thallium(I) sulfate (Riedel de Haën A.G.) with a diluted solution of sodium tetraphenylborate (Merck), followed by filtration and washing of the precipitate with distilled water until the thallium ions did not react. The precipitate was dried in the room atmosphere. The thermograms of sodium and thallium tetraphenylborates (*9*) show a good thermal stability, the loss of substance being observed up to 200 °C.

Measurements were carried out on a gas chromatograph Fractovap Model C (Carlo-Erba, Milano), with a flame ionization detector. Nitrogen was used as carrier gas. The solution peaks were recorded using a Speedomax G 0–1 mV (Leeds & Northrup). The different components were introduced in the chromatographic column using a Terumo microsyringe of 1 μl. Each component was separately introduced (0.1 μl) in the chromatographic column. All the chemical compounds used as standards were of chromatographic purity. Phenylacetylene, phenyl *tert*-butylacetylene and benzo-*tert*-butylcyclobutene were synthetized and identified by means of elemental analysis, IR spectra, and NMR measurements.

The olefin retention was studied using chromatographic columns of aluminum with internal diameter of 4 mm and a length of 6 m. The columns were filled with thallium and sodium tetraphenylborates deposited in the proportion of 25% on hexamethyl-silanized Chromosorb W 30–60 mesh. The retention data for aromatic hydrocarbons were determined on thermostable glass columns with internal diameter of 3.6 mm and a length of 1.4 m.

The stationary phases were solved in acetone and deposited in proportion of 15% on hexamethyl-silanized Chromosorb W 60–80 mesh.

The chromatographic columns were filled by tapping and conditioned in a carrier gas flow at 180 °C for 12 hr.

RESULTS AND DISCUSSIONS

Table I gives the relative retentions, calculated against *n*-pentane at 58 °C, of several olefins on columns with sodium and thallium tetraphenylborates. Table I also gives the relative retentions of some aliphatic hydrocarbons having boiling points (*10*) close to those of the olefins.

The similar relative retentions of olefins and saturated hydrocarbons having close boiling points, obtained with sodium tetraphenylborate show the lack of noticeable interaction between the stationary phase and the components.

The olefins and especially diene hydrocarbons are strongly retained on thallium(I) tetraphenylborate. This interaction is due to thallium(I) ions having low-lying d-orbitals which can form partial covalent bonds with the π-orbitals of the adsorbed molecules.

Cyclopentadiene does not elute from the column of thallium tetraphenylborate under our conditions (column temperature 58 °C, carrier gas flow 20.1 ml/min).

Table II gives the relative retentions of some aromatic hydrocarbons and their derivatives, calculated referred to *n*-decane at 129 °C. The substances elute generally on the column of sodium tetraphenylborate in the increasing order of their boiling points. Higher differences in the relative retentions of the aromatic hydrocarbons on the column of thallium tetraphenylborate comparative to that of sodium, should be due to the thallium(I) ions which are able to interact with the π-orbitals of the aromatic hydrocarbons.

The presence of an ethinyl radical in the phenylacetylene causes the lowering of the aromatic character of the molecule which explains its relative retention, practically the same on both chromatographic columns.

The introduction of a *tert*-butyl radical in the molecule of phenylacetylene causes differences between the relative retentions on the chromatographic columns.

(1) R. A. Bernhard, *Anal. Chem.*, **34**, 1576 (1962).
(2) M. H. Klouwen and R. J. Heide, *J. Chromatogr.*, **7**, 297 (1962).
(3) J. Herling, J. Shabtai, and E. Gil-Av, *J. Chromatogr.*, **8**, 349 (1962).
(4) E. Smith and R. Ohlson, *Acta. Chem. Scand.*, **16**, 351 (1962).
(5) M. Muhlstadt, *Chem. Ber.*, **93**, 2638 (1960).
(6) G. P. Cartoni *et al.*, "Gas Chromatography 1960," R. P. W. Scott, Ed., Butterworths, London, 1960, p 273–93.
(7) B. T. Guran and L. B. Rogers, *J. Gas. Chromatogr.*, **3**, 269 (1965).
(8) D. V. Banthorpe, C. Gatford, and B. R. Hollebone, *J. Gas. Chromatogr.*, **6**, 61 (1968).
(9) G. E. Baiulescu and V. A. Ilie, *Anal. Chem.*, **44**, 1490 (1972).
(10) "Dictionary of Organic Compounds," I. Heilbron and H. M. Bunbury, Ed., Russian ed., Izd. I. L., Moscow, 1949.

Table I. Relative Retentions (Referred to *n*-Pentane at 58 °C) of Some Olefins on Columns with $NaB(C_6H_5)_4$ and $TlB(C_6H_5)_4$

Compound	Boiling point, °C	$NaB(C_6H_5)_4$	$TlB(C_6H_5)_4$
1,3-Butadiene	−2.6	0.35	0.65
n-Butane	−0.5	0.29	0.31
2-Methylbutadiene-1,3	35.0	1.10	1.76
n-Pentane	36.0	1.00	1.00
cis-2-Pentene	37.0	1.14	1.24
2-Methyl-2-butene	38.6	1.20	1.38
Cyclopentadiene	41–42	1.36	—
4-Methyl-*trans*-2-pentene	53.9	2.18	2.35
2,3-Dimethyl-1,3-butadiene	69–70	3.29	6.00
n-Hexane	68.9	3.15	3.00

Table II. Relative Retentions (Referred to *n*-Decane at 129 °C) on Columns with $NaB(C_6H_5)_4$ and $TlB(C_6H_5)_4$

Compound	Boiling point, °C	$NaB(C_6H_5)_4$	$TlB(C_6H_5)_4$
Benzene	80.08	0.06	0.18
Cyclohexane	81.0	0.06	0.06
Toluene	110.6	0.24	0.41
Ethylbenzene	135.5	0.43	0.70
o-Xylene	144.1	0.47	0.94
m-Xylene	139.3	0.46	0.83
p-Xylene	138.0	0.46	0.76
Styrene	145.0	0.47	0.75
Phenylacetylene	142–144	0.56	0.60
Isopropylbenzene	152.0	0.57	1.01
Mesitylene	164.8	0.86	1.57
tert-Butylbenzene	168.0	0.91	1.59
1-Methyl-4-isopropylbenzene	177.0	1.11	1.71
n-Decane	174.0	1.00	1.00
Naphthalene	218.0	3.74	5.98
Phenyl-*tert*-butylacetylene	72°/2 mm.	2.56	8.59
Benzo-*tert*-butyl-cyclobutene	57°/1 mm.	1.90	3.77
p-Di-*tert*-butyl-benzene	236.5	6.69	17.23
n-Tridecane	234.0	5.90	7.66
1-Methyl-naphthalene	241.0	5.65	10.30
2-Methyl-naphthalene	240–242	6.74	10.76
Hexamethyl-benzene	264.0	9.04	18.69
Diphenyl	254–255	14.93	17.38
n-Pentadecane	270.5	20.81	32.20

Table IV. Entropy Changes for Selected Compounds, Calculated Using log *K* Values at 129 °C[a]

Compound	ΔS		$\Delta S/\Delta H$	
	$NaB(C_6H_5)_4$	$TlB(C_6H_5)_4$	Na	Tl
1-Methyl-4-isopropylbenzene	−27.2	−38.5	2.65	2.45
Naphthalene	−29.9	−33.3	2.54	2.37
Phenyl-*tert*-butylacetylene	−29.9	−42.8	2.56	2.38
Benzo-*tert*-butylcyclobutene	−27.2	−38.0	2.60	2.41
p-Di-*tert*-butylbenzene	−35.3	−45.8	2.49	2.36
1-Methylnaphthalene	−32.1	−38.1	2.51	2.36
n-Decane	−29.2	−32.3	2.64	2.48
n-Pentadecane	−41.8	−43.9	2.43	2.33

[a] The entropy changes are in units of cal/deg. mole.

Table III gives the logarithms of the capacity ratios and the adsorption heats of some compounds on sodium and thallium tetraphenylborates. The adsorption heats were calculated from the slope of the plotted straight lines log *K* *vs.* $1/T \times 10^4$.

The adsorption heat of *n*-pentadecane on thallium tetraphenylborate was estimated for log *K* at 156 °C = 0.900.

The straight line slopes were calculated by means of the least squares method. The standard error of the slope has been estimated using the regression analysis.

The adsorption heat values of various components on thallium tetraphenylborate were higher than those of the same components on a column of sodium tetraphenylborate. The differences were significant especially in the case of the aromatic hydrocarbons and their derivatives, which may be explained by the interaction ability of Tl(I) ion with these components.

Relative changes in entropies of adsorption were calculated assuming that the capacity ratios were directly proportional to the thermodynamic adsorption constant K_a (*11*) in order to make relative, but not absolute comparisons (Table IV).

The relative entropy changes for the selected compounds are higher on the column of thallium tetraphenylborate compared to that of sodium, the highest differences being observed with the aromatic compounds.

The ratios $\Delta S/\Delta H$ are lower on thallium tetraphenylborate than on the sodium tetraphenylborate and decrease for the superior homologs implying that heats of adsorption increased more rapidly than the corresponding values for entropies.

(11) J. E. Heveran and L. B. Rogers, *J. Chromatogr.*, **25**, 213 (1966).

Table III. Log Capacity Ratios for Some Compounds Eluted from $NaB(C_6H_5)_4$, $TlB(C_6H_5)_4$ Columns and Their Heats of Adsorption, Kcal/mole

Compound	$NaB(C_6H_5)_4$				$TlB(C_6H_5)_4$			
	log *K*, 106 °C	log *K*, 129 °C	log *K*, 146 °C	$-\Delta H$	log *K*, 106 °C	log *K*, 129 °C	log *K*, 146 °C	$-\Delta H$
1-Methyl-4-isopropylbenzene	−0.435	−0.814	−0.996	10.28 ± 0.87	0.763	0.256	−0.104	15.68 ± 0.37
Naphthalene	0.121	−0.288	−0.527	11.79 ± 0.41	1.192	0.799	0.409	14.03 ± 1.55
Phenyl-*tert*-butylacetylene	−0.050	−0.453	−0.690	11.65 ± 0.37	1.492	0.956	0.493	17.96 ± 1.32
benzo-*tert*-butylcyclobutene	−0.219	−0.584	−0.794	10.46 ± 0.41	1.083	0.599	0.207	15.77 ± 0.87
p-Di-*tert*-butylbenzene	0.432	−0.036	−0.348	14.17 ± 0.14	1.883	1.259	0.809	19.42 ± 0.46
1-Methylnaphthalene	0.362	−0.109	−0.338	12.80 ± 1.05	1.578	1.035	0.689	16.13 ± 0.18
n-Decane	−0.469	−0.861	−1.075	11.06 ± 0.59	0.435	0.022	−0.287	13.02 ± 0.46
n-Pentadecane	1.061	0.457	0.119	17.18 ± 0.82	...	1.530	1.087	18.87 ± 1.07

CONCLUSIONS

The present paper shows that the olefins and aromatic hydrocarbons are selectively retained on columns of thallium tetraphenylborate compared to those of sodium tetraphenylborate. The stronger retention of these compounds on the column of thallium tetraphenylborate should be due to the possible interaction between thallium d-orbitals and the π-orbitals of unsaturated hydrocarbons.

Therefore, the thallium tetraphenylborate may be used as selective stationary phase for the separation of hydrocarbons.

RECEIVED for review January 28, 1974. Accepted June 4, 1974.

Determination of Long Chain Fatty Acids as 2-Naphthacyl Esters by High Pressure Liquid Chromatography and Mass Spectrometry

M. J. Cooper and M. W. Anders

Department of Pharmacology, University of Minnesota, Minneapolis, Minn. 55455

Long chain polyunsaturated fatty acids have assumed increased importance in recent years; in particular, some C_{20} acids are known precursors of the biologically important prostaglandins. A number of analytical methods have been employed for the determination of fatty acids. For example, microdiffusion and gas chromatography have been used for the analysis of short and medium chain fatty acids (*1*) and Umeh (*2*) described the gas chromatographic analysis of C_2–C_{20} acids as their *p*-bromophenacyl and *p*-phenylphenacyl esters. Ehrsson (*3*) reported the gas chromatographic detection of C_4–C_{10} acids as their pentafluorobenzyl derivatives. Recently, the gas chromatography–mass spectrometry of C_1–C_{20} acids as their benzyl esters was reported (*4*). Mikeš *et al.* (*5*) used high pressure liquid chromatography (HPLC) with complex-forming stationary phases for C_{18} fatty acid methyl esters. Grünert and Bässler (*6*) reported the gas chromatographic analysis of fatty acid methyl esters.

Derivatives have been widely employed in gas chromatographic analysis to improve chromatographic properties and to increase the sensitivity of detection. It is apparent, however, that derivatives should be useful in liquid chromatographic analysis for the same purposes. Henry *et al.* (*7*) and Papa and Turner (*8*) have employed 2,4-dinitrophenylhydrazone derivatives for the HPLC analysis of various carbonyl compounds and Fitzpatrick and Siggia (*9*) described the preparation and analysis of benzoate derivatives of hydroxy steroids. Fluorigenic labeling has also been employed in HPLC analysis (*10, 11*). Dunham and Anders (*12*) reported the base-catalyzed conversion of prostaglandin E to B to enhance the sensitivity of detection for HPLC analysis.

(1) J. W. A. Meijer and L. Hessing-Brand, *Clin. Chim. Act.* **43,** 215 (1973).
(2) E. O. Umeh, *J. Chromatogr.*, **56,** 29 (1971).
(3) H. Ehrsson, *Acta Pharm. Suecica*, **8,** 113 (1971).
(4) U. Hintze, H. Roper, and G. Gercken, *J. Chromatogr.*, **87,** 481 (1973).
(5) F. Mikeš, V. Schurig, and E. Gil-Av, *J. Chromatogr.*, **83,** 91 (1973).
(6) A. Grunert and K. H. Bassler, *Fresenius' Z. Anal. Chem.*, **267,** 342 (1973).
(7) R. A. Henry, J. A. Schmit, and J. F. Dieckman, *J. Chromatogr. Sci.*, **9,** 513 (1971).
(8) L. J. Papa and L. P. Turner, *J. Chromatogr. Sci.*, **10,** 747 (1972).
(9) F. A. Fitzpatrick and S. Siggia, *Anal. Chem.*, **45,** 2310 (1973).
(10) R. W. Frei and J. F. Lawrence, *J. Chromatogr.*, **83,** 321 (1973).
(11) R. W. Frei, J. F. Lawrence, J. Hope, and R. M. Cassidy, *J. Chromatogr. Sci.*, **12,** 40 (1974).
(12) E. W. Dunham and M. W. Anders, *Prostaglandins*, **4,** 85 (1973).

We report here the HPLC analysis of unsaturated C_{18} and C_{20} fatty acids. Since the methylene interrupted polyunsaturated acids show no specific ultraviolet absorption, the 2-naphthacyl esters were prepared. The structures of the derivatives were confirmed by both electron impact (EI) and chemical ionization (CI) mass spectrometry (MS).

EXPERIMENTAL

Reagents. Reagent grade solvents were used without further purification. 2-Naphthacyl bromide (α-bromo-2′-acetonaphthone) and *N,N*-diisopropylethylamine were obtained from Aldrich Chemical Company. Dihomo-γ-linolenic acid was obtained from the Hormel Institute, and oleic acid from Calbiochem; all other fatty acids were purchased from Sigma Chemical Company.

Derivatization Procedure. The acid (10 μmoles), 2-naphthacyl bromide (20 μmoles), and *N,N*-diisopropylethylamine (40 μmoles) were dissolved in 1 ml of dimethylformamide. The reaction mixture was heated at 60° for 10 minutes, at which time the reaction was complete. An aliquot of the reaction mixture was injected into the liquid chromatograph.

For the MS analyses, the esters were prepared on a larger scale. Acid (100 μmoles), 2-naphthacyl bromide (92 μmoles), and *N,N*-diisopropylethylamine (184 μmoles) were dissolved in 10 ml of dimethylformamide and stirred for 20 hr at room temperature. The solvent was removed *in vacuuo* at 50°, the residue was dissolved in ethyl acetate and washed with sodium bicarbonate solution followed by water and dried over sodium sulfate. The ethyl acetate solution was evaporated to dryness leaving the derivatives as oils at room temperature; only 2-naphthacyl oleate was a crystalline compound. The derivatives were recrystallized from ether at −20°. Since the methylene interrupted polyunsaturated acids are very prone to oxidation, the reaction and work-up were conducted under nitrogen and all vessels were protected from light.

High Speed Liquid Chromatography. Analyses were conducted using a chromatograph fabricated in this laboratory. A Varian constant pressure, gas driven reservoir/pump was employed with nitrogen as the pressurizing gas. A Pharmacia 1205 UV monitor measured absorbance at 254 nm. The column was a 3-ft × 0.07-in. i.d. stainless steel tube packed with Corasil-C_{18} (Waters Associates). Methanol:water (85:15) served as the eluent and a flow rate of 12 ml/hr was obtained at a pressure of 300 psig. The solvents were degassed by boiling just before use. Samples were injected directly onto the column.

Mass Spectrometry. A Finnigan 1015 quadrupole mass spectrometer was used. The ionizing current and voltage were 50 μA and 50 eV, respectively, when EI spectra were recorded. CI spectra were recorded using methane as the reactant gas; the source parameters were 500 μA and 100 eV. The scan time was 10 sec. All samples were introduced through the solid probe and the spectra were recorded at probe and ion source temperatures of 200°.

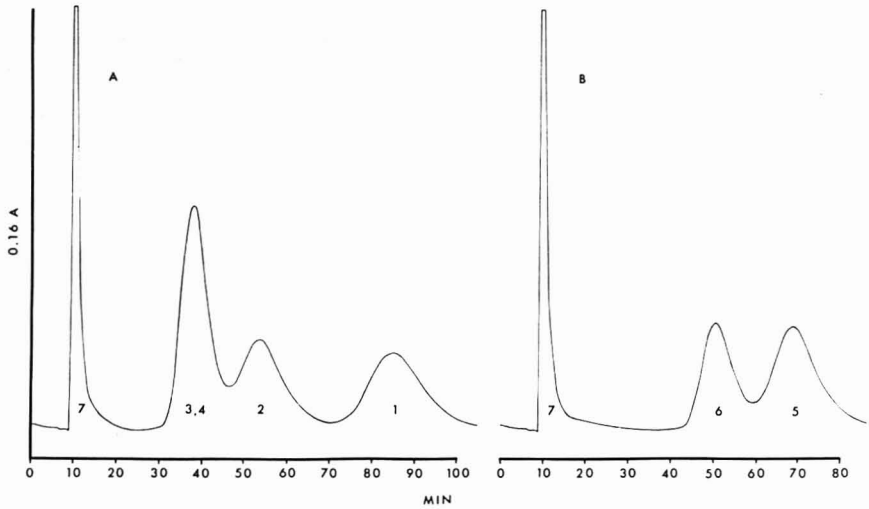


Figure 1. HPLC of C_{18} acids (*A*) and C_{20} acids (*B*) as 2-naphthacyl esters

Peak 1, oleic; peak 2, linoleic ; peak 3,4, α- and γ-linolenic; peak 5, dihomo-γ-linolenic; peak 6, arachidonic; peak 7, 2-naphthacyl bromide. Conditions: column, 3-ft × 0.07-in. i.d. Corasil-C_{18}; eluent, methanol:water (85:15); flow rate, 12 ml/hr at 300 psig

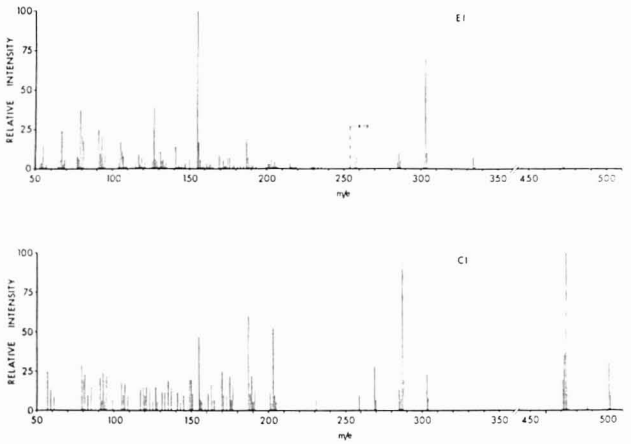


Figure 2. EI (upper) and CI (lower) mass spectra of 2-naphthacyl arachidonate

Operating parameters: EI, 50 μA and 50 eV; CI, methane reactant gas, 500 μA and 100 eV; scan time, 10 sec.; probe and ion source temperature, 200°

RESULTS AND DISCUSSION

Since the fatty acids investigated here show no UV absorption at 254 nm, where the absorbance monitor normally functions, strongly UV-absorbing derivatives were prepared. The 2-naphthacyl esters proved particularly useful in this respect. Although the λ_{max} for these esters was 247–248 nm with log ϵ values of about 4.5, the log ϵ values at 254 nm were about 4.1. This is sufficient to provide nanogram sensitivities.

Good chromatographic properties of the naphthacyl esters were observed using a reversed phase column and methanol-water as the eluent. Figure 1*A* shows the chromatography of C_{18} acids, namely oleic, linoleic, α-, and γ-linolenic. Fatty acids differing by the presence of double bonds were well resolved; however, the positional isomers, α- and γ-linolenic acids, could not be resolved. The chromatography of the C_{20} acids, dihomo-γ-linolenic and arachidonic acid, which differ by the presence of a double bond, is shown in Figure 1*B*; again, good resolution was obtained. In all cases, the derivatizing reagent elutes early and presents no interference.

The optimum conditions for the resolution of mixtures of

Table I. EI and CI Mass Spectral Data of 2-Naphthacyl Esters of Fatty Acids[a]

Ester	Probable structure of observed fragments								
	$[M + 29]^+$	$[M + 15]^+$	$[M + 1]^+$	$[M]^+$	$[RCOO]^+$,[b] $(M - 169)$	$[RCO]^+$ $(M - 185)$	$[NapCH(OH)=CH\,OH]^+$,[c]	$[NapC(=OH)—CH_2]^+$	$[NapCO]^+$	$[Nap]^+$
Oleate EI	. . .	. . .	. . .	450 (0.2)	. . .	265 (3.6)	187 (34)	170 (11)	155 (100)	127 (7)
CI	479 (19)	465 (3)	451 (100)	450 (16)	. . .	265 (30)	187 (38)	170 (7)	155 (32)	127 (5)
Linoleate EI	. . .	. . .	. . .	448 (0.4)	279 (4)	263 (13)	187 (13)	170 (12)	155 (100)	127 (13)
CI	477 (23)	463 (5)	449 (40)	448 (17)	279 (8)	263 (100)	187 (42)	. . .	155 (21)	. . .
α-Linolenate EI	. . .	. . .	. . .	446 (5)	277 (8)	261 (2)	187 (16)	170 (14)	155 (100)	127 (22)
CI	475 (20)	461 (2)	447 (90)	446 (20)	277 (10)	261 (100)	187 (18)	. . .	155 (16)	. . .
γ-Linolenate EI	. . .	. . .	. . .	446 (1.4)	277 (16)	261 (3)	187 (12)	170 (27)	155 (100)	127 (6)
CI	475 (10)	461 (1)	447 (37)	446 (11)	277 (10)	261 (100)	187 (42)	170 (13)	155 (40)	127 (22)
Dihomo-γ-linolenate EI	. . .	. . .	. . .	474 (0.9)	305 (10)	289 (2)	187 (15)	170 (17)	155 (100)	127 (29)
CI	503 (13)	489 (1)	475 (100)	474 (34)	305 (20)	289 (82)	187 (30)	170 (10)	155 (42)	127 (6)
Arachidonate EI	. . .	. . .	. . .	472 (0.3)	303 (7)	287 (0.4)	187 (19)	170 (8)	155 (100)	127 (40)
CI	501 (30)	487 (3)	473 (100)	472 (36)	303 (23)	287 (95)	187 (60)	170 (25)	155 (47)	127 (15)

[a] Values are shown as *m/e* (relative intensity). [b] R refers to the hydrocarbon moiety. [c] Nap refers to the 2-naphthyl moiety.

fatty acid derivatives necessitated rather long retention times. However, when only one acid was being assayed, the time of analysis could be shortened considerably by using increased flow rates. Even with substantially higher flow rates, the derivatizing reagent peak was always well separated from the esters.

The lower limit of detection was 4 ng of ester. Plots of concentration *vs.* absorbance were linear in the range of 4–90 ng.

The esters were stable for at least six days when kept in the usual reaction mixture at room temperature.

In liquid chromatography, as in gas chromatography, it is important that the structures of the derivatives be determined. Therefore, the EI and CI mass spectra were recorded for all the esters studied; these data are summarized in Table I. Figure shows both the EI and CI mass spectra of a representative derivative, namely 2-naphthacyl arachidonate. As can be seen from the data in Table I and Figure 2, the EI mass spectra show very weak molecular ions with relative intensities of 0.2 to 5%. Ions which have diagnostic value were found in all cases at $[M - 169]^+$ and $[M - 185]^+$; these represent $[RCOO]^+$ and $[RCO]^+$, respectively, where R refers to the hydrocarbon moiety. In all esters, the base peak was found at *m/e* 155 which comprises the $[NapCO]^+$ ion where Nap refers to the 2-naphthyl group. This is to be expected as resonance stabilization highly favors this species. Another characteristic fragment at *m/e* 127 could result from the loss of CO from $[NapCO]^+$ to give the $[Nap]^+$ ion. In addition, all esters showed rather prominent ions at *m/e* 187 and *m/e* 170 which may be attributed to the protonated species $[NapCH(OH)=CHOH]^+$ and $[NapC(=OH)—CH_2]^+$, respectively.

As expected, the CI spectra, with methane as the reactant gas, yielded different results. Molecular ions were more prominent in all cases with relative intensities of 11–35%. Large peaks were also seen for the $[M + 29]^+$ and $[M + 1]^+$ species; indeed, in the cases of oleate, dihomo-γ-linolenate and arachidonate, the quasi-molecular ion comprised the base peak. Much less prominent, but of diagnostic value, was the $[M + 15]^+$ ion, which could be detected in all cases. The $[M - 169]^+$ and $[M - 185]^+$ fragments, corresponding to $[RCOO]^+$ and $[RCO]^+$, respectively, were also generally more prominent than in the EI spectra. The $[M - 185]^+$ ion formed the base peak in the case of linoleate and linolenates. In contrast, the fragments at *m/e* 127, 155, 170, and 187, which could be attributed to various naphthyl species, were much less abundant in the CI spectra than in the EI spectra. Characteristic hydrocarbon fragments were also seen in the range of *m/e* 50–200 (data not shown in Table I) in both the EI and CI modes though they were less prominent in the latter case. These fragments are also seen in the EI spectra methyl esters of C_{18} acids (*13*) though the relative intensities vary. Furthermore, it can be seen that β-cleavage to the ester carbonyl with McLafferty rearrangement, which could give a fragment at *m/e* 228 is absent. The corresponding peak at *m/e* 74 is present to a greater or lesser extent in the case of C_{18} methyl esters (*13*).

CONCLUSIONS

The method described here offers ease of derivatization and the 2-naphthacyl esters possess excellent chromatographic and chromophoric properties. Furthermore, the method could be applicable to the analysis of other carboxylic acids. The sensitivity of detection, which lies in the na-

(13) G. Odham and E. Stenhagen, "Biochemical Applications of Mass Spectrometry," G. R. Waller, Ed., Wiley-Interscience, New York, N.Y., 1972, p 221.

nogram range, also suggests application to biological problems.

Derivatization procedures, which have proved to be most useful in gas chromatographic analysis, will undoubtedly prove to be similarly useful in liquid chromatographic analysis. In the work presented here, compounds possessing no appreciable UV-absorbance were converted into intensely absorbing derivatives. In other cases, it may be possible to augment the absorptivities of weakly absorbing compounds. Finally, it should be possible, by selection of proper substituents in the 2-naphthacyl bromides, to form derivatives which absorb even more intensely at 254 nm where commercially available absorbance monitors operate most effectively.

ACKNOWLEDGMENT

The authors thank Adrian Swanson for recording the mass spectra and Jerry Soechting for the art work.

RECEIVED for review April 5, 1974. Accepted June 24, 1974. This research was supported by U.S. Public Health Service, National Institutes of Health, Grant No. GM 15477.

Gas Chromatographic Analysis of Ambient Air for Light Hydrocarbons Using a Chemically Bonded Stationary Phase

H. H. Westberg, R. A. Rasmussen, and M. Holdren

Air Pollution Research, Engineering Research Division, Washington State University, Pullman, Wash. 99163

Several reports have appeared recently which describe the use of chemically bonded stationary phases in gas chromatographic columns (*1–3*). These packing materials consist of spherical silica particles in which the surface hydroxyl groups have been replaced by an organic function. For example, the esterification of silica beads (Porasils) with alcohols provides a useful stationary phase. These materials exhibit many qualities which are highly desirable for trace analysis—namely, good thermal stability, high efficiency separations, and sharp, symmetrical peaks. The theory and methods of preparation of these types of materials have been recently reviewed (*4*).

Our interest in this type of packing arose as a consequence of the need for a simple, yet highly efficient gas chromatographic column for light hydrocarbon (C_2–C_5) analysis in ambient air. The purpose of this note is to describe the attainment of this goal through the use of the chemically bonded stationary phase *n*-octane/Porasil C.

EXPERIMENTAL

Apparatus. Gas chromatographic work was performed on a Perkin-Elmer 990 dual flame instrument equipped with a subambient accessory. The normal carrier gas flow system was modified to include the freezeout trap and valve illustrated in Figure 1.

Matched pairs of 20-ft × 1/16-in. stainless steel Durapak *n*-octane/Porasil C columns were prepared by the standard pressure packing technique. Both 80–100 mesh and 100–120 mesh material was packed in this manner.

Drying loops were prepared by packing 18- × 1/4-in. copper tubes with 20–60 mesh anhydrous potassium carbonate. These water filters were activated by heating (120°) overnight while purging with a dry gas.

The sampling trap shown in Figure 1 is a 6- × 1/8-in. stainless steel tube packed with 60-mesh glass beads.

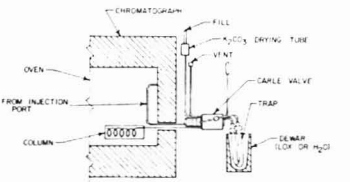


Figure 1. Freezeout trap and inlet system to gas chromatograph

Reagents. The standards employed were obtained from Scott Research Laboratories in small pressurized cans.

Liquid oxygen and nitrogen were purchased in 150-liter low-pressure Dewar containers.

Durapak materials were purchased from Waters Associates.

Procedures. Typical ambient air analyses were performed as follows. The trap illustrated in Figure 1 was submerged in liquid oxygen with the valve placed in the fill position. The air sample was then admitted into the trap by syringe injection. In the meantime, the column oven had been cooled to −70°. The valve was then switched so that the carrier gas (helium, 7 ml/min) swept the contents of the trap onto the head of the cold Durapak column. The liquid oxygen Dewar was replaced with one of hot water to assist the transfer process. A slight base-line disturbance was normally encountered within the first three to four minutes. When a stable base line was regained, the temperature program was initiated. With *n*-octane/Porasil C columns, the temperature was increased from −70° to 65° at 16°/min with a hold at the higher temperature for about 25 minutes. At the end of a run, higher molecular weight material was removed by heating at approximately 120 °C for 15 minutes.

When large volumes (500–1000 ml) of ambient air were analyzed, it was necessary to reduce the moisture content by passing the air through a potassium carbonate drying tube before concentration in the freezeout loop.

RESULTS AND DISCUSSION

During the past few years we have been concerned with the measurement of light hydrocarbons under atmospheric conditions. In many cases, this involved separating and

(1) J. N. Little, W. A. Dark, P. W. Farlinger, and K. J. Bommbaugh, *J. Chromatogr. Sci.*, **8**, 647 (1970).
(2) F. W. Karasek, *Res./Develop.*, **22**, 34 (June 1971).
(3) "Durapak," Brochures of Waters Associates, Inc., Framingham, Mass. 01701.
(4) D. C. Locke, *J. Chromatogr. Sci.*, **11**, 120 (1973).

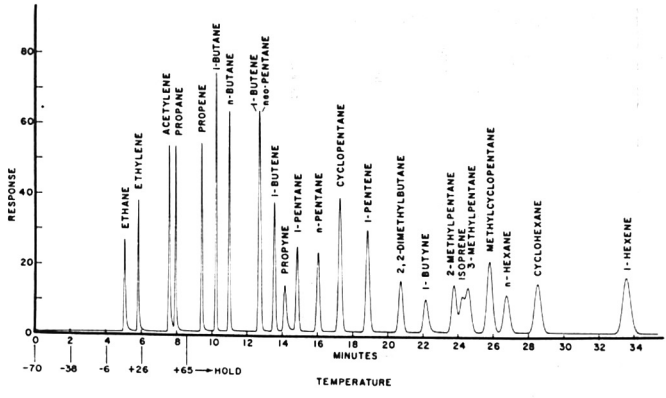


Figure 2. Durapak (*n*-octane/Porasil C) separation of a standard light hydrocarbon (C_2–C_6) mixture

quantitating only ethylene and/or acetylene. Recently, however, it became desirable to examine in detail the spectrum of all C_2 to C_5 hydrocarbon compounds in ambient air. Porapak N was sufficient for the original work since it gave good ethylene, ethane, and acetylene separation. It failed, however, to separate the "enes" from the "anes" in C_3 and above molecular weight groups. Thus, propene and propane were superimposed as were *n*-butane and 1-butene.

Examination of the literature showed a wide variety of techniques and column types have been employed for light hydrocarbon analysis. Generally, packed columns of $\frac{1}{8}$-in. o.d. are used, encompassing many different combinations of support materials and stationary phases. Over-all resolution has been poor and emphasis has focused on optimum separation of compounds over a narrow range (*i.e.*, ethane, ethylene, and acetylene). Currently, complicated mixtures of liquid phases (*5*), use of multiple columns (*6*), critical optimum temperature parameters and, in many cases, the operation of two or more gas chromatographs (*7*) are used to achieve good chromatograms.

Most of our ambient air analyses are preformed in mobile field units which undergo frequent site changes. Under these conditions, it is essential to have the simplest system possible in order to minimize maintenance problems. Therefore we sought a simple one substrate-in one column-in one chromatograph type system capable of providing the required resolution.

The few previous reports of Durapak materials being used for light hydrocarbon analysis appeared promising since good separation of mixtures was observed (*1, 3*).

We prepared a set of 20-ft × $\frac{1}{16}$-in. Durapak *n*-octane/Porasil C columns and found extremely good resolution for C_5 and below hydrocarbon mixtures. Figure 2 shows the capabilities of this column for separating a standard gaseous mixture (10 ng/peak). This was achieved by optimizing the temperature-programmed range and rate of oven temperature increase. By freezing (−70 °C) components on the head of the column, a "slug" start is effected. A range of −70 to 65 °C elutes light hydrocarbons up to *n*-hexane within 30 minutes. The programmed rate of temperature increase is best determined by optimizing separation within the ethane–ethylene and acetylene–propane peak pairs. A slow temperature increase improves the ethane and eth-

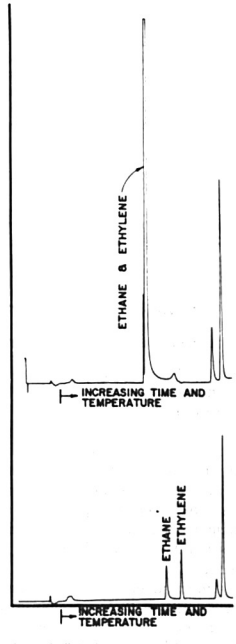


Figure 3. Illustration of disturbance to ethane and ethylene peaks caused by excess moisture

Top: Ambient air sample without water removed. Bottom: Ambient air sample passed through anhydrous potassium carbonate prior to analysis

(5) E. R. Stephens, Statewide Air Pollution Research Center, Riverside, Calif., personal communication, 1974.
(6) E. R. Stephens and F. R. Burleson, *J. Air Pollut. Contr. Ass.*, **19**, 929 (1969).
(7) S. L. Kopozynski, W. A. Lonneman, T. Winfield, and R. Seila, *Environ. Sci. Technol.*, **8**, 229 (1974).

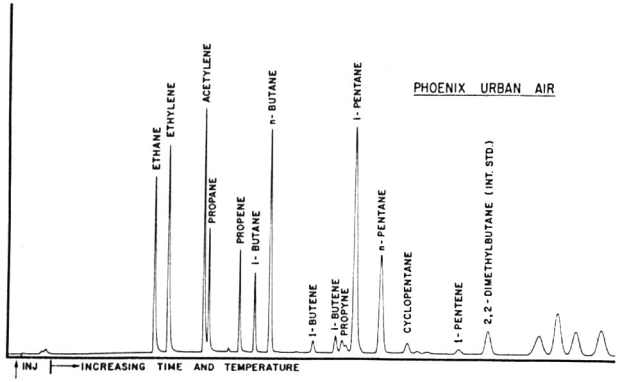


Figure 4. Light hydrocarbons measured in ambient air sample collected in downtown Phoenix, Arizona

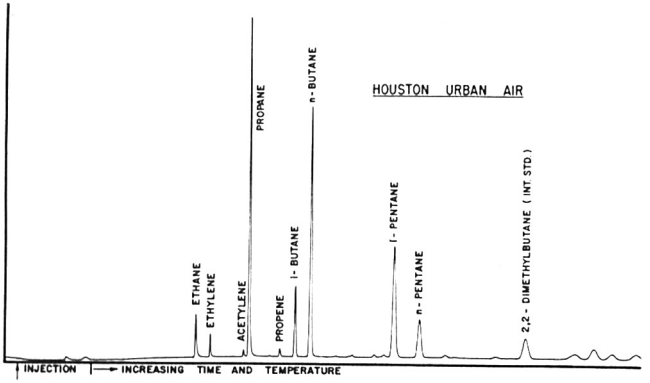


Figure 5. Light hydrocarbons measured in ambient air sample collected near ship channel in Houston, Texas

ylene resolution but has the opposite effect on acetylene and propane. Generally, we have found 16°/min provides the best over-all resolution.

Difficulty was encountered when we attempted to use the system for large-volume ambient air samples. The ethylene and ethane peaks were disturbed such that accurate quantitation was not possible. This is illustrated in Figure 3. Since water is a prevalent component of ambient air, it was the most logical source of trouble, especially in light of the reported instability of the chemically bonded esters (Si–O–C) to hydrolysis (*8*).

Considerable time and effort were expended searching for the proper water filter. Short pre-columns of molecular sieve, silica gel, etc. removed the water but, in all cases, disrupted peak shape and resolution throughout the entire chromatogram. Only in the case of anhydrous potassium carbonate could sufficient water be removed and yet retain the good peak shape and resolution as well as obtain 100% transmittance of the light hydrocarbons. By using an 18- × ¼-in. tube packed with anhydrous potassium carbonate, approximately 10 liters of air (50% RH) could be processed before the filter lost its effectiveness.

This technique has performed satisfactorily under a wide variety of field conditions. Figures 4 and 5 show typical chromatograms of atmospheric samples analyzed in this manner.

It is obvious from these ambient air chromatograms that all the characteristics required for high-quality trace analysis are inherent in the Durapak column: 1) resolution—even isomeric butanes are well resolved; 2) peak shape—allows accurate quantitation; 3) stable base line—the chromatograms shown in Figures 4 and 5 were obtained at an instrument attenuation of 16X (maximum sensitivity of 1X = 5×10^{-12} AFS). The attenuation can be lowered to 4X with little effect on the base line. This allows us to routinely measure individual light hydrocarbon concentrations as low as 0.5 ppb. In addition, the columns are very durable and reproducibility of different column pairs is excellent. Probably the most important feature of the system, as a whole, is its simplicity and compatibility with a mobile field sampling trailer.

We feel that this analysis technique will prove valuable as a standard method for ambient air light hydrocarbon analysis.

RECEIVED for review March 5, 1974. Accepted June 3, 1974. The research upon which this paper is based was performed in conjunction with Coordinating Research Council Project No. CAPA-11-71 and Environmental Protection Agency contract No. 68-02-1232.

(8) J. J. Kirkland and J. J. De Stefano, *J. Chromatogr. Sci.*, **8**, 309 (1970).

Synthesis of Reproducible Tin(IV) Based Ion Exchangers: Separation of Lanthanum(III) from Yttrium(III), Europium(III), and Lutetium(III)

Mohsin Qureshi, Rajendra Kumar, and Veena Sharma

Chemical Laboratories, Aligarh Muslim University, Aligarh, U.P., India

During recent years, there has been considerable interest in the crystalline synthetic inorganic ion-exchangers (*1–4*). However, amorphous inorganic ion-exchangers also offer some attractive features which make them especially suitable for analytical work. Amorphous ion exchangers are easier to prepare, and they show selectivities which are different from those of their crystalline counterparts. Thus, the uptake of ions on crystalline zirconium phosphate is in the order $Li^+ > Na^+ > K^+ > Rb^+ > Cs^+$, while on the amorphous material, the reverse is true. The studies on the crystalline exchangers are also complicated by the hysteresis phenomena resulting from the facts of mixed phases during exchange.

To make an effective use of the amorphous materials two problems should be tackled: Their reproducibility should be improved; a critical comparative evaluation should be made of the various ion exchangers prepared under the same conditions; and the ion-exchange potential of these materials should be established for some difficult separations.

Comparative studies of various exchangers are rather few. Szirtes (*5*) made an interesting study of the phosphates of Ti, Zr, and Th. Qureshi and coworkers compared the ion-exchange properties of the tungstate, arsenate, antimonate, selenite, and molybdate of Ti(IV) (*6*). They, however, examined those phases of the above exchangers which were reported to be the most stable in each case. Qureshi and coworkers also made a comparative study of the hydroxide, arsenate, molybdate, antimonate, and tungstate of Cr(III) (*7*). They prepared these compounds by mixing 0.1*M* Cr(III) solution with a 0.1*M* solution of the appropriate anion in the volume ratio of 1:2 at pH $\simeq$ 7. The ion-exchange capacity of a material generally increases with decrease in pH (*8*). Therefore, it is more useful to prepare the ion-exchange material at a low pH. Such a study is now reported for the antimonate, selenite, arsenate, tungstate, and molybdate of Sn(IV).

There are three most difficult problems in the separation of cations: Separation of alkali metals; separation of alkaline earths; and separation of lanthanide. Numerous solutions of the first two problems have been proposed using inorganic ion-exchangers, but as far as we are aware very few studies have been reported on the lanthanides (*9*).

We have, therefore, in this communication examined the reproducibility of some Sn(IV) exchangers and we have used one of them for some binary separation of lanthanide ions.

EXPERIMENTAL

Apparatus. pH measurements and spectrophotometric studies were done with Elico pH meter model LI-10, Bausch and Lomb Spectronic 20 Colorimeter and shaking with a SICO temperature controlled shaker.

Reagents. Stannic chloride pentahydrate (pure, Poland) sodium arsenate heptahydrate (Riedel), sodium tungstate (AR) sodium molybdate (May & Baker), sodium selenite (Riedel) and potassium pyroantimonate (BDH) were used. All other reagents used were of analytical grade. Chlorides of rare earth metals were prepared by dissolving oxides (BDH) in hydrochloric acid.

Procedure. *Preparation of Ion-Exchange Material.* These materials were prepared by mixing 0.25*M* stannic chloride solution with 0.25*M* sodium arsenate, sodium tungstate, sodium selenite, sodium molybdate, and potassium pyroantimonate in the volume ratio of 1:1 at pH $\simeq$ 0. The precipitate obtained was divided in each case into two parts. One part was allowed to stand for 24 hr at room temperature, and the other part was refluxed with the mother liquor for 24 hr. After attaining room temperature, samples were washed by decantation, filtered off, and washed with 0.1*M* HCl and then with acetone. The gel was dried at 40 °C. The dry product broke down into small particles when immersed in water. Approximately 40 grams of the exchanger was converted into the hydrogen form by treatment with 100 ml of 1.0*M* nitric acid and finally washed with demineralized water. The exchanger dissolved to some extent during this treatment. Finally, the exchangers were washed with demineralized water to remove excess acid and again dried at 40 °C.

Chemical Composition. A 0.20-gram of the exchanger was dissolved in hydrochloric acid. After reduction with lead, tin was titrated with potassium dichromate (*10*). Arsenic and antimony were determined titrimetrically with potassium thiocyanate (*10*) and potassium iodide (*11*), respectively. Tungsten and molybdenum were determined as lead tungstate and molybdate (*12, 13*). Selenium was separated by sulfur dioxide treatment and determined gravimetrically as selenium metal (*14*).

Dissolution of Sn(IV) Exchangers. A 0.5-gram portion of the exchanger was shaken in a flask with 50 ml of the solution concerned in a temperature controlled shaker for 6 hr until equilibrium was reached. The undissolved portion of the exchanger was removed by filteration. Tin, arsenic, tungsten, selenium, molybdenum, and antimony were determined in the filtrate spectrophotometrically as earlier (*10–14*). The results are given in Figure 1.

Ion-Exchange Capacity. The ion-exchange capacity of the various materials determined by the standard method (*15*) is given in Tables I and II.

Distribution Coefficients Studies. Distribution coefficients of lanthanide ions were determined in nitric acid solutions of varying pH. For this purpose, 0.5 gram of the exchanger was shaken with 50 ml of the solution for 6 hr. The amount of the cation in the solution was determined by titration with EDTA and the K_d values were calculated from the equation:

$$K_d = \frac{I - F}{F} \times \frac{50}{0.5} \text{ ml/g} \qquad (1)$$

Where I is the volume of EDTA consumed by the original solution and F is the volume of EDTA consumed after equilibrium. The results are given in Table III.

(1) A. Clearfield and J. A. Stynes, *J. Inorg. Nucl. Chem.*, **24**, 117 (1964).
(2) A. Clearfield, G. D. Smith, and B. Hammond, *J. Inorg. Nucl. Chem.*, **30**, 277 (1968).
(3) G. Alberti and E. Torracca, *J. Inorg. Nucl. Chem.*, **30**, 3075 (1968).
(4) U. Constantino and A. Gasperoni, *J. Chromatogr.*, **51**, 289 (1970).
(5) L. Szirtes, L. Zsinka, K. B. Zaborenko, and B. Z. Iofa, *Acta Chem. Acad Sci. Hung.*, **54**, 215 (1967).
(6) M. Qureshi, N. Zehra, S. A. Nabi, and V. Kumar, *Talanta*, **20**, 609 (1973).
(7) M. Qureshi, R. Kumar, and H. S. Rathore, *Talanta*, **19**, 1377 (1972).
(8) M. Qureshi, J. P. Gupta, and V. Sharma, *Talanta*, In press.
(9) A. M. Trofimov, G. N. Kovalev, and V. G. Pitalev, *Radiokhimiya*, **9**, 409 (1967).
(10) M. Qureshi, H. S. Rathore, and R. Kumar, *J. Chem. Soc. (A)*, 1986 (1970).
(11) M. Qureshi, V. Kumar, and N. Zehra, *J. Chromatogr.*, **67**, 351 (1972).
(12) M. Qureshi and K. G. Varshney, *J. Inorg. Nucl. Chem.*, **30**, 3081 (1968).
(13) M. Qureshi and J. P. Rawat, *J. Inorg. Nucl. Chem.*, **30**, 305 (1968).
(14) M. Qureshi and S. A. Nabi, *Talanta*, **19**, 1033 (1972).
(15) O. Samuelson, Diss. Tekn. Hogskolan, Stockholm, 1944.

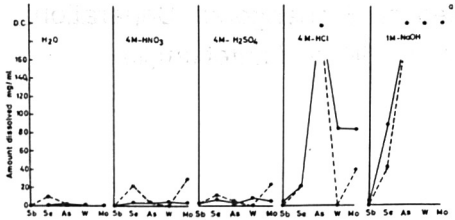


Figure 1a. Chemical dissolution of unrefluxed Sn(IV) ion exchangers

—●— Cation. - -●- - Anion. D.C. = Dissolved completely

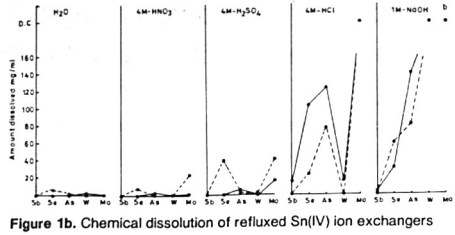


Figure 1b. Chemical dissolution of refluxed Sn(IV) ion exchangers

—●— Cation. - -●- - Anion. D.C. = Dissolved completely

Table I. Some Properties of Refluxed and Unrefluxed Arsenate, Antimonate, Molybdate, Tungstate, and Selenite of Sn(IV)

Ion-exchange material[a]	Color	Chemical composition, cation/anion	IEC, mequiv/gram
Sn-As(R)	White	1:0.90	1.56
Sn-As(UR)	White	1:0.78	1.25
Sn-Sb(R)	Blackish green	1:1.99	0.82
Sn-Sb(UR)	Blackish green	1:1.83	0.63
Sn-Mo(R)	Yellowish green	1:2.27	1.40
Sn-Mo(UR)	Yellowish green	1:2.16	1.12
Sn-W(R)	Pale yellow	1:1.51	0.98
Sn-W(UR)	Pale yellow	1:1.50	0.56
Sn-Se(R)	Pinkish white	1:0.62	0.80
Sn-Se(UR)	Pinkish white	1:0.44	0.75

[a] Sn-As = Stannic arsenate, Sn-Sb = Stannic antimonate, Sn-Mo = Stannic molybdate, Sn-W = Stannic tungstate, Sn-Se = Stannic selenite, (R) = Refluxed, (UR) = Unrefluxed, and IEC = Ion-exchange capacity.

Column Preparation. For separation studies, a 30- × 0.39-cm bore glass column was used and 2 grams of stannic selenite was put in the column with glass-wool support. The column was washed with demineralized water and the amount of cation added to the column was less than 3% of the experimental ion-exchange capacity of the ion exchanger. The flow rate of effluent was 8–9 drop/min. All the cations other than lanthanum were eluted with 4% NH_4NO_3 in 0.04*M* HNO_3 and finally lanthanum was eluted with 4% NH_4NO_3 in 1.5*M* HNO_3. The cations were determined by EDTA titration and no interference due to the dissolved anions was observed. All other details were similar to those reported earlier (*10–14*).

Heat Treatment. The ion-exchange material dried at 40 °C was heated at different temperatures in the muffle furnace for 1 hr, and the ion-exchange capacity was determined. The results are given in Figure 2.

pH-Titrations. pH Titrations were carried out by the method of Topp and Pepper (*16*).

(16) N. E. Topp and K. W. Pepper, *J. Chem. Soc.*, 3299 (1949).

Table II. Effect of Refluxing on Arsenate, Antimonate, Molybdate, Tungstate, and Selenite of Sn(IV)

Ion-exchange material	IEC mequiv/gram		K_d values × 10^{-2} at pH ≃ 5, ml/g					
			Mg^{2+}		Mn^{2+}		Al^{3+}	
	UR	R	UR	R	UR	R	UR	R
Sn-As	1.60, 1.25, 1.05	1.56	>96.5, 29.0, 38.0	38.0	10.8, 20.1, 22.6	>46.2	26.0, 15.0, 24.0	>134.0
Sn-Sb	0.91, 0.63, 0.82	0.82	38.0, >96.5, >96.5	>96.5	10.8, 23.0, 22.6	>46.2	>134.0, 17.0, 26.0	>134.0
Sn-Mo	1.16, 1.12, 1.00	1.18	29.0, 38.0, 45.0	>96.5	>46.2, 20.1, 10.8	22.6	15.0, >134.0, 26.0	26.0
Sn-W	0.96, 0.30, 0.56	0.98	38.0, 29.0, 95.0	45.0	>46.2, >46.2, >46.2	>46.2	15.0, 17.0, 133.0	>134.0
Sn-Se	1.12, 0.63, 0.75	0.83	95.0, 38.0, 29.0	45.0	>46.2, >46.2, >46.2	>46.2	15.0, 17.0, >134.0	>134.0

Table III. Distribution Coefficient of Metal Ion at Different pH Values on Sn(IV) Arsenate, Antimonate, Molybdate, Tungstate and Selenite at 25 ± 1 °C, K_d × 10^{-2} ml/g

S. No.	Metal ion	Sn-As		Sn-Sb		Sn-Mo		Sn-W		Sn-Se	
		pH 1	2	0	1	1	2	0	1	1	2
1.	Y^{3+}	1.60	66.60	0.29	66.60	1.82	168.0	0.05	32.00	0.22	27.17
2.	La^{3+}	0.47	219.00	0.43	43.00	0.76	219.0	0.17	6.33	6.33	219.00
3.	Ce^{3+}	26.10	202.00	0.40	82.20	1.54	202.0	0.13	19.30	6.26	202.00
4.	Pr^{3+}	0.44	209.00	0.40	11.08	2.21	209.0	0.03	82.60	0.81	208.00
5.	Nd^{3+}	0.30	52.50	0.42	7.56	1.38	213.0	0.08	27.53	0.44	84.60
6.	Sm^{3+}	0.28	197.00	0.37	121.30	0.53	197.0	0.01	67.80	0.40	196.00
7.	Eu^{3+}	0.04	77.00	0.45	8.75	1.88	194.0	0.01	6.10	0.32	7.00
8.	Gd^{3+}	0.68	36.80	0.50	24.20	2.15	188.0	0.12	11.60	0.22	9.80
9.	Tb^{3+}	0.04	66.60	0.34	21.53	2.10	168.0	0.02	5.76	0.27	5.15
10.	Dy^{3+}	0.33	79.00	0.41	25.66	1.95	199.0	0.27	3.70	0.29	9.00
11.	Ho^{3+}	0.29	47.50	0.34	24.20	1.36	193.0	0.10	4.97	0.29	8.70
12.	Er^{3+}	0.28	75.80	0.38	11.80	1.10	191.0	0.09	11.80	0.28	11.80
13.	Tm^{3+}	0.56	23.80	0.48	19.66	2.10	242.0	0.25	16.71	0.29	8.90
14.	Lu^{3+}	0.35	13.81	0.43	16.93	1.19	218.0	0.18	8.96	0.19	3.86

Table IV. Separation of La^{3+} from Y^{3+}, Eu^{3+}, and Lu^{3+} on Stannic Selenite

S. No.	Sample	Eluent	Taken, μg	Found, μg	Error, %
1.	Y^{3+}	4% NH_4NO_3 in 0.04*M* HNO_3	1076	1039	−3.4
	La^{3+}	4% NH_4NO_3 in 1.5*M* HNO_3	2010	1978	−3.4
2.	Eu^{3+}	4% NH_4NO_3 in 0.04*M* HNO_3	958	995	+3.9
	La^{3+}	4% NH_4NO_3 in 1.5*M* HNO_3	1427	1427	±0.0
3.	Lu^{3+}	4% NH_4NO_3 in 0.04*M* HNO_3	1501	1522	+0.7
	La^{3+}	4% NH_4NO_3 in 1.5*M* HNO_3	2010	2075	+3.2

Separations. Quantitative separation of La^{3+} from Y^{3+}, Eu^{3+}, and Lu^{3+} has been achieved on the stannic selenite columns. The results are given in Table IV.

DISCUSSION

It was shown in our earlier paper that on refluxing with mother liquor, tantalum antimonate (*17*) shows reproducible characteristics. Every exchanger reported here was synthesized three times and its ion-exchange capacity as well as K_d value was determined. All three values are given in Table II for unrefluxed samples. However, for refluxed samples, only one value is given because, on repeating the experiment, the value did not change by more than 0.03. The results in Table II indicate that refluxing improves the reproducibility in the ion-exchange properties of the Sn(IV) salts studied here. This is an important advantage since it is not always possible to crystallize the ion exchange material. It is clear from the results given in Table I that on refluxing, the anion content of the exchanger increases in every case and therefore the ion-exchange capacity of the refluxed sample is always greater than that of the unrefluxed sample.

Stability in aqueous media is also a useful property of the ion exchange material. Stannic arsenate is very stable in water, 4*M* HNO_3, and 4*M* H_2SO_4. The non-refluxed sample dissolved completely in 4*M* HCl and 1*N* NaOH. The refluxed samples, however, do not decompose completely and are therefore slightly more stable in the last two solvents. The great increase in solubility in 4*M* HCl is due to the high complex forming ability of the chloride ions. Stannic antimonate is an outstanding example of stability. This material is equally stable in 4*M* HCl and 1*N* NaOH and, hence, a number of useful separations can be achieved on its columns. Various HCl systems were used since other ion exchangers dissolve in HCl. This property will enable the use of HCl for numerous important and interesting separations. NaOH can be used to precipitate a cation on tin ion exchange columns. Stannic antimonate could be very good for these studies. Molybdate is the most unstable of the various materials tried and is useful only in the aqueous media. The same conclusion was obtained in our earlier paper (*6*) where we had compared the dissolution of the various Ti(IV) salts, and we had concluded that molybdate is the least stable. There is little to choose between the tungstate and arsenate in H_2O, 4*M* HNO_3, and 4*M* H_2SO_4. However, in 4*M* HCl, the tungstate is more stable than the arsenate and, in this case also, refluxing improves stability of the material. The selenite is also very stable in water, 4*M* HNO_3, and 4*M* H_2SO_4. It is not stable in 4*M* HCl and 1*N* NaOH. In 4*M* HCl, the tin release increases on refluxing. This is an exceptional behavior because in almost all other cases refluxing decreases chemical dissolution.

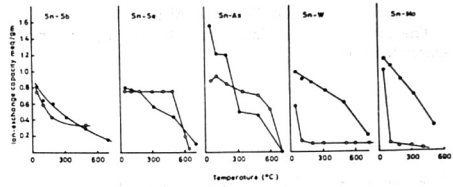


Figure 2. (Ion-exchange capacity) at different temperatures of Sn(IV) ion exchangers

—●— This work. —O— SnSb (*11*), SnSe (*14*), SnAs (*10*), SnW (*12*), SnMo (*13*)

The pH titration curves of Sn(IV) compounds give one inflection point, showing the monofunctional behavior of the exchanger, which differs from the stannic selenite and titanium selenite prepared in our laboratory. During the pH titration, stannic arsenate and stannic selenite dissolved completely in flasks containing more than 8 mmoles per liter of OH^-.

The effect of temperature on ion-exchange capacity is shown in Figure 2. In all cases, there is a regular decrease in the ion-exchange capacity except in the case of arsenate where the decrease in capacity takes place in two steps. This may be due to the fact that there are two types of OH groups—*i.e.*, those which condense before 300 °C and those which condense after 500 °C. If 0.4 mequiv/gram is taken arbitrarily as the useful limit of an ion exchange material, than stannic arsenate can be used up to 530 °C, stannic tungstate up to 600 °C, stannic antimonate up to 400 °C, stannic molybdate up to 450 °C, stannic selenite up to 500 °C. The tungstate is therefore the most thermally stable material.

To demonstrate the utility of these materials, rare earth cations were chosen because of their obvious importance in analytical chemistry. Stannic selenite was selected because there was a significant difference in K_d values of these ions on this exchanger (Table III). At pH 1, the order of K_d values is $La^{3+} > Ce^{3+} > Pr^{3+} \ldots Lu^{3+}$. The same order is predicted on the basis of the hydrated radii. La^{3+} has been separated from Lu^{3+} using a citrate buffer and a strong cation exchange resin. Lu^{3+}, being the smallest ion, forms a more stable complex while La^{3+}, being a large ion, forms a less stable complex and is eluted in the end. The same separation has been achieved on stannic selenite columns using a simple nitrate buffer which shows the superiority of inorganic ion exchangers. Since the sequence of elution into the citrate buffer is the same as into the nitrate buffer, a similar explanation may hold good in the later case also.

These studies have resulted in the preparation of new phases of some ion exchangers which are more stable and have a larger capacity. The best sample of stannic molybdate synthesized by Qureshi and coworkers (*18*) had Sn/Mo ratio of 1.99, its precipitation pH was ≃ 1.0, capacity 0.54 mequiv/gram, and chemical dissolution 0.68 mg/50 ml in water. The sample described here has a Sn/Mo ratio of 0.40; chemical dissolution, 0.30 mg/50 ml; and capacity, 1.40 mequiv/gram. Similarly, the stannic tungstate described here is more stable and has a higher capacity than the one described earlier.

(17) M. Qureshi, J. P. Gupta, and V. Sharma, *Anal. Chem.*, **45**, 1901 (1973).

(18) M. Qureshi, K. Husain, and J. P. Gupta, *J. Chem. Soc. (A)*, 29 (1971).

ACKNOWLEDGMENT

The authors are grateful to W. Rahman for providing research facilities.

Received for review October 30, 1973. Accepted March 29, 1974. Financial assistance to R.K. and V.S. by the U.G.C. (India) is gratefully acknowledged.

Sampling Errors in the Quantitation of Petroleum in Boston Harbor Water

S. M. Ahmed, M. D. Beasley, A. C. Efromson, and Ronald A. Hites[1]

Department of Chemical Engineering, Massachusetts Institute of Technology, Cambridge, Mass. 02139

The petroleum content of many effluents which are discharged into the environment (tanker ballast water and refinery waste water, for example) is limited by state or federal regulations. The enforcement of these regulations depends on the existence of reliable analytical methods for determining oil-in-water concentration. Many such methods are available: they make use of gravimetry (*1*); volumetry (*2*); infrared (*3–6*), ultraviolet (*7*) and fluorescence (*7*) spectrophotometry; and gas chromatography (*4, 8, 9*). Among these techniques, the infrared spectrophotometric method seems to be the most popular (*5*). Despite its widespread use, however, there are no data available on its reliability in practice. Therefore, the precision and accuracy of this method have been studied using the Boston Inner Harbor as the test case and using two techniques of oil pre-concentration—namely, carbon tetrachloride extraction (*1*) and polyurethane foam adsorption (*10*).

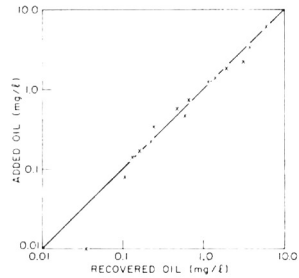


Figure 1. Oil concentration as determined by infrared spectrophotometric technique *vs.* known concentration

EXPERIMENTAL

All glassware was cleaned by washing with detergent and hot water followed by washing with concentrated chromic acid solution at about 90 °C. The glassware was then thoroughly rinsed with distilled water, dried in an oven at 175 °C, and washed with carbon tetrachloride (ACS reagent grade, sulfur-free).

Carbon Tetrachloride Extraction. The water samples (1 liter each) were obtained by submerging an open glass sample bottle upright to the desired depth and allowing it to fill. These bottles were then sealed with aluminum foil held secure with a screw cap. All samples were preserved with 3 ml of concentrated sulfuric acid, refrigerated, and extracted within 30 hours after being obtained. Once in the laboratory, the sample was poured into a 2 l. separatory funnel and 30 ml of carbon tetrachloride was used to wash the bottle from which the sample was removed. This same carbon tetrachloride was then used to extract the water sample. After 30-sec agitation and a 3-min settling period, the nonaqueous phase was drained through a funnel containing about 30 grams of anhydrous sodium sulfate over a glass wool plug and collected in a 100-ml volumetric flask. This rinsing and extraction procedure was repeated twice more. The sodium sulfate was rinsed with 5 ml of carbon tetrachloride which was added to the extracts and the volumetric flask was made up to 100.0 ml.

Infrared spectra were taken of these extracts in a 10.0-mm cell with NaCl windows. Solutions were transferred via a Pasteur pipet, washing the cell twice with the solution to be observed before filling. Spectra were scanned from 3400 cm^{-1} to 2500 cm^{-1} using 5 to 10 times expansion of the percent transmission scale. The C–H stretching band at 2930 cm^{-1} was used for analysis. The absorptivity at this wavelength as calibrated with a motor oil (SAE 30 weight) was 3.39 l. $g^{-1}cm^{-1}$. A typical procedural blank corresponded to an oil concentration of less than 0.010 mg/l.

Samples used in the recovery study were produced by adding known weights of the motor oil to sample bottles which were then filled about ¼ full with distilled water and shaken. Concentrated sulfuric acid (2.5 ml) was added, the bottles were filled with distilled water and immediately processed as described above.

Polyurethane Foam Adsorption. The foam adsorption method was implemented as described previously (*10*). In brief, 10 to 50 liters of sea water were passed through a foam disk (8-cm diameter, 4 cm thick, 100 pores/in.) and then the retained oil was extracted in a Soxhlet apparatus with carbon tetrachloride. This extract was measured as described above. It was necessary to clean new disks by Soxhlet extraction with carbon tetrachloride for four to six hours to reduce blank analyses to acceptable levels. It has previously been shown that recoveries of known concentrations of oil were greater than 85% for those concentrations above 5 mg/l. (*10*); lower concentrations were not studied (*10*).

RESULTS AND DISCUSSION

To determine the performance of the carbon tetrachloride extraction method itself devoid of any sampling errors, a recovery study was carried out. Solutions of oil in water of known concentrations were prepared as described above

[1]To whom correspondence should be addressed.

(1) ASTM Procedure No. D2778-70, "Solvent Extraction of Organic Matter from Water," ASTM Standards, Part 23.
(2) L. E. Hearn, 164th National Meeting of the American Chemical Society, New York, N.Y., August 1972.
(3) R. G. Simard, I. Hasegawa, W. Bandaruk, and C. E. Headington, *Anal. Chem.*, **10**, 1384 (1951).
(4) R. Jeltes and W. A. M. den Tonkelaar, *Water Res.*, **6**, 271 (1972).
(5) R. A. Brown, T. D. Searl, J. J. Elliott, B. G. Phillips, D. E. Brandon, and P. H. Monaghan, Proceedings of 1973 Conference on Prevention and Control of Oil Spills, Washington, D.C., p. 505.
(6) M. Gruenfeld, *Environ. Sci. Technol.*, **7**, 636 (1973).
(7) E. M. Levy, *Water Res.*, **5**, 723 (1971).
(8) R. Jeltes and R. Veldink, *J. Chromatogr.*, **27**, 242 (1967).
(9) R. Jeltes, Water Res., **3**, 931 (1969).
(10) P. Schatzberg and D. F. Jackson, *U.S. Coast Guard Rep.*, **No. 734209.9**, Washington, D.C., November 1972.

Table I. Samples Taken from Boston Inner Harbor

Sample No.	Station location[a]	Date	Time	Sheen condition
1A	*a*	July 26, 1973	11:00 a.m.	Light to heavy
2A	*b*	July 26, 1973	11:30 a.m.	None
1B	*a*	Aug. 3, 1973	11:30 a.m.	Very heavy
2B	*b*	Aug. 3, 1973	10:30 a.m.	None
3B	*c*	Aug. 3, 1973	11:00 a.m.	None
1C	*a*	Aug. 16, 1973	10:30 a.m.	None to light
2C	*b*	Aug. 16, 1973	11:30 a.m.	None

[a] Station locations were as follows: (*a*) 1.4 miles up Chelsea Creek (oil unloading site); (*b*) junction of Chelsea Creek and Mystic River; (*c*) 0.4 miles up Chelsea Creek.

Table II. Oil Concentration in Boston Harbor Water (mg/l.)

Sample No.[a]	Surface (0–5 cm)	Subsurface (25–35 cm)
1A	0.631	0.029
	1.54	<0.025
	0.407	<0.025
	0.708	0.394
	0.793	0.698
	Av. 0.816	0.234
	Rel std dev[b] 53%	130%
	Confid. lim.[c] 0.4–1.2	0.0–0.5
2A	0.213	0.143
	0.030	0.089
	0.197	0.308
	0.320	0.072
	Av. 0.190	0.153
	Rel std dev 63%	72%
	Confid. lim. 0.1–0.3	0.0–0.3
1C	0.546	0.074
	0.256	0.254
	0.306	0.096
	<0.025	0.034
	Av. 0.283	0.114
	Rel std dev 75%	84%
	Confid. lim. 0.0–0.5	0.0–0.2
2C	0.153	0.077
	0.296	0.060
	0.368	0.269
	0.138	0.366
	Av. 0.239	0.193
	Rel std dev 46%	78%
	Confid. lim. 0.1–0.4	0.0–0.4

Average rel std dev = 75%

[a] See Table I. [b] Relative standard deviation of a single measurement. [c] 90% confidence limits of mean. [d] The average of all 34 values is 0.292 mg/l. with a 95% confidence limit of 0.104 mg/l.

and analyzed. These results are shown in Figure 1; excluding the one point of lowest concentration, the average recovery is 101% and the average error is 13%. Therefore, the method itself seems quite reliable since the quantity of oil in the sample bottle can be determined with a relative standard deviation of less than 15% for concentrations exceeding about 0.05 mg/l.

The descriptions of the various samples taken from the Boston Inner Harbor are given in Table I. All samples were analyzed by the carbon tetrachloride extraction procedure and those samples taken at station numbers 1B, 2B, 3B, 1C, and 2C were also analyzed by the foam adsorption procedure to compare the two methods.

Samples were taken in replicate at stations 1A, 2A, 1C, and 2C at two depths: surface (0–5 cm) and subsurface (25–35 cm). All replicate samples at a given station and depth were taken simultaneously (±30 sec) and from within an area of about one square meter. The analyses of these samples is shown in Table II.

Table III. Comparison of Oil Concentrations Determined Using Different Preconcentration Techniques (Surface Samples Only)

Sample No.[a]	CCl_4 extraction mg/l.	Foam adsorption mg/l.	Ratio
1B	84.1	7.2	11.7
2B	0.10	0.08	1.25
3B	0.21	0.03	7.0
1C	0.283[b]	0.19	1.5
2C	0.239[b]	0.07	3.4
		Av.	5.0

[a] See Table I. [b] Average of four values (see Table II).

The relative standard deviations for each set of replicates ranges from 46 to 130% with the average being 75%; this variability is far in excess of the variability of the analytical procedure itself (15%). This error must, therefore, be associated with sampling from a heterogeneous system such as oil in water.

A model of this oil in water system will serve to quantitate the natural variability which is necessary to produce this observed variability in the measurement (75%). The model assumes that the oil is coated on, or in some way associated with, the particulate matter in the Harbor water and that there are N of these particles per liter of water. If each particle has X milligrams of oil associated with it, the measured oil concentration C is given by

$$C = NX \tag{1}$$

and therefore the relative standard deviation S_c of C is approximately

$$S_c = (S_N^2 + S_X^2 + S_A^2)^{1/2} \tag{2}$$

where S_N, S_X, and S_A are the relative standard deviations of the number of particles N, of the weight per particle X, and of the analytical procedure, respectively. If it is assumed that $S_N = S_X$, $S_c = 75\%$, and $S_A = 15\%$; then $S_N = S_X = 52\%$. In other words, if the density of particles (N) and the oil per particle (X) have a relative standard deviation of 52%, the measured concentration would have a relative standard deviation of 75%. This magnitude of variability in the natural system seems quite modest considering the polluted state of Boston Inner Harbor.

A detailed examination of Table II shows that only the 1A surface sample differs significantly from all the others. This sample was taken in an area located close to an oil unloading complex and on a day when a light to heavy sheen was observed on the water. With this one exception, the ambient oil concentration observed in this study was less than 0.5 mg/l. Furthermore, the lack of significant differences in Table II, particularly between corresponding surface and subsurface samples and between different locations, indicates that the sampling error effectively obscures the expected variation in oil concentration due to tides, currents, and depth.

Comparative data for the extraction and foam adsorption preconcentration methods are given in Table III. In all cases, the oil concentration resulting from the foam technique is the lower of the two values; in fact, it is low by a factor of five on the average. Although there are sampling errors associated with both techniques (which may well account for the scatter in the ratios), it is clear that the foam technique has a much lower collection efficiency than liq-

uid–liquid extraction and is, therefore, a less useful procedure.

CONCLUSIONS

There are, in principle, two major ways of reducing the large sampling error that was observed—namely, replicate samples and larger sample sizes. These two methods do not, however, have an equal effect on the overall precision (S_c) To demonstrate this effect, the following assumption is made: the number of particles per unit volume (N) is quite small and, thus, follows a Poisson distribution. If this is the case, the relative standard deviation of N is given by

$$S_N = \frac{100\sqrt{N}}{N} \quad (3)$$

Therefore, the overall precision resulting from n replicate analyses is

$$S_c' = \left(\frac{10^4}{nN} + \frac{S_X^2 + S_A^2}{n}\right)^{1/2} \quad (4)$$

One can now see what the effects of replication and sample size are. In the extreme, as n becomes infinitely large S_c' approaches zero. However, as sample size (and thus N) becomes infinitely large, S_c' approaches $[(S_X^2 + S_A^2)/n]^{1/2}$ which, if S_X = 52% and S_A = 15%, is 54% for a single analysis. In other words, the overall precision is limited by the analytical error (S_A) and the variability of the weight of oil on the individual particles (S_X) and, therefore, increasing sample size will not be worthwhile if these values are at all high. Increasing the number of replicates, however, directly improves the overall precision by a factor of $n^{1/2}$ over that of a single analysis.

An example may make these concepts more concrete. For the data reported above S_c = 75%, n = 1, we see that N = 3.71 l.$^{-1}$. Increasing the sample size to one gallon (3.785 l.) and analyzing three samples gives an increased precision of 35%. Keeping the sample size at one liter but analyzing four samples gives $S_c' = 75\%/\sqrt{4} = 37\%$. Clearly this latter case may be preferred from a practical point of view since less total water needs to be transported.

Finally, a few cautionary words concerning the designation of exactly what is being measured should be said. The infrared method discussed here is not measuring petroleum *per se* but rather is quantitating the abundance of aliphatic C–H bonds present in compounds which can be extracted from sea water by carbon tetrachloride. Obviously, this includes many naturally occurring lipids which are not due to petroleum, fatty acids for example. The other methods cited above are similarly non-specific; fluorescence spectrophotometry (7), for example, will respond to chlorophyll as well as the aromatic hydrocarbons in petroleum. Therefore, it is important to interpret all such quantitative measurements of petroleum-in-water in light of the known, or suspected, identities of the compounds which are present.

RECEIVED for review March 7, 1974. Accepted June 27, 1974. This work was supported by the United States Coast Guard, Contract Number DOT-CG-31862-A, and by the M.I.T. Undergraduate Research Opportunity Program.

Triplet State Acidity Constants for Hydroxy and Amino Substituted Anthraquinones and Related Compounds

Comparison of Phosphorescence and Transient Triplet Absorption Measurements

H. H. Richtol and B. R. Fitch

Department of Chemistry, Rensselaer Polytechnic Institute, Troy, N.Y. 12181

Many studies have been performed on the determination of acidity constants in the singlet excited state. Far fewer have been done on triplet state acidity constants (pK_T).

For the measurement of acidity constants in the triplet state, Jackson and Porter (*1*) have applied essentially the same methods, using flash spectroscopy, that have been used for the measurement of pK values in the excited singlet state (*2*). The energy changes needed for Förster (*2*) cycle calculations were determined directly from the short wavelength limit of the phosphorescence spectra (*1*) of the two forms. For the direct determination of pK_T, the concentrations of the triplets of the two forms in various solutions were compared by flash absorption spectroscopy. They applied this method to several compounds and found the pK_T values were intermediate between pK (ground state) and pK_S (excited singlet state) although generally much closer to the former. Others (*3, 4*) have applied flash photolysis to the determination of ionization constants of certain dyes with good success.

In this paper, acidity constants of the lowest triplet state have been determined for some hydroxy-substituted anthraquinones, fluorenes, and fluorenones by two different methods. In the first method, the triplet state is populated by flash photolysis and the acid–base equilibrium is studied spectrophotometrically as a function of pH. Lifetime studies are also an aid in interpreting the ensuing equilibrium. In the second method, the difference between acidity constants in the triplet and ground states is calculated from energy levels of the acid and base obtained from phosphorescence spectra.

(1) G. Jackson and G. Porter, *Proc. Roy. Soc., Ser. A*, **260**, 13 (1961).
(2) Th. Förster, *Z. Elektrochem.*, **54**, 42(1950).
(3) J. Faure, R. Bonneau, and J. Joussot-Dubien, *Photochem. Photobiol.*, **6**, 331 (1967).
(4) J. Faure and J. Joussot-Dubien, *J. Chim. Phys.*, **63**, 621 (1966).

Table I. Summary of Triplet State Acidity Constants

Compound	pK_G	pK_T (flash photolysis)	$pK_T(\nu_a$ max, ν_b max $cm^{-1} \times 10^4)$ (phosphorescence)
1-Hydroxyanthraquinone	9.3	8.8	8.9 (1.805, 1.786)
2-Hydroxyanthraquinone	7.1	6.7	6.1 (2.13, 1.83)
1-Aminoanthraquinone	0.5	−1.0	−0.3 (1.85, 1.81)
2-Aminoanthraquinone	0.8	−0.1	−0.5 (1.87, 1.81)
1-Hydroxyfluorene	9.3	8.4	8.7 (2.29, 2.24)
2-Hydroxyfluorene	9.1	8.1	7.8 (2.30, 2.24)
9-Hydroxyfluorene	14.6		13.5 (2.29, 2.24)
2-Aminofluorene	4.3	3.4	3.0 (2.29, 2.23)
4-Hydroxy-9-fluorenone	8.4		6.7 (1.89, 1.81)
1-Amino-9-fluorenone	−0.3		−1.5 (2.04, 1.98)

EXPERIMENTAL

Matheson Coleman and Bell spectrograde methanol and U.S.P. absolute ethanol were used as solvents without further purification. Dioxane was distilled over lithium aluminum hydride in a nitrogen atmosphere and stored in a dark bottle under nitrogen. This prevented detectable peroxide formation for more than two weeks. The purification of the solvents is described elsewhere (*5*).

Room temperature transient spectra were obtained using a cylindrical cell with two optically flat polished windows. The solution chamber was 22 mm in diameter and had a 10-cm path length. To the cell inlet, a 10-mm (i.d.) section of Pyrex tubing bent at right angles was connected to a 100-ml bulb. Above the right angle bend was a constriction to permit convenient sealing and above a 18/9 ball joint with a grease trap, which was connected to the vacuum rack. Approximately 50 ml of solution to be deaerated would be introduced into the degassing bulb. The bulb with attached cell was connected to the vacuum rack, and the solution was degassed six times by repeated freeze–pump–thaw cycles. After the sixth pumping cycle with the solution still frozen, the entire assembly was removed from the vacuum rack by sealing off the stem at the constriction.

A cell for low temperature luminescence measurements was described by one of the authors (*6*).

The solvent was a buffered 33% dioxane–water mixture. Buffer solutions of 33% dioxane–water in the pH range 1–14 were prepared by using appropriate mixtures of the following in deionized water solutions: HCl, HOAc, NaOAc, KH_2PO_4, NaOH, H_3BO_3. Each buffer was brought up to constant ionic strength by adding an appropriate amount of KCl. For very weak bases, Hammett indicators were used in H_2SO_4–H_2O mixtures. The hydrogen ion concentration of the various buffers employed was measured using an Orion Model 801 digital millivoltmeter in conjunction with a glass electrode and a saturated KCl calomel electrode. Calibration was made with Harleco standard buffer solutions. The solvent mixture chosen was a compromise due to the high solute solubility in dioxane and low solubility in water. Ground state p*K* values obtained by a spectroscopic technique (*7*) agree well with literature values (*8, 9*) taken in ethanol–water systems.

The flash photolysis unit employed in this work is the same one previously used by Strong and Perano (*10*). All flash photolysis results were obtained at ambient temperature. Solvents were required which form clear glasses at liquid nitrogen temperatures, which show no significant phosphorescence and which could be used for the study of strongly acidic and basic solutions. Water is unsuitable since it cracks badly at low temperatures. The following solvents were eventually used: ethanol + potassium hydroxide for basic spectra and sulfuric acid + ethanol for acidic spectra.

Absorption spectra were measured on a Beckman DK-2A recording spectrophotometer or a Beckman DU spectrophotometer. The fluorescence spectrophotometer is described elsewhere (*11*).

(5) H. H. Richtol and B. R. Fitch, *Anal. Chem.*, **46**, 1749 (1974).
(6) H. H. Richtol and F. H. Klappmeier, *Appl. Spectrosc.*, **18**, 113 (1964).
(7) R. A. Robinson and A. I. Biggs, *Trans. Faraday Soc.*, **51**, 901 (1955).
(8) H. Treadwell and G. Schwarzenbach, *Helv. Chim. Acta.*, **11**, 386 (1928).
(9) P. H. Grantham, E. K. Weisberger, and J. H. Weisberger, *J. Org. Chem.*, **26**, 1008 (1961).
(10) R. L. Strong and J. Perano, *J. Amer. Chem. Soc.*, **89**, 2535 (1967).
(11) H. H. Richtol and F. H. Klappmeier, *J. Chem. Phys.*, **44**, 1519 (1966).

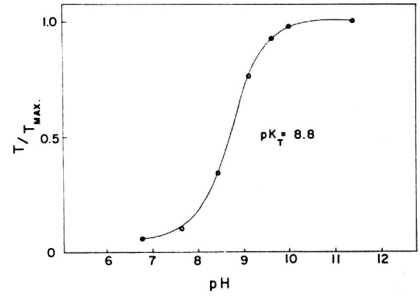


Figure 1. Plot of T/T_{max} *vs.* pH for 1-hydroxyanthraquinone

RESULTS

The corrected maxima for the acid and base forms of the observed phosphorescence spectra of the compounds studied are assumed to be an equal amount below the 0–0 bands and were used to calculate pK_T (*2*). The results are given in Table I. The short wavelength limits of the acidic and basic forms were also used to calculate pK_T and these results gave similar values of pK_T. Also presented in Table I are the pK_T values obtained by flash photolysis. In this method, the triplet absorbance ratio T/T_{max} is plotted *vs.* pH, where T_{max} is the transient absorbance maximum of, for example, the acidic form and T is the transient absorbance value at pH's different than the maximum. A typical plot is shown in Figure 1 for 1-hydroxyanthraquinone. Table II contains the wavelength maxima of the transients studied in this paper. Seven of the compounds gave good transient spectra in both acidic and basic forms, while three could not be studied by flash spectroscopy because no transient was observed.

The kinetic data associated with the decay of the acidic and basic forms of the transients are presented in Table III. The decay rate constants were all found to be first order and are, within reasonable limits, equal for the acidic and basic forms.

DISCUSSION

Phosphorescence is mainly observed in rigid media, conditions under which acid–base equilibrium cannot quickly be established after excitation. Therefore, methods based

Table II. Spectral Data for the Acidic and Basic Transients

Compound	λ_{max}, nm	
	Acid transient	Basic transient
1-Hydroxyanthraquinone	445, 490	470, 730
2-Hydroxyanthraquinone	440, 550, 655	450, 770
1-Aminoanthraquinone	395, 500, 640	410, 650
2-Aminoanthraquinone	360, 510, 560	380, 640
1-Hydroxyfluorene	360, 510, 560	390, 470, 580
2-Hydroxyfluorene	360, 560	380, 585
2-Aminofluorene	370, 600	380, 410, 430, 520

Table III. Calculated Kinetic Data for Observed Transients

Compound	Acid transient		Basic transient	
	Rate constant, sec^{-1}	Lifetime × 10^3, sec	Rate constant, sec^{-1}	Lifetime × 10^3, sec
1-Hydroxyanthraquinone	412	2.4	343	2.9
2-Hydroxyanthraquinone	421	2.4	398	2.5
1-Aminoanthraquinone	942	1.1	792	1.3
2-Aminoanthraquinone	663	1.5	645	1.6
1-Hydroxyfluorene	8150	0.12	7740	0.13
2-Hydroxyfluorene	10,820	0.09	8940	0.11
2-Aminofluorene	1150	0.87	1060	0.94

on intensity measurements have not been used for pK_T values. However, the Förster (*12*) cycle was used to determine the pK_T values from the phosphorescence spectra. Since the probability of singlet → triplet transitions is extremely small, absorption measurements were not attempted, but phosphorescence emission gives some information about the energy of the 0–0 transitions of the acidic and basic forms. In the case of the fluorene derivatives, phosphorescence spectra had well-defined vibrational structure which made the short wavelength band rather easily identifiable and hence allowed a reasonable estimation of the 0–0 transition. The application of the Förster cycle for these compounds gave precise values for the acidity constants in the triplet state. In several other compounds identification of the 0–0 transition was difficult. For the anthraquinones and fluorenones in this work, evaluations of 0–0 transitions were performed with fair success and comparison with results from flash experiments was quite good (*cf.*, Table I).

All the transient spectra studied are assumed to be triplets, since all the spectra were quenched by oxygen and decay by first-order kinetics. Further evidence that these were most probably triplets were shown by the quenching of biacetyl phosphorescence (*13*) in deaerated fluid solution. The quenching constants were of the order of magnitude observed by Sandros and Bäckström (*14*) for triplet quenching of biacetyl.

Consider an acid–base equilibrium in the ground state (S_0) between protonated, $AH(S_0)$, and deprotonated, $A^-(S_0)$, forms. A high intensity flash excites a portion of the molecules into the various singlet excited states. Direct excitation into the triplet is neglected. Depending on the acidity conditions, the presence of buffer, and the various rate constants involved, a new equilibrium will be established or at least partly established (*15*) in the excited singlet state (S_1) between $AH(S_1)$ and $A^-(S_1)$. According to the ratio of intersystem crossing and fluorescence quantum yields of the two species, a fraction of $AH(S_1)$ will intersystem cross to the triplet state (T_1). In a buffered (B) solution, it has been shown (*1*, *16*) that the following equilibrium will usually be established in a time smaller than the mean lifetime of the triplet state:

$$AH(T_1) + B \underset{k_b}{\overset{k_a}{\rightleftharpoons}} A^-(T_1) + BH^+$$

where k_a and k_b, the forward and backward rate constants are much faster than the triplet lifetimes. The rate constants and decay lifetimes presented in Table III are within an experimental error of ±10%, about equal for the acidic and basic forms of each compound. This indicates that the lifetimes are independent of pH and of the concentration of the particular acidic or basic species. The lifetimes are dependent only upon the equilibrium reaction, which is apparently established much more rapidly than the decay characteristics of the xenon flash lamps (~10^{-5} sec). The apparent rate constant observed is the sum of all rate processes involved. Since the rate constant appears independent of pH, the rate measured is most likely the apparent over-all rate constant.

In the calculation of results, absorptivities of the triplet–triplet absorption bands of the acid and basic forms were assumed to be equal at the maxima of the bands under consideration. As Jackson and Porter (*1*) have shown, the influence of this assumption on the final value of pK_T is negligible.

On comparison of the acidity constants obtained in this work with those found in the literature (*1*), we find that for molecules containing the hydroxyl or the amino groups, the

(12) Th. Förster, in "Photochemistry in the Liquid and Solid States," F. Daniels, Ed., John Wiley & Sons, Inc., New York, N.Y., 1960.
(13) B. R. Fitch, Ph.D. Dissertation, Rensselaer Polytechnic Institute, Troy, N.Y., 1973.
(14) K. Sandros and H. L. J. Bäckström, *Acta. Chem. Scand.*, **16**, 958 (1962).
(15) N. Lasser and J. Feitelson, *J. Phys. Chem.*, **77**, 1011 (1973).
(16) L. Lindqvist, *Ark. Kemi*, **16**, 79 (1960).

acidity is always increased in both the excited singlet state and the triplet state. However, the pK_T usually lies much closer to the ground state value than does the excited singlet state acidity constant.

The excited state acidity constants in the triplet state showed a much smaller dependence on the type of compound under investigation. The values obtained were always within two pK units of the values measured for the ground state, which is an agreement with the results obtained by other authors (*1, 17*). For the singlet excited state acidity constants, variations of from 5 to 20 pK units from the ground state are known (*18*).

RECEIVED for review February 19, 1974. Accepted June 17, 1974.

(17) S. G. Schulman, L. B. Sanders, and J. D. Winefordner, *Photochem. Photobiol.*, **13,** 381 (1971).
(18) H. H. Jaffe, D. L. Beveridge, and L. Jones, *J. Amer. Chem. Soc.*, **86,** 2932 (1964).

Potential Sources of Analytical Error in the Erythrocytic δ-Aminolevulinic Acid Dehydratase Test for Lead Exposure

Theo. J. Kneip, Norman Cohen, and Virginia Rulon

New York University Medical Center, 550 First Avenue, New York, N.Y. 10016

The determination of δ-aminolevulinic acid dehydratase activity (ALA-D) in erythrocytes is one of the most sensitive tests proposed for screening large populations of children potentially exposed to lead. Despite the excellent sensitivity of ALA-D to lead exposures as shown by Hernberg (*1, 2*) for normal and elevated levels of blood lead concentration, and the relatively simple spectrophotometric equipment required for its analysis, the test has not been widely adopted for routine use. The occurrence of erratic and widely variable ALA-D values, as observed in this as well as other laboratories (*3*), has been one cause for the unpopularity of this test. A second factor for the lack of acceptance is the unavailability of the purified enzyme for the determination of quantitative calibration curves.

Present studies employing this test are part of a broad research program designed to elucidate dose-response relationships for lead exposures for controlled ingestion of leaded compounds by infant baboons (*4*). Baboons are exposed to lead by intravenous injection of lead chloride or by forced feeding of various doses of lead acetate, paint pigment (lead hydroxycarbonate), powdered paint containing a lead drier compound (lead octoate), or lead octoate dissolved in olive oil. Several clinical and biochemical indices of lead exposure are routinely monitored and evaluated with respect to the duration and magnitude of the lead dose rate as well as to the accumulated lead body burden.

EXPERIMENTAL

Activity of ALA-D is determined in hemolyzed whole blood by the method of Granick (*5*) with two modifications. Hemolysis is achieved by immersing the sample tube in a Dry Ice–acetone mixture for 10 minutes, eliminating the use of the saponin. Mercuric chloride is not used in the Erhlich's reagent, and is replaced by *N*-ethylmaleimide (*6*) in the trichloroacetic acid reagent to prevent sulfhydryl interference in the subsequent color development step. The porphobilinogen (PBG) formed by condensation of two molecules of δ-aminolevulinic acid (δ-ALA) through the catalytic action of ALA-D is measured spectrophotometrically with a Beckman Model DB spectrophotometer and expressed as nmol PBG/mlRBC/hr.

RESULTS AND DISCUSSION

The ALA-D test was difficult to control throughout the early history of the lead toxicity study. Early values for erythrocytic ALA-D in infant baboons ingesting lead compounds over a wide range of dose rates, showed considerable scatter and almost no correlation to the magnitude of their lead exposures. When it was noted that ALA-D values were more variable in blood collected in heparinized 5-ml glass Vacutainer tubes than in blood collected in 10-ml glass Vacutainer tubes, a study of the sampling procedure was initiated. (All the glass Vacutainer tubes are products of Becton-Dickinson. The polystyrene tubes are products of Falcon Plastics. Both producers are Divisions of Becton-Dickinson and Co., Rutherford, N.J.).

Three types of tubes and two types of stoppers were subsequently employed for blood collection: polystyrene tubes, 10-ml glass tubes with amber or green stoppers, and 5-ml glass tubes with amber stoppers. The amber rubber stoppers are used for those tubes certified to contain no more than 1 μg lead per tube—*i.e.*, "minimal lead." Tubes with green rubber stoppers are not certified as "minimal lead."

Blood samples were collected from animals exposed to lead at three different dose levels. For example, B-31 (a 4½-yr old male weighing 13.3 kg) and B-330 (a 5-yr old female weighing 6.3 kg) had been ingesting lead as lead acetate as the dose rate of 16.1 mg Pb/kg/day over a period of 7 to 8 months. The animal B-556 (a 1-yr old female weighing 2.3 kg) had been ingesting lead in the form of lead octoate drier in dried paint solids at the rate of 100 μg Pb/kg/day over a period of 3½ months. The blood lead concentrations of the samples drawn during this investigation were extremely high for B-330 and B-31, and in the range of normal human values for B-556 and B-650 (a 1½ yr old female weighing 4 kg) which was not exposed to any lead compound.)

Values for ALA-D were determined in aliquots of blood transferred from a single plastic syringe into the different types of collection tubes. To prevent initial blood-stopper contact, the stopper was removed from the tube before the blood was transferred from the syringe. The blood was allowed to flow down the inside wall of the tube and was

(1) S. Hernberg and J. Nikkanen, *Lancet*, **1,** 64 (1970).
(2) S. Hernberg, S. Tola, J. Nikkanen, and S. Valkonen, *Arch. Environ. Health*, **25,** 109 (1973).
(3) B. G. King, % Dr. Dale Ruthig, Environmental Health Services Division, Center for Disease Control, Atlanta, Ga. 30333, personal communication, 1974.
(4) N. Cohen, T. J. Kneip, V. Rulon, and D. H. Goldstein, "Environmental Health Perspectives," Experimental Issue 7, DHEW Pub. NIH 74-218, U.S. Government Printing Office, Washington, D.C., 1974, p 161
(5) S. Granick, S. Sassa, J. L. Granick, R. D. Levere, and A. Kappas, *Proc. Nat. Acad. Sci. US*, **69,** 2285 (1972).
(6) H. B. Burch, and A. L. Siegel, *Clin. Chem.*, **17,** 1038 (1971).

Table I. Sample Container Effects on Measured ALA-D Values in Baboon Blood (Values in nmol PBG/ml RBC/hr)

Animal No.	Date	Poly-styrene tube	10-ml Glass tube: Amber stopper	Error, %[a]	No stopper	Error, %[a]	Green stopper	Error, %[a]	No stopper	Error, %[a]
B-31	5/9	32	359	1020	122	280	779	2330	54	69
B-330		33	352	970	141	330	1024	3000	75	127
Average error, %				995		305		2665		98
B-31	5/16	30	39	30	30	0	435	1350	30	0
B-330		47	30	−36	30	−36	412	777	30	−36
B-556		235	406	73	250	6	506	115	287	22
B-650		330	437	32	331	0.3	503	52	376	14
Average error, %				25		7.4		573		0

[a] Error, % = $(\text{ALA-D}_{\text{glass}} - \text{ALA-D}_{\text{polystyrene}})/\text{ALA-D}_{\text{polystyrene}} \times 100$.

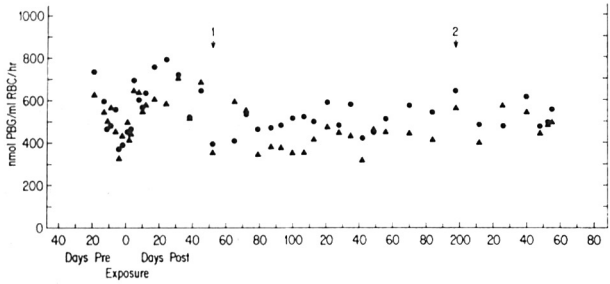


Figure 1. δ-Aminolevulinic acid dehydratase variations for control animals

Animals: B-131 (●); B-145 (▲). (1) Routine use of 10-ml "minimal lead" tubes without stopper contact. (2) Routine use of polystyrene tubes sealed with parafilm

mixed by manually rotating the tube in an upright position for 15–20 seconds to dissolve the heparin. In this way, contact was avoided between the blood and the lubricated area where the stopper had originally been. After a volume of blood necessary to run the assay was taken from the sample, the stopper was replaced. The tube was then inverted for a period of three minutes to allow the blood to contact the stopper. While a totally consistent pattern was not obtained, it is clear from the data in Table I that stopper contact often resulted in values with a positive bias—*i.e.*, values greater than those obtained without stopper contact.

Continued evaluation of the difference between 5-ml and 10-ml amber-stoppered tubes confirmed the results. During these intercomparisons, however, clotting was observed in some of the 5-ml tubes, so that a further modification of the sampling procedure was necessary. The walls of the plastic syringe into which the blood sample is drawn are now rinsed with a solution of sodium heparin ("Liquaemin Sodium '10'," 1cm^3 = 1000 USP units, Organon, Inc., West Orange, N.J.) before the needle is inserted into the vein. No clotting problem has been observed when blood taken in this manner is transferred to a "minimal lead" tube from which the stopper has been removed or to a polystyrene tube, and is mixed by rotating as previously described. The tubes are then covered with parafilm for transfer to the laboratory.

As can be seen in Figures 1 through 3, the ALA-D activity of animals having normal or elevated blood lead levels has been strongly affected by this sampling problem. The sporadic nature of the effect is seen initially by the improvement observed for some time while using 10-ml "minimal lead" tubes without stopper contact, and subsequent interference as shown at day 182 in Figure 2 and at day 64 in Figure 3. The animals represented in Figure 3 had begun exposure after the original change in the sampling procedure.

As it was believed that a new problem had developed, a complete recheck of the ALA substrate and repreparation of all reagents was performed. Only one lot of 10-ml "minimal lead" tubes had been used since refinement of the sampling procedure. It was finally determined by the further intercomparisons shown in Table II that the 10-ml tubes were variable from box to box within the same lot.

Subsequent to this discovery, polystyrene tubes have been used for all blood sample collections after ascertaining that this change would not interfere in the blood lead determination. The change to polystyrene tubes resulted in a return to ALA-D values representative of those expected for both exposed and unexposed animals.

The per cent error due to blood collection in the glass tubes is plotted in Figure 4 and can be seen to be a function of the actual enzyme activity—*i.e.*, that observed in blood collected in polystyrene tubes. (The dashed line shows a theoretical curve calculated from an assumed hypothetical value in polystyrene of 300, 200, 100, 50, and 25 nmol PBG/ml RBC/hr and a hypothetical constant value of 400 nmol PBG/ml RBC/hr. for glass sample tubes.) The excellent fit of the curve to the actual experimental data is indicative of the complete restoration of ALA-D activity regardless of the magnitude of the original inhibition due to lead.

Table II. Sample Container Effects on Measured ALA-D Values in Baboon Blood (Values in nmol PBG/ml RBC/hr)

Animal No.	Date	Polystyrene tube	10-ml Glass, no stopper	5-ml Glass, no stopper	Difference, %[a]	Error, %[b]
B-31	6/12	N.A.[c]	31	210	577	...
B-330	6/12	N.A.	29	253	772	...
B-159	6/12	N.A.	356	500	40	...
B-179	6/12	N.A.	371	353	−5	...
B-199	6/12	N.A.	366	319	−12	...
B-642	6/12	N.A.	330	336	2	...
B-652	6/12	N.A.	345	475	38	...
B-191	9/12	161	231	...	...	43
B-191	9/14	154	387	...	...	151
B-191	9/18	167	499	...	...	199
B-654	9/12	85	148	...	...	74
B-654	9/18	129	333	...	...	158
B-656	9/12	150	176	...	...	17
B-656	9/14	180	266	...	...	48
B-656	9/13	131	287	...	...	119

[a] Difference, % = (ALA-D_{10ml} − ALA-D_{5ml})/ALA-D_{5ml} × 100. [b] Error, % = (ALA-D_{glass} − ALA-$D_{polystyrene}$)/ALA-$D_{polystyrene}$ × 100. [c] N.A. = Tubes not available, no data obtained.

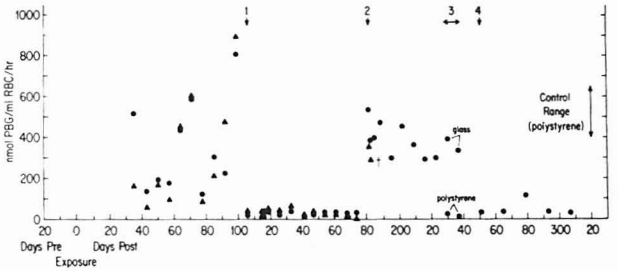


Figure 2. δ-Aminolevulinic acid dehydratase variations for animals exposed to lead acetate (16.1 mg Pb/kg/day)

Animals: B-153 (●); B-542 (▲); † Indicates death of B-524. (1) Routine use of 10-ml "minimal lead" tubes without stopper contact. (2) Reappearance of interference. (3) Experimental intercomparison of 10-ml "minimal lead" glass tubes without stopper contact and polystyrene tubes. (4) Routine use of polystyrene tubes sealed with parafilm

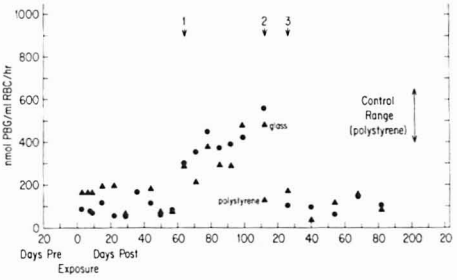


Figure 3. δ-Aminolevulinic acid dehydratase variations for animals exposed to lead hydroxycarbonate (8.2 mg Pb/kg/day)

Animals: B-189 (●); B-610 (▲). (1) First appearance of interference. (2) Experimental intercomparison of 10-ml "minimal lead" glass tubes without stopper contact and polystyrene tubes. (3) Routine use of polystyrene tubes sealed with parafilm

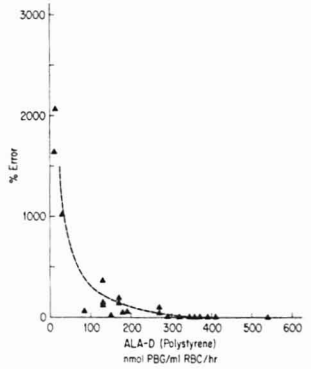


Figure 4. Per cent error in δ-aminolevulinic acid dehydratase activity due to blood collection in glass tubes

The problems encountered in measuring ALA-D activity in the study have all been caused by interferences inherent in the sampling system. In addition to excessive scatter at "normal" ALA-D activity levels, numerous incorrect "normal" activities have been found. These values would all appear as false negative results since they occurred for animals known to have elevated blood lead concentrations. It is possible that materials in the rubber stoppers containing chelating functional groups could remove lead from an enzyme–metal complex, thereby reactivating the enzyme much as is done intentionally with dithiothreitol (*5*). Furthermore, the glass tubes used to avoid lead interference are acid washed and, in this way, an active surface may be produced which could remove the lead from the ALA-D by adsorption or ion exchange reactions.

The recommended sample handling procedure developed in this study requires drawing venous blood into a plastic syringe which is prerinsed with a solution of sodium heparin. The sample is then transferred to a polystyrene tube, which is covered with parafilm, and kept at 4 °C for a maximum of two hours (*7*) before removal of 200 μl of whole blood for ALA-D analysis by the method of Granick.

CONCLUSIONS

It is obvious from these results that considerable care in sample handling must be taken in any screening program which attempts to measure erythrocytic ALA-D activity. Significant problems could be encountered in a program where both blood lead and ALA-D were to be measured in screening children for lead exposure. The "minimal lead" Vacutainer sample tubes, which would normally be used to prevent lead contamination and resulting false positive blood lead values, are a significant source of interference in the ALA-D test.

The interference as observed in this study would produce a large fraction of false negative ALA-D values when these results were compared to elevated blood lead values. In order to avoid this problem, it is imperative to use a noninterfering sample collection tube. Any contact with materials capable of reactivating the enzyme must be avoided, and only the polystyrene tubes appear to be free of interfering substances. In extensive use of these tubes, no problem has been found in the determination of blood lead, ALA-D, or free erythrocytic porphyrin.

(7) D. Prpic-Majic, P. K. Mueller, V. C. Lew, and S. Twiss, *Amer. Ind. Hyg. Ass. J.*, **34**, 315 (1973).

ACKNOWLEDGMENT

The authors gratefully acknowledge the technical assistance of John Gorczynski and Peter Mallon. The support of the entire staff of the Laboratory for Experimental Medicine and Surgery in Primates (LEMSIP) of the New York University Medical Center is appreciated.

RECEIVED for review March 4, 1974. Accepted June 14, 1974. This investigation was supported by Contract No. 73-22 from the Consumer Product Safety Commission, Grant No. U 2274, from the Health Research Council of New York City, and is part of a Center program supported by the National Institute of Environmental Health Sciences, Grant ES 00260.

Kinetic Study of the Stabilities of Chloromethyl Methyl Ether and Bis(Chloromethyl) Ether in Humid Air

James C. Tou and George J. Kallos

Analytical Laboratories, Dow Chemical U.S.A., Midland, Mich. 48640

Chloromethyl methyl ether (CMME) is one of the most commonly used chloromethylating agents in the manufacture of commercial ionic resins and bis(chloromethyl) ether (bis-CME), a strong carcinogen (*1*, *2*), is known to be one of the impurities present in CMME. Possible industrial exposure to these simple molecules has been of great concern. An analytical technique for monitoring parts-per-billion levels of bis-CME in air has, therefore, been developed (*3*). However, monitoring techniques for CMME in air have not been reported to the best of our knowledge. A recent kinetic study of their hydrolysis in aqueous solution showed that both CMME (*4*) and bis-CME (*5*) hydrolyzed very fast with half-lives in the order of <1 sec (extrapolated to pure water) and 10–20 sec, respectively. This indicates that these two compounds cannot exist in aqueous media for any extended period of time. However, their stabilities in air have not been studied.

The present investigation was undertaken to help understand the chemical properties of these two hazardous chemicals which could be present in our occupational environment. This study involves the stabilities of CMME and bis-CME in humid air as determined by the kinetics of their hydrolysis rates. The results of this study are also important in assessing the validation of the analytical determinations of these two molecules in air.

EXPERIMENTAL

In the study of the hydrolysis rates in a glass system, a three-neck round-bottom 5-l. flask was used and immersed in a well controlled thermal bath. A fifteen-head silicone fiber probe (*6*) was installed in the flask through a ground glass joint and connected (with ¼-in. Teflon tubing) to a cycloidal mass spectrometer which was used for analysis. The design and the properties of the probe were described elsewhere (*6*). A septum was placed on one of the three necks and used for injecting samples or for evacuating the

(1) B. L. Van Duuren, A. Sivak, B. M. Goldschmidt, C. Katz, and S. Milchonne, *J. Nat. Cancer Inst.*, **43**, 481 (1969).
(2) S. Laskin, M. Kuschner, R. T. Drew, V. P. Cappielle, and N. Nelson, *Arch. Environ. Health*, **23** (8), 135 (1971).
(3) L. A. Shadoff, G. J. Kallos, and J. S. Woods, *Anal. Chem.*, **45**, 2341 (1973).
(4) T. C. Jones and E. R. Thornton, *J. Amer. Chem. Soc.*, **89**, 4863 (1967).
(5) J. C. Tou, L. B. Westover, and L. F. Sonnabend, *J. Phys. Chem.*, **78**, 1096 (1974).
(6) L. B. Westover, J. C. Tou, and J. H. Mark, *Anal. Chem.*, **46**, 568 (1974).

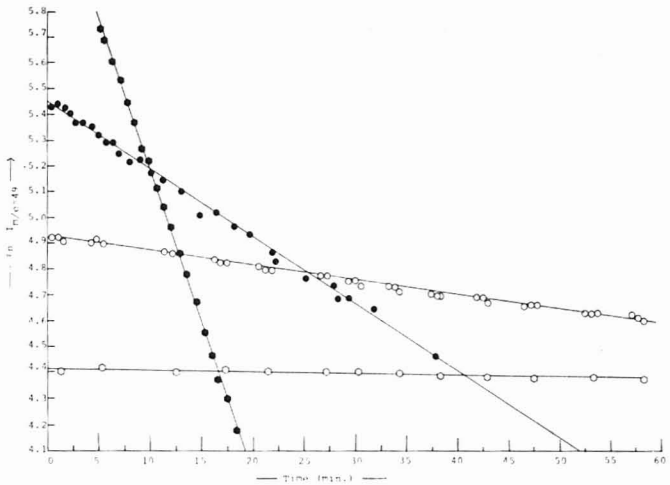


Figure 1. Hydrolysis rate plot of chloromethyl methyl ether in a glass system

O dry air (~ 0.06% H_2O), 25 °C. • 1.7% H_2O, 25 °C. ● 2.2% H_2O, 25 °C. ○ m/e = 57 from isooctane

flask. The third neck was used as a thermometer well. At the beginning of an experiment, the flask was evacuated and flushed several times with purified air dried with a molecular sieve, and then conditioned with the dry air for about an hour. The humid air was prepared by injecting an appropriate amount of de-ionized water into the flask through the septum. The air in the flask was stirred with a magnetic bar and small glass beads for one hour. Five milliliters of the humid air so prepared were removed using a syringe for checking the humidity by the P_2O_5 electrolytic method (7) (Our system was designed by G. F. Crable of our laboratories.). The recorded humidity was taken as the average of determinations before, during, and after each experiment. The accuracy of each determination is better than ±10%. Either 0.5 μl or 2.5 μl of the compounds to be studied was injected into the flask, which yielded the initial concentrations of about 22 ppm or 110 ppm, respectively. The intensities of the characteristic ion peaks of the compound produced by the mass spectrometer were recorded as a function of time with a Sargent-Welch recorder having sensitivity ranging from 1–100 mV.

In the study of the surface effect on the rate of hydrolysis, an identical flask having the inner surface fused with ground glass was used to increase the surface-to-volume ratio. Also used in the study were a 5-l. Teflon (Du Pont) bag and a 5-l. Saran (Dow) bag with and without the inner surface being coated with Fe_2O_3 powder. The bags were purchased from Fluorodynamic Corp., Newark, Del., and Anspec Co., Ann Arbor, Mich., respectively. The experiments involving the use of the bags were carried out only at ambient temperature with different humidities. The fiber probe was installed in the bags through the provided neck and the humid air in the bags was prepared in the same manner as previously described. The mixing was achieved using a Teflon-coated magnet stirrer only. The samples were injected into the bag through the wall. The hole caused by the syringe punctuation was immediately sealed with a piece of Scotch Brand tape (3M Co., St. Paul, Minn.) after the sample injections.

RESULTS AND DISCUSSION

Chloromethyl Methyl Ether (CMME). The most intense ion peak in the mass spectrum of CMME is at m/e 45 (rel. int. 100%), generated from the decomposition of the molecular ions, $[ClCH_2OCH_3]\cdot^+ \rightarrow CH_2{=}{}^+O\text{-}CH_3 + \cdot Cl$. The ion at m/e 45 is known to be a very common ion from many oxygen-containing compounds (8). To avoid any possible interference from the anticipated hydrolysis products, the second most intense peaks at m/e 49 (rel. int. 17%) and 51 (rel. int. 6.7%) due to the ions, $^{35}Cl^+{=}CH_2$ and $^{37}Cl^+{=}CH_2$, respectively, were monitored as an indication of the change of the concentration of CMME. The concentration time curve shows an initial increase to its maximum in about one minute and then an exponential decay. The increase at the beginning of the curve is caused by the combined effects of the initial sample mixing and the reaction taking place. The exponential decay of the peak intensity indicates the occurrence of a pseudo unimolecular reaction. The diminishing of the intensity of the peaks to the background level at time approaching infinity reveals that there was no serious interference from either the reaction product(s) or the foreign components present in the system. The observed decay of the $CH_2{=}Cl^+$ ion peak intensity may also indicate that the reaction involves a nucleophilic attack of a water molecule on the α-carbon substituted with a chlorine atom. The detection limit of CMME with use of the present technique is estimated to be 1–0.5 ppm based on the peak at m/e 49 or about 0.05–0.03 ppm if based on the peak at m/e 45.

In the pseudo-unimolecular reaction, the plot of the log concentration (or peak intensity) *vs.* time should yield a straight line. Therefore, the rate of the reaction can be calculated from the slope of the straight line. As an example, Figure 1 shows several rate plots at different water concentrations in the glass system. The data points were taken after the completion of mixing. Also shown in Figure 1 is the intensity of the peak at m/e 57 from isooctane, which was loaded into the reaction flask with CMME for checking any possible variations of the instrument sensitivity during the kinetic runs. As expected, no noticeable change of the peak height was observed. The amount of water used in the dry air runs was calculated to be approximately 0.06%. It is

(7) D. E. Smith and C. H. Zimmerli, "Electrochemical Methods of Process Analysis," Chapter 5, Part 2, Instrument Society of America, Pittsburgh, 1972.

(8) F. W. McLafferty, "Mass Spectral Correlations," *Advan. Chem. Ser.*, American Chemical Society, Washington, D.C., 1963.

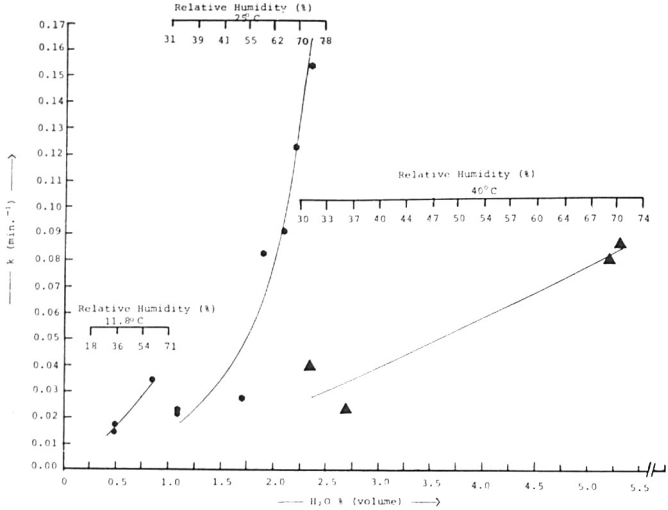


Figure 2. Humidity effect on the hydrolysis rates of chloromethyl methyl ether in a glass system.

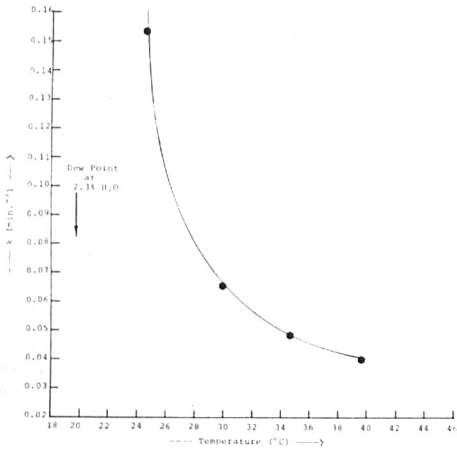


Figure 3. Temperature effect on the hydrolysis rates of chloromethyl methyl ether in a glass system at 2.3% H_2O concentration

obvious that a higher humidity leads to a steeper slope, and therefore, a higher rate of reaction. This indicates that the reaction must involve water molecules in the system and that hydrolysis is taking place. Within experimental accuracy, no significant difference was found in the rate of hydrolysis at the initial concentrations of 28 and 110 ppm. The expected trend of the dependence of rates on water concentration is also shown in Figure 2, where the humidity effect on the hydrolysis rates of CMME in a glass system was studied at several different temperatures. The hydrolysis rates were also investigated as a function of temperature. The results are shown in Figure 3. As the temperature increases, the rate of hydrolysis decreases. This strongly suggests that the hydrolysis reaction has taken place on the glass surface instead of in the gas phase. It is known that there are two types of water on the glass surface—physically adsorbed and chemically hydrated (*9*). The amount of water on the surface is expected to be inversely proportional to the temperature. However, the amount of water adsorbed is so small (*10*) that no gross effect on the water content in gas phase should be observed in the humidity determination.

For further investigation of these surface hydrolysis reactions, two approaches were taken and are discussed below.

Increase of the Surface to Volume Ratio. To increase the surface-to-volume ratio, ground glass was fused onto the inner surface of a glass reactor. The hydrolysis rate was determined and compared with that obtained from a normal glass reactor under similar conditions. The data are shown in Table I. The rate increases by a factor of approximately four when the surface-to-volume ratio is increased as described.

Change of the Construction Material of the Reactor. The rates of hydrolysis were also determined near ambient temperature at different water concentrations in reactors made of Teflon, Saran, and ferric oxide powder-coated Saran. The results of the determinations are compared in Table I. The rates of hydrolysis vary markedly depending upon the reactor construction materials, in the following order: ferric oxide powder-coated Saran > glass > Teflon > Saran.

All the above data strongly suggest that the hydrolysis reaction of CMME is surface-catalyzed. The rate of hydrolysis taking place in the gas phase must be considered to be slower than, or comparable to, that determined in the Saran reactor.

The rates of hydrolysis of CMME reported by R. W.

(9) K. Erents and G. Carter, *Vacuum*, **15**, 573 (1965).
(10) T. Yoshimori, S. Ishiwari, Y. Watanabe, T. Harada, and S. Yamada, *Nippon Kinzoku Gakkaishi*, **35**, 808 (1971); *Chem. Abstr.*, **75**, 115500 d.

Table I. Surface Effect on the Gaseous Hydrolysis Rates of Chloromethyl Methyl Ether (A) and Bis(Chloromethyl) Ether (B) Near Ambient Temperature

Compounds	Reactor material	Temperature, °C	Water concentration, % by volume	Relative humidity, %	k(min^{-1})	$t_{1/2}$(min)
A	Glass	25	1.7	53	0.028	25
		25	2.2	69	0.12	5.8
	Fused ground glass	26	1.6	47	0.12	5.8
	Teflon	27	1.5	42	0.0059	120
		25	1.9	60	0.014	50
		25	2.1	65	0.035	20
	Saran	29	1.6	39	0.0018	390
		25	2.0	62	0.0058	120
		29	2.2	54	0.0060	120
	F_2O_3 powder-coated Saran	25	1.1	35	0.042	17
		25	2.3	72	0.31	2.3
B	Glass	25	2.2	67	0.00057	1200 (20 hr)
	Fused ground glass	25	2.6	81	0.00047	1500 (25 hr)
	Fe_2O_3-powder coated Saran	23	1.2	42	0.0013	540 (9.0 hr)
		23	2.3	81	0.0016	430 (7.2 hr)

Nichols and R. F. Merritt (*11*) are very close to those determined presently in the glass system. Based on our findings, the stability data on CMME cannot be extrapolated from a glass system (*11*) to atmospheric environment.

Bis(chloromethyl) Ether (Bis-CME). The most intense ion peak in the mass spectrum of bis-CME is at m/e 79, generated from the decomposition $[ClCH_2OCH_2Cl]\cdot^+ \rightarrow ClCH_2O^+{=}CH_2 + Cl\cdot$. Both the ion, $^{35}ClCH_2O^+{=}CH_2$, at m/e 79 and its isotopic ion $^{37}ClCH_2{-}O^+{=}CH_2$ at m/e 81 were monitored. The rates of hydrolysis were determined in reactors made of glass, fused ground glass, and ferric oxide powder-coated Saran near the ambient temperatures at water concentrations between 1.2–2.6%. The data obtained are shown in Table I. The surface effect on the rate of hydrolysis of bis-CME is in the same direction as shown in the case of CMME. The rate is faster in the ferric oxide-coated Saran reactor than in the glass reactors. Bis-CME was found to be much more stable than CMME. The upper limit of the rate of hydrolysis of bis-CME in gas phase is less than 0.00047 min^{-1}, (or $t_{1/2} > 25$ hours).

CONCLUSION

The rates of hydrolysis for CMME and bis-CME were measured in humid air, and the rates of reaction ranged between 0.31–0.0018 min^{-1} for CMME and between 0.0016–0.00047 min^{-1} for bis-CME depending upon the type of the reactor surface. A strong surface effect on the rate of hydrolysis was observed in the following decreasing order: ferric oxide powder-coated Saran > glass > Teflon > Saran. Therefore, the upper limits of the rates of hydrolysis taking place in gas phase were 0.0018 min^{-1} and 0.00047 min^{-1} for CMME and bis-CME, respectively, at water concentrations 1.6 and 2.6%, respectively, near ambient temperature. Also the rate of hydrolysis was slower at lower water concentrations. Because of the strong surface effect on the rate of hydrolysis of CMME, the material of construction of any analytical devices and the residence time of CMME in the devices prior to analysis have to be considered in order to determine the true (or approaching to true) level of CMME in air. On the other hand, bis-CME is quite stable. Therefore, no serious problem in monitoring its level in air is anticipated.

ACKNOWLEDGMENT

The authors express their sincere gratitude to W. B. Crummett, L. B. Westover, G. F. Crable, and R. A. Nyquist for their encouragement and valuable discussions.

RECEIVED for review February 28, 1974. Accepted June 13, 1974.

(11) R. W. Nichols and R. F. Merritt, *J. Nat. Cancer Inst.*, **50**, 1373 (1973).

Effect of Ethyl Chloroformate on the Dye Binding Capacity of Protein

Louis Sandler

Fishing Industry Research Institute, University of Cape Town, Rondebosch 7700, Cape, South Africa

F. L. Warren

Natural Products Research Laboratory, University of Cape Town, Rondebosch 7700, Cape, South Africa

The present communication is concerned with a simplified method for the determination of lysine in protein by measuring the amount of acid dye which combines with the protein before and after masking the basic terminal amino group of lysine. The difference would then give the amount of dye which combined with the lysine and, hence, the amount of lysine itself. This differential dye binding determination avoids the lengthy hydrolysis of the protein necessary in other methods, and offers a simple and rapid technique for a routine determination of lysine in protein material.

The theoretical basis of the method rests on the observation of Chapman, Greenberg, and Schmidt (*1*) that the amount of certain acid dyes which combines with protein shows a correlation with the amount of arginine, histidine, and lysine in the protein. This is attributed to salt formation between the acid dye and the guanidine group in arginine, the imidazole group in histidine, and the ϵ-amino group of lysine. The difference in the amount of dye which would combine with the protein after masking the amino group of lysine would be equivalent to the amount of arginine and histidine. The departure from exact quantitativity in the experiments of Chapman *et al.* (*1*) may be attributed to secondary factors such as the reaction of the dye to other groups in, and to adsorption on, the protein. These factors would cancel out in any difference method provided that the reagent used to mask the ϵ-amino group of lysine did not modify the protein itself by reacting with other groups or cause cross-linking.

The reagent of choice should accordingly be of small molecular size to avoid steric hindrance to reaction of the dye with the basic groups, react quantitatively at low temperatures with the ϵ-amino group, and not modify the basic properties of the imidazole group of histidine or the guanidine group of arginine. The reaction of nitrous acid on gelatin according to Chapman *et al.* (*1*) not only deaminized lysine but also affected other parts of the molecule as shown by the low dye-binding value after the reaction. This is in accordance with the decrease in the amount of arginine and histidine content of protein on deamination found by Skraup (*2*) and by Dunn and Lewis (*3*) and also with the report of Sekine (*4*) that the guanidine group of arginine is attacked with nitrous acid. Experiments by Fraenkel-Conrat and Cooper (*5*) showed that phthalic anhydride had almost the same affect as nitrous acid on the dye binding capacity of hoof powder. Further the anhydride of a dicarboxylic acid would leave a free carboxylic group which could form a zwitterion with the basic groups.

Chloroformic ester was selected for study since under mild conditions it forms substituted urethanes with amino groups of amino acids; and although it reacts with the imidazole group of histidine (*6*) the imidazole-*N*-carboxylate is basic (*7*) and the azolide would be readily hydrolized (*8*). Experiments have been carried out with fish meal in the first instance as lysine values are required as a measure of quality, and amino acid analyses were readily available. Reaction conditions have been designed to analyze this material, and modifications of practical detail may be necessary for other protein substances. The practical procedure in its present form is, for example, inapplicable to gelatin which solidifies on the addition of the buffer solution at 4 °C; and the sensitivity of the method could preclude its extension to protein material of very low lysine content. The method has been applied successfully to soya meal (Table IV and V), although a larger sample was used to operate at the sensitive part of our colorimeter scale. For all insoluble protein, fine grinding (80 to 100 mesh) is a prerequisite to allow intimate reaction of the reagents.

Table I. Amount of Dye (mg) Taken up by Defatted Fish Meal (120 mg) at pH 2.2 and 40 °C with and without Wetting Agent (Tween 80) for Different Times

Time, min	Without Tween	With Tween
5	16.0, 15.2	18.0, 20.4
10	20.0, 20.0	20.8, 22.4
15	24.8, 22.4	23.4, 23.6
20	24.0, 23.6	25.2, 24.8

Table II. Effect of Time and Temperature of the Reaction with Ethyl Chloroformate on Fish Meal at pH 8.5 on the Amount of Dye Taken up in 15 min at 40 °C and pH 2.2 (A undefatted, B defatted samples)

		Dye used up (mg/120 mg sample)		
Temp °C	Reaction time, min	A 1855	A 1856	A 1916
4	5	8.2	8.5	7.3
4	90	10.1	10.1	8.1
4	6 (hr)	10.0	10.1	8.3
10	5	9.8	9.8	8.2
20	5	10.2	10.3	8.7
50	5	10.5	10.6	8.7
		B		
4	0	12.0		
	5	10.6		
	15	10.6		
	30	10.0		
	60	9.8		
	240	10.6–12.0		
20	15	10.2		
	30	12.0		
	60	12.0		

(1) L. M. Chapman, D. M. Greenberg, and C. L. A. Schmidt, *J. Biol. Chem.*, **72**, 707 (1927).
(2) H. Skraup, *Monatsh. Chem.*, **27**, 631 (1906).
(3) M. S. Dunn and H. B. Lewis, *J. Biol. Chem.*, **49**, 327 (1929).
(4) H. Sekine quoted from *Chem. Abstr.*, **15**, 343 (1921).
(5) H. Fraenkel-Conrat and M. Cooper, *J. Biol. Chem.*: **154**, 239 (1944).
(6) H. J. Uhlig and P. Heitmann, *Acta Biol. Med. Germ.*, **28** (3), 431 (1972).
(7) W. John, *Ber.*, **68**, 2283 (1935).
(8) H. A. Staab, *Chem. Ber.*, **89**, 1927 (1956).

Table III. Concentration in mM/100 mg of Sample Derived from an Aminogram of a Sample of Fish Meal before (B) and after (A) Treatment with Ethyl Chloroformate

	Lysine	Histidine	Arginine
B	40.5	11.3	25.8
B	36.9	10.8	23.4
B	38.8	10.6	24.4
Average	38.7	10.9	24.5
A	41.1	13.3	24.6
A	39.9	12.2	23.8
A	36.4	7.1	22.2
A	37.5	7.8	22.5
Average	38.8	10.1	25.5

Simple amines, which do not form a precipitate with the dye, will not influence the determination. The end amino groups of the protein will behave similarly to the amino group of lysine; but the number is considered small relative to the number of lysine moieties in the protein under discussion. The end groups could be significant in proteins of smaller molecular weight ("solubles") which are sometimes added to fish protein before drying; but exploratory estimations with varying quantities of solubles did not show any significant differences.

EXPERIMENTAL

Dye Reagent. Recrystallized and analytically pure sodium salt of acid orange-12 (mol wt 350; 1.3 g) in 0.05*M* phosphate buffer (1 liter) was used.

Phosphate Buffer. Potassium dihydrogen phosphate (3.4 g), 85% phosphoric acid (1.7 ml), glacial acetic acid (60 ml), propionic acid (1 ml), and oxalic acid (2 g) and the solution were made up to 1 liter.

Carbonate Buffer. Anhydrous sodium carbonate in 8% sodium hydrogen carbonate to give pH 8.5 was used.

Reaction of Dye with Fish Meal Protein. A finely milled sample (80 to 100 mesh) of meal (120 mg) was moistened with 0.5*M* sodium hydroxide (1 ml). After 15 minutes, the reagent dye (40 ml) was added, the mixture stirred for 20 min at 40 °C and cooled. Hyflo Super cel filter aid (120 mg) was added, and the solution was filtered through glass wool filter paper. An aliquot of the filtrate (15 ml) was diluted with phosphate buffer (15 ml) and the concentration of dye determined on a Beckman Model C Colorimeter at 475 nm previously calibrated.

Reaction of Fish Meal with Ethyl Chloroformate and Then with Dye. Finely milled fish meal (120 mg) moistened with carbonate buffer (1 ml) was cooled to 0 to 4 °C and cooled ethyl chloroformate (0.5 ml) added. The reaction mixture was maintained at 0 to 4 °C with occasional stirring for 20 minutes. Phosphate buffer (20 ml) and then reagent dye solution (20 ml) were added and allowed to react at 40 °C for 20 minutes and the dye concentration determined as above.

RESULTS AND DISCUSSION

For the estimation to be satisfactory, the following conditions would have to be satisfied: (i) the dye binding capacity of the sample must be reproducible, (ii) the carbethoxylation with chloroformate must proceed at a reasonable rate to completion, (iii) the dye binding capacity of the sample and of the carbethoxylated sample must be complete under conditions which preclude hydrolysis of the latter, and (iv) the protein shall not be modified other than by forming a simple derivative with the reagent.

(i) *The rate of dye uptake* at pH 2.2 was slow at 20 °C compared with that at 40 °C at which temperature the reaction reached equilibrium between 15–20 minutes. The addition of a wetting agent accelerated the immediate uptake; but the overall reaction time was not changed (Table I). Accordingly, all measurements of dye binding were carried out for 20 minutes at pH 2.2 and 40 °C.

(ii) *The rate of reaction with ethyl chloroformate* with protein was studied under the condition of dye binding established in (i). Table II shows that at 4 °C, the reaction time of 20–40 minutes is sufficient to attain constancy; and this value remains unaltered for a further one hour. After four hours, there is some increase in dye uptake, less consistency in results, and the limiting value approaches that of the unacylated dye. This increase after the initial decrease is attributed to slow hydrolysis of the carbethoxy derivative. The reaction at room temperature attained the same value in 15 minutes, but did not remain constant.

(iii) The agreement between amount of dye bound and the histidine and arginine content is indicative of little hydrolysis of the carbethoxylated lysine (See Table IV).

(iv) The action of chloroformic ester on the fish meal cannot be more than one of simple substitution, removable on hydrolysis, since an aminogram of a sample of protein before and after treatment with ethyl chloroformate showed no significant difference (Table III).

The results obtained by dye binding and by aminogram analysis are shown in Table IV. There is a close agreement between the difference Δ in equivalent dye binding capaci-

Table IV. Comparison of Amount of Dye Bound at pH 2.2 and 40 °C for 20 Minutes of Different Fish Meals before and after Treatment with Ethyl Chloroformate at pH 8.5 and 4 °C for *t* minutes. Series A, undefatted meal, *t* = 5; Series B, defatted meal, *t* = 30

	Aminogram, mmol amino acids/120 mg sample					Dye bound, mmol dye/120 mg sample		
Sample	Lysine	Histidine	Arginine	LHA	HA	Fish meal	Acylated fish meal	Δ
A1745	44.4	15.6	22.8	83	38	91	47	44
1773	50.4	14.4	28.8	94	43	94	45	49
1820	40.8	12.0	22.8	76	35	83	43	40
1854	38.4	14.4	21.6	74	36	86	37	49
1880	40.8	10.8	19.2	71	30	83	44	39
Average	43	13	23	80	36	87	43	44
B17273	36.6	10.4	21.4	68.4	31.8	70	33	37
17677	35.6	10.0	20.3	65.9	30.3	67	29	38
17680	42.1	11.5	20.5	78.1	36.0	74	35	39
17681	38.8	10.8	24.1	73.6	34.8	70	36	34
17275	46.5	10.3	29.45	86.3	39.8	87	43	44
Average	40.0	10.6	23.1	74.5	34.5	73.6	37.1	38
	mmol amino acids/150 mg sample					mmol dye/150 mg sample		
B Soya meal	30.1	12.7	29.3	72.1	42.0	74.3	41.1	33
B Cashew	17.1	7.8	33.9	58.8	41.7	65.1	42.9	22

Table V. Amount of Lysine in a Sample of Fish Meal Compared with the Difference in Amount of Dye Bound (Calculated as Lysine) by Untreated and Treated (Chloroformate) Fish Meal

Sample	Lysine, %, aminogram	Carpenter, 'available' lysine, %		Differential dye binding, calcd as lysine, %
		Found	Corrected × 1.14	
A1745	5.3	5.1	5.8	5.3
1773	6.0	5.1	5.8	5.9
1820	4.9	3.9	4.5	4.8
1854	4.6	5.6	6.4	5.9
1880	4.9	3.5	4.0	4.7
Average	5.1	4.6	5.3	5.3
B17273	4.4	4.1	4.6	4.4
17677	4.3	4.5	5.1	4.7
17680	5.0	4.2	4.8	4.7
17681	4.7	3.8	4.3	4.0
17275	5.6	3.8	4.3	5.5
Average	4.8	4.1	4.6	4.7
Overall average	4.95	4.35	4.95	5.0
B Soya meal	3.0	...	...	3.1
B Cashew	1.6	...	...	2.2

ty (EDBC) for fish meal protein before and after treatment with ethyl chloroformate and the molar quantity of lysine in the sample. The EDBC of the untreated and treated fish meal approximates to the total equivalents of the three basic amino acids (LHA) and of histidine and arginine (HA), respectively. The variation is attributed to other dye-binding capacities in the particular sample of fish meal.

CONCLUSION

The difference in the amount of dye bound, calculated as lysine, for different fish meals, and for a sample of soya meal, before and after treatment with ethyl chloroformate is shown in relation to the amount of lysine in the sample, determined by amino acid analysis and the "available" lysine by Carpenter's method (*9*) without correction and with correction (*10*) in Table V. The agreement would indicate the use of differential dye binding capacity for the routine determination of lysine as being quicker and simpler than the elegant Carpenter's method or aminogram analysis.

ACKNOWLEDGMENT

The authors thank O. A. M. Lewis (Department of Botany, U.C.T.) for all aminograms and I. M. Moodie for lysine determinations by Carpenter's method; the Director, FIRI, for permission to publish these results; and the C.S.I.R. for financial assistance.

RECEIVED for review September 24, 1973. Accepted April 23, 1974.

(9) K. J. Carpenter, *Biochem.*, **77**, 604 (1960).
(10) I. M. Moodie, *Fishing Ind. Res. Inst., Annu. Rep.*, **24**, 23 (1970).

Evaluation of an Ozone Photometer for Ambient Ozone Measurements

Leo Zafonte, William Long, and James N. Pitts, Jr.[1]

Statewide Air Pollution Research Center, University of California—Riverside, Riverside, Calif. 92502

Recent emphasis on the development of new analytical techniques for environmental quality studies has resulted in the development of new analytical techniques for the atmospheric monitoring of ozone. Noted developments in this area were the uses of the ultraviolet absorption (*1*) and the ethylene chemiluminescent (*2*) and the nitric oxide chemiluminescent techniques (*3, 4*). In the course of investigations at the Statewide Air Pollution Research Center, the Dasibi Environmental Model 1003A ozone photometer was evaluated for use as a routine airborne, atmospheric monitor. This report gives the results of several testing procedures which were used to determine the instrumental response, calibration, and linearity. A complete description of the actual experimental results obtained by the use of the instrument in an airborne monitoring program can be found elsewhere (*5*).

EXPERIMENTAL

The Model 1003A ozone photometer (Dasibi Environmental Corp., Glendale, Calif.) used in these tests is a self-contained unit with a digital readout whose operation is based upon the physical measurement of the absorption of ultraviolet light at 2537Å by ozone in a single absorption chamber 14 inches long. This particular unit was of special manufacture for operation on small aircraft. The modifications included a sample flow rate increase to 2.7 liters per minute, higher than the standard flow rate of 1.0 liter/minute, in order to accommodate a faster measurement time. The optical bench was strengthened by the manufacturer to minimize possible susceptibility to vibration, and the circuit boards were held in place with detents to minimize slippage. Also, the absorption cell is approximately one half the length of those in units currently being produced. In other respects, this unit was identical to the standard version.

[1] Author to whom correspondence should be addressed.

(1) Lloyd D. Bowman and Richard F. Horak, "A Continuous Ultraviolet Absorption Ozone Photometer," Paper No. 7430. Presented at the Meeting of the Instrumentation Society of America, May 1972, pp 103–108.
(2) Gary J. Warren and Gordon Babcock, *Rev. Sci. Instrum.*, **41**, 280 (1970).
(3) Donald H. Stedman, Eric E. Daby, Fredrick Stuhl, and Hiromi Niki, *Air Pollut. Contr. Ass.*, **22**, 260 (1972).
(4) Arthur Fontijn, Alberto J. Sabadell, and Richard J. Ronco, *Anal. Chem.*, **42**, 575 (1970).
(5) Hermilo R. Gloria, James N. Pitts, Jr., Joseph V. Behar, Gary E. Bradburn, and Leo Zafonte, "Airborne Measurement of Air Pollution Chemistry and Transport. I. Initial Survey of Major Air Basins in California, Report No. 1," The Statewide Air Pollution Research Center, University of California, Riverside, Calif. 92502.

Ozone measurements with this instrument are updated every 11 seconds and are based on two half-cycle (5.5 seconds each) integration periods. During the first or reference half-cycle, atmospheric air is first passed through a catalytic scrubber to remove ozone before entering the light chamber. The scrubber consists of manganese dioxide coated on an open structure to minimize pressure drop and particulate collection. At this high flow rate, the cell is purged of previously contained gases within three seconds, after which a digital light intensity measurement is made over a total integration period of approximately one second. This integration time is accurately determined with a quartz crystal frequency source and retained in memory for the second half-cycle.

The accuracy of this instrument calibration is dependent on a calibration count for the reference light measurement, which is determined by the potassium iodide technique. It should be noted that the reference integration interval is varied in such a way as to reproduce automatically the same total integrated light measurement in each reference half-cycle. Therefore, the ozone calibration remains constant and linear at all times, depending only on the selectivity of the ozone scrubber.

During the second or measurement half-cycle, the atmospheric air containing ozone is passed directly into the light chamber. After purging the cell of deozonized air from the previous half-cycle, a light measurement is made by integrating the intensity over precisely the same time period established during the first half-cycle and is retained in memory. Assuming ozone to be the only gas removed by the scrubber, the difference in the light intensity measurement can be related by Beer's law to the ozone concentration because the integration times during both the reference and the measurement half-cycles are identical. In this manner, long term perturbations (greater than 11 seconds) such as light intensity variations due to source fluctuations, window solarization, and Rayleigh scattering are cancelled out in the digital subtraction process.

At the fractional change in light measurements obtained by this technique (10^{-3} to 10^{-6}), the Beer–Lambert law can be expressed in a linear fashion to a close approximation. Thus, ozone measurements are expected to be linear with concentration as an inherent feature of this technique.

RESULTS AND DISCUSSIONS

Calibration Accuracy and Linearity. The instrument was calibrated for accuracy using the standard potassium iodide technique. The instrument was in operation for at least one hour prior to the calibration and was often running overnight. Figure 1 gives the cumulative results of several calibrations which were run over a period of several months. The solid circles indicate the points which were verified against potassium iodide (a primary calibration) while the open circles give the comparative determinations by the Dasibi ozone monitor and a Mast ozone meter which were simultaneously sampling a stream of ozone (a secondary calibration). In this case, the Mast ozone meter was a bench unit routinely kept in good operating condition for such secondary calibration checks. Because of drift characteristics of the ozone source, the reliability of each calibration is 0.02 ppm.

For comparison to the data, the solid line in Figure 1 has a slope of 1.00. The best fitted linear function to these data has a slope of 1.016 ± 0.017. These results indicate that the calibration accuracy is within the manufacturer's specifications. The standard error in the slope of ±0.017 we feel to be very good in view of the fact that two different calibration techniques were used on several occasions over a long period of time. We feel that this error is due to differences in calibration technique rather than to nonlinearity in the actual measurement.

Response Time. The unit was tested for its response to a step ozone input in the following manner. An ozone calibrator (Model 1505, Dasibi Environmental, Inc.) was placed on the input line within two inches of the inlet port. The UV lamp in the calibrator was turned on and permitted to stabilize for 30 min with the instrument in operation. After the warm-up period, the adjustable sleeve around the photolysis lamp within the calibrator was closed and the ozone reading was observed to decrease to zero. In each test, the sleeve was quickly adjusted to an arbitrary setting at the start of the 11-second measurement period (as indicated by the light on the front panel of the instrument) and the data given in Table I below were recorded at each 11-second interval. The data indicate that the instrument had an average response of 98% within one measurement period (11 seconds) to the step ozone input. During four of the tests, the instrument response was 98% or better while the fifth test (No. 4, Table I) indicated response of 94% during this period. Further testing showed the pen-ray lamp on the ozone source to be temperature sensitive, and that ozone equilibrium was not immediately established at the time the sleeve around the quartz tube (on the calibrator) was withdrawn. Therefore, this lower response factor is most probably the result of the testing procedure rather than an instrumental characteristic.

Because of the two-step measurement technique used in this instrument, it is not practical to define an instrument response time; more properly, the term delay time should be used. The data in Table I indicate that the delay time is a maximum of 11 seconds for 98% response. However, in actual practice, the difference between the time of the ozone measurement and its display is only 1–2 seconds because the measurement time falls within the later half-cycle operational mode. This time will vary only slightly because the integration time varies only slightly with each measurement and, therefore, it need not be considered for routine ground-based monitoring where changes over a period of several minutes are of interest. In airborne monitoring, however, the delay time must be known for each instrument for accurate work.

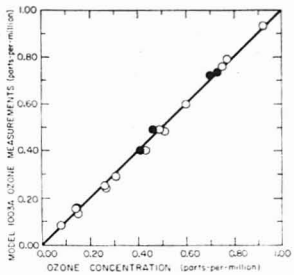


Figure 1. Calibration data for the Dasibi Environmental Model 1003A ozone photometer

(●) indicates the primary calibration points (KI Technique); (O) indicates the secondary calibration points utilizing a calibrated Mast ozone meter. A linear least squares treatment of the data points yielded a fitted slope of 1.016 ± 0.017 and an intercept of −0.005 ppm

Table I. Dasibi Model 1003A Response to a Step Ozone Input

Time, sec	Test 1	Test 2	Test 3	Test 4	Test 5	Av response, %
0	0.0	0.0	0.0	0.0	0.0	00.0
11	0.043	0.134	0.370	0.618	0.633	98.3
22	0.043	0.139	0.372	0.634	0.637	99.8
33	0.043	0.137	0.371	0.634	0.636	99.5
44	0.044	0.143	0.373	0.632	0.637	100.6
55	0.042	0.141	0.373	0.634	0.635	99.7
66	0.043	0.141	0.373	0.631	0.637	99.9
77	0.044	0.142	0.373	0.633	0.635	100.6
88	0.044	0.142	0.373	0.630	0.636	100.4

Maintenance. In the course of our studies, relatively little maintenance was required to keep the instrument in calibration. The long-path cell was periodically cleaned with ethanol each month during use to minimize ozone losses within the cell, a ten-minute operation. This procedure had no effect on the calibration and served to increase the light intensity reaching the detector and thus to reduce the integration period. Because an ultraviolet absorption technique is used, no accessory gases or solutions were required and the calibration was independent of small changes in the atmospheric gas flow rate. The ozone scrubber should be periodically changed as recommended by the manufacturer to eliminate the possibility for low ozone readings.

Airborne Operation. In airborne use, two important factors which must be overcome are aircraft vibration and tilt for noise-free and effective operation. With liquid-based measurement techniques, these factors tend to disrupt the flow of the measuring liquid and may cause noise excursions on the output recorder. Under the operating environment of a twin-engine aircraft (Cessna 401), this instrument has proved itself to be insensitive to these factors except during severe turbulence after which recovery was observed to occur in one 11-second measurement period. At a ground speed of 180 mph, the ozone measurements are integrated over a distance of 0.05 mile, with new readings every 0.5 mile.

Based on studies at ambient concentrations, there were no apparent interferences due to nitrogen dioxide, hydrocarbons, or sulfur dioxide. Possible interference would depend upon such factors as the value of the absorption and scattering cross sections at 2537Å and the selectivity of the ozone scrubber. The sample intake was located in the aircraft nose approximately four feet in front of the propeller plane to eliminate exhaust-hydrocarbon interferences, and no further interferences were observed in the course of our studies. The general agreement of the Model 1003 ozone measurements and the Mast total oxidants meter during each flight indicates that the levels of photochemically generated aerosols which were encountered did not introduce an observable change in the ozone reading. On one occasion an O_3–ethylene chemiluminescent monitor was flown with the Model 1003, and readings of both instruments were generally in agreement within 0.01 ppm of ozone at the low ozone concentrations that were encountered.

CONCLUSIONS

Based on the data presented in this report, the following conclusions can be made. The accuracy, repeatability and linearity of the ultraviolet absorption technique are satisfactory for atmospheric monitoring. The unit responded to within 98% of the step ozone input within one measurement period (11 seconds). The instrument proved itself to be sufficiently rugged and reliable for routine airborne operation. The use of the ultraviolet absorption technique results in a lower maintenance requirement as compared to liquid techniques for ozone measurement and either a comparable or lower maintenance requirement as compared to ethylene chemiluminescent techniques.

ACKNOWLEDGMENT

The authors express their appreciation to the Ames Research Center of the National Aeronautics and Space Administration and, particularly, to Hermilo R. Gloria of NASA for the opportunity to evaluate this instrument during airborne operation.

RECEIVED for review December 26, 1973. Accepted May 20, 1974. Specific reference to brand names of instruments does not imply endorsement by the University of California Statewide Air Pollution Research Center at Riverside.

CORRESPONDENCE

Beryllium Content of NBS Standard Reference Orchard Leaves

Sir: A recent paper (*1*) indicated the presence of volatile beryllium compounds in National Bureau of Standards Orchard Leaves (SRM 1571), and in air samples taken from a beryllium machining facility. Samples of Orchard Leaves digested with nitric and sulfuric acids in an open beaker, or dry-ashed in an oxygen plasma furnace at 150 °C, gave only 16% and 7%, respectively, of the beryllium content found when the leaves were digested under reflux with nitric and sulfuric acids (0.11 ± 0.01 ppm Be). Relatively large amounts of beryllium were detected in a Dry Ice cold trap inserted between the plasma furnace and the vacuum pump. The analytical method used involved gas chromatographic measurement of the beryllium trifluoroacetylacetone complex extracted into benzene.

This report (*1*) contained several surprising results. Among these was the observation that volatile beryllium compounds were present both in Orchard Leaves and in air samples taken from a beryllium machining factory. Also, the volatile beryllium compound detected in Orchard Leaves was so inert that it distilled from concentrated mineral acid mixtures, yet apparently underwent complete chemical exchange with trifluoroacetylacetone (Htfa) when shaken for 15 min with a benzene solution of Htfa. This type of behavior is certainly unusual, and is not shown by any known beryllium compound (*2, 3*). For example, the beryllium complexes of acetylacetone and its fluorinated derivatives are very volatile and thermally stable, yet they are readily wet-ashed in an open beaker without any loss of beryllium (*4–6*).

Over the past ten years, a very large number of environmental samples have been analyzed for beryllium in our laboratory, after either wet-ashing in open beakers or dry-ashing at temperatures up to 800 °C (*7*). If undetected

(1) M. S. Black and R. E. Sievers, *Anal. Chem.*, **45**, 1773 (1973).

(2) L. E. Smythe and T. M. Florence, "Recent Advances in the Analytical Chemistry of Beryllium," in "Progress in Nuclear Energy," C. E. Crouthamel, Ed., Series IX, Vol. 3, part 6, Pegamon Press, New York, N.Y., 1963.

(3) D. A. Everest, "The Chemistry of Beryllium," Elsevier, Amsterdam, 1964.

(4) J. D. Cosgrove, J. Morgan, and P. Pakalns, *Australian At. Energy Comm. Rept.* **AAEC/TM 87** (1961).

(5) C. W. Sill and C. P. Willis, *Anal. Chem.*, **31**, 598 (1959).

(6) J. K. Foreman, T. A. Gough, and E. A. Walker, *Analyst (London)*, **95**, 797 (1970).

(7) W. R. Meehan and L. E. Smythe, *Environ. Sci. Technol.*, **1**, 839 (1967).

volatile beryllium compounds are indeed present in most environmental materials, our results would be invalid. Black and Sievers' paper also raises serious questions about health and safety aspects of the handling of beryllium and its compounds. We therefore set out to carefully check the beryllium content of NBS Orchard Leaves.

EXPERIMENTAL

Ashing Procedures. Samples of NBS Orchard Leaves (5 grams), taken directly from a freshly opened bottle, were ashed by the following methods:

(*a*) Dry ashing in platinum dishes in an air muffle at temperatures of 450, 600, or 800 °C for a period of 6 hours. The ash was dissolved in 50 ml of 10*M* HCl and 20 ml of 72% $HClO_4$, then fumed. The $HClO_4$ was diluted, 2.5 ml of 9*M* H_2SO_4 added, and the solution filtered through a No. 41 Whatman paper. The filtrate and residue were analyzed for beryllium by fluorimetry.

(*b*) Wet ashing in an open 250-ml beaker with 55 ml of 15*M* HNO_3 and 15 ml of 18*M* H_2SO_4, as described by Black and Sievers (*1*). After oxidation was complete, the solution was diluted and filtered. The small siliceous residue was washed, then the paper and precipitate ashed in a platinum dish over a gas burner. The residue was treated with HF + $HClO_4$, taken to fumes of $HClO_4$, then diluted. The original filtrate and solution of the residue were analyzed for beryllium.

(*c*) Wet digestion in a 250-ml flask fitted with a 50-cm reflux condenser, using HNO_3 + H_2SO_4 and the procedure described by Black and Sievers (*1*). After 4 hr of reflux, the digestion did not appear to be complete; traces of oil could be seen floating on the surface and emulsified with the acids. Additional digestion under reflux gave no improvement, and complete destruction of organic matter was achieved only after the refluxed solution was transferred to a beaker and taken to fumes of H_2SO_4 with occasional additions of HNO_3 to prevent charring. The residual H_2SO_4 was diluted, filtered, and analysed as described in (*b*).

(*d*) Wet digestion under complete reflux with a Gorsuch apparatus. An all-glass Gorsuch apparatus (*8*), consisting of a 250-ml round-bottomed flask, a 50-ml reservoir above the flask, and a 40-cm reflux condenser, was used to achieve complete destruction of the Orchard Leaves under total reflux. A 2-way tap between the flask and reservoir allowed the distillate to either return to the flask, be collected in the reservoir, or be run off to a separate receiver. The Gorsuch apparatus has been used successfully for the wet ashing of volatile complexes of mercury and selenium (*8*). A 5-gram portion of Orchard Leaves was digested in this apparatus for 4 hr using the same conditions as in (*c*). A thermometer positioned just above the liquid surface showed that a maximum temperature of 125 °C was reached while refluxing. After 4 hr, the tap was closed so that the nitric acid distillate collected in the reservoir. When all the nitric acid had been distilled from the flask and collected, it was run off into a beaker and reserved for analysis. The temperature was raised until the sulfuric acid fumed and destruction of organic matter was complete. A few small additions of nitric acid were made down the condenser to prevent charring. The small volume of distillate which collected in the reservoir during this final operation was added to the nitric acid previously collected. The nitric and sulfuric acid fractions were then analyzed separately for beryllium.

(*e*) Wet digestion under complete reflux with a Gorsuch apparatus connected to a Dry Ice cold trap. The experiment described in (*d*) was repeated, but an all-glass lead-off tube was connected to the top of the reflux condenser via a B29 joint, and led to a 3-cm × 3-cm diam. glass trap immersed in a beaker of powdered Dry Ice. The trap was in position throughout the heating period and, at the end of the experiment, both it and the lead-off tube were rinsed with 6*M* HNO_3 to dissolve any volatile beryllium compounds collected (*1*). This solution was analyzed for beryllium along with the two other acid fractions.

Fluorimetric Analysis. Beryllium was determined by the well-known morin fluorimetric method (*4, 5*). The beryllium acetylacetonate complex was extracted with chloroform in the presence of EDTA to mask interfering metals. After destruction of the beryllium complex by fuming with HNO_3 + $HClO_4$ + H_2SO_4, the beryllium–morin complex was formed and measured fluorimetrically. A Perkin-Elmer Model 203 fluorescence spectrophotometer was used with an excitation wavelength of 365 nm and an analyzer wavelength of 518 nm. The beryllium calibration curve was linear from zero to at least 1 μg Be per 50 ml of final solution. Blanks were carried through the entire analytical procedures. Beryllium spikes were added to 5-gram portions of Orchard Leaves at the start of analysis to determine overall per cent recovery.

Emission Spectrographic Analysis. Emission spectrography was used in an attempt to detect volatile beryllium compounds in Orchard Leaves, and to provide an independent method for the determination of total beryllium content.

In the first series of experiments, samples of Orchard Leaves were arced directly, and compared with beryllium-in-graphite standards (Spex G standards), which contained 0.01 to 1 ppm Be. The spectrographic conditions were as follows: spectrograph, 3.4-m plane grating Ebert (Jarrell-Ash); grating angle, 9.45°; reciprocal linear dispersion, 2.5 Å/mm; slit, 2 × 0.02 mm; gap, 4 mm; source, 10 A dc arc; anode, sample, shallow crater electrode similar to National type L4031; cathode, 60° pointed 6.15-mm diam. rod, National SPK grade; emulsion, Kodak SA3; development, 4 min Kodak D-19, 4-min fix.

In the second series of experiments, 20-mg portions of Orchard Leaves were loaded into the bottom of deep crater electrodes, and a boiler cap (*9*) fitted. The electrodes had thermocouple leads sealed into the wall just above the charge so that its temperature could be measured during arcing. Two charge temperatures, 400 and 200 °C, were achieved by using 4.75-mm i.d. electrodes which were 19 mm and 35 mm deep, respectively. The samples were arced at 10 A, and moving plate spectra recorded for each 10 sec of a 60-sec exposure, using the same conditions as in the first series of experiments but with a 0.03-mm slit. Any volatile beryllium compounds from the sample would have to emerge through the hole in the boiler cap and enter the plasma. To prove that a volatile beryllium compound would be detected by the boiler cap electrode technique, 20-mg portions of graphite were weighed into the deep crater electrodes and spiked with aliquots of a solution of beryllium acetylacetonate in chloroform. Beryllium was easily detected at both 200 and 400 °C, and a limit of detection of 5×10^{-4} μg Be was estimated. With a 20-mg sample charge, this corresponds to a limit of detection of 0.025 ppm volatile beryllium in the sample.

Gas Chromatography. A 5-gram portion of Orchard Leaves was refluxed for 4 hr with HNO_3 + H_2SO_4 as described by Black and Sievers (*1*). The solution was diluted to 100-ml, and 10-ml aliquots taken for extraction with Htfa. The extractions were carried out exactly as recommended by Black and Sievers. The Pierce Chemical Co. Htfa was vacuum distilled before use because it was found that the as-received Htfa gave large interfering chromatographic peaks. Pure $Be(tfa)_2$ was synthesized from the distilled ligand (theor., 2.86% Be; found, 2.76% Be) and solutions of the complex were prepared in benzene in order to calibrate the gas chromatograph. The chromatograph used was a Hewlett-Packard Model 5750 equipped with a ^{63}Ni source electron capture detector. The column, support, stationary phase, and temperatures were identical to those used by Black and Sievers (*1*), but the carrier gas was 4%, rather than 10%, CH_4 in Ar, with a flow rate of 42 ml/min.

RESULTS AND DISCUSSION

The fluorimetric results, corrected for moisture content determined on a separate sample, are shown in Table I. There was no significant difference between the results obtained using a wide variety of dry ashing and wet ashing procedures. The mean result for acid soluble beryllium of 0.0213 ± 0.0035 ppm Be (1 σ) in NBS Standard Reference Orchard Leaves (dry basis) is similar to the figure of 0.017 ± 0.003 ppm Be found by Black and Sievers when the sample was digested in an open beaker. Our observation that no beryllium is lost by muffle ashing at temperatures as high as 800 °C was not unexpected, because the most likely product of the dry ashing of an organic beryllium compound is the highly refractory oxide, BeO (*2*). No beryllium was detected in the nitric acid distillates using the Gorsuch apparatus, or in the dry ice trap leading from the condenser.

Emission spectrographic analysis with a shallow crater

(8) T. T. Gorsuch, *Analyst (London)*, **84**, 135 (1959).

(9) G. H. Morrison, Ed., "Trace Analysis," Interscience, New York, N.Y., 1965.

Table I. Beryllium in NBS Orchard Leaves

Ashing procedure	Be in Orchard Leaves, ppm[a,b]	Recovery of spike, %[c]
(*a*) Dry ashing, 450 °C	0.019, 0.019[d]	101
600 °C	0.017[e]	
800 °C	0.023, 0.027	
siliceous residue	0.008	
(*b*) Open beaker, $HNO_3 + H_2SO_4$	0.027, 0.025, 0.018, 0.020	94, 95
siliceous residue	0.009, 0.009	
method blank	<0.002[f]	
(*c*) Refluxed with $HNO_3 + H_2SO_4$ for 4 hr, then fumed in open beaker	0.019	
(*d*) Gorsuch apparatus, $HNO_3 + H_2SO_4$		
HNO_3	<0.002	
H_2SO_4	0.020	
(*e*) Gorsuch apparatus with dry ice trap, $HNO_3 + H_2SO_4$		
HNO_3	<0.002, <0.002[g]	
H_2SO_4	0.021, 0.022[g]	95
trap	<0.002, <0.002[g]	

[a] Results are for separate 5-gram weighings, and have been corrected for moisture content of 5.9% (24 hr at 90 °C). [b] Results do not include Be in siliceous residue. [c] 0.5 μg Be spike added at start of analysis. [d] Ash = 9.6%. [e] Ash = 7.2%. [f] Limit of detection. [g] These three results were obtained on a second sample of Orchard Leaves received from NBS 6 months after the first sample.

electrode gave a limit of detection of 0.02 ppm Be using graphite standards. No beryllium could be dectected in the Orchard Leaves by this technique. To check the unlikely possibility that beryllium compounds were present which were so volatile that they escaped the plasma, the sample was also analyzed using a deep crater electrode fitted with a boiler cap. Again, no beryllium was detected in Orchard Leaves and, by comparison with beryllium acetylacetonate standards, it was concluded that the content of volatile beryllium compounds must be less than 0.025 ppm Be.

Gas chromatographic analysis of pure solutions of $Be(tfa)_2$ in benzene gave well-defined peaks with a retention time of 4.9 min. However, we were unable to determine beryllium in the Orchard Leaves extracts because of the presence of very large interfering peaks which occurred close to the beryllium peak. These interfering peaks were not present in blanks or standards carried through the same analytical procedure, and appear to result from the extraction of some of the undestroyed organic matter which is still visibly present after prolonged refluxing of Orchard Leaves with nitric and sulfuric acids.

As a result of our fluorimetric and emission spectrographic studies, we have concluded that NBS Standard Reference Orchard Leaves has a total beryllium content (acid soluble + siliceous residue) of 0.030 ± 0.004 ppm Be (dry basis) and that the sample contains no beryllium compounds which are volatile below 800 °C. Two separate sample bottles of Orchard Leaves, received six months apart, were analyzed for beryllium and no significant difference was found (Table I). The high results obtained in the earlier study (*1*), and the identification of very volatile beryllium compounds in Orchard Leaves, may have been due to undestroyed organic matter interfering with the gas chromatographic measurement technique.

ACKNOWLEDGMENT

We would like to thank S. Dilli of the University of New South Wales for providing the gas chromatograph facilities.

T. M. Florence
Yvonne J. Farrar
L.S. Dale
G. E. Batley

Chemical Technology Division
Australian Atomic Energy Commission Research Establishment
Lucas Heights, New South Wales, Australia

RECEIVED for review December 4, 1973. Accepted April 8, 1974.

Comments on Ratio Matching

Sir: Anders (*1*) proposed a new statistical method for discovering the generic relationship among samples. Though intuitively appealing, the ratio matching technique for discovering the generic relationship among samples suffers from lack of logic foundation and mathematical consistency. In this paper, the method is reviewed and then criticized. Techniques for analyzing this kind of data are also suggested.

The method can well be explained by his own example. Suppose we have two sets of sediment samples; one from a Michigan waterway (sample A) and the other from a California waterway (sample B). Each sample consists of concentrations of eight chemical elements As, Sb, Cu, Zn, Au, Cd, Hg, and Cr. The concentration ratios "x_{ij}" for a sample are formed by dividing the concentration of each element by that of some other elements. That is,

(1) O. U. Anders, *Anal. Chem.*, **44**, 1930 (1972).

$$\{x_{ij}\}_A =$$

$$\begin{bmatrix} (As/As)_A & & & \\ (Sb/As)_A & (Sb/Sb)_A & & \\ (Cu/As)_A & (Cu/Sb)_A & (Cu/Cu)_A & \\ (Zn/As)_A & (Zn/Sb)_A & (Zn/Cu)_A & \\ (Au/As)_A & (Au/Sb)_A & (Au/Cu)_A & \\ (Cd/As)_A & \cdots\cdots\cdots\cdots\cdots\cdots & & \\ (Hg/As)_A & & & \\ (Cr/As)_A & & & Cr/Cr)_A \end{bmatrix}$$

Similarly, the concentration ratio matrix for the sample B can be formed.

The comparison of the ratios obtained for two samples A and B can be carried out by forming the ratio of the ratio of two ratio matrices. That is,

$$\{y_{ij}(AB)\} =$$

$$\begin{bmatrix} \dfrac{(As/As)_A}{(As/As)_B} & & \\ \dfrac{(Sb/As)_A}{(Sb/As)_B} & \dfrac{(Sb/Sb)_A}{(Sb/Sb)_B} & \\ \dfrac{(Cu/As)_A}{(Cu/As)_B} & \dfrac{(Cu/Sb)_A}{(Cu/Sb)_B} & \dfrac{(Cu/Cu)_A}{(Cu/Cu)_B} \\ \cdot\quad\cdots\cdots\cdots & \cdots\cdots\cdots & \cdots\cdots\cdots\cdots\cdots \end{bmatrix}$$

To find the correlation between sample A and sample B, Anders suggested the following criterion. Compute the proportion of non-diagonal components $y_{ij}(AB)$ lying in the interval (M^{-1}, M) where M is an arbitrarily selected constant. This proportion is denoted by Z_{AB} and is called correlation number of samples A and B. If Z_{AB} is large, then sample A and B are announced generically related; otherwise they are considered genericqally unrelated.

In his original example, Anders took 80 samples from a Michigan waterway and 11 samples from a California waterway. Based on these samples, he constructed empirical distribution functions for correlation numbers of different types, and subsequently he used these distributions functions to assert the statistical significance of the correlation between two samples of a given type.

Several samples may be simultaneously computed and tested using Anders' method. For instance, if we have three samples, A, B, and C, then we have a correlation matrix

$$\{Z_{kl}\} = \begin{bmatrix} 1 & & \\ Z_{AB} & 1 & \\ Z_{AC} & Z_{BC} & 1 \end{bmatrix}$$

COMMENTS ON RATIO MATCHING TECHNIQUE

Intuitively, the ratio matching appears reasonable because if two samples are generically related, then y_{ij} should be close to 1. Implicitly he assumes there is an unknown variable Y_{ij} which has some probability distribution with a mean equal to 1. The computed y_{ij}'s are random samples for the variable Y_{ij}. In spite of its intuitive attraction, the method suffers from lack of logic foundation and mathematical consistency.

1. Having only eight concentrations in a sample, we subsequently reproduce 28 ratios which are to be used for constructing a statistical test. It is conceivable, that if this kind of combination were allowed, we could have infinitely many ratios by choosing different methods of combination. In fact, if we denote eight concentrations by $(x_1, x_2, x_3, \ldots, x_8)$, then there are infinitely many ways to define a function $f(x_1, x_2, \ldots, x_8)$. For instance, if we define $f_{21}(x_1, x_2, \ldots, x_8) = x_2/x_1 = x_{21}$ etc., then we have the ratio matching proposed by Anders. However, there is no reason that we have to restrict ourselves to simple ratios.

2. For the example of eight concentrations, out of 28 ratios there are 7 ratios with As as denominator, 6 ratios with Sb as denominator, 5 ratios with Cu as denominator, 4 ratios with Zn as the denominator, 3 ratios with Au as denominator, 2 ratios with Cd as denominator, 1 ratio with Hg as denominator and none with Cr as denominator. If these chemical elements are rearranged in a different order, then we have a different set of ratios which in turn generate a different correlation number between two samples. In Anders' example 1, if the order is As, Sb, Cu, Zn, Au, Hg, and Cr, then correlation numbers among three samples (for $M = 1.3$) are

	A	B	C
A	1		
B	0.11	1	
C	0.32	0.54	1

If the order is Hg, Cr, As, Au, Sb, Cd, Zn, and Cu, then correlation numbers among the three samples are

	A	B	C
A	1		
B	0.11	1	
C	0.21	0.54	1

There are 40,320 possible order arrangements for eight chemical elements and thus the same number of correlation matrices exists. This lack of consistency is a serious shortcoming of the ratio matching.

3. For the matching criterion (M^{-1}, M) to be logical, y_{ij}'s must be independently and identically distributed. This is clearly not attainable since two ratios with the same denominator are usually correlated even if two numerators are not correlated. In particular, they are positively correlated if concentrations involved in the ratios are uncorrelated (see Appendix).

4. It is illogical to assert the statistical significance level by using the distribution function constructed from a set of samples while the same set of samples is to be used in the statistical test.

CONCLUDING REMARKS

For the sediment experiment considered by Anders, we can take eight concentrations $(x_1, x_2, \ldots, x_8)$ as a vector observation from a certain multivariate population. As indicated in Anders' paper, several authors have pointed out that the ratios of the concentrations of elements in two samples lend themselves better than the concentrations themselves to establish their common origin. Alternatively, we can consider $(y_1, y_2, \ldots, y_8)$, where $y_i = x_i/\Sigma x_j$, as an ob-

servation from a multivariate population. To discover the generic relationship between two geographical locations, replicate samples at each location should be taken. Then the problem becomes one of the statistical classification analyses. More specifically, it is the subject clustering (not attribute clustering) as described by Green, Frank, and Robinson (*2*). An excellent review article of classification is by Cormack (*3*). It seems worthwhile to mention that one of the techniques is to apply factor analysis on subjects (locations). Factor analysis on attributes have been used by several chemists (*4*).

APPENDIX

Let X, Y, and Z be three uncorrelated random variables with means μ_x, μ_y, μ_z and variances σ_x^2, σ_y^2, σ_z^2. We shall show the following theorem.

Theorem. Correlation between two ratios Y/X and Z/X is given by

$$\frac{\mu_y\mu_z\sigma_x^2}{[(\mu_y^2\sigma_x^2 + \mu_x^2\sigma_y^2)(\mu_z^2\sigma_x^2 + \mu_x^2\sigma_z^2)]^{1/2}}$$

Proof: Let $dx = (x - \mu_x)/\mu_x$ and similarly defined for dy and dz. Then

$$Y/X = (\mu_y/\mu_x)(1 + dy)/(1 + dx)$$

$$= (\mu_y/\mu_x)(1 + dy)(1 - dx + (dx)^2 + \ldots)$$

Similarly,

$$Z/X = (\mu_z/\mu_x)(1 + dz)/(1 + dx)$$

$$= (\mu_z/\mu_x)(1 + dz)(1 - dx + (dx)^2 + \ldots)$$

Taking expectation and retaining only the first and second moments, we have

$$\mathrm{Cov}(Y/X, Z/X) = E(Y/X \cdot Z/X) - E(Y/X)E(Z/X)$$

$$= (\mu_y\mu_z/\mu_x^2)(\sigma_x^2/\mu_x^2)$$

$$\mathrm{Var}(Y/X) = E[(Y/X)^2] - [E(Y/X)]^2$$

$$= (\mu_y^2/\mu_x^2)(\sigma_x^2/\mu_x^2 + \sigma_y^2/\mu_y^2)$$

and

$$\mathrm{Var}(Z/X) = E(Z/X)^2] - [E(Z/X)]^2$$

$$= (\mu_z^2/\mu_x^2)(\sigma_x^2/\mu_x^2 + \sigma_z^2/\mu_z^2)$$

Thus

$$\mathrm{Corr}(Y/X, Z/X) = \frac{\mu_y\mu_z\sigma_x^2}{[(\mu_y^2\sigma_x^2 + \mu_x^2\sigma_y^2)(\mu_z^2\sigma_x^2 + \mu_x^2\sigma_z^2)]^{1/2}}$$

C. W. Chen

Mathematics Department
University of Maine at Orono
Orono, Me. 04473

RECEIVED for review January 21, 1974. Accepted July 8, 1974.

(2) B. E. Green, R. E. Frank, and P. J. Robinson, *Management Sci.*, **13**, 387 (1967).
(3) R. M. Cormack, *Roy. Stat. Soc. A*, **134**, 321 (1971).
(4) P. H. Weiner and J. F. Parcher, *Anal. Chem.*, **45**, 302 (1973).

AIDS FOR ANALYTICAL CHEMISTS

Simple Device for Improving the Production of Coiled Glass Capillary Columns

Eugene Reiner and James W. Weaver

Center for Disease Control, Public Health Service, U.S. Department of Health, Education, and Welfare, Atlanta, Ga. 30333

At present, the use of glass capillary columns in gas chromatography is increasing because of the many advantages of this material over metal (*1–3*). Since the cost of commercially available uncoated glass columns is high, most workers elect to make their own, either with home-built or commercially constructed glass-drawing machines (*4*).

In using a capillary glass-drawing device, troubles are usually encountered when the initial straight portion of capillary tubing (Figure 1,A) passes through the rollers (Figure 1,B) and on through the heated coiling tube (Figure 1,C). Some of these troubles can be traced to inefficient lubrication of the heated coiling tube (graphite is the commonly used lubricant). Either too much or too little graphite can cause bits of glass to break off in the heated coil-forming tube. As a result, the tube clogs, and the entire op-

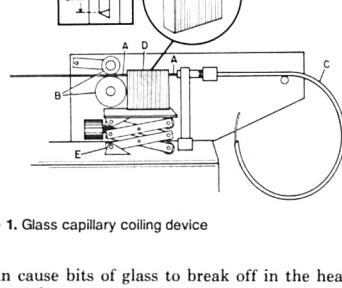


Figure 1. Glass capillary coiling device

(1) M. Novotny and A. Zlatkis, *Chromatogr. Rev.*, **14**, 1 (1971).
(2) M. d'Aubigne, C. Landault, and G. Guiochon, *Chromatographia*, **4**, 309 (1971).
(3) A. L. German and E. C. Horning, *J. Chromatogr. Sci.*, **11**, 76 (1973).
(4) D. H. Desty, J. N. Haresnape, and B. H. F. Whyman, *Anal. Chem.*, **32**, 302 (1960).

eration comes to a halt. The accumulated glass fragments and graphite must then be removed.

A simple expedient, which we have used advantageously, consists of placing a trough (Figure 1,D) filled with graphite immediately in front of the coiling tube. As the straight portion of capillary burrows through the trough, small portions of graphite cling to the glass, thus assuring constant, adequate lubrication. To avoid getting graphite inside the glass tubing, the first few coils should be severed.

For glass drawing machines operating in the vertical mode, a small cylinder with slots cut into the side from top to bottom and filled with graphite, should serve the same purpose.

The trough (Figure 1,D insert) consists of a block of aluminum (4.5 × 4.0 × 1.3 cm), with a slot milled 3 mm wide and 6 mm deep. The block is supported by a small laboratory jack (Figure 1,E).

With the former arrangement, starting with borosilicate glass tubing (122 cm long × 0.8-cm o.d. × 0.3-cm i.d.), wastage is kept to such a minimum that 62–68 meter lengths of coiled capillary tubes (0.95 mm-o.d. × 0.34-mm i.d.) are consistently attained.

In addition, since column efficiency increases with column length, longer columns are frequently desirable. By using shrinkable Teflon tubing, capable of operating at temperatures to 327°, several coiled sections of glass capillaries can be joined together without loss of efficiency.

ACKNOWLEDGMENT

Thanks are due to Edgar Biel, Instructional Media Division, CDC, for the drawing which appears in this communication.

RECEIVED for review June 11, 1974. Accepted July 22, 1974.

Glass-Immobilized 8-Hydroxyquinoline for Separation of Trace Metals from Base Electrolytes Used for Anodic Stripping Analysis

E. D. Moorhead and P. H. Davis

Departments of Chemical Engineering and Chemistry, University of Kentucky, Lexington, Ky. 40506

That anodic stripping voltammetry (ASV) provides a rapid and convenient method for the measurement of trace levels of amalgam-forming heavy metals is well known (*1*). However, the very high sensitivity of the ASV technique can produce problems arising from the purity of available solvents and reagents when the sample constituents fall into the parts per billion (ppb) or sub-ppb range. This complication is further accentuated if the material to be analyzed contains a mixture of trace metals, since separation of the complex response due to the sample from that produced by contaminants in the base, or supporting, electrolyte is difficult, and substantially compromises analytical speed and convenience.

Absolute reagent purity is a virtually unattainable ideal. Even with the purest of available chemicals and conscientious attention to problems of laboratory handling and storage, *ad hoc* contaminant levels in the ASV test solution may far exceed those in the original sample.

A frequently employed, straightforward method of reducing the effect of background interferences involves the use of extremely dilute supporting electrolytes and modern, three-electrode instrumentation with provision for IR compensation. If more concentrated base electrolytes are required for the analysis step, it is customary to clean up such solutions beforehand, using controlled-potential electrolysis at a mercury pool cathode (*2*).

In a recent study of the phase-selective anodic stripping analysis of gallium, we were confronted with the need to substantially reduce trace metal impurities from stock supporting electrolytes 2.0*M* to 6.0*M* in NaSCN. Concentrated thiocyanate is required in order to obtain polarographic reversibility of gallium (*3*), which ruled out using a very dilute salt as supporting electrolyte. Purification by controlled-potential electrolysis proved to be an unsuitable solution in this case because of the appearance of anode-generated thiocyanate oxidation products. The long electrolysis period required for purification produced yellow oxidation products even when the anode compartment was well isolated using a fine porosity glass frit diaphragm.

To circumvent these difficulties, an alternative purification approach was adopted in which the concentrated thiocyanate, contaminated primarily with Zn, Pb, Cd, and Cu, was passed through a 6-mm × 41-mm glass column packed with 7.16 cm^3 (wet) of Corning CPG-550 microporous glass beads, the surface area of which contained a coating of immobilized 8-hydroxyquinoline ("oxine") as metal chelating agent (Pierce Chemical Co.). The CPG-oxine had a pore diameter, average particle diameter, and surface area of 550 Å, 177–840 micrometers, and 70 m^2 gm^{-1}, respectively; its exchange capacity in milliequivalents of amine per gram was 0.03. As in the case of bulk separations of metals using oxine, retention of metals by immobilized oxine appears to be strongly pH dependent.

Following the manufacturer's recommendations, the column packing was first conditioned by elution with 1.0*M* HCl in an attempt to displace any residual metal, and then flushed with *ca.* 50 ml of quadruply-distilled water. In a trial run, a neutral solution 2.0*M* in NaSCN was passed through the column. Analysis of the effluent using the phase-selective ASV technique (*4*) revealed a substantial increase in Cu content, with Pb, Cd, and Zn essentially unchanged.

It is the manufacturer's recommendation that alkaline solutions, especially strongly alkaline solutions, should not be employed with the immobilized oxine if quantitative regeneration of separated metal is to be expected. As this was not an important consideration in the present application, it was decided to operate the column at pH > 7 to maximize retention of the trace metal constituents.

(1) E. Barendrecht in "Electroanalytical Chemistry—A Series of Advances," Vol. 2, A. J. Bard, Ed., Marcel Dekker, New York, N.Y., 1967, p 53.

(2) J. J. Lingane, "Electroanalytical Chemistry," Interscience, New York, N.Y., 1958.

(3) E. D. Moorhead, *J. Amer. Chem. Soc.*, **87**, 2503 (1965).

(4) E. D. Moorhead and P. H. Davis, *Anal. Chem.*, **45**, 2178 (1973).

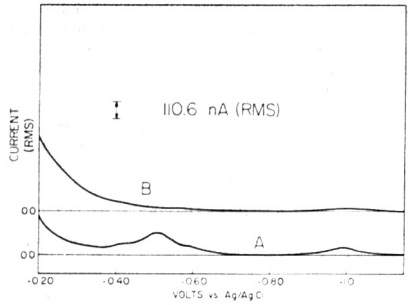


Figure 1. The effect of glass-immobilized 8-hydroxyquinoline on removal of trace metals from concentrated NaSCN as measured by phase-selective anodic stripping

Solution: 2.0*M* NaSCN. Frequency ≐ 50 Hz; applied voltage = 10 mV (rms); plating time = 5.0 min at −1.15 volts *vs.* Ag/AgCl; rest period = 30 sec; electrode area = 0.041 cm^2; T = 303 °K

Elution Procedure. After elution with a 25-ml volume of 1.0*M* HCl, the fresh column packing was washed with a 100-ml volume of quadruply-distilled water. An unbuffered solution 6.0*M* in NaSCN was then adjusted to pH 9 with NaOH and placed in an aspirator bottle. This reservoir was then connected to the head of the column through a glass needle–septum arrangement.

Initial aliquots of effluent gave a measured pH of 6.4. However, the pH gradually increased with time, and after passage of 450 ml of 6.0*M* NaSCN, the pH had risen to 8.5. In this initial step of purification, the first 25 ml of effluent were discarded and the remaining 425-ml volume collected in a receiver protected from laboratory air and dust.

After a second adjustment with NaOH to increase its pH to 9.0, the solution collected from the first run was passed through the column again—and once again the first 25 ml of effluent were discarded.

The level of trace impurities in both the original and twice purified NaSCN was monitored [after dilution from 6.0*M* to 2.0*M*] with ac phase-selective anodic stripping voltammetry using a Kemula-type micrometer hanging mercury drop electrode [Metrohm E-410].

Figure 1 provides a comparison of results obtained for the diluted solution. Curve *A* depicts impurity peaks which were obtained for the unpurified NaSCN. The addition to this solution of known metal ions tentatively identified the grouping of peaks at −0.5 volt *vs.* Ag/AgCl as due to Pb, Cu, and Cd, while the peak at −1.0 volt is due to zinc. In view of the care taken with these solutions and the use of quadruply distilled water, the curve *A* peaks are probably representative of the intrinsic heavy-metal impurity in the NaSCN salt. From a standard addition experiment, the zinc impurity in the solid salts was estimated to be 81 ppb.

On the other hand, curve *B* shows the result of passing this same solution twice through the bed of CPG-oxine beads. Virtually no evidence remains of the trace impurities at −0.5 volt *vs.* Ag/AgCl, and there is evidence of considerable reduction in the trace zinc at −1.0 volt.

Unlike ion exchange resins whose swelling characteristics normally vary considerably with ionic strength, the microporous glass packing appeared in this sense to be unaffected physically by use of concentrated salt. The material, which ordinarily appears a light ruby red in color, turned darker red in the presence of alkaline thiocyanate. Elution with HCl restored the material to its original color. The packing seemed unaffected by alkaline pH, although its ability to exchange metal quantitatively was untested.

In the present study, elution with 6.0*M* NaSCN resulted in the very slow flow rate of 25 ml hr^{-1}. Rather than working as a disadvantage, this enabled a system to be set up to process large quantities of material unattended, and obviated the usual necessity to commit electrochemical cells and potentiostats for prolonged periods. From our exploratory use of the glass-immobilized oxine, we conclude that the material represents a simple, convenient, alternative device for clearing supporting electrolytes of unwanted trace metals, and should prove useful for preparing stocks of alkali metal base electrolytes.

Received for review February 22, 1974. Accepted April 15, 1974.

PRODUCT CAPSULES

Scan this list for products of interest. Then, circle the indicated numbers on the adjacent reply card and selected literature from advertisers in the previous issue will be sent to you.

No.	Product
301	Amplifiers; Power Supplies
302	Balances
303	Baths; Circulators
304	Books
305	Centrifuges
306	Chemicals; Reagents
307	Chromatography, Gas
308	Chromatography, Liquid
309	Chromatography, Thin Layer
310	Computers; Calculators
311	Cryogenic; Refrigeration
312	Elemental Analyzers
313	Filters
314	Furniture
315	Labware, Glass & Plastic
316	Lasers
317	Microscopes
318	Mixers; Stirrers; Blenders; Grinders; Mills
319	Nuclear Instruments
320	Ovens; Furnaces; Heaters
321	Photometers; Colorimeters
322	Polarographic Instruments
323	pH Meters; Ion Meters; Titrators; Electrodes
324	Pipets; Dispensers; Fraction Collectors
325	Recorders; Integrators
326	Pumps; Valves; Fittings
327	Spectrometers, Atomic Absorption
328	Spectrometers, Fluorescence
329	Spectrometers, Infrared
330	Spectrometers, Mass
331	Spectrometers, NMR
332	Spectrometers, UV/VIS
333	Spectrometers, X-Ray
334	Temperature Instruments
335	Thermal Analyzers
336	Vacuum Equipment

MEMO

Send for the new expanded list of Spex High-Purity Compounds which now include halides, nitrates, sulfates and sulfides . . . many water soluble, ideal for standard solutions.

SPEX INDUSTRIES, INC. • BOX 798, METUCHEN, N.J. 08840 • ☎(201)-549-7144

CIRCLE 220 ON READER SERVICE CARD

FIRST CLASS
Permit No. 25682
Philadelphia, Pa.
19101

BUSINESS REPLY CARD

No postage stamp necessary if mailed in the United States

POSTAGE WILL BE PAID BY

ANALYTICAL CHEMISTRY

P. O. Box #8660

Philadelphia, Pennsylvania 19101

Analytical Chemistry

OCTOBER 1974

Valid through JAN. 31, 1975

NEW PRODUCTS, CHEMICALS, LITERATURE: 401 402 403 404 405 406 407 408 409 410 411 412 413 414 415
416 417 418 419 420 421 422 423 424 425 426 427 428 429 430 431 432 433 434 435 436 437 438 439 440 441 442
443 444 445 446 447 448 449 450 451 452 453 454 455 456 457 458 459 460 461 462 463 464 465 466 467 468 469
470 471 472 473 474 475 476 477 478 479 480 481 482 483 484 485 486 487 488 489 490 491 492 493 494 495 496

ADVERTISED PRODUCTS: 1 2 3 4 5 6 7 8 9 10 11 12 13 14 15 16 17 18 19
20 21 22 23 24 25 26 27 28 29 30 31 32 33 34 35 36 37 38 39 40 41 42 43 44 45 46
47 48 49 50 51 52 53 54 55 56 57 58 59 60 61 62 63 64 65 66 67 68 69 70 71 72 73
74 75 76 77 78 79 80 81 82 83 84 85 86 87 88 89 90 91 92 93 94 95 96 97 98 99 100
101 102 103 104 105 106 107 108 109 110 111 112 113 114 115 116 117 118 119 120 121 122 123 124 125 126 127
128 129 130 131 132 133 134 135 136 137 138 139 140 141 142 143 144 145 146 147 148 149 150 151 152 153 154
155 156 157 158 159 160 161 162 163 164 165 166 167 168 169 170 171 172 173 174 175 176 177 178 179 180 181
182 183 184 185 186 187 188 189 190 191 192 193 194 195 196 197 198 199 200 201 202 203 204 205 206 207 208
209 210 211 212 213 214 215 216 217 218 219 220 221 222 223 224 225 226 227 228 229 230 231 232 233 234 235
236 237 238 239 240 241 242 243 244 245 246 247 248 249 250 251 252 253 254 255 256 257 258 259 260 261 262

PRODUCT CAPSULES: 301 302 303 304 305 306 307 308 309 310 311 312 313 314 315 316 317 318 319 320
321 322 323 324 325 326 327 328 329 330 331 332 333 334 335 336 337 338 339 340

Name_____ Position_____

Company_____

Street_____

City_____ State_____ Zip_____

USE . . .

these postage paid reply cards for free data on all products advertised in this issue.

Analytical Chemistry **OCTOBER 1974** Valid through JAN. 31, 1975

NEW PRODUCTS, CHEMICALS, LITERATURE: 401 402 403 404 405 406 407 408 409 410 411 412 413 414 415
416 417 418 419 420 421 422 423 424 425 426 427 428 429 430 431 432 433 434 435 436 437 438 439 440 441 442
443 444 445 446 447 448 449 450 451 452 453 454 455 456 457 458 459 460 461 462 463 464 465 466 467 468 469
470 471 472 473 474 475 476 477 478 479 480 481 482 483 484 485 486 487 488 489 490 491 492 493 494 495 496

ADVERTISED PRODUCTS: 1 2 3 4 5 6 7 8 9 10 11 12 13 14 15 16 17 18 19
20 21 22 23 24 25 26 27 28 29 30 31 32 33 34 35 36 37 38 39 40 41 42 43 44 45 46
47 48 49 50 51 52 53 54 55 56 57 58 59 60 61 62 63 64 65 66 67 68 69 70 71 72 73
74 75 76 77 78 79 80 81 82 83 84 85 86 87 88 89 90 91 92 93 94 95 96 97 98 99 100
101 102 103 104 105 106 107 108 109 110 111 112 113 114 115 116 117 118 119 120 121 122 123 124 125 126 127
128 129 130 131 132 133 134 135 136 137 138 139 140 141 142 143 144 145 146 147 148 149 150 151 152 153 154
155 156 157 158 159 160 161 162 163 164 165 166 167 168 169 170 171 172 173 174 175 176 177 178 179 180 181
182 183 184 185 186 187 188 189 190 191 192 193 194 195 196 197 198 199 200 201 202 203 204 205 206 207 208
209 210 211 212 213 214 215 216 217 218 219 220 221 222 223 224 225 226 227 228 229 230 231 232 233 234 235
236 237 238 239 240 241 242 243 244 245 246 247 248 249 250 251 252 253 254 255 256 257 258 259 260 261 262

PRODUCT CAPSULES: 301 302 303 304 305 306 307 308 309 310 311 312 313 314 315 316 317 318 319 320
321 322 323 324 325 326 327 328 329 330 331 332 333 334 335 336 337 338 339 340

Name_____ Position_____

Company_____

Street_____

City_____ State_____ Zip_____

FIRST CLASS
Permit No. 25682
Philadelphia, Pa.
19101

BUSINESS REPLY CARD
No postage stamp necessary if mailed in the United States

POSTAGE WILL BE PAID BY

ANALYTICAL CHEMISTRY
P. O. Box #8660
Philadelphia, Pennsylvania 19101

PRODUC CAPSULI

Scan this list for of interest. Then, c indicated numbers adjacent reply card lected literature fro tisers in the previo will be sent to you.

No.	Product
301	Amplifiers; Power
302	Balances
303	Baths; Circulators
304	Books
305	Centrifuges
306	Chemicals; Reage
307	Chromatography,
308	Chromatography,
309	Chromatography,
310	Computers; Calcul
311	Cryogenic; Refrige
312	Elemental Analyze
313	Filters
314	Furniture
315	Labware, Glass &
316	Lasers
317	Microscopes
318	Mixers; Stirrers; Bl Grinders; Mills
319	Nuclear Instrumen
320	Ovens; Furnaces;
321	Photometers; Colorimeters
322	Polarographic Inst
323	pH Meters; Ion Me Titrators; Electr
324	Pipets; Dispensers Fraction Collect
325	Recorders; Integra
326	Pumps; Valves; Fit
327	Spectrometers, At Absorption
328	Spectrometers, Fluorescence
329	Spectrometers, Inf
330	Spectrometers, Ma
331	Spectrometers, NM
332	Spectrometers, UV
333	Spectrometers, X-
334	Temperature Instr
335	Thermal Analyzers
336	Vacuum Equipmer

approved

:otal organic carbon
volatile organic carbon
:otal carbon

The Dohrmann DC-50 organic analyzer

makes *all* of these measurements accurately nd rapidly. Based on proven, EPA *approved** nethods, it avoids interferences and undesire- able pyrolysis reactions that historically have resulted in significant errors.





- DIRECT READOUT: Four-digit presentation shows carbon content directly in mg/liter or ppm. *No recorder needed!*
- DIRECT MEASUREMENT: A single sample injection gives either Organic Carbon or Total Carbon content ***directly, not by difference.***
- INDEPENDENT MEASUREMENT: Volatile Organics are determined separately from Total Organics to aid in source identification.

- RELIABLE MEASUREMENTS: Determines important, lightweight volatiles such as low molecular weight alcohols and ketones, normally lost by acidification and sparging.
- FAST: 5 minutes per determination
- ACCURATE: Repeatability of ± 1 mg/liter or ± 2%
- WIDE RANGE: 1 to 2,000 mg/liter (ppm) without dilution
- PRICE: $7,875, including start-up assistance and operator training

EPA's evaluation:
"... Overall the unit performed in a most satisfactory manner. Detection limit was 0.5 to 1.0 mg C/l, working range was 1 to 2,000 mg C/l... Excellent comparisons were obtained in practically all cases. Thus, the Dohrmann DC-50 appears to be an acceptable alternative for measuring total organic carbon in water and wastes."

Newsletter No. 15, AQCL, NERC, EPA
Cincinnati, Ohio 45268

* ENVIRONMENTAL PROTECTION AGENCY, WATER PROGRAMS, Guidelines Establishing Test Procedures for Analysis of Pollutants. FEDERAL REGISTER Vol. 38, No. 199, Part II, Oct. 16, 1973.

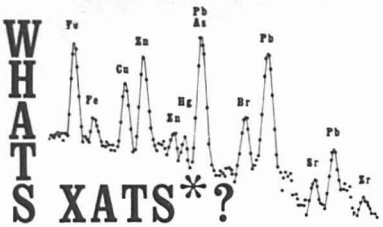
for brochures, reprints, or dates and locations of seminars, contact:

ENVIROTECH

DOHRMANN

3240 Scott Boulevard
Santa Clara, California 95050
Telephone (408) 249-6000
Telex 346 395

CIRCLE 56 ON READER SERVICE CARD



WHAT'S XATS*?

THE NEW MULTIELEMENT ANALYSIS SERVICE

for

AIR PARTICULATES • HEAVY METALS IN WATER • TRACE ELEMENT SCREENING • WEAR DEBRIS IN OILS • GEOLOGICAL, PLANT AND TISSUE SAMPLES

*X-ray Analysis of Thin Specimens — a new approach to non-destructive elemental analysis of solids and liquids for all elements above magnesium.

Only $25 per sample for 10 elements!

FOR INFORMATION CONTACT: JOHN RHODES

COLUMBIA SCIENTIFIC INDUSTRIES
Applied Research Division
P.O. Box 6190, Austin, Texas 78762 (512) 926-1530

CIRCLE 35 ON READER SERVICE CARD

FAMOUS SCIENTISTS NEW CASSETTES

ENERGY

- ☐ **Cleaning a Dirty Fuel** H. Feldman
  From Wastes to Energy H. Feldman
- ☐ **Energy: A Critique**
  Dr. Dean Abrahamson
  Puzzles of Air Pollution
  Arthur Levy
- ☐ **Antidote to the Energy Crisis**
  George Long
  Chemicals In the Environment
  Dr. Samuel Epstein

ENVIRONMENT

- ☐ **The Damaged Air-I**
- ☐ **The Damaged Air-II**
- ☐ **The Struggle for Clean Water-I**
- ☐ **The Struggle for Clean Water-II**
- ☐ **Water Supply of the Future**
  Dr. I. Kugelman
  The Secrets of Salmon
  Dr. A. Hasler
- ☐ **New Weapons Against Insects**
  Dr. G. Staal & Dr. J. Siddall
  Moths, Drugs, & Pheromones
  Dr. W. Roelofs

BIO-MEDICAL

- ☐ **Chemistry of the Mind-Schizophrenia**
  Dr. Larry Stein
  Chemistry of the Mind-Depression
  Dr. Joel Elkes
- ☐ **Early Prenatal Diagnosis of Genetic Disease** Dr. M. L. Moss
  From Mother to Child
  Dr. M. Horning & Dr. R. Hill
- ☐ **Nature's Own Toxicants in Foods**
  Dr. J. M. Coon
  Added, Not Intended
  Dr. H. Kraybill

SCIENCE

- ☐ **Wine From Native American Grapes-I** Dr. A. Rice
  Wine From Native American Grapes-II Dr. A. Rice
- ☐ **Probing Creation** Dr. M. A. Coler
  New Directions in U.S. Science
  Dr. W. McElroy
- ☐ **Chemicals Combating Cancer**
  Dr. D. Grassetti
  Chemical Essence of Beer & Ale
  Dr. R. Palamand

	ACS Members	Nonmembers
Single Cassette	$5.59	$6.59
Any Eight Cassettes	$4.20/cassette	$5.20/cassette

Any 20 or more cassettes to one address $4.00/cassette

10% DISCOUNT if payment accompanies order

Order From: American Chemical Society, 1155 16th Street, N.W. Washington, D.C. 20036. ATTN: A. Poulos

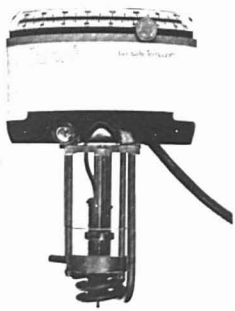
---

Bath circulators Don't settle for second best!

Techne bath immersion circulators are first rate. Three units, each of which stirs, heats, pumps and controls the temperature of the bath liquid. Self contained instruments. Clip to practically any laboratory vessel and you have a constant temperature bath.

Control precision ±0.01 °C. Units with built-in overheat and liquid level cut out systems. Units for high temperature 200 °C operation.

Techne circulators combine high precision and rugged dependability in a way which is unique. See for yourself!



For free 16 page constant temperature bath catalog write to Techne Incorporated, 661 Brunswick Pike, Princeton, New Jersey 08540 or call (609) 452-9275.

Techne

. . . leaders in constant temperature baths

AVAILABLE THROUGH MAJOR LABORATORY SUPPLY HOUSES.

CIRCLE 222 ON READER SERVICE CARD

Never Before SO_2 Specific

Direct, clean, and specific. That's the way you measure SO_2 stack emissions with the new state-of-the-art Model 40 Pulsed Fluorescent Analyzer from Thermo Electron.

No flames, consumable reactants, or hazardous bottled gases are required. The Model 40 has 5 full scale ranges from 0.5 to 5000 ppm with precision to 0.5%. It demonstrates linear response through the full range, excellent stability, and freedom from interference. Never before has measurement been so specific. Pulse us for details.

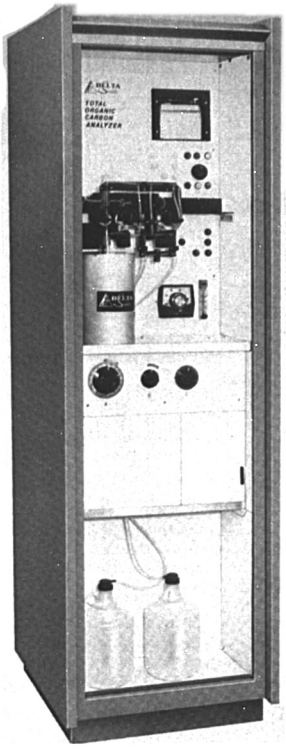


Thermo Electron
CORPORATION

Environmental Instruments Division
85 First Avenue, Waltham, Mass. 02154 / (617) 890-8700

CIRCLE 226 ON READER SERVICE CARD

New Products



Total Carbon Analyzer

Model 8055 total organic carbon analyzer features a nephelometric sensor to analyze unfiltered waste and water samples. Range can be extended from 0–1 to 0–5000 mg/l. or higher. Tests take 5 min, and programming includes total carbon, inorganic carbon, and volatile and nonvolatile organic carbon. Delta Scientific Corp. **405**



Electrophoresis Scanning System

The system pictured includes scanner, computing integrator, and analog recorder all in one modular unit. Transmittance and reflectance scanning for protein electrophoresis strips and thin-layer chromatograms is featured. Scan speeds include 1, 2, 3, and 6 cm/min/automatic fast return with a maximum length of scan of 200 mm. The computing integrator has a maximum storage capacity of 31 fractions with a maximum computation time of 1000 msec. Precision of the analog recorder includes ±0.25% accuracy and better than 0.1% reproducibility. Further specifications are provided in an 8-p brochure. Camag Inc. **401**

Glucose and Blood Urea Nitrogen Analyzer

System 1 glucose/BUN analyzer is a benchtop instrument fully automated from sample pickup through self-calibration to final answer in mg/dl. STAT samples can be inserted with readout in 64 sec. Features include self-calibration against a known standard, automatic detection and flagging of false positives and negatives, and throughput of 112 results/hr. The turntable accommodates up to 40 discrete samples with sample volume of 14 μl/test. Beckman Instruments **403**



New Products



Sulfur Detector

Lab-X 100, offered by Telsec Instruments Ltd., is one of a series of analyzers for detecting elements in the oil, chemical, and mineral industries. Optimum analytical time is 50 sec in the concentration range from 100 ppm to 100% with a typical detection limit of 15 ppm. The X-ray fluorescence system requires no careful sample weighing and permits solid, liquid, or powder forms to be analyzed. Analex Ltd., P.O. Box 2, Didcot, OX 11 9NA, England

Hemoglobin in Blood

Fisher digital hemophotometer rapidly and reliably measures hemoglobin in blood with precision of 0.2 grams of hemoglobin per 100 ml. The unit is designed and tested for use with classical methodologies that employ cyanmethemoglobin determination at 540 nm. The digital model accepts specimens diluted 1:251 and contains an additional switch to convert and utilize samples diluted 1:501. Calibration is held to within ±0.2 g-Hb for extended periods of time. Fisher Scientific Co. 424

Gas Partitioner

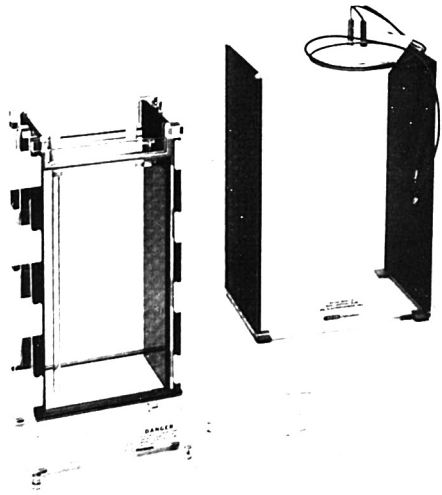
Model 1200 gas partitioner analyzes fixed gases and hydrocarbons with a dual-column, dual-detector configuration. A partition column separates hydrocarbons, whereas an adsorption column separates fixed gases such as oxygen, nitrogen, and carbon monoxide. Accuracy is ±2°C throughout the operating temperature range, and liquid samples with boiling ranges up to 250°C may be handled. Accessories provide for the routine analysis of natural gas and reactive gas mixtures. Fisher Scientific Co. 419

Fast Detection System

Model 509 high-frequency lock-in amplifier is capable of detecting short-lived phenomena from flash photolysis or other pulse-type stimuli. A wide-band preamplifier provides 25 dB gain from below 20 Hz to over 15 MHz, and an internal gate which attenuates video signals during the pulse permits examination of events occurring as soon as 2 μsec after the stimulus. The model was originally designed for use with the company's GHz EPR spectrometer and is priced at $4500. Micro-Now Instrument Co. 416

Solid Materials Microanalysis System

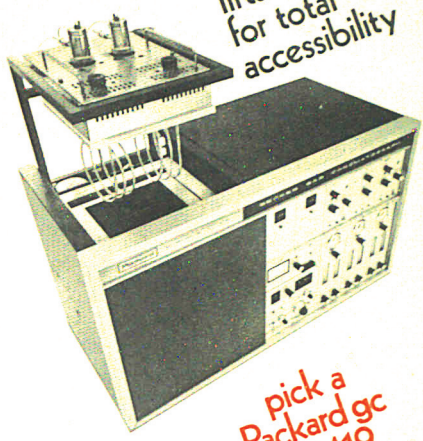
Microanalytical systems for in situ measurements of the relative abundances of stable or radioactive nuclides within solid materials are now available. The systems analyze gases (by mass spectrometry or counting) which are released by laser volatilization from selective portions of a sample. Sensitivities of less than 10^{-6} atoms are readily attainable for many nuclides. Prices vary with sensitivity specifications. Megrue Associates 411



Gel Electrophoresis Cells

Two dual vertical slab electrophoresis cells for analytical and preparative work are being offered with adjustable slab thickness of 0.75, 1.5, or 3.0 mm. Model 220 has a slab length of 100 mm for routine research, and Model 221 has a slab length of 280 mm for high-resolution work and separation of RNA fragments. Model 220 is priced at $545, and Model 221 at $755, complete with all components to make two 20-well slabs. Bio-Rad Laboratories 406

the unique gc



Packard presents the remarkable Model 419 Gas Chromatograph with the exclusive lift-top oven. The entire analytical package—inlets, columns, detectors—lifts up to give 360° eye level access for quick changing of columns or can be lifted off for rapid exchange of analytical systems. Large column oven with digital control of temperature parameters from −150°C to 500°C . . . a true proportional cryogenic attachment . . . and the unique multiflex injection system are only a few of the total flexibility features of the 419. And with every 419 comes Packard's world-wide sales and service organization. Write for additional information—request Bulletin 1192.

Packard

pick a Packard gc the 419

GAS CHROMATOGRAPHS

Packard

PACKARD INSTRUMENT COMPANY, INC.
2200 WARRENVILLE RD. • DOWNERS GROVE, ILLINOIS 60515
PACKARD INSTRUMENT INTERNATIONAL S. A.
TALSTRASSE 39 • 8001 ZURICH, SWITZERLAND
SUBSIDIARIES OF AMBAC INDUSTRIES, INC.

CIRCLE 190 ON READER SERVICE CARD

From ELECTRO-NUCLEONICS, INC.

Controlled-Pore Glass Chromatography

PERMEATION / EXCLUSION PACKINGS
AFFINITY-SUPPORTS • HIGH-SPEED GPC PACKINGS
PREPACKED COLUMNS

Controlled-Pore Glass (CPG)
- For permeation/exclusion chromatography
- Twelve narrowly controlled pore sizes: 40 to 3000Å
- Separation range: 10^3 to 10^6 M.W.
- Use aqueous or organic solvents
- Pore size unaffected by eluant, pH, pressure, temperature
- Flow rates up to 100x faster than soft gels
- Unaffected by concentrated acids, corrosive solvents, detergents
- Easily cleaned, reused, sterilized; immune to biological attack
- No preswelling required; fast packing

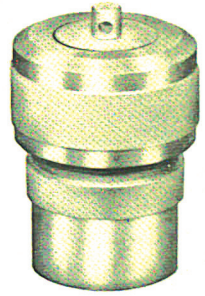
Affinity-Supports
- Controlled-Pore Glass matrix: rigid, chemically inert, use aqueous or organic solvents
- Attach ligands, enzymes, hormones, antibodies, antigens
- Available functional groups: alkylamine, arylamine, carboxyl

Speed-Pore™ Packings
- For high-speed permeation chromatography
- Porous quartz-glass chemically modified to eliminate adsorption
- Use aqueous or solvent systems
- Pore sizes: 40, 75, 170, 240, 700, 2000Å

Redi-Pak™ Columns
- Prepacked with Controlled-Pore Glass (autoclavable)
- Septum end-closures for sterile connections, and injection; ideal for pathogens
- Use or store in any position
- Available empty for use with any rigid column packing

ELECTRO-NUCLEONICS, INC.
368 Passaic Ave., Fairfield, N.J. 07006 / Tel. (201) 227-6700 / Telex 138302

CIRCLE 68 ON READER SERVICE CARD



THE PARR ACID DIGESTION BOMB

The rapid and safe way to dissolve inorganic samples in HF, HCl or HNO_3, or to digest organic materials in strong alkalis or oxidizing acids with complete sample recovery.

Samples are held in a 25 ml, thick walled Teflon* cup which is not attacked by the acid charge. This cup is confined within a sturdy stainless steel bomb from which it is easily removed for sample recovery and washing. No wrenches or clamps are needed to produce a tight seal.



Ask for PARR Bulletin 4745 describing this rapid method for dissolving difficult samples.

*duPont TFE fluorocarbon resin.

PARR INSTRUMENT COMPANY
211 Fifty-Third St. Moline, Ill. 61265
(309) 762-7716

CIRCLE 187 ON READER SERVICE CARD

Choose the right method and the best equipment to achieve superior results.

1. TECHNIQUES AND APPLICATIONS OF PLASMA CHEMISTRY
Edited by John R. Hollahan, **Tegal Corporation** and Alexis T. Bell, **University of California, Berkeley**

Analysts . . . Technicians . . . Scientists and Engineers . . . learn how to apply the most successful applications of plasma chemistry to your work in organic chemistry, polymer, chemistry, biology, electronics and materials science.

1974 (Sept.) 416 pages $22.50

2. DETERMINATION OF GASEOUS ELEMENTS IN METALS
Edited by Laben M. Melnick, **United States Steel Corporation,** Lynn L. Lewis, **General Motors Corporation** and Ben D. Holt, **Argonne National Laboratory**

21 experts give you a firm grasp of the underlying principles of the behavior of gases in metals, and show you how to choose the best method and instrumentation to determine gases in all common and many uncommon metals.

1974 720 pages $39.95

3. REGISTRY OF MASS SPECTRA DATA Four Volumes
By the late Einar Stenhagen, Sixten Abrahamsson, **University of Goteborg,** and Fred W. McLafferty, **Cornell University**

This is the most **complete** and **accurate** source of mass spectral data ever compiled! It equips you with the best mass spectra of **18,806 different compounds** arranged for quick and easy reference. Compounds are arranged by structural type as well as by molecular weight and elemental composition.

1974 3392 pages $250.00 (sold only as a set)

Mail this coupon to:
WILEY-INTERSCIENCE, Dept. 313
Grand Central Station, New York, N.Y.

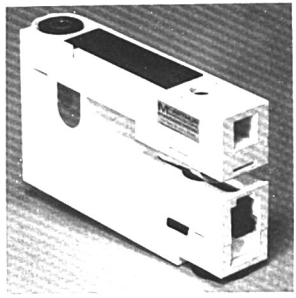
Please send me the book(s) I have checked below.
☐ My check (money order) for $ _____ is enclosed.
☐ Please bill me. (Restricted to the continental United States.)
☐ Please send me a list of local bookstores carrying your titles.
☐ 1. (40628-7) @ $22.50
☐ 2. (59328-1) @ $39.95
☐ 3. (82115-2) @ $250.00

Name _____
Title _____
Firm (College) _____
Address _____
City _____
State _____ Zip _____

Please add state and local taxes where applicable. Prices subject to change without notice. A4736WI

CIRCLE 256 ON READER SERVICE CARD

New Products



Pocket Microscope

The McArthur microscope features 5 × 3 × 1-in. dimensions and precision compound optics, providing overall magnifications of 80×, 200×, and using a special eyepiece, 400×. A battery-powered light source is standard. Three versions are available, including the polarizing model and triple-objective model. The standard unit is priced at $84.50. Imanex International 402

Portable Calibration System

Model 320 calibration system can be operated on internal rechargeable nickel–cadmium batteries, a 12-V automotive system, or 110-V ac. Designed for the exclusive use of permeation tubes, the unit's factory-set temperature is 35°C, and the permeation tube can be maintained within 0.1°C of the set point with a meter readout for temperature verification. An internal pumping system produces a resettable, continuously variable dilution flow with a range of 300–1500 ml/min. Analytical Instrument Development, Inc. 420

Vinyl Chloride Detection

A new system for the detection of vinyl chloride features a flasher assembly with electrical heater to provide energy to flash the collected sample from absorption tube to gas chromatograph. Vinyl chloride can be monitored in concentrations as low as 50 ppb, well below OSHA's proposed detection standard. Bendix Corp. 422

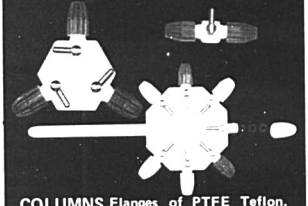
For more information on listed items, circle the appropriate numbers on one of our Readers' Service Cards

High Performance LIQUID CHROMATOGRAPHY PRODUCTS



CONNECTORS Make it easy on yourself. You no longer need to have every tubing connector available. The new unique Unimetrics Omnifit Universal Connector allows you to connect tubing of glass, metal or plastic in any combination of these materials in sizes from 3mm to 11 mm O.D. The connectors are chemically inert, autoclavable, and leak-tight to 600 psi.

VALVES PTFE Teflon with EN58J Stainless Steel Valve Keys. Two-way, three-way, and seven-way valves. Chemically inert, no dead space, autoclavable, each channel has variable diameter fittings to connect tubing up to 3.95mm O.D., and pressure rated at 250 psi. Many combinations of switching possible to run numerous identical columns.



COLUMNS Flanges of PTFE Teflon. High Sensitivity with cross section of 0.33 cm^2. Seven lengths from 10mm to 1500mm. Jackets for temperature control.



KITS Versatile selection of components to construct a variety of column systems.

CATALOGS Please request

Unimetrics CORPORATION
1853 Raymond Avenue
Anaheim, Calif. 92801
714-879-3777

CIRCLE 236 ON READER SERVICE CARD

Tracer Gas Vapor Detector

SF-6 gas detector/chromatograph detects traces of sulfur hexafluoride tracer and other halogens in minute concentrations. Detection is by an electron capture detector. The unit is capable of operating from rechargeable batteries for field use, and the detection probe is made of nonsparking brass and glass fiber and has a water trap. Ion Track Instruments, Inc. 426

CO_2 Monitor/Controller

Model 20-450 monitor/controller measures and regulates the percent carbon dioxide content of incubators. Featured are direct reading of the co_2 concentration, direct dial setting of desired concentration, all solid-state circuitry, decreased CO_2 consumption, and accuracy to $\pm 0.25\%$ CO_2 in air. Single unit price: $580; double unit price: $990. GOW-MAC Instrument Co. 433

Particulate Metals in Air

Air microsampler for sampling particulate metals in air traps airborne particulates on a millipore filter and analyzes the sample by atomic absorption spectrophotometry. Analysis time takes 3 min, including sample collection. Lead concentrations as low as 0.1 $\mu g/m^3$ and cadmium levels as low as 0.0008 $\mu g/m^3$ can be measured routinely. Varian Associates 412

Vinyl Chloride Detector

This simple-to-use gas detector kit is designed to measure 5–500-ppm vinyl chloride in the atmosphere as well as the atmospheric levels of 82 hazardous gases. Precise samples are drawn into the reagent-filled tube by means of a precision-calibrated pump. Vinyl chloride tube # 132B has a lower detection level of 1 ppm. Matheson Gas Products 418

Automatic Gradient Former

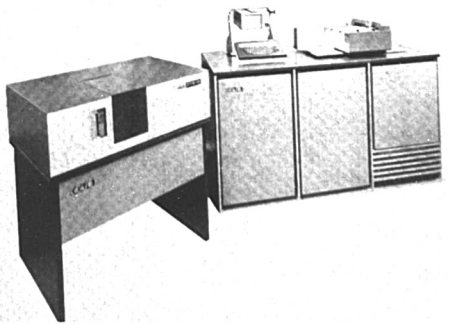
The Mixograd forms linear, concave, convex, or complex gradients of pH, concentration, etc., by combining two liquids in continuously varying proportions. A gradient profile is drawn on millimeter graph paper, cut to shape, and repeated with perfect reproducibility with the aid of an electronic profile-following device. Included are a built-in column rinse timer, automatic shut-off, and a peak detector to interrupt the gradient. Gilson Medical Electronics, Inc. 408

Tubular Furnace

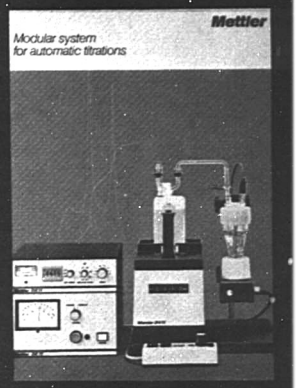
Model 1700 HTF horizontal furnace features 1650°C maximum temperature and a new type heating element for instant servicing. The 3-in. diameter furnace is especially suited to sintering, ceramic firing, brazing, annealing, and crystal-growing applications. CM Manufacturing Co. 415

Fourier Transform IR Spectrophotometer

FTS-15 FT infrared spectrophotometer provides a high-resolution interferometer, high-speed minicomputer, and fourth-generation FT/IR software. Resolution to 0.25 cm^{-1} is selectable from a silent magnetic keyboard. Features include an alphanumeric graphic display, printout on a digital plotter, and a light pen and interactive display scope. The double-beam spectrophotometer with improved signal-to-noise ratio (S/N) is priced at $79,950. Digilab, Inc. 407



So much more automatic titration capability...



it takes these 8 pages to tell about it.

The multi-purpose Mettler Automatic Titrator actually offers more automatic titration capability than any other comparable system.

You can carry out automatic end point titration, recording titration, pH or pIon stat procedures. Its accuracy and versatility meet the exacting demands of the research laboratory. Its ease of operation makes it ideal for the quality control lab. For continuous automatic control, just start it up and press a button. Programming controls are simple. Rapidly interchangeable burettes in 1, 10, 20 and 50 ml snap-in and snap-out of the drive to speed titrant changes.

The Mettler Automatic Titrator meets all potentiometric needs with aqueous and nonaqueous solutions, and provides direct entry into data processing systems. For more information, circle the number.

Mettler

CIRCLE 160 ON READER SERVICE CARD

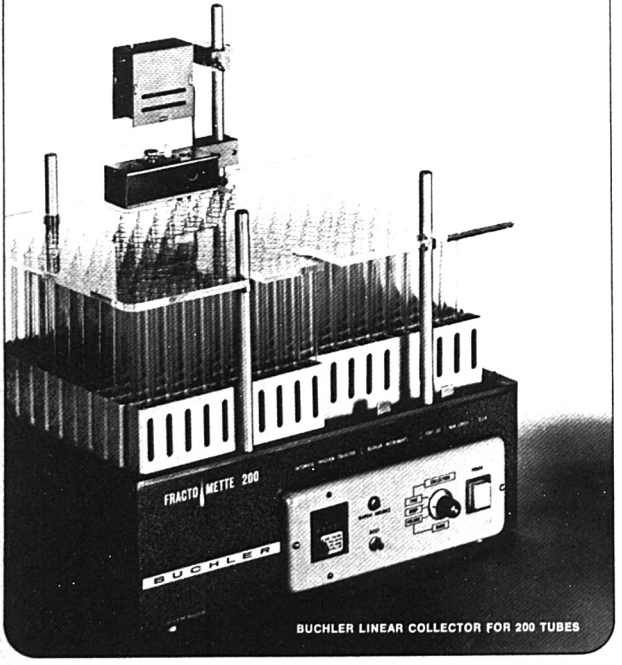
Considering a Fraction Collector?

Consider Buchler.

Liquid chromatography, density gradients, electrophoresis . . . anywhere a versatile, automatic fraction collector is required, Buchler has the exact model. Linear, circular, long run, short run, sectional, micro . . . you name it, we make it.
Buchler Fraction Collectors offer a choice of collection methods, solid state electronics for cold room use, refrigeration options, and ease of conversion for changes in application. We believe Buchler Fraction Collectors are — dollar for dollar — the best value on the market. So if you're collecting fractions without collecting our literature, you could be missing something. Write today for complete information.

SEARLE **Buchler Instruments**

Division of Searle Analytic Inc.
1327 Sixteenth Street
Fort Lee New Jersey 07024



BUCHLER LINEAR COLLECTOR FOR 200 TUBES

CIRCLE 28 ON READER SERVICE CARD

New Products



pH/Conductivity Analyzer

Model 4403 offers pH measurements from 0 to 14, readable to two places, and five conductivity ranges between 0–1.4 and 0–140,000 μohms/cm. Specific ion measurements (optional) may also be read either in millivolts or pH. Liquid crystal digital readout is featured. The 9 × 10 × 8-in. analyzer is available in 110 or 220-V 50/60-Hz models and is priced at $773. Markson Science, Inc. 404

Trace Analyses Electroanalytical System

Model 174A/315 automated electroanalytical system is capable of providing part-per-billion analysis of metals, anions, organics, pollutants, and pharmaceuticals, utilizing a polarographic analyzer and automated electroanalysis controller. Automatic operation deaerates and blankets the sample solution, preconditions the working electrode, initiates and terminates the scan, times critical steps in the run, controls the stirrer, provides duplicate or triplicate runs, and controls strip chart advance. Priced at $4570. Princeton Applied Research Corp. 413

Laboratory Recorder

Model 447 oscillograph includes one 14-channel magnet bank, resistor mounting board, and a remote control and record intensity control. The unit has a full 8-in. peak-to-peak deflection and records up to 42 traces. Features include 12 standard recording speeds ranging from 0.1 to 100 in./sec and a frequency response of 5000 Hz. Optional features and equipment are available. Hathaway Industries, Inc. 414

Radioimmunoassay Test Materials

IMMO PHASE solid-phase RIA test systems include antibody preparation, standards, reference controls, and tracer material. Standards and reference controls are lyophilized, and the antibody tubes are stable for a minimum of 120 days. Beta (^{3}H) Digoxin and Gamma (^{125}I) Digoxin are available now, and Insulin, T_3, and Angiotensin I will be available soon. Corning 421

Bio-Oxidation System

A new bench scale bio-oxidation system for experimentation in municipal and industrial waste treatment consists of the console cabinet, glass apparatus, support stand, 5-ft length of silicone tubing for each pump, and fittings. The system provides for continuous flow for uniform organic loading, metered aeration, positive suspended solids control, and hydraulic loading similar to full-scale systems. Cole-Parmer Instrument Co. 425

Portable Analyzer/Chromatograph

The portable OVA organic vapor analyzer detects, measures, and analyzes hazardous gases present in most industries. Operation is continous for 8 hr, and a built-in gas chromatographic system with flame ionization detector permits on-the-spot qualitative analysis when required. The unit features 1-ppm sensitivity (methane), with a response time of 2 sec. Applications include leak detection in gas handling equipment and toxic vapor measurements for compliance with OSHA requirements, among others. Century Systems Corp. 409

Grain Quality Analyzer

Model 31 grain analyzer determines percent protein, oil, water, and other constituents of grain by utilizing a patented tilting filter technique with high-speed scanning capability and modification of a previously well-known principle in infrared light absorption. Interchangeable calibration cards and an internal computer system allow a different portion of the spectrum to be read for alternate determinations. Complete specifications and accuracy/precision data are provided in the company's brochures. Applications include measuring the quality of beer, wines, margarine, and butter. Neotec Corp. 417

Dielectric Spectrometer

UNIRELAX is a modular system for performing dynamic dielectric, dynamic mechanical, thermomechanical, differential thermal, and dynamic depolarization analyses on polymeric plastics and ceramics. The system consists of a basic main frame containing temperature control instruments and a test cell holder to which may be added a wide variety of test cells for exploring internal stresses and voids, curing behavior of polymers from the monomer stage onward, etc. Tetrahedron Associates, Inc. 423

Portable Total Hydrocarbon Analyzer

Model 550 has a completely heated sampling probe and detector to avoid condensation of the organic compounds to be sampled. The hand-held unit incorporates a digital readout with concentration in ppm of hydrocarbons in the air being sampled. Featured are a recorder output, an audible flame-out alarm, a concentration alarm, and a minimum of 8-hr operation in the portable mode. Analytical Instrument Development, Inc. 410

Electron Capture Detector

Model-140 wide-range EC detector system can be adapted to any existing gas chromatograph, permitting continuous linear measurements of common pesticides and other electron-capturing substances to be made over a five-decade dynamic range. The detector operates in a patented variable-frequency pulsed mode and provides a pulsed output signal, whose frequency change is proportional to the concentration of the gas being measured, and a dc output voltage proportional to the differential pulse repetition frequency. Analog Technology Corp. 427

Syringe Pump

Model 314 high-pressure liquid chromatography syringe pump delivers 200 kg/cm^2 in constant flow from 0.8 to 200 ml/hr. Total capacity is 375 ml. Construction is of single-stroke steel with precision bearings. An electronic digital pressure monitor/regulator is available as an optional accessory. Instrumentation Specialties Co. 430

For more information on listed items, circle the appropriate numbers on one of our Readers' Service Cards



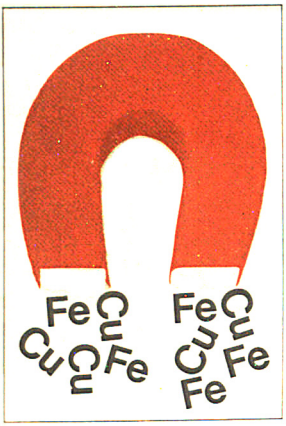
Want to automatically determine melting and boiling points without any possibility of misinterpreting results? Determine exact melting ranges of polymer films and fibers, liquid crystal preparations, and sub-microgram quantities of organic compounds using thermal microscopy? Obtain digital dropping points of lubricants, food fats, paraffins and waxes? Softening points of fats, coal tar pitches, polymers and resins? The new generation of instruments, the modular Mettler FP system, will do them all faster, easier, more accurately.

There's a separate Mettler FP furnace for each application. All provide high-precision, electronically controlled, linear (to ±0.1°C) heating and cooling with extremely fast response over the −20 to +300°C range. Temperatures at which significant thermal events occur are digitally displayed. Accurate, reliable platinum resistance sensors, closely matched by Mettler, enable you to choose the furnace which precisely suits your needs. For detailed information, circle the number.

Mettler

CIRCLE 161 ON READER SERVICE CARD

Chelex 100 vs. heavy metals.



[fatal attraction]

Chelex 100, Bio-Rad's chelating exchange resin, shows a high specific affinity for the ions of copper, iron, and other heavy metals. It's ideally suited for **removing, concentrating,** or **analyzing** trace amounts of these metals, even in the presence of large quantities of sodium and potassium.

Chelex 100's diverse applications include: **analysis** of trace metals in natural waters, reagents, biochemicals, and physiological solutions • **removal** of trace metals from reagents, culture media, soils, buffers and enzyme systems • **recovery** of metals from process streams • **chromatography** of closely-related metals • **concentration** of trace metals for atomic absorption or anodic stripping voltammetry analyses.

Call or write for bulletin 114.

BIO-RAD Laboratories
32nd and Griffin Avenue
Richmond, CA 94804
Phone (415) 234-4130

Also in: Rockville Centre, N.Y.; Mississauga, Ontario; London; Munich; Milan.

CIRCLE 21 ON READER SERVICE CARD

New Products

Data Acquisition Systems

Two multichannel scanning/digitizing systems for data monitoring, logging, and transmission have just been introduced which feature complete, complementary digital output formats that permit wide-range equipment compatibility and simultaneous use. Model DAS-1AV has a unique algebraic-averaging feature for long-term monitoring of fluctuating parameters found in ecological surveys, erratic processes, and high noise/signal situations. Model DAS-16 data-acquisition/telemetry system is designed for monitoring, collecting, and recording vital data from remotely controlled, unattended installations via a central/satellite network. FX Systems Corp. 434

Sample Transport System

This automatic sample transport is a pneumatically operated system which is capable of accommodating 44 samples placed in 11 magazines. Sample volumes range from 20 to 250 ml, and the system can be used with all Mettler titrator modules. Features include interchangeable buret heads, with 1, 10, 20, and 50-ml volume sizes. Once set up, the 44 samples are titrated completely automatically. Titration results are completed with a desk-top calculator. Mettler Instrument Co. 428

IR Exhaust Performance Analyzers

This line of analyzers is used to measure the hydrocarbon and carbon monoxide content of internal combustion engines and provide rapid, accurate detection of ignition and carburetor problems. The new automotive test equipment features easy-to-read meters, separate HC and CO readouts, fast measurements, easy calibration, and 10-min warm-up. The equipment will be utilized for testing conformance with emission regulations and control requirements. Barnes Engineering Co. 432

For more information on listed items, circle the appropriate numbers on one of our Readers' Service Cards

Chemicals

Catalyst

Catalyst R3-11, used in the purification of gases and liquids in laboratories and manufacturing, removes oxygen from gases and liquids and oxidizes hydrogen and carbon monoxide contained in inert gases. Composition is approximately 30% copper in highly dispersed form. Operating temperature of the pellet-form catalyst is 0–250°C, and prices range from $12 for 250 grams to $15.95/kg for 100 kg. Chemical Dynamics Corp. 435

Isotope-Labeled Compounds

Approximately 100 new stable isotope-labeled amino acids, carbohydrates, drugs, lipids, and steroids are now available, including such compounds as cholesterol (4-^{13}C), oleic acid (9,10-^{13}C), glucose (1-^{13}C), and a number of resolved C-13 and N-15 labeled amino acids. A catalog is available listing the compounds and other intermediates. Koch Isotopes 438

Diagnostic Reagents

A line of accurately standardized Hematall reagents has been specially formulated and use-tested for Coulter counter systems. Included are an isotonic diluent, lysing agents, and detergents for removing lysing agents and cellular debris. All are given a one-year performance guarantee. Fisher Scientific Co. 439

Sucrose, Density Gradient Grade

A special grade of sucrose for density gradient centrifugation is available for preparing sucrose gradients for separating RNA preparations. Specifications include less than 5-ppm heavy metals and negligible RNAase activity. The material is chromatographically homogeneous in NRC-recommended paper systems. EM Laboratories, Inc. 437

Packing Materials Sample Kit

A liquid chromatography column packing materials sample kit permits the chromatographer to pick the optimum material for his application without the expense of purchasing large quantities of other materials. Packings included span a wide range of polarities, and sufficient amounts of each material (four in all) are provided to pack two 2-mm i.d. × 61-cm columns with each material. The kit is priced at $155. Empty column assembly, $45. Waters Associates, Inc. 436

Manufacturers' Literature

Surface and Thin-Film Analysis

A 15-p brochure of the company's systems, components, and lab services for surface and thin-film analysis lists complete systems such as the Auger electron spectroscopy unit, thin-film analyzer, and scanning Auger microprobe. Included are sections on software, quality control, analytical services, and a catalog of accessories. Physical Electronics Industries, Inc. 448

Hydrogen Analysis

"Current Peaks" engineering quarterly, 6 p, describes a new GC technique for measuring hydrogen in any sample, utilizing the company's dual carrier gas system. Also featured are articles on improved methods for trace CO and vinyl chloride detection. Carle Instruments, Inc. 474

Instrument Applications

Varian Instrument Applications, Vol 8, No. 2, 16 p, features articles on optimization of the electron capture detector, trace metal determinations in hair, and fluorescence excitation and analysis. Instruments featured include the 8500 liquid chromatograph and the CFT-20 carbon-13 NMR spectrometer. Varian Associates 462

Automated Materials Analyzer

Bulletin 7262, 12 p, discusses the AMA-40 modular system for automating a wide variety of manual analytical techniques such as sample dissolution or extraction, filtration, sample pipeting and aliquot transfer, etc. The modular system combines discrete sample, wet chemistry batch analysis with analytical instrumentation for simultaneous multiple analyses. Beckman Instruments 464

Clinical Laboratory Products

Bulletin 7500, 16 p, summarizes the company's total line of health care laboratory equipment, including enzyme activity analyzers, glucose/BUN analyzers, electrophoresis systems, and instruments for radioimmunoassay, cardiopulmonary applications, and vascular analysis. Beckman Instruments 469

Biochemical Research Products

Bulletin 6500, 12 p, summarizes Beckman's line of instrumentation and chemical products for biochemical research. Illustrated descriptions and specifications of instruments, bioproducts, and chemicals are included. Beckman Instruments 453

Thin-Layer Chromatography

Telechrom Topics, Vol 1, No. 2, 4 p, is a bimonthly publication which features new product descriptions and application information. This issue features a device to alert the researcher when plate development is complete and an article on amine and steroid separations. Applied Science Laboratories, Inc. 471

Calculator Guide

A 16-p booklet, called the "Executive's No-Nonsense Guide to Computing Calculators," describes types of calculators and relates computing powers of each to the readers' needs. Recent developments and differences in capabilities among various types of calculators are discussed. Hewlett-Packard Co. 445

Table-Top Centrifuge

Bulletin 6303, 1 p, describes a new miniature centrifuge for spinning down blood samples and precipitates from micro samples in less than 60 sec. The unit can accommodate 250 and 400-μl tubes, permitting 30 and 48-tube maximum capacity runs, respectively. 1.5-ml tubes may also be used. Beckman Instruments 447

Radioimmunoassay Catalog Supplement

An updated supplement, 1 p, announces the availability of a new intermediate for rapid labeling of proteins to high specific activity with ^{125}I. Also listed are a number of RIA labeled antigen and unlabeled antibody components. Calatomic 449

Data Systems for Mass Spectrometers

A 12-p brochure describes the DS50 system for use with modern GC/MS instruments. Features include fast data acquisition with real time mass determination and Interscan reports, double or single-beam operation, full range of high and low-resolution analytical reports, and a wide range of available peripherals. AEI Scientific Apparatus 450

This is the heart of the Mettler DSC System.



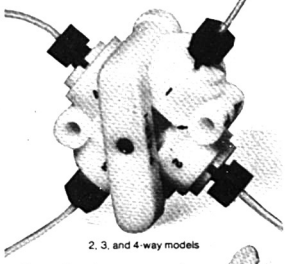
The vapor-deposited, thin-film thermopile sensor at the heart of the Mettler scanning calorimeter is revolutionary for a commercial instrument. As a sensor it is fast and responsive—assures excellent heat contact with crucibles. It is ideally suited for accurate purity determinations, as well as heat of fusion, specific heat, and many more measurements.

The modular TA 2000 DSC system offers everything you want in thermal analysis. It is more sensitive and reproducible than most comparable instruments. It offers 0.17 millicalories per second full scale sensitivity. And calorimetric reproducibility of ±0.5%. Noise level is less than ±1 microcalorie per second. Temperature range covers −20 to 500°C, with precision of ±0.1°C, and isothermal fluctuations of ±0.002°C. Extremely linear selectable heating and cooling rates in steps of 0.1°C. Temperature programs can be controlled remotely. It is completely computer compatible. For your copy of the 8-page Mettler TA 2000 brochure, circle the number.

Mettler

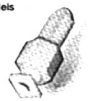
CIRCLE 162 ON READER SERVICE CARD

ALTEX®
MINIATURE
VALVES
AND
FITTINGS



2, 3, and 4-way models

Every inert component you need to quickly construct any liquid or gas flow system.



- ☐ CHEMICALLY INERT
- ☐ ZERO DEAD VOLUME
- ☐ LEAK TIGHT TO 500 PSI
- ☐ MATE PERFECTLY WITH GLASS-METAL-PLASTIC



Compatible with other micro-plumbing components, the Altex system includes: Tees and Crosses, Luer Adapters, Couplings, Stainless-steel and Glass Tube Adapters, Plugs, Pipe Connectors, TEFLON Tubing and Flanging Tool.

Also . . . a complete line of Liquid Chromatography Columns and Sample Injection Valves.





COMPLETE CATALOG on request

ANALTECH
75 Blue Hen Drive
Newark, Delaware 19711
(302) 737-6960
CIRCLE 7 ON READER SERVICE CARD

Manufacturers' Literature

Portable NO_x Meter

Model 2200 portable chemiluminescent NO, NO_2, and NO_x meter is described in a 2-p brochure which includes complete specifications, pricing, and delivery information. The unit weighs 12 lb, is A-C or battery powered, and is capable of measuring NO, NO_2, and NO_x levels accurately to within 5 ppb with a precision of ±1% of full scale. EPA ranges of 0–5.0 ppm are covered. McMillan Electronics 451

Sample Concentrators

Publication No. 439, an 8-p brochure, describes the complete line of Minicon disposable concentrators for rapid enrichment of dilute macrosolute mixtures in the clinical or biomedical research laboratory. Unique features and operating principles are described, applications data are included, and electrophoresis patterns are illustrated. Amicon Corp. 454

Thin-Layer Chromatography

Publication No. JJ-6, entitled "Thin-layer Chromatography with Eastman Chromagram Sheet and Developing Apparatus," serves as an introduction to the company's line of TLC products. Tables of R_f values and descriptions of visualization reagents and techniques are included. Eastman Kodak Co. 455

AA Accessory

A 4-p brochure discusses the HGA-2100 improved graphite furnace for use with atomic absorption spectrophotometers to increase their sensitivity while simplifying trace determinations. Perkin-Elmer Corp. 452

Fluorometric Analysis

Fluorescence News, Vol 8, No. 2, 8 p, features a technical report on fluorometric methods of analysis on silicon rubber pads by Herbert K. Y. Lau and G. G. Guilbault. Other information on new fluorescence systems and a bibliography of recent articles are included. American Instrument Co. 457

For more information on listed items, circle the appropriate numbers on one of our Readers' Service Cards

Geological Research

A 12-p technical manual describes and illustrates new procedures for rapid automatic precision lapping of 30-μ rock sections, including application notes. Hacker Instruments, Inc. 446

Spectrophotometers

An 18-p brochure describes the company's 700 Series spectrophotometer systems and accessories and includes a complete table of instrumentation specifications. Included are digital electronic controllers for UV–VIS spectrophotometers, ratio recording and fluorescence spectrophotometers, and detector and light source modules. GCA/McPherson Instruments 458

Water Testing

Product bulletin 323, "Water Testing with Gelman Filters—Biological Testing/Suspended Solids Testing," offers complete procedures for water testing with the membrane filtration technique. An expanded listing of current references documenting use of these filters is included. Gelman Instrument Co. 459

Thin-Layer Chromatography

A 7-p brochure describes how to get better TLC results through the concept of PMD—Programmed Multiple Development. The method is described in detail, as well as R_f and resolution, spot reconcentration effect, sensitivity and efficiency, tolerance to overloading, and independence from spotting technique. Regis Chemical Co. 460

GC Bibliography

A new gas chromatography bibliography of Porapak applications contains over 190 entries and covers more than 60 application areas. Specific chemical classes and types of separations are indexed for easy reference. Waters Associates 461

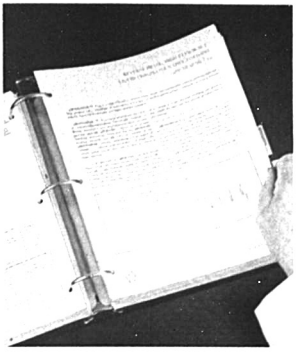
Affinity Chromatography

BIO-RADiations No. 16, a 4-p technical periodical, features affinity chromatography materials, and describes the use of Bio-Gel P. References to applications of the polyacrylamide gel filtration medium are included. Bio-Rad Laboratories 467

SO_2 Analyzer

A 4-p brochure on the Model 43 pulsed fluorescent analyzer for ambient air concentrations of SO_2 describes principles of operation and full specifications and capabilities. A schematic diagram of instrumentation is presented. Thermo Electron Corp. 470

from Waters/the Liquid Chromatography People



required reading

for better, faster chromatographic separations

Consider Waters' library of liquid chromatography information your resource for solving separations problems. We've got factual, concise, and helpful monographs on a wide variety of topics. They are yours for the asking. Send for our complete Applications Index today. And if your separations problem is more pressing, give us a call; we'll do our best to help you.

WATERS ASSOCIATES

137 Maple Street, Milford, Mass. 01757
Telephone (617) 478-2000
The Liquid Chromatography People
CIRCLE 252 ON READER SERVICE CARD

Manufacturers' Literature

Indicator and Test Papers

"pH Indicator Papers, Test Papers and Visocolor Test Kits for Analysis of Water and Waste Water," 23 p, is the company's 7th annual catalog edition covering this product group. Test kits for the determination of contaminants in water include those for ammonium, chromate, detergents, phosphate, and silicon dioxide. Gallard-Schlesinger 472

Thermocouple Applications

Bulletin 1111 DB 9, 11 p, includes recent information on types of thermocouples, proper calibration and applications, limits of error, temperature ranges and limitations of various types, wire gauge sizes, and information on protection tubes. Several valuable tables and a temperature conversion guide are included. Barber-Colman Co. 465

Analytical Kits

Brochure No. 310, 15 p, lists a complete line of radioimmunoassay and competitive protein binding assay kits, controls, and supplies. Twenty-one kits are listed, and summaries of the tests are provided. Also featured are elevated control serums, a nuclear counting system for "in vitro" tests, and liquid scintillation counting reagents. Fisher Scientific Co. 468

Monochromator Attachment

A 6-p brochure describes Model 665 double-beam attachment and ratio recording electronics for converting GCA/McPherson VUV–UV–VIS and IR monochromators into double-beam spectrophotometers. Model 782 logarithmic ratiometer, part of the electronics, is also featured. GCA/McPherson Instrument 476

Power Supplies Catalog

A new 130-p 1974 catalog and handbook on stabilized power supplies has just been published containing simplified schematic and mechanical drawings of more than 30 power supply designs encompassing hundreds of separate models. The handbook section discusses ferroresonance, measurement techniques, thermal design criteria, multiunit interconnections, etc. Kepco, Inc. 463

Serious lock-in, ridiculous price:

$1050.*



*U.S. domestic price.

- 0.5 Hz to 150 kHz frequency range
- 10 μV full-scale sensitivity
- 100 nV, 100 pV, and 0.1 pA sensitivity with optional plug-in preamps
- 60 dB (1000x) dynamic reserve plus pushbutton high- and low-pass filters for 106 dB (200,000x)
- Optional bandpass/notch plug-in
- Does 2f measurements even with its own optional plug-in oscillator
- Time constants down to 250 μsec

The Ortec 9501's wide-band dynamic reserve enables it to measure signals accurately in the presence of high noise overloads. Its reference circuitry is automatic-tracking with precise, fast-setting phase controls. And it has advanced, multi-purpose triggering capabilities. For complete technical data, contact your nearby Ortec representative or Ortec Incorporated, 110 Midland Road, Oak Ridge, Tenn. 37830. (615) 482-4411.

ORTEC
AN EG&G COMPANY

© ORTEC 5924
CIRCLE 180 ON READER SERVICE CARD

LABORATORY SUPPLY CENTER

Acenaphthylene • p-Aminohippuric Acid • Aurin • 4-Bromopyridine HCl
tert-Butyl Chloride • Cellobiose • α-Chloralose • Cresol Red & Na
m-Cresyl Acetate • Cuprous Bromide • 2,4-Diaminophenol DiHCl
Dichloroacetic Acid • 2,6-Dichloroindophenol, Na • 2,2'-Dipyridyl
Esculin • Levulinic Acid • Levulose • Mercuric Potassium Iodide
3-Methyl Glutaric Anhydride • Orcinol • Phenol Red & Sodium Salt
Potassium Acid Phthalate • Reinecke Salt • Sodium Dithionate
Sodium Tetraphenylboron • Succinimide • o-Vanillin • Xanthone

Write for our NEW Products List of over 3,000 chemicals

Tel.: 516-273-0900 TWX: 510-227-6230

EASTERN CHEMICAL
Division of GUARDIAN CHEMICAL CORP.
BOX 2500 K
HAUPPAUGE, N. Y. 11787

Do You Need....
90% CARBON-13?
For lowest prices, call (415) 234-4130
or write for our newest isotope catalog.
BIO-RAD Laboratories
32nd & Griffin, Richmond, CA 94804

Do you need?
OPTICAL SHIFT REAGENT
$Eu(TFC)_3$ 1 g $30.00
BIO-RAD Laboratories
32nd & Griffin Ave., Richmond, CA 94804

POLLUTION STUDIES
- AIR, WATER & INDUSTRIAL ENVIRONMENTS
- CONTAMINATION IN FOOD & PACKAGING

Write for Brochure
GOLLOB ANALYTICAL SERVICE CORP
46 Industrial Road,
Berkeley Heights, N. J.
07922
201-464-3331

Rates Available
on Request
ANALYTICAL CHEMISTRY
50 West State Street
Westport, Ct. 06880
203-226-7131

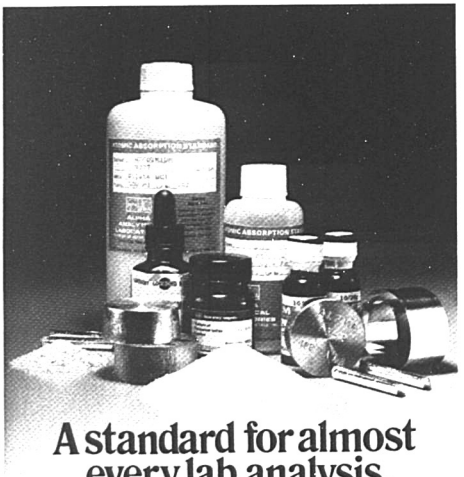
CABLE ADDRESS: SACTEX PROMPT SHIPMENT

Lithium Metaborate $LiBO_2$ Anhydrous*

Faster fusions at lower temperatures. Less damage to platinumware. Lower blanks. Easier dissolution after the fusion. Photometric and titrimetric measurements may be made directly on the dissolved fusions.

*It is imperative that ANHYDROUS $LiBO_2$ be used for fusions to prevent expansion when heated!

SAC
SOUTHWESTERN ANALYTICAL CHEMICALS
BOX 485 — AUSTIN, TEX
AREA 512 444-3626
—literature on request



A standard for almost every lab analysis.

Spectrochemical standards, both nonferrous and ferrous; atomic absorption standards; high-purity metals and metal salts; water and waste-water analysis reagents; laboratory reagents and chemicals, including inorganics, organics, pesticides, plasticizers, surfactants. And more. Send for our free catalog.

alpha analytical laboratories Inc.
Division of Alpha Metals Inc.
57 Freeman Street, Newark, New Jersey 07105 (201) 589-7150

CIRCLE 3 ON READER SERVICE CARD

Purity levels less than 0.1 ppm total ash



If this were ordinary graphite we'd use an ordinary package.

You're looking at a unique new package developed by POCO Graphite that's anything but ordinary.

First, it's made of graphite. Second, it's purified. Third, it's wrapped and sealed in plastic film.

Because of our new package, you can now specify purity levels less than 0.1 ppm total ash in all spectroscopic electrodes made by POCO from isotropic graphite.

If purity is one of your problems, you can solve it with the new POCO Graphite package which is purified with the electrodes inside.

Our new package doesn't cost you extra, it's standard with all rod-type preforms made from isotropic graphite.

That's the only thing ordinary about POCO Graphite Spectroscopic electrodes.

Poco Graphite, Inc.
A Union Oil Company of California subsidiary
1601 South State Street, Decatur, Texas 76234
Telephone (817) 627-2121 • TWX 910-890-5724

union 76 POCO

CIRCLE 196 ON READER SERVICE CARD

The
CRYSTAL-CLEAR
DROP
...symbol of reliable

ULTRA-HIGH-PURITY SOLVENTS

from
BURDICK & JACKSON
LABORATORIES

Ask for Data Sheet BJ-25
"Distilled-in-Glass" Solvents
BJ-21 Liquid Scintillation
Counting

BURDICK
& JACKSON
LABORATORIES, INC.
MUSKEGON, MICHIGAN 49442 (616)726-3171

CIRCLE 22 ON READER SERVICE CARD

FREE CATALOG Describes Harvard's line of pumps for moving fluids in small volumes precisely and reliably. These pumps handle flows ranging from 0.05 ml. per hour to over 2 liters per minute, in such diverse applications as drug infusion, batch sampling and pilot plant studies.



SMALL-VOLUME PUMPS

Mail coupon to:
Harvard Apparatus
Department B07
P.O. Box 24
Millis, Mass. 02054
Or call (617) 376-2986

Please send the Harvard Pump Catalog to:

Name_____

Dept._____

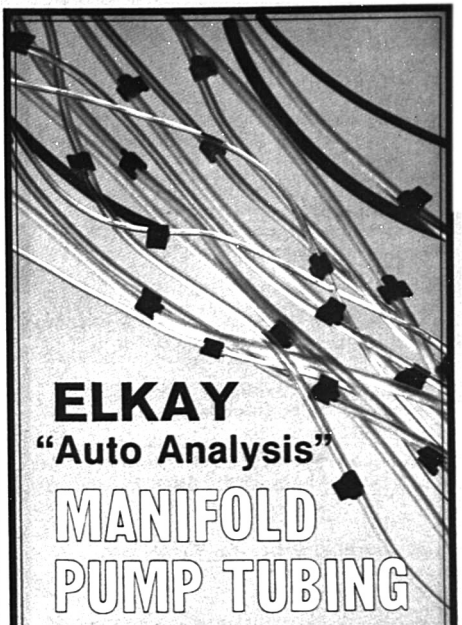
Institution_____

Address_____

City_____ State_____ Zip_____

HARVARD APPARATUS

CIRCLE 116 ON READER SERVICE CARD



ELKAY
"Auto Analysis"
MANIFOLD PUMP TUBING

1. **Standard**
2. **Acid Flexible**
3. **Solvent Flexible**

Quality assured by Elkay's exacting standards. All tubing continuously monitored for consistent flow, performance and efficiency. Elkay's new optical comparator evaluates all tubing for specification accuracy.

NOTE:
Solvent flexible tubing is specially formulated to yield longer pumping life when solvents are used. Acid flexible tubing is designed for pumping strong acids.

Immediate Delivery

ELKAY
PRODUCTS, INC.
95 Grand St., Worcester, Mass. 01610
Tel: (617) 757-4435

CIRCLE 69 ON READER SERVICE CARD

Future Articles

Silica-Containing Cross-Linked Polymer as Highly Efficient and Thermally Stable Stationary Phase for Gas Chromatography
Wilhelm Bruening, I. M. R. de Andrade Bruening, and A. L. Scofield

Alternating Current Linear Sweep and Cylic Voltammetry at a Dropping Mercury Electrode with Phase-Selective Fundamental and Second Harmonic Detection
H. Blutstein and A. M. Bond

Real-Time System for Microsecond-Range Acquisition and Processing of Fast Spectrometric Data
J. A. Miller, P. Levoir, J. C. Fontaine, F. Garnier, and J. E. Dubois

Steady State Current Analysis for Kinetic Studies Using Twin Packed Graphite Electrodes
J. H. Strohl and J. Hern

Direct Measurement of $E'_{1/2}$ with Reversible and EC Electrode Processes by Second Harmonic Alternating Current Polarography and Voltammetry
Alan M. Bond and Donald E. Smith

Solvent Extraction for Use with Flame Atomic Absorption Spectrometry
John D. Kinrade and Jon C. Van Loon

Determination of Magnesium Oxide in Finely Divided Magnesium Metal
T. A. Hiller and V. A. Stenger

Cold-Tap Preconcentration Method for the Determination of Mercury in Sea Water and in Other Natural Materials
William F. Fitzgerald, W. Berry Lyons, and Carlton D. Hunt

Factors Influencing the Kinetics of Ligand Substitution Reactions of Nickel(II) and Cobalt(II) Ions in Acetonitrile as Solvent
P. K. Chattopadhyay and J. F. Coetzee

Direct Analysis of Water Samples for Organic Pollutants with Gas Chromatography–Mass Spectrometry
Lawrence E. Harris, William L. Budde, and James W. Eichelberger

Programmed Sedimentation Field-Flow Fractionation
Frank J. F. Yang, Marcus N. Myers, and J. Calvin Giddings

Sedimentation Field-Flow Fractionation
J. Calvin Giddings, Frank J. F. Yang, and Marcus N. Myers

Selective Modulation: A New Instrumental Approach to the Fluorimetric Analysis of Mixtures without Separation
T. C. O'Haver and W. M. Parks

Application of Numerical Taxonomy Techniques to the Choice of Optimal Sets of Solvents in Thin Layer Chromatography
Desire L. Massart and Henri De Clercq



RECIPROCATING SHAKERS

Eberbach continuous duty laboratory shakers are designed for the exacting requirements of research and for general purpose shaking. A wide range of available carriers adds to their versatility. They are sturdy machines providing a maximum of reliability. Speeds are variable and are not affected by normal line voltage fluctuations or loading within specified limits.

Cat. **5850**—speed 20-240, adjustable stroke, 11½ x 12 x 9½". For 115v, 50/60 Hz, Power Unit Only . . $362.00

Cat. **5900**—speed 60-240, adjustable stroke, 39 x 20 x 10". For 115v 60Hz, Power Unit Only $629.00

Cat. **6000**—speed 60-260, fixed stroke, 24½ x 13½ x 10". For 115v, 60 Hz Power Unit Only. $433.00

One and Two speed shakers also available.

Eberbach CORPORATION
P.O. BOX 1024
ANN ARBOR, MICHIGAN
48106

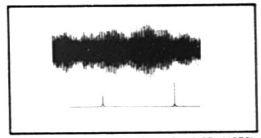
CIRCLE 71 ON READER SERVICE CARD

NICOLET nmr data systems...

for routine research problems and advanced applications

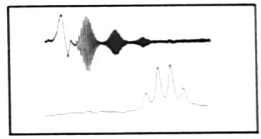
The Nicolet 1080 and NMR-80 data acquisition and analysis systems are in use worldwide in solving not only routine research problems but also in advancing the frontiers of nmr knowledge. These data systems are highly regarded for their timing accuracy, sensitivity, continuous display capabilities and general versatility in the conception and execution for new experiments. Some of these are:

STOCHASTIC RESONANCE — This technique involves random noise modulation of the rf excitation frequency, leading to a broadband excitation whose response is measured and Fourier transformed much as in conventional pulsed-FT nmr. Its principal advantage lies in the fact that much less rf power is needed to excite the chemical shift range of interest and that it has the same Fellgett's advantage of FT nmr.



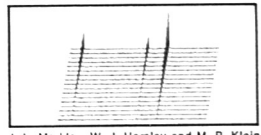
R. R. Ernst, *J. Mag. Res.* 3 10-27 (1970); R. Kaiser, *J. Mag. Res.* 3 28-40, (1970); J. Cooper and R. Addleman, 13th Experimental Nmr Conference (1972); E. Lippmaa, private communication.

RAPID SCAN NMR — In this technique, a spectral region is swept at a rate much greater than allowed for by slow passage conditions and the resulting ringing spectrum correlated with a spectrum of a single ringing line or of a theoretical line. Its principal advantage lies in the ability to acquire data rapidly even in the presence of strong solvent lines, without requiring that these lines be part of the signal averaged data.



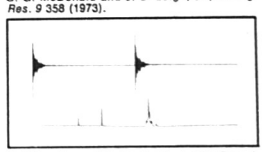
J. Dadok and R. F. Sprecher, 13th and 14th Experimental Nmr Conferences (1972, 1973); E. Becker, paper in press.

HOMOSPOIL T_1 SEQUENCE — This sequence allows the rapid measurement of long T_1's without the long $5xT_1$ waiting period needed by the inversion-recovery sequence. It is accomplished by a -(90-spoil-tau-90-sample-spoil)- sequence.



J. L. Markley, W. J. Horsley and M. P. Klein *J. Phys. Chem.* 55 3604 (1971); R. Freeman and H. D. W. Hill, *Ibid.* 54 April (1971); G. G. McDonald and J. S. Leigh, Jr., *J. Mag. Res.* 9 358 (1973).

QUADRATURE DETECTION NMR — This technique allows $\sqrt{2}$ enhancement over conventional pulsed nmr since the rf carrier can be placed in the center of the spectral region and dual phase detectors used to receive the response. The two resulting free induction decays are Fourier transformed using a complex transform which results in a single frequency domain spectrum.



J. Schaeffer and E. O. Stejskal, 15th Experimental Nmr Conference (1974), and *J. Mag. Res.* March (1974) (in press). J. D. Ellett, et al. *Adv. Mag. Res.* 5 117 (1971)

Please phone or write for details on these applications or to discuss how the versatile NMR-80 data system may be used for your experiments. Complete systems start at $20,000. If you are already a Nicolet data system user, you may order free software for the above techniques from our Nicolet Users Society (NUS) library.

NICOLET INSTRUMENT CORPORATION
5225 Verona Road
Madison, Wisconsin 53711
Telephone: 608/271-3333

CIRCLE 173 ON READER SERVICE CARD



Series 3000
over $4,000

Ever wish for a top-loader that eliminated dialing-in of weights and guessing at the readout? The fully automatic new Sartorius 3000 is such a balance. Electronic display of indicated weight (no readout error!) and completely automatic weight compensation (no dialing-in of weights!) combine to speed up weighings by as much as 50%. BCD output for connection to data processing equipment is built-in. The Sartorius 3000 comes in two weighing ranges: Model 3014 has 1,000g capacity with 0.01g readability; Model 3015, with 160g capacity, is the only fully automatic top-loader readable to 0.001g.

The electronic Sartorius 3000 costs over $4,000, but not every laboratory needs a balance as sophisticated as this. In fact, two reasons why the 3000 might not interest you at all are our Series 1100 and 2250 top loaders. These Sartorius 'workhorses' are tops in value and performance for virtually all routine weighings.

The 1104 is a compact, economical torsion balance with 1,000g capacity, 0.1g accuracy, built-in 500g optical taring, and costs only $495. The Series 2250 offers capacities from 160 to 5,000g, all-digital readouts, large, clear numerals, built-in taring, exceptional stability, plus many optional features. Prices begin at $1,000.

Whichever Sartorius you're interested in, we'll gladly send literature. Just write: Sartorius Balances Div., Brinkmann Instruments, Cantiague Rd., Westbury, N.Y. 11590.

Two reasons why the sophisticated new, electronic Sartorius 3000 might not interest you.



Series 1100
$495 & up

Series 2250
$1,000 & up

sartorius balances

CIRCLE 26 ON READER SERVICE CARD